THE UNIVERSITY OF NEWCASTLE

FACULTY OF SCIENCE AND IT

SCHOOL OF ENVIRONMENTAL AND LIFE SCIENCES

Thesis title:

SMALL MOLECULE INHIBITORS OF THE HEDGEHOG SIGNALLING PATHWAY AS CANCER SUPPRESSING AGENTS

Thesis submitted in fulfilment of the requirement for the award of the degree of

DOCTOR OF PHILOSOPHY

(BIOLOGICAL SCIENCES)

BY

Nguyen Trieu Trinh

M.S.

Supervisors: Prof. Adam McCluskey

Prof. Eileen A. McLaughlin

Dr. Christopher P. Gordon

April 2016

Statements of originality and authorship

I hereby certify that this thesis contains no material which has been accepted for the award of any other degree or diploma in any University or other tertiary institution and, to the best of my knowledge and belief, contains no material previously published or written by another person, except where due reference has been made in the text. I give consent to the final version of my thesis being made available worldwide when deposited in the University's Digital Repository, subject to the provisions of the Copyright Act 1968.

Furthermore, I hereby certify that the work embodied in this thesis contains published journal articles of which I am the first author. I have included as part of the thesis a written statement, endorsed by my primary supervisor, attesting to my contribution to the joint publications.

Nguyen Trieu Trinh
29 April 2016

Acknowledgements

First, I would like to warmly thank all of my supervisors Prof. Adam McCluskey, Prof. Eileen A. McLaughlin and Dr. Christopher P. Gordon for teaching, supporting and guiding me through this amazing journey. Adam, without you I wouldn't be here in this beautiful city, and there would be no story to tell. I am lucky to be in your very well-equipped lab, where I have met wonderful people and developed my expertise in organic chemistry. I really appreciate all of your support, guiding and generosity during my research. Eileen, I will never forget the way you quickly and positively manage things, that's something so specific. Big issues become small and the small ones disappear when working with you, and that was always my privilege. It's my great honour to be a member of your lab, where people are so experienced, dedicated, and very supportive to guide me through the interesting biological assays. And Chris, you are so special, you taught me from the very beginning steps of my journey. Your explanations were quite simple to understand, and they have nurtured my passion and confidence in chemistry. You are an awesome teacher with whom every student would love to work with. You are always helping me and I am very grateful for that.

I would like to acknowledge my Prime Minister's Australia Asia Postgraduate Endeavour Awards, for giving me this precious chance to do high ranking research, as well as experience the exciting multicultural environment in Australia.

Thank you to all my friends and colleagues for supporting me in my research:

- *McCluskey's group*: Kelly, Jen, Peter, Laura, Cec, Fiona, Andrew L., Andrew S., Joey, Brad, Ahmed, Lacey, Mohamed, Mark R, Mark T, and Azadeh.
- *McLaughlin's group*: Ilana, Victoria, Kate, Jessie, Nicole, and Bettina. Special thanks to Ilana and Victoria who were patient enough to teach me how to do the biological assays, and Kate for valuable comments on my drafts.

Special thanks to the technical and administrative staffs, who always quickly supported me whenever I was in need of anything: Ben, Monica, Nathan, Michael, Stene, Steven, Vicky, Anna, and Andrea. Your help certainly made my life a lot easier.

And lastly, it's never enough to thank my beloved family: My wife Anh Le and my little girl Liuda Trinh, who are always supporting, sacrificing, and believing in me; my Mother, brothers, sister, and my late Dad who always take pride in me. Without you I am nothing. Thank you all so much.

Statement of contribution

I hereby certify that this thesis is submitted in the form of a series of published/submitted papers of which I am the first author. I have included as part of the thesis a written statement from each senior co-author; and endorsed by the Faculty Assistant Dean of Research Training, attesting to my contribution to the following joint publications:

1. Trinh TN, McLaughlin EA, Gordon CP, McCluskey A. Hedgehog Signalling Pathway inhibitors as cancer suppressing agents. MedChemComm 2014; 5(2): 117-33.
2. Trinh TN, Hizartzidis L, Lin AJS, Harman DG, McCluskey A, Gordon CP. An efficient continuous flow approach to furnish furan-based biaryls. *Organic & Biomolecular Chemistry,* 2014; 12(47): 9562-71.
3. Trinh TN, McLaughlin EA, Gordon CP, Bernstein IR, Pye V, Cossar P, Sakoff JA, and McCluskey A. Quinolone-1-(2*H*)-ones as Hedgehog Signalling Pathway Inhibitors, *Organic & Biomolecular Chemistry,* 2016*,* 14*,* 6304-6315.
4. Trinh TN, McCluskey A. A multi-component access to 1,3-thiazine-6-phenylimino-5-carboxylates. *Tetrahedron Letters*, 2016, 57, 3256-3259.
5. Trinh TN, McLaughlin EA, Gordon CP, Bernstein IR, Pye V, Redgrove KA, and McCluskey A. Small molecules inhibitors of Gli transcriptional factors of the Hedgehog Signalling Pathway. Submitted to *Organic & Biomolecular Chemistry* in October 2016.

Nguyen Trieu Trinh

Date: 02/11/2016

Statement of contribution of others

I, Adam McCluskey, attest that Research Higher Degree candidate Nguyen Trieu Trinh was responsible for the design and development of synthetic procedures, synthesis, and purification of synthesised analogues, biological testings, and the writing of publication manuscripts for the paper/publications entitled:

- Trinh TN, McLaughlin EA, Gordon CP, McCluskey A. Hedgehog Signalling Pathway inhibitors as cancer suppressing agents. MedChemComm 2014; 5(2): 117-33.
- Trinh TN, Hizartzidis L, Lin AJS, Harman DG, McCluskey A, Gordon CP. An efficient continuous flow approach to furnish furan-based biaryls. *Organic & Biomolecular Chemistry,* 2014; 12(47): 9562-71.
- Trinh TN, McLaughlin EA, Gordon CP, Bernstein IR, Pye V, Cossar P, Sakoff JA, and McCluskey A. Quinolone-1-(2*H*)-ones as Hedgehog Signalling Pathway Inhibitors, *Organic & Biomolecular Chemistry,* 2016*,* 14*,* 6304-6315.
- Trinh TN, McCluskey A. A multi-component access to 1,3-thiazine-6-phenylimino-5-carboxylates. *Tetrahedron Letters*, 2016, 57, 3256-3259.
- Trinh TN, McLaughlin EA, Gordon CP, Bernstein IR, Pye V, Redgrove KA, and McCluskey A. Small molecules inhibitors of Gli transcriptional factors of the Hedgehog Signalling Pathway. Submitted to *Organic & Biomolecular Chemistry* in October 2016.

Adam McCluskey

Signature of Co-author Full name of Co-author

Date: 2 November 2016

Nguyen Trieu Trinh

(Signature of Candidate) Full name of Candidate

Date: 2 Nov 2016

Signature of Assistant Dean of Research Training (ADRT) Full name of ADRT

Date:

I, Eileen McLaughlin, attest that Research Higher Degree candidate Nguyen Trieu Trinh was responsible for the design and development of synthetic procedures, synthesis, and purification of synthesised analogues, biological testings, and the writing of publication manuscripts for the paper/publications entitled:

- Trinh TN, McLaughlin EA, Gordon CP, McCluskey A. Hedgehog Signalling Pathway inhibitors as cancer suppressing agents. MedChemComm 2014; 5(2): 117-33.
- Trinh TN, McLaughlin EA, Gordon CP, Bernstein IR, Pye V, Cossar P, Sakoff JA, and McCluskey A. Quinolone-1-(2*H*)-ones as Hedgehog Signalling Pathway Inhibitors, *Organic & Biomolecular Chemistry,* 2016*,* 14*,* 6304-6315.
- Trinh TN, McLaughlin EA, Gordon CP, Bernstein IR, Pye V, Redgrove KA, and McCluskey A. Small molecules inhibitors of Gli transcriptional factors of the Hedgehog Signalling Pathway. Submitted to *Organic & Biomolecular Chemistry* in October 2016.

Eileen Anne McLaughlin

Signature of Co-author | Full name of Co-author

Date: 02/11/16

Nguyen Trieu Trinh

(Signature of Candidate) | Full name of Candidate

Date: 03/11/16

Signature of Assistant Dean of Research Training (ADRT) | Full name of ADRT

Date:

I, Christopher Gordon, attest that Research Higher Degree candidate Nguyen Trieu Trinh was responsible for the design and development of synthetic procedures, synthesis, and purification of synthesised analogues, biological testings, and the writing of publication manuscripts for the paper/publications entitled:

- Trinh TN, McLaughlin EA, Gordon CP, McCluskey A. Hedgehog Signalling Pathway inhibitors as cancer suppressing agents. MedChemComm 2014; 5(2): 117-33.
- Trinh TN, Hizartzidis L, Lin AJS, Harman DG, McCluskey A, Gordon CP. An efficient continuous flow approach to furnish furan-based biaryls. *Organic & Biomolecular Chemistry,* 2014; 12(47): 9562-71.
- Trinh TN, McLaughlin EA, Gordon CP, Bernstein IR, Pye V, Cossar P, Sakoff JA, and McCluskey A. Quinolone-1-(2*H*)-ones as Hedgehog Signalling Pathway Inhibitors, *Organic & Biomolecular Chemistry,* 2016*,* 14*,* 6304-6315.
- Trinh TN, McLaughlin EA, Gordon CP, Bernstein IR, Pye V, Redgrove KA, and McCluskey A. Small molecules inhibitors of Gli transcriptional factors of the Hedgehog Signalling Pathway. Submitted to *Organic & Biomolecular Chemistry* in October 2016.

Christopher Gordon

Signature of Co-author | Full name of Co-author

Date: 6/11/2016

Nguyen Trieu Trinh

(Signature of Candidate) | Full name of Candidate

Date:

Signature of Assistant Dean of Research Training (ADRT) | Full name of ADRT

Date:

I, Ilana Bernstein, attest that Research Higher Degree candidate Nguyen Trieu Trinh was responsible for the design and development of synthetic procedures, synthesis, and purification of synthesised analogues, biological testings, and the writing of publication manuscripts for the paper/publications entitled:

- Trinh TN, McLaughlin EA, Gordon CP, Bernstein IR, Pye V, Cossar P, Sakoff JA, and McCluskey A. Quinolone-1-(2*H*)-ones as Hedgehog Signalling Pathway Inhibitors, *Organic & Biomolecular Chemistry,* 2016, 14, 6304-6315.
- Trinh TN, McLaughlin EA, Gordon CP, Bernstein IR, Pye V, Redgrove KA, and McCluskey A. Small molecules inhibitors of Gli transcriptional factors of the Hedgehog Signalling Pathway. Submitted to *Organic & Biomolecular Chemistry* in October 2016.

ILANA BERNSTEIN

Signature of Co-author

Full name of Co-author

Date: 03/11/16

Nguyen Trieu Trinh

(Signature of Candidate)

Full name of Candidate

Date: 3 Nov 2016

Signature of Assistant Dean of Research Training (ADRT)

Full name of ADRT

Date:

I, Jennette Sakoff, attest that Research Higher Degree candidate Nguyen Trieu Trinh was responsible for the design and development of synthetic procedures, synthesis, and purification of synthesised analogues, biological testings, and the writing of publication manuscripts for the paper/publications entitled:

- Trinh TN, McLaughlin EA, Gordon CP, Bernstein IR, Pye V, Cossar P, Sakoff JA, and McCluskey A. Quinolone-1-(2*H*)-ones as Hedgehog Signalling Pathway Inhibitors, *Organic & Biomolecular Chemistry,* 2016*,* 14*,* 6304-6315.

Signature of Co-author

Full name of Co-author

Jennette A Sakoff PhD
Chief Hospital Scientist
Department of Medical Oncology
Calvary Mater Newcastle Hospital,
NSW

Date: 02/11/2016

Nguyen Trieu Trinh

(Signature of Candidate)

Full name of Candidate

Date: 03 Nov 2016

Signature of Assistant Dean of Research Training (ADRT)

Full name of ADRT

Date:

I, Peter Cossar, attest that Research Higher Degree candidate Nguyen Trieu Trinh was responsible for the design and development of synthetic procedures, synthesis, and purification of synthesised analogues, biological testings, and the writing of publication manuscripts for the paper/publications entitled:

- Trinh TN, McLaughlin EA, Gordon CP, Bernstein IR, Pye V, Cossar P, Sakoff JA, and McCluskey A. Quinolone-1-(2*H*)-ones as Hedgehog Signalling Pathway Inhibitors, *Organic & Biomolecular Chemistry,* 2016, 14, 6304-6315.

Peter. J Cossar

Sígnature of Co-author — Full name of Co-author

Date: 2.11.16

Nguyen Trieu Trinh

(Signature of Candidate) — Full name of Candidate

Date: 3 Nov 2016

Signature of Assistant Dean of Research Training (ADRT) — Full name of ADRT

Date:

I, Lacey Hizartzidis, attest that Research Higher Degree candidate Nguyen Trieu Trinh was responsible for the design and development of synthetic procedures, synthesis, and purification of synthesised analogues, and the writing of publication manuscripts for the paper/publications entitled:

- Trinh TN, Hizartzidis L, Lin AJS, Harman DG, McCluskey A, Gordon CP. An efficient continuous flow approach to furnish furan-based biaryls. *Organic & Biomolecular Chemistry,* 2014; 12(47): 9562-71.

Signature of Co-author

Lacey Hizartzidis
Full name of Co-author

Date: 02/11/2016

(Signature of Candidate)

Nguyen Trieu Trinh
Full name of Candidate

Date: 3 Nov 2016

Signature of Assistant Dean Training (ADRT)

Full name of ADRT

Date: of Research

Contents

ABSTRACT

Among various options to treat cancers, targeting the signalling pathways that are differentially expressed in specific cancer cells has developed as a promising approach. Whilst huge benefits of targeted therapies have been obtained with less severe side effects and higher survival rates than past experiences with traditional cytotoxic chemotherapy, the application of selective targeting is hindered and in part determined by the knowledge of the molecular biology of each cancer. Cancers are so diverse in nature expressing distinctive signalling pathways or components, whose biological elucidation is challenging but invaluable to the development of cancer treatment. In this respect, the Hedgehog Signalling Pathway (HSP) has become as an attractive target in a number of human cancers thanks to its unique mechanism of activity.

The HSP plays a pivotal role in the spatial and temporal regulation of cell proliferation and differentiation. Conversely aberrant Hh signalling is involved in Gorlin syndrome, basal cell carcinoma (the most common cancer in the world), and more than one third of all human medulloblastoma cases. In all of these cases, it is believed that deregulated Hh signalling leads to increased cell proliferation and tumour formation. Inhibition of the Hedgehog Signalling Pathway, is a recently validated anti-cancer drug target, with vismodegib (GDC-0449, Erivedge®) and sonidegib (LDE225, Odomzo®), approved by the U.S. Food and Drug Administration for treatment of early and advanced basal cell carcinomas.

We developed three new scaffolds of small molecule inhibitors of the HSP. The first scaffold consisted of 11 quinolone-2-(1*H*)-ones developed from a sequential Ugi-Knoevenagel reaction pathway (Chapter 3). These analogues not only express their anti-hedgehog activity through the significant inhibition of Gli_2 at both *gene* and protein expression in SAG-activated Shh LIGHT 2 cells at 10 and 25 μM, respectively, but are able to suppress a panel of nine human HSP expressing cancer cells (GI_{50} from 2.9 to 18.0 μM). Whilst the exact mechanism remains to be determined, it is probable the inhibition observed is occurring downstream of Smo, due to its activity in the presence of SAG, a potent Smo activator.

Subsequent second and third generation analogues were developed on the quinolone-2-(1*H*)-one pharmacophore, which highlighted the importance of a C3-tethered indole moiety. These new scaffolds were built on tryptophan (9 analogues, Chapter 4) and benzo[1,3]dioxol-5-ylmethyl-[2-(1*H*-indol-3-yl)-ethyl]-amine derivatives (11 analogues, Chapter 4) displaying superior inhibitory activity against Gli protein expression with the best inhibitors displaying submicromolar IC_{50} (Chapter 4). Noteworthy, active compounds from the second and third libraries displayed inhibitory activity downstream of Smo, which circumvents the resistance issues experienced by the Smo inhibitors currently in use.

We discovered the fourth library of 1,3-thiazine-6-phenylimino-5-carboxylates in a multicomponent one pot synthesis (12 analogues, Chapter 5). These analogues display structural similarities to HPI-1, a non-selective Gli inhibitor, and thus may present themselves as HSP inhibitors. Current biological evaluation is going on to investigate their anti-hedgehog properties.

Additionally, using flow technique we have synthesised the potent Smo inhibitor LDE-225, as well as a number of aldehydes containing the furan-based biaryl motif (Chapter 2). This motif is available in biological active compounds, including the HSP inhibitors, and thus presents an opportunity to develop new scaffolds of HSP inhibitors.

ABBREVIATIONS

° C	Degrees Celsius
^{13}C	Carbon-13 nuclear magnetic resonance spectroscopy
^{1}H	Proton nuclear magnetic resonance spectroscopy
3CR	Three component reaction
4CR	Four component reaction
A2780	Human ovarian carcinoma cell line
Ac	Acetate
Acetone-*d6*	Deuterated acetone
ACN	Acetonitrile
AcOH	Acetic acid
Ar	Aromatic
BCC	Basal cell carcinoma
BCL2	B-cell CLL/lymphoma 2
BE2-C	Human neuroblastoma cell line
BMI1	B lymphoma Mo-MLV insertion region 1 homolog
BRD4	Bromodomain-containing protein 4
bs	Broad singlet (NMR)
C3H10T1/2	Mouse mesenchymal cell line
CatCart™	Catalyst cartridges for use in ThalesNano flow reactors
$CDCl_3$	Deuterated chloroform
CK1	Casein kinase 1
CML	Chronic myeloid leukaemia
CSC	Cancer stem cell
d	Doublet (NMR)
dd	doublet of doublet (NMR)
Dhh	Desert hedgehog
DIPEA	Diisopropylamine
DMSO	Dimethyl sulfoxide
DMSO-d_6	Deuterated dimethyl sulfoxide
DNA	Deoxyribonucleic acid
DU145	Human prostate carcinoma cell line
ELK1	ETS-like gene 1
EtOAc	Ethyl acetate

EtOH	Ethanol
FC	FibreCat
Fmoc	Fluorenylmethyloxycarbonyl chloride
g	Gram
GI_{50}	Concentration of drug that reduces cell growth by 50% relative to an untreated control
$Gli_{1,2,3}$	Glioma-associated oncogene homolog 1,2,3
GLI	Glioma-associated protein
GSK3β	Glycogen synthase kinase 3β
h	Hour
H460	Human lung carcinoma cell line
HATU	1-[Bis(dimethylamino)methylene]-1*H*-1,2,3-triazolo[4,5-b]pyridinium 3-oxide hexafluorophosphate
HCl	Hydrochloric acid
H-Cube Pro™	Flow hydrogenation reactor
HDAC	Histone Deacetylase (HDACs) enzymes
Hh	Hedgehog
Hhat	Hedgehog acyltransferase
Hip	Hedgehog interacting protein
HPI	Hedgehog signalling pathway inhibitor
HPLC	High performance liquid chromatography
HRMS	High resolution mass spectra
HSP	Hedgehog signalling pathway
HT29	Human colorectal carcinoma cell line
Hz	Hertz
IC_{50}	Concentration of a drug required to reduce enzyme/protein activity by 50%
Ihh	Indian hedgehog
IR	Infra-red
J	Coupling constant in Hz
LRMS	Low resolution mass spectra
LXR	Liver X receptor
M	Molar
m	Multiplet (NMR)
MCF-7	Human breast adenocarcinoma cell line
MeOH	Methanol

MHz	Mega Hertz
MIA-Paca-2	Human Pancreatic carcinoma cell line
Min	Minute
mL	Millilitre
mL.min^{-1}	Millilitre per minute
mmol	Millimole
mp	Melting point
MS	Mass Spectrometry
MSX2	Homeobox msh-like
NANOG	Early embryo specific expression NK-type homeobox protein
NanoHHI	HPI-1 encapsulated by nanoparticles
NFkB	Nuclear factor kappa-light-chain-enhancer of activated B cells
NIH 3T3	Mouse embryo fibroblast cell line
nm	Nanometre
nM	Nanomolar
NMR	Nuclear magnetic resonance
N-Myc	Myelocytomatosis viral oncogene homolog
NOESY	Nuclear Overhauser effect spectroscopy
PANC1	Human pancreatic carcinoma, epithelial-like cell line
Pd Tetrakis	Palladium Tetrakis catalyst
$Pd(OH)_2/C$	Palladium hydroxide/Carbon hydrogenation catalyst
Pd/C	Palladium/Carbon hydrogenation catalyst
$PdCl_2(PPh3)_2$-DVB	Bis-triphenylphosphine CatCart™ catalyst
PDE4	Phosphodiesterase 4
PGF	Prostaglandin F
PI3/ALK/Mtor	Phosphoinositide 3-kinase pathway
PKA	Protein kinase A
ppm	Parts per million
PTCH1	Hedgehog ligand receptor patched 1
Ptch1	Gene of hedgehog ligand receptor patched
PTM	Post translational modification
q	Quartet (NMR)
RAS/RAF/MEK/ERK	Mitogen-activated protein kinases pathway
RP-HPLC	Reverse phase High performance liquid chromatography
Rt	Room temperature
Rt	Retention time

RTK	Receptor tyrosine kinases
s	Singlet (NMR)
SAG	Smoothened agonist
Shh	Sonic hedgehog
SHH LIGHT2	Fibroblast reporter cell line
Smo	Smoothened protein
SNAIL	Zinc-finger transcription factors
SUFU	Suppressor of fused protein
SW480	Human colorectal carcinoma
t	Triplet (NMR)
TBAA	Tetrabutylammonium acetate
TBAF	Tetrabutylammonium fluoride
TCAM-2	Seminoma cell line
TEA	Triethylamine
TGF-β	Transforming growth factor β
TLC	Thin layer chromatography
TM3	Murine testis Leydig cell line
TNF	Tumour necrosis factor
UV	Ultraviolet light
VEGF	Vascular endothelial growth factor
W	Watts
WIP1	Nuclear Ser/Thr phosphatase
Wnt	Wingless-related integration site
X-Cube™	Flow Reactor
δ	Chemical shift in parts per million
µM	Micromolar

I. CHAPTER ONE: Literature review

1.1. Introduction

Since its discovery in the fruit fly (*Drosophila melanogaster)* in 1980, the development of Hedgehog Signalling Pathway (HSP) inhibitors has been the focus of significant research as a potential treatment for human cancers [1]. Under homeostatic conditions, the HSP is crucial to embryogenesis, where it controls the spatial and temporal regulation of cell proliferation, differentiation, and tissue patterning [2, 3]. However, abnormal activation of this pathway results in the formation of cancer stem cells [4, 5], and subsequently the development of a variety of human cancers, including basal cell carcinoma,[6] medulloblastoma [7-9], cancers of the pancreas [10], prostate [11], lung [12, 13], colon [14], stomach [15], breast [16, 17], and ovary [18 4, 5]. Consequently, targeting the HSP has become an attractive approach for the treatment of cancer, leading to a great number of HSP inhibitors being developed in recent years [19].

Our review on the HSP is included in the following paper. In this paper, we described the development of various classes of HSP inhibitors, their limitations and highlighted Gli transcription factors as the desired target to develop next generation of inhibitors. In addition, current advances regarding recent development in HSP inhibitors are updated.

MedChemComm

REVIEW

View Article Online

Hedgehog signalling pathway inhibitors as cancer suppressing agents

Cite this: DOI: 10.1039/c3md00334e

Trieu N. Trinh,[a] Eileen A. McLaughlin,[b] Christopher P. Gordon[a] and Adam McCluskey*[a]

The Hedgehog (Hh) signalling pathway plays a pivotal role in the spatial and temporal regulation of cell proliferation and differentiation. By controlling the correct maturation of developing tissues and ensuring attainment of the correct size, position and the presence of fully functioning cellular structures, the Hh plays a pivotal role in development. Conversely aberrant Hh signalling is involved in Gorlin syndrome, basal cell carcinoma (the most common cancer in the world), and more than one third of all human medulloblastoma cases. In all of these cases, it is believed that deregulated Hh signalling leads to increased cell proliferation and tumour formation. Inhibition of the Hedgehog signalling pathway, is a recently validated anti-cancer drug target, with vismodegib (Erivedge™), approved by the U.S. Food and Drug Administration for the treatment of adult basal cell carcinoma. In this perspective we outline the current state of Hh pathway inhibitors with a particular focus on potential limitations of upstream Hh pathway inhibition in relation to resistance mutations and crosstalk pathways. Together, these limitations indicate that inhibition of downstream components, specifically the Gli family of transcription factors, may represent a next generation approach to suppress tumours associated with aberrant Hh pathway signalling.

Received 30th October 2013
Accepted 4th December 2013

DOI: 10.1039/c3md00334e

www.rsc.org/medchemcomm

Introduction

The Hedgehog signalling pathway

The Hedgehog (Hh) gene was first identified in *Drosophila melanogaster* and has subsequently been identified in numerous vertebrates, including humans.[2,3] The Hh pathway has been shown to play a crucial role in embryogenesis by controlling cell proliferation, differentiation and tissue patterning. These important functions include correct left-right asymmetry; development of the nervous system, skeleton, skin, muscles, eyes, lungs, teeth, limbs and differentiation of sperm and cartilage.[4] In adults, the Hh pathway is significantly down-regulated and limited to the maintenance of stem cells in the hemopoietic system, neural system, mammary glands as well as tissue repair, regeneration in hair follicles and skin cells.[5]

Given the significant role the Hh pathway plays in cell proliferation, differentiation and tissue patterning, it is unsurprising that abnormalities or mutations within the Hh pathway lead to severe consequences. During embryogenesis, inadequate activation of the pathway may result in cyclopia, defects in ventral neural tube, somite, foregut patterning, severe lamb malfunction, absence of ribs, failure of lung branching and holoprosencephaly,[6-9] bone defects[10] and male infertility.[11] In contrast, aberrant up-regulation of the pathway has been shown to be a critical factor in initiating and maintaining tumour growth and survival. In both adults and children, up-regulation of the Hh pathway has been linked to Gorlin syndrome (nevoid basal cell carcinoma syndrome)[12] basal cell carcinoma,[13] medulloblastoma[14-16] and also with a wide range of other cancers including cancers of the pancreas,[17] prostate,[18] lungs,[19,20] colon,[21] stomach,[22] breast,[23,24] ovarian and especially, stem cell cancer.[25,26] Consequently, Hh pathway inhibition has become an attractive chemotherapeutic target.

Hh pathway mechanisms

The activity of the Hh pathway is characterized by its dependence on Hh ligands which are produced in secreting cells. These ligands activate or inhibit downstream signalling in receiving cells (Fig. 1). In secreting cells, premature Hh proteins undergo a number of chemical transformations. This maturation process includes an autocatalytic cleavage from the precursor, an attachment of a cholesterol or endogenous steroids moieties to the C-terminal,[27] and an amide coupling of the palmytoyl-CoA to the N-terminal of the Hh protein which generate the fully active Hh ligand (Fig. 1).[28] Mature Hh ligands are secreted with the aid of Disp, a transmembrane protein on the secreting cell. Evidence suggests that the released Hh ligands reach the receiving cells *via* numerous mechanisms including active transport[29] and passive diffusion.[30] In the absence of Hh ligands, the 'off state' for receiving cells, Ptch catalytically inhibits Smo and prevents entry to the cilium where it is believed to inhibit various protein

[a]Chemistry, Centre for Chemical Biology, The University of Newcastle, Callaghan, NSW 2308, Australia. E-mail: Adam.McCluskey@Newcastle.edu.au; Fax: +61 2 4921 5472; Tel: +61 2 4921 5472

[b]Biology, Priority Research Centre for Chemical Biology, The University of Newcastle, University Drive, Callaghan, NSW 2308, Australia

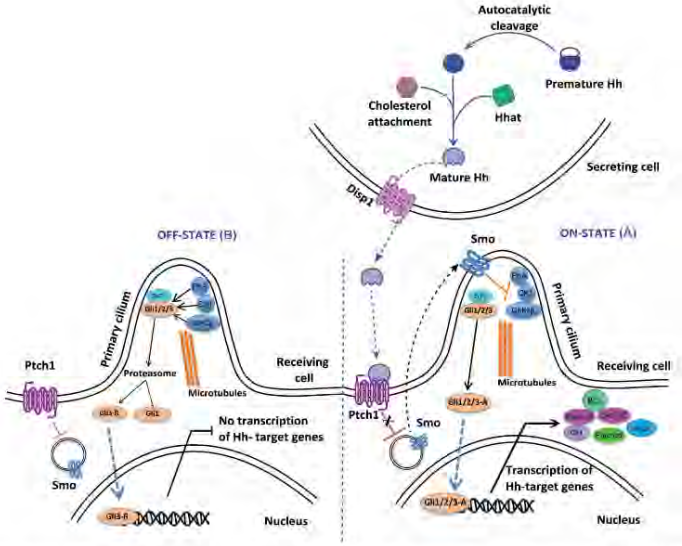

Fig. 1 *The Hedgehog signalling pathway mechanism.* (A) In secreting cells, Hh pro-proteins undergo a number of post translational modifications. This maturation process includes an autocatalytic cleavage from the precursor, an attachment of a cholesterol or endogenous steroid moiety to the C-terminal[27] and an amide coupling of the palmytoyl-CoA to the N-terminal of the Hh protein which generate the fully active Hh ligand at the plasma membrane.[30] Mature Hh ligands are secreted with the help of Disp1, a trans-plasma membrane protein located on the secreting cell. (B) In the absence of Hh-ligands (off-state), smoothened (Smo) is inhibited by Patched 1 (Ptch1) and does not enter the cilium. Consequently, the complex SuFu–Gli1,2,3 is phosphorylated by various kinases (PKA, GSK-3β, CK1) and results in truncated inactive forms (Gli2,3-R). Gli3-R travels to the nucleus and inhibits the transcription of Hh target genes. In the presence of Hh-ligands binding to and inhibiting Ptch1 (on-state), Smo is released to the primary cilium, where it inhibits PKA, GSK-3β and CK1. Consequently, no phosphorylation over Gli–SuFu complex occurs and Gli1,2,3 remain in full-length active forms (Gli1,2,3-A). These active forms of Gli travel to the nucleus and induce the expression of Hh target genes.

kinases, including PKA, GSK-3β and CK1 (Fig. 1).[31] As a result, the Gli family of transcription factors (Gli1, 2, and 3), which are the effectors of the system, in complex with SuFu (a negative inhibitor of the vertebrate Hh pathway) are phosphorylated stepwise by a number of protein kinases (PKA, GSK-3β and CK1).[32] These phosphorylation events results in proteosomal cleavage where Gli-2 is degraded to Gli2-R,[33] Gli3 is degraded to Gli3-R (limited proteolysis) while Gli1 remains full length.[34] Simultaneously, the inhibitory protein SuFu sequesters the remaining unprocessed cytoplasmic Gli such that only inactive Gli travels to the nucleus and inhibits the transcription of Hh target genes.[35,36] Typical Hh target genes include the components of the pathway itself (PTCH, GLI1) and cell proliferation and differentiation (Cyclin D, E, Wnt, N-Myc),[37–39] angiogenesis (VEGF),[40] survival (BCL2),[41] epithelial–mesenchymal transition (SNAIL, ELK1, MSX2),[42,43] invasiveness (osteopontin),[44] and self-renewal (BMI1, NANOG) factors.[45,46]

In the presence of Hh ligands, the 'on-state', the ligands bind to Ptch resulting in Smo activation. Once activated, Smo travels to the cilium where it inhibits the phosphorylation of the Gli–SuFu complex leading to the generation of active forms of Gli (Gli1-A, Gli2-A, Gli3-A). The activated forms of Gli travel to the nucleus and induce the transcription of Hh target genes.

Hh signalling pathway in cancer

Abnormally constitutive Hh pathway activation in cancer can be categorised as either: Hh ligand-independent, or Hh ligand-dependent. Hh ligand independent (Type I) cancer is characterized by a number of mutations of different components of the Hh pathway, which results in aberrant signalling (Fig. 2).

Ptch mutations

Ptch loss of function mutations have been described at high frequency in various disorders including patients with Gorlin syndrome, and those who are predisposed to basal cell carcinoma, medulloblastoma and rhabdomyosarcoma.[47–50] These mutations include deletions, insertions or nonsense mutations in Ptch proteins, which result in Ptch's inability to inhibit Smo and aberrant up-regulation of Hh signalling (Fig. 2).

Smo mutations

Smo gain of function mutations up-regulate Hh signalling by continuously generating active forms of Gli, which is typically associated with sporadic basal cell carcinoma and other skin abnormalities (Fig. 2).[51–53]

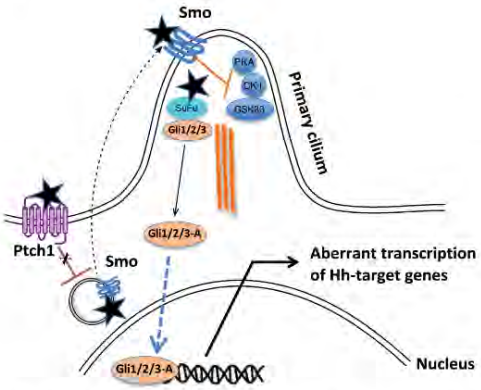

Fig. 2 Type I cancer – Hh ligand independent. Loss-of-function in Ptch1 or gain-of-function in Smo mutations activate Smo prior to cilium entry and subsequent inhibition of PKA, GSK-3β and CK1 in the absence of Hh-ligands, which results in aberrant the Hh pathway activation. Loss-of-function in SuFu mutations can enable more frequent nucleus entering of active Gli to or reduce the export of active Gli out of the nucleus, all of which lead to aberrant the Hh pathway activation. Star symbol represents mutations.

SuFu mutations

SuFu regulates Gli activity exogenously sequestering Gli in the cytoplasm and endogenously by repressing Gli transcription within the nucleus.[35,36,54] Multiple SuFu inactivating mutations are known to result in the nuclear accumulation of Gli proteins. This results in constitutive Hh signalling in patients, especially children, with medulloblastoma.[55–58] Alternatively, inactivated SuFu is no longer capable of retaining unprocessed full-length Gli-proteins in the cytoplasm, resulting in more frequent entry of active Gli proteins to the nucleus, and induction of aberrant constitutive the Hh pathway (Fig. 2).[35]

Hh ligand dependent (Type II) cancer is characterized by a "typical" the Hh pathway in terms of its functioning *i.e.* without any mutations in the signalling components. Thus the aberrant Hh signalling results instead from the continuous receipt of Hh ligands. Depending on the Hh-ligand source, it is further subdivided into three models: *autocrine–juxtacrine*, *paracrine* and *reverse paracrine* (Fig. 3). Theoretically, these models have the potential to occur independently or in combination.

Autocrine–juxtacrine model

The autocrine–juxtacrine model promotes tumour growth; typically resulting in prostate,[59] lung[60] and colon cancers;[61] by having a ligand both secreted and responded to by the same/neighbouring tumour cells (Fig. 3). Given that this model does not involve mutations within any of the components of the Hh pathway it is anticipated that these cancers should be effectively controlled by the use of Hh pathway inhibitors at different positions of the pathway, including Hh ligand, Smo and Gli inhibitors.

Paracrine model

The paracrine model enables the development of tumour angiogenesis, invasiveness and metastasis resulting in prostate,[62] hepatocellular carcinomas,[63] pancreatic and colorectal cancers (Fig. 3).[64] Cancer cell secreted Hh ligands interact with and activate the surrounding normal stromal cells (endothelial cells, epithelial cells, fibroblasts and immune cells) activating stromal. Crucially this model does not necessarily display some standard components of the pathway, including Smo. Consequently, Smo inhibitors may not be effective against these cancers.

Reverse paracrine model

The reverse paracrine model is a variation of the paracrine type (Fig. 3). It has been observed in B-cell lymphoma, multiple myeloma and leukemia patients, where Hh ligands are excreted by the stromal microenvironment and activate the Hh pathway

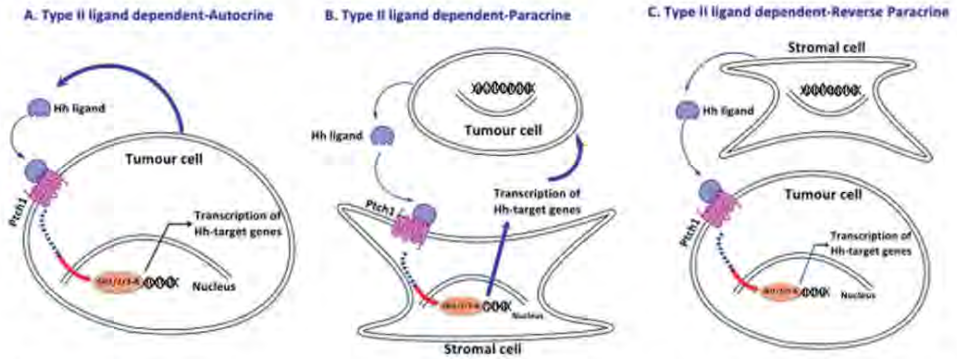

Fig. 3 Type II cancers – Hh ligand dependent. (A) *Autocrine–juxtacrine model*: Hh ligand is both produced and responded to the same cancer cell. (B) *Paracrine model*: tumour produces Hh ligands, which activate the Hh pathway in surrounding stromal cells. As a result, stromal cells produce necessary components back to the tumour. Evidence indicates that this results in aberrant growth, invasion and metastasis. (C) *Reverse paracrine model*: stromal cells secrete Hh ligands that activate the Hh pathway in tumour.

in cancer cells.[65,66] This subtype highlights the role of the tumour microenvironment,[67,68] and that Hh pathway inhibitor dosing should be carefully considered as they target both cancer cells and its stromal microenvironment.

Targeting the Hh pathway in cancers

Assessing the inhibitory activities of small molecules within the Hh pathway

Given the diverse range of cells that secrete or respond to Hedgehog proteins, and the diverse range of cancers that result from aberrant signalling, it is unsurprising that a raft of cellular models to examine the Hh pathway have been established. Whilst a complete account of currently utilised models falls outside the scope of this perspective, an overview of a number of cell types and assays techniques utilised is presented in Table 1.

As outlined in Table 1, a significant number of inhibitor identification programs have utilised cell viability or proliferation assays such as the MTT or the bromodeoxyuridine BrdU assays, respectively. Further, a number of luciferase reporter cell lines have been engineered such as NIH 3T3 and SHH LIGHT2 cells which carry a transfected Gli-reporter construct. Moreover a homogeneous assay system that measures changes in fluorescence polarization that accompany cholesterol-dependent auto-cleavage of Hh proteins has recently been reported.[69] In contrast the luciferase assays which provide a means of examining events between Smo and Gli activation, this assay provides insights to Hh auto-cleavage and esterification with cholesterol in the initial step of the pathway.

Hh pathway inhibitors functioning upstream of Smo - inhibitors of the post-translational maturation of Hh ligands

During Hh post-translation maturation (PTM) cholesterol attaches to the newly auto-catalytically cleaved hedgehog ligand and then Hhat (Hedgehog acyltransferase) mediates subsequent attachment of a palmitate molecule. Combined, this results in signalling competent hedgehog ligand.[80,81] Cholesterol attachment is required for the activation of liver X receptors (LXR).[82]

LXR activation in M2-10B4 marrow stromal cells by cholesterol analogues **1** and **2** inhibits Hh pathway activation by SHh ligands (Fig. 4).[81] The depletion of cholesterol under the activation of LXR may occur on a Hh protein, and indirectly affect hedgehog ligands' maturation leading to mature hedgehog ligand deficiency. This is consistent with the observation that the same activator was not able inhibit the Hh pathway when activated by Smo agonist purmorphamine.[83] This interactivity between LXR and the Hh pathway may partially explain the anti cancer and anti proliferation properties of LXR activation,[84,85] in addition to their traditional anti atherogenic effects.[82]

The maturation of hedgehog ligands also occurs at the Hhat mediated pamitoylation step. The thiopiperidyl RU-SKI 43 (**3**) Hhat inhibitor blocks SHh palmitoylation *in vitro* and Gli activation in NIH 3T3 cells (IC_{50} = 10 μM).[69] Further investigations in SHH LIGHT2, Su /Fu , and C3H10T1/2 cell lines demonstrated that Hhat inhibitors reduced the production of mature SHh ligands.[69] The inhibitory effect of (**3**) on the Hh pathway cannot be rescued in SHH-transfected cells with SAG or SHh, suggesting the possibility of off targets effects.[69]

Table 1 Overview of representative cell lines and cellular assays models currently utilised to examine Hh pathway inhibition

Cell lines	Origin	Regulator	Assay	Reference
NIH 3T3	Mouse embryonic fibroblast cells	Activated by SHh	Gli-luciferase	69
SHH LIGHT2	NIH/3T3 cells were co-transfected with GLI-responsive firefly luciferase reporter and other reporters	Activated by SHh or SAG	Gli-luciferase	69–72
C3H10/T1/2	Mouse pluripotent mesenchymal cells	Activated by SHh, Hh responsive but non-dependent	Gli-luciferase, cytotoxicity	73–75
TM3	Mouse testis Leydig cells	Activated by SHh	Luciferase assay	76
TMHh12	Not specified	Activated by SAG	Smo binding, Gli-luciferase	77
SuFu null MEFs	Mouse embryonic fibroblast without SuFu	Without SuFu, Hh target genes are highly expressed	Quantitative PCR	78
22Rv1	Prostate carcinoma	Available with elevated Gli1 level	Bromodeoxyuridine	78
PANC1	Pancreatic adenocarcinoma cells	Available with elevated Hh components, including Ptch, SuFu, Gli1,2 level	Bromodeoxyuridine, cytotoxicity	73 and 78
Rh30	Rhabdomyosarcoma cell line	Available with high overexpression of Gli1 genes	Gli-luciferase	79
HaCaT	Human keratinocyte cells	Expressing GLI1 under tetracycline control	Cytotoxicity, Gli-luciferase	73
DU145	Prostate cancer	Available with elevated Hh components, including Ptch, SuFu, Gli1,2 level	Cytotoxicity	73

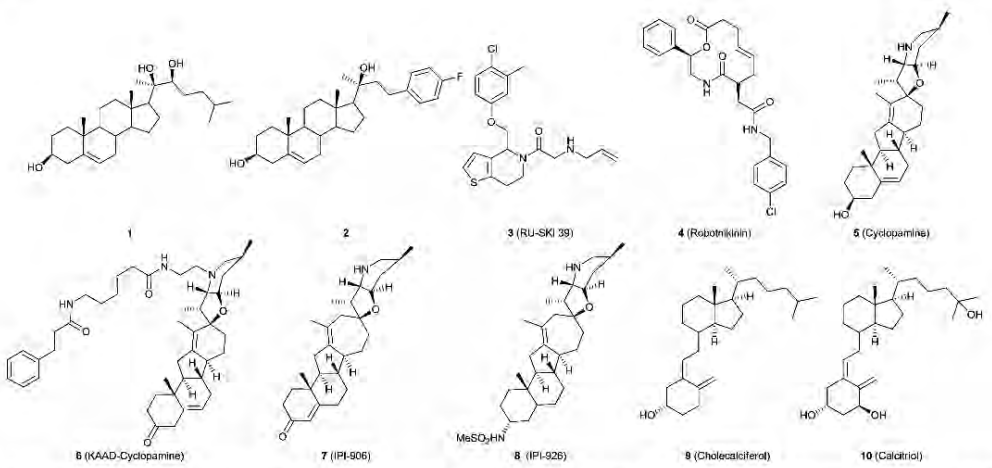

Fig. 4 Hedgehog pathway inhibitors targeting upstream of Smo, the LXR's agonists (1) and (2), Hhat inhibitor (3), and Hh-ligand inhibitor (4) and the cyclopamine scaffold of Smo inhibitors cyclopamine (5), KAAD-cyclopamine (6), IPI-906 (7) and IPI-926 (8) along with the vitamin D3 analogues cholecalciferol (9) and calcitriol (10).

Hh ligand inhibitors

Robotnikinin (**4**) inhibits the Hh pathway by binding with the hedgehog ligand which induces a conformational change thus preventing binding to Ptch1 (Fig. 4). In SHH LIGHT2 cells, human primary keratinocytes, and a synthetic model of human skin, **4** displayed substantial repression of SHh-induced Gli1 and Gli2 transcripts.[72] Currently the only other reported competitive inhibitor of the Hh ligand is a monoclonal antibody, 5E1, which blocks binding of SHh ligands to Ptch1 through binding at the pseudo-active site groove of SHh.[86] The 5E1 monoclonal antibody has been largely used to elucidate the hedgehog biology.

Smo inhibitors

There has been a rapid increase in the number of Smo inhibitors identified, through targeted synthesis and high throughput screening (HTS) efforts, making them the current largest class of the Hh pathway inhibitors.

Natural product inhibitors and derivatives

Cyclopamine (**5**), a natural steroidal alkaloid extracted from the corn lily *Veratrum californicum*,[87] has been considered the classical inhibitor of the Hh pathway, acting by directly binding to Smo (Fig. 4).[88] However, despite promising Hh antagonistic and anticancer effects in various xenograft models,[61,80,89] and in basal cell carcinoma patients,[90] the unfavourable pharmaceutical properties (poor water solubility, low pH instability), have limited the development of this compound class as clinical agents.[91] KAAD-cyclopamine (**6**), IPI609 (**7**) and IPI-926 (**8**), are representative of more drug like cyclopamine analogues (Fig. 5).[92,93] IPI-609 (**7**) inhibited SHH-induced differentiation of C3H10/T1/2 cells to osteoblasts with EC_{50} of 200 nM.[93,94] Sulfonamide substituted IPI-926 (**8**) showed superior potency to IPI-609 with improved pharmacokinetics and metabolic stability over cyclopamine. Further IPI-926 induced tumour regression in mice ligand-independent medulloblastoma,[95] as well as inhibited lung and pancreatic xenografts' growth.[96] Additionally a number of vitamin D3 analogues, such as cholecalciferol (**9**) and calcitriol (**10**), have been identified as Hh pathway antagonists.[97] In models of clear cell renal carcinoma **9**, at a concentration of 50 nM, decreased cell density in a time- and concentration-dependent manner up to 90% within 24 h.[97]

Benzimidazoles, arylpyridines, pyrrolopyridine and quinazolines

From murine cell (C3H10T1/2) based HTS a series of benzimidazoles, including compound **9**, were identified as nanomolar potent the Hh pathway.[98] Lead optimization of **9** afforded GDC-0449 (vismodegib) (**12**).[99] Vismodegib (**12**) is the first FDA approved Hh pathway inhibitor, for the treatment of adult BCC.[1] In terms of mechanism of action, vismodegib binds to the extracellular domain of SMO and significantly inhibits downstream hedgehog signalling.[100] NVP-LDE225 (erismodegib) (**13**, Fig. 4) has also emerged as a promising Smo inhibitor displaying potent in cell activity (IC_{50} = 8 nM in TM3 cells) as well as favourable pharmacokinetics properties in animal models.[76] Further, a series of pyrrolo[3,2-*c*]pyridine were recently reported with one of these analogues TAK-441 (**14**), (Gli-luc reporter IC_{50} = 4.6 nM) is currently undergoing investigation in clinical trials.[101] In a related study a number of quinazolines were discovered including XL-139 (**15**) and the majority of compounds in this series displayed single digit nanomolar activity.[102]

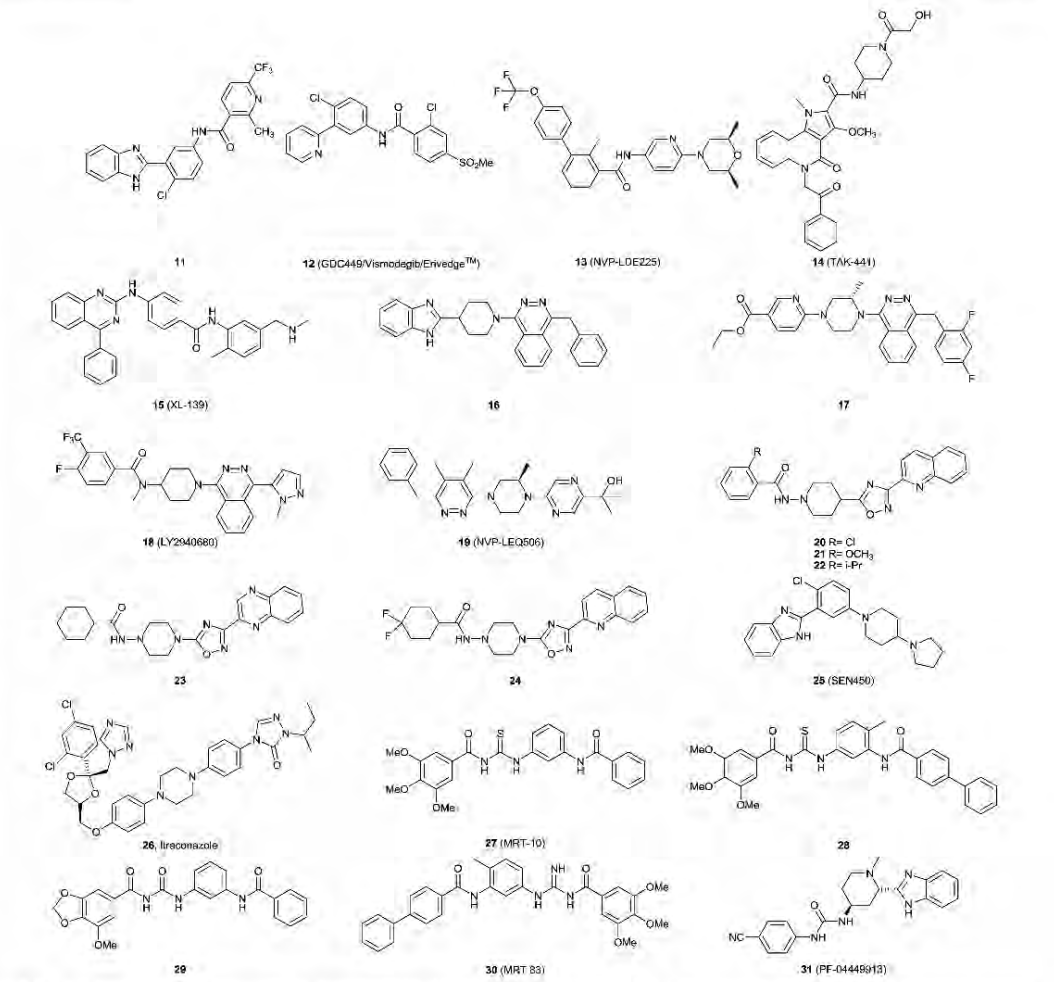

Fig. 5 First generation Smo inhibitors, the benzimidazole (**11**), and pyridine (**12**) and (**13**), the phthaladines (**16–18**), and the second generation Smo inhibitor (**19**). Piperidines (**20–22**, **25**) and piperazines (**23** and **24**). The *N*-acylthioureas (**27**) and (**28**), *N*-acylurea (**29**), and *N*-acylguanidine (**30**) along with urea based analogue PF-04449913 (**31**).

Phthaladines

The phthaladines **16**, **17**, and **18** have been reported to be 0.1–10 μM inhibitors, *via* Smo targeting of the Hh pathway activated by SAG inTMHh12 cells (Fig. 5).[77] LY2940680 (**18**) not only inhibits Smo in the human medulloblastoma cell line (Daoy) and murine C3H10T1/2 cell line, but also counteracts the effects in D473H, a Smo mutant.[103] Preclinical data on Ptch$^{+/-}$ p53$^{-/-}$ transgenic mice, which spontaneously develop medulloblastoma, revealed rapid anti-tumour activity and improved survival rate.[103] Second generation of phthaladine analogues such as NVP-LEQ506 (**19**) display improved potency in a Gli-luc assay, low hERG channel binding and enhanced solubility have been reported. *In vitro* analysis revealed that **19** inhibited Hh signalling in a human cell line (HEPM) as measured by Gli mRNA with an IC_{50} ~6-fold more potent than NVP-LDE225 (**13**). Moreover **19** was evaluated in C3H10T1/2 luciferase reporter cells transfected with a Smo D473H expression vector which conferred resistance to vismodegib (**12**) in a medulloblastoma patient after an initial response. Analogue **19** retained good potency with an IC_{50} <100 nM.[104]

Piperidines and piperazines

From HTS piperidines **20–22** were identified as potent Smo inhibitors (Fig. 8).[70] SAR development led to piperazines such as **23** and **24**, which displayed high efficacy against the Hh pathway

in the SHH LIGHT2 cell line displaying IC_{50} values of 5 nM, and 25 nM, respectively. Unfortunately oxidative metabolism of the oxadizole ring resulted in high clearance rates.[70] SEN450 (**25**) is representative of an additional series of piperidine based Smo inhibitors. This compound is efficacious (IC_{50} – 23 nM), and effects reduction in tumour volume in the Hh pathway expressing glioblastoma multiforme xenograft models.[105] An additional piperazine displaying Hh pathway inhibitory activity is the triazole based antifungal agent itraconazole (**26**) which displayed an IC_{50} of 55 nM against medulloblastoma cells.[106]

N-Acylthioureas, *N*-acylureas and *N*-acylguanidines

From the lead thiourea MRT-10 (**27**) the *N*-acylurea and *N*-acylguanidine series of Smo inhibitors were developed. Amongst these were compounds **28** (IC_{50} = 60 nM), **29** (IC_{50} = 25 nM), and MRT-83 (**30**) (IC_{50} = 11 nM), with inhibitory activity measured against the Hh pathway SHH LIGHT2 and C3H10T1/2 cell lines (Fig. 5).[107] An additional urea based analogue displaying activity in the Hh pathway is PF-04449913 (**31**). This analogue displays an IC_{50} of 5 nM (Gli-luciferase reporter C3H10T1/2) and is currently under investigation in clinical trials.[108]

Potential limitations of upstream Hh pathway inhibitors

Thus, whilst upstream inhibition of the Hh pathway has afforded some promising agents, evidence is emerging that downstream components of the pathway, and other interacting pathways, can compensate for inhibitory activity elicited by upstream inhibitors. For example the effectors of Hh signalling, particularly the Gli family of transcription factors, are regulated by other signalling pathways and thus the activity of Smo and Ptch inhibitors can be overridden.

Interactions of the Hh pathway with other signalling pathways – the big crosstalk picture

Crosstalk with the TGF-β pathway

Similar to Hh pathways, the TGF-β signalling pathway plays a crucial role in the embryonic development and both share overlapping functions including cell differentiation, cell growth control, tissue repair and regeneration.[109,110] Consequently, dysregulation of TGF-β signalling pathway also leads to the development of various cancers.[109,110] It has been recently identified that both pathways share the same powerful effector, Gli2.[111,112]

Gli proteins were previously regarded as effectors of the Hh pathway only, but there is increasing evidence that the TGF-β pathway controls Gli expression and activation through induction of Gli2 expression independently of the Hh pathway in human keratinocytes,[113] and by repressing PKA activity and thus indirectly elevated the number of full-length active Gli proteins in human melanoma cells (Fig. 6).[114] This provides potential insights to resistance development mechanisms associated

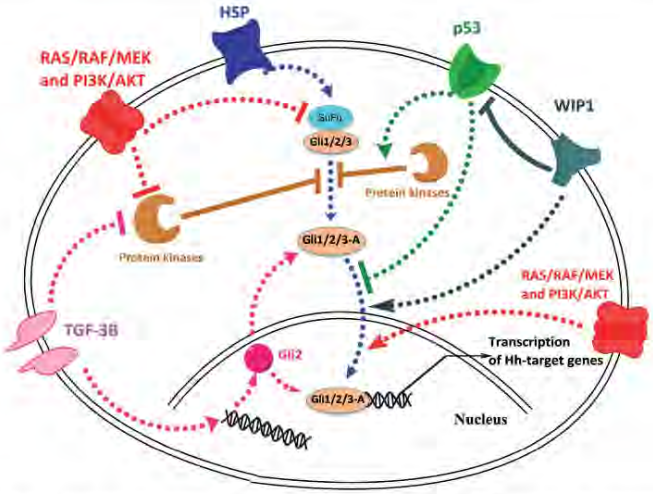

Fig. 6 *Crosstalk between the Hh pathway and other oncogenic signalling pathways.* TGF-3β induces Gli2 expression in the nucleus independently of the HSP, and inhibits PKA, which results in the presence of more full-length Gli. RAS/RAF/MEK/ERK and PI3K/AKT/Mtor pathways share the same initiating components (PGF, RTKs and RAS). These pathways inhibit SuFu and the phosphorylation of PKA and GSK-3β over Gli. Evidence indicates that they enhance Gli1 transcriptional activity and increase its nuclear localisation. P53 pathway activates the phosphorylation of Gli1 into repressor form and reducing its nuclear localisation and protein levels. WIP1 increases Gli1 transcriptional activity, nuclear localisation, and protein stability, possibly by inhibiting p53.

with current Hh pathway inhibitors and may be exploited to create better chemotherapeutics. This also explains how cancer cells, usually lacking of primary cilium formations, can still induce Hh pathway without mutations in the ciliary Hh components including Smo.[115]

Crosstalk with p53 and WIP1 pathways

The p53 pathway is either suppressed or subject to loss of function mutations in multiple cancers. In the context of Hh pathway, p53 inhibits human Gli1 transcriptional activity by either reducing its nuclear localisation and protein levels or, by activating phosphorylation of Gli1 into its repressor form. Conversely, up-regulation of Gli1 represses p53 activity.[46] The oncogenic phosphatase WIP1, a p53 inhibitor, has been shown to enhance Gli1 function in human cancer cells (melanomas, breast cancer) by increasing its transcriptional activity, nuclear localisation, and protein stability. Further WIP1 has been shown to, maintain tumour growth and cancer stem cell renewal in the Hh pathway cancers.[116] WIP1 can dephosphorylate and inhibit a wide range of important targets p53, p38MAPK, ATM/ATR, Chk1/2, all of which contribute to the complete or partial inactivation of the p53 pathway (Fig. 6). As a result of reduced p53 activity and the mutual inhibitory relationship between p53 and Gli1, it is likely that WIP1 modulates Gli1 activity through p53 pathway inhibition.

Crosstalk with RAS/RAF/MEK/ERK and PI3K/AKT/mTOR pathways

Given the ability to promote cancer cells survival, proliferation, invasion and inhibition of apoptosis, the abnormal activation of the RAS/RAF/MEK/ERK and PI3K/AKT/mTOR signalling pathways play an important role in the development cancers.[117,118] The PI3K/AKT and RAS/MEK pathways share the same initiating components PGF, RTKs and RAS. These enhance Gli1 transcriptional activity, increase nuclear localisation, whilst at the same time antagonising the inhibitory effects of SuFu, PKA and GSK3β over Gli (Fig. 6).[89,119–121]

The need for next generation Hh pathway inhibitors

LXR activators, Hhat inhibitors, robotnikinin and the monoclonal antibody 5E1 act as upstream antagonists at the level of hedgehog ligand production and binding. They could be a valid option for hedgehog related cancers activated by overexpressed hedgehog ligands, but not for those whose aberrant activation of the Hh pathway is due to downstream lesions of the pathway. For instance, robotnikinin loses inhibition over the Hh pathway in cells missing Ptch1 receptors or when Smo is activated by its agonists SAG or purmorphamine.[72] Consequently, the sensitivity of these inhibitors functioning upstream of Smo is preserved only to cancers dependent on Hh ligands.

With respect to Smo inhibitors, despite being the largest class with more than 30 on going clinical trials, they possess several limitations. Firstly, from the chemical point of view, these Smo inhibitors can be categorized into a handful of structurally similar classes, including benzimidazoles, pyridines, pyridazines, piperidines, phthaladines, and piperazines. The inhibitors in each group share core structural similarities. Thus, acquired resistance against one inhibitor may result in resistance against the entire class. Secondly, most Smo inhibitors are ineffective against the ligand-dependent cancer models, in which Smo proteins are not displayed in cancer cells, but rather in the surrounding stromal microenvironment. Here, Smo inhibitors alone would be predicted to give no direct short-term tumour regression, but a long-term benefit in survival rate may be achieved due to the depletion of the Hh pathway in stromal microenvironment. This limitation, theoretically, should be overcome when combining Smo inhibitors with standard anticancer therapies. This approach is currently being applied in a number of clinical trials. Finally, up-regulation of the Hh pathway due to any incident downstream of Smo will obviously render the tumour resistant to all of existing Smo inhibitors and further upstream inhibitors. One such example is the amplification of Gli transcription factors, which originates from the complicated crosstalk of the Hh pathway and other oncogenic signalling pathways (Fig. 8). Indeed, current clinical trials are highlighting these flaws.

Clinical experiences with Hh pathway inhibitors targeting Smo

Vismodegib/GDC-0449

Phase I evaluation of vismodegib (**12**) revealed that only patients with BCC or medulloblastoma, which are Hh-ligand independent cancers, were completely or partially sensitive to vismodegib.[122] In the same study, patients with other types of cancers, including ovarian, colorectal and pancreatic cancer displayed at best arrested cancer progression. No mutations or alterations in the Hh pathway in these patients were identified, which suggested a paracrine the Hh pathway scenario. This evidence indicated that the feedback from the surrounding stromal microenvironment supported the tumour growth regardless of the use of vismodegib and to a greater extent, other Smo inhibitors. Phase II trial in patients with locally advanced or metastatic BCC showed a total response rate of 30% and 63% of stable disease in metastatic patients; and 43% of total response with 40% of stable disease in locally advanced BCC patients.[123] Vismodegib is the first-in-class the Hh pathway FDA approved inhibitor, but its application is strictly limited to adult patients with BCC.

Despite these promising results, vismodegib resistance has been reported in one patient with metastatic medulloblastoma after a preliminary positive response.[124] This resistance was enacted through a D473H mutation in Smo which prevented vismodegib–Smo binding while, maintaining the aberrant Hh signalling.[124,125]

IPI-926 (saridegib)

In a Phase I study of patients with locally advanced or metastatic solid tumours, IPI-926 (**8**) exhibited low levels of side effects and

showed evidence of clinical activity in BCC patients.[125] Combination approaches with gemcitabine and IPI-926 in a Phase Ib study of metastatic pancreatic cancer patients were positive with good tolerance and limited toxicity.[126] However IPI-926 was less effective than gemcitabine or a placebo, terminating the metastatic pancreatic cancer Phase II study.[127] This may have been a result of Hh up-regulation in both in the tumour and stromal microenvironment. Additional clinical trials with IPI-926 are on going in patients with chondrosarcoma and myelofibrosis are on going, but the likelihood of success is questionable as these conditions are not considered to be mutation driven.[127]

NVP-LDE225

One Phase I trial was conducted in patients with advanced solid tumours to determine the maximum tolerated dose of NVP-LDE225 (**13**), with additional assessments of its pharmacokinetics, pharmacodynamics, and potential efficacy.[128] NVP-LDE-225 was shown to be well tolerated up to 800 mg (mg kg^{-1}) and displayed preliminary evidence of activity of reducing Gli-1 mRNA expression in one medulloblastoma patient. However their was also evidence of several resistance mechanisms in other animal models of medulloblastoma.[129] The resistance may come from separate mechanisms, including the amplification of Gli2, an aberrant up-regulation of the PI3K signalling pathway and Smo mutations.[130]

Thus, these current clinical trials suggest that inhibition of the Hh pathway further downstream of Smo may be more effective against Smo resistant cancers and others caused by the overexpression of Hh ligands. In addition, compelling evidence of the complicated crosstalk between the Hh pathway and other oncogenic pathways highlights the crucial role of the Gli transcription factors as the unique link of the crosstalk (Fig. 4). Consequently, there has been increasing interest in the creation of the new inhibitors targeting at Gli transcription level. These inhibitors are likely to be sensitive against not only Smo resistant cancers, but also others generated by several oncogenic pathways.

Next generation Hh pathway inhibitors – the Gli inhibitors

GANT-61 and GANT-58

As previously alluded to, given the Gli family are the effectors of the Hh pathway and other oncogenic pathways, Gli inhibitors pose as attractive chemotherapeutic agents. Two of the first Gli inhibitors described were GANT-61 (**32**) and GANT-58 (**33**) (Fig. 6). Both compounds dependently interfere with Gli1 and Gli2-mediated transcription and suppressed Hh signalling in SHH LIGHT2 (SAG-activated) and SuFu null MEFs cell lines, suggesting their inhibitory activity lies downstream of Smo and SuFu.[78] The selectivity towards the Hh pathway was confirmed relative to other oncogenic pathways, including TNF signalling/NFκB activation, RAS/RAF/MEK/ERK, and glucocorticoid receptor gene transactivation. GANT-61 and GANT-58 inhibited growth of cyclopamine resistant Hh-dependent cancer cell lines PANC1 (pancreatic adenocarcinoma) and 22Rv1 (prostate carcinoma). This efficacy was reproducible in human xenografts models in mice. GANT-61 is also cytotoxic to a panel of seven human neuroblastoma cells with growth inhibition values (GI_{50}) between 5.82 and 12.4 μM. Significantly, GANT-61 inhibited neuroblastoma growth in mouse xenografts in which Smo inhibitors had no effect.[130] GANT-61 was more efficacious than the Smo inhibitor cyclopamine in six human colon cancer cell lines, and inhibited pancreatic cancer stem cell growth *in vitro* and in NOD/SCID/IL2R gamma null mice xenograft models.[131,132]

The mechanism by which GANT-61 and GANT-58 inhibit the Hh pathway at the Gli level is unknown. Current evidence suggests that GANT-61, but not GANT-58, induces modification of Gli1 and prevents it from binding to the DNA promoter.[78] As these compounds inhibit both Gli1 and Gli2, with Gli2 being intricately involved in bone development,[133,134] possible implications for their use in therapy may include serious bone defects, especially in children.

HPI-1, HPI-2, HPI-3, HPI-4 and NanoHHI

A screen of 122 755 compounds was conducted to find candidates which could block the SAG-induced Hh pathway activation in SHH LIGHT2 cells.[71] Four structurally diverse leads displaying IC_{50} values of <10 μM (HPI-1 to HPI-4) (**34–37**) were identified (Fig. 7).[71]

HPI-1, -2, -3, and -4 were active against Ptch$^{-/-}$, SuFu$^{-/-}$ cell lines consistent with Hh pathway inhibition downstream of Smo and SuFu. They were inactive against PKA and other Hh pathway associated oncogenic signalling pathways, including the PI3K/AKT/MTOR, RAS/RAF/MEK/ERK and the Wnt pathways.[71] In NIH 3T3 cells, which overexpress Gli proteins, HPI-1 (**34**) and HPI-2 (**35**) inhibited Gli1 and Gli2 functions, but no significant inhibition was noted with HPI-3 (**36**) and HPI-4 (**37**).[71,78] Each of the Hh pathway inhibitors analogues operate *via* a unique mechanism of action distinct from other known Gli-mediated transcription inhibitors, including GANT-61 (**32**), GANT-58 (**33**), zerumbone (**44**), arcyriaflavin C (**48**), and physalin F (**50**) (Fig. 8). HPI-1 (**34**) was thought to inhibit both endogenous and exogenous Gli1/Gli2 activity independently of the primary cilium. HPI-2 (**35**) and HPI-3 (**36**) appeared to counteract the activation of Gli into active forms in the primary cilium. HPI-4 (**37**) was believed to disrupt the ciliogenesis, leading to the malfunction of Gli's ciliary processes.[71] These mechanisms are currently speculative.

Encapsulation of HPI-1 (**34**) (NanoHHI) in polymeric nanoparticles enhanced aqueous solubility and bioavailability.[135] NanoHHI actively inhibited the Smo mutant allograft of mouse medulloblastoma, and dramatically down-regulated mGli as well as Hh target genes. NanoHHI in combination with gemcitabine significantly hampered the growth of orthotropic Pa03C pancreatic cancer when compared with gemcitabine alone.[135] This pancreatic cancer, possibly having the ligand-dependent and paracrine type of Hh pathway activation, could express

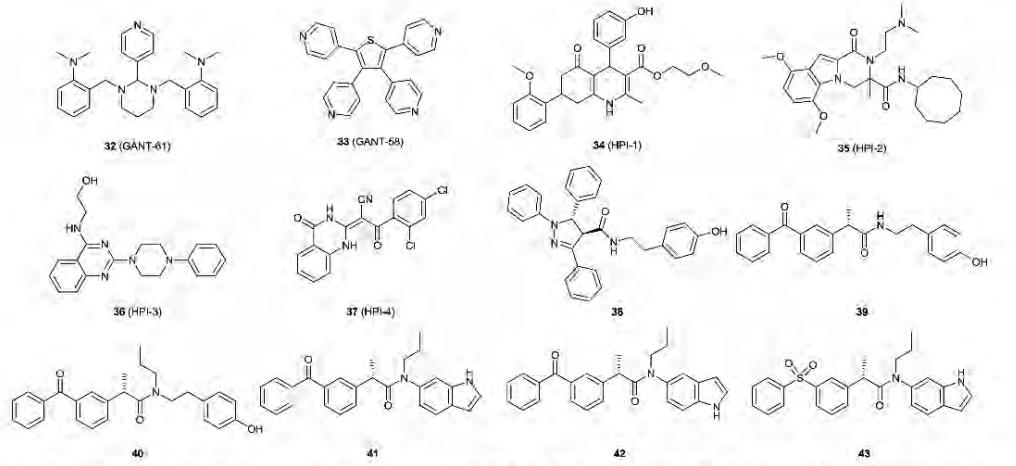

Fig. 7 Chemical structures of Gli-mediated transcription inhibitors GANT-61 (**32**) and GANT-58 (**33**); the Gli-mediated transcription inhibitors HPI-1, HPI-2, HPI-3, and HPI-4 (**34–37**), the lead Gli inhibitor (**38**) and the ketoprofen analogues (**39–43**).

resistance to the Smo inhibitor IPI-926 (**8**) as discussed above. NanoHHI resulted in no hematologic side effects or biochemical abnormalities during administration.[135]

Ketoprofen derivatives

Rationally designed from lead Gli inhibitor **38**,[136] to specifically inhibit Gli1, analogues **39** and **40** selectively inhibited Gli1-mediated transcription over that of Gli2, with IC_{50} values of 11.4 μM and 6.9 μM, respectively in C3H10T1/2 cells.[137] The phenol moiety was believed to promote metabolism in liver microsomes. Accordingly a phenol-to-indole bioisosteric replacement strategy was implemented yielding **41** and **42** with enhanced drug characteristics, including improved liver microsome stability, greater Gli1 selectivity and good membrane permeability. Both **41** and **42** inhibit exogenous and endogenous Gli1-mediated transcription in C3H10T1/2 and Rh30 cell lines, respectively.[79]

Replacement of the ketone carbonyl moiety with a ether, amide, sulphonamide, or sulfone generated several candidates with equipotent activity, including **43**, which lacked the phototoxicity linked to the ketoprofen moiety (Fig. 8).[138] Thus far, **43** is the most promising candidate in this class of Hh pathway inhibitors displaying enhanced stability and low toxicity. The mechanism of action is currently unknown, but **43** does not inhibit the promotors of Gli1-mediated transcription, Dyrk1a or HDAC-1 inhibitors.[139,140]

Natural products displaying inhibition of Gli-mediated transcription

A wide range of natural product based Gli-mediated transcription inhibitors have been reported.[73,141,142] Among the first natural products Gli1 and Gli2 inhibitors identified were zerumbone (**44**), zerumbone epoxide (**45**), staurosporinone (**46**), 6-hydroxystaurosporinone (**47**), arcyriaflavin C (**48**), 6-dihydroxyarcyriaflavin A (**49**), physalin F (**50**) and B (**51**) (Fig. 8).[143] These compounds inhibited the Hh pathway target proteins, including Ptch, Gli1 and BCL2 (anti-apoptosis protein) in HaCaT and PANC1 cells, respectively. SAR studies highlighted the importance of α,β-unsaturated carbonyl group in the zerumbones (**44** and **45**),[144] as well as the indole NH moieties in **46–49**.[143]

The pentacyclic triterpenes colubrinic acid (**52**), betulinic acid (**53**) and alphitolic acid (**54**), were isolated from *Zizyphus cambodiana* and subsequently identified as Gli inhibitors. Compounds **52** and **53** inhibited the expression of Ptch, Gli1, Gli2 and Bcl in HaCaT and PANC1 cell lines, respectively. Further investigations on the cytotoxicity over other cell lines expressing the Hh pathway (DU145 and C3H10T1/2) demonstrated that C3H10T1/2, an Hh responsive but not reliant cell line, were less sensitive to the compounds' cytotoxic activity. This is indeed positive in terms of selectivity, as these compounds have limited effects on normal cell lines.[73,144] Taepeenin D (**55**), (+)-drim-8-ene (**56**) and a glycoside quercetin (**57**) were isolated from *Acacia pennata* and displayed GI_{50} values of Gli-mediated transcriptional inhibition in HaCaT cells 1.6, 13.5 and 10.5 μM, respectively. These inhibitors dose dependently reduced Ptch and Bcl expression in HaCaT and PANC1 cells, but only **55** could reduce the exogenous Gli1 protein level in same cells.[73,145] Gli inhibitors have also been identified from *Excoecaria agallocha* (Euphorbiaceae) and *Adenium obesum* (Apocynaceae). *Excoecaria agallocha* afforded **58–60** as 0.5, 19.1 and 2.0 μM potent inhibitors, respectively, of Gli1-mediated transcription in HaCaT cells with selective toxicity for PANC1 and DU145 cells over the normal cells C3H10T1/2. Further,

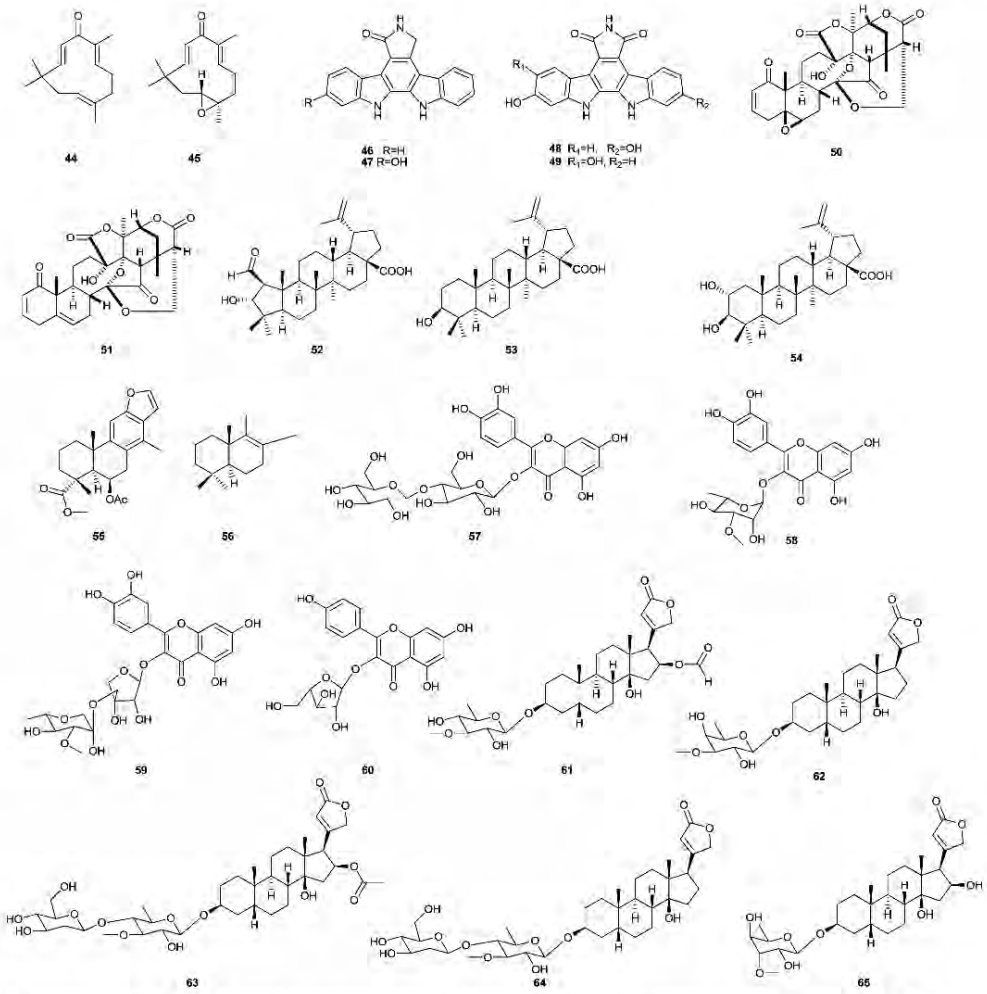

Fig. 8 Structures of natural Gli-mediated transcription inhibitors (**44–51**) and of natural Gli-mediated transcription inhibitors (**52–65**).

compound **58** was confirmed to inhibit the translocation of Gli1 into the nucleus, as well as the expression of Hh proteins Ptch and Bcl in PANC1 cells.[43,143] Examination of *Adenium obesum*, identified up to 17 cardiac glycosides as potent Gli1-mediated transcriptional inhibitors with IC_{50} values from 0.11–2.4 μM. Screening against PANC1, DU145 and HaCaT cell lines indicated that these analogues were selectively cytotoxic to the PANC1 and DU145 cancer cells, while sparing the normal cell (HaCaT). Among these, compounds **61–65** clearly decreased Ptch and BCL2 proteins at 0.25 μM in PANC1 cells; and compounds **62–65** also decreased Ptch mRNA at 0.25 μM (Fig. 8).[141]

Obstacles to the development of chemotherapeutics from Hh pathway inhibitors

Acquired resistance to Hh inhibitors

One of the most important attributes of cancer cells is their unique ability to quickly generate resistance to any therapeutic agents or stressed conditions. A comparison between the genomes of a malignant melanoma and a normal cell line from the same person revealed over 33 000 nucleotide substitutions, 66 micro insertion/deletions and 37 rearrangements.[146] Not all

of these mutations were anticipated to develop cancers due to the self-repairing functions. Thus, despite the highly specific molecular level targeting by Hh pathway inhibitors, they are vulnerable to resistance. Resistance against the Smo inhibitor GDC-0449 (Erivedge™), through a D473H Smo mutation, was the first such case reported.[124,125] Point mutations in Smo and other crosstalk mechanisms resulted in Smo resistance against NVP-LDE225 *via* an alternative mechanism to that observed with GDC-0449.[129]

Gli transcription level inhibitors are expected to resolve a number of issues associated with the resistance of Smo inhibitors, as they are the last effector of the Hh pathway. Based on new insights into the complicated crosstalk of the Hh pathway with other oncogenic pathways, it may be appropriate to target indirect inhibition of Gli by removing/enhancing the supporting/inhibiting activity from corresponding pathways. Consistent with this is the evidence that PI3/ALK inhibitors in murine xenografts result in about a 50% reduction in the Smo and Gli protein levels. This may occur by the rescue of GSK3β-phosphorylation, as GSK3β-phosphorylation promotes proteosomal degradation of Smo and Gli proteins.[129]

Serious side effects

The crucial role of the Hh pathway, particularly in early development suggests that non physiological inhibition may give rise to significant side effects. The adult Hh pathway is less pronounced and the toxicity may be mild in those self-renewing tissues such as bone marrow, gut and skin. Common side effects of vismodegib (Erivedge™) in adult patients include digestive disorders (diarrhoea, constipation, and decreased appetite), tiredness, hair loss, and muscle spasms. However, in children, the consequences can be very severe in the skeletal system. Indeed, experiments in young mice treated with Hh pathway inhibitors resulted in serious bone defects, including premature differentiation of chondrocytes, thinning of cortical bone, and fusion of the growth plate. Unfortunately, these bone defects could not be compensated by administering parathyroid hormone-related protein (PTHrP), whose function is to maintain chondrocytes in a proliferative state.[147]

An acceptable solution to these limitations remains elusive. However, one potential approach may be selective targeting of Gli1, instead of Gli2 and Gli3. Gli2 has been reported to induce PTHrP promoter activity, as well as PTHrP protein production, while Gli1 showed no regulation in PTHrP promoter activity.[124] Gli1 mutants are viable and normal while Gli2 and Gli3 mutants showed from severe bone, nervous system defects to lethal consequences in mice.[148] Importantly Gli2, not Gli1, interacts with and up-regulates the expression and function of Runx2, which involves in osteoblast differentiation in mesenchymal cell line (C3H10T1/2).[149] This suggests that a selective inhibition in Gli1 may minimize the defects in the skeletal system in children treated with the HPIs. Moreover HPI-1 nanoparticle incorporated NanoHHI showed no evidence of hematologic or biochemical abnormalities.[135] It is possible that the combination of nano-encapsulation and specific targeting of Gli1 may allow Hh signalling pathway inhibitors to fulfil their considerable promise as anti cancer agents.

Conclusion

The rapid identification and development of hedgehog inhibitors has benefitted from HTS cell-based assays. However the lead optimisation is hampered at the testing stage in living systems, as it is getting more complex, possibly enhanced by multiple interactions with the microenvironment and different endocrine regulators. Furthermore, different cancers can display different types of the Hh pathway with varying crosstalk combinations, which may largely complicate the development of an effective therapeutic. As a result, despite the fact that thousands of patented and non-patented promising Hh pathway inhibitors have been developed, only one product has successfully reached the clinic (Erivedge™). Many others have been suspended in the clinical trials, when new obstacles emerged in the *in vivo* systems, significantly higher than initial expectations.

Identification of a unique target in the Hh pathway expressed in cancer cells but not in normal cell remains elusive.[130] Fortunately, in this respect, the Gli1 transcription factor has emerged as the "gold target": it is the requisite final effector of the Hh pathway but is not involved in a majority developmental processes unlike Gli2, which is a mainstay of skeletal development. Thus, selective inhibitors of the Gli1-transcription factor are expected to counteract any hedgehog-dependant cancers, irrespectively of their origin or being resistant to up-stream components' inhibitors, while displaying fewer side effects. Preliminary inhibitors of Gli1-mediated transcription have been developed with promising anti-cancer properties and their mechanisms of activity are being characterised.[71,78,151]

Abbreviations

BCC	Basal cell carcinoma
BCL2	B-cell CLL/lymphoma 2
BMI1	B lymphoma Mo-MLV insertion region 1 homolog
C3H10T1/2	Mesenchymal cell line
CK1	Casein kinase 1
CML	Chronic myeloid leukaemia
CSC	Cancer stem cell
Dhh	Desert hedgehog
DU145 cell line	Prostate cancer cell line
ELK1	ETS like gene 1
Gli1,2,3	Glioma-associated oncogene homolog 1,2,3
GSK3β	Glycogen synthase kinase 3β
Hh	Hedgehog
Hhat	Hedgehog acyltransferase
Hip	Hedgehog interacting protein
HPI	Hedgehog signalling pathway inhibitor
HSP	Hedgehog signalling pathway
Ihh	Indian hedgehog
LXR	Liver X receptor

MSX2	Homeobox msh-like
NANOG	Early embryo specific expression NK-type homeobox protein
NanoHH	HPI-1 encapsulated by nanoparticles
NFκB	Nuclear factor kappa light-chain-enhancer of activated B cells
NIH 3T3 cell line	Mouse embryonic fibroblast cell line
N-Myc	Myelocytomatosis viral oncogene homolog
PANC1 cell line	Human pancreatic carcinoma, epithelial like cell line
PGF	Prostaglandin F
PI3/ALK/Mtor	Phosphoinositide 3-kinase pathway
PKA	Protein kinase A
Ptch	Hedgehog ligand receptor patched
PTM	Post translational modification
RAS/RAF/MEK/ERK	Mitogen-activated protein kinases pathway
RTK	Receptor tyrosine kinases
SAG	Smoothened agonist
SHh	Sonic hedgehog
SHH LIGHT2	Cell line
Smo	Smoothened protein
SNAIL	Zinc-finger transcription factors
SuFu	Suppressor of fused
TGF-β	Transforming growth factor β
TM3 cell line	Murine testis Leydig cell line
TNF	Tumour necrosis factor
VEGF	Vascular endothelial growth factor
WIP1	Nuclear Ser/Thr phosphatase
Wnt	Wingless-related integration site

Acknowledgements

The authors thank the NHMRC (Australia) for project support and T.N.T. is the recipient of a Prime Minister's Australia Asia Postgraduate Award.

References

1 FDA approves new treatment for most common type of skin cancer, http://www.fda.gov/NewsEvents/Newsroom/PressAnnouncements/ucm289545.htm.
2 C. Nusslein-Volhard and E. Wieschaus, *Nature*, 1980, **287**, 795–801.
3 D. Huangfu and K. V. Anderson, *Development*, 2006, **133**, 3–14.
4 P. Heretsch, L. Tzagkaroulaki and A. Giannis, *Bioorg. Med. Chem.*, 2010, **18**, 6613–6624.
5 M. Evangelista, H. Tian and F. J. de Sauvage, *Clin. Cancer Res.*, 2006, **12**, 5924–5928.
6 E. Belloni, M. Muenke, E. Roessler, G. Traverso, J. Siegel-Bartelt, A. Frumkin, H. F. Mitchell, H. Donis-Keller, C. Helms, A. V. Hing, H. H. Heng, B. Koop, D. Martindale, J. M. Rommens, L. C. Tsui and S. W. Scherer, *Nat. Genet.*, 1996, **14**, 353–356.
7 C. Chiang, Y. Litingtung, E. Lee, K. E. Young, J. L. Corden, H. Westphal and P. A. Beachy, *Nature*, 1996, **383**, 407–413.
8 Y. Litingtung, L. Lei, H. Westphal and C. Chiang, *Nat. Genet.*, 1998, **20**, 58–61.
9 C. V. Pepicelli, P. M. Lewis and A. P. McMahon, *Curr. Biol.*, 1998, **8**, 1083–1086.
10 B. St-Jacques, M. Hammerschmidt and A. P. McMahon, *Genes Dev.*, 1999, **13**, 2072–2086.
11 M. J. Bitgood, L. Shen and A. P. McMahon, *Curr. Biol.*, 1996, **6**, 298–304.
12 W. Feng, I. Choi, E. Clouthier David, L. Niswander and T. Williams, *Genesis*, 2013, **51**, 677–689.
13 E. H. Epstein, *Nat. Rev. Cancer*, 2008, **8**, 743–754.
14 D. G. Evans, P. A. Farndon, L. D. Burnell, H. R. Gattamaneni and J. M. Birch, *Br. J. Cancer*, 1991, **64**, 959–961.
15 T. Pietsch, A. Waha, A. Koch, J. Kraus, S. Albrecht, J. Tonn, N. Sorensen, F. Berthold, B. Henk, N. Schmandt, H. K. Wolf, A. von Deimling, B. Wainwright, G. Chenevix-Trench, O. D. Wiestler and C. Wicking, *Cancer Res.*, 1997, **57**, 2085–2088.
16 C. Raffel, R. B. Jenkins, L. Frederick, D. Hebrink, B. Alderete, D. W. Fults and C. D. James, *Cancer Res.*, 1997, **57**, 842–845.
17 S. P. Thayer, M. Pasca di Magliano, P. W. Heiser, C. M. Nielsen, D. J. Roberts, G. Y. Lauwers, Y. P. Qi, S. Gysin, C. Fernandez-del Castillo, V. Yajnik, B. Antoniu, M. McMahon, A. L. Warshaw and M. Hebrok, *Nature*, 2003, **425**, 851–856.
18 S. S. Karhadkar, G. S. Bova, N. Abdallah, S. Dhara, D. Gardner, A. Maitra, J. T. Isaacs, D. M. Berman and P. A. Beachy, *Nature*, 2004, **431**, 707–712.
19 D. N. Watkins, D. M. Berman, S. G. Burkholder, B. Wang, P. A. Beachy and S. B. Baylin, *Nature*, 2003, **422**, 313–317.
20 Z. Yuan, J. A. Goetz, S. Singh, S. K. Ogden, W. J. Petty, C. C. Black, V. A. Memoli, E. Dmitrovsky and D. J. Robbins, *Oncogene*, 2007, **26**, 1046–1055.
21 D. Qualtrough, A. Buda, W. Gaffield, A. C. Williams and C. Paraskeva, *Int. J. Cancer*, 2004, **110**, 831–837.
22 D. M. Berman, S. S. Karhadkar, A. Maitra, R. Montes De Oca, M. R. Gerstenblith, K. Briggs, A. R. Parker, Y. Shimada, J. R. Eshleman, D. N. Watkins and P. A. Beachy, *Nature*, 2003, **425**, 846–851.
23 S. Mukherjee, N. Frolova, A. Sadlonova, Z. Novak, A. Steg, G. P. Page, D. R. Welch, S. M. Lobo-Ruppert, J. M. Ruppert, M. R. Johnson and A. R. Frost, *Cancer Biol. Ther.*, 2006, **5**, 674–683.
24 M. Kasper, V. Jaks, M. Fiaschi and R. Toftgaard, *Carcinogenesis*, 2009, **30**, 903–911.
25 A. Po, E. Ferretti, E. Miele, E. De Smaele, A. Paganelli, G. Canettieri, S. Coni, L. Di Marcotullio, M. Biffoni, L. Massimi, C. Di Rocco, I. Screpanti and A. Gulino, *EMBO J.*, 2010, **29**, 2646–2658.
26 M. Zbinden, A. Duquet, A. Lorente-Trigos, S. N. Ngwabyt, I. Borges and A. Ruiz i Altaba, *EMBO J.*, 2010, **29**, 2659–2674.
27 R. K. Mann and P. A. Beachy, *Biochim. Biophys. Acta*, 2000, **1529**, 188–202.

28 J. A. Buglino and M. D. Resh, in *Vitamins & Hormones*, ed. L. Gerald, Academic Press, 2012, vol. 88, pp. 229–252.
29 D. Panakova, H. Sprong, E. Marois, C. Thiele and S. Eaton, *Nature*, 2005, **435**, 58–65.
30 Y. Bellaiche, I. The and N. Perrimon, *Nature*, 1998, **394**, 85–88.
31 J. Taipale, M. K. Cooper, T. Maiti and P. A. Beachy, *Nature*, 2002, **418**, 892–896.
32 R. V. Pearse, 2nd, L. S. Collier, M. P. Scott and C. J. Tabin, *Dev. Biol.*, 1999, **212**, 323–336.
33 N. Bhatia, S. Thiyagarajan, I. Elcheva, M. Saleem, A. Dlugosz, H. Mukhtar and V. S. Spiegelman, *J. Biol. Chem.*, 2006, **281**, 19320–19326.
34 H. Sasaki, Y. Nishizaki, C. Hui, M. Nakafuku and H. Kondoh, *Development*, 1999, **126**, 3915–3924.
35 P. Kogerman, T. Grimm, L. Kogerman, D. Krause, A. B. Unden, B. Sandstedt, R. Toftgard and P. G. Zaphiropoulos, *Nat. Cell Biol.*, 1999, **1**, 312–319.
36 S. Y. Cheng and S. Yue, *Adv. Cancer Res.*, 2008, **101**, 29–43.
37 A. M. Kenney and D. H. Rowitch, *Mol.Cell. Biol.*, 2000, **20**, 9055–9067.
38 J. L. Mullor, N. Dahmane, T. Sun and A. Ruiz i Altaba, *Curr. Biol.*, 2001, **11**, 769–773.
39 A. M. Kenney, M. D. Cole and D. H. Rowitch, *Development*, 2003, **130**, 15–28.
40 R. Pola, L. E. Ling, M. Silver, M. J. Corbley, M. Kearney, R. B. Pepinsky, R. Shapiro, F. R. Taylor, D. P. Baker, T. Asahara and J. M. Isner, *Nat. Med.*, 2001, **7**, 706–711.
41 G. Regl, M. Kasper, H. Schnidar, T. Eichberger, G. W. Neill, M. P. Philpott, H. Esterbauer, C. Hauser-Kronberger, A. M. Frischauf and F. Aberger, *Cancer Res.*, 2004, **64**, 7724–7731.
42 X. Li, W. Deng, C. D. Nail, S. K. Bailey, M. H. Kraus, J. M. Ruppert and S. M. Lobo-Ruppert, *Oncogene*, 2006, **25**, 609–621.
43 H. Ohta, K. Aoyagi, M. Fukaya, I. Danjoh, A. Ohta, N. Isohata, N. Saeki, H. Taniguchi, H. Sakamoto, T. Shimoda, T. Tani, T. Yoshida and H. Sasaki, *Br. J. Cancer*, 2009, **100**, 389–398.
44 S. Das, L. G. Harris, B. J. Metge, S. Liu, A. I. Riker, R. S. Samant and L. A. Shevde, *J. Biol. Chem.*, 2009, **284**, 22888–22897.
45 C. Leung, M. Lingbeek, O. Shakhova, J. Liu, E. Tanger, P. Saremaslani, M. van Lohuizen and S. Marino, *Nature*, 2004, **428**, 337–341.
46 B. Stecca and A. Ruiz i Altaba, *EMBO J.*, 2009, **28**, 663–676.
47 H. Hahn, C. Wicking, P. G. Zaphiropoulous, M. R. Gailani, S. Shanley, A. Chidambaram, I. Vorechovsky, E. Holmberg, A. B. Unden, S. Gillies, K. Negus, I. Smyth, C. Pressman, D. J. Leffell, B. Gerrard, A. M. Goldstein, M. Dean, R. Toftgard, G. Chenevix-Trench, B. Wainwright and A. E. Bale, *Cell*, 1996, **85**, 841–851.
48 R. L. Johnson, A. L. Rothman, J. Xie, L. V. Goodrich, J. W. Bare, J. M. Bonifas, A. G. Quinn, R. M. Myers, D. R. Cox, E. H. Epstein Jr and M. P. Scott, *Science*, 1996, 272, 1668–1671.
49 J. Xie, R. L. Johnson, X. Zhang, J. W. Bare, F. M. Waldman, P. H. Cogen, A. G. Menon, R. S. Warren, L. C. Chen, M. P. Scott and E. H. Epstein, Jr, *Cancer Res.*, 1997, **57**, 2369–2372.
50 N. Soufir, B. Gerard, M. Portela, A. Brice, M. Liboutet, P. Saiag, V. Descamps, D. Kerob, P. Wolkenstein, I. Gorin, C. Lebbe, N. Dupin, B. Crickx, N. Basset-Seguin and B. Grandchamp, *Br. J. Cancer*, 2006, **95**, 548–553.
51 J. Xie, M. Murone, S.-M. Luoh, A. Ryan, Q. Gu, C. Zhang, J. M. Bonifas, C.-W. Lam, M. Hynes, A. Goddard, A. Rosenthal, E. H. Epstein, Jr and F. J. de Sauvage, *Nature*, 1998, **391**, 90–92.
52 T. Yan, M. Angelini, B. A. Alman, I. L. Andrulis and J. S. Wunder, *Clin. Orthop. Relat. Res.*, 2008, **466**, 2184–2189.
53 F. J. De Sauvage, Mutant smoothened and methods of using the same, *US Pat.* 20120039893, 2012.
54 S. Y. Cheng and J. M. Bishop, *Proc. Natl. Acad. Sci. U. S. A.*, 2002, **99**, 5442–5447.
55 M. D. Taylor, L. Liu, C. Raffel, C.-C. Hui, T. G. Mainprize, X. Zhang, R. Agatep, S. Chiappa, L. Gao, A. Lowrance, A. Hao, A. M. Goldstein, T. Stavrou, S. W. Scherer, W. T. Dura, B. Wainwright, J. A. Squire, J. T. Rutka and D. Hogg, *Nat. Genet.*, 2002, **31**, 306–310.
56 L. Brugieres, G. Pierron, A. Chompret, B. Bressac-de Paillerets, F. Di Rocco, P. Varlet, A. Pierre-Kahn, O. Caron, J. Grill and O. Delattre, *J. Med. Genet.*, 2010, 47, 142–144.
57 I. Slade, A. Murray, S. Hanks, A. Kumar, L. Walker, D. Hargrave, J. Douglas, C. Stiller, L. Izatt and N. Rahman, *Fam. Cancer*, 2011, **10**, 337–342.
58 L. Brugieres, A. Remenieras, G. Pierron, P. Varlet, S. Forget, V. Byrde, J. Bombled, S. Puget, O. Caron, C. Dufour, O. Delattre, B. Bressac-de Paillerets and J. Grill, *J. Clin. Oncol.*, 2012, **30**, 2087–2093.
59 M. Chen, M. Tanner, A. C. Levine, E. Levina, P. Ohouo and R. Buttyan, *Cell Cycle*, 2009, **8**, 149–157.
60 S. Singh, Z. Wang, F. D. Liang, K. E. Black, J. A. Goetz, R. Tokhunts, C. Giambelli, J. Rodriguez-Blanco, J. Long, E. Lee, K. J. Briegel, P. A. Bejarano, E. Dmitrovsky, A. J. Capobianco and D. J. Robbins, *Cancer Res.*, 2011, **71**, 4454–4463.
61 F. Varnat, A. Duquet, M. Malerba, M. Zbinden, C. Mas, P. Gervaz and A. Ruiz i Altaba, *EMBO Mol. Med.*, 2009, **1**, 338–351.
62 L. Fan, C. V. Pepicelli, C. C. Dibble, W. Catbagan, J. L. Zarycki, R. Laciak, J. Gipp, A. Shaw, M. L. G. Lamm, A. Munoz, R. Lipinski, J. B. Thrasher and W. Bushman, *Endocrinology*, 2004, **145**, 3961–3970.
63 I. S. Chan, C. D. Guy, Y. Chen, J. Lu, M. Swiderska-Syn, G. A. Michelotti, G. Karaca, G. Xie, L. Kruger, W.-K. Syn, B. R. Anderson, T. A. Pereira, S. S. Choi, A. S. Baldwin and A. M. Diehl, *Cancer Res.*, 2012, 72, 6344–6350.
64 R. L. Yauch, S. E. Gould, S. J. Scales, T. Tang, H. Tian, C. P. Ahn, D. Marshall, L. Fu, T. Januario, D. Kallop, M. Nannini-Pepe, K. Kotkow, J. C. Marsters, L. L. Rubin and F. J. de Sauvage, *Nature*, 2008, **455**, 406–410.
65 C. Dierks, J. Grbic, K. Zirlik, R. Beigi, N. P. Englund, G.-R. Guo, H. Veelken, M. Engelhardt, R. Mertelsmann,

J. F. Kelleher, P. Schultz and M. Warmuth, *Nat. Med.*, 2007, **13**, 944–951.
66 G. V. Hegde, K. J. Peterson, K. Emanuel, A. K. Mittal, A. D. Joshi, J. D. Dickinson, G. J. Kollessery, R. G. Bociek, P. Bierman, J. M. Vose, D. D. Weisenburger and S. S. Joshi, *Mol. Cancer Res.*, 2008, **6**, 1928–1936.
67 J. Jiang and C. C. Hui, *Dev. Cell*, 2008, **15**, 801–812.
68 S.-Q. Jiang and H. Paulus, *J. Biomol. Screening*, 2010, **15**, 1082–1087.
69 E. Petrova, J. Rios-Esteves, O. Ouerfelli, J. F. Glickman and M. D. Resh, *Nat. Chem. Biol.*, 2013, **9**, 247–249.
70 G. Dessole, P. Jones, L. L. Bufi, E. Muraglia, J. M. Ontoria and C. Torrisi, 1,2,4-Oxadiazole substituted piperidine and piperazine derivatives as Smo antagonists, WO 2010013037 A1, 2008.
71 J. M. Hyman, A. J. Firestone, V. M. Heine, Y. Zhao, C. A. Ocasio, K. Han, M. Sun, P. G. Rack, S. Sinha, J. J. Wu, D. E. Solow-Cordero, J. Jiang, D. H. Rowitch and J. K. Chen, *Proc. Nat. Acad. Sci. U. S. A.*, 2009, **106**, 14132–14137.
72 B. Z. Stanton, L. F. Peng, N. Maloof, K. Nakai, X. Wang, J. L. Duffner, K. M. Taveras, J. M. Hyman, S. W. Lee, A. N. Koehler, J. K. Chen, J. L. Fox, A. Mandinova and S. L. Schreiber, *Nat. Chem. Biol.*, 2009, **5**, 154–156.
73 M. A. Arai, C. Tateno, T. Hosoya, T. Koyano, T. Kowithayakorn and M. Ishibashi, *Bioorg. Med. Chem.*, 2008, **16**, 9420–9424.
74 J. L. Gunzner, D. P. Sutherlin, M. S. Stanley, L. Bao, G. Castanedo, R. L. Lalonde, S. Wang, M. E. Reynolds, S. J. Savage, K. Malesky and M. S. Dina, Pyridyl inhibitors of hedgehog signalling, WO 2009126863 A2, 2008.
75 N. Mahindroo, C. Punchihewa and N. Fujii, *J. Med. Chem.*, 2009, **52**, 3829–3845.
76 S. Pan, X. Wu, J. Jiang, W. Gao, Y. Wan, D. Cheng, D. Han, J. Liu, N. P. Englund, Y. Wang, S. Peukert, K. Miller-Moslin, J. Yuan, R. Guo, M. Matsumoto, A. Vattay, Y. Jiang, J. Tsao, F. Sun, A. C. Pferdekamper, S. Dodd, T. Tuntland, W. Maniara, J. F. Kelleher, III, Y. M. Yao, M. Warmuth, J. Williams and M. Dorsch, *ACS Med. Chem. Lett.*, 2010, **1**, 130–134.
77 M. Dai, F. He, R. K. Jain, R. Karki, J. Kelleher, III, J. Lei, L. Llamas, M. A. McEwan, K. Miller-Moslin, L. B. Perez, S. Peukert and N. Yusuff, Organic compounds and their uses, WO/2008/110611, 2008.
78 M. Lauth, A. Bergstroem, T. Shimokawa and R. Toftgard, *Proc. Natl. Acad. Sci. U. S. A.*, 2007, **104**, 8455–8460.
79 N. Mahindroo, M. C. Connelly, C. Punchihewa, L. Yang, B. Yan and N. Fujii, *Bioorg. Med. Chem.*, 2010, **18**, 4801–4811.
80 R. K. Mann and P. A. Beachy, *Annu. Rev. Biochem.*, 2004, **73**, 891–923.
81 J. A. Buglino and M. D. Resh, *J. Biol. Chem.*, 2008, **283**, 22076–22088.
82 M. Baranowski, *J. Physiol. Pharmacol.*, 2008, **59**, 31–55.
83 W. K. Kim, V. Meliton, K. W. Park, C. Hong, P. Tontonoz, P. Niewiadomski, J. A. Waschek, S. Tetradis and F. Parhami, *Mol. Endocrinol.*, 2009, **23**, 1532–1543.
84 C.-P. Chuu, J. M. Kokontis, R. A. Hiipakka and S. Liao, *J. Biomed. Sci.*, 2007, **14**, 543–553.
85 J. Belltowski, *Clin. Lipidol.*, 2011, **6**, 137–141.
86 H. R. Maun, X. Wen, A. Lingel, F. J. de Sauvage, R. A. Lazarus, S. J. Scales and S. G. Hymowitz, *J. Biol. Chem.*, 2010, **285**, 26570–26580.
87 R. F. Keeler, *Teratology*, 1970, **3**, 169–173.
88 J. K. Chen, J. Taipale, M. K. Cooper and P. A. Beachy, *Genes Dev.*, 2002, **16**, 2743–2748.
89 B. Stecca, C. Mas, V. Clement, M. Zbinden, R. Correa, V. Piguet, F. Beermann and I. A. A. Ruiz, *Proc. Natl. Acad. Sci. U. S. A.*, 2007, **104**, 5895–5900.
90 S. Tabs and O. Avci, *Eur. J. Dermatol.*, 2004, **14**, 96–102.
91 C. Mas and A. Ruiz i Altaba, *Biochem. Pharmacol.*, 2010, **80**, 712–723.
92 P. A. Beachy, J. K. Chen and A. J. Taipale, Regulators of the Hedgehog pathway, compositions and uses related thereto, *US Pat.* 7,098,196, 2006.
93 M. R. Tremblay, M. Nevalainen, S. J. Nair, J. R. Porter, A. C. Castro, M. L. Behnke, L.-C. Yu, M. Hagel, K. White, K. Faia, L. Grenier, M. J. Campbell, J. Cushing, C. N. Woodward, J. Hoyt, M. A. Foley, M. A. Read, J. R. Sydor, J. K. Tong, V. J. Palombella, K. McGovern and J. Adams, *J. Med. Chem.*, 2008, **51**, 6646–6649.
94 G. van der Horst, H. Farih-Sips, C. W. G. M. Lowik and M. Karperien, *Bone*, 2003, **33**, 899–910.
95 M. R. Tremblay, A. Lescarbeau, M. J. Grogan, E. Tan, G. Lin, B. C. Austad, L.-C. Yu, M. L. Behnke, S. J. Nair, M. Hagel, K. White, J. Conley, J. D. Manna, T. M. Alvarez-Diez, J. Hoyt, C. N. Woodward, J. R. Sydor, M. Pink, J. MacDougall, M. J. Campbell, J. Cushing, J. Ferguson, M. S. Curtis, K. McGovern, M. A. Read, V. J. Palombella, J. Adams and A. C. Castro, *J. Med. Chem.*, 2009, **52**, 4400–4418.
96 V. Travaglione, presented in part at the ASMS Conference, Denver, 2008.
97 V. Dormoy, C. Beraud, V. Lindner, C. Coquard, M. Barthelmebs, D. Brasse, D. Jacqmin, H. Lang and T. Massfelder, *Carcinogenesis*, 2012, **33**, 2084–2093.
98 K. D. Robarge, S. A. Brunton, G. M. Castanedo, Y. Cui, M. S. Dina, R. Goldsmith, S. E. Gould, O. Guichert, J. L. Gunzner, J. Halladay, W. Jia, C. Khojasteh, M. F. T. Koehler, K. Kotkow, H. La, R. L. La Londe, K. Lau, L. Lee, D. Marshall, J. C. Marsters, L. J. Murray, C. Qian, L. L. Rubin, L. Salphati, M. S. Stanley, J. H. A. Stibbard, D. P. Sutherlin, S. Ubhayaker, S. Wang, S. Wong and M. Xie, *Bioorg. Med. Chem. Lett.*, 2009, **19**, 5576–5581.
99 J. Gunzner, D. Sutherlin, M. Stanley, L. Bao, G. Castanedo, R. Lalonde, S. Wang, M. Reynolds, S. Savage, K. Malesky and M. Dina, Pyridyl inhibitors of Hedgehog signalling, US2012/009480 A1, 2011.
100 C. M. Rudin, *Clin. Cancer Res.*, 2012, **18**, 3218–3222.
101 T. Ohashi, Y. Oguro, T. Tanaka, Z. Shiokawa, Y. Tanaka, S. Shibata, Y. Sato, H. Yamakawa, H. Hattori, Y. Yamamoto, S. Kondo, M. Miyamoto, M. Nishihara,

Y. Ishimura, H. Tojo, A. Baba and S. Sasaki, *Bioorg. Med. Chem.*, 2012, **20**, 5507–5517.
102 R. Tremblay Martin, M. Nesler, R. Weatherhead and C. Castro Alfredo, *Expert Opin. Ther. Pat.*, 2009, **19**, 1039–1056.
103 C. Wang, H. Wu, V. Katritch, G. W. Han, X. P. Huang, W. Liu, F. Y. Liu, B. L. Roth, V. Cherezov and R. C. Stevens, *Nature*, 2013, **497**, 338–343.
104 S. Peukert, F. He, M. Dai, R. Zhang, Y. Sun, K. Miller-Moslin, M. McEwan, B. Lagu, K. Wang, N. Yusuff, A. Bourret, A. Ramamurthy, W. Maniara, A. Amaral, A. Vattay, A. Wang, R. Guo, J. Yuan, J. Green, J. Williams, S. Buonamici, F. Kelleher Joseph, 3rd and M. Dorsch, *ChemMedChem*, 2013, **8**, 1261–1265.
105 P. Ferruzzi, F. Mennillo, A. De Rosa, C. Giordano, M. Rossi, G. Benedetti, R. Magrini, G. Pericot Mohr, V. Miragliotta, L. Magnoni, E. Mori, R. Thomas, P. Tunici and A. Bakker, *Int. J. Cancer*, 2012, **131**, E33–E44.
106 J. Kim, B. T. Aftab, J. Y. Tang, D. Kim, A. H. Lee, M. Rezaee, J. Kim, B. Chen, E. M. King, A. Borodovsky, G. J. Riggins, E. H. Epstein, P. A. Beachy and C. M. Rudin, *Cancer Cell*, 2013, **23**, 23–34.
107 A. Solinas, H. Faure, H. Roudaut, E. Traiffort, A. Schoenfelder, A. Mann, F. Manetti, M. Taddei and M. Ruat, *J. Med. Chem.*, 2012, **55**, 1559–1571.
108 M. J. Munchhof, Q. Li, A. Shavnya, G. V. Borzillo, T. L. Boyden, C. S. Jones, S. D. LaGreca, L. Martinez-Alsina, N. Patel, K. Pelletier, L. A. Reiter, M. D. Robbins and G. T. Tkalcevic, *ACS Med. Chem. Lett.*, 2012, **3**, 106–111.
109 R. Derynck, R. J. Akhurst and A. Balmain, *Nat. Genet.*, 2001, **29**, 117–129.
110 P. M. Siegel and J. Massague, *Nat. Rev. Cancer*, 2003, **3**, 807–820.
111 D. Javelaud, M. J. Pierrat and A. Mauviel, *FEBS Lett.*, 2012, **586**, 2016–2025.
112 C. Y. Perrot, D. Javelaud and A. Mauviel, *Pharmacol. Therapeut.*, 2013, **137**, 183–199.
113 S. Dennler, J. Andre, F. Verrecchia and A. Mauviel, *J. Biol. Chem.*, 2009, **284**, 31523–31531.
114 M.-J. Pierrat, V. Marsaud, A. Mauviel and D. Javelaud, *J. Biol. Chem.*, 2012, **287**, 17996–18004.
115 M. Chen, R. Carkner and R. Buttyan, *Expert Rev. Endocrinol. Metab.*, 2011, **6**, 453–467.
116 S. Pandolfi, V. Montagnani, J. Y. Penachioni, M. C. Vinci, B. Olivito, L. Borgognoni and B. Stecca, *Oncogene*, 2013, **32**, 4737–4747.
117 M. Cully, H. You, A. J. Levine and T. W. Mak, *Nat. Rev. Cancer*, 2006, **6**, 184–192.
118 M. Raman, W. Chen and M. H. Cobb, *Oncogene*, 2007, **26**, 3100–3112.
119 J. G. Monzon and J. Dancey, *OncoTargets Ther.*, 2012, **5**, 31–46.
120 B. Ramaswamy, Y. Lu, K.-Y. Teng, G. Nuovo, X. Li, L. Shapiro Charles and S. Majumder, *Cancer Res.*, 2012, **72**, 5048–5059.
121 N. A. Riobo, *Proc. Nat. Acad. Sci. U. S. A.*, 2006, **103**, 4505–4510.
122 P. M. LoRusso, C. M. Rudin, J. C. Reddy, R. Tibes, G. J. Weiss, M. J. Borad, C. L. Hann, J. R. Brahmer, I. Chang, W. C. Darbonne, R. A. Graham, K. L. Zerivitz, J. A. Low and D. D. Von Hoff, *Clin. Cancer Res.*, 2011, **17**, 2502–2511.
123 A. Sekulic, M. R. Migden, A. E. Oro, L. Dirix, K. Lewis, J. D. Hainsworth, J. A. Solomon, S. Yoo, S. T. Arron, P. A. Friedlander, E. Marmur, C. M. Rudin, A. L. S. Chang, J. A. Low, A. B. Mueller, R. L. Yauch, J. C. Reddy and A. Hauschild, *Melanoma Res.*, 2011, **21**, pe9, DOI: 10.1097/01.cmr.0000399448.65869.b7.
124 C. M. Rudin, C. L. Hann, J. Laterra, R. L. Yauch, C. A. Callahan, L. Fu, T. Holcomb, J. Stinson, S. E. Gould, B. Coleman, P. M. LoRusso, D. D. von Hoff, F. J. de Sauvage and J. A. Low, Treatment of medulloblastoma with hedgehog pathway inhibitor GDC-0449, Report 1533-1406, Sidney Kimmel Comprehensive Cancer Center, Johns Hopkins University, Baltimore, MD 21231, USA, 2009.
125 R. L. Yauch, G. J. P. Dijkgraaf, B. Alicke, T. Januario, C. P. Ahn, T. Holcomb, K. Pujara, J. Stinson, C. A. Callahan, T. Tang, J. F. Bazan, Z. Kan, S. Seshagiri, C. L. Hann, S. E. Gould, J. A. Low, C. M. Rudin and F. J. de Sauvage, *Science*, 2009, **326**, 572–574.
126 D. A. Richards, J. Stephenson, B. M. Wolpin, C. Becerra, J. T. Hamm, W. A. Messersmith, S. Devens, J. Cushing, T. Schmalbach and C. S. Fuchs, *J. Clin. Oncol.*, 2012, **30**, 213.
127 M. Allison, *Nat. Biotechnol.*, 2012, **30**, 203.
128 J. Rodon Ahnert, J. Baselga, H. A. Tawbi, Y. Shou, C. Granvil, J. Dey, M. M. Mita, A. L. Thomas, D. D. Amakye and A. C. Mita, *J. Clin. Oncol.*, 2010, **28**, 2500.
129 S. Buonamici, J. Williams, M. Morrissey, A. Wang, R. Guo, A. Vattay, K. Hsiao, J. Yuan, J. Green, B. Ospina, Q. Yu, L. Ostrom, P. Fordjour, D. L. Anderson, J. E. Monahan, J. F. Kelleher, S. Peukert, S. Pan, X. Wu, S. M. Maira, C. Garcia-Echeverria, K. J. Briggs, D. N. Watkins, Y. M. Yao, C. Lengauer, M. Warmuth, W. R. Sellers and M. Dorsch, *Sci. Transl. Med.*, 2010, **2**, 51ra70.
130 M. Wickstroem, C. Dyberg, T. Shimokawa, J. Milosevic, N. Baryawno, O. M. Fuskevag, R. Larsson, P. Kogner, P. G. Zaphiropoulos and J. I. Johnsen, *Int. J. Cancer*, 2013, **132**, 1516–1524.
131 J. Fu, M. Rodova, S. K. Roy, J. Sharma, K. P. Singh, R. K. Srivastava and S. Shankar, *Cancer Lett.*, 2013, **330**, 22–32.
132 T. Mazumdar, J. DeVecchio, T. Shi, J. Jones, A. Agyeman and J. A. Houghton, *Cancer Res.*, 2011, **71**, 1092–1102.
133 S. Liu, G. Dontu, D. Mantle Ilia, S. Patel, N.-S. Ahn, W. Jackson Kyle, P. Suri and S. Wicha Max, *Cancer Res.*, 2006, **66**, 6063–6071.
134 J. A. Sterling, B. O. Oyajobi, B. Grubbs, S. S. Padalecki, S. A. Munoz, A. Gupta, B. Story, M. Zhao and G. R. Mundy, *Cancer Res.*, 2006, **66**, 7548–7553.
135 V. Chenna, C. Hu, D. Pramanik, B. T. Aftab, C. Karikari, N. R. Campbell, S.-M. Hong, M. Zhao, M. A. Rudek, S. R. Khan, C. M. Rudin and A. Maitra, *Mol. Cancer Ther.*, 2012, **11**, 165–173.

136 B. He, N. Fujii, L. You, Z. Xu and D. M. Jablons, Targeting GLI proteins in human cancer by small molecules, *US Pat.* 7714014, 2006.
137 N. Mahindroo, M. C. Connelly, C. Punchihewa, H. Kimura, M. P. Smeltzer, S. Wu and N. Fujii, *J. Med. Chem.*, 2009, **52**, 4277–4287.
138 M. Actis, M. C. Connelly, A. Mayasundari, C. Punchihewa and N. Fujii, *Biopolymers*, 2011, **95**, 24–30.
139 G. Canettieri, L. Di Marcotullio, A. Greco, S. Coni, L. Antonucci, P. Infante, L. Pietrosanti, E. De Smaele, E. Ferretti, E. Miele, M. Pelloni, G. De Simone, E. M. Pedone, P. Gallinari, A. Giorgi, C. Steinkuhler, L. Vitagliano, C. Pedone, M. E. Schinin, I. Screpanti and A. Gulino, *Nat. Cell Biol.*, 2010, **12**, 132–142.
140 J. Mao, *J. Biol. Chem.*, 2002, **277**, 35156–35161.
141 M. A. Arai, C. Tateno, T. Koyano, T. Kowithayakorn, S. Kawabe and M. Ishibashi, *Org. Biomol. Chem.*, 2011, **9**, 1133–1139.
142 Y. Rifai, M. A. Arai, T. Koyano, T. Kowithayakorn and M. Ishibashi, *J. Nat. Prod.*, 2010, **73**, 995–997.
143 T. Hosoya, M. A. Arai, T. Koyano, T. Kowithayakorn and M. Ishibashi, *ChemBioChem*, 2008, **9**, 1082–1092.
144 A. Murakami, D. Takahashi, T. Kinoshita, K. Koshimizu, H. W. Kim, A. Yoshihiro, Y. Nakamura, S. Jiwajinda, J. Terao and H. Ohigashi, *Carcinogenesis*, 2002, **23**, 795–802.
145 Y. Rifai, M. A. Arai, S. K. Sadhu, F. Ahmed and M. Ishibashi, *Bioorg. Med. Chem. Lett.*, 2011, **21**, 718–722.
146 E. D. Pleasance, R. K. Cheetham, P. J. Stephens, D. J. McBride, S. J. Humphray, C. D. Greenman, I. Varela, M.-L. Lin, G. R. Ordonez, G. R. Bignell, K. Ye, J. Alipaz, M. J. Bauer, D. Beare, A. Butler, R. J. Carter, L. Chen, A. J. Cox, S. Edkins, P. I. Kokko-Gonzales, N. A. Gormley, R. J. Grocock, C. D. Haudenschild, M. M. Hims, T. James, M.-M. Jia, Z. Kingsbury, C. Leroy, J. Marshall, A. Menzies, L. J. Mudie, Z.-M. Ning, T. Royce, O. B. Schulz-Trieglaff, A. Spiridou, L. A. Stebbings, L. Szajkowski, J. Teague, D. Williamson, L. Chin, M. T. Ross, P. J. Campbell, D. R. Bentley, P. A. Futreal and M. R. Stratton, *Nature*, 2010, **463**, 191–196.
147 J. L. Brechbiel, J. M. Y. Ng and T. Curran, *Toxicol. Pathol.*, 2011, **39**, 478–485.
148 H. L. Park, C. Bai, K. A. Platt, M. P. Matise, A. Beeghly, C. C. Hui, M. Nakashima and A. L. Joyner, *Development*, 2000, **127**, 1593–1605.
149 A. Shimoyama, M. Wada, F. Ikeda, K. Hata, T. Matsubara, A. Nifuji, M. Noda, K. Amano, A. Yamaguchi, R. Nishimura and T. Yoneda, *Mol. Biol. Cell*, 2007, **18**, 2411–2418.
150 A. Quintas-Cardama, H. Kantarjian and J. Cortes, *Nat. Rev. Clin. Oncol.*, 2009, **6**, 535–543.

1.2. Updates on recent development of HSP's inhibitors

1.2.1 Smo inhibitors

Since 2014, a number of additional Smo inhibitors have been reported. Further derivatives from the benzimdidazole scaffold, represented by (**3**), were identified as Smo inhibitors though the potency was not disclosed [20]. Most recently, a series of piperidinyl pyridazine derivatives were prepared as potent Smo inhibitors displaying low nanomolar potency in inhibiting Gli signalling in NIH3T3 (Mouse Embryo Fibroblast) cell line as illustrated by (**4**) [21]. In another area, more derivatives based on vitamin D3 scaffold have been reported, with (**5**) displaying low micromolar inhibition over Smo in HEK293T (Human Embryonic Kidney 293) cells at a different binding site from those of Cyclopamine or vismodegib (Erivedge®) [22-24] (Figure 1).

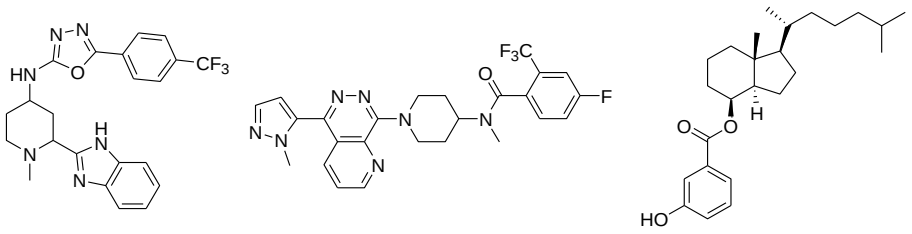

3 **4** (IC_{50} = 0.4 nM) **5** (IC_{50} = 0.74 ± 0.1 µM)

Figure 1. Structures of benzimidazole (**3**), piperidinyl pyridazine (**4**) and vitamin D3 (**5**) derivatives as Smo inhibitors.

1.2.2. Inhibitors targeting Gli transcription factors

As a more robust and complete inhibition of the HSP [19], Gli inhibition has attracted greater attention, with an increased number of Gli inhibitors developed. Interestingly, besides the direct targeting on Gli, a number of indirect strategies to inhibit Gli signalling have been developed. These include the modulation of interacting signalling pathways/proteins that tightly regulate the HSP to suppress Gli expression.

1.2.2.1. Direct Gli inhibitors

As outlined in our review, a number of Gli inhibitors originated from natural sources. Recently, Glabrescione B (**6**) [25] (Figure 2), an isoflavone naturally occurring in *Derris glabrescens*, is purported to directly bind to Gli_1 and inhibiting the Gli_1-DNA complex in Smo $^{-/-}$ MEF (Smo deficient Mouse Embryonic Fibroblast) cells. Promisingly, Glabrescione B effectively inhibited several tumours, *in vivo,* including Gli-dependent allograft of spontaneous MBs from Ptch $^{+/-}$

mice, orthotopic xenograft of Daoy MB cells at 35 mg/kg; and allograft of ASZ001 BCC cells at 50 mg/kg [25].

In other studies, lead compounds from *Artocarpus communis* (**7**) [26], *Hyptis suaveolens* (**8**) [26], *Withania somnifera* (**9**) [27], and *Crinum asiaticum* (**10**) [28] (Figure 2) displayed low micromolar activity from 0.5 µM to 14.6 µM inhibiting exogenous Gli_1 mediated transcription activity in tetracycline controlled HaCaT cells. These compounds were selectively cytotoxic against HSP expressing human pancreatic (PANC1) and prostate (DU145) cancer cells, while showing lower levels of activity against C3H10T1/2, a normal cell line in which Hh signalling is active but does not contribute to abnormal cell survival. Furthermore, using the electron mobility shift assay (EMSA) [27], compound (**9**) was found to disrupt the Gli-DNA interaction at 100 µM (Figure 2).

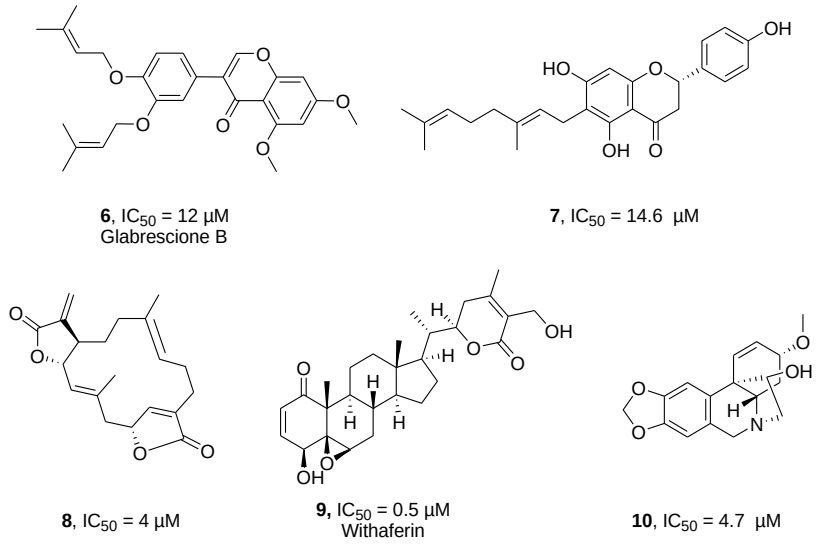

Figure 2. Structures of natural products that target Gli transcription factors.

1.2.2.2. Indirect Gli inhibitors

a. Activators of the mitogen-activated protein kinase (MAPK) pathway

The activation of GPCR GPR39 receptor by a number of cyclohexyl-methyl aminopyrimidines (CMAPs), represented by **11**, triggered activation of the MAPK pathway and led to the suppression of Gli signalling. Evidence showed that **11** displayed low nanomolar potency in inhibiting Gli luciferase reporter in TM3 cells treated with 1 nM and 25 nM of Smo agonist Ag1.5, respectively [29, 30] (Figure 3).

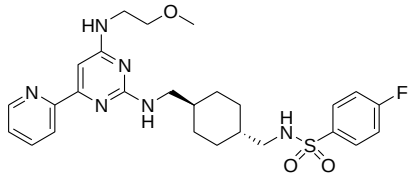

11, IC_{50} = 4 nM

Figure 3. Structures of CMAPs, represented by **11**.

b. Activators of Protein Kinase A (PKA) and Cyclin-suppressing kinase 1 (CSK1α)

As previously outlined in our published review, PKA and CSK1α negatively regulate the HSP downstream of Smo by phosphorylating $GLI_{2,3}$ leading to their proteosomal cleavage, and subsequent inhibition of Gli signalling [31]. In this respect, several activators of the PKA and/or CSK1α have been identified as indirect inhibitors of Gli signalling, including eggmanone (**12)** and imiquimod (**13)** targeting PKA[32, 33] and pyrvinium (**14**) acting on CSK1α [34, 35] (Figure 4).

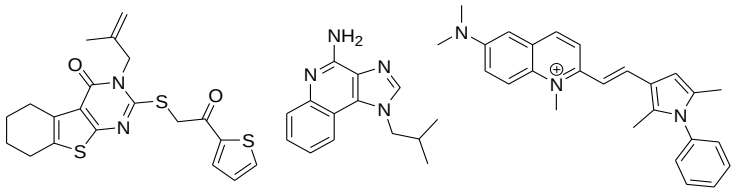

12, low micromolar potency
Eggmanone

13
Imiquimod

14, IC_{50} = 10 nM
Pyrvinium

Figure 4. Structures of PKA activators eggmanone (**12**), imiquimod (**13**), and CSK1α activator pyrvinium (**14**)

Eggmanone (**12**) at 10 μM effectively inhibited transcription levels of *Gli1* and *Ptch1* in $Sufu^{-/-}$ mouse embryonic fibroblasts (MEFs), demonstrating activity independently of Smo. Further investigation demonstrated that eggmanone (**12**) selectively antagonised phosphodiesterase 4 (PDE4), leading to PKA activation and subsequent Gli signalling blockade.

Imiquimod (**13**) was initially developed as an immune stimulating product, topically used in the treatment of small superficial basal cell carcinomas (BCCs) [36, 37]. Subsequent investigation demonstrated imiquimod (**13**) induced phosphorylation of Gli into repressor forms by binding to andenosine receptors, thereby activating PKA.[38] This interaction resulted in the downregulation of Gli_1 mRNA and protein levels in murine BCC cells and Hh-responsive human cancer cells [33].

Moreover, pyrvinium (**14**), originally developed as an anti-pinworm drug, has recently been linked as a potent and selective stimulator of the CSK1α [35]. This finding suggested an anti-HSP property which was confirmed *in vitro* by the significant inhibition of Gli signalling in Shh-LIGHT 2 cells (IC_{50} = 10 nM), and *in vivo* through attenuating the growth of the allograft of spontaneous MBs from $Ptch^{+/-}$ mice at 0.8 mg/kg [35].

c. Epigenetic inhibitors

Gli signalling can also be constrained by influencing several epigenetic enzymes which play a crucial role in the gene expression. One such enzyme is the bromodomain-containing protein 4 (BRD4), functioning as an enhancer of the HSP through direct occupation of the $Gli_{1,2}$ promoter [39]. Consequently inhibition of BRD4 by JQ1 (**15**) [39] and I-BET151 (**16**) [40] significantly suppressed Gli signalling independently of Smo at nanomolar potency (Figure 5).

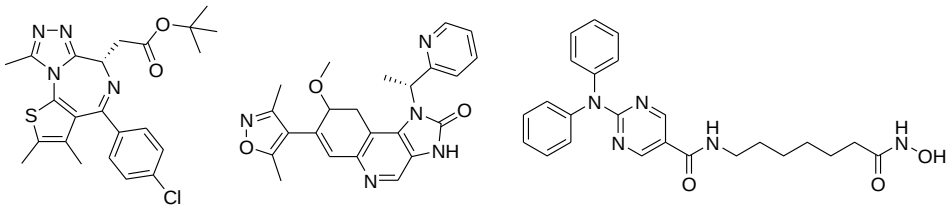

15, IC_{50} = (50 -150) nM
JQ1

16, IC_{50} = 31 nM
I-BET151

17
ACY-1215

Figure 5. Structures of epigenetic inhibitors (**15**–**17**).

Another epigenetic target are the Histone Deacetylase (HDACs) enzymes. Under HDACs' influence, $Gli_{1,2}$ are deacetylated into active forms capable of initiating Gli signalling [41, 42]. Accordingly, inhibitors of HDACs, such as ACY-1215 (**17**) [43], can act as HSP antagonists by inducing the hyperacetylation of $Gli_{1,2}$ leading to the blockage of Gli transcriptional activity [44-46]. Interestingly, ACY-1215 effectively reduced tumour growth in an allograft of primary SmoA1 MB cells (MB99-1 cells) at 50 mg/kg making it a promising lead in the treatment of Hh related cancers [43, 47] (Figure 5).

1.3. Conclusions and project aims

The detailed exploration of the HSP has afforded an array of molecular targets for chemotherapeutic interventions. The number of strategies to inhibit Gli signalling continues to expand both directly within the HSP's components and beyond through interacting signalling pathways and related protein modulators. In this aspect, a good source of lead compounds with differential mechanisms of activity have been produced and their clinical trials are ongoing.

Despite being the largest and most advanced class of analogues, Smo inhibitors face several limitations, which prompted the need to develop next generations of inhibitors targeting mechanisms downstream of Smo. Current approaches include direct inhibition of Gli, or activation of negative regulators of hedgehog signalling such as PKA and CSK1α, or the inhibition of relating epigenetic enzymes.

Hence the key aims of this research are to:

1. Develop new scaffolds of small molecules sharing core structural similarities with reported HSP inhibitors.

2. Investigate these scaffolds' biological activity using broad cytotoxicity testing (MTT assay), as well as specific investigations on their activity against Gli *gene* (qPCR assay) and protein expression (Gli−Luciferase assay) within the HSP.

3. Investigate on the possibility that these scaffolds inhibit the HSP downstream of Smo *via* the Gli−luciferase assay.

4. Make use of flow chemistry to generate libraries of potential scaffolds for subsequent biological screening.

1.4. Updated references

1. C. Nusslein-Volhard and E. Wieschaus, *Nature*, 1980, **287**, 795-801.

2. A. P. McMahon, P. W. Ingham and C. J. Tabin, *Current Topics in Developmental Biology*, 2003, **53**, 1-114, 111

3. P. W. Ingham and A. P. McMahon, *Genes and Development*, 2001, **15**, 3059-3087.

4. M. Zbinden, A. Duquet, A. Lorente-Trigos, S.-N. Ngwabyt, I. Borges and A. Ruiz i Altaba, *EMBO Journal*, 2010, **29**, 2659-2674.

5. A. Po, E. Ferretti, E. Miele, E. De Smaele, A. Paganelli, G. Canettieri, S. Coni, L. Di Marcotullio, M. Biffoni, L. Massimi, C. Di Rocco, I. Screpanti and A. Gulino, *EMBO Journal*, 2010, **29**, 2646-2658.

6. E. H. Epstein, *Nature Reviews Cancer*, 2008, **8**, 743-754.

7. C. Raffel, R. B. Jenkins, L. Frederick, D. Hebrink, B. Alderete, D. W. Fults and C. D. James, *Cancer Research*, 1997, **57**, 842-845.

8. T. Pietsch, A. Waha, A. Koch, J. Kraus, S. Albrecht, J. Tonn, N. Sorensen, F. Berthold, B. Henk, N. Schmandt, H. K. Wolf, A. von Deimling, B. Wainwright, G. Chenevix-Trench, O. D. Wiestler and C. Wicking, *Cancer Research*, 1997, **57**, 2085-2088.

9. D. G. Evans, P. A. Farndon, L. D. Burnell, H. R. Gattamaneni and J. M. Birch, *British Journal of Cancer*, 1991, **64**, 959-961.

10. S. P. Thayer, M. Pasca di Magliano, P. W. Heiser, C. M. Nielsen, D. J. Roberts, G. Y. Lauwers, Y. P. Qi, S. Gysin, C. Fernandez-del Castillo, V. Yajnik, B. Antoniu, M. McMahon, A. L. Warshaw and M. Hebrok, *Nature*, 2003, **425**, 851-856.

11. S. Karhadkar Sunil, G. S. Bova, N. Abdallah, S. Dhara, D. Gardner, A. Maitra, T. J. Isaacs, M. D. Berman and A. P. Beachy, *Nature*, 2004, **431**, 707-712.

12. Z. Yuan, J. A. Goetz, S. Singh, S. K. Ogden, W. J. Petty, C. C. Black, V. A. Memoli, E. Dmitrovsky and D. J. Robbins, *Oncogene*, 2007, **26**, 1046-1055.

13. D. N. Watkins, M. D. Berman, G. S. Burkholder, B. Wang, A. P. Beachy and B. S. Baylin, *Nature*, 2003, **422**, 313-317.

14. D. Qualtrough, A. Buda, W. Gaffield, C. Williams Ann and C. Paraskeva, *International Journal of Cancer,* 2004, **110**, 831-837.

15. M. D. Berman, S. S. Karhadkar, A. Maitra, R. Montes De Oca, R. M. Gerstenblith, K. Briggs, R. A. Parker, Y. Shimada, R. Eshleman James, D. N. Watkins and A. P. Beachy, *Nature*, 2003, **425**, 846-851.

16. M. Kasper, V. Jaks, M. Fiaschi and R. Toftgaard, *Carcinogenesis*, 2009, **30**, 903-911.

17. S. Mukherjee, N. Frolova, A. Sadlonova, Z. Novak, A. Steg, G. P. Page, D. R. Welch, S. M. Lobo-Ruppert, J. M. Ruppert, M. R. Johnson and A. R. Frost, *Cancer Biology & Therapy*, 2006, **5**, 674-683.

18. X. Chen, A. Horiuchi, N. Kikuchi, R. Osada, J. Yoshida, T. Shiozawa and I. Konishi, *Cancer Science*, 2007, **98**, 68-76.

19. T. N. Trinh, E. A. McLaughlin, C. P. Gordon and A. McCluskey, *MedChemComm*, 2014, **5**, 117-133.

20. M. Bingham, R. Armer, A. Morrison, A. McCarroll, A. Belfield, I. Bhamra, A. Tuffnell, J. Beadle, and M. Shah. *Preparation benzimidazole derivatives and their use as Hedgehog Signalling Pathway inhibitors for treating cancer and other* diseases. *Application: GB Pat.,* 2013-18461, 2519344, 2015.

21. R. Armer, M. Bingham, I. Bhamra, J. Beadle, and A. McCarroll. *Preparation of piperidinyl pyridazine derivatives as Hedgehog Signalling Pathway inhibitors useful in cancer therapy. Application: GB Pat.,* 2014-12660, 2528298, 2016.

22. A. M. DeBerardinis, D. S. Raccuia, E. N. Thompson, C. A. Maschinot and M. Kyle Hadden, *European Journal of Medicinal Chemistry*, 2015, **93**, 156-171.

23. U. Banerjee, A. M. DeBerardinis and M. K. Hadden, *Bioorganic & Medicinal Chemistry*, 2015, **23**, 548-555.

24. A. M. DeBerardinis, D. J. Madden, U. Banerjee, V. Sail, D. S. Raccuia, D. De Carlo, S. M. Lemieux, A. Meares and M. K. Hadden, *Journal of Medicinal Chemistry*, 2014, **57**, 3724-3736.

25. P. Infante, M. Mori, R. Alfonsi, F. Ghirga, F. Aiello, S. Toscano, C. Ingallina, M. Siler, D. Cucchi, A. Po, E. Miele, D. D'Amico, G. Canettieri, E. De Smaele, E. Ferretti, I. Screpanti, G. U. Barretta, M. Botta, B. Botta, A. Gulino and L. Di Marcotullio, *EMBO Journal*, 2015, **34**, 200-217.

26. M. A. Arai, K. Uchida, S. K. Sadhu, F. Ahmed, T. Koyano, T. Kowithayakorn and M. Ishibashi, *Bioorganic & Medicinal Chemistry*, 2015, **23**, 4150-4154.

27. T. Yoneyama, M. A. Arai, S. K. Sadhu, F. Ahmed and M. Ishibashi, *Bioorganic & Medicinal Chemistry Letters*, 2015, **25**, 3541-3544.

28. M. A. Arai, R. Akamine, S. K. Sadhu, F. Ahmed and M. Ishibashi, *Journal of Natural Medicines*, 2015, **69**, 538-542.

29. F. Bassilana, A. Carlson, J. A. Da Silva, B. Grosshans, S. Vidal, V. Beck, B. Wilmeringwetter, L. A. Llamas, T. B. Showalter, P. Rigollier, A. Bourret, A. Ramamurthy, X. Wu, F. Harbinski, S. Plonsky, L. Lee, H. Ruffner, P. Grandi, M. Schirle, J. Jenkins, A. W. Sailer, T. Bouwmeester, J. A. Porter, V. Myer, P. M. Finan, J. A. Tallarico, J. F. Kelleher, III, K. Seuwen, R. K. Jain and S. J. Luchansky, *Nature Chemical Biology*, 2014, **10**, 343-349.

30. M. Frank-Kamenetsky, X. M. Zhang, S. Bottega, O. Guicherit, H. Wichterle, H. Dudek, D. Bumcrot, F. Y. Wang, S. Jones, J. Shulok, L. L. Rubin and J. A. Porter, *Journal of Biology*, 2002, **1**, doi 10.1186/1475-4924-1-10.

31. J. Taipale, M. K. Cooper, T. Maiti and P. A. Beachy, *Nature*, 2002, **418**, 892-896.

32. C. H. Williams, J. E. Hempel, J. Hao, A. Y. Frist, M. M. Williams, J. T. Fleming, G. A. Sulikowski, M. K. Cooper, C. Chiang and C. C. Hong, *Cell Reports*, 2015, **11**, 43-50.

33. F. Wolff, A. Loipetzberger, W. Gruber, F. Aberger, A. M. Frischauf and H. Esterbauer, *Oncogene*, 2013, **32**, 5574-5581.

34. B. Li, C. A. Flaveny, C. Giambelli, D. L. Fei, L. Han, B. I. Hang, F. Bai, X.-H. Pei, V. Nose, O. Burlingame, A. J. Capobianco, D. Orton, E. Lee and D. J. Robbins, *PLoS One*, 2014, **9**, e101969/101961-e101969/101969, 101969 pp.

35. B. Li, D. L. Fei, C. A. Flaveny, N. Dahmane, V. Baubet, Z. Wang, F. Bai, X.-H. Pei, J. Rodriguez-Blanco, B. Hang, D. Orton, L. Han, B. Wang, A. J. Capobianco, E. Lee and D. J. Robbins, *Cancer Research*, 2014, **74**, 4811-4821.

36. B. Drobits, M. Holcmann, N. Amberg, M. Swiecki, R. Grundtner, M. Hammer, M. Colonna and M. Sibilia, *Journal of Clinical Investigation*, 2012, **122**, 575-585.

37. F. Lacarrubba, M. C. Potenza, S. Gurgone and G. Micali, *Journal of Dermatological Treatment*, 2011, **22**, 353-358.

38. M. P. Schoen, M. Schoen and K.-N. Klotz, *Journal of Investigative Dermatology*, 2006, **126**, 1338-1347.

39. Y. Tang, S. Gholamin, S. Schubert, M. I. Willardson, A. Lee, P. Bandopadhayay, G. Bergthold, S. Masoud, B. Nguyen, N. Vue, B. Balansay, F. Yu, S. Oh, P. Woo, S. Chen, A. Ponnuswami, M. Monje, S. X. Atwood, R. J. Whitson, S. Mitra, S. H. Cheshier, J. Qi, R. Beroukhim, J. Y. Tang, R. Wechsler-Reya, A. E. Oro, B. A. Link, J. E. Bradner and Y.-J. Cho, *Nature Medicine*, 2014, **20**, 732-740.

40. J. Long, B. Li, J. Rodriguez-Blanco, C. Pastori, C.-H. Volmar, C. Wahlestedt, A. Capobianco, F. Bai, X.-H. Pei, N. G. Ayad and D. J. Robbins, *Journal of Biological Chemistry*, 2014, **289**, 35494-35502.

41. E. De Smaele, L. Di Marcotullio, M. Moretti, M. Pelloni, M. A. Occhione, P. Infante, D. Cucchi, A. Greco, L. Pietrosanti, J. Todorovic, S. Coni, G. Canettieri, E. Ferretti, R. Bei, M. Maroder, I. Screpanti and A. Gulino, *Neoplasia*, 2011, **13**, 374-385.

42. G. Canettieri, L. Di Marcotullio, A. Greco, S. Coni, L. Antonucci, P. Infante, L. Pietrosanti, E. De Smaele, E. Ferretti, E. Miele, M. Pelloni, G. De Simone, E. M. Pedone, P. Gallinari, A. Giorgi, C. Steinkuhler, L. Vitagliano, C. Pedone, M. E. Schinin, I. Screpanti and A. Gulino, *Nature Cell Biology*, 2010, **12**, 132-142.

43. P. K. Dhanyamraju, P. S. Holz, F. Finkernagel, V. Fendrich and M. Lauth, *Molecular Cancer Therapeutics*, 2015, **14**, 727-739.

44. S. Coni, L. Antonucci, D. D'Amico, L. Di Magno, P. Infante, E. De Smaele, G. Giannini, L. Di Marcotullio, I. Screpanti, A. Gulino and G. Canettieri, *PLoS One*, 2013, **8**, e65718.

45. A. Gulino, L. Di Marcotullio, G. Canettieri, E. De Smaele and I. Screpanti, *Vitamin and Hormones*, 2012, **88**, 211-227.

46. G. Canettieri, L. Di Marcotullio, A. Greco, S. Coni, L. Antonucci, P. Infante, L. Pietrosanti, E. De Smaele, E. Ferretti, E. Miele, M. Pelloni, G. De Simone, E. M. Pedone, P. Gallinari, A. Giorgi, C. Steinkuehler, L. Vitagliano, C. Pedone, M. E. Schinin, I. Screpanti and A. Gulino, *Nature Cell Biology*, 2010, **12**, 132-142.

47. P. Infante, R. Alfonsi, B. Botta, M. Mori and L. Di Marcotullio, *Trends in Pharmacological Sciences*, 2015, **36**, 547-558.

II. CHAPTER TWO

Flow synthesis towards current HSP inhibitors

2.1. Introduction

In our previous review of the current HSP inhibitors, the Smo inhibitor NVP-LDE225 (Sonidegib) was among the most potent exhibiting the low nanomolar activity [1]. After passing all clinical requirements, NVP-LDE225 has recently been approved for the treatment of advanced basal cell carcinoma under the name Odomzo® [2] (Figure 1, compound **1**). Hence, we proposed that NVP-LDE225 would suit as an ideal control compound for our hedgehog project's development. In addition, we were interested in the furan-based biaryl motifs (Figure 1, structure **2**) that are available in a number of compounds expressing inhibitory activity against the HSP [3, 4].

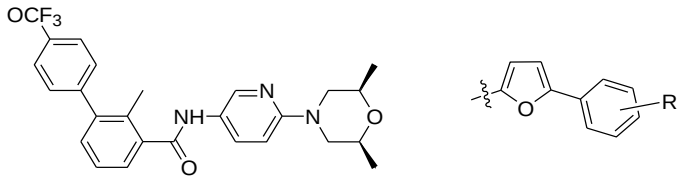

1 **2**

Figure 1. Structures of NVP-LDE225 (**1**, Odomzo®) and the furanyl biaryl motif (**2**).

Subsequently, we initiated our hedgehog research by establishing the synthesis protocol to afford NVP-LDE225, and the furan-based biaryl motifs. The synthesis of both requires a C − C coupling step, which typically involves the use of Pd-based catalysts in Suzuki-coupling conditions. While the traditional batch synthesis affords from good to excellent yields, a common issue relating to the leaching of Pd impurities into the final products poses as a major concern, particularly in the pharmaceutical industry [5-9]. Therefore, we aimed at using flow techniques to address this question.

The huge advantages of flow *vs* batch synthesis have been widely reported. These include controlled reaction parameters such as temperature, pressure, and flow rate, as well as creating safer environment for operators in dealing with toxic or hazardous reagents [10, 11]. In addition, one added value of the flow techniques is the potential to minimize the level of catalyst impurities in the final products thanks to the use of immobilised solid supported catalysts. Subsequently, we developed a flow chemistry methodology using a range of solid supported precursors to $L_2Pd(0)$ catalysts, known as FibreCats® [5-9] on our flow system ThalesNano X-Cube™ to successfully synthesize NVP-LDE225 and the furan-based biaryl derivatives with negligible level of Pd leaching. The details of our flow approach are included in the following paper, with the supporting information provided in the Appendix to Chapter 2 (please see Chapter 8, page 144).

Organic & Biomolecular Chemistry

PAPER

An efficient continuous flow approach to furnish furan-based biaryls†

Trieu N. Trinh,[a] Lacey Hizartzidis,[a] Andrew J. S. Lin,[a] David G. Harman,[b,c] Adam McCluskey*[a] and Christopher P. Gordon*‡[a]

Cite this: *Org. Biomol. Chem.*, 2014, **12**, 9562

Received 1st August 2014,
Accepted 10th October 2014

DOI: 10.1039/c4ob01641f

www.rsc.org/obc

Suzuki cross-couplings of 5-formyl-2-furanylboronic acid with activated or neutral aryl bromides were performed under continuous flow conditions in the presence of $(Bu)_4N^+F^-$ and the immobilised *t*-butyl based palladium catalyst CatCart™ FC1032™. Deactivated aryl bromides and activated aryl chlorides were cross-coupled with 5-formyl-2-furanylboronic in the presence of $(Bu)_4N^+OAc^-$ using the bis-triphenylphosphine CatCart™ $PdCl_2(PPh_3)_2$-DVB. Initial evidence indicates the latter method may serve as a universal approach to conduct Suzuki cross-couplings with the protocol successfully employed in the synthesis of the current gold standard Hedgehog pathway inhibitor LDE225.

Introduction

The furan-based biaryl motif is an intriguing molecular framework which serves as a pivotal core for a range of bioactive molecules. The furan biaryl motif is an integral feature of a number of kinase inhibitors including pan-Pim (**1**)[1] and class I phosphoinositide 3-kinase[2] inhibitors (**2**), a family of Bcl-xL inhibitors (**3**),[3] HIV-1 fusion inhibitors (**4**),[4] in addition to a class of antibacterial agents (**5**)[5] (Fig. 1). However, of particular interest to our research, the furan-based biaryl motif forms the core of a number of small molecules possessing inhibitory activity within the Hedgehog signalling pathway such as **6**.[6–8]

It is unknown if the diverse bioactivities of furan-biaryl based molecules are related to unique molecular recognitions or is simply a reflection of the scaffold being overrepresented in high-throughput-screening libraries. Nevertheless, a noteworthy feature of the furanyl–biaryl scaffold is that in contrast to the majority of biaryl molecular frameworks, modelling[9] and crystallographic data[10] demonstrate that this system preferentially adopts a planar conformation (Fig. 2).

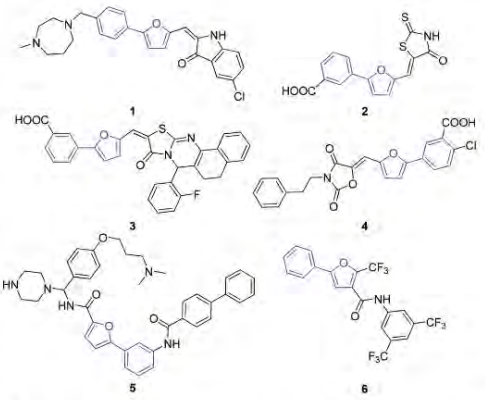

Fig. 1 Illustrative examples of bioactive compounds constructed around the furanyl–biaryl core. Structure of the pan-Pim (**1**)[1] and class I phosphoinositide 3-kinase (**2**)[2] inhibitors, along with the Bcl-xL inhibitor (**3**),[3] the HIV-1 fusion inhibitors (**4**),[4] the gram-negative antibacterial agent (**5**), and the Hedgehog signalling pathway inhibitor (**6**).[6,7]

Given the abundance of furanyl–biaryl analogues in the literature it is unsurprising that synthetic methodologies to access the scaffold have been extensively reported. Typical approaches involve the use of a furanylboronic acid or furanyl-bromide in Suzuki cross-coupling conditions with a range of Pd-based catalysts including $Pd(OAc)_2$,[2,11–17] $PdCl_2(PPh_3)_2$,[18–20] $Pd(PPh_3)_4$,[18–26] $Pd_2(dba)_3$,[27] and $Pd(OH)_2$.[28]

Whilst these methodologies typically afford the furanyl–biaryl scaffold in good to excellent yields a common problem faced, particularly by the pharmaceutical industry, in using

[a]*Chemistry, Centre for Chemical Biology, The University of Newcastle, University Drive, Callaghan, NSW 2308, Australia. E-mail: Adam.McCluskey@newcastle.edu.au; Fax: +61 (0)249 215472; Tel: +61 (0)249 216486*

[b]*Office of the Deputy Vice-Chancellor (Research and Development), University of Western Sydney, Penrith, NSW 2751, Australia*

[c]*Molecular Medicine Research Group, School of Medicine, Building 30, University of Western Sydney, Goldsmith Avenue, Campbelltown, NSW 2560, Australia*

†Electronic supplementary information (ESI) available: GS MS chromatographic traces, ^1H and ^{13}C NMR spectra. See DOI: 10.1039/c4ob01641f

‡Present address: Nanoscale Organisation and Dynamics Group, School of Science and Health, University of Western Sydney, Locked Bag 1797, Penrith South DC, Australia. E-mail: c.gordon2@uws.edu.au; Fax: +61 (02) 4620 3025; Tel: +61 (02) 4620 3201.

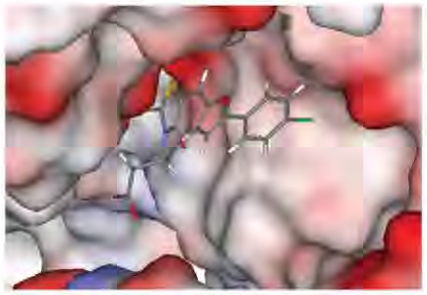

Fig. 2 Co-crystallised structure of 3-(5-[5-(4-chloro-phenyl)-furan-2-ylmethylene]-4-oxo-2-thioxo-thiazolidin-3-yl)-propionic acid with the *Bacillus anthracis* lethal factor metalloproteinase. This structure indicates that in contrast to the majority of biaryl systems the furanyl–biaryl motif adopts a planar conformation (*PDB accession code 1ZXV.pdb*).[10]

homogeneous catalysts is the removal of residual Pd from catalyst leaching.[29–33] This has in part been negated by the use of immobilised solid supported catalysts that can be simply partitioned from reaction mixtures. To this end, a suite of solid supported precursors to $L_2Pd(0)$ catalysts, known as FibreCats® are now commercially available.[29–33] A number of these FibreCats® systems are available in pre-packed cartridges which are compatible with a number of flow reactors including the ThalesNano X-Cube™. Further various flow systems utilising a range of immobilised catalysts have previously been successfully utilised to conduct a number of cross-coupling reactions.[34–37] Herein we report the development of a FibreCats® compatible flow chemistry methodology that provides a robust and expedient means of accessing furanyl–biaryl based analogues as building blocks for drug development programs.

Results and discussion

Our primary interest in the furan-based biaryl motif relates to our current interest in developing a series of Hedgehog signalling pathway inhibitors. To this end our primary aim was to develop a series of furfural-based analogues, *e.g.* 7 (Scheme 1), as the aldehyde moiety readily permits further synthetic manipulations. To this end, our investigations commenced with flowing a methanolic solution of 5-formyl-2-furanylboronic acid (**8**), 3-bromobenzyl alcohol (**9**), and three equivalents of $(Bu)_4N^+F^-$ through an X-cube™ charged with an FC1001 FibreCat® at 0.5 mL min^{-1} at a temperature of 80 °C (Scheme 1). This equated to a 2.2 min catalyst residence time.

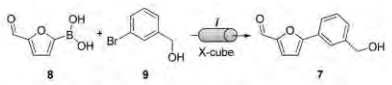

8 9 7

Scheme 1 *Reagents and conditions*: (*i*) 5-formyl-2-furanylboronic acid (**8**) (1 mmol), 3-bromobenzyl alcohol (**9**) (1 mmol), $(Bu)_4N^+F^-$ (3 mmol), MeOH (30 mL), FibreCat® 1001, X-Cube™, 0.5 mL min^{-1}, and 80 °C.

The effect of recycling through the catalyst was evaluated by HPLC-MS analysis.

The initial reaction conditions gave a 1 : 1.2 ratio of **7** to **9** obtained after a single cycle (Table 1), increasing to 2 : 1 after 4 cycles using FibreCat® 1001. However, given that the Suzuki reaction coupling efficiencies can be significantly affected by the ligand utilised, we investigated a number of alternative FibreCat® columns (Table 1, entries 2–4). Each FibreCat® catalyst furnished the desired Suzuki reaction with relatively high efficiencies with Pd-Tetrakis providing the most efficient coupling with a near 4 : 1 ratio of **7** to **9** afforded within two catalyst cycles (Table 1, entry 4).

Further improvements in the Pd-Tetrakis coupling efficiency were noted on increasing reaction temperature to 120 °C with a 1 : 0.08 ratio of **7** : **9** observed at a 0.5 mL min^{-1} flow rate (a 1.3 min catalyst residence time) (Fig. 3b). However, at $T > 100$ °C increased aryl-bromide homocoupling with the excessive formation of **10** observed at 140 °C (Fig. 3b). Increased reaction pressures at 80 °C afforded similar results, with pressures above 60 bar enhancing the formation of both **7** and **10** (Fig. 3c). At elevated pressure the aryl-bromide homocoupled product **10** was the major product.

Given the undesired production of **10**, we re-examined FC1032™ (Table 1, entry 3). While not as effective as Pd-Tetrakis, it did produce a higher level of coupling selectivity with only trace levels of homocoupled product after 4 catalyst cycles. Consequently FC1032™ was subjected to a temperature screen as with Pd-Tetrakis (Scheme 1 & Table 2). Optimisation of the reaction temperature and flow rate revealed near quantitative conversion to **7** at 120 °C and 0.5 mL min^{-1}. After two catalyst cycles (2.6 min retention time) only trace levels of starting material (**9**) and homocoupled (**10**) were evident (Table 2). Workup furnished the desired product **7** in a 93% isolated yield, which compares favourably with the reported batch yield of 88%.[38] Further, consistent with the previous studies which examined palladium leaching,[29,30] ICP MS analysis demonstrated negligible levels of palladium leaching with a maximum total recoverable palladium content of 5.2 ppm observed for a crude sample of compound **7**. As context the European Agency for the Evaluation of Medicines states that for oral administration the permitted daily exposure of class A1 metals such as palladium should not exceed 10 mg kg^{-1} and thus the Pd content of **7** is within this guideline.[39,40]

While the optimised protocol efficiently furnished **7**, the practicality of this continuous flow approach could only be judged by amenability to aryl bromide variations. Thus, the coupling of a small library of aryl bromides, sulfonamide based aryl bromides, and an amide based aryl bromide was investigated. The data presented in Table 3 illustrates the utility of FC1032™, $(Bu)_4N^+F^-$, at a flow rate of 0.5 mL min^{-1}, over two catalyst cycles and temperature of 120 °C in furnishing a small library in excellent isolated yields (82–92%).

Given our success with FC1032™ we next turned our attention to the Suzuki cross-coupling of deactivated aryl bromides such as 4-bromophenol (**13**, Scheme 2). The synthesis

Table 1 Ratio of 7 and 9 peak areas obtained after subsequent cycles through various FibreCat® catalysts. Reagents and conditions are as per Scheme 1

			Number of catalyst cycles			
			Ratio of 7 : 9[a]			
Entry	Pd-ligand	FibreCat®	1	2	3	4
1	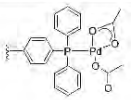	FC1001™	1 : 1.2	1 : 0.7	1 : 0.5	1 : 0.4
2	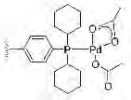	FC1007™	1 : 1.3	1 : 0.7	1 : 0.4	1 : 0.2
3	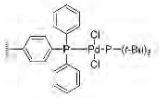	FC1032™	1 : 0.7	1 : 0.4	1 : 0.3	1 : 0.2
4	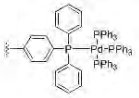	Pd-Tetrakis	1 : 0.4	1 : 0.3	1 : 0.3	1 : 0.2

[a] Ratio of peak areas determined by HPLC analysis at 220 nm.

of the desired analogue **14** had been previously reported *via* coupling of 4-iodophenol and **8** using Pd-Tetrakis to afford **14** in an 87% yield,[19] however, equivalent Pd-Tetrakis coupling with 4-bromophenol (**13**) gave **14** in only 10%.[2] Using our flow protocol resulted in an improvement on the batch synthesis with an approximate 30% conversion (and 23% isolated yield) of **14** after three catalyst cycles (Table 3, entry 1). This however, was not the near quantitative yields obtained with the more activated aryl bromides (**9a–f**). Given that our prior studies with Pd-Tetrakis highlighted increasing homocoupled product with increased temperature and pressures, our initial reaction optimisation examined the effect of varying the tetrabutylammonium salt which has previously been observed to impart subtle variations on cross-coupling yields.[41]

Varying the halogen counterion from –F to –Cl, –Br and –I resulted in reduced coupling efficiencies (Table 4, entries 2–5), as with the BF_4^- (Table 4, entry 5), and HSO_4^- salts (Table 4, entry 6). However, the use of $(Bu)_4N\ OAc^-$ (Table 4, entry 7) resulted in improved coupling efficiency with a near to 80% conversion after a single catalyst cycle. Presumably the excess acetate ions activate the boronic acid (as is the case with K_2CO_3), and halogen abstraction from the first organopalladium intermediate in the Suzuki cycle.

Binary mixtures of $(Bu)_4N^+F^-$ and Cs_2CO_3 improved the efficiency of the cross coupling from 0.46 : 1 with $(Bu)_4N^+F^-$ alone (Table 4, entry 1) to 0.2 : 1 (Table 4, entry 8). The binary combination of $(Bu)_4N\ OAc^-$ and Cs_2CO_3 gave a coupling efficiency ratio of 0.21 : 1, essentially identical to that of $(Bu)_4N^+OAc^-$ alone (Table 4, entries 9 and 7 respectively), supporting the hypothesized additional role of the ^-OAc. Performing the cross-coupling reaction with only Cs_2CO_3 the yield of **14** was reduced to ~20% whilst the aryl bromide homocoupled product was obtained in a 52% yield confirming the crucial nature of the tetrabutylammonium salt.

Using $(Bu)_4N^+OAc^-$ in conjunction with FC1032™ gave **14** in a 72% yield from **13**. However other deactivated aryl bromides such as the dimethylamino analogues **15a** and **15b**, the methoxy analogue **15c**, and the indole **15d**, aryl chlorides **15e** and **15f** gave unacceptably low levels of the desired cross coupled products (Table 5).

We consequently investigated the more activated CatCart™ $PdCl_2(PPh_3)_2$-DVB catalysts which has been shown to be highly effective in Sonogashira couplings.[42] The flow coupling steps were optimised as before with the CatCart™ $PdCl_2(PPh_3)_2$-DVB catalyst and we noted that clean coupling, with near quantitative conversions was accomplished at 120 °C, after three catalyst cycles at 0.3 mL min^{-1} (Table 5).

We subsequently used this protocol to effect the cross-coupling of **16** and **17** and gained expedient access to the potent smoothened inhibitor LDE225 (**18**) which is a crucial component of our Hedgehog pathway inhibitor development program (Scheme 3).

Thus whilst increasing catalyst retention time and catalysts cycles significantly enhanced coupling efficiencies of deacti-

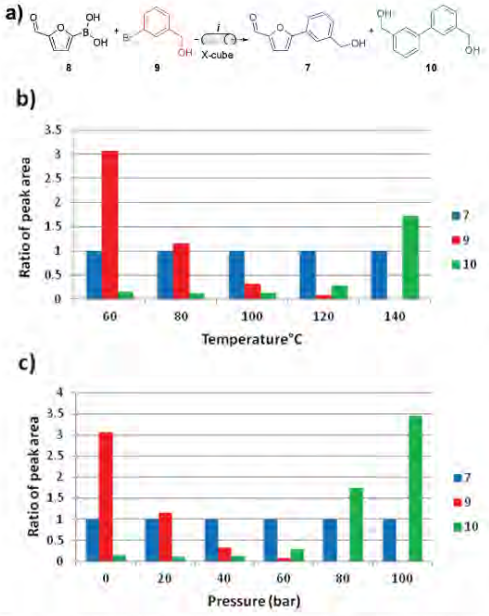

Fig. 3 (a) *Reagents and conditions*: (*i*) 5-formyl-2-furanylboronic acid (**8**) (1 mmol), 3-bromobenzyl alcohol (**9**) (1 mmol), $(Bu)_4N^+F^-$ (3 mmol), and MeOH (30 mL) at 0.5 mL min^{-1}, Pd-tetrakis; (b) Comparison of the relative quantities of aryl bromide (**9**), desired product (**7**), and aryl bromide homocoupled (**10**) product returned at temperatures of 60 to 140 °C with 0 bar pressure; (c) Comparison of the relative quantities of aryl bromide (**9**), desired product (**7**), and aryl bromide homocoupled product returned at pressures of 0 to 100 bar at 80 °C. HPLC analysis conducted at 220 nm. Maximum total recoverable Pd content by ICP MS analysis 5.2 ppm.

Table 2 Temperature screen using FC1032™ at 0 bar pressure. Reagents and conditions are as per Fig. 3

	Ratio of peak area after two cycles[a]		
Temperature (°C)	**7**	**9**	**10**
60	1	7.8	0
80	1	1.1	0
100	1	0.37	0
120	1	0.05	0

[a] Ratio of peak areas determined HPLC analysis at 220 nm. Maximum total recoverable Pd content by ICP MS analysis 5.2 ppm.

vated aryl-bromides and aryl-chlorides, we were cognisant that these conditions may promote increased levels of palladium leaching. However as outlined in Table 6, negligible levels of palladium leaching were observed with a maximum total recoverable Pd content by ICP MS analysis of 5.2 ppm for **15d**, 5.2 ppm for **15e**, whilst the remainder of samples analysed contenting less than 1 ppm palladium content.

Table 3 Suzuki cross-couplings using a series of aryl bromides (**9a–f**) with FC1032™[a]

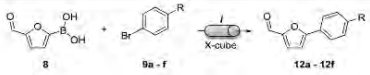

Compound	R	Conversion (%)	Isolated yield (%)
12a		96	87
12b		95	82
12c		90	91
12d		95	85
12e		91	87
12f	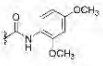	98	92

[a] *Reagents and conditions*: 5-formyl-2-furanylboronic acid (**8**) (1 mmol), aryl bromides (**9a–9f**) (1 mmol), $(Bu)_4N^+F^-.3H_2O$ (3 mmol), MeOH, FC1032™, X-Cube™, and 0.5 mL min^{-1} over two catalyst cycles.

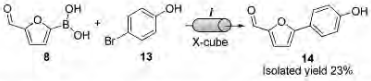

Scheme 2 *Reagents and conditions*: (*i*) 5-formyl-2-furanylboronic acid (**8**) (1 mmol), 4-bromophenol benzyl alcohol (**13**) (1 mmol), $(Bu)_4N^+F^-.3H_2O$ (3 mmol), MeOH (30 mL), FC1032™, X-Cube™, 0.5 mL min^{-1}, and 120 °C.

Table 4 Tetrabutylammonium salt screen using FC1032™

		Ratio of peak area[a]	
Entry	Tetrabutylammonium salt	**13**	**14**
1	$(Bu)_4N^+F^-$	0.46	1
2	$(Bu)_4N^+Cl^-$	0.65	1
3	$(Bu)_4N^+Br^-$	21.82	1
4	$(Bu)_4N^+I^-$	30.11	1
5	$(Bu)_4N^+BF_4^-$	2.47	1
6	$(Bu)_4N^+HSO_4^-$	1.51	1
7	$(Bu)_4N^+OAc^-$	0.22	1
8	$(Bu)_4N^+F^- + Cs_2CO_3$	0.20	1
9	$(Bu)_4N^+OAc^- + Cs_2CO_3$	0.24	1

[a] Ratio of peak areas determined by HPLC analysis at 220 nm.

Conclusion

A combination of un-distilled methanol, $(Bu)_4^+OAc^-$, 5-formyl-2-furanylboronic acid, an activated or neutral aryl bromide,

Table 5 Suzuki couplings with deactivated aryl bromides and aryl chlorides

	Aryl halide	Product[a]	Percent conversion[b]	
			FC1032™	$PdCl_2(PPh_3)_2$-DVB
15a		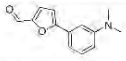	28	96
15b		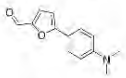	12	87
15c	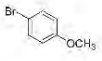	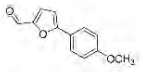	16	92
15d		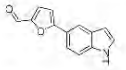	16	92
15e	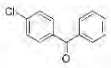	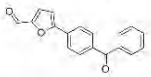	<5	83
15f		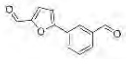	<5	87

[a] *Reagents and conditions*: (i) 5-formyl-2-furanylboronic acid (1 mmol), aryl halide (1 mmol), $(Bu)_4N^+OAc^-$ (3 mmol), MeOH (30 mL), X-Cube™, 0.3 mL min^{-1}, and 120 °C, three catalyst cycles. [b] Percentage conversion determined by HPLC analysis at 220 nm.

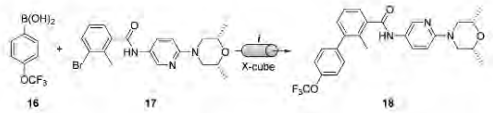

Scheme 3 *Reagents and conditions*: (*i*) 4-(trifluoromethoxy)phenylboronic acid (**16**), 3-bromo-*N*-(6-((2*R*,6*S*)-2,6-dimethylmorpholino)pyridin-3-yl)-2-methylbenzamide (**17**), $(Bu)_4N^+OAc^-$, MeOH (30 mL), $PdCl_2(PPh_3)_2$-DVB, 0.3 mL min^{-1}, and 120 °C.

along with the X-cube™ continuous flow reactor charged with the *t*-butyl based palladium catalyst FC1032™ efficiently afforded Suzuki cross-coupled products in excellent yield (>80%) with negligible homocoupling observed. In relation to deactivated aryl bromides or aryl chlorides the use of a more active Pd-based catalyst such as $PdCl_2(PPh_3)_2$-DVB, provided efficient coupling to the desired products. This optimised continuous flow Suzuki cross-coupling methodology appears amenable with a range of boronic acids. However, we note that when CatCart™ $PdCl_2(PPh_3)_2$-DVB was employed to perform the initial cross-coupling investigation (*i.e.* Scheme 1), as was the case with Pd-Tetrakis, a significant (~30%) amount of aryl bromide homocoupling product was observed. Consequently we propose that FC1032™ serves as a more effective catalyst for the cross-coupling of activated or neutral aryl bromides. We have used this protocol to provide expedient access to the potent smoothened inhibitor LDE225 (**18**). Significantly, negligible palladium leaching was observed with the immobilised catalysts[29,31] and thus this continuous flow Suzuki cross-coupling protocol is ideally suited to medicinal chemistry research programs. We are currently investigating the versatility of these

Table 6 Total recoverable trace palladium by ICP MS of selected samples

	Product[a]	$PdCl_2(PPh_3)_2$-DVB (yield %)	Palladium content[a]
15a	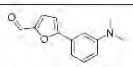	96	0.65 ppm
15c	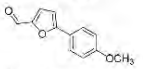	92	0.48 ppm
15e	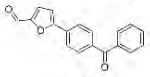	83	0.72 ppm
18	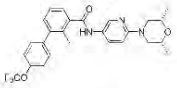	87	5.2 ppm

[a] ICP MS analysis was conducted by the Australian National Measurement Institute.

conditions with other palladium catalysed cross-coupling reactions and the outcomes of these investigations will be reported in due course.

Experimental section

All reagents were purchased from Sigma Aldrich and were used without purification, with the exception of furfural, which was distilled through glass prior to use. Solvents were bulk, and distilled through glass prior to use.

^{1}H and ^{13}C NMR spectra were recorded on a Bruker Advance™ AMX 400 MHz spectrometer at 400.13 and 100.62 MHz, respectively. Chemical shifts (δ) are reported in parts per million (ppm) measured to relative the internal standards. Coupling constants (J) are expressed in hertz (Hz). Mass spectra were recorded on a Shimadzu LCMS 2010 EV using a mobile phase of 1 : 1 acetonitrile–H_2O with 0.1% formic acid. Gas chromatography-mass spectrometry (GC-MS) was performed on a Shimadzu GC-MS QP2010 EI/NCI System equipped with a ZB-5MS capillary column of 5% phenylarylene stationary phase. High-resolution mass spectra (HRMS) were determined on a Micromass QToF2 spectrometer using polyethylene glycol or polypropylene glycol as lockmass. Monoisotopic molecular masses were calculated utilising ChemDraw Ultra 8.0.

Analytical HPLC traces were obtained using a Shimadzu system possessing a SIL-20A auto-sampler, dual LC-20AP pumps, CBM-20A bus module, CTO-20A column heater, and a SPD-20A UV/vis detector. This system was fitted with an Alltima™ C18 5u 150 mm × 4.6 mm column with solvent A: 0.06% TFA in water and solvent B: 0.06% TFA in CH_3CN–H_2O (90 : 10). In each case HPLC traces were acquired at a flow rate of 2.0 mL min^{-1}, gradient 10–100 (%B), curve = 6, over 15.0 min, with detection at 220 nm and 265 nm.

Where applicable, melting points were recorded on a Buchi Melting Point M-565. IR spectra were recorded on a PerkinElmer Spectrum Two™ FTIR Spectrometer. Thin layer chromatography (TLC) was performed on Merck 60 F254 pre-coated aluminium plates with a thickness of 0.2 mm. Column chromatography was performed under 'flash' conditions on Merck silica gel 60 (230–400 mesh).

ICP MS analysis was conducted by the Australian National Measurement Institute 105 Delhi Road, North Ryde NSW 2113 (http://www.measurement.gov.au).

Biphenyl-3,3′-diyldimethanol (10) and 5-(3-(hydroxymethyl) phenyl)furan-2-carbaldehyde (7)

A solution of (3-bromophenyl)methanol (0.28 mL, 2.3 mmol), 5-formyl-2-furanylboronic acid (0.32 g, 2.3 mmol) and TBAF (2.16 g, 6.86 mmol) was diluted with MeOH (30 mL) to afford a 0.05 M solution. This solution was flowed through an X-Cube™ fitted with a Fibrecat®1001 catalyst at flow rate of 0.5 mL min^{-1}, at a temperature of 80 °C, and 0 bar pressure for 2 h (*i.e.* total of two catalyst cycles). The eluent was concentrated *in vacuo*, diluted with DCM (30 mL), washed with 1 M HCl (2 × 30 mL), dried ($MgSO_4$), concentrated *in vacuo*, and the crude was subjected to flash silica gel chromatography (1 : 1 EtOAc–hexanes) to afford biphenyl-3,3′-diyldimethanol (**10**) as a colourless oil (0.01 g, 3%). LRMS (ESI+) m/z 215(M + 1). ^{1}H NMR (400 MHz, $CDCl_3$) δ 7.61 (s, 1H), 7.54 (d, J = 7.7 Hz, 1H), 7.44 (t, J = 7.6 Hz, 1H), 7.36 (d, J = 7.5 Hz, 1H), 4.76 (d, J = 7.7 Hz, 2H); ^{13}C NMR (101 MHz, $CDCl_3$) δ 141.4, 141.3, 129.0, 129.0, 126.5, 126.0, 125.8, 65.4; RP-HPLC Alltima™ C18 5u 150 mm × 4.6 mm, 10–100% B in 15 min, t_R 10.39 min. Continued elution (1 : 1 EtOAc–hexanes) afforded 5-(3-(hydroxymethyl)-phenyl)furan-2-carbaldehyde (7) as an orange oil (0.37 g, 82%). LRMS (ESI+) m/z 203 (M + 1); HRMS (ES+) for $C_{12}H_{11}O_3$; calculated 201.0630, found 202.0681; ^{1}H NMR (400 MHz, $CDCl_3$) δ 9.51 (s, 1H), 7.74 (s, 1H), 7.67–7.57 (m, 1H), 7.32 (m, 2H), 7.25 (d, J = 3.7 Hz, 1H), 6.76 (d, J = 3.7 Hz, 1H), 4.67 (s, 2H). ^{13}C NMR (101 MHz, $CDCl_3$) δ 177.34, 159.5, 151.8, 142.1, 129.0 (C × 2), 128.9, 128.2, 124.3, 123.6, 107.9, 77.5, 77.2, 76.9, 64.4. RP-HPLC Alltima™ C18 5u 150 mm × 4.6 mm, 10–100% B in 15 min, t_R 9.10 min.

5-(4-Acetylphenyl)-2-furancarboxaldehyde (12a)

General procedure 1. A solution of 4-bromoanisole (0.40 g, 2.1 mmol), 5-formyl-2-furanylboronic acid (0.30 g, 2.1 mmol) and TBAF (2.16 g, 6.86 mmol) was diluted with MeOH (30 mL) to afford a 0.05 M solution. This solution was flowed through an X-Cube™ fitted with a FC1032™ catalyst at flow rate of 0.5 mL min^{-1}, at a temperature of 120 °C, and 0 bar pressure for 2 h (*i.e.* total of two catalyst cycles). The eluent was concentrated *in vacuo*, diluted with DCM (30 mL), washed with 1 M HCl (2 × 30 mL), dried ($MgSO_4$), concentrated *in vacuo*, and the crude was subjected to flash silica gel chromatography (1 : 1 EtOAc–hexanes) to afford 5-(4-acetylphenyl)-2-furancarboxaldehyde (**12a**) as a yellow oil (0.36 g, 87%). LRMS (ESI+) m/z 215 (M + 1); HRMS (ES+) for $C_{13}H_{11}O_3$; calculated 215.0630, found 214.0637; ^{1}H NMR ($CDCl_3$, 400 MHz); δ 9.60 (s, 1H), 7.77 (d, J = 8.9 Hz, 2H), 7.30 (d, J = 3.7 Hz, 1H), 6.96 (d, J = 8.9 Hz, 2H), 6.72 (d, J = 3.7 Hz, 1H), 3.86 (s, 3H); ^{13}C NMR ($CDCl_3$, 101 MHz): δ 176.9, 160.91, 159.8, 151.6, 129.0, 127.0, 121.8, 114.1, 106.3, 55.4; RP-HPLC Alltima™ C18 5u 150 mm × 4.6 mm, 10–100% B in 15 min, t_R 14.26 min.

2-(4-(5-Formylfuran-2-yl)phenyl)acetonitrile (12b)

Compound (**12b**) was synthesised as described in general procedure 1 from 4-bromoacetonitrile (0.44 g, 2.2 mmol), 5-formyl-2-furanylboronic acid (0.31 g, 2.2 mmol) and TBAF (2.04 g, 6.7 mmol). The crude reaction mixture was subjected to flash silica chromatography (4 : 1 Hex–EtOAc) to afford **12b** as an orange solid (0.38 g, 82%). LRMS (ESI+) m/z 212 (M + 1); HRMS (ES+) for $C_{13}H_{10}NO_2$; calculated 212.0630, found 212.0637; ^{1}H NMR ($CDCl_3$, 400 MHz): δ 9.67 (s, 1H), 7.84 (d, J = 8.4 Hz, 2H), 7.43 (d, J = 8.5 Hz, 2H), 7.33 (d, J = 3.7 Hz, 1H), 6.87 (d, J = 3.7 Hz, 1H), 3.81 (s, 2H); ^{13}C NMR ($CDCl_3$, 101 MHz): δ 177.3, 158.37, 152.2, 131.3, 128.9, 128.6, 126.0, 108.2,23.6. RP-HPLC Alltima™ C18 5u 150 mm × 4.6 mm, 10–100% B in 15 min, t_R 14.27 min.

5-(4-Methylphenyl)-2-furancarboxaldehyde (12c)

Compound **12c** was prepared utilising general procedure 1,4-bromotoluene (0.28 mL, 2.3 mmol), 5-formyl-2-furanylboronic acid (0.32 g, 2.3 mmol), TBAF (2.16 g, 6.86 mmol), and MeOH (30 mL). The eluent was concentrated *in vacuo* and the crude material was diluted with DCM (30 mL) and washed with 1 M HCl (2 × 30 mL). The organic layer was dried ($MgSO_4$), and concentrated *in vacuo* to yield an oil which was further purified using flash chromatography (1 : 9 EtOAc–hexanes) to afford 5-(4-methylphenyl)-2-furancarboxaldehyde as an orange oil/solid (0.39 g, 91%) m.p. 50–56 °C. LRMS (ESI+) *m/z* 187 (M + 1); HRMS (ES+) for $C_{12}H_{11}O_2$; calculated 187.0681, found 186.0678; ^{1}H NMR ($CDCl_3$; 400 MHz): δ 9.63 (s, 1H), 7.72 (d, J = 8.2 Hz, 2H), 7.31 (d, J = 3.7 Hz, 1H), 7.25 (d, J = 8.9 Hz, 2H), 6.78 (d, J = 3.7 Hz, 1H), 2.39 (s, 3H); ^{13}C NMR ($CDCl_3$, 101 MHz): δ 177.1, 159.8, 151.8, 140.0, 129.7, 126.3, 125.3, 107.1, 21.5; RP-HPLC Alltima™ C18 5u 150 mm × 4.6 mm, 10–100% B in 15 min, t_R 17.41 min.

5-(Dimethylamino)-*N*-(4-(5-formylfuran-2-yl)phenyl)-naphthalene-1-sulfonamide (12d)

Compound **12d** was prepared utilising general procedure 1, and *N*-(4-bromophenyl)-5-(dimethylamino)naphthalene-1-sulfonamide (0.92 g, 2.3 mmol), 5-formyl-2-furanylboronic acid (0.32 g, 2.3 mmol), TBAF (2.16 g, 6.86 mmol), and MeOH (30 mL). The eluent was concentrated *in vacuo*, the crude material was diluted with DCM (30 mL) and washed with 1 M HCl (2 × 30 mL). The organic layer was dried ($MgSO_4$), and concentrated *in vacuo* to yield an oil which was further purified using flash chromatography (5 : 1 EtOAc–hexanes) to afford 5-(4-methylphenyl)-2-furancarboxaldehyde as an yellow oil/solid (0.82 g, 87%). LRMS (ESI+) *m/z* 421 (M + 1); HRMS (ES+) for $C_{23}H_{21}N_2O_3S$; calculated 421.1144, found 421.1144; ^{1}H NMR (400 MHz, $CDCl_3$) δ 9.55 (s, 1H), 8.51 (d, J = 8.4 Hz, 1H), 8.46–8.25 (m, 2H), 8.13 (s, 1H), 7.56–7.51 (m, 1H), 7.50 (d, J = 8.7 Hz, 2H), 7.47–7.42 (m, 1H), 7.23 (d, J = 3.7 Hz, 1H), 7.16 (d, J = 7.9 Hz, 1H), 7.09 (d, J = 8.7 Hz, 2H), 6.62 (d, J = 3.7 Hz, 1H), 2.85 (s, 6H). ^{13}C NMR ($CDCl_3$, 101 MHz): δ 177.2, 158.9, 151.7, 138.2, 134.1, 132.1, 131.0, 130.4, 129.7, 129.6, 128.7, 126.3, 125.0, 123.2, 122.7, 120.3, 115.5, 111.1, 107.3, 45.4; RP-HPLC Alltima™ C18 5u 150 mm × 4.6 mm, 10–100% B in 15 min, t_R 9.60 min.

***N*-(4-(5-Formylfuran-2-yl)phenyl)benzenesulfonamide (12e)**

Compound **12e** was prepared utilising general procedure 1, and *N*-(4-bromophenyl)benzenesulfonamide (0.77 g, 2.3 mmol), 5-formyl-2-furanylboronic acid (0.32 g, 2.3 mmol), TBAF (2.16 g, 6.86 mmol), and MeOH (30 mL). The eluent was concentrated *in vacuo*, the crude material was diluted with DCM (30 mL) and washed with 1 M HCl (2 × 30 mL). The organic layer was dried ($MgSO_4$), and concentrated *in vacuo* to yield an oil which was further purified using flash chromatography (4 : 1 EtOAc–hexanes) to afford *N*-(4-(5-formylfuran-2-yl)phenyl)benzenesulfonamide as an yellow oil/solid (0.65 g, 87%). LRMS (ESI+) *m/z* 328 (M + 1); HRMS (ES+) for $C_{17}H_{13}NO_4S$; calculated 328.0565, found 327.0556; ^{1}H NMR (400 MHz, $CDCl_3$) δ 9.61 (s, 1H), 7.85–7.78 (m, 2H), 7.69 (d, J = 8.7 Hz, 2H), 7.55 (t, J = 7.4 Hz, 1H), 7.46 (t, J = 7.7 Hz, 2H), 7.30 (d, J = 3.7 Hz, 1H), 7.26 (s, 1H), 7.18 (d, J = 8.7 Hz, 3H), 6.76 (d, J = 3.7 Hz, 1H); ^{13}C NMR (101 MHz, $CDCl_3$) δ 177.0, 158.6, 151.89, 138.8, 137.8, 129.2, 127.2, 126.6, 125.8, 121.1 (C × 2), 107.6. RP-HPLC Alltima™ C18 5u 150 mm × 4.6 mm, 10–100% B in 15 min, t_R 15.58 min.

***N*-(2,4-Dimethoxyphenyl)-4-(5-formylfuran-2-yl)benzamide (12f)**

Compound **12f** was synthesised utilising general procedure 1, 4-bromo-*N*-(2,4-dimethoxyphenyl)benzamide (0.73 g, 2.2 mmol), 5-formyl-2-furanylboronic acid (0.31 g, 2.2 mmol) and TBAF (2.14 g, 6.6 mmol) to afford *N*-(2,4-dimethoxyphenyl)-4-(5-formylfuran-2-yl)benzamide as a light brown solid (0.71. g, 92%). LRMS (ESI−) *m/z* 352 (M − 1); HRMS (ES−) for $C_{20}H_{18}NO_5$; calculated 352.1107, found 352.1113; ^{1}H NMR (400 MHz, DMSO-d6): δ 9.66 (s, 1H), 9.54 (s, NH), 8.09 (d, J = 8.3 Hz, 2H), 8.01 (d, J = 8.4 Hz, 2H), 7.70 (d, J = 3.8 Hz, 1H), 7.48 (d, J = 8.6 Hz, 1H), 7.45 (d, J = 3.7 Hz, 1H), 6.67 (d, J = 2.6 Hz, 1H), 6.55 (dd, J = 8.7, 2.6 Hz, 1H), 3.81 (s, 3H), 3.79 (s, 3H); ^{13}C NMR (400 MHz, DMSO-d6): δ 178.6, 164.8, 158.5, 157.6, 154.1, 152.6, 135.55, 131.6, 128.9, 127.1, 125.3, 120.0, 110.7, 104.7, 99.4, 56.2, 55.8; RP-HPLC Alltima™ C18 5u 150 mm × 4.6 mm, 10–100% B in 15 min, t_R 18.12 min.

5-(4-Hydroxyphenyl)-2-furancarboxaldehyde (14)

Compound **14** was synthesised utilising general procedure **1**,4-bromophenol (0.38 g, 2.3 mmol), 5-formyl-2-furanylboronic acid (0.32 g, 2.3 mmol) and TBAF (2.10 g, 6.9 mmol). The crude was subjected to silica gel chromatography (4 : 1 EtOAc–Hex) to afford 5-(4-hydroxyphenyl)-2-furancarboxaldehyde as an orange oil/solid (0.09 g, 30%). LRMS (ESI−) *m/z* 187 (M − 1); HRMS (ES−) for $C_{11}H_7O_3$; calculated 187.0473, found 187.0468; ^{1}H NMR ($CDCl_3$, 400 MHz): δ 9.60 (s, 1H), 7.73 (d, J = 8.8 Hz, 2H), 7.31 (d, J = 3.7 Hz, 1H), 6.92 (d, J = 8.8 Hz, 2H), 6.71 (d, J = 3.7 Hz, 1H); ^{13}C NMR ($CDCl_3$, 101 MHz): δ 176.9, 157.1, 128.0, 127.3, 122.0, 116.0, 115.6, 106.3. RP-HPLC Alltima™ C18 5u 150 mm × 4.6 mm, 10–100% B in 15 min, t_R 10.68 min.

5-(3-(Dimethylamino)phenyl)-2-furancarboxaldehyde (15a)

General procedure 2. A solution of 3-bromo-*N*,*N*-dimethylaniline (0.28 mL, 2.3 mmol), 5-formyl-2-furanylboronic acid (0.32 g, 2.3 mmol) and TBAA (2.08 g, 6.86 mmol) was diluted with MeOH (30 mL) to afford a 0.05 M solution. This solution was flowed through an X-Cube™ fitted with a CatCart® $PdCl_2(PPh_3)_2$-DVB catalyst at flow rate of 0.3 mL min^{-1}, at a temperature of 120 °C, and 0 bar pressure for 3 h (*i.e.* total of three catalyst cycles). The eluent was concentrated *in vacuo*, diluted with DCM (30 mL) and washed with 1 M HCl (2 × 30 mL), dried ($MgSO_4$), concentrated *in vacuo*, and the crude was subjected to flash silica gel chromatography (7 : 1 EtOAc–hexanes) to afford 5-(3-(dimethylamino)phenyl)-2-furancarboxaldehyde as a colourless oil (0.43 g, 87%). LRMS (ESI+)

m/z 216 (M + 1); HRMS (ES+) for $C_{13}H_{14}NO_2$; calculated 216.0946, found 216.0942; ^{1}H NMR (DMSO-d6, 400 MHz): δ 9.59 (s, 1H), 7.64 (d, J = 3.7 Hz, 1H), 7.30 (d, J = 7.9 Hz, 1H), 7.27 (d, J = 3.7 Hz, 1H), 7.16 (d, J = 7.6 Hz, 1H), 7.13 (d, J = 2.0 Hz, 1H), 6.81 (dd, J = 8.3, 2.4 Hz, 1H), 2.97 (s, 6H). ^{13}C NMR (DMSO-d6, 101 MHz): δ 178.1, 159.7, 151.9, 151.2, 130.2, 129.7, 114.3, 113.5, 109.0, 108.5, 40.5. RP-HPLC Alltima™ C18 5u 150 mm × 4.6 mm, 10–100% B in 15 min, t_R 9.60 min.

5-(4-(Dimethylamino)phenyl)-2-furancarboxaldehyde (15b)

Compound **15b** was synthesised utilising general procedure **2** and 4-bromo-*N*,*N*-dimethylaniline (0.46 g, 2.3 mmol), 5-formyl-2-furanylboronic acid (0.32 g, 2.3 mmol) and TBAA (2.08 g, 6.90 mmol). The crude was subject to flash silica gel chromatography (7 : 1 EtOAc–Hex) to afford 5-(4-(dimethylamino) phenyl)-2-furancarboxaldehyde as a yellow solid (0.43 g, 87%). M.p. 96–98 °C (Lit m.p.: 95–98 °C). LRMS (ESI$^-$) *m/z* 216 (M + 1); HRMS (ES+) for $C_{13}H_{14}NO_2$; calculated 216.0946, found 216.0950; ^{1}H NMR (DMSO-d6, 400 MHz): δ 9.48 (d, J = 3.2 Hz, 1H), 7.69 (dd, J = 8.2, 3.6 Hz, 2H), 7.59 (t, J = 3.8 Hz, 1H), 7.00 (t, J = 3.9 Hz, 1H), 6.81 (dd, J = 8.3, 3.4 Hz, 2H), 3.00 (d, J = 3.2 Hz, 6H); ^{13}C NMR (DMSO-d6, 101 MHz): δ 176.9, 160.6, 151.6, 151.1, 126.9, 116.4, 112.5, 106.0; RP-HPLC Alltima™ C18 5u 150 mm × 4.6 mm, 10–100% B in 15 min, t_R 10.68 min.

5-(4-Methoxyphenyl)-2-furancarboxaldehyde (15c)

Compound **15c** was synthesised utilised general procedure **2**, 4-bromoanisole (0.41 g, 2.2 mmol), 5-formyl-2-furanylboronic acid (0.31 g, 2.2 mmol) and TBAA (1.99 g, 6.6 mmol). The crude was subjected to flash silica gel chromatography (5 : 1 Hex–EtOAc) to afford 5-(4-methoxyphenyl)-2 furancarboxaldehyde as a pale yellow oil (0.42 g, 92%). LRMS (ESI$^-$) *m/z* 201 (M − 1); HRMS (ES−) for $C_{12}H_9O_3$; calculated 201.0630, found 201.0637; ^{1}H NMR ($CDCl_3$, 400 MHz): δ 9.60 (s, 1H), 7.77 (d, J = 8.9 Hz, 2H), 7.30 (d, J = 3.7 Hz, 1H), 6.96 (d, J = 8.9 Hz, 2H), 6.72 (d, J = 3.7 Hz, 1H), 3.86 (s, 3H); ^{13}C NMR ($CDCl_3$, 101 MHz): δ 176.9, 160.91, 159.8, 151.6, 129.0, 127.0, 121.8, 114.4, 106.3, 55.4; RP-HPLC Alltima™ C18 5u 150 mm × 4.6 mm, 10–100% B in 15 min, t_R 18.92 min.

5-(1*H*-Indol-6-yl)-2-furancarboxaldehyde (15d)

Compound **15d** was synthesised utilising general procedure **2**, 6-bromo-1*H*-indole (0.41 g, 2.1 mmol), 5-formyl-2-furanylboronic acid (0.29 g, 2.1 mmol) and TBAA (1.90 g, 6.3 mmol). The crude was subjected to flash silica gel chromatography (3 : 1 EtOAc–Hex) to afford 5-(1*H*-indol-6-yl)-2-furancarboxaldehyde as an off-white solid (0.48. g, 83%). LRMS (ESI$^-$) *m/z* 212 (M + 1); HRMS (ES+) for $C_{13}H_{10}NO_2$; calculated 212.0633, found 212.0635; ^{1}H NMR ($CDCl_3$, 400 MHz): δ 9.61 (s, 1H), 8.43 (s, NH), 7.95 (s, 1H), 7.68 (d, J = 8.3 Hz, 1H), 7.54 (dd, J = 8.3, 1.4 Hz, 1H), 7.34 (d, J = 3.7 Hz, 1H), 7.33–7.31 (m, 1H), 6.83 (d, J = 3.7 Hz, 1H), 6.60–6.56 (m, 1H). ^{13}C NMR ($CDCl_3$, 101 MHz): δ 176.8, 161.3, 151.6, 135.9, 129.2, 126.5, 122.9, 121.2, 117.7, 108.4, 106.8, 103.1; RP-HPLC Alltima™ C18 5u 150 mm × 4.6 mm, 10–100% B in 15 min, t_R 15.58 min.

5-(4-Benzoylphenyl)-2-furancarboxaldehyde (15e)

Compound **15e** was synthesised using general procedure **2**, (4-chlorophenyl)(phenyl)methanone (0.41 g, 2.2 mmol), 5-formyl-2-furanylboronic acid (0.31 g, 2.2 mmol) and TBAF (1.99 g, 6.60 mmol). The crude was subjected to flash silica gel chromatography (4 : 1 Hex–EtOAc) to afford 5-(4-benzoylphenyl)-2-furancarboxaldehyde as a off-white solid (0.38. g, 87%). LRMS (ESI$^+$) *m/z* 277 (M + 1); HRMS (ES+) for $C_{18}H_{13}O_3$; calculated 277.0786, found 277.0791; ^{1}H NMR (DMSO-d6, 100 MHz): δ 9.67 (s, 1H), 8.05 (d, J = 8.4 Hz, 2H), 7.86 (d, J = 8.4 Hz, 2H), 7.78–7.75 (m, 2H), 7.73–7.69 (m, 2H), 7.59 (t, J = 7.6 Hz, 2H), 7.48 (d, J = 3.8 Hz, 1H); ^{13}C NMR ($CDCl_3$, 101 MHz): δ 195.5, 178.7, 157.3, 152.8, 137.7, 137.3, 133.3, 132.6, 131.0, 130.1, 129.1, 125.4, 111.3; RP-HPLC Alltima™ C18 5u 150 mm × 4.6 mm, 10–100% B in 15 min, t_R 18.21 min.

5-(3-Formylphenyl)furan-2-carbaldehyde (15f)

Compound **15f** was synthesised using general procedure, 3-chlorobenzaldehyde (0.28 g, 2.0 mmol), 5-formyl-2-furanylboronic acid (0.28 g, 2.0 mmol) and TBAF (1.81 g, 6.0 mmol). The crude was subjected to flash silica gel chromatography (9 : 1 Hex–EtOAc) to afford 5-(4-benzoylphenyl)-2-furancarboxaldehyde as a off-white solid (0.34. g, 85%). LRMS (ESI$^-$) *m/z* 199 (M − 1); HRMS (ES−) for $C_{12}H_7O_3$; calculated 199.0473, found 199.0482; ^{1}H NMR (400 MHz, DMSO) δ 10.11 (s, 1H), 9.66 (s, 1H), 8.38 (s, 1H), 8.21 (d, J = 7.9 Hz, 1H), 7.98 (d, J = 7.6 Hz, 1H), 7.76 (t, J = 7.7 Hz, 1H), 7.70 (d, J = 3.7 Hz, 1H), 7.46 (d, J = 3.7 Hz, 1H); ^{13}C NMR (101 MHz, DMSO) δ 193.33, 178.61, 157.24, 152.51, 137.38, 131.03, 130.65, 130.63, 129.99, 126.09, 125.91, 125.67, 110.34; RP-HPLC Alltima™ C18 5u 150 mm × 4.6 mm, 10–100% B in 15 min, t_R 10.68 min.

N-(6-((2*S*,6*R*)-2,6-Dimethylmorpholino)pyridin-3-yl)-2-methyl-4′-(trifluoromethoxy)biphenyl-3-carboxamide (LDE225) (18)

Compound **18** was synthesised using general procedure 2, 3-bromo-*N*-(6-((2*R*,6*S*)-2,6-dimethylmorpholino)pyridin-3-yl)-2-methylbenzamide (0.48 g, 1.2 mmol), 4-(trifluoromethoxy)-phenylboronic acid (0.25 g, 1.2 mmol), and TBAF (1.08 g, 3.6 mmol). The crude was subjected to flash silica gel chromatography (9 : 1 DCM–MeOH) to afford LDE225 as a off-white solid (0.55 g, 94%). LRMS (ESI$^+$) *m/z* 486 (M + 1); ^{1}H NMR (400 MHz, DMSO-d6) δ 10.25 (s, 1H), 8.43 (d, J = 2.4 Hz, 1H), 7.94 (dd, J = 9.1, 2.5 Hz, 1H), 7.47 (s, 4H), 7.42–7.25 (m, 2H), 6.86 (d, J = 9.1 Hz, 1H), 4.06 (d, J = 12.0 Hz, 2H), 3.67–3.54 (m, 2H), 2.41–2.27 (m, 2H), 2.22 (s, 3H), 1.16 (d, J = 6.2 Hz, 6H); ^{13}C NMR (101 MHz, DMSO-d6) δ 0.19, 156.18, 148.00, 141.40, 140.63, 139.87, 139.05, 132.53, 131.52, 131.14, 130.66, 127.49, 127.05, 126.26, 121.85, 121.38, 119.31, 107.32, 71.32, 51.25, 19.30, 17.71;193.33, 178.61, 157.24, 152.51, 137.38, 131.03, 130.65, 130.63, 129.99, 126.09, 125.91, 125.67, 110.34; RP-HPLC Alltima™ C18 5u 150 mm × 4.6 mm, 10–100% B in 15 min, t_R 17.41 min.

Acknowledgements

This project is supported by the Australian Cancer Research Foundation, and the Australian Research Council. CPG is the recipient of an ARC DECRA fellowship. LH acknowledges the receipt of a Postgraduate Scholarship from the University of Newcastle. T.N.T. is the recipient of a Prime Minister's Australia Asia Postgraduate Award.

Notes and references

1 M. Haddach, J. Michaux, M. K. Schwaebe, F. Pierre, S. E. O'Brien, C. Borsan, J. Tran, N. Raffaele, S. Ravula, D. Drygin, A. Siddiqui-Jain, L. Darjania, R. Stansfield, C. Proffitt, D. Macalino, N. Streiner, J. Bliesath, M. Omori, J. P. Whitten, K. Anderes, W. G. Rice and D. M. Ryckman, *ACS Med. Chem. Lett.*, 2012, **3**, 135–139.

2 V. Pomel, J. Klicic, D. Covini, D. D. Church, J. P. Shaw, K. Roulin, F. Burgat-Charvillon, D. Valognes, M. Camps, C. Chabert, C. Gillieron, B. Francon, D. Perrin, D. Leroy, D. Gretener, A. Nichols, P. A. Vitte, S. Carboni, C. Rommel, M. K. Schwarz and T. Rueckle, *J. Med. Chem.*, 2006, **49**, 3857–3871.

3 Y. Feng, X. Ding, T. Chen, L. Chen, F. Liu, X. Jia, X. Luo, X. Shen, K. Chen, H. Jiang, H. Wang, H. Liu and D. Liu, *J. Med. Chem.*, 2010, **53**, 3465–3479.

4 S. Jiang, S. R. Tala, H. Lu, P. Zou, I. Avan, T. S. Ibrahim, N. E. Abo-Dya, A. Abdelmajeid, A. K. Debnath and A. R. Katritzky, *Bioorg. Med. Chem. Lett.*, 2011, **21**, 6895–6898.

5 E. A. Jefferson, P. P. Seth, D. E. Robinson, D. K. Winter, A. Miyaji, L. M. Risen, S. A. Osgood, M. Bertrand and E. E. Swayze, *Bioorg. Med. Chem. Lett.*, 2004, **14**, 5257–5261.

6 L. M. Fung, K. W. H. Chan and C. A. Swindlehurst, *Application: WO Pat*, 2011-US39377 2011156321, 2011.

7 M. K. Hadden, *Expert Opin. Ther. Pat.*, 2013, **23**, 345–361.

8 T. N. Trinh, E. A. McLaughlin, C. P. Gordon and A. McCluskey, *MedChemComm*, 2014, **5**, 117–133.

9 M. K. Dahlgren, P. Schyman, J. Tirado-Rives and W. L. Jorgensen, *J. Chem. Inf. Model.*, 2013, **53**, 1191–1199.

10 M. Forino, S. Johnson, T. Y. Wong, D. V. Rozanov, A. Y. Savinov, W. Li, R. Fattorusso, B. Becattini, A. J. Orry, D. Jung, R. A. Abagyan, J. W. Smith, K. Alibek, R. C. Liddington, A. Y. Strongin and M. Pellecchia, *Proc. Natl. Acad. Sci. U. S. A.*, 2005, **102**, 9499–9504.

11 M. Eisenmann, H. Steuber, M. Zentgraf, M. Altenkaemper, R. Ortmann, J. Perruchon, G. Klebe and M. Schlitzer, *ChemMedChem*, 2009, **4**, 809–819.

12 M. R. Kumar, K. Park and S. Lee, *Adv. Synth. Catal.*, 2010, **352**, 3255–3266.

13 T. Mino, Y. Shirae, M. Sakamoto and T. Fujita, *J. Org. Chem.*, 2005, **70**, 2191–2194.

14 G. A. Molander and L. Iannazzo, *J. Org. Chem.*, 2011, **76**, 9182–9187.

15 M. L. N. Rao, D. K. Awasthi and J. B. Talode, *Synlett*, 2012, 1907–1912.

16 J. G. A. Walton, S. V. Chankeshwara and M. Bradley, *Application: WO Pat*, 2011-GB658 2011135303, 2011.

17 J. Yang, S. Liu, J.-F. Zheng and J. Zhou, *Eur. J. Org. Chem.*, 2012, **2012**, 6248–6259.

18 D. Balachari, L. Quinn and G. A. O'Doherty, *Tetrahedron Lett.*, 1999, **40**, 4769–4773.

19 T. Hosoya, H. Aoyama, T. Ikemoto, Y. Kihara, T. Hiramatsu, M. Endo and M. Suzuki, *Bioorg. Med. Chem.*, 2003, **11**, 663–673.

20 S. Murasawa, K. Iuchi, S. Sato, T. Noguchi-Yachide, M. Sodeoka, T. Yokomatsu, K. Dodo, Y. Hashimoto and H. Aoyama, *Bioorg. Med. Chem.*, 2012, **20**, 6384–6393.

21 M. E. Jung, J.-M. Ku, L. Du, H. Hu and R. A. Gatti, *Bioorg. Med. Chem. Lett.*, 2011, **21**, 5842–5848.

22 B. Martin-Matute, C. Nevado, D. J. Cardenas and A. M. Echavarren, *J. Am. Chem. Soc.*, 2003, **125**, 5757–5766.

23 K. L. Milkiewicz, D. J. Parks and T. Lu, *Tetrahedron Lett.*, 2003, **44**, 4257–4260.

24 A. Mitsch, P. Wissner, K. Silber, P. Haebel, I. Sattler, G. Klebe and M. Schlitzer, *Bioorg. Med. Chem.*, 2004, **12**, 4585–4600.

25 F. Moreau, N. Desroy, J. M. Genevard, V. Vongsouthi, V. Gerusz, G. Le Fralliec, C. Oliveira, S. Floquet, A. Denis, S. Escaich, K. Wolf, M. Busemann and A. Aschenbrenner, *Bioorg. Med. Chem. Lett.*, 2008, **18**, 4022–4026.

26 J. K. Yano, T. T. Denton, M. A. Cerny, X. Zhang, E. F. Johnson and J. R. Cashman, *J. Med. Chem.*, 2006, **49**, 6987–7001.

27 W.-M. Dai, Y. Li, Y. Zhang, K. W. Lai and J. Wu, *Tetrahedron Lett.*, 2004, **45**, 1999–2001.

28 M. Parisien, D. Valette and K. Fagnou, *J. Org. Chem.*, 2005, **70**, 7578–7584.

29 T. J. Colacot, W. A. Carole, B. A. Neide and A. Harad, *Organometallics*, 2008, **27**, 5605–5611.

30 W. Carole and T. J. Colacot, *Chim. Oggi*, 2010, **28**, XXIII–XXV.

31 T. J. Colacot, *Top. Catal.*, 2008, **48**, 91–98.

32 C. C. C. Johansson Seechurn, M. O. Kitching, T. J. Colacot and V. Snieckus, *Angew. Chem., Int. Ed.*, 2012, **51**, 5062–5085.

33 H. Li, C. C. C. Johansson Seechurn and T. J. Colacot, *ACS Catal.*, 2012, **2**, 1147–1164.

34 T. N. Glasnov and C. O. Kappe, *Adv. Synth. Catal.*, 2010, **352**, 3089–3097.

35 W. Solodenko, H. Wen, S. Leue, F. Stuhlmann, G. Sourkouni-Argirusi, G. Jas, H. Schoenfeld, U. Kunz and A. Kirschning, *Eur. J. Org. Chem.*, 2004, 3601–3610.

36 G. O. D. Estrada, M. C. Flores, J. F. M. da Silva, R. O. M. A. de Souza and L. S. M. e Miranda, *Tetrahedron Lett.*, 2012, **53**, 4166–4168.

37 T. Noel, S. Kuhn, A. J. Musacchio, K. F. Jensen and S. L. Buchwald, *Angew. Chem., Int. Ed.*, 2011, **50**, 5943–5946.
38 J. F. A. Lacrampe, R. W. Connors, C. Y. Ho, A. Richardson, E. J. E. Freyne, P. J. J. Buijnsters and A. C. Bakker, *Application: WO Pat*, 2003-EP50293 2004007499, 2004.
39 E. Margui, K. Van Meel, R. Van Grieken, A. Buendia, C. Fontas, M. Hidalgo and I. Queralt, *Anal. Chem.*, 2009, **81**, 1404–1410.
40 Committee for medicinal products for human use (CHMP). *Doc. No. EMEA/CHMP/SWP/4446/2000); European Medicines Agency: London, U.K., February 2008*, 2008.
41 C. K. Y. Lee, A. B. Holmes, S. V. Ley, I. F. McConvey, B. Al-Duri, G. A. Leeke, R. C. D. Santos and J. P. K. Seville, *Chem. Commun.*, 2005, 2175–2177.
42 B. Borcsek, G. Bene, G. Szirbik, G. Dorman, R. Jones, L. Urge and F. Darvas, *ARKIVOC*, 2012, 186–195.

2.2. Updated references

1. S. Pan, X. Wu, J. Jiang, W. Gao, Y. Wan, D. Cheng, D. Han, J. Liu, N. P. Englund, Y. Wang, S. Peukert, K. Miller-Moslin, J. Yuan, R. Guo, M. Matsumoto, A. Vattay, Y. Jiang, J. Tsao, F. Sun, A. C. Pferdekamper, S. Dodd, T. Tuntland, W. Maniara, J. F. Kelleher, III, Y.-m. Yao, M. Warmuth, J. Williams and M. Dorsch, *ACS Med. Chem. Lett.*, 2010, **1**, 130-134.
2. FDA approves new treatment for most common form of advanced skin cancer, http://www.fda.gov/NewsEvents/Newsroom/PressAnnouncements/ucm455862.htm).
3. L. M. Fung, C. A. Swindlehurst, K. W. H. Chan and R. W. Sullivan, *Application: WO Pat.,* 2013-US72303 2014085633, 2014.
4. M. K. Hadden, *Expert Opinion on Therapeutic Patents*, 2013, **23**, 345-361.
5. H. Li, C. C. C. Johansson Seechurn and T. J. Colacot, *ACS Catalysis*, 2012, **2**, 1147-1164.
6. C. C. C. Johansson Seechurn, M. O. Kitching, T. J. Colacot and V. Snieckus, *Angewandte Chemie, International Edition*, 2012, **51**, 5062-5085.
7. W. Carole and T. J. Colacot, *Chimica Oggi*, 2010, **28**, XXIII-XXV.
8. T. J. Colacot, W. A. Carole, B. A. Neide and A. Harad, *Organometallics*, 2008, **27**, 5605-5611.
9. T. J. Colacot, *Topics in Catalysis*, 2008, **48**, 91-98.
10. R. Porta, M. Benaglia and A. Puglisi, *Organic Process Research & Development*, 2016, **20**, 2-25.
11. D. T. McQuade and P. H. Seeberger, *Journal of Organic Chemistry*, 2013, **78**, 6384-6389.

III. CHAPTER THREE

Quinolone-1-(2*H*)-ones as Hedgehog Signalling Pathway Inhibitors

3.1. Introduction

In relation to the key project aim of developing scaffolds with inhibitory activity beyond Smo, we turned our attention to the previously reported Gli inhibitor HPI-4 (**1**) [1]. Considered as a non-selective inhibitor of the Gli family of transcription factors, HPI-4 contained a number of structural features present within a family of quinolone-1-(2*H*)-ones previously described from our laboratories (exemplified by **2**; Figure 1) [2]. Hence the initial phase of the project focused on this scaffold in a bid to determine whether it posed as a potential lead compound.

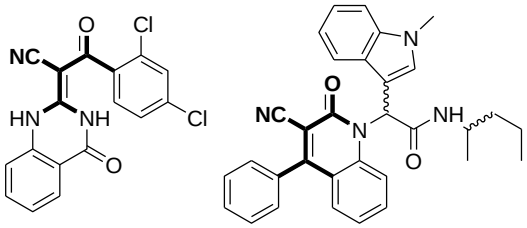

1
HPI-4

2

Figure 1. N-(sec-butyl)-2-(3-cyano-2-oxo-4-phenylquinolin-1-(2*H*)-yl)-2-(1-methyl-1*H*-indol-3-yl)acetamide (**2**) from our laboratory with the bolded structure sections reflecting the structural similarities with the Gli inhibitor HPI-4 (**1**).

To assess the potential of the quinolone-1-(*2H*)-one scaffold as HSP inhibitors, we developed a multi-screen pathway which included a broad cytotoxicity testing (MTT assay) to more specific assays (Gli-luciferase and qPCR assays). This combined screening resulted in three active compounds capable of inhibiting $Ptch_1$ and Gli_2 gene expression and subsequent inhibition of the Gli protein expression in Shh LIGHT 2 cell line. Moreover, these analogues demonstrated good cytotoxicity against a panel of nine human HSP expressing cancer cell lines. The results of this combined screening are included in the following paper, with the supporting information provided in the Appendix to Chapter 3 (please see Chapter 8, page 188).

Organic & Biomolecular Chemistry

PAPER

View Article Online
View Journal | View Issue

Cite this: Org. Biomol. Chem., 2016, 14, 6304

Quinolone-1-(2*H*)-ones as hedgehog signalling pathway inhibitors†

Trieu N. Trinh,[a] Eileen A. McLaughlin,‡[b] Mohammed K. Abdel-Hamid,[a,c] Christopher P. Gordon,[d] Ilana R. Bernstein,[b] Victoria Pye,[b] Peter Cossar,[a] Jennette A. Sakoff[e] and Adam McCluskey*[a]

Received 21st March 2016,
Accepted 20th May 2016

DOI: 10.1039/c6ob00606j

www.rsc.org/obc

A series of quinolone-2-(1*H*)-ones derived from the Ugi-Knoevenagel three- and four-component reaction were prepared exhibiting low micromolar cytotoxicity against a panel of eight human cancer cell lines known to possess the Hedgehog Signalling Pathway (HSP) components, as well as the seminoma TCAM-2 cell line. A focused SAR study was conducted and revealed core characteristics of the quinolone-2-(1*H*)-ones required for cytotoxicity. These requirements included a C3-tethered indole moiety, an indole C5-methyl moiety, an aliphatic tail or an ester, as well as an additional aromatic moiety. Further investigation in the SAG-activated Shh-LIGHT2 cell line with the most active analogues: 2-(3-cyano-2-oxo-4-phenylquinolin-1(2*H*)-yl)-2-(1-methyl-1*H*-indol-3-yl)-*N*-(pentan-2-yl)acetamide (**5**), 2-(3-cyano-2-oxo-4-phenylquinolin-1(2*H*)-yl)-2-(5-methyl-1*H*-indol-3-yl)-*N*-(pentan-2-yl)acetamide (**23**) and ethyl (2-(3-cyano-2-oxo-4-phenylquinolin-1(2*H*)-yl)-2-(5-methyl-1*H*-indol-3-yl)acetyl)glycinate (**24**) demonstrated a down regulation of the HSP *via* a reduction in Gli expression, and in the mRNA levels of $Ptch_1$ and Gli_2. Analogues **5**, **23** and **24** returned in cell inhibition values of 11.6, 2.9 and 3.1 μM, respectively, making this new HSP-inhibitor pharmacophore amongst the most potent non-Smo targeted inhibitors thus far reported.

Introduction

The Hedgehog (Hh) signalling pathway (HSP) plays a pivotal role in embryogenesis by controlling the spatial and temporal regulation of cell proliferation, differentiation, and tissue patterning.[1,2] Aberrant Hh signalling in humans can initiate the development of a diverse range of human cancers, including basal cell carcinoma,[3] medulloblastoma,[4–6] cancers of the pancreas,[7] prostate,[8] lung,[9,10] colon,[11] stomach,[12] breast,[13,14] ovary[15] and perhaps most problematically the formation of cancer stem cells.[16,17] Consequently, suppressing the HSP is an attractive and recently validated chemotherapeutic target with two inhibitors targeting the Smoothened (Smo) protein, Vismodegib (1, GDC-0449, Erivedge®) and Sonidegib (2, LDE225, Odomzo®) (Fig. 1), approved by FDA for the treatment of early and advanced basal cell carcinomas.[18,19]

The activation and suppression of the HSP involves an intricate interplay between proteins, both within the HSP and with associated signalling networks including the TGF-β, p53, WIP1, PI3K/AKT and RAS/MEK pathways. Briefly, the canonical HSP functions in a hierarchical manner, in which a Hedgehog ligand (Sonic, Desert or Indian hedgehog protein) binds to the membrane receptor $Patched_1$ ($Ptch_1$), resulting in the activation of the Smo protein and subsequent release of active Glioma-Associated Oncogene Homolog transcriptional factors (Gli_{1-3}) into the nucleus.[1,2,20] These Gli transcription factors

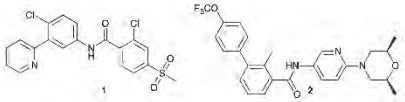

Fig. 1 Chemical structures of the Smo inhibitors Vismodegib (1, GDC-0449, Erivedge®) and Sonidegib (2, LDE225, Odomzo®) approved by FDA for the treatment of early and advanced basal cell carcinomas.[18,19]

[a]Chemistry, Priority Research Centre for Chemical Biology, University of Newcastle, University Drive, Callaghan, NSW 2308, Australia. E-mail: Adam.McCluskey@newcastle.edu.au; Fax: +61(2)49 215472; Tel: +61(2)49 216486
[b]Biology, Priority Research Centre for Chemical Biology, University of Newcastle, University Drive, Callaghan, NSW 2308, Australia
[c]Department of Medicinal Chemistry, Faculty of Pharmacy, Assiut University, Assiut 71526, Egypt
[d]Nanoscale Organization and Dynamics Group, School of Science and Health, University of Western Sydney, Penrith South DC, NSW, Australia
[e]Department of Medical Oncology, Calvary Mater Hospital, Edith Street, Waratah, NSW 2298, Australia

† Electronic supplementary information (ESI) available: NMR, IR, mass spectra, and HPLC peaks. See DOI: 10.1039/c6ob00606j

‡ Current Address: School of Biological Sciences, University of Auckland, Auckland, New Zealand.

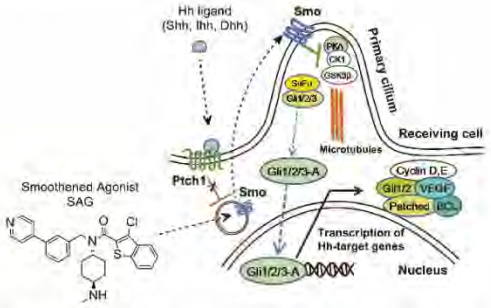

Fig. 2 The canonical HSP is initiated by the binding of the Hedgehog ligand (Sonic, Desert or Indian) to the membrane receptor $Ptch_1$, resulting in the activation of Smo protein and release of active Gli transcriptional factors (Gli_{1-3}) into the nucleus, culminating in the transcription of Hh-target genes.[20] Alternatively, the HSP can be activated directly at the Smo level by using SAG (3).[22]

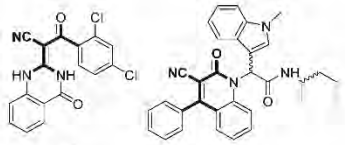

Fig. 3 *N*-(sec-Butyl)-2-(3-cyano-2-oxo-4-phenylquinolin-1-(2*H*)-yl)-2-(1-methyl-1*H*-indol-3-yl)acetamide (5) from our laboratory with the bolded structure sections reflecting the structural similarities with the Gli inhibitor HPI-4 (4).

facilitate the transcription of Hh target genes, including the components of the HSP Gli_1, Gli_2, $Ptch_1$, and $Ptch_2$.[21] Alternatively, the HSP can be activated directly at the Smo level *via* a synthetic Smo agonist (3, SAG) (Fig. 2).[22]

The hierarchical character of the HSP affords several opportunities to suppress the pathway including the inhibition of Hedgehog–ligand–$Ptch_1$ interactions,[23,24] inhibition of the Smo protein[22,25–35] or further downstream such as the inhibition of the Gli transcription factors.[36–46] At present the most clinically advanced HSP inhibitor compounds target Smo. These clinical studies have identified limitations to this approach including the development of acquired resistance resulting from Smo mutations and compensatory amplification of Gli_2 transcription factors by the aforementioned interacting pathways.[20] Targeting the HSP further downstream of Smo at the Gli transcription factor level, and/or indirectly at interacting signalling pathways may constitute a more robust strategy for treating HSP related cancers.[20,13]

Given our ongoing interest in the development of small molecule HSP inhibitors[20,47] our attention was drawn to the previously reported HIP-4 (4).[43] Considered as a non-selective inhibitor of the Gli family of transcription factors, HIP-4 contained a number of structural features present within a family of quinolone-2-(1*H*)-ones recently reported from our laboratories (exemplified by 5; Fig. 3).[48]

To assess the potential of quinolone-1-(2*H*)-one scaffold as HSP inhibitors, we first evaluated their cytotoxicity in a double-filter screening against a panel of eight human cancer cell lines possessing components of the HSP (Table 1; entries 1–8), and one seminoma cancer cell line (TCAM-2) (Table 1; entry 9).

The TCAM-2 cell line, in addition to expressing the HSP (ESI†), possesses the active PI3K signalling pathway[49] and the aberrantly up-regulated mitogen-activated protein kinase signalling pathway (RAS/RAF/MEK/ERK) due to a mutation at the BRAF gene (V600E).[50–52] Together these signalling pathways create a complex loop facilitating the non-canonical activation of Gli activity downstream of Smo.[47,49,53] Thus the TCAM-2 cell line provides a valuable filter to identify potential Gli transcription factor inhibitors, with this (we believe) to be the first such use of this system. Active compounds from our double-filter cytotoxicity screening approach would be further evaluated in SAG-activated Sonic Hedgehog-(Shh) LIGHT 2 cell line model for their potential to suppress the HSP using Dual Luciferase Reporter (DLR), Reverse Transcription PCR (RT-PCR) and Quantitative PCR (qPCR) assays.

Results and discussion

A targeted library of quinolone-1-(2*H*)-ones retaining the highlighted pharmacophore of 4 (Fig. 3) was prepared using our

Table 1 Human cancer cell lines known to possess the HSP

Entry	Cell Line	Cell Type	HSP components expressed	Ref.
1	HT29	Colorectal carcinoma	Ihh, Shh, $Ptch_1$, Smo, $Gli_{1,2,3}$, Hhip at mRNA levels	54
2	SW480	Colorectal carcinoma	Shh, Ptch, Smo, Sufu, $Gli_{2,3}$, Hhip at mRNA levels	55
3	MCF-7	Breast adenocarcinoma	Ihh, Shh, Dhh, $Ptch_1$, Smo, $Gli_{1,2}$ at mRNA levels	14
4	A2780	Ovarian carcinoma	Shh, Dhh, Ptch, Smo, Gli_1 at mRNA and protein levels	15
5	H460	Lung carcinoma	Smo, $Ptch_1$, Gli_1 at mRNA levels	56 and 57
6	DU145	Prostate carcinoma	$Ptch_1$, $Gli_{1,2}$ at mRNA levels	58 and 59
7	BE2-C	Neuroblastoma	Shh, Smo, Gli_2 at protein levels	60
8	MIA-Paca-2	Pancreatic carcinoma	Shh, $Ptch_{1,2}$, Smo, $Gli_{1,2}$ at mRNA levels	61 and 62
9	TCAM-2	Seminoma	$Ptch_1$, Smo, Sufu, Gli_3, and Gli_1 at mRNA levels	ESI
			Expression of PI3 pathway	49
			Mutation at BRAF gene, overexpression of RAS/RAF/MEK/ERK pathway	51, 50 and 52

previously reported sequential Ugi-Knoevenagel protocol.[48] In a typical synthesis, a methanolic solution of 2-aminobenzophenone (**6**), 4-chlorobenzaldehyde (**7**), cyanoacetic acid (**8**) and ethyl isocyanoacetate (**9**) in methanol was stirred at room temperature for 48 h, followed by chromatographic separation of the desired product (**10**) (Scheme 1).[48] Using this approach eleven exemplars were generated, of which five (**5**, **12**, **14**–**16**, Table 2) were obtained as a mixture of diastereomers (see Experimental).

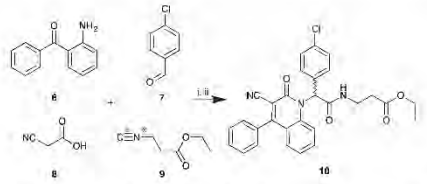

Scheme 1 Synthesis of quinolone-2-(1*H*)-ones. Reagents and Conditions: (i) MeOH, rt; (ii) spontaneous.[48]

Attempts to separate individual diastereomers proved unsuccessful. However using Willoughby *et al.*'s computational approach we identified the relative configuration of the major isomers in each instance.[63] With analogues **14**–**16** the geometry was optimised and free energy calculated using Density Functional Theory and B3LYP (6-31+G(d,p) basis set) approaches. This theory level was used to calculate the ^{1}H NMR shifts of each conformer and to predict the more abundant diasteroisomer obtained synthetically. Data relating to analogues **14**–**16** showed distinguishable ^{1}H NMR peaks for each pair of diastereomersfor the two methyl and the methylene moieties of the 2-pentyl substituent. Comparison of the *R*,*R*/*S*,*S* and *R*,*S*/*S*,*R* pairs as well as their computed ^{1}H NMR chemical shifts (ESI, Table S1†) showed favourable DFT energies for the *R*,*S*/*S*,*R* pair compared to *R*,*R*/*S*,*S* (difference of 1.6–4.3 kcal mol^{-1}) in all instances. This was consistent with the observed ^{1}HNMR shifts for the major product and the cal-

Table 2 Evaluation of the cytotoxicity of the quinolin-2-(1*H*)-ones analogues (**5**, **10**–**19**) against a panel of eight hedgehog signalling pathway expressing cancer cell lines. Values are the percentage of growth inhibition at 25 μM drug concentration

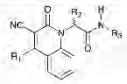

Compound	R_1	R_2	R_3	HT29[a]	SW480[a]	MCF-7[b]	A2780[c]	H460[d]	Du145[e]	BE2-C[f]	MIA[g]
5				79 ± 2	99 ± 5	92 ± 2	96 ± 2	84 ± 4	94 ± 4	92 ± 2	92 ± 2
10				49 ± 2	43 ± 3	62 ± 3	51 ± 2	43 ± 7	22 ± 2	42 ± 0	41 ± 2
11				42 ± 3	57 ± 1	60 ± 5	38 ± 5	32 ± 4	28 ± 4	43 ± 6	45 ± 10
12				34 ± 6	46 ± 1	65 ± 2	39 ± 6	26 ± 7	18 ± 2	41 ± 2	39 ± 15
13				11 ± 7	2 ± 5	20 ± 3	27 ± 3	4 ± 4	<0	8 ± 3	16 ± 10
14				11 ± 6	7 ± 2	11 ± 4	29 ± 3	5 ± 5	<0	<0	14 ± 11
15				46 ± 1	47 ± 5	29 ± 3	31 ± 1	28 ± 7	<0	42 ± 3	36 ± 2
16				85 ± 0	77 ± 3	90 ± 2	96 ± 1	>100	63 ± 4	>100	81 ± 0
17				18 ± 3	3 ± 9	17 ± 3	35 ± 1	14 ± 12	<0	<0	19 ± 3
18				38 ± 3	26 ± 7	45 ± 5	42 ± 3	26 ± 17	21 ± 5	16 ± 1	30 ± 3
19				6 ± 2	6 ± 3	9 ± 9	19 ± 6	9 ± 5	4 ± 5	2 ± 7	14 ± 5

[a] HT29 and SW480 (colon carcinoma). [b] MCF-7 (breast carcinoma). [c] A2780 (ovarian carcinoma). [d] H460 (lung carcinoma). [e] Du145 (prostate carcinoma). [f] BE2-C (neuroblastoma). [g] MIA (pancreatic carcinoma).

Table 3 Evaluation of the cytotoxicity, GI_{50} values (μM), of compounds **5** and **16** against a panel of nine human HSP expressing cancer cell lines. GI_{50} is the concentration of drug that reduces cell growth by 50%

Compound	HT29[a]	SW480[a]	MCF-7[b]	A2780[c]	H460[d]	Du145[e]	BE2-C[f]	MIA[g]	TCAM-2[h]
5	5.3 ± 0.3	11 ± 1	4.6 ± 1.1	3.9 ± 0.3	5.2 ± 0.1	13 ± 0	3.6 ± 0.1	6.0 ± 0.1	11.6 ± 0.6
16	8.7 ± 0.5	17 ± 1	7.9 ± 1	7.5 ± 0.6	11 ± 1	18 ± 1	7.3 ± 0.3	13 ± 1	>100

[a] HT29 and SW480 (colon carcinoma). [b] MCF-7 (breast carcinoma). [c] A2780 (ovarian carcinoma). [d] H460 (lung carcinoma). [e] Du145 (prostate carcinoma). [f] BE2-C (neuroblastoma). [g] MIA (pancreatic carcinoma). [h] TCAM-2 (seminoma).

Table 4 Synthesis results and the evaluation of the cytotoxicity of the second focused library against the TCAM-2 cell line. Values are the percentage of growth inhibition at 10 μM drug concentration and GI_{50} were determined where the growth inhibition >50% (ESI) reagents and conditions: (i) MeOH, rt, 24 h

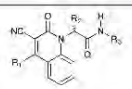

Compound	R_1	R_2	R_3	Yield (%)	TCAM-2% inhibition at 10 μM	TCAM-2 GI_{50} (μM)
5				38	52	11.6 ± 0.6
20				13	21	—
21				11	41	—
22				36	<0	—
23				46	72	2.9 ± 0
24				34	66	3.1 ± 0.4
25				46	28	—
26				26	45	—
27				50	44	—
28				33	<0	—
29				47	41	—
30				26	44	

culated chemical shifts for *R,S/S,R* pair of enantiomers. This 11 component library was screened against our panel of eight human cancer cell lines and the data presented in Table 2.

Analysis of the data presented in Table 2 showed analogues **5** and **16** as the most promising at the 25 μM drug concentration evaluated. The C3-tethered indole group (**5**) was shown to be crucial for activity, while its replacement by either a 4-methoxyphenyl (**12**) or phenyl moiety (**14**) resulted in a significant decrease in inhibition. All other analogues displayed modest (30–75%) to negligible growth inhibition (<30%) (Table 2). The two most promising analogues (**5** and **16**) proceeded to full dose response evaluation (Table 3).

The data in Table 3 shows **5** and **16** to be potent broad spectrum cytotoxic agents with GI_{50} values of 3.6–11 and 7.3–18 μM for respectively. However examination of these two analogues in TCAM-2 cells revealed **16** to be inactive (GI_{50} > 100 μM), while the indole-based **5** displayed excellent growth inhibition (GI_{50} = 11.6 ± 0.6 μM). These data and those presented in Table 2 support retention of the indole moiety as a key pharmacophore in this study. To further investigate this hypothesis we developed a second indole moiety based focused library, assembled *via* our Ugi-Knoevenagel approach (Scheme 1). Given the differential activity noted with the TCAM-2 cell line, these new indole based analogues were screened directly in this cell line only and the data presented in Table 4. This represents the first such use of TCAM-2 cells in the development of HSP inhibitors.

Analysis of the DLR assay data indicated moderate suppression (55, 54 and 31%) of Gli expression at the protein level by **5**, **23** and **24** respectively relative to the DMSO and SAG-treated controls (Fig. 4). This inhibition over Gli protein expression does not always result from the suppression of the HSP due to the complex crosstalk of interacting signalling pathways sharing Gli_2 as the same effector.[20]

Thus, the mRNA level of HSP components in SAG-activated Shh-LIGHT2 cell line was probed using a combination of Reverse Transcription PCR (RT-PCR) and Quantitative PCR (qPCR) assays. Of the individual HSP components identified at the mRNA level by RT-PCR, only *Ptch*$_1$ and *Gli*$_2$ exhibited significant up-regulation under SAG-stimulation (ESI†) and thus became our targets. Unlike previous reports, we found no evidence for Gli_1 expression under the conditions evaluated herein.[61,65] The outcomes of our qPCR analysis of $Ptch_1$ and

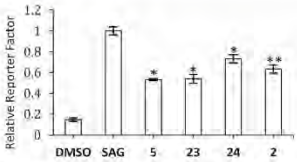

Fig. 4 Effect of compounds **5**, **23**, and **24** at 25 μM and Sonidegib (**2**) at 100 nM concentration on the suppression Gli expression in Shh-LIGHT2 cells activated with 100nM SAG. Treatments were performed in triplicate. *P < 0.05, **P < 0.001 compared with SAG control.

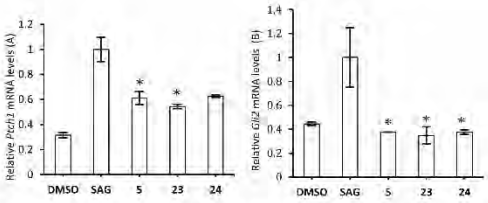

Fig. 5 Effect of compounds **5**, **23**, and **24** at 10 μM concentration on mRNA levels of *Ptch*$_1$ (A) and *Gli*$_2$ (B) in Shh-LIGHT2 cells activated with 100nM SAG. Treatments were performed in triplicate. * P < 0.05 compared to SAG controls.

Table 5 Evaluation of compounds **5**, **23**, and **24** (10 μM) on $Ptch_1$ and Gli_2 mRNA levels in SAG-activated Shh-LIGHT 2 cells. Values are the approximate percentage reduction relative to the DMSO and SAG-treated controls

	Percent change in $Ptch_1$ and Gli_2 mRNA levels (%)	
Compound	$Ptch_1$	Gli_2
5	57	112
23	67	117
24	55	112

Gli_2 post treatment at 10 μM of **5**, **23** and **24** are shown in Fig. 5.

As illustrated in Fig. 5 both *Ptch*$_1$ and *Gli*$_2$ mRNA levels were significantly suppressed by compounds **5**, **23**, and **24** at 10 μM treatments. To clarify the data presented in Fig. 5 the percent inhibition of *Ptch*$_1$ and *Gli*$_2$ mRNA levels were calculated (Table 5), in which the inhibition of mRNA levels of *Gli*$_2$ appeared to be larger than 100%. This may arise as a result of the compounds not only suppressing the elevated mRNA levels of *Gli*$_2$ induced by SAG, but also inhibition of *Gli*$_2$ in inactivated Shh LIGHT2 cells. Together, these results indicate that compounds **5**, **23**, and **24** exhibited suppressive activity over the HSP in Shh LIGHT2 through the inhibition of *Ptch*$_1$ at mRNA level and Gli_2 at both mRNA and protein levels.

Conclusions

We have successfully identified a new scaffold of HSP inhibitors derived from the Ugi-Knoevenagel products. At inhibitor concentration of 10 μM, these quinolone-2-(1*H*)-one analogues can effectively inhibit the mRNA levels of $Ptch_1$ and Gli_2 in Sonic Hedgehog LIGHT2 cell line stimulated with 100nM SAG. Of note, selected compounds demonstrated good cytotoxicity (GI_{50} from 2.9 to 18.0 μM) against a panel of eight human cancer cell lines, as well as the mutant seminoma TCAM-2 cell line, all of which are known to possess the HSP's components (Table 3). Whilst the exact mechanism remains to be determined, our data is consistent with inhibition downstream of

Smo due to the fact that it is valid in the presence of SAG, a potent Smo activator. Moreover, the analogues reported herein suppress Gli_2 mRNA level in non-activated Shh LIGHT 2 cells also supports a downstream of Smo inhibition. Inhibition of Smo does not display this phenotype. Furthermore, a preliminary quinolone-2-(1*H*)-one pharmacophore required to elicit the cytotoxicity profile has been established. Apparent crucial structural features include an indole moiety at R_2 which is tethered to the remainder of the scaffold through the C3 position. Moreover, the presence of bulky aliphatic groups within R_3 of the scaffold appears to be required to endow cytotoxicity against the TCAM-2 cell line. These valuable data undoubtedly will enable us to exploit the current pharmacophore to develop next generation analogues with superior properties to combat the hedgehog signalling related cancers. The results of these efforts will be reported in due course.

Experimental section

Biology

Cell culture and stock solutions. Stock solutions were prepared as follows and stored at −20 °C: related compounds were stored as 40 mM solutions in DMSO. All cell lines were cultured at 37 °C in an automated CO_2 (5%) incubator (HERA cell 150, Thermo Scientific).

HT29, SW480 (colon carcinomas), MCF-7 (breast carcinoma), A2780 (ovarian carcinoma), H460 (lung carcinoma), A431 (skin carcinoma), DU145 (prostate carcinoma), BEC-2 (neuroblastoma), SJ-G2 (glioblastoma) and MIA (pancreatic carcinoma) cell lines were maintained in Dulbecco's modified Eagle's medium (Trace Biosciences, Australia) supplemented with 10% foetal bovine serum, 10 mM sodium bicarbonate, penicillin (100 IU mL^{-1}), streptomycin (100 mg mL^{-1}), and glutamine (4 mM).

TCAM-2 cell line (testis carcinoma) was maintained in Hyclone RPMI 1640 medium (GE Healthcare Life Sciences) supplemented with 10% foetal bovine serum (Gibco®), penicillin (100 IU mL^{-1}) (Gibco®), streptomycin (100 mg mL^{-1}) (Gibco®) and glutamine (4 mM) (Gibco®).

Shh LIGHT2 cell line (derived from NIH-3T3 fibroblast cell line) was maintained in Gibco® Dulbecco's modified Eagle's medium (Thermo Fisher Scientific) supplemented with 10% foetal bovine serum (FBS), glutamine (4 mM), Zeocin® (0.15 mg mL^{-1}, Invitrogen), Geneticin® (0.4 mg mL^{-1}, Thermo Fisher Scientific).

In vitro growth inhibition assay

Protocol 1 (HT29, SW480, MCF-7, A2780, H460, DU145, BEC-2 and MIA cell lines). Cells in logarithmic growth were transferred to 96-well plates. Cytotoxicity was determined by plating cells in duplicate in 100 μL medium at a density of 2500–4000 cells per well. On day 0, (24 h after plating) when the cells were in logarithmic growth, 100 μL medium with or without the test agent was added to each well. After 72 h drug exposure growth inhibitory effects were evaluated using the MTT (3-[4,5-dimethylthiazol-2-yl]-2,5-diphenyl-tetrazolium bromide) assay and absorbance read at 540 nm. Percentage growth inhibition was determined at a fixed drug concentration of 25 μM. A value of 100% is indicative of total cell growth inhibition. Those analogues showing appreciable percentage growth inhibition underwent further dose response analysis allowing for the calculation of a GI_{50} value. This value is the drug concentration at which cell growth is 50% inhibited based on the difference between the optical density values on day 0 and those at the end of drug exposure.

Protocol 2 (TCAM-2 cell line). Cells in logarithmic growth were transferred to 96-well plates in triplicates at 2500 cells per well in 200 μL media and cultured in the automated CO_2 (5%) incubator. When the cells reach to about 80% confluency, old media were removed and replaced with 100 μL fresh media containing testing agents (at 10 μM), as well as DMSO and 1% Triton X as controls. Cells were further incubated for another 72 h and were evaluated using the MTT assay with the absorbance at 550 nm. The growth inhibition was calculated based on the differences in the optical densities between those treated by various agents (10 μM) and controls by DMSO and 1% Triton X treatments. Only those agents which expressed a growth inhibition greater than 60% were further subjected to full dose response evaluation (GI_{50} values).

Dual luciferase reporter assay

Shh-LIGHT2 cells in logarithmic growth were transferred to 96-well plate (3000 cells per well) and cultured to confluency. The Shh-LIGHT2 cells were then grown in DMEM containing 0.5% FBS, 4 mM glutamine, 0.15 mg mL^{-1} Zeocin®, 0.4 mg mL^{-1} Geneticin®, and combinations of 100 nM SAG (Smo agonist), with different testing compounds (**5**, **23**, and **24**) at 25 μM each. The SAG-free DMSO treated (25 μM), and SAG-included Sonidegib (100 nM) treated cells were used as controls. Treatments were done in triplicates. After the cells were cultured for another 45 h in the automated CO_2 (5%) incubator, the resulting firefly and Renilla luciferase activities were measured using a Dual Luciferase Reporter kit (Promega) and a BMG Labtech Pherastar microplate reader (Thermo Fisher Scientific).

RNA extraction

Total RNA was isolated from cultured cells using two rounds of a modified acid guanidinium thiocyanate-phenol-chloroform protocol:[66] washed cells resuspended in lysis buffer (4 M guanidinium thiocyanate, 25 mM sodium citrate, 0.5% sarkosyl, 0.72% β-mercaptoethanol). RNA was isolated by phenol/chloroform extraction and isopropanol precipitated.

Reverse transcription PCR (RT-PCR) and quantitative PCR (qPCR)

Reverse transcription was performed with 2 μg of isolated RNA, 500 ng oligo(dT)15 primer, 40 U of RNasin, 0.5 mM dNTPs, and 20 U of M-MLV-Reverse Transcriptase (Promega). Total RNA was DNase treated prior to reverse transcription to remove genomic DNA. Reverse transcription reactions were

Table 6 Primer sequences used in qPCR assay

	Forward sequence (5′–3′)	Reverse sequence (5′–3′)	Annealing temp. (°C)
Human gene			
Gli$_2$	ATCTCTTGCCACCATTCCAT	GGACAGAATGAGGCTCGTAA	60
Smo	CTGCCACTTCTACGACTTCT	GGCCTGACATAGCACATAGT	56
Sufu	GACCCCTTGGACTATGTTAG	CTGATGTAGTGCCAGTGCTC	55
Ptch$_1$	CCCTCACGTCCATCAGCAAT	AACACCACTACTACCGCTGC	58
Mouse gene			
Gli$_2$	TCCAGTCAATGGTTCTGTCC	TGGCTCAGCATCGTCACTTC	60
Gli$_3$	GGCCGTTACCATTATGATCC	CTGAGGCTGCAGTGGGATTA	60
Shh	TGCTTTGTAACCGCCACTTT	CGCTGCTAGGTGCACTTTTA	61
Smo	GAACTCCAATCGCTACCCTG	ATCTGCTCGGCAAACAATCT	60
Sufu	GACCCCTTGGACTATGTTAG	CTGATGTAGTGCCAGTGCTC	55
Ptch$_1$	CATAGCTGCCCAGTTCAAGT	GGTCGTAAAGTAGGTGCTGG	55

verified by β-actin RT-PCR using cDNA amplified with GoTaq Flexi (Promega). qPCR was performed using SYBR Green GoTaq qPCR master mix (Promega) according to manufacturer's instructions on LightCycler 96 SW 1.0 (Roche). Primer sequences have been supplied (Table 6). Reactions were performed on cDNA equivalent to 50 ng of total RNA and carried out for 45 amplification cycles. SYBR® Green fluorescence was measured after the extension step at the end of each amplification cycle and quantified using LightCycler Analysis Software (Roche). For each sample, a replicate omitting the reverse transcription step was undertaken as a negative control. qPCR data was normalized to the house-keeping control *Cyclophilin*. Experiments were replicated at least 3 times prior to statistical assessment. Each PCR was performed on at least 3 separate cell isolations, of which a representative PCR or an average is shown (ESI†).

Statistical analysis

Statistical analysis was performed using *F*-test and *t*-test in Excel 2013. $^*P < 0.05$, $^{**}P < 0.001$, $^{***}P < 0.0001$.

Chemistry

All reagents were purchased from Sigma-Aldrich, Matrix Scientific or Lancaster Synthesis and were used without purification. All solvents were re-distilled from glass prior to use.

^{1}H and ^{13}C NMR spectra were recorded on a Brüker Advance™ AMX 400 MHz spectrometer at 400.13 and 100.62 MHz, respectively. Chemical shifts (δ) are reported in parts per million (ppm) measured to relative the internal standards. Coupling constants (J) are expressed in hertz (Hz). Mass spectra were recorded on a Shimadzu LCMS 2010 EV using a mobile phase of 1 : 1 acetonitrile–H_2O with 0.1% formic acid. High resolution mass spectra (HRMS) were determined using nanoflow reversed phased Liquid Chromatography (Dionex Ultimate 3000 RSLCnano, Thermo Fischer Scientific) coupled directly to a High Resolution mode equipped, Q-Exactive Plus Hybrid Quadrupole-Orbitrap Mass Spectrometer (Thermo Fischer Scientific). This system was fitted with 5 μm C18 nanoViper trap column (100 μm × 2 cm, Acclaim PepMap100, Thermo) for desalting and pre-concentration, and separation was then performed at 300 nl min^{-1} over an EASY-Spray PepMap column (3 μm C18, 75 μm × 15 cm) utilising a gradient of 2–99% buffer B (80% acetonitrile, 0.1% formic acid) over 25 minutes.

Analytical HPLC traces were obtained using a Shimadzu system possessing a SIL-20A auto-sampler, dual LC-20AP pumps, CBM-20A bus module, CTO-20A column heater, and a SPD-20A UV/vis detector. This system was fitted with an Alltima™ C18 5 μm 150 mm × 4.6 mm column with solvent A: 0.06% trifluoroacetic acid (TFA) in water and solvent B: 0.06% TFA in CH_3CN–H_2O (90 : 10). In each case HPLC traces were acquired at a flow rate of 2.0 mL min^{-1}, gradient 10–100 (%B), over 15.0 min, with detection at 220 nm and 254 nm.

Melting points were recorded on a Büchi Melting Point M-565. IR spectra were recorded on a PerkinElmer Spectrum Two™ FTIR Spectrometer with the UATR accessories. Thin layer chromatography (TLC) was performed on Merck 60 F254 pre-coated aluminium plates with a thickness of 0.2 mm. Column chromatography was performed under 'flash' conditions on Merck silica gel 60 (230–400 mesh).

Experimental data

Compounds **5** and **10**–**19** were prepared as described in ref. 48. The relative configuration for the obtained products was assigned computationally as follow: each of the initial geometry of each analogue (**14**–**16**) was built using the molecular builder of Molecular Operating Environment (MOE). Each molecule was relaxed using the semi-empirical AM1 method in MOE with a root mean square (rms) gradient of 0.01. Each analogue was subjected to conformational analysis using Stochastic Conformational Search method. The most stable conformation for each analogue was retained and saved as a mol2 file format. Each conformer was subjected to geometry optimization at DFT level of theory using B3LYP function with the 6-31+G(d,p) basis set. At this stage the DFT energy was calculated. The optimized structures were used for the calculation of NMR chemical shifts (relative to TMS) using the GIAO (gauge-independent (or including) atomic orbitals) method and the B3LYP functional with the 6-311+G(2d,p) basis set. The calculated DFT energy and ^{1}HNMR chemical shifts for selected peaks were used for assigning the configuration for the major and minor isomeric products (ESI, Table S1†).

2-(3-Cyano-2-oxo-4-methylquinolin-1(2*H*)-yl)-2-(1-methyl-1*H*-indol-3-yl)-*N*-(pentan-2-yl)acetamide (20). General procedure: A solution of MeOH (5.0 mL), 2-aminoacetophenone (0.148 mL, 1.23 mmol) and 1-methyl-1*H*-indole-3-carboxaldehyde (0.196 g, 1.23 mmol) was stirred at room temperature for 0.5 h. To the stirred solution was added cyanoacetic acid (0.105 g, 1.23 mmol) followed by the addition of 2-pentylisocyanide (0.152 mL, 1.23 mmol). The reaction mixture was stirred at room temperature for 24 h and the crude material was subjected to silica gel column chromatography (1 : 4 hexanes–EtOAc) to afford 4 (70 mg, 13%) as an off white solid (mp 243–245 °C).

IR (cm^{-1}): 3246 (NH), 3083 (CH), 2972 (CH), 2229 (CN), 1637 (CO); the ^1H NMR displays a mixture of isomers, with the ratio 1.35 : 1.0 calculated at 0.74 and 0.60 ppm, respectively. ^1H is reported as a whole without splitting due to the complex overlapping. All peaks detected in ^{13}C are reported. ^1H NMR (400 MHz, DMSO-d_6) δ 7.91 (d, J = 8.2 Hz, 1H), 7.83–7.69 (m, 2H), 7.67–7.51 (m, 2H), 7.47–7.35 (m, 3H), 7.29 (dd, J = 9.8, 5.4 Hz, 1H), 7.13 (t, J = 7.6 Hz, 1H), 7.01 (t, J = 7.4 Hz, 1H), 3.98–3.86 (m, 1H), 3.75 (s, 3H), 2.75 (d, J = 3.2 Hz, 3H), 1.54–1.15 (m, 4H), 0.93–0.87 (m, 3H), 0.77–0.56 (m, 2H); ^{13}C NMR (101 MHz, DMSO-d_6) δ 167.4, 166.8, 159.2, 159.2, 158.3, 158.3, 139.1, 136.6, 136.5, 133.3, 133.2, 130.9, 130.81, 127.7, 127.6, 127.6, 123.4, 121.9, 120.1, 120.1, 119.8, 118.9, 118.1, 118.1, 116.2, 110.4, 107.7, 106.2, 106.1, 106.1, 60.2, 53.8, 53.7, 52.9, 45.3, 45.2, 38.3, 38.0, 33.0 (C × 2), 27.4, 26.8, 21.2, 21.1, 20.8, 19.6, 19.1, 18.8, 14.6, 14.3, 14.2, 11.2, 10.8; LRMS (ESI–) m/z 440, 520 $[M + DMSO + 2H]^+$ 100%. HRMS (ES+) for $C_{27}H_{28}N_4O_3Na$; calculated 463.2110, found 463.2104; RP-HPLC Alltima™ C18 5 μm 150 mm × 4.6 mm, 10–100% B in 15 min, R_t min = 7.07, 93%.

2-(3-Cyano-2-oxo-4-phenylquinolin-1(2*H*)-yl)-2-(1*H*-indol-3-yl)-*N*-(pentan-2-yl)acetamide (21). Synthesized utilizing the general procedure described above, from 2-aminobenzophenone (0.252 g, 1.28 mmol), indole-3-carboxaldehyde (0.186 g, 1.28 mmol), cyanoacetic acid (0.109 g, 1.28 mmol) and 2-pentylisocyanide (0.158 mL, 1.28 mmol) in MeOH (5.0 mL) to afford 6 (0.07 g, 11%) as an off white solid (mp 182–183 °C).

IR (cm^{-1}): 3420 (NH), 2229 (CN), 1678 (CONH), 1646 (CON); the ^1H NMR displays a mixture of isomers, with the ratio 5.5 : 1.0 calculated at 3.96 and 3.72 ppm, respectively. ^1H is reported as a whole without splitting due to the complex overlapping. All peaks detected in ^{13}C are reported ^1H NMR (400 MHz, DMSO-d_6) δ 11.26 (s, 1H), 7.85 (s, 2H), 7.73–7.32 (m, 10H), 7.29–6.87 (m, 4H), 3.96 (s, 1H), 1.84–0.09 (m, 11H); ^{13}C NMR (101 MHz, DMSO) δ 167.4, 166.8, 160.1, 159.3, 140.1, 136.2, 136.1, 134.1, 133.3, 130.4, 129.3, 129.2, 129.1, 127.4, 127.3, 127.0, 126.9, 123.5, 122.0, 119.9, 119.8, 118.8, 118.6, 116.0, 112.2, 108.5, 106.0, 54.3, 54.2, 53.0, 45.4, 45.3, 38.4, 38.2, 27.4, 26.9, 21.1, 20.9, 19.6, 19.2, 14.4, 14.2, 11.3, 10.8; LRMS (ESI+) m/z 488, 489 $[M + H]^+$, 40%. HRMS (ES+) for $C_{31}H_{28}N_4O_2$; calculated 489.2285, found 489.2284; RP-HPLC Phenomenex Onyx™ Monolithic C18 5 μm 100 mm × 4 mm, 10–100% B in 15 min, R_t min = 12.24, 100%.

2-(3-Cyano-2-oxo-4-phenylquinolin-1(2*H*)-yl)-2-(1*H*-indol-5-yl)-*N*-(pentan-2-yl)acetamide (22). Synthesized utilizing the general procedure described above, from 2-aminobenzophenone (0.267 g, 1.35 mmol), indole-5-carboxaldehyde (0.197 g, 1.35 mmol), cyanoacetic acid (0.115 g, 1.35 mmol) and 2-pentylisocyanide (0.167 mL, 1.35 mmol) in MeOH (5.0 mL) to afford 6 (0.238 g, 36%) as an off white solid (mp 271–272 °C).

IR (cm^{-1}): 3403 (NH), 3338 (NH), 2956 (CH), 2235(CN), 1647 (CO); the ^1H NMR displays a mixture of isomers, with the ratio 2.45 : 1.0 calculated at 0.74 and 0.64 ppm, respectively. ^1H is reported as a whole without splitting due to the complex overlapping. All peaks detected in ^{13}C are reported ^1H NMR (400 MHz, DMSO-d_6) δ 11.13 (s, 1H), 7.89 (dd, J = 14.3, 8.1 Hz, 1H), 7.71–7.52 (m, 7H), 7.52–7.44 (m, 1H), 7.41–7.29 (m, 2H), 7.26–7.01 (m, 4H), 6.40 (d, J = 1.8 Hz, 1H), 3.91 (dd, J = 13.4, 7.0 Hz, 1H), 1.59–1.19 (m, 3H), 1.16–0.99 (m, 2H), 0.99–0.84 (m, 3H), 0.81–0.55 (m, 2H).

^{13}C NMR (101 MHz, DMSO-d_6) δ 167.5, 167.0, 166.9, 160.1, 160.0, 159.4, 140.6, 135.6, 134.2, 134.2, 133.1, 133.0, 130.4, 129.3 (C × 2), 129.2 (C × 2), 129.1, 129.1, 128.0, 126.5, 126.5, 125.8, 125.7, 125.6, 123.5, 121.8, 120.1, 120.1, 120.0, 119.1, 119.0, 116.0, 116.0, 111.9, 111.9, 106.3, 106.3, 106.2, 101.8, 101.7, 61.3, 61.1, 61.1, 52.8, 45.3, 45.2, 38.3, 38.2, 27.2, 26.8, 21.2, 20.9, 19.5, 19.0, 14.4, 14.3, 11.1, 10.6; LRMS (ESI–) m/z −488, 520 $[M + CH_3OH - H]$ 95%. HRMS (ES+) for $C_{31}H_{28}N_4O_2$; calculated 489.2285, found 489.2284.

RP-HPLC Alltima™ C18 5 μm 150 mm × 4.6 mm, 10–100% B in 15 min, R_t min = 7.07, >98%.

2-(3-Cyano-2-oxo-4-phenylquinolin-1(2*H*)-yl)-2-(5-methyl-1*H*-indole-3-yl)-*N*-(pentan-2-yl) acetamide (23). Synthesized utilizing the general procedure described above, from 2-aminobenzophenone (0.378 g, 1.92 mmol), 5-methyl-1*H*-indole carbaldehyde (0.305 g, 1.92 mmol), cyanoacetic acid (0.163 g, 1.92 mmol), and 2-pentylisocyanide (0.237 mL, 1.92 mmol) to afford 23 (0.445 g, 46%) as an off white solid (mp 178–180 °C).

IR (cm^{-1}): 3427 (br NH), 2962(CH), 2236 (CN), 1645(CON); the ^1H NMR displays a mixture of isomers, with the ratio 2.1 : 1.0 calculated at 0.77 and 0.68 ppm, respectively. ^1H is reported as a whole without splitting due to the complex overlapping. All peaks detected in ^{13}C are reported ^1H NMR (400 MHz, DMSO-d_6) δ 11.13 (d, J = 4.9 Hz, 1H), 7.90–7.37 (m, 10H), 7.29–7.16 (m, 4H), 6.92 (d, J = 8.3 Hz, 1H), 4.03–3.87 (m, 1H), 2.34 (s, 3H), 1.57–1.20 (m, 3H), 1.20–0.86 (m, 5H), 0.82–0.60 (m, 3H); ^{13}C NMR (101 MHz, DMSO-d_6) δ 167.5, 166.9, 160.1, 160.1, 159.3, 140.1, 140.1, 134.6, 134.6, 134.5, 134.1, 133.3, 130.4, 129.4, 129.2, 129.1, 128.2, 128.1, 127.5, 127.5, 126.8, 126.6, 123.5, 119.9, 118.5, 118.4, 118.3, 116.0, 111.9, 107.9, 107.9, 106.0, 105.9, 54.5, 54.4, 52.9, 45.4, 45.2, 38.4, 38.2, 27.3, 26.9, 21.9, 21.1, 20.9, 19.6, 19.2, 14.4, 14.2, 11.2, 10.8; LRMS (ESI–) m/z 502, 521 $[M + NH_4]^+$ 40%. HRMS (ES+) for $C_{32}H_{30}N_4O_2$; calculated 503.2442, found 503.2444; RP-HPLC Alltima™ C18 5 μm 150 mm × 4.6 mm, 10–100% B in 15 min, R_t min = 10.89, 100%.

Ethyl-[2-(3-Cyano-2-oxo-4-phenyl-2*H*-quinolin-1-yl)-2-(5-methyl-1*H*-indol-3-yl)-acetamido]-acetate (24). Synthesized utilizing the general procedure described above, from 2-aminobenzophe-

none (0.390 g, 1.98 mmol), 5-methyl-indole-3-carboxaldehyde (0.315 g, 1.98 mmol), cyanoacetic acid (0.168 g, 1.98 mmol) and ethyl isocyanoacetate (0.216 mL, 1.98 mmol) in MeOH (5.0 mL) to afford **9** (0.347 g, 34%) as a greenish solid (mp 199–200 °C).

IR (cm^{-1}): 3423 (NH), 3410 (NH), 2232 (CN), 1731 (COO), 1673 (CON); ^{1}H NMR (400 MHz, DMSO-d_6) δ 11.21 (d, J = 1.8 Hz, 1H), 8.53 (s, 1H), 7.83 (d, J = 8.7 Hz, 1H), 7.72–7.48 (m, 8H), 7.32–7.17 (m, 4H), 6.92 (d, J = 8.3 Hz, 1H), 4.14 (q, J = 7.1 Hz, 2H), 4.02–3.84 (m, 2H), 2.34 (s, 3H), 1.22 (t, J = 7.1 Hz, 3H); ^{13}C NMR (101 MHz, DMSO-d_6) δ 170.2, 168.4, 160.3, 159.3, 139.7, 134.5, 134.1, 133.5, 130.5, 129.4, 129.4, 129.4, 129.1, 129.0, 128.3, 127.5, 127.1, 123.7 (C × 2), 119.9, 118.5, 118.2, 115.8, 111.9, 107.3, 105.8, 61.0, 53.8, 41.9, 21.9, 14.6; LRMS (ESI+) m/z 518, 541 $[M + Na - H]^+$ 60%. HRMS (ES+) for $C_{31}H_{26}N_4O_4$; calculated 519.2027, found 519.2026; RP-HPLC Alltima™ C18 5 μm 150 mm × 4.6 mm, 10–100% B in 15 min, R_t min = 13.72, >97%.

Ethyl-[2-(3-cyano-2-oxo-4-phenyl-2*H*-quinolin-1-yl)-2-(1*H*-indol-3-yl)-acetamido]-acetate (25). Synthesized utilizing the general procedure described above, from 2-aminobenzophenone (0.366 g, 1.86 mmol), 1*H*-indole carbaldehyde (0.269 g, 1.86 mmol), cyanoacetic acid (0.157 g, 1.86 mmol), and ethyl isocyanoacetate (0.202 mL, 1.86 mmol) to afford **25** (0.30 g, 46%) as an off white solid (mp 179.3–180.5 °C).

IR (cm^{-1}): 3420 (NH), 2236 (CN), 1737 (COO), 1686 (CONH), 1646 (CON); ^{1}H NMR (400 MHz, DMSO-d_6) δ 11.35 (s, 1H), 8.58 (s, 1H), 7.93–7.75 (m, 2H), 7.75–7.45 (m, 8H), 7.39 (d, J = 8.0 Hz, 1H), 7.21 (d, J = 3.7 Hz, 2H), 7.15–6.91 (m, 2H), 4.25–4.06 (m, 2H), 4.04–3.80 (m, 2H), 1.22 (t, J = 7.0 Hz, 3H); ^{13}C NMR (101 MHz, DMSO-d_6) δ 170.2, 168.4, 160.3, 159.3, 139.7, 136.1, 134.0, 133.5, 130.5, 129.5, 129.4 (C × 2), 129.3 (C × 2), 129.2, 129.0, 127.3, 123.7, 122.1, 120.0 (C × 2), 118.6, 118.5, 115.9, 112.2, 107.8, 105.8, 61.1, 53.7 41.9, 14.6; LRMS (ESI+) m/z 504, 505 $[M + H]^+$, 100%. HRMS (ES+) for $C_{30}H_{24}N_4O_4$; calculated 505.1870, found 505.1869; RP-HPLC Phenomenex Onyx™ Monolithic C18 5 μm 100 mm × 4 mm, 10–100% B in 15 min, R_t min = 11.09, 100%.

Ethyl-[2-(3-cyano-2-oxo-4-phenyl-2*H*-quinolin-1-yl)-2-(1-methyl-indole-3-yl)-acetamido]-acetate (26). Synthesized utilizing the general procedure described above, from 2-aminobenzophenone (0.281 g, 1.43 mmol), 1-methyl-indole-3-carboxaldehyde (0.227 g, 1.43 mmol), cyanoacetic acid (0.121 g, 1.43 mmol) and ethyl isocyanoacetate (0.156 mL, 1.43 mmol) in MeOH (5.0 mL). The crude material was subjected to silica gel column chromatography (1 : 1 hexanes–EtOAc) to afford **26** (0.192 g, 26%) as an off white solid (mp 209–211 °C).

IR (cm^{-1}): 3422 (NH), 2920 (CH), 2229 (CN), 1743 (COO), 1639 (CON); ^{1}H NMR (400 MHz, DMSO-d_6) δ 8.53 (bs, 1H), 7.85 (d, J = 8.8 Hz, 1H), 7.75 (s, 1H), 7.70–7.48 (m, 7H), 7.43 (d, J = 8.2 Hz, 1H), 7.25–7.19 (m, 2H), 7.17 (t, J = 7.2 Hz, 1H), 7.06 (t, J = 7.2 Hz, 1H), 4.12 (q, J = 7.1 Hz, 2H), 3.90 (d, J = 6.6 Hz, 2H), 3.79 (s, 3H), 1.20 (t, J = 7.1 Hz, 3H); ^{13}C NMR (101 MHz, DMSO-d_6) δ 170.1, 168.3, 160.3, 159.2, 139.6, 136.5, 134.0, 133.7, 131.4, 130.5, 129.5, 129.4 (C × 2), 129.2, 129.0, 127.7, 123.7, 122.1, 120.1, 120.0, 118.9, 118.2, 115.9, 110.5, 106.8, 105.9, 105.9, 61.0, 41.9, 33.2, 14.6; LRMS (ESI−) m/z 518, 540 $[M + Na - H]^-$, 100%. HRMS (ES+) for $C_{31}H_{26}N_4O_4$; calculated 519.2027, found 519.2027; RP-HPLC Alltima™ C18 5 μm 150 mm × 4.6 mm, 10–100% B in 15 min, R_t min = 14.26, >98%.

Ethyl-3-[2-(3-cyano-2-oxo-4-phenyl-2*H*-quinolin-1-yl)-2-(1-methyl-1*H*-indol-3-yl)-acetylamino]-propionate (27). Synthesized utilizing the general procedure described above, from 2-aminobenzophenone (0.186 g, 0.94 mmol), 1-methyl-indole-3-carboxaldehyde (0.15 g, 0.94 mmol), cyanoacetic acid (0.08 g, 0.94 mmol) and ethyl isocyanopropionate (0.12 mL, 0.94 mmol) in MeOH (5.0 mL) to afford **27** (0.149 g, 50%) as a white solid (mp 267–268 °C).

IR (cm^{-1}): 3410 (NH), 2232 (CN), 1725 (COO), 1686 (CON); ^{1}H NMR (400 MHz, DMSO-d_6) δ 8.05 (bs, 1H), 7.83 (d, J = 8.7 Hz, 1H), 7.71–7.56 (m, 6H), 7.56–7.47 (m, 2H), 7.45–7.38 (m, 2H), 7.26–7.20 (m, 2H), 7.17 (t, J = 7.2 Hz, 1H), 7.06 (t, J = 7.2 Hz, 1H), 4.03 (q, J = 7.1 Hz, 2H), 3.78 (s, 3H), 3.42–3.35 (m, 2H), 2.57–2.44 (m, 2H), 1.16 (t, J = 7.1 Hz, 3H); ^{13}C NMR (101 MHz, DMSO-d_6) δ 171.7, 167.7, 160.1, 159.0, 139.9, 136.5, 134.1, 133.8, 131.3, 130.5, 129.6, 129.4, 129.2, 129.0, 127.8, 123.7, 122.1, 120.0, 119.9, 119.0, 117.8, 115.9, 110.5, 107.1, 106.1, 60.4, 54.1, 35.9, 34.0, 33.1, 14.5; LRMS (ESI+) m/z 532, 287 $[M + ACN + 2H]^{2+}$ 100%. HRMS (ES+) for $C_{16}H_{11}N_2O^+$ (main fragment); calculated 247.087, found 247.0865; RP-HPLC Alltima™ C18 5 μm 150 mm × 4.6 mm, 10–100% B in 15 min, R_t min = 14.46, >95%.

Ethyl-2-(2-(5-chloro-indole (1*H*)-3-yl)-2-(3-cyano-2-oxo-4-phenyl-1(2*H*)-quinolin-yl)-acetamido)-acetate (28). Synthesized utilizing the general procedure described above, from 2-aminobenzophenone (0.478 g, 2.4 mmol), 5-chloro-indole-3-carboxaldehyde (0.434 g, 2.4 mmol), cyanoacetic acid (0.204 g, 2.4 mmol) and ethyl isocyanoacetate (0.271 mL, 2.4 mmol) in MeOH (5.0 mL) to afford **28** (0.435 g, 33%) as a yellowish precipitate (mp 201–203 °C).

IR (cm^{-1}): 3415 (NH), 3406 (NH), 2236 (CN), 1736 (COO), 1671 (CON); ^{1}H NMR (400 MHz, DMSO-d_6) (isomeric mixture) δ 11.54 (d, J = 1.4 Hz, 1H), 8.53 (s, 1H), 7.82 (dd, J = 11.9, 5.5 Hz, 2H), 7.71–7.61 (m, 4H), 7.61–7.5 (m, 4H), 7.42 (d, J = 8.6 Hz, 1H), 7.29–7.18 (m, 2H), 7.12 (dd, J = 8.6, 1.7 Hz, 1H), 4.14 (q, J = 7.0 Hz, 2H), 3.93 (qd, J = 17.2, 5.8 Hz, 2H), 1.22 (t, J = 7.1 Hz, 3H); ^{13}C NMR (101 MHz, DMSO-d_6) δ 170.1, 168.2, 160.4, 159.2, 139.6, 134.6, 134.0, 133.7, 130.5, 129.6(C × 2), 129.4, 129.2, 129.0 (C × 2), 128.5, 124.5, 123.8, 122.0, 120.1, 118.3 (C × 2), 118.2, 115.8, 113.8, 107.8, 106.0, 61.0, 42.0, 14.6; LRMS (ESI+) m/z 538, 292 $[M + 2Na]^{2+}$, 60%. HRMS for $C_{30}H_{23}ClN_4O_4$; calculated 539.1481, found 539.1481; RP-HPLC Alltima™ C18 5 μm 150 mm × 4.6 mm, 10–100% B in 15 min, R_t min = 14.07, >99%.

***N*-*tert*-Butyl-2-(3-cyano-2-oxo-4-phenyl-2*H*-quinolin-1-yl)-2-(5-methyl-1*H*-indol-3-yl)-acetamide (29).** Synthesized utilizing the general procedure described above, from 2-aminobenzophenone (0.359 g, 1.83 mmol), 5-methyl-indole-3-carboxaldehyde (0.290 g, 1.83 mmol), cyanoacetic acid (0.156 g, 1.83 mmol) and *tert*-butyl isocyanide (0.207 mL, 1.83 mmol) in MeOH (5.0 mL) to afford **29** (0.419 g, 47%) as a white solid (mp 196–198 °C).

IR (cm^{-1}): 3427(NH), 2978 (CH), 2228 (CN), 1650 (CON); ^1H NMR (400 MHz, DMSO-d_6) (isomeric mixture) δ 11.13 (d, J = 4.9 Hz, 1H), 7.90–7.37 (m, 10H), 7.29–7.16 (m, 4H), 6.92 (d, J = 8.3 Hz, 1H), 4.03–3.87 (m, 1H), 2.34 (s, 3H), 1.57–1.20 (m, 3H), 1.20–0.86 (m, 5H), 0.82–0.60 (m, 3H); ^{13}C NMR (101 MHz, DMSO) (isomeric mixture) δ 167.5, 166.9, 160.1, 160.1, 159.3, 140.1, 140.1, 134.6, 134.6, 134.5, 134.1, 133.3, 130.4, 129.4, 129.2, 129.1, 128.2, 128.1, 127.5, 127.5, 126.8, 126.6, 23.5, 19.9, 118.48, 118.4, 118.3, 116.0, 111.9, 107.9, 107.9, 106.0, 105.9, 54.5, 54.4, 52.9, 45.4, 45.2, 38.4, 38.2, 27.3, 26.9, 21.9, 21.1, 20.9, 19.6, 19.2, 14.4, 14.2, 11.2, 10.8; LRMS (ESI−) m/z 488, 243 $[M - 2H]^{2+}$, 90%. HRMS for $C_{31}H_{28}N_4O_2$; calculated 489.2285, found 489.2283; RP-HPLC Alltima™ C18 5μm 150 mm × 4.6 mm, 10–100% B in 15 min, R_t min = 14.59, >95%.

***N*-*tert*-Butyl-2-(3-cyano-2-oxo-4-phenyl-2*H*-quinolin-1-yl)-2-(1-methyl-1*H*-indole-3-yl)-acetamide (30).** Synthesized utilizing the general procedure described above, from 2-aminobenzophenone (0.311 g, 1.58 mmol), 1-methyl-indole-3-carboxaldehyde (0.251 g, 1.58 mmol), cyanoacetic acid (0.134 g, 1.58 mmol) and *tert*-butyl isocyanide (0.178 mL, 1.58 mmol) in MeOH (5.0 mL) to afford **29** (0.200 g, 26%) as a white solid (mp 232–234 °C).

IR (cm^{-1}): 3357 (NH), 2979 (CH), 2229 (CN), 1650 (CO); ^1H NMR (400 MHz, DMSO) δ 7.89 (d, J = 8.8 Hz, 1H), 7.68–7.46 (m, 9H), 7.43 (d, J = 7.8 Hz, 2H), 7.22–7.13 (m, 3H), 7.06 (t, J = 7.4 Hz, 1H), 3.79 (s, 3H), 1.32 (s, 9H); ^{13}C NMR (101 MHz, DMSO) δ 166.66, 160.13, 159.17, 140.28, 136.75, 134.09, 133.34, 130.54, 130.42, 129.31 (C × 3), 129.15 (C × 2), 127.48, 123.52, 122.17, 119.99, 119.78, 119.04, 118.55, 115.91, 110.53, 108.04, 105.89, 54.94, 51.57, 33.09, 28.83 (C × 3); LRMS (ESI+) m/z 488, 243 $[M - 2H]^{2+}$, 100%. HRMS (ES+) for $C_{31}H_{28}N_4O_2$; calculated 489.2285, found 489.2287; RP-HPLC Alltima™ C18 5 μm 150 mm × 4.6 mm, 10–100% B in 15 min, R_t min = 7.03, 96%.

More information on the synthesis and characterization of the analogues can be found in the ESI.†

Acknowledgements

The authors thank the NHMRC (Australia) for project support, Nathan Druery Smith (Analytical and Biomolecular Research Facility at the University of Newcastle) for the HRMS data, James K. Chen for helpful discussions and T. N. T. is the recipient of a Prime Minister's Australia Asia Postgraduate Endeavour Award.

References

1 A. P. McMahon, P. W. Ingham and C. J. Tabin, *Curr. Top. Dev. Biol.*, 2003, **53**, 1–114.
2 P. W. Ingham, *Genes Dev.*, 2001, **15**, 3059–3087.
3 E. H. Epstein, *Nat. Rev. Cancer*, 2008, **8**, 743–754.
4 C. Raffel, R. B. Jenkins, L. Frederick, D. Hebrink, B. Alderete, D. W. Fults and C. D. James, *Cancer Res.*, 1997, **57**, 842–845.
5 T. Pietsch, A. Waha, A. Koch, J. Kraus, S. Albrecht, J. Tonn, N. Sorensen, F. Berthold, B. Henk, N. Schmandt, H. K. Wolf, A. von Deimling, B. Wainwright, G. Chenevix-Trench, O. D. Wiestler and C. Wicking, *Cancer Res.*, 1997, **57**, 2085–2088.
6 D. G. Evans, P. A. Farndon, L. D. Burnell, H. R. Gattamaneni and J. M. Birch, *Br. J. Cancer*, 1991, **64**, 959–961.
7 S. P. Thayer, M. Pasca di Magliano, P. W. Heiser, C. M. Nielsen, D. J. Roberts, G. Y. Lauwers, Y. P. Qi, S. Gysin, C. Fernandez-del Castillo, V. Yajnik, B. Antoniu, M. McMahon, A. L. Warshaw and M. Hebrok, *Nature*, 2003, **425**, 851–856.
8 S. Karhadkar Sunil, G. S. Bova, N. Abdallah, S. Dhara, D. Gardner, A. Maitra, T. Isaacs John, M. Berman David and A. Beachy Philip, *Nature*, 2004, **431**, 707–712.
9 Z. Yuan, J. A. Goetz, S. Singh, S. K. Ogden, W. J. Petty, C. C. Black, V. A. Memoli, E. Dmitrovsky and D. J. Robbins, *Oncogene*, 2007, **26**, 1046–1055.
10 D. N. Watkins, M. Berman David, G. Burkholder Scott, B. Wang, A. Beachy Philip and B. Baylin Stephen, *Nature*, 2003, **422**, 313–317.
11 D. Qualtrough, A. Buda, W. Gaffield, C. Williams Ann and C. Paraskeva, *Int. J. Cancer*, 2004, **110**, 831–837.
12 D. M. Berman, S. S. Karhadkar, A. Maitra, R. Montes De Oca, M. R. Gerstenblith, K. Briggs, A. R. Parker, Y. Shimada, J. R. Eshleman, D. N. Watkins and P. A. Beachy, *Nature*, 2003, **425**, 846–851.
13 M. Kasper, V. Jaks, M. Fiaschi and R. Toftgaard, *Carcinogenesis*, 2009, **30**, 903–911.
14 S. Mukherjee, N. Frolova, A. Sadlonova, Z. Novak, A. Steg, G. P. Page, D. R. Welch, S. M. Lobo-Ruppert, J. M. Ruppert, M. R. Johnson and A. R. Frost, *Cancer Biol. Ther.*, 2006, **5**, 674–683.
15 X. Chen, A. Horiuchi, N. Kikuchi, R. Osada, J. Yoshida, T. Shiozawa and I. Konishi, *Cancer Sci.*, 2007, **98**, 68–76.
16 M. Zbinden, A. Duquet, A. Lorente-Trigos, S.-N. Ngwabyt, I. Borges and A. Ruiz i Altaba, *EMBO J.*, 2010, **29**, 2659–2674.
17 A. Po, E. Ferretti, E. Miele, E. De Smaele, A. Paganelli, G. Canettieri, S. Coni, L. Di Marcotullio, M. Biffoni, L. Massimi, C. Di Rocco, I. Screpanti and A. Gulino, *EMBO J.*, 2010, **29**, 2646–2658.
18 FDA approves new treatment for most common form of advanced skin cancer, http://www.fda.gov/NewsEvents/Newsroom/PressAnnouncements/ucm455862.htm.
19 FDA approves new treatment for most common type of skin cancer http://www.fda.gov/NewsEvents/Newsroom/PressAnnouncements/ucm289545.htm.
20 T. N. Trinh, E. A. McLaughlin, C. P. Gordon and A. McCluskey, *MedChemComm*, 2014, **5**, 117–133.
21 R. Nanta, D. Kumar, D. Meeker, M. Rodova, P. J. Van Veldhuizen, S. Shankar and R. K. Srivastava, *Oncogenesis*, 2013, **2**, e42, DOI: 10.1038/oncsis.2013.5.

22 J. K. Chen, J. Taipale, K. E. Young, T. Maiti and P. A. Beachy, *Proc. Natl. Acad. Sci. U. S. A.*, 2002, **99**, 14071–14076.
23 R. Maun Henry, X. Wen, A. Lingel, J. de Sauvage Frederic, A. Lazarus Robert, J. Scales Suzie and G. Hymowitz Sarah, *J. Biol. Chem.*, 2010, **285**, 26570–26580.
24 B. Z. Stanton, L. F. Peng, N. Maloof, K. Nakai, X. Wang, J. L. Duffner, K. M. Taveras, J. M. Hyman, S. W. Lee, A. N. Koehler, J. K. Chen, J. L. Fox, A. Mandinova and S. L. Schreiber, *Nat. Chem. Biol.*, 2009, **5**, 154–156.
25 J. Kim, B. T. Aftab, J. Y. Tang, D. Kim, A. H. Lee, M. Rezaee, J. Kim, B. Chen, E. M. King, A. Borodovsky, G. J. Riggins, E. H. Epstein, P. A. Beachy and C. M. Rudin, *Cancer Cell*, 2013, **23**, 23–34.
26 A. Solinas, H. Faure, H. Roudaut, E. Traiffort, A. Schoenfelder, A. Mann, F. Manetti, M. Taddei and M. Ruat, *J. Med. Chem.*, 2012, **55**, 1559–1571.
27 T. Ohashi, Y. Oguro, T. Tanaka, Z. Shiokawa, Y. Tanaka, S. Shibata, Y. Sato, H. Yamakawa, H. Hattori, Y. Yamamoto, S. Kondo, M. Miyamoto, M. Nishihara, Y. Ishimura, H. Tojo, A. Baba and S. Sasaki, *Bioorg. Med. Chem.*, 2012, **20**, 5507–5517.
28 M. J. Munchhof, Q. Li, A. Shavnya, G. V. Borzillo, T. L. Boyden, C. S. Jones, S. D. LaGreca, L. Martinez-Alsina, N. Patel, K. Pelletier, L. A. Reiter, M. D. Robbins and G. T. Tkalcevic, *ACS Med. Chem. Lett.*, 2012, **3**, 106–111.
29 S. Pan, X. Wu, J. Jiang, W. Gao, Y. Wan, D. Cheng, D. Han, J. Liu, N. P. Englund, Y. Wang, S. Peukert, K. Miller-Moslin, J. Yuan, R. Guo, M. Matsumoto, A. Vattay, Y. Jiang, J. Tsao, F. Sun, A. C. Pferdekamper, S. Dodd, T. Tuntland, W. Maniara, J. F. Kelleher III, Y.-m. Yao, M. Warmuth, J. Williams and M. Dorsch, *ACS Med. Chem. Lett.*, 2010, **1**, 130–134.
30 B He, N Fujii, L MYou, Z Xu and D M. Jablons, Dihydropyrazolecarboxamides and their preparation, pharmaceutical compositions and use in the targeting GLI proteins in human cancer by small molecules, *WO Pat*, 2009-GB509262010013037, 2010.
31 M. R. Tremblay, A. Lescarbeau, M. J. Grogan, E. Tan, G. Lin, B. C. Austad, L.-C. Yu, M. L. Behnke, S. J. Nair, M. Hagel, K. White, J. Conley, J. D. Manna, T. M. Alvarez-Diez, J. Hoyt, C. N. Woodward, J. R. Sydor, M. Pink, J. MacDougall, M. J. Campbell, J. Cushing, J. Ferguson, M. S. Curtis, K. McGovern, M. A. Read, V. J. Palombella, J. Adams and A. C. Castro, *J. Med. Chem.*, 2009, **52**, 4400–4418.
32 K. D. Robarge, S. A. Brunton, G. M. Castanedo, Y. Cui, M. S. Dina, R. Goldsmith, S. E. Gould, O. Guichert, J. L. Gunzner, J. Halladay, W. Jia, C. Khojasteh, M. F. T. Koehler, K. Kotkow, H. La, R. L. La Londe, K. Lau, L. Lee, D. Marshall, J. C. Marsters, L. J. Murray, C. Qian, L. L. Rubin, L. Salphati, M. S. Stanley, J. H. A. Stibbard, D. P. Sutherlin, S. Ubhayaker, S. Wang, S. Wong and M. Xie, *Bioorg. Med. Chem. Lett.*, 2009, **19**, 5576–5581.
33 M. R. Tremblay, M. Nevalainen, S. J. Nair, J. R. Porter, A. C. Castro, M. L. Behnke, L.-C. Yu, M. Hagel, K. White, K. Faia, L. Grenier, M. J. Campbell, J. Cushing, C. N. Woodward, J. Hoyt, M. A. Foley, M. A. Read, J. R. Sydor, J. K. Tong, V. J. Palombella, K. McGovern and J. Adams, *J. Med. Chem.*, 2008, **51**, 6646–6649.
34 V. Travaglione, C. Peacock, J. MacDougall, K. McGovern, J. Cushing, L. C. Yu, M. Trudeau, V. Palombella, J. Adams, J. Hierman, J. Rhodes, W. Devereux and D. N. Watkins, A novel HH pathway inhibitor, IPI-926, delays recurrence post-chemotherapy in a primary human SCLC xenograft model, *99th AACR Annual Meeting*, 2008, p. 4611.
35 M. Dai, F. He, R. K. Jain, R. Karki, J. F. Kelleher, J. Lei, L. Llamas, M. A. McEwan, K. Miller-Moslin, L. B. Perez, S. Peukert and N. Yusuff, Nitrogen-containing heterocyclic organic compounds as inhibitors of the hedgehog pathway and their preparation and use in the treatment of diseases. *WO Pat*, 2008-EP530402008110611, 2008.
36 J. Fu, M. Rodova, S. K. Roy, J. Sharma, K. P. Singh, R. K. Srivastava and S. Shankar, *Cancer Lett.*, 2013, **330**, 22–32.
37 Y. Rifai, M. A. Arai, S. K. Sadhu, F. Ahmed and M. Ishibashi, *Bioorg. Med. Chem. Lett.*, 2011, **21**, 718–722.
38 T. Mazumdar, J. DeVecchio, T. Shi, J. Jones, A. Agyeman and J. A. Houghton, *Cancer Res.*, 2011, **71**, 1092–1102.
39 M. A. Arai, C. Tateno, T. Koyano, T. Kowithayakorn, S. Kawabe and M. Ishibashi, *Org. Biomol. Chem.*, 2011, **9**, 1133–1139.
40 M. Actis, M. C. Connelly, A. Mayasundari, C. Punchihewa and N. Fujii, *Biopolymers*, 2011, **95**, 24–30.
41 N. Mahindroo, M. C. Connelly, C. Punchihewa, L. Yang, B. Yan and N. Fujii, *Bioorg. Med. Chem.*, 2010, **18**, 4801–4811.
42 N. Mahindroo, C. Punchihewa and N. Fujii, *J. Med. Chem.*, 2009, **52**, 3829–3845.
43 J. M. Hyman, A. J. Firestone, V. M. Heine, Y. Zhao, C. A. Ocasio, K. Han, M. Sun, P. G. Rack, S. Sinha, J. J. Wu, D. E. Solow-Cordero, J. Jiang, D. H. Rowitch and J. K. Chen, *Proc. Natl. Acad. Sci. U. S. A.*, 2009, **106**, 14132–14137.
44 T. Hosoya, M. A. Arai, T. Koyano, T. Kowithayakorn and M. Ishibashi, *ChemBioChem*, 2008, **9**, 1082–1092.
45 M. A. Arai, C. Tateno, T. Hosoya, T. Koyano, T. Kowithayakorn and M. Ishibashi, *Bioorg. Med. Chem.*, 2008, **16**, 9420–9424.
46 M. Lauth, A. Bergstroem, T. Shimokawa and R. Toftgard, *Proc. Natl. Acad. Sci. U. S. A.*, 2007, **104**, 8455–8460.
47 T. N. Trinh, L. Hizartzidis, A. J. S. Lin, D. G. Harman, A. McCluskey and C. P. Gordon, *Org. Biomol. Chem.*, 2014, **12**, 9562–9571.
48 C. P. Gordon, K. A. Young, L. Hizartzidis, F. M. Deane and A. McCluskey, *Org. Biomol. Chem.*, 2011, **9**, 1419.
49 H. Ajj, A. Chesnel, S. Pinel, F. Plenat, S. Flament and H. Dumond, *PLoS One*, 2013, **8**, e61758.
50 E. R. Cantwell-Dorris, J. J. O'Leary and O. M. Sheils, *Mol. Cancer Therap.*, 2011, **10**, 385–394.
51 J. de Jong, H. Stoop, A. J. M. Gillis, R. Hersmus, R. J. H. L. M. van Gurp, G.-J. M. van de Geijn, E. van Drunen, H. B. Beverloo, D. T. Schneider, J. K. Sherlock,

J. Baeten, S. Kitazawa, E. J. van Zoelen, K. van Roozendaal, J. W. Oosterhuis and L. H. J. Looijenga, *Genes, Chromosomes Cancer.*, 2008, **47**, 185–196.

52 H. Davies, G. R. Bignell, C. Cox, P. Stephens, S. Edkins, S. Clegg, J. Teague, H. Woffendin, M. J. Garnett, W. Bottomley, N. Davis, E. Dicks, R. Ewing, Y. Floyd, K. Gray, S. Hall, R. Hawes, J. Hughes, V. Kosmidou, A. Menzies, C. Mould, A. Parker, C. Stevens, S. Watt, S. Hooper, R. Wilson, H. Jayatilake, B. A. Gusterson, C. Cooper, J. Shipley, D. Hargrave, K. Pritchard-Jones, N. Maitland, G. Chenevix-Trench, G. J. Riggins, D. D. Bigner, G. Palmieri, A. Cossu, A. Flanagan, A. Nicholson, J. W. C. Ho, S. Y. Leung, S. T. Yuen, B. L. Weber, H. F. Seigler, T. L. Darrow, H. Paterson, R. Marais, C. J. Marshall, R. Wooster, M. R. Stratton and P. A. Futreal, *Nature*, 2002, **417**, 949–954.

53 B. Stecca, C. Mas, V. Clement, M. Zbinden, R. Correa, V. Piguet, F. Beermann and I. A. A. Ruiz, *Proc. Natl. Acad. Sci. U. S. A.*, 2007, **104**, 5895–5900.

54 A. N. Yoshimoto, C. Bernardazzi, A. Jose, V. Carneiro, C. C. S. Elia, C. A. Martinusso, G. M. Ventura, M. T. L. Castelo-Branco and H. S. P. de Souza, *PLoS One*, 2012, **7**, e45332.

55 G. Chatel, C. Ganeff, N. Boussif, L. Delacroix, A. Briquet, G. Nolens and R. Winkler, *Int. J. Cancer*, 2007, **121**, 2622–2627.

56 G. Bosco-Clement, F. Zhang, Z. Chen, H. M. Zhou, H. Li, I. Mikami, T. Hirata, A. Yagui-Beltran, N. Lui, H. T. Do, T. Cheng, H. H. Tseng, H. Choi, L. T. Fang, I. J. Kim, D. Yue, C. Wang, Q. Zheng, N. Fujii, M. Mann, D. M. Jablons and B. He, *Oncogene*, 2014, **33**, 2087–2097.

57 Y. Shi, X. Fu, Y. Hua, Y. Han, Y. Lu and J. Wang, *PLoS One*, 2012, **7**, e33358.

58 N. Bansal, N. J. Farley, L. Wu, J. Lewis, H. Youssoufian and J. R. Bertino, *Mol. Cancer Ther.*, 2015, **14**, 23–30.

59 T. Sheng, C. Li, X. Zhang, S. Chi, N. He, K. Chen, F. McCormick, Z. Gatalica and J. Xie, *Mol. Cancer*, 2004, **3**, 29.

60 L. Mao, Y.-P. Xia, Y.-N. Zhou, R.-L. Dai, X. Yang, S.-J. Duan, X. Qiao, Y.-W. Mei, B. Hu and H. Cui, *Cancer Sci.*, 2009, **100**, 1848–1855.

61 B. N. Singh, J. Fu, R. K. Srivastava and S. Shankar, *PLoS One*, 2011, **6**, e27306.

62 J. Taipale, J. K. Chen, M. K. Cooper, B. Wang, R. K. Mann, L. Milenkovic, M. P. Scotts and P. A. Beachy, *Nature*, 2000, **106**, 1005–1009.

63 P. H. Willoughby, M. J. Jansma and T. R. Hoye, *Nat. Protoc.*, 2014, **9**, 643–660.

64 Y. Tang, S. Gholamin, S. Schubert, M. I. Willardson, A. Lee, P. Bandopadhayay, G. Bergthold, S. Masoud, B. Nguyen, N. Vue, B. Balansay, F. Yu, S. Oh, P. Woo, S. Chen, A. Ponnuswami, M. Monje, S. X. Atwood, R. J. Whitson, S. Mitra, S. H. Cheshier, J. Qi, R. Beroukhim, J. Y. Tang, R. Wechsler-Reya, A. E. Oro, B. A. Link, J. E. Bradner and Y.-J. Cho, *Nat. Med.*, 2014, **20**, 732–740.

65 P. G. Rack, J. Ni, A. Y. Payumo, V. Nguyen, J. A. Crapster, V. Hovestadt, M. Kool, D. T. W. Jones, J. K. Mich, A. J. Firestone, S. M. Pfister, Y.-J. Cho and J. K. Chen, *Proc. Natl. Acad. Sci. U. S. A.*, 2014, **111**, 11061–11066.

66 A. P. Sobinoff, V. Pye, B. Nixon, S. D. Roman and E. A. McLaughlin, *Toxicol. Sci.*, 2010, **118**, 653–666.

3.2. References

1. J. M. Hyman, A. J. Firestone, V. M. Heine, Y. Zhao, C. A. Ocasio, K. Han, M. Sun, P. G. Rack, S. Sinha, J. J. Wu, D. E. Solow-Cordero, J. Jiang, D. H. Rowitch and J. K. Chen, *Proceedings of the National Academy of Sciences USA*, 2009, **106**, 14132-14137.
2. C. P. Gordon, K. A. Young, L. Hizartzidis, F. M. Deane and A. McCluskey, *Organic & Biomolecular Chemistry*, 2011, **9**, 1419.

IV. CHAPTER FOUR

Next generation inhibitors of the HSP: Targeting the Gli transcription factors

4.1. Introduction

In Chapter 3, we identified several small molecule inhibitors of the HSP based on the quinolone-1-(2*H*)-one scaffold (Figure 1). Displaying cytotoxicity against a number of human cancer cell lines expressing the HSP (Chapter 3, Table 1, page 57), these compounds demonstrated their anti-hedgehog properties through inhibiting Gli protein (Chapter 3, Figure 4, page 60) and *gene* expression (Chapter 3, Figure 5, page 60) in SAG-activated Shh LIGHT 2 cell line.

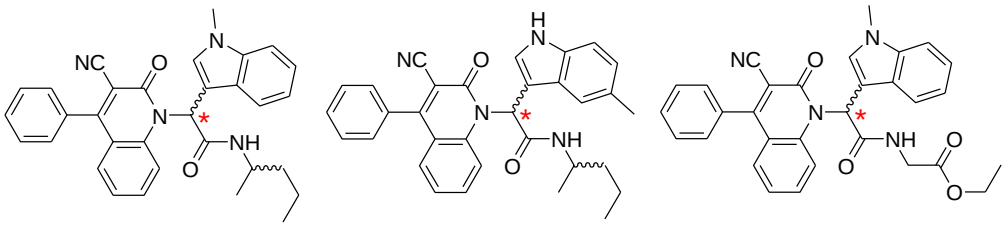

Figure 1. Quinolone-1-(2*H*)-ones **1-3** exhibit inhibitory activity against the HSP with the percent inhibition of GLI protein expression in SAG-activated Shh LIGHT 2 cell line -55%, -54%, and -31%, respectively (Chapter 3, Table 5, page 60).

It is uncertain whether these compounds directly target Smo or act downstream of the protein, as evidence indicates Smo may have multiple binding sites [1]. Whilst these analogues presented as promising lead compounds, an obvious limitation is that the reaction sequence affords a diastereomeric or racemic mixture [2]. However, the SAR from this initial series pointed to a requirement of an indole tethered at C3 to produce cytotoxicity (Chapter 3, page 59). Therefore, we believed that utilisation of tryptophan moieties may provide a means of accessing enantiopure analogues. To this end, a series of compounds generated from L-tryptophan were proposed (i.e. compound **4**, Figure 2). Further a series based on the benzo[1,3]dioxol-5-ylmethyl-[2-(1*H*-indol-3-yl)-ethyl]-amine scaffold, which lack a stereocentre (i.e. compound **5**, Figure 2) were also earmarked for synthesis. Both scaffolds possess a C3-tethered indole ring with controlled stereochemistry and can be easily modified to adopt the Ugi-Knoevenagel pharmacophore's features as shown in Figure 2.

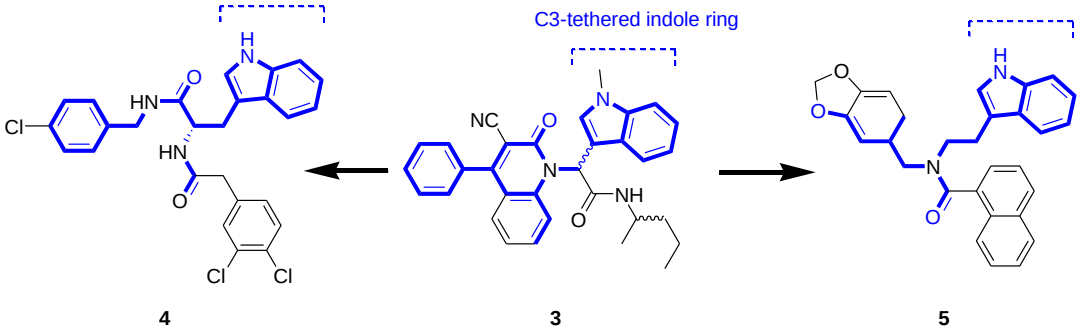

Figure 2. New scaffolds (represented by compounds **4** and **5**) were developed from the Ugi-Knoevenagel pharmacophore (compound **3**). Highlighted in blue structures present the structural similarities including the C3-tethered indole ring as the foundation for the subsequent development.

The inhibitory activity of these scaffolds is reported in the following publication submitted to *Organic and Biomolecular Chemistry* in October 2016. The supporting information is provided in the Appendix to Chapter 2 (please see Chapter 8, page 280).

Journal Name

ARTICLE

Small molecules inhibitors of Gli transcriptional factors of the Hedgehog Signalling Pathway

Received 00th January 20xx,

Accepted 00th January 20xx

DOI: 10.1039/x0xx00000x

www.rsc.org/

Trieu N. Trinh,[a] Eileen A. McLaughlin,[b†] Christopher P. Gordon,[a§] Ilana R. Bernstein,[b] Victoria A Pye, [b] Kate A. Redgrove, [b] and Adam McCluskey [a*]

Leveraging our quinolone-1-(2*H*)-ones we have developed two new classes of hedgehog signalling pathway inhibitors based on: L-tryptophan and benzo[1,3]dioxol-5-ylmethyl-[2-(1*H*-indol-3-yl)-ethyl]-amine. Synthesis of focused compound libraries identified six L-tryptophan based inhibitors of Gli and two stimulators at 10 μM concentration. 2,4-Dichloro- **13** and indole **16** suppressed mRNA expression of *Ptch*$_1$ in Shh LIGHT2 cells, with **13** suppressing and **16** stimulating *Gli*$_1$ mRNA expression. Focused library development of the benzo[1,3]dioxol-5-ylmethyl-[2-(1*H*-indol-3-yl)-ethyl]-amine afforded two sub-micro molar potent inhibitors of Gli expression with 5-methoxy-1*H*-indole-2-carboxylic acid benzo[1,3]dioxol-5-ylmethyl-[2-(1*H*-indol-3-yl)-ethyl]-amide **29** and 5-chloro-1*H*-indole-2-carboxylic acid benzo[1,3]dioxol-5-ylmethyl-[2-(1*H*-indol-3-yl)-ethyl]-amide **30** returning IC_{50} values of 0.5 and 0.24 μM, respectively. Neither **29** nor **30** acted directly on Smo with our data supporting inhibition of the HSP downstream of Smo.

Introduction

Since its discovery in the fruit fly (*Drosophila melanogaster)* in 1980, the Hedgehog Signalling Pathway (HSP) has been the focus of significant research as a potential target for next generation chemotherapeutic agents.[1] Under homeostatic conditions, the HSP is crucial to embryogenesis whereby it controls the spatial and temporal regulation of cell proliferation, differentiation, and tissue patterning.[2,3] However, abnormal activation of this pathway results in the formation of cancer stem cells,[4,5] and subsequent development of a variety of human cancers including basal cell carcinoma,[6] medulloblastoma,[7-9] cancers of the pancreas,[10] prostate,[11] lung,[12,13] colon,[14] stomach,[15] breast,[16,17] and ovary.[18] Consequently, targeting the HSP has become an attractive approach for the treatment of cancer and hence numerous HSP inhibitors have been developed in recent years.[19] Currently two HSP inhibitors, Vismodegib (**1**, GDC-0449, Erivedge®) and Sonidegib (**2**, LDE225, Odomzo®) (Figure 1), are in clinical use for the treatment of early and advanced basal cell carcinomas.[20, 21] These HSP inhibitors target the Smoothened (Smo) protein which results in downstream inhibition within the HSP.

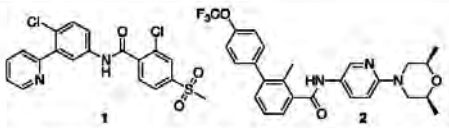

Figure 1. Chemical structures of the Smo inhibitors Vismodegib (1, GDC-0449, Erivedge®) and Sonidegib (2, LDE225, Odomzo®) approved by FDA for the treatment of early and advanced basal cell carcinomas.[20, 21]

In addition to Smo targeting, there are additional points in the HSP suitable for therapeutic intervention. The canonical HSP is hierarchical in nature, with a Hedgehog (Hh) ligand (either Sonic (Shh), Desert (Dhh) or Indian (Ihh) hedgehog protein) binding to the membrane receptor Patched$_1$ (Ptch$_1$) which subsequently activates the Smo protein and results in the release of active Glioma-Associated Oncogene Homolog transcriptional factors (Gli$_{1-3}$) into the cell nucleus.[2,3,19] These Gli transcription factors facilitate the transcription of Hh target genes, including the HSP components: Gli$_1$, Gli$_2$, Ptch$_1$ and Ptch$_2$.[22] Alternatively, the HSP can be activated directly at the Smo level by the synthetic Smo agonist (e.g., SAG) (Figure 2).[23] Suppression of abnormal HSP activation is possible through targeting the Hh-ligand-Ptch$_1$ interactions [24,25], Smo protein [23, 26-36] or further downstream of Smo through Gli transcription factor inhibition.[37-47] At present, the significant proportion of the most clinically advanced HSP inhibitor compounds target Smo. However, resistance to this inhibition has recently been observed, due in part to Smo mutations,[48, 49] or more commonly through the non-canonical overexpression of Gli$_2$ transcription factors by crosstalk with the TGF-β, p53, WIP1, PI3K/AKT and RAS/MEK pathways.[2, 3, 19, 50] Thus it is hypothesised that targeting the HSP further downstream of

[a] Chemistry, Priority Research Centre for Chemical Biology, University of Newcastle, University Drive Callaghan NSW 2308, Australia. * Phone: +61(2)49 216486; Fax: +61(2)49 215472; Email: Adam.McCluskey@newcastle.edu.au
[b] Biology, Priority Research Centre for Chemical Biology, University of Newcastle, University Drive Callaghan NSW 2308, Australia
[§] Nanoscale Organization and Dynamics Group, School of Science and Health, University of Western Sydney, Penrith South DC, NSW, Australia.
[†] Current Address: School of Biological Sciences, University of Auckland, Auckland, New Zealand.

Electronic Supplementary Information (ESI) available: NMR, IR and HPLC chromatographic traces. See DOI: 10.1039/x0xx00000x

Smo at the Gli transcription factors level and/or indirectly through interacting signalling pathways may present a more robust strategy for the treatment of HSP related cancers.[19, 44]

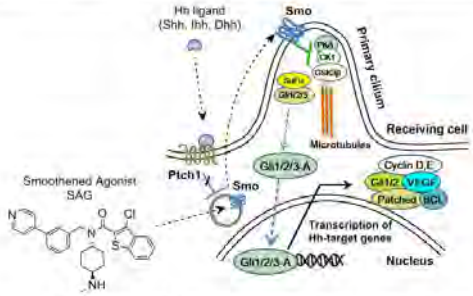

Figure 2. The canonical HSP is initiated by the binding of the Hh-ligand (Dhh, Shh, or Ihh) to the membrane receptor $Ptch_1$, resulting in the activation of Smo protein and releasing of active Gli transcriptional factors (Gli_{1-3}) into the nucleus. Consequently, the transcription of Hh target genes was activated.[20] Alternatively, the HSP can be activated directly at Smo level via SAG.[22] Figure reproduced from reference 51.

To this end we previously reported the development of a series of quinolone-1-(2*H*)-ones HSP inhibitors.[51] These analogues were active in human cancer cell lines expressing the HSP, and mediated their effects by inhibiting the overexpression of $Ptch_1$ and Gli_2 mRNA transcript in Shh LIGHT2 cells.[51] However, it is not known if these compounds directly target Smo or act downstream of the protein, as evidence indicates Smo may have multiple binding sites.[23] Additionally, the quinolone-1-(2*H*)-one scaffold presented key limitations for further development including uncontrolled product stereochemistry and the formation of undesired 3-component Ugi adducts.[51] Thus herein we report on the development of two new scaffolds based on our quinolone-1-(2*H*)-one pharmacophore (Figure 3).

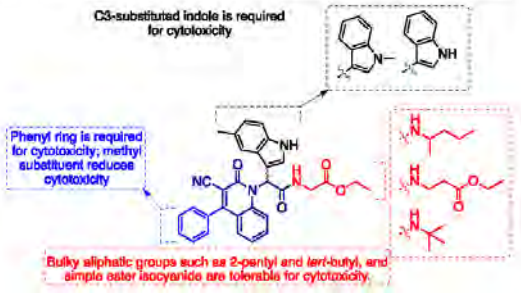

Figure 3. The Ugi-Knoevenagel pharmacophore with key features required for cytotoxicity in HSP expressing cancer cell lines highlighted.

Results and Discussion

From the examination of the previously developed quinolone-1-(2*H*)-one pharmacophore two potential new scaffolds were proposed with the potential to abrogate the aforementioned limitations (Figure 4). These scaffolds were based on **L**-Tryptophan and benzo[**1,3**]dioxol-5-ylmethyl-[2-(1*H*-indol-3-yl)-ethyl]-amine, which would provide access to analogues exemplified by **6** and **7**, respectively (Figure 4).

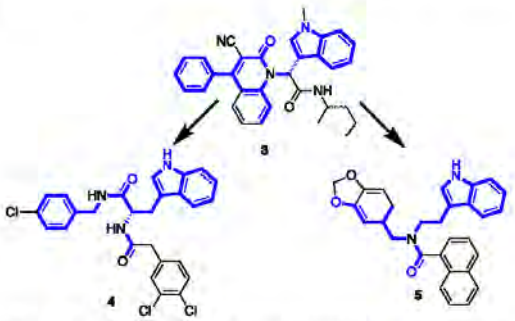

Figure 4. New scaffolds represented by (4) and (5) developed from the existing Ugi-Knoevenagel pharmacophore (e.g. 3). The blue highlighted moieties represent areas of structural similarity across the three scaffolds.

The investigation of scaffold **4** commenced with the synthesis of a focused library of eight L-tryptophan based analogues whereby Fmoc-L-Tryptophan **6** was initially treated with 4-chlorobenzylamine **7** under amide coupling conditions (HATU) to afford **8**. Subsequent Fmoc deprotection (20% piperidine / DMF) and HATU coupling with 3,4-dichlorobenzoic acid **10** gave *N*-(4-chlorobenzyl)-2-[2-(3,4-dichlorophenyl)-acetylamino]-3-(1*H*-indol-3-yl)-propionamide **4** in good yield (Scheme 1). Utilising this general procedure an additional seven selected benzoic acids were coupled with **8** generating the desired L-tryptophan based library (Table 1) which were subsequently biologically evaluated against the HSP.

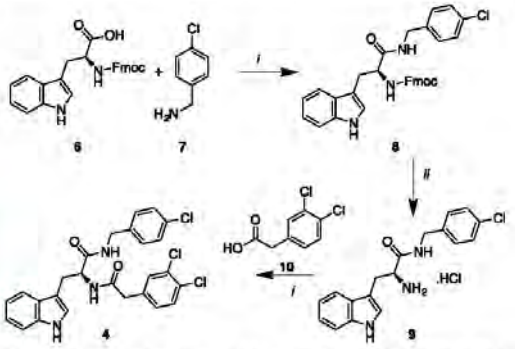

Scheme 1. Reagents and conditions: (i) 1.5 eq. HATU, 3eq. DIPEA, DMF, RT; (ii) 20 % piperidine in DMF and subsequent 1M hydrochloric acid wash.

As the level of dependence on the HSP varies from cell line to cell line, cytotoxicity may not be a direct measure of HSP activity. Consequently the L-tryptophan based analogues were screened for their inhibition of total Gli protein expression using the Dual Luciferase Reporter (DLR) assay in Shh LIGHT2 cells as previously reported.[52] As outlined in Table 1 preliminary screening of the L-tryptophan based analogues

4, and **11-17** was conducted at 10 μM compound concentration.

Table 1. Percentage inhibition of Gli protein expression in 100 nM SAG-activated Shh LIGHT2 cells by L-Tryptophan analogues 4 and 11-17 at 10 μM compound concentration.

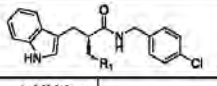

R_1	Inhibition (%)	R_1	Inhibition (%)
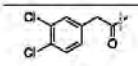 **4**	66	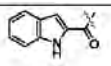 **14**	86
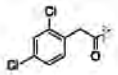 **11**	83	 **15**	71
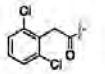 **12**	-38	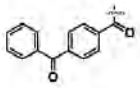 **16**	-105
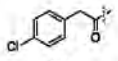 **13**	64	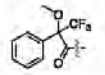 **17**	26

This initial screen indicated that the L-tryptophan analogues **4**, **11**, **13-15** and **17** display an inhibitory effect whilst **12** and **16** elicit a stimulating effect on Gli protein expression compared to SAG and DMSO controls (Table 1). The efficacy of those analogues inhibiting Gli expression ranged from 26% (**17**) to 86% (**14**) while the observed stimulation was -38% (**12**) and -105% (**16**). Hence in relation to initial structure-activity-relationship (SAR) data the presence of a 4-Cl moiety appears to impart high levels of inhibition (**4**, **11** and **13**), whereas a 3,5-di-Cl disposition elicits a stimulatory effect (**12**). In terms of inhibition simple aromatic moieties are tolerated with indole (**14**) and napthyl (**15**) moieties displaying potency excellent inhibition whereas the introduction the trifluomethoxyphenyl moiety (**17**) shows a significant activity loss relative to **14** and **15**.

However as previously noted,[51] the observed Gli inhibitory activity may be a result of off-target action. Thus we examined the *mRNA* expression of HSP components in Shh LIGHT 2 cells on treatment with **4** and **11-17** at 10 μM with SAG stimulation (100 nM). Of the HSP components detected at the *mRNA* level, only $Ptch_1$ and Gli_2 exhibited significant over-expression,[51] while no clear expression of Gli_1 in Shh LIGHT2 cells was detected as previously reported.[53, 54] Focusing on the most potent analogues **11** and **14**, we examined the effect of 10 μM compound dosing on the expression of $Ptch_1$ and Gli_2 by qPCR assay, again in SAG activated Shh LIGHT 2 cells. Both compounds significantly suppressed mRNA levels of *Ptch1* (Figure 6A,B), but only **11** showed inhibition of Gli_2 expression (Figure 6C). Surprisingly, **14** displayed a slight activation of Gli_2 (21%) (Figure 6D). These data in combination with analogue **14** exhibiting complete inhibition of total Gli protein expression (Table 1) suggests that **14** may target Gli translation or act at a post translation level. Despite the apparent divergence in mode of action, both **11** and **14** demonstrated significant inhibition within the HSP.

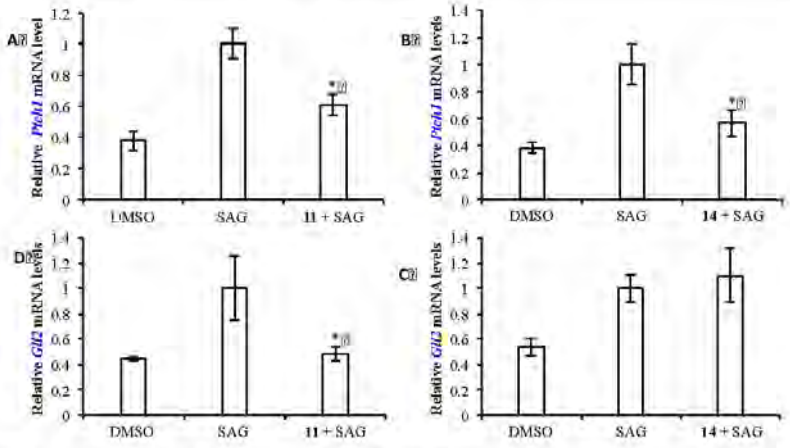

Figure 6. The normalised effect of treatment of 100 nM SAG-activated Shh LIGHT 2 cells on the expression of, A) $Ptch_1$ with 10 μM 11; B) $Ptch_1$ with 10 μM 14, C) A) Gli_2 with 10 μM 13; and D) Gli_2 with 10 μM 14. All experiments were performed in triplicate. * = $P < .05$ relative to SAG treatment.

Having developed **14** as an inhibitor of Gli expression in the Shh LIGHT 2 cell line, the role of stereochemistry was investigated. The D-stereoisomer **14a** was synthesised as described in Scheme 1 from Fmoc-D-Tryptophan. Chiral HPLC

analysis was consistent with no epimerisation during synthesis. Dual luciferase reporter (DLR) assay evaluation of **14a** indicated a modest increase in Gli protein expression inhibition compared with **14**, *viz* 99% vs 84% (ESI†). This suggests only a minor impact of stereochemistry at this point of engagement with the binding site.

In addition to the suppressors **11** and **14**, compound **16** which functioned to up-regulate Gli was also examined using the same assay. Consistent with the DLR data (Figure 7A), the combination of **16** and SAG in resulted in significantly higher Gli_2 expression (93%) relative to cells treated with SAG only (Figure 7B), with a smaller increase in $Ptch_1$ expression also observed (42%) (Figure 7C). To elucidate whether **16** could act as a potential HSP activator like SAG, the compound was screened using the DLR assay in Shh LIGHT2 cells across a number of concentrations in the absence of SAG. Interestingly, results showed that **16** alone had no activating effect on Gli protein expression (Figure 7D), indicating a synergistic activating effect between **16** and SAG, which in combination afforded the best activation (Figure 7A).

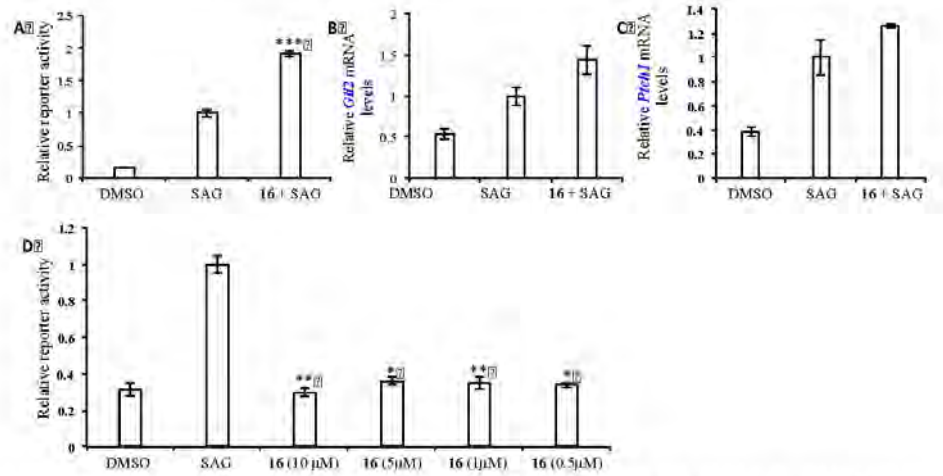

Figure 7. A: Relative Gli protein level treated by the combination of SAG (100 nM) and **16 (10 μM). B** and **C:** mRNA levels of Gli_2 and $Ptch_1$ in Shh LIGHT 2 cells under the treatment of the combination of SAG (100 nM) and **16 (10 μM), respectively. D:** Relative Gli protein level in Shh LIGHT2 cells treated by **16 at different concentrations from 10 to 0.5 μM with** no SAG added. In all assays (A, B, C, and D) SAG (100 nM) and DMSO were used as controls. ***P* < .05, ****P* < .001 compared to SAG treatment.

Investigation of the second scaffold, the benzo[1,3]dioxol-5-ylmethyl-[2-(1*H*-indol-3-yl)-ethyl]-amine derivatives, was conducted concurrently with the L-Tryptophan analogues. In this instance synthesis commenced with the treatment of commercially available C3-indole tethered benzo[1,3]dioxol-5-ylmethyl-[2-(1*H*-indol-3-yl)-ethyl]-amine HBr salt **18**. HATU/DIPEA mediated amide coupling of **18** with naphthalene-1-carboxylic acid **19** afforded after chromatographic purification the desired naphthalene-1-carboxylic acid benzo[1,3]dioxol-5-ylmethyl-[2-(1*H*-indol-3-yl)-ethyl]-amide **5** as the sole product (Scheme 2).

Variation of the acid moiety (**19**) allowed rapid access to a targeted library of benzo[1,3]dioxol-5-ylmethyl-[2-(1*H*-indol-3-yl)-ethyl]-amine derivatives (**5** and **20-26**). Of note within this library NMR analysis suggested the presence of atropoisomers in analogues **5** and **23-26**. This was supported by variable temperature and 1D selective NOESY NMR experiments with **5** which showed peak coalescence and signal behaviour consistent with atropoisomerisation (ESI†). Despite extensive investigation we were unable to separate these isomers. Nonetheless subsequent DLR assay evaluation of this library was conducted at 10 μM compound concentration.

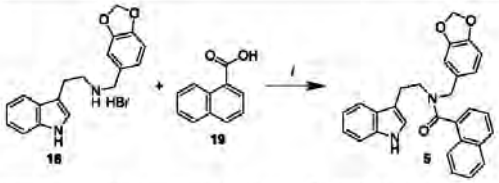

Scheme 2. Reagents and Conditions: i) 1.5 eq. HATU, 3eq. DIPEA, DMF, RT, 48h.

Table 2. Percentage inhibition of Gli expression in 100 nM SAG-activated Shh LIGHT2 cells by benzo[1,3]dioxol-5-ylmethyl-[2-(1*H*-indol-3-yl)-ethyl]-amine derivatives analogues **5** and **20-26** at 10 μM compound concentration.

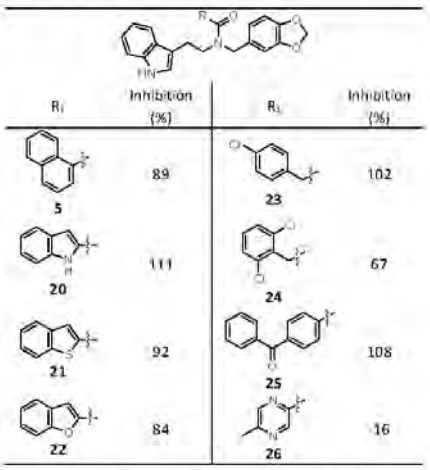

As outlined in Table 2 the DLR assay data for this series indicated that each analogue affected Gli protein expression. Inhibition of Gli expression ranged from modest (**24**; 67%) to excellent (**5**, **20-23**, **25**; 84% to 111%). Bis-indoly-**20** returned the highest inhibition with bioisosteric modifications to benzofuran (**22**) or benzothiophene (**221**) resulting in a slight decrease Gli expression inhibition (**111**%, 84% and 92% respectively). Alterations to the aromatic moiety were significant with 2,6-dichlorobenzoyl **24** showing a marked potency reduction (67%). However, activity could be restored with the removal one, and repositioning of the other, chlorine moiety to C4 with **23** (102%). This data was consistent with that observed for L-Tryptophan analogues **4**, **11** and **13** where the introduction of a C4-Cl moiety imparted good to excellent inhibition of Gli expression (Table 1). Combined, this strongly supports C4-derivatization of the benzoyl moiety as beneficial to Gli inhibition. A similar outcome was observed with the C4 –benzoyl substituted **25** (108%). The C1-tethered napthyl **5** displayed a decrease in activity (89%), while the electron rich system of 5-methyl-pyrazine-2-carboxyl **26** resulted in stimulation (16%) of Gli protein expression (Table 2). It is also worthy to note that the inhibition of **20**, **23**, and **25** appeared to be larger than 100%. This may arise as a result of the compounds not only suppressing the elevated Gli protein levels induced by SAG, but also inhibition of this protein in inactivated Shh **LIGHT2** cells (Table 2).

As with the L-tryptophan series the two compounds displaying the highest inhibitory activity (e.g. **20** and **25**), were further investigated for their ability to affect $Ptch_1$ and Gli_2 expression in SAG-activated Shh **LIGHT2** cells at 10 μM compound concentration (Figure 9).

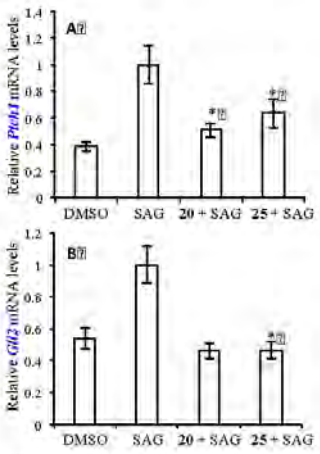

Figure 8. Relative *mRNA* levels of $Ptch_1$ (A) and Gli_2 (B) treated by the combination of SAG (100 nM) with **20** and **25** **at 10 μM. Treatments were performed** in triplicate. * $P <$ 0.05 compared to SAG treatments.

The data in Figure 8 is consistent with **20** and **25** showing significant inhibition of $Ptch_1$ expression, eliciting 80% and 59%, inhibition respectively (Figure 8A). In regards to Gli_2, compounds **20** and **25** displayed an inhibitory activity of 117% and 116%, respectively compared to controls (Figure 8B). These results support **20** and **25** targeting the HSP through $Ptch_1$ and Gli_2 gene suppression.

Given that unlike **25**, **20** did not display atropisomeric characteristics under NMR analysis it was selected as the lead for the next benzo[1,3]dioxol-5-ylmethyl-[2-(1*H*-indol-3-yl)-ethyl]-amine based targeted library. Subsequent analogues were prepared as described in Scheme 2 to afford analogues **27-29** which were evaluated in the DLR assay at 2.5 μM compound concentration (Table 3).

Table 3. Percentage inhibition of Gli expression in 100 nM SAG-activated Shh LIGHT2 cells by benzo[1,3]dioxol-5-ylmethyl-[2-(1*H*-indol-3-yl)-ethyl]-amine derivatives analogues **20**, **27-29** at 2.5 μM compound concentration, and IC_{50} values (μM).

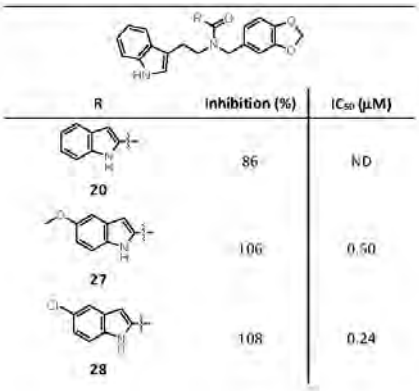

 29	76	ND

As outlined in Table 3, introduction of a methoxy (**27**, 106%; IC_{50} = 0.5 μM) or a chlorine (**28**, 108%; IC_{50} = 0.24 μM) substituent resulted in analogues more potent than **20** (Table 3). Indole tethered regiochemistry modification to C5 with **29** was detrimental to activity (76%).

Possible Mechanism of action

Together with the tryptophan derivatives, the benzo[1,3]dioxol-5-ylmethyl-[2-{1*H*-indol-3-yl)-ethyl]-amine represent two new HSP inhibitor scaffolds. Whilst these compounds displayed clear inhibition of Gli protein expression in the presence of SAG, a biochemically and functionally competitive agent against the majority of Smo inhibitors, it was also possible that these analogues targeted Smo by interaction remote to the SAG binding site.[23, 44, 55] However based on our DLR assays with **14a** and **28** we hypothesized that the target for these compound is downstream of Smo. Based on the elevated level of Gli protein in SAG-activated Shh LIGHT 2 cells, compounds that are able to significantly counteract this protein accumulation would therefore promote themselves as inhibitors targeting the HSP downstream of Smo. During the DLR assay, Shh LIGHT 2 cells were initially activated by 100 nM SAG for 12, 24, and 36 h respectively before **14a** and **28** were added at 2.5 μM each, and the assay read at 48 h. A control assay was performed using only SAG to monitor the accumulation of Gli protein after the cells had been treated for 12, 24 and 36 h respectively (Figure 9).

SAG stimulated accumulation of Gli protein in Shh LIGHT 2 cells was rapid with Gli expression doubling after 12 h reaching a five-fold increase after 24 h. The rate of increase then slowed between 24 to 36 h, reaching a plateau after 48 h (Figure 9;). Under these conditions, **14a** and **28** strongly inhibited Gli expression. This is consistent with these analogues acting independently of Smo (i.e. not binding to Smo) as direct Smo inhibition would not be expected to dramatically reduce the large accumulation of Gli protein observed (Figure 9). In a similar manner, the classic Smo inhibitor, cyclopamine, failed to inhibit pathway activation through Gli2 overexpression in NIH-3T3 cells.[52] Additionally, KAAD-cyclopamine displayed mutual antagonism with SAG only when administered simultaneously in Shh LIGHT2 and/or SmoA1 LIGHT2 cells.[23] Combined this data supports the supposition that **14a** and **28** inhibit the HSP by regulating Gli gene and protein expression, downstream of Smo. This significantly increases their potential as lead compounds in the development of HSP inhibitors as anti-cancer agents given the emerging resistance to current Smo targeting inhibitors.[19]

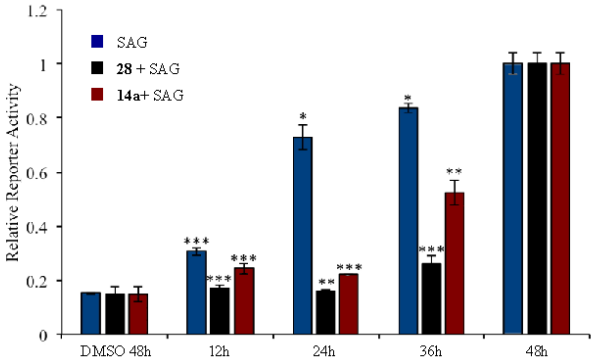

Figure 9. Shown is the normalized 48 h development of Gli protein in the DLR assay in Shh LIGHT 2 cells. The cells were differently treated with either SAG only (100 nM,), or a combination of SAG (100 nM) and the compound of interest (**14a** or **28**), in which SAG was pre-treated for 12, 24, or 36 h before **14a** or **28** at 2.5 μM each was added. Controls for each treatment were the 48 h treatments of DMSO and SAG (100 nM), respectively. Treatments were performed in triplicate. * $P < .05$, ** $P < .001$, *** $P < .0001$ compared to SAG-48h controls.

Conclusion

Building on our previously reported quinolone-1-{2*H*)-one pharmacophore,[51] two series of the tryptophan and benzo[1,3]dioxol-5-ylmethyl-[2-{1*H*-indol-3-yl)-ethyl]-amine derivatives demonstrated enhanced inhibition of the HSP. A number of analogues within these series' significantly increased inhibitory activity on the HSP as observed through Gli gene and protein expression in Shh LIGHT2 at low concentrations. The mechanism of action was determined to be downstream of Smo, which has the potential to circumvent the resistance issues emerging with the current classes of clinically used Smo inhibitors. The evidence presented in this study strongly suggests that these compounds inhibit Gli_2 expression through transcription and translation, and subsequently, that the protein profile of these molecules is altered. Regarding the chemical properties, the

stereochemistry has been approached using pure D- or L-Tryptophan derivatives, but further studies are required to classify the atropoisomerism that occurred sporadically through a number of the benzo[1,3]dioxol-5-ylmethyl-[2-(1*H*-indol-3-yl)-ethyl]-amine derivatives, most likely due to the sterically hindered rotations.[56]

Experimental

Biology

Cell culture and stock solutions

Stock solutions were prepared as follows and stored at -20ºC: Related compounds were stored as 50 mM solutions in DMSO. All cell lines were cultured at 37ºC in an automated CO_2 (5%) incubator (HERA cell 150, Thermo Scientific).

Shh LIGHT2 cell line (derived from NIH-3T3 fibroblast cell line) was maintained in Gibco® Dulbecco's modified Eagle's medium (Thermo Fisher Scientific) supplemented with 10% foetal bovine serum (FBS), glutamine (4 mM), Zeocin® (0.15 mgmL, Invitrogen), Genetecin® (0.4 mg/mL, Thermo Fisher Scientific).

Dual Luciferase Reporter assay

Shh-LIGHT2 cells in logarithmic growth were transferred to 96-well plate (3000 cells/well) and cultured to confluency. The Shh-LIGHT2 cells were grown in DMEM containing 0.5% FBS, 4 mM glutamine, 0.15 mg/mL Zeocin®, 0.4 mg/mL Genetecin®, and then co-cultured with combinations of 100 nM SAG, and/or our novel compounds in concentrations from 2.5 to 10 µM. The SAG- free DMSO treated (2.5 to 10 µM), and SAG-included Sonidegib (100 nM) treated cells were used as controls. Treatments were done in triplicates. After the cells were cultured for a further 45 h in an automated CO_2 (5%) incubator, the resulting firefly and Renilla luciferase activities were measured using a Dual Luciferase Reporter kit (Promega) and a BMG Labtech Pherastar microplate reader (Thermo Fisher Scientific).

RNA Extraction

Total RNA was isolated from cultured cells using two rounds of a modified acid guanidinium thiocyanate-phenol-chloroform protocol:[57] washed cells resuspended in lysis buffer (4 M guanidinium thiocyanate, 25 mM sodium citrate, 0.5% sarkosyl, 0.72% β-mercaptoethanol) as previously described.[58]

Reverse Transcription PCR (RT-PCR) and Quantitative PCR (qPCR)

Reverse transcription was performed with 2 µg of isolated RNA, 500 ng oligo(dT)15 primer, 40 U of RNäsin, 0.5 mM dNTPs, and 20 U of M-MLV-Reverse Transcriptase (Promega). Total RNA was DNase treated prior to reverse transcription to remove genomic DNA. Reverse transcription reactions were verified by *β-actin* RT-PCR using cDNA amplified with GoTaq Flexi (Promega). qPCR was performed using SYBR Green GoTaq qPCR master mix (Promega) according to manufacturer's instructions on LightCycler 96 SW 1.0 (Roche). Primer sequences have been supplied (Table 6). Reactions were performed on cDNA equivalent to 50 ng of total RNA and carried out for 45 amplification cycles. SYBR® Green fluorescence was measured after the extension step at the end of each amplification cycle and quantified using LightCycler Analysis Software (Roche). For each sample, a replicate omitting the reverse transcription step was undertaken as a negative control. qPCR data was normalized to the house-keeping control *Cyclophilin*. Experiments were replicated at least 3 times prior to statistical assessment. Each PCR was performed on at least 3 separate cell isolations, of which a representative PCR or an average is shown. We have previously reported the primer sequences for this PCR (ESI†).[51]

Statistical analysis

Statistical analysis was performed using F-test and t-test in Excel 2013. * $P < .05$, ** $P < .001$, *** $P < .0001$.

Chemistry

All reagents were purchased from Sigma-Aldrich, Matrix Scientific, ABCR GmbH, ChemPep, or AK Scientific, and were used without purification. All solvents were re-distilled from glass prior to use.

^1H, ^{13}C NMR, temperature variable, and 1D selective NOESY spectra were recorded on a Brüker Advance™ AMX 400 MHz spectrometer at 400.1 and 100.6 MHz, respectively. Chemical shifts (δ) are reported in parts per million (ppm) measured to relative the internal standards. Coupling constants (*J*) are expressed in hertz (Hz). Low resolution mass spectra were recorded on a Shimadzu LCMS 2010 EV using a mobile phase of 1 : 1 acetonitrile–H_2O with 0.1% formic acid. High resolution mass spectra (HRMS) were determined using nanoflow reversed phased Liquid Chromatography (Dionex Ultimate 3000 RSLCnano, Thermo Fischer Scientific) coupled directly to a High Resolution mode equipped, Q-Exactive Plus Hybrid Quadrupole-Orbitrap Mass Spectrometer (Thermo Fischer Scientific). This system was fitted with 5 µm C18 nanoViper trap column (100 µm x 2cm, Acclaim PepMap100, Thermo) for desalting and pre-concentration, and separation was then performed at 300 nL.min^{-1} over an EASY-Spray PepMap column (3 µm C18, 75 µm x 15 cm) utilising a gradient of 2-99% Buffer B (80% Acetonitrile, 0.1% Formic Acid) over 25 minutes.

Analytical HPLC traces were obtained using a Shimadzu system possessing a SIL-20A auto-sampler, dual LC-20AP pumps, CBM-20A bus module, CTO-20A column heater, and a SPD-20A UV/vis detector. This system was fitted with an Alltima™ C18 5 µm 150 mm × 4.6 mm column with solvent A: 0.06% trifluoroacetic acid (TFA) in water and solvent B: 0.06% TFA in CH_3CN–H_2O (90 : 10). Chiral resolution was performed on the same system using ChiralPak®AD-H 5 µm 250 mm x 4.6 mm chiral column with solvent A: 100% methanol and B: 100% acetonitrile. In normal resolution, HPLC traces were acquired at a flow rate of 2.0 mL.min^{-1}, gradient 10 –100 (%B), over 15.0 min, with detection at 220 nm and 254 nm. In chiral resolution mode, HPLC traces were acquired at a flow rate of 0.2 mL.min^{-1}, gradient 10 (%A) and 90 (%B) over 85 min, with at 220 nm and 254 nm. Where applicable UPLC traces were obtained using the Agilent Technologies 1260 Infinity UPLC system. This system was fitted with an Agilent Zorbax SB-C18 1.8 µm, 2.1 x 50 mm, column with the solvent A: 0.1% formic

acid in water and solvent B: 0.1% formic acid in CH_3CN–H_2O (90 : 10). In each case UPLC traces were acquired at a flow rate of 0.6 mL.min^{-1} using an isocratic run at 80% or 50% solvent B.

Melting points were recorded on a Büchi Melting Point M-565. IR spectra were recorded on a PerkinElmer Spectrum Two™ FTIR Spectrometer with the UATR accessories. Thin layer chromatography (TLC) was performed on Merck 60 F254 pre-coated aluminium plates with a thickness of 0.2 mm. Column chromatography was performed under 'flash' conditions on Merck silica gel 60 (230–400 mesh).

Synthesis of L-Tryptophan intermediate (9)

2-Amino-*N*-(4-chlorobenzyl)-3-(1*H*-indol-3-yl)-propionamide (9). A solution of dimethylformamide (DMF) (30.0 mL), Fmoc-L-Tryptophan **6** (3.65 g, 8.55 mmol), HATU (4.88 g, 12.83 mmol) and 4-chlorobenzylamine **7** (1.04 mL, 8.55 mmol) was stirred at room temperature until completely dissolved. To the stirred solution was added diisopropylethylamine (DIPEA) (4.46 mL, 25.65 mmol) and the reaction mixture was stirred overnight. DMF was then removed and the crude was dissolved in ethyl acetate (60 mL) and washed with 1M HCl (3 x 20 mL). The precipitate was treated with 20% piperidine in CH_3CN (20 mL) for 3 h. The CH_3CN was removed *in vacuo* and the residue taken up in ethyl acetate (40 mL) and washed with 1M HCl (3 x 20 mL) and allowed to stand for 48 h at which time the solid was collected to afford **9** (1.71 g, 55%) as an off white solid (MP 254.5 – 255 °C).

IR (cm^{-1}): 3253 (NH), 2858 (CH- aliphatic), 1659 (CON), 738 (CH-aromatic); ^{1}H NMR (400 MHz, DMSO-d_6) δ 11.08 (s, 1H), 9.07 (t, J = 5.8 Hz, 1H), 8.32 (s, 3H), 7.66 (d, J = 7.9 Hz, 1H), 7.40 (d, J = 8.1 Hz, 1H), 7.30 (d, J = 8.4 Hz, 2H), 7.21 (d, J = 2.2 Hz, 1H), 7.10 (dd, J = 15.9, 7.8 Hz, 3H), 7.01 (t, J = 7.4 Hz, 1H), 4.26 (ddd, JAX = 38.6, J_{BX} = 15.4, J_{AB} = 5.8 Hz, 2H), 4.04 (t, J = 7.1 Hz, 1H), 3.22 (ddd, J'_{AX} = 30.8, J'_{BX} = 14.4, J'_{AB} =7.1 Hz, 2H); ^{13}C NMR (400 MHz, DMSO-d_6) δ 169.0, 137.9, 136.7, 131.9, 129.5 (Cx2), 128.6 (Cx2), 127.5, 125.3, 121.6, 119.0, 111.9, 107.5, 53.4, 42.0, 31.2, 27.8; LRMS (APCI$^+$) m/z 327, 328 [M+H]$^+$, 100%. HRMS (ES+) for $C_{18}H_{18}ClN_3O$, calculated 328.1211, found 328.1210.

***Note**: This protocol with the replacing Fmoc-L-Tryptophan by Fmoc-D-Tryptophan affords the D-Tryptophan derivative **9a** which demonstrates same chemical and physical properties to **9**, including NMR spectra.

Synthesis of L-Tryptophan derivatives using (9) as the starting material

***N*-(4-Chlorobenzyl)-2-[2-(3,4-dichlorophenyl)-acetylamino]-3-(1*H*-indol-3-yl)-propionamide (4): General procedure A**: A DMF solution (10 mL) of the freshly prepared **9** (0.37 g, 1.01 mmol), HATU (0.58 g, 1.52 mmol), and (3,4-dichlorophenyl)-acetic acid (0.21 g, 1.01 mmol) was stirred at room temperature to complete dissolution. To the stirred solution was added DIPEA (0.37 mL, 3.03 mmol) and the reaction mixture was stirred overnight. DMF was then removed and the crude material was subjected to silica gel column chromatography (1:4 hexanes–EtOAc) to afford **4** (0.18 g, 35%) as a white solid (mp 208 – 209 °C).

IR (cm^{-1}): 3410 (NH), 3277 (NH), 3068 (CH), 1636 (CON); ^{1}H NMR (400 MHz, DMSO-d_6) δ 10.84 (s, 1H), 8.56 (t, J = 8.0 Hz, 1H), 8.43 (d, J = 8.1 Hz, 1H), 7.60 (d, J = 7.9 Hz, 1H), 7.47 (d, J = 8.2 Hz, 1H), 7.42 (d, J = 1.8 Hz, 1H), 7.35 (d, J = 8.1 Hz, 1H), 7.28 (d, J = 8.4 Hz, 2H), 7.16 – 7.02 (m, 5H), 6.97 (t, J = 7.1 Hz, 1H), 4.59 (dd, J = 8.0, 12.0 Hz, 1H), 4.24 (ddd, $J_{A'X'}$ = $J_{B'X'}$ = 8.0, $J_{A'B'}$= 16 Hz, 2H), 3.47 (s, 2H), 3.05 (ddd*, J_{AX} = 4.0, J_{BX} = 8.0, J_{AB} = 16.0 Hz, 2H); ^{13}C NMR (101 MHz, DMSO-d_6) δ 171.9, 169.6, 138.7, 138.0, 136. 6, 131.6, 131.5, 131.0, 130.6, 129.8, 129.4, 129.2 (2C), 128.5 (2C), 127.7, 124.2, 121.4, 119.0, 118.7, 111.8, 110.4, 54.2, 41.8, 41.2, 28.5; LRMS (ESI$^+$) m/z: 513, 514 [M+H]$^+$, 95%. HRMS (ES$^+$) for $C_{26}H_{22}Cl_3N_3O_2$, calculated 514.0850, found 514.0850; RP-HPLC Alltima™ C18 5 µm 150 mm x 4.6 mm, 10–100% B in 15 min, R_t = 14.31 min, 100%.

***N*-(4-Chlorobenzyl)-2-[2-(2,4-dichlorophenyl)-acetylamino]-3-(1*H*-indol-3-yl)-propionamide (11).** Synthesized utilizing the general procedure A described above, from **9** (0.152 g, 0.42 mmol), HATU (0.239 g, 0.63 mmol), (2,4-dichlorophenyl)-acetic acid (0.086 g, 0.42 mmol), and DIPEA (0.22 mL, 1.26 mmol) in DMF (5.0 mL) to afford **11** (0.055 g, 24%) as an off white solid (MP 207 – 208 °C); IR (cm^{-1}): 3410 (NH), 3280 (NH), 3065 (CH), 1642 (CON); ^{1}H NMR (400 MHz, DMSO-d_6) δ 10.85 (s, 1H), 8.54 (t, J = 4.0 Hz, 1H), 8.40 (d, J = 8.2 Hz, 1H), 7.62 (d, J = 7.8 Hz, 1H), 7.53 (d, J = 2.1 Hz, 1H), 7.36 (d, J = 8.1 Hz, 1H), 7.33 – 7.23 (m, 3H), 7.12 (ddd, J = 22.2, 12.5, 7.8 Hz, 5H), 6.98 (t, J = 7.4 Hz, 1H), 4.63 (dd, J = 8.0, 16.0 Hz, 1H), 4.25 (ddd, $J_{A'X'}$ = $J_{B'X'}$ = 4.0, $J_{A'B'}$= 16 Hz, 2H), 3.60 (s, 2H), 3.07 (ddd, J_{AX} = 4.0, J_{BX}= 8.0, J_{AB}= 16.0 Hz, 2H); ^{13}C NMR (101 MHz, DMSO-d_6) δ 171.9, 168.9, 138.8, 136.6, 135.0, 133.9, 133.3, 132.3, 131.6, 129.3 (2C), 128.8, 128.5 (2C) 127.7, 127.4, 124.2, 121.3, 119.0, 118.7, 111.7, 110.4, 54.2, 41.8, 31.0, 28.5; LRMS (APCI$^+$) m/z 513, 514 [M+1H]$^+$ 50%. HRMS (ES$^+$) for $C_{26}H_{22}Cl_3N_3O_2$, calculated 514.0850, found 514.0850; RP-HPLC Alltima™ C18 5 µm 150 mm x 4.6 mm, 10–100% B in 15 min, R_t =14.38 min, 99.2%.

***N*-(4-Chlorobenzyl)-2-[2-(2,6-dichlorophenyl)-acetylamino]-3-(1*H*-indol-3-yl)-propionamide (12).** Synthesized utilizing the general procedure A described above, from **9** (0.148 g, 0.41 mmol), HATU (0.228 g, 0.6 mmol), (2,6-dichlorophenyl)-acetic acid (0.082 g, 0.41 mmol) and DIPEA (0.21 mL, 1.2 mmol) in DMF (5.0 mL) to afford **12** (0.08 g, 40%) as a white solid (MP 265 – 256 °C).

IR (cm^{-1}): 3410 (NH), 3292 (NH), 3252 (NH), 1641 (CON); ^{1}H NMR (400 MHz, DMSO-d_6) δ 10.85 (s, 1H), 8.49 (t, J = 4.0 Hz, 1H), 8.40 (d, J = 8.2 Hz, 1H), 7.60 (d, J = 7.9 Hz, 1H), 7.41 (d, J = 7.9 Hz, 2H), 7.34 (d, J = 8.1 Hz, 1H), 7.28 (ddd, J = 8.6, 4.7, 2.5 Hz, 3H), 7.13 (d, J = 2.2 Hz, 1H), 7.11 – 7.03 (m, 3H), 7.00 – 6.94 (m, 1H), 4.60 (dd, J = 8.0 Hz, 1H), 4.24 (ddd, $J_{A'X'}$ = 8.0, $J_{B'X'}$ = 4.0, $J_{A'B'}$= 16 Hz, 2H), 3.84 (q, J = 16.3 Hz, 2H), 3.07 (ddd, J_{AX} = 6, J_{BX} = 8.0, J_{AB}= 12 Hz, 2H); ^{13}C NMR (101 MHz, DMSO-d_6) δ 171.9, 167.8, 138.7, 136.5, 136.0 (2C), 133.1, 131.6, 129.6, 129.2 (2C), 128.5 (2C), 128.5 (2C), 127.8, 124.1, 121.3, 118.9, 118.7, 111.7, 110.4, 54.3, 41.8, 37.9, 28.6; LRMS (ESI$^+$) m/z 513, 514 [M+H]$^+$ 95%. HRMS (ES$^+$) for $C_{26}H_{22}Cl_3N_3O_2$, calculated 514.0850, found 514.0850; RP-HPLC Alltima™ C18 5

µm 150 mm x 4.6 mm, 10–100% B in 15 min, R_t = 6.54 min, 100%.

***N*-(4-Chlorobenzyl)-2-[2-(4-chlorophenyl)-acetylamino]-3-(1*H*-indol-3-yl)-propionamide (13).** Synthesized utilizing the general procedure A described above, from **9** (0.142 g, 0.39 mmol), HATU (0.223 g, 0.59 mmol), (4-chlorophenyl)-acetic acid (0.067 g, 0.39 mmol) and DIPEA (0.20 mL, 1.17 mmol) in DMF (5.0 mL) to afford **13** (0.06 g, 32%) as a white solid (MP 205.2 – 206.3 ºC).

IR (cm^{-1}): 3410 (NH), 3292 (NH), 3061 (CH), 1635 (CON); ^1H NMR (400 MHz, DMSO-d_6) δ 10.84 (s, 1H), 8.55 (t, *J* = 6.0 Hz, 1H), 8.38 (d, *J* = 8.2 Hz, 1H), 7.60 (d, *J* = 7.9 Hz, 1H), 7.36 (d, *J* = 8.1 Hz, 1H), 7.32 – 7.21 (m, 4H), 7.16 – 7.01 (m, 6H), 7.01 – 6.90 (m, 1H), 4.59 (dd, *J* = 8 Hz, 1H), 4.23 (ddd, $J_{A'X'}$ = 8, $J_{B'X'}$ = 6.0, $J_{A'B'}$= 16 Hz, 2H), 3.44 (dd, *J* = 19.8, 14.4 Hz, 2H), 3.05 (ddd, J_{AX} = 6, J_{BX} = 8, J_{AB} = 16 Hz, 2H); ^{13}C NMR (101 MHz, DMSO-d_6) δ 172.0, 170.0, 138.7, 136.6, 135.8, 131.6, 131.4, 131.3 (2C), 129.2 (2C), 128.5 (2C), 128.4 (2C), 127.7, 124.2, 121.4, 119.0, 118.7, 111.7, 110.4, 54.1, 41.8, 41.7, 28.5; LRMS (ESI^+) m/z 479, 480 $[M+H]^+$, 100%; HRMS (ES^+) for $C_{26}H_{23}Cl_2N_3O_2$, calculated 480.1240, found 480.1240; RP-HPLC Alltima™ C18 5 µm 150 mm x 4.6 mm, 10–100% B in 15 min, R_t =13.69 min, 100%.

1*H*-Indole-2-carboxylic acid [1-(4-chlorobenzylcarbamoyl)-2-(1*H*-indol-3-yl)-ethyl]-amide (14 L-isomer). Synthesised utilizing the general procedure A described above, from **9** (0.142 g, 0.40 mmol), HATU (0.227 g, 0.60 mmol), 1*H*-Indole-2-carboxylic acid (0.064 g, 0.40 mmol) and DIPEA (0.21 mL, 1.19 mmol) in DMF (5.0 mL) to afford **14** (0.097 g, 50%) as a white solid (mp 229.5 – 230.7 ºC).

IR (cm^{-1}): 3422 (NH), 3381 (NH), 3316 (NH), 1630 (CON); ^1H NMR (400 MHz, DMSO-d_6) δ 11.53 (s, 1H), 10.80 (s, 1H), 8.70 (t, *J* = 6.0 Hz, 1H), 8.57 (d, *J* = 8.1 Hz, 1H), 7.71 (d, *J* = 7.8 Hz, 1H), 7.62 (d, *J* = 8.0 Hz, 1H), 7.41 (d, *J* = 8.2 Hz, 1H), 7.33 (dd, *J* = 7.7, 5.5 Hz, 3H), 7.25 – 7.14 (m, 5H), 7.09 – 6.96 (m, 3H), 4.80 (dd, *J* = 9.2, 5.0 Hz, 1H), 4.31 (dd, $J_{A'X'}$ =$J_{B'X'}$ = 6.0, $J_{A'B'}$= 16.0 Hz, 2H), 3.24 (ddd, J_{AX} = 5.0, J_{BX} = 9.6, J_{AB} = 14.4 Hz, 2H); ^{13}C NMR (101 MHz, DMSO-d_6) δ 172.3, 161.5, 138.9, 136.9, 136.5, 131.7, 129.3 (2C), 128.6 (C), 127.7, 127.5, 124.3, 123.8, 122.0, 121.4, 120.2, 119.0, 118.7, 112.7, 111.8, 110.8, 103.8, 54.5, 41.9, 28.2; LRMS ($APCI^+$) m/z 470, 471 $[M+1H]^+$, 90%; HRMS (ES^+) for $C_{27}H_{23}ClN_4O_2$ calculated 471.1582, found 471.1582; RP-HPLC Alltima™ C18 5 µm 150 mm x 4.6 mm, 10–100% B in 15 min, R_t = 13.35 min, 100%.

1*H*-Indole-2-carboxylic acid [1-(4-chlorobenzylcarbamoyl)-2-(1*H*-indol-3-yl)-ethyl]-amide (14a D-isomer). Synthesised utilizing the general procedure A described above, from **9a** (0.249 g, 0.69 mmol), HATU (0.39 g, 1.03 mmol), 1*H*-Indole-2-carboxylic acid (0.11 g, 0.69 mmol) and DIPEA (0.36 mL, 2.05 mmol) in DMF (5.0 mL) to afford **14a** (0.156 g, 48%) as a white solid (MP 227 – 227.5 ºC).

IR (cm^{-1}): 3420 (NH), 3382 (NH), 3325 (NH), 1630 (CONH), 1656 (CON), 737 (CH-aromatic); ^1H NMR (400 MHz, DMSO-d_6) δ 11.53 (s, 1H), 10.81 (d, *J* = 1.6 Hz, 1H), 8.71 (t, *J* = 6.0 Hz, 1H), 8.58 (d, *J* = 8.1 Hz, 1H), 7.72 (d, *J* = 7.8 Hz, 1H), 7.63 (d, *J* = 8.0 Hz, 1H), 7.45 – 7.39 (m, 1H), 7.37 – 7.30 (m, 3H), 7.26 – 7.14 (m, 5H), 7.11 – 6.95 (m, 3H), 4.82 (dd, *J* = 9.2, 5.2 Hz, 1H), 4.32 (dd, $J_{A'X'}$ =$J_{B'X'}$ = 6.0, $J_{A'B'}$= 16.0 Hz, 2H), 3.23 (ddd, J_{AX} = 5.2, J_{BX} = 9.6, J_{AB} = 14.4 Hz, 2H); ^{13}C NMR (101 MHz, DMSO-d_6) δ 172.3, 161.5, 138.9, 136.9, 136.6, 131.8, 131.7, 129.3 (2C), 128.6 (2C), 127.7, 127.5, 124.3, 123.8, 122.0, 121.4, 120.2, 119.0, 118.7, 112.7, 111.8, 110.8, 103.9, 54.5, 42.0, 28.2; LRMS (ESI^+) 470, 470 $[M+H]^+$, 80%. HRMS (ES^+) for $C_{27}H_{23}ClN_4O_2$ calculated 471.1582, found 471.15844; RP-HPLC Alltima™ C18 5 µm 150 mm x 4.6 mm, 10 – 100% B in 15 min, R_t = 6.44 min, 100%.

Naphthalene-1-carboxylic acid [1-(4-chlorobenzylcarbamoyl)-2-(1*H*-indol-3-yl)-ethyl]-amide (15). Synthesized utilizing the general procedure A described above, from **9** (0.105 g, 0.29 mmol), HATU (0.17 g, 0.43 mmol), naphthalene-1-carboxylic acid (0.05 g, 0.29 mmol) and DIPEA (0.15 mL, 0.87 mmol) in DMF (5.0 mL) to afford **15** (0.057 g, 41%) as a white solid (MP 165.7 – 166.5 ºC).

IR (cm^{-1}): 3398 (NH), 3268 (NH), 3049 (CH), 1627 (CON), 739 (CH-aromatic); ^1H NMR (400 MHz, DMSO-d_6) δ 10.89 (s, 1H), 8.73–8.67 (m, 2H) (overlapped two NH amides), 8.02 – 7.86 (m, 3H), 7.74 (d, *J* = 7.8 Hz, 1H), 7.57 – 7.47 (m, 3H), 7.47 – 7.32 (m, 4H), 7.27 (d, *J* = 8.5 Hz, 3H), 7.11 (dd, *J* = 11.1, 3.9 Hz, 1H), 7.02 (dd, *J* = 11.0, 3.9 Hz, 1H), 4.93 (ddd, *J* = 9.3, 5.2 Hz, 1H), 4.37 (ddd, $J_{A'X'}$ =$J_{B'X'}$ = 8.0, $J_{A'B'}$= 16.0 Hz, 2H), 3.23 (ddd, J_{AX} = 5.2, J_{BX}= 9.6, J_{AB} = 14.4 Hz, 2H); ^{13}C NMR (101 MHz, DMSO-d_6) δ 172.3, 169.0, 139.0, 136.7, 135.0, 133.5, 131.7, 130.2 (2C), 129.4 (2C), 128.6 (3C), 127.8, 126.9, 126.6, 126.0, 125.8, 125.3, 124.4, 121.4, 119.1, 118.7, 111.8, 110.7, 54.8, 42.0, 28.1; LRMS ($APCI^+$) m/z 481, 482 $[M+1H]^+$, 90%; HRMS (ES^+) for $C_{29}H_{24}ClN_3O_2$, calculated 482.1630, found 482.1630; RP-HPLC Alltima™ C18 5 µm 150 mm x 4.6 mm, 10 – 100% B in 15 min, R_t = 13.62 min, 99.1%.

4-Benzoyl-*N*-[1-(4-chlorobenzylcarbamoyl)-2-(1*H*-indol-3-yl)-ethyl]-benzamide (16). Synthesized utilizing the general procedure A described above, from **9** (0.179 g, 0.49 mmol), HATU (0.28 g, 0.74 mmol), 4-benzoylbenzoic acid (0.11 g, 0.49 mmol) and DIPEA (0.26 mL, 1.48 mmol) in DMF (5.0 mL) to afford **16** (0.127 g, 45%) as a white solid (MP 202 – 202.5 ºC).

IR (cm^{-1}): 3440 (NH), 3304 (NH), 1662 (CO), 1632 (CON), 743 (CH-aromatic); ^1H NMR (400 MHz, DMSO-d_6) δ 10.80 (s, 1H), 8.80 (d, *J* = 8.0 Hz, 1H), 8.68 (t, *J* = 5.9 Hz, 1H), 8.00 (d, *J* = 8.4 Hz, 2H), 7.81 – 7.66 (m, 6H), 7.58 (t, *J* = 7.6 Hz, 2H), 7.33 (dd, *J* = 8.2, 3.5 Hz, 3H), 7.21 (dd, *J* = 9.2, 5.3 Hz, 3H), 7.03 (dt, *J* = 30.0, 7.0 Hz, 2H), 4.81 (dd, *J* = 9.3, 5.2 Hz, 1H), 4.30 (ddd, $J_{A'X'}$ = 5.6, $J_{B'X'}$ = 4.4, $J_{A'B'}$= 15.6 Hz, 2H), 3.25 (ddd, J_{AX} = 5.2, J_{BX} = 9.7, J_{AB} = 14.4 Hz, 2H); ^{13}C NMR (101 MHz, DMSO-d_6) δ 195.9, 172.1, 166.0, 139.7, 138.9, 137.8, 137.1, 136.6, 133.5, 131.7, 130.2 (2C), 129.8 (2C), 129.3 (2C), 129.1 (2C), 128.6 (2C), 128.2 (2C), 127.7, 124.2, 121.4, 119.0, 118.7, 111.8, 110.8, 55.0, 42.0, 28.0; LRMS ($APCI^+$) m/z 535, 536 $[M+1H]^+$, 20%; HRMS (ES^+), for $C_{32}H_{26}ClN_3O_3$, calculated 536.1735, found 536.1735; RP-HPLC Alltima™ C18 5 µm 150 mm x 4.6 mm, 10–100% B in 15 min, R_t = 14.14 min, 100%.

***N*-[1-(4-Chlorobenzylcarbamoyl)-2-(1*H*-indol-3-yl)-ethyl]-3,3,3-trifluoro-2-methoxy-2-phenylpropionamide (17).** Synthesized utilizing the general procedure A described above, from **9** (0.157 g, 0.43 mmol), HATU (0.25 g, 0.65 mmol), 3,3,3-

trifluoro-2-methoxy-2-phenylpropionic acid (0.1 g, 0.43 mmol) and DIPEA (0.23 mL, 1.30 mmol) in DMF (5.0 mL) to afford **17** (0.171 g, 45%) as a white solid (MP 171– 172 ºC).

IR (cm^{-1}): 3310 (NH), 2925 (CH), 1657 (CON), 741 (CH-aromatic); ^{1}H NMR (400 MHz, DMSO-d_6) δ 10.82 (s, 1H), 8.70 (t, J = 8.0 Hz, 1H), 8.17 (d, J = 8.5 Hz, 1H), 7.62 (d, J = 7.9 Hz, 1H), 7.43 – 7.32 (m, 4H), 7.30 – 7.18 (m, 4H), 7.13 – 7.01 (m, 3H), 7.01 – 6.90 (m, 2H), 4.81 (dd, J = 8.0, 4.0 Hz, 1H), 4.32 (ddd, $J_{A'X'}$ = 6.0, $J_{B'X'}$ = 8.0, $J_{A'B'}$= 16.0 Hz, 2H), 3.27 (s, 3H), 3.15 (ddd, J_{AX} = 4, J_{BX} = 8, J_{AB} = 16.0 Hz, 2H); ^{13}C NMR (101 MHz, DMSO-d_6) δ 171.4, 165.6, 138.6, 136.6, 132.8, 131.8, 129.8, 129.4 (4C), 128.7 (2C), 128.6 (4C), 127.8, 124.4, 121.4, 119.0, 118.7, 111.7, 109.9, *84.4, 84.2, 83.9, 83.7*, 55.2, 53.8, 42.0, 28.1. **Note*: CF_3 splitting is detected at 84.0 (q, J = 25.3 Hz) (*italic*); LRMS (APCI$^+$) m/z 543, 544 [M+ H]$^+$, 50%; HRMS (ES$^+$) for $C_{28}H_{25}ClF_3N_3O_3$, calculated 543.1646, found 544.16105; RP-HPLC Alltima™ C18 5µm 150 mm x 4.6 mm, 10–100% B in 15 min, R_t = 14.53 min, 100%.

Synthesis of benzo[1,3]dioxol-5-ylmethyl-[2-(1*H*-indol-3-yl)-ethyl]-amine derivatives

Naphthalene-1-carboxylic acid benzo[1,3]dioxol-5-ylmethyl-[2-(1*H*-indol-3-yl)-ethyl]-amide (5). General procedure B: A DMF solution (10 mL) of benzo[1,3]dioxol-5-ylmethyl-[2-(1*H*-indol-3-yl)-ethyl]-amine hydrobromide **18** (0.138 g, 0.37 mmol), HATU (0.21 g, 0.55 mmol), and naphthalene-1-carboxylic acid **19** (0.063 g, 0.37 mmol) was stirred at room temperature to complete dissolution. To the stirred solution was added DIPEA (0.19 mL, 1.10 mmol) and the reaction mixture was stirred overnight. DMF was then removed *in vacuo* and the crude material was subjected to silica gel column chromatography (1:4 hexanes–EtOAc) to afford **5** (0.11 g, 67%) as a white solid (mp 199 – 200 °C).

IR (cm^{-1}): 3215 (NH), 1608 (CON), 743 (CH- aromatic); *Proton and carbon spectra displays an atropisomeric property of compound **7**, with the approximate ratio 1:0.66 calculated based on the proton benzodioxole C**H**$_2$ peaks at 6.05 and 5.97 ppm, respectively. As the spectra is complex with both splitting and overlapping, the proton NMR is reported separately for splitting peaks where possible. In case of complex overlapping (aromatic region), the proton NMR is assigned as a whole. Carbon peaks are all included. This format will be applied to all atropisomeric mixtures. ^{1}H NMR (400 MHz, DMSO-d_6) δ 10.91 (s, 0.67H), 10.71 (s, 1H), 8.07 – 7.89 (m, 3.33H), 7.75 – 7.64 (m, 1H), 7.64 – 7.44 (m, 7H), 7.42 – 7.16 (m, 3.3H), 7.14 – 7.06 (m, 1.67H), 7.06 – 6.78 (m, 5.33H), 6.71 – 6.56 (m, 2.33H), 6.39 (d, J = 7.9 Hz, 1H), 6.05 (s, 2H), 5.97 (s, 1.33H), 5.01 – 4.70 (m, 2H), 4.26 –4.02 (m, 2H), 3.43 (d, J = 20.9 Hz, 0.67H), 3.26 – 2.98 (m, 3.33H), 2.91 –2.66 (m, 2H); ^{13}C NMR (101 MHz, DMSO-d_6) δ 170.4, 170.0, 148.0, 148.0, 147.1, 147.0, 136.8, 136.4, 135.1, 135.0, 133.5 133.4, 132.3, 130.7, 129.5, 129.2, 129.0, 128.9, 128.9, 127.7, 127.5, 127.1, 126.9, 125.8, 125.0, 124.7, 124.1, 123.6, 123.3, 122.1, 121.5, 121.3, 121.1, 118.9, 118.8, 118.5, 118.0, 111.9, 111.8, 111.7, 110.7, 109.1, 108.8, 108.7, 108.1, 101.5, 51.8, 49.2, 47.1, 44.5, 24.9, 23.1; LRMS (APCI$^+$) m/z 448, 449 [M+1H]$^+$, 100%. HRMS (ES$^+$) for $C_{29}H_{24}N_2O_3$, calculated 449.1860, found 449.1859; RP-HPLC Alltima™ C18 5 µm 150 mm x 4.6 mm, 10–100% B in 15 min, R_t = 18.06 min, 100%.

1*H*-Indole-2-carboxylic acid benzo[1,3]dioxol-5-ylmethyl-[2-(1*H*-indol-3-yl)-ethyl]-amide (20). Synthesized utilizing the general procedure B described above, from benzo[1,3]dioxol-5-ylmethyl-[2-(1*H*-indol-3-yl)-ethyl]-amine hydrobromide **18** (0.18 g, 0.48 mmol), HATU (0.27 g, 0.72 mmol), 1*H*-Indole-2-carboxylic acid (0.077 g, 0.48 mmol) and DIPEA (0.25 mL, 1.43 mmol) in DMF (5.0 mL) to afford **20** (0.14 g, 67%) as a white solid (MP 198 – 199 ºC).

IR (cm^{-1}): 3440 (NH), 3274 (NH), 1620 (CON), 742 (CH-aromatic); ^{1}H NMR (400 MHz, DMSO-d_6) δ 11.72 (s, 1H), 10.86 (s, 1H), 7.72 – 7.29 (m, 4H), 7.20 (dd, J = 9.2, 4.8 Hz, 2H), 7.13 – 6.58 (m, 7H), 6.01 (s, 2H), 4.81 (bs, 2H), 3.76 (bs, 2H), 3.09 (s, 2H); ^{13}C NMR (101 MHz, DMSO-d_6) δ 163.7, 148.1, 147.0, 136.7, 136.4, 131.9, 130.5, 127.5, 123.8, 123.3, 121.9, 121.5, 120.2, 118.8, 118.7, 112.5, 111.9, 111.2, 108.8, 107.7, 103.7, 101.5, 52.4, 48.6, 47.7, 24.7, 23.3; LRMS (APCI$^+$) m/z 437, 438 [M+1], 70%; HRMS (ES$^+$) for $C_{27}H_{23}N_3O_3$, calculated 438.1812, found 439.1811; RP-HPLC Alltima™ C18 5 µm 150 mm x 4.6 mm, 10–100% B in 15 min, R_t = 14.68 min, 100%.

Benzo[*b*]thiophene-2-carboxylic acid benzo[1,3]dioxol-5-ylmethyl-[2-(1*H*-indol-3-yl)-ethyl]-amide (21). Synthesized utilizing the general procedure B described above, from benzo[1,3]dioxol-5-ylmethyl-[2-(1*H*-indol-3-yl)-ethyl]-amine hydrobromide **18** (0.183 g, 0.49 mmol), HATU (0.28 g, 0.73 mmol), benzo[*b*]thiophene-2-carboxylic acid (0.087 g, 0.49 mmol) and DIPEA (0.25 mL, 1.46 mmol) in DMF (5.0 mL) to afford **21** (0.12 g, 53%) as a white solid (MP 166 – 167 ºC).

IR (cm^{-1}): 3331 (NH), 1627 (CON), 738 (CH-aromatic); ^{1}H NMR (400 MHz, DMSO-d_6) δ 10.85 (s, 1H), 8.00 (d, J = 8.2 Hz, 1H), 7.81 (s, 1H), 7.70 – 6.64 (m, 11H), 6.02 (s, 2H), 4.73 (s, 2H), 3.65 (s, 2H), 3.12 – 2.91 (m, 2H); ^{13}C NMR (101 MHz, DMSO-d_6) δ 164.5, 148.1, 147.0, 139.7, 139.1, 137.7, 136.6, 131.5, 127.5, 126.32, 125.3 (2C), 125.2, 123.5, 122.9, 121.5 (2C), 118.7 (2C), 118.6, 111.9, 110.9, 108.8, 101.5, 49.6, 48.4, 24.7; LRMS (APCI$^+$) m/z 454, 455 [M+H]$^+$, 100%; HRMS (ES$^+$) for $C_{27}H_{22}N_2O_3S$, calculated 455.1424, found 455.1423; RP-HPLC Alltima™ C18 5 µm 150 mm x 4.6 mm, 10 – 100% B in 15 min, R_t = 14.97 min, 100%.

Benzofuran-2-carboxylic acid benzo[1,3]dioxol-5-ylmethyl-[2-(1*H*-indol-3-yl)-ethyl]-amide (22). Synthesized utilizing the general procedure B described above, from benzo[1,3]dioxol-5-ylmethyl-[2-(1*H*-indol-3-yl)-ethyl]-amine hydrobromide **18** (0.212 g, 0.57 mmol), HATU (0.32 g, 0.85 mmol), benzofuran-2-carboxylic acid (0.091 g, 0.57 mmol) and DIPEA (0.30 mL, 1.69 mmol) in DMF (5.0 mL) to afford **22** (0.156 g, 63%) as a white solid (MP 173 – 173.6 ºC).

IR (cm^{-1}): 3316 (NH), 1627 (CON), 737 (CH-aromatic); ^{1}H NMR (400 MHz, DMSO-d_6) δ 10.83 (s, 1H), 7.72 (d, J = 5.8 Hz, 1H), 7.62 (d, J = 8.3 Hz, 1H), 7.58 – 7.26 (m, 5H), 7.19 – 6.71 (m, 6H), 6.01 (s, 2H), 4.72 (s, 2H), 3.91 –3.51 (m, 2H), 3.05 (s, 2H); ^{13}C NMR (101 MHz, DMSO-d_6) δ 154.4, 149.3, 148.0, 147.0, 136.7, 131.7, 129.0, 127.4, 127.2, 126.9, 124.1, 123.6, 122.9, 122.0, 121.4, 118.7, 118.5, 112.2, 111.9, 111.1, 109.0, 108.8, 101.5, 48.7, 48.8, 25.1; LRMS (APCI$^{+/-}$) m/z 438, 439

[M+H]+, 100%; HRMS (ES+) for $C_{27}H_{22}N_2O_4$, calculated 439.1652, found 439.1652; RP-HPLC Alltima™ C18 5 µm 150 mm x 4.6 mm, 10 – 100% B in 15 min, R_t = 7.12 min, 100%.

***N*-Benzo[1,3]dioxol-5-ylmethyl-4-chloro-*N*-[2-(1*H*-indol-3-yl)-ethyl]-benzamide (23).** Synthesized utilizing the general procedure B described above, from benzo[1,3]dioxol-5-ylmethyl-[2-(1*H*-indol-3-yl)-ethyl]-amine hydrobromide **18** (0.134 g, 0.36 mmol), HATU (0.205 g, 0.53 mmol), 4-chlorobenzoic acid (0.056 g, 0.36 mmol) and DIPEA (0.187 mL, 1.08 mmol) in DMF (5.0 mL) to afford **23** (0.09 g, 58%) as a white solid (MP 132 – 133 ºC).

IR (cm^{-1}): 3203 (NH), 1626 (CON), 1500 (C–C aromatic), 1251 (C-N), 747 (C-H aromatic); This is a mixture of atropoisomers of compound **23** with the ratio approximately 2.0 : 1.2 calculated on the CH_2 splitting peaks at 2.93 and 2.84 ppm of the proton NMR. As the spectra is complex with both splitting and overlapping, the proton NMR is reported separately for splitting peaks where possible. In case of complex overlapping (aromatic region), the proton NMR is assigned as a whole. ^{1}H NMR (400 MHz, DMSO-d_6) δ 10.89 (s, 1H), 10.78 (s, 0.6H), 7.53 – 7.45 (m, 1.7H), 7.40 – 7.32 (m, 2.6H), 7.32 – 7.26 (m, 2.4H), 7.23 (d, *J* = 8.4 Hz, 1.2H), 7.14 (d, *J* = 1.9 Hz, 1H), 7.11 – 7.90 (m, 6H), 6.87 (m, 1.6H), 6.81 – 6.63 (m, 3.3H), 6.00 (s, 1.2H), 5.98 (s, 2H), 4.52 (s, 2H), 4.48 (s, 1.2H), 3.75 (s, 1.1H), 3.53 (s, 2.1H), 3.52–3.43 (m, 3.2H), 2.92 (t, *J* = 7.2 Hz, 2H), 2.88 – 2.79 (m, 1.2H); ^{13}C NMR (101 MHz, DMSO-d_6) δ 170.1 and 170.0 (1C), 147.6 and 147.4 (1C), 146.5 and 146.3 (1C), 136.2 (1C), 135.1 and 135.0 (1C), 132.1, 131.3 and 131.2 (2C), 131.1 and 130.9 (1C), 128.1 and 127.9 (2C), 127.1 and 127.0 (1C), 123.4, 122.7, 121.2 and 121.1 (1C), 120.9 and 120.2 (1C), 118.5 and 118.3 (1C), 118.2 and 118.1 (1C), 111.5 and 111.4 (1C), 110.9, 108.3 and 108.1 (1C), 107.4, 101.0 and 100.9 (1C), 50.8 and 47.1 (1C), 47.5 and 46.4 (1C), 38.9 and 38.3 (1C), 23.8 and 23.0 (1C); LRMS (APCI+) m/z 446, 447 $[M+H]^+$ 100%. HRMS (ES+) calculated for $C_{26}H_{23}ClN_2O_3$ 446.1397, found 447.1467; RP-HPLC Alltima™ C18 5 µm 150 mm x 4.6 mm, 10–100% B in 15 min, R_t = 14.76 min, 100%.

***N*-Benzo[1,3]dioxol-5-ylmethyl-2,6-dichloro-*N*-[2-(1H-indol-3-yl)-ethyl]-benzamide (24).** Synthesized utilizing the general procedure B described above, from benzo[1,3]dioxol-5-ylmethyl-[2-(1*H*-indol-3-yl)-ethyl]-amine hydrobromide **18** (0.123 g, 0.33 mmol), HATU (0.186 g, 0.49 mmol), (2,6-dichlorophenyl)-acetic acid (0.067 g, 0.33 mmol) and DIPEA (0.17 mL, 0.98 mmol) in DMF (5.0 mL) to afford **24** (0.100 g, 65%) as a white solid (MP 157 – 158 ºC).

IR (cm^{-1}): 3280 (NH), 2937 (CH), 1626 (CON), 739 (CH-aromatic); This is a mixture of atropoisomers of compound **24** with the ratio approximately 2.0 : 1.3 calculated on the CH_2 splitting peaks at 5.99 and 6.02 ppm of the proton NMR. ^{1}H NMR (400 MHz, DMSO-d_6) δ 10.90 (s, 1H), 10.80 (s, 0.7H), 7.59 – 7.25 (m, 8.3H), 7.21 (d, *J* = 2.2 Hz, 1H), 7.10 (s, 0.3H), 7.07 (dd, *J* = 15.0, 8.0 Hz, 2H), 7.03 – 6.91 (m, 2.3H), 6.88 (d, *J* = 7.7 Hz, 1.7H), 6.83 – 6.75 (m, 2.7H), 6.02 (s, 1.3H), 5.99 (s, 2H), 4.61 (s, 1.3H), 4.53 (s, 2H), 4.04 (s, 1.3H), 3.87 (s, 2H), 3.65 (t, *J* = 7.2 Hz, 2H), 3.58 – 3.44 (m, 1.3H), 3.04 (t, *J* = 7.1 Hz, 2H), 2.97 – 2.80 (m, 1.3H); ^{13}C NMR (101 MHz, DMSO-d_6) δ 168.2, 168.0, 148.1, 147.9, 147.0, 146.8, 136.8, 136.7, 135.9, 135.9, 133.7, 133.6, 132.5, 131.8, 129.6, 129.5, 128.5, 128.4, 127.6, 127.5, 124.0, 123.2, 121.5, 121.4, 120.5, 118.9, 118.7, 118.7, 118.5, 112.0, 111.8, 111.1, 108.9, 108.6, 107.8, 101.5, 101.4, 51.1, 47.9, 47.7, 47.5, 36.7, 35.9, 24.2, 23.6; LRMS (ESI+) m/z 481, 481$[M]^+$, 100; HRMS (ES+) for $C_{26}H_{22}Cl_2N_2O_3$, calculated 481.1080, found 481.1079; RP-HPLC Alltima™ C18 5 µm 150 mm x 4.6 mm, 10–100% B in 15 min, R_t = 18.81 min, 100%.

***N*-Benzo[1,3]dioxol-5-ylmethyl-4-benzoyl-*N*-[2-(1*H*-indol-3-yl)-ethyl]-benzamide (25).** Synthesized utilizing the general procedure B described above, from benzo[1,3]dioxol-5-ylmethyl-[2-(1*H*-indol-3-yl)-ethyl]-amine hydrobromide **18** (0.143 g, 0.38 mmol), HATU (0.22 g, 0.57 mmol), 4-benzoylbenzoic acid (0.086 g, 0.38 mmol) and DIPEA (0.20 mL, 1.14 mmol) in DMF (5.0 mL) to afford **25** (0. 077 g, 40%) as a white solid (MP 181.2 – 181.7 ºC).

IR (cm^{-1}): 3191 (NH), 2990 (CH), 1643 (CON), 742 (CH-aromatics); This is a mixture of atropoisomers of compound **25** with the ratio approximately 2.0 : 0.9 calculated on the CH_2 splitting peaks at 4.75 and 6.02 ppm of the proton NMR; ^{1}H NMR (400 MHz, DMSO-d_6) δ 10.83 (d, *J* = 10.1 Hz, 1.5H), 7.85 – 7.66 (m, 5.5H), 7.58 (dt, *J* = 18.2, 8.8 Hz, 6.5H), 7.41 – 7.17 (m, 4H), 7.11 – 6.85 (m, 7.5H), 6.84 – 6.56 (m, 2H), 6.01 (d, *J* = 13.2 Hz, 3H), 4.75 (s, 2H), 4.32 (s, 0.9H), 3.60 (d, *J* = 7.1 Hz, 1H), 3.36 – 3.30 (overlapped by water) (m, 2.5H), 3.03 (d, *J* = 7.1 Hz, 1H), 2.88 (t, *J* = 7.1 Hz, 2H); ^{13}C NMR (101 MHz, DMSO-d_6) δ 195.6, 170.6, 148.0, 146.9, 140.9, 137.4, 137.2, 136.6, 133.4, 132.0, 130.1, 130.0, 129.1, 127.4, 127.1, 126.8, 123.7, 121.8, 121.4, 118.7, 118.6, 118.1, 111.9, 110.8, 108.8, 108.7, 101.4, 52.4, 49.1, 46.9, 45.5, 24.2, 23.1; LRMS (APCI+/-) m/z 502, 503 [M+1], 100%; HRMS (ES+) for $C_{32}H_{26}N_2O_4$, calculated 503.1965, found 503.1964; RP-HPLC Alltima™ C18 5 µm 150 mm x 4.6 mm, 10–100% B in 15 min, R_t = 17.71 min, 100 %.

5-Methylpyrazine-2-carboxylic acid benzo[1,3]dioxol-5-ylmethyl-[2-(1*H*-indol-3-yl)-ethyl]-amide (26). Synthesized utilizing the general procedure B described above, from benzo[1,3]dioxol-5-ylmethyl-[2-(1*H*-indol-3-yl)-ethyl]-amine hydrobromide **18** (0.197 g, 0.53 mmol), HATU (0.30 g, 0.79 mmol), 5-methylpyrazine-2-carboxylic acid (0.072 g, 0.53 mmol) and DIPEA (0.28 mL, 1.58 mmol) in DMF (5.0 mL) to afford **26** (0. 047 g, 22%) as a white solid (MP 132 – 133 ºC).

IR (cm^{-1}): 3316 (NH), 1632 (CON), 1632 (CON), 739 (CH-aromatic); This is a mixture of atropoisomers of compound **26** with the ratio approximately 2 : 1 calculated on the CH_2 splitting peaks at 4.71 and 4.46 ppm of the proton NMR; ^{1}H NMR (400 MHz, DMSO-d_6) δ 10.83 (s, 0.5H), 10.77 (s, 1H), 8.75 (d, *J* = 1.2 Hz, 0.5H), 8.56 (s, 0.5H), 8.34 (s, 1H), 8.19 (d, *J* = 1.3 Hz, 1H), 7.52 (d, *J* = 7.8 Hz, 0.5H), 7.34 (d, *J* = 8.1 Hz, 0.7H), 7.25 (d, *J* = 8.1 Hz, 1.2H), 7.16 (d, *J* = 2.0 Hz, 0.7H), 7.11 – 7.02 (m, 1.8H), 7.02 – 6.79 (m, 8H), 6.75 (d, *J* = 7.9 Hz, 0.5H), 6.01 (s, 2H), 5.99 (s, 0.8H), 4.71 (s, 2H), 4.46 (s, 1H), 3.60 (dt, *J* = 15.8, 7.5 Hz, 3.2H), 2.92 (dt, *J* = 13.8, 7.5 Hz, 3.2H), 2.54 (s, 1.8H), 2.41 (s, 3.2); ^{13}C NMR (101 MHz, DMSO-d_6) δ 167.2, 166.8, 155.0, 154.2, 147.9, 147.4, 147.1, 147.0, 146.9, 143.7, 143.2, 143.0, 142.0, 136.7, 136.6, 131.9, 131.3, 127.6, 127.1, 123.6, 123.3, 121.8, 121.6, 121.5, 121.3, 118.7, 118.5, 118.1,

111.9, 111.7, 110.9, 108.8, 108.7, 108.6, 108.5, 101.5, 101.4, 52.0, 48.6, 47.8, 46.192, 24.4, 23.1, 21.7, 21.5; LRMS (APCI +/-) m/z 414, 415 $[M+H]^+$, 100%; HRMS (ES^+) for $C_{24}H_{22}N_4O_5$, calculated 415.17647, found 415.17611; RP-HPLC Alltima™ C18 5 µm 150 mm x 4.6 mm, 10–100% B in 15 min, R_t = 12.40 min, 100%.

5-Methoxy-1*H*-indole-2-carboxylic acid benzo[1,3]dioxol-5-ylmethyl-[2-(1*H*-indol-3-yl)-ethyl]-amide (27). Synthesized utilizing the general procedure B described above, from benzo[1,3]dioxol-5-ylmethyl-[2-(1*H*-indol-3-yl)-ethyl]-amine hydrobromide **18** (0.193 g, 0.51 mmol), HATU (0.29 g, 0.77 mmol), 5-methoxy-1*H*-indole-2-carboxylic acid (0.098 g, 0.51 mmol) and DIPEA (0.27 mL, 1.54 mmol) in DMF (5.0 mL) to afford **27** (0. 149 g, 62%) as an off white solid (MP 202 – 202.5 ºC).

IR (cm^{-1}): 3439 (NH), 3258(NH), 1612 (CON), 1450 (C-C ring), 738 (C-H aromatic); ^1H NMR (400 MHz, DMSO-d_6) δ 11.57 (s, 1H), 10.86 (s, 1H), 7.68-7.26 (m, 3H), 7.19 (s, 1H), 7.13 – 6.48 (m, 8H), 6.01 (s, 2H), 4.81 (s, 2H), 3.73 (s, 5H), 3.08 (s, 2H); ^{13}C NMR (101 MHz, DMSO-d_6) δ 163.6, 154.2, 148.1, 146.9, 136.7, 132.0, 131.6, 130.8, 127.8, 127.6, 123.3, 121.5 (2C), 118.8 (2C), 115.0, 113.4, 111.9, 108.8, 103.5 (2C), 102.4, 101.5, 65.4, 55.7, 48.5, 48.1, 23.6; LRMS (ESI^+) m/z 467, 467 $[M]^+$, 100%; HRMS (ES^+) for $C_{28}H_{25}N_3O_4$, calculated 468.1918, found 468.1919; RP-HPLC Alltima™ C18 5 µm 150 mm x 4.6 mm, 10 – 100% B in 15 min, R_t = 6.92 min, 100%.

5-Chloro-1*H*-indole-2-carboxylic acid benzo[1,3]dioxol-5-ylmethyl-[2-(1*H*-indol-3-yl)-ethyl]-amide (28). Synthesized utilizing the general procedure B described above, from benzo[1,3]dioxol-5-ylmethyl-[2-(1*H*-indol-3-yl)-ethyl]-amine hydrobromide **18** (0.21 g, 0.56 mmol), HATU (0.32 g, 0.83 mmol), 5-chloro-1*H*-indole-2-carboxylic acid (0.11 g, 0.56 mmol) and DIPEA (0.29 mL, 1.69 mmol) in DMF (5.0 mL) to afford **28** (0.17 g, 64%) as an off white solid (MP 194 – 194.5 ºC).

IR (cm^{-1}): 3433 (NH), 3265 (NH), 1612 (CON), 739 (CH-aromatic); ^1H NMR (400 MHz, DMSO-d_6) δ 11.93 (*s*, 1H), 10.87 (s, 1H), 7.73 – 7.26 (m, 4H), 7.25 – 7.13 (m, 2H), 7.08 (t, *J* = 7.5 Hz, 1H), 7.02 – 6.60 (m, 5H), 6.02 (s, 2H), 4.79 (br s, 2H), 3.74 (br s, 2H), 3.08 (s, 2H); ^{13}C NMR (101 MHz, DMSO-d_6) δ 163.4, 148.1, 147.0, 136.7, 134.8, 132.1, 128.5, 127.5, 124.7, 123.9 (2C), 123.4, 121.5, 121.4, 121.0, 118.8 (2C), 118.7, 114.1, 111.9, 108.8, 103.2 (2C), 101.5, 52.4, 48.9, 48.6, 47.6, 24.7, 23.4; *Note : Signs of atropisomers for aliphatic CH_2, in which 52.38 and 48.59 are the splitting of 1 C (Ar-$\underline{C}H_2$-N-); 48.91 and 47.58 are the splitting of (CH_2-$\underline{C}H_2$-N-), and 24.68, 23.41 are the splitting of ($\underline{C}H_2$-CH_2-N-); LRMS (ESI^+) m/z 471, 471 $[M]^+$, 50%; HRMS (ES^+) for $C_{27}H_{22}ClN_3O_3$, calculated 472.1423, found 472.1422; UPLC: Mobile phase A = 100% H_2O with 0.1% formic acid; Mobile phase B = 90% ACN : 10% H_2O and 0.1% formic acid; RP-HPLC Agilent Zorbax SB-C18 1.8 µm, 50 mm x 2.1 mm, isocratic 80% mobile phase B at 0.6 mL/min in 8 minutes, R_t = 5.05 min, 100%.

1*H*-Indole-5-carboxylic acid benzo[1,3]dioxol-5-ylmethyl-[2-(1*H*-indol-3-yl)-ethyl]-amide (29). Synthesized utilizing the general procedure B described above, from benzo[1,3]dioxol-5-ylmethyl-[2-(1*H*-indol-3-yl)-ethyl]-amine hydrobromide **18** (0.20 g, 0.54 mmol), HATU (0.31 g, 0.80 mmol), 1*H*-indole-5-carboxylic acid (0.087 g, 0.54 mmol) and DIPEA (0.28 mL, 1.61 mmol) in DMF (5.0 mL) to afford **29** (0.158 g, 67%) as an off white solid (MP 162.5 – 163 ºC).

IR (cm^{-1}): 3638 (NH), 3227 (NH), 1614 (CON), 740 (CH-aromatic); ^1H NMR (400 MHz, DMSO-d_6) δ 11.29 (s, 1H), 10.78 (s, 1H), 7.61 (s, 1H), 7.51 – 7.39 (m, 2H), 7.56 – 6.38 (m, 9H), 6.47 (s, 1H), 6.01 (s, 2H), 4.87 – 4.29 (m, 2H), 3.65 – 3.45 (m, 2H), 3.12 – 2.70 (m, 2H); ^{13}C NMR (101 MHz, DMSO-d_6) δ 186.0, 172.8, 148.0, 146.9, 136.6, 136.5, 127.8, 127.5, 127.0, 123.3, 121.4, 120.4, 119.1, 118.6, 111.8, 111.7, 108.7, 102.2, 101.4, 49.1, 47.3, 45.6, 24.6, 23.4. *Note: Signs of atropoisomers for aliphatic CH_2, in which 47.3 is the splitting of 1 C (Ar-$\underline{C}H_2$-N-); 49.1 and 45.6 are the splitting of (CH_2-$\underline{C}H_2$-N-); 24.6 and 23.4 are the splitting of ($\underline{C}H_2$-CH_2-N-). Peak at 49.3 ppm is among the impurities; LRMS (ESI^+) m/z 437, 437 $[M]^+$, 70%; HRMS (ES^+) for $C_{27}H_{23}N_3O_3$, calculated 438.1812, found 438.1812; RP-HPLC Alltima™ C18 5 µm 150 mm x 4.6 mm, 10–100% B in 15 min, R_t = 6.48 min, 96%.

Acknowledgements

The authors thank the NHMRC (Australia) for project support, Nathan D. Smith (Analytical and Biomolecular Research Facility at the University of Newcastle) for the HRMS data, James K. Chen for helpful discussions and T.N.T. is the recipient of a Prime Minister's Australia Asia Postgraduate Endeavour Award.

References

1. C. Nusslein-Volhard and E. Wieschaus, *Nature*, 1980, **287**, 795-801.
2. A. P. McMahon, P. W. Ingham and C. J. Tabin, *Curr. Topics Devel. Biol.*, 2003, **53**, 1-114, 111
3. P. W. Ingham and A. P. McMahon, *Genes Devel.*, 2001, **15**, 3059-3087.
4. M. Zbinden, A. Duquet, A. Lorente-Trigos, S.-N. Ngwabyt, I. Borges and A. Ruiz i Altaba, *EMBO J.*, 2010, **29**, 2659-2674.
5. A. Po, E. Ferretti, E. Miele, E. De Smaele, A. Paganelli, G. Canettieri, S. Coni, L. Di Marcotullio, M. Biffoni, L. Massimi, C. Di Rocco, I. Screpanti and A. Gulino, *EMBO J.*, 2010, **29**, 2646-2658.
6. E. H. Epstein, *Nat. Rev. Cancer*, 2008, **8**, 743-754.
7. C. Raffel, R. B. Jenkins, L. Frederick, D. Hebrink, B. Alderete, D. W. Fults and C. D. James, *Cancer Res.*, 1997, **57**, 842-845.
8. T. Pietsch, A. Waha, A. Koch, J. Kraus, S. Albrecht, J. Tonn, N. Sorensen, F. Berthold, B. Henk, N. Schmandt, H. K. Wolf, A. von Deimling, B. Wainwright, G. Chenevix-Trench, O. D. Wiestler and C. Wicking, *Cancer Res.*, 1997, **57**, 2085-2088.
9. D. G. Evans, P. A. Farndon, L. D. Burnell, H. R. Gattamaneni and J. M. Birch, *Br. J. Cancer*, 1991, **64**, 959-961.
10. S. P. Thayer, M. Pasca di Magliano, P. W. Heiser, C. M. Nielsen, D. J. Roberts, G. Y. Lauwers, Y. P. Qi, S. Gysin, C. Fernandez-del Castillo, V. Yajnik, B. Antoniu, M. McMahon, A. L. Warshaw and M. Hebrok, *Nature*, 2003, **425**, 851-856.
11. S. Karhadkar Sunil, G. S. Bova, N. Abdallah, S. Dhara, D. Gardner, A. Maitra, T. Isaacs John, M. Berman David and A. Beachy Philip, *Nature*, 2004, **431**, 707-712.
12. Z. Yuan, J. A. Goetz, S. Singh, S. K. Ogden, W. J. Petty, C. C. Black, V. A. Memoli, E. Dmitrovsky and D. J. Robbins, *Oncogene*, 2007, **26**, 1046-1055.

13. D. N. Watkins, M. Berman David, G. Burkholder Scott, B. Wang, A. Beachy Philip and B. Baylin Stephen, *Nature*, 2003, **422**, 313-317.
14. D. Qualtrough, A. Buda, W. Gaffield, C. Williams Ann and C. Paraskeva, *Int. J. Cancer*, 2004, **110**, 831-837.
15. M. Berman David, S. Karhadkar Sunil, A. Maitra, R. Montes De Oca, R. Gerstenblith Meg, K. Briggs, R. Parker Antony, Y. Shimada, R. Eshleman James, D. N. Watkins and A. Beachy Philip, *Nature*, 2003, **425**, 846-851.
16. M. Kasper, V. Jaks, M. Fiaschi and R. Toftgaard, *Carcinogenesis*, 2009, **30**, 903-911.
17. S. Mukherjee, N. Frolova, A. Sadlonova, Z. Novak, A. Steg, G. P. Page, D. R. Welch, S. M. Lobo-Ruppert, J. M. Ruppert, M. R. Johnson and A. R. Frost, *Cancer Biol. Ther.*, 2006, **5**, 674-683.
18. X. Chen, A. Horiuchi, N. Kikuchi, R. Osada, J. Yoshida, T. Shiozawa and I. Konishi, *Cancer Sci.*, 2007, **98**, 68-76.
19. T. N. Trinh, E. A. McLaughlin, C. P. Gordon and A. McCluskey, *MedChemComm*, 2014, **5**, 117-133.
20. FDA approves new treatment for most common form of advanced skin cancer, http://www.fda.gov/NewsEvents/Newsroom/PressAnnouncements/ucm455862.htm).
21. FDA approves new treatment for most common type of skin cancer http://www.fda.gov/NewsEvents/Newsroom/PressAnnouncements/ucm289545.htm).
22. R. Nanta, D. Kumar, D. Meeker, M. Rodova, P. J. Van Veldhuizen, S. Shankar and R. K. Srivastava, *Oncogenesis*, 2013, **2**, e42.
23. J. K. Chen, J. Taipale, K. E. Young, T. Maiti and P. A. Beachy, *Proc. Nat. Acad. Sci. USA*, 2002, **99**, 14071-14076.
24. E. Petrova, J. Rios-Esteves, O. Ouerfelli, J. F. Glickman and M. D. Resh, *Nat. Chem. Biol.*, 2013, **9**, 247-249.
25. H. R. Maun, X. Wen, A. Lingel, F. J. de Sauvage, R. A. Lazarus, S. J. Scales and S. G. Hymowitz, *J. Biol. Chem.*, 2010, **285**, 26570-26580.
26. G. Bosco-Clement, F. Zhang, Z. Chen, H. M. Zhou, H. Li, I. Mikami, T. Hirata, A. Yagui-Beltran, N. Lui, H. T. Do, T. Cheng, H. H. Tseng, H. Choi, L. T. Fang, I. J. Kim, D. Yue, C. Wang, Q. Zheng, N. Fujii, M. Mann, D. M. Jablons and B. He, *Oncogene*, 2014, **33**, 2087-2097.
27. A. Solinas, H. Faure, H. Roudaut, E. Traiffort, A. Schoenfelder, A. Mann, F. Manetti, M. Taddei and M. Ruat, *J. Med. Chem.*, 2012, **55**, 1559-1571.
28. T. Ohashi, Y. Oguro, T. Tanaka, Z. Shiokawa, Y. Tanaka, S. Shibata, Y. Sato, H. Yamakawa, H. Hattori, Y. Yamamoto, S. Kondo, M. Miyamoto, M. Nishihara, Y. Ishimura, H. Tojo, A. Baba and S. Sasaki, *Bioorg. Med. Chem.*, 2012, **20**, 5507-5517.
29. M. J. Munchhof, Q. Li, A. Shavnya, G. V. Borzillo, T. L. Boyden, C. S. Jones, S. D. LaGreca, L. Martinez-Alsina, N. Patel, K. Pelletier, L. A. Reiter, M. D. Robbins and G. T. Tkalcevic, *ACS Med. Chem. Lett.*, 2012, **3**, 106-111.
30. S. Pan, X. Wu, J. Jiang, W. Gao, Y. Wan, D. Cheng, D. Han, J. Liu, N. P. Englund, Y. Wang, S. Peukert, K. Miller-Moslin, J. Yuan, R. Guo, M. Matsumoto, A. Vattay, Y. Jiang, J. Tsao, F. Sun, A. C. Pferdekamper, S. Dodd, T. Tuntland, W. Maniara, J. F. Kelleher, III, Y.-M. Yao, M. Warmuth, J. Williams and M. Dorsch, *ACS Med. Chem. Lett.*, 2010, **1**, 130-134.
31. He, Biao; Fujii, Naoaki; MYou, Liang; Xu, Zhidong; Jablons, David M. *Dihydropyrazolecarboxamides and their preparation, pharmaceutical compositions and use in the targeting GLI proteins in human cancer by small molecules.* Application: WO Pat., 2009-GB50926 2010013037, 2010.
32. M. R. Tremblay, A. Lescarbeau, M. J. Grogan, E. Tan, G. Lin, B. C. Austad, L.-C. Yu, M. L. Behnke, S. J. Nair, M. Hagel, K. White, J. Conley, J. D. Manna, T. M. Alvarez-Diez, J. Hoyt, C. N. Woodward, J. R. Sydor, M. Pink, J. MacDougall, M. J. Campbell, J. Cushing, J. Ferguson, M. S. Curtis, K. McGovern, M. A. Read, V. J. Palombella, J. Adams and A. C. Castro, *J. Med. Chem.*, 2009, **52**, 4400-4418.
33. K. D. Robarge, S. A. Brunton, G. M. Castanedo, Y. Cui, M. S. Dina, R. Goldsmith, S. E. Gould, O. Guichert, J. L. Gunzner, J. Halladay, W. Jia, C. Khojasteh, M. F. T. Koehler, K. Kotkow, H. La, R. L. La Londe, K. Lau, L. Lee, D. Marshall, J. C. Marsters, L. J. Murray, C. Qian, L. L. Rubin, L. Salphati, M. S. Stanley, J. H. A. Stibbard, D. P. Sutherlin, S. Ubhayaker, S. Wang, S. Wong and M. Xie, *Bioorg. Med. Chem. Lett.*, 2009, **19**, 5576-5581.
34. M. R. Tremblay, M. Nevalainen, S. J. Nair, J. R. Porter, A. C. Castro, M. L. Behnke, L.-C. Yu, M. Hagel, K. White, K. Faia, L. Grenier, M. J. Campbell, J. Cushing, C. N. Woodward, J. Hoyt, M. A. Foley, M. A. Read, J. R. Sydor, J. K. Tong, V. J. Palombella, K. McGovern and J. Adams, *J. Med. Chem.*, 2008, **51**, 6646-6649.
35. V. Travaglione, C. Peacock, J. MacDougall, K. McGovern, J. Cushing, L. C. Yu, M. Trudeau, V. Palombella, J. Adams, J. Hierman, J. Rhodes, W. Devereux, and D.N. Watkins. *A novel HH pathway inhibitor, IPI-926, delays recurrence postchemotherapy in a primary human SCLC xenograft model*. 99th AACR Annual Meeting. 2008. p. 4611.8.
36. M. Dai, F. He, R. KJain, R. Karki, J. F. Kelleher, J. Lei, L. Llamas, M. A. McEwan, K. Miller-Moslin, L. B. Perez, S. Peukert, and N. Yusuff. *Nitrogen-containing heterocyclic organic compounds as inhibitors of the hedgehog pathway and their preparation and use in the treatment of diseases.* Application: WO Pat., 2008-EP53010 2008110611, 2008.
37. J. Fu, M. Rodova, S. K. Roy, J. Sharma, K. P. Singh, R. K. Srivastava and S. Shankar, *Cancer Lett.*, 2013, **330**, 22-32.
38. Y. Rifai, M. A. Arai, S. K. Sadhu, F. Ahmed and M. Ishibashi, *Bioorg. Med. Chem. Lett.*, 2011, **21**, 718-722.
39. T. Mazumdar, J. DeVecchio, T. Shi, J. Jones, A. Agyeman and J. A. Houghton, *Cancer Res.*, 2011, **71**, 1092-1102.
40. M. A. Arai, C. Tateno, T. Koyano, T. Kowithayakorn, S. Kawabe and M. Ishibashi, *Org. Biomol. Chem.*, 2011, **9**, 1133-1139.
41. M. Actis, M. C. Connelly, A. Mayasundari, C. Punchihewa and N. Fujii, *Biopolymers*, 2011, **95**, 24-30.
42. N. Mahindroo, M. C. Connelly, C. Punchihewa, L. Yang, B. Yan and N. Fujii, *Bioorg. Med. Chem.*, 2010, **18**, 4801-4811.
43. N. Mahindroo, C. Punchihewa and N. Fujii, *J. Med. Chem.*, 2009, **52**, 3829-3845.
44. J. M. Hyman, A. J. Firestone, V. M. Heine, Y. Zhao, C. A. Ocasio, K. Han, M. Sun, P. G. Rack, S. Sinha, J. J. Wu, D. E. Solow-Cordero, J. Jiang, D. H. Rowitch and J. K. Chen, *Proc. Nat. Acad. Sci. USA*, 2009, **106**, 14132-14137.
45. T. Hosoya, M. A. Arai, T. Koyano, T. Kowithayakorn and M. Ishibashi, *ChemBioChem*, 2008, **9**, 1082-1092.
46. M. A. Arai, C. Tateno, T. Hosoya, T. Koyano, T. Kowithayakorn and M. Ishibashi, *Bioorg. Med. Chem.*, 2008, **16**, 9420-9424.
47. M. Lauth, A. Bergstroem, T. Shimokawa and R. Toftgard, *Proc. Nat. Acad. Sci. USA*, 2007, **104**, 8455-8460.
48. G. J. P. Dijkgraaf, B. Alicke, L. Weinmann, T. Januario, K. West, Z. Modrusan, D. Burdick, R. Goldsmith, K. Robarge, D. Sutherlin, S. J. Scales, S. E. Gould, R. L. Yauch and F. J. de Sauvage, *Cancer Res.*, 2011, **71**, 435-444.
49. R. L. Yauch, G. J. P. Dijkgraaf, B. Alicke, T. Januario, C. P. Ahn, T. Holcomb, K. Pujara, J. Stinson, C. A. Callahan, T. Tang, J. F. Bazan, Z. Kan, S. Seshagiri, C. L. Hann, S. E. Gould, J. A. Low, C. M. Rudin and F. J. de Sauvage, *Science*, 2009, **326**, 572-574.
50. S. Buonamici, J. Williams, M. Morrissey, A. Wang, R. Guo, A. Vattay, K. Hsiao, J. Yuan, J. Green, B. Ospina, Q. Yu, L. Ostrom, P. Fordjour, D. L. Anderson, J. E. Monahan, J. F.

Kelleher, S. Peukert, S. Pan, X. Wu, S. M. Maira, C. Garcia-Echeverria, K. J. Briggs, D. N. Watkins, Y. M. Yao, C. Lengauer, M. Warmuth, W. R. Sellers and M. Dorsch, *Sci. Transl. Med.*, 2010, **2**, 51ra70-51ra70.

51. T. N. Trinh, E. A. McLaughlin, M. K. Abdel-Hamid, C. P. Gordon, I. R. Bernstein, V. Pye, P. Cossar, J. A. Sakoff and A. McCluskey, *Org. Biomol. Chem.*, 2016, DOI: 10.1039/c6ob00606j.
52. J. Taipale, J. K. Chen, M. K. Cooper, B. Wang, R. K. Mann, L. Milenkovic, M. P. Scotts and P. A. Beachy, *Nature*, 2000, **406**, 1005-1009.
53. Y. Tang, S. Gholamin, S. Schubert, M. I. Willardson, A. Lee, P. Bandopadhayay, G. Bergthold, S. Masoud, B. Nguyen, N. Vue, B. Balansay, F. Yu, S. Oh, P. Woo, S. Chen, A. Ponnuswami, M. Monje, S. X. Atwood, R. J. Whitson, S. Mitra, S. H. Cheshier, J. Qi, R. Beroukhim, J. Y. Tang, R. Wechsler-Reya, A. E. Oro, B. A. Link, J. E. Bradner and Y.-J. Cho, *Nature Med.*, 2014, **20**, 732-740.
54. P. G. Rack, J. Ni, A. Y. Payumo, V. Nguyen, J. A. Crapster, V. Hovestadt, M. Kool, D. T. W. Jones, J. K. Mich, A. J. Firestone, S. M. Pfister, Y.-J. Cho and J. K. Chen, *Proc. Nat. Acad. Sci. USA*, 2014, **111**, 11061-11066.
55. M. Frank-Kamenetsky, M. Zhang Xiaoyan, S. Bottega, O. Guicherit, H. Wichterle, H. Dudek, D. Bumcrot, Y. Wang Frank, S. Jones, J. Shulok, L. Rubin Lee and A. Porter Jeffery, *J. Biol.*, 2002, **1**, 10.
56. S. R. LaPlante, L. D. Fader, K. R. Fandrick, D. R. Fandrick, O. Hucke, R. Kemper, S. P. F. Miller and P. J. Edwards, *J. Med. Chem.*, 2011, **54**, 7005-7022.
57. P. Chomczynski and N. Sacchi, *Nature Prot.*, 2006, **1**, 581-585.
58. A. P. Sobinoff, V. Pye, B. Nixon, S. D. Roman and E. A. McLaughlin, *Toxicological Sci.*, 2010, **118**, 653-666.

4.2. References

1. J. K. Chen, J. Taipale, K. E. Young, T. Maiti and P. A. Beachy, *Proceedings of the National Academy of Sciences USA,* 2002, **99**, 14071-14076.

2. C. P. Gordon, K. A. Young, L. Hizartzidis, F. M. Deane and A. McCluskey, *Organic & Biomolecular Chemistry*, 2011, **9**, 1419.

V. CHAPTER FIVE

Discovery of the 1,3-thiazine-6-phenylimino-5-carboxylate analogues

5.1. Introduction

In our screening program for potential small molecule inhibitors of the HSP, we discovered a series of 12 1,3-thiazine-6-phenylimino-5-carboxylate analogues, represented by **1**, which displays core structural similarities to HPI-1 (**2**) [1], a non-selective inhibitor of the HSP (Figure 1).

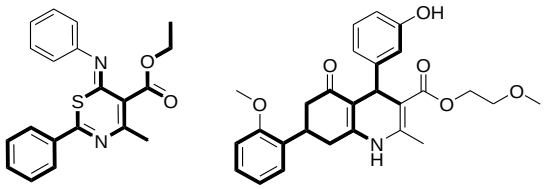

1 **2** HPI -1

Figure 1. Structural similarities of 1,3-thiazine-6-phenylimino-5-carboxylate analogues, represented by **1**, with HPI-1 (**2**)

Mechanistically, HPI-1 (**2**) is supposed to inhibit the whole ciliary process and thus leads to the inhibition of both exogenous and endogenous Gli signalling [1]. Hence, these analogues may present as a new scaffold of inhibitors targeting the HSP downstream of Smo. This Chapter introduces how we discovered these 1,3-thiazine-6-phenylimino-5-carboxylates in a one pot synthesis. The discovery of this scaffold is included in the following paper. The supporting information is included as Appendix to Chapter 5 (please see Chapter 8, page 443).

The biological evaluation of these analogues is going on and results will be reported in due course.

Tetrahedron Letters 57 (2016) 3256–3259

Contents lists available at ScienceDirect

Tetrahedron Letters

journal homepage: www.elsevier.com/locate/tetlet

A multicomponent access to 1,3-thiazine-6-phenylimino-5-carboxylates

Trieu N. Trinh, Adam McCluskey *

Chemistry, Centre for Chemical Biology, School of Environmental & Life Sciences, The University of Newcastle, University Drive, Callaghan, NSW 2308, Australia

ARTICLE INFO

Article history:
Received 8 April 2016
Revised 12 May 2016
Accepted 1 June 2016
Available online 2 June 2016

Keywords:
Multicomponent reaction
Isothiocyanate
1,3-Thiazine
Anhydride
Ethyl 3-aminocrotonate

ABSTRACT

The multicomponent reaction of ethyl 3-aminocrotonate (**1**), substituted phenylisothiocyanates (**2a–i**) and acetic anhydride (**7**), afforded facile access to a series of substituted 1,3-thiazine-6-phenylimino-5-carboxylates under mild conditions in 15–65% yields. Limited tolerance for modification of the anhydride moiety was noted with a significant reduction in yield for propionic and trifluoroacetic anhydrides. The use of benzoic anhydride favoured a two-component coupling product.

Introduction

Isothiocyanate multicomponent reactions (MCRs) have proved to be extremely versatile entry points to a wide array of novel biologically active scaffolds.[1–4] MCRs, by virtue of this simplicity and the diversity of potential individual components can permit the exquisite positioning of key pharmacophoric moieties in the correct chemical space to enable critical interactions within protein binding sites.[5–11]

The use of a one-pot MCR is particularly appealing, especially in light of the increasing drivers towards sustainable synthetic methodologies and approaches with high atom economy.[12–15] We were particularly interested in a recent report from Vasu and co-workers that detailed the one-pot MCR synthesis of quinazolin-2-yl-tetrasubstituted thiophenes.[16] While the thiophene moiety has had widespread use in medicinal chemistry, it was the transient formation of the ammonium thiolate zwitterion (**4**) in the postulated mechanism that attracted our initial attention (Scheme 1).[17–19]

Examination of Vasu's proposed mechanism, suggested that replacement of the activated halide by acetic anhydride would permit in situ trapping of the anion, which would then follow a similar sequence of intramolecular additions to yield compounds such as **6**, or possibly those lacking the exocyclic $-NH_2$ (from loss of NH_3).[16] Thus our interest lay in the possible generation of a family

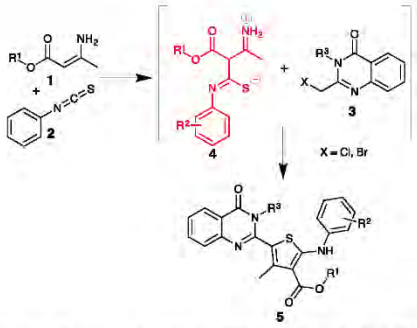

Scheme 1. Reagents and conditions: THF/CH_3CN (1:1), 45–50 °C, DMF.

of phenylimino-1,3-oxathiane-5-carboxylates (Fig. 1), a scaffold that is currently very poorly described in the chemical literature.[20]

Ethyl 3-aminocrotonate (**1**) was stirred with phenylisothiocyanate (**2**) under a nitrogen atmosphere followed by the addition of acetic anhydride (**7**). TLC analysis showed clear evidence for the consumption of starting materials, however, examination of the crude NMR showed no evidence of a NH_2 moiety, nor did the FTIR spectrum. No NH stretch was observed, but there was clear evidence of the ester C=O ($\nu_{C=O}$ 1728 cm^{-1}) and additional signals in the aromatic region of the NMR spectrum. Rather than the

* Corresponding author. Tel.: +61 (0)249216486; fax: +61 (0)249215472.
E-mail address: Adam.McCluskey@newcastle.edu.au (A. McCluskey).

http://dx.doi.org/10.1016/j.tetlet.2016.06.007
0040-4039/

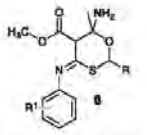

Figure 1. Representative example of a phenylimino-1,3-oxathiane-5-carboxylate.

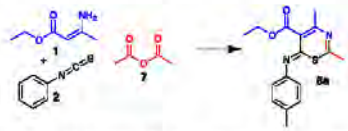

Scheme 2. Synthesis of 1,3-thiazine **8a**. Reagents and conditions: CH_3CN, 24 h, RT, under N_2.

proposed phenylimino-1,3-oxathiane-5-carboxylate, all spectroscopic evidence was consistent with the synthesis of a similarly poorly described scaffold, 2,4-dimethyl-6-phenylimino-6*H*-[1,3] thiazine-5-carboxylic acid ethyl ester (**8a**) which was isolated in a 65% yield (Scheme 2).[21]

Most probably the observed 1,3-thiazine-6-phenylimino-5-carboxylate (**8a**) arose via the coupling of ethyl 3-aminocrotonate with phenyl isothiocyanate to yield the ammonium thiolate zwitterion (**10**). The thiolate was intercepted by the addition of acetic anhydride and following acetate loss and H-abstraction, yielded enamine (**12**). Cyclisation to the thiazine results from an amine mediated nucleophilic attack on the carbonyl moiety followed by intramolecular proton transfer and subsequent loss of water to give the protonated 1,3-thiazine-6-phenylimino-5-carboxylate (**15**). Carboxylate H-abstraction from **15** gives **8a**. This mechanism differs from Vasu's only in the final stages where the loss of ammonia is not favoured over intramolecular condensation with the carbonyl moiety (Fig. 2).

The use of a variety of substituted isothiocyanates afforded 1,3-thiazines **8a–8i** in low (15%, **8i**; Table 1, entry 9) to good (65%, **8a**;

Table 1
Synthesis of substituted 1,3-thiazin-6-imino-5-carboxylates **8a–8i**

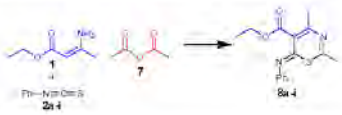

Entry	R	Product	Yield (%)
1		**8a**	65
2		**8b**	19
3		**8c**	50
4		**8d**	64
5		**8e**	35
6		**8f**	20
7		**8g**	29
8		**8h**	29
9	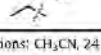	**8i**	15

Reagents and conditions: CH_3CN, 24 h, RT, under N_2.

entry 1) yields. The introduction of a bromine substituent (64%, **8d**; entry 4) was well tolerated with no change in yield (65% vs 64%), but strong electron withdrawing substituents, e.g., 4-CF_3 (35%, **8e**; entry 5) and 3,5-Cl_2 (20%, **8f**; entry 6) resulted in a significant

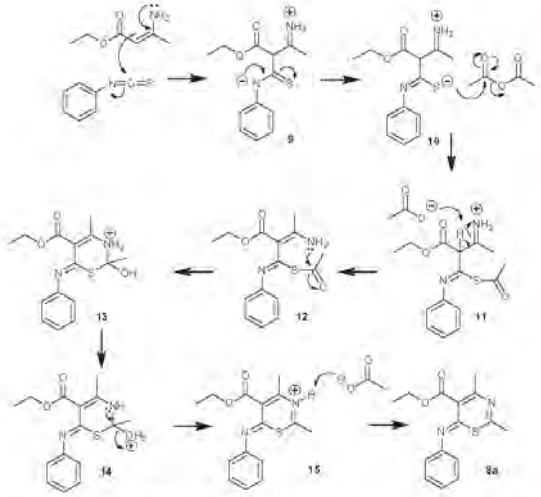

Figure 2. Proposed mechanism for the formation of 1,3-thiazine-5-carboxylate from the one-pot MCR of ethyl 3-aminocrotonates, phenylisothiocyanate and acetic anhydride.

Table 2
Synthesis of substituted 1,3-thiazin-6-imines **8j–8l** using propionic, benzoic and trifluoroacetic anhydrides

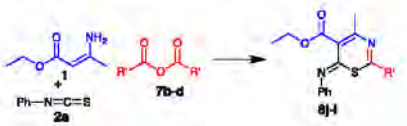

Entry	R'	Product	Yield (%)
1	CH_2CH_3 **7b**	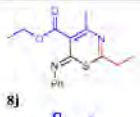 **8j**	29
2	**7c**	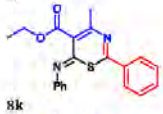 **8k**	4
3	CF_3 **7d**	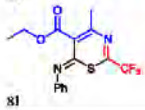 **8l**	12

Reagents and conditions: CH_3CN, 24 h, RT, under N_2.

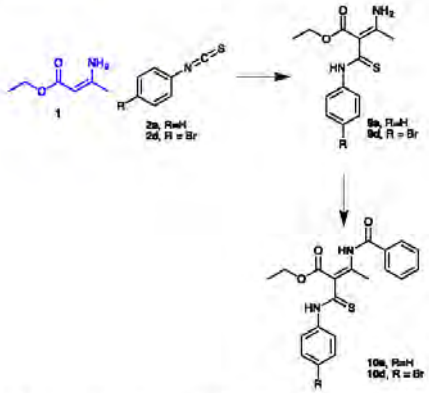

Scheme 3. Reagents and conditions: CH_3CN, benzoic anhydride, 24 h, RT, under N_2.

reduction in yield. Both 3,4-methylenedioxy and 2-naphthyl isothiocyanates were reasonably tolerated with yields of 29% and 29%, respectively (**8g** and **8h**; entries 7 and 8). Alkyl substituted phenyl isothiocyanates gave variable outcomes with 4-CH_3 and 4-CH$(CH_3)_2$ products isolated in yields of 19% and 50%, respectively (**8b** and **8c**; entries 2 and 3). Alkyl isothiocyanates were not well tolerated with the 1,3-thiazene-5-carboxylate originating from ethyl isothiocyanate obtained in low yield (15%, **8i**; entry 9). The addition of additional equivalents of EtNCS failed to increase the yield. The poor results in this instance meant that we did not further explore the use of alkyl isothiocyanates.

This path to 1,3-thiazine-6-phenylimino-5-carboxylates, unlike that reported by Vugts and co-workers,[3] and Glasnov and co-workers[22] does not require the use of harsh reagents (*n*-BuLi) nor low temperatures (−78 °C; to generate the phosphonate anion) and thus represents a significantly more facile entry point.

To further explore the scope of this reaction we next examined modifications of the anhydride moiety. We examined the use of propionic, benzoic and trifluoroacetic anhydride and while 1,3-thiazine-6-imino-5-carboxylates **8j–8l** were isolated, they were typically in very low yields (4–29%; Table 2). This most likely is a consequence of the multiple roles that the anhydride moiety plays during the course of this reaction, including as an electrophile, with the corresponding carboxylate then acting as a base. In Vasu's original report thiolate attack on a range of 2-halomethyl quinazolinones released a halide that subsequently acted as a base (in the same manner as the carboxylate herein). While we did not explore this possibility, it does suggest that access to substituted 1,3-thazin-6-imines may be possible via a range of acyl chlorides and bromides.

In the case of benzoic anhydride, we further explored this reaction with phenyl- and 4-bromophenyl isothiocyanate. In both instances the addition of the initial isothiocyanate (**2a** and **2d**) to ethyl 3-aminocrotonate (**1**) proceeded well with the thioamides **9a** and **9d** formed in good yield (~70%). However, only limited evidence of thiolate interception was noted with the major isolated products arising from benzoylation of the free amino moiety being **10a** and **10d** (28%) (Scheme 3), these thioamides were isolated as a mixture of *cis* and *trans* isomers.[23]

Conclusions

The reaction of ethyl 3-aminocrotonate (**1**), a range of phenyl isothiocyanates (**2a–m**) and acetic anhydride has provided rapid access to 1,3-thiazine-6-phenylimino-5-carboxylates that avoids the use of strong bases and restrictive reaction conditions.[21,3,22] This synthesis, while tolerant of the phenyl isothiocyanate substituent, has limited tolerance for modifications to the anhydride moiety. In the case of benzoic anhydride, preference for the generation of the *N*-benzoyl analogues was observed. Notwithstanding, the multicomponent synthesis of 1,3-thiazine-6-phenylimino-5-carboxyates was accomplished in low to good yields in a simple process requiring only stirring at room temperature.

Acknowledgements

The authors thank the NHMRC (Australia) for project support and T.N.T. is the recipient of a Prime Minister's Australia Asia Postgraduate Endeavour Award.

Supplementary data

Supplementary data (full experimental detail and copies of ^1H and ^{13}C NMR spectra and LCMS evaluation for compounds **8a–8j** and **10a** and **10d**) associated with this article can be found, in the online version, at http://dx.doi.org/10.1016/j.tetlet.2016.06.007.

References and notes

1. Ranjan, A.; Mandal, A.; Verande, S. G.; Deshe, D. H. *Chem. Commun.* **2015**, 14215–14218.
2. Martínez-Ariza, G.; Avaz, M.; Medda, F.; Hulme, C. *J. Org. Chem.* **2014**, *79*, 5153–5162.
3. Vugts, D. J.; Koningstein, M. M.; Schmitz, R. F.; de Kanter, F. J. J.; Groen, M. B.; Orru, R. V. A. *Chem. Eur. J.* **2006**, *12*, 7178–7189.
4. Rostami Charati, F.; Hassankhani, A.; Hosseini, Z. *Comb. Chem. High Throughput Screening* **2012**, *15*, 822–825.
5. Zarganes-Tzitzikas, T.; Chandgude, A. L.; Dömling, A. *Chem. Rev.* **2015**, *15*, 981–996.
6. Bellucci, M. C.; Sani, M.; Sganappa, A.; Volonterio, A. *ACS Comb. Sci.* **2014**, *16*, 711–720.
7. Méndez, Y.; Pérez-Labrada, K.; González-Bacerio, J.; Valdés, C.; de los Chávez, M. Á.; Osuna, J.; Charli, J.-L.; Pascual, I.; Rivera, D. G. *ChemMedChem* **2014**, *9*, 2351–2359.

8. Monfardini, I.; Huang, J.-W.; Beck, B.; Cellitti, J. F.; Pellecchia, M.; Dömling, A. *J. Med. Chem.* **2011**, *54*, 890–900.
9. Gordon, C. P.; Young, K. A.; Hizartzidis, L.; Deane, F. M.; McCluskey, A. *Org. Biomol. Chem.* **2011**, *9*, 1419–1428.
10. Gordon, C. P.; Young, K. A.; Robertson, M. J.; Hill, T. A.; McCluskey, A. *Tetrahedron* **2011**, *67*, 554–561.
11. Di Micco, S.; Vitale, R.; Pellecchia, M.; Rega, M. F.; Riva, R.; Basso, A.; Bifulco, G. *J. Med. Chem.* **2009**, *52*, 7856–7867.
12. Shaaban, S.; Abdel-Wahab, B. F. *Mol. Divers.* **2016**, *20*, 233–254.
13. Zhang, X.; Li, D.; Fan, X.; Wang, X.; Li, X.; Qu, G.; Wang, J. *Mol. Divers.* **2009**, *14*, 159–167.
14. Isambert, N.; Duque, M. D. M. S.; Plaquevent, J.-C.; Génisson, Y.; Rodriguez, J.; Constantieux, T. *Chem. Soc. Rev.* **2011**, *40*, 1347–1357.
15. El Asri, Z.; Génisson, Y.; Guillen, F.; Baslé, O.; Isambert, N.; del Mar Sanchez Duque, M.; Ladeira, S.; Rodriguez, J.; Constantieux, T.; Plaquevent, J.-C. *Green Chem.* **2011**, *13*, 2549–2552.
16. Jalani, H. B.; Kaila, J. C.; Baraiya, A. B.; Pandya, A. N.; Sudarsanam, V.; Vasu, K. K. *Tetrahedron Lett.* **2010**, *51*, 5686–5689.
17. Corona, A.; Desantis, J.; Massari, S.; Distinto, S.; Masaoka, T.; Sabatini, S.; Esposito, F.; Manfroni, G.; Maccioni, E.; Cecchetti, V.; Pannecouque, C.; Le Grice, S. F. J.; Tramontano, E.; Tabarrini, O. *ChemMedChem* **2016**. http://dx.doi.org/10.1002/cmdc.201600015.
18. Toth, P. M.; Lieber, S.; Scheer, F. M.; Schumann, T.; Schober, Y.; Nockher, W. A.; Adhikary, T.; Müller-Brüsselbach, S.; Müller, R.; Diederich, W. E. *ChemMedChem* **2016**, *11*, 488–496.
19. Lindenschmidt, C.; Krane, D.; Vortherms, S.; Hilbig, L.; Prinz, H.; Müller, K. *Eur. J. Med. Chem.* **2016**, *110*, 280–290.
20. Yin, H.; Crowder, R. J.; Jones, J. P.; Anders, M. W. *Chem. Res. Toxicol.* **1996**, *9*, 140–146.
21. General procedure of synthesis, represented by **8a**: *2,4-Dimethyl-6-phenylimino-6H-[1,3]thiazine-5-carboxylic acid ethyl ester.* A mixture of ethyl 3-aminocrotonate (0.3 mL, 2.373 mmol) and phenylisothiocyanate (**2a**) (0.283 mL, 2.373 mmol) was stirred, under solvent free conditions, at room temperature overnight under a nitrogen atmosphere. To the stirred mixture was added acetic anhydride (0.26 mL, 2.61 mmol) and acetonitrile (5 mL). The reaction mixture was stirred for 24 h at room temperature and the crude material was subjected to silica gel chromatography (1:4 ethyl acetate/petroleum ether) to afford **8a** (0.41 g, 65%) as a bright yellow solid (mp 145.3–146.5 °C). IR (cm^{-1}): 2984 (CH), 1728 (COO), 1231 (CO). ^1H NMR (400 MHz, $CDCl_3$) δ 7.65–7.43 (m, 3H), 7.25–7.09 (m, 2H), 4.42 (q, J = 7.1 Hz, 2H), 2.31 (s, 3H), 2.22 (s, 3H), 1.39 (t, J = 7.1 Hz, 3H). ^{13}C NMR (400 MHz, $CDCl_3$) δ 183.0, 166.1, 159.2, 153.9, 140.6, 132.3, 130.5 (C × 2), 129.7, 127.1 (C × 2), 62.0, 25.1, 21.9, 14.0. LRMS (ESI$^+$) m/z 288, 288 [M] + 40%. HRMS (ES$^+$), calculated for $C_{15}H_{16}N_2O_2S$ 288.0932; RP-HPLC Alltima™ C_{18} 5 μm 150 mm × 4.6 mm, 10–100% B in 15 min, R_t = 5.19 min, 100%.
22. Glasnov, T. N.; Vuigts, D. J.; Koningstein, M. M. *QSAR Comb. Chem.* **2006**, *25*, 509–518.
23. Wiberg, K. B. *Acc. Chem. Res.* **1999**, *32*, 922–929.

5.2. References

1. J. M. Hyman, A. J. Firestone, V. M. Heine, Y. Zhao, C. A. Ocasio, K. Han, M. Sun, P. G. Rack, S. Sinha, J. J. Wu, D. E. Solow-Cordero, J. Jiang, D. H. Rowitch and J. K. Chen, *Proceedings of the National Academy of Sciences USA*, 2009, **106**, 14132-14137.

VI. CHAPTER SIX

Conclusions and future directions

Starting from the Gli inhibitor HPI-4 [1], we have subsequently developed three new scaffolds of small molecule inhibitors of the HSP. Additionally we developed and optimised a multiscreen pathway to identify HSP inhibitors. However this still remains a significant bottleneck to project development. These included preliminary (MTT assays) to specific testings (DLR and qPCR assays). An example is the Gli-luciferase assay, which needs approximately 6−7 days to finish starting from cell culturing, assay running, to data processing. Despite this fact, the outcomes are promising with all three types of analogues active against the HSP, and our best Gli inhibitors displaying IC_{50} in the sub-micromolar range (Chapter 4, compounds **27** and **28**).

The first scaffold examination consisted of 11 quinolone-2-(1*H*)-ones developed from the Ugi-Knoevenagel reaction (Chapter 3). These analogues not only express their anti-hedgehog activity through the significant inhibition of Gli_2 at both *gene* and protein expression in SAG-activated Shh LIGHT 2 cells at 10 and 25 μM, respectively, but are able to suppress a panel of nine human HSP expressing cancer cells (GI_{50} from 2.9 to 18.0 μM). Whilst the exact mechanism remains to be determined, it is probable the inhibition observed is occurring downstream of Smo, due to its activity in the presence of SAG, a potent Smo activator. This scaffold, however, provides negligible control over stereochemistry and often results in significant formation of undesired 3-component adducts, which may limit the utility of the scaffold in further drug development.

Consequently, the second and the third scaffolds of HSP inhibitors were developed on the quinolone-2-(1*H*)-one pharmacophore, which highlighted the importance of a C3-tethered indole moiety. These new scaffolds were built on tryptophan (9 analogues, Chapter 4) and benzo[1,3]dioxol-5-ylmethyl-[2-(1*H*-indol-3-yl)-ethyl]-amine derivatives (11 analogues, Chapter 4) displaying superior inhibitory activity against Gli protein expression at low micromolar activity in comparison to the quinolone-2-(1*H*)-ones. In the tryptophan scaffold, the introduction of the chlorine atoms was preliminarily aimed at circumventing the poor solubility noted in quinolone-2-(1*H*)-ones. However, in the benzo[1,3]dioxol-5-ylmethyl-[2-(1*H*-indol-3-yl)-ethyl]-amine scaffold which displayed a promising solubility profile, the superior activity of the Cl-derivative *vs* the lead compound (Chapter 4, compounds **28** vs **20**) potentially suggested the influence of the chlorine substitution in the ligand-protein interactions [2].

Noteworthy, active compounds from the second and third libraries displayed inhibitory activity downstream of Smo, which circumvents the resistance issues experienced by the Smo inhibitors currently in use. Regarding the chemical properties, the stereochemistry has been approached using pure D- or L-tryptophan derivatives, but further studies are required to classify the atropisomerism that occurred sporadically through a number of the benzo[1,3]dioxol-5-

ylmethyl-[2-(1*H*-indol-3-yl)-ethyl]-amine derivatives, most likely due to the sterically hindered rotations [3].

We subsequently discovered the fourth library of 1,3-thiazine-6-phenylimino-5-carboxylates (12 analogues, Chapter 5), which displayed structural similarities to HPI-1[1]. Current biological evaluation is going on to investigate their anti-hedgehog properties. Results will be reported in due course.

In relation to improving analogue synthesis, we have developed a number of aldehydes containing the furan-based biaryl motif using a flow chemistry approach (Chapter 2). This motif is present in a number of biological active compounds, including the HSP inhibitors. Hence our future studies will focus on exploiting this motif by building up new scaffolds, in which the C3-tethered indole moiety in the three scaffolds will be replaced by these furanyl-biaryl aldehydes using flow techniques, and investigating their activity within the HSP.

Concurrently, in terms of further developing our current best hits, we will determine if the effects observed in the Shh LIGHT 2 mouse fibroblast cell line are consistent across human cancer cell lines expressing the HSP, in order to validate the potential of these compounds as drug candidates.

6.1. References

1. J. M. Hyman, A. J. Firestone, V. M. Heine, Y. Zhao, C. A. Ocasio, K. Han, M. Sun, P. G. Rack, S. Sinha, J. J. Wu, D. E. Solow-Cordero, J. Jiang, D. H. Rowitch and J. K. Chen, *Proceedings of the National Academy of Sciences USA*, 2009, **106**, 14132-14137.
2. E. Parisini, P. Metrangolo, T. Pilati, G. Resnati and G. Terraneo, *Chemical Society Reviews*, 2011, **40**, 2267-2278.
3. S. R. LaPlante, L. D. Fader, K. R. Fandrick, D. R. Fandrick, O. Hucke, R. Kemper, S. P. F. Miller and P. J. Edwards, *Journal of Medicinal Chemistry*, 2011, **54**, 7005-7022.

VII. CHAPTER SEVEN

EXPERIMENTAL SECTION

7.1. General chemistry

All reagents were purchased from Sigma-Aldrich, Matrix Scientific, ABCR GmbH, ChemPep, or AK Scientific, and were used without purification. All solvents were re-distilled from glass prior to use.

^{1}H, ^{13}C NMR, temperature variable, and 1D selective NOESY spectra were recorded on a Brüker Advance™ AMX 400 MHz spectrometer at 400.13 and 100.62 MHz, respectively. Chemical shifts (δ) are reported in parts per million (ppm) measured to relative the internal standards. Coupling constants (*J*) are expressed in hertz (Hz). Low resolution mass spectra were recorded on a Shimadzu LCMS 2010 EV using a mobile phase of 1 : 1 acetonitrile – H_2O with 0.1% formic acid. High resolution mass spectra (HRMS) were determined using nanoflow reversed phased Liquid Chromatography (Dionex Ultimate 3000 RSLCnano, Thermo Fischer Scientific) coupled directly to a High Resolution mode equipped, Q-Exactive Plus Hybrid Quadrupole-Orbitrap Mass Spectrometer (Thermo Fischer Scientific). This system was fitted with 5 µm C18 nanoViper trap column (100 µm x 2 cm, Acclaim PepMap100, Thermo) for desalting and pre-concentration, and separation was then performed at 300 nl/min over an EASY-Spray PepMap column (3 µm C18, 75 µm x 15 cm) utilising a gradient of 2-99% Buffer B (80% acetonitrile, 0.1% formic Acid) over 25 minutes.

Analytical HPLC traces were obtained using a Shimadzu system possessing a SIL-20A auto-sampler, dual LC-20AP pumps, CBM-20A bus module, CTO-20A column heater, and a SPD-20A UV/vis detector. This system was fitted with an Alltima™ C18 5 µm 150 mm × 4.6 mm column with solvent A: 0.06% trifluoroacetic acid (TFA) in water and solvent B: 0.06% TFA in CH_3CN–H_2O (90 : 10). Chiral resolution was performed on the same system using ChiralPak®AD-H 5 µm 250 mm x 4.6 mm chiral column with solvent A: 100% methanol and B: 100% acetonitrile. In normal resolution, HPLC traces were acquired at a flow rate of 2.0 mL min^{-1}, gradient 10 –100 (%B), over 15.0 min, with detection at 220 nm and 254 nm. In chiral resolution, HPLC traces were acquired at a flow rate of 0.2 mL min^{-1}, gradient 10 (%A) and 90 (%B) over 85 min, with at 220 nm and 254 nm. Where applicable UPLC traces were obtained using the Agilent Technologies 1260 Infinity UPLC system. This system was fitted with an Agilent Zorbax SB-C18 1.8 µm, 2.1 x 50 mm, column with the solvent A: 0.1% formic acid in water and solvent B: 0.1% formic acid in CH_3CN–H_2O (90 : 10). In each case UPLC traces were acquired at a flow rate of 0.6 mL/min using an isocratic run at 80% or 50% solvent B.

Melting points were recorded on a Büchi Melting Point M-565. IR spectra were recorded on a PerkinElmer Spectrum Two™ FTIR Spectrometer with the UATR (Universal Attenuated Total Reflectance) accessories. Thin layer chromatography (TLC) was performed on Merck 60 F254

pre-coated aluminium plates with a thickness of 0.2 mm. Column chromatography was performed under 'flash' conditions on Merck silica gel 60 (230–400 mesh).

7.2. Biological investigations

7.2.1. Cell culture and stock solutions

Stock solutions were prepared as follows and stored at -20ºC: Related compounds were stored as 40 mM solutions in DMSO. All cell lines were cultured at 37ºC in an automated CO_2 (5%) incubator (HERA cell 150, Thermo Scientific).

HT29, SW480 (colon carcinomas), MCF-7 (breast carcinoma), A2780 (ovarian carcinoma), H460 (lung carcinoma), A431 (skin carcinoma), DU145 (prostate carcinoma), BEC-2 (neuroblastoma), SJ-G2 (glioblastoma) and MIA (pancreatic carcinoma) cell lines were maintained in Dulbecco's modified Eagle's medium (Trace Biosciences, Australia) supplemented with 10% foetal bovine serum, 10 mM sodium bicarbonate, penicillin (100 IU/mL), streptomycin (100 mg/mL), and glutamine (4 mM).

TCAM-2 cell line (testis carcinoma) was maintained in Hyclone RPMI 1640 medium (GE Healthcare Life Sciences) supplemented with 10% foetal bovine serum (Gibco®), penicillin (100 IU/mL) (Gibco®), streptomycin (100 mg/mL) (Gibco®) and glutamine (4 mM) (Gibco®).

Shh LIGHT2 cell line (derived from NIH-3T3 fibroblast cell line) was maintained in Gibco® Dulbecco's modified Eagle's medium (Thermo Fisher Scientific) supplemented with 10% foetal bovine serum (FBS), glutamine (4 mM), Zeocin® (0.15 mg/mL, Invitrogen), Genetecin® (0.4 mg/mL, Thermo Fisher Scientific).

7.2.2. In vitro growth inhibition assay

Protocol 1 (HT29, SW480, MCF-7, A2780, H460, DU145, BEC-2 and MIA cell lines)

Cells in logarithmic growth were transferred to 96-well plates. Cytotoxicity was determined by plating cells in duplicate in 100 µL medium at a density of 2500-4000 cells/well. On day 0, (24 h after plating) when the cells were in logarithmic growth, 100 µL medium with or without the test agent was added to each well. After 72 h drug exposure growth inhibitory effects were evaluated using the MTT (3-[4,5-dimethylthiazol-2-yl]-2,5-diphenyl-tetrazolium bromide) assay and absorbance read at 540 nm. The percentage growth inhibition was determined at a fixed drug concentration of 25 µM. A value of 100% is indicative of total cell growth inhibition. Those analogues showing appreciable percentage growth inhibition underwent further dose response analysis allowing for the calculation of a GI_{50} value. This value is the drug concentration at which cell growth is 50% inhibited based on the difference between the optical density values on day 0 and those at the end of drug exposure.

Protocol 2 (TCAM-2 cell line)

Cells in logarithmic growth were transferred to 96-well plates in triplicate at 2500 cells/well in 200 µL media and cultured in the automated CO_2 (5%) incubator. When the cells reach to about 80% confluency, old media were removed and replaced with 100 µL fresh media containing testing agents (at 10 µM), as well as DMSO and 1% Triton X as controls. Cells were further incubated for another 72 h and were evaluated using the MTT assay with the absorbance at 550 nm. The growth inhibition was calculated based on the differences in the optical densities between those treated by various agents (10 µM) and controls by DMSO and 1% Triton X treatments. Only those agents which expressed a growth inhibition greater than 60% were further subjected to full dose response evaluation (GI_{50} values).

7.2.3. Dual Luciferase Reporter assay

Shh-LIGHT2 cells in logarithmic growth were transferred to 96-well plate (3000 cells/well) and cultured to confluency. The Shh-LIGHT2 cells were grown in DMEM containing 0.5% FBS, 4 mM glutamine, 0.15 mg/mL Zeocin®, 0.4 mg/mL Genetecin®, and then co-cultured with combinations of 100 nM SAG, and/or our novel compounds in concentrations from 2.5 to 10 µM. The SAG- free DMSO treated (2.5 to 10 µM), and SAG-included Sonidegib (100 nM) treated cells were used as controls. Treatments were perforemed in triplicate. After the cells were cultured for a further 45 h in an automated CO_2 (5%) incubator, the resulting firefly and Renilla luciferase activities were measured using a Dual Luciferase Reporter kit (Promega) and a BMG Labtech Pherastar microplate reader (Thermo Fisher Scientific).

7.2.4. RNA Extraction

Total RNA was isolated from cultured cells using two rounds of a modified acid guanidinium thiocyanate-phenol-chloroform protocol [1]. Washed cells were resuspended in lysis buffer (4 M guanidinium thiocyanate, 25 mM sodium citrate, 0.5% sarkosyl, 0.72% β-mercaptoethanol) as previously described [2].

7.2.5. Reverse Transcription PCR (RT-PCR) and Quantitative PCR (qPCR)

Reverse transcription was performed with 2 µg of isolated RNA, 500 ng oligo(dT)15 primer, 40 U of RNasin, 0.5 mM dNTPs, and 20 U of M-MLV-Reverse Transcriptase (Promega). Total RNA was DNase treated prior to reverse transcription to remove genomic DNA. Reverse transcription reactions were verified by *β-actin* RT-PCR using cDNA amplified with GoTaq Flexi (Promega). qPCR was performed using SYBR Green GoTaq qPCR master mix (Promega) according to the manufacturer instructions on LightCycler 96 SW 1.0 (Roche). Primer sequences have been supplied (Table 6). Reactions were performed on cDNA equivalent to 50

ng of total RNA and carried out for 45 amplification cycles. SYBR® Green fluorescence was measured after the extension step at the end of each amplification cycle and quantified using LightCycler Analysis Software (Roche). For each sample, a replicate omitting the reverse transcription step was undertaken as a negative control. qPCR data was normalized to the house-keeping control *Cyclophilin*. Experiments were replicated at least 3 times prior to statistical assessment. Each PCR was performed on at least 3 separate cell isolations, of which a representative PCR or an average is shown (Table 1).

Table 1. Primer sequences used in qPCR assay.

Human gene			
	Forward Sequence (5'-3')	**Reverse Sequence (5'-3')**	**Annealing Temp (ºC)**
Gli_2	ATCTCTTGCCACCATTCCAT	GGACAGAATGAGGCTCGTAA	60
Smo	CTGCCACTTCTACGACTTCT	GGCCTGACATAGCACATAGT	56
SuFu	GACCCCTTGGACTATGTTAG	CTGATGTAGTGCCAGTGCTC	55
$Ptch_1$	CCCTCACGTCCATCAGCAAT	AACACCACTACTACCGCTGC	58
Mouse gene			
Gli_2	TCCAGTCAATGGTTCTGTCC	TGGCTCAGCATCGTCACTTC	60
Gli_3	GGCCGTTACCATTATGATCC	CTGAGGCTGCAGTGGGATTA	60
Shh	TGCTTTGTAACCGCCACTTT	CGCTGCTAGGTGCACTTTTA	61
Smo	GAACTCCAATCGCTACCCTG	ATCTGCTCGGCAAACAATCT	60
SuFu	GACCCCTTGGACTATGTTAG	CTGATGTAGTGCCAGTGCTC	55
$Ptch_1$	CATAGCTGCCCAGTTCAAGT	GGTCGTAAAGTAGGTGCTGG	55

7.2.6. Statistical analysis

Statistical analysis was performed using F-test and t-test in Excel 2013. * *P* < *.05,* ** *P* < *.001,* *** *P* < *.0001.*

7.3. Synthesis data

7.3.1. Synthesis of the furan based biaryls (Chapter 2)

*Biphenyl-3,3'-diyldimethanol (**10**) and 5-(3-(hydroxymethyl)phenyl)furan-2-carbaldehyde (**7**)*

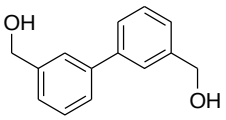

$C_{14}H_{14}O_2$

A solution of (3-bromophenyl)methanol (0.28 mL, 2.3 mmol), 5-formyl-2-furanylboronic acid (0.32 g, 2.3 mmol) and TBAF (2.16 g, 6.86 mmol) was diluted with MeOH (30 mL) to afford a 0.05 M solution. This solution was flowed through an X-Cube™ fitted with a Fibrecat®1001 catalyst at flow rate of 0.5 mL/min, at a temperature of 80 °C, and 0 bar pressure for 2 h (i.e. total of two catalyst cycles). The eluent was concentrated *in vacuo*, diluted with DCM (30 mL), washed with 1 M HCl (2 x 30 mL), dried ($MgSO_4$), concentrated *in vacuo*, and the crude was subjected to flash silica gel chromatography (1:1 EtOAc:Hexane) to afford biphenyl-3,3'-diyldimethanol (**10**) as a colourless oil (0.01 g, 3 %). LRMS (ESI+) m/z 215 (M+H). ^{1}H NMR (400 MHz, $CDCl_3$) δ 7.61 (s, 1H), 7.54 (d, *J* = 7.7 Hz, 1H), 7.44 (t, *J* = 7.6 Hz, 1H), 7.36 (d, *J* = 7.5 Hz, 1H), 4.76 (d, *J* = 7.7 Hz, 2H); ^{13}C NMR (101 MHz, $CDCl_3$) δ 141.4, 141.3, 129.0, 129.0, 126.5, 126.0, 125.8, 65.4; RP-HPLC Alltima™ C18 5 µm 150 mm x 4.6 mm, 10-100 % B in 15 min, R_t = 10.39 min.

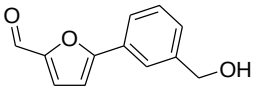

$C_{12}H_{10}O_3$

Continued elution (1:1 EtOAc:Hexane) afforded 5-(3-(hydroxymethyl)phenyl)furan-2-carbaldehyde (**7**) as an orange oil (0.37 g, 82 %). LRMS (ESI+) m/z 203 (M+H); HRMS (ES+) for $C_{12}H_{11}O_3$; calculated 201.0630, found 202.0681; ^{1}H NMR (400 MHz, $CDCl_3$) δ 9.51 (s, 1H), 7.74 (s, 1H), 7.67 – 7.57 (m, 1H), 7.32 (m, 2H), 7.25 (d, *J* = 3.7 Hz, 1H), 6.76 (d, *J* = 3.7 Hz, 1H), 4.67 (s, 2H). ^{13}C NMR (101 MHz, $CDCl_3$) δ 177.34, 159.5, 151.8, 142.1, 129.0 (C x 2), 128.9, 128.2, 124.3, 123.6, 107.9, 77.5, 77.2, 76.9, 64.4. RP-HPLC Alltima™ C18 5 µm 150 mm x 4.6 mm, 10-100 % B in 15 min, R_t = 9.10 min.

*5-(4-Acetylphenyl)-2-furancarboxaldehyde (**12a**)*

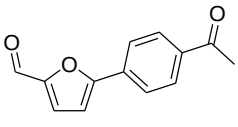

$C_{13}H_{10}O_3$

General procedure 1: A solution of 4-bromoanisole (0.40 g, 2.1 mmol), 5-formyl-2-furanylboronic acid (0.30 g, 2.1 mmol) and TBAF (2.16 g, 6.86 mmol) was diluted with MeOH (30 mL) to afford a 0.05 M solution. This solution was flowed through an X-Cube™ fitted with a Fibrecat®1032 catalyst at flow rate of 0.5 mL/min, at a temperature of 120 °C, and 0 bar pressure for 2 h (i.e. total of two catalyst cycles). The eluent was concentrated *in vacuo*, diluted with DCM (30 mL), washed with 1 M HCl (2 x 30 mL), dried ($MgSO_4$), concentrated *in vacuo*, and the crude was subjected to flash silica gel chromatography (1:1 EtOAc:Hexane) to afford 5-(4-acetylphenyl)-2-furancarboxaldehyde (**12a**) as a yellow oil (0.36 g, 87 %). LRMS (ESI+) m/z 215 (M+H); HRMS (ES+) for $C_{13}H_{11}O_3$; calculated 215.0630, found 214.0637; ^{1}H NMR ($CDCl_3$, 400 MHz); δ 9.60 (s, 1H), 7.77 (d, *J* = 8.9 Hz, 2H), 7.30 (d, *J* = 3.7 Hz, 1H), 6.96 (d, *J* = 8.9 Hz, 2H), 6.72 (d, *J* = 3.7 Hz, 1H), 3.86 (s, 3H); ^{13}C NMR ($CDCl_3$, 101 MHz): δ 176.9, 160.91, 159.8, 151.6, 129.0, 127.0, 121.8, 114.4, 106.3, 55.4; RP-HPLC Alltima™ C18 5 μm 150 mm x 4.6 mm, 10-100 % B in 15 min, R_t = 14.26 min.

*2-(4-(5-Formylfuran-2-yl)phenyl)acetonitrile (**12b**)*

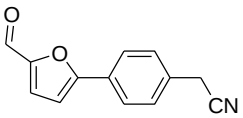

$C_{13}H_9NO_2$

Compound (**12b**) was synthesised as described in general procedure 1 from 4-bromoacetonitrile (0.44 g, 2.2 mmol), 5-formyl-2-furanylboronic acid (0.31 g, 2.2 mmol) and TBAF (2.04 g, 6.7 mmol). The crude reaction mixture was subjected to flash silica chromatography (1:4 EtOAc:Hexane:) to afford **12b** as an orange solid (0.38 g, 82 %). LRMS (ESI+) m/z 212 (M+H); HRMS (ES+) for $C_{13}H_{10}NO_2$; calculated 212.0630, found 212.0637; ^{1}H NMR ($CDCl_3$, 400 MHz): δ 9.67 (s, 1H), 7.84 (d, *J* = 8.4 Hz, 2H), 7.43 (d, *J* = 8.5 Hz, 2H), 7.33 (d, *J* = 3.7 Hz, 1H), 6.87 (d, *J* = 3.7 Hz, 1H), 3.81 (s, 2H); ^{13}C NMR ($CDCl_3$, 101 MHz): δ 177.3, 158.37, 152.2, 131.3, 128.9, 128.6, 126.0, 108.2, 23.6. RP-HPLC Alltima™ C18 5 μm 150 mm x 4.6 mm, 10-100 % B in 15 min, R_t = 14.27 min.

*5-(4-Methylphenyl)-2-furancarboxaldehyde (**12c**)*

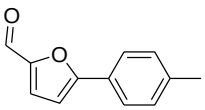

$C_{12}H_{10}O_2$

Compound **12c** was prepared utilising general procedure 1, 4-bromotoluene (0.28 mL, 2.3 mmol), 5-formyl-2-furanylboronic acid (0.32 g, 2.3 mmol), TBAF (2.16 g, 6.86 mmol), and MeOH (30 mL). The eluent was concentrated *in vacuo* and the crude material was diluted with DCM (30

mL) and washed with 1 M HCl (2 x 30 mL). The organic layer was dried ($MgSO_4$), and concentrated *in vacuo* to yield an oil which was further purified using flash chromatography (1:9 EtOAc:Hexane) to afford 5-(4-methylphenyl)-2-furancarboxaldehyde as an orange solid (0.39 g, 91 %) m.p 50-56 °C. LRMS (ESI+) m/z 187 (M+H); HRMS (ES+) for $C_{12}H_{11}O_2$; calculated 187.0681, found 186.0678; ^{1}H NMR ($CDCl_3$, 400 MHz): δ 9.63 (s, 1H), 7.72 (d, *J* = 8.2 Hz, 2H), 7.31 (d, *J* = 3.7 Hz, 1H), 7.25 (d, *J* = 8.9 Hz, 2H), 6.78 (d, *J* = 3.7 Hz, 1H), 2.39 (s, 3H); ^{13}C NMR ($CDCl_3$, 101 MHz): δ 177.1, 159.8, 151.8, 140.0, 129.7, 126.3, 125.3, 107.1, 21.5; RP-HPLC Alltima™ C18 5 μm 150 mm x 4.6 mm, 10-100 % B in 15 min, R_t = 17.41 min.

*5-(Dimethylamino)-N-(4-(5-formylfuran-2-yl)phenyl)naphthalene-1-sulfonamide (**12d**)*

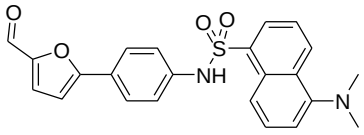

$C_{23}H_{20}N_2O_4S$

Compound **12d** was prepared utilising general procedure 1, and *N*-(4-bromophenyl)-5-(dimethylamino)naphthalene-1-sulfonamide (0.92 g, 2.3 mmol), 5-formyl-2-furanylboronic acid (0.32 g, 2.3 mmol), TBAF (2.16 g, 6.86 mmol), and MeOH (30 mL). The eluent was concentrated *in vacuo*, the crude material was diluted with DCM (30 mL) and washed with 1 M HCl (2 x 30 mL). The organic layer was dried ($MgSO_4$), and concentrated *in vacuo* to yield an oil which was further purified using flash chromatography (5:1 EtOAc:Hexane) to afford 5-(4-methylphenyl)-2-furancarboxaldehyde as a yellow oil (0.82 g, 87 %). LRMS (ESI+) m/z 421 (M+H); HRMS (ES+) for $C_{23}H_{21}N_2O_4S$; calculated 421.1144, found 421.1144; ^{1}H NMR (400 MHz, $CDCl_3$) δ 9.55 (s, 1H), 8.51 (d, *J* = 8.4 Hz, 1H), 8.46 – 8.25 (m, 2H), 8.13 (s, 1H), 7.56 – 7.51 (m, 1H), 7.50 (d, *J* = 8.7 Hz, 2H), 7.47 – 7.42 (m, 1H), 7.23 (d, *J* = 3.7 Hz, 1H), 7.16 (d, *J* = 7.9 Hz, 1H), 7.09 (d, *J* = 8.7 Hz, 2H), 6.62 (d, *J* = 3.7 Hz, 1H), 2.85 (s, 6H). ^{13}C NMR ($CDCl_3$, 101 MHz): δ 177.2, 158.9, 151.7, 138.2, 134.1, 132.1, 131.0, 130.4, 129.7, 129.6, 128.7, 126.3, 125.0, 123.2, 122.7, 120.3, 115.5, 111.1, 107.3, 45.4; RP-HPLC Alltima™ C18 5 μm 150 mm x 4.6 mm, 10-100 % B in 15 min, R_t = 9.60 min.

*N-(4-(5-Formylfuran-2-yl)phenyl)benzenesulfonamide (**12e**)*

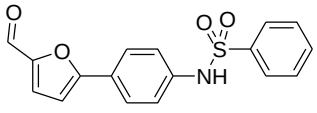

$C_{17}H_{13}NO_4S$

Compound **12e** was prepared utilising general procedure 1, and *N*-(4-bromophenyl)benzenesulfonamide (0.77 g, 2.3 mmol), 5-formyl-2-furanylboronic acid (0.32 g, 2.3 mmol), TBAF (2.16 g, 6.86 mmol), and MeOH (30 mL). The eluent was concentrated *in vacuo*, the crude material was diluted with DCM (30 mL) and washed with 1 M HCl (2 x 30 mL). The organic layer was dried ($MgSO_4$), and concentrated *in vacuo* to yield an oil which was further purified using flash chromatography (4:1 EtOAc:Hexane) to afford *N*-

(4-(5-formylfuran-2-yl)phenyl)benzenesulfonamide as an yellow oil(0.65 g, 87 %). LRMS (ESI+) m/z 328 (M+H); HRMS (ES+) for $C_{17}H_{14}NO_4S$; calculated 328.0565, found 327.0556; ^{1}H NMR (400 MHz, $CDCl_3$) δ 9.61 (s, 1H), 7.85 – 7.78 (m, 2H), 7.69 (d, *J* = 8.7 Hz, 2H), 7.55 (t, *J* = 7.4 Hz, 1H), 7.46 (*t*, *J* = 7.7 Hz, 2H), 7.30 (d, *J* = 3.7 Hz, 1H), 7.26 (s, 1H), 7.18 (d, *J* = 8.7 Hz, 3H), 6.76 (d, *J* = 3.7 Hz, 1H); ^{13}C NMR (101 MHz, $CDCl_3$) δ 177.0, 158.6, 151.89, 138.8, 137.8, 129.2, 127.2, 126.6, 125.8, 121.1 (Cx2), 107.6. RP-HPLC Alltima™ C18 5 μm 150 mm x 4.6 mm, 10-100 % B in 15 min, R_t = 15.58 min.

*N-(2,4-Dimethoxyphenyl)-4-(5-formylfuran-2-yl)benzamide (**12f**)*

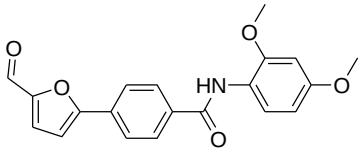

$C_{20}H_{17}NO_5$

Compound **12f** was synthesised utilising general procedure 1, 4-bromo-*N*-(2,4-dimethoxyphenyl)benzamide (0.73 g, 2.2 mmol), 5-formyl-2-furanylboronic acid (0.31 g, 2.2 mmol) and TBAF (2.14 g, 6.6 mmol) to afford *N*-(2,4-dimethoxyphenyl)-4-(5-formylfuran-2-yl)benzamide as a light brown solid (0.71 g, 92 %). LRMS (ESI-) m/z 352 (M-H); HRMS (ES-) for $C_{20}H_{18}NO_5$; calculated 352.1107, found 352.1113; ^{1}H NMR (400 MHz, DMSO-d_6): δ 9.66 (s, 1H), 9.54 (s, NH), 8.09 (d, *J* = 8.3 Hz, 2H), 8.01 (d, *J* = 8.4 Hz, 2H), 7.70 (d, *J* = 3.8 Hz, 1H), 7.48 (d, *J* = 8.6 Hz, 1H), 7.45 (d, *J* = 3.7 Hz, 1H), 6.67 (d, *J* = 2.6 Hz, 1H), 6.55 (dd, *J* = 8.7, 2.6 Hz, 1H), 3.81 (s, 3H), 3.79 (s, 3H); ^{13}C NMR (400MHz, DMSO-d_6): δ 178.6, 164.8, 158.5, 157.6, 154.1, 152.6, 135.55, 131.6, 128.9, 127.1, 125.3, 120.0, 110.7, 104.7, 99.4, 56.2, 55.8; RP-HPLC Alltima™ C18 5 μm 150 mm x 4.6 mm, 10-100 % B in 15 min, R_t = 18.12 min.

*5-(4-Hydroxyphenyl)-2-furancarboxaldehyde (**14**)*

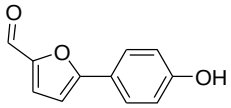

$C_{11}H_8O_3$

Compound **14** was synthesised utilising general procedure 1, 4-bromophenol (0.38 g, 2.3 mmol), 5-formyl-2-furanylboronic acid (0.32 g, 2.3 mmol) and TBAF (2.10 g, 6.9 mmol). The crude was subjected to silica gel chromatography (4:1 EtOAc:Hexane) to afford 5-(4-hydroxyphenyl)-2-furancarboxaldehyde as an orange solid (0.09 g, 30 %). LRMS (ESI-) m/z 187 (M-H); HRMS (ES-) for $C_{11}H_7O_3$; calculated 187.0473, found 187.0468; ^{1}H NMR ($CDCl_3$, 400 MHz): δ 9.60 (s, 1H), 7.73 (d, *J* = 8.8 Hz, 2H), 7.31 (d, *J* = 3.7 Hz, 1H), 6.92 (d, *J* = 8.8 Hz, 2H), 6.71 (d, *J* = 3.7 Hz, 1H); ^{13}C NMR ($CDCl_3$, 101 MHz): δ 176.9, 157.1, 128.0, 127.3, 122.0, 116.0, 115.6, 106.3. RP-HPLC Alltima™ C18 5 μm 150 mm x 4.6 mm, 10-100 % B in 15 min, R_t = 10.68 min.

*5-(3-(Dimethylamino)phenyl)-2-furancarboxaldehyde (**15a**)*

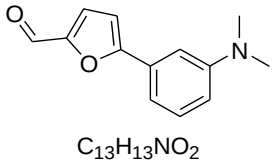

General Procedure 2: A solution of 3-bromo-*N*,*N*-dimethylaniline (0.28 mL, 2.3 mmol), 5-formyl-2-furanylboronic acid (0.32 g, 2.3 mmol) and TBAA (2.08 g, 6.86 mmol) was diluted with MeOH (30 mL) to afford a 0.05 M solution. This solution was flowed through an X-Cube™ fitted with a CatCart® $PdCl_2(PPh_3)_2$-DVB catalyst at flow rate of 0.3 mL/min, at a temperature of 120 °C, and 0 bar pressure for 3 h (i.e. total of three catalyst cycles). The eluent was concentrated *in vacuo*, diluted with DCM (30 mL) and washed with 1 M HCl (2 x 30 mL), dried ($MgSO_4$), concentrated *in vacuo*, and the crude was subjected to flash silica gel chromatography (7:1 EtOAc:Hexane) to afford 5-(3-(dimethylamino)phenyl)-2-furancarboxaldehyde as a colourless oil (0.43 g, 87 %). LRMS (ESI+) m/z 216 (M+H); HRMS (ES+) for $C_{13}H_{14}NO_2$; calculated 216.0946, found 216.0942; ^{1}H NMR (DMSO-d_6, 400 MHz): δ 9.59 (s, 1H), 7.64 (d, *J* = 3.7 Hz, 1H), 7.30 (d, *J* = 7.9 Hz, 1H), 7.27 (d, *J* = 3.7 Hz, 1H), 7.16 (d, *J* = 7.6 Hz, 1H), 7.13 (d, *J* = 2.0 Hz, 1H), 6.81 (dd, *J* = 8.3, 2.4 Hz, 1H), 2.97 (s, 6H). ^{13}C NMR (DMSO-d_6, 101 MHz): δ 178.1, 159.7, 151.9, 151.2, 130.2, 129.7, 114.3, 113.5, 109.0, 108.5, 40.5. RP-HPLC Alltima™ C18 5 μm 150 mm x 4.6 mm, 10-100 % B in 15 min, R_t = 9.60 min.

*5-(4-(Dimethylamino)phenyl)-2-furancarboxaldehyde (**15b**)*

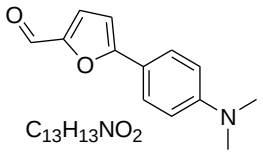

Compound **15b** was synthesised utilising general procedure 2 and 4-bromo-*N*,*N*-dimethylaniline (0.46 g, 2.3 mmol), 5-formyl-2-furanylboronic acid (0.32 g, 2.3 mmol) and TBAA (2.08 g, 6.90 mmol). The crude was subject to flash silica gel chromatography (7:1 EtOAc:Hexane) to afford 5-(4-(dimethylamino)phenyl)-2-furancarboxaldehyde as a yellow solid (0.43 g, 87 %). M.p. 96-98 °C. LRMS (ESI-) m/z 216 (M+H); HRMS (ES+) for $C_{13}H_{14}NO_2$; calculated 216.0946, found 216.0950; ^{1}H NMR (DMSO-d_6, 400 MHz): δ 9.48 (d, *J* = 3.2 Hz, 1H), 7.69 (dd, *J* = 8.2, 3.6 Hz, 2H), 7.59 (t, *J* = 3.8 Hz, 1H), 7.00 (t, *J* = 3.9 Hz, 1H), 6.81 (dd, *J* = 8.3, 3.4 Hz, 2H), 3.00 (d, *J* = 3.2 Hz, 6H); ^{13}C NMR (DMSO-d_6, 101 MHz): δ 176.9, 160.6, 151.6, 151.1, 126.9, 116.4, 112.5, 106.0; RP-HPLC Alltima™ C18 5 μm 150 mm x 4.6 mm, 10-100 % B in 15 min, R_t = 10.68 min.

*5-(4-Methoxyphenyl)-2-furancarboxaldehyde (**15c**)*

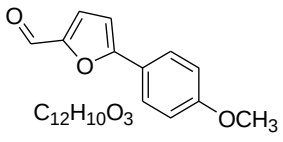

Compound **15c** was synthesised utilised general procedure 2, 4-bromoanisole (0.41 g, 2.2 mmol), 5-formyl-2-furanylboronic acid (0.31 g, 2.2 mmol) and TBAA (1.99 g, 6.6 mmol). The crude was

subjected to flash silica gel chromatography (1:5 EtOAc:Hexane) to afford 5-(4-methoxyphenyl)-2 furancarboxaldehyde as a pale yellow oil (0.42 g, 92 %). LRMS (ESI-) m/z 201 (M-H); HRMS (ES-) for $C_{12}H_9O_3$; calculated 201.0630, found 201.0637; ^{1}H NMR ($CDCl_3$, 400 MHz): δ 9.60 (s, 1H), 7.77 (d, *J* = 8.9 Hz, 2H), 7.30 (d, *J* = 3.7 Hz, 1H), 6.96 (d, *J* = 8.9 Hz, 2H), 6.72 (d, *J* = 3.7 Hz, 1H), 3.86 (s, 3H); ^{13}C NMR ($CDCl_3$, 101 MHz): δ 176.9, 160.9, 159.8, 151.6, 129.0, 127.0, 121.8, 114.4, 106.3, 55.4; RP-HPLC Alltima™ C18 5 μm 150 mm x 4.6 mm, 10-100 % B in 15 min, R_t = 18.92 min.

*5-(1H-Indol-6-yl)-2-furancarboxaldehyde (**15d**)*

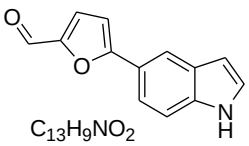

Compound **15d** was synthesised utilising general procedure 2, 6-bromo-1*H*-indole (0.41 g, 2.1 mmol), 5-formyl-2-furanylboronic acid (0.29 g, 2.1 mmol) and TBAA (1.90 g, 6.3 mmol). The crude was subjected to flash silica gel chromatography (3:1 EtOAc:Hexane) to afford 5-(1*H*-indol-6-yl)-2-furancarboxaldehyde as an off-white solid (0.48. g, 83 %). LRMS (ESI+) m/z 212 (M+H); HRMS (ES+) for $C_{13}H_{10}NO_2$; calculated 212.0633, found 212.0635; ^{1}H NMR ($CDCl_3$, 400 MHz): δ 9.61 (s, 1H), 8.43 (s, NH), 7.95 (s, 1H), 7.68 (d, *J* = 8.3 Hz, 1H), 7.54 (dd, *J* = 8.3, 1.4 Hz, 1H), 7.34 (d, *J* = 3.7 Hz, 1H), 7.33 – 7.31 (m, 1H), 6.83 (d, *J* = 3.7 Hz, 1H), 6.60 – 6.56 (m, 1H). ^{13}C NMR ($CDCl_3$, 101 MHz): δ 176.8, 161.3, 151.6, 135.9, 129.2, 126.5, 122.9, 121.2, 117.7, 108.4, 106.8, 103.1; RP-HPLC Alltima™ C18 5 μm 150 mm x 4.6 mm, 10-100 % B in 15 min, R_t = 15.58 min.

*5-(4-Benzoylphenyl)-2-furancarboxaldehyde (**15e**)*

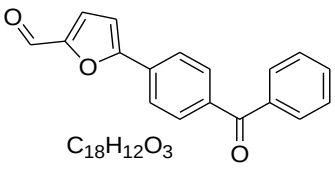

Compound **15e** was synthesised using general procedure 2, (4-chlorophenyl)(phenyl)methanone,(0.41 g, 2.2 mmol), 5-formyl-2-furanylboronic acid (0.31 g, 2.2 mmol) and TBAF (1.99 g, 6.60 mmol). The crude was subjected to flash silica gel chromatography (1:4 EtOAc:Hexane) to afford 5-(4-benzoylphenyl)-2-furancarboxaldehyde as an off-white solid (0.38 g, 87 %). LRMS (ESI+) m/z 277 (M+H); HRMS (ES+) for $C_{18}H_{13}O_3$; calculated 277.0786, found 277.0791; ^{1}H NMR (DMSO-d_6, 100 MHz): δ 9.67 (s, 1H), 8.05 (d, *J* = 8.4 Hz, 2H), 7.86 (d, *J* = 8.4 Hz, 2H), 7.78 – 7.75 (m, 2H), 7.73 – 7.69 (m, 2H), 7.59 (t, *J* = 7.6 Hz, 2H), 7.48 (d, *J* = 3.8 Hz, 1H); ^{13}C NMR ($CDCl_3$, 101 MHz): δ 195.5, 178.7, 157.3, 152.8, 137.7, 137.3, 133.3, 132.6, 131.0, 130.1, 129.1, 125.4, 111.3; RP-HPLC Alltima™ C18 5 μm 150 mm x 4.6 mm, 10-100 % B in 15 min, R_t = 18.21 min.

*5-(3-Formylphenyl)furan-2-carbaldehyde (**15f**)*

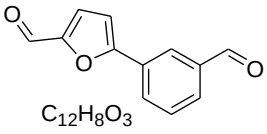

Compound **15f** was synthesised using general procedure, 3-chlorobenzaldehyde (0.28 g, 2.0 mmol), 5-formyl-2-furanylboronic acid (0.28 g, 2.0 mmol) and TBAF (1.81 g, 6.0 mmol). The crude was subjected to flash silica gel chromatography (9:1 Hexane:EtOAc) to afford 5-(4-benzoylphenyl)-2-furancarboxaldehyde as a of white solid (0.34. g, 85 %). LRMS (ESI-) m/z 199 (M-H); HRMS (ES-) for $C_{12}H_7O_3$; calculated 199.0473, found 199.0482; ^{1}H NMR (400 MHz, DMSO-d_6) δ 10.11 (s, 1H), 9.66 (s, 1H), 8.38 (s, 1H), 8.21 (d, J = 7.9 Hz, 1H), 7.98 (d, J = 7.6 Hz, 1H), 7.76 (t, J = 7.7 Hz, 1H), 7.70 (d, J = 3.7 Hz, 1H), 7.46 (d, J = 3.7 Hz, 1H); ^{13}C NMR (101 MHz, DMSO-d_6) δ 193.3, 178.6, 157.2, 152.5, 137.4, 131.0, 130.7, 130.6, 130.0, 126.1, 125.9, 125.7, 110.3; RP-HPLC Alltima™ C18 5 µm 150 mm x 4.6 mm, 10-100 % B in 15 min, R_t = 10.68 min.

*N-(6-((2S,6R)-2,6-Dimethylmorpholino)pyridin-3-yl)-2-methyl-4'-trifluoromethoxy) biphenyl-3-carboxamide (LDE225) (**18**)*

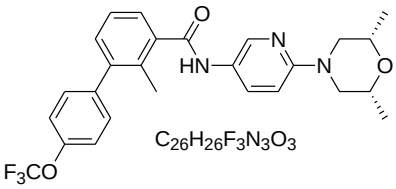

Compound **18** was synthesised using general procedure 2, 3-bromo-*N*-(6-((2R,6S)-2,6-dimethylmorpholino)pyridin-3-yl)-2-methylbenzamide (0.48 g, 1.2 mmol), 4-(trifluoromethoxy)phenylboronic acid (0.25 g, 1.2 mmol), and TBAF (1.08 g, 3.6 mmol). The crude was subjected to flash silica gel chromatography (9:1 DCM:MeOH) to afford LDE225 as an off-white solid (0.55 g, 94 %). LRMS (ESI+) m/z 486 (M+H); ^{1}H NMR (400 MHz, DMSO-d_6) δ 10.25 (s, 1H), 8.43 (d, J = 2.4 Hz, 1H), 7.94 (dd, J = 9.1, 2.5 Hz, 1H), 7.47 (s, 4H), 7.42 – 7.25 (m, 2H), 6.86 (d, J = 9.1 Hz, 1H), 4.06 (d, J = 12.0 Hz, 2H), 3.67 – 3.54 (m, 2H), 2.41 – 2.27 (m, 2H), 2.22 (s, 3H), 1.16 (d, J = 6.2 Hz, 6H); ^{13}C NMR (101 MHz, DMSO-d_6) δ 168.2, 156.2, 148.0, 141.4, 140.6, 139.9, 139.1, 132.5, 131.5, 131.1, 130.7, 127.5, 127.1, 126.3, 121.9, 121.4, 119.3, 107.3, 71.3, 51.3, 19.3, 17.7;193.3, 178.6, 157.2, 152.5, 137.4, 131.0, 130.7, 130.6, 130.0, 126.1, 125.9, 125.7, 110.3; RP-HPLC Alltima™ C18 5 µm 150 mm x 4.6 mm, 10-100 % B in 15 min, R_t = 17.41 min.

7.3.2. Synthesis of the quinolone-1-(2*H*)-ones (Chapter 3)

*2-(3-Cyano-2-oxo-4-methylquinolin-1(2H)-yl)-2-(1-methyl-1H-indol-3-yl)-N-(pentan-2-yl)acetamide (**20**)*

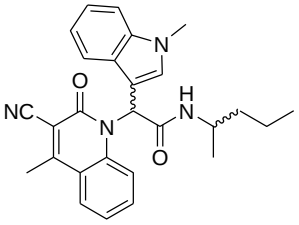

$C_{27}H_{28}N_4O_2$

General procedure 3: A solution of MeOH (5.00 mL), 2-aminoacetophenone (0.148 mL, 1.23 mmol) and 1-methyl-1*H*-indole-3-carboxaldehyde (0.196 g, 1.23 mmol) was stirred at room temperature for 0.5 h. To the stirred solution was added cyanoacetic acid (0.105 g, 1.23 mmol) followed by the addition of 2-pentylisocyanide (0.152 mL, 1.23 mmol). The reaction mixture was stirred at room temperature for 24 h and the crude material was subjected to silica gel column chromatography (1:4 Hexane–EtOAc) to afford **20** (70 mg, 13%) as an off white solid (mp 243-245°C). IR (cm^{-1}): 3246 (NH), 3083 (CH), 2972 (CH), 2229 (CN), 1637 (CO); The ^1H NMR displays a mixture of isomers, with the ratio 1.35 : 1.0 calculated at 0.74 and 0.60 ppm, respectively. ^1H is reported as a whole without splitting due to the complex overlapping. All peaks detected in ^{13}C are reported. ^1H NMR (400 MHz, DMSO-d_6) δ 7.91 (d, J = 8.2 Hz, 1H), 7.83 – 7.69 (m, 2H), 7.67 – 7.51 (m, 2H), 7.47 – 7.35 (m, 3H), 7.29 (dd, J = 9.8, 5.4 Hz, 1H), 7.13 (t, J = 7.6 Hz, 1H), 7.01 (t, J = 7.4 Hz, 1H), 3.98-3.86 (m, 1H), 3.75 (s, 3H), 2.75 (d, J = 3.2 Hz, 3H), 1.54 – 1.15 (m, 4H), 0.93-0.87 (m, 3H), 0.77-0.56 (m, 2H); ^{13}C NMR (101 MHz, DMSO-d_6) δ 167.4, 166.8, 159.2, 159.2, 158.3, 158.3, 139.1, 136.6, 136.5, 133.3, 133.2, 130.9, 130.81, 127.7, 127.6, 127.6, 123.4, 121.9, 120.1, 120.1, 119. 8, 118.9, 118.1, 118.1, 116.2, 110.4, 107.7, 106.2, 106.1, 106.1, 60.2, 53.8, 53.7, 52.9, 45.3, 45.2, 38.3, 38.0, 33.0 (Cx2), 27.4, 26.8, 21.2, 21.1, 20.8, 19.6, 19.1, 18.8, 14.6, 14.3, 14.2, 11.2, 10.8; LRMS (ESI-) m/z 440, 520 $[M+DMSO+2H]^+$ 100%. HRMS (ES+) for $C_{27}H_{28}N_4O_2Na$; calculated 463.2110, found 463.2104; RP-HPLC Alltima™ C18 5 µm 150 mm x 4.6 mm, 10–100% B in 15 min, R_t = 7.07 min, 93 %.

*2-(3-Cyano-2-oxo-4-phenylquinolin-1(2H)-yl)-2-(1H-indol-3-yl)-N-(pentan-2-yl)acetamide (**21**)*

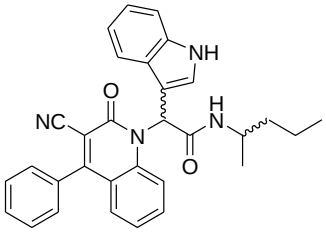

$C_{31}H_{28}N_4O_2$

Synthesized utilizing the general procedure 3 described above, from 2-aminobenzophenone (0.252 g, 1.28 mmol), indole-3-carboxaldehyde (0.186g, 1.28 mmol), cyanoacetic acid (0.109 g, 1.28 mmol) and 2-pentylisocyanide (0.158 mL, 1.28 mmol) in MeOH (5.00 mL) to afford **21** (0.07 g, 11%) as an off white solid (mp 182–183 ºC). IR (cm^{-1}): 3420 (NH), 2229 (CN), 1678 (CONH), 1646 (CON); The ^1H NMR displays a mixture of isomers,

with the ratio 5.5 : 1.0 calculated at 3.96 and 3.72 ppm, respectively. ^{1}H is reported as a whole without splitting due to the complex overlapping. All peaks detected in ^{13}C are reported ^{1}H NMR (400 MHz, DMSO-d_6) δ 11.26 (s, 1H), 7.85 (s, 2H), 7.73 – 7.32 (m, 10H), 7.29 – 6.87 (m, 4H), 3.96 (s, 1H), 1.84 – 0.09 (m, 11H); ^{13}C NMR (101 MHz, DMSO-d_6) δ 167.4, 166.8, 160.1, 159.3, 140.1, 136.2, 136.1, 134.1, 133.3, 130.4, 129.3, 129.2, 129.1, 127.4, 127.3, 127.0, 126.9, 123.5, 122.0, 119.9, 119.8, 118.8, 118.6, 116.0, 112.2, 108.5, 106.0, 54.3, 54.2, 53.0, 45.4, 45.3, 38.4, 38.2, 27.4, 26.9, 21.1, 20.9, 19.6, 19.2, 14.4, 14.2, 11.3, 10.8; LRMS (ESI+) m/z 488, 489 $[M+H]^+$, 40%. HRMS (ES+) for $C_{31}H_{28}N_4O_2$; calculated 489.2285, found 489.2284; RP-HPLC Phenomenex Onyx™ Monolithic C18 5 µm 100 mm x 4 mm, 10–100% B in 15 min, R_t = 12.24 min, 100 %.

*2-(3-Cyano-2-oxo-4-phenylquinolin-1(2H)-yl)-2-(1H-indol-5-yl)-N-(pentan-2-yl)acetamide (**22**)*

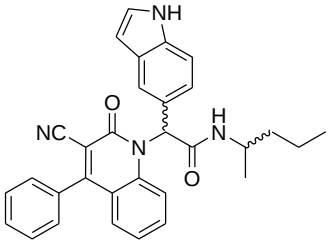

$C_{31}H_{28}N_4O_2$

Synthesized utilizing the general procedure 3 described above, from 2-aminobenzophenone (0.267 g, 1.35 mmol), indole-5-carboxaldehyde (0.197g, 1.35 mmol), cyanoacetic acid (0.115 g, 1.35 mmol) and 2-pentylisocyanide (0.167 mL, 1.35 mmol) in MeOH (5.0 mL) to afford **22** (0.238 g, 36%) as an off white solid (mp 271–272 ºC). IR (cm^{-1}): 3403 (NH), 3338 (NH), 2956 (CH), 2235 (CN), 1647 (CO); The ^{1}H NMR displays a mixture of isomers, with the ratio 2.45 : 1.0 calculated at 0.74 and 0.64 ppm, respectively. ^{1}H is reported as a whole without splitting due to the complex overlapping. All peaks detected in ^{13}C are reported ^{1}H NMR (400 MHz, DMSO-d_6) δ 11.13 (s, 1H), 7.89 (dd, J = 14.3, 8.1 Hz, 1H), 7.71 – 7.52 (m, 7H), 7.52 – 7.44 (m, 1H), 7.41 – 7.29 (m, 2H), 7.26 – 7.01 (m, 4H), 6.40 (d, J = 1.8 Hz, 1H), 3.91 (dd, J = 13.4, 7.0 Hz, 1H), 1.59 – 1.19 (m, 3H), 1.16 – 0.99 (m, 2H), 0.99 – 0.84 (m, 3H), 0.81-0.55 (m, 2H); ^{13}C NMR (101 MHz, DMSO-d_6) δ 167.5, 167.0, 166.9, 160.1, 160.0, 159.4, 140.6, 135.6, 134.2, 134.2, 133.1, 133.0, 130.4, 129.3 (C x 2), 129.2 (C x 2), 129.1, 129.1, 128.0, 126.5, 126.5, 125.8, 125.7, 125.6, 123.5, 121.8, 120.1, 120.1, 120.0, 119.1, 119.0, 116.0, 116.0, 111.9, 111.9, 106.3, 106.3, 106.2, 101.8, 101.7, 61.3, 61.1, 61.1, 52.8, 45.3, 45.2, 38.3, 38.2, 27.2, 26.8, 21.2, 20.9, 19.5, 19.0, 14.4, 14.3, 11.1, 10.6; LRMS (ESI-) m/z - 488, 520 $[M+CH_3OH-H]$ 95%. HRMS (ES+) for $C_{31}H_{28}N_4O_2$; calculated 489.2285, found 489.2284. RP-HPLC Alltima™ C18 5 µm 150 mm x 4.6 mm, 10–100% B in 15 min, R_t = 7.07 min, >98 %.

*2-(3-Cyano-2-oxo-4-phenylquinolin-1(2H)-yl)-2-(5-methyl-1H-indole-3-yl)-N-(pentan-2-yl) acetamide (**23**)*

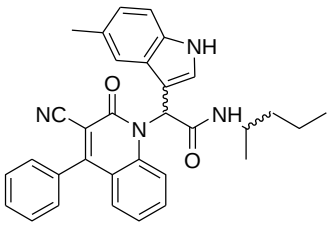

$C_{32}H_{30}N_4O_2$

Synthesized utilizing the general procedure 3 described above, from 2-aminobenzophenone (0.378 g, 1.92 mmol), 5-methyl-1*H*-indole carbaldehyde (0.305 g, 1.92 mmol), cyanoacetic acid (0.163 g, 1.92 mmol), and 2-pentylisocyanide (0.237 mL, 1.92 mmol) to afford **23** (0.445 g, 46%) as an off white solid (mp 178–180 ºC). IR (cm^{-1}): 3427 (br NH), 2962 (CH), 2236 (CN), 1645 (CON); The ^1H NMR displays a mixture of isomers, with the ratio 2.1 : 1.0 calculated at 0.77 and 0.68 ppm, respectively. ^1H is reported as a whole without splitting due to the complex overlapping. All peaks detected in ^{13}C are reported ^1H NMR (400 MHz, DMSO-d_6) δ 11.13 (d, J = 4.9 Hz, 1H), 7.90 – 7.37 (m, 10H), 7.29-7.16 (m, 4H), 6.92 (d, J = 8.3 Hz, 1H), 4.03 – 3.87 (m, 1H), 2.34 (s, 3H), 1.57 – 1.20 (m, 3H), 1.20 – 0.86 (m, 5H), 0.82-0.60 (m, 3H); ^{13}C NMR (101 MHz, DMSO-d_6) δ 167.5, 166.9, 160.1, 160.1, 159.3, 140.1, 140.1, 134.6, 134.6, 134.5, 134.1, 133.3, 130.4, 129.4, 129.2, 129.1, 128.2, 128.1, 127.5, 127.5, 126.8, 126.6, 123.5, 119.9, 118.5, 118.4, 118.3, 116.0, 111.9, 107.9, 107.9, 106.0, 105.9, 54.5, 54.4, 52.9, 45.4, 45.2, 38.4, 38.2, 27.3, 26.9, 21.9, 21.1, 20.9, 19.6, 19.2, 14.4, 14.2, 11.2, 10.8; LRMS (ESI-) m/z 502, 521 $[M+NH_4]^+$ 40%. HRMS (ES+) for $C_{32}H_{30}N_4O_2$; calculated 503.2442, found 503.2444; RP-HPLC Alltima™ C18 5 μm 150 mm x 4.6 mm, 10–100% B in 15 min, R_t = 10.89 min, 100%.

*Ethyl-[2-(3-cyano-2-oxo-4-phenyl-2H-quinolin-1-yl)-2-(5-methyl-1H-indol-3-yl)-acetamido]-acetate (**24**)*

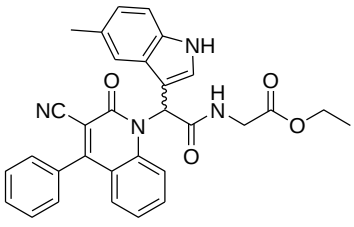

$C_{31}H_{26}N_4O_4$

Synthesized utilizing the general procedure 3 described above, from 2-aminobenzophenone (0.390 g, 1.98 mmol), 5-methyl-indole-3-carboxaldehyde (0.315g, 1.98 mmol), cyanoacetic acid (0.168 g, 1.98 mmol) and ethyl isocyanoacetate (0.216 mL, 1.98 mmol) in MeOH (5.0 mL) to afford **24** (0.347 g, 34%) as a greenish solid (mp 199-200 °C). IR (cm^{-1}): 3423 (NH), 3410 (NH), 2232 (CN), 1731 (COO), 1673 (CON); ^1H NMR (400 MHz, DMSO-d_6) δ 11.21 (d, J = *1*.8 Hz, 1H), 8.53 (s, 1H), 7.83 (d, J = 8.7 Hz, 1H), 7.72 – 7.48 (m, 8H), 7.32 – 7.17 (m, 4H), 6.92 (d, J = 8.3 Hz, 1H), 4.14 (q, J = 7.1 Hz, 2H), 4.02-3.84 (m, 2H), 2.34 (s, 3H), 1.22 (t, J = 7.1 Hz, 3H); ^{13}C NMR (101 MHz, DMSO-d_6) δ 170.2, 168.4, 160.3, 159.3, 139.7, 134.5, 134.1, 133.5, 130.5, 129.4, 129.4, 129.4, 129.1, 129.0, 128.3, 127.5, 127.1, 123.7 (C x 2), 119.9, 118.5, 118.2, 115.8, 111.9, 107.3, 105.8, 61.0, 53.8, 41.9, 21.9,

14.6; LRMS (ESI+) m/z518, 541 $[M+Na-H]^+$ 60%. HRMS (ES+) for $C_{31}H_{26}N_4O_4$; calculated 519.2027, found 519.2026; RP-HPLC Alltima™ C18 5 µm 150 mm x 4.6 mm, 10–100% B in 15 min, R_t = 13.72 min, > 97%.

*Ethyl-[2-(3-cyano-2-oxo-4-phenyl-2H-quinolin-1-yl)-2-(1H-indol-3-yl)-acetamido]-acetate (**25**)*

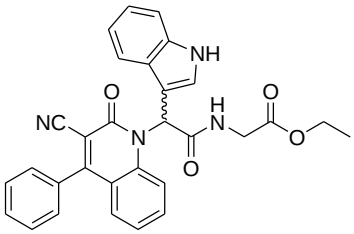

$C_{30}H_{24}N_4O_4$

Synthesized utilizing the general procedure 3 described above, from 2-aminobenzophenone (0.366 g, 1.86 mmol), 1*H*-indole carbaldehyde (0.269 g, 1.86 mmol), cyanoacetic acid (0.157 g, 1.86 mmol), and ethyl isocyanoacetate (0.202 mL, 1.86 mmol) to afford **25** (0.30 g, 46%) as an off white solid (mp 179.3-180.5 °C). IR (cm^{-1}): 3420 (NH), 2236 (CN), 1737 (COO), 1686 (CONH), 1646 (CON); ^{1}H NMR (400 MHz, DMSO-d_6) δ 11.35 (s, 1H), 8.58 (s, 1H), 7.93 – 7.75 (m, 2H), 7.75-7.45 (m, 8H), 7.39 (d, J = 8.0 Hz, 1H), 7.21 (d, J = 3.7 Hz, 2H), 7.15-6.91 (m, 2H), 4.25 – 4.06 (m, 2H), 4.04-3.80 (m, 2H), 1.22 (t, J = 7.0 Hz, 3H); ^{13}C NMR (101 MHz, DMSO-d_6) δ 170.2, 168.4, 160.3, 159.3, 139.7, 136.1, 134.0, 133.5, 130.5, 129.5, 129.4 (C x 2), 129.3 (C x 2), 129.2, 129.0, 127.3, 123.7, 122.1, 120.0 (C x 2), 118.6, 118.5, 115.9, 112.2, 107.8, 105.8, 61.1, 53.7 41.9, 14.6; LRMS (ESI+) m/z 504, 505 $[M+H]^+$, 100%. HRMS (ES+) for $C_{30}H_{24}N_4O_4$; calculated 505.1870, found 505.1869; RP-HPLC Phenomenex Onyx™ Monolithic C18 5 µm 100 mm x 4 mm, 10–100% B in 15 min, R_t = 11.09 min, 100%.

*Ethyl-[2-(3-cyano-2-oxo-4-phenyl-2H-quinolin-1-yl)-2-(1-methylindole-3-yl)-acetamido]-acetate (**26**)*

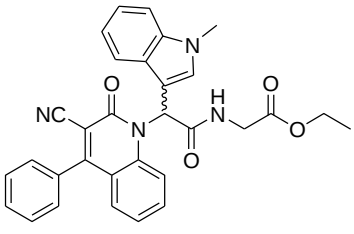

$C_{31}H_{26}N_4O_4$

Synthesized utilizing the general procedure 3 described above, from 2-aminobenzophenone (0.281 g, 1.43 mmol), 1-methyl-indole-3-carboxaldehyde (0.227 g, 1.43 mmol), cyanoacetic acid (0.121 g, 1.43 mmol) and ethyl isocyanoacetate (0.156 mL, 1.43 mmol) in MeOH (5.0 mL). The crude material was subjected to silica gel column chromatography (1:1 Hexane–EtOAc) to afford **26** (0.192 g, 26%) as an off white solid (mp 209-211°C). IR (cm^{-1}): 3422 (NH), 2920 (CH), 2229 (CN), 1743 (COO), 1639 (CON); ^{1}H NMR (400 MHz, DMSO-d_6) δ 8.53 (bs, 1H), 7.85 (d, J = 8.8 Hz, 1H), 7.75 (s, 1H), 7.70 – 7.48 (m, 7H), 7.43 (d, J = 8.2 Hz, 1H), 7.25 – 7.19 (m, 2H), 7.17 (t, J = 7.2 Hz, 1H), 7.06 (t, J = 7.2 Hz, 1H), 4.12 (q, J = 7.1 Hz, 2H), 3.90 (d, J = 6.6 Hz, 2H), 3.79 (s, 3H), 1.20 (t, J = 7.1 Hz, 3H); ^{13}C NMR (101 MHz, DMSO-d_6) δ 170.1, 168.3,

160.3, 159.2, 139.6, 136.5, 134.0, 133.7, 131.4, 130.5, 129.5, 129.4 (C x 2), 129.2, 129.0, 127.7, 123.7, 122.1, 120.1, 120.0, 118.9, 118.2, 115.9, 110.5, 106.8, 105.9, 105.9, 61.0, 41.9, 33.2, 14.6; LRMS (ESI-) m/z 518, 540 $[M+ Na-H]^+$, 100%. HRMS (ES+) for $C_{31}H_{26}N_4O_4$; calculated 519.2027, found 519.2027; RP-HPLC Alltima™ C18 5 µm 150 mm x 4.6 mm, 10–100% B in 15 min, R_t = 14.26 min, >98%.

*Ethyl-3-[2-(3-cyano-2-oxo-4-phenyl-2H-quinolin-1-yl)-2-(1-methyl-1H-indol-3-yl)-acetylamino]-propionate (**27**)*

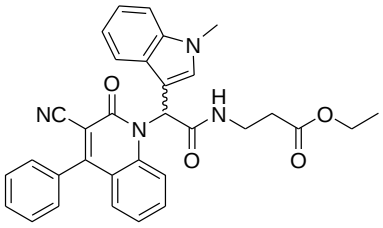

$C_{32}H_{28}N_4O_4$

Synthesized utilizing the general procedure 3 described above, from 2-aminobenzophenone (0.186 g, 0.94 mmol), 1-methyl-indole-3-carboxaldehyde (0.15g, 0.94 mmol), cyanoacetic acid (0.08 g, 0.94 mmol) and ethyl isocyanopropionate (0.12 mL, 0.94 mmol) in MeOH (5.0 mL) to afford **27** (0.149 g, 50%) as a white solid (mp 267-268°C). IR (cm^{-1}): 3410 (NH), 2232 (CN), 1725 (COO), 1686 (CON); ^{1}H NMR (400 MHz, DMSO-d_6) δ 8.05 (bs, 1H), 7.83 (d, J = 8.7 Hz, 1H), 7.71 – 7.56 (m, 6H), 7.56 – 7.47 (m, 2H), 7.45-7.38 (m, 2H), 7.26 – 7.20 (m, 2H), 7.17 (t, J = 7.2 Hz, 1H), 7.06 (t, J = 7.2 Hz, 1H), 4.03 (q, J = 7.1 Hz, 2H), 3.78 (s, 3H), 3.42 – 3.35 (m, 2H), 2.57-2.44 (m, 2H), 1.16 (t, J = 7.1 Hz, 3H); ^{13}C NMR (101 MHz, DMSO-d_6) δ 171.7, 167.7, 160.1, 159.0, 139.9, 136.5, 134.1, 133.8, 131.3, 130.5, 129.6, 129.4, 129.2, 129.0, 127.8, 123. 7, 122.1, 120.0, 119.9, 119.0, 117.8, 115.9, 110. 5, 107.1, 106.1, 60.4, 54.1, 35.9, 34.0, 33.1, 14.5; LRMS (ESI+) m/z 532, 287 $[M+ACN+ 2H]^{2+}$ 100%. HRMS (ES+) for $C_{16}H_{11}N_2O^+$ (main fragment); calculated 247.0870, found 247.0870; RP-HPLC Alltima™ C18 5 µm 150 mm x 4.6 mm, 10–100% B in 15 min, R_t = 14.46 min, > 95%.

*Ethyl-2-(2-(5-chloro-indole(1H)-3-yl)-2-(3-cyano-2-oxo-4-phenyl-1(2H)-quinolin-yl)-acetamido)-acetate (**28**)*

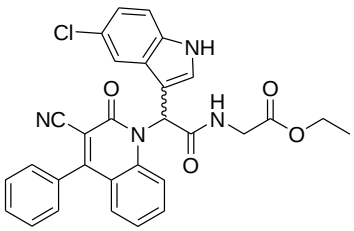

$C_{30}H_{23}ClN_4O_4$

Synthesized utilizing the general procedure 3 described above, from 2-aminobenzophenone (0.478 g, 2.4 mmol), 5-chloro-indole-3-carboxaldehyde (0.434g, 2.4 mmol), cyanoacetic acid (0.204 g, 2.4 mmol) and ethyl isocyanoacetate (0.271 mL, 2.4 mmol) in MeOH (5.0 mL) to afford **28** (0.435 g, 33%) as a yellowish solid (mp 201–203°C). IR (cm^{-1}): 3415 (NH), 3406 (NH), 2236 (CN), 1736 (COO), 1671 (CON); ^{1}H NMR (400 MHz, DMSO-d_6) (isomeric mixture) δ 11.54 (d, J = 1.4 Hz, 1H), 8.53 (s, 1H), 7.82 (dd, J = 11.9, 5.5 Hz, 2H), 7.71 – 7.61 (m, 4H), 7.61-7.5 (m, 4H), 7.42 (d, J =

8.6 Hz, 1H), 7.29 – 7.18 (m, 2H), 7.12 (dd, *J* = 8.6, 1.7 Hz, 1H), 4.14 (q, *J* = 7.0 Hz, 2H), 3.93 (qd, *J* = 17.2, 5.8 Hz, 2H), 1.22 (t, *J* = 7.1 Hz, 3H); ^{13}C NMR (101 MHz, DMSO-d_6) δ 170.1, 168.2, 160.4, 159.2, 139.6, 134.6, 134.0, 133.7, 130.5, 129.6 (C x 2), 129.4, 129.2, 129.0 (C x 2), 128.5, 124.5, 123.8, 122.0, 120.1, 118.3 (Cx2), 118.2, 115.8, 113.8, 107.8, 106.0, 61.0, 42.0, 14.6; LRMS (ESI+) m/z 538, 292 $[M+2Na]^{2+}$, 60%. HRMS for $C_{30}H_{23}ClN_4O_4$; calculated 539.1481, found 539.1481; RP-HPLC Alltima™ C18 5 µm 150 mm x 4.6 mm, 10–100% B in 15 min, R_t = 14.07 min, >99%.

*N-tert-Butyl-2-(3-cyano-2-oxo-4-phenyl-2H-quinolin-1-yl)-2-(5-methyl-1H-indol-3-yl)-acetamide (**29**)*

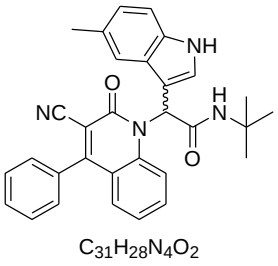

$C_{31}H_{28}N_4O_2$

Synthesized utilizing the general procedure 3 described above, from 2-aminobenzophenone (0.359 g, 1.83 mmol), 5-methyl-indole-3-carboxaldehyde (0.290g, 1.83 mmol), cyanoacetic acid (0.156 g, 1.83 mmol) and *tert*-butyl isocyanide (0.207 mL, 1.83 mmol) in MeOH (5.0 mL) to afford **29** (0.419g, 47%) as a white solid (mp 196-198°C). IR (cm^{-1}): 3427 (NH), 2978 (CH), 2228 (CN), 1650 (CON); ^{1}H NMR (400 MHz, DMSO-d_6) (isomeric mixture) δ 11.13 (d, *J* = 4.9 Hz, 1H), 7.90 – 7.37 (m, 10H), 7.29-7.16 (m, 4H), 6.92 (d, *J* = 8.3 Hz, 1H), 4.03 – 3.87 (m, 1H), 2.34 (s, 3H), 1.57 – 1.20 (m, 3H), 1.20 –0.86 (m, 5H), 0.82-0.60 (m, 3H); ^{13}C NMR (101 MHz, DMSO-d_6) δ 167.5, 166.9, 160.1, 160.1, 159.3, 140.1, 140.1, 134.6, 134.6, 134.5, 134.1, 133.3, 130.4, 129.4, 129.2, 129.1, 128.2, 128.1, 127.5, 127.5, 126.8, 126.6, 23.5, 19.9, 118.48, 118.4, 118.3, 116.0, 111.9, 107.9, 107.9, 106.0, 105.9, 54.5, 54.4, 52.9, 45.4, 45.2, 38.4, 38.2, 27.3, 26.9, 21.9, 21.1, 20.9, 19.6, 19.2, 14.4, 14.2, 11.2, 10.8; LRMS (ESI-) m/z 488, 243 $[M-2H]^{2+}$, 90%. HRMS for $C_{31}H_{28}N_4O_2$; calculated 489.2285, found 489.2283; RP-HPLC Alltima™ C18 5 µm 150 mm x 4.6 mm, 10–100% B in 15 min, R_t = 14.59 min, >95%.

*N-tert-Butyl-2-(3-cyano-2-oxo-4-phenyl-2H-quinolin-1-yl)-2-(1-methyl-1H-indole-3-yl)-acetamide (**30**)*

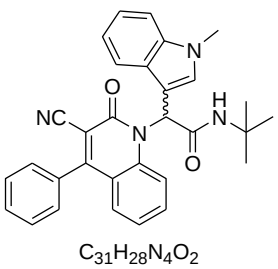

$C_{31}H_{28}N_4O_2$

Synthesized utilizing the general procedure 3 described above, from 2-aminobenzophenone (0.311 g, 1.58 mmol), 1-methyl-indole-3-carboxaldehyde (0.251g, 1.58 mmol), cyanoacetic acid (0.134 g, 1.58 mmol) and *tert*-butyl isocyanide (0.178 mL, 1.58 mmol) in MeOH (5.0 mL) to afford **29** (0.200 g, 26%) as a white solid (mp 232-234°C). IR (cm^{-1}): 3357 (NH), 2979 (CH), 2229 (CN), 1650 (CO); ^{1}H NMR (400 MHz, DMSO-d_6) δ 7.89 (d, *J* = 8.8 Hz, 1H), 7.68 – 7.46

(m, 9H), 7.43 (d, J = 7.8 Hz, 2H), 7.22-7.13 (m, 3H), 7.06 (t, J = 7.4 Hz, 1H), 3.79 (s, 3H), 1.32 (s, 9H); ^{13}C NMR (101MHz, DMSO-d_6) δ 166.66, 160.13, 159.17, 140.28, 136.75, 134.09, 133.34, 130.54, 130.42, 129.31 (C x 3), 129.15 (C x 2), 127.48, 123.52, 122.17, 119.99, 119.78, 119.04, 118.55, 115.91, 110.53, 108.04, 105.89, 54.94, 51.57, 33.09, 28.83 (C x 3); LRMS (ESI+) m/z 488, 243 $[M-2H]^{2+}$, 100%. HRMS (ES+) for $C_{31}H_{28}N_4O_2$; calculated 489.2285, found 489.2287; RP-HPLC Alltima™ C18 5µm 150 mm x 4.6 mm, 10–100% B in 15 min, R_t = 7.03 min, 96%.

7.3.3. Synthesis of the tryptophan and indole based analogues (Chapter 4)

Synthesis of tryptophan derivatives

*2-Amino-N-(4-chlorobenzyl)-3-(1H-indol-3-yl)-propionamide (**9**)*

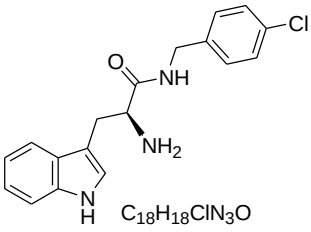

A solution of dimethylformamide (DMF) (30.0 mL), Fmoc-L-tryptophan (3.65 g, 8.55 mmol), HATU (4.88 g, 12.83 mmol) and 4-chloro-benzylamine (1.04 mL, 8.55 mmol) was stirred at room temperature to complete dissolution. To the stirred solution was added diisopropylethylamine (DIPEA) (4.46 mL, 25.65 mmol) and the reaction mixture was stirred overnight. DMF was then removed and the crude was dissolved in ethyl acetate, which was subsequently washed three times by 1M hydrochloric) acid (50.00 mL) forming milky precipitate. The precipitate without further purification was filtered and stirred in 20% piperidine in acetonitrile (20 mL) for three hours. Acetonitrile was subsequently removed by evaporation *in vacuo* and the crude was re-dissolved in ethyl acetate. The ethyl acetate solution was washed three times by 1M hydrochloric acid and left for 48 h for recrystallization to afford **9** (1.55 g, 50%) as an off white solid (mp. 254.5 − 255 °C). IR (cm^{-1}): 3253 (NH), 2858 (CH- aliphatics), 1659 (CON), 738 (CH-aromatics). ^{1}H NMR (400 MHz, DMSO-d_6) δ 11.08 (s, 1H), 9.07 (t, J = 5.8 Hz, 1H), 8.32 (s, 3H), 7.66 (d, J = 7.9 Hz, 1H), 7.40 (d, J = 8.1 Hz, 1H), 7.30 (d, J = 8.4 Hz, 2H), 7.21 (d, J = 2.2 Hz, 1H), 7.10 (dd, J = 15.9, 7.8 Hz, 3H), 7.01 (t, J = 7.4 Hz, 1H), 4.26 (ddd, J_{AX} = 38.6, J_{BX} = 15.4, J_{AB} = 5.8 Hz, 2H), 4.04 (t, J = 7.1 Hz, 1H), 3.22 (ddd, J'_{AX} = 30.8, J'_{BX} = 14.4, J'_{AB} =7.1 Hz, 2H). ^{13}C NMR (400 MHz, DMSO-d_6) δ 169.0, 137.9, 136.7, 131.9, 129.5 (C x 2), 128.6 (C x 2), 127.5, 125.3, 121.6, 119.0, 111.9, 107.5, 53.4, 42.0, 31.2, 27.8. LRMS (APCI+) m/z 327, 328 $[M+H, ^{35}Cl]^+$, 100%. HRMS (ES+) for $C_{18}H_{18}ClN_3O$, calculated 328.1211, found 328.1210.

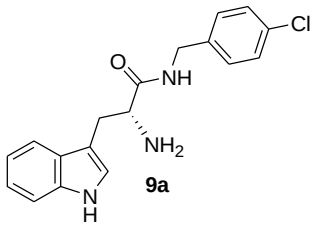

9a

***Note**: Using exactly the same protocol and replacing Fmoc-L-tryptophan by Fmoc-D-tryptophan affords the D-tryptophan derivative **9a** which displayed the same chemical and physical properties to **11**, including NMR spectra.*

Synthesis of L-tryptophan derivatives using (9) as the starting material

N-(4-Chlorobenzyl)-2-[2-(3,4-dichlorophenyl)-acetylamino]-3-(1H-indol-3-yl)-propionamide ***(4)***

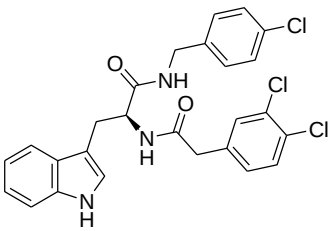

$C_{26}H_{22}Cl_3N_3O_2$

General procedure A: A DMF solution (10 mL) of the freshly prepared **9** (0.37 g, 1.01 mmol), HATU (0.58 g, 1.52 mmol), and (3,4-dichlorophenyl)-acetic acid (0.21 g, 1.01 mmol) was stirred at room temperature to complete dissolution. To the stirred solution was added DIPEA (0.37 mL, 3.03 mmol) and the reaction mixture was stirred overnight. DMF was then removed and the crude material was subjected to silica gel column chromatography (1:4 Hexane–EtOAc) to afford **4** (0.18 g, 35%) as a white solid (mp 208 − 209 °C). IR (cm^{-1}): 3410 (NH), 3277 (NH), 3068 (CH), 1636 (CON). ^{1}H NMR (400 MHz, DMSO-d_6) δ 10.84 (s, 1H), 8.56 (t, J = 8.0 Hz, 1H), 8.43 (d, J = 8.1 Hz, 1H), 7.60 (d, J = 7.9 Hz, 1H), 7.47 (d, J = 8.2 Hz, 1H), 7.42 (d, J = 1.8 Hz, 1H), 7.35 (d, J = 8.1 Hz, 1H), 7.28 (d, J = 8.4 Hz, 2H), 7.16 – 7.02 (m, 5H), 6.97 (t, J = 7.1 Hz, 1H), 4.59 (dd, J = 8.0, 12.0 Hz, 1H), 4.24 (ddd, $J_{A'X'} = J_{B'X'}$ = 8.0, $J_{A'B'}$ = 16 Hz, 2H), 3.47 (s, 2H), 3.05 (ddd, J_{AX} = 4.0, J_{BX} = 8.0, J_{AB} = 16.0 Hz, 2H). ^{13}C NMR (101 MHz, DMSO-d_6) δ 171.9, 169.6, 138.7, 138.0, 136. 6, 131.6, 131.5, 131.0, 130.6, 129.8, 129.4, 129.2 (C x 2), 128.5 (C x 2), 127.7, 124.2, 121.4, 119.0, 118.7, 111.8, 110.4, 54.2, 41.8, 41.2, 28.5. LRMS (ESI+) m/z: 513, 514 $[M+H, {}^{35}Cl]^+$, 95%. HRMS (ES+) for $C_{26}H_{22}Cl_3N_3O_2$, calculated 514.0850, found 514.0850. RP-HPLC Alltima™ C18 5 µm 150 mm x 4.6 mm, 10–100% B in 15 min, R_t =14.31 min, 100%.

N-(4-Chlorobenzyl)-2-[2-(2,4-dichlorophenyl)-acetylamino]-3-(1H-indol-3-yl)-propionamide ***(11)***

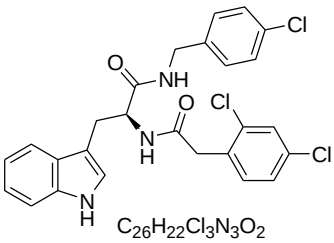

$C_{26}H_{22}Cl_3N_3O_2$

Synthesized utilizing the general procedure A described above, from **9** (0.152 g, 0.42 mmol), HATU (0.239 g, 0.63 mmol), (2,4-dichlorophenyl)-acetic acid (0.086 g, 0.42 mmol), and DIPEA (0.22 mL, 1.26 mmol) in DMF (5.0 mL) to afford **11** (0.055 g,

24%) as an off white solid (mp 207 − 208 °C). IR (cm^{-1}): 3410 (NH), 3280 (NH), 3065 (CH), 1642 (CON). ^{1}H NMR (400 MHz, DMSO-d_6) δ 10.85 (s, 1H), 8.54 (t, J = 4.0 Hz, 1H), 8.40 (d, J = 8.2 Hz, 1H), 7.62 (d, J = 7.8 Hz, 1H), 7.53 (d, J = 2.1 Hz, 1H), 7.36 (d, J = 8.1 Hz, 1H), 7.33 – 7.23 (m, 3H), 7.12 (ddd, J = 22.2, 12.5, 7.8 Hz, 5H), 6.98 (t, J = 7.4 Hz, 1H), 4.63 (dd, J = 8.0, 16.0 Hz, 1H), 4.25 (ddd, $J_{A'X'} = J_{B'X'}$ = 4.0, $J_{A'B'}$= 16 Hz, 2H), 3.60 (s, 2H), 3.07 (ddd, J_{AX} = 4.0, J_{BX}= 8.0, J_{AB}= 16.0 Hz, 2H). ^{13}C NMR (101 MHz, DMSO-d_6) δ 171.9, 168.9, 138.8, 136.6, 135.0, 133.9, 133.3, 132.3, 131.6, 129.3 (C x 2), 128.8, 128.5 (C x 2) 127.7, 127.4, 124.2, 121.3, 119.0, 118.7, 111.7, 110.4, 54.2, 41.8, 31.0, 28.5. LRMS (APCI+) m/z 513, 514 $[M+1H]^+$ 50%. HRMS (ES+) for $C_{26}H_{22}Cl_3N_3O_2$, calculated 514.0850, found 514.0850. RP-HPLC Alltima™ C18 5 µm 150 mm x 4.6 mm, 10–100% B in 15 min, R_t =14.38 min, 99.2%

N-(4-Chlorobenzyl)-2-[2-(2,6-dichlorophenyl)-acetylamino]-3-(1H-indol-3-yl)-propionamide ***(12)***

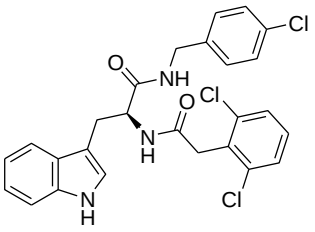

$C_{26}H_{22}Cl_3N_3O_2$

Synthesized utilizing the general procedure A described above, from **9** (0.148 g, 0.41 mmol), HATU (0.228 g, 0.6 mmol), (2,6-dichlorophenyl)-acetic acid (0.082 g, 0.41 mmol) and DIPEA (0.21 mL, 1.2 mmol) in DMF (5.0 mL) to afford **12** (0.08 g, 40%) as a white solid (mp 265 − 256 °C). IR (cm^{-1}): 3410 (NH), 3292 (NH), 3252 (NH), 1641 (CON). ^{1}H NMR (400 MHz, DMSO-d_6) δ 10.85 (s, 1H), 8.49 (t, J = 4.0 Hz, 1H), 8.40 (d, J = 8.2 Hz, 1H), 7.60 (d, J = 7.9 Hz, 1H), 7.41 (d, J = 7.9 Hz, 2H), 7.34 (d, J = 8.1 Hz, 1H), 7.28 (ddd, J = 8.6, 4.7, 2.5 Hz, 3H), 7.13 (d, J = 2.2 Hz, 1H), 7.11 – 7.03 (m, 3H), 7.00 – 6.94 (m, 1H), 4.60 (dd, J = 8.0 Hz, 1H), 4.24 (ddd, $J_{A'X'}$ = 8.0, $J_{B'X'}$ = 4.0, $J_{A'B'}$= 16 Hz, 2H), 3.84 (q, J = 16.3 Hz, 2H), 3.07 (ddd, J_{AX} = 6, J_{BX} = 8.0, J_{AB}= 12 Hz, 2H). ^{13}C NMR (101 MHz, DMSO-d_6) δ 171.9, 167.8, 138.7, 136.5, 136.0 (Cx2), 133.1, 131.6, 129.6, 129.2 (C x 2), 128.5 (C x 2), 128.5 (C x 2), 127.8, 124.1, 121.3, 118.9, 118.7, 111.7, 110.4, 54.3, 41.8, 37.9, 28.6. LRMS (ESI+) m/z 513, 514 $[M+H]^+$ 95%. HRMS (ES+) for $C_{26}H_{22}Cl_3N_3O_2$, calculated 514.0850, found 514.0850. RP-HPLC Alltima™ C18 5 µm 150 mm x4.6 mm, 10–100% B in 15 min, R_t = 6.54 min, 100%

*N-(4-Chlorobenzyl)-2-[2-(4-chlorophenyl)-acetylamino]-3-(1H-indol-3-yl)-propionamide (**13**)*

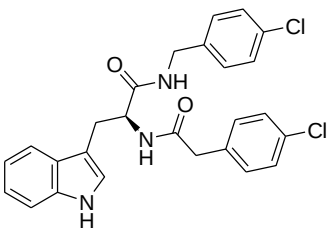

$C_{26}H_{23}Cl_2N_3O_2$

Synthesized utilizing the general procedure A described above, from **9** (0.142 g, 0.39 mmol), HATU (0.223 g, 0.59 mmol), (4-chlorophenyl)-acetic acid (0.067 g, 0.39 mmol) and DIPEA (0.20

mL, 1.17 mmol) in DMF (5.0 mL) to afford **13** (0.06 g, 32%) as a white solid (mp 205.2 − 206.3 ºC). IR (cm^{-1}): 3410 (NH), 3292 (NH), 3061 (CH), 1635 (CON). ^{1}H NMR (400 MHz, DMSO-d_6) δ 10.84 (s, 1H), 8.55 (t, J = 6.0 Hz, 1H), 8.38 (d, J = 8.2 Hz, 1H), 7.60 (d, J = 7.9 Hz, 1H), 7.36 (d, J = 8.1 Hz, 1H), 7.32 – 7.21 (m, 4H), 7.16 – 7.01 (m, 6H), 7.01 – 6.90 (m, 1H), 4.59 (dd, J = 8 Hz, 1H), 4.23 (ddd, $J_{A'X'}$ = 8, $J_{B'X'}$ = 6.0, $J_{A'B'}$= 16 Hz, 2H), 3.44 (dd, J = 19.8, 14.4 Hz, 2H), 3.05 (ddd, J_{AX} = 6, J_{BX} = 8, J_{AB} = 16 Hz, 2H). ^{13}C NMR (101 MHz, DMSO-d_6) δ 172.0, 170.0, 138.7, 136.6, 135.8, 131.6, 131.4, 131.3 (C x 2), 129.2 (C x 2), 128.5 (C x 2), 128.4 (C x 2), 127.7, 124.2, 121.4, 119.0, 118.7, 111.7, 110.4, 54.1, 41.8, 41.7, 28.5. LRMS (ESI+) m/z 479, 480 $[M+H]^+$, 100%. HRMS (ES+) for $C_{26}H_{23}Cl_2N_3O_2$, calculated 480.1240, found 480.1240. RP-HPLC Alltima™ C18 5 µm 150 mm x 4.6 mm, 10–100% B in 15 min, R_t = 13.69 min, 100%

1H-Indole-2-carboxylic acid [1-(4-chlorobenzylcarbamoyl)-2-(1H-indol-3-yl)-ethyl]-amide ***(14_ L-isomer)***

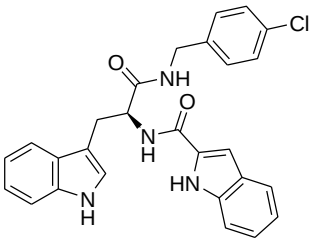

$C_{27}H_{23}ClN_4O_2$

Synthesized utilizing the general procedure A described above, from **9** (0.142 g, 0.40 mmol), HATU (0.227 g, 0.60 mmol), 1*H*-indole-2-carboxylic acid (0.064 g, 0.40 mmol) and DIPEA (0.21 mL, 1.19 mmol) in DMF (5.0 mL) to afford **14** (0.097 g, 50%) as a white solid (mp 229.5 − 230.7 ºC). IR (cm^{-1}): 3422 (NH), 3381 (NH), 3316 (NH), 1630 (CON). ^{1}H NMR (400 MHz, DMSO-d_6) δ 11.53 (s, 1H), 10.80 (s, 1H), 8.70 (t, J = 6.0 Hz, 1H), 8.57 (d, J = 8.1 Hz, 1H), 7.71 (d, J = 7.8 Hz, 1H), 7.62 (d, J = 8.0 Hz, 1H), 7.41 (d, J = 8.2 Hz, 1H), 7.33 (dd, J = 7.7, 5.5 Hz, 3H), 7.25 – 7.14 (m, 5H), 7.09 – 6.96 (m, 3H), 4.80 (dd, J = 9.2, 5.0 Hz, 1H), 4.31 (dd, $J_{A'X'}$ =$J_{B'X'}$ = 6.0, $J_{A'B'}$= 16.0 Hz, 2H), 3.24 (ddd, J_{AX} = 5.0, J_{BX} = 9.6, J_{AB} = 14.4 Hz, 2H). ^{13}C NMR (101 MHz, DMSO-d_6) δ 172.3, 161.5, 138.9, 136.9, 136.5, 131.7, 129.3 (C x 2), 128.6 (C x 2), 127.7, 127.5, 124.3, 123.8, 122.0, 121.4, 120.2, 119.0, 118.7, 112.7, 111.8, 110.8, 103.8, 54.5, 41.9, 28.2 LRMS (APCI+) m/z 470, 471 $[M+1H]^+$, 90%. HRMS (ES+) for $C_{27}H_{23}ClN_4O_2$ calculated 471.1582, found 471.1582. RP-HPLC Alltima™ C18 5 µm 150 mm x 4.6 mm, 10–100% B in 15 min, R_t = 13.35 min, 100%.

1H-Indole-2-carboxylic acid [1-(4-chlorobenzylcarbamoyl)-2-(1H-indol-3-yl)-ethyl]-amide ***(14a_ D-isomer)***

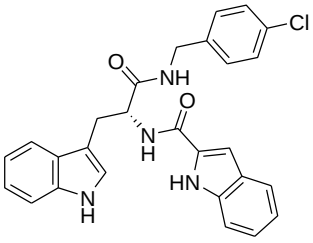

$C_{27}H_{23}ClN_4O_2$

Synthesized utilizing the general procedure A described above, from **9a** (0.249 g, 0.69 mmol), HATU (0.39 g, 1.03 mmol), 1*H*-indole-2-carboxylic acid (0.11 g, 0.69 mmol) and DIPEA (0.36 mL, 2.05 mmol) in DMF (5.0 mL) to afford **14a** (0.156 g, 48%) as a white solid (mp 227 − 227.5 ºC). IR (cm^{-1}): 3420 (NH), 3382 (NH), 3325 (NH), 1630 (CONH), 1656 (CON), 737 (CH-aromatics). ^{1}H NMR (400 MHz, DMSO-d_6) δ 11.53 (s, 1H), 10.81 (d, J = 1.6 Hz, 1H), 8.71 (t, J = 6.0 Hz, 1H), 8.58 (d, J = 8.1 Hz, 1H), 7.72 (d, J = 7.8 Hz, 1H), 7.63 (d, J = 8.0 Hz, 1H), 7.45 – 7.39 (m, 1H), 7.37 – 7.30 (m, 3H), 7.26 – 7.14 (m, 5H), 7.11 – 6.95 (m, 3H), 4.82 (dd, J = 9.2, 5.2 Hz, 1H), 4.32 (dd, $J_{A'X'}$ =$J_{B'X'}$ = 6.0, $J_{A'B'}$= 16.0 Hz, 2H), 3.23 (ddd, J_{AX} = 5.2, J_{BX} = 9.6, J_{AB} = 14.4 Hz, 2H). ^{13}C NMR (101 MHz, DMSO-d_6) δ 172.3, 161.5, 138.9, 136.9, 136.6, 131.8, 131.7, 129.3 (C x 2), 128.6 (C x 2), 127.7, 127.5, 124.3, 123.8, 122.0, 121.4, 120.2, 119.0, 118.7, 112.7, 111.8, 110.8, 103.9, 54.5, 42.0, 28.2. LRMS (ESI+) 470, 470 [M+H, ^{35}Cl]$^+$, 80%. HRMS (ES+) for $C_{27}H_{23}ClN_4O_2$ calculated 471.1582. RP-HPLC Alltima™ C18 5 µm 150 mm x 4.6 mm, 10–100% B in 15 min, R_t = 6.44 min, 100%

Naphthalene-1-carboxylic acid [1-(4-chlorobenzylcarbamoyl)-2-(1H-indol-3-yl)-ethyl]-amide ***(15)***

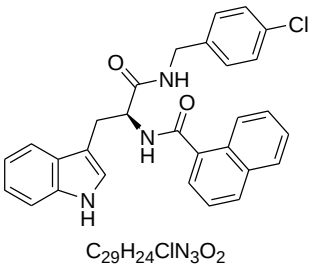

$C_{29}H_{24}ClN_3O_2$

Synthesized utilizing the general procedure A described above, from **9** (0.105 g, 0.29 mmol), HATU (0.17 g, 0.43 mmol), naphthalene-1-carboxylic acid (0.05 g, 0.29 mmol) and DIPEA (0.15 mL, 0.87 mmol) in DMF (5.0 mL) to afford **15** (0.057 g, 41%) as a white solid (mp 165.7 − 166.5 ºC). IR (cm^{-1}): 3398 (NH), 3268 (bp NH), 3049 (CH), 1627 (CON), 739 (CH-aromatics). ^{1}H NMR (400 MHz, DMSO-d_6) δ 10.89 (s, 1H), 8.73−8.67 (m, 2H) (overlapped two NH amides), 8.02 – 7.86 (m, 3H), 7.74 (d, J = 7.8 Hz, 1H), 7.57 – 7.47 (m, 3H), 7.47 – 7.32 (m, 4H), 7.27 (d, J = 8.5 Hz, 3H), 7.11 (dd, J = 11.1, 3.9 Hz, 1H), 7.02 (dd, J = 11.0, 3.9 Hz, 1H), 4.93 (ddd, J = 9.3, 5.2 Hz, 1H), 4.37 (ddd, $J_{A'X'}$ =$J_{B'X'}$ = 8.0, $J_{A'B'}$= 16.0 Hz, 2H), 3.23 (ddd, J_{AX} = 5.2, J_{BX}= 9.6, J_{AB} = 14.4 Hz, 2H). ^{13}C NMR (101 MHz, DMSO-d_6) δ 172.3, 169.0, 139.0, 136.7, 135.0, 133.5, 131.7, 130.2 (C x 2), 129.4 (C x 2), 128.6 (C x 3), 127.8, 126.9, 126.6, 126.0, 125.8, 125.3, 124.4, 121.4, 119.1, 118.7, 111.8, 110.7, 54.8, 42.0, 28.1. LRMS (APCI+) m/z 481, 482 [M+H, ^{35}Cl]$^+$, 90%. HRMS (ES+) for $C_{29}H_{24}ClN_3O_2$, calculated 482.1630, found 482.1630. RP-HPLC Alltima™ C18 5 µm 150 mm x 4.6 mm, 10–100% B in 15 min, R_t = 13.62 min, 99.1%

*4-Benzoyl-N-[1-(4-chlorobenzylcarbamoyl)-2-(1H-indol-3-yl)-ethyl]-benzamide (**16**)*

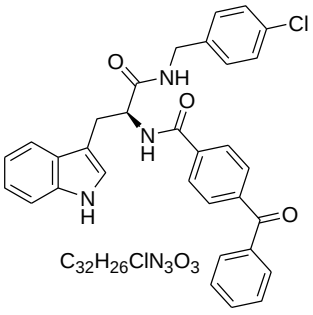

Synthesized utilizing the general procedure A described above, from **9** (0.179 g, 0.49 mmol), HATU (0.28 g, 0.74 mmol), 4-benzoylbenzoic acid (0.11 g, 0.49 mmol) and DIPEA (0.26 mL, 1.48 mmol) in DMF (5.0 mL) to afford **16** (0.127 g, 45%) as a white solid (mp 202 − 202.5 ºC). IR (cm^{-1}): 3440 (NH), 3304 (NH), 1662 (CO), 1632 (CON), 743 (CH-aromatics). ^{1}H NMR (400 MHz, DMSO-d_6) δ 10.80 (s, 1H), 8.80 (d, J = 8.0 Hz, 1H), 8.68 (t, J = 5.9 Hz, 1H), 8.00 (d, J = 8.4 Hz, 2H), 7.81 – 7.66 (m, 6H), 7.58 (t, J = 7.6 Hz, 2H), 7.33 (dd, J = 8.2, 3.5 Hz, 3H), 7.21 (dd, J = 9.2, 5.3 Hz, 3H), 7.03 (dt, J = 30.0, 7.0 Hz, 2H), 4.81 (dd, J = 9.3, 5.2 Hz, 1H), 4.30 (ddd, $J_{A'X'}$ = 5.6, $J_{B'X'}$ = 4.4, $J_{A'B'}$= 15.6 Hz, 2H), 3.25 (ddd, J_{AX} = 5.2, J_{BX} = 9.7, J_{AB} = 14.4 Hz, 2H). ^{13}C NMR (101 MHz, DMSO-d_6) δ 195.9, 172.1, 166.0, 139.7, 138.9, 137.8, 137.1, 136.6, 133.5, 131.7, 130.2 (C x 2), 129.8 (C x 2), 129.3 (C x 2), 129.1 (C x 2), 128.6 (C x 2), 128.2 (C x 2), 127.7, 124.2, 121.4, 119.0, 118.7, 111.8, 110.8, 55.0, 42.0, 28.0. LRMS (APCI+) m/z 535, 536 [M+H, ^{35}Cl]$^+$, 20%. HRMS (ES+), for $C_{32}H_{26}ClN_3O_3$, calculated 536.1735, found 536.1735. RP-HPLC Alltima™ C18 5 µm 150 mm x 4.6 mm, 10–100% B in 15 min, R_t = 14.14 min, 100%

*N-[1-(4-Chlorobenzylcarbamoyl)-2-(1H-indol-3-yl)-ethyl]-3,3,3-trifluoro-2-methoxy-2-phenyl-propionamide (**17**)*

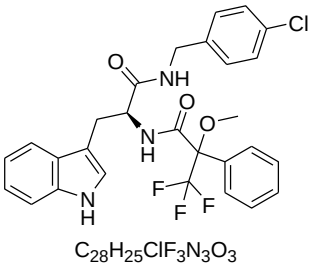

Synthesized utilizing the general procedure A described above, from **9** (0.157 g, 0.43 mmol), HATU (0.25 g, 0.65 mmol), 3,3,3-trifluoro-2-methoxy-2-phenylpropionic acid (0.10 g, 0.43 mmol) and DIPEA (0.23 mL, 1.30 mmol) in DMF (5.0 mL) to afford **17** (0.171 g, 45%) as a white solid (mp 171− 172 ºC). IR (cm^{-1}): 3310 (bp,NH), 2925 (CH), 1657 (CON), 741 (CH-aromatics). ^{1}H NMR (400 MHz, DMSO-d_6) δ 10.82 (s, 1H), 8.70 (t, J = 8.0 Hz, 1H), 8.17 (d, J = 8.5 Hz, 1H), 7.62 (d, J = 7.9 Hz, 1H), 7.43 – 7.32 (m, 4H), 7.30 – 7.18 (m, 4H), 7.13 – 7.01 (m, 3H), 7.01 – 6.90 (m, 2H), 4.81 (dd, J = 8.0, 4.0 Hz, 1H), 4.32 (ddd, $J_{A'X'}$ = 6.0, $J_{B'X'}$ = 8.0, $J_{A'B'}$= 16.0 Hz, 2H), 3.27 (s, 3H), 3.15 (ddd, J_{AX} = 4, J_{BX} = 8, J_{AB} = 16.0 Hz, 2H). ^{13}C NMR (101 MHz, DMSO-d_6) δ 171.4, 165.6, 138.6, 136.6, 132.8, 131.8, 129.8, 129.4 (C x 4), 128.7 (C x 2), 128.6 (C x 4), 127.8, 124.4, 121.4, 119.0, 118.7, 111.7, 109.9, *84.4, 84.2, 83.9, 83.7*, 55.2, 53.8, 42.0, 28.1. [**Note*: CF_3 splitting is detected at 84.0 ppm (q, J = 25.3 Hz) (*italic numbers*)]. LRMS (APCI+)

m/z 543, 544 [M+H, $^{35}Cl]^+$, 50%. HRMS (ES+) for $C_{28}H_{25}ClF_3N_3O_3$, calculated 543.1646, found 544.1611. RP-HPLC Alltima™ C18 5µm 150 mm x 4.6 mm, 10–100% B in 15 min, R_t = 14.53, 100%

Synthesis of benzo[1,3]dioxol-5-ylmethyl-[2-(1*H*-indol-3-yl)-ethyl]-amine derivatives

*Naphthalene-1-carboxylic acid benzo[1,3]dioxol-5-ylmethyl-[2-(1H-indol-3-yl)-ethyl]-amide (**5**)*

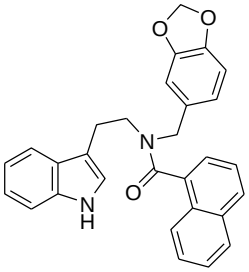

$C_{29}H_{24}N_2O_3$

General procedure B: A DMF solution (10 mL) of benzo[1,3]dioxol-5-ylmethyl-[2-(1*H*-indol-3-yl)-ethyl]-amine hydrobromide (**18**) (0.138 g, 0.37 mmol), HATU (0.21 g, 0.55 mmol), and naphthalene-1-carboxylic acid (0.063 g, 0.37 mmol) was stirred at room temperature to complete dissolution. To the stirred solution was added DIPEA (0.19 mL, 1.10 mmol) and the reaction mixture was stirred overnight. DMF was then removed and the crude material was subjected to silica gel column chromatography (1:4 Hexane–EtOAc) to afford **5** (0.11 g, 67%) as a white solid (mp 199 − 200 °C). IR (cm^{-1}): 3215 (NH), 1608 (CON), 743 (CH- aromatics). **Proton and carbon spectra displays an atropisomeric property of compound **7**, with the approximate ratio 1:0.66 calculated based on the proton benzodioxole C$\underline{H_2}$ peaks at 6.05 and 5.97 ppm, respectively. As the mixture cannot be separated forming 1 HPLC peak, the question as to which atropisomer is dominant or less remains to be determined. As the spectra is complex with both splitting and overlapping, the proton NMR is reported separately for splitting peaks where possible. In case of complex overlapping (aromatic region), the proton NMR is assigned as a whole. Carbon peaks are all included. This format will be applied to all atropisomeric mixtures.* ^{1}H NMR (400 MHz, DMSO-d_6) δ 10.91 (s, 0.67H), 10.71 (s, 1H), 8.07 – 7.89 (m, 3.33H), 7.75 – 7.64 (m, 1H), 7.64 – 7.44 (m, 7H), 7.42 – 7.16 (m, 3.3H), 7.14 – 7.06 (m, 1.67H), 7.06 – 6.78 (m, 5.33H), 6.71 – 6.56 (m, 2.33H), 6.39 (d, J = 7.9 Hz, 1H), 6.05 (s, 2H), 5.97 (s, 1.33H), 5.01 – 4.70 (m, 2H), 4.26 −4.02 (m, 2H), 3.43 (d, J = 20.9 Hz, 0.67H), 3.26 – 2.98 (m, 3.33H), 2.91 −2.66 (m, 2H). ^{13}C NMR (101 MHz, DMSO-d_6) δ 170.4, 170.0, 148.0, 148.0, 147.1, 147.0, 136.8, 136.4, 135.1, 135.0, 133.5 133.4, 132.3, 130.7, 129.5, 129.2, 129.0, 128.9, 128.9, 127.7, 127.5, 127.1, 126.9, 125.8, 125.0, 124.7, 124.1, 123.6, 123.3, 122.1, 121.5, 121.3, 121.1, 118.9, 118.8, 118.5, 118.0, 111.9, 111.8, 111.7, 110.7, 109.1, 108.8, 108.7, 108.1, 101.5, 51.8, 49.2, 47.1, 44.5, 24.9, 23.1. LRMS (APCI +) m/z 448, 449 $[M+1H]^+$, 100%. HRMS (ES+) for $C_{29}H_{24}N_2O_3$, calculated 449.1860, found 449.1859. RP-HPLC Alltima™ C18 5 µm 150 mm x 4.6 mm, 10–100% B in 15 min, R_t = 18.06 min, 100%.

*1H-Indole-2-carboxylic acid benzo[1,3]dioxol-5-ylmethyl-[2-(1H-indol-3-yl)-ethyl]-amide (**20**)*

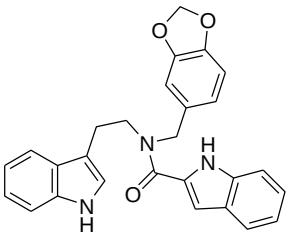

$C_{27}H_{23}N_3O_3$

Synthesized utilizing the general procedure B described above, from benzo[1,3]dioxol-5-ylmethyl-[2-(1*H*-indol-3-yl)-ethyl]-amine hydrobromide (**20**) (0.18 g, 0.48 mmol), HATU (0.27 g, 0.72 mmol), 1*H*-Indole-2-carboxylic acid (0.077 g, 0.48 mmol) and DIPEA (0.25 mL, 1.43 mmol) in DMF (5.0 mL) to afford **20** (0.14 g, 67%) as a white solid (mp 198 − 199 ºC). IR (cm^{-1}): 3440 (NH), 3274 (NH), 1620 (CON), 742 (CH-aromatics). ^{1}H NMR (400 MHz, DMSO-d_6) δ 11.72 (s, 1H), 10.86 (s, 1H), 7.72 – 7.29 (m, 4H), 7.20 (dd, J = 9.2, 4.8 Hz, 2H), 7.13 – 6.58 (m, 7H), 6.01 (s, 2H), 4.81 (bs, 2H), 3.76 (bs, 2H), 3.09 (s, 2H). ^{13}C NMR (101 MHz, DMSO-d_6) δ 163.7, 148.1, 147.0, 136.7, 136.4, 131.9, 130.5, 127.5, 123.8, 123.3, 121.9, 121.5, 120.2, 118.8, 118.7, 112.5, 111.9, 111.2, 108.8, 107.7, 103.7, 101.5, 52.4, 48.6, 47.7, 24.7, 23.3. LRMS (APCI+) m/z 437, 438 [M+1], 70%. HRMS (ES+) for $C_{27}H_{23}N_3O_3$, calculated 438.1812, found 439.1811. RP-HPLC Alltima™ C18 5 µm 150 mm x 4.6 mm, 10–100% B in 15 min, R_t = 14.68 min, 100%.

*Benzo[b]thiophene-2-carboxylic acid benzo[1,3]dioxol-5-ylmethyl-[2-(1H-indol-3-yl)-ethyl]-amide (**21**)*

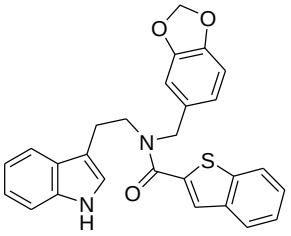

$C_{27}H_{22}N_2O_3S$

Synthesized utilizing the general procedure B described above, from benzo[1,3]dioxol-5-ylmethyl-[2-(1*H*-indol-3-yl)-ethyl]-amine hydrobromide (**18**) (0.183 g, 0.49 mmol), HATU (0.28 g, 0.73 mmol), benzo[*b*]thiophene-2-carboxylic acid (0.087 g, 0.49 mmol) and DIPEA (0.25 mL, 1.46 mmol) in DMF (5.0 mL) to afford **21** (0.12 g, 53%) as a white solid (mp 166 − 167 ºC). IR (cm^{-1}): 3331 (NH), 1627 (CON), 738 (CH-aromatics). ^{1}H NMR (400 MHz, DMSO-d_6) δ 10.85 (s, 1H), 8.00 (d, J = 8.2 Hz, 1H), 7.81 (s, 1H), 7.70 – 6.64 (m, 11H), 6.02 (s, 2H), 4.73 (s, 2H), 3.65 (s, 2H), 3.12 – 2.91 (m, 2H). ^{13}C NMR (101 MHz, DMSO-d_6) δ 164.5, 148.1, 147.0, 139.7, 139.1, 137.7, 136.6, 131.5, 127.5, 126.32, 125.3 (C x 2), 125.2, 123.5, 122.9, 121.5 (C x 2), 118.7 (C x 2), 118.6, 111.9, 110.9, 108.8, 101.5, 49.6, 48.4, 24.7. LRMS **(**APCI+) m/z 454, 455 [M+H]+, 100%. HRMS (ES+) for $C_{27}H_{22}N_2O_3S$, calculated 455.1424, found 455.1423. RP-HPLC Alltima™ C18 5 µm 150 mm x 4.6 mm, 10–100% B in 15 min, R_t = 14.97 min, 100%.

*Benzofuran-2-carboxylic acid benzo[1,3]dioxol-5-ylmethyl-[2-(1H-indol-3-yl)-ethyl]-amide (**22**)*

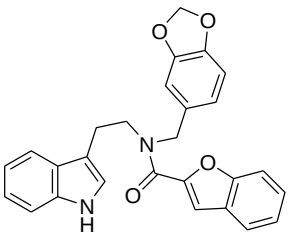

$C_{27}H_{22}N_2O_4$

Synthesized utilizing the general procedure B described above, from benzo[1,3]dioxol-5-ylmethyl-[2-(1*H*-indol-3-yl)-ethyl]-amine hydrobromide **(18)** (0.212 g, 0.57 mmol), HATU (0.32 g, 0.85 mmol), benzofuran-2-carboxylic acid (0.091 g, 0.57 mmol) and DIPEA (0.30 mL, 1.69 mmol) in DMF (5.0 mL) to afford **22** (0.156 g, 63%) as a white solid (mp 173 − 173.6 ºC). IR (cm^{-1}): 3316 (NH), 1627 (CON), 737 (CH-aromatics). ^{1}H NMR (400 MHz, DMSO-d_6) δ 10.83 (s, 1H), 7.72 (d, J = 5.8 Hz, 1H), 7.62 (d, J = 8.3 Hz, 1H), 7.58 – 7.26 (m, 5H), 7.19 – 6.71 (m, 6H), 6.01 (s, 2H), 4.72 (s, 2H), 3.91 −3.51 (m, 2H), 3.05 (s, 2H). ^{13}C NMR (101 MHz, DMSO-d_6) δ 154.4, 149.3, 148.0, 147.0, 136.7, 131.7, 129.0, 127.4, 127.2, 126.9, 124.1, 123.6, 122.9, 122.0, 121.4, 118.7, 118.5, 112.2, 111.9, 111.1, 109.0, 108.8, 101.5, 48.7, 48.8, 25.1. LRMS **(**APCI+/-) m/z 438, 439 $[M+H]^+$, 100%. HRMS (ES+) for $C_{27}H_{22}N_2O_4$, calculated 439.1652, found 439.1652. RP-HPLC Alltima™ C18 5 µm 150 mm x 4.6 mm, 10–100% B in 15 min, R_t = 7.12 min, 100%.

*N-Benzo[1,3]dioxol-5-ylmethyl-4-chloro-N-[2-(1H-indol-3-yl)-ethyl]-benzamide (**23**)*

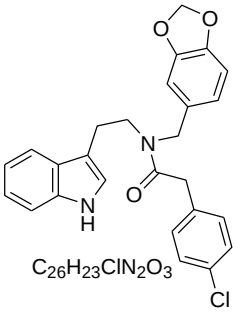

$C_{26}H_{23}ClN_2O_3$

Synthesized utilizing the general procedure B described above, from benzo[1,3]dioxol-5-ylmethyl-[2-(1*H*-indol-3-yl)-ethyl]-amine hydrobromide **(18)** (0.134 g, 0.36 mmol), HATU (0.205 g, 0.53 mmol), 4-chlorobenzoic acid (0.056 g, 0.36 mmol) and DIPEA (0.187 mL, 1.08 mmol) in DMF (5.0 mL) to afford **23** (0.09 g, 58%) as a white solid (mp 132 − 133 ºC). IR (cm^{-1}): 3203 (NH), 1626 (CON), 1500 (C=C aromatic), 1251 (C-N), 747 (C-H aromatic). *This is a mixture of atropisomers of compound **25** with the ratio approximately 2.0 : 1.2 calculated on the CH_2 splitting peaks at 2.93 and 2.84 ppm of the proton NMR. The exact structure for each of the atropisomer remains to be confirmed. As the spectra are complex with both splitting and overlapping, the proton NMR is reported separately for splitting peaks where possible. In case of complex overlapping (aromatic region), the proton NMR is assigned as a whole.* ^{1}H NMR (400 MHz, DMSO-d_6) δ 10.89 (s, 1H), 10.78 (s, 0.6H), 7.53 −7.45 (m, 1.7H), 7.40 – 7.32 (m, 2.6H), 7.32 – 7.26 (m, 2.4H), 7.23 (d, J = 8.4 Hz, 1.2H), 7.14 (d, J = 1.9 Hz, 1H), 7.11 −7.90 (m, 6H), 6.87 (m, 1.6H), 6.81 – 6.63 (m, 3.3H), 6.00 (s, 1.2H), 5.98 (s, 2H), 4.52 (s, 2H), 4.48 (s, 1.2H), 3.75 (s, 1.1H), 3.53 (s, 2.1H), 3.52 −3.43 (m, 3.2H), 2.92 (t, J = 7.2 Hz, 2H), 2.88 – 2.79 (m, 1.2H). ^{13}C NMR (101 MHz, DMSO-d_6) δ 170.1 and 170.0 (C x 1), 147.6 and 147.4 (C x 1)), 146.5 and 146.3 (C x 1), 136.2 (C x 1), 135.1 and 135.0 (C x 1), 132.1, 131.3 and 131.2 (C x 2), 131.1 and 130.9 (C

x 1), 128.1 and 127.9 (C x 1), 127.1 and 127.0 (C x 1), 123.4, 122.7, 121.2 and 121.1 (C x 1), 120.9 and 120.2 (C x 1, 118.5 and 118.3 (C x 1), 118.2 and 118.1 (C x 1), 111.5 and 111.4 (C x 1), 110.9, 108.3 and 108.1 (C x 1), 107.4, 101.0 and 100.9 (C x 1), 50.8 and 47.1 (C x 1), 47.5 and 46.4 (C x 1), 38.9 and 38.3 (C x 1), 23.8 and 23.0 (C x 1). LRMS (APCI+) m/z 446, 447 [M+H, $^{35}Cl]^+$ 100%. HRMS (ES+) calculated for $C_{26}H_{23}ClN_2O_3$ 446.1397, found 447.1467. RP-HPLC Alltima™ C18 5 µm 150 mm x 4.6 mm, 10–100% B in 15 min, R_t = 14.76 min, 100%.

*N-Benzo[1,3]dioxol-5-ylmethyl-2,6-dichloro-N-[2-(1H-indol-3-yl)-ethyl]-benzamide (**24**)*

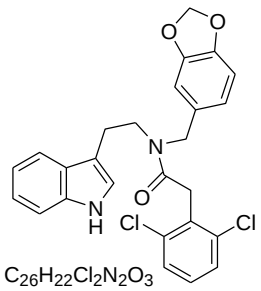

$C_{26}H_{22}Cl_2N_2O_3$

Synthesized utilizing the general procedure B described above, from benzo[1,3]dioxol-5-ylmethyl-[2-(1*H*-indol-3-yl)-ethyl]-amine hydrobromide **(18)** (0.123 g, 0.33 mmol), HATU (0.186 g, 0.49 mmol), (2,6-dichlorophenyl)-acetic acid (0.067 g, 0.33 mmol) and DIPEA (0.17 mL, 0.98 mmol) in DMF (5.0 mL) to afford **24** (0.100 g, 65%) as a white solid (mp 157 − 158 ºC). IR (cm^{-1}): 3280 (NH), 2937 (CH), 1626 (CON), 739 (CH-aromatics). *This is a mixture of atropisomers of compound **24** with the ratio approximately 2.0 : 1.3 calculated on the CH_2 splitting peaks at 5.99 and 6.02 ppm of the proton NMR.* ^{1}H NMR (400 MHz, DMSO-d_6) δ 10.90 (s, 1H), 10.80 (s, 0.7H), 7.59 – 7.25 (m, 8.3H), 7.21 (d, *J* = 2.2 Hz, 1H), 7.10 (s, 0.3H), 7.07 (dd, *J* = 15.0, 8.0 Hz, 2H), 7.03 – 6.91 (m, 2.3H), 6.88 (d, *J* = 7.7 Hz, 1.7H), 6.83 – 6.75 (m, 2.7H), 6.02 (s, 1.3H), 5.99 (s, 2H), 4.61 (s, 1.3H), 4.53 (s, 2H), 4.04 (s, 1.3H), 3.87 (s, 2H), 3.65 (t, *J* = 7.2 Hz, 2H), 3.58 – 3.44 (m, 1.3H), 3.04 (t, *J* = 7.1 Hz, 2H), 2.97 – 2.80 (m, 1.3H). ^{13}C NMR (101 MHz, DMSO-d_6) δ 168.2, 168.0, 148.1, 147.9, 147.0, 146.8, 136.8, 136.7, 135.9, 135.9, 133.7, 133.6, 132.5, 131.8, 129.6, 129.5, 128.5, 128.4, 127.6, 127.5, 124.0, 123.2, 121.5, 121.4, 120.5, 118.9, 118.7, 118.7, 118.5, 112.0, 111.8, 111.1, 108.9, 108.6, 107.8, 101.5, 101.4, 51.1, 47.9, 47.7, 47.5, 36.7, 35.9, 24.2, 23.6. LRMS (ESI+) m/z 480, 481[M+H, $^{35}Cl]^+$, 100%. HRMS (ES+) calculated for $C_{26}H_{22}Cl_2N_2O_3$ 480.1007, found 481.1080. RP-HPLC Alltima™ C18 5 µm 150 mm x 4.6 mm, 10–100% B in 15 min, R_t = 18.81 min, 100%.

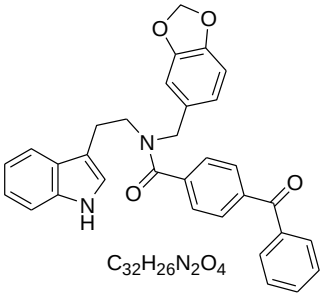

$C_{32}H_{26}N_2O_4$

*N-Benzo[1,3]dioxol-5-ylmethyl-4-benzoyl-N-[2-(1H-indol-3-yl)-ethyl]-benzamide (**25**)*

Synthesized utilizing the general procedure B described above, from benzo[1,3]dioxol-5-ylmethyl-[2-(1*H*-indol-3-yl)-ethyl]-amine hydrobromide **(18)** (0.143 g, 0.38 mmol), HATU (0.22 g, 0.57 mmol), 4-benzoylbenzoic acid (0.086 g, 0.38 mmol) and DIPEA

(0.20 mL, 1.14 mmol) in DMF (5.0 mL) to afford **25** (0. 077 g, 40%) as a white solid (mp 181.2 − 181.7 ºC). IR (cm^{-1}): 3191 (NH), 2990 (CH), 1643 (CON), 742 (CH-aromatics). *This is a mixture of atropisomers of compound **25** with the ratio approximately 2.0 : 0.9 calculated on the CH_2 splitting peaks at 4.75 and 6.02 ppm of the proton NMR.* ^{1}H NMR (400 MHz, DMSO-d_6) δ 10.83 (d, *J* = 10.1 Hz, 1.5H), 7.85 – 7.66 (m, 5.5H), 7.58 (dt, *J* = 18.2, 8.8 Hz, 6.5H), 7.41 – 7.17 (m, 4H), 7.11 – 6.85 (m, 7.5H), 6.84 – 6.56 (m, 2H), 6.01 (d, *J* = 13.2 Hz, 3H), 4.75 (s, 2H), 4.32 (s, 0.9H), 3.60 (d, *J* = 7.1 Hz, 1H), 3.36 – 3.30 (overlapped by water) (m, 2.5H), 3.03 (d, *J* = 7.1 Hz, 1H), 2.88 (t, *J* = 7.1 Hz, 2H). ^{13}C NMR (101 MHz, DMSO-d_6) δ 195.6, 170.6, 148.0, 146.9, 140.9, 137.4, 137.2, 136.6, 133.4, 132.0, 130.1, 130.0, 129.1, 127.4, 127.1, 126.8, 123.7, 121.8, 121.4, 118.7, 118.6, 118.1, 111.9, 110.8, 108.8, 108.7, 101.4, 52.4, 49.1, 46.9, 45.5, 24.2, 23.1. LRMS (APCI+/-) m/z 502, 503 $[M+H]^+$, 100%. HRMS (ES+) for $C_{32}H_{26}N_2O_4$, calculated 503.1965, found 503.1964. RP-HPLC Alltima™ C18 5 μm 150 mm x 4.6 mm, 10–100% B in 15 min, R_t = 17.71 min, 100 %.

*5-Methyl-pyrazine-2-carboxylic acid benzo[1,3]dioxol-5-ylmethyl-[2-(1H-indol-3-yl)-ethyl]-amide (**26**)*

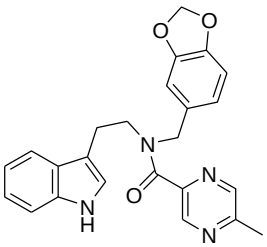

$C_{24}H_{22}N_4O_3$

Synthesized utilizing the general procedure B described above, from benzo[1,3]dioxol-5-ylmethyl-[2-(1*H*-indol-3-yl)-ethyl]-amine hydrobromide **(18)** (0.197 g, 0.53 mmol), HATU (0.30 g, 0.79 mmol), 5-methylpyrazine-2-carboxylic acid (0.072 g, 0.53 mmol) and DIPEA (0.28 mL, 1.58 mmol) in DMF (5.0 mL) to afford **26** (0. 047 g, 22%) as a white solid (mp 132 − 133 ºC). IR (cm^{-1}): 3316 (NH), 1632 (CON), 1632 (CON), 739 (CH-aromatic). *This is a mixture of atropisomers of compound **26** with the ratio approximately 2 : 1 calculated on the CH_2 splitting peaks at 4.71 and 4.46 ppm of the proton NMR.* ^{1}H NMR (400 MHz, DMSO-d_6) δ 10.83 (s, 0.5H), 10.77 (s, 1H), 8.75 (d, *J* = 1.2 Hz, 0.5H), 8.56 (s, 0.5H), 8.34 (s, 1H), 8.19 (d, *J* = 1.3 Hz, 1H), 7.52 (d, *J* = 7.8 Hz, 0.5H), 7.34 (d, *J* = 8.1 Hz, 0.7H), 7.25 (d, *J* = 8.1 Hz, 1.2H), 7.16 (d, *J* = 2.0 Hz, 0.7H), 7.11 – 7.02 (m, 1.8H), 7.02 – 6.79 (m, 8H), 6.75 (d, *J* = 7.9 Hz, 0.5H), 6.01 (s, 2H), 5.99 (s, 0.8H), 4.71 (s, 2H), 4.46 (s, 1H), 3.60 (dt, *J* = 15.8, 7.5 Hz, 3.2H), 2.92 (dt, *J* = 13.8, 7.5 Hz, 3.2H), 2.54 (s, 1.8H), 2.41 (s, 3.2). ^{13}C NMR (101 MHz, DMSO-d_6) δ 167.2, 166.8, 155.0, 154.2, 147.9, 147.4, 147.1, 147.0, 146.9, 143.7, 143.2, 143.0, 142.0, 136.7, 136.6, 131.9, 131.3, 127.6, 127.1, 123.6, 123.3, 121.8, 121.6, 121.5, 121.3, 118.7, 118.5, 118.1, 111.9, 111.7, 110.9, 108.8, 108.7, 108.6, 108.5, 101.5, 101.4, 52.0, 48.6, 47.8, 46.192, 24.4, 23.1, 21.7, 21.5. LRMS (APCI +/-) m/z 414, 415 $[M+H]^+$, 100%. HRMS (ES+) for $C_{24}H_{22}N_4O_3$, calculated 415.1765, found 415.1761. RP-HPLC Alltima™ C18 5 μM 150 mm x 4.6 mm, 10–100% B in 15 min, R_t = 12.40 min, 100%.

*5-Methoxy-1H-indole-2-carboxylic acid benzo[1,3]dioxol-5-ylmethyl-[2-(1H-indol-3-yl)-ethyl]-amide (**27**)*

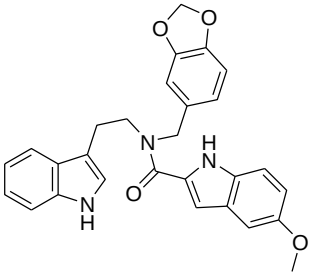

$C_{28}H_{25}N_3O_4$

Synthesized utilizing the general procedure B described above, from benzo[1,3]dioxol-5-ylmethyl-[2-(1*H*-indol-3-yl)-ethyl]-amine hydrobromide **(18)** (0.193 g, 0.51 mmol), HATU (0.29 g, 0.77 mmol), 5-methoxy-1*H*-indole-2-carboxylic acid (0.098 g, 0.51 mmol) and DIPEA (0.27 mL, 1.54 mmol) in DMF (5.0 mL) to afford **27** (0. 149 g, 62%) as an off white solid (mp 202 − 202.5 ºC). IR (cm^{-1}): 3439 (NH), 3258 (NH), 1612 (CON), 1450 (C-C ring), 738 (C-H aromatics). ^{1}H NMR (400 MHz, DMSO-d_6) δ 11.57 (s, 1H), 10.86 (s, 1H), 7.68-7.26 (m, 3H), 7.19 (s, 1H), 7.13 – 6.48 (m, 8H), 6.01 (s, 2H), 4.81 (s, 2H), 3.73 (s, 5H), 3.08 (s, 2H). ^{13}C NMR (101 MHz, DMSO-d_6) δ 163.6, 154.2, 148.1, 146.9, 136.7, 132.0, 131.6, 130.8, 127.8, 127.6, 123.3, 121.5 (C x 2), 118.8 (C x 2), 115.0, 113.4, 111.9, 108.8, 103.5 (C x 2), 102.4, 101.5, 65.4, 55.7, 48.5, 48.1, 23.6. LRMS (ESI+) m/z 467, 467 $[M]^+$, 100%. HRMS (ES+) for $C_{28}H_{25}N_3O_4$, calculated 468.1918, found 468.1919. RP-HPLC Alltima™ C18 5 μm 150 mm x 4.6 mm, 10–100% B in 15 min, R_t = 6.92 min, 100%.

*5-Chloro-1H-indole-2-carboxylic acid benzo[1,3]dioxol-5-ylmethyl-[2-(1H-indol-3-yl)-ethyl]-amide (**28**)*

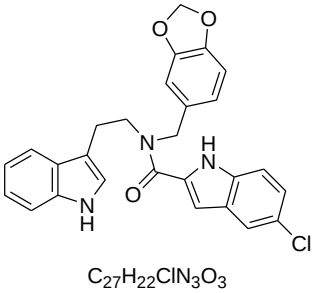

$C_{27}H_{22}ClN_3O_3$

Synthesized utilizing the general procedure B described above, from benzo[1,3]dioxol-5-ylmethyl-[2-(1*H*-indol-3-yl)-ethyl]-amine hydrobromide **(18)** (0.21 g, 0.56 mmol), HATU (0.32 g, 0.83 mmol), 5-chloro-1*H*-indole-2-carboxylic acid (0.11 g, 0.56 mmol) and DIPEA (0.29 mL, 1.69 mmol) in DMF (5.0 mL) to afford **28** (0.17 g, 64%) as an off white solid (mp 194 − 194.5 ºC). IR (cm^{-1}): 3433 (NH), 3265 (NH), 1612 (CON), 739 (CH-aromatics). ^{1}H NMR (400 MHz, DMSO-d_6) δ 11.93 (s, 1H), 10.87 (s, 1H), 7.73 – 7.26 (m, 4H), 7.25 – 7.13 (m, 2H), 7.08 (t, J = 7.5 Hz, 1H), 7.02 – 6.60 (m, 5H), 6.02 (s, 2H), 4.79 (br.s, 2H), 3.74 (br.s, 2H), 3.08 (s, 2H). ^{13}C NMR (101 MHz, DMSO-d_6) δ 163.4, 148.1, 147.0, 136.7, 134.8, 132.1, 128.5, 127.5, 124.7, 123.9 (C x 2), 123.4, 121.5, 121.4, 121.0, 118.8 (C x 2), 118.7, 114.1, 111.9, 108.8, 103.2 (C x 2), 101.5, 52.4, 48.9, 48.6, 47.6, 24.7, 23.4. **Note* : Signs of atropisomers for aliphatic CH_2, in which *52.38 and 48.59 are the splitting of 1 C (Ar-$\underline{C}H_2$-N-); 48.91 and 47.58 are the splitting of (CH_2-$\underline{C}H_2$-N-), and 24.68, 23.41 are the splitting of ($\underline{C}H_2$-CH_2-N-).* LRMS (ESI+) m/z 471, 471 [M]+, 50%.

HRMS (ES+) for $C_{27}H_{22}ClN_3O_3$, calculated 472.1423, found 472.1422. RP-UPLC Agilent Zorbax SB-C18 1.8 µm, 50 mm x 2.1 mm, isocratic 80% mobile phase B at 0.6 mL/min in 8 minutes, R_t = 5.05 min, 100%.

*1H-Indole-5-carboxylic acid benzo[1,3]dioxol-5-ylmethyl-[2-(1H-indol-3-yl)-ethyl]-amide (**29**)*

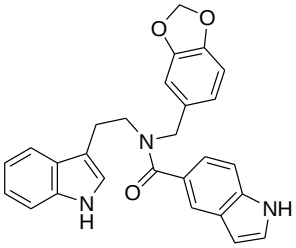

$C_{27}H_{23}N_3O_3$

Synthesized utilizing the general procedure B described above, from benzo[1,3]dioxol-5-ylmethyl-[2-(1*H*-indol-3-yl)-ethyl]-amine hydrobromide **(18)** (0.20 g, 0.54 mmol), HATU (0.31 g, 0.80 mmol), 1*H*-indole-5-carboxylic acid (0.087 g, 0.54 mmol) and DIPEA (0.28 mL, 1.61 mmol) in DMF (5.0 mL) to afford **29** (0.158 g, 67%) as an off white solid (mp 162.5 − 163 ºC). IR (cm^{-1}): 3638 (NH), 3227 (NH), 1614 (CON), 740 (CH-aromatics). ^{1}H NMR (400 MHz, DMSO-d_6) δ 11.29 (s, 1H), 10.78 (s, 1H), 7.61 (s, 1H), 7.51 – 7.39 (m, 2H), 7.56 – 6.38 (m, 9H), 6.47 (s, 1H), 6.01 (s, 2H), 4.87 – 4.29 (m, 2H), 3.65 – 3.45 (m, 2H), 3.12 – 2.70 (m, 2H). ^{13}C NMR (101 MHz, DMSO-d_6) δ 186.0, 172.8, 148.0, 146.9, 136.6, 136.5, 127.8, 127.5, 127.0, 123.3, 121.4, 120.4, 119.1, 118.6, 111.8, 111.7, 108.7, 102.2, 101.4, 49.1, 47.3, 45.6, 24.6, 23.4. **Note*: Signs of atropisomers for aliphatic CH_2, in which *47.3 is the splitting of 1 C (Ar-$\underline{C}H_2$-N-); 49.1 and 45.6 are the splitting of (CH_2-$\underline{C}H_2$-N-); 24.6 and 23.4 are the splitting of ($\underline{C}H_2$-CH_2-N-). Peak at 49.3 ppm is among the impurities.* LRMS (ESI+) m/z 437, 437 $[M]^+$, 70%. HRMS (ES+) for $C_{27}H_{23}N_3O_3$, calculated 438.1812, found 438.1812. RP-HPLC Alltima™ C18 5 µm 150 mm x 4.6 mm, 10–100% B in 15 min, R_t = 6.48 min, 96%.

7.3.4. Synthesis of the 1,3-thiazine-6-phenylimino-5-carboxylates (Chapter 5)

*2,4-Dimethyl-6-phenylimino-6H-[1,3]thiazine-5-carboxylic acid ethyl ester (**8a**)*

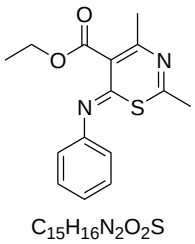

$C_{15}H_{16}N_2O_2S$

A mixture of ethyl 3-aminocrotonate (0.3 mL, 2.373 mmol) and phenyisothiocyanate (**2a**) (0.283 mL, 2.373 mmol) was stirred, under solvent free conditions, at room temperature overnight under nitrogen. To the stirred mixture was added acetic anhydride (0.26 mL, 2.61 mmol) and acetonitrile (5 mL). The reaction mixture was stirred for 24h at room temperature and the crude material was subjected to silica gel chromatography [1:4 ethyl acetate : petroleum ether (b.p 40-60 ºC)] to afford **8a** (0.41 g, 65%) as a bright yellow precipitate (mp 145.3-146.5 ºC). IR (cm^{-1}): 2984 (CH), 1728

(COO), 1231 (CO). ^{1}H NMR (400 MHz, $CDCl_3$) δ 7.65 – 7.43 (m, 3H), 7.25 – 7.09 (m, 2H), 4.42 (q, *J* = 7.1 Hz, 2H), 2.31 (s, 3H), 2.22 (s, 3H), 1.39 (t, *J* = 7.1 Hz, 3H). ^{13}C NMR (400 MHz, $CDCl_3$) δ 183.0, 166.1, 159.2, 153.9, 140.6, 132.3, 130.5 (C x 2), 129.7, 127.1 (C x 2), 62.0, 25.1, 21.9, 14.0. LRMS (ESI+) m/z 288, 288 $[M]^+$ + 40%. HRMS (ES+) for $C_{15}H_{16}N_2O_2S$, calculated 289.1005, found 289.1004; RP-HPLC Alltima™ C18 5 µm 150 mm x 4.6 mm, 10-100% B in 15 min, R_t = 5.19 min, 100%.

*2,4-Dimethyl-6-(4'-tolylimino)-6H-[1,3]thiazine-5-carboxylic acid ethyl ester (**8b**)*

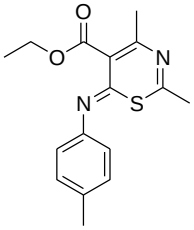

$C_{16}H_{18}N_2O_2S$

Synthesized utilising the general procedure above, from 3-aminocrotonate (0.3 mL, 2.373 mmol), 4-methylphenyl isothiocyanate (**2b**) (0.52, 3.560 mmol), and acetic anhydride (0.448 mL, 4.746 mmol) in acetonitrile (5.0 mL) to afford **8b** (0.132 g, 19%) as a yellow solid (mp 166.7-167.5 ºC). IR (cm^{-1}): 2975 (CH), 1733 (COO), 1232 (CO); ^{1}H NMR (400 MHz, $CDCl_3$) δ 7.36 (d, *J* = 8.1 Hz, 2H), 7.05 (d, *J* = 8.3 Hz, 2H), 4.42 (q, *J* = 7.1 Hz, 2H), 2.43 (s, 3H), 2.30 (s, 3H), 2.22 (s, 3H), 1.39 (t, *J* = 7.1 Hz, 3H) ^{13}C NMR (101 MHz, $CDCl_3$) δ 183.1, 166.1, 159.5, 153.9, 139.9, 138.0, 132.3, 131.1 (C x 2), 126.7 (C x 2), 62.0, 25.1, 21.9, 21.4, 14.0. LRMS (ESI+) m/z 302, 302 $[M]^+$ 100%; HRMS (ES+) for $C_{16}H_{18}N_2O_2S$, calculated 303.1162, found 303.1160; RP-HPLC Alltima™ C18 5 µm 150 mm x 4.6 mm, 10–100% B in 15 min, R_t = 6.81 min, 100%.

*6-(4-Isopropylphenylimino)-2,4-dimethyl-6H-[1,3]thiazine-5-carboxylic acid ethyl ester (**8c**)*

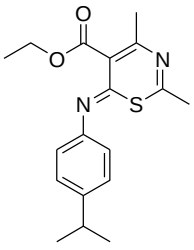

$C_{18}H_{22}N_2O_2S$

Synthesized utilising the general procedure above, from 3-aminocrotonate (0.3 mL, 2.373 mmol), 4-isopropylphenyl isothiocyanate (0.42 mL, 2.373 mmol) and acetic anhydride (0.448 mL, 4.746 mmol) in acetonitrile (5.0 mL) to afford **8c** (0.393 g, 50%) as a yellow solid (mp 113.8-114.6 ºC). IR (cm^{-1}): 2989 (CH), 1727 (COO), 1233 (CO); ^{1}H NMR (400 MHz, $CDCl_3$) δ 7.40 (d, *J* = 8.3 Hz, 2H), 7.08 (d, *J* = 8.4 Hz, 2H), 4.40 (q, *J* = 7.1 Hz, 2H), 3.03-2.90 (m, 1H), 2.29 (s, 3H), 2.21 (s, 3H), 1.37 (t, *J* = 7.1 Hz, 3H), 1.29 (d, *J* = 6.9 Hz, 6H). ^{13}C NMR (101 MHz, $CDCl_3$) δ 183.0, 166.1, 159.5, 153.7, 150.3, 138.1, 132.18, 128.4 (C x 2), 126.7 (C x 2), 61.9, 33.7, 25.1, 23.8 (C x 2), 21.8, 14.0 LRMS (ESI+) m/z 330, 330 [M]+ 100%; HRMS (ES^+) for $C_{18}H_{22}N_2O_2S$, calculated 331.1475, found 331.1470; RP-HPLC Alltima™ C18 5 µm 150 mm x 4.6 mm, 10-100% B in 15 min, R_t = 7.55 min, 94%.

6-(4-Bromophenylimino)-2,4-dimethyl-6H-[1,3]thiazine-5-carboxylic acid ethyl ester ***(8d)***

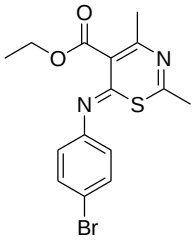

$C_{15}H_{15}BrN_2O_2S$

Synthesized utilising the general procedure above, from 3-aminocrotonate (0.3 mL, 2.373 mmol), 4-bromopheny isothiocyanate (**2d**) (0.508 g, 2.373 mmol), and acetic anhydride (0.448 mL, 4.746 mmol) in acetonitrile (5.0 mL) to afford **8d** (0.556 g, 64%) as a yellow solid (mp 178-179 ºC). IR (cm^{-1}): 2994 (CH), 1729 (COO), 1239 (CO). ^1H NMR (400 MHz, Acetone-d_6) δ 7.85 – 7.71 (m, 2H), 7.45 – 7.35 (m, 2H), 4.31 (q, J = 7.1 Hz, 2H), 2.26 (s, 3H), 2.21 (s, 3H), 1.32 (t, J = 7.1 Hz, 3H). ^{13}C NMR (400 MHz, Acetone-d_6) δ 182.7, 165.5, 159.5, 153.7, 140.4, 133.3 (C x 2), 131.9, 129.9 (C x 2), 122.8, 61.2, 24.6, 21.1, 13.4; LRMS (ESI_+) m/z 366, 368 $[M+2H]^+$ 100%; HRMS (ES_+) for $C_{15}H_{15}BrN_2O_2S$, calculated 367.0110, found 367.0110 [M+ H; ^{79}Br, $^{81}Br]^+$; RP-HPLC Alltima™ C18 5 µm 150 mm x 4.6 mm, 10–100% B in 15 min, R_t = 7.14 min, 100%.

*2,4-Dimethyl-6-(4-trifluoromethylphenylimino)-6H-[1,3]thiazine-5-carboxylic acid ethyl ester (****8e****)*

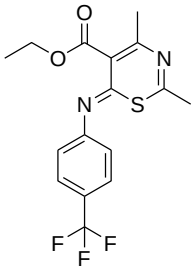

$C_{16}H_{15}F_3N_2O_2S$

Synthesized utilising the general procedure above, from 3-aminocrotonate (0.3 mL, 2.373 mmol), 4-trifluorophenyl isothiocyanate (**2e**) (0.489 g, 2.373 mmol) and acetic anhydride (0.678 mL, 7.119 mmol) in acetonitrile (5.0 mL) to afford **8e** (0.300 g, 35%) as a yellow solid (mp 125.7-126.5 ºC). IR (cm^{-1}): 2982 (CH), 1728 (COO), 1235 (CO); ^1H NMR (400 MHz, $CDCl_3$) δ 7.84 (d, J = 8.4 Hz, 2H), 7.35 (d, J = 8.3 Hz, 2H), 4.41 (q, J = 7.1 Hz, 2H), 2.32 (s, 3H), 2.21 (s, 3H), 1.38 (t, J = 7.1 Hz, 3H). ^{13}C NMR (101 MHz, $CDCl_3$) δ 182.8, 165.9, 158.5, 154.3, 143.5, 143.5, 132.3, 131.8 (q, J = 33.33 Hz, 1H), 128.1 (C x 2), 127.7 (C x 2) (q, J = 4.04 Hz, 2H), 123.4 (q, J = 273 Hz, 1H), 62.1, 25.1, 21.9, 14.0; LRMS (ESI^+) m/z 356, 356 $[M]^+$ 100%; HRMS (ES^+) for $C_{15}H_{15}F_3N_2O_2S$, calculated 357.0879, found 357.0886; RP-HPLC Alltima™ C18 5 µm 150 mm x4.6 mm, 10–100% B in 15 min, R_t = 7.22 min, 95%.

*6-(3,5-Dichlorophenylimino)-2,4-dimethyl-6H-[1,3]thiazine-5-carboxylic acid ethyl ester (****8f****)*

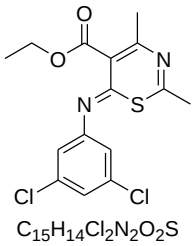

$C_{15}H_{14}Cl_2N_2O_2S$

Synthesized utilising the general procedure above, from 3-aminocrotonate (0.283 mL, 1.857 mmol), 3,5-dichlorolphenyl isothiocyanate (0.379 g, 1.857 mmol) and acetic anhydride (0.448 mL,

4.746 mmol) in acetonitrile (5.0 mL) to afford **8f** (0.123 g, 20%) as a yellow solid (mp 184.3-185.1ºC). IR (cm^{-1}): 3070 (CH), 2982 (CH), 1720 (COO), 1243 (CO); ^1H NMR (400 MHz, $CDCl_3$) δ 7.51 (t, *J* = 1.8 Hz, 1H), 7.14 (d, *J* = 1.8 Hz, 2H), 4.41 (q, *J* = 7.1 Hz, 2H), 2.29 (d, *J* = 7.4 Hz, 6H), 1.38 (t, *J* = 7.1 Hz, 3H). ^{13}C NMR (101 MHz, $CDCl_3$) δ 182.7, 165.7, 158.3, 154.2, 141.9, 136.8 (C x 2), 132.3, 130.2, 126.3 (C x 2), 62.1, 25.1, 21.9, 14.0 LRMS (ESI+) m/z 356, 356 $[M]^+$ 100%; HRMS (ES+) for $C_{15}H_{15}Cl_2N_2O_2S$, calculated 357.0226, found 357.0226; RP-HPLC Alltima™ C18 5 µm 150 mm x 4.6 mm, 10–100% B in 15 min, R_t = 7.53 min, 96%.

*6-(Benzo[1,3]dioxol-5-ylimino)-2,4-dimethyl-6H-[1,3]thiazine-5-carboxylic acid ethyl ester (**8g**)*

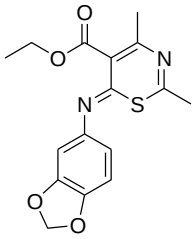

$C_{16}H_{16}N_2O_4S$

Synthesized utilising the general procedure above, from 3-aminocrotonate (0.177 mL, 1.395 mmol), 3,4-methylenedioxyphenyl isothiocyanate (**2g**) (0.25 g, 1.395 mmol) and acetic anhydride (0.448 mL, 4.746 mmol) in acetonitrile (5.0 mL) to afford **8g** (0.134 g, 29%) as a yellow solid (mp 146.5-147.3 ºC). IR (cm^{-1}): 2982 (CH), 1733 (COO), 1250 (CO) ^1H NMR (400 MHz, $CDCl_3$) δ 6.94 (d, *J* = 7.9 Hz, 1H), 6.66 – 6.60 (m, 2H), 6.08 (d, *J* = 4.9 Hz, 2H), 4.42 (q, *J* = 7.1 Hz, 2H), 2.32-2.26 (m, 6H), 1.39 (t, *J* = 7.1 Hz, 3H); ^{13}C NMR (101 MHz, $CDCl_3$) δ 183.3, 166.1, 159.7, 153.8, 149.3, 148.6, 134.0, 132.2, 120.5, 109.4, 108.0 5, 102.3, 62.0, 25.0, 21.9, 14.0; LRMS (ESI+) m/z 332, 332 $[M]^+$ 100%; HRMS (ES+) for $C_{16}H_{16}N_2O_4S$, calculated 333.0904, found 333.0902; RP-HPLC Alltima™ C18 5 µm 150 mm x 4.6 mm, 10-100% B in 15 min, R_t = 6.39 min, 100%.

*2,4-Dimethyl-6-(naphthalen-1-ylimino)-6H-[1,3]thiazine-5-carboxylic acid ethyl ester (**8h**)*

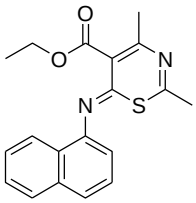

$C_{19}H_{18}N_2O_2S$

Synthesized utilising the general procedure above, from 3-aminocrotonate (0.28 mL, 2.216 mmol), 1-naphthyl isothiocyanate (**2h**) (0.41 g, 2.216 mmol) and acetic anhydride (0.419 mL, 4.431 mmol) in acetonitrile (5.0 mL) to afford **8h** (0.218 g, 29%) as a yellow solid (mp 162.1-163ºC). IR (cm^{-1}): 2982 (CH), 1726 (COO), 1239 (CO); ^1H NMR (400 MHz, $CDCl_3$) δ 7.99 (d, *J* = 8.3 Hz, 1H), 7.95 (dd, *J* = 6.9, 2.2 Hz, 1H), 7.64 – 7.48 (m, 3H), 7.45 – 7.40 (m, 1H), 7.37 (dd, *J* = 7.3, 0.7 Hz, 1H), 4.51 – 4.32 (m, 2H), 2.37 (s, 3H), 2.13 (s, 3H), 1.39 (t, *J* = 7.1 Hz, 3H); ^{13}C NMR (400 MHz, $CDCl_3$) δ 183.1, 166.2, 160.0, 154.0, 137.0, 134.6, 132.4, 130.2, 129.0, 128.2, 128.1, 127.1, 125.9, 125.5, 121.4, 62.0, 24.4, 22.0, 14.1; LRMS (ESI+) m/z 338, 338 $[M]^+$

100%; HRMS (ES+) for $C_{19}H_{18}N_2O_2S$, calculated 339.1162, found 339.1160; RP-HPLC Alltima™ C18 5 µm 150 mm x 4.6 mm, 10-100% B in 15 min, R_t = 7.12 min, 100%.

*6-Ethylimino-2,4-dimethyl-6H-[1,3]thiazine-5-carboxylic acid ethyl ester (**8i**)*

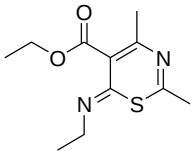

$C_{11}H_{16}N_2O_2S$

Synthesized utilising the general procedure above, from 3-aminocrotonate (0.3 mL, 2.373 mmol), ethyl isothiocyanate (0.206 mL, 2.373 mmol) and acetic anhydride (0.448 mL, 4.746 mmol) in acetonitrile (5.0 mL) to afford **8i** (0.084 g, 15%) as a yellow solid (mp 112.5-113.4 ºC). IR (cm^{-1}): 2969 (CH), 1732 (COO), 1267 (CO); ^{1}H NMR (400 MHz, $CDCl_3$) δ 4.72-4.61 (m, 2H), 4.53 – 4.33 (m, 2H), 2.69 (s, 3H), 2.22 (s, 3H), 1.48-1.37 (m, 6H); ^{13}C NMR (400 MHz, $CDCl_3$) δ 181.0, 166.3, 158.6, 153.4, 132.5, 61.9, 45.8, 23.8, 21.6, 14.0, 11.8; LRMS (ESI+) m/z 240, 240 $[M]^+$ 100%; HRMS (ES+) for $C_{11}H_{16}N_2O_2S$, calculated 241.1005, found 241.1003; RP-HPLC Alltima™ C18 5 µm 150 mm x 4.6 mm, 10-100% B in 15 min, R_t = 5.83 min, 94%.

*2-Ethyl-4-methyl-6-phenylimino-6H-[1,3]thiazine-5-carboxylic acid ethyl ester (**8k**)*

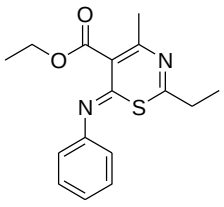

$C_{16}H_{18}N_2O_2S$

Synthesized utilising the general procedure above, from 3-aminocrotonate (0.098 mL, 0.774 mmol), phenyl isothiocyanate (0.093 mL, 0.775 mmol) and propanoic anhydride (0.197 mL, 1.55 mmol) in acetonitrile (5.0 mL) to afford **8k** (0.041 g, 17%) as a yellow solid (mp 87.5-88.3 ºC). IR (cm^{-1}): 2988 (CH), 1728 (COO), 1237 (CO); ^{1}H NMR (400 MHz, $CDCl_3$) δ 7.59 – 7.47 (m, 3H), 7.20 – 7.13 (m, 2H), 4.42 (q, *J* = 7.1 Hz, 2H), 2.40 (d, *J* = 7.4 Hz, 2H), 2.33 (s, 3H), 1.39 (t, *J* = 7.1 Hz, 3H), 1.15 (t, *J* = 7.4 Hz, 3H); ^{13}C NMR (101 MHz, $CDCl_3$) δ 183.1, 166.3, 162.9, 154.1, 40.0, 132.1, 130.3 (C x 2), 130.0, 127.4 (C x 2), 62.0, 30.1, 22.0, 14.0, 11.4; LRMS (ESI^+) m/z 302, 302 $[M]^+$ 100%; HRMS (ES^+) for $C_{16}H_{18}N_2O_2S$, calculated 303.1162, found 303.1157; RP-HPLC Alltima™ C_{18} 5 µm 150 mm x4.6 mm, 10-100% B in 15 min, R_t = 6.91 min, 100%.

*4-Methyl-2-phenyl-6-phenylimino-6H-[1,3]thiazine-5-carboxylic acid ethyl ester (**8l**)*

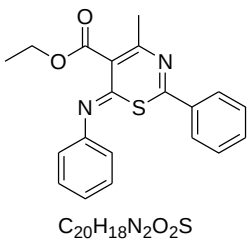

$C_{20}H_{18}N_2O_2S$

Synthesized utilising the general procedure above, from 3-aminocrotonate (0.3 mL, 2.373 mmol), phenyl isothiocyanate (0.283 mL, 2.373 mmol) and benzoic anhydride (0.895 mL, 4.746 mmol) in acetonitrile (5.0 mL) to afford **8l** (0.030 g, 4%) as a yellow solid (mp 252-252.5ºC). IR (cm^{-1}): 2982 (CH), 1725 (COO), 1231 (CO); ^{1}H NMR (400 MHz, $CDCl_3$) δ 7.35 – 7.17 (m, 8H), 7.15 – 7.03 (m, 2H), 4.47 (q, *J* = 7.1 Hz, 2H), 2.40 (s, 3H), 1.42 (t, *J* = 7.1 Hz, 3H); ^{13}C

NMR (101 MHz, $CDCl_3$) δ 183.2, 166.1, 159.7, 153.8, 140.1, 134.5, 132.9, 129.9, 129.3 (C x 2), 129.2, 128.9 (C x 2), 128.7 (C x 2), 128.1 (C x 2), 62.2, 22.0, 14.1 LRMS (ESI+) m/z 350, 350 $[M]^+$ 100%; HRMS (ES+) for $C_{20}H_{18}N_2O_2S$, calculated 351.1162, found 351.1157; RP-HPLC Alltima™ C18 5 µm 150 mm x 4.6 mm, 10-100% B in 15 min, R_t = 7.26 min, 100%.

*4-Methyl-6-phenylimino-2-trifluoromethyl-6H-[1,3]thiazine-5-carboxylic acid ethyl ester (TP92B5) (**8m**)*

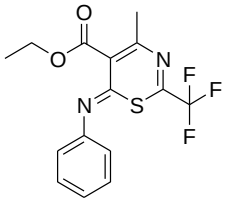

$C_{15}H_{13}F_3N_2O_2S$

Synthesized utilising the general procedure above, from 3-aminocrotonate (0.2 mL, 1.583 mmol), phenyl isothiocyanate (0.189 mL, 1.583 mmol) and benzoic anhydride (0.447 mL, 3.166 mmol) in acetonitrile (5.0 mL) to afford **8m** (0.060 g, 12%) as a yellow solid (mp 101.2-102.6 ºC). IR (cm^{-1}): 2982 (CH), 1733 (COO), 1225 (CO); ^1H NMR (400 MHz, $CDCl_3$) δ 7.61 – 7.47 (m, 3H), 7.22-7.16 (m, 2H), 4.43 (q, *J* = 7.1 Hz, 2H), 2.38 (s, 3H), 1.39 (t, *J* = 7.1 Hz, 3H); ^{13}C NMR (101 MHz, $CDCl_3$) δ 184.2, 164.9, 151.6, 146.4, 146.0, 137.0, 135.9, 130.5, 129.6, 129.0, 128.5, 128.5, 124.0, 121.5, 121.4, 121.1, 118.6, 115.9, 62.4, 21.6, 14.0; LRMS (ESI+) m/z 342, 342 $[M]^+$ 100%; HRMS (ES+) for $C_{15}H_{13}F_3N_2O_2S$, calculated 343.0723, found 343.0721; RP-HPLC Alltima™ C18 5 µm 150 mm x 4.6 mm, 10-100% B in 15 min, R_t = 7.48 min, 92%.

*Ethyl (E)-3-benzamido-2-(phenylcarbamothioyl)but-2-enoate (**10a**)*

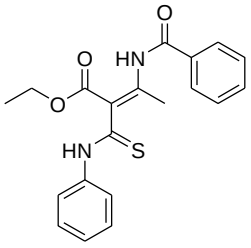

$C_{20}H_{20}N_2O_3S$

Synthesized utilising the general procedure above, from 3-aminocrotonate (0.3 mL, 2.373 mmol), phenyl isothiocyanate (0.28 mL, 2.373 mmol) and benzoic anhydride (0.895 mL, 4.746 mmol) in acetonitrile (5.0 mL) to afford **10a** (0.248 g, 28%) as a yellow solid. IR (cm^{-1}): 3185 (NH), 1697 (COO), 1665 (CON), 1234 (CO). The product is detected as a mixture of isomers in ^1H NMR, with the ratio 2.3 : 1.0 calculated at 2.68 and 2.65 ppm, respectively. The ^1H NMR is reported as a whole due to complex overlapping. All ^{13}C NMR peaks are reported. ^1H NMR (400 MHz, $CDCl_3$) δ 12.49 (d, *J* = 8.2 Hz, 1H), 10.03 (d, *J* = 46.0 Hz, 1H), 7.91 (dd, *J* = 10.6, 4.5 Hz, 3H), 7.61 – 7.04 (m, 7H), 4.19 – 3.90 (m, 2H), 2.66 (d, *J* = 11.6 Hz, 3H), 1.19 (dt, *J* = 14.5, 7.1 Hz, 3H); ^{13}C NMR (101 MHz, $CDCl_3$) δ 198.7, 194.3, 166.9, 166.6, 166.2, 165.8, 153.0, 151.4, 139.0, 138.4, 133.9, 133.6, 132.8, 132.6, 130.1, 129.5, 129.1 (2C x 2), 129.0 (C x 2), 128.9, 128.8, 128.5, 127.7, 127.6 (C x 2), 127.3, 127.0, 123.0, 122.9 (2C x 2), 116.3, 111.0, 61.3, 61.3, 19.4, 18.8, 14.1, 14.0; LRMS (ESI+) m/z 368, 369 $[M+H]^+$ 100%; HRMS (ES+) for $C_{20}H_{20}N_2O_3S$, calculated 369.1267, found 369.1270; RP-UPLC Agilent Zorbax SB™ C18 1.8 µm 50 mm x 2.1 mm, isocratic 50% B (9:1 ACN: Water) in 6 min, R_t = 4.1 min, 100% at 210, 254 and 320 nm.

*Ethyl (E)-3-benzamido-2-((4-bromophenyl)carbamothioyl)but-2-enoate (**10b**)*

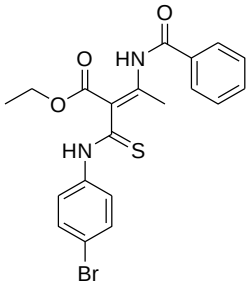

$C_{20}H_{19}BrN_2O_3S$

Synthesized utilising the general procedure above, from 3-aminocrotonate (0.3 mL, 2.373 mmol), 4-bromopheny isothiocyanate (**2d**) (0.508 g, 2.373 mmol) and benzoic anhydride (0.895 mL, 4.746 mmol) in acetonitrile (5.0 mL) to afford **10b** (0.30 g, 28%) as a yellow soild. IR (cm^{-1}): 3296 (NH), 1683 (COO), 1661 (CON), 1240 (CO). The product is detected as a mixture of isomers in ^{1}H NMR, with the ratio 12.8 : 1.0 calculated at 2.55 and 2.47 ppm, respectively. The ^{1}H NMR is reported as a whole due to complex overlapping. All ^{13}C NMR peaks are reported. ^{1}H NMR (400 MHz, DMSO-d_6) δ 12.31 (s, 1H), 12.11 (s, 1H), 8.01 – 7.83 (m, 4H), 7.74 – 7.06 (m, 5H), 4.28 – 4.06 (m, 2H), 2.55 (s, 2.7H), 2.47 (s, 0.2H), 1.25 – 1.05 (m, 3H); ^{13}C NMR (400 MHz, DMSO-d_6) δ 193.9, 167.3, 165.4, 150.7, 139.2, 134.1, 133.3, 132.1 (C x 2), 129.7 (C x 2), 127.7 (C x 2), 125.0 (C x 2), 118.8, 116.5, 61.4, 18.8, 14.5; LRMS (ESI+) m/z 446, 447 [M+ H; ^{79}Br, $^{81}Br]^{+}$ 100%; HRMS (ES+) for $C_{20}H_{19}BrN_2O_3S$, calculated 447.0373, found 447.0370 [M+ H; ^{79}Br, $^{81}Br]^{+}$; RP-UPLC Agilent Zorbax SB™ C18 1.8 µm 50 mm x 2.1 mm, isocratic 80% B (9:1 ACN: Water) in 6 min, R_t = 0.72 min, 100% at 210, 254 and 320 nm.

7.4. References

1. P. Chomczynski and N. Sacchi, *Nature Protocols*, 2006, **1**, 581-585.
2. A. P. Sobinoff, V. Pye, B. Nixon, S. D. Roman and E. A. McLaughlin, *Toxicological Sciences*, 2010, **118**, 653-666.

VIII. CHAPTER EIGHT

SUPPORTING INFORMATION

8.1. Appendix to Chapter 2

Electronic Supplementary Material (ESI) for Organic & Biomolecular Chemistry.

Supporting Data for An Efficient Continuous Flow Approach to Furnish Furan-Based Biaryls

Trieu N. Trinh,[a] Lacey Hizartzidis,[a] Andrew J. S. Lin,[a] David G. Harman,[b,c] Adam McCluskey,[a,*] and Christopher P. Gordon[a,d,*]

[a] Chemistry, Centre for Chemical Biology, The University of Newcastle, University Drive, Callaghan NSW 2308, Australia. Phone: +61 (0)249 216486; Fax: +61 (0)249 215472; E-mail: Adam.McCluskey@newcastle.edu.au

[b] Office of the Deputy Vice-Chancellor, University of Western Sydney, Penrith NSW 2751 Australia.

[c] Molecular Medicine Research Group, School of Medicine, Building 30, University of Western Sydney, Goldsmith Avenue, Campbelltown, NSW 2560, Australia

[d] Present address: Nanoscale Organisation and Dynamics Group, School of Science and Health, University of Western Sydney, Locked Bag 1797, Penrith South DC, Australia. E-mail: c.gordon2@uws.edu.au, Fax: +61 (02) 4620 3025, Tel: +61 (02) 4620 3201.

Abstract

Suzuki cross-couplings of 5-formyl-2-furanylboroic acid with activated or neutral aryl bromides were performed under continuous flow conditions in the presence of tetrabutylammonium fluoride and immobilised *t*-butyl based palladium catalyst CatCart™ FC1032. Deactivated aryl bromides and aryl chlorides were cross-coupled with 5-formyl-2-furanylboroic in the presence of tetrabutylammonium acetate using the bis-tripehnylphosphine CatCart™ $PdCl_2(PPh_3)_2$-DVB which efficiently furnished a series of decorated aldehyde based building blocks. Initial evidence indicates the latter method my serve as a universal approach to conduct Suzuki cross-couplings as it was employed in the successful synthesis of the current gold standard hedgehog pathway inhibitor LDE225.

Graphical Abstract

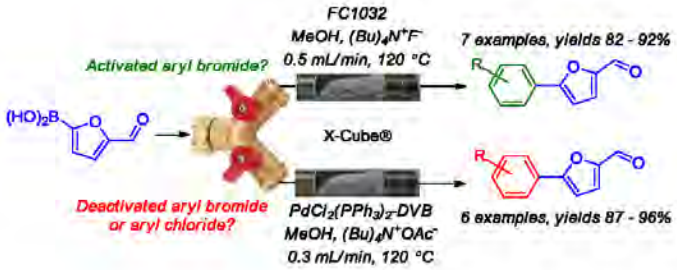

Supporting Information

S1. General Chemistry

All reagents were purchased from Sigma Aldrich and were used without purification, with the exception of furfural, which was distilled through glass prior to use. Solvents were bulk, and distilled through glass prior to use.

^{1}H and ^{13}C NMR spectra were recorded on a Bruker Advance™ AMX 400 MHz spectrometer at 400.13 and 100.62 MHz, respectively. Chemical shifts (δ) are reported in parts per million (ppm) measured to relative the internal standards. Coupling constants (J) are expressed in Hertz (Hz). Mass spectra were recorded on a Shimadzu LCMS 2010 EV using a mobile phase of 1:1 acetonitirle:H2O with 0.1 % formic acid. Gas chromatography-mass spectrometry (GC-MS) was performed on a Shimadzu GC-MS QF2010 EI/NCI System equipped with a ZB-5MS capillary column of 5% phenyl-arylene stationary phase. High-resolution mass spectra (HRMS) were determined on a Micromass QTof2 spectrometer using polyethylene glycol or polypropylene glycol as lockmass. Monoisotopic molecular masses were calculated utilising ChemDraw Ultra 8.0.

Analytical HPLC traces were obtained using a Shimadzu system possessing a SIL-20A auto-sampler, dual LC-20AP pumps, CBM-20A bus module, CTO-20A column heater, and a SPD-20A UV/vis detector. This system was fitted with an Alltima™ C18 5u 150 mm x 4.6 mm column with solvent A: 0.06% TFA in water and solvent B: 0.06% TFA in CH_3CN:H_2O (90:10). In each case HPLC traces were acquired at a flow rate of 2.0 mL/min, gradient 10-100 (%B), curve = 6, over 15.0 mins, with detection at 220 nm and 265 nm.

Where applicable, melting points were recorded on a BUCHI Melting Point M-565. IR spectra were recorded on a PerkinElmer Spectrum Two™ FTIR Spectrometer. Thin layer chromatography (TLC) was performed on Merck 60 F254 pre-coated aluminium plates with a thickness of 0.2 mm. Column chromatography was performed under 'flash' conditions on Merck silica gel 60 (230-400 mesh).

ICP analysis was conducted by the Australian National Measurement Institute 105 Delhi Road, North Ryde NSW 2113 (www.measurement.gov.au)

S2. Initial Synthesis of Compound 10

Biphenyl-3,3'-diyldimethanol (10) and 5-(3-(hydroxymethyl)phenyl)furan-2-carbaldehyde (7)

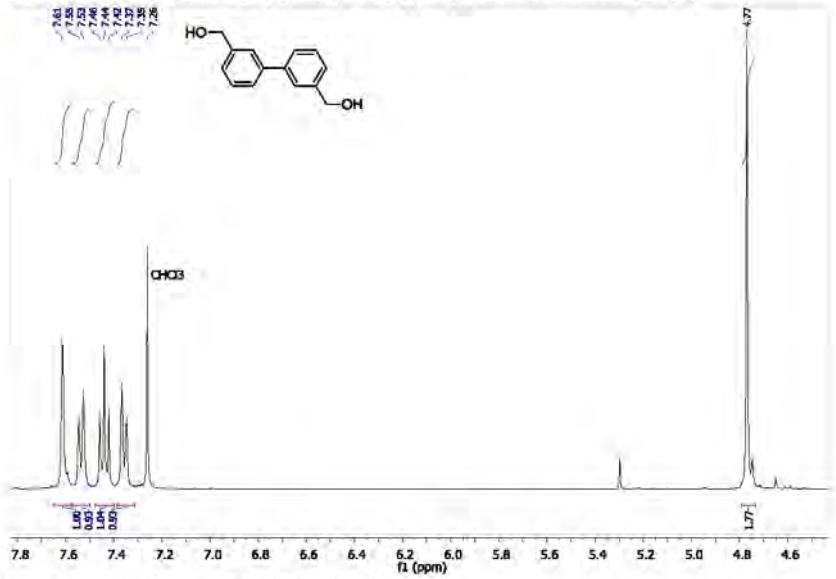

Figure S1: ^{1}H NMR spectrum of compound **10**, solvent $CDCl_3$.

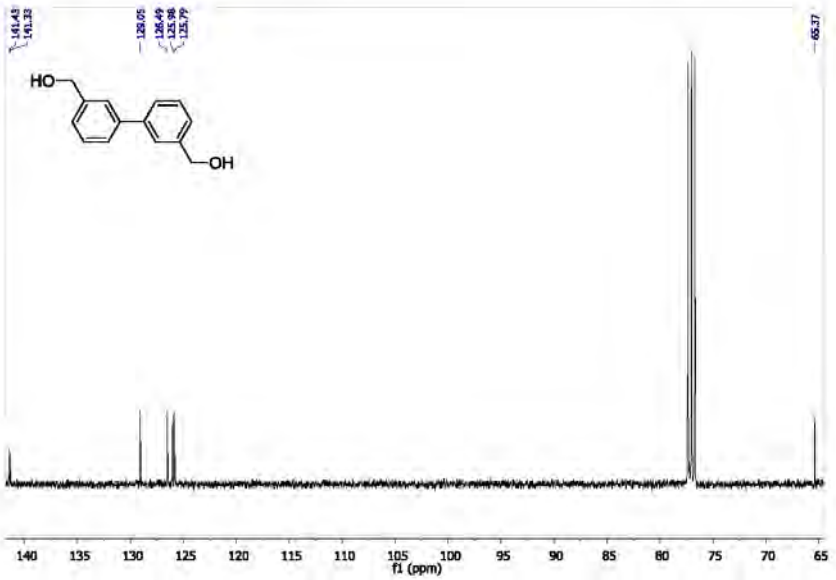

Figure S2: ^{13}C NMR spectrum of compound **10**, solvent $CDCl_3$.

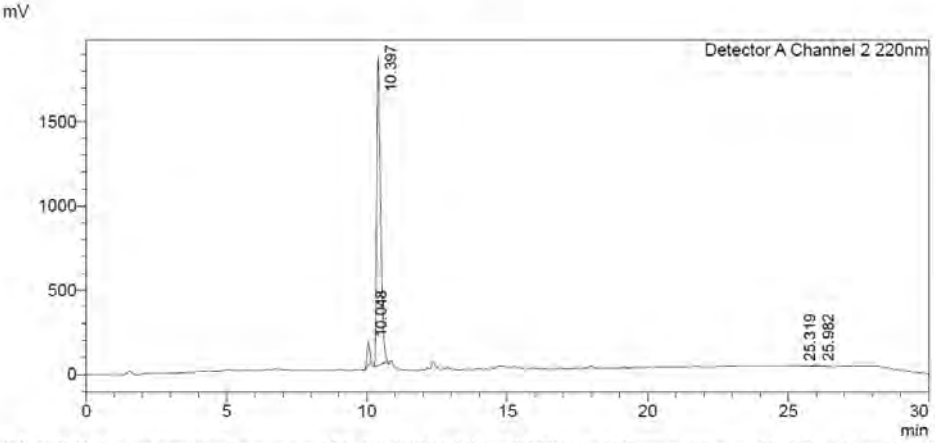

Figure S3: HPLC chromatogram of compound **10**, RP-HPLC Alltima™ C18 5u 150mm x 4.6 mm, 10-100 % B in 15 min.

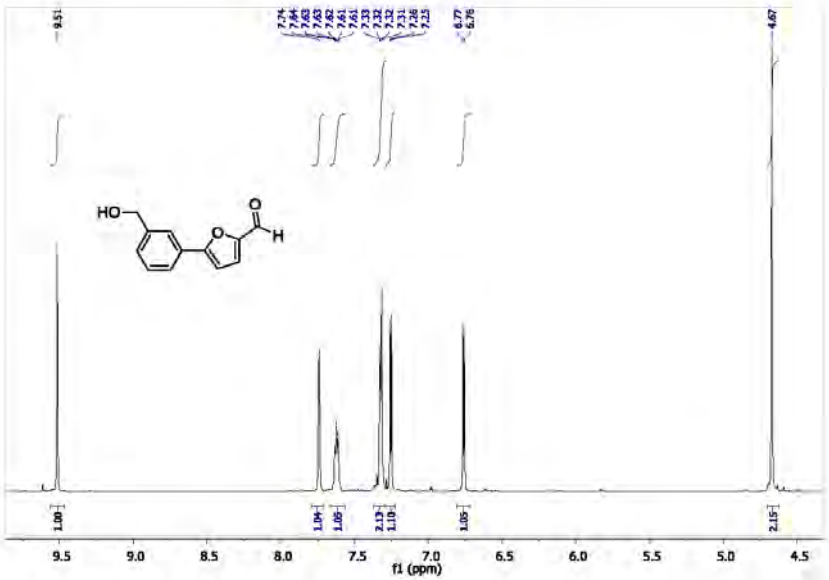

Figure S4: ^{1}H NMR spectrum of compound **7**, solvent $CDCl_3$.

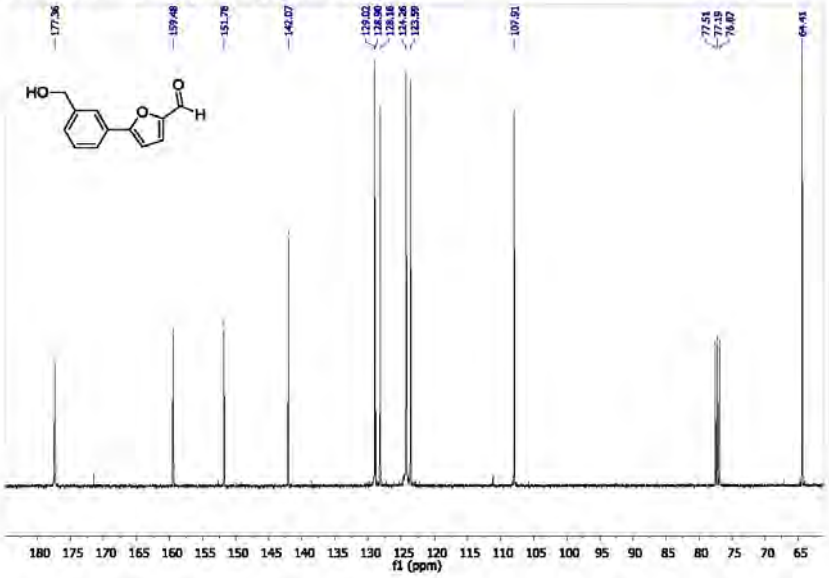

Figure S5: ^{13}C NMR spectrum of compound **7**, solvent $CDCl_3$.

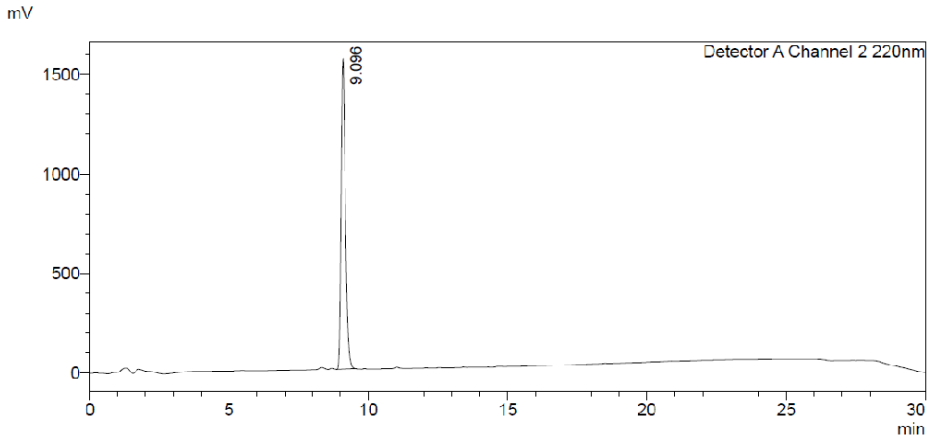

Figure S6: HPLC chromatogram of compound **7**, RP-HPLC Alltima™ C18 5u 150mm x 4.6 mm, 10-100 % B in 15 min

S3. Initial Catalyst Screening Optimisation Investigations

The optimisation investigations were performed in accordance with the protocol outlined for the initial synthesis of compound **9** (i.e. section S2) with the only variation being the catalyst employed.

Table S1: Ratio of **7** and **9** peak areas obtained after subsequent cycles FibreCat® 1001. ***Reagents and conditions***: (*i*) 5-formyl-2-furanylboroic acid (1 mmol), 3-bromobenzyl alcohol (1 mmol), tetrabutylammonium fluoride trihydrate (3 mmol), and MeOH (30 mL) at 0.5 mL/min, and 80 °C.

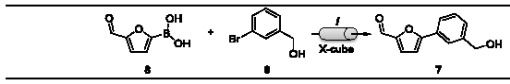

8 **9** **7**

Entry	Pd-Ligand	FibreCat®	Number of catalyst cycles Ratio of 7 : 9[a] 1	2	3	4
1	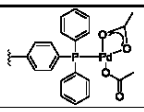	FC1001	1:1.2	1:0.7	1:0.5	1:0.4

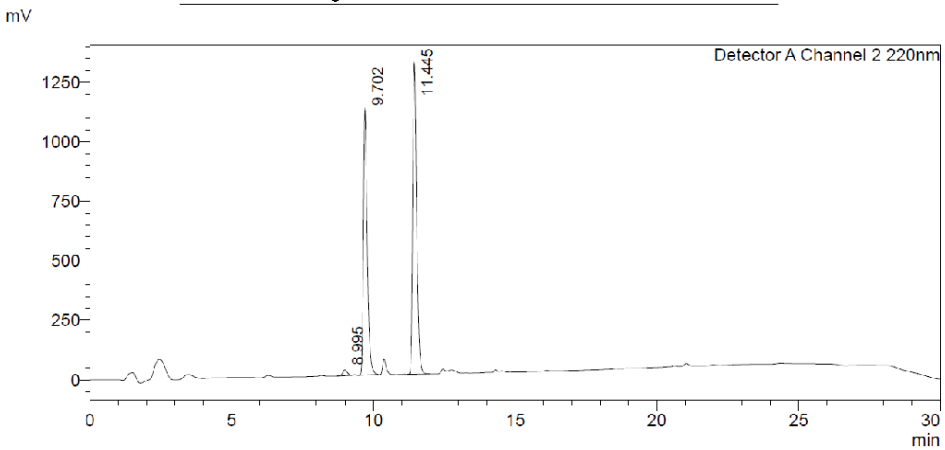

Figure S7: HPLC chromatogram of the reaction mixture outlined in table S1 after a single catalyst cycle. RP-HPLC Alltima™ C18 5u 150mm x 4.6 mm, 10-100 % B in 15 min.

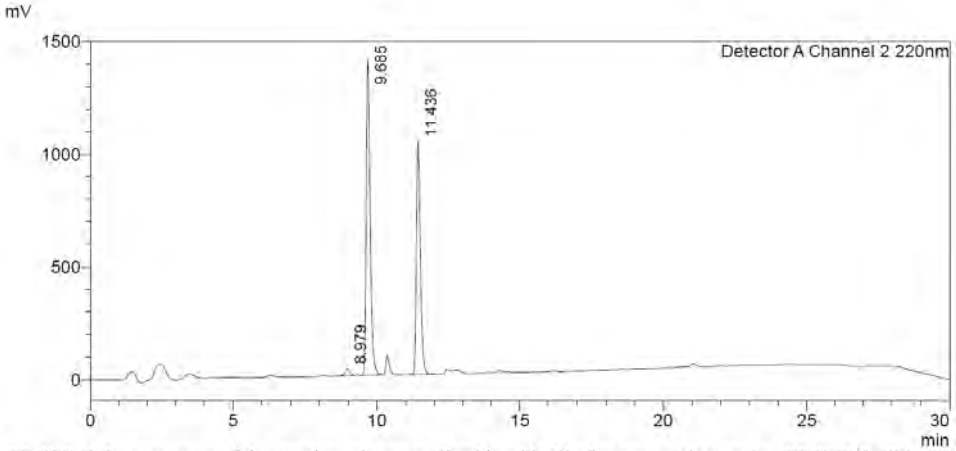

Figure S8: HPLC chromatogram of the reaction mixture outlined in table S1 after two catalyst cycles. RP-HPLC Alltima™ C18 5u 150mm x 4.6 mm, 10-100 % B in 15 min.

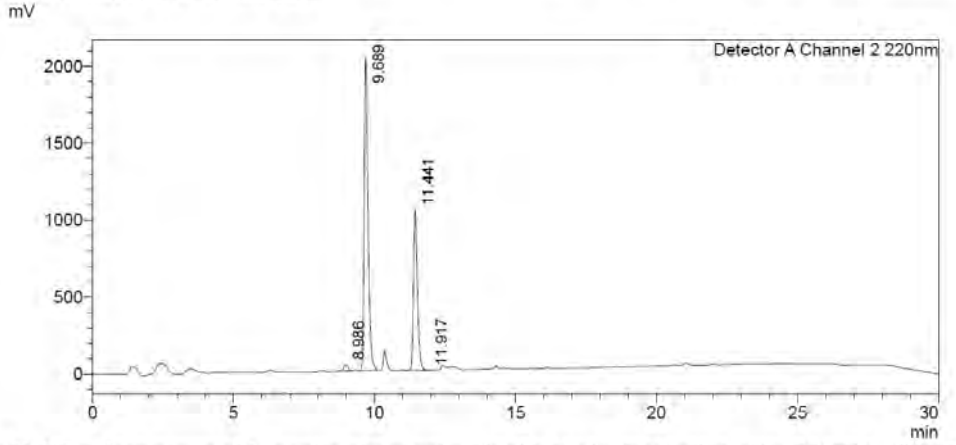

Figure S8: HPLC chromatogram of the reaction mixture outlined in table S1 after three catalyst cycles. RP-HPLC Alltima™ C18 5u 150mm x 4.6 mm, 10-100 % B in 15 min.

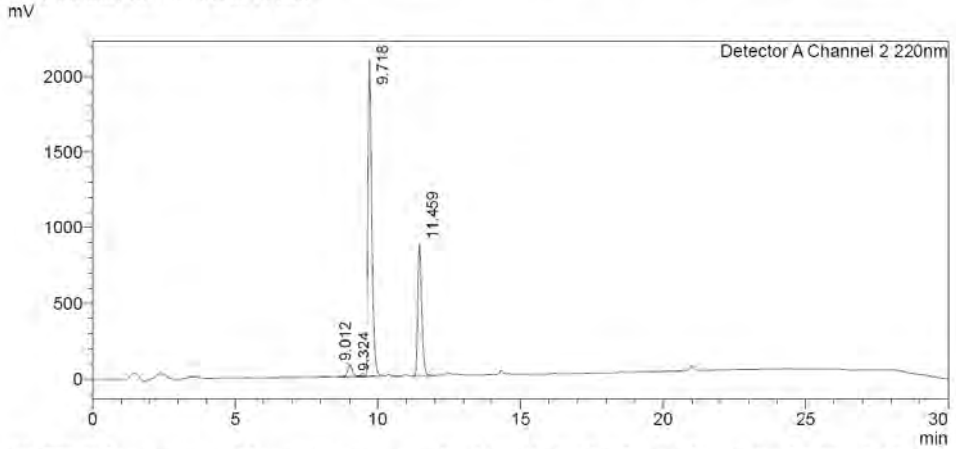

Figure S9: HPLC chromatogram of the reaction mixture outlined in table S1 after four catalyst cycles. RP-HPLC Alltima™ C18 5u 150mm x 4.6 mm, 10-100 % B in 15 min.

Table S2: Ratio of **7** and **9** peak areas obtained after subsequent cycles FibreCat® 1007. ***Reagents and conditions***: (*i*) 5-formyl-2-furanylboroic acid (1 mmol), 3-bromobenzyl alcohol (1 mmol), tetrabutylammonium fluoride trihydrate (3 mmol), and MeOH (30 mL) at 0.5 mL/min, and 80 °C.

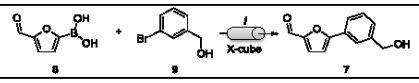

Entry	Pd-Ligand	FibreCat®	Number of catalyst cycles Ratio of 7 : 9[a] 1	2	3	4
2	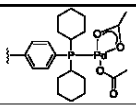	FC1007	1:1.3	1:0.7	1:0.4	1:0.2

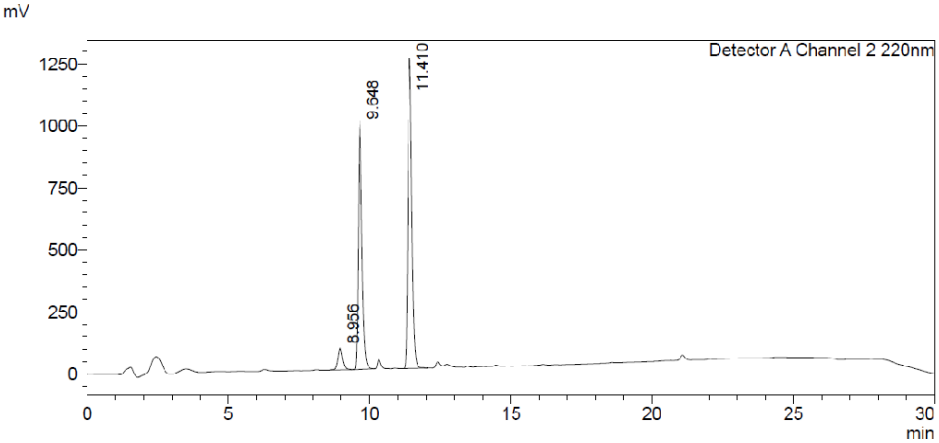

Figure S10: HPLC chromatogram of the reaction mixture outlined in table S2 after a single catalyst cycle. RP-HPLC Alltima™ C18 5u 150mm x 4.6 mm, 10-100 % B in 15 min.

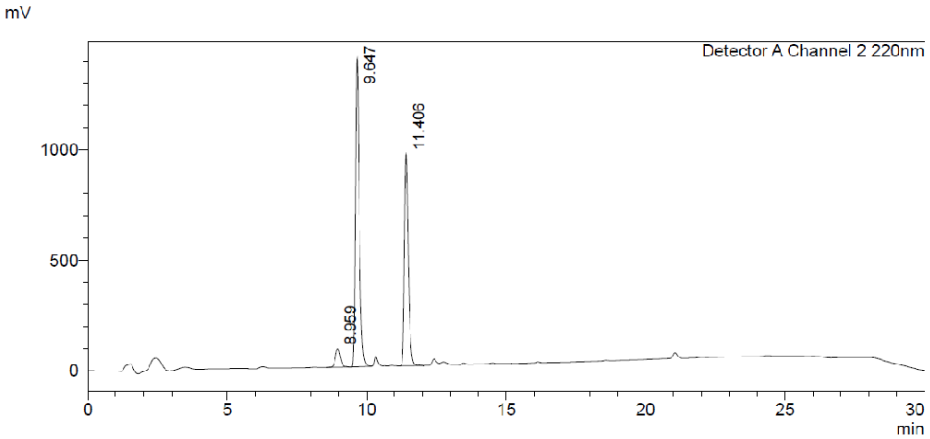

Figure S11: HPLC chromatogram of the reaction mixture outlined in table S2 after two catalyst cycles. RP-HPLC Alltima™ C18 5u 150mm x 4.6 mm, 10-100 % B in 15 min.

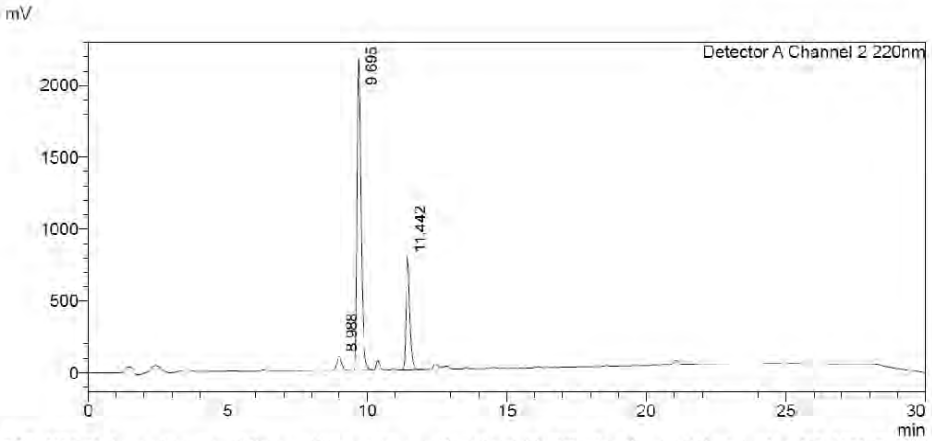

Figure S12: HPLC chromatogram of the reaction mixture outlined in table S2 after three catalyst cycles. RP-HPLC Alltima™ C18 5u 150mm x 4.6 mm, 10-100 % B in 15 min.

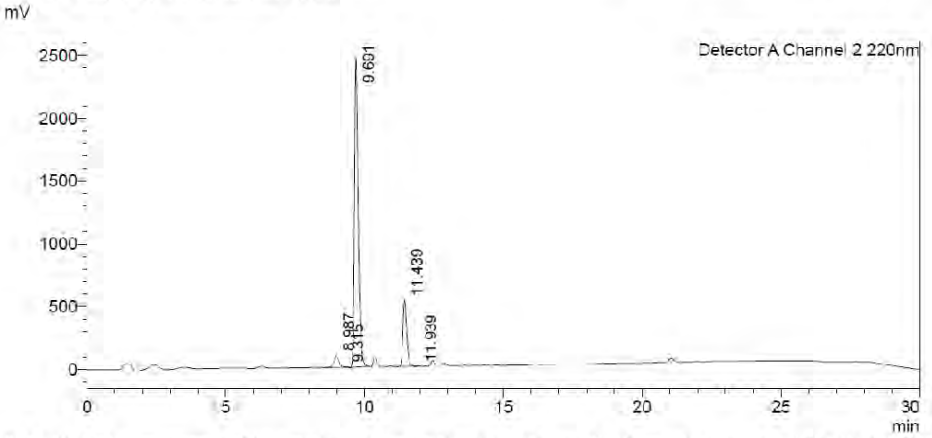

Figure S13: HPLC chromatogram of the reaction mixture outlined in table S2 after four catalyst cycles. RP-HPLC Alltima™ C18 5u 150mm x 4.6 mm, 10-100 % B in 15 min.

Table S3: Ratio of **7** and **9** peak areas obtained after subsequent cycles FibreCat® 1032. ***Reagents and conditions***: (*i*) 5-formyl-2-furanylboroic acid (1 mmol), 3-bromobenzyl alcohol (1 mmol), tetrabutylammonium fluoride trihydrate (3 mmol), and MeOH (30 mL) at 0.5 mL/min, and 80 °C.

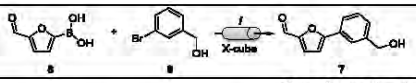

8 9 7

Entry	Pd-Ligand	FibreCat®	Number of catalyst cycles Ratio of 7 : 9[a] 1	2	3	4
3	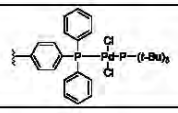	FC1032	1:0.7	1:0.4	1:0.3	1:0.2

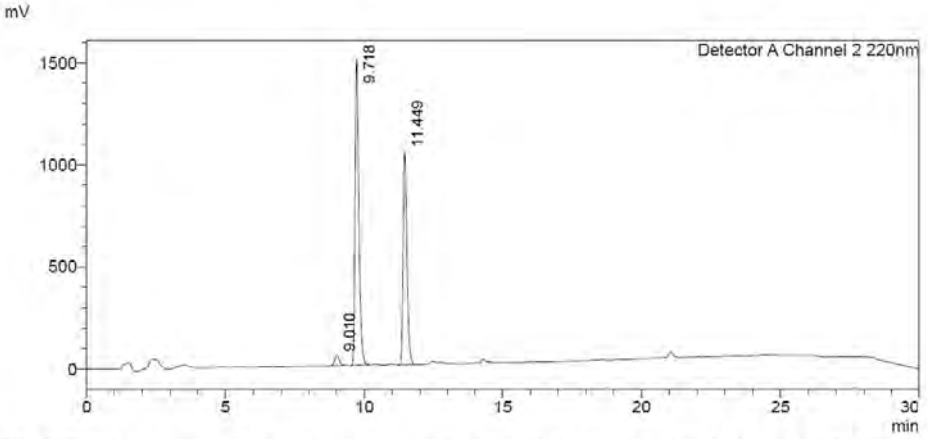

Figure S14: HPLC chromatogram of the reaction mixture outlined in table S3 after a single catalyst cycle. RP-HPLC Alltima™ C18 5u 150mm x 4.6 mm, 10-100 % B in 15 min.

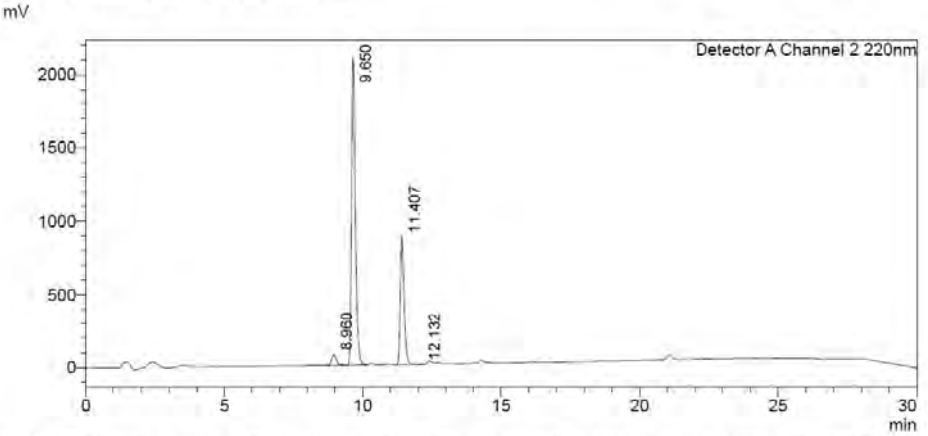

Figure S15: HPLC chromatogram of the reaction mixture outlined in table S3 after two catalyst cycles. RP-HPLC Alltima™ C18 5u 150mm x 4.6 mm, 10-100 % B in 15 min.

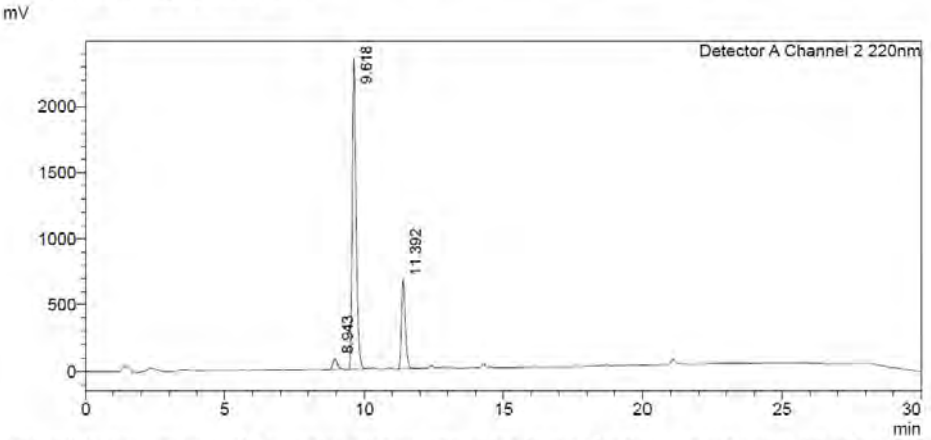

Figure S16: HPLC chromatogram of the reaction mixture outlined in table S3 after three catalyst cycles. RP-HPLC Alltima™ C18 5u 150mm x 4.6 mm, 10-100 % B in 15 min.

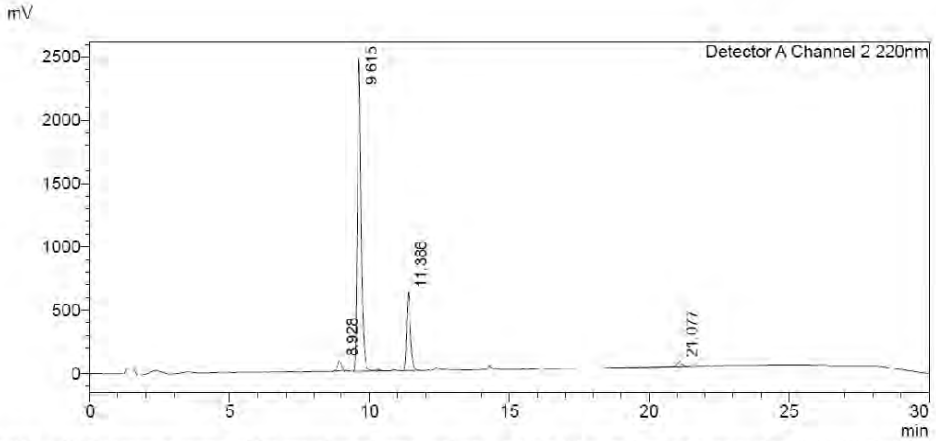

Figure S17: HPLC chromatogram of the reaction mixture outlined in table S3 after four catalyst cycles. RP-HPLC Alltima™ C18 5u 150mm x 4.6 mm, 10-100 % B in 15 min.

Table S4: Ratio of **7** and **9** peak areas obtained after subsequent cycles FibreCat® Pd-tetrakis. ***Reagents and conditions***: (***i***) 5-formyl-2-furanylboroic acid (1 mmol), 3-bromobenzyl alcohol (1 mmol), tetrabutylammonium fluoride trihydrate (3 mmol), and MeOH (30 mL) at 0.5 mL/min, and 80 °C.

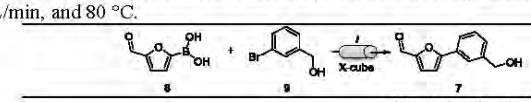

Entry	Pd-Ligand	FibreCat®	Number of catalyst cycles Ratio of 7 : 9[a]			
			1	2	3	4
4	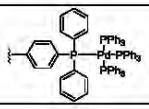	Pd-Tetrakis	1:0.4	1:0.3	1:0.3	1:0.2

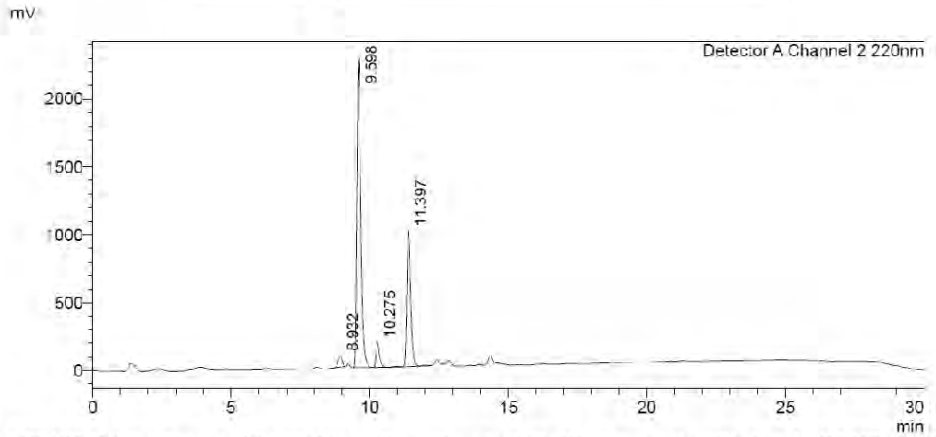

Figure S18: HPLC chromatogram of the reaction mixture outlined in table S4 after a single catalyst cycle. RP-HPLC Alltima™ C18 5u 150mm x 4.6 mm, 10-100 % B in 15 min.

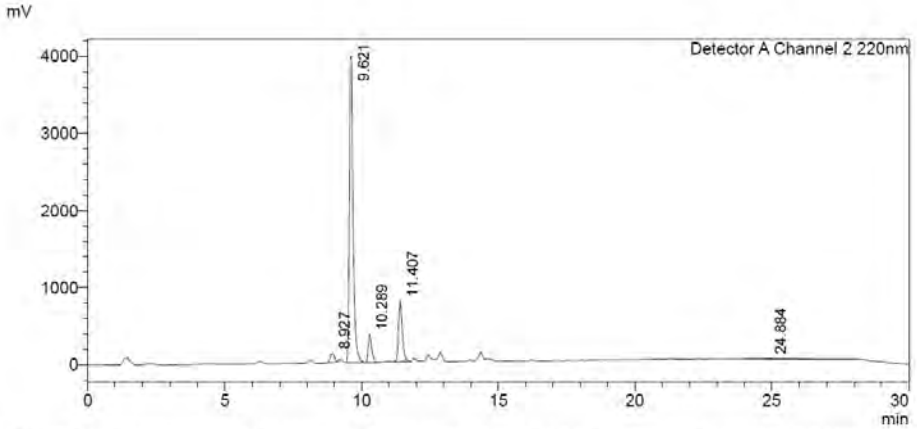

Figure S19: HPLC chromatogram of the reaction mixture outlined in table S4 after two catalyst cycles. RP-HPLC Alltima™ C18 5u 150mm x 4.6 mm, 10-100 % B in 15 min.

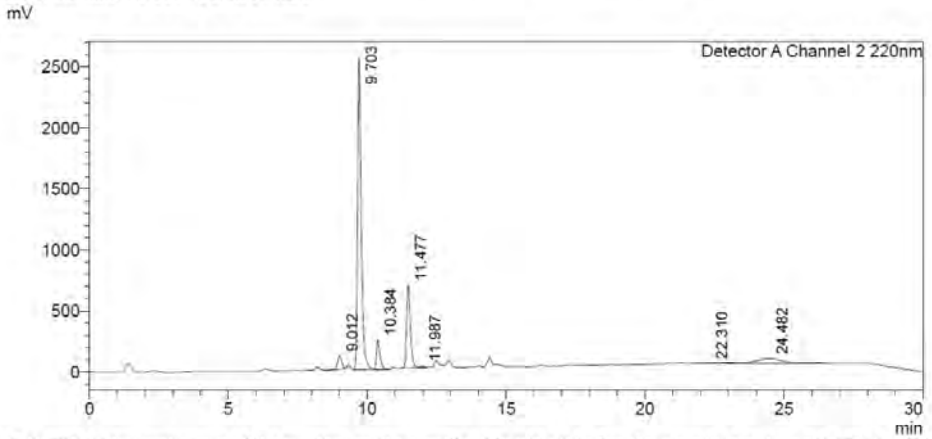

Figure S19: HPLC chromatogram of the reaction mixture outlined in table S4 after three catalyst cycles. RP-HPLC Alltima™ C18 5u 150mm x 4.6 mm, 10-100 % B in 15 min.

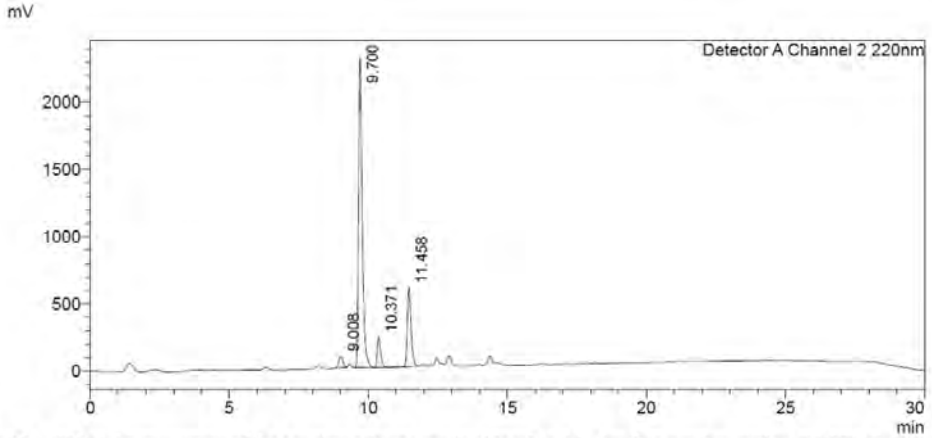

Figure S20: HPLC chromatogram of the reaction mixture outlined in table S4 after four catalyst cycles. RP-HPLC Alltima™ C18 5u 150mm x 4.6 mm, 10-100 % B in 15 min.

S4. Investigation of Temperature Variations Using Pd-Tetrakis

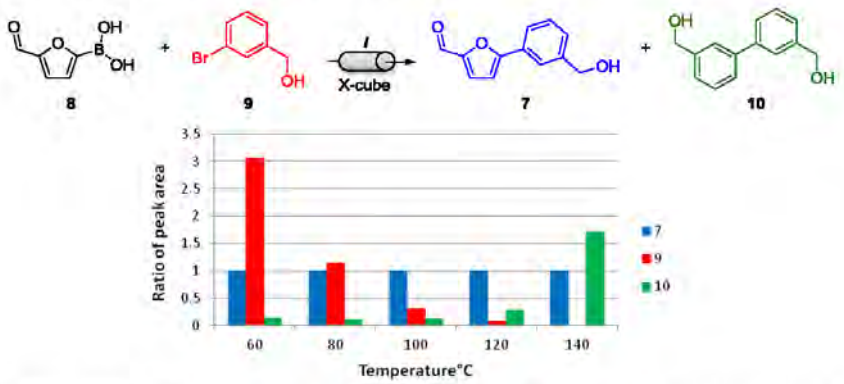

Figure S21: ***Reagents and conditions***: (*i*) 5-formyl-2-furanylboroic acid (1 mmol), 3-bromobenzyl alcohol (1 mmol), tetrabutylammonium fluoride trihydrate (3 mmol), and MeOH (30 mL) at 0.5 mL/min, Pd-tetrakis; **b**) Comparison of the relative quantities of aryl bromide (**9**), desired product (7), and aryl bromide homocoupled product retuned at temperatures of 60 to 140 °C with 0 bar pressure (*Note: ratio of peak areas determined at 220 nm*).

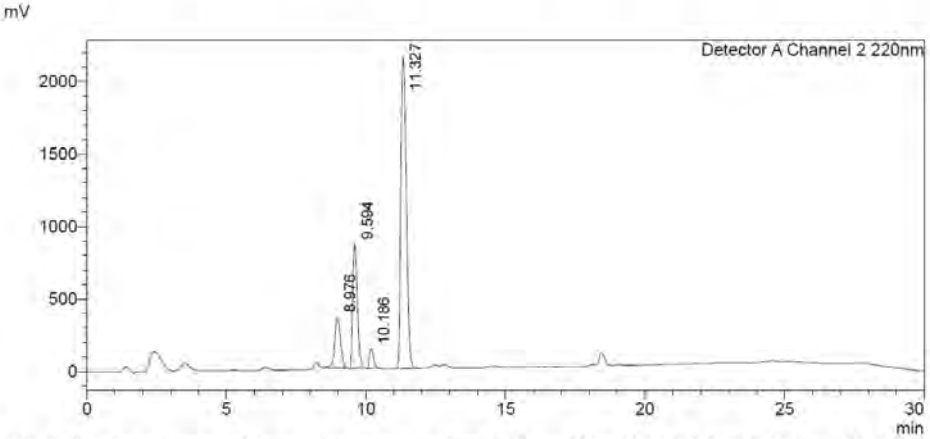

Figure S22: HPLC chromatogram of the reaction mixture outlined in figure S21at 60 °C. RP-HPLC Alltima™ C18 5u 150mm x 4.6 mm, 10-100 % B in 15 min.

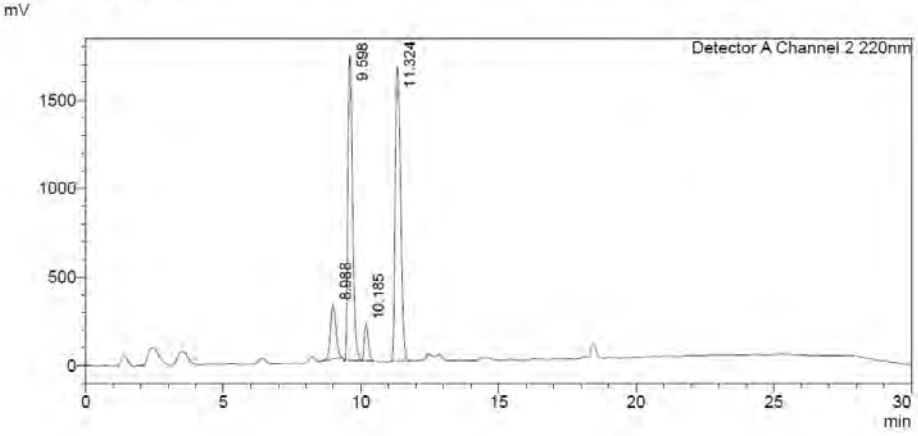

Figure S23: HPLC chromatogram of the reaction mixture outlined in figure S21at 80 °C. RP-HPLC Alltima™ C18 5u 150mm x 4.6 mm, 10-100 % B in 15 min.

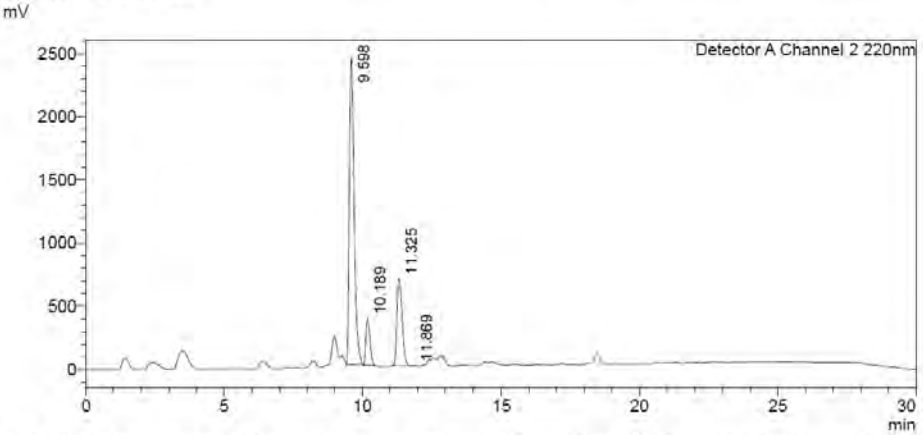

Figure S24: HPLC chromatogram of the reaction mixture outlined in figure S21at 100 °C. RP-HPLC Alltima™ C18 5u 150mm x 4.6 mm, 10-100 % B in 15 min.

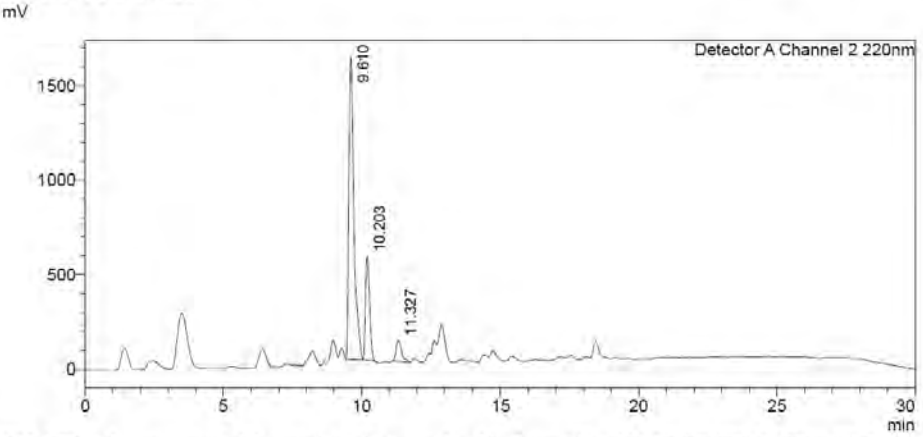

Figure S25: HPLC chromatogram of the reaction mixture outlined in figure S21at 120 °C. RP-HPLC Alltima™ C18 5u 150mm x 4.6 mm, 10-100 % B in 15 min.

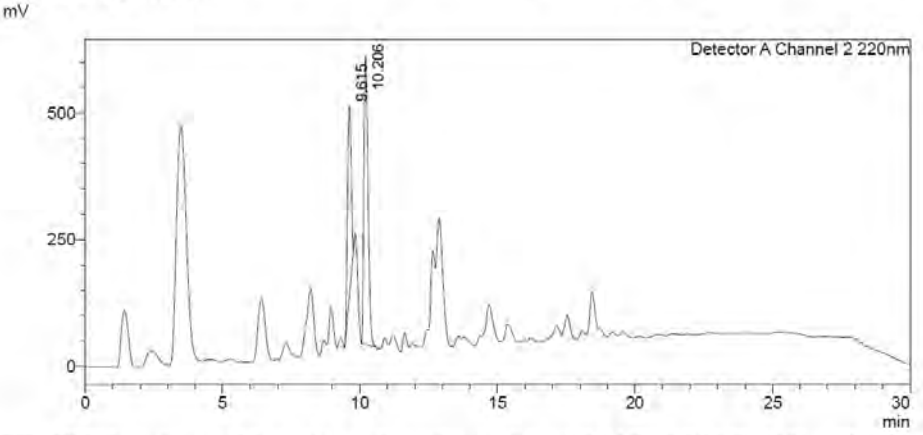

Figure S26: HPLC chromatogram of the reaction mixture outlined in figure S21at 140 °C. RP-HPLC Alltima™ C18 5u 150mm x 4.6 mm, 10-100 % B in 15 min.

S5. Investigation of Pressure Variations Using Pd-Tetrakis

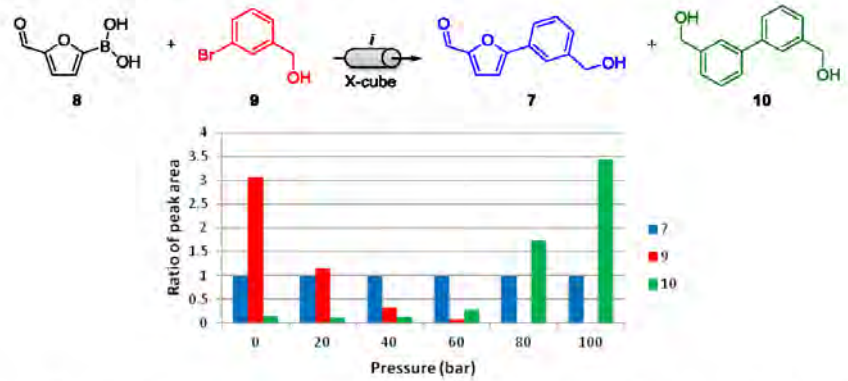

Figure S27: **a**) ***Reagents and conditions***: (*i*) 5-formyl-2-furanylboroic acid (1 mmol), 3-bromobenzyl alcohol (1 mmol), tetrabutylammonium fluoride trihydrate (3 mmol), and MeOH (30 mL) at 0.5 mL/min, Pd-tetrakis; **b**) Comparison of the relative quantities of aryl bromide (**9**), desired product (**7**), and aryl bromide homocoupled product retuned at pressures of 0 to 100 bar at 80 °C (*Note: ratio of peak areas determined at 220 nm*).

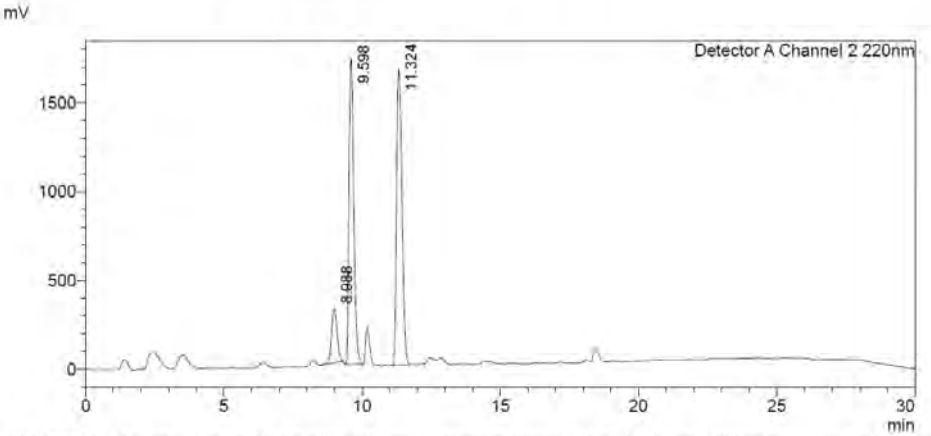

Figure S28: HPLC chromatogram of the reaction mixture outlined in figure S27 at 80 °C and 20 bar pressure. RP-HPLC Alltima™ C18 5u 150mm x 4.6 mm, 10-100 % B in 15 min.

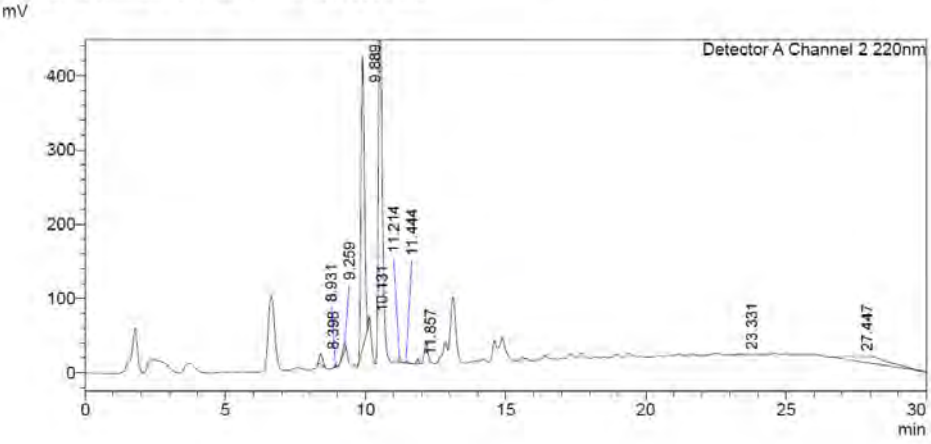

Figure S29: HPLC chromatogram of the reaction mixture outlined in figure S27 at 80 °C and 40 bar pressure. RP-HPLC Alltima™ C18 5u 150mm x 4.6 mm, 10-100 % B in 15 min.

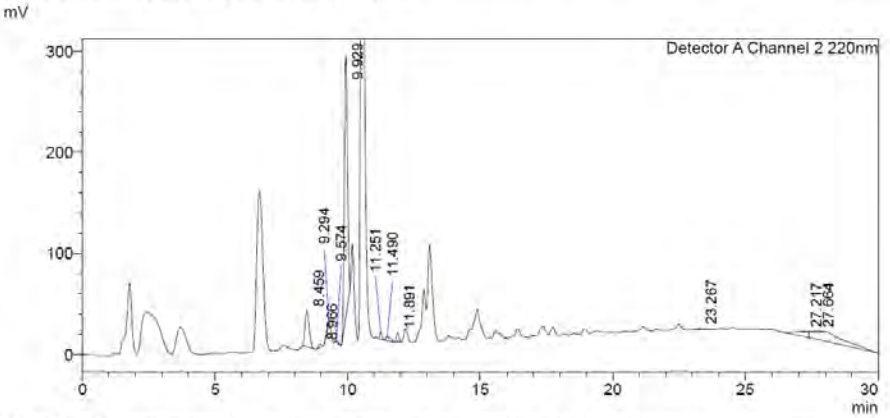

Figure S30: HPLC chromatogram of the reaction mixture outlined in figure S27 at 80 °C and 60 bar pressure. RP-HPLC Alltima™ C18 5u 150mm x 4.6 mm, 10-100 % B in 15 min.

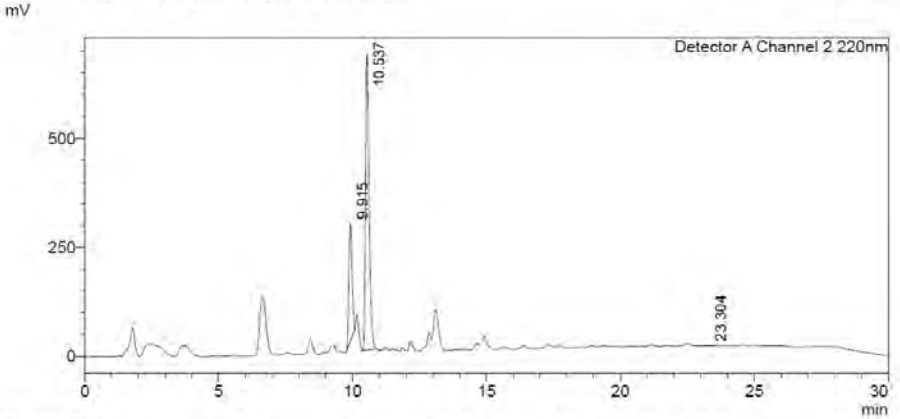

Figure S31: HPLC chromatogram of the reaction mixture outlined in figure S27 at 80 °C and 80 bar pressure. RP-HPLC Alltima™ C18 5u 150mm x 4.6 mm, 10-100 % B in 15 min.

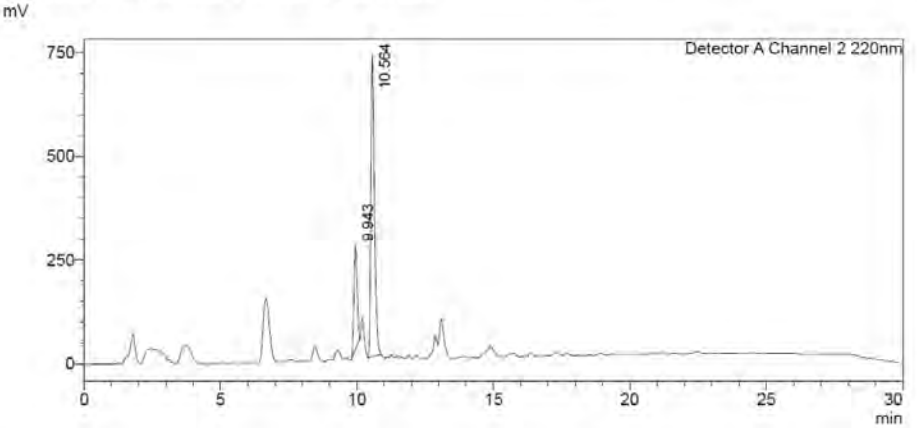

Figure S32: HPLC chromatogram of the reaction mixture outlined in figure S27 at 80 °C and 100 bar pressure. RP-HPLC Alltima™ C18 5u 150mm x 4.6 mm, 10-100 % B in 15 min.

S15

S6. General Procedure 1 using $(Bu)_4N^+F^-$ and FC1032™

5-(4-acetylphenyl)-2-furancarboxaldehyde (12a)

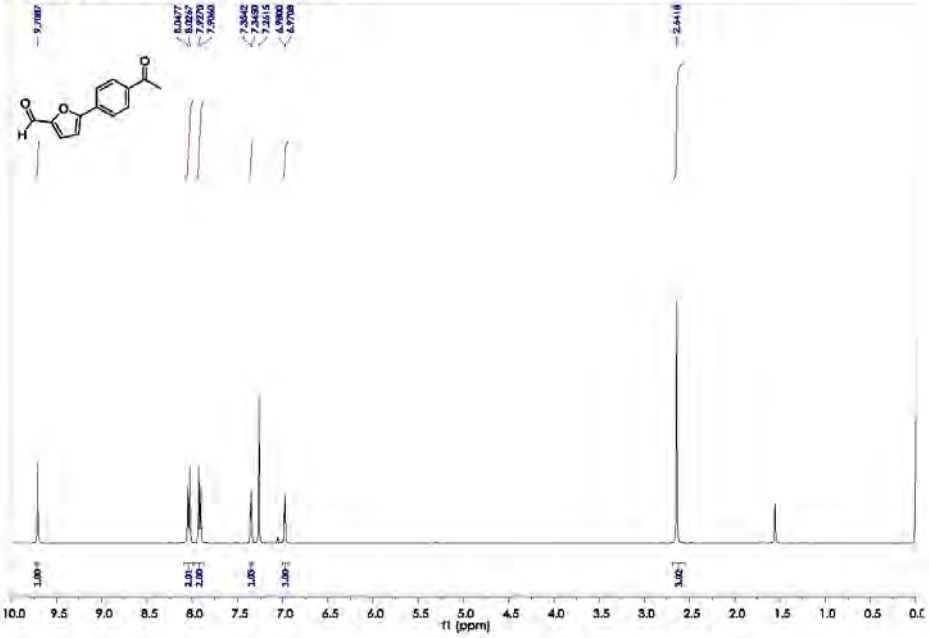

Fig S33: ^{1}H NMR Spectrum ($CDCl_3$, 400 MHz) of 5-(4-acetylphenyl)-2-furancarboxaldehyde (**12a**)

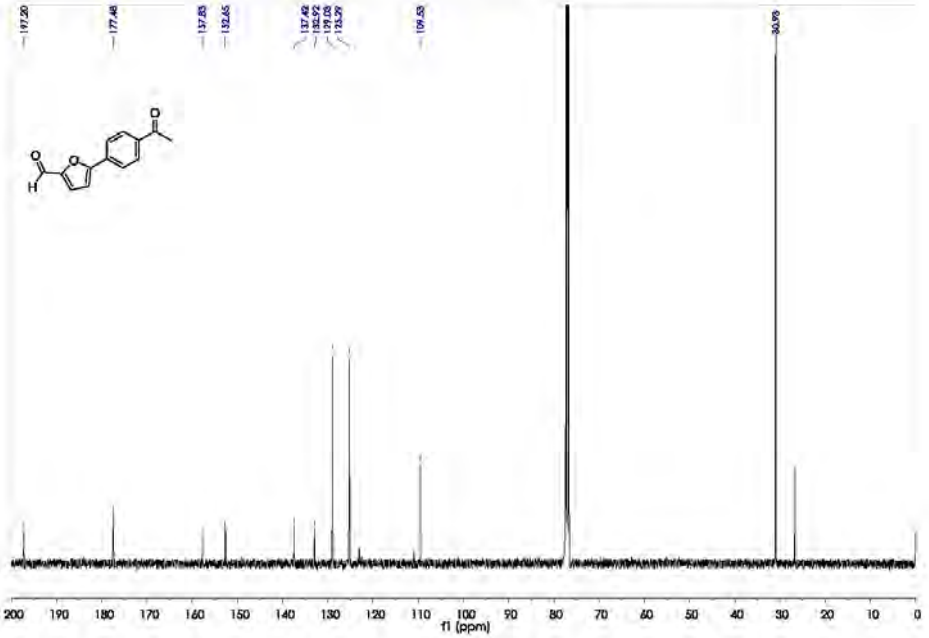

Fig S34: ^{13}C NMR Spectrum ($CDCl_3$, 400 MHz) of 5-(4-acetylphenyl)-2-furancarboxaldehyde (**12a**).

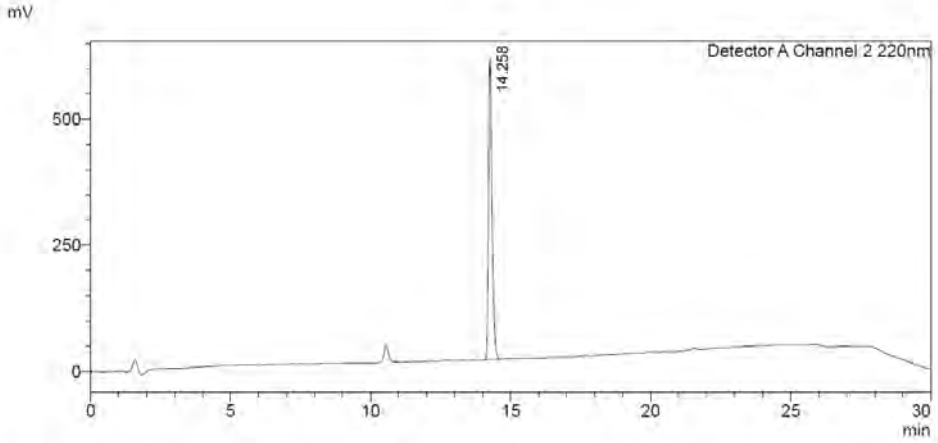

Figure S35: HPLC chromatogram of compound **12a**, RP-HPLC Alltima™ C18 5u 150mm x 4.6 mm, 10-100 % B in 15 min.

2-(4-(5-formylfuran-2-yl)phenyl)acetonitrile (12b)

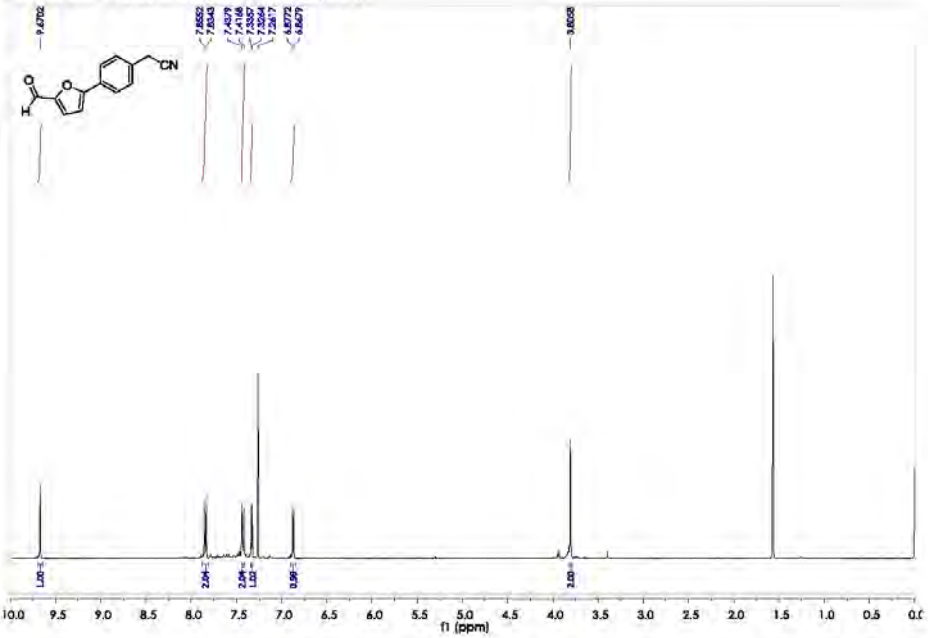

Fig S36: ^{1}H NMR Spectrum ($CDCl_3$, 400 MHz) of 2-(4-(5-formylfuran-2-yl)phenyl)acetonitrile (**12b**)

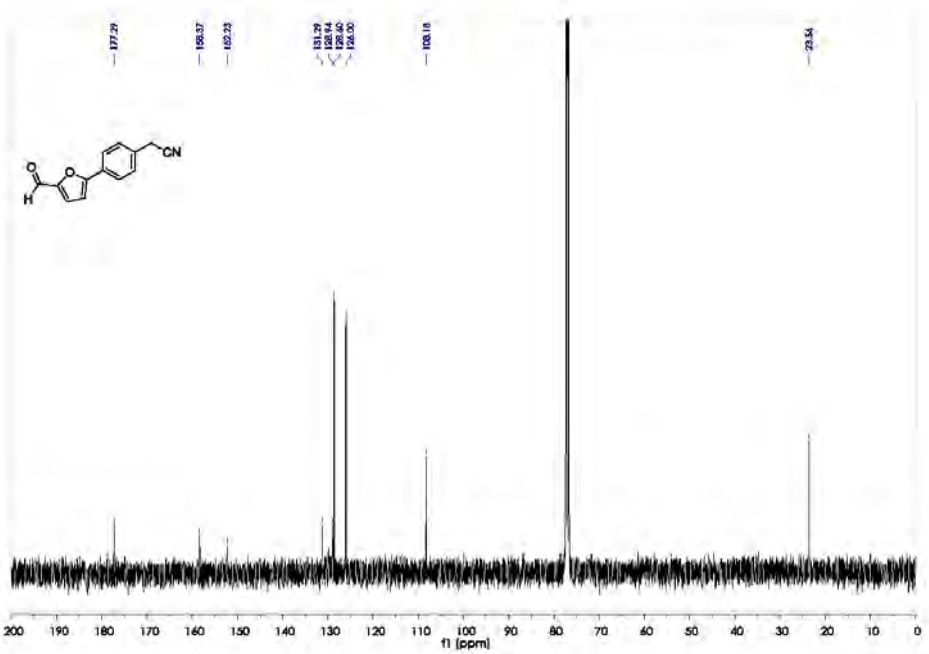

Fig S37: ^{13}C NMR Spectrum ($CDCl_3$, 101 MHz) of 2-(4-(5-formylfuran-2-yl)phenyl)acetonitrile (**12b**)

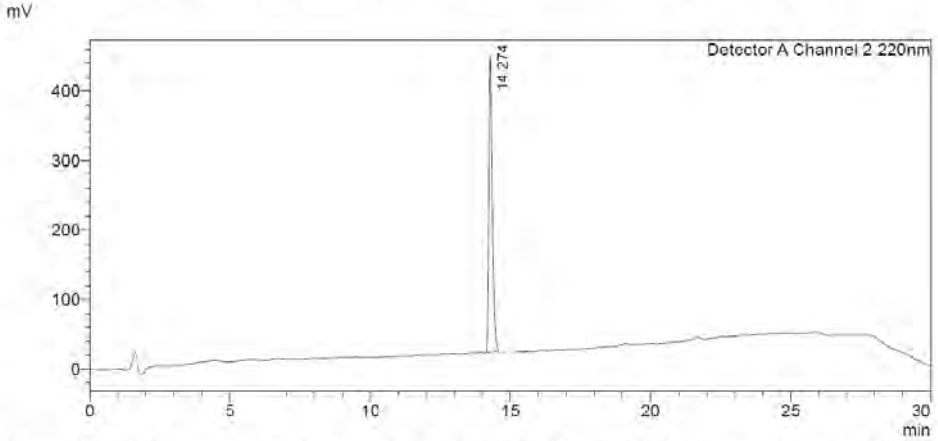

Figure S38: HPLC chromatogram of compound **12b**, RP-HPLC Alltima™ C18 5u 150mm x 4.6 mm, 10-100 % B in 15 min.

5-(4-Methylphenyl)-2-furancarboxaldehyde (12c)

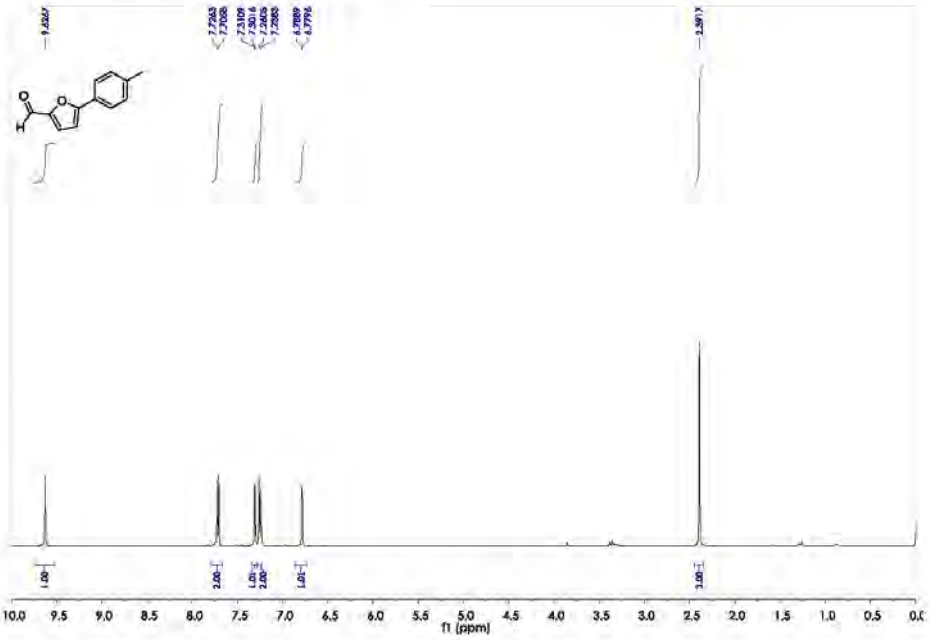

Fig S39: ^{1}H NMR Spectrum ($CDCl_3$, 400 MHz) of 5-(4-Methylphenyl)-2-furancarboxaldehyde (**12c**)

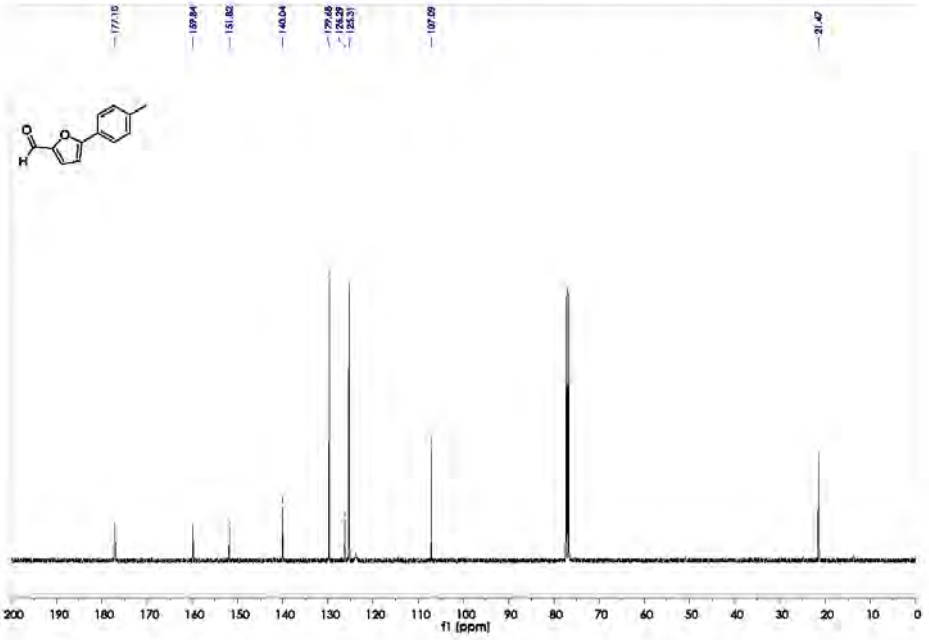

Fig S40: ^{13}C NMR Spectrum ($CDCl_3$, 101 MHz) of 5-(4-Methylphenyl)-2-furancarboxaldehyde (**12c**)

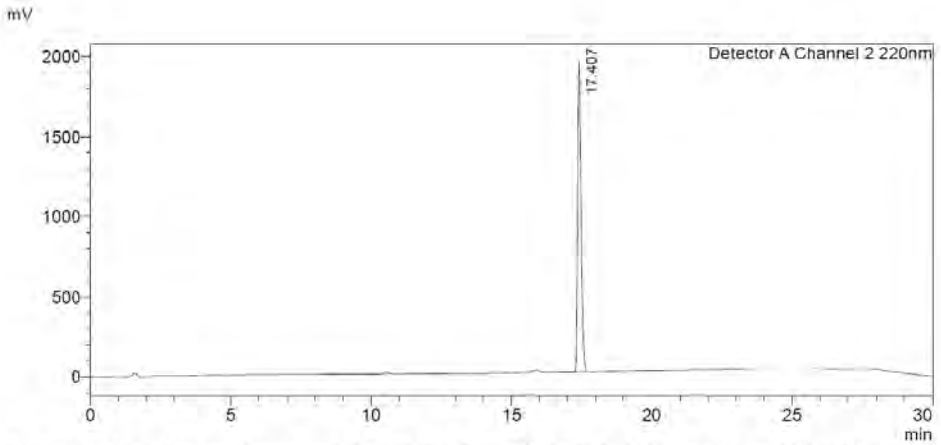

Figure S41: HPLC chromatogram of compound **12c**, RP-HPLC Alltima™ C18 5u 150mm x 4.6 mm, 10-100 % B in 15 min.

5-(dimethylamino)-N-(4-(5-formylfuran-2-yl)phenyl)naphthalene-1-sulfonamide (12d)

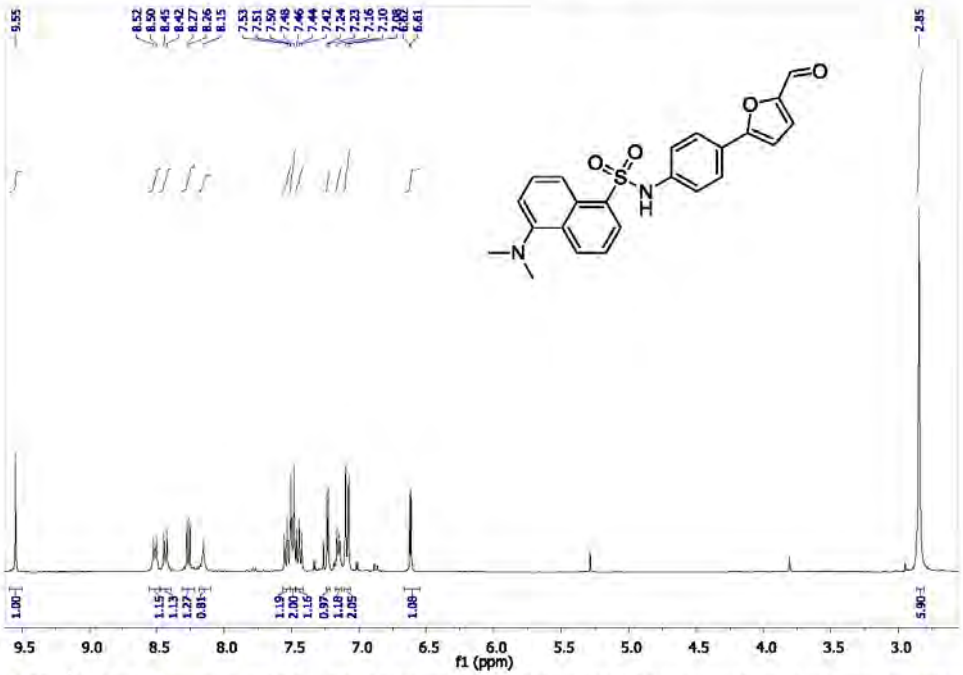

Figure S42: ^{1}H NMR Spectrum ($CDCl_3$, 400 MHz) of 5-(dimethylamino)-N-(4-(5-formylfuran-2-yl)phenyl)naphthalene-1-sulfonamide (**12d**).

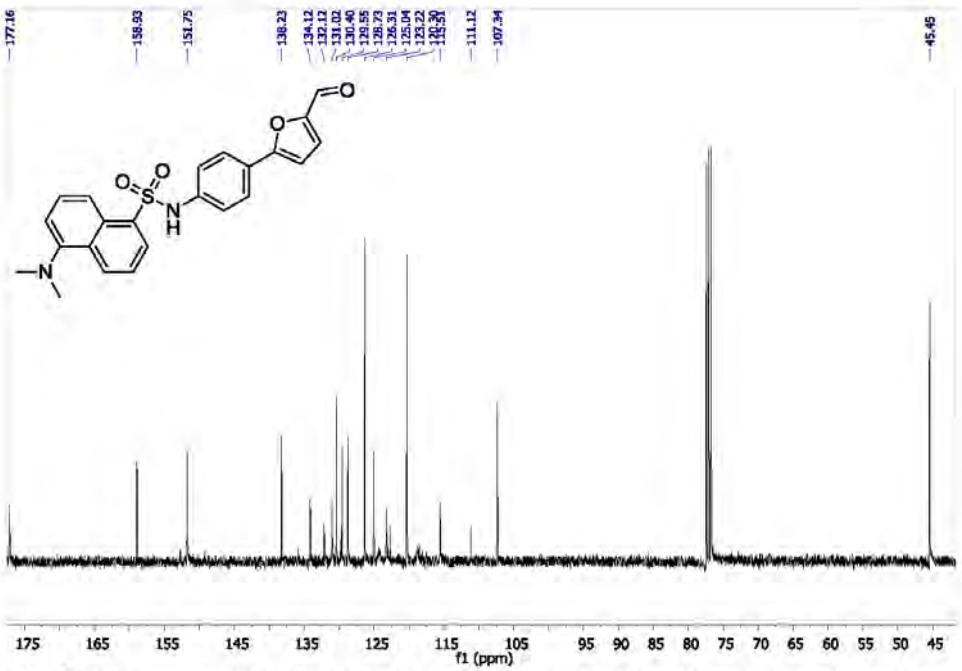

Figure S43: ^{13}C NMR Spectrum ($CDCl_3$, 101 MHz) of 5-(dimethylamino)-N-(4-(5-formylfuran-2-yl)phenyl)naphthalene-1-sulfonamide (**12d**).

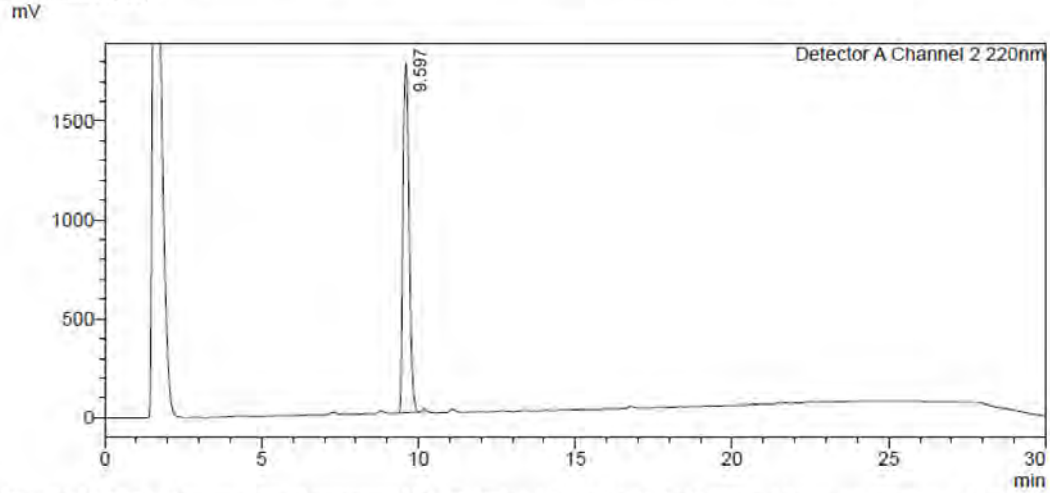

Figure S44: HPLC chromatogram of compound **12d**. RP-HPLC Alltima™ C18 5u 150mm x 4.6 mm, 10-100 % B in 15 min.

N-(4-(5-formylfuran-2-yl)phenyl)benzenesulfonamide (12e)

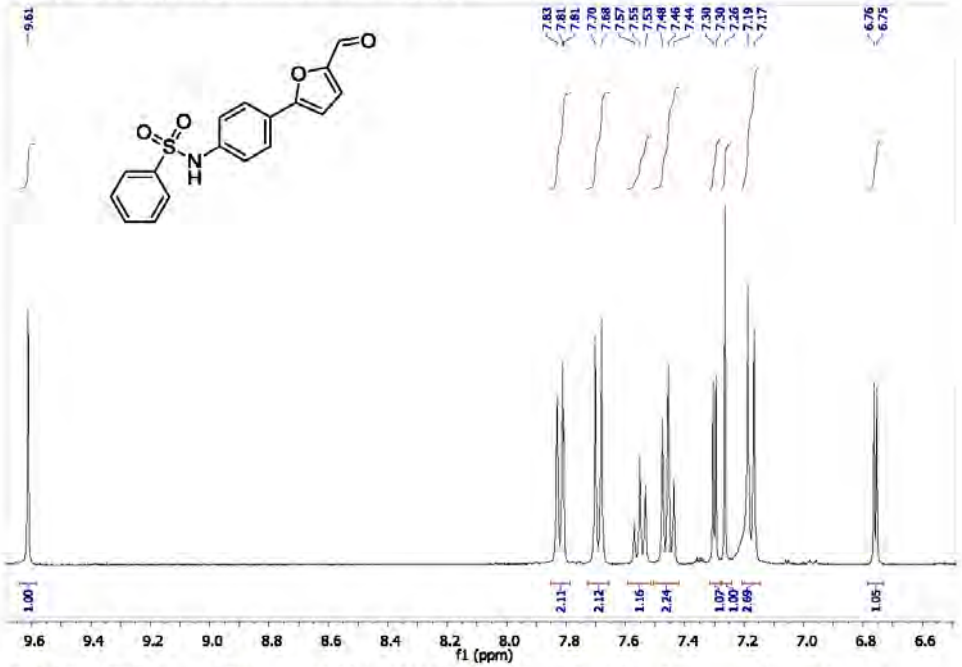

Figure S45: ^{1}H NMR Spectrum ($CDCl_3$, 400 MHz) of *N*-(4-(5-formylfuran-2-yl)phenyl)benzenesulfonamide (**12e**).

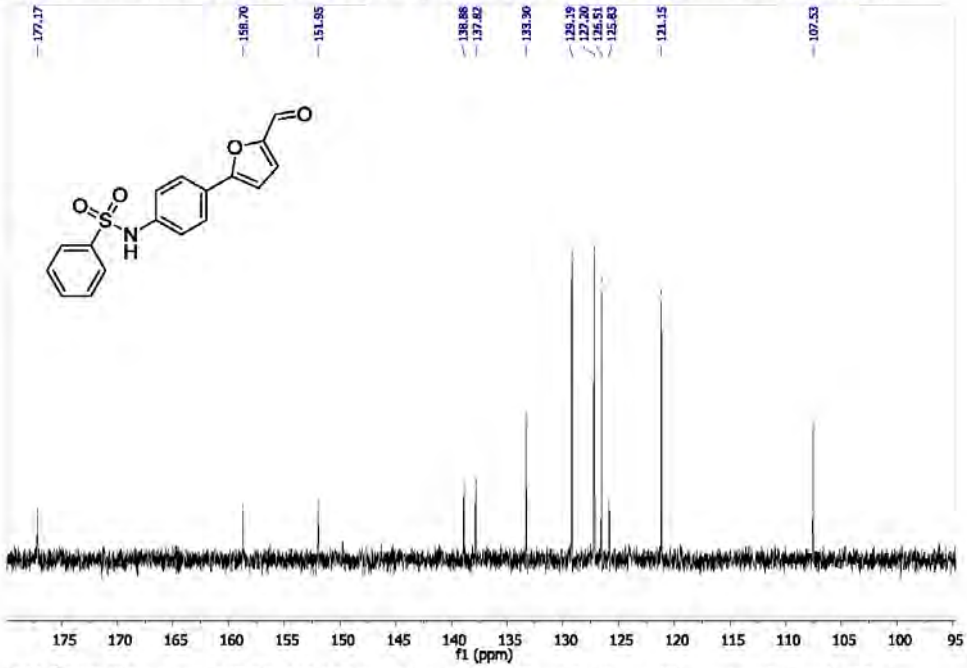

Figure S46: ^{1}C NMR Spectrum ($CDCl_3$, 101 MHz) of *N*-(4-(5-formylfuran-2-yl)phenyl)benzenesulfonamide (**12e**).

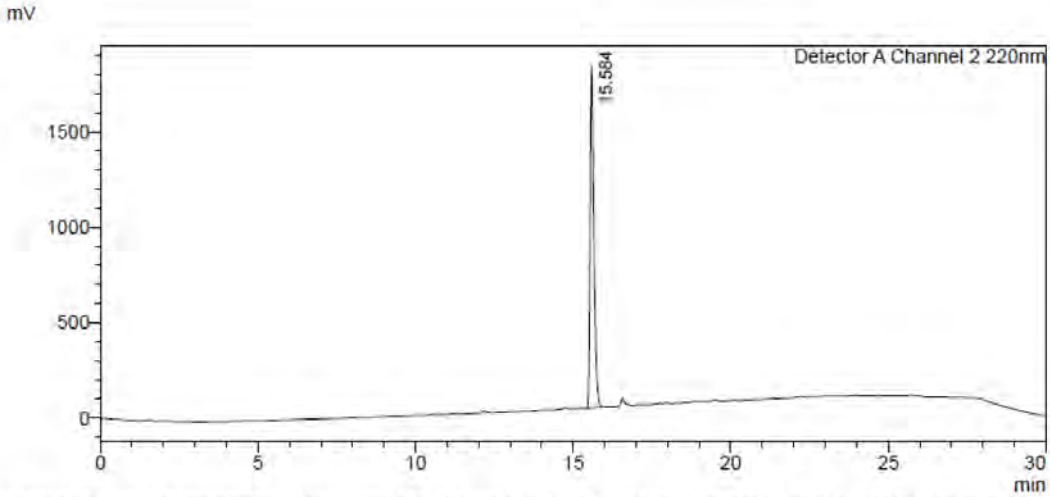

Figure S47: HPLC chromatogram of compound **12e**, RP-HPLC Alltima™ C18 5u 150mm x 4.6 mm, 10-100 % B in 15 min.

***N*-(2,4-dimethoxyphenyl)-4-(5-formylfuran-2-yl)benzamide (12f)**

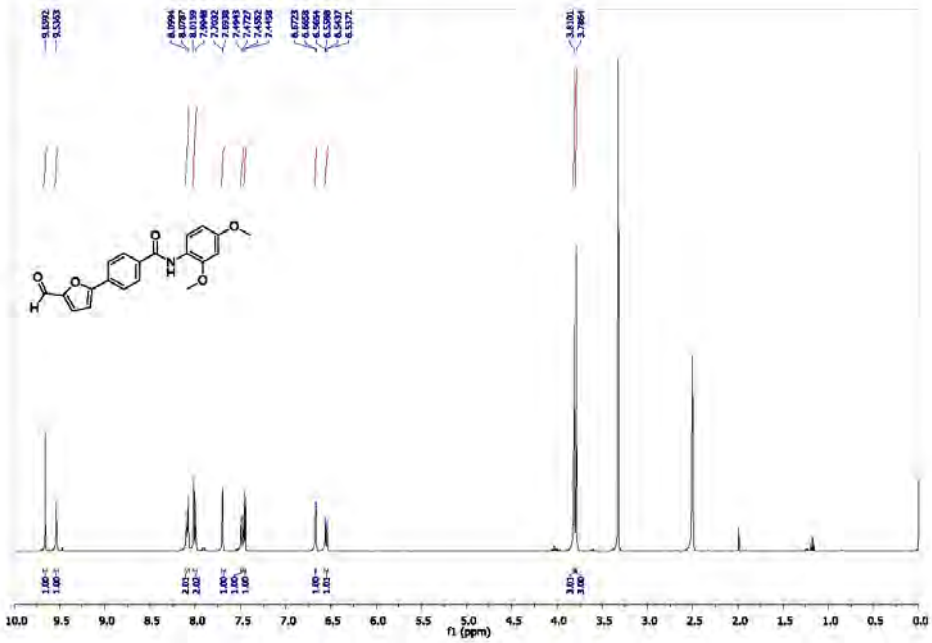

Figure S48: ^{1}H NMR Spectrum (DMSO-d6, 400 MHz) of *N*-(2,4-dimethoxyphenyl)-4-(5-formylfuran-2-yl)benzamide (**12f**).

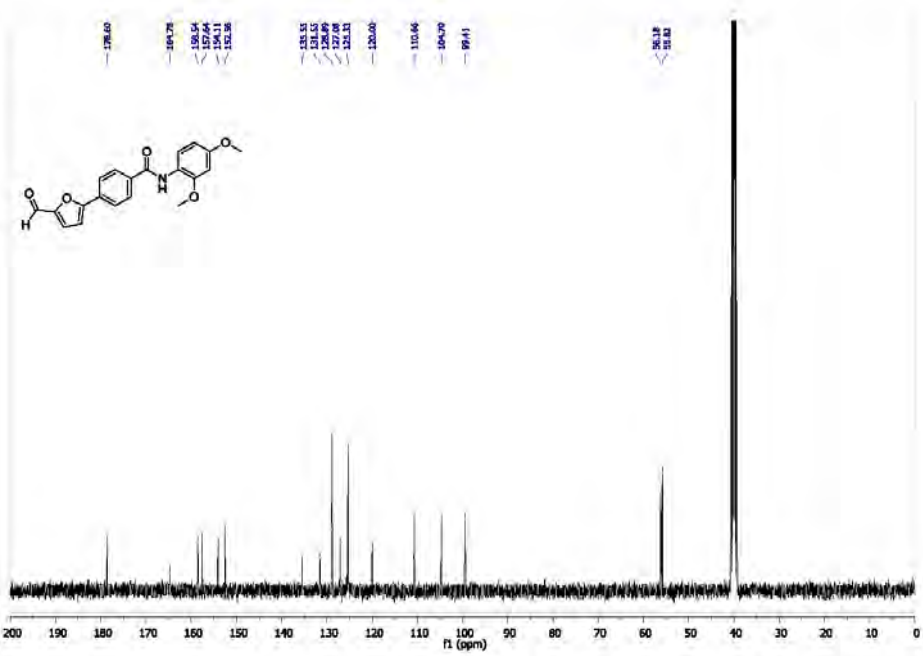

Figure S49: ^{13}C NMR Spectrum (DMSO-d6, 101 MHz) of 5-(4-benzoylphenyl)-2-furancarboxaldehyde (**12f**)

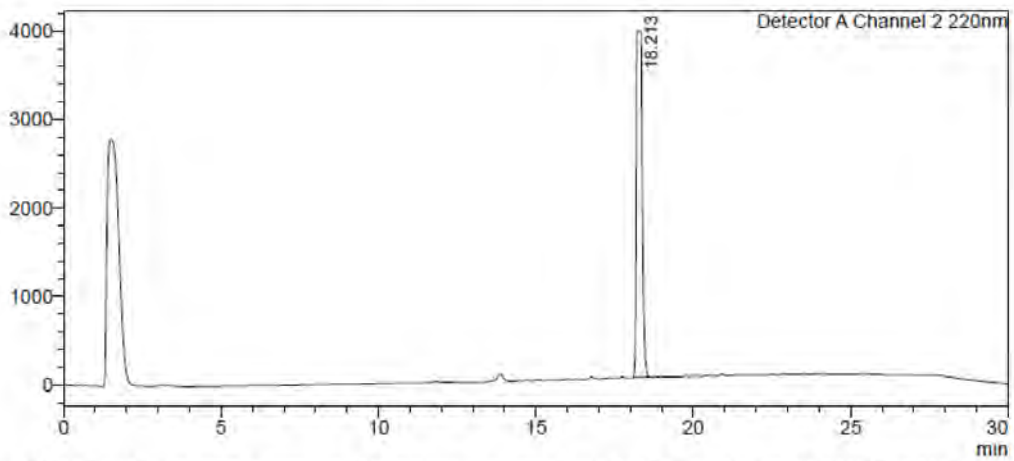

Figure S50: HPLC chromatogram of compound **12f**, RP-HPLC Alltima™ C18 5u 150mm x 4.6 mm, 10-100 % B in 15 min.

S7. Tetrabutylammonium Salt Counterion Variations with FC1032™

5-(4-hydroxyphenyl)-2-furancarboxaldehyde (14)

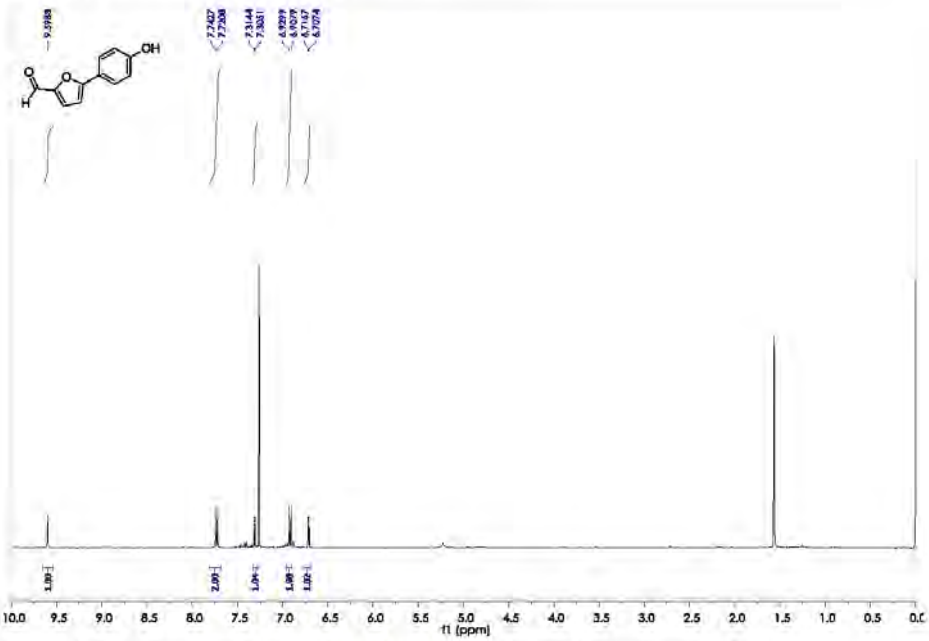

Figure S51: ^{1}H NMR Spectrum ($CDCl_3$, 400 MHz) of 5-(4-hydroxyphenyl)-2-furancarboxaldehyde (**14**).

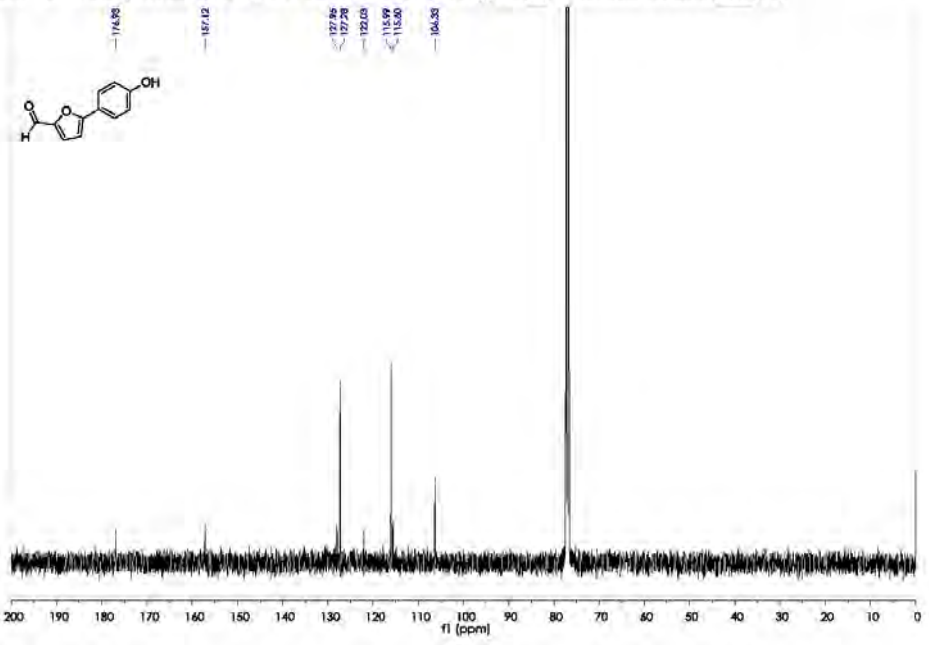

Figure S52: ^{13}C NMR Spectrum ($CDCl_3$, 101 MHz) of 5-(4-hydroxyphenyl)-2-furancarboxaldehyde (**14**).

Table S5: Tetrabutylammonium salt screen using FibreCat® 1032. ***Reagents and Conditions***: (*i*) 5-formyl-2-furanylboroic acid (1 mmol), 4-bromophenol benzyl (**13**) (1 mmol), tetrabutylammonium fluoride trihydrate (3 mmol), MeOH (30 mL), FibreCat® 1032, X-Cube™, 0.5 mL/min, and 120 °C.

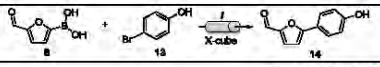

Entry	Tetrabutylammonium salt	Ratio of Peak Area[a]	
		13	14
1	$(Bu)_4N^+F^-$	0.46	1

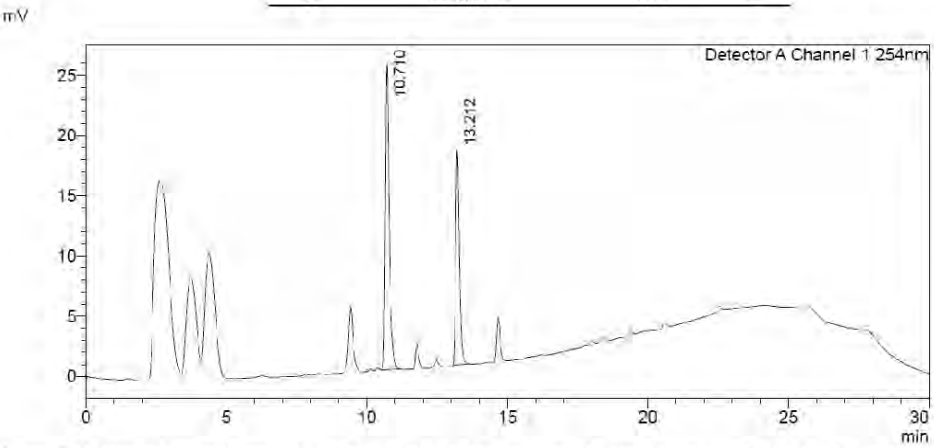

Figure S53: HPLC chromatogram of the crude material obtained from the reaction outlined in table S5 with the peak at 10.7 mins corresponding to the desired product **14** whilst the peak at 13.2 mins corresponds to the aryl bromide starting material **13**. RP-HPLC Alltima™ C18 5u 150mm x 4.6 mm, 10-100 % B in 15 min.

Table S6: Tetrabutylammonium salt screen using FibreCat® 1032. ***Reagents and Conditions***: (*i*) 5-formyl-2-furanylboroic acid (1 mmol), 4-bromophenol benzyl (**13**) (1 mmol), tetrabutylammonium fluoride trihydrate (3 mmol), MeOH (30 mL), FibreCat® 1032, X-Cube™, 0.5 mL/min, and 120 °C.

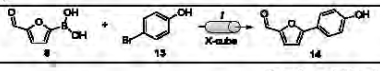

Entry	Tetrabutylammonium salt	Ratio of Peak Area[a]	
		13	14
2	$(Bu)_4N^+Cl^-$	0.65	1

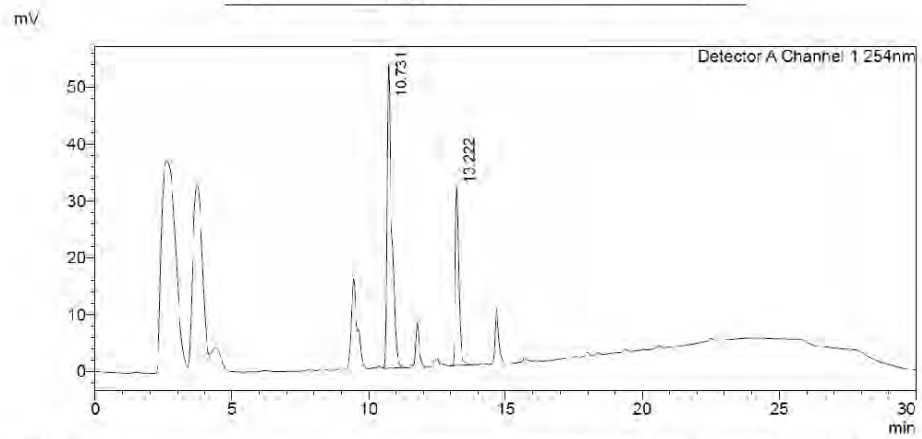

Figure S54: HPLC chromatogram of the crude material obtained from the reaction outlined in table S6 with the peak at 10.7 mins corresponding to the desired product **14** whilst the peak at 13.2 mins corresponds to the aryl bromide starting material **13**. RP-HPLC Alltima™ C18 5u 150mm x 4.6 mm, 10-100 % B in 15 min.

Table S7: Tetrabutylammonium salt screen using FibreCat® 1032. ***Reagents and Conditions***: (*i*) 5-formyl-2-furanylboroic acid (1 mmol), 4-bromophenol benzyl (**13**) (1 mmol), tetrabutylammonium fluoride trihydrate (3 mmol), MeOH (30 mL), FibreCat® 1032, X-Cube™, 0.5 mL/min, and 120 °C.

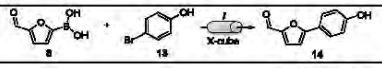

Entry	Tetrabutylammonium salt	Ratio of Peak Area[a]	
		13	14
3	$(Bu)_4N^+Br^-$	21.82	1

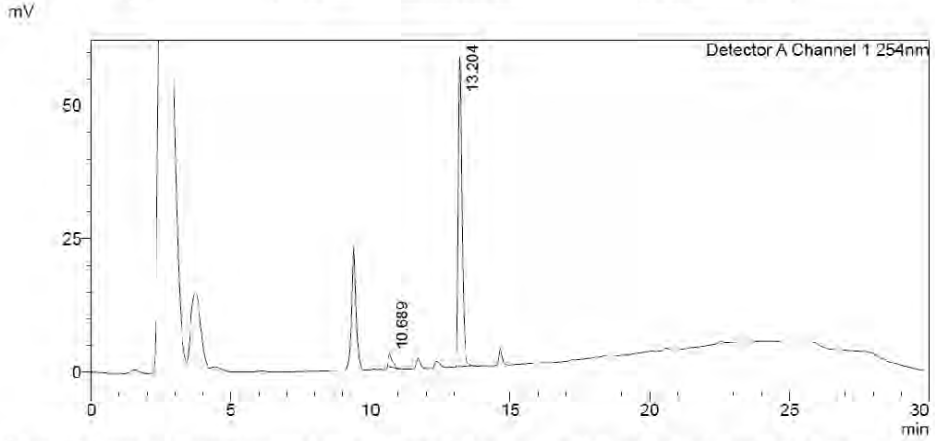

Figure S55: HPLC chromatogram of the crude material obtained from the reaction outlined in table S7 with the peak at 10.7 mins corresponding to the desired product **14** whilst the peak at 13.2 mins corresponds to the aryl bromide starting material **13**. RP-HPLC Alltima™ C18 5u 150mm x 4.6 mm, 10-100 % B in 15 min.

Table S8: Tetrabutylammonium salt screen using FibreCat® 1032. ***Reagents and Conditions***: (*i*) 5-formyl-2-furanylboroic acid (1 mmol), 4-bromophenol benzyl (**13**) (1 mmol), tetrabutylammonium fluoride trihydrate (3 mmol), MeOH (30 mL), FibreCat® 1032, X-Cube™, 0.5 mL/min, and 120 °C.

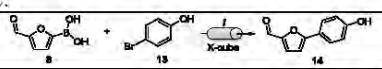

Entry	Tetrabutylammonium salt	Ratio of Peak Area[a]	
		13	14
4	$(Bu)_4N^+I^-$	30.11	1

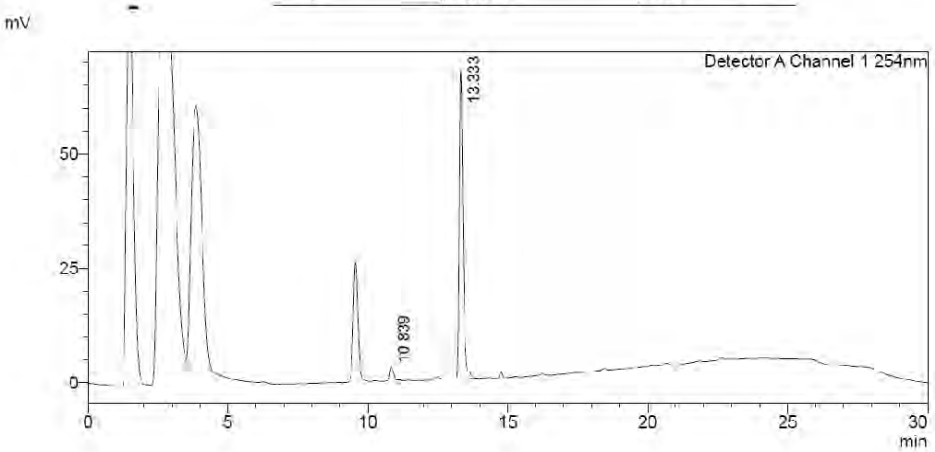

Figure S56: HPLC chromatogram of the crude material obtained from the reaction outlined in table S8 with the peak at 10.8 mins corresponding to the desired product **14** whilst the peak at 13.3 mins corresponds to the aryl bromide starting material **13**. RP-HPLC Alltima™ C18 5u 150mm x 4.6 mm, 10-100 % B in 15 min.

Table S9: Tetrabutylammonium salt screen using FibreCat® 1032. ***Reagents and Conditions***: (*i*) 5-formyl-2-furanylboroic acid (1 mmol), 4-bromophenol benzyl (**13**) (1 mmol), tetrabutylammonium fluoride trihydrate (3 mmol), MeOH (30 mL), FibreCat® 1032, X-Cube™, 0.5 mL/min, and 120 °C.

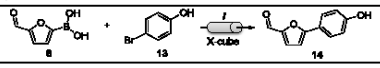

Entry	Tetrabutylammonium salt	Ratio of Peak Area[a]	
		13	**14**
5	$(Bu)_4N^+BF_4^-$	2.47	1

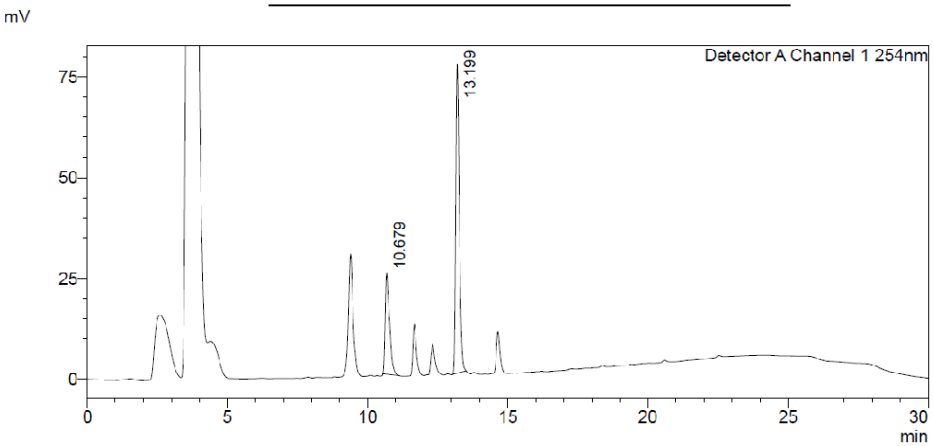

Figure S57: HPLC chromatogram of the crude material obtained from the reaction outlined in table S9 with the peak at 10.7 mins corresponding to the desired product **14** whilst the peak at 13.2 mins corresponds to the aryl bromide starting material **13**. RP-HPLC Alltima™ C18 5u 150mm x 4.6 mm, 10-100 % B in 15 min.

Table S10: Tetrabutylammonium salt screen using FibreCat® 1032. ***Reagents and Conditions***: (*i*) 5-formyl-2-furanylboroic acid (1 mmol), 4-bromophenol benzyl (**13**) (1 mmol), tetrabutylammonium fluoride trihydrate (3 mmol), MeOH (30 mL), FibreCat® 1032, X-Cube™, 0.5 mL/min, and 120 °C.

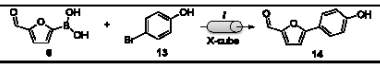

Entry	Tetrabutylammonium salt	Ratio of Peak Area[a]	
		13	**14**
6	$(Bu)_4N^+HSO_4^-$	1.51	1

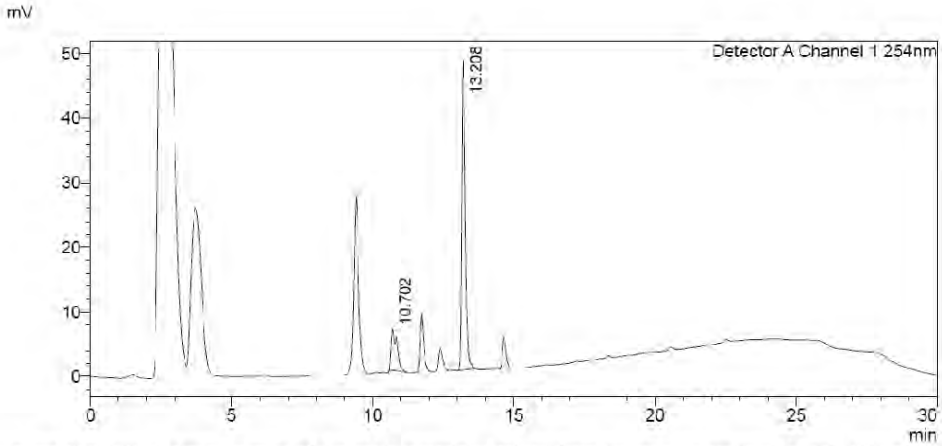

Figure S58: HPLC chromatogram of the crude material obtained from the reaction outlined in table S10 with the peak at 10.7 mins corresponding to the desired product **14** whilst the peak at 13.2 mins corresponds to the aryl bromide starting material **13**. RP-HPLC Alltima™ C18 5u 150mm x 4.6 mm, 10-100 % B in 15 min.

Table S11: Tetrabutylammonium salt screen using FibreCat® 1032. ***Reagents and Conditions***: (*i*) 5-formyl-2-furanylboroic acid (1 mmol), 4-bromophenol benzyl (**13**) (1 mmol), tetrabutylammonium fluoride trihydrate (3 mmol), MeOH (30 mL), FibreCat® 1032, X-Cube™, 0.5 mL/min, and 120 °C.

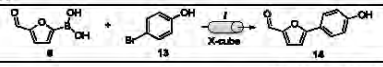

Entry	Tetrabutylammonium salt	Ratio of Peak Area[a]	
		13	14
7	$(Bu)_4N^+OAc^-$	0.22	1

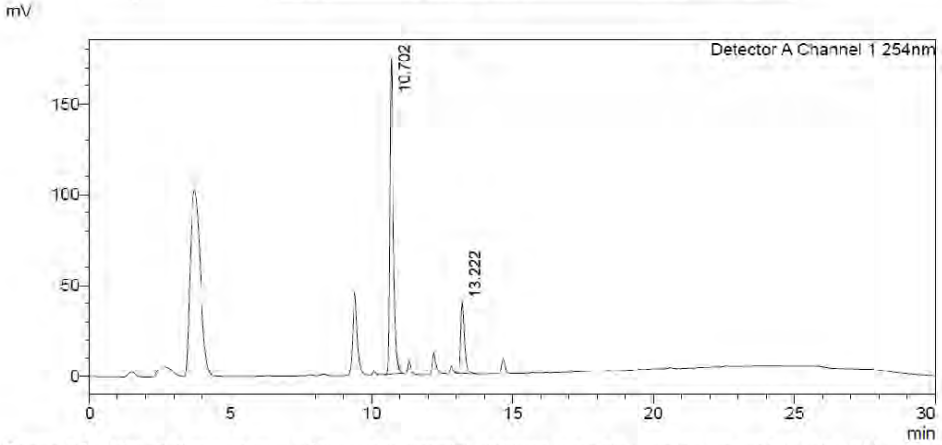

Figure S59: HPLC chromatogram of the crude material obtained from the reaction outlined in table S11 with the peak at 10.7 mins corresponding to the desired product **14** whilst the peak at 13.2 mins corresponds to the aryl bromide starting material **13**. RP-HPLC Alltima™ C18 5u 150mm x 4.6 mm, 10-100 % B in 15 min.

Table S12: Tetrabutylammonium salt screen using FibreCat® 1032. ***Reagents and Conditions***: (***i***) 5-formyl-2-furanylboroic acid (1 mmol), 4-bromophenol benzyl (**13**) (1 mmol), tetrabutylammonium fluoride trihydrate (3 mmol), MeOH (30 mL), FibreCat® 1032, X-Cube™, 0.5 mL/min, and 120 °C.

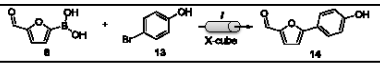

Entry	Tetrabutylammonium salt	Ratio of Peak Area[a]	
		13	14
8	$(Bu)_4N^+F^- + Cs_2CO_3$	0.20	1

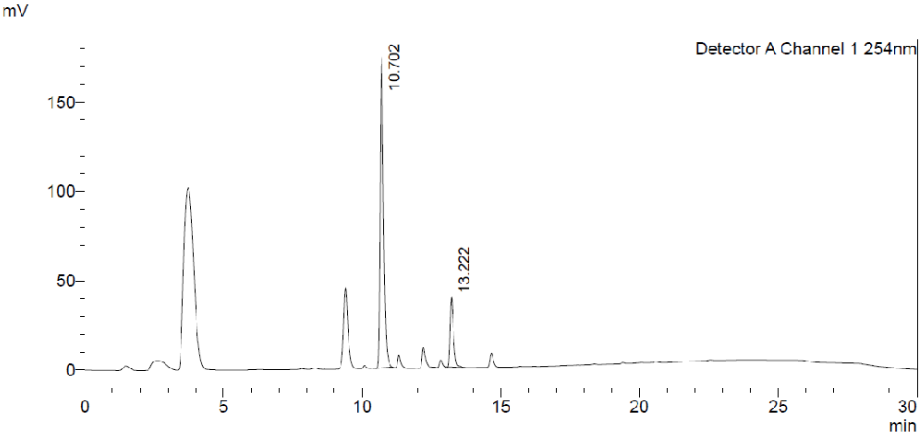

Figure S60: HPLC chromatogram of the crude material obtained from the reaction outlined in table S12 with the peak at 10.7 mins corresponding to the desired product **14** whilst the peak at 13.2 mins corresponds to the aryl bromide starting material **13**. RP-HPLC Alltima™ C18 5u 150mm x 4.6 mm, 10-100 % B in 15 min.

Table S13: Tetrabutylammonium salt screen using FibreCat® 1032. ***Reagents and Conditions***: (***i***) 5-formyl-2-furanylboroic acid (1 mmol), 4-bromophenol benzyl (**10**) (1 mmol), tetrabutylammonium fluoride trihydrate (3 mmol), MeOH (30 mL), FibreCat® 1032, X-Cube™, 0.5 mL/min, and 120 °C.

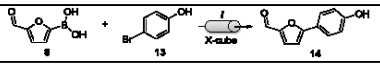

Entry	Tetrabutylammonium salt	Ratio of Peak Area[a]	
		13	14
9	$(Bu)_4N^+OAc^- + Cs_2CO_3$	0.24	1

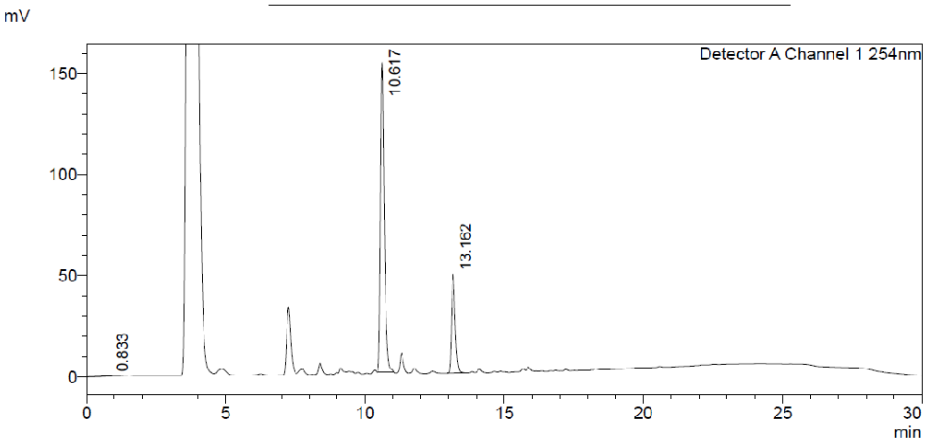

Figure S61: HPLC chromatogram of the crude material obtained from the reaction outlined in table S13 with the peak at 10.6 mins corresponding to the desired product **14** whilst the peak at 13.2 mins corresponds to the aryl bromide starting material **13**. RP-HPLC Alltima™ C18 5u 150mm x 4.6 mm, 10-100 % B in 15 min.

S8. General Procedure 2 using $(Bu)_4N$+OAc- with CatCart™ $PdCl_2(PPh_3)_2$-DVB

5-(3-(dimethylamino)phenyl)-2-furancarboxaldehyde (15a)

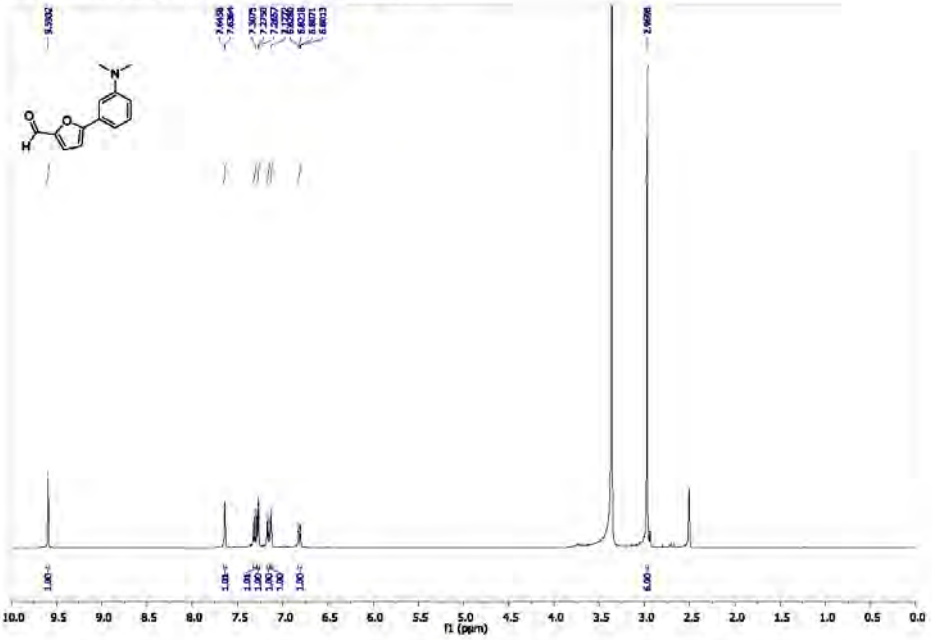

Figure S62: ^{1}H NMR Spectrum (DMSO-d6, 400 MHz) of 5-(3-(dimethylamino)phenyl)-2-furancarboxaldehyde (**15a**)

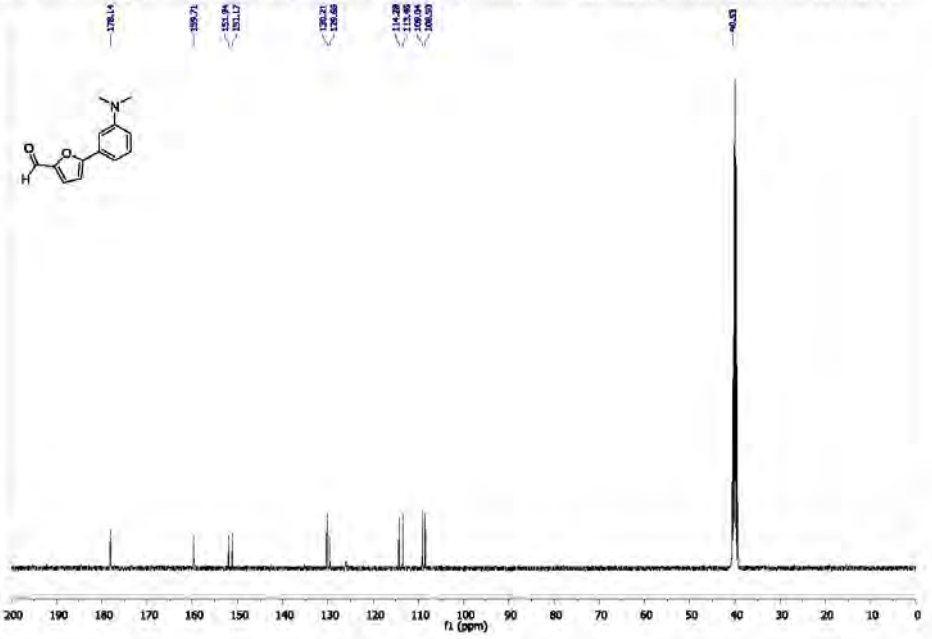

Figure S63: ^{13}C NMR Spectrum (DMSO-d6, 101 MHz) of 5-(3-(dimethylamino)phenyl)-2-furancarboxaldehyde (**15a**).

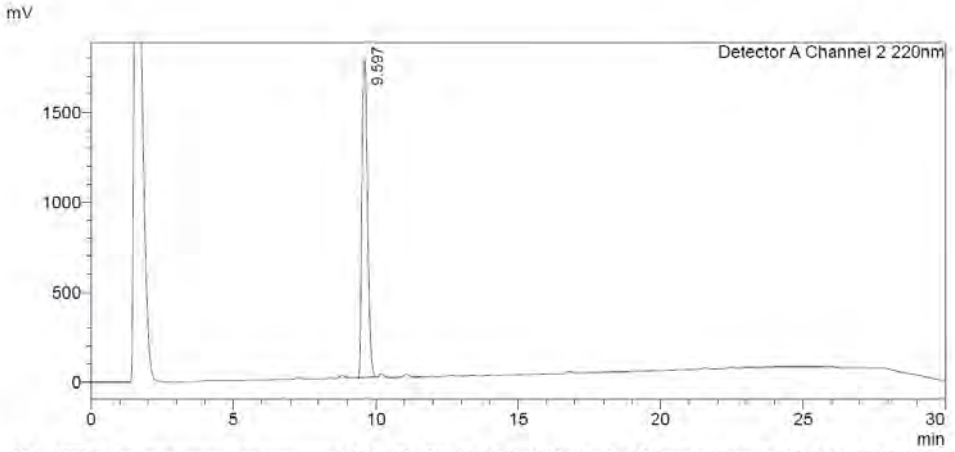

Figure S64: HPLC chromatogram of compound **15a**, RP-HPLC Alltima™ C18 5u 150mm x 4.6 mm, 10-100 % B in 15 min.

5-(4-(dimethylamino)phenyl)-2-furancarboxaldehyde (15b)

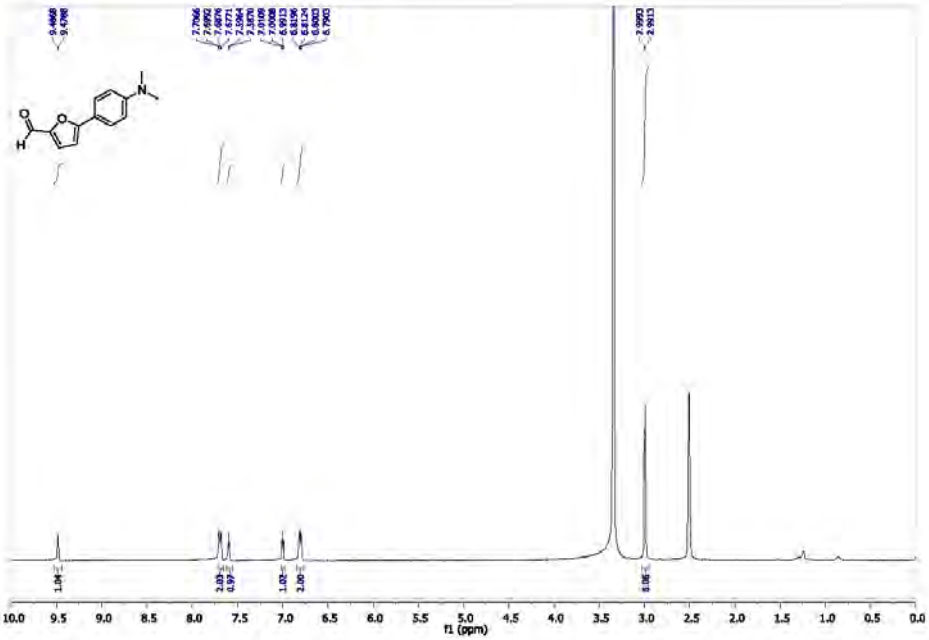

Figure S65: ^{1}H NMR Spectrum (DMSO-d6, 400 MHz) of 5-(4-(dimethylamino)phenyl)-2-furancarboxaldehyde (**15b**)

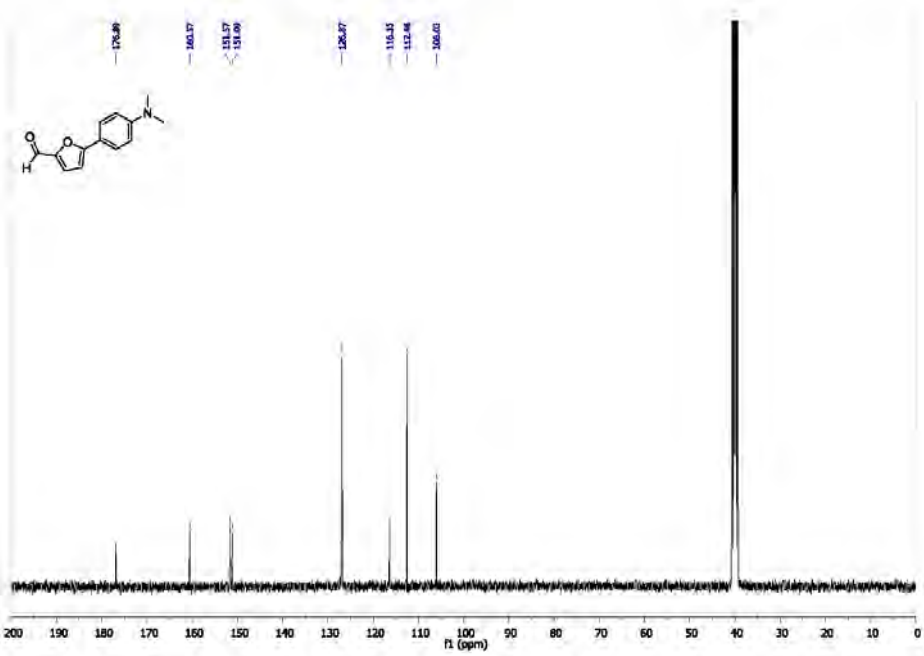

Figure S66: ^{13}C NMR Spectrum (DMSO-d6, 101 MHz) of 5-(4-(dimethylamino)phenyl)-2-furancarboxaldehyde (**15b**).

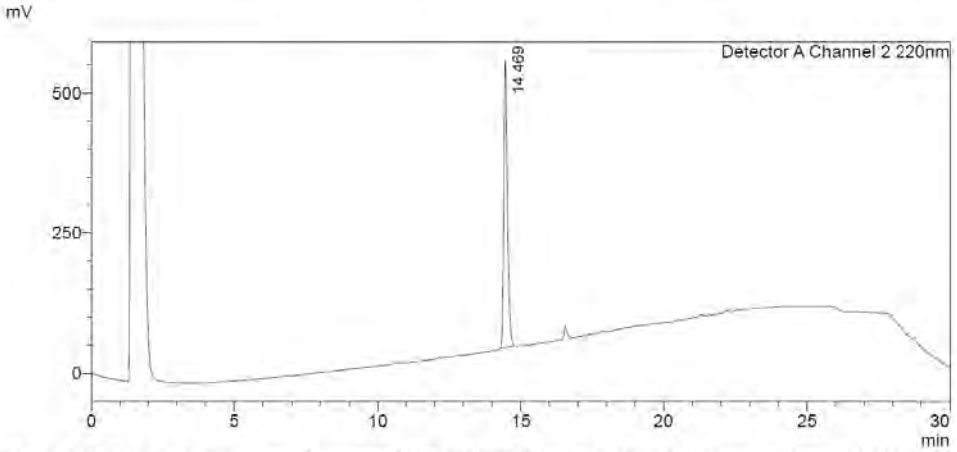

Figure S67: HPLC chromatogram of compound **15b**, RP-HPLC Alltima™ C18 5u 150mm x 4.6 mm, 10-100 % B in 15 min.

5-(4-methoxyphenyl)-2-furancarboxaldehyde (15c)

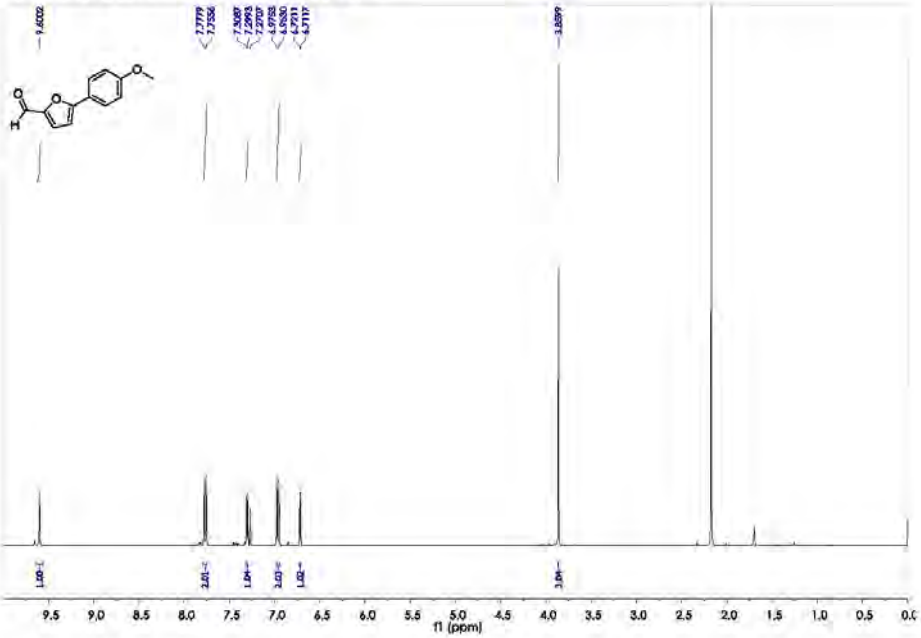

Fig S68: ^{1}H NMR Spectrum ($CDCl_3$, 400 MHz) of 5-(4-methoxyphenyl)-2-furancarboxaldehyde (**15c**).

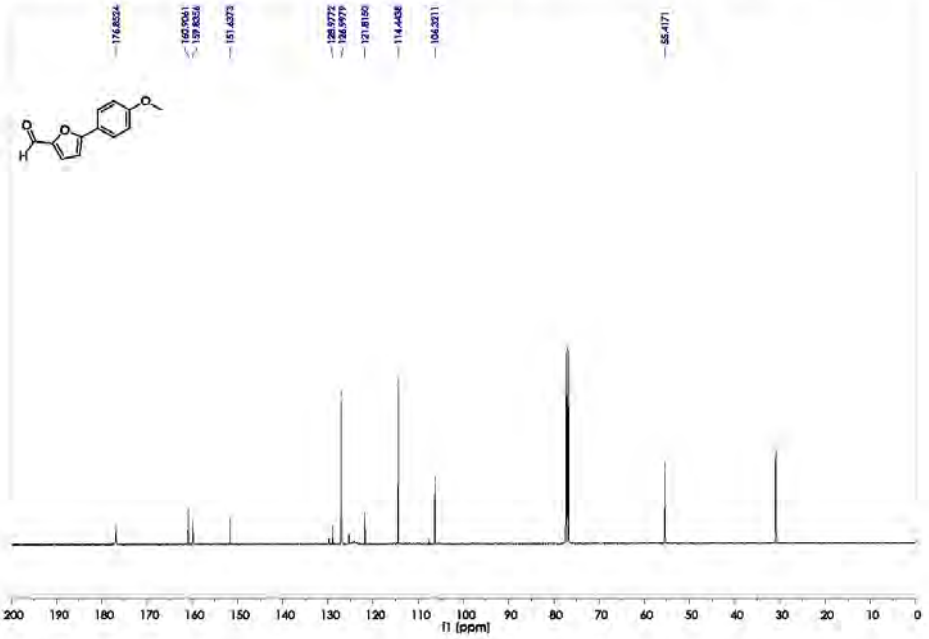

Figure S69: ^{13}C NMR Spectrum ($CDCl_3$, 101 MHz) of 5-(4-methoxyphenyl)-2-furancarboxaldehyde (**15c**).

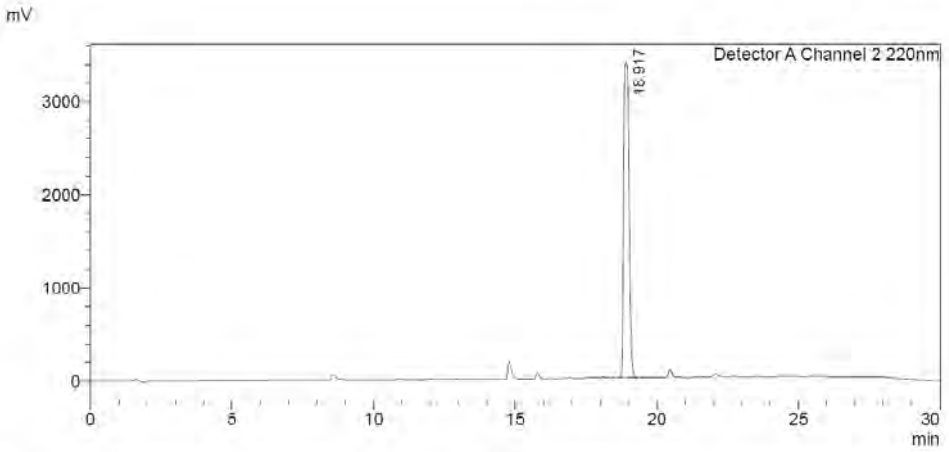

Figure S70: HPLC chromatogram of compound **15c**, RP-HPLC Alltima™ C18 5u 150mm x 4.6 mm, 10-100 % B in 15 min.

5-(1*H*-indol-6-yl)-2-furancarboxaldehyde (15d)

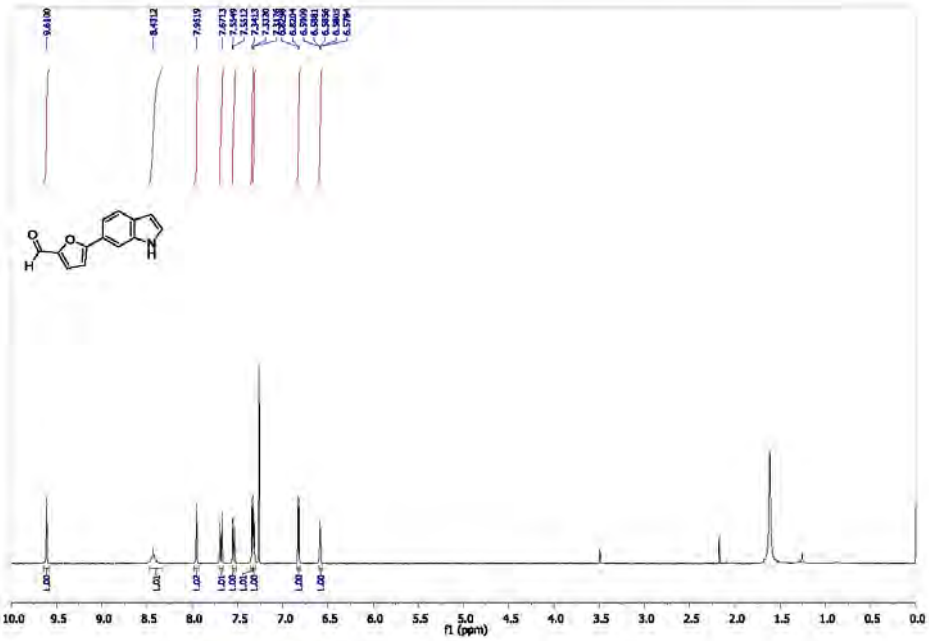

Figure S71: ^{1}H NMR Spectrum ($CDCl_3$, 400 MHz) of 5-(1*H*-indol-6-yl)-2-furancarboxaldehyde (**15d**).

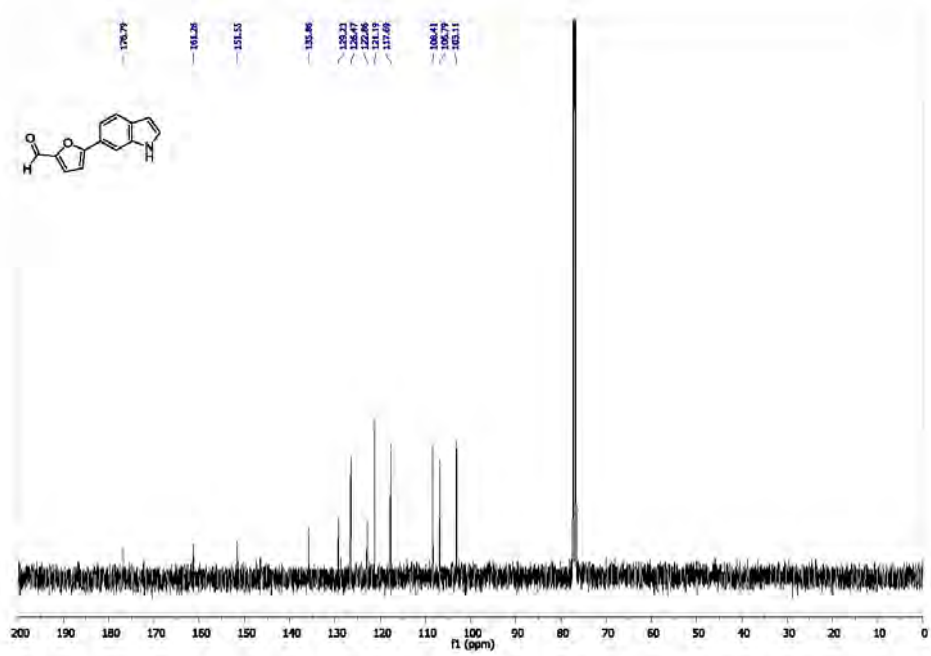

Figure S72: ^{13}C NMR Spectrum ($CDCl_3$, 101 MHz) of 5-(1*H*-indol-6-yl)-2-furancarboxaldehyde (**15d**).

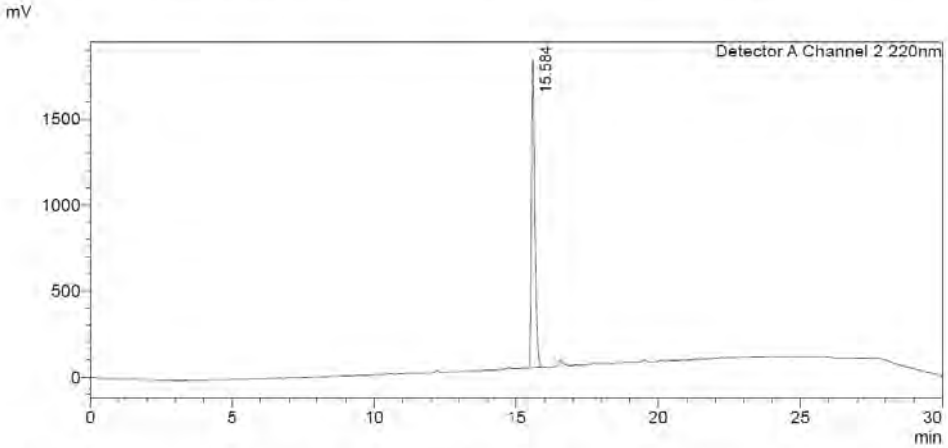

Figure S73: HPLC chromatogram of compound **15d**, RP-HPLC Alltima™ C18 5u 150mm x 4.6 mm, 10-100 % B in 15 min.

5-(4-benzoylphenyl)-2-furancarboxaldehyde (15e)

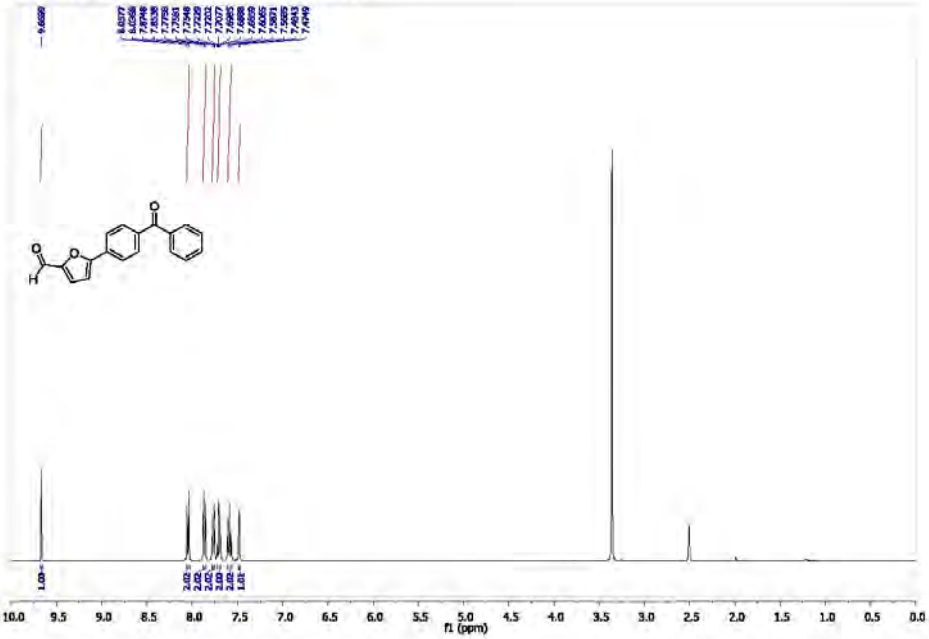

Figure S74 : ^{1}H NMR Spectrum (DMSO-d6, 400 MHz) of 5-(4-benzoylphenyl)-2-furancarboxaldehyde (**15e**).

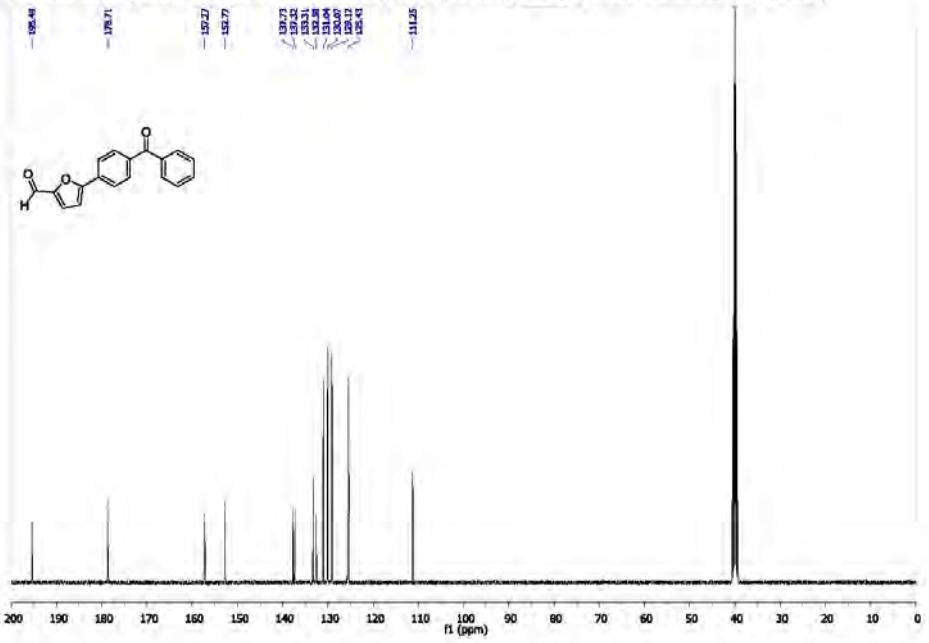

Figure S75: ^{13}C NMR Spectrum (DMSO-d6, 101 MHz) of 5-(4-benzoylphenyl)-2-furancarboxaldehyde (**15e**).

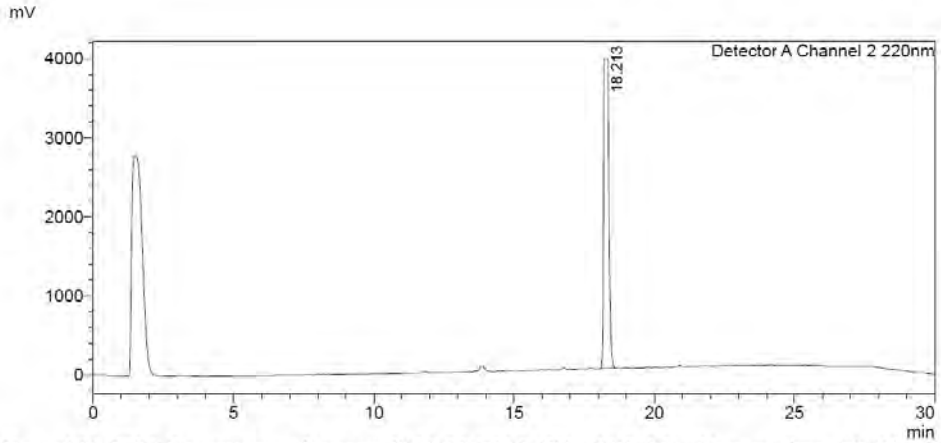

Figure S76: HPLC chromatogram of compound **15d**, RP-HPLC Alltima™ C18 5u 150mm x 4.6 mm, 10-100 % B in 15 min.

5-(3-formylphenyl)furan-2-carbaldehyde (15f)

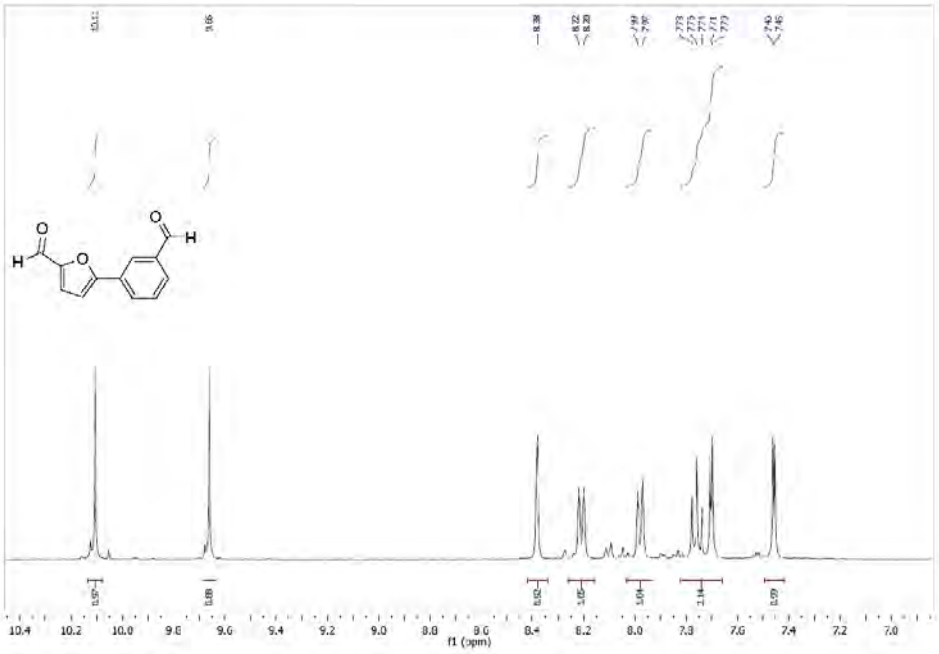

Figure S77 : ^{1}H NMR Spectrum (DMSO-d6, 400 MHz) of 5-(3-formylphenyl)furan-2-carbaldehyde (**15f**).

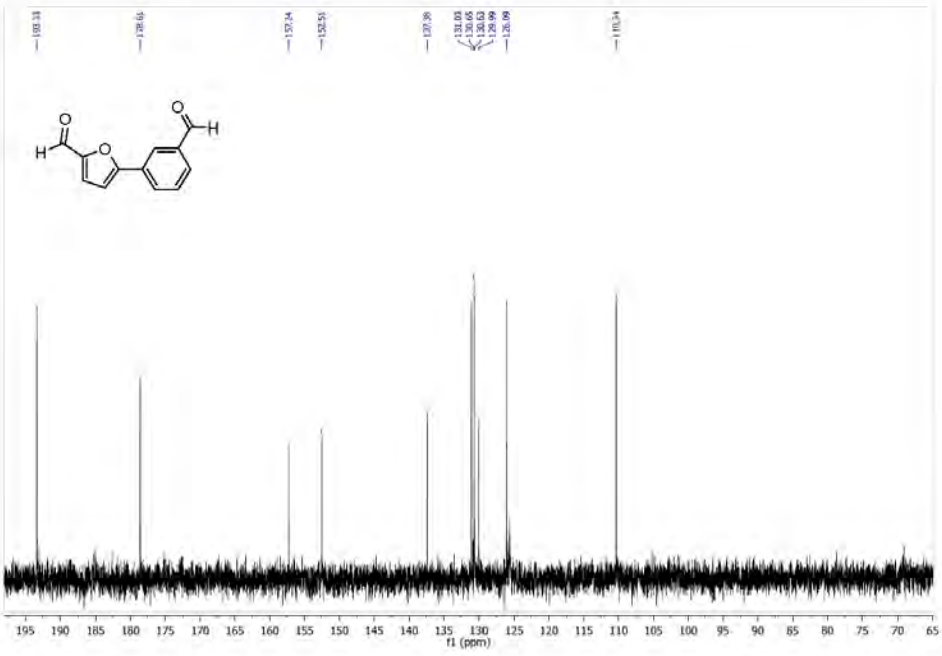

Figure S78: ^{13}C NMR Spectrum (DMSO-d6, 101 MHz) of 5-(3-formylphenyl)furan-2-carbaldehyde (**15f**).

***N*-(6-((2S,6R)-2,6-dimethylmorpholino)pyridin-3-yl)-2-methyl-4'-(trifluoromethoxy)biphenyl-3-carboxamide (LDE225) (18)**

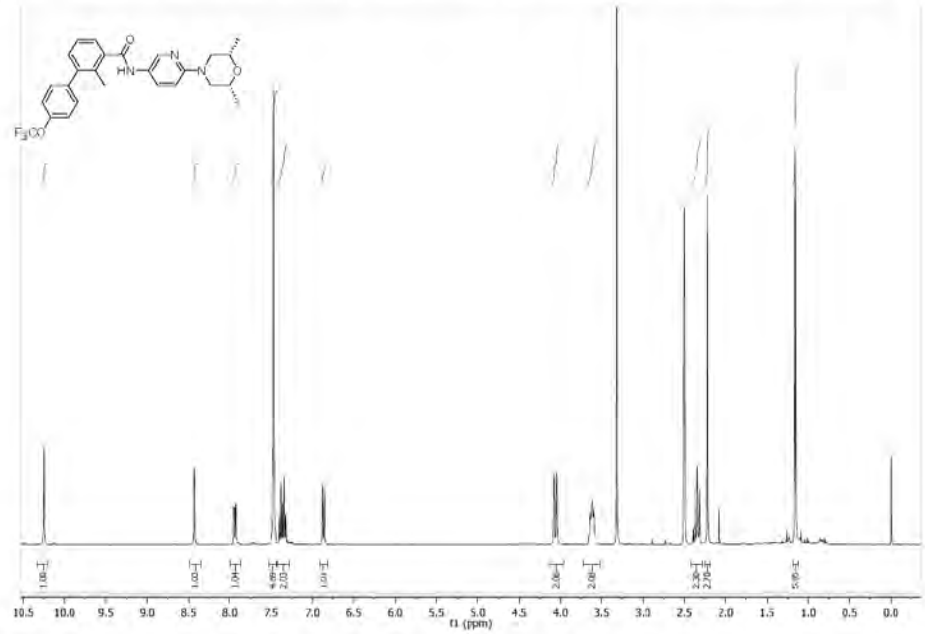

Figure S80: ^{1}H NMR Spectrum (DMSO-d6, 400 MHz) of *N*-(6-((2S,6R)-2,6-dimethylmorpholino)pyridin-3-yl)-2-methyl-4'-(trifluoromethoxy)biphenyl-3-carboxamide (**18**).

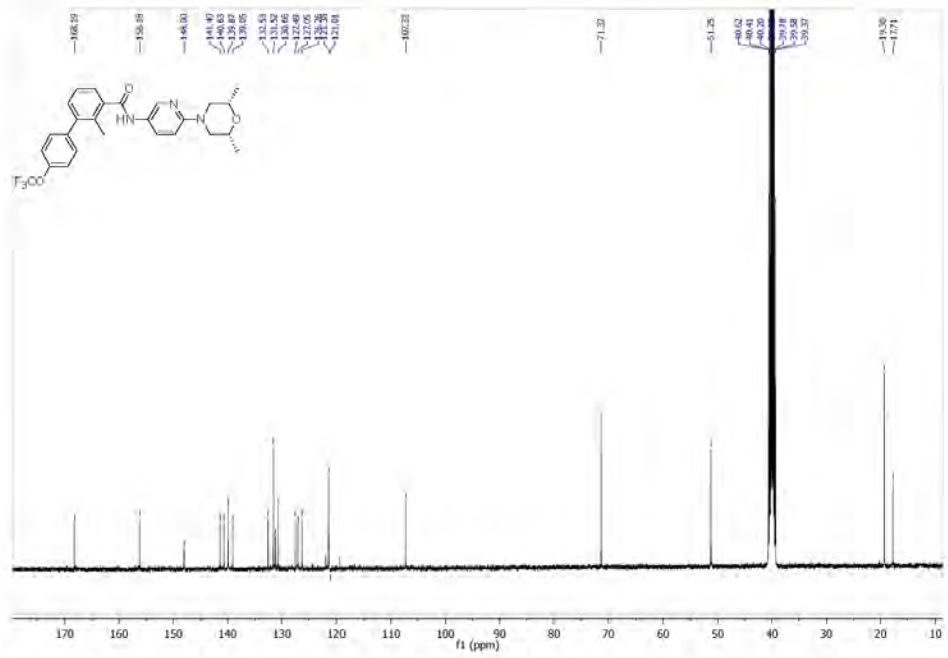

Figure S81: ^{13}C NMR Spectrum (DMSO-d6, 101 MHz) of 5 *N*-(6-((2S,6R)-2,6-dimethylmorpholino)pyridin-3-yl)-2-methyl-4'-(trifluoromethoxy)biphenyl-3-carboxamide (**18**).

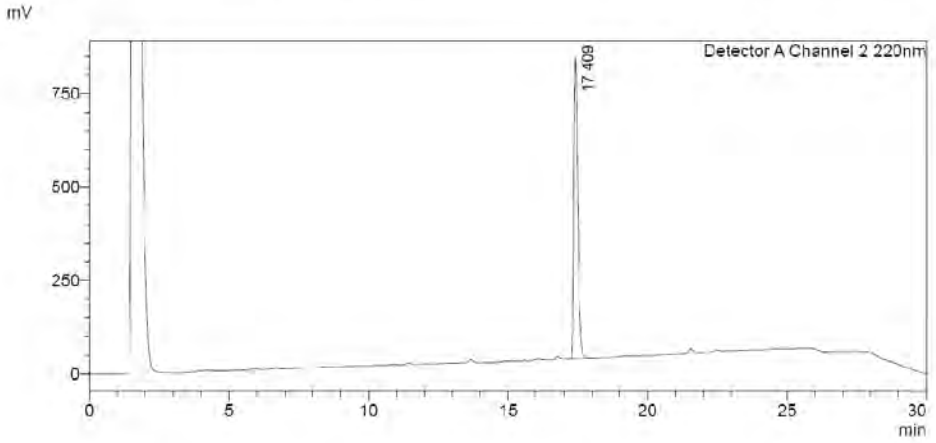

Figure S82: HPLC chromatogram of compound **18**, RP-HPLC Alltima™ C18 5u 150mm x 4.6 mm, 10-100 % B in 15 min.

Australian Government
National Measurement Institute

QUALITY ASSURANCE REPORT

Client: **UNIVERSITY OF WESTERN SYDNEY**

NMI QA Report No: **UNIW32/140910T1** **Sample Matrix:** Liquid
Solid

Analyte	Method	LOR	Blank	Duplicates			Recoveries	
				Sample	Duplicate	RPD	LCS	Matrix Spike
		ug/L	ug/L	ug/L	ug/L	%	%	
Inorganics Section				**N14/022318**				**N14/022318**
Palladium	NT2.49	1	<1	42	43	2	104	100
		mg/kg	mg/kg	mg/kg	mg/kg			
Palladium	NT2.49	0.5	<0.5	ND	ND	ND	104	ND

Filename = K:\inorganics\Quality System\QA Reports\TE\QAR2014\Food & Mis\

Legend:
Acceptable recovery is 75-120%.
Acceptable RPDs on duplicates is 44% at concentrations >5 times LOR. Greater RPD may be expected at <5 times LOR.
LOR = Limit Of Reporting
RPD = Relative Percent Difference
LCS = Laboratory Control Sample.
ND = Not Determined
NA = Not Applicable
#: Spike level is less than 50% of the sample's concentration, hence the recovery data is not reliable.
**: reference value not available

Comments:
Results greater than ten times LOR have been rounded to two significant figures.

Signed:

Dr Michael Wu
Inorganics Manager, NMI-North Ryde
Date: **26/09/2014**

Australian Government

National Measurement Institute

REPORT OF ANALYSIS

Report No. RN1038128

Client	: UNIVERSITY OF WESTERN SYDNEY	**Job No.**	: UNIW32/140910
	SCHOOL OF MEDICINE - BUILDING 30	**Quote No.**	: QT-02021
	CAMPBELLTOWN CAMPUS	**Order No.**	:
	CAMPBELLTOWN NSW 2560	**Date Sampled**	:
		Date Received	: 10-SEP-2014
Attention	DAVID HARMAN	**Sampled By**	: CLIENT
Project Name :			
Your Client Services Manager	: RICHARD COGHLAN	**Phone**	: (02) 94490161

Lab Reg No.	Sample Ref	Sample Description
N14/022316	TP8B4	LIQUID
N14/022317	TP174B3	LIQUID
N14/022318	TP188B3	LIQUID

Lab Reg No.		N14/022316	N14/022317	N14/022318		
Sample Reference	Units	TP8B4	TP174B3	TP188B3		
Filtered Trace Elements by ICP						
Palladium	ug/L	39	29	43		

N14/022316
- N14/022318
Method Used: NMI NT 2.49.

Ling Shuang Lu, Analyst
Inorganics - NSW
Accreditation No. 198

26-SEP-2014

NATA
ACCREDITED FOR TECHNICAL COMPETENCE

Accredited for compliance with ISO/IEC 17025.
This report shall not be reproduced except in full.
Results relate only to the sample(s) tested.

This Report supersedes reports: *RN1038125*

Australian Government

National Measurement Institute

REPORT OF ANALYSIS

Report No. RN1038127

Client	: UNIVERSITY OF WESTERN SYDNEY	**Job No.**	: UNIW32/140910
	SCHOOL OF MEDICINE - BUILDING 30	**Quote No.**	: QT-02021
	CAMPBELLTOWN CAMPUS	**Order No.**	:
	CAMPBELLTOWN NSW 2560	**Date Sampled**	:
		Date Received	: 10-SEP-2014
Attention	DAVID HARMAN	**Sampled By**	: CLIENT
Project Name :			
Your Client Services Manager	: RICHARD COGHLAN	**Phone**	: (02) 94490161

Lab Reg No.	Sample Ref	Sample Description
N14/022313	TP15B4	SOLID
N14/022314	TP176B3	SOLID
N14/022315	TP188B3	SOLID

Lab Reg No.		N14/022313	N14/022314	N14/022315		
Sample Reference	Units	TP15B4	TP176B3	TP188B3		Method
Total Recoverable Trace Elements by ICP						
Palladium	mg/kg	5.2	340	52		NT2_49

Ling Shuang Lu, Analyst
Inorganics - NSW
Accreditation No. 198

26-SEP-2014

ACCREDITED FOR TECHNICAL COMPETENCE

Accredited for compliance with ISO/IEC 17025.
This report shall not be reproduced except in full.
Results relate only to the sample(s) tested.

This Report supersedes reports: *RN1038058*

Australian Government

National Measurement Institute

REPORT OF ANALYSIS

Report No. RN1038127

Client	: UNIVERSITY OF WESTERN SYDNEY	**Job No.**	: UNIW32/140910
	SCHOOL OF MEDICINE - BUILDING 30	**Quote No.**	: QT-02021
	CAMPBELLTOWN CAMPUS	**Order No.**	:
	CAMPBELLTOWN NSW 2560	**Date Sampled**	:
		Date Received	: 10-SEP-2014
Attention	DAVID HARMAN	**Sampled By**	: CLIENT
Project Name :			
Your Client Services Manager	: RICHARD COGHLAN	**Phone**	: (02) 94490161

Lab Reg No.	Sample Ref	Sample Description
N14/022313	TP15B4	SOLID
N14/022314	TP176B3	SOLID
N14/022315	TP188B3	SOLID

Lab Reg No.		N14/022313	N14/022314	N14/022315		
Sample Reference	Units	TP15B4	TP176B3	TP188B3		Method
Total Recoverable Trace Elements by ICP						
Palladium	mg/kg	5.2	340	52		NT2_49

Ling Shuang Lu, Analyst
Inorganics - NSW
Accreditation No. 198

26-SEP-2014

ACCREDITED FOR TECHNICAL COMPETENCE

This Report supersedes reports: *RN1038058*

8.2. Appendix to Chapter 3

8.2.1 Biological investigation

§ Components of the HSP detected in TCAM-2 cell line

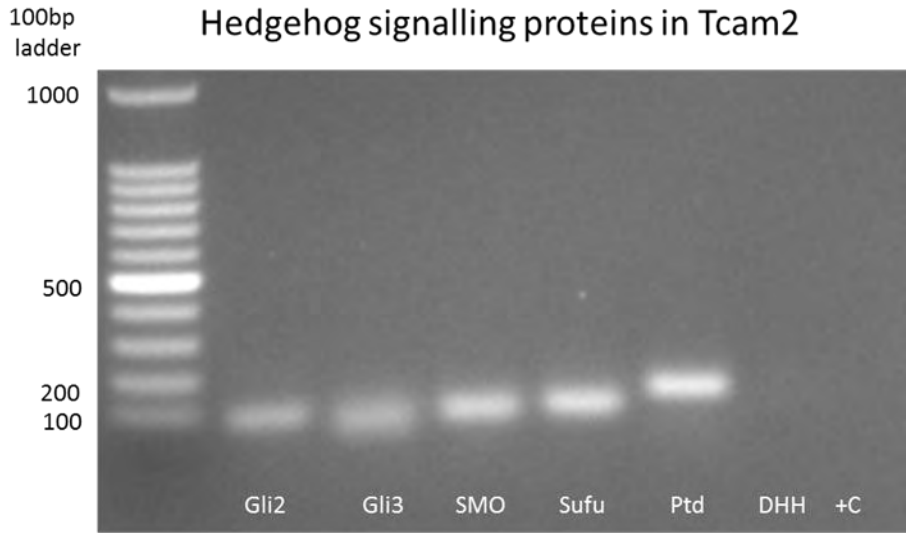

§ Cytotoxicity of indole analogues against TCAM-2 cells

Table 4. Cytotoxicity (**compounds 7b, 40 − 50**) at 10 µM concentration against TCAM-2 cell line was measured after 72 hours of incubation, with DMSO and Triton X (Red) (1%) as controls. Only compounds **5**, **23**, and **24** expressed a growth inhibition greater than 50% and were further investigated for their dose responses to generate the GI_{50} (n=2)

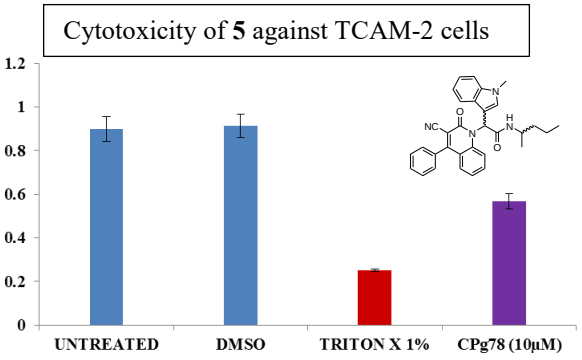

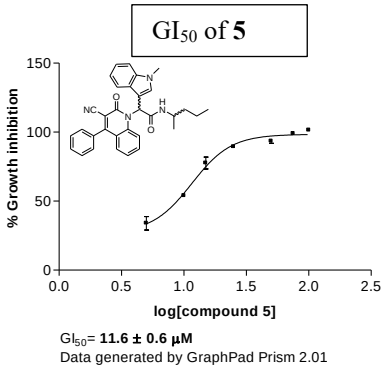

Cytotoxicity of **20** against TCAM-2 cells

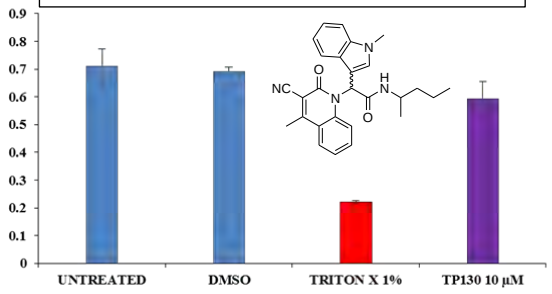

Cytotoxicity of **21** against TCAM-2 cells

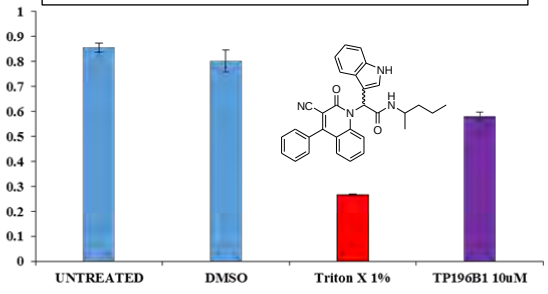

Cytotoxicity of **22** against TCAM-2 cells

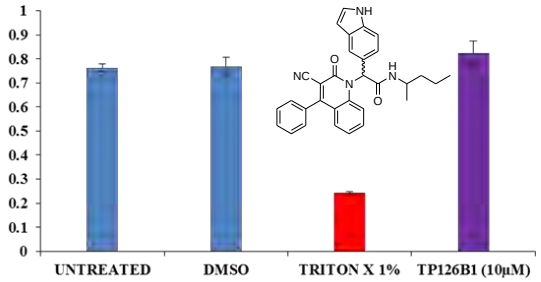

Cytotoxicity of **25** against TCAM-2 cells

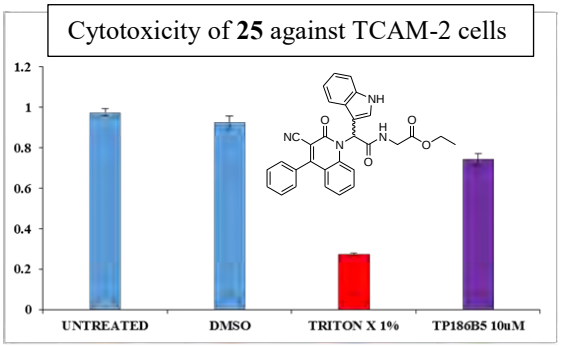

Cytotoxicity of **23** against TCAM-2 cells

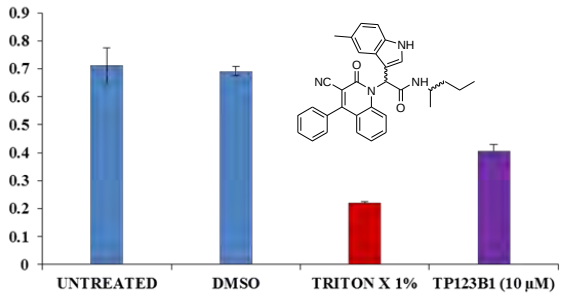

GI_{50} of **23**

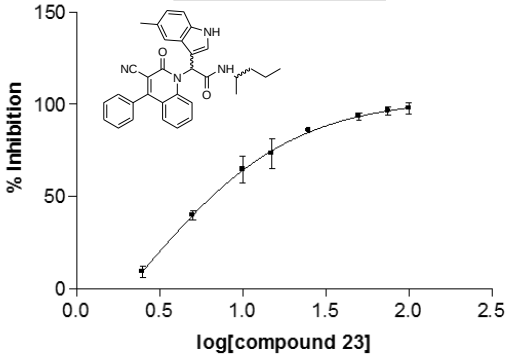

GI_{50} = **2.9 ± 0.0 µM**
Data generated by GraphPad Prism 2.01

Cytotoxicity of **24** against TCAM-2 cells

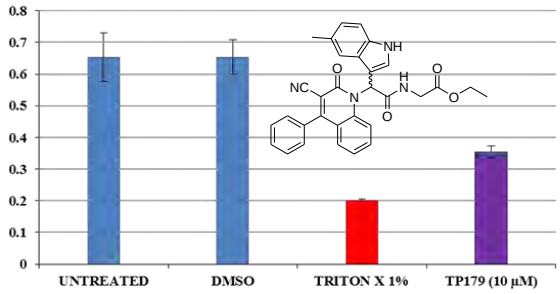

GI_{50} of **24**

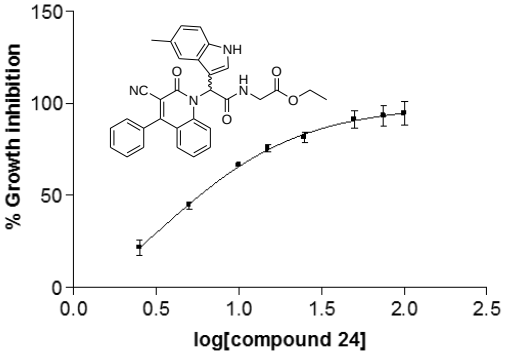

GI_{50} = **3.1 ± 0.4 µM**

Data generated by GraphPad Prism 2.01

Cytotoxicity of **26** against TCAM-2 cells

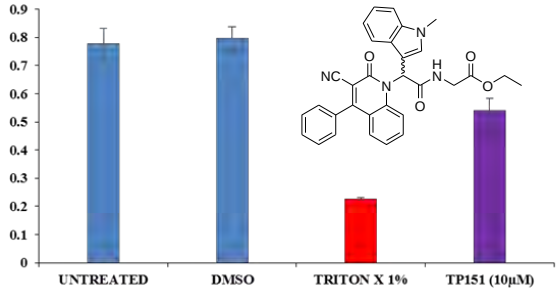

Cytotoxicity of **27** against TCAM-2 cells

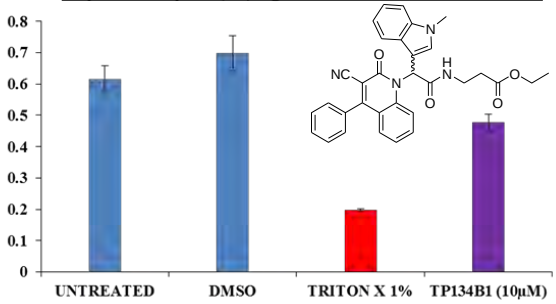

Cytotoxicity of **28** against TCAM-2 cells

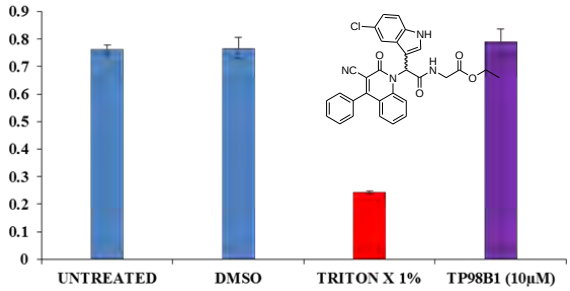

Cytotoxicity of **29** against TCAM-2 cells

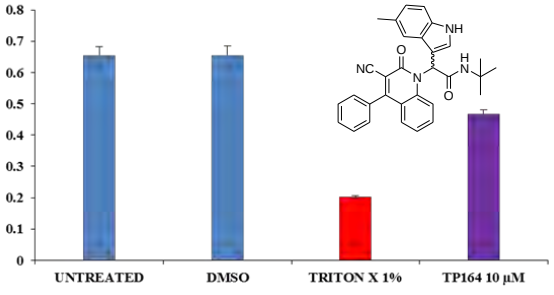

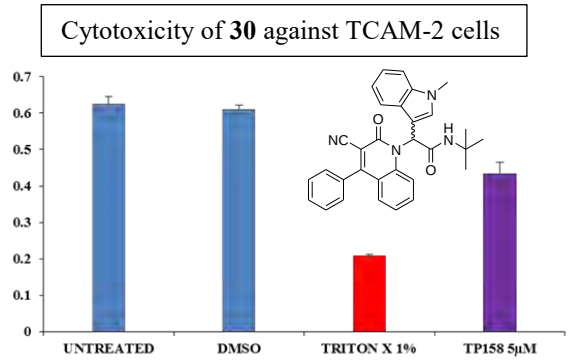

§ Negligible cytotoxicity of 5, 23, and 24 against Shh LIGHT 2 cell line up to 50 µM concentration. Thus, in the DLR assay these compounds were screen at 25 µM

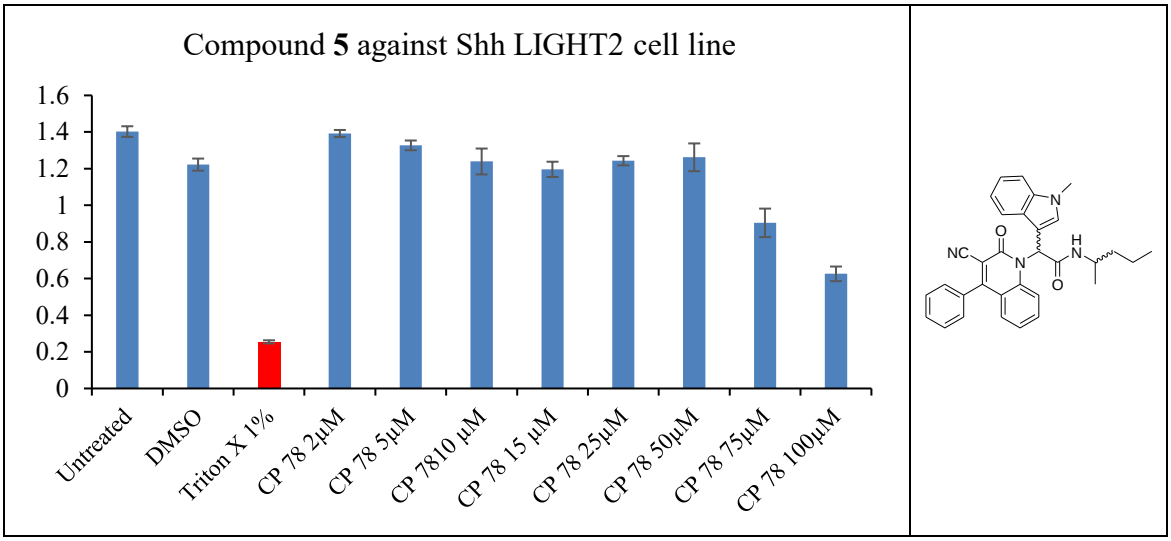

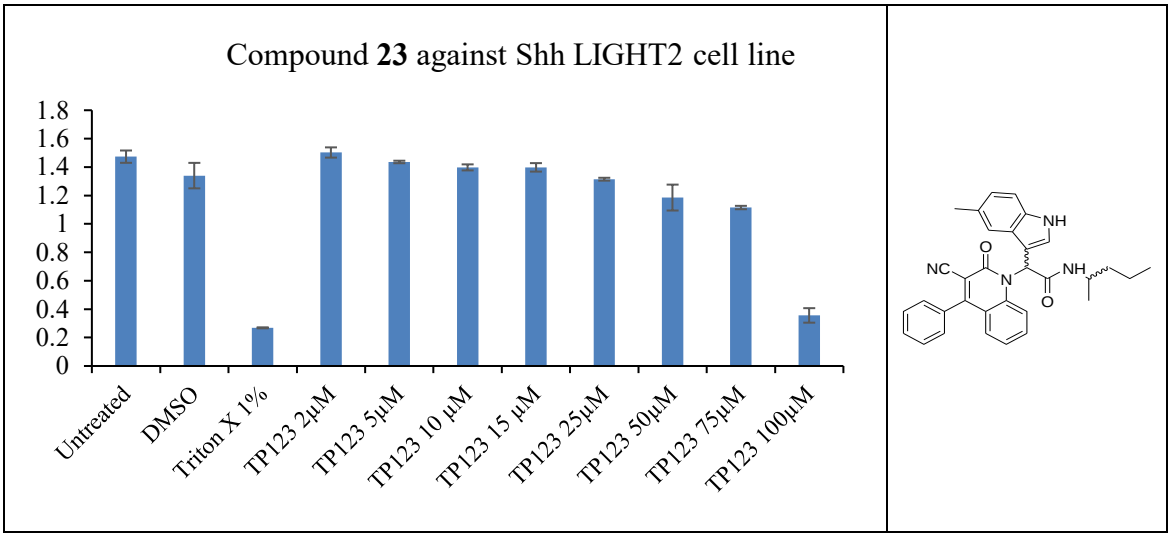

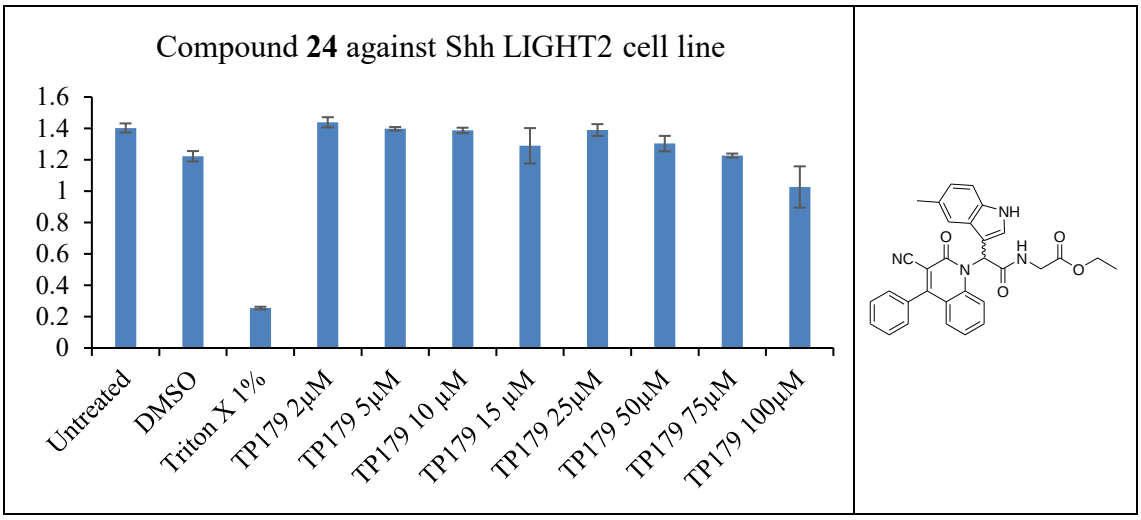
Compound 24 against Shh LIGHT2 cell line
1.6
1.4
1.2
1
0.8
0.6
0.4
0.2
0
Untreated
DMSO
Triton X 1%
TP179 2µM
TP179 5µM
TP179 10 µM
TP179 15 µM
TP179 25µM
TP179 50µM
TP179 75µM
TP179 100µM
NH
NC
O
N
H
N
O
O
O

§ Genes expression of *Ptch₁*, *Sufu*, *Smo*, *Gli₂* and *Gli₃* in Shh LIGHT2 cell line activated by 100 nM SAG.

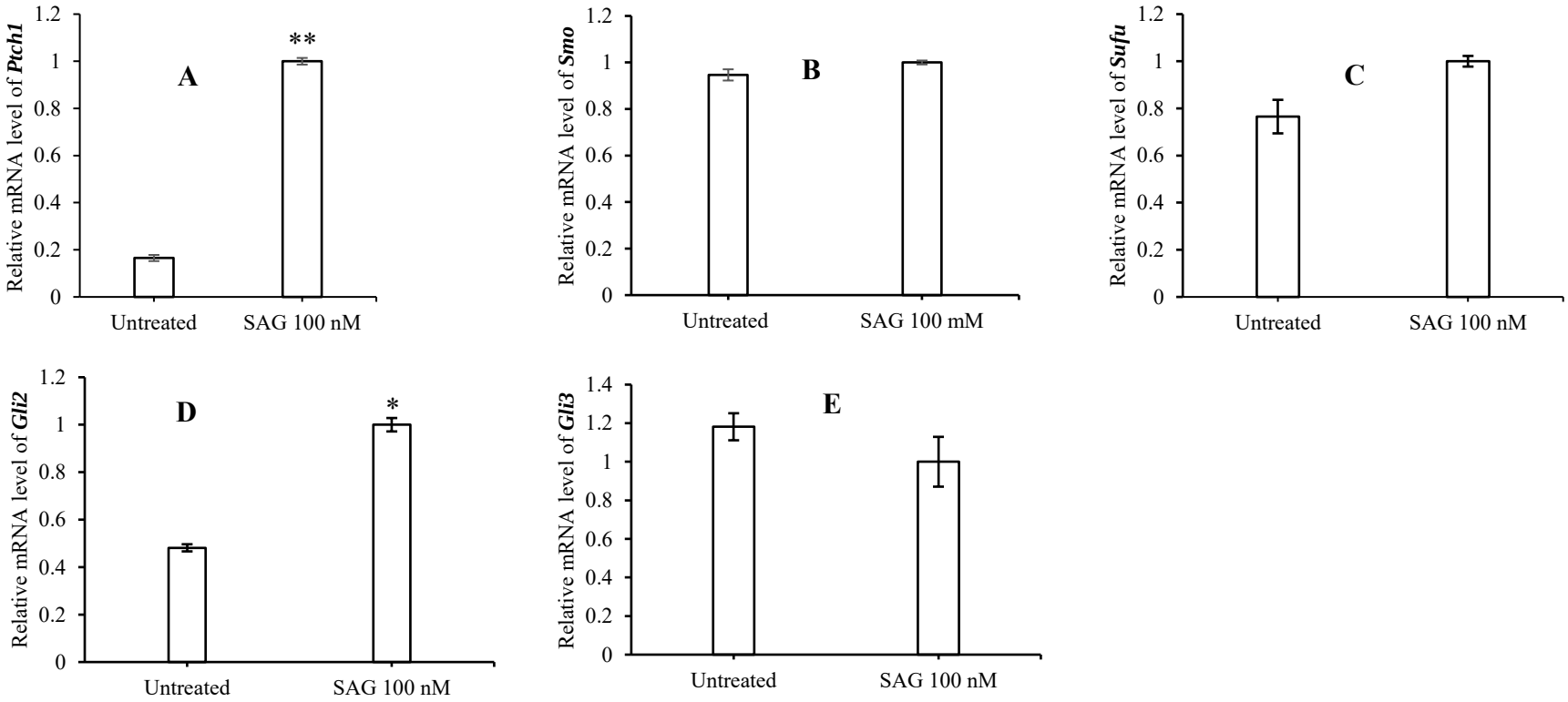

Figure. Relative *gene* expression of *Ptch1* **(A)**, *Smo* **(B)**, *Sufu* **(C)**, *Gli2* **(D)**, and *Gli3* **(E)** in Shh LIGHT 2 cell line activated by SAG (100 nM). All treatments were performed in triplicate. **P* < .05, ***P* < .001 compared to untreated controls.

§ Statistical analysis

Chapter 3_Figure 4	GLI expression compared to SAG control		
	SAG	**5** + SAG	Compound 5 = CP78
	0.190985668	0.062391	
	0.190888798	0.100727	
	0.1789335	0.098295	

F-Test Two-Sample for Variances			t-Test: Two-Sample Assuming Equal Variances		
	Variable 1	*Variable 2*		*Variable 1*	*Variable 2*
Mean	0.087137754	0.186935989	Mean	0.087137754	0.186935989
Variance	0.000460767	4.80322E-05	Variance	0.000460767	4.80322E-05
Observations	3	3	Observations	3	3
df	2	2	Pooled Variance	0.0002544	
F	9.592875957		Hypothesized Mean Difference	0	
P(F<=f) one-tail	0.094403069		df	4	
F Critical one-tail	19		t Stat	-7.663201671	
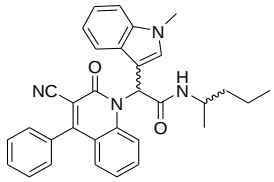			P(T<=t) one-tail	0.000779324	
			t Critical one-tail	2.131846786	
			P(T<=t) two-tail	0.001558649	
			t Critical two-tail	2.776445105	
			*P < .05		

Chapter 3_Figure 4	GLI expression compared to SAG control		
	SAG	**23** + SAG	Compound 23 = TP123B1
	0.190985668	0.117323579	
	0.190888798	0.090150714	
	0.1789335		

F-Test Two-Sample for Variances			t-Test: Two-Sample Assuming Equal Variances		
	Variable 1	*Variable 2*		*Variable 1*	*Variable 2*
Mean	0.103737	0.186935989	Mean	0.103737147	0.186935989
Variance	0.000369	4.80322E-05	Variance	0.000369182	4.80322E-05
Observations	2	3	Observations	2	3
df	1	2	Pooled Variance	0.000155082	
F	7.68614		Hypothesized Mean Difference	0	
P(F<=f) one-tail	0.109203		df	3	
F Critical one-tail	18.51282		t Stat	-7.318580807	
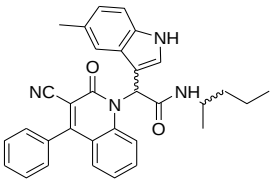			P(T<=t) one-tail	0.002634596	
			t Critical one-tail	2.353363435	
			P(T<=t) two-tail	0.005269193	
			t Critical two-tail	3.182446305	
			*P < .05		

Chapter 3_Figure 4		GLI expression compared to SAG control			
		SAG	**24** + SAG	**Compound 24 = TP179B1**	
		0.190986	0.138624		
		0.190889	0.129131		
		0.178934	0.143547		
F-Test Two-Sample for Variances			t-Test: Two-Sample Assuming Equal Variances		
	Variable 1	*Variable 2*		*Variable 1*	*Variable 2*
Mean	0.137100906	0.186936	Mean	0.137101	0.186936
Variance	5.36941E-05	4.8E-05	Variance	5.37E-05	4.8E-05
Observations	3	3	Observations	3	3
df	2	2	Pooled Variance	5.09E-05	
F	1.117877324		Hypothesized Mean Difference	0	
P(F<=f) one-tail	0.47217088		df	4	
F Critical one-tail	19		t Stat	-8.55813	
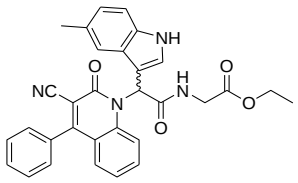			P(T<=t) one-tail	0.000512	
			t Critical one-tail	2.131847	
			P(T<=t) two-tail	0.001024	
			t Critical two-tail	2.776445	
			*P < .05		

Chapter 3_Figure 4		**GLI expression compared to SAG control**			
		SAG	Sonidegib + SAG	**Sonidegib = LDE225**	
		0.190986	0.125976		
		0.190889	0.119023		
		0.178934	0.111083		
F-Test Two-Sample for Variances			t-Test: Two-Sample Assuming Equal Variances		
	Variable 1	*Variable 2*		*Variable 1*	*Variable 2*
Mean	0.118694	0.186936	Mean	0.118694	0.186936
Variance	5.55E-05	4.8E-05	Variance	5.55E-05	4.8E-05
Observations	3	3	Observations	3	3
df	2	2	Pooled Variance	5.18E-05	
F	1.156147		Hypothesized Mean Difference	0	
P(F<=f) one-tail	0.46379		df	4	
F Critical one-tail	19		t Stat	-11.6147	
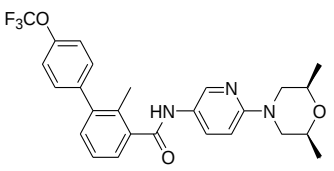			P(T<=t) one-tail	0.000157	
			t Critical one-tail	2.131847	
			P(T<=t) two-tail	0.000314	
			t Critical two-tail	2.776445	
			**P < .001		

Genes expression of HSP components in Shh LIGHT 2 activated by 100 nM SAG		***Ptch1*** expression compared to DMSO control			
		DMSO	SAG		
		0.001011	0.00548611	**Smo Agonist SAG**	
		0.000833	0.00567958		
F-Test Two-Sample for Variances			t-Test: Two-Sample Assuming Equal Variances		
	Variable 1	*Variable 2*		*Variable 1*	*Variable 2*
Mean	0.005583	0.000922	Mean	0.005583	0.000922
Variance	1.87E-08	1.59E-08	Variance	1.87E-08	1.59E-08
Observations	2	2	Observations	2	2
df	1	1	Pooled Variance	1.73E-08	
F	1.176714		Hypothesized Mean Difference	0	
P(F<=f) one-tail	0.47413		df	2	
F Critical one-tail	161.4476		t Stat	35.4273	
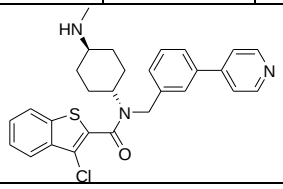			P(T<=t) one-tail	0.000398	
			t Critical one-tail	2.919986	
			P(T<=t) two-tail	0.000796	
			t Critical two-tail	4.302653	
			* *P* < .001		

Genes expression of HSP components in Shh LIGHT 2 activated by 100 nM SAG		***Gli2*** expression compared to DMSO control		
		DMSO	SAG	
		0.00016	0.000309	**Smo agonist SAG**
		0.000148	0.000331	
F-Test Two-Sample for Variances			t-Test: Two-Sample Assuming Unequal Variances	
	Variable 1	*Variable 2*		*Variable 1*	*Variable 2*
Mean	0.000154	0.00032	Mean	0.000154	0.00032
Variance	6.89E-11	2.46E-10	Variance	6.89E-11	2.46E-10
Observations	2	2	Observations	2	2
df	1	1	Hypothesized Mean Difference	0	
F	0.280316		df	2	
P(F<=f) one-tail	0.309988		t Stat	-13.2308	
F Critical one-tail	0.006194		P(T<=t) one-tail	0.002832	
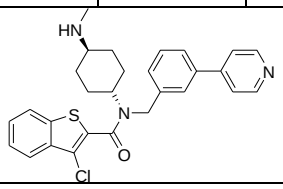			t Critical one-tail	2.919986	
			P(T<=t) two-tail	0.005664	
			t Critical two-tail	4.302653	
			* *P* < .05		

Chapter 3_ Figure 5A	***Ptch1*** expression compared to SAG control		
	SAG	**5** + SAG	**Compound 5 = CP78**

		0.006992	0.002108		
		0.005601	0.003377		
		0.005083	0.003826		
F-Test Two-Sample for Variances			t-Test: Two-Sample Assuming Unequal Variances		
	Variable 1	*Variable 2*		*Variable 1*	*Variable 2*
Mean	0.005892	0.003104	Mean	0.005892	0.003104
Variance	9.75E-07	7.94E-07	Variance	9.75E-07	7.94E-07
Observations	3	3	Observations	3	3
df	2	2	Hypothesized Mean Difference	0	
F	1.22749		df	4	
P(F<=f) one-tail	0.448936		t Stat	3.632142	
F Critical one-tail	19		P(T<=t) one-tail	0.011059	
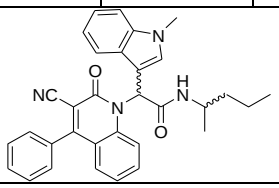			t Critical one-tail	2.131847	
			P(T<=t) two-tail	0.022118	
			t Critical two-tail	2.776445	
			* *P* < .05		

Chapter 3_ Figure 5A	***Ptch1*** expression compared to SAG control			
	SAG	Compound **23** + SAG		**Compound 23 = TP123B1**
	0.006992	0.003285		
	0.005601	0.003129		
	0.005083			
F-Test Two-Sample for Variances		t-Test: Two-Sample Assuming Unequal Variances		
	Variable 1	*Variable 2*	*Variable 1*	*Variable 2*
Mean	0.005892379	0.003207	0.005892	0.003207
Variance	9.74593E-07	1.21E-08	9.75E-07	1.21E-08
Observations	3	2	3	2
df	2	1	Hypothesized Mean Difference	0
F	80.53566287		df	2
P(F<=f) one-tail	0.07855013		t Stat	4.668237
F Critical one-tail	199.5		P(T<=t) one-tail	0.021476
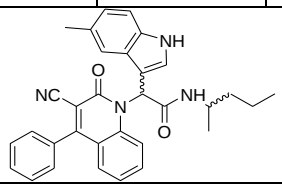			t Critical one-tail	2.919986
			P(T<=t) two-tail	0.042953
			t Critical two-tail	4.302653
			* P < .05	

Chapter 3_ Figure 5A	***Ptch1*** expression compared to SAG control				
	SAG	Compound **24** + SAG			
	0.006992	0.003721		**Compound 24 = TP179B1**	
	0.005601	0.005263			
	0.005083	0.003645			
F-Test Two-Sample for Variances			t-Test: Two-Sample Assuming Equal Variances		
	Variable 1	*Variable 2*		*Variable 1*	*Variable 2*

Mean	0.005892	0.00421	Mean	0.005892	0.00421
Variance	9.75E-07	8.33E-07	Variance	9.75E-07	8.33E-07
Observations	3	3	Observations	3	3
df	2	2	Pooled Variance	9.04E-07	
F	1.169611		Hypothesized Mean Difference	0	
P(F<=f) one-tail	0.460912		df	4	
F Critical one-tail	19		t Stat	2.167848	
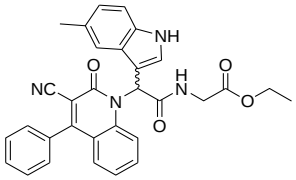			P(T<=t) one-tail	0.048021	
			t Critical one-tail	2.131847	
			P(T<=t) two-tail	0.096041	
			t Critical two-tail	2.776445	
			P = .09		

Chapter 3_ Figure 5B			***Gli*$_2$ expression compared to SAG treatment**		
			SAG	Compound **5** +SAG	
			0.00292	0.000844275	**Compound 5 = CP78**
			0.002752	0.000850147	
			0.002025		
F-Test Two-Sample for Variances			t-Test: Two-Sample Assuming Unequal Variances		
	Variable 1	*Variable 2*		*Variable 1*	*Variable 2*
Mean	0.002565596	0.000847	Mean	0.002566	0.000847
Variance	2.26544E-07	1.72E-11	Variance	2.27E-07	1.72E-11
Observations	3	2	Observations	3	2
df	2	1	Hypothesized Mean Difference	0	
F	13138.70305		df	2	
P(F<=f) one-tail	0.006168797		t Stat	6.252876	
F Critical one-tail	199.5		P(T<=t) one-tail	0.012318	
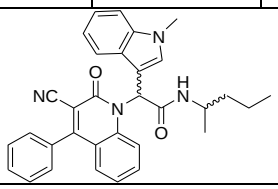			t Critical one-tail	2.919986	
			P(T<=t) two-tail	0.024635	
			t Critical two-tail	4.302653	
			*P < .05		

Chapter 3_ Figure 5B			***Gli*$_2$ expression compared to SAG control**		
			SAG	Compound **23** + SAG	
			0.00262	0.000983	**Compound 23 = TP123B1**
			0.002152	0.000589	
			0.001925		
F-Test Two-Sample for Variances			t-Test: Two-Sample Assuming Equal Variances		
	Variable 1	*Variable 2*		*Variable 1*	*Variable 2*
Mean	0.002232	0.000786	Mean	0.002232262	0.000786
Variance	1.26E-07	7.78E-08	Variance	1.25676E-07	7.78E-08

Observations	3	2	Observations	3	2
df	2	1	Pooled Variance	1.09733E-07	
F	1.614394		Hypothesized Mean Difference	0	
P(F<=f) one-tail	0.486286		df	3	
F Critical one-tail	199.5		t Stat	4.782435678	
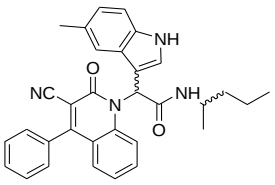			P(T<=t) one-tail	0.008690299	
			t Critical one-tail	2.353363435	
			P(T<=t) two-tail	0.017380598	
			t Critical two-tail	3.182446305	
			* *P* < .05		

Chapter 3_ Figure 5B	***Gli*$_2$ expression compared to SAG control**	
	SAG	Compound **24** + SAG
	0.00262	0.000793
	0.002152	0.000899
	0.001925	
		t-Test: Two-Sample Assuming Equal Variances

Compound 24 = TP179B1

F-Test Two-Sample for Variances				*Variable 1*	*Variable 2*
			Mean	0.002232	0.000846
	Variable 1	*Variable 2*	Variance	1.26E-07	5.56E-09
Mean	0.002232	0.000846	Observations	3	2
Variance	1.26E-07	5.56E-09	Pooled Variance	8.56E-08	
Observations	3	2	Hypothesized Mean Difference	0	
df	2	1	df	3	
F	22.62334		t Stat	5.189598	
P(F<=f) one-tail	0.147048		P(T<=t) one-tail	0.006948	
F Critical one-tail	199.5		t Critical one-tail	2.353363	
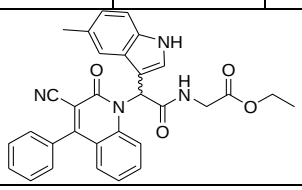			P(T<=t) two-tail	0.013895	
			t Critical two-tail	3.182446	
			* *P* < .05		

8.2.2. Compounds characterization

§ Synthesis summary of the quinolone-1-(2*H*)-ones using the Ugi-Knoevenagel reaction

Appendix for Table 2 & 4. Isolated yields of quinolin-1-(2*H*)-ones (**5**, **10**–**30**) (the Ugi 4CR products) and structural differentiations using the ^{1}H NMR , IR spectra and base cations in HRMS $[M+H]^{+}$ and $[M-H]^{-}$. ***Reagents and conditions:*** (***i***) MeOH, rt, 24 h.

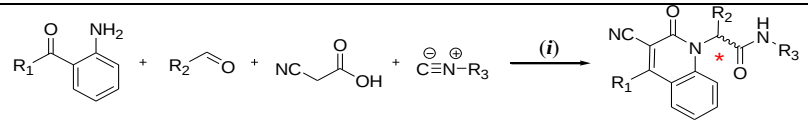

Entry	Compound Codes	R_1	R_2	R_3	Yield %	^{1}H of CH* (ppm)	IR of −CN (cm^{-1})	Mass Peak (*m/z*)
1	**5**		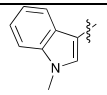		38	6.94 – 6.88 (m)	2227	502.2369 $[M+H]^{+}$
2	**10**		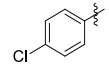	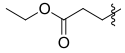	25	6.85 (bs)	2230	513.1455 $[M-H, {}^{35}Cl]^{-}$
3	**11**		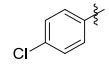		56	6.95 (s)	2229	498.1483 $[M-H, {}^{35}Cl]^{-}$
4	**12**		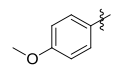		68	6.94 – 6.88 (m)	2228	480.2207 $[M+H]^{+}$
5	**13**		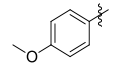		37	6.92 (d)	2229	480.1636 $[M-H]^{-}$

6	**14**		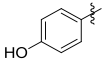		71	6.74 (d)	2231	464.2052 $[M-H]^-$
7	**15**		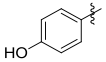		66	6.69 (d)	2230	402.1895 $[M-H]^-$
8	**16**		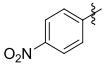		26	7.29 – 7.18 (m)	2227	431.1798 $[M-H]^-$
9	**17**		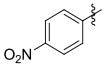		49	6.25 (s)	2225	473.2267 $[M-H]^-$
10	**18**		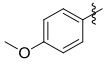		68	6.94 – 6.84 (m)	2227	458.2522 $[M-H]^-$
11	**19**		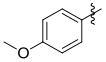		49	7.1 (bs)	2228	418.1481 $[M-H]^-$
12	**20**		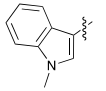		13	7.39 – 7.43 (m)	2229	463.2104 $[M+H]^+$
13	**21**		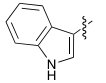		11	7.46 − 7.54 (m)	2229	489.2284 $[M+H]^+$
14	**22**		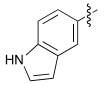		36	7.15 – 7.20 (m)	2235	489.2284 $[M+H]^+$
15	**23**		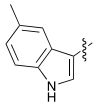		46	7.41 – 7.47 (m)	2236	503.2444 $[M+H]^+$

16	**24**		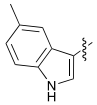	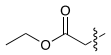	34	7.55 − 7.59 (m)	2232	519.2026 $[M+H]^+$
17	**25**			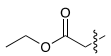	46	7.65 – 7.67 (m)	2236	505.1869 $[M+H]^+$
18	**26**			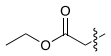	26	7.57 – 7.60 (m)	2226	519.2027 $[M+H]^+$
19	**27**			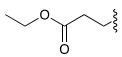	50	7.38 – 7.41 (m)	2232	287 $[M+ACN+2H]^{2+}$
20	**28**		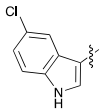	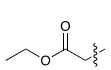	33	7.53 – 7.58 (m)	2236	539.1481 $[M+H, {}^{35}Cl]^+$
21	**29**				47	7.40 – 7.43 (m)	2228	489.2283 $[M+H]^+$
22	**30**		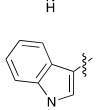		26	7.40 (s)	2229	489.2287 $[M+H]^+$

Compound 20

Compound Name: 2-(3-cyano-2-oxo-4-methylquinolin-1(2*H*)-yl)-2-(1-methyl-1*H*-indol-3-yl)-*N*-(pentan-2-yl)acetamide

Obtained Weight & Yield: 70 mg, 13%

Appearance: Off white precipitate

Solubility: EtOAc, Acetone, ACN

Melting Point: 243-245 ˚C

TLC Conditions: EtOAc/Hexane (50/50)

IR Analysis: νmax/cm^{-1}

3246 (NH), 3083 (CH), 2972 (CH), 2229 (CN), 1637 (CO).

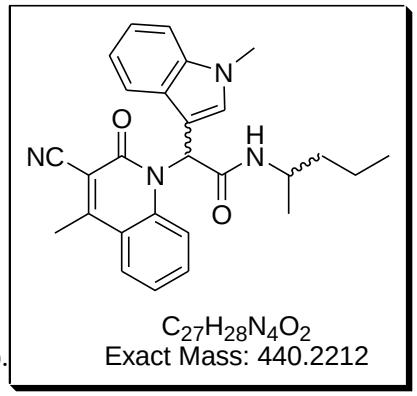

The ^{1}H NMR displays a mixture of isomers, with the ratio 1.35 : 1.0 calculated at 0.74 and 0.60 ppm, respectively. ^{1}H is reported as a whole without splitting due to the complex overlapping. All peaks detected in ^{13}C are reported.

^{1}H NMR Analysis:

^{1}H NMR (400 MHz, DMSO-d_6) δ 7.91 (d, J = 8.2 Hz, 1H), 7.83 – 7.69 (m, 2H), 7.67 – 7.51 (m, 2H), 7.47 – 7.35 (m, 3H), 7.29 (dd, J = 9.8, 5.4 Hz, 1H), 7.13 (t, J = 7.6 Hz, 1H), 7.01 (t, J = 7.4 Hz, 1H), 3.98-3.86 (m, 1H), 3.75 (s, 3H), 2.75 (d, J = 3.2 Hz, 3H), 1.54 – 1.15 (m, 4H), 0.93-0.87 (m, 3H), 0.77-0.56 (m, 2H).

^{13}C NMR Analysis: (Sign of isomers)

^{13}C NMR (101 MHz, DMSO-d_6) δ 167.4, 166.8, 159.2, 159.2, 158.3, 158.3, 139.1, 136.6, 136.5, 133.3, 133.2, 130.9, 130.81, 127.7, 127.6, 127.6, 123.4, 121.9, 120.1, 120.1, 119. 8, 118.9, 118.1, 118.1, 116.2, 110.4, 107.7, 106.2, 106.1, 106.1, 60.2, 53.8, 53.7, 52.9, 45.3, 45.2, 38.3, 38.0, 33.0 (Cx2), 27.4, 26.8, 21.2, 21.1, 20.8, 19.6, 19.1, 18.8, 14.6, 14.3, 14.2, 11.2, 10.8

HPLC: RP-HPLC Alltima™ C18 5 μm 150 mm x 4.6 mm, 10–100% B in 15 min, R_t = 7.07 min, 93 %

Mass Spectral Analysis

LRMS (ESI-) m/z 440, 520 $[M+DMSO+2H]^+$ 100%. HRMS (ES+) for $C_{27}H_{28}N_4O_2Na$; calculated 463.2110, found 463.2104.

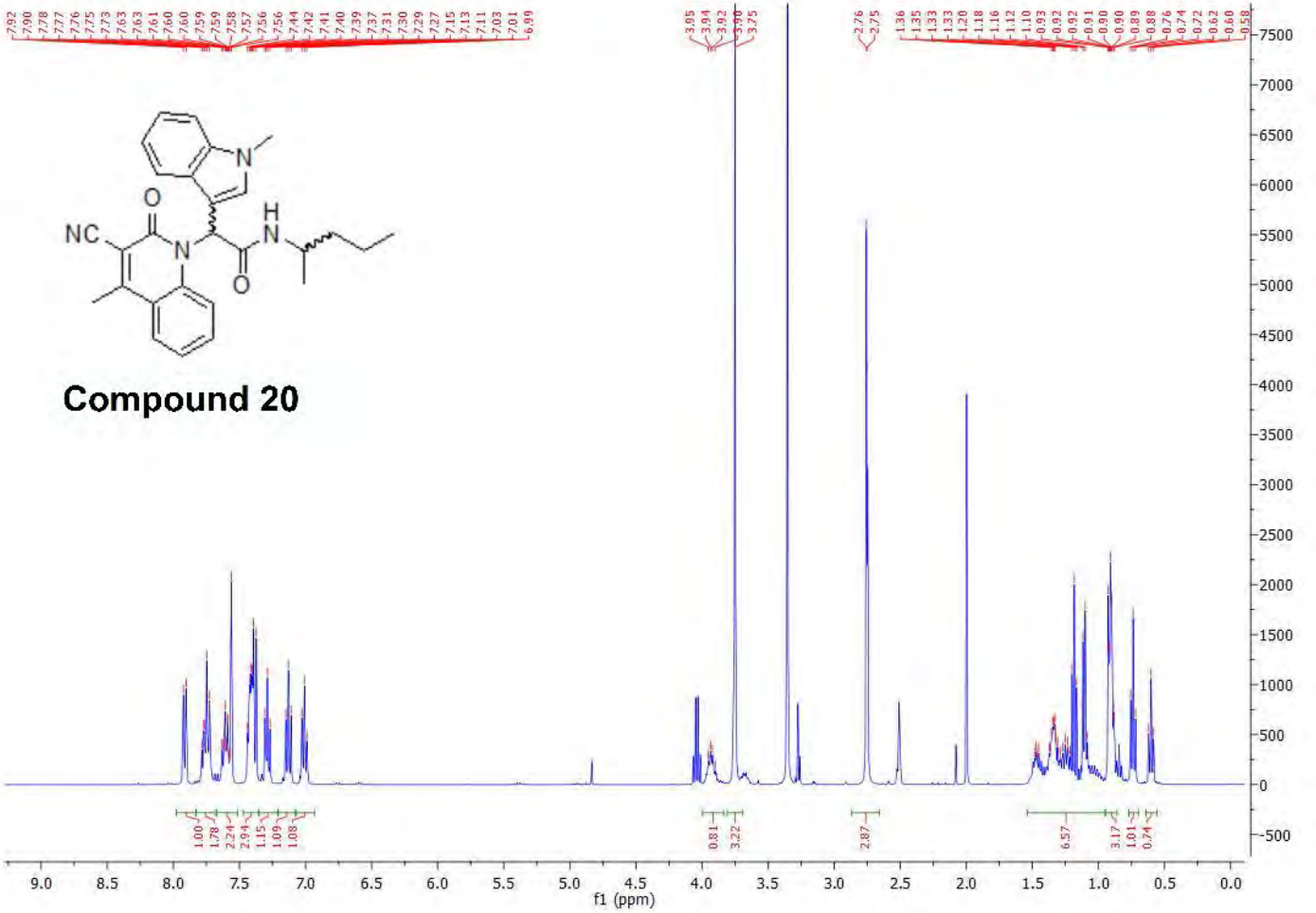
Compound 20
f1 (ppm)

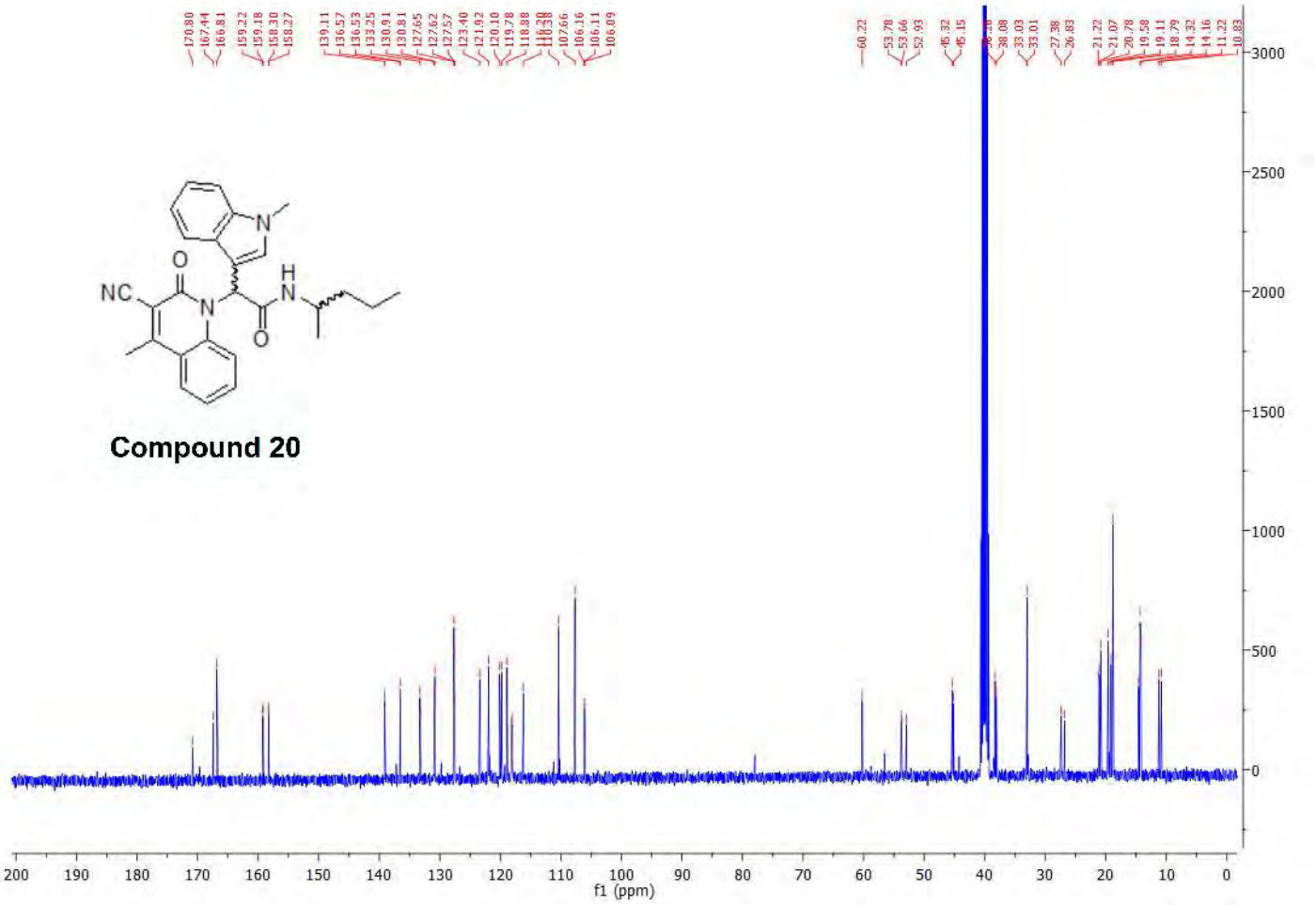
170.80
167.44
166.81
159.22
159.18
158.30
158.27
139.11
136.57
136.53
133.25
130.91
130.81
127.65
127.62
127.57
123.40
121.92
120.10
119.78
118.88
107.66
106.16
106.11
106.09
60.22
53.78
53.66
52.93
45.32
45.15
38.08
33.03
33.01
27.38
26.83
21.22
21.07
20.78
19.58
19.11
18.79
14.32
14.16
11.22
10.83
NC
O
N
H
N
O
Compound 20
3000
2500
2000
1500
1000
500
0
200
190
180
170
160
150
140
130
120
110
100
90
80
70
60
50
40
30
20
10
0
f1 (ppm)

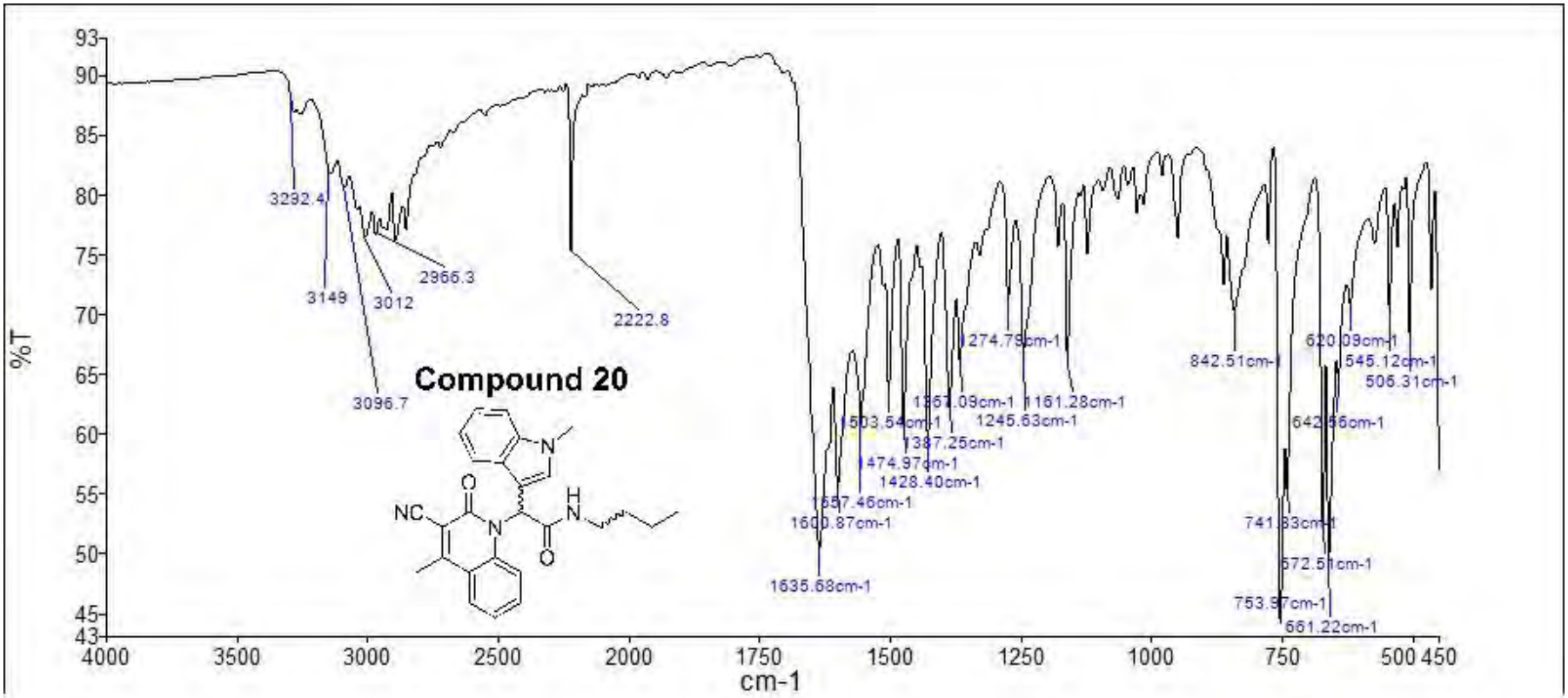
Compound 20
%T
cm-1
3292.4
3149
3096.7
3012
2966.3
2222.8
1635.68cm-1
1600.87cm-1
1557.46cm-1
1503.54cm-1
1474.97cm-1
1428.40cm-1
1387.25cm-1
1361.09cm-1
1274.79cm-1
1245.63cm-1
1161.28cm-1
842.51cm-1
741.83cm-1
753.97cm-1
672.51cm-1
661.22cm-1
642.56cm-1
620.09cm-1
545.12cm-1
506.31cm-1
NC
O
N
H
O

==== Shimadzu LCMSsolution Analysis Report ====

Acquired by	: Admin
Sample Name	: TP130B1 Pre E
Sample ID	:
Vail #	: 43
Injection Volume	: 30 uL
Data File Name	: TP130B1 Pre E.lcd
Method File Name	: Econosphere C18 EPS 5u lot 50195421 part 70070 150mm id 4.6mm.lcm
Batch File Name	: 2015 Ugi Knoevenagel products continue.lcb
Report File Name	: DefaultLCMS.lcr
Data Acquired	: 10/20/2015 3:15:53 PM
Data Processed	: 10/20/2015 3:42:46 PM

<Chromatogram>

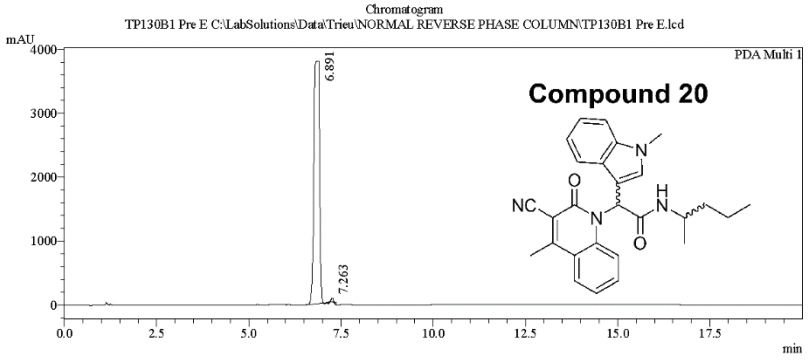

1 PDA Multi 1 / 254nm 4nm
2 PDA Multi 2 / 220nm 4nm

PeakTable

PDA Ch1 254nm 4nm

Peak#	Ret. Time	Area	Height	Area %	Height %
1	6.891	39983729	3798093	99.645	98.361
2	7.263	142482	63301	0.355	1.639
Total		40126210	3861394	100.000	100.000

PeakTable

PDA Ch2 220nm 4nm

Peak#	Ret. Time	Area	Height	Area %	Height %
1	6.901	50404388	3863757	92.871	94.834
2	7.263	3868877	610468	7.129	5.166
Total		54273265	4474225	100.000	100.000

==== Shimadzu LCMSsolution Data Report ====

<Chromatogram>

Sample Information

Acquired by	: Admin
Date Acquired	: 7/21/2015 11:49:47 AM
Sample Type	: Unknown
Level#	: 0
Sample Name	: TP130B1S2
Sample ID	:
ISTD Amount	: (Level1 Conc.)
Sample Amount	: 1
Dilution Factor	: 1
Tray#	: 1
Vial#	: 43
Injection Volume	: 5
Data File	: TP130B1S2.lcd
Method File	: FIA-ESI_Scan(-).lcm
Original Method	: C:\LabSolutions\Data\Kelly\FIA-ESI_Scan(-).lcm
Report Format	: DefaultLCMS.lcr
Tuning File	: C:\LabSolutions\LCsolution\Log\Tuning\Autotune_030908.lct
Processed by	: Admin
Modified Date	: 7/21/2015 11:51:18 AM

Compound 20

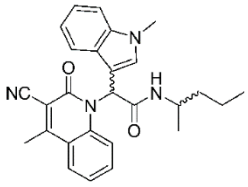

Chromatogram

TP130B1S2 C:\LabSolutions\Data\Trieu\NORMAL REVERSE PHASE COLUMN\ESI POSITIVE\SECOND AND THIRD\TP130B1S2.lcd

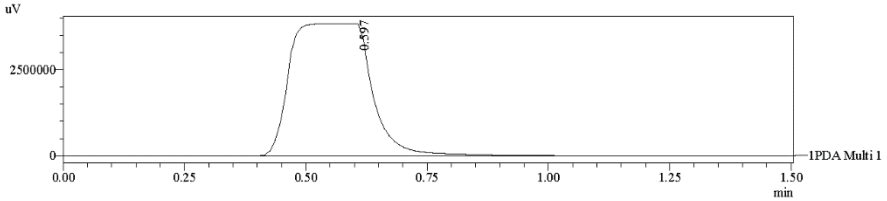

1 PDA Multi 1 / 254nm 4nm

<Spectrum>

Retention Time:0.880(Scan#:89)
Max Peak:630 Base Peak:256.80(2022293)
Spectrum:Averaged 0.640-1.400(65-141)
Background:Averaged 0.120-0.528(13-53) Polarity:Pos Segment1 - Event1

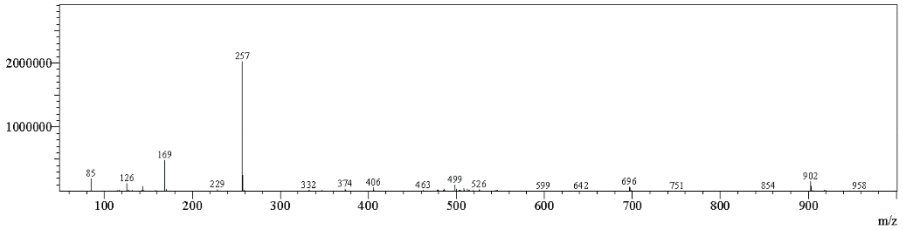

Retention Time:0.870(Scan#:88)
Max Peak:658 Base Peak:520.35(150059)
Spectrum:Averaged 0.650-1.410(66-142)
Background:Averaged 0.130-0.528(14-54) Polarity:Neg Segment1 - Event2

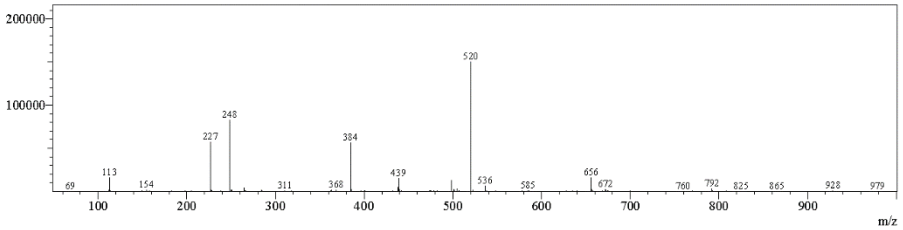

C:¥LabSolutions¥Data¥Trieu¥NORMAL REVERSE PHASE COLUMN¥ESI POSITIVE¥SECOND AND THIRD¥TP130B1S2.lcd

Compound	Chemical Formula	Predicted monoisotopic neutral MW	Predicted MH+	MH+ Measured	Main MS Ions	Main MS/MS Fragments
TP130B1	$C_{27}H_{28}N_4O_2$	440.2212	441.2285	n/a	463.21036(+Na) 257.16466 (fragment)	257.1652 207.5034

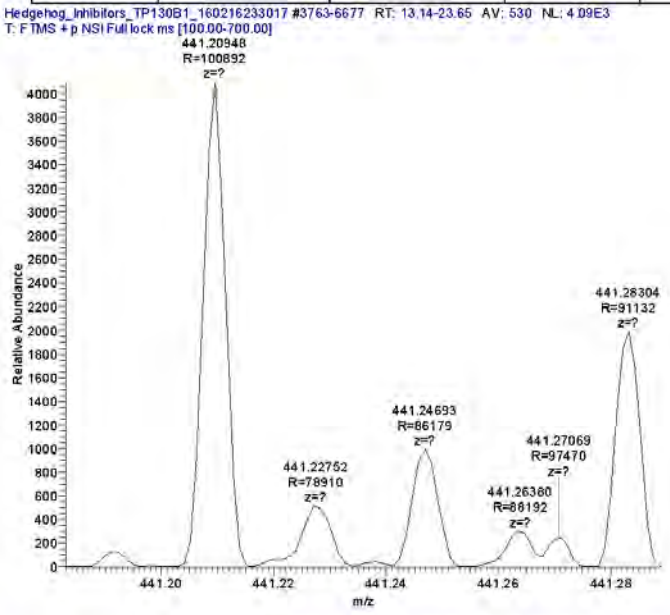

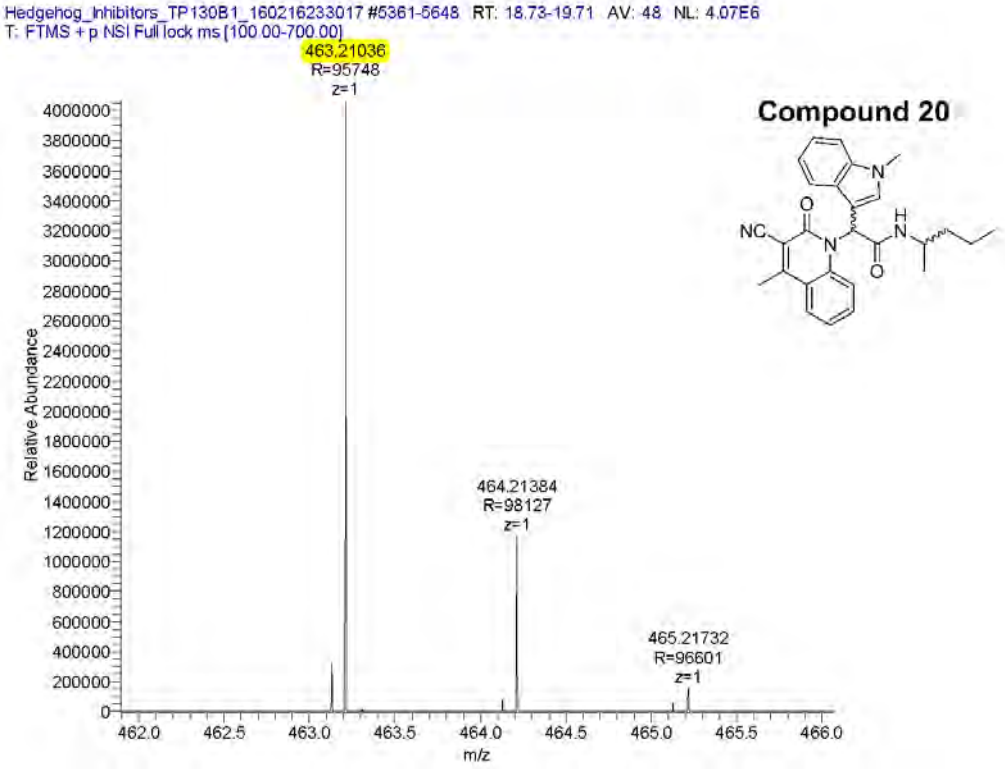

Compound 20

Compound 21

Compound Name: 2-(3-cyano-2-oxo-4-phenylquinolin-1(2*H*)-yl)-2-(1*H*-indol-3-yl)-*N*-(pentan-2-yl)acetamide

Obtained Weight & Yield: 70 mg, 11 %

Appearance: Off white precipitate

Solubility: EtOAc, ACN

Melting Point: 182-183 ˚C

TLC Conditions: EtOAc/Hexane (50/50)

IR Analysis: νmax/cm^{-1}

3420 (NH), 2229 (CN), 1678 (CONH), 1646 (CON)

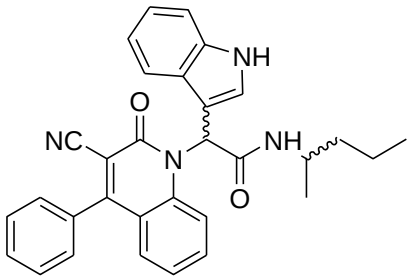

$C_{31}H_{28}N_4O_2$
Mol. Wt.: 488.5796

The ^{1}H NMR displays a mixture of isomers, with the ratio 5.5 : 1.0 calculated at 3.96 and 3.72 ppm, respectively. ^{1}H is reported as a whole without splitting due to the complex overlapping. All peaks detected in ^{13}C are reported

^{1}H NMR Analysis:

^{1}H NMR (400 MHz, DMSO-d_6) δ 11.26 (s, 1H), 7.85 (s, 2H), 7.73 – 7.32 (m, 10H), 7.29 – 6.87 (m, 4H), 3.96 (s, 1H), 1.84 – 0.09 (m, 11H).

^{13}C NMR Analysis:

^{13}C NMR (101 MHz, DMSO-d_6) δ 167.4, 166.8, 160.1, 159.3, 140.1, 136.2, 136.1, 134.1, 133.3, 130.4, 129.3, 129.2, 129.1, 127.4, 127.3, 127.0, 126.9, 123.5, 122.0, 119.9, 119.8, 118.8, 118.6, 116.0, 112.2, 108.5, 106.0, 54.3, 54.2, 53.0, 45.4, 45.3, 38.4, 38.2, 27.4, 26.9, 21.1, 20.9, 19.6, 19.2, 14.4, 14.2, 11.3, 10.8.

HPLC:

RP-HPLC Phenomenex Onyx™ Monolithic C18 5 µm 100 mm x 4 mm, 10–100% B in 15 min, R_t = 12.24 min, 100 %

Mass Spectral Analysis: LRMS (ESI+) m/z 488, 489 $[M+H]^+$, 40%. HRMS (ES+) for $C_{31}H_{28}N_4O_2$; calculated 489.2285, found 489.2284.

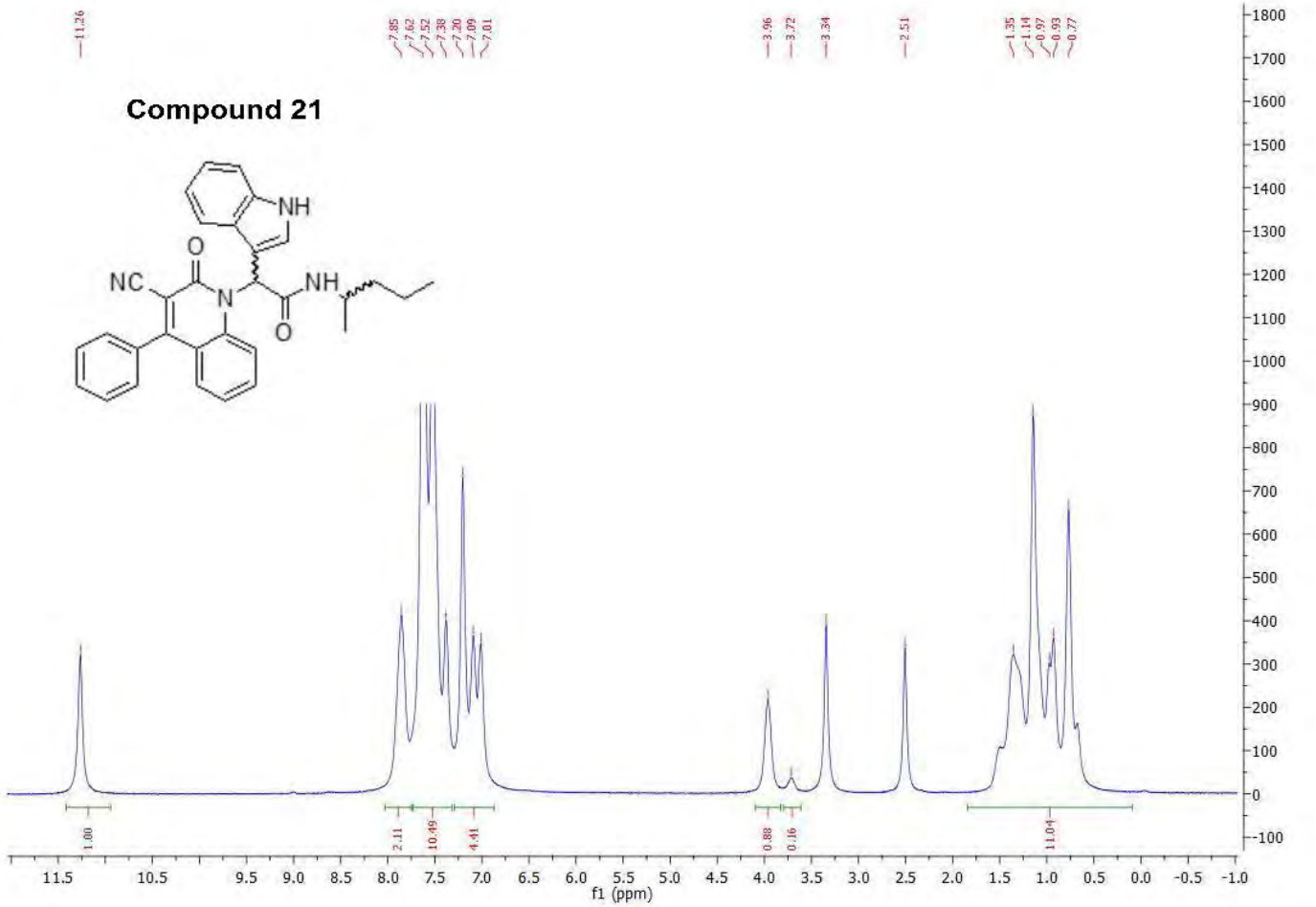
Compound 21
NH
O
NC
N
NH
O
11.26
7.85
7.62
7.52
7.38
7.20
7.09
7.01
3.96
3.72
3.34
2.51
1.35
1.14
0.97
0.93
0.77
1.00
2.11
10.49
4.41
0.88
0.16
11.04
f1 (ppm)

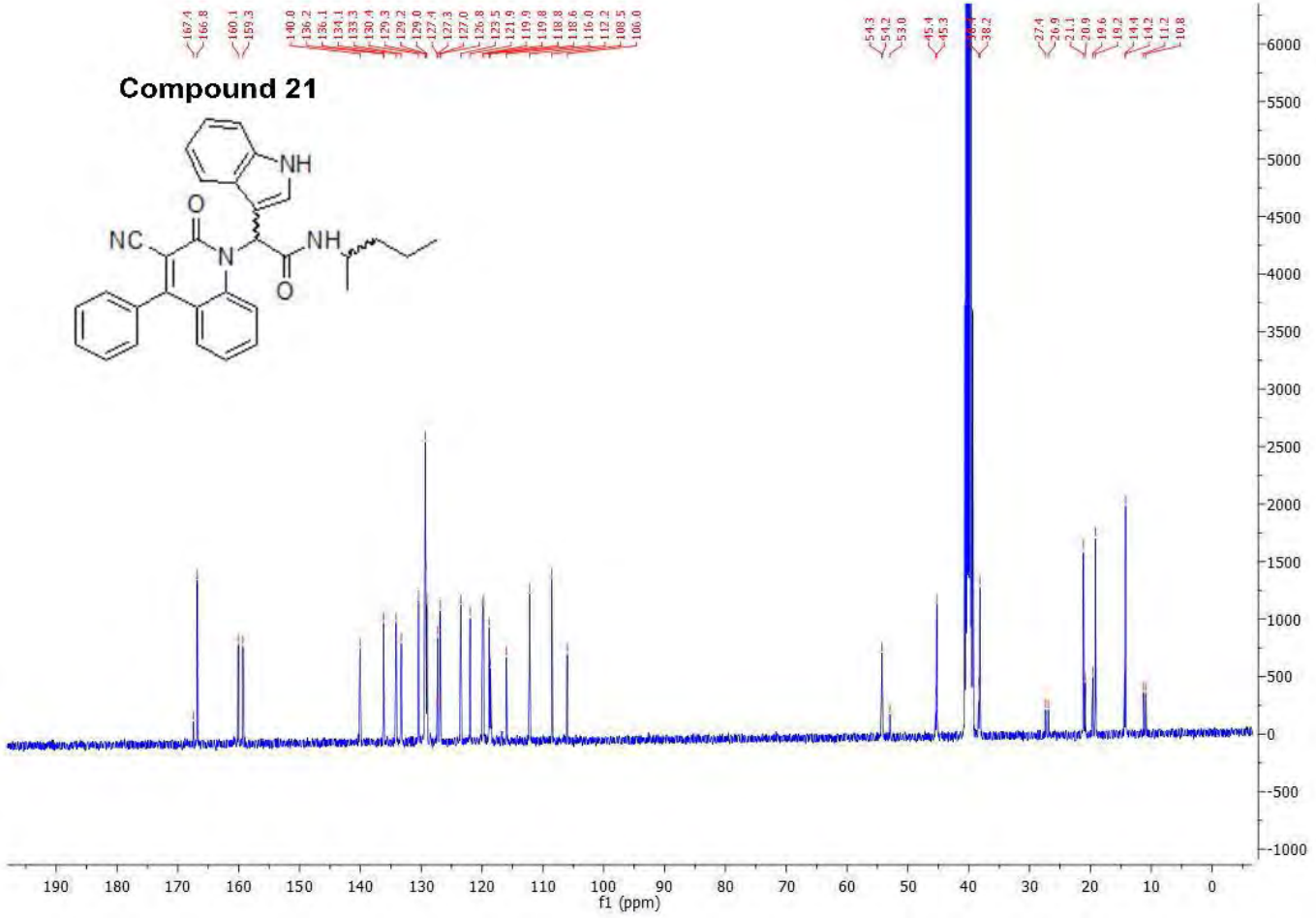
Compound 21
NH
O
NC
N
NH
O
f1 (ppm)

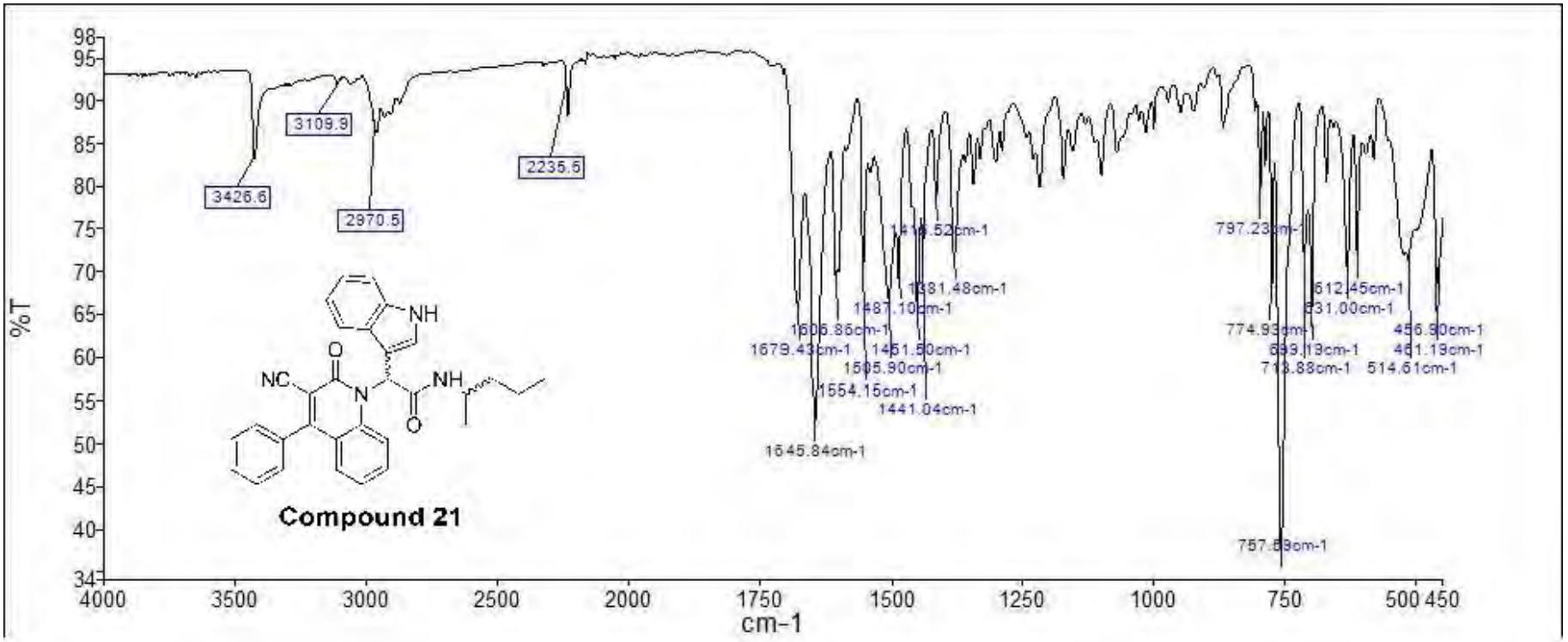
%T
cm-1
3426.6
3109.9
2970.5
2235.6
1645.84cm-1
1679.43cm-1
1606.86cm-1
1554.15cm-1
1505.90cm-1
1487.10cm-1
1451.50cm-1
1441.04cm-1
1381.48cm-1
757.69cm-1
774.93cm-1
797.23cm-1
612.45cm-1
631.00cm-1
699.19cm-1
713.88cm-1
456.90cm-1
461.19cm-1
514.61cm-1
NC
O
N
NH
O
NH
Compound 21

Data File C:\CHEM32\...EMO\PURIFIED TR S EPI AND S LUG AIPS 2016-01-05 09-33-14\033-3401.D
Sample Name: TP169B1

```
Acq. Operator   : Simi120102015                  Seq. Line :  34
Acq. Instrument : LC1260                         Location : Vial 33
Injection Date  : 1/6/2016 2:48:47 AM                 Inj :  1
                                                Inj Volume : 10.000 µl
Acq. Method     : C:\CHEM32\1\DATA\DEMO\PURIFIED TR S EPI AND S LUG AIPS 2016-01-05 09-
                  33-14\10 TO 100 OV 15MIN 10UL.M
Last changed    : 12/10/2015 4:12:43 PM by Simi120102015
Analysis Method : C:\CHEM32\1\DATA\DEMO\PURIFIED TR S EPI AND S LUG AIPS 2016-01-05 09-
                  33-14\10 TO 100 OV 15MIN 20UL.M (Sequence Method)
Last changed    : 1/6/2016 10:52:32 AM by Simi120102015
                  (modified after loading)
```

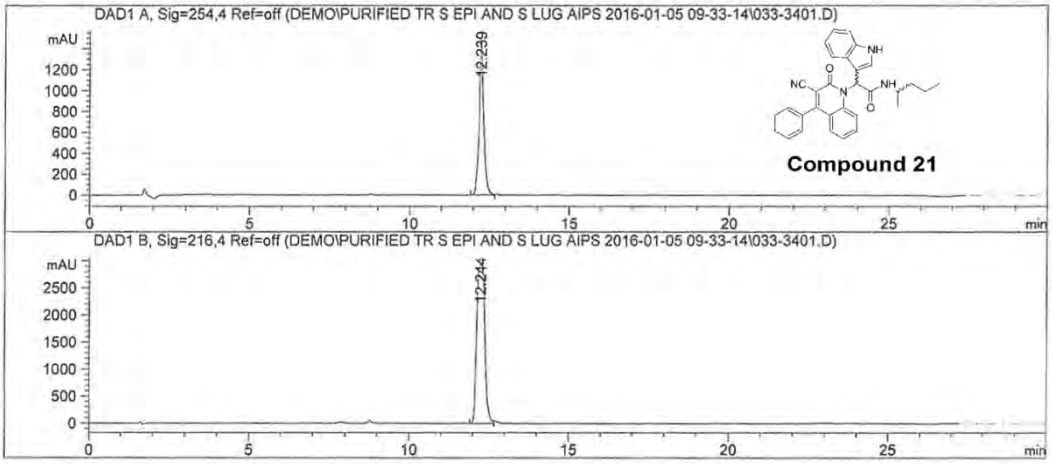

Area Percent Report

```
Sorted By             :      Signal
Multiplier:                  :      1.0000
Dilution:                    :      1.0000
Use Multiplier & Dilution Factor with ISTDs
```

Signal 1: DAD1 A, Sig=254,4 Ref=off

Peak #	RetTime [min]	Type	Width [min]	Area [mAU*s]	Height [mAU]	Area %
1	12.239	BV	0.1407	1.49408e4	1493.16357	100.0000
Totals :				1.49408e4	1493.16357	

Signal 2: DAD1 B, Sig=216,4 Ref=off

Peak #	RetTime [min]	Type	Width [min]	Area [mAU*s]	Height [mAU]	Area %
1	12.244	BV	0.2858	5.21904e4	2930.83984	100.0000

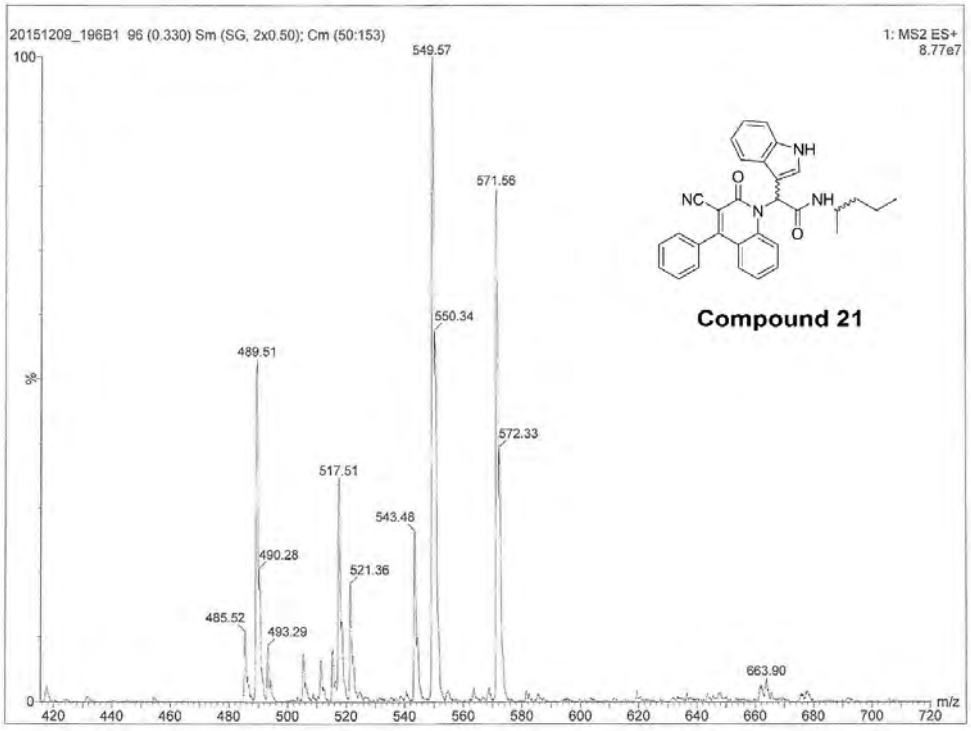
20151209_196B1 96 (0.330) Sm (SG, 2x0.50); Cm (50:153)
1: MS2 ES+
8.77e7
100
%
0
549.57
571.56
550.34
489.51
572.33
517.51
543.48
490.28
521.36
485.52
493.29
663.90
420
440
460
480
500
520
540
560
580
600
620
640
660
680
700
720
m/z
NH
O
NC
N
NH
O
Compound 21

Compound	Chemical Formula	Predicted monoisotopic neutral MW	Predicted MH+	MH+ Measured	Main MS Ions	Main MS/MS Fragments
TP 196B1	$C_{31}H_{28}N_4O_2$	488.2212	489.2285	489.2284	243.14903 (fragment) 489.2284	243.1486 86.0970 489.3408

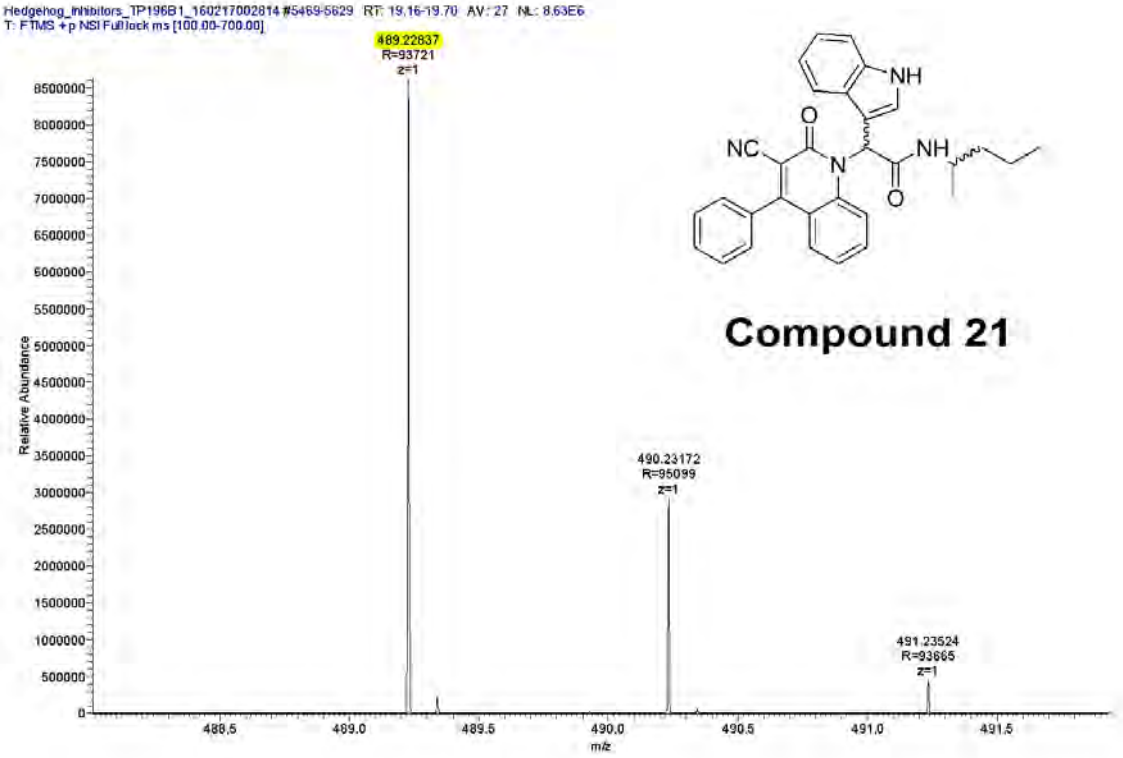

Compound 22

Compound Name: 2-(3-cyano-2-oxo-4-phenylquinolin-1(2*H*)-yl)-2-(1*H*-indol-5-yl)-*N*-(pentan-2-yl)acetamide

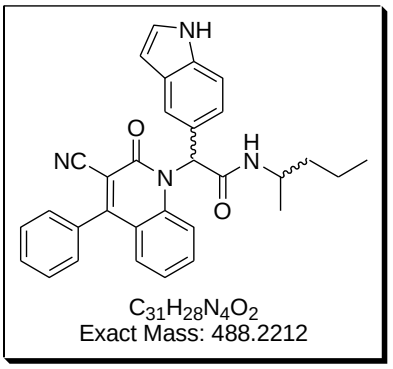

$C_{31}H_{28}N_4O_2$
Exact Mass: 488.2212

Obtained Weight & Yield: 0.238, 36%

Appearance: Off white precipitate

Solubility: DMSO, not in Aceton, MeOH, EtOAc

Melting Point: 271-272 ˚C

TLC Conditions: EtOAc/Hexane (50/50)

IR Analysis: ν_{max}/cm^{-1}
3403 (NH), 3338 (NH), 2956 (CH), 2235 (CN), 1647 (CO).

The ^{1}H NMR displays a mixture of isomers, with the ratio 2.45 : 1.0 calculated at 0.74 and 0.64 ppm, respectively. ^{1}H is reported as a whole without splitting due to the complex overlapping. All peaks detected in ^{13}C are reported.

^{1}H NMR Analysis:
^{1}H NMR (400 MHz, DMSO-d_6) δ 11.13 (s, 1H), 7.89 (dd, J = 14.3, 8.1 Hz, 1H), 7.71 – 7.52 (m, 7H), 7.52 – 7.44 (m, 1H), 7.41 – 7.29 (m, 2H), 7.26 – 7.01 (m, 4H), 6.40 (d, J = 1.8 Hz, 1H), 3.91 (dd, J = 13.4, 7.0 Hz, 1H), 1.59 – 1.19 (m, 3H), 1.16 – 0.99 (m, 2H), 0.99 – 0.84 (m, 3H), 0.81-0.55 (m, 2H).

^{13}C NMR Analysis:
^{13}C NMR (101 MHz, DMSO-d_6) δ 167.5, 167.0, 166.9, 160.1, 160.0, 159.4, 140.6, 135.6, 134.2, 134.2, 133.1, 133.0, 130.4, 129.3 (C x 2), 129.2 (C x 2), 129.1, 129.1, 128.0, 126.5, 126.5, 125.8, 125.7, 125.6, 123.5, 121.8, 120.1, 120.1, 120.0, 119.1, 119.0, 116.0, 116.0, 111.9, 111.9, 106.3, 106.3, 106.2, 101.8, 101.7, 61.3, 61.1, 61.1, 52.8, 45.3, 45.2, 38.3, 38.2, 27.2, 26.8, 21.2, 20.9, 19.5, 19.0, 14.4, 14.3, 11.1, 10.6

HPLC:
RP-HPLC Alltima™ C18 5 μm 150 mm x 4.6 mm, 10–100% B in 15 min, R_t = 7.07 min, 98.6%

Mass Spectral Analysis (Low res): LRMS (ESI-) m/z - 488, 520 [M+CH_3OH-H] 95%. HRMS (ES+) for $C_{31}H_{28}N_4O_2$; calculated 489.2285, found 489.2284.

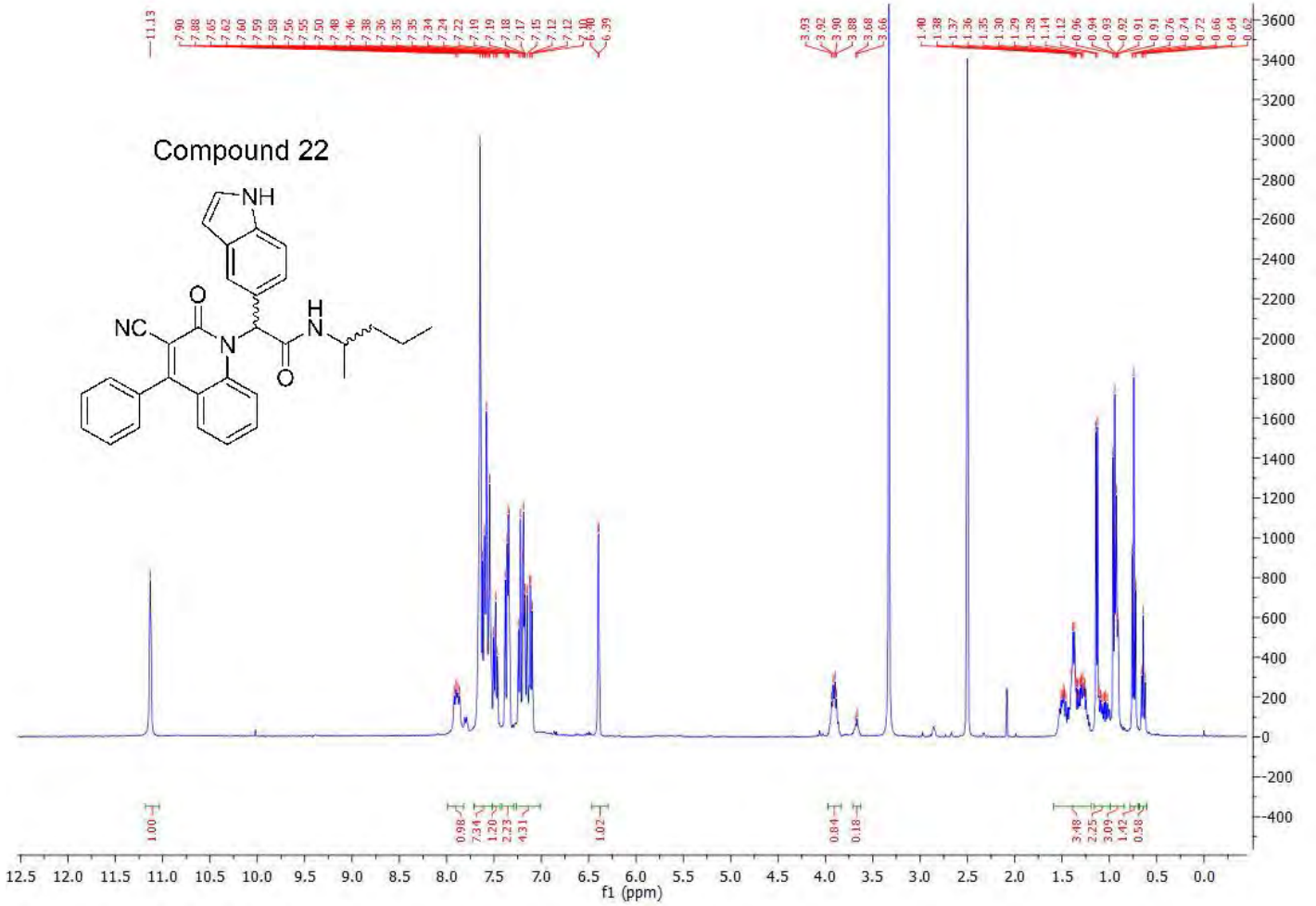
Compound 22
NH
NC
O
N
H
N
O
f1 (ppm)

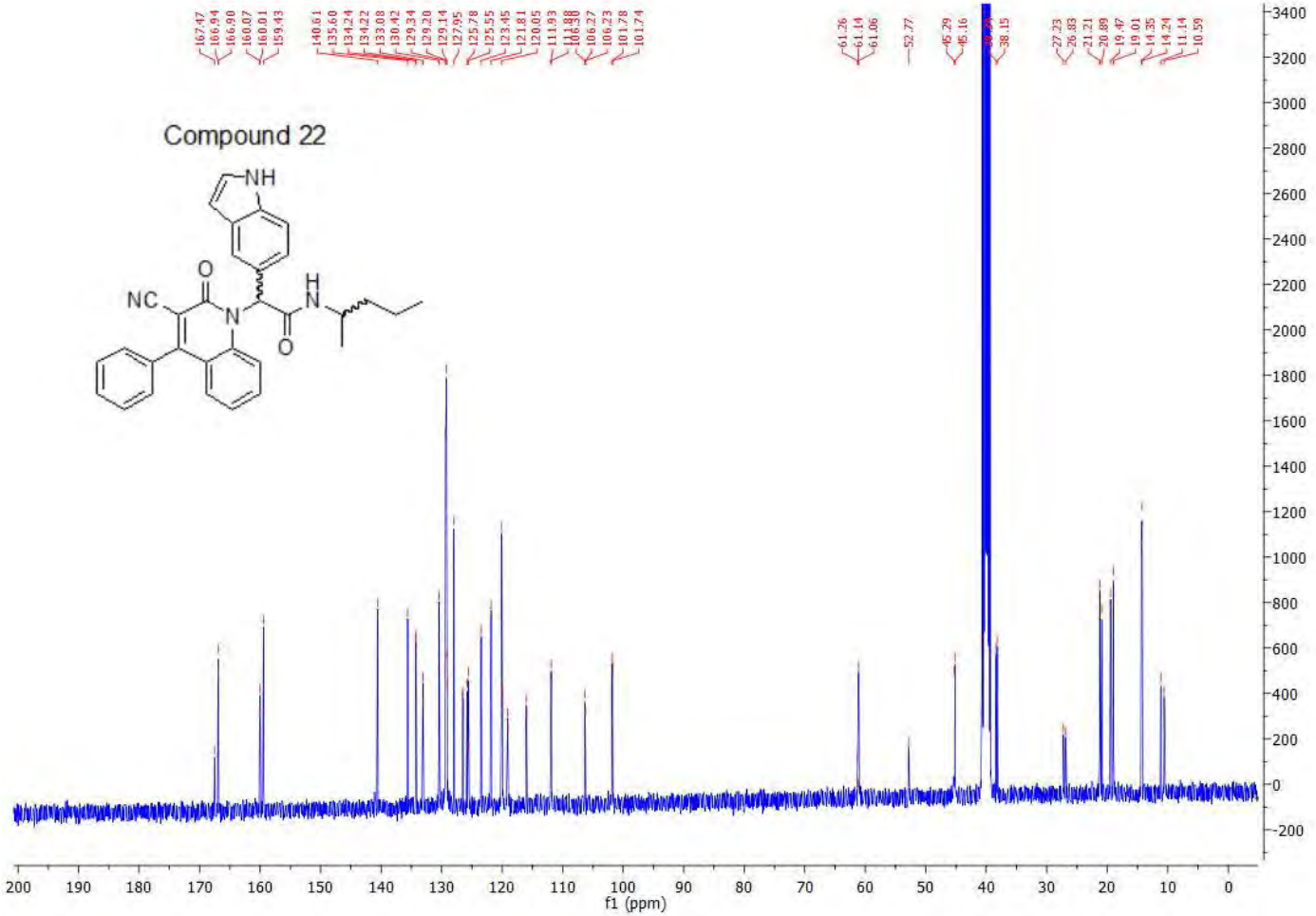
Compound 22
NH
O
NC
N
H
N
O
f1 (ppm)

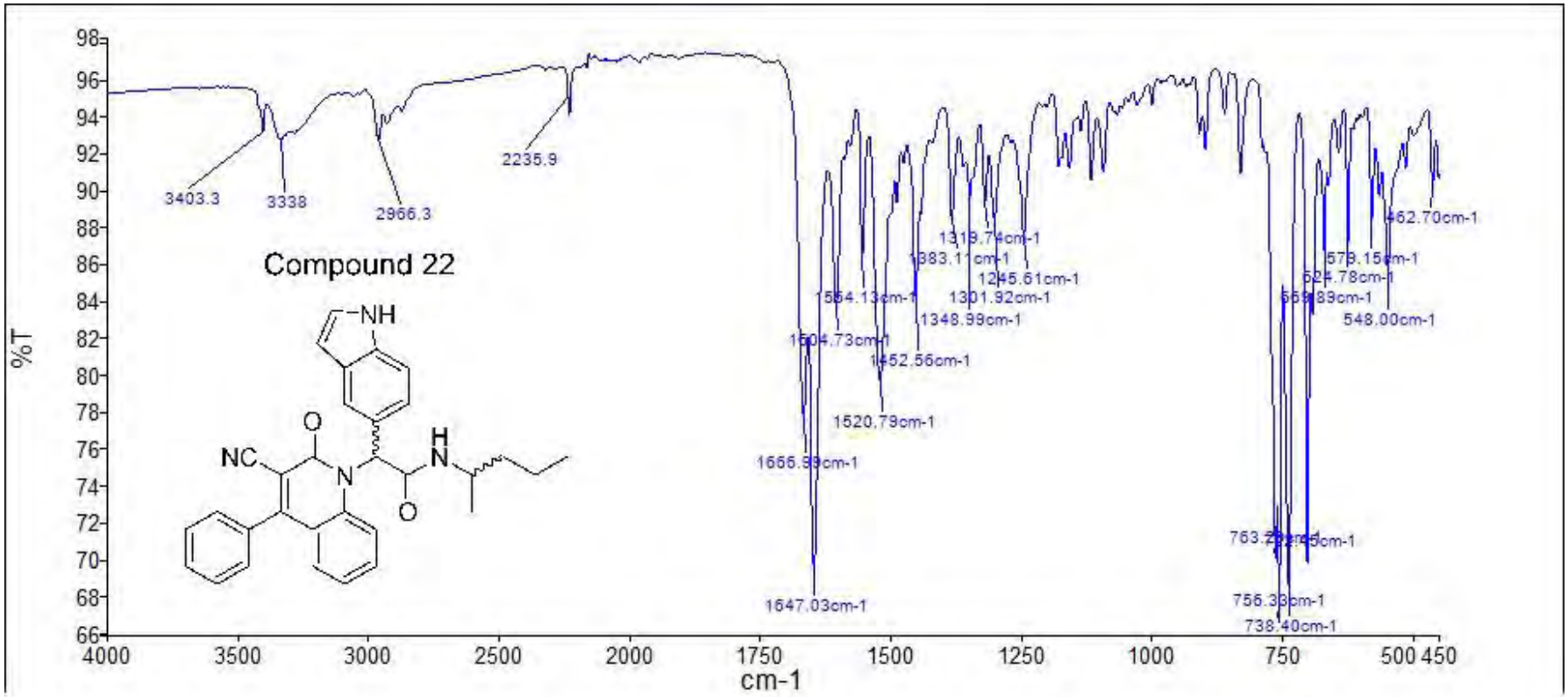
Compound 22
%T
cm-1
3403.3
3338
2966.3
2235.9
1666.39cm-1
1647.03cm-1
1604.73cm-1
1554.13cm-1
1520.79cm-1
1452.56cm-1
1383.11cm-1
1348.99cm-1
1319.74cm-1
1301.92cm-1
1245.61cm-1
756.33cm-1
738.40cm-1
573.15cm-1
548.00cm-1
462.70cm-1
NC
O
N
H
N
O

==== Shimadzu LCMSsolution Analysis Report ====

Acquired by	: Admin
Sample Name	: TP126B1 Old
Sample ID	:
Vail #	: 53
Injection Volume	: 30 uL
Data File Name	: TP126B1 Old .lcd
Method File Name	: Econosphere C18 EPS 5u lot 50195421 part 70070 150mm id 4.6mm.lcm
Batch File Name	: 2015 Ugi Knoevenagel products continue.lcb
Report File Name	: DefaultLCMS.lcr
Data Acquired	: 9/16/2015 12:47:50 PM
Data Processed	: 10/15/2015 10:07:01 AM

Compound 22

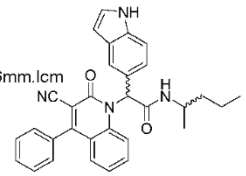

<Chromatogram>

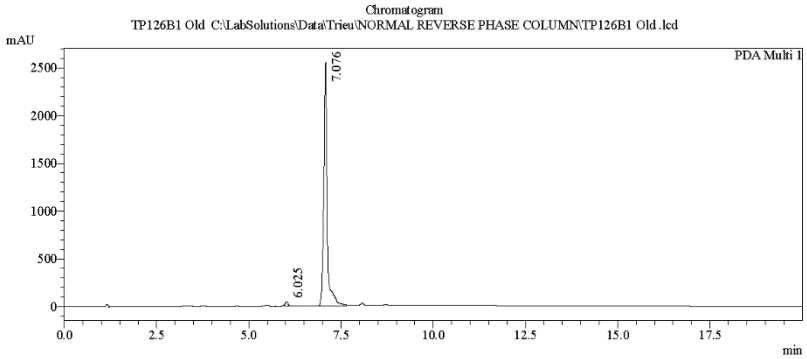

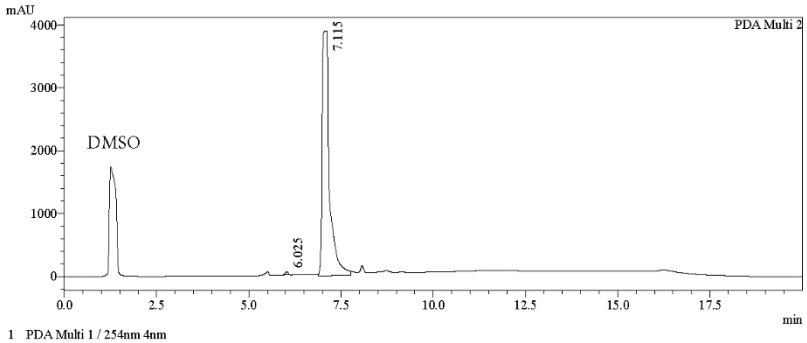

1 PDA Multi 1 / 254nm 4nm
2 PDA Multi 2 / 220nm 4nm

PeakTable

PDA Ch1 254nm 4nm

Peak#	Ret. Time	Area	Height	Area %	Height %
1	6.025	224446	44876	1.347	1.724
2	7.076	16434733	2558207	98.653	98.276
Total		16659179	2603083	100.000	100.000

PeakTable

PDA Ch2 220nm 4nm

Peak#	Ret. Time	Area	Height	Area %	Height %
1	6.025	218499	45903	0.403	1.166
2	7.115	54050292	3891227	99.597	98.834
Total		54268791	3937130	100.000	100.000

==== Shimadzu LCMSsolution Data Report ====

<Chromatogram>

Sample Information

Acquired by	: Admin
Date Acquired	: 7/23/2015 6:26:49 PM
Sample Type	: Unknown
Level#	: 0
Sample Name	: TP126B1
Sample ID	:
ISTD Amount	: (Level1 Conc.)
Sample Amount	: 1
Dilution Factor	: 1
Tray#	: 1
Vial#	: 59
Injection Volume	: 5
Data File	: TP126B2.lcd
Method File	: FIA-ESI_Scan(-).lcm
Original Method	: C:\LabSolutions\Data\Kelly\FIA-ESI_Scan(-).lcm
Report Format	: DefaultLCMS.lcr
Tuning File	: C:\LabSolutions\LCsolution\Log\Tuning\Autotune_030908.lct
Processed by	: Admin
Modified Date	: 7/23/2015 6:28:20 PM

Chromatogram

TP126B1 C:\LabSolutions\Data\Trieu\NORMAL REVERSE PHASE COLUMN\UGI MASS ESI NEGATIVE SCAN\TP126B2.lcd

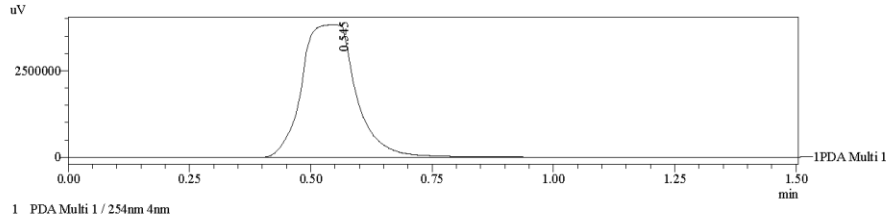

1 PDA Multi 1 / 254nm 4nm

<Spectrum>

Retention Time:0.820(Scan#:83)
Max Peak:535 Base Peak:156.55(669410)
Spectrum:Averaged 0.620-1.300(63-131)
Background:Averaged 0.100-0.454(11-47) Polarity:Pos Segment1 - Event1

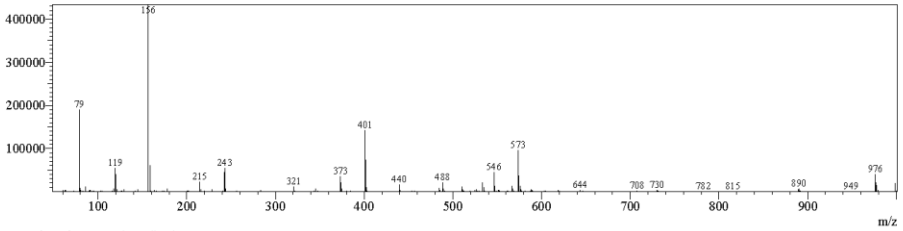

Retention Time:0.810(Scan#:82)
Max Peak:523 Base Peak:226.55(72741)
Spectrum:Averaged 0.630-1.310(64-132)
Background:Averaged 0.110-0.454(12-48) Polarity:Neg Segment1 - Event2

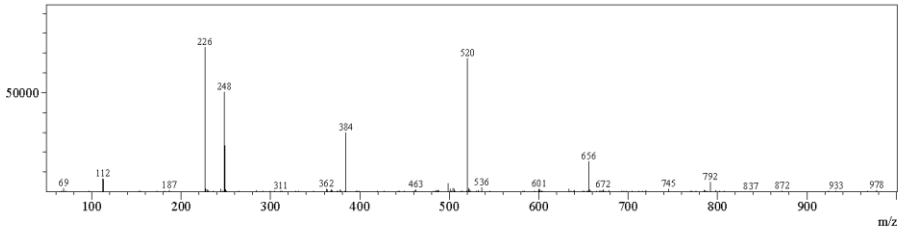

C:¥LabSolutions¥Data¥Trieu¥NORMAL REVERSE PHASE COLUMN¥UGI MASS ESI NEGATIVE SCAN¥TP126B2.lcd

Compound	Chemical Formula	Predicted monoisotopic neutral MW	Predicted MH+	MH+ Measured	Main MS Ions	Main MS/MS Fragments
TP126B1	$C_{31}H_{28}N_4O_2$	488.2212	489.2285	489.2284	402.1253 243.14907 (fragment) 489.2284	402.1245 374.1294 215.1574

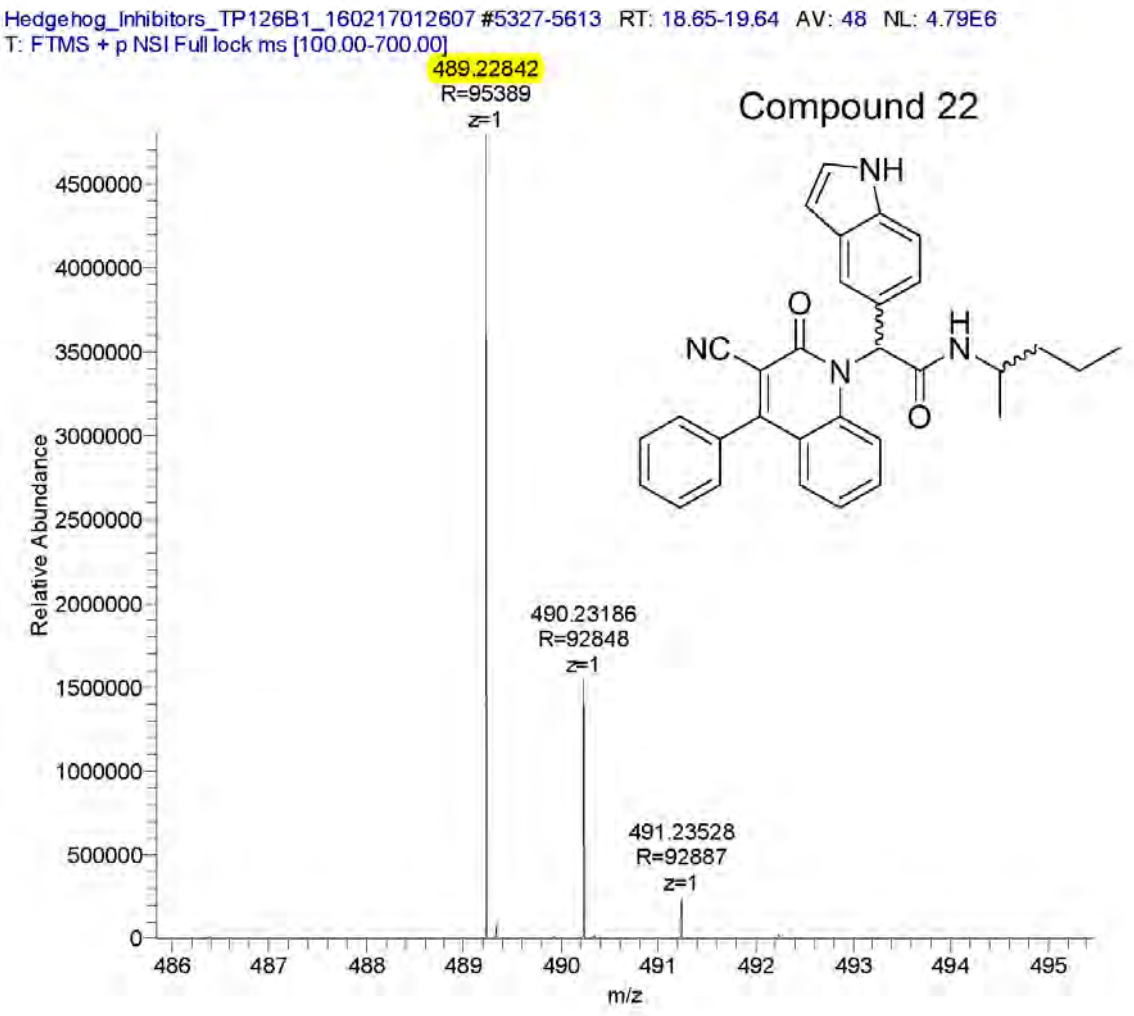

Compound 23

Compound Name: 2-(3-cyano-2-oxo-4-phenylquinolin-1(2*H*)-yl)-2-(5-methyl-1*H*-indole-3-yl)-*N*-(pentan-2-yl)acetamide

Obtained Weight & Yield: 0.445g, 46%

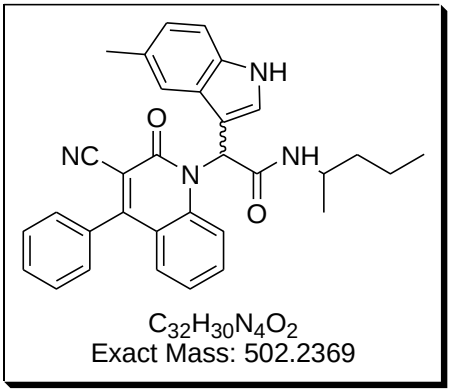

Appearance: Off-white precipitate

Solubility: EtOAc, Acetone, ACN

Melting Point: 178-180 ˚C

TLC Conditions: EtOAc/Hexane (50/50)

IR Analysis: ν_{max}/cm^{-1}
3427 (bp NH), 2962 (CH), 2236 (CN), 1645 (CON)

The ^{1}H NMR displays a mixture of isomers, with the ratio 2.1 : 1.0 calculated at 0.77 and 0.68 ppm, respectively. ^{1}H is reported as a whole without splitting due to the complex overlapping. All peaks detected in ^{13}C are reported

^{1}H NMR Analysis:

^{1}H NMR (400 MHz, DMSO-d_6) δ 11.13 (d, J = 4.9 Hz, 1H), 7.90 – 7.37 (m, 10H), 7.29-7.16 (m, 4H), 6.92 (d, J = 8.3 Hz, 1H), 4.03 – 3.87 (m, 1H), 2.34 (s, 3H), 1.57 – 1.20 (m, 3H), 1.20 – 0.86 (m, 5H), 0.82-0.60 (m, 3H).

^{13}C NMR Analysis: (Sign of isomers)

^{13}C NMR (101 MHz, DMSO-d_6) δ 167.5, 166.9, 160.1, 160.1, 159.3, 140.1, 140.1, 134.6, 134.6, 134.5, 134.1, 133.3, 130.4, 129.4, 129.2, 129.1, 128.2, 128.1, 127.5, 127.5, 126.8, 126.6, 123.5, 119.9, 118.5, 118.4, 118.3, 116.0, 111.9, 107.9, 107.9, 106.0, 105.9, 54.5, 54.4, 52.9, 45.4, 45.2, 38.4, 38.2, 27.3, 26.9, 21.9, 21.1, 20.9, 19.6, 19.2, 14.4, 14.2, 11.2, 10.8

HPLC:
RP-HPLC Alltima™ C18 5 μm, 150 mm x 4.6 mm, 10–100% B in 15 min, R_t =10.89 min, 100%.

Mass Spectral Analysis (Low res): LRMS (ESI-) m/z 502, 521 $[M+NH_4]^+$ 40%. HRMS (ES+) for $C_{32}H_{30}N_4O_2$; calculated 503.2442, found 503.2444.

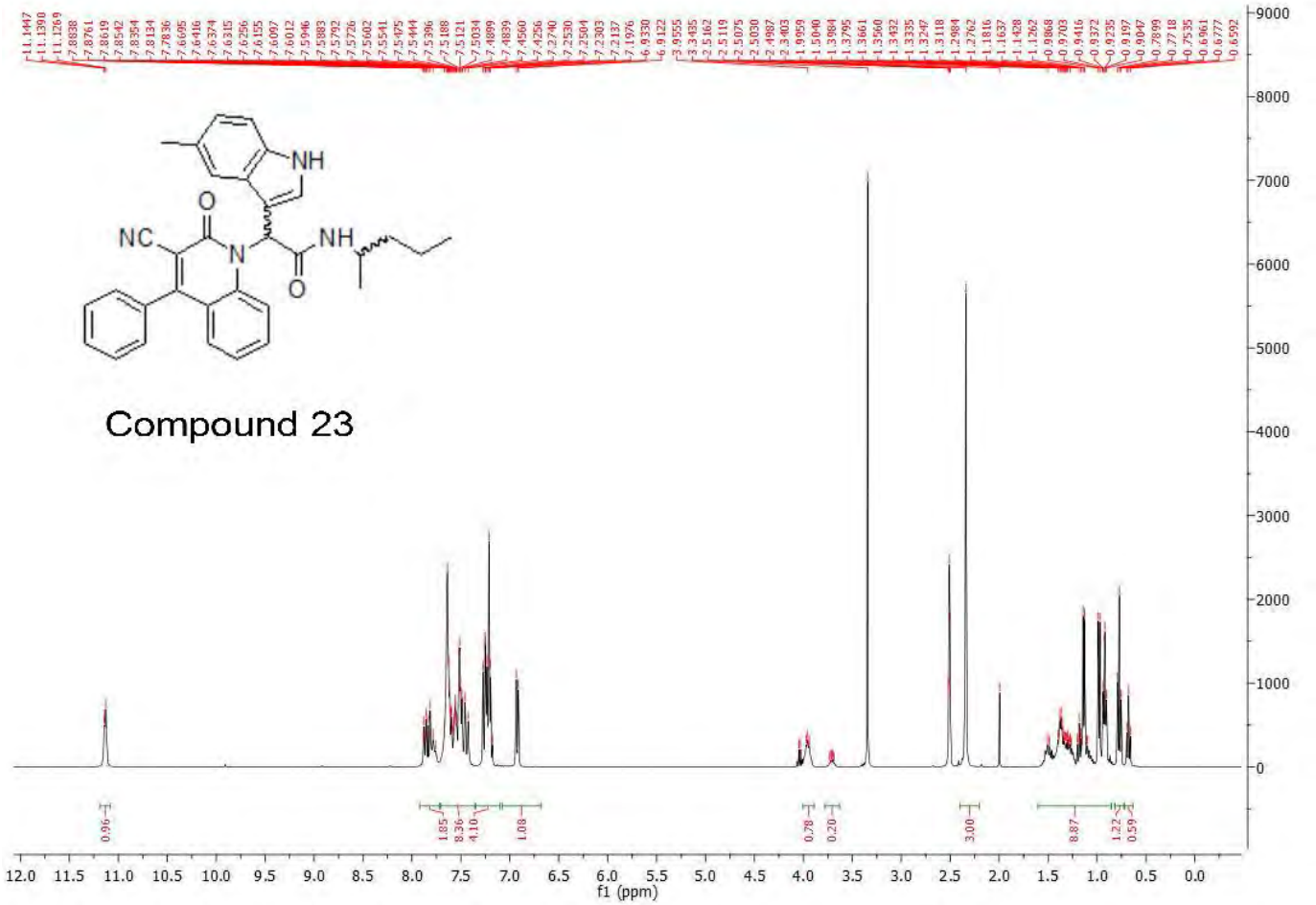
NH
O
NC
N
NH
O
Compound 23
f1 (ppm)

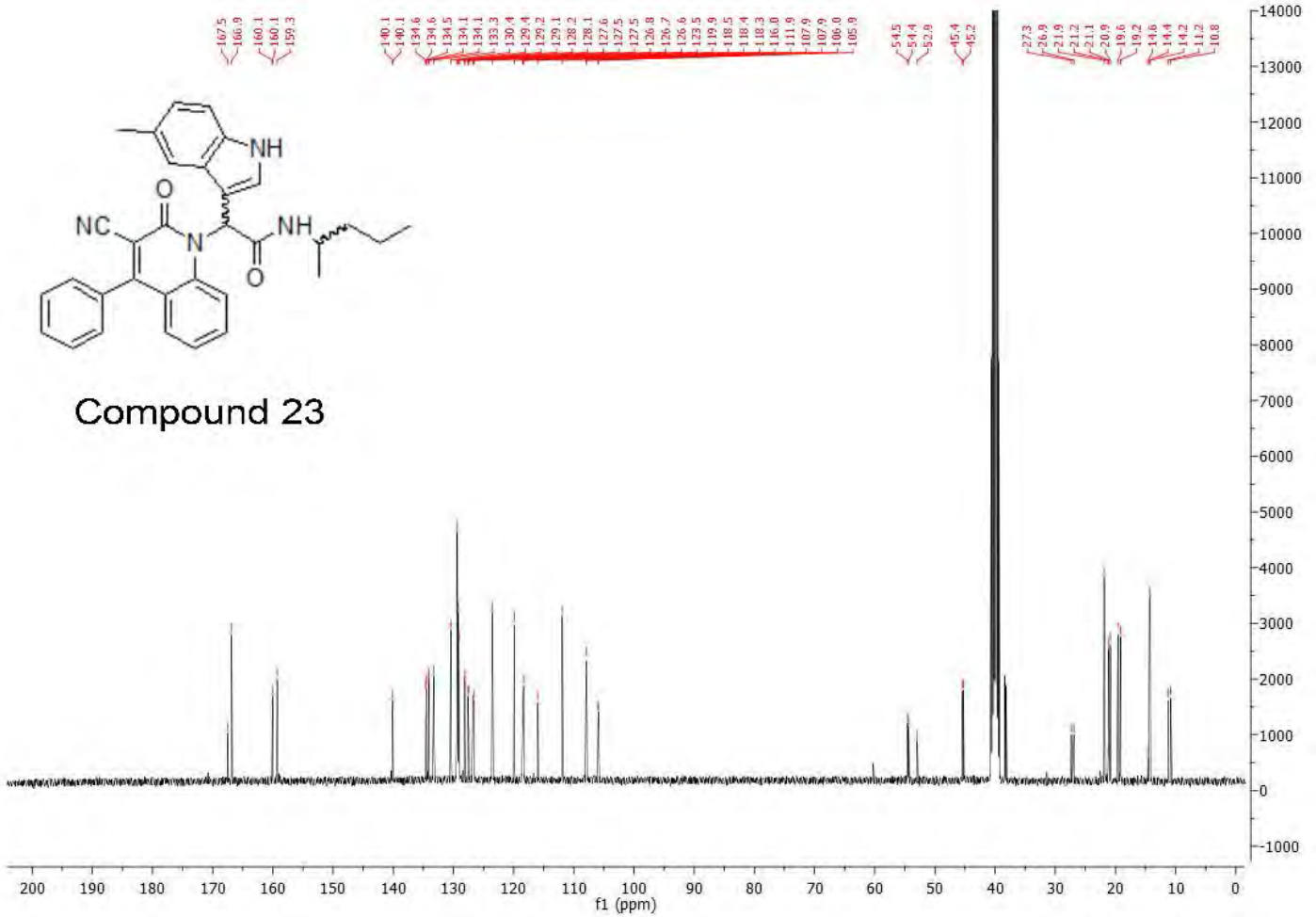
NH
O
NC
N
NH
O
Compound 23
f1 (ppm)

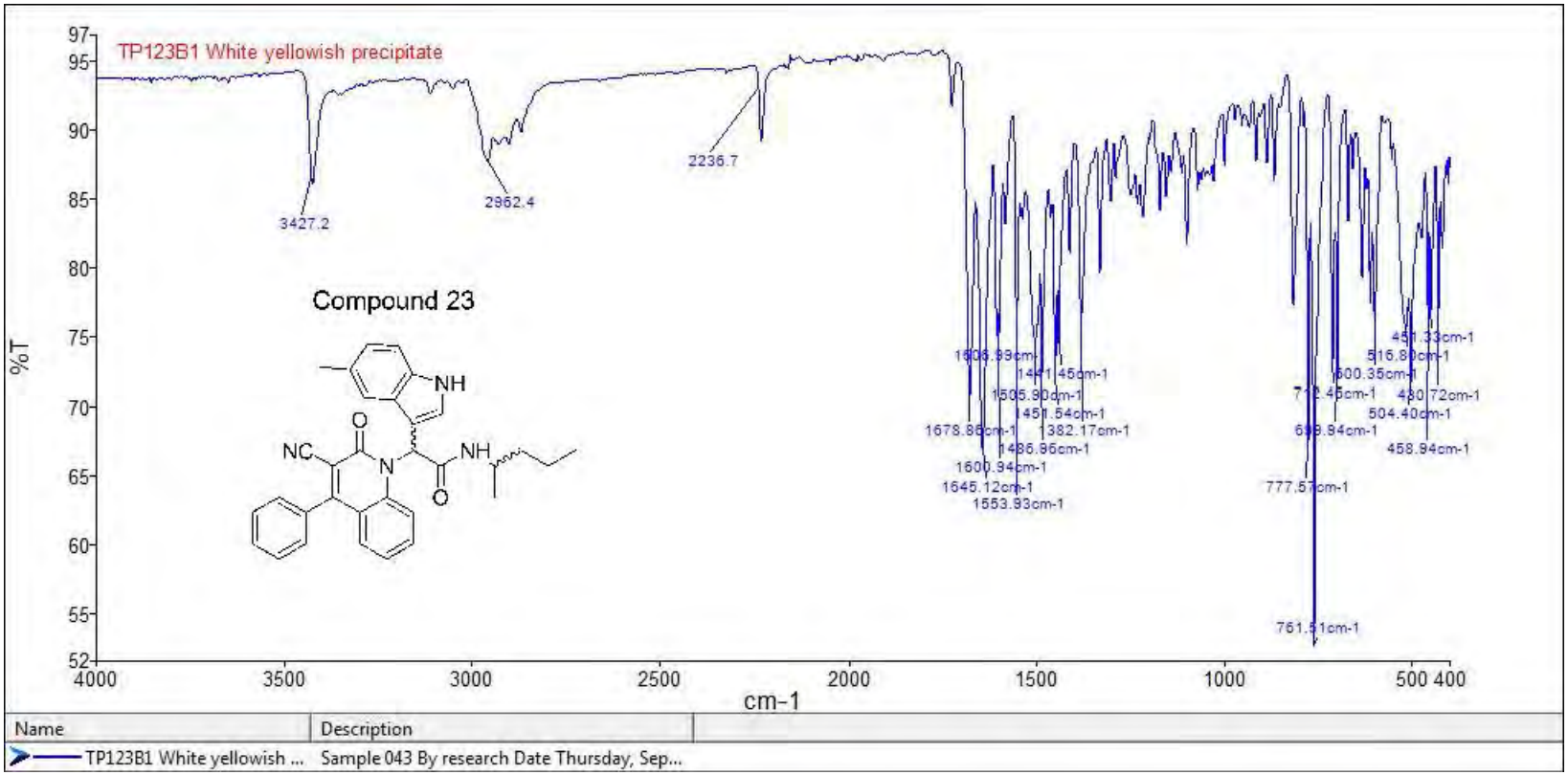
TP123B1 White yellowish precipitate
Compound 23
%T
cm-1
3427.2
2962.4
2236.7
1678.86cm-1
1645.12cm-1
1600.94cm-1
1553.93cm-1
1505.90cm-1
1486.96cm-1
1451.54cm-1
1441.45cm-1
1382.17cm-1
777.51cm-1
761.51cm-1
712.45cm-1
699.94cm-1
600.35cm-1
516.80cm-1
504.40cm-1
480.72cm-1
458.94cm-1
451.33cm-1
Name
Description
TP123B1 White yellowish ...
Sample 043 By research Date Thursday, Sep...

SHIMADZU LabSolutions Analysis Report

<Sample Information>

Sample Name	: TP123B1 E		
Sample ID	: TP123B1 E		
Data Filename	: TP123B1 E.lcd		
Method Filename	: 30-100 over 15 mins.lcm		
Batch Filename	: TP174-176B3 10-100 over 15mins.lcb		
Vial #	: 1-10	Sample Type	: Unknown
Injection Volume	: 15 uL		
Date Acquired	: 8/08/2014 1:33:34 PM	Acquired by	: System Administrator
Date Processed	: 8/08/2014 2:03:35 PM	Processed by	: System Administrator

<Chromatogram>

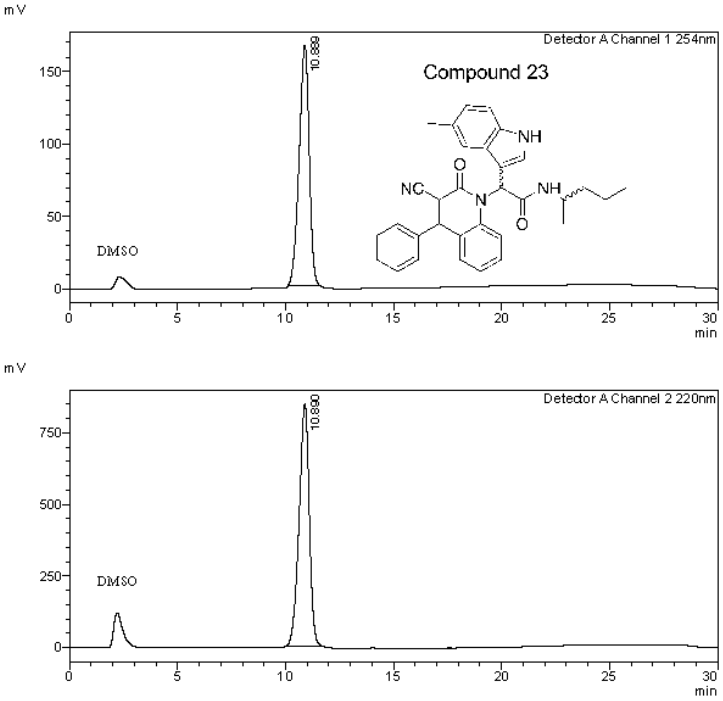

<Peak Table>

Detector A Channel 1 254nm

C:\LabSolutions\Data\Project1\TRIEU\TP123B1 E.lcd

2

Peak#	Ret. Time	Area	Height	Conc.	Unit	Mark	Name
1	10.889	5320260	165568	100.000		M	
Total		5320260	165568				

Detector A Channel 2 220nm

Peak#	Ret. Time	Area	Height	Conc.	Unit	Mark	Name
1	10.890	27640600	846427	100.000		M	
Total		27640600	846427				

==== Shimadzu LCMSsolution Data Report ====

<Chromatogram>

Sample Information

Acquired by	: Admin
Date Acquired	: 10/13/2015 12:57:05 PM
Sample Type	: Unknown
Level#	: 0
Sample Name	: TP123B1Re-ve
Sample ID	:
ISTD Amount	: (Level1 Conc.)
Sample Amount	: 1
Dilution Factor	: 1
Tray#	: 1
Vial#	: 30
Injection Volume	: 10
Data File	: TP123B1Re-ve.lcd
Method File	: FIA-ESI_Scan(-).lcm
Original Method	: C:\LabSolutions\Data\Jen Baker\FIA-ESI_Scan(-).lcm
Report Format	: DefaultLCMS.lcr
Tuning File	: C:\LabSolutions\Data\AutoTuning\Autotune_ESI_26AUG15.lct
Processed by	: Admin
Modified Date	: 10/13/2015 12:58:37 PM

Compound 23

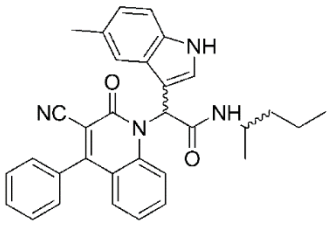

Chromatogram
TP123B1Re-ve C:\LabSolutions\Data\Jen Baker\TP123B1Re-ve.lcd

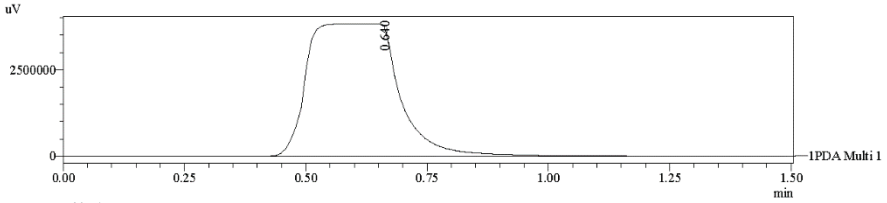

1 PDA Multi 1 / 254nm 4nm

<Spectrum>

Retention Time:0.620(Scan#:63)
Max Peak:593 Base Peak:298.10(423998)
Spectrum:Averaged 0.620-1.400(63-141)
Background:Averaged 0.020-0.606(3-61) Polarity:Pos Segment1 - Event1

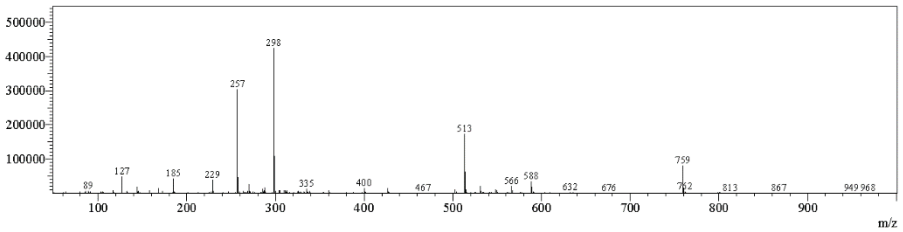

Retention Time:0.950(Scan#:96)
Max Peak:570 Base Peak:227.25(217681)
Spectrum:Averaged 0.630-1.410(64-142)
Background:Averaged 0.030-0.606(4-62) Polarity:Neg Segment1 - Event2

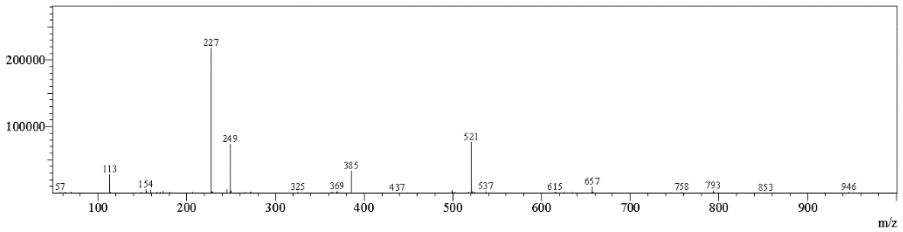

C:¥LabSolutions¥Data¥Jen Baker¥TP123B1Re-ve.lcd

Compound	Chemical Formula	Predicted monoisotopic neutral MW	Predicted MH+	MH+ Measured	Main MS Ions	Main MS/MS Fragments
TP123B1	$C_{32}H_{30}N_4O_2$	502.2369	503.2442	503.2444	257.16473 (fragment) 247.0866 (fragment)	257.1653 86.0971 144.0811

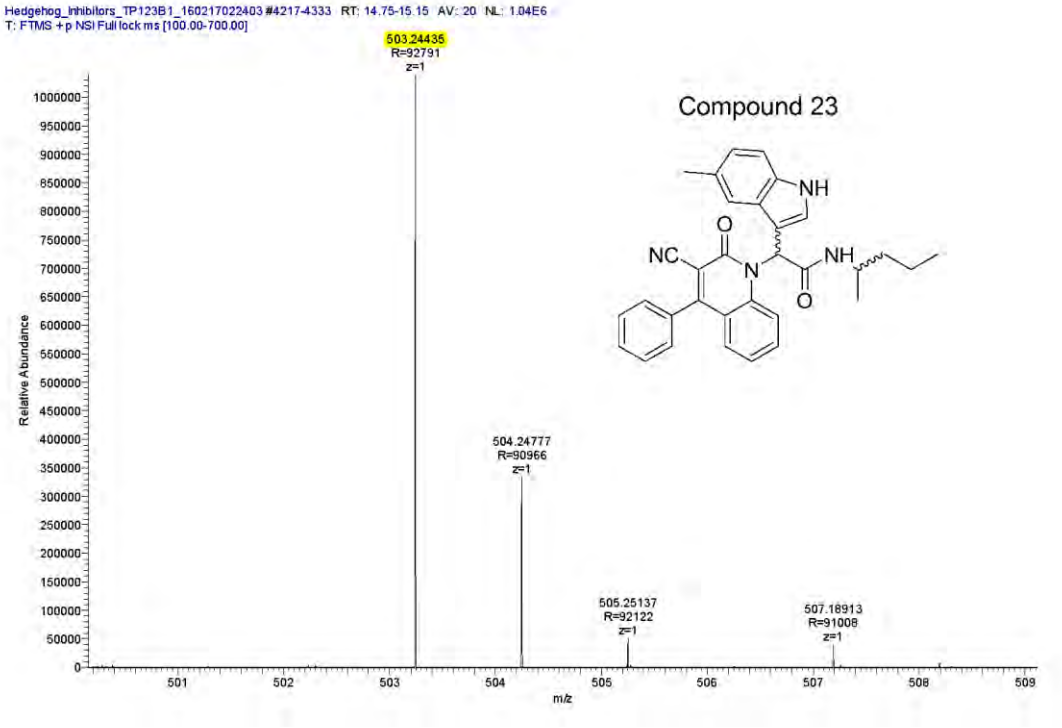

Compound 24

Compound Name: Ethyl-[2-(3-cyano-2-oxo-4-phenyl-2*H*-quinolin-1-yl)-2-(5-methyl-1*H*-indol-3-yl)-acetamido]-acetate

Obtained Weight & Yield: 0.347g, 34%

Appearance: Greenish precipitate

Solubility: EtOAc, ACN

Melting Point: 199-200 ˚C

TLC Conditions: EtOAc/Hexane (50/50)

IR Analysis: νmax/cm^{-1}

3423 (NH), 3410 (NH), 2232 (CN), 1731 (COO), 1673 (CON)

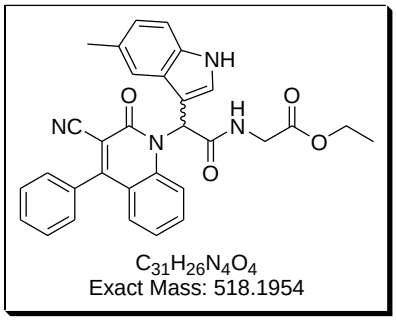

$C_{31}H_{26}N_4O_4$
Exact Mass: 518.1954

^{1}H NMR Analysis:

^{1}H NMR (400 MHz, DMSO-d_6) δ 11.21 (d, J = 1.8 Hz, 1H), 8.53 (s, 1H), 7.83 (d, J = 8.7 Hz, 1H), 7.72 – 7.48 (m, 8H), 7.32 – 7.17 (m, 4H), 6.92 (d, J = 8.3 Hz, 1H), 4.14 (q, J = 7.1 Hz, 2H), 4.02-3.84 (m, 2H), 2.34 (s, 3H), 1.22 (t, J = 7.1 Hz, 3H).

^{13}C NMR Analysis:

^{13}C NMR (101 MHz, DMSO-d_6) δ 170.2, 168.4, 160.3, 159.3, 139.7, 134.5, 134.1, 133.5, 130.5, 129.4, 129.4, 129.4, 129.1, 129.0, 128.3, 127.5, 127.1, 123.7 (C x 2), 119.9, 118.5, 118.2, 115.8, 111.9, 107.3, 105.8, 61.0, 53.8, 41.9, 21.9, 14.6.

HPLC:

RP-HPLC Alltima™ C18 5 µm, 150 mm x 4.6 mm, 10–100% B in 15 min, R_t =13.72 min, 97.9% (254nm and 220nm).

Mass Spectral Analysis: LRMS (ESI+) m/z518, 541 $[M+Na-H]^+$ 60%. HRMS (ES+) for $C_{31}H_{26}N_4O_4$; calculated 519.2027, found 519.2026.

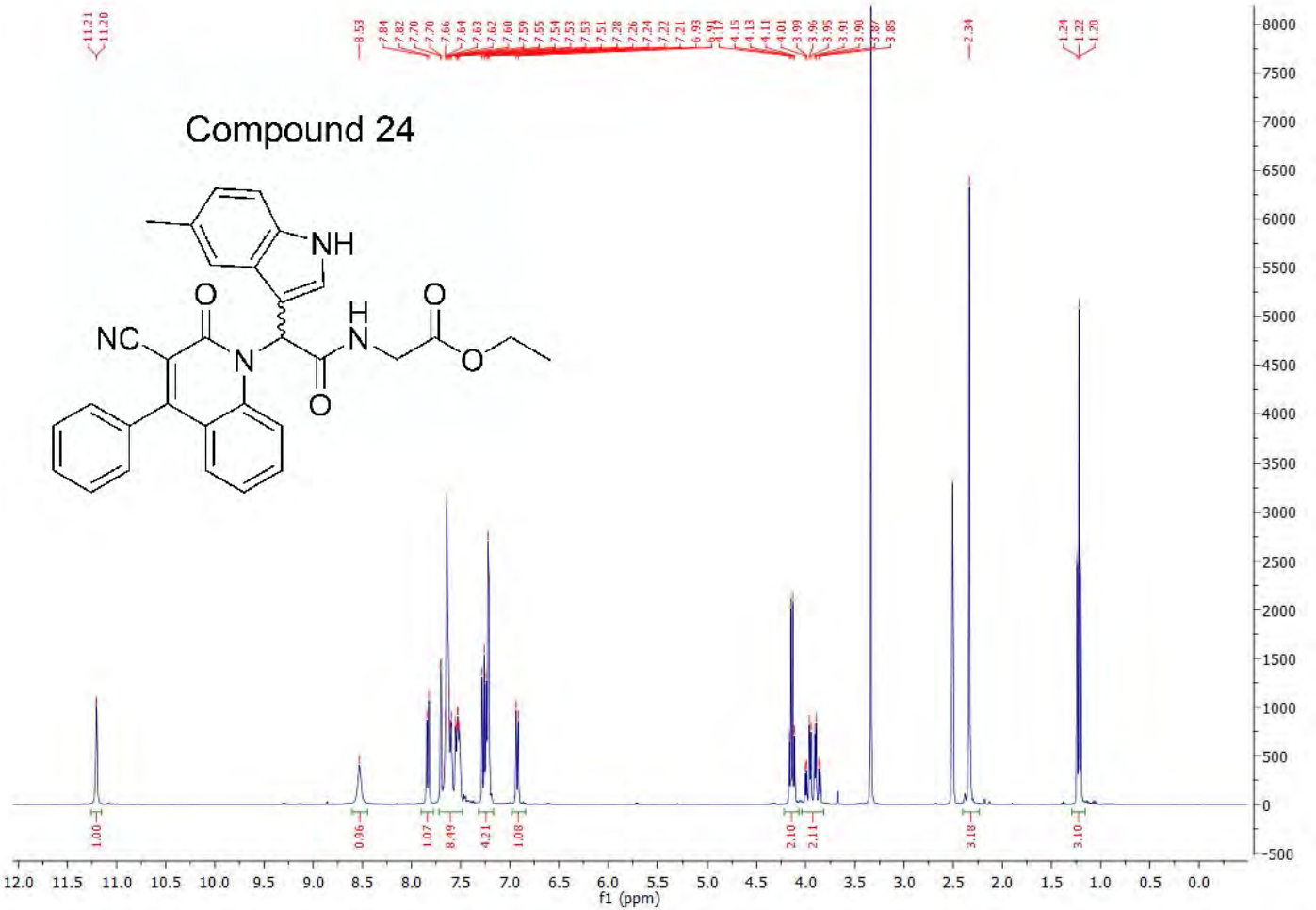
Compound 24
NH
O
NC
N
H
N
O
O
O
11.21
11.20
8.53
7.84
7.82
7.70
7.70
7.66
7.64
7.63
7.62
7.60
7.59
7.55
7.54
7.53
7.53
7.51
7.28
7.26
7.24
7.22
7.21
6.93
4.17
4.15
4.13
4.11
4.01
3.99
3.96
3.95
3.91
3.90
3.87
3.85
2.34
1.24
1.22
1.20
1.00
0.96
1.07
8.49
4.21
1.08
2.10
2.11
3.18
3.10
f1 (ppm)

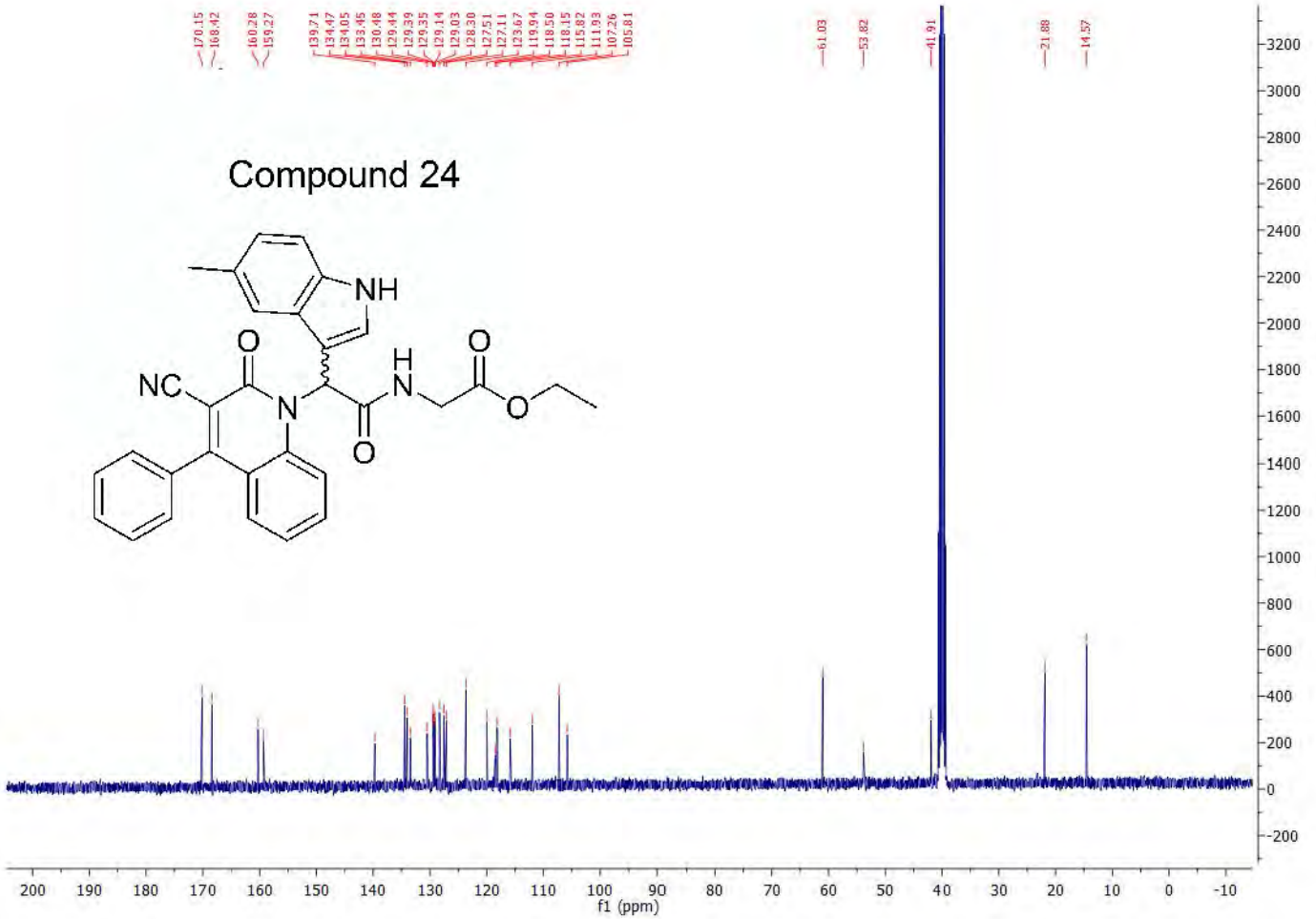
Compound 24
NH
O
NC
N
H
N
O
O
O
170.15
168.42
160.28
159.27
139.71
134.47
134.05
133.45
130.48
129.44
129.39
129.35
129.14
129.03
128.30
127.51
127.11
123.67
119.94
118.50
118.15
115.82
111.93
107.26
105.81
61.03
53.82
41.91
21.88
14.57
3200
3000
2800
2600
2400
2200
2000
1800
1600
1400
1200
1000
800
600
400
200
0
-200
200 190 180 170 160 150 140 130 120 110 100 90 80 70 60 50 40 30 20 10 0 -10
f1 (ppm)

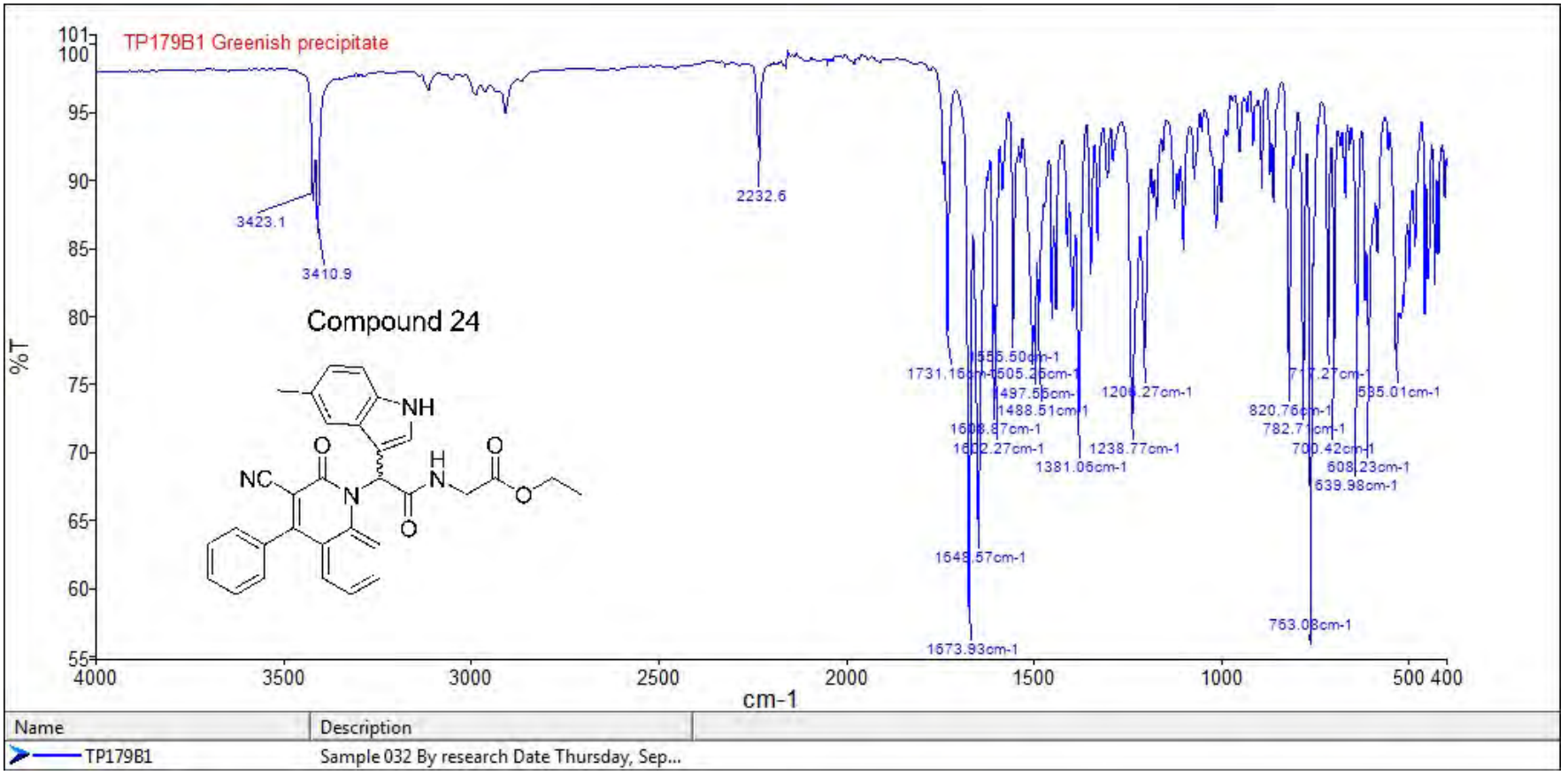
TP179B1 Greenish precipitate
Compound 24
%T
cm-1
3423.1
3410.9
2232.6
1731.16cm-1
1673.93cm-1
1649.57cm-1
1602.27cm-1
1488.51cm-1
1381.06cm-1
1238.77cm-1
820.76cm-1
763.08cm-1
700.42cm-1
639.98cm-1
608.23cm-1
535.01cm-1
Name
Description
TP179B1
Sample 032 By research Date Thursday, Sep...

SHIMADZU LabSolutions **Analysis Report**

<Sample Information>

Sample Name	: TP179B1		
Sample ID	: TP179B1		
Data Filename	: TP179B1.lcd		
Method Filename	: 10-100 over 15 mins.lcm		
Batch Filename	: TRIEU Second Third Generation and New pro.lcb		
Vial #	: 1-17	Sample Type	: Unknown
Injection Volume	: 30 uL		
Date Acquired	: 8/09/2014 2:39:27 PM	Acquired by	: System Administrator
Date Processed	: 8/09/2014 3:09:29 PM	Processed by	: System Administrator

<Chromatogram>

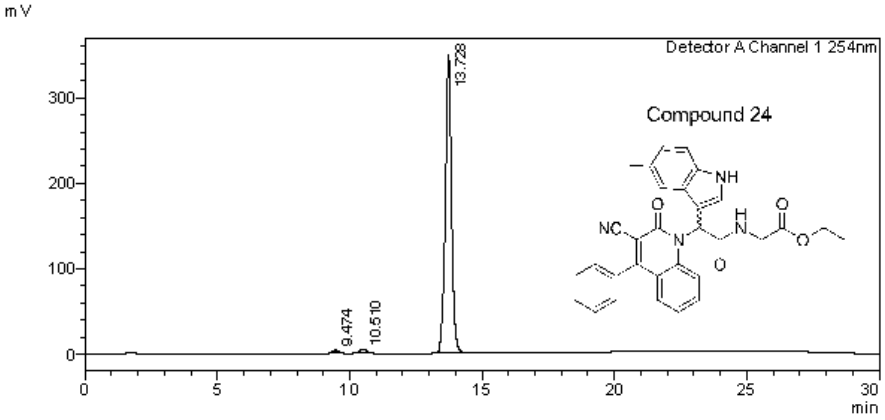

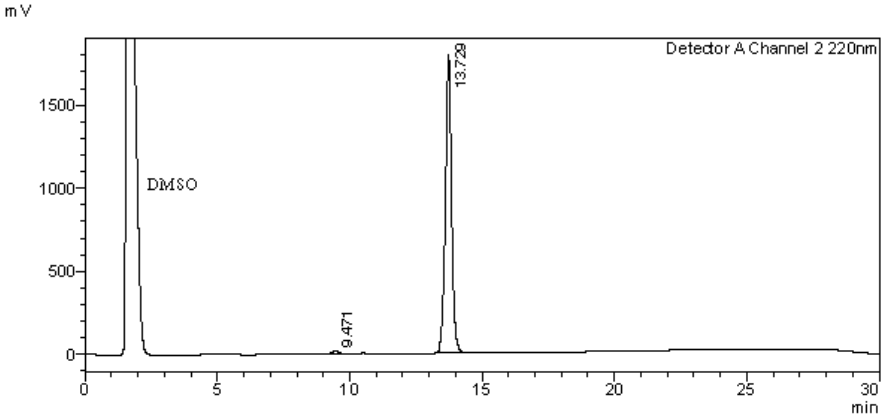

<Peak Table>

Detector A Channel 1 254nm

Peak#	Ret. Time	Area	Height	Conc.	Unit	Mark	Name
1	9.474	50354	3410	0.891		M	
2	10.510	63506	3798	1.124		M	
3	13.728	5535547	348160	97.985		M	
Total		5649407	355368				

Detector A Channel 2 220nm

Peak#	Ret. Time	Area	Height	Conc.	Unit	Mark	Name
1	9.471	275545	15893	0.956		M	
2	13.729	28561970	1790048	99.044		M	
Total		28837515	1805941				

==== Shimadzu LCMSsolution Data Report ====

<Chromatogram>

Sample Information

Acquired by	: Admin
Date Acquired	: 7/24/2015 9:57:16 AM
Sample Type	: Unknown
Level#	: 0
Sample Name	: TP179B1
Sample ID	:
ISTD Amount	: (Level1 Conc.)
Sample Amount	: 1
Dilution Factor	: 1
Tray#	: 1
Vial#	: 52
Injection Volume	: 15
Data File	: TP179B2.lcd
Method File	: FIA-ESI_Scan(+).lcm
Original Method	: C:\LabSolutions\Data\Trieu\Mass spec files\FIA-ESI_Scan(+).lcm
Report Format	: DefaultLCMS.lcr
Tuning File	: C:\LabSolutions\LCsolution\Log\Tuning\Autotune_030908.lct
Processed by	: Admin
Modified Date	: 7/24/2015 9:58:48 AM

Compound 24

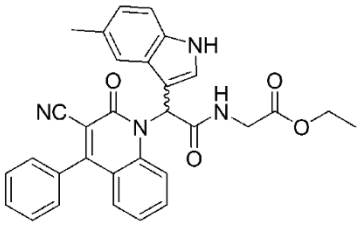

Chromatogram

TP179B1 C:\LabSolutions\Data\Trieu\NORMAL REVERSE PHASE COLUMN\ESI POSITIVE\UGI KNOEVENAGEL\TP179B2.lcd

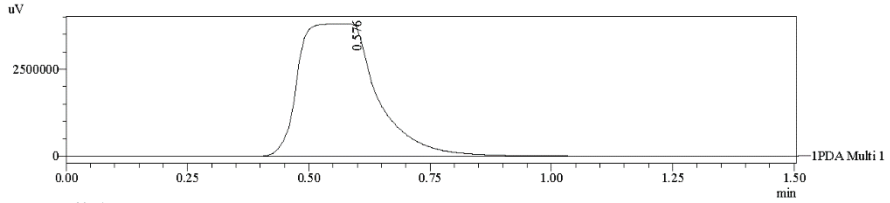

1 PDA Multi 1 / 254nm 4nm

<Spectrum>

Retention Time:0.980(Scan#:99)
Max Peak:323 Base Peak:272.70(128022)
Spectrum:Averaged 0.640-1.200(65-121)
Background:Averaged 0.120-0.515(13-53) Polarity:Pos Segment1 - Event1

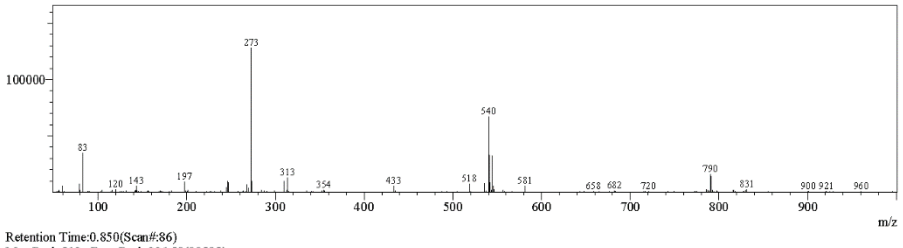

Retention Time:0.850(Scan#:86)
Max Peak:512 Base Peak:226.50(88595)
Spectrum:Averaged 0.650-1.210(66-122)
Background:Averaged 0.130-0.515(14-54) Polarity:Neg Segment1 - Event2

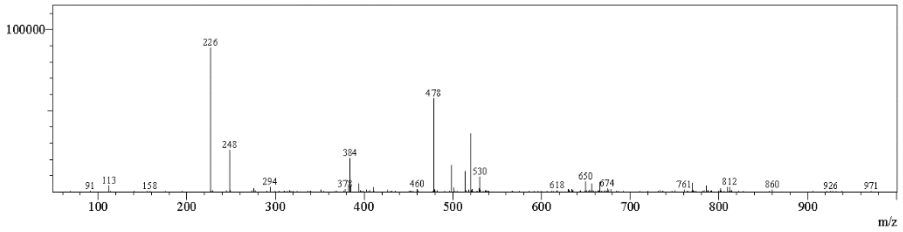

C:¥LabSolutions¥Data¥Trieu¥NORMAL REVERSE PHASE COLUMN¥ESI POSITIVE¥UGI KNOEVENAGEL¥TP179B2.lcd

Compound	Chemical Formula	Predicted monoisotopic neutral MW	Predicted MH+	MH+ Measured	Main MS Ions	Main MS/MS Fragments
TP179B1	$C_{31}H_{26}N_4O_4$	518.1954	519.2027	519.2026	273.12305 (fragment) 536.22908(+NH4) 519.2026	273.1237 245.1288

Hedgehog_Inhibitors_TP179B1_160217032158 #5152-5295 RT: 18.01-18.49 AV: 24 NL: 1.22E7
T: FTMS + p NSI Full lock ms [100.00-700.00]

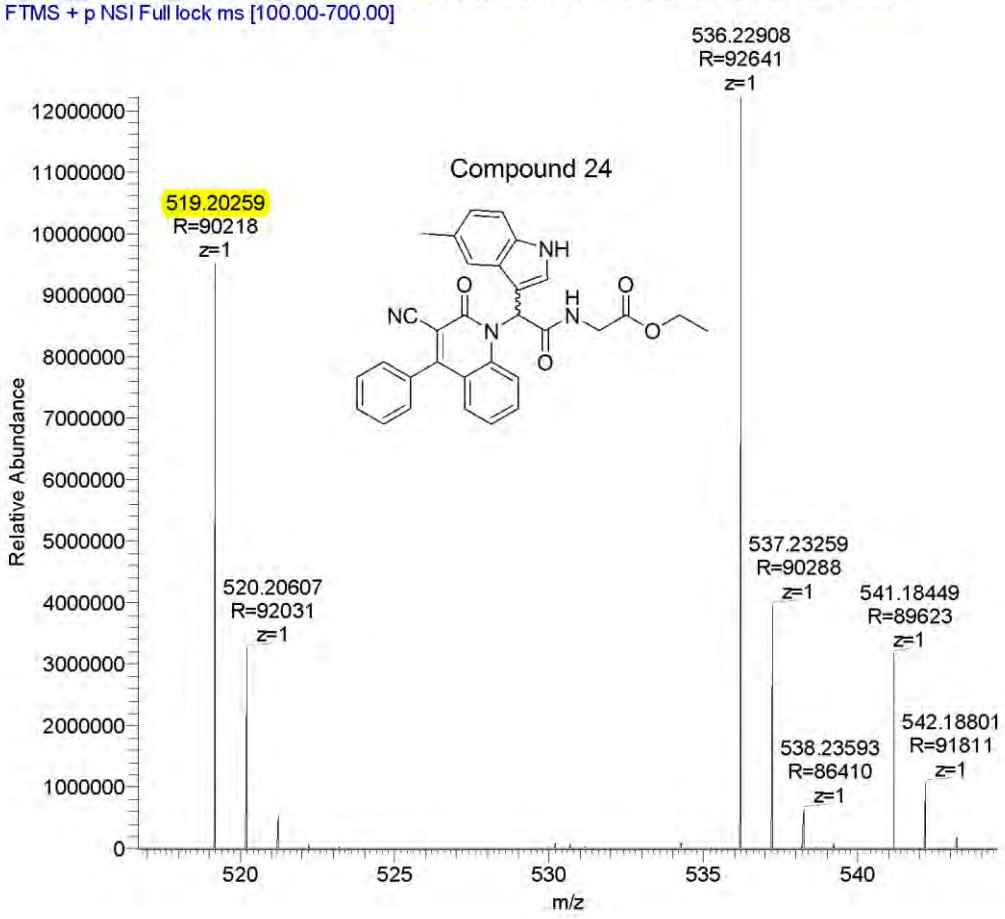

Compound 25

Compound Name: Ethyl-[2-(3-cyano-2-oxo-4-phenyl-2*H*-quinolin-1-yl)-2-(1*H*-indol-3-yl)-acetamido]-acetate

Obtained Weight & Yield: 0.3 g, 32%

Appearance: Offwhite precipitate

Solubility: EtOAc, ACN

Melting Point: 179.3-180.5 ˚C

TLC Conditions: EtOAc/Hexane (50/50)

IR Analysis: νmax/cm^{-1}

3420 (NH), 2236 (CN), 1737 (COO), 1686 (CONH), 1646 (CON)

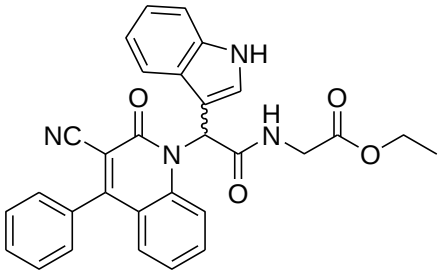

$C_{30}H_{24}N_4O_4$
Mol. Wt.: 504.5360

^{1}H NMR Analysis:

^{1}H NMR (400 MHz, DMSO-d_6) δ 11.35 (s, 1H), 8.58 (s, 1H), 7.93 – 7.75 (m, 2H), 7.75-7.45 (m, 8H), 7.39 (d, *J* = 8.0 Hz, 1H), 7.21 (d, *J* = 3.7 Hz, 2H), 7.15-6.91 (m, 2H), 4.25 – 4.06 (m, 2H), 4.04-3.80 (m, 2H), 1.22 (t, *J* = 7.0 Hz, 3H).

^{13}C NMR Analysis:

^{13}C NMR (101 MHz, DMSO-d_6) δ 170.2, 168.4, 160.3, 159.3, 139.7, 136.1, 134.0, 133.5, 130.5, 129.5, 129.4 (C x 2), 129.3 (C x 2), 129.2, 129.0, 127.3, 123.7, 122.1, 120.0 (C x 2), 118.6, 118.5, 115.9, 112.2, 107.8, 105.8, 61.1, 53.7 41.9, 14.6.

HPLC:

RP-HPLC Phenomenex Onyx™ Monolithic C18 5 μm, 100 mm x 4 mm, 10–100% B in 15 min, R_t = 11.09 min, 100%.

Mass Spectral Analysis: LRMS (ESI+) m/z 504, 505 $[M+H]^+$, 100%. HRMS (ES+) for $C_{30}H_{24}N_4O_4$; calculated 505.1870, found 505.1869.

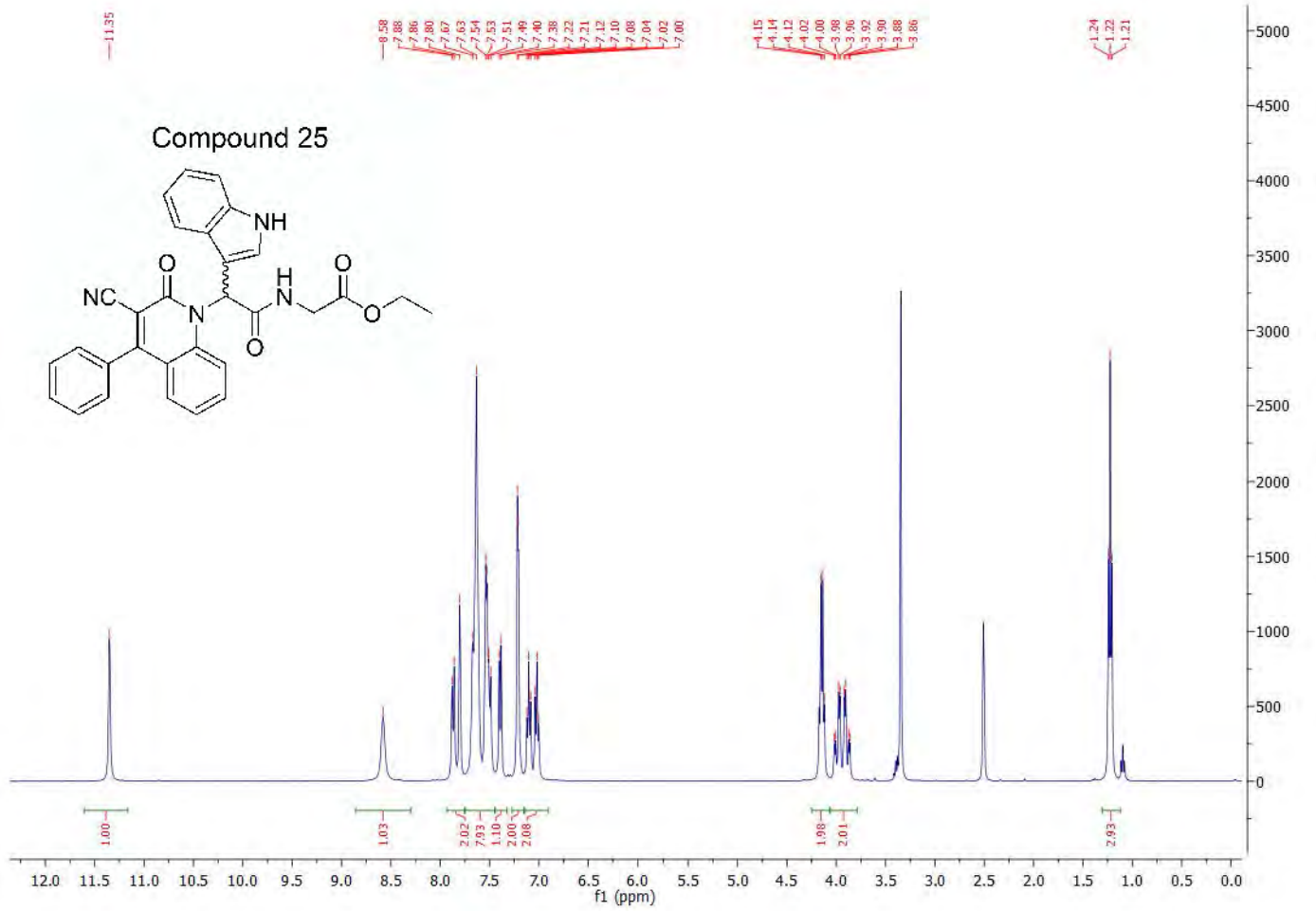
Compound 25
NH
NC
O
N
H
N
O
O
O
11.35
8.58
7.88
7.86
7.80
7.67
7.63
7.54
7.53
7.51
7.49
7.40
7.38
7.22
7.21
7.12
7.10
7.08
7.04
7.02
7.00
4.15
4.14
4.12
4.02
4.00
3.98
3.96
3.92
3.90
3.88
3.86
1.24
1.22
1.21
1.00
1.03
2.02
7.03
1.10
2.00
2.08
1.98
2.01
2.93
f1 (ppm)

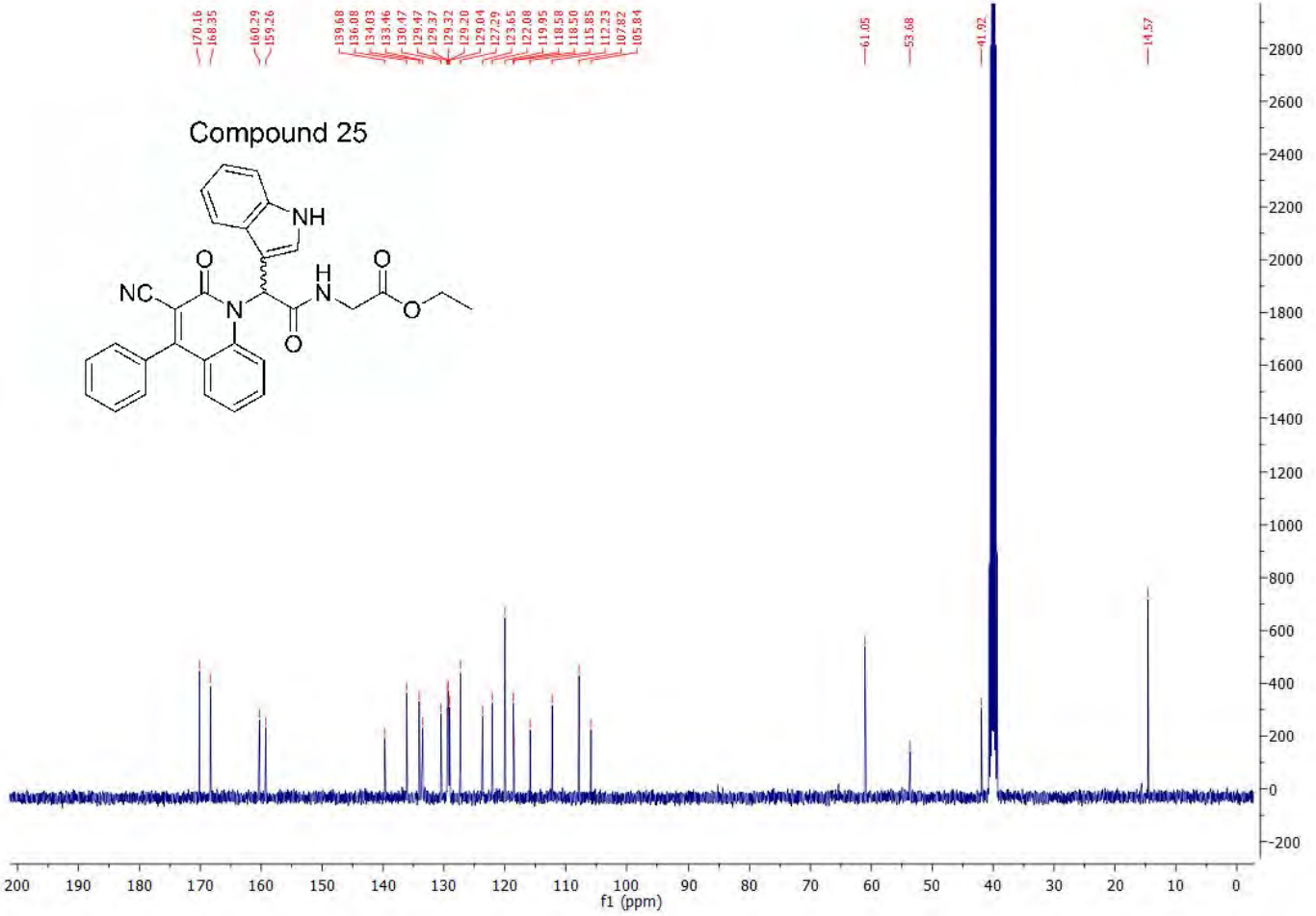
Compound 25
NH
O
NC
N
H
N
O
O
O
170.16
168.35
160.29
159.26
139.68
136.08
134.03
133.46
130.47
129.47
129.37
129.32
129.20
129.04
127.29
123.65
122.08
119.95
118.58
118.50
115.85
112.23
107.82
105.84
61.05
53.68
41.92
14.57
2800
2600
2400
2200
2000
1800
1600
1400
1200
1000
800
600
400
200
0
-200
200 190 180 170 160 150 140 130 120 110 100 90 80 70 60 50 40 30 20 10 0
f1 (ppm)

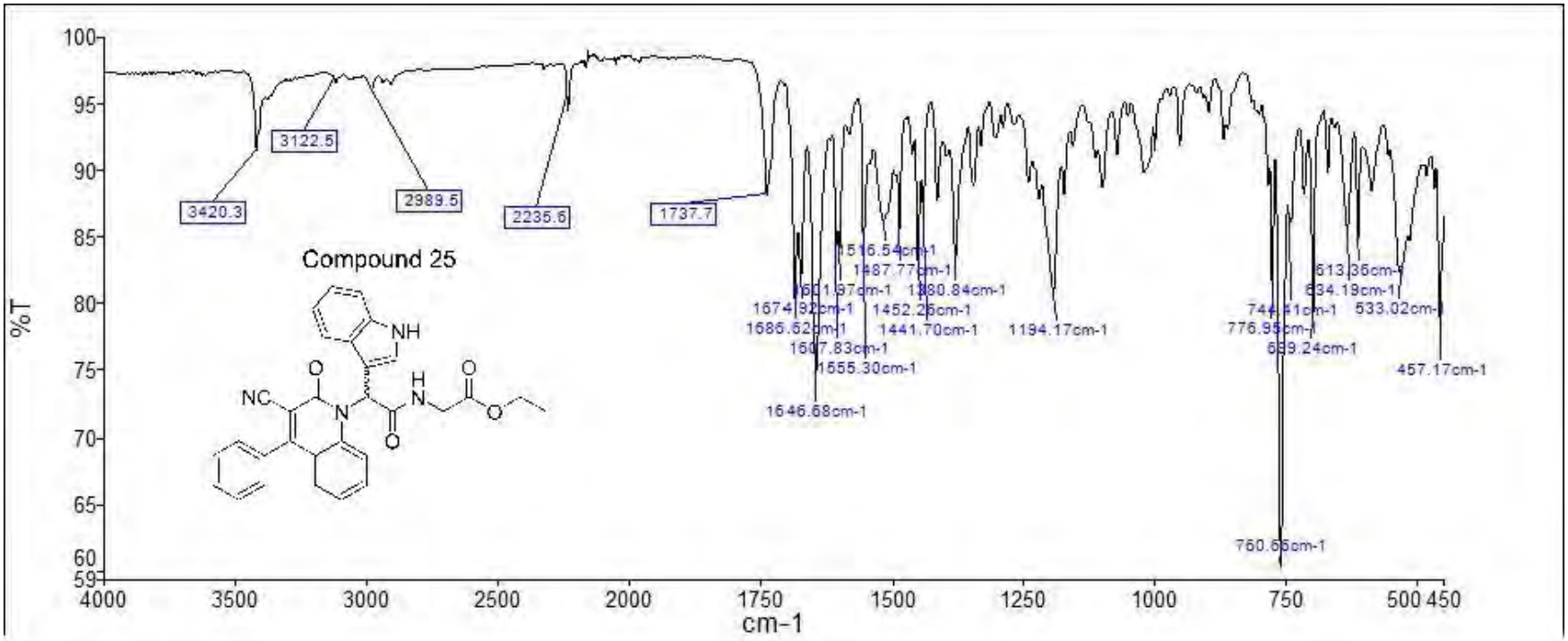
Compound 25
%T
cm-1
3420.3
3122.5
2989.5
2235.6
1737.7
1516.54cm-1
1487.77cm-1
1674.92cm-1
1452.26cm-1
1685.62cm-1
1441.70cm-1
1194.17cm-1
1607.83cm-1
1555.30cm-1
1646.68cm-1
744.41cm-1
776.95cm-1
513.36cm-1
634.19cm-1
533.02cm-1
457.17cm-1
760.66cm-1

Data File C:\CHEM32\...EMO\PURIFIED TR S EPI AND S LUG AIPS 2016-01-05 09-33-14\034-3501.D
Sample Name: TP186B5

Acq. Operator	: Simi120102015	Seq. Line	: 35
Acq. Instrument	: LC1260	Location	: Vial 34
Injection Date	: 1/6/2016 3:19:44 AM	Inj	: 1
		Inj Volume	: 10.000 µl
Acq. Method	: C:\CHEM32\1\DATA\DEMO\PURIFIED TR S EPI AND S LUG AIPS 2016-01-05 09-33-14\10 TO 100 OV 15MIN 10UL.M		
Last changed	: 12/10/2015 4:12:43 PM by Simi120102015		
Analysis Method	: C:\CHEM32\1\DATA\DEMO\PURIFIED TR S EPI AND S LUG AIPS 2016-01-05 09-33-14\10 TO 100 OV 15MIN 20UL.M (Sequence Method)		
Last changed	: 1/6/2016 10:52:32 AM by Simi120102015 (modified after loading)		

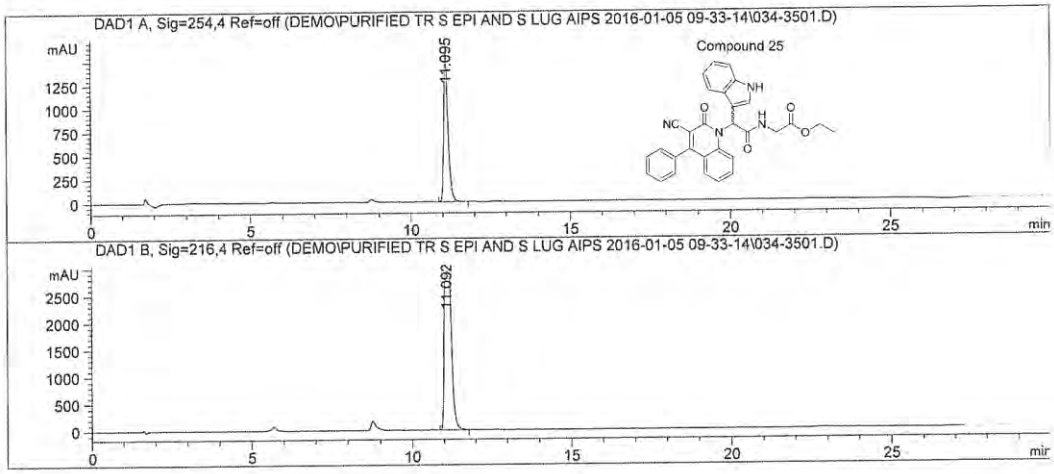

Area Percent Report

Sorted By : Signal
Multiplier: : 1.0000
Dilution: : 1.0000
Use Multiplier & Dilution Factor with ISTDs

Signal 1: DAD1 A, Sig=254,4 Ref=off

Peak #	RetTime [min]	Type	Width [min]	Area [mAU*s]	Height [mAU]	Area %
1	11.095	BB	0.1291	1.49871e4	1664.42249	100.0000
Totals :				1.49871e4	1664.42249	

Signal 2: DAD1 B, Sig=216,4 Ref=off

Peak #	RetTime [min]	Type	Width [min]	Area [mAU*s]	Height [mAU]	Area %
1	11.092	BV	0.2252	4.76297e4	2936.25610	100.0000

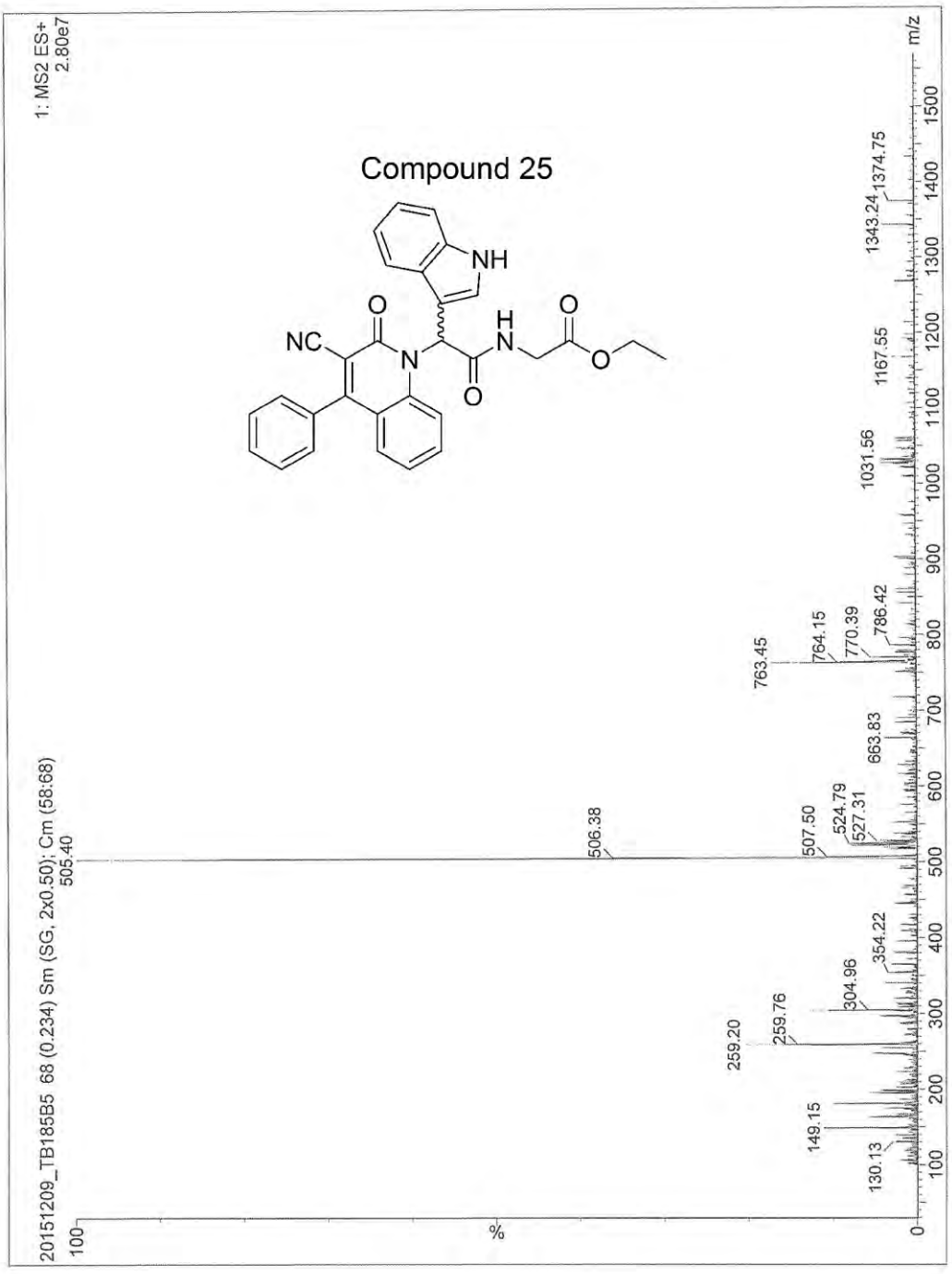
Compound 25
NC
O
N
H
N
O
O
O
NH
1: MS2 ES+
2.80e7
20151209_TB185B5 68 (0.234) Sm (SG, 2x0.50); Cm (58:68)
505.40
100
%
0
m/z
130.13
149.15
259.20
259.76
304.96
354.22
506.38
507.50
524.79
527.31
663.83
763.45
764.15
770.39
786.42
1031.56
1167.55
1343.24
1374.75

Compound	Chemical Formula	Predicted monoisotopic neutral MW	Predicted MH+	MH+ Measured	Main MS Ions	Main MS/MS Fragments
TP 18685	$C_{30}H_{24}N_4O_4$	504.1797	505.1870	505.1869	259.1074 (fragment) 505.1867 522.21336 (+NH4)	259.1080 231.1131

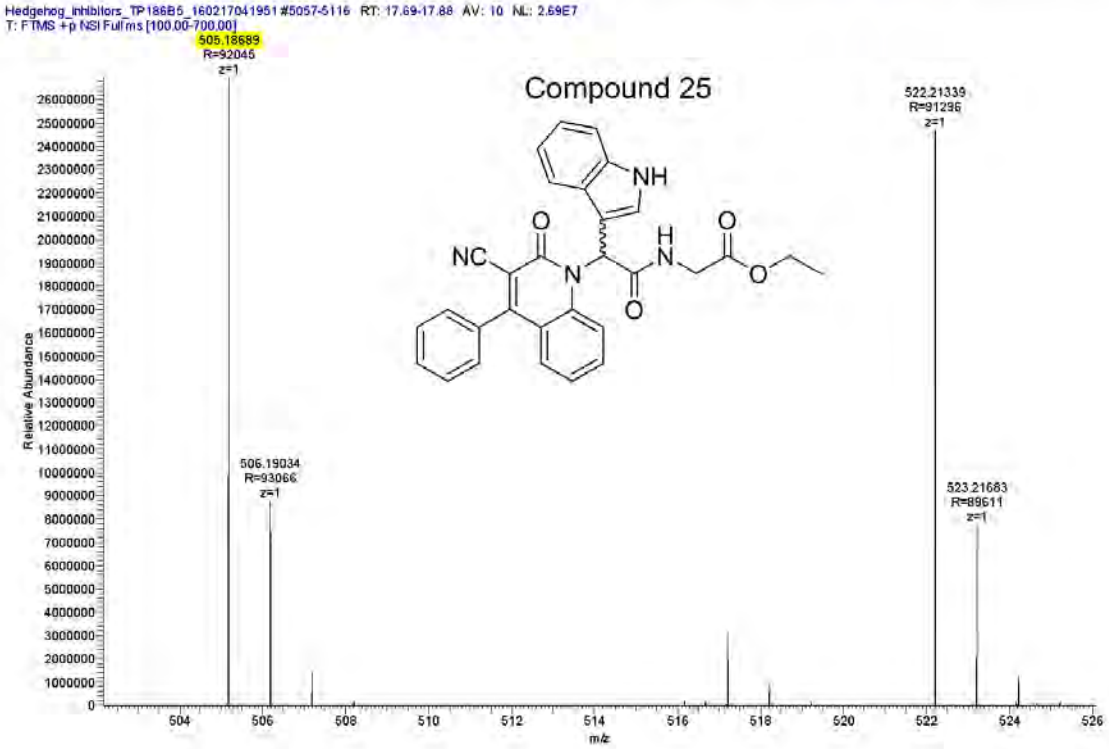

Compound 26

Compound Name: Ethyl-[2-(3-cyano-2-oxo-4-phenyl-2*H*-quinolin-1-yl)-2-(1-methylindole-3-yl)-acetamido]-acetate

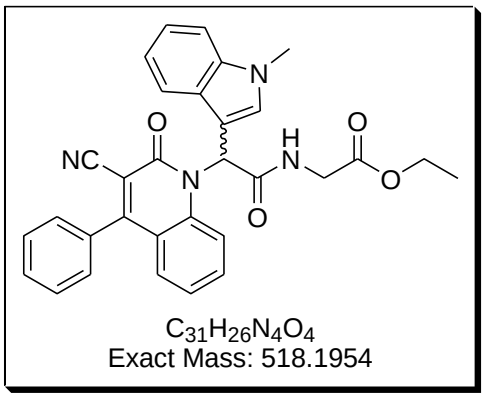

$C_{31}H_{26}N_4O_4$
Exact Mass: 518.1954

Obtained Weight & Yield: 0.192g, 27%

Appearance: Off white precipitate

Solubility: EtOAc, Acetone, ACN

Melting Point: 209-211 ˚C

TLC Conditions: EtOAc/Hexane (50/50)

IR Analysis: νmax/cm^{-1}

IR 3422 (NH), 2920 (CH), 2229 (CN), 1743 (COO), 1639 (CON).

^{1}H NMR Analysis:

1H NMR (400 MHz, DMSO-*d*$_6$) δ 8.53 (bs, 1H), 7.85 (d, *J* = 8.8 Hz, 1H), 7.75 (s, 1H), 7.70 – 7.48 (m, 7H), 7.43 (d, *J* = 8.2 Hz, 1H), 7.25 – 7.19 (m, 2H), 7.17 (t, *J* = 7.2 Hz, 1H), 7.06 (t, *J* = 7.2 Hz, 1H), 4.12 (q, *J* = 7.1 Hz, 2H), 3.90 (d, *J* = 6.6 Hz, 2H), 3.79 (s, 3H), 1.20 (t, *J* = 7.1 Hz, 3H).

^{13}C NMR Analysis: (Sign of isomers)

^{13}C NMR (101 MHz, DMSO-*d*$_6$) δ 170.1, 168.3, 160.3, 159.2, 139.6, 136.5, 134.0, 133.7, 131.4, 130.5, 129.5, 129.4 (Cx2), 129.2, 129.0, 127.7, 123.7, 122.1, 120.1, 120.0, 118.9, 118.2, 115.9, 110.5, 106.8, 105.9, 105.9, 61.0, 41.9, 33.2, 14.6.

HPLC:

RP-HPLC Alltima™ C18 5 μm 150 mm x 4.6 mm, 10–100% B in 15 min R_t =14.26 min, 98.10%

Mass Spectral Analysis (Low res): LRMS (ESI-) m/z 518, 540 $[M+ Na-H]^+$, 100%. HRMS (ES+) for $C_{31}H_{26}N_4O_4$; calculated 519.2027, found 519.2027.

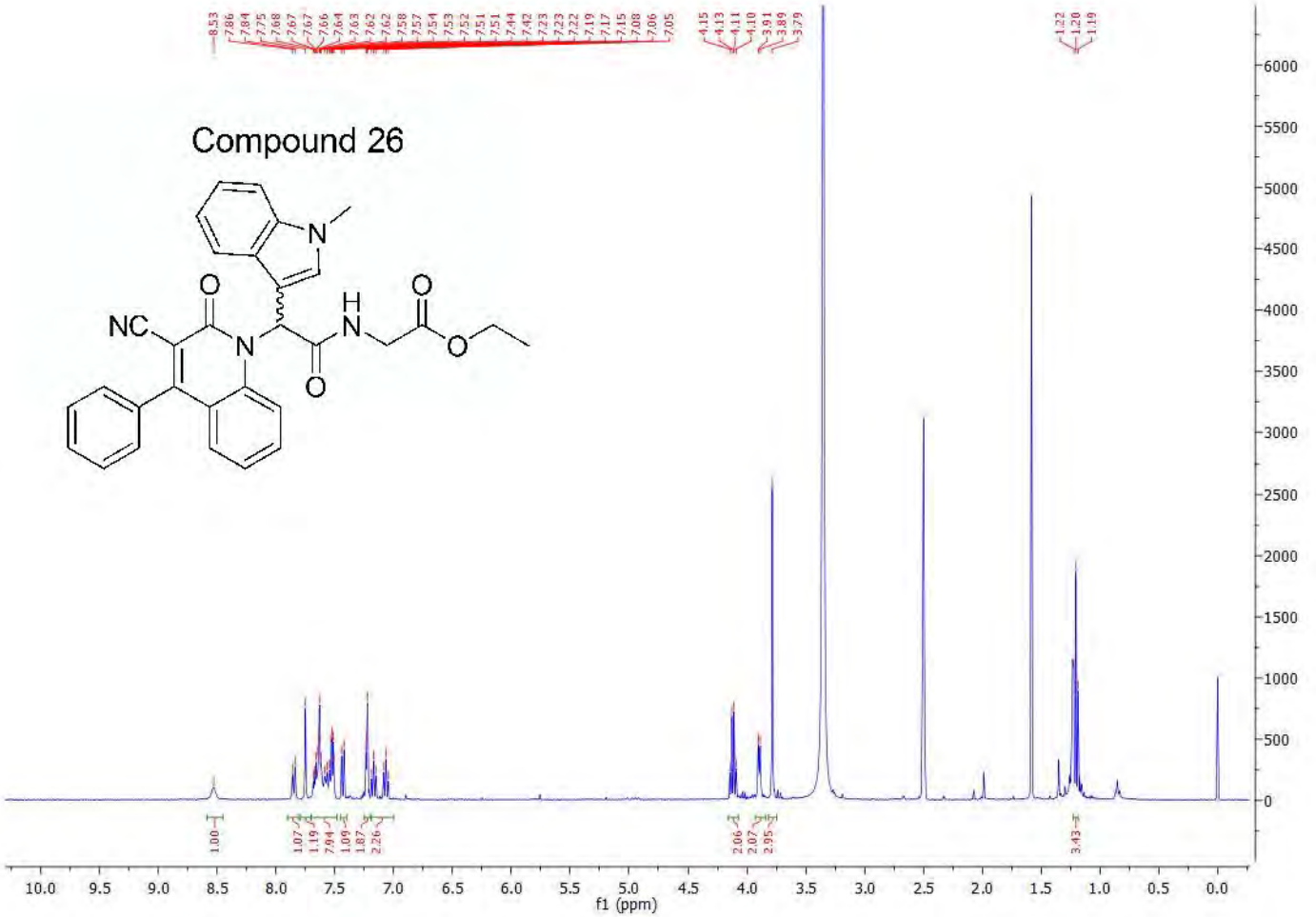
Compound 26
NC
O
N
O
H
N
O
O
f1 (ppm)

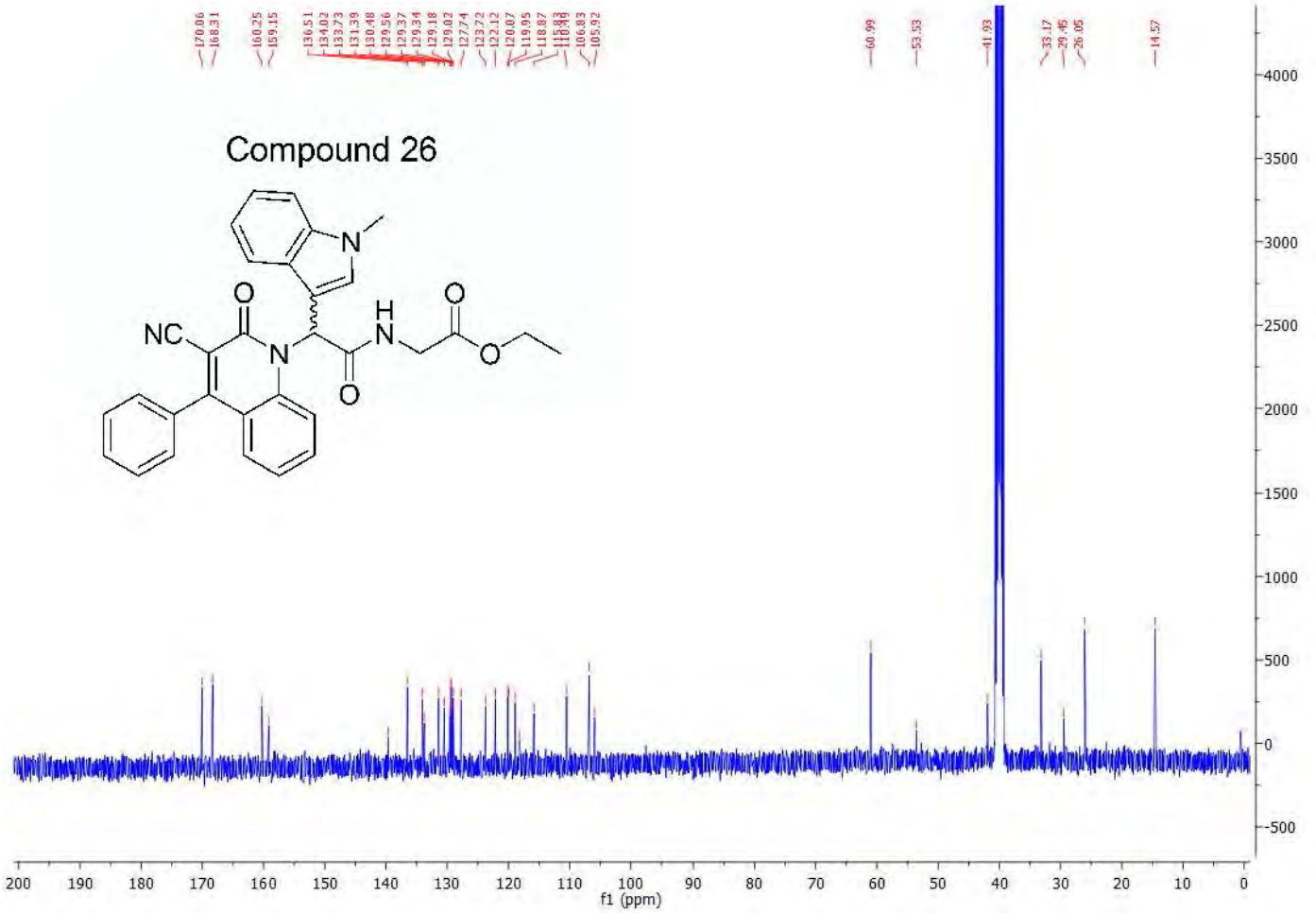
Compound 26
NC
O
N
O
H
N
O
O
170.06
168.31
160.25
159.15
136.51
134.02
133.73
131.39
130.48
129.56
129.37
129.34
129.18
129.02
127.74
123.72
122.12
120.07
119.95
118.87
106.83
105.92
60.99
53.53
41.93
33.17
29.45
26.05
14.57
4000
3500
3000
2500
2000
1500
1000
500
0
-500
200
190
180
170
160
150
140
130
120
110
100
90
80
70
60
50
40
30
20
10
0
f1 (ppm)

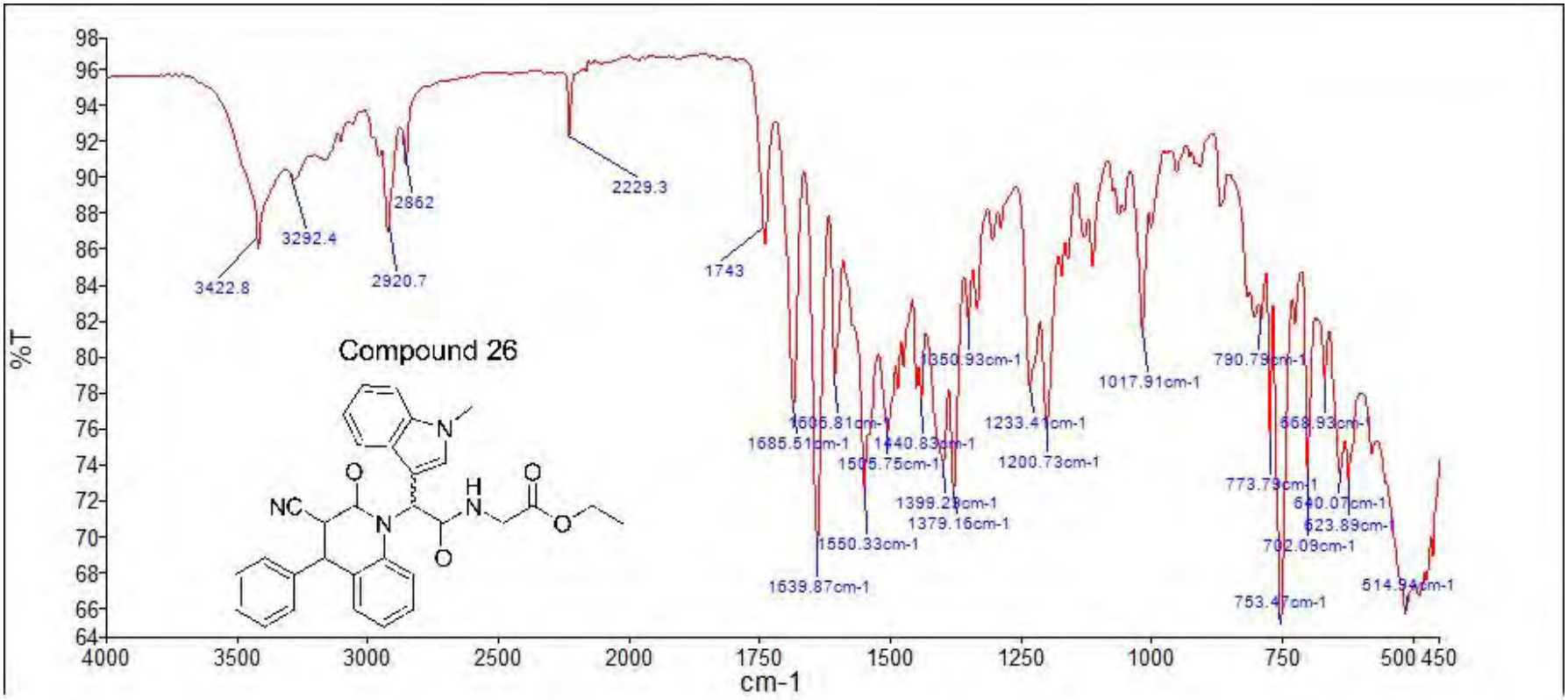
Compound 26
%T
cm-1
3422.8
3292.4
2862
2920.7
2229.3
1743
1685.51cm-1
1639.87cm-1
1550.33cm-1
1233.41cm-1
1200.73cm-1
1017.91cm-1
790.79cm-1
773.79cm-1
753.47cm-1
702.09cm-1
668.93cm-1
640.07cm-1
623.89cm-1
514.94cm-1

SHIMADZU LabSolutions **Analysis Report**

<Sample Information>

Sample Name	: TP151B1		
Sample ID	: TP151B1		
Data Filename	: TP151B1.lcd		
Method Filename	: 10-100 over 15 mins.lcm		
Batch Filename	: TRIEU Second Third Generation and New pro.lcb		
Vial #	: 1-20	Sample Type	: Unknown
Injection Volume	: 30 uL		
Date Acquired	: 8/09/2014 4:10:39 PM	Acquired by	: System Administrator
Date Processed	: 8/09/2014 4:40:41 PM	Processed by	: System Administrator

<Chromatogram>

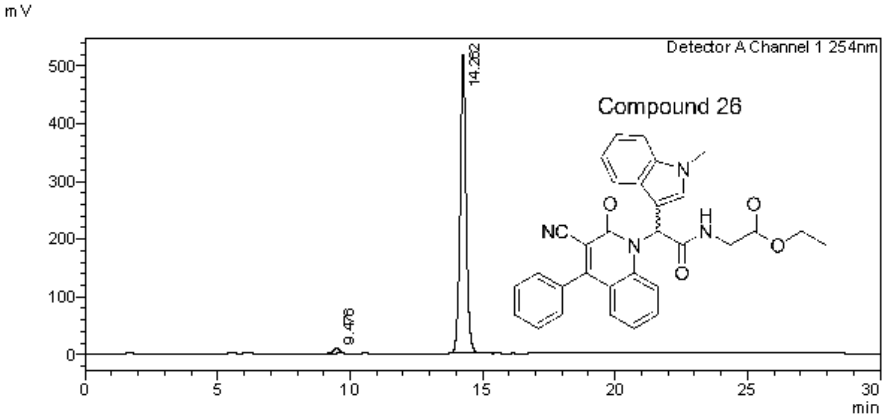

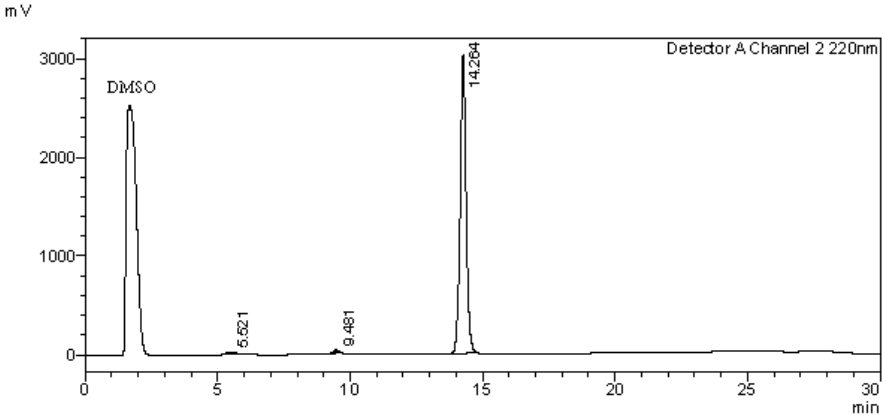

<Peak Table>

Detector A Channel 1 254nm

C:\LabSolutions\Data\Project1\TRIEU\TP151B1.lcd

Peak#	Ret. Time	Area	Height	Conc.	Unit	Mark	Name
1	9.476	152369	9271	1.856		M	
2	14.262	8055967	516482	98.144		M	
Total		8208335	525753				

Detector A Channel 2 220nm

Peak#	Ret. Time	Area	Height	Conc.	Unit	Mark	Name
1	5.521	466598	20316	0.980		M	
2	9.481	434968	31398	0.913		M	
3	14.264	46731373	3017885	98.107		M	
Total		47632939	3069600				

==== Shimadzu LCMSsolution Data Report ====

<Chromatogram>

Sample Information

Acquired by	: Admin
Date Acquired	: 7/23/2015 6:19:19 PM
Sample Type	: Unknown
Level#	: 0
Sample Name	: TP151B1
Sample ID	:
ISTD Amount	: (Level1 Conc.)
Sample Amount	: 1
Dilution Factor	: 1
Tray#	: 1
Vial#	: 56
Injection Volume	: 5
Data File	: TP151B2.lcd
Method File	: FIA-ESI_Scan(-).lcm
Original Method	: C:\LabSolutions\Data\Kelly\FIA-ESI_Scan(-).lcm
Report Format	: DefaultLCMS.lcr
Tuning File	: C:\LabSolutions\LCsolution\Log\Tuning\Autotune_030908.lct
Processed by	: Admin
Modified Date	: 7/23/2015 6:20:50 PM

Compound 26

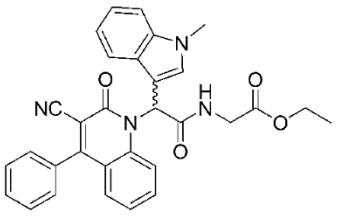

Chromatogram

TP151B1 C:\LabSolutions\Data\Trieu\NORMAL REVERSE PHASE COLUMN\UGI MASS ESI NEGATIVE SCAN\TP151B2.lcd

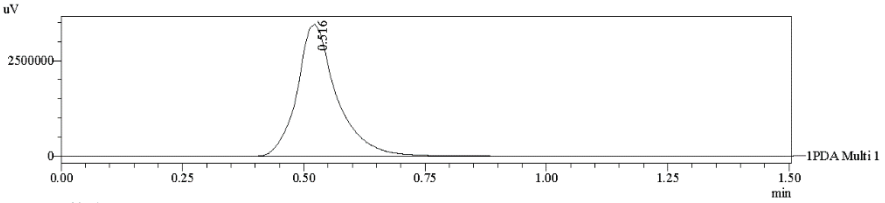

1 PDA Multi 1 / 254nm 4nm

<Spectrum>

Retention Time:0.800(Scan#:81)
Max Peak:652 Base Peak:272.55(274674)
Spectrum:Averaged 0.640-1.300(65-131)
Background:Averaged 0.120-0.399(13-41) Polarity:Pos Segment1 - Event1

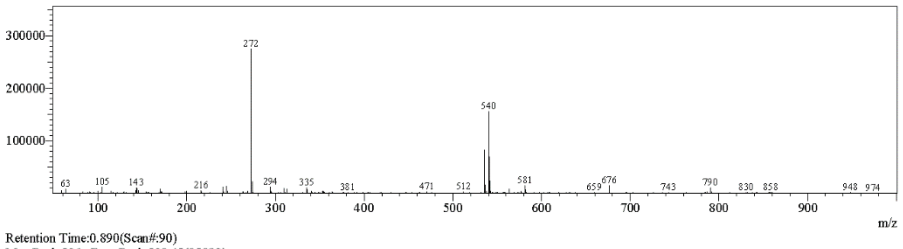

Retention Time:0.890(Scan#:90)
Max Peak:526 Base Peak:520.45(85932)
Spectrum:Averaged 0.650-1.310(66-132)
Background:Averaged 0.130-0.399(14-42) Polarity:Neg Segment1 - Event2

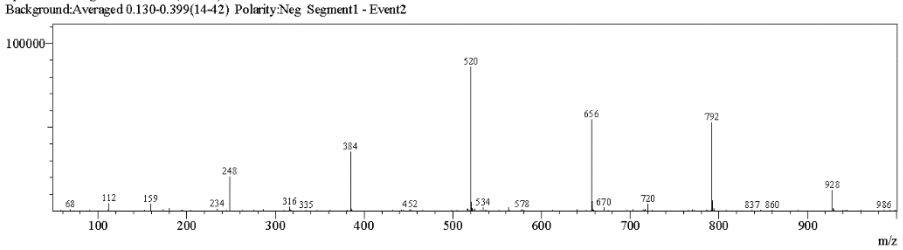

C:¥LabSolutions¥Data¥Trieu¥NORMAL REVERSE PHASE COLUMN¥UGI MASS ESI NEGATIVE SCAN¥TP151B2.lcd

Compound	Chemical Formula	Predicted monoisotopic neutral MW	Predicted MH+	MH+ Measured	Main MS Ions	Main MS/MS Fragments
TP151B1	$C_{31}H_{26}N_4O_4$	518.1949	519.2027	519.2027*	273.1231 (fragment) 536.2292 (+Na) 541.1845 (+NH4)	273.1235

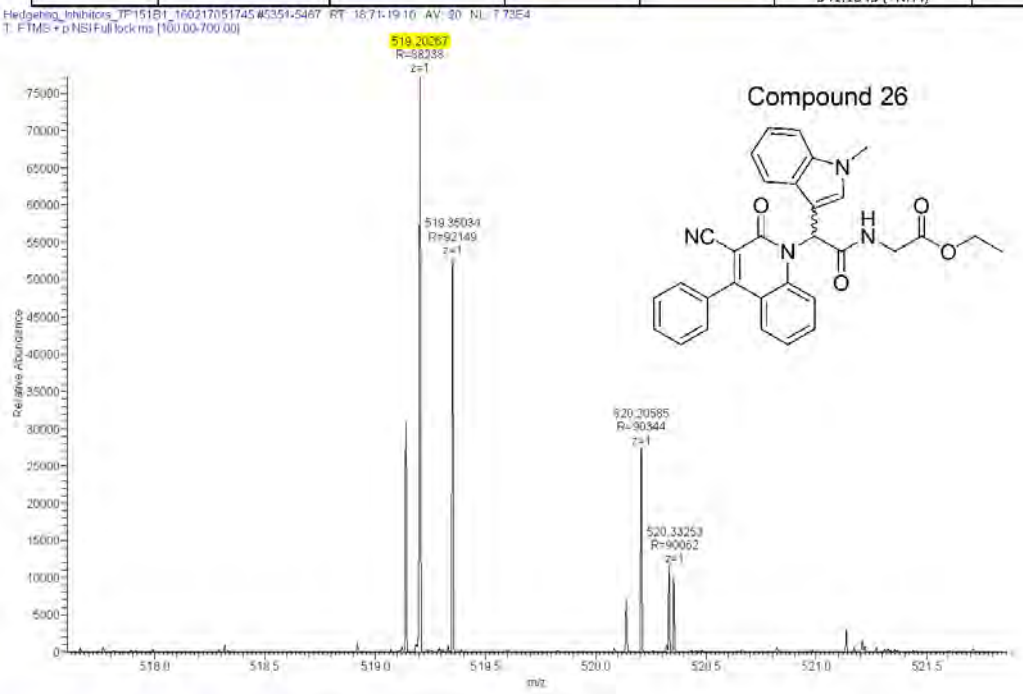

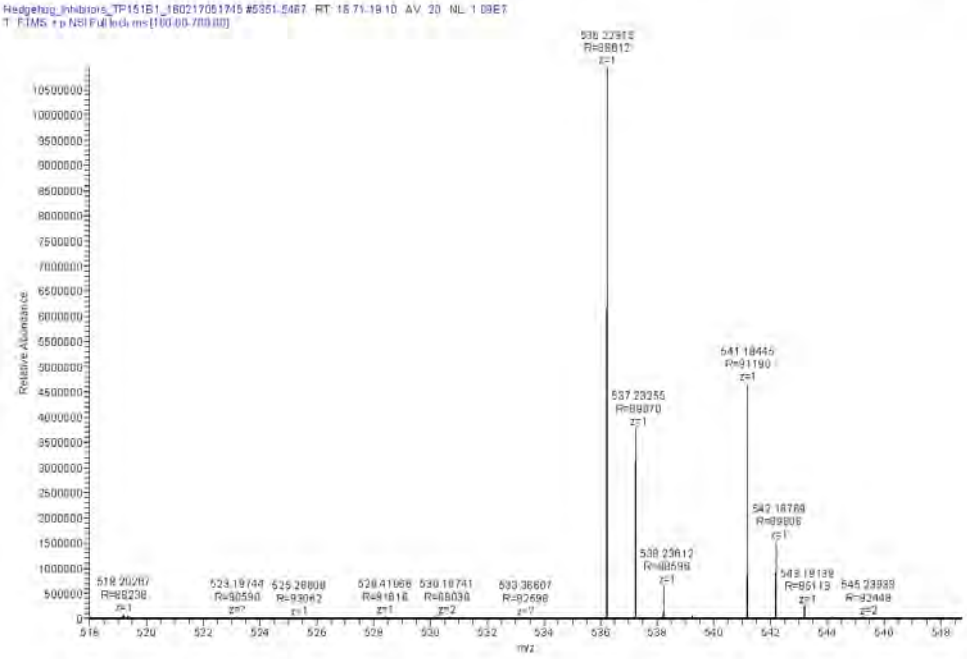

Compound 27

Compound Name: Ethyl-3-[2-(3-cyano-2-oxo-4-phenyl-2*H*-quinolin-1-yl)-2-(1-methyl-1*H*-indol-3-yl)-acetylamino]-propionate

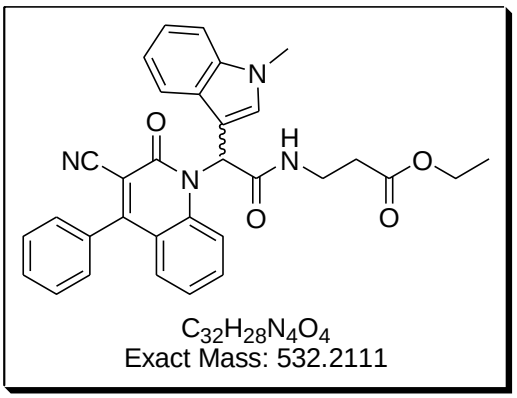

Obtained Weight & Yield: 0.149g, 50%

Appearance: White precipitate

Solubility: EtOAc, Acetone, ACN

Melting Point: 267-268 ˚C

TLC Conditions: EtOAc/Hexane (50/50)

IR Analysis: νmax/cm^{-1}

3410 (NH), 2232 (CN), 1710 (COO), 1686 (CON)

^{1}H NMR Analysis:

^{1}H NMR (400 MHz, DMSO-*d*$_6$) δ 8.05 (bs, 1H), 7.83 (d, *J* = 8.7 Hz, 1H), 7.71 – 7.56 (m, 6H), 7.56 – 7.47 (m, 2H), 7.45-7.38 (m, 2H), 7.26 – 7.20 (m, 2H), 7.17 (t, *J* = 7.2 Hz, 1H), 7.06 (t, *J* = 7.2 Hz, 1H), 4.03 (q, *J* = 7.1 Hz, 2H), 3.78 (s, 3H), 3.42 – 3.35 (m, 2H), 2.57-2.44 (m, 2H), 1.16 (t, *J* = 7.1 Hz, 3H).

^{13}C NMR Analysis:

^{13}C NMR (101 MHz, DMSO-*d*$_6$) δ 171.7, 167.7, 160.1, 159.0, 139.9, 136.5, 134.1, 133.8, 131.3, 130.5, 129.6, 129.4, 129.2, 129.0, 127.8, 123. 7, 122.1, 120.0, 119.9, 119.0, 117.8, 115.9, 110. 5, 107.1, 106.1, 60.4, 54.1, 35.9, 34.0, 33.1, 14.5

HPLC:

RP-HPLC Alltima™ C18 5 μm 150 mm x 4.6 mm, 10–100% B in 15 min, R_t =14.46 min, 95.8%

Mass Spectral Analysis: LRMS (ESI+) m/z 532, 287 $[M+ACN+ 2H]^{2+}$ 100%. HRMS (ES+) for $C_{16}H_{11}N_2O^+$ (main fragment); calculated 247.0870, found 247.0865

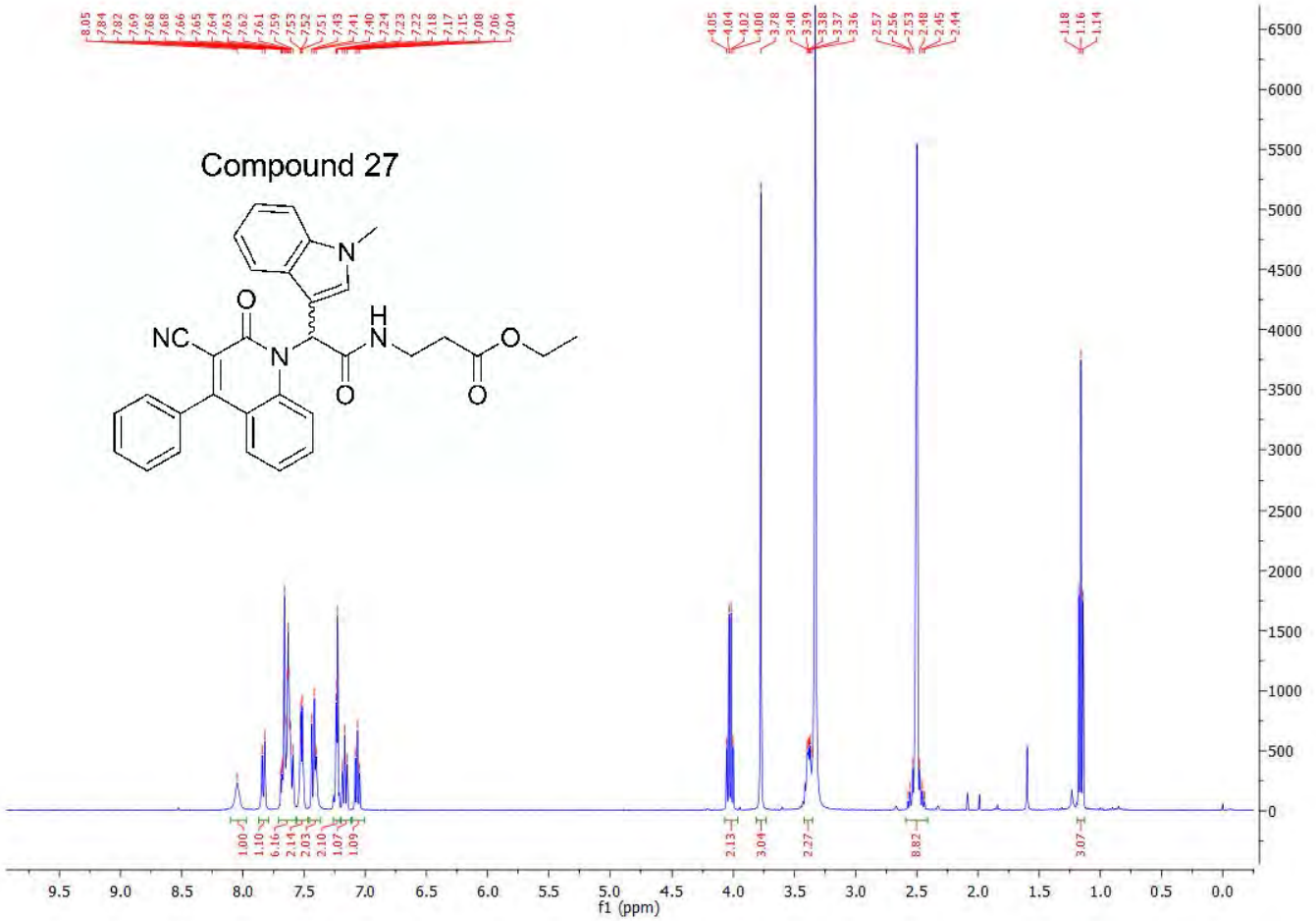
Compound 27
NC
O
N
H
N
O
O
O
f1 (ppm)

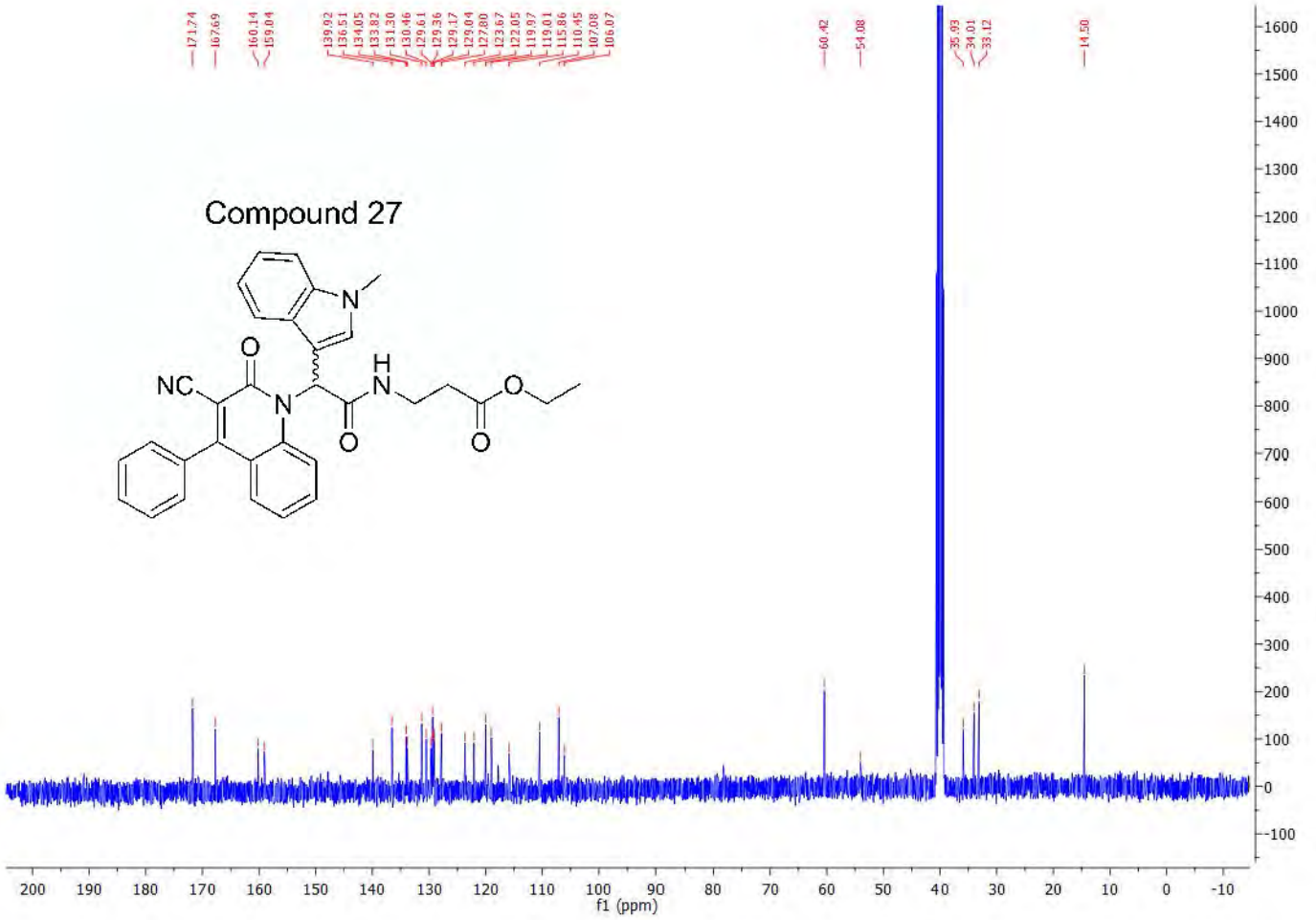
Compound 27
NC
O
N
H
N
O
O
O
171.74
167.69
160.14
159.04
139.92
136.51
134.05
133.82
131.30
130.46
129.61
129.36
129.17
129.04
127.80
123.67
122.05
119.97
119.01
115.86
110.45
107.08
106.07
60.42
54.08
35.93
34.01
33.12
14.50
f1 (ppm)

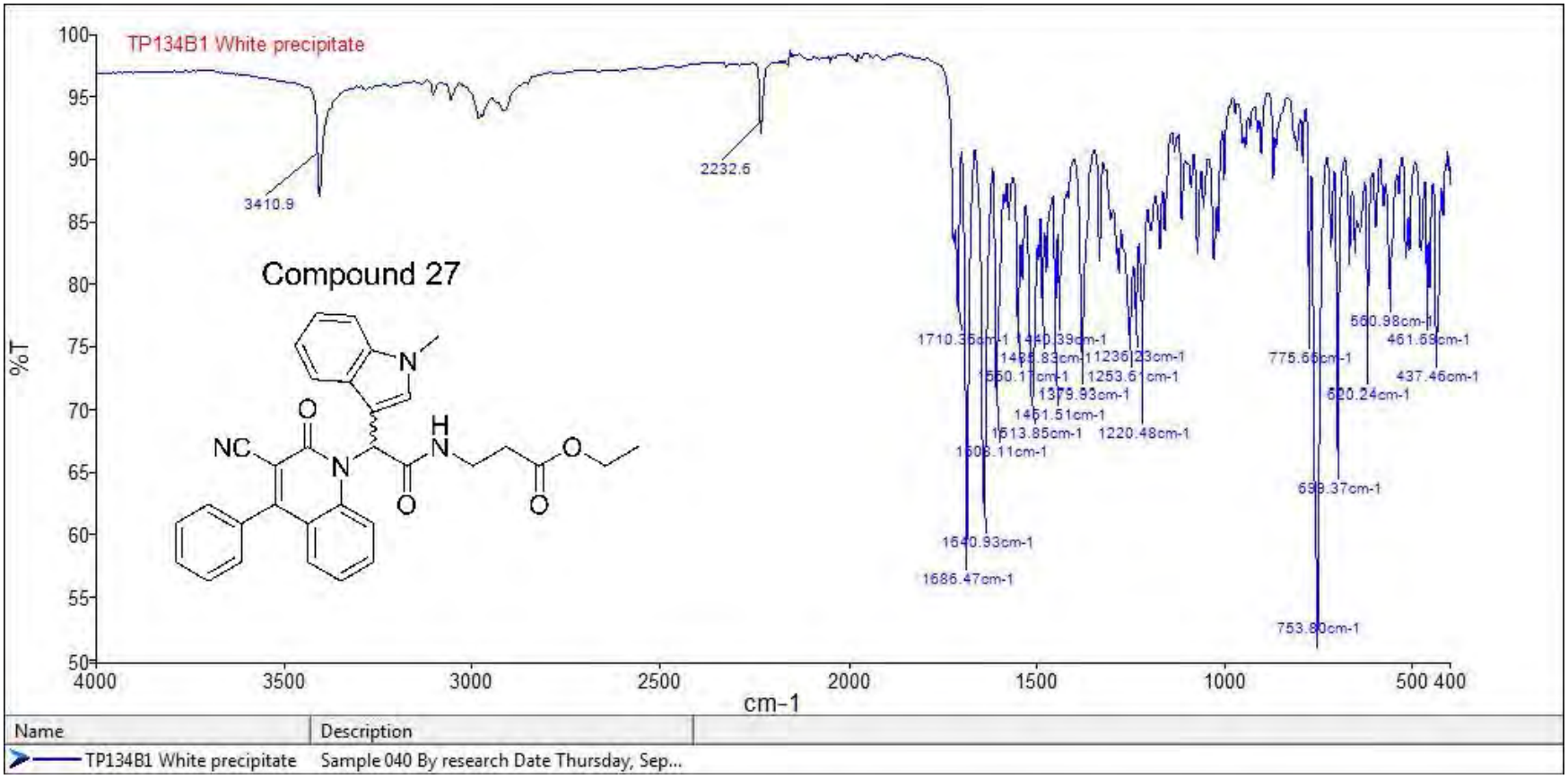
TP134B1 White precipitate
Compound 27
3410.9
2232.6
1710.35cm-1
1640.39cm-1
1496.83cm-1
1236.23cm-1
1560.11cm-1
1253.61cm-1
1379.93cm-1
1451.51cm-1
1513.85cm-1
1220.48cm-1
1608.11cm-1
1640.93cm-1
1686.47cm-1
775.66cm-1
660.98cm-1
461.69cm-1
437.46cm-1
620.24cm-1
639.37cm-1
753.80cm-1
%T
cm-1
Name
Description
TP134B1 White precipitate
Sample 040 By research Date Thursday, Sep...

SHIMADZU LabSolutions Analysis Report

<Sample Information>

Sample Name	: TP134B1		
Sample ID	: TP134B1		
Data Filename	: TP134B1.lcd		
Method Filename	: 10-100 over 15 mins.lcm		
Batch Filename	: TRIEU Second Third Generation and New pro.lcb		
Vial #	: 1-29	Sample Type	: Unknown
Injection Volume	: 30 uL		
Date Acquired	: 8/09/2014 8:44:24 PM	Acquired by	: System Administrator
Date Processed	: 8/09/2014 9:14:26 PM	Processed by	: System Administrator

<Chromatogram>

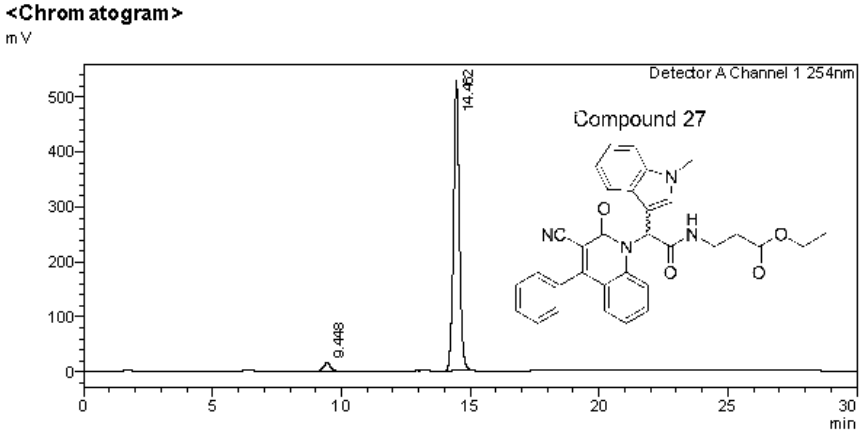

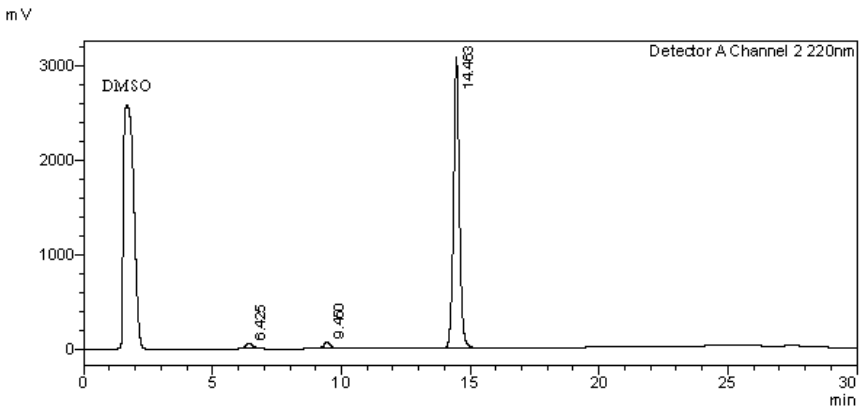

<Peak Table>

Detector A Channel 1 254nm

Peak#	Ret. Time	Area	Height	Conc.	Unit	Mark	Name
1	9.448	276842	16046	3.236		M	
2	14.462	8277664	527452	96.764		M	
Total		8554507	543498				

Detector A Channel 2 220nm

Peak#	Ret. Time	Area	Height	Conc.	Unit	Mark	Name
1	6.425	1115783	49239	2.232		M	
2	9.450	980758	61730	1.962		M	
3	14.463	47898085	3070407	95.806		M	
Total		49994626	3181376				

==== Shimadzu LCMSsolution Data Report ====

<Chromatogram>

Sample Information

Acquired by	: Admin
Date Acquired	: 7/24/2015 9:33:05 AM
Sample Type	: Unknown
Level#	: 0
Sample Name	: TP134B1
Sample ID	:
ISTD Amount	: (Level1 Conc.)
Sample Amount	: 1
Dilution Factor	: 1
Tray#	: 1
Vial#	: 51
Injection Volume	: 5
Data File	: TP134B2.lcd
Method File	: FIA-ESI_Scan(+).lcm
Original Method	: C:\LabSolutions\Data\Trieu\Mass spec files\FIA-ESI_Scan(+).lcm
Report Format	: DefaultLCMS.lcr
Tuning File	: C:\LabSolutions\LCsolution\Log\Tuning\Autotune_030908.lct
Processed by	: Admin
Modified Date	: 7/24/2015 9:34:36 AM

Compound 27

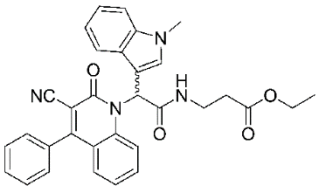

Chromatogram

TP134B1 C:\LabSolutions\Data\Trieu\NORMAL REVERSE PHASE COLUMN\ESI POSITIVE\UGI KNOEVENAGEL\TP134B2.lcd

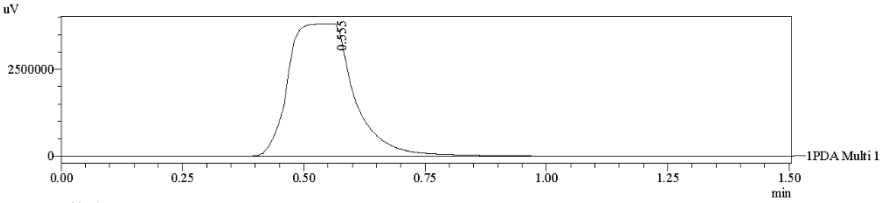

1 PDA Multi 1 / 254nm 4nm

<Spectrum>

Retention Time:0.900(Scan#:91)
Max Peak:331 Base Peak:286.65(253957)
Spectrum:Averaged 0.600-1.160(61-117)
Background:Averaged 0.140-0.493(15-51) Polarity:Pos Segment1 - Event1

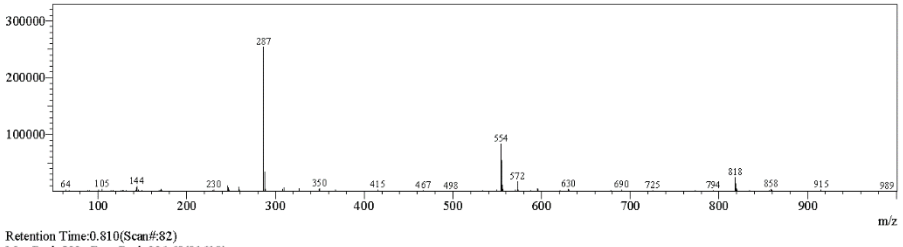

Retention Time:0.810(Scan#:82)
Max Peak:522 Base Peak:226.60(81618)
Spectrum:Averaged 0.610-1.170(62-118)
Background:Averaged 0.150-0.493(16-52) Polarity:Neg Segment1 - Event2

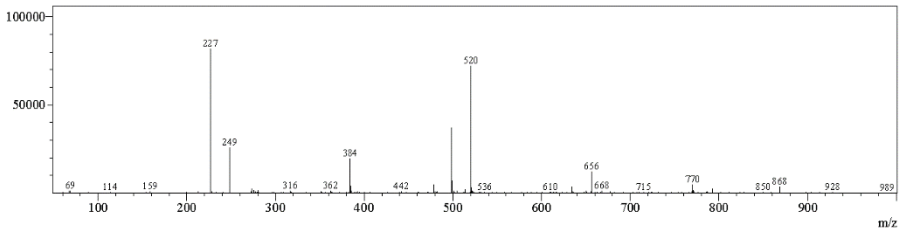

C:¥LabSolutions¥Data¥Trieu¥NORMAL REVERSE PHASE COLUMN¥ESI POSITIVE¥UGI KNOEVENAGEL¥TP134B2.lcd

Compound	Chemical Formula	Predicted monoisotopic neutral MW	Predicted MH+	MH+ Measured	Main MS Ions	Main MS/MS Fragments
TP134B1	$C_{32}H_{28}N_4O_4$	532.2111	533.2183	n/a	247.0865	247.087^

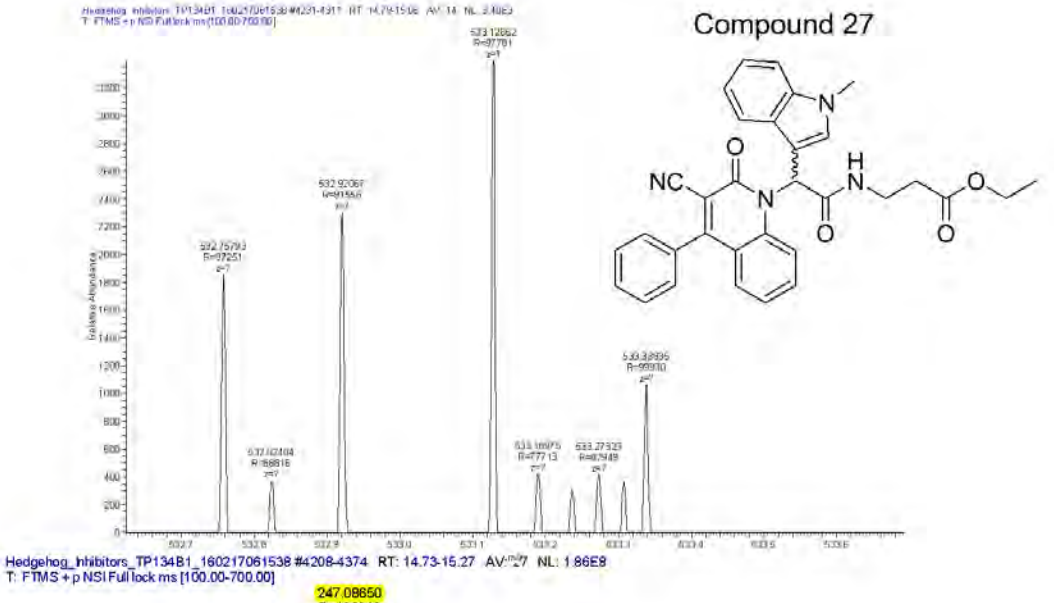

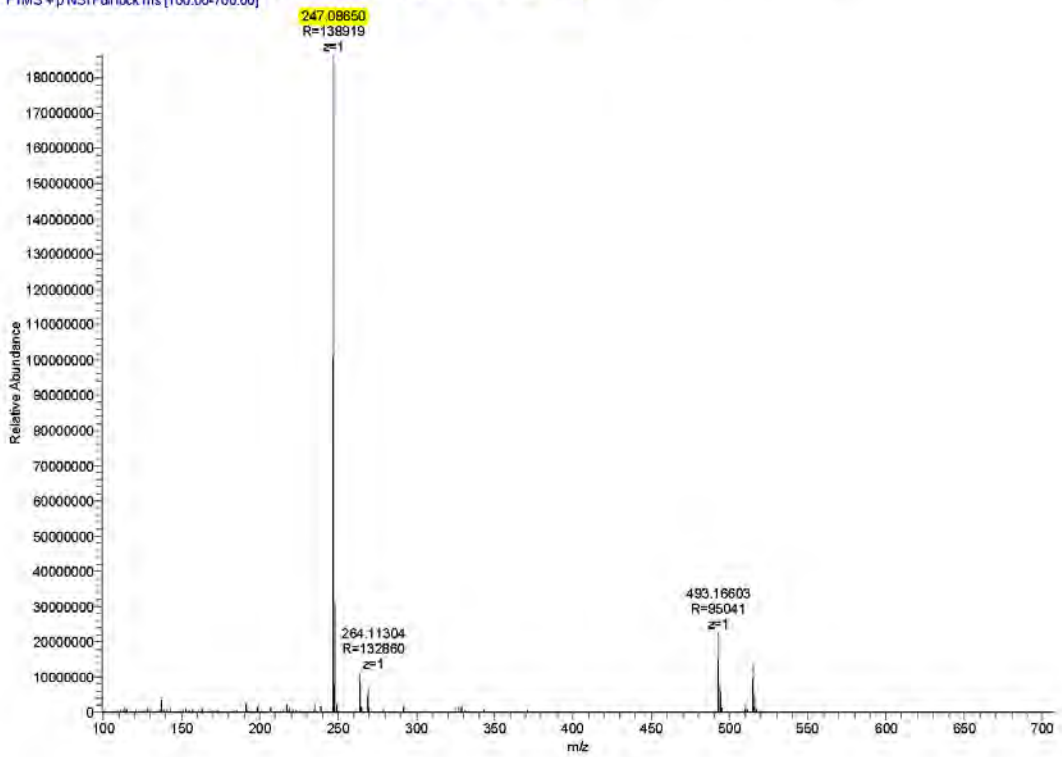

Compound 28

Compound Name: Ethyl-2-(2-(5-chloro- indole (1*H*)-3-yl)-2-(3-cyano-2-oxo-4-phenyl-1(2*H*)-quinolin-yl)-acetamido)-acetate

Obtained Weight & Yield: 0.435g, 33%

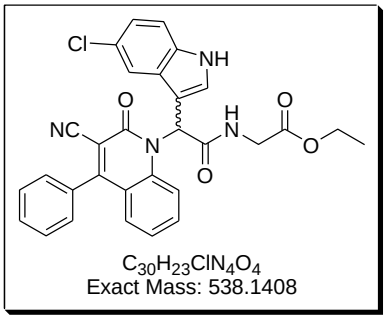

Appearance: Light yellow precipitate

Solubility: DMSO, partially soluble in Acetone, not in $CHCl_3$

Melting Point: 201-203 ˚C

TLC Conditions: EtOAc/Hexane (50/50)

IR Analysis: ν_{max}/cm^{-1}
3415 (NH), 3406 (NH), 2236 (CN), 1736 (COO), 1671 (CON)

^{1}H NMR Analysis:

^{1}H NMR (400 MHz, DMSO-*d*$_6$) δ 11.54 (d, *J* = 1.4 Hz, 1H), 8.53 (s, 1H), 7.82 (dd, *J* = 11.9, 5.5 Hz, 2H), 7.71 – 7.61 (m, 4H), 7.61-7.5 (m, 4H), 7.42 (d, *J* = 8.6 Hz, 1H), 7.29 – 7.18 (m, 2H), 7.12 (dd, *J* = 8.6, 1.7 Hz, 1H), 4.14 (q, *J* = 7.0 Hz, 2H), 3.93 (qd, *J* = 17.2, 5.8 Hz, 2H), 1.22 (t, *J* = 7.1 Hz, 3H).

^{13}C NMR Analysis:

^{13}C NMR (101 MHz, DMSO-*d*$_6$) δ 170.1, 168.2, 160.4, 159.2, 139.6, 134.6, 134.0, 133.7, 130.5, 129.6(C x 2), 129.4, 129.2, 129.0 (C x 2), 128.5, 124.5, 123.8, 122.0, 120.1, 118.3 (C x 2), 118.2, 115.8, 113.8, 107.8, 106.0, 61.0, 42.0, 14.6

HPLC:
RP-HPLC Alltima™ C18 5 μm 150 mm x 4.6 mm, 10–100% B in 15 min, R_t =14.07 min, 99.4%

Mass Spectral Analysis: LRMS (ESI+) m/z 538, 292 $[M+2Na]^{2+}$, 60%. HRMS for $C_{30}H_{23}ClN_4O_4$; calculated 539.1481, found 539.1481

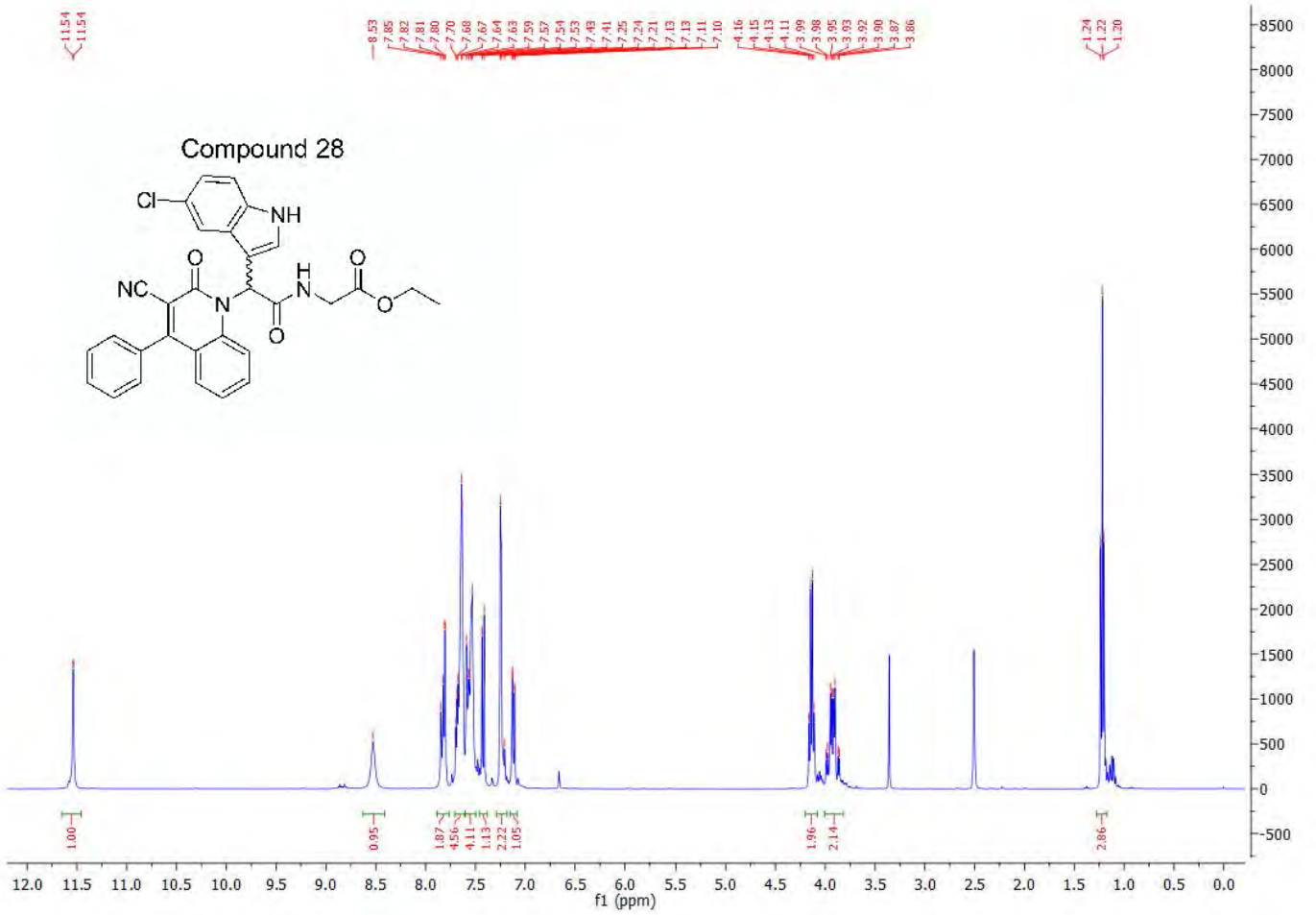
Compound 28
Cl
NH
NC
N
H
N
O
O
O
O
f1 (ppm)

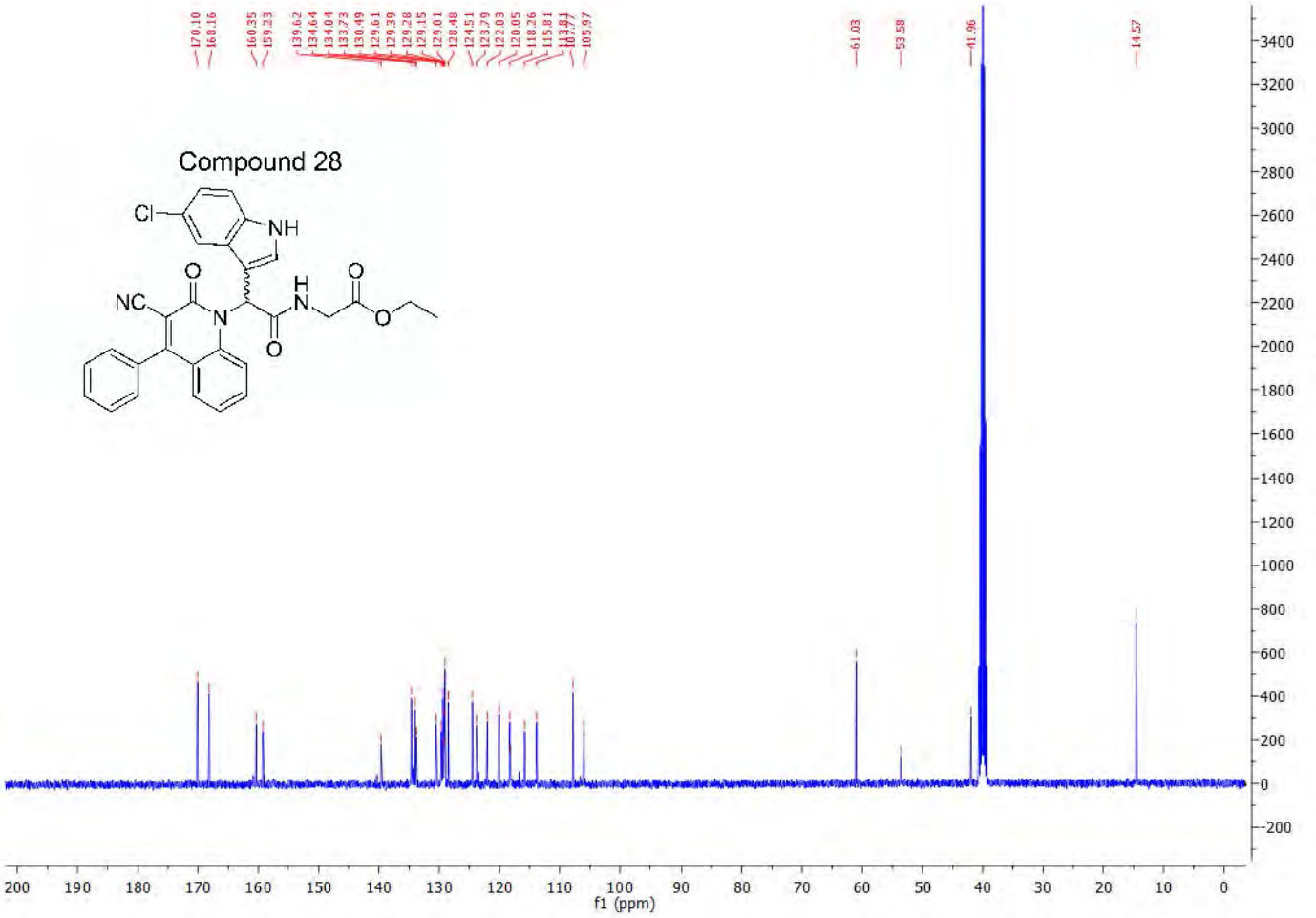
Compound 28
Cl
NH
NC
O
N
H
N
O
O
O
170.10
168.16
160.35
159.33
139.62
134.64
134.04
133.73
130.49
129.61
129.39
129.28
129.15
129.01
128.48
124.51
123.79
122.03
120.05
118.26
115.81
105.97
61.03
53.58
41.96
14.57
3400
3200
3000
2800
2600
2400
2200
2000
1800
1600
1400
1200
1000
800
600
400
200
0
-200
200 190 180 170 160 150 140 130 120 110 100 90 80 70 60 50 40 30 20 10 0
f1 (ppm)

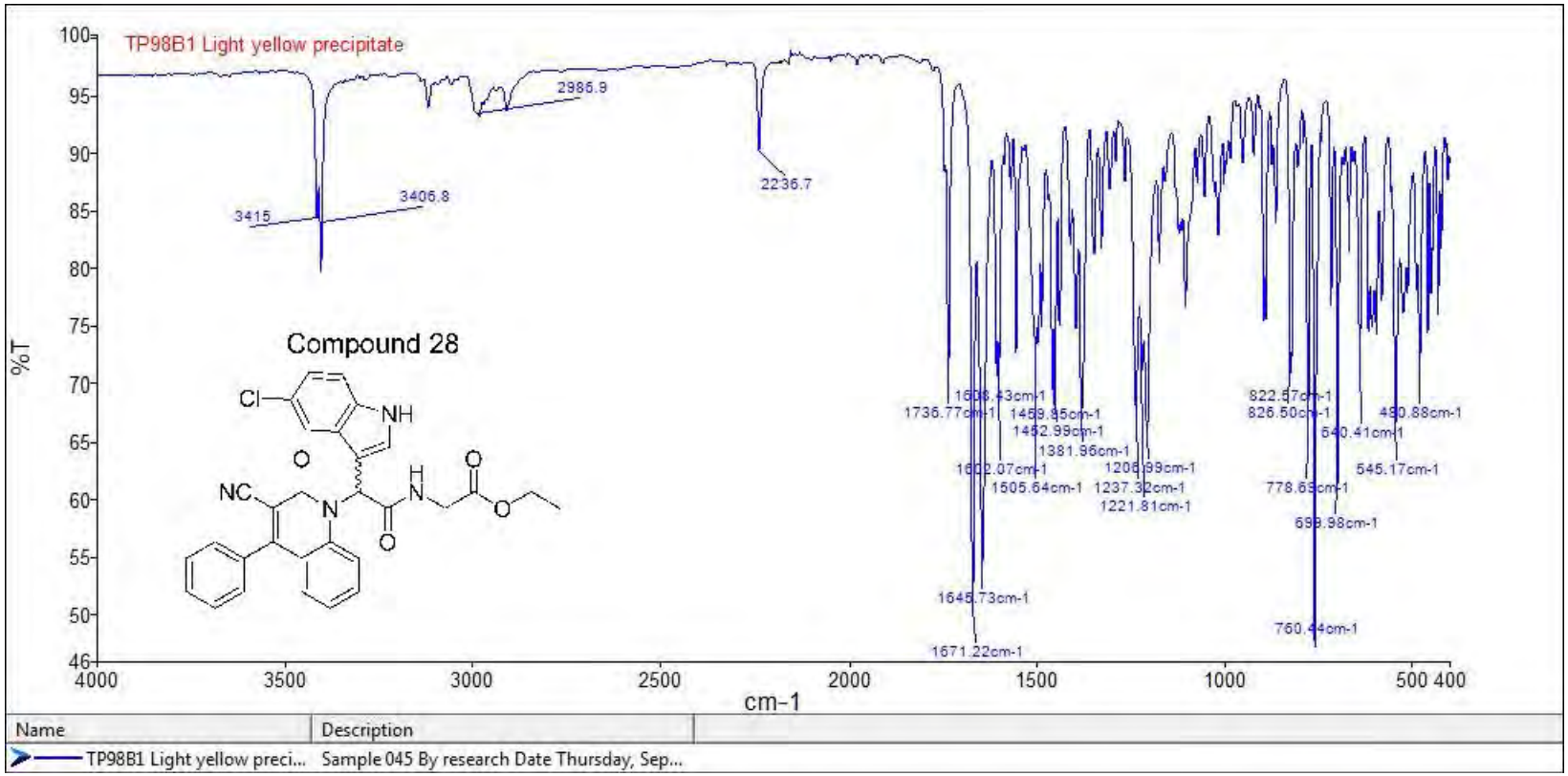
TP98B1 Light yellow precipitate
Compound 28
%T
cm-1
2986.9
3415
3406.8
2236.7
1736.77cm-1
1645.73cm-1
1671.22cm-1
1602.07cm-1
1505.64cm-1
1459.85cm-1
1452.99cm-1
1381.96cm-1
1206.99cm-1
1237.32cm-1
1221.81cm-1
822.57cm-1
826.50cm-1
778.69cm-1
760.44cm-1
699.98cm-1
640.41cm-1
545.17cm-1
480.88cm-1
Name
Description
TP98B1 Light yellow preci...
Sample 045 By research Date Thursday, Sep...

SHIMADZU LabSolutions Analysis Report

<Sample Information>

Sample Name	: TP98B1		
Sample ID	: TP98B1		
Data Filename	: TP98B1.lcd		
Method Filename	: 10-100 over 15 mins.lcm		
Batch Filename	: TRIEU Second Third Generation and New pro.lcb		
Vial #	: 1-24	Sample Type	: Unknown
Injection Volume	: 30 uL		
Date Acquired	: 8/09/2014 6:12:18 PM	Acquired by	: System Administrator
Date Processed	: 8/09/2014 6:42:19 PM	Processed by	: System Administrator

<Chromatogram>

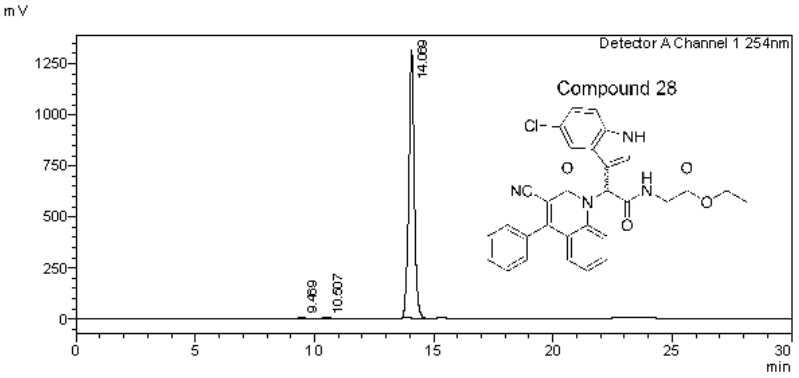

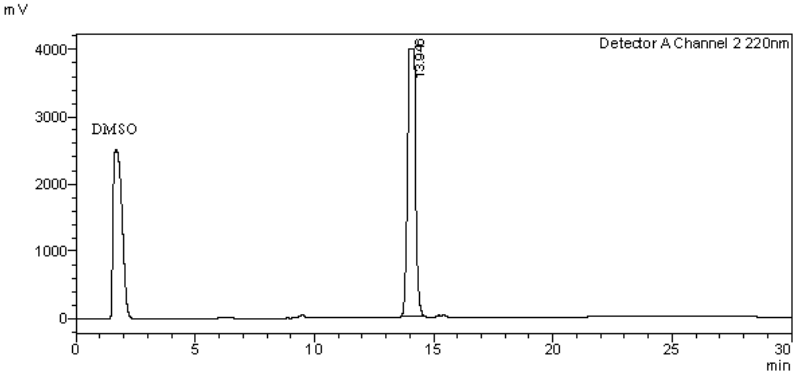

<Peak Table>

Detector A Channel 1 254nm

Peak#	Ret. Time	Area	Height	Conc.	Unit	Mark	Name
1	9.469	71153	6488	0.340		M	
2	10.507	52847	4013	0.252		M	
3	14.069	20821958	1310947	99.408		M	
Total		20945959	1321448				

Detector A Channel 2 220nm

Peak#	Ret. Time	Area	Height	Conc.	Unit	Mark	Name
1	13.946	93602997	3968571	100.000		M	
Total		93602997	3968571				

==== Shimadzu LCMSsolution Data Report ====

<Chromatogram>

Sample Information

Acquired by	: Admin
Date Acquired	: 7/24/2015 10:02:15 AM
Sample Type	: Unknown
Level#	: 0
Sample Name	: TP98B1
Sample ID	:
ISTD Amount	: (Level1 Conc.)
Sample Amount	: 1
Dilution Factor	: 1
Tray#	: 1
Vial#	: 57
Injection Volume	: 15
Data File	: TP98B2.lcd
Method File	: FIA-ESI_Scan(+).lcm
Original Method	: C:\LabSolutions\Data\Trieu\Mass spec files\FIA-ESI_Scan(+).lcm
Report Format	: DefaultLCMS.lcr
Tuning File	: C:\LabSolutions\LCsolution\Log\Tuning\Autotune_030908.lct
Processed by	: Admin
Modified Date	: 7/24/2015 10:03:47 AM

Compound 28

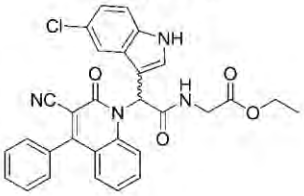

Chromatogram

TP98B1 C:\LabSolutions\Data\Trieu\NORMAL REVERSE PHASE COLUMN\ESI POSITIVE\UGI KNOEVENAGEL\TP98B2.lcd

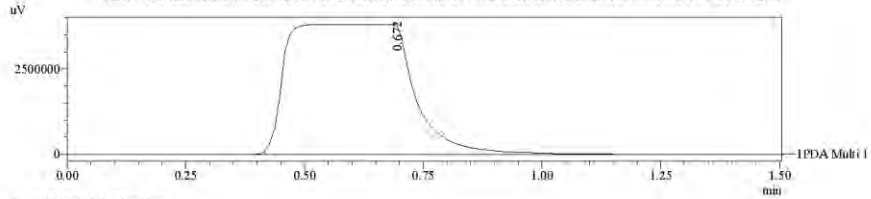

1 PDA Multi 1 / 254nm 4nm

<Spectrum>

Retention Time:0.880(Scan#:89)
Max Peak:304 Base Peak:453.55(102202)
Spectrum:Averaged 0.620-1.200(63-121)
Background:Averaged 0.120-0.534(13-55) Polarity:Pos Segment1 - Event1

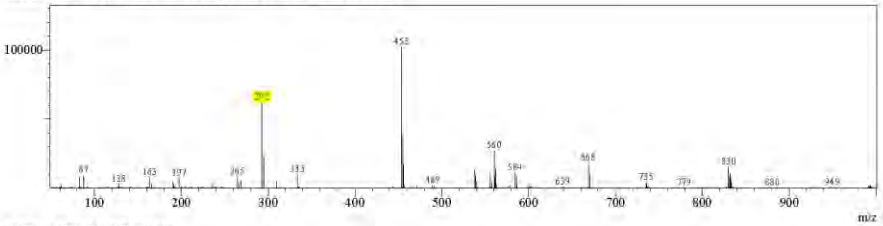

Retention Time:0.890(Scan#:90)
Max Peak:639 Base Peak:478.35(192464)
Spectrum:Averaged 0.630-1.210(64-122)
Background:Averaged 0.130-0.534(14-56) Polarity:Neg Segment1 - Event2

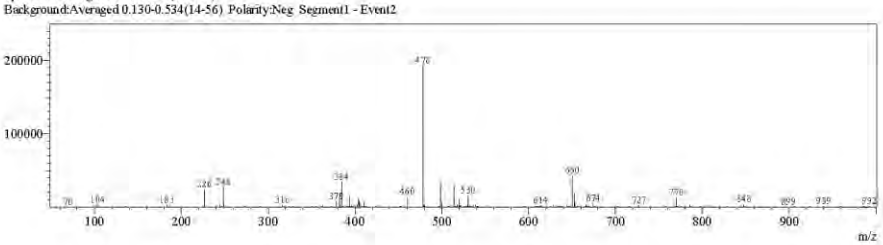

C:¥LabSolutions¥Data¥Trieu¥NORMAL REVERSE PHASE COLUMN¥ESI POSITIVE¥UGI KNOEVENAGEL¥TP98B2.lcd

Compound	Chemical Formula	Predicted monoisotopic neutral MW	Predicted MH+	MH+ Measured	Main MS Ions	Main MS/MS Fragments
TP98B1	$C_{30}H_{23}ClN_4O_4$	538.1408	539.1481	539.1481	539.1481 556.17458 (+NH4)	293.0692 265.0742

Hedgehog_Inhibitors_TP98B1_160217071332 #5060-5428 RT: 17.70-18.96 AV: 61 NL: 9.76E5
T: FTMS + p NSI Full lock ms [100.00-700.00]

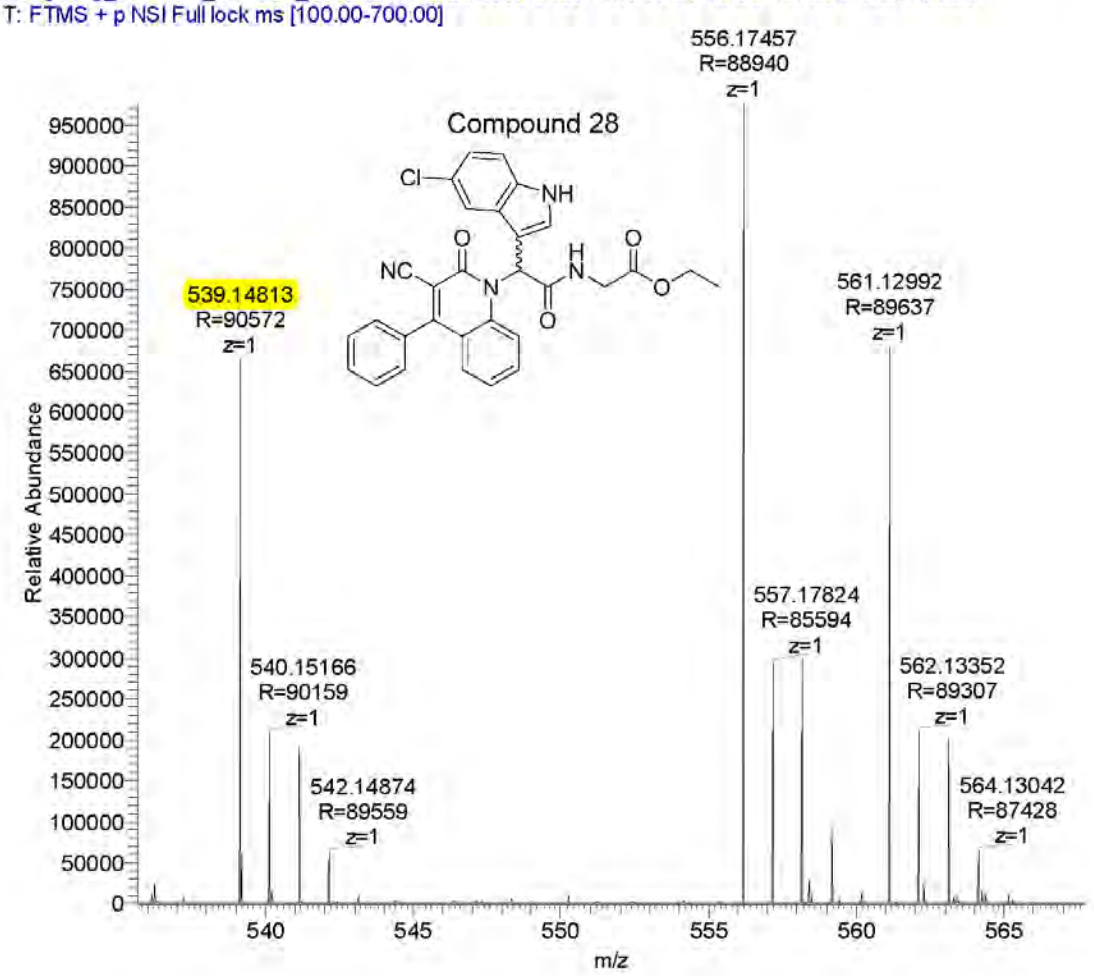

Compound 29

Compound Name: *N*-tert-Butyl-2-(3-cyano-2-oxo-4-phenyl-2*H*-quinolin-1-yl)-2-(5-methyl-1*H*-indole-3-yl)-acetamide

Obtained Weight & Yield: 0.419g, 47.6%

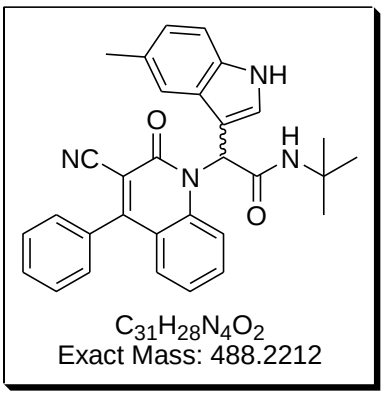

Appearance: Yellowish precipitate

Solubility: EtOAc, Acetone, ACN

Melting Point: 196-198 ˚C

TLC Conditions: EtOAc/Hexane (50/50)

IR Analysis: ν_{max}/cm^{-1}
3427 (NH), 2978 (CH), 2228 (CN), 1650 (CON)

^{1}H NMR Analysis: (Sign of isomers)

^{1}H NMR (400 MHz, DMSO-d_6) δ 11.13 (d, J = 4.9 Hz, 1H), 7.90 – 7.37 (m, 10H), 7.29-7.16 (m, 4H), 6.92 (d, J = 8.3 Hz, 1H), 4.03 – 3.87 (m, 1H), 2.34 (s, 3H), 1.57 – 1.20 (m, 3H), 1.20 – 0.86 (m, 5H), 0.82-0.60 (m, 3H).

^{13}C NMR Analysis: (Sign of isomers)
^{13}C NMR (101 MHz, DMSO-d_6) δ 167.5, 166.9, 160.1, 160.1, 159.3, 140.1, 140.1, 134.6, 134.6, 134.5, 134.1, 133.3, 130.4, 129.4, 129.2, 129.1, 128.2, 128.1, 127.5, 127.5, 126.8, 126.6, 23.5, 19.9, 118.48, 118.4, 118.3, 116.0, 111.9, 107.9, 107.9, 106.0, 105.9, 54.5, 54.4, 52.9, 45.4, 45.2, 38.4, 38.2, 27.3, 26.9, 21.9, 21.1, 20.9, 19.6, 19.2, 14.4, 14.2, 11.2, 10.8.

HPLC:
RP-HPLC Alltima™ C18 5 μm 150 mm x 4.6 mm, 10–100% B in 15 min, R_t =14.59 min, 95.3%

Mass Spectral Analysis: LRMS (ESI-) m/z 488, 243 $[M-2H]^{2+}$, 90%. HRMS for $C_{31}H_{28}N_4O_2$; calculated 489.2285, found 489.2283.

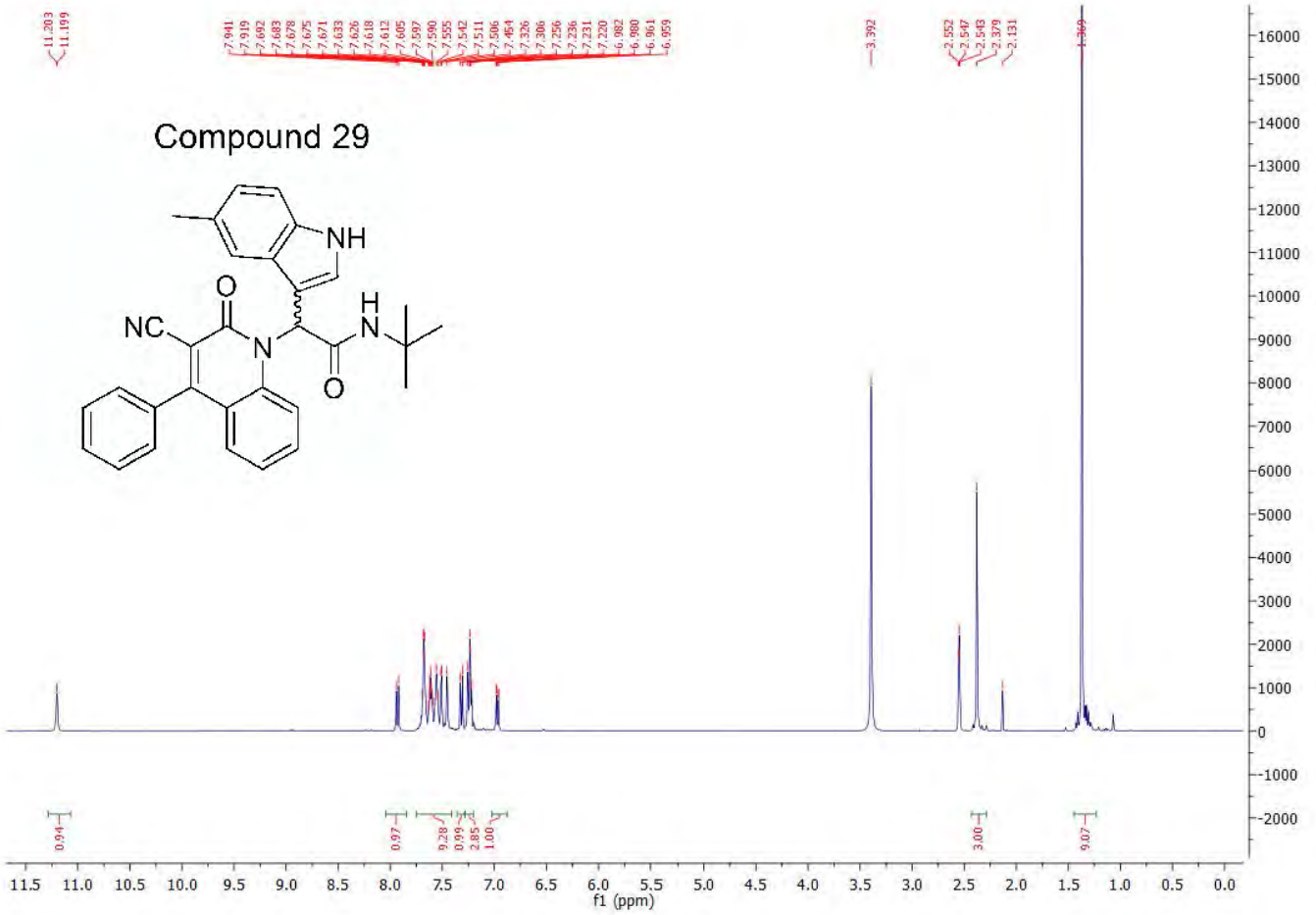
Compound 29
NH
O
NC
N
H
N
O
f1 (ppm)

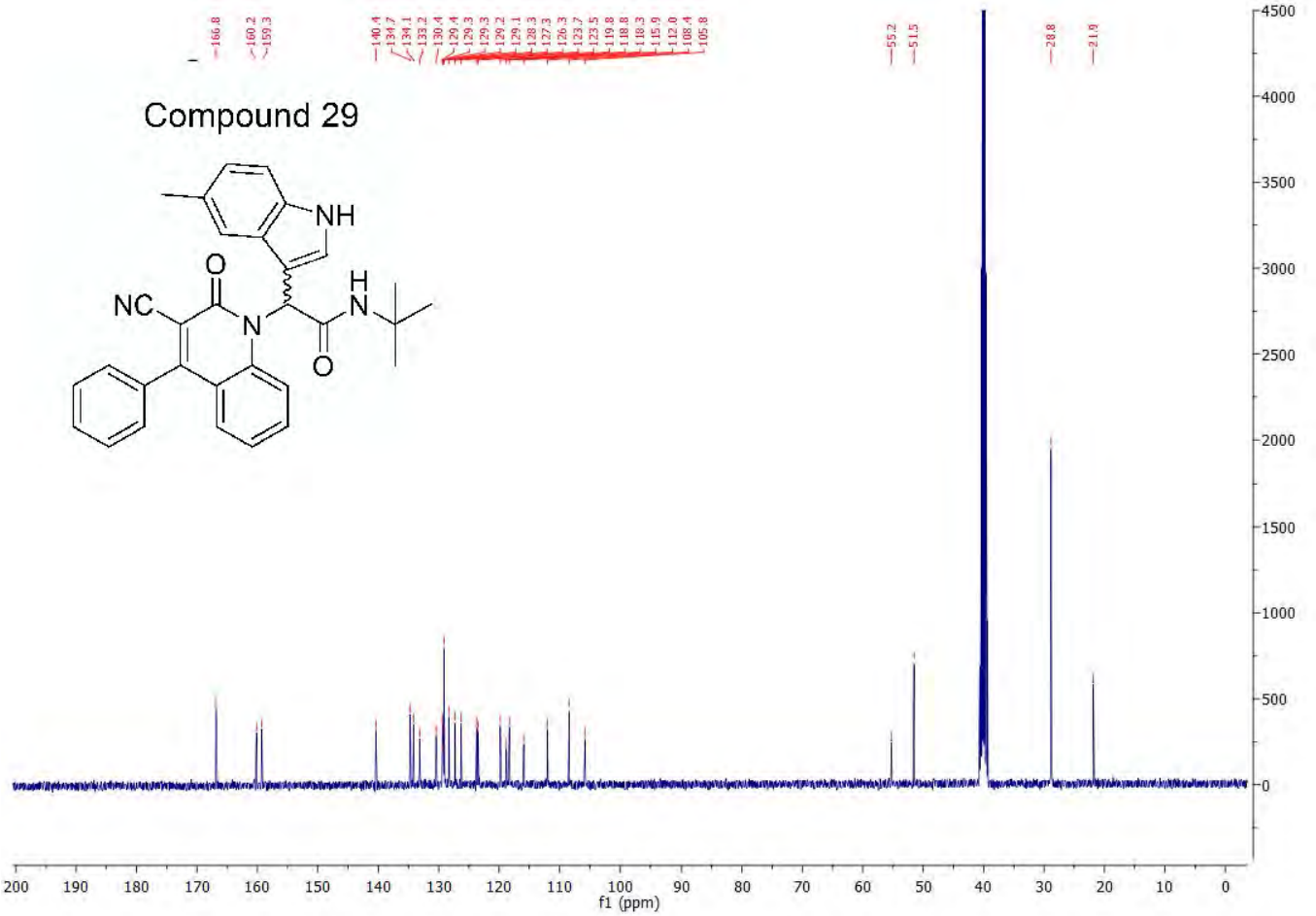
Compound 29
NH
O
NC
N
H
N
O
166.8
160.2
159.3
140.4
134.7
134.1
133.2
130.4
129.4
129.3
129.3
129.2
129.1
128.3
127.3
126.3
123.7
123.5
119.8
118.8
118.3
115.9
112.0
108.4
105.8
55.2
51.5
28.8
21.0
4500
4000
3500
3000
2500
2000
1500
1000
500
0
200 190 180 170 160 150 140 130 120 110 100 90 80 70 60 50 40 30 20 10 0
f1 (ppm)

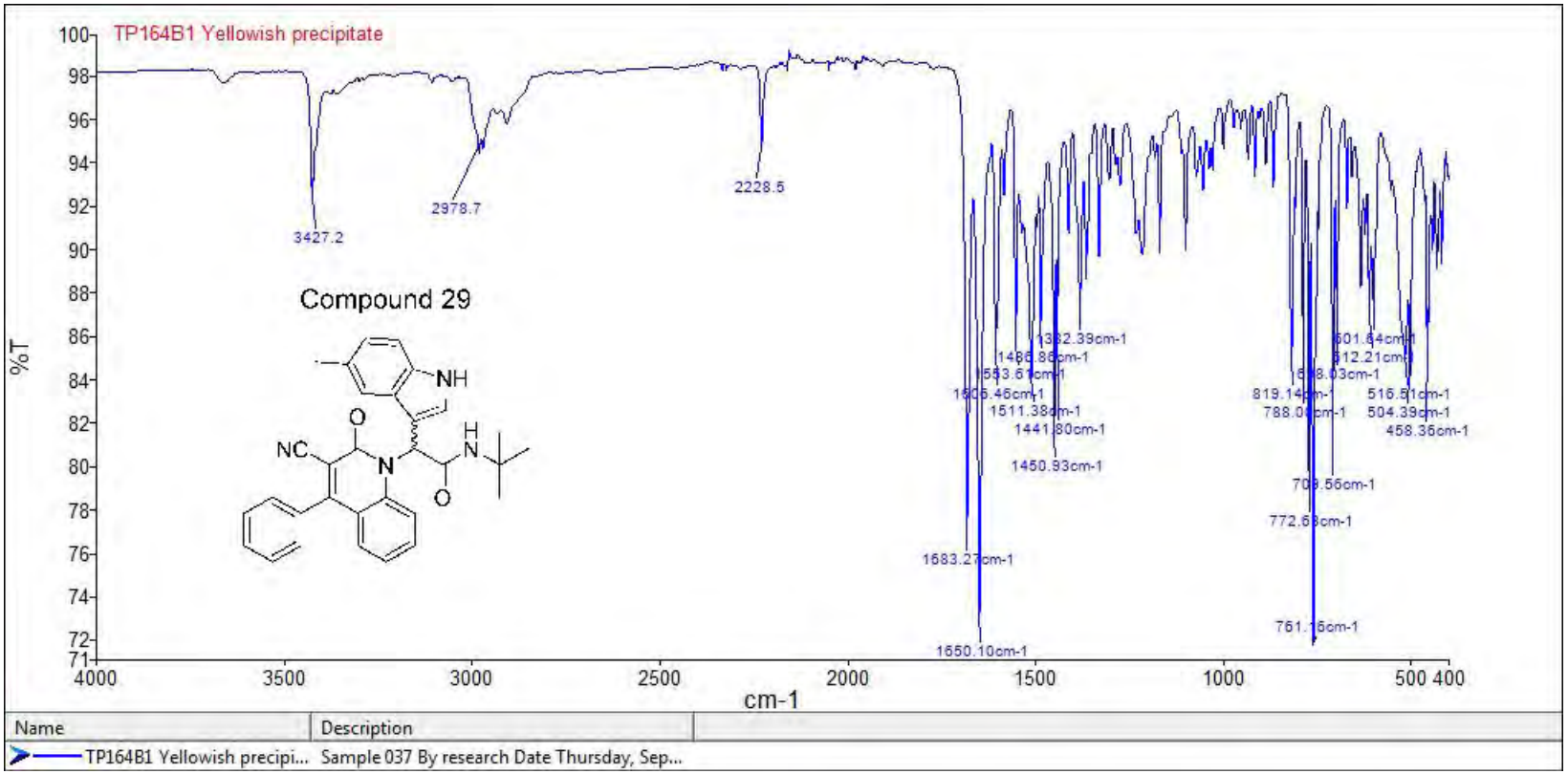
TP164B1 Yellowish precipitate
%T
cm-1
3427.2
2978.7
2228.5
1683.27cm-1
1650.10cm-1
1606.46cm-1
1511.38cm-1
1450.93cm-1
1441.80cm-1
1382.39cm-1
1486.86cm-1
1553.61cm-1
819.14cm-1
788.04cm-1
709.56cm-1
772.68cm-1
761.16cm-1
601.64cm-1
612.21cm-1
648.03cm-1
516.51cm-1
504.39cm-1
458.36cm-1
Compound 29
NH
O
NC
N
H
N
O
Name
Description
TP164B1 Yellowish precipi...
Sample 037 By research Date Thursday, Sep...

SHIMADZU LabSolutions **Analysis Report**

<Sample Information>

Sample Name	: TP164B1		
Sample ID	: TP164B1		
Data Filename	: TP164B1.lcd		
Method Filename	: 10-100 over 15 mins.lcm		
Batch Filename	: TRIEU Second Third Generation and New pro.lcb		
Vial #	: 1-18	Sample Type	: Unknown
Injection Volume	: 30 uL		
Date Acquired	: 8/09/2014 3:09:52 PM	Acquired by	: System Administrator
Date Processed	: 15/10/2015 12:06:52 PM	Processed by	: System Administrator

<Chromatogram>

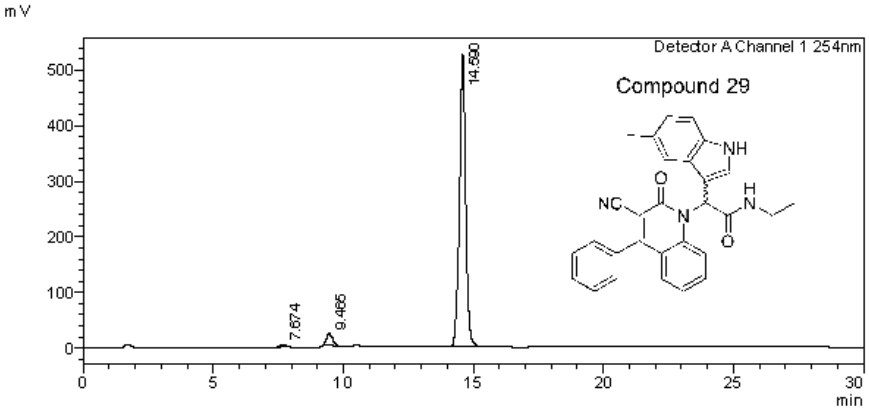

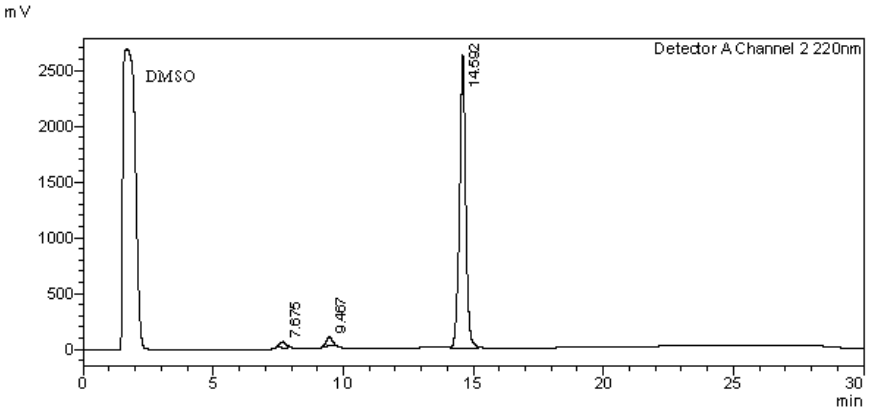

<Peak Table>

Detector A Channel 1 254nm

C:\LabSolutions\Data\Project1\TRIEU\TP164B1.lcd

Peak#	Ret. Time	Area	Height	Area%	Height%
1	7.674	67733	4325	0.741	0.784
2	9.465	341004	21316	3.730	3.865
3	14.590	8733695	525880	95.529	95.351
Total		9142431	551520	100.000	100.000

Detector A Channel 2 220nm

Peak#	Ret. Time	Area	Height	Area%	Height%
1	7.675	959320	56291	2.066	2.032
2	9.467	1187096	80692	2.556	2.913
3	14.592	44292928	2633164	95.378	95.055
Total		46439343	2770146	100.000	100.000

==== Shimadzu LCMSsolution Data Report ====

<Chromatogram>

Sample Information

Acquired by	: Admin
Date Acquired	: 7/23/2015 6:24:19 PM
Sample Type	: Unknown
Level#	: 0
Sample Name	: TP164B1
Sample ID	:
ISTD Amount	: (Level1 Conc.)
Sample Amount	: 1
Dilution Factor	: 1
Tray#	: 1
Vial#	: 58
Injection Volume	: 5
Data File	: TP164B2.lcd
Method File	: FIA-ESI_Scan(-).lcm
Original Method	: C:\LabSolutions\Data\Kelly\FIA-ESI_Scan(-).lcm
Report Format	: DefaultLCMS.lcr
Tuning File	: C:\LabSolutions\LCsolution\Log\Tuning\Autotune_030908.lct
Processed by	: Admin
Modified Date	: 7/23/2015 6:25:50 PM

Compound 29

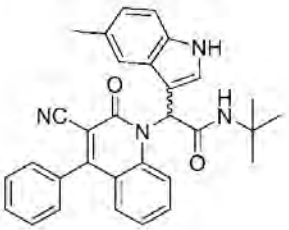

Chromatogram

TP164B1 C:\LabSolutions\Data\Trieu\NORMAL REVERSE PHASE COLUMN\UGI MASS ESI NEGATIVE SCAN\TP164B2.lcd

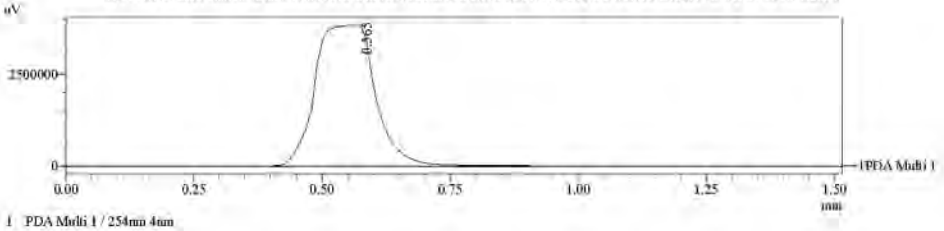

1 PDA Multi 1 / 254nm 4nm

<Spectrum>

Retention Time:0.840(Scan#:85)
Max Peak:554 Base Peak:156.50(4321178)
Spectrum:Averaged 0.640-1.280(65-129)
Background:Averaged 0.180-0.560(19-57) Polarity:Pos Segment1 - Event1

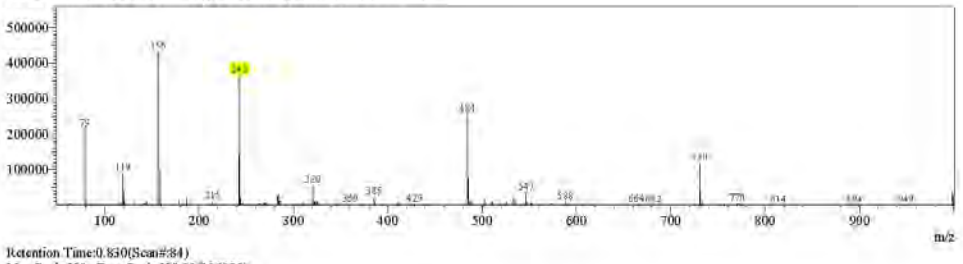

Retention Time:0.830(Scan#:84)
Max Peak:589 Base Peak:520.30(113099)
Spectrum:Averaged 0.650-1.290(66-130)
Background:Averaged 0.190-0.560(20-58) Polarity:Neg Segment1 - Event2

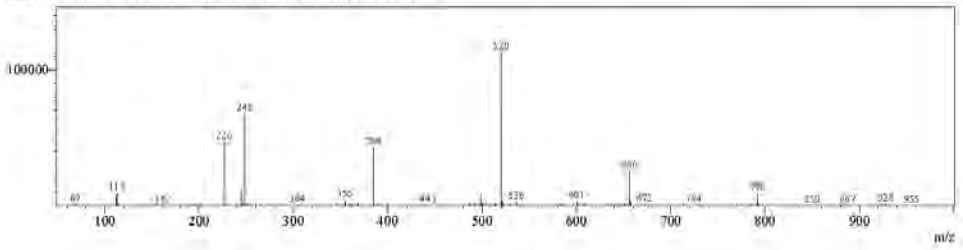

C:¥LabSolutions¥Data¥Trieu¥NORMAL REVERSE PHASE COLUMN¥UGI MASS ESI NEGATIVE SCAN¥TP164B2.lcd

Compound	Chemical Formula	Predicted monoisotopic neutral MW	Predicted MH+	MH+ Measured	Main MS Ions	Main MS/MS Fragments
TP164B1	$C_{31}H_{28}N_4O_2$	488.2212	489.2285	489.2283	243.149 (fragment) 489.2283	243.1496 187.0870 489.3408

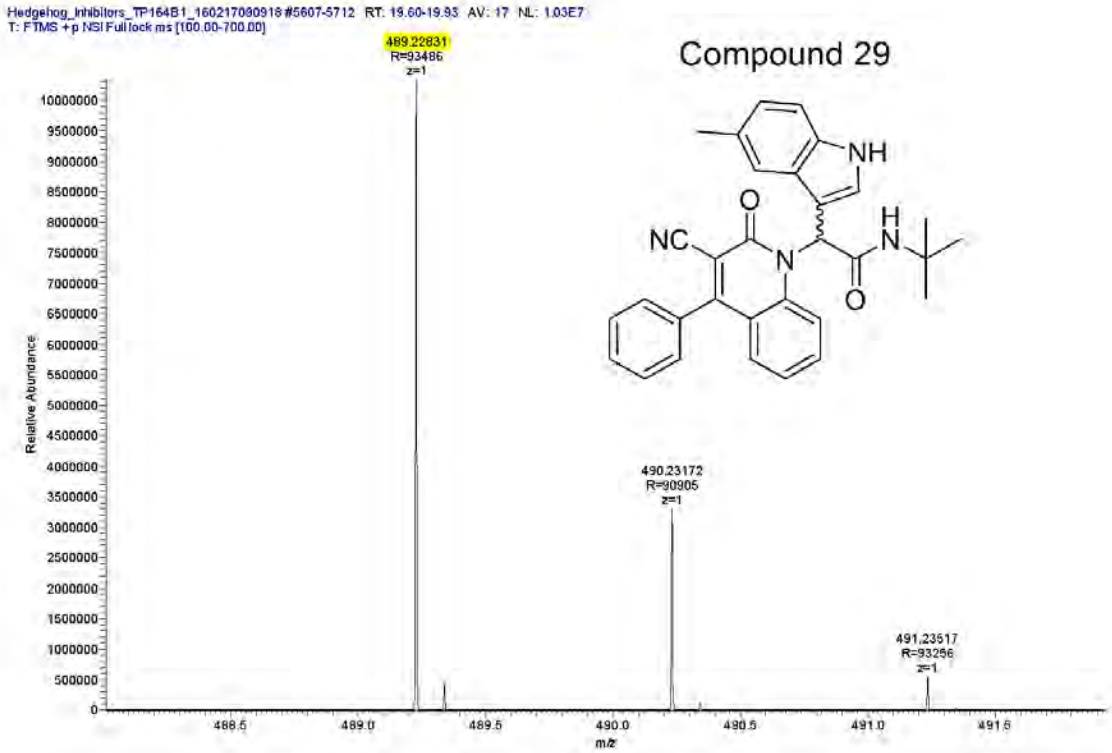

Compound 30

Compound Name: *N*-tert-Butyl-2-(3-cyano-2-oxo-4-phenyl-2*H*-quinolin-1-yl)-2-(1-methyl-1*H*-indole-3-yl)-acetamide

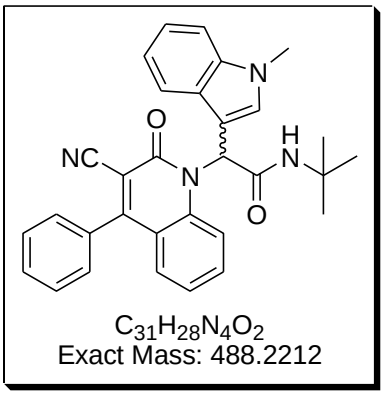

Obtained Weight & Yield: 0.2g, 27%

Appearance: White precipitate

Solubility: Acetone, ACN

Melting Point: 232-234 ˚C

TLC Conditions: EtOAc/Hexane (50/50)

IR Analysis: ν_{max}/cm^{-1}
3357 (NH), 2979 (CH), 2229 (CN), 1650 (CO).

^{1}H NMR Analysis:

^{1}H NMR (400 MHz, DMSO-d_6) δ 7.89 (d, J = 8.8 Hz, 1H), 7.68 – 7.46 (m, 9H), 7.43 (d, J = 7.8 Hz, 2H), 7.22-7.13 (m, 3H), 7.06 (t, J = 7.4 Hz, 1H), 3.79 (s, 3H), 1.32 (s, 9H).

^{13}C NMR Analysis:

136.75, 134.1, 133.3, 130.5, 130.4, 129.3 (C x 3), 129.2 (C x 2), 127.58, 123.5, 122.2, 120.0, 119.8, 119.0, 118.6, 115.9, 110.5, 108.0, 105.9, 54.9, 51.6, 33.1, 28.8 (C x 3).

HPLC:
RP-HPLC Alltima™ C18 5 μm 150 mm x 4.6 mm, 10–100% B in 15 min, R_t = 7.03 min, 96.7%

Mass Spectral Analysis: LRMS (ESI+) m/z 488, 243 $[M-2H]^{2+}$, 100%. HRMS (ES+) for $C_{31}H_{28}N_4O_2$; calculated 489.2285, found 489.2287.

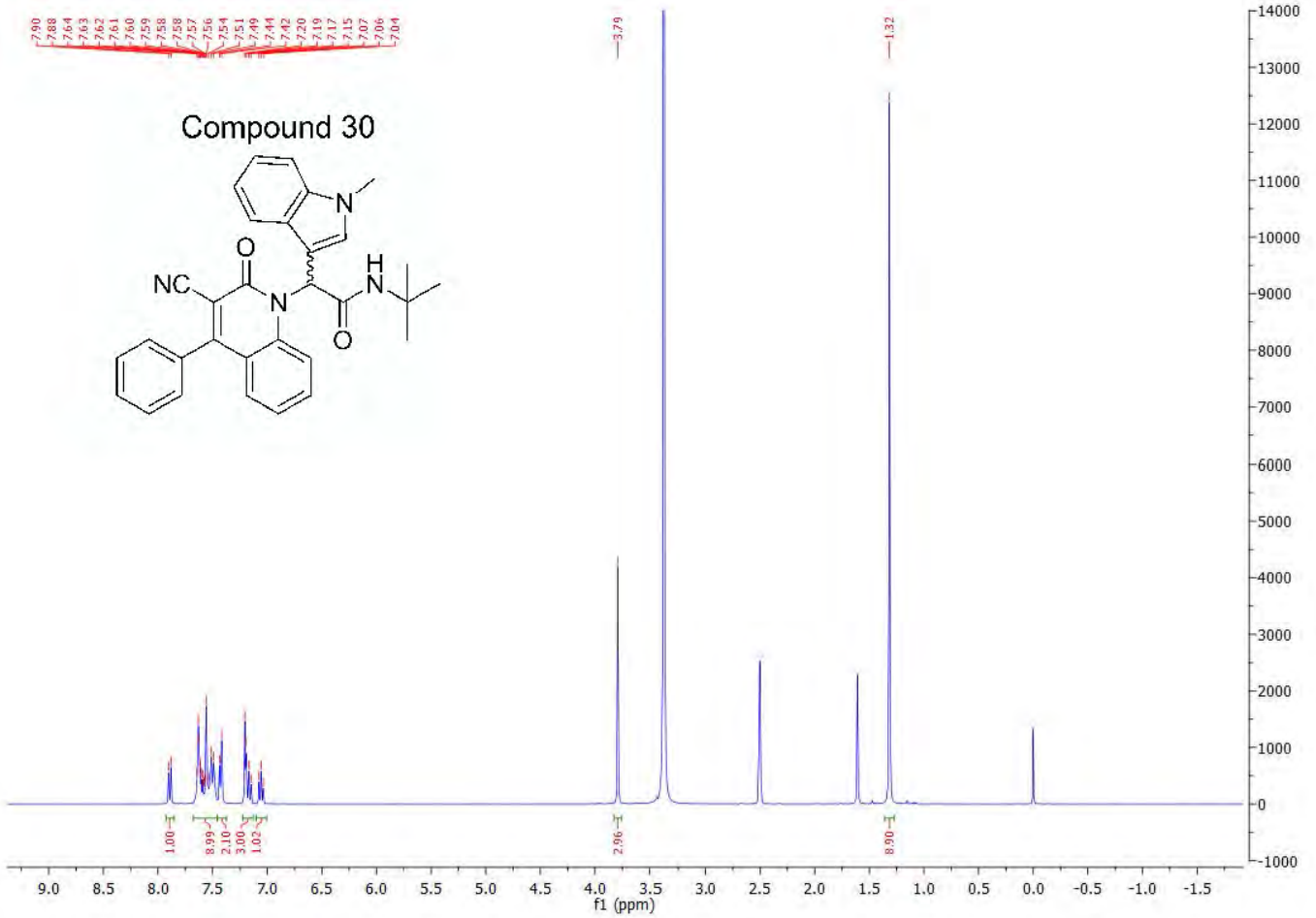
Compound 30
NC
O
N
H
N
O
f1 (ppm)

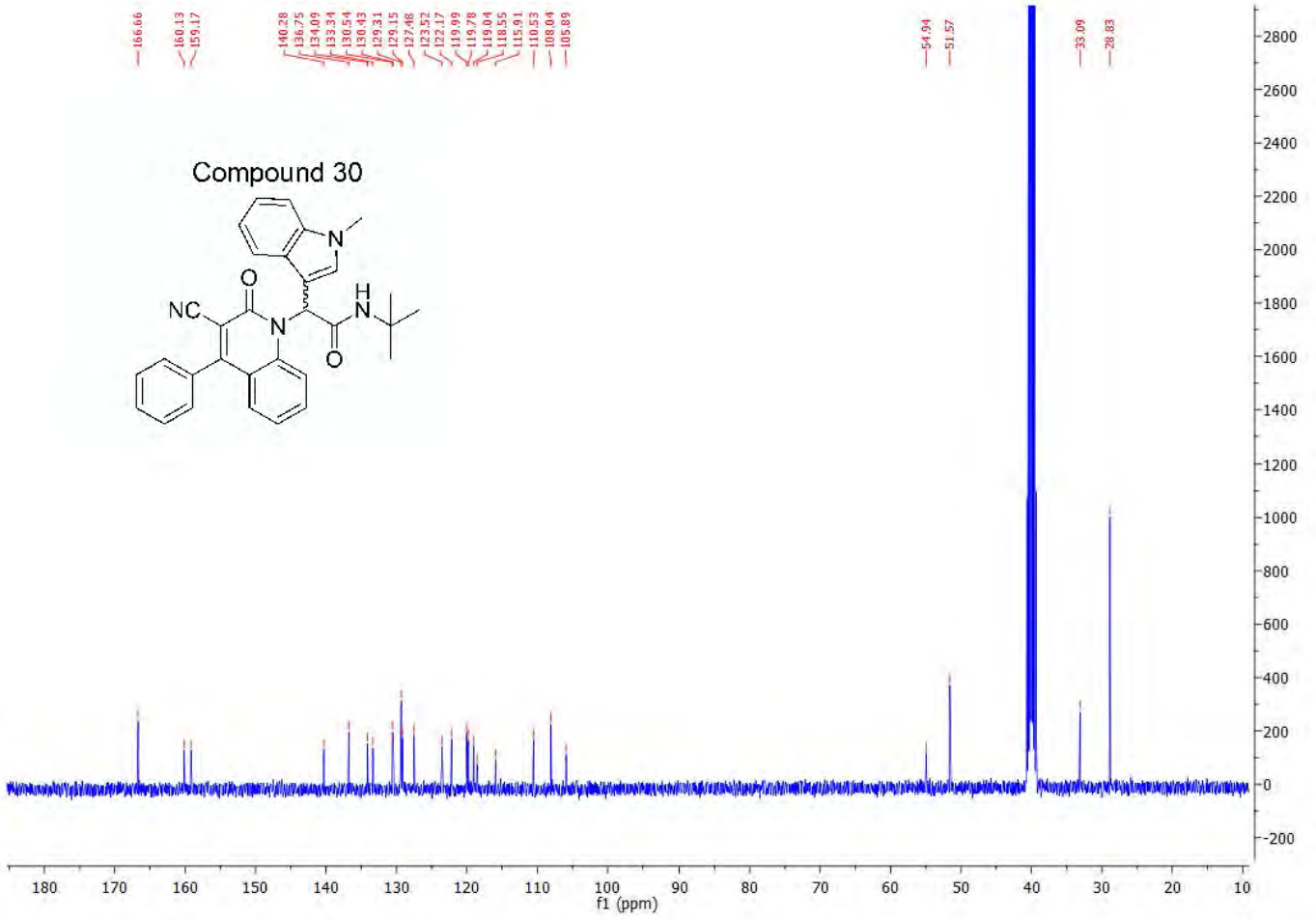
166.66
160.13
159.17
140.28
136.75
134.09
133.34
130.54
130.43
129.31
129.15
127.48
123.52
122.17
119.99
119.78
119.04
118.55
115.91
110.53
108.04
105.89
54.94
51.57
33.09
28.83
Compound 30
NC
O
N
O
H
N
f1 (ppm)

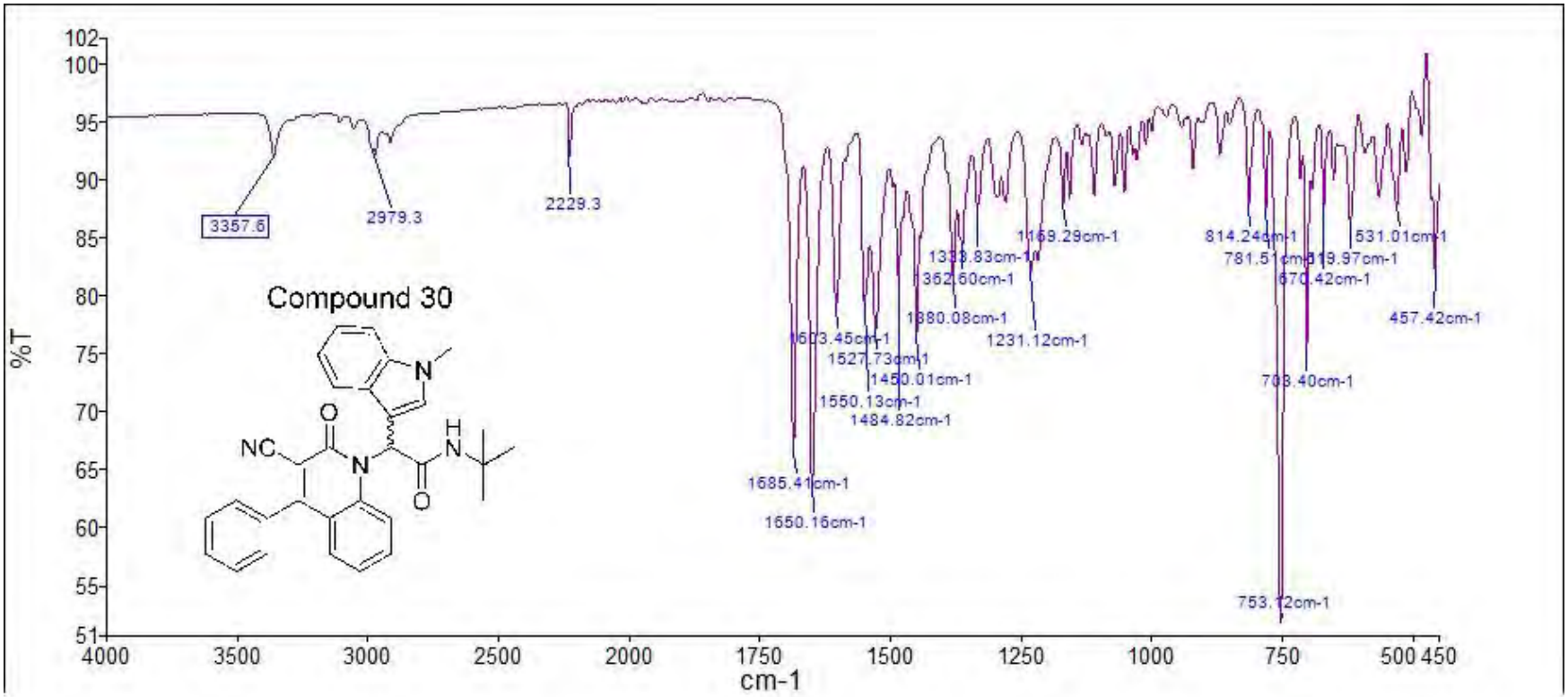
Compound 30
%T
cm-1
3357.6
2979.3
2229.3
1685.41cm-1
1650.16cm-1
1623.45cm-1
1527.73cm-1
1550.13cm-1
1484.82cm-1
1450.01cm-1
1380.08cm-1
1362.60cm-1
1333.83cm-1
1231.12cm-1
1169.29cm-1
814.24cm-1
781.51cm-1
753.12cm-1
703.40cm-1
670.42cm-1
531.01cm-1
457.42cm-1

==== Shimadzu LCMSsolution Analysis Report ====

Acquired by	: Admin
Sample Name	: TP158B1 Old
Sample ID	:
Vail #	: 56
Injection Volume	: 30 uL
Data File Name	: TP158B1 Old.lcd
Method File Name	: Econosphere C18 EPS 5u lot 50195421 part 70070 150mm id 4.6mm.lcm
Batch File Name	: 2015 Ugi Knoevenagel products continue.lcb
Report File Name	: DefaultLCMS.lcr
Data Acquired	: 9/16/2015 1:49:14 PM
Data Processed	: 10/15/2015 11:30:54 AM

<Chromatogram>

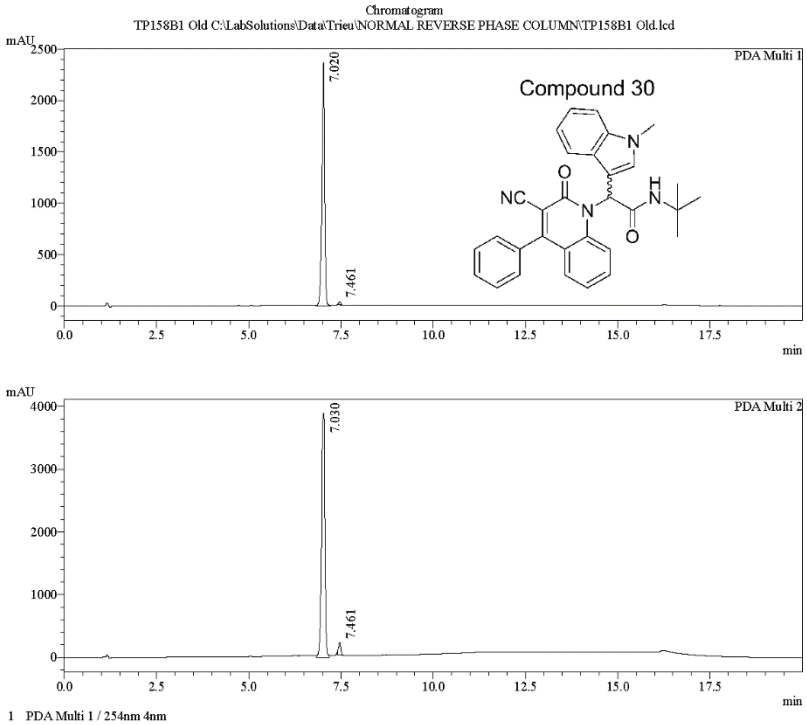

1 PDA Multi 1 / 254nm 4nm
2 PDA Multi 2 / 220nm 4nm

PeakTable

PDA Ch1 254nm 4nm

Peak#	Ret. Time	Area	Height	Area %	Height %
1	7.020	12152785	2372981	99.066	98.712
2	7.461	114628	30955	0.934	1.288
Total		12267413	2403936	100.000	100.000

PeakTable

PDA Ch2 220nm 4nm

Peak#	Ret. Time	Area	Height	Area %	Height %
1	7.030	25077202	3887009	96.782	95.000
2	7.461	833821	204563	3.218	5.000
Total		25911023	4091572	100.000	100.000

==== Shimadzu LCMSsolution Data Report ====

<Chromatogram>

Sample Information

Acquired by	: Admin
Date Acquired	: 7/24/2015 9:38:01 AM
Sample Type	: Unknown
Level#	: 0
Sample Name	: TP158B1
Sample ID	:
ISTD Amount	: (Level1 Conc.)
Sample Amount	: 1
Dilution Factor	: 1
Tray#	: 1
Vial#	: 54
Injection Volume	: 5
Data File	: TP158B2.lcd
Method File	: FIA-ESI_Scan(+).lcm
Original Method	: C:\LabSolutions\Data\Trieu\Mass spec files\FIA-ESI_Scan(+).lcm
Report Format	: DefaultLCMS.lcr
Tuning File	: C:\LabSolution\LCsolution\Log\Tuning\Autotune_030908.lct
Processed by	: Admin
Modified Date	: 7/24/2015 9:39:34 AM

Compound 30

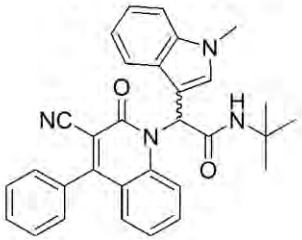

Chromatogram

TP158B1 C:\LabSolutions\Data\Trieu\NORMAL REVERSE PHASE COLUMN\ESI POSITIVE\UGI KNOEVENAGEL\TP158B2.lcd

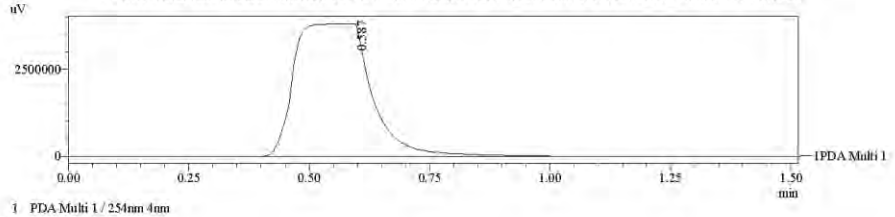

1 PDA Multi 1 / 254nm 4nm

<Spectrum>

Retention Time:0.880(Scan#:89)
Max Peak:311 Base Peak:242.65(349222)
Spectrum:Averaged 0.620-1.280(63-129)
Background:Averaged 0.200-0.509(21-51) Polarity:Pos Segment1 - Event1

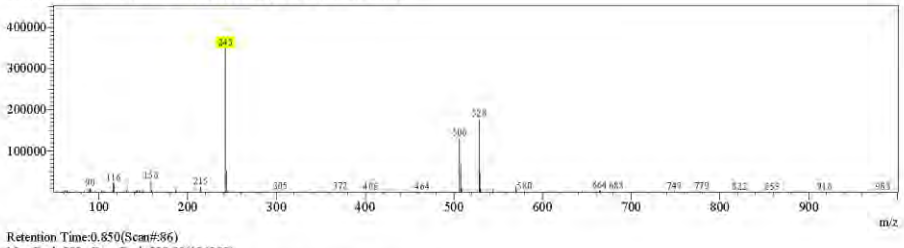

Retention Time:0.850(Scan#:86)
Max Peak:502 Base Peak:520.30(124282)
Spectrum:Averaged 0.630-1.290(64-130)
Background:Averaged 0.210-0.509(22-52) Polarity:Neg Segment1 - Event2

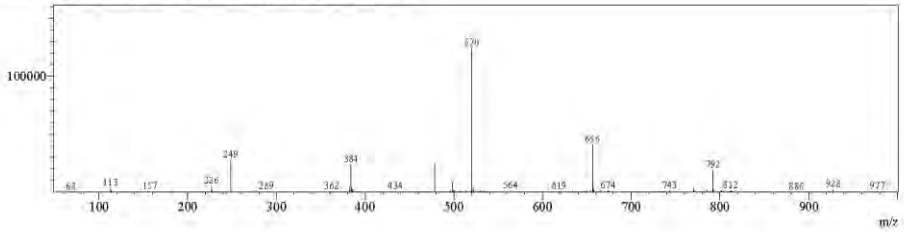

C:¥LabSolutions¥Data¥Trieu¥NORMAL REVERSE PHASE COLUMN¥ESI POSITIVE¥UGI KNOEVENAGEL¥TP158B2.lcd

Compound	Chemical Formula	Predicted monoisotopic neutral MW	Predicted MH+	MH+ Measured	Main MS Ions	Main MS/MS Fragments
TP158B1	$C_{31}H_{28}N_4O_2$	488.2212	489.2285	489.2287*	243.14917 (fragment)	243.149^

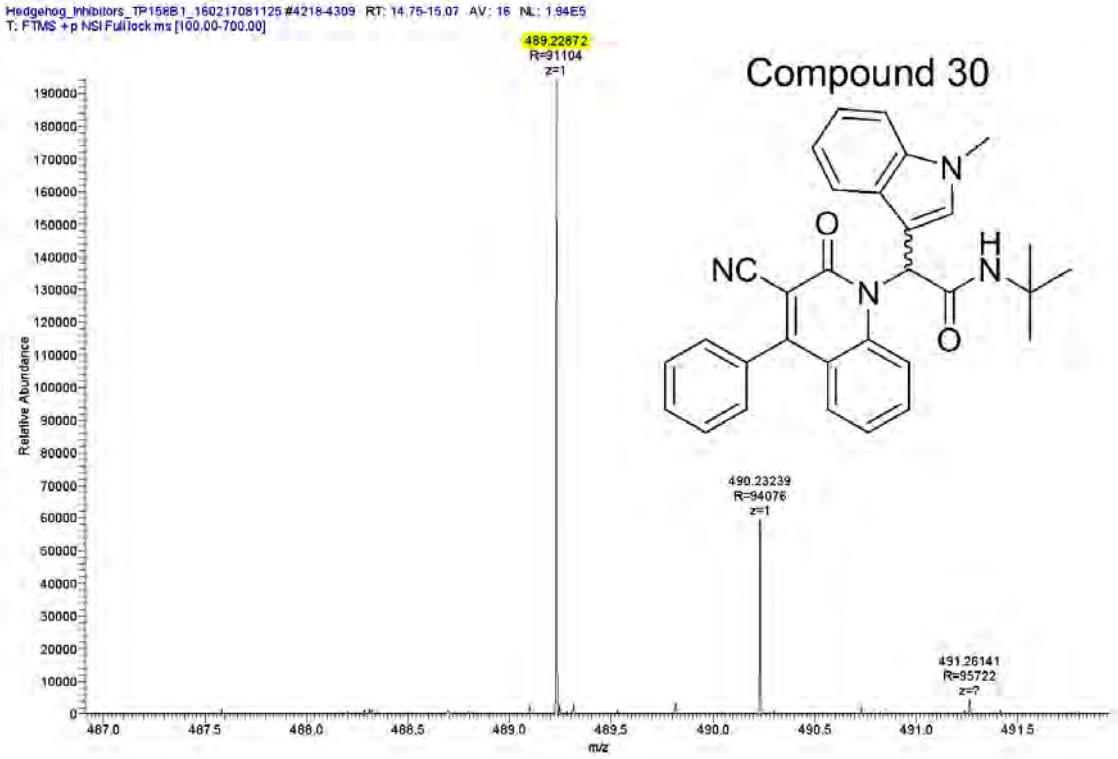

8.3. Appendix to Chapter 4

8.3.1. Biological investigation

Statistical analysis

Chapter 4, table 1	GLI protein expression		TP90B2 = **4**
	SAG	Compound 4 + SAG	
	0.049881677	0.026802303	
	0.045816634	0.025896196	
	0.046748108	0.025204239	

F-Test Two-Sample for Variances			t-Test: Two-Sample Assuming Equal Variances		
	Variable 1	*Variable 2*		*Variable 1*	*Variable 2*
Mean	0.04748214	0.025967579	Mean	0.04748214	0.025967579
Variance	4.53525E-06	6.42274E-07	Variance	4.53525E-06	6.42274E-07
Observations	3	3	Observations	3	3
df	2	2	Pooled Variance	2.58876E-06	
F	7.061231487		Hypothesized Mean Difference	0	
P(F<=f) one-tail	0.124050525		df	4	
F Critical one-tail	19		t Stat	16.37692008	
	Equal		P(T<=t) one-tail	4.06887E-05	
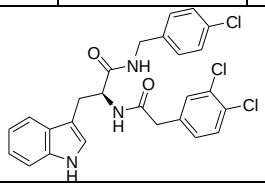			t Critical one-tail	2.131846786	
			P(T<=t) two-tail	8.13774E-05	
			t Critical two-tail	2.776445105	
			** P < .001		

Chapter 4, table 1		SAG	**17** + SAG		TP90B4 = **17**
		0.049881677	0.034917546		
		0.045816634	0.042979856		
		0.046748108			
F-Test Two-Sample for Variances		t-Test: Two-Sample Assuming Unequal Variances			
	Variable 1	*Variable 2*		*Variable 1*	*Variable 2*
Mean	0.04748214	0.038948701	Mean	0.047482	0.038949
Variance	4.53525E-06	3.25004E-05	Variance	4.54E-06	3.25E-05
Observations	3	2	Observations	3	2
df	2	1	Hypothesized Mean Difference	0	
F	0.139544202		df	1	
P(F<=f) one-tail	0.115801611		t Stat	2.024784	
F Critical one-tail	0.05401662		P(T<=t) one-tail	0.146021	
	Unequal		t Critical one-tail	6.313752	
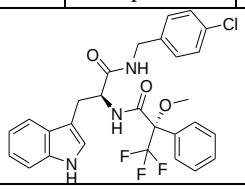			P(T<=t) two-tail	0.292043	
			t Critical two-tail	12.7062	
			P= .29, No significant difference		

Chapter 4, table 1		**GLI protein expression**			TP152B4 = **13**
		SAG	**13** + SAG		
		0.049882	0.026827		
		0.045817	0.026603		
		0.046748			
F-Test Two-Sample for Variances			t-Test: Two-Sample Assuming Equal Variances		
	Variable 1	*Variable 2*		*Variable 1*	*Variable 2*
Mean	0.047482	0.026715	Mean	0.047482	0.026715
Variance	4.54E-06	2.5E-08	Variance	4.54E-06	2.5E-08
Observations	3	2	Observations	3	2
F	181.3226		Hypothesized Mean Difference	0	
P(F<=f) one-tail	0.05244		df	3	
F Critical one-tail	199.5		t Stat	13.06499	
	equal		P(T<=t) one-tail	0.000484	
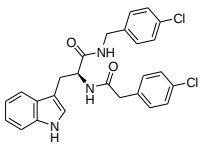			t Critical one-tail	2.353363	
			P(T<=t) two-tail	0.000968	
			t Critical two-tail	3.182446	
			**P < .001		

Chapter 4, table 1		GLI protein expression		
		SAG	**16** + SAG	
		0.159728698	0.279471191	TP67B4 = **16**
		0.149875215	0.287654457	
		0.142709665	0.293284354	

F-Test Two-Sample for Variances			t-Test: Two-Sample Assuming Equal Variances		
	Variable 1	*Variable 2*		*Variable 1*	*Variable 2*
Mean	0.150771192	0.286803334	Mean	0.150771192	0.286803334
Variance	7.3014E-05	4.82442E-05	Variance	7.3014E-05	4.82442E-05
Observations	3	3	Observations	3	3
F	1.513425338		Hypothesized Mean Difference	0	
P(F<=f) one-tail	0.39786342		df	4	
F Critical one-tail	19		t Stat	-21.3966969	
Equal			P(T<=t) one-tail	1.41071E-05	
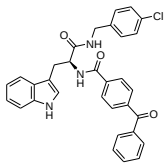			t Critical one-tail	2.131846786	
			P(T<=t) two-tail	2.82141E-05	
			t Critical two-tail	2.776445105	
			*** P < .0001		

Chapter 4, table 1		GLI protein expression		
		SAG	**14** + SAG	
		0.159728698	0.048306285	TP93B4 = **14**
		0.149875215	0.045140059	
		0.142709665	0.039920679	

F-Test Two-Sample for Variances			t-Test: Two-Sample Assuming Equal Variances		
	Variable 1	*Variable 2*		*Variable 1*	*Variable 2*
Mean	0.150771192	0.044455674	Mean	0.150771192	0.044455674
Variance	7.3014E-05	1.79309E-05	Variance	7.3014E-05	1.79309E-05
Observations	3	3	Observations	3	3
F	4.071966173		Hypothesized Mean Difference	0	
P(F<=f) one-tail	0.197162198		df	4	
F Critical one-tail	19		t Stat	19.30937692	
Equal			P(T<=t) one-tail	2.11994E-05	
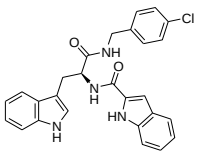			t Critical one-tail	2.131846786	
			P(T<=t) two-tail	4.23987E-05	
			t Critical two-tail	2.776445105	
			*** P < .0001		

Chapter 4, table 1	GLI protein expression		
	SAG	**15** + SAG	
	0.159728698	0.056977657	TP95B4 = **15**
	0.149875215	0.05986236	
	0.142709665	0.065104256	

F-Test Two-Sample for Variances			t-Test: Two-Sample Assuming Equal Variances		
	Variable 1	*Variable 2*		*Variable 1*	*Variable 2*
Mean	0.150771192	0.060648091	Mean	0.150771192	0.060648091
Variance	7.3014E-05	1.69734E-05	Variance	7.3014E-05	1.69734E-05
Observations	3	3	Observations	3	3
df	2	2	Pooled Variance	4.49937E-05	
F	4.301661077		Hypothesized Mean Difference	0	
P(F<=f) one-tail	0.18862013		df	4	
F Critical one-tail	19		t Stat	16.45530501	
Equal			P(T<=t) one-tail	3.99282E-05	
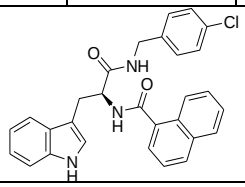			t Critical one-tail	2.131846786	
			P(T<=t) two-tail	7.98564E-05	
			t Critical two-tail	2.776445105	
			*** P < .0001		

Chapter 4, table 1	GLI protein expression		
	SAG	**12** + SAG	
	0.159728698	0.179834193	TP150B4 = **12**
	0.149875215	0.200700038	
	0.142709665	0.219379435	

F-Test Two-Sample for Variances			t-Test: Two-Sample Assuming Equal Variances		
	Variable 1	*Variable 2*		*Variable 1*	*Variable 2*
Mean	0.199971222	0.150771192	Mean	0.150771192	0.199971222
Variance	0.000391355	7.3014E-05	Variance	7.3014E-05	0.000391355
Observations	3	3	Observations	3	3
df	2	2	Pooled Variance	0.000232184	
P(F<=f) one-tail	0.157232661		df	4	
F Critical one-tail	19		t Stat	-3.954526016	
Equal			P(T<=t) one-tail	0.008377152	
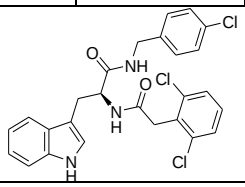			t Critical one-tail	2.131846786	
			P(T<=t) two-tail	0.016754305	
			t Critical two-tail	2.776445105	
			* P < .05		

Chapter 4, table 1		GLI protein expression		TP70B4 = **11**	
		SAG	**11** + SAG		
		0.107998	0.028305424		
		0.102026	0.033503471		
F-Test Two-Sample for Variances			t-Test: Two-Sample Assuming Equal Variances		
	Variable 1	*Variable 2*		*Variable 1*	*Variable 2*
Mean	0.105012201	0.030904	Mean	0.105012	0.030904
Variance	1.78308E-05	1.35E-05	Variance	1.78E-05	1.35E-05
Observations	2	2	Observations	2	2
df	1	1	Pooled Variance	1.57E-05	
F	1.319836796		Hypothesized Mean Difference	0	
P(F<=f) one-tail	0.455974259		df	2	
F Critical one-tail	161.4476388		t Stat	18.72081	
Equal			P(T<=t) one-tail	0.001421	
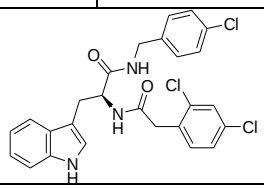			t Critical one-tail	2.919986	
			P(T<=t) two-tail	0.002841	
			t Critical two-tail	4.302653	
			* P < .05		

Chapter 4_ Figure 6A		*Ptch1* expression compared to SAG treatment		Compound 11= TP70B4	
		SAG	SAG + **11**		
		0.006992	0.00296		
		0.005601	0.003496		
		0.005083	0.004304		
F-Test Two-Sample for Variances			t-Test: Two-Sample Assuming Equal Variances		
	Variable 1	*Variable 2*		*Variable 1*	*Variable 2*
Mean	0.005892	0.003587	Mean	0.005892	0.003587
Variance	9.75E-07	4.58E-07	Variance	9.75E-07	4.58E-07
Observations	3	3	Observations	3	3
df	2	2	Pooled Variance	7.16E-07	
F	2.129241		Hypothesized Mean Difference	0	
P(F<=f) one-tail	0.319566		df	4	
F Critical one-tail	19		t Stat	3.336499	
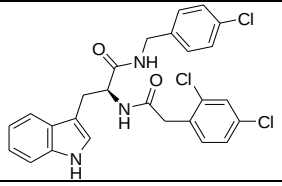			P(T<=t) one-tail	0.014465	
			t Critical one-tail	2.131847	
			P(T<=t) two-tail	0.02893	
			t Critical two-tail	2.776445	
			*P < .05		

Chapter 4_ Figure 6C	*Gli*$_2$ expression compared to SAG treatment		
	SAG	**11** + SAG	**Compound 11= TP70B4**
	0.00292	0.001262	
	0.002752	0.00085	
	0.002025	0.001145	

F-Test Two-Sample for Variances			t-Test: Two-Sample Assuming Equal Variances		
	Variable 1	*Variable 2*		*Variable 1*	*Variable 2*
Mean	0.002566	0.001086	Mean	0.002566	0.001086
Variance	2.27E-07	4.51E-08	Variance	2.27E-07	4.51E-08
Observations	3	3	Observations	3	3
df	2	2	Pooled Variance	1.36E-07	
F	5.026114		Hypothesized Mean Difference	0	
P(F<=f) one-tail	0.165944		df	4	
F Critical one-tail	19		t Stat	4.917768	
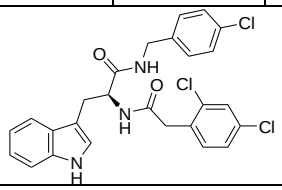			P(T<=t) one-tail	0.003971	
			t Critical one-tail	2.131847	
			P(T<=t) two-tail	0.007942	
			t Critical two-tail	2.776445	
			* *P* < .05		

Chapter 4_ Figure 6D	***Gli*$_2$ expression compared to SAG treament**		
	SAG	SAG + **14**	**Compound 14 = TP93B4**
	0.000622	0.001211	
	0.000766	0.000745	
	0.001011		

F-Test Two-Sample for Variances			t-Test: Two-Sample Assuming Equal Variances		
	Variable 1	*Variable 2*		*Variable 1*	*Variable 2*
Mean	0.000978	0.0008	Mean	0.000978	0.0008
Variance	1.08E-07	3.86E-08	Variance	1.08E-07	3.86E-08
Observations	2	3	Observations	2	3
df	1	2	Pooled Variance	6.18E-08	
F	2.804829		Hypothesized Mean Difference	0	
P(F<=f) one-tail	0.235963		df	3	
F Critical one-tail	18.51282		t Stat	0.784536	
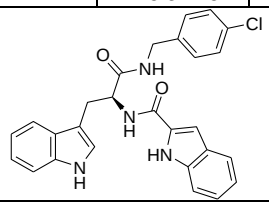			P(T<=t) one-tail	0.244987	
			t Critical one-tail	2.353363	
			P(T<=t) two-tail	0.489973	
			t Critical two-tail	3.182446	
			No significant difference *P* = .48		

Chapter 4_ Figure 6B	***Ptch*$_1$ expression compared to SAG treatments**		
	SAG	**14** + SAG	**Compound 14 = TP93B4**
	0.004279	0.002781	
	0.004419	0.001785	
	0.003508		

F-Test Two-Sample for Variances			t-Test: Two-Sample Assuming Equal Variances		
	Variable 1	Variable 2		Variable 1	Variable 2
Mean	0.002283	0.004069	Mean	0.002283	0.004069
Variance	4.97E-07	2.41E-07	Variance	4.97E-07	2.41E-07
Observations	2	3	Observations	2	3
df	1	2	Pooled Variance	3.26E-07	
F	2.061438		Hypothesized Mean Difference	0	
P(F<=f) one-tail	0.287565		df	3	
F Critical one-tail	18.51282		t Stat	-3.42506	
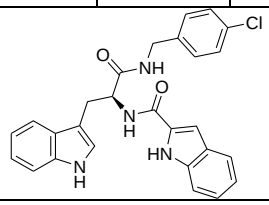			P(T<=t) one-tail	0.020844	
			t Critical one-tail	2.353363	
			P(T<=t) two-tail	0.041688	
			t Critical two-tail	3.182446	
			* P < .05		

Chapter 4_ Figure 7A	GLI expression compared to SAG treatment		
	SAG	**16** + SAG	Compound 16 = TP 67B4
	0.1597287	0.2794712	
	0.1498752	0.2876545	
	0.1427097	0.2932844	

F-Test Two-Sample for Variances			t-Test: Two-Sample Assuming Equal Variances		
	Variable 1	*Variable 2*		*Variable 1*	*Variable 2*
Mean	0.150771192	0.2868033	Mean	0.1507712	0.2868033
Variance	7.3014E-05	4.824E-05	Variance	7.301E-05	4.824E-05
Observations	3	3	Observations	3	3
df	2	2	Pooled Variance	6.063E-05	
F	1.513425338		Hypothesized Mean Difference	0	
P(F<=f) one-tail	0.39786342		df	4	
F Critical one-tail	19		t Stat	21.396697	
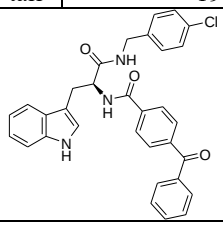			P(T<=t) one-tail	1.411E-05	
			t Critical one-tail	2.1318468	
			P(T<=t) two-tail	2.821E-05	
			t Critical two-tail	2.7764451	
			*** *P < .0001*		

Chapter 4_ Figure 7C	***Ptch*$_1$ expression compared to SAG treatment**		
	SAG	**16** + SAG	Compound 16 = TP67B4
	0.004279	0.005013	
	0.004419	0.005154	
	0.003508		

F-Test Two-Sample for Variances			t-Test: Two-Sample Assuming Equal Variances		
	Variable 1	*Variable 2*		*Variable 1*	*Variable 2*
Mean	0.004069	0.005084	Mean	0.004069	0.005084
Variance	2.41E-07	9.93E-09	Variance	2.41E-07	9.93E-09
Observations	3	2	Observations	3	2
df	2	1	Pooled Variance	1.64E-07	
F	24.2494		Hypothesized Mean Difference	0	
P(F<=f) one-tail	0.142136		df	3	
F Critical one-tail	199.5		t Stat	-2.74744	
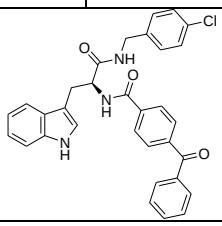			P(T<=t) one-tail	0.035447	
			t Critical one-tail	2.353363	
			P(T<=t) two-tail	0.070894	
			t Critical two-tail	3.182446	
			P =.07 No statistically significant difference		

Chapter 4_ Figure 7B	***Gli2* expression compared to SAG treatment**

		SAG	**16** + SAG		
		0.00062234	0.00147	**Compound 16 = TP67B4**	
		0.0007662	0.001084		
		0.001011			
F-Test Two-Sample for Variances			t-Test: Two-Sample Assuming Equal Variances		
	Variable 1	*Variable 2*		*Variable 1*	*Variable 2*
Mean	0.001276766	0.00079985	Mean	0.001276766	0.00079985
Variance	7.46539E-08	3.8613E-08	Variance	7.46539E-08	3.8613E-08
Observations	2	3	Observations	2	3
df	1	2	Pooled Variance	5.06265E-08	
F	1.933394495		Hypothesized Mean Difference	0	
P(F<=f) one-tail	0.29890562		df	3	
F Critical one-tail	18.51282051		t Stat	2.321914136	
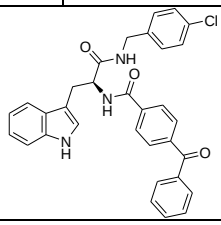			P(T<=t) one-tail	0.051452075	
			t Critical one-tail	2.353363435	
			P(T<=t) two-tail	0.10290415	
			t Critical two-tail	3.182446305	
			P = .1 No statistically significant difference		

Chapter 4_ Figure 7D		**GLI protein expression compared to SAG treatment**			
		SAG	**16**	**Compound 16 (10 µM)**	
		0.049881677	0.01346169		
		0.045816634	0.01502132		
		0.046748108			
F-Test Two-Sample for Variances			t-Test: Two-Sample Assuming Equal Variances		
	Variable 1	*Variable 2*		*Variable 1*	*Variable 2*
Mean	0.04748214	0.0142415	Mean	0.04748214	0.0142415
Variance	4.53525E-06	1.2162E-06	Variance	4.5352E-06	1.216E-06
Observations	3	2	Observations	3	2
df	2	1	Pooled Variance	3.4289E-06	
F	3.728948245		Hypothesized Mean Difference	0	
P(F<=f) one-tail	0.343849832		df	3	
F Critical one-tail	199.5		t Stat	19.6644668	
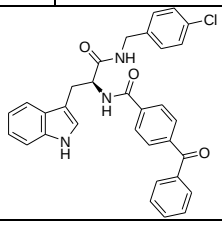			P(T<=t) one-tail	0.00014367	
			t Critical one-tail	2.35336343	
			P(T<=t) two-tail	0.00028734	
			t Critical two-tail	3.18244631	
			***P < .001*		

Chapter 4_ Figure 7D	GLI protein expression compared to SAG treatment		
	SAG	**16**	**Compound 16 (5 µM)**
	0.049881677	0.017292	
	0.045816634	0.016201	
	0.046748108	0.01791	

F-Test Two-Sample for Variances			t-Test: Two-Sample Assuming Equal Variances		
	Variable 1	*Variable 2*		*Variable 1*	*Variable 2*
Mean	0.04748214	0.017134668	Mean	0.017135	0.014242
Variance	4.53525E-06	7.48681E-07	Variance	7.49E-07	1.22E-06
Observations	3	3	Observations	3	2
df	2	2	Pooled Variance	9.05E-07	
F	6.057649322		Hypothesized Mean Difference	0	
P(F<=f) one-tail	0.141690236		df	3	
F Critical one-tail	19		t Stat	3.332365	
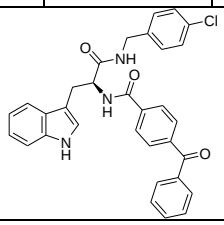			P(T<=t) one-tail	0.02232	
			t Critical one-tail	2.353363	
			P(T<=t) two-tail	0.04464	
			t Critical two-tail	3.182446	
			* *P* < .05		

Chapter 4_ Figure 7D	GLI protein expression compared to SAG treatment		
	SAG	**16**	**Compound 16 (1 µM)**
	0.04988168	0.015585203	
	0.04581663	0.017794278	
	0.04674811		

F-Test Two-Sample for Variances			t-Test: Two-Sample Assuming Equal Variances		
	Variable 1	*Variable 2*		*Variable 1*	*Variable 2*
Mean	0.04748214	0.01668974	Mean	0.04748214	0.0166897
Variance	4.53525E-06	2.44E-06	Variance	4.5352E-06	2.44E-06
Observations	3	2	Observations	3	2
df	2	1	Pooled Variance	3.8368E-06	
F	1.858702953		Hypothesized Mean Difference	0	
P(F<=f) one-tail	0.460413847		df	3	
F Critical one-tail	199.5		t Stat	17.2205789	
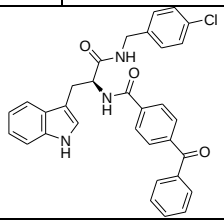			P(T<=t) one-tail	0.00021333	
			t Critical one-tail	2.35336343	
			P(T<=t) two-tail	0.00042666	
			t Critical two-tail	3.18244631	
			**P < .001		

Chapter 4_ Figure 7D		GLI protein expression compared to SAG treatment			
		SAG	**16**	Compound 16 (0.5 µM)	
		0.049881677	0.015478332		
		0.045816634	0.016334621		
		0.046748108	0.016149237		
F-Test Two-Sample for Variances			t-Test: Two-Sample Assuming Unequal Variances		
	Variable 1	*Variable 2*		*Variable 1*	*Variable 2*
Mean	0.04748214	0.015987397	Mean	0.047482	0.015987
Variance	4.53525E-06	2.02952E-07	Variance	4.54E-06	2.03E-07
Observations	3	3	Observations	3	3
df	2	2	Hypothesized Mean Difference	0	
F	22.34640589		df	2	
P(F<=f) one-tail	0.042833145		t Stat	25.06064	
F Critical one-tail	19		P(T<=t) one-tail	0.000794	
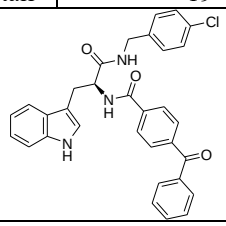			t Critical one-tail	2.919986	
			P(T<=t) two-tail	0.001588	
			t Critical two-tail	4.302653	
			*P < .05		

Chapter 4		GLI protein expression compared to SAG treatment		
		SAG	**14** + SAG	Compound 14 = TP93B4
		0.220042695	0.062541147	
		0.224185924	0.060026468	
		0.227006267		
F-Test Two-Sample for Variances			t-Test: Two-Sample Assuming Equal Variances	
	Variable 1	*Variable 2*		*Variable 1*	*Variable 2*
Mean	0.2237449	0.0612838	Mean	0.223744962	0.0612838
Variance	1.22687E-05	3.16181E-06	Variance	1.22687E-05	3.16181E-06
Observations	3	2	Observations	3	2
df	2	1	Pooled Variance	9.23305E-06	
F	3.880271302		Hypothesized Mean Difference	0	
P(F<=f) one-tail	0.337858226		df	3	
F Critical one-tail	199.5		t Stat	58.56897261	
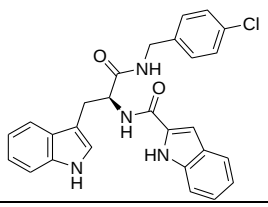			P(T<=t) one-tail	5.48255E-06	
			t Critical one-tail	2.353363435	
			P(T<=t) two-tail	1.09651E-05	
			t Critical two-tail	3.182446305	
			***P < .0001		

Chapter 4	GLI protein expression compared to SAG treatment				
	SAG	**14a** + SAG	Compound 14a = TP154B5		
	0.220042695	0.03075343			
	0.224185924	0.031741495			
	0.227006267	0.031291395			
F-Test Two-Sample for Variances			t-Test: Two-Sample Assuming Unequal Variances		
	Variable 1	*Variable 2*		*Variable 1*	*Variable 2*
Mean	0.223744962	0.031262107	Mean	0.223745	0.031262
Variance	1.22687E-05	2.44712E-07	Variance	1.23E-05	2.45E-07
Observations	3	3	Observations	3	3
df	2	2	Hypothesized Mean Difference	0	
F	50.13519261		df	2	
P(F<=f) one-tail	0.019556003		t Stat	94.24653	
F Critical one-tail	19		P(T<=t) one-tail	5.63E-05	
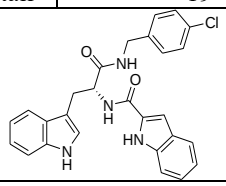			t Critical one-tail	2.919986	
			P(T<=t) two-tail	0.000113	
			t Critical two-tail	4.302653	
			**P < .001		

Chapter 4_Figure 16A	GLI expression compared to SAG treatment				
	SAG	**5** + SAG	Compound 5 = TP114B4		
	0.159728698	0.024331616			
	0.149875215	0.052961019			
	0.142709665				
F-Test Two-Sample for Variances			t-Test: Two-Sample Assuming Equal Variances		
	Variable 1	*Variable 2*		*Variable 1*	*Variable 2*
Mean	0.038646317	0.150771192	Mean	0.038646317	0.150771192
Variance	0.000409821	7.3014E-05	Variance	0.000409821	7.3014E-05
Observations	2	3	Observations	2	3
df	1	2	Pooled Variance	0.000185283	
F	5.612918291		Hypothesized Mean Difference	0	
P(F<=f) one-tail	0.141344856		df	3	
F Critical one-tail	18.51282051		t Stat	9.023493375	
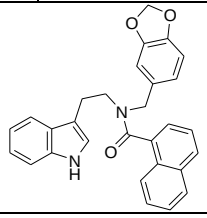			P(T<=t) one-tail	0.001436947	
			t Critical one-tail	2.353363435	
			P(T<=t) two-tail	0.002873894	
			t Critical two-tail	3.182446305	
			*P < .05		

Chapter 4_Figure 16A	GLI expression compared to SAG treatment

		SAG	**5** + SAG	**Compound 33 = TP28B5**	
		0.159728698	0.03407596		
		0.149875215	0.032712635		
		0.142709665			
F-Test Two-Sample for Variances			t-Test: Two-Sample Assuming Equal Variances		
	Variable 1	*Variable 2*		*Variable 1*	*Variable 2*
Mean	0.150771192	0.033394298	Mean	0.150771192	0.033394298
Variance	7.3014E-05	9.29328E-07	Variance	7.3014E-05	9.29328E-07
Observations	3	2	Observations	3	2
df	2	1	Pooled Variance	4.89857E-05	
F	78.56642383		Hypothesized Mean Difference	0	
P(F<=f) one-tail	0.079522304		df	3	
F Critical one-tail	199.5		t Stat	18.37123611	
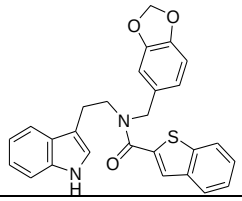			P(T<=t) one-tail	0.000175959	
			t Critical one-tail	2.353363435	
			P(T<=t) two-tail	0.000351919	
			t Critical two-tail	3.182446305	
			** P < .001		

Chapter 4, table 2		**GLI expression compared to SAG treatment**			
		SAG	**22** + SAG	**Compound 22 = TP31B5**	
		0.1597287	0.0439865		
		0.1498752	0.0433821		
		0.1427097	0.0441348		
F-Test Two-Sample for Variances			t-Test: Two-Sample Assuming Unequal Variances		
	Variable 1	*Variable 2*		*Variable 1*	*Variable 2*
Mean	0.150771192	0.0438345	Mean	0.1507712	0.0438345
Variance	7.3014E-05	1.59E-07	Variance	7.301E-05	1.59E-07
Observations	3	3	Observations	3	3
df	2	2	Hypothesized Mean Difference	0	
F	459.2192304		df	2	
P(F<=f) one-tail	0.002172877		t Stat	21.652709	
F Critical one-tail	19		P(T<=t) one-tail	0.0010631	
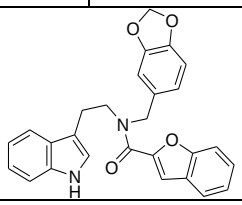			t Critical one-tail	2.9199856	
			P(T<=t) two-tail	0.0021261	
			t Critical two-tail	4.3026527	
			* P < .05		

Chapter 4, table 2	**GLI expression compared to SAG treatment**		
	SAG	**23** + SAG	**Compound 23 = TP142B4**

		0.159728698	0.019299269		
		0.149875215	0.020845687		
		0.142709665	0.016022084		
F-Test Two-Sample for Variances			t-Test: Two-Sample Assuming Equal Variances		
	Variable 1	*Variable 2*		*Variable 1*	*Variable 2*
Mean	0.15077119	0.01872234	Mean	0.150771192	0.01872234
Variance	7.3014E-05	6.06641E-06	Variance	7.3014E-05	6.06641E-06
Observations	3	3	Observations	3	3
df	2	2	Pooled Variance	3.95402E-05	
F	12.03576841		Hypothesized Mean Difference	0	
P(F<=f) one-tail	0.07671201		df	4	
F Critical one-tail	19		t Stat	25.71940371	
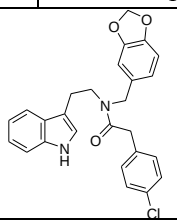			P(T<=t) one-tail	6.78755E-06	
			t Critical one-tail	2.131846786	
			P(T<=t) two-tail	1.35751E-05	
			t Critical two-tail	2.776445105	
			*** P < .0001		

Chapter 4, table 2	**GLI expression compared to SAG treatment**		
	SAG	**24** + SAG	**Compound 24 = TP140B4**
	0.1597287	0.0651874	
	0.1498752	0.0625071	
	0.1427097	0.0682888	

F-Test Two-Sample for Variances			t-Test: Two-Sample Assuming Equal Variances		
	Variable 1	*Variable 2*		*Variable 1*	*Variable 2*
Mean	0.150771192	0.0653278	Mean	0.1507712	0.0653278
Variance	7.3014E-05	8.372E-06	Variance	7.301E-05	8.372E-06
Observations	3	3	Observations	3	3
df	2	2	Pooled Variance	4.069E-05	
F	8.721455962		Hypothesized Mean Difference	0	
P(F<=f) one-tail	0.10286525		df	4	
F Critical one-tail	19		t Stat	16.404579	
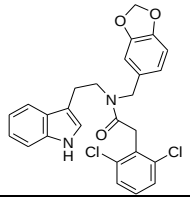			P(T<=t) one-tail	4.042E-05	
			t Critical one-tail	2.1318468	
			P(T<=t) two-tail	8.084E-05	
			t Critical two-tail	2.7764451	
			*** P < .0001		

Chapter 4, table	**GLI expression compared to SAG treatment**		
	SAG	**25**+ SAG	**Compound 25 = TP37B4**
	0.159728698	0.014188853	
	0.149875215	0.013219172	

		0.142709665			
F-Test Two-Sample for Variances			t-Test: Two-Sample Assuming Equal Variances		
	Variable 1	*Variable 2*		*Variable 1*	*Variable 2*
Mean	0.150771192	0.013704013	Mean	0.150771192	0.013704013
Variance	7.3014E-05	4.70141E-07	Variance	7.3014E-05	4.70141E-07
Observations	3	2	Observations	3	2
df	2	1	Pooled Variance	4.88327E-05	
F	155.3023402		Hypothesized Mean Difference	0	
P(F<=f) one-tail	0.056649752		df	3	
F Critical one-tail	199.5		t Stat	21.48665482	
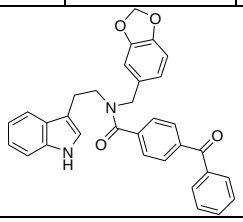			P(T<=t) one-tail	0.000110296	
			t Critical one-tail	2.353363435	
			P(T<=t) two-tail	0.000220591	
			t Critical two-tail	3.182446305	
			** P < .001		

Chapter 4, table	**GLI expression compared to SAG treatment**		**Compound 26 = TP34B5**
	SAG	**26**+ SAG	
	0.1597287	0.1677918	
	0.1498752	0.1762933	
	0.1427097	0.1701978	

F-Test Two-Sample for Variances			t-Test: Two-Sample Assuming Equal Variances		
	Variable 1	*Variable 2*		*Variable 1*	*Variable 2*
Mean	0.150771192	0.1714277	Mean	0.1507712	0.1714277
Variance	7.3014E-05	1.92E-05	Variance	7.301E-05	1.92E-05
Observations	3	3	Observations	3	3
df	2	2	Pooled Variance	4.611E-05	
F	3.8021767		Hypothesized Mean Difference	0	
P(F<=f) one-tail	0.208238901		df	4	
F Critical one-tail	19		t Stat	-3.7257281	
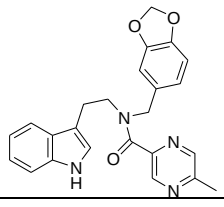			P(T<=t) one-tail	0.0101863	
			t Critical one-tail	2.1318468	
			P(T<=t) two-tail	0.0203725	
			t Critical two-tail	2.7764451	
			* P < .05		

Chapter 4	GLI expression compared to SAG treatment

Chapter 4, table 2	GLI protein expression compared to SAG treatment				
	SAG	**20** + SAG	**Compound 20 = TP111B4**		
	0.1174	0.0084			
	0.1080	0.0076			
	0.1020				
F-Test Two-Sample for Variances		t-Test: Two-Sample Assuming Equal Variances			
	Variable 1	*Variable 2*		*Variable 1*	*Variable 2*
Mean	0.109141557	0.007990237	Mean	0.109141557	0.0079902
Variance	6.00701E-05	3.07902E-07	Variance	6.00701E-05	3.079E-07
Observations	3	2	Observations	3	2
df	2	1	Pooled Variance	4.01494E-05	
F	195.0951801		Hypothesized Mean Difference	0	
P(F<=f) one-tail	0.050559868		df	3	
F Critical one-tail	199.5		t Stat	17.48729593	
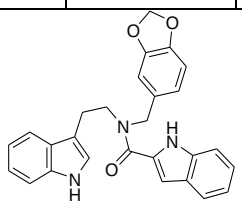			P(T<=t) one-tail	0.00020379	
			t Critical one-tail	2.353363435	
			P(T<=t) two-tail	0.000407581	
			t Critical two-tail	3.182446305	
			** $P < .001$		

Chapter 4	SAG	Sonidegib + SAG		
	0.159728698	0.029175821	**Sonidegib**	
	0.149875215	0.028473746		
	0.142709665			
F-Test Two-Sample for Variances		t-Test: Two-Sample Assuming Unequal Variances		
	Variable 1	*Variable 2*	*Variable 1*	*Variable 2*
Mean	0.150771192	0.028824783	0.150771192	0.028824783
Variance	7.3014E-05	2.46454E-07	7.3014E-05	2.46454E-07
Observations	3	2	3	2
df	2	1	Hypothesized Mean Difference	0
F	296.25764		df	2
P(F<=f) one-tail	0.041047248		t Stat	24.65642074
F Critical one-tail	199.5		P(T<=t) one-tail	0.000820427
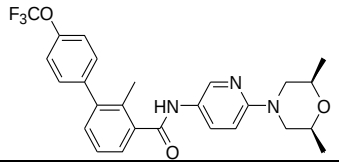			t Critical one-tail	2.91998558
			P(T<=t) two-tail	0.001640854
			t Critical two-tail	4.30265273
			*P < .05	

Chapter 4, Figure 8A	***Ptch1* expression compared with SAG treatment**		
	SAG	**20** + SAG	**Compound 20 = TP111B4**
	0.003508	0.001785	
	0.004419	0.002323	
	0.004279		

F-Test Two-Sample for Variances			t-Test: Two-Sample Assuming Equal Variances		
	Variable 1	*Variable 2*		*Variable 1*	*Variable 2*
Mean	0.00406852	0.002054	Mean	0.004069	0.002054
Variance	2.4086E-07	1.45E-07	Variance	2.41E-07	1.45E-07
Observations	3	2	Observations	3	2
df	2	1	Pooled Variance	2.09E-07	
F	1.66529569		Hypothesized Mean Difference	0	
P(F<=f) one-tail	0.48053652		df	3	
F Critical one-tail	199.5		t Stat	4.830171	
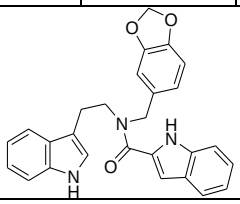			P(T<=t) one-tail	0.008458	
			t Critical one-tail	2.353363	
			P(T<=t) two-tail	0.016917	
			t Critical two-tail	3.182446	
			* P < .05		

Chapter 4, Figure 8A	***Ptch1* expression compared with SAG treatment**		
	SAG	**25**+ SAG	**Compound 25 = TP137B4**
	0.003508	0.002705	
	0.004419	0.002438	
	0.004279		

F-Test Two-Sample for Variances			t-Test: Two-Sample Assuming Equal Variances		
	Variable 1	*Variable 2*		*Variable 1*	*Variable 2*
Mean	0.004068519	0.002572	Mean	0.004069	0.002572
Variance	2.40864E-07	3.57E-08	Variance	2.41E-07	3.57E-08
Observations	3	2	Observations	3	2
df	2	1	Pooled Variance	1.72E-07	
F	6.750005712		Hypothesized Mean Difference	0	
P(F<=f) one-tail	0.262612762		df	3	
F Critical one-tail	199.5		t Stat	3.948177	
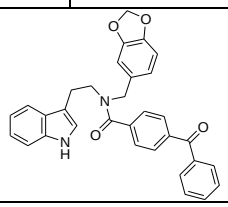			P(T<=t) one-tail	0.01449	
			t Critical one-tail	2.353363	
			P(T<=t) two-tail	0.028979	
			t Critical two-tail	3.182446	
			* P < .05		

Chapter 4, Figure 8B	***Gli2* expression compared with SAG treatment**		
	SAG	**20** + SAG	**Compound 20 = TP111B4**
	0.000766195	0.000357	
	0.001011001	0.000459	
	0.001011001		

F-Test Two-Sample for Variances			t-Test: Two-Sample Assuming Equal Variances		
	Variable 1	*Variable 2*		*Variable 1*	*Variable 2*
Mean	0.000889	0.000408097	Mean	0.000889	0.000408
Variance	3E-08	5.13171E-09	Variance	3E-08	5.13E-09
Observations	2	2	Observations	2	2
df	1	1	Pooled Variance	1.75E-08	
F	5.839157		Hypothesized Mean Difference	0	
P(F<=f) one-tail	0.249793		df	2	
F Critical one-tail	161.4476		t Stat	3.627246	
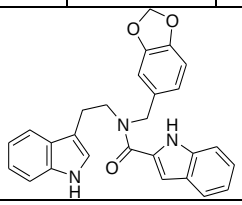			P(T<=t) one-tail	0.034155	
			t Critical one-tail	2.919986	
			P(T<=t) two-tail	0.06831	
			t Critical two-tail	4.302653	
			P = 0.07		

Chapter 4, Figure 8B	***Gli2* expression compared with SAG treatment**		
	SAG	**25** + SAG	**Compound 25= TP137B4**
	0.000766	0.000367	
	0.001011	0.00036	
	0.001011		

F-Test Two-Sample for Variances			t-Test: Two-Sample Assuming Unequal Variances		
	Variable 1	*Variable 2*		*Variable 1*	*Variable 2*
Mean	0.000929	0.000364	Mean	0.000929	0.000364
Variance	2E-08	2.86E-11	Variance	2E-08	2.86E-11
Observations	3	2	Observations	3	2
df	2	1	Hypothesized Mean Difference	0	
F	698.5176		df	2	
P(F<=f) one-tail	0.026745		t Stat	6.924872	
F Critical one-tail	199.5		P(T<=t) one-tail	0.010111	
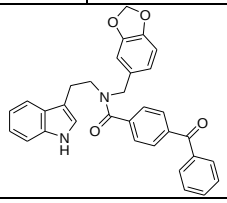			t Critical one-tail	2.919986	
			P(T<=t) two-tail	0.020223	
			t Critical two-tail	4.302653	
			* P < .05		

Chapter 4_ Figure 19	**GLI expression compared to SAG treatment at 48h**

		SAG for 12h	SAG for 48h		
		0.040488886	0.129164	**Smo agonist 12h**	
		0.043146551	0.140141		
		0.039622697	0.1337336		
F-Test Two-Sample for Variances			t-Test: Two-Sample Assuming Equal Variances		
	Variable 1	*Variable 2*		*Variable 1*	*Variable 2*
Mean	0.134346188	0.041086045	Mean	0.134346188	0.041086
Variance	3.0405E-05	3.37183E-06	Variance	3.0405E-05	3.37E-06
Observations	3	3	Observations	3	3
df	2	2	Pooled Variance	1.68884E-05	
F	9.017347504		Hypothesized Mean Difference	0	
P(F<=f) one-tail	0.099826825		df	4	
F Critical one-tail	19		t Stat	27.79375337	
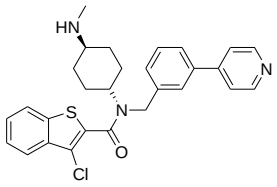			P(T<=t) one-tail	4.98418E-06	
			t Critical one-tail	2.131846786	
			P(T<=t) two-tail	9.96836E-06	
			t Critical two-tail	2.776445105	
			*** P < .0001		

Chapter 4, Figure 9		**GLI expression compared to SAG treatment at 48h**			
		SAG for 24h	SAG for 48h	**Smo agonist 24h**	
		0.1000273	0.129163972		
		0.09081273	0.140140963		
		0.10296968	0.13373363		
F-Test Two-Sample for Variances			t-Test: Two-Sample Assuming Equal Variances		
	Variable 1	*Variable 2*		*Variable 1*	*Variable 2*
Mean	0.097936569	0.13434619	Mean	0.097937	0.134346
Variance	4.02262E-05	3.0405E-05	Variance	4.02E-05	3.04E-05
Observations	3	3	Observations	3	3
df	2	2	Pooled Variance	3.53E-05	
F	1.323013713		Hypothesized Mean Difference	0	
P(F<=f) one-tail	0.430475289		df	4	
F Critical one-tail	19		t Stat	-7.50375	
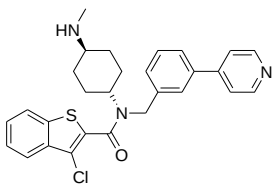			P(T<=t) one-tail	0.000844	
			t Critical one-tail	2.131847	
			P(T<=t) two-tail	0.001688	
			t Critical two-tail	2.776445	
			* P < .05		

Chapter 4, Figure 9	**GLI expression compared to SAG treatment at 48h**		
	SAG for 36h	SAG for 48h	**Smo agonist 36h**

		0.113911824	0.129164		
		0.110760819	0.140141		
			0.133734		
F-Test Two-Sample for Variances			t-Test: Two-Sample Assuming Equal Variances		
	Variable 1	*Variable 2*		*Variable 1*	*Variable 2*
Mean	0.134346	0.112336322	Mean	0.134346	0.112336
Variance	3.04E-05	4.96442E-06	Variance	3.04E-05	4.96E-06
Observations	3	2	Observations	3	2
df	2	1	Pooled Variance	2.19E-05	
F	6.124588		Hypothesized Mean Difference	0	
P(F<=f) one-tail	0.27473		df	3	
F Critical one-tail	199.5		t Stat	5.149204	
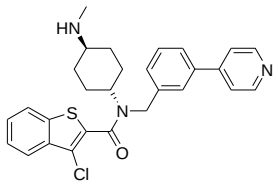			P(T<=t) one-tail	0.007099	
			t Critical one-tail	2.353363	
			P(T<=t) two-tail	0.014198	
			t Critical two-tail	3.182446	
			* P < .05		

Chapter 4, Figure 9	**GLI expression compared to 48h SAG control**		
	SAG	**14a** + SAG 12h	**Compound 14a = TP154B5** **12h**
	0.120289	0.026454	
	0.124113	0.030987	
	0.114701	0.029956	

F-Test Two-Sample for Variances			t-Test: Two-Sample Assuming Equal Variances		
	Variable 1	*Variable 2*		*Variable 1*	*Variable 2*
Mean	0.119701171	0.029132	Mean	0.119701	0.029132
Variance	2.24043E-05	5.65E-06	Variance	2.24E-05	5.65E-06
Observations	3	3	Observations	3	3
df	2	2	Pooled Variance	1.4E-05	
F	3.967881723		Hypothesized Mean Difference	0	
P(F<=f) one-tail	0.201293037		df	4	
F Critical one-tail	19		t Stat	29.61887	
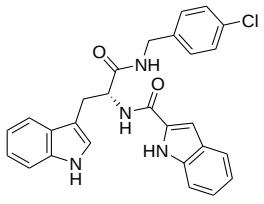			P(T<=t) one-tail	3.87E-06	
			t Critical one-tail	2.131847	
			P(T<=t) two-tail	7.74E-06	
			t Critical two-tail	2.776445	
			*** P < .0001		

Chapter 4, Figure 9	**GLI expression compared to 48h SAG control**		
	SAG	**14a** + SAG 24h	**Compound 14a =**

		0.120289	0.026661	**TP154B5** **24h**	
		0.124113	0.026548		
		0.114701	0.034577		
F-Test Two-Sample for Variances			t-Test: Two-Sample Assuming Equal Variances		
	Variable 1	*Variable 2*		*Variable 1*	*Variable 2*
Mean	0.119701171	0.029262	Mean	0.119701	0.029262
Variance	2.24043E-05	2.12E-05	Variance	2.24E-05	2.12E-05
Observations	3	3	Observations	3	3
df	2	2	Pooled Variance	2.18E-05	
F	1.057337219		Hypothesized Mean Difference	0	
P(F<=f) one-tail	0.486065187		df	4	
F Critical one-tail	19		t Stat	23.72491	
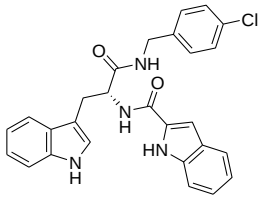			P(T<=t) one-tail	9.36E-06	
			t Critical one-tail	2.131847	
			P(T<=t) two-tail	1.87E-05	
			t Critical two-tail	2.776445	
			*** P < .0001		

Chapter 4, Figure 9			GLI expression compared to 48h SAG control		
		SAG	**14a** + SAG 36h	**Compound 14a = TP154B5** **36h**	
		0.120289	0.068748		
		0.124113	0.058246		
		0.114701	0.060572		
F-Test Two-Sample for Variances			t-Test: Two-Sample Assuming Equal Variances		
	Variable 1	*Variable 2*		*Variable 1*	*Variable 2*
Mean	0.062522002	0.119701	Mean	0.062522	0.119701
Variance	3.04241E-05	2.24E-05	Variance	3.04E-05	2.24E-05
Observations	3	3	Observations	3	3
df	2	2	Pooled Variance	2.64E-05	
F	1.35795558		Hypothesized Mean Difference	0	
P(F<=f) one-tail	0.424096199		df	4	
F Critical one-tail	19		t Stat	-13.6259	
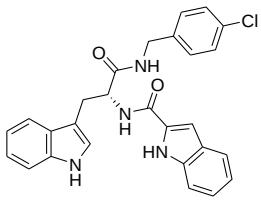			P(T<=t) one-tail	8.4E-05	
			t Critical one-tail	2.131847	
			P(T<=t) two-tail	0.000168	
			t Critical two-tail	2.776445	
			** P < .001		

Chapter 4, Figure 9	**GLI expression compared to 48h SAG control**		
	SAG	**28**+ SAG 12h	**Compound 28 = TP142B5** **12h**
	0.120289313	0.021721638	
	0.124112936	0.019857728	
	0.114701264	0.019129766	

F-Test Two-Sample for Variances			t-Test: Two-Sample Assuming Equal Variances		
	Variable 1	*Variable 2*		*Variable 1*	*Variable 2*
Mean	0.119701171	0.020236377	Mean	0.119701171	0.020236
Variance	2.24043E-05	1.78698E-06	Variance	2.24043E-05	1.79E-06
Observations	3	3	Observations	3	3
df	2	2	Pooled Variance	1.20957E-05	
F	12.53752335		Hypothesized Mean Difference	0	
P(F<=f) one-tail	0.073868755		df	4	
F Critical one-tail	19		t Stat	35.02679172	
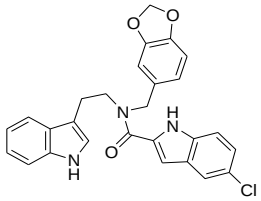			P(T<=t) one-tail	1.98227E-06	
			t Critical one-tail	2.131846786	
			P(T<=t) two-tail	3.96455E-06	
			t Critical two-tail	2.776445105	
			*** P < .0001		

Chapter 4, Figure 9	**GLI expression compared to 48h SAG control**		
	SAG	**28**+ SAG 24h	**Compound 28 = TP142B5 24h**
	0.120289	0.020181	
	0.124113	0.019004	
	0.114701	0.019066	

F-Test Two-Sample for Variances			t-Test: Two-Sample Assuming Unequal Variances		
	Variable 1	*Variable 2*		*Variable 1*	*Variable 2*
Mean	0.119701	0.019417	Mean	0.119701	0.019417
Variance	2.24E-05	4.39E-07	Variance	2.24E-05	4.39E-07
Observations	3	3	Observations	3	3
df	2	2	Hypothesized Mean Difference	0	
F	51.03879		df	2	
P(F<=f) one-tail	0.019216		t Stat	36.34236	
F Critical one-tail	19		P(T<=t) one-tail	0.000378	
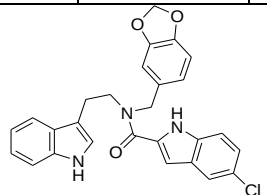			t Critical one-tail	2.919986	
			P(T<=t) two-tail	0.000756	
			t Critical two-tail	4.302653	
			** *P* < .001		

Chapter 4, Figure 9	**GLI expression compared to 48h SAG control**		
	SAG	**28**+ SAG 36h	**Compound 28 = TP142B5 36h**
	0.120289	0.038341	
	0.124113	0.029004	
	0.114701	0.033952	

F-Test Two-Sample for Variances			t-Test: Two-Sample Assuming Equal Variances		
	Variable 1	*Variable 2*		*Variable 1*	*Variable 2*
Mean	0.119701	0.033766	Mean	0.119701	0.033766

Variance	2.24E-05	2.18E-05	Variance	2.24E-05	2.18E-05
Observations	3	3	Observations	3	3
df	2	2	Pooled Variance	2.21E-05	
F	1.026736		Hypothesized Mean Difference	0	
P(F<=f) one-tail	0.493404		df	4	
F Critical one-tail	19		t Stat	22.38193	
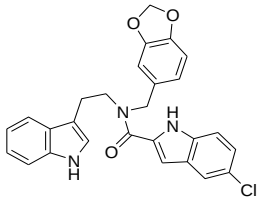			P(T<=t) one-tail	1.18E-05	
			t Critical one-tail	2.131847	
			P(T<=t) two-tail	2.36E-05	
			t Critical two-tail	2.776445	
			*** *P < .0001*		

8.3.2. Compounds characterization

A. The tryptophan derivatives

COMPOUND 4

Compound Name: *N*-(4-Chloro-benzyl)-2-[2-(3,4-dichloro-phenyl)-acetylamino]-3-(1*H*-indole-3-yl)-propionamide

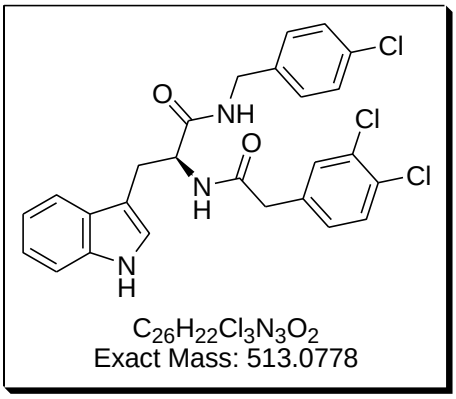

Obtained Weight & Yield: 182 mg, 35%

Appearance: White floppy precipitate

Solubility: EtOAc, Acetone

Melting Point: 208 − 209 ºC

TLC Conditions: EtOAc/Hexane (50/50)

IR Analysis: νmax/cm^{-1}

3410 (NH), 3277 (NH), 3068 (CH), 1636 (CON)

^{1}H NMR Analysis:

^{1}H NMR (400 MHz, DMSO-d_6) δ 10.84 (s, 1H), 8.56 (t, J = 8.0 Hz, 1H), 8.43 (d, J = 8.1 Hz, 1H), 7.60 (d, J = 7.9 Hz, 1H), 7.47 (d, J = 8.2 Hz, 1H), 7.42 (d, J = 1.8 Hz, 1H), 7.35 (d, J = 8.1 Hz, 1H), 7.28 (d, J = 8.4 Hz, 2H), 7.16 – 7.02 (m, 5H), 6.97 (t, J = 7.1 Hz, 1H), 4.59 (dd, J = 8.0, 12.0 Hz, 1H), 4.24 (ddd, $J_{A'X'} = J_{B'X'}$ = 8.0, $J_{A'B'}$ = 16 Hz, 2H), 3.47 (s, 2H), 3.05 (ddd, J_{AX} = 4.0, J_{BX} = 8.0, J_{AB} = 16.0 Hz, 2H).

^{13}C NMR Analysis:

^{13}C NMR (101 MHz, DMSO-d_6) δ 171.9, 169.6, 138.7, 138.0, 136. 6, 131.6, 131.5, 131.0, 130.6, 129.8, 129.4, 129.2 (C x 2), 128.5 (C x 2), 127.7, 124.2, 121.4, 119.0, 118.7, 111.8, 110.4, 54.2, 41.8, 41.2, 28.5.

HPLC: RP-HPLC Alltima™ C18 5 µm 150 mm x 4.6 mm, 10–100% B in 15 min, R_t =14.31 min, 100%.

Mass Spectral Analysis: LRMS (ESI+) m/z: 513, 514 [M+H, ^{35}Cl]$^{+}$, 95%. HRMS (ES+) for $C_{26}H_{22}Cl_3N_3O_2$, calculated 514.0850, found 514.0850.

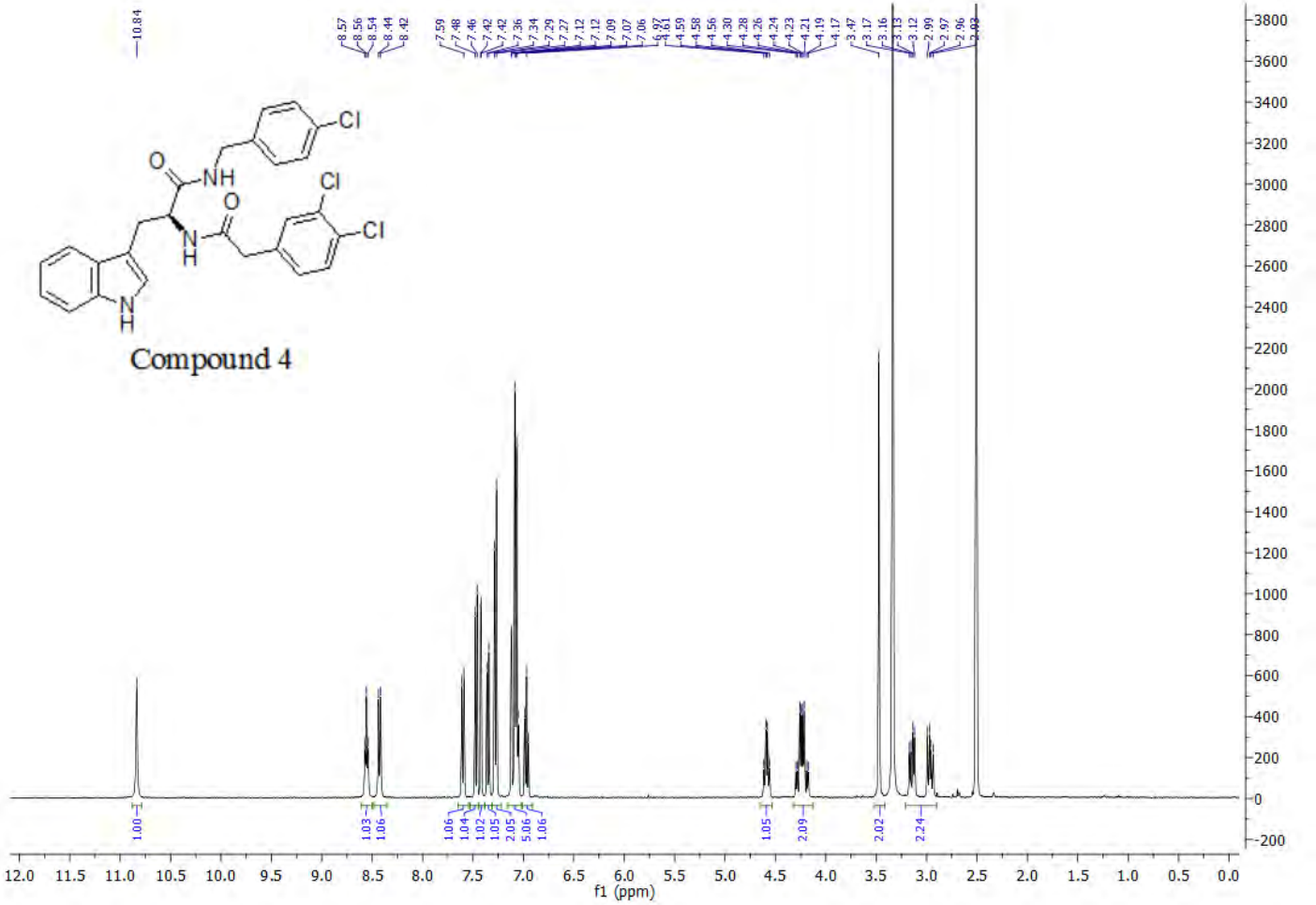
Cl
O
NH
Cl
O
N
H
Cl
N
H
Compound 4
f1 (ppm)

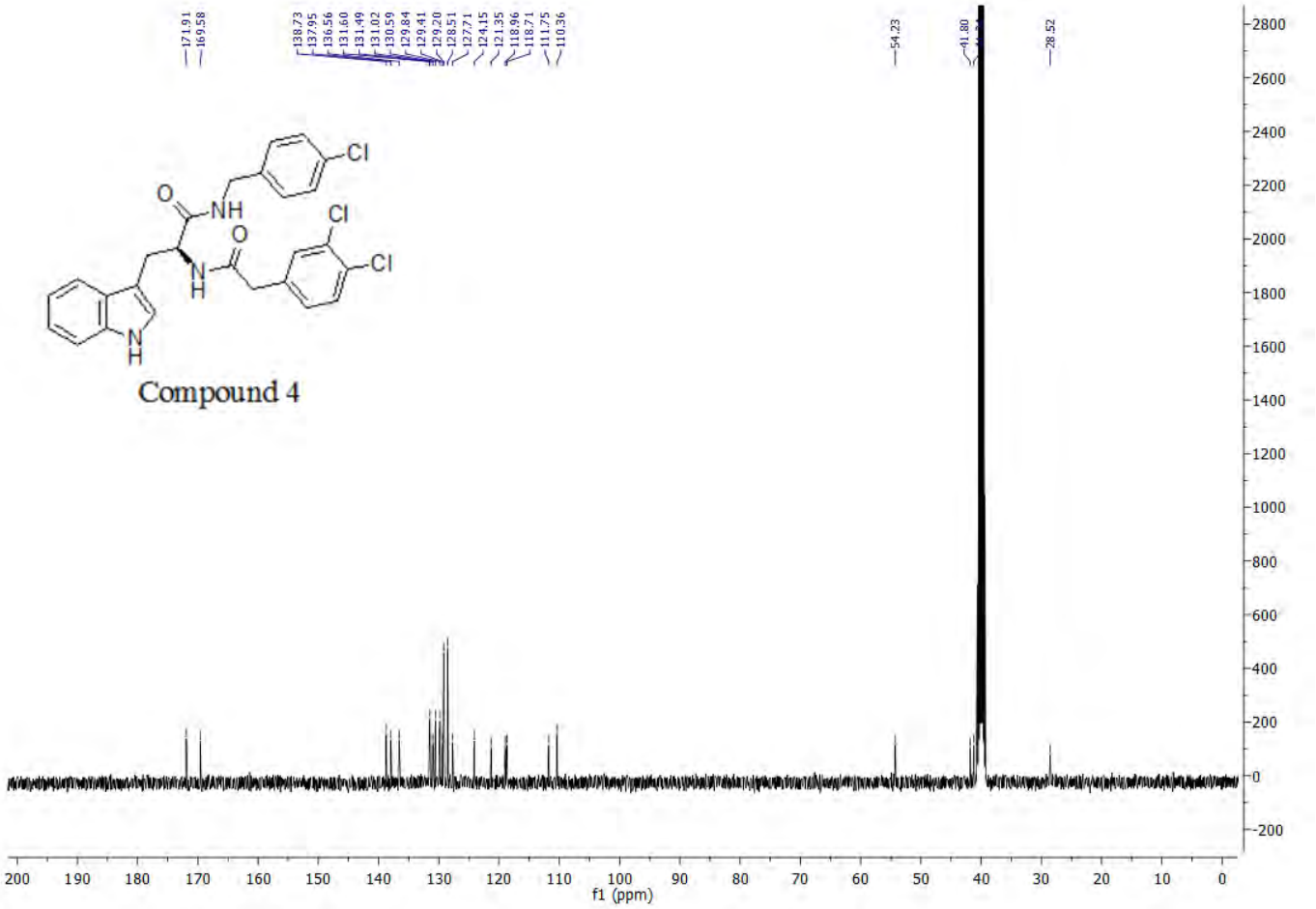
171.91
169.58
138.73
137.95
136.56
131.60
131.49
131.02
130.59
129.84
129.41
129.20
128.51
127.71
124.15
121.35
118.96
118.71
111.75
110.36
54.23
41.80
28.52
Cl
Cl
Cl
O
NH
O
N
H
N
H
2800
2600
2400
2200
2000
1800
1600
1400
1200
1000
800
600
400
200
0
-200
200 190 180 170 160 150 140 130 120 110 100 90 80 70 60 50 40 30 20 10 0
f1 (ppm)

Compound 4

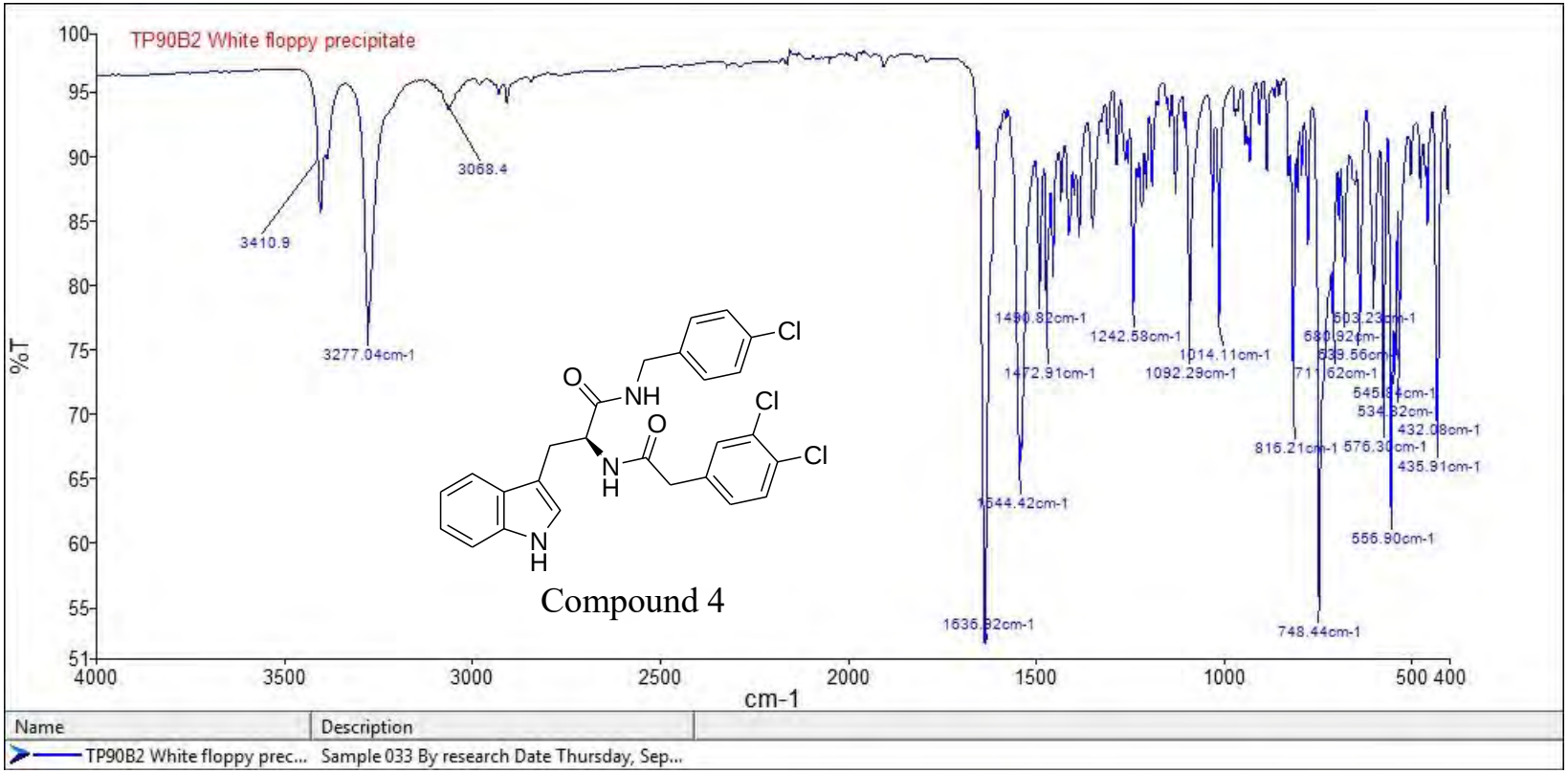
TP90B2 White floppy precipitate
%T
cm-1
3410.9
3277.04cm-1
3068.4
1636.32cm-1
1544.42cm-1
1472.91cm-1
1450.82cm-1
1242.58cm-1
1092.29cm-1
1014.11cm-1
816.21cm-1
748.44cm-1
711.62cm-1
556.90cm-1
435.91cm-1
Cl
Cl
Cl
O
NH
O
N
H
N
H
Name
Description
TP90B2 White floppy prec...
Sample 033 By research Date Thursday, Sep...

Compound 4

SHIMADZU LabSolutions **Analysis Report**

<Sample Information>

Sample Name	: TP90B2		
Sample ID	: TP90B2		
Data Filename	: TP90B2.lcd		
Method Filename	: 10-100 over 15 mins.lcm		
Batch Filename	: TRIEU Second Third Generation and New pro.lcb		
Vial #	: 1-13	Sample Type	: Unknown
Injection Volume	: 30 uL		
Date Acquired	: 8/09/2014 12:37:44 PM	Acquired by	: System Administrator
Date Processed	: 8/09/2014 1:07:46 PM	Processed by	: System Administrator

<Chromatogram>

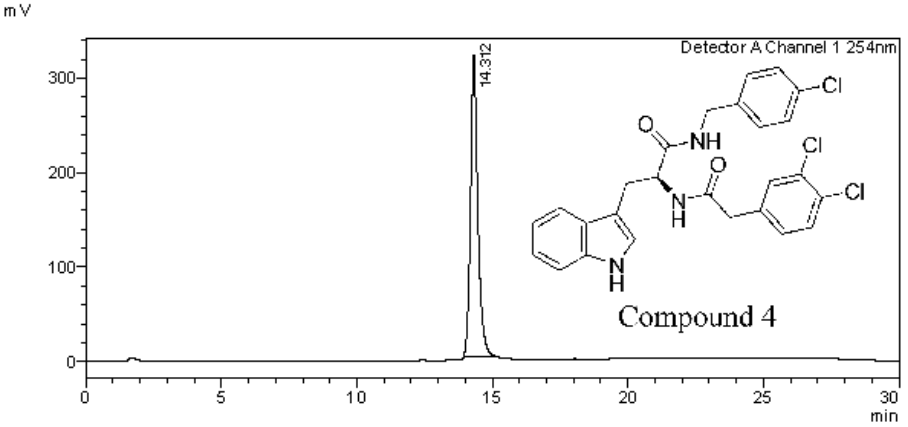

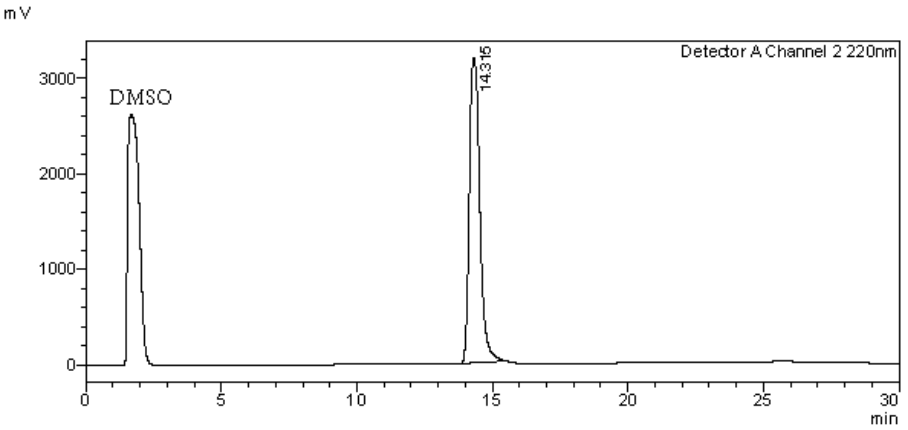

<Peak Table>

Detector A Channel 1 254nm

Peak#	Ret. Time	Area	Height	Conc.	Unit	Mark	Name
1	14.312	6013393	319119	100.000		M	
Total		6013393	319119				

Detector A Channel 2 220nm

Peak#	Ret. Time	Area	Height	Conc.	Unit	Mark	Name
1	14.315	86479206	3184442	100.000		M	
Total		86479206	3184442				

==== Shimadzu LCMSsolution Data Report ====

<Chromatogram>

Sample Information

Acquired by	: Admin
Date Acquired	: 9/22/2015 1:12:57 PM
Sample Type	: Unknown
Level#	: 0
Sample Name	: TP90B2
Sample ID	:
ISTD Amount	: (Level1 Conc.)
Sample Amount	: 1
Dilution Factor	: 1
Tray#	: 1
Vial#	: 42
Injection Volume	: 5
Data File	: TP90B2.lcd
Method File	: FIA-ESI_Scan(+).lcm
Original Method	: C:\LabSolutions\Data\Kelly\FIA-ESI_Scan(+).lcm
Report Format	: DefaultLCMS.lcr
Tuning File	: C:\LabSolutions\Data\AutoTuning\Autotune_ESI_26AUG15.lct
Processed by	: Admin
Modified Date	: 9/22/2015 1:14:28 PM

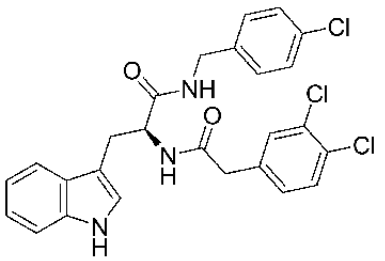

Compound 4

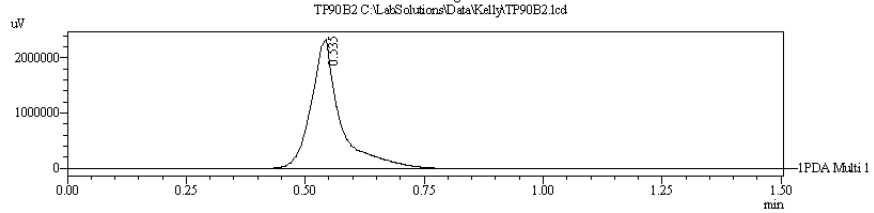

1 PDA Multi 1 / 254nm 4nm

<Spectrum>

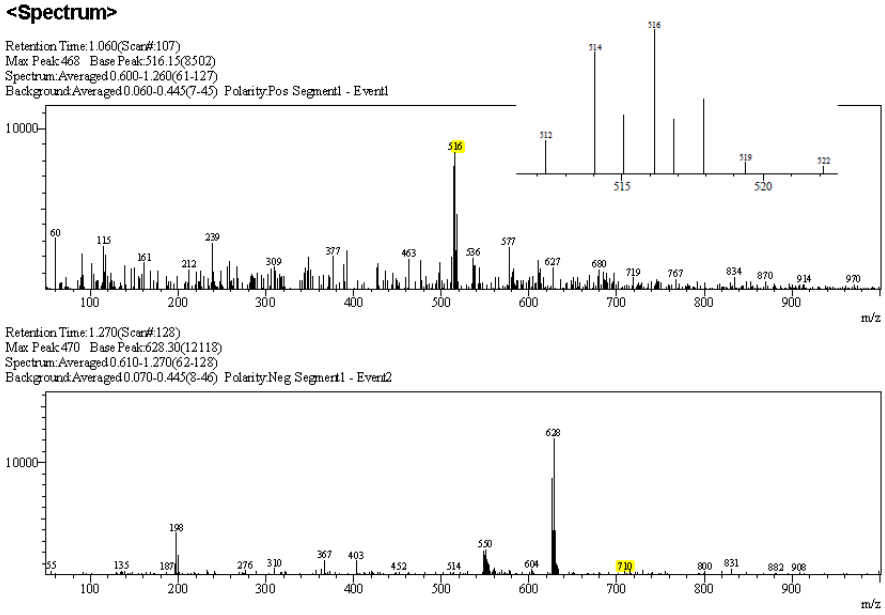

C:¥LabSolutions¥Data¥Kelly¥TP90B2.lcd

Compound	Chemical Formula	Predicted monoisotopic neutral MW	Predicted MH+	MH+ Measured	Main MS Ions	Main MS/MS Fragments
TP 90B2	$C_{26}H_{22}Cl_3N_3O_2$	513.0778	514.0850	514.08498	514.08498*	373.0510 345.0560 159.0920

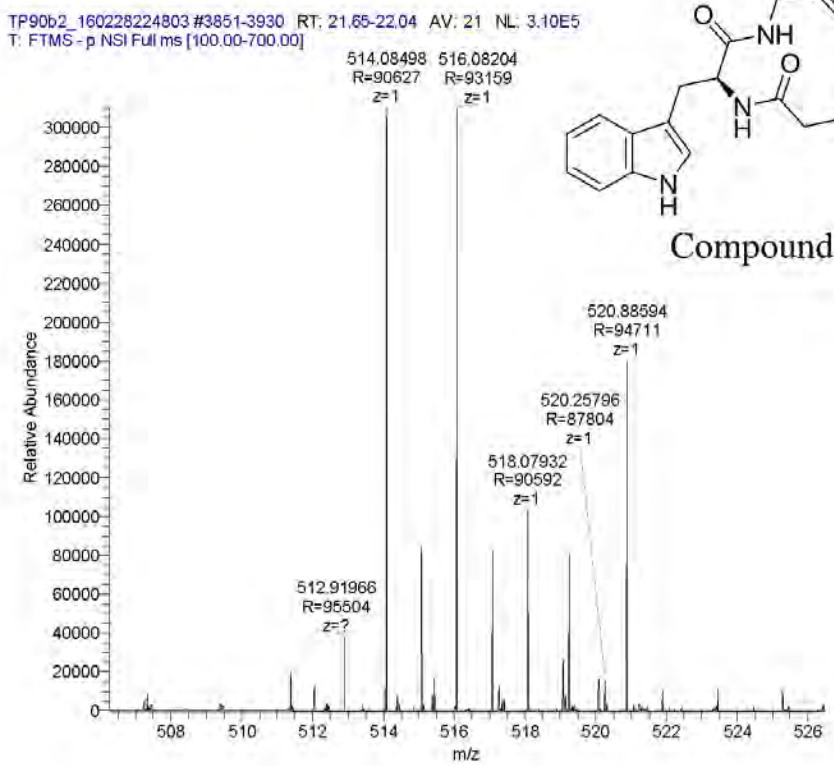

COMPOUND 11

Compound Name: *N*-(4-Chloro-benzyl)-2-[2-(2,4-dichloro-phenyl)-acetylamino]-3-(1*H*-indol-3-yl)-propionamide

Obtained Weight & Yield: 55 mg, 24%

Appearance: Milky precipitate

Solubility: EtOAc, Acetone, ACN

Melting Point: 207-208 ºC

TLC Conditions: EtOAc/Hexane (50/50)

IR Analysis: νmax/cm^{-1}

3410 (NH), 3280 (NH), 3065 (CH), 1642 (CON)

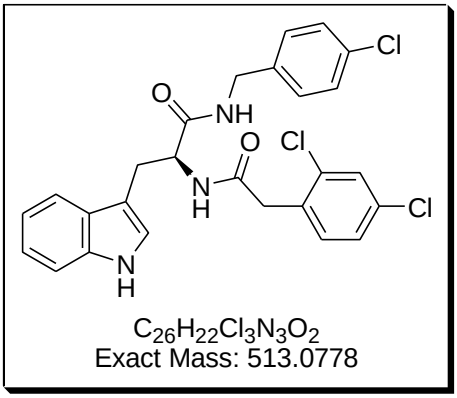

^{1}H NMR Analysis:

^{1}H NMR (400 MHz, DMSO-d_6) δ (400 MHz, DMSO-d_6) δ 10.85 (s, 1H), 8.54 (t, J = 4.0 Hz, 1H), 8.40 (d, J = 8.2 Hz, 1H), 7.62 (d, J = 7.8 Hz, 1H), 7.53 (d, J = 2.1 Hz, 1H), 7.36 (d, J = 8.1 Hz, 1H), 7.33 – 7.23 (m, 3H), 7.12 (ddd, J = 22.2, 12.5, 7.8 Hz, 5H), 6.98 (t, J = 7.4 Hz, 1H), 4.63 (dd, J = 8.0, 16.0 Hz, 1H), 4.25 (ddd, $J_{A'X'}$ = $J_{B'X'}$ = 4.0, $J_{A'B'}$= 16 Hz, 2H), 3.60 (s, 2H), 3.07 (ddd, J_{AX} = 4.0, J_{BX}= 8.0, J_{AB}= 16.0 Hz, 2H).

^{13}C NMR Analysis:

^{13}C NMR (101 MHz, DMSO-d_6) δ 171.9, 168.9, 138.8, 136.6, 135.0, 133.9, 133.3, 132.3, 131.6, 129.3 (C x 2), 128.8, 128.5 (C x 2) 127.7, 127.4, 124.2, 121.3, 119.0, 118.7, 111.7, 110.4, 54.2, 41.8, 31.0, 28.5.

HPLC:

RP-HPLC Alltima™ C18 5 µm 150 mm x 4.6 mm, 10–100% B in 15 min, R_t =14.38 min, 99.2%.

Mass Spectral Analysis: LRMS (APCI+) m/z 513, 514 [M+H, ^{35}Cl]$^+$ 50%. HRMS (ES+) for $C_{26}H_{22}Cl_3N_3O_2$, calculated 514.0850, found 514.0850.

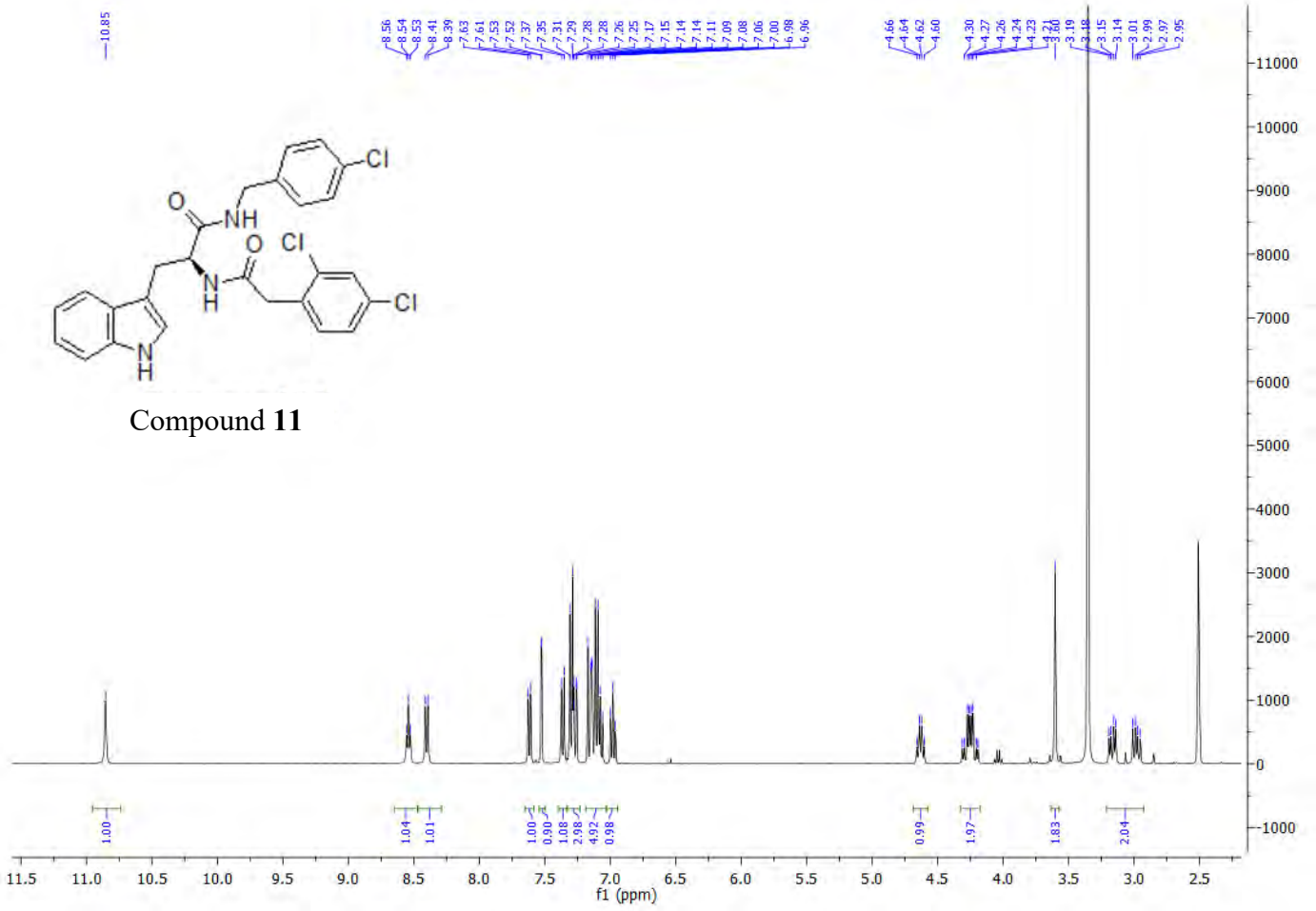

Compound **11**

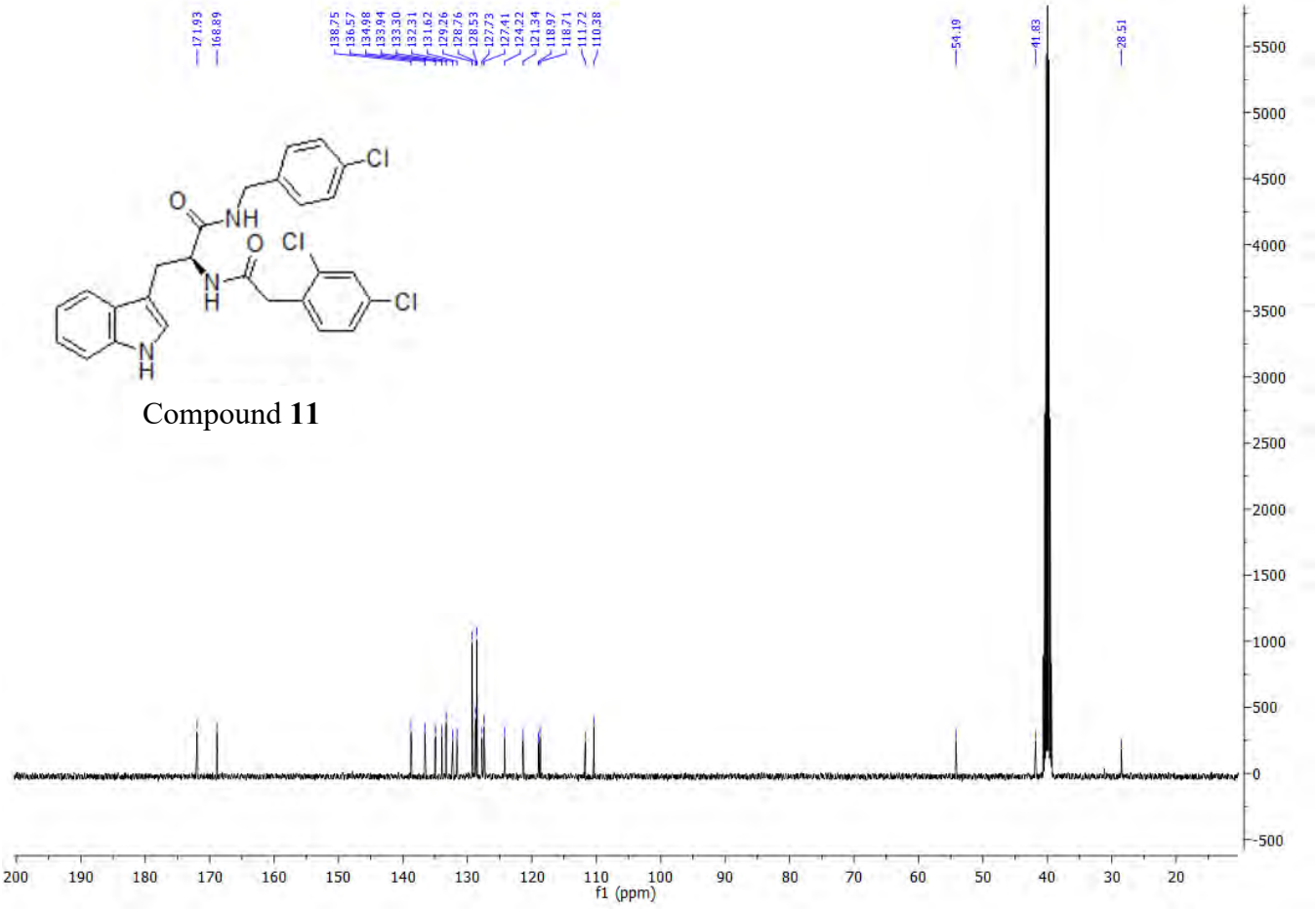
171.93
168.89
138.75
136.57
134.98
133.94
133.30
132.31
131.62
129.26
128.76
128.53
127.73
127.41
124.22
121.34
118.97
118.71
111.72
110.38
54.19
41.83
28.51
Cl
O
NH
O
Cl
N
H
Cl
N
H
5500
5000
4500
4000
3500
3000
2500
2000
1500
1000
500
0
-500
200
190
180
170
160
150
140
130
120
110
100
90
80
70
60
50
40
30
20
f1 (ppm)

Compound **11**

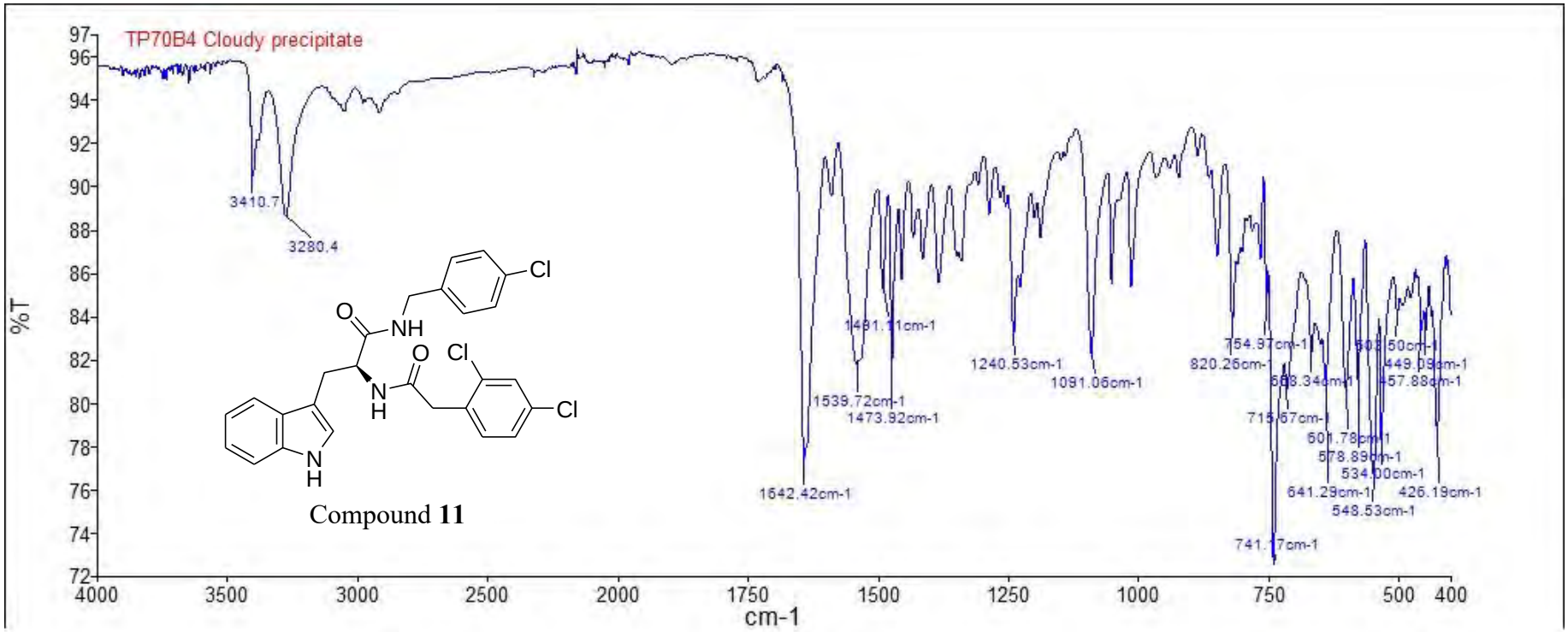
TP70B4 Cloudy precipitate
%T
cm-1
3410.7
3280.4
1642.42cm-1
1539.72cm-1
1473.92cm-1
1491.11cm-1
1240.53cm-1
1091.06cm-1
754.97cm-1
820.26cm-1
741.17cm-1
715.67cm-1
601.78cm-1
578.89cm-1
534.00cm-1
641.29cm-1
548.53cm-1
426.19cm-1
449.09cm-1
457.88cm-1
O
NH
O
Cl
N
H
Cl
Cl
N
H

Compound **11**

SHIMADZU LabSolutions **Analysis Report**

<Sample Information>

Sample Name	: TP70B4		
Sample ID	: TP70B4		
Data Filename	: TP70B4.lcd		
Method Filename	: 10-100 over 15 mins.lcm		
Batch Filename	: TP174-176B3 10-100 over 15mins.lcb		
Vial #	: 1-10	Sample Type	: Unknown
Injection Volume	: 15 uL		
Date Acquired	: 6/08/2014 2:02:15 PM	Acquired by	: System Administrator
Date Processed	: 6/08/2014 2:32:16 PM	Processed by	: System Administrator

<Chromatogram>

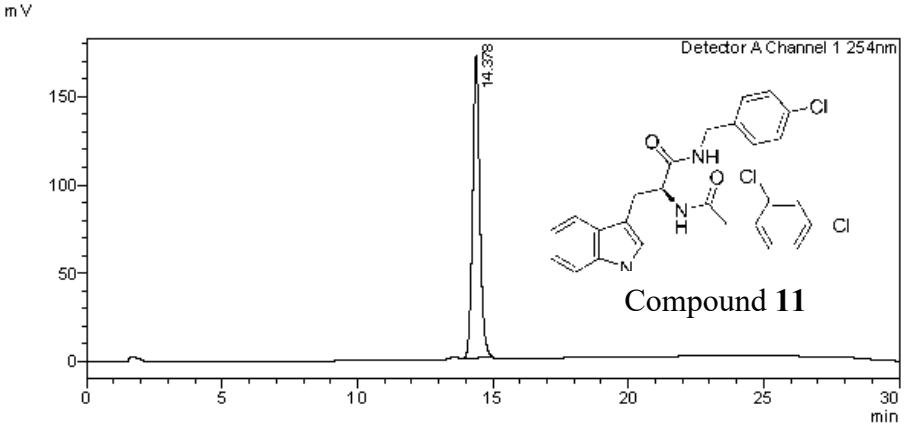

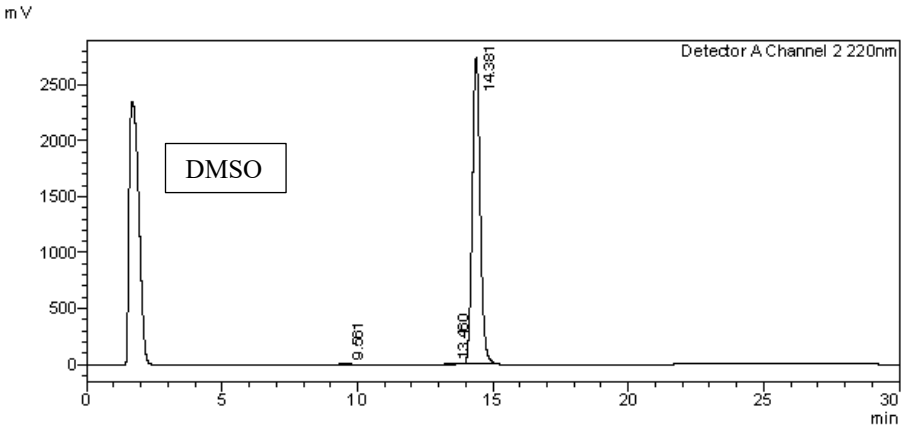

<Peak Table>

Detector A Channel 1 254nm

Peak#	Ret. Time	Area	Height	Conc.	Unit	Mark	Name
1	14.378	3170425	171341	100.000		M	
Total		3170425	171341				

Detector A Channel 2 220nm

Peak#	Ret. Time	Area	Height	Conc.	Unit	Mark	Name
1	9.561	242696	10679	0.435		M	
2	13.460	159035	7012	0.285		M	
3	14.381	55380338	2728386	99.280		M	
Total		55782069	2746078				

==== Shimadzu LCMSsolution Data Report ====

<Chromatogram>

Sample Information

Acquired by	: Admin
Date Acquired	: 11/18/2014 2:34:14 PM
Sample Type	: Unknown
Level#	: 0
Sample Name	: TP70B4_APCI+
Sample ID	:
ISTD Amount	: (Level1 Conc.)
Sample Amount	: 1
Dilution Factor	: 1
Tray#	: 1
Vial#	: 14
Injection Volume	: 10
Data File	: TP70B4_APCI+.lcd
Method File	: FIA-APCI_scan(+).lcm
Original Method	: C:\LabSolutions\Data\Pete\FIA-APCI_scan(+).lcm
Report Format	: DefaultLCMS.lcr
Tuning File	: C:\LabSolutions\LCsolution\Log\Tuning\Autotune_030908.lct
Processed by	: Admin
Modified Date	: 11/18/2014 2:35:47 PM

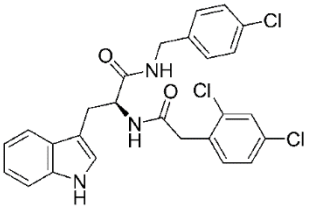

Compound **11**

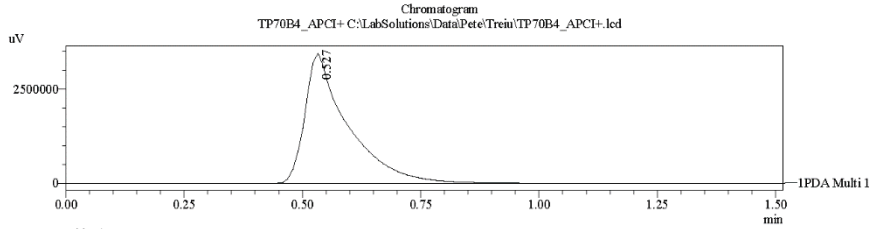

1 PDA Multi 1 / 254nm 4nm

<Spectrum>

Retention Time:0.680(Scan#:69)
Max Peak:742 Base Peak:168.75(583984)
Spectrum:Averaged 0.480-1.080(49-109)
Background:Averaged 0.100-0.332(11-35) Polarity:Pos Segment1 - Event1

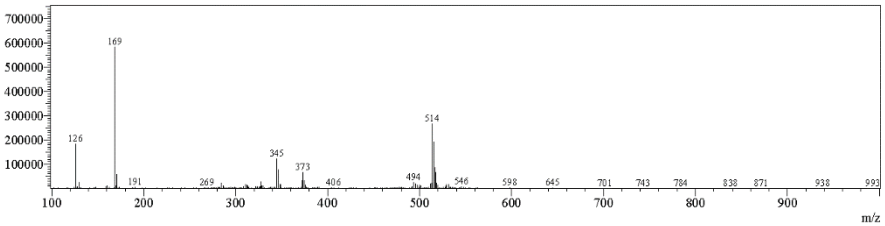

Retention Time:0.550(Scan#:56)
Max Peak:713 Base Peak:112.60(383929)
Spectrum:Averaged 0.490-1.090(50-110)
Background:Averaged 0.110-0.332(12-36) Polarity:Neg Segment1 - Event2

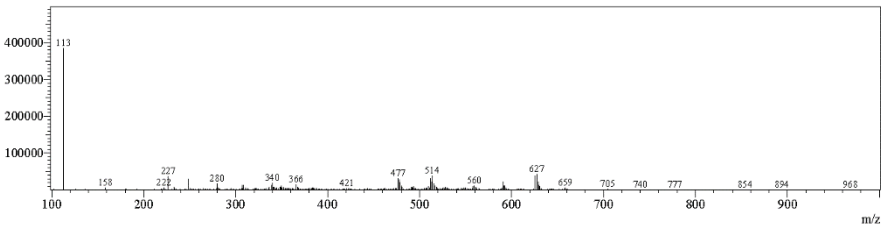

C:¥LabSolutions¥Data¥Pete¥Treiu¥TP70B4_APCI+.lcd

Compound	Chemical Formula	Predicted monoisotopic neutral MW	Predicted MH+	MH+ Measured	Main MS Ions	Main MS/MS Fragments
TP 70B4	$C_{26}H_{22}Cl_3N_3O_2$	513.0778	514.0850	514.0850	514.08496*	373.0512 345.0560 159.0920

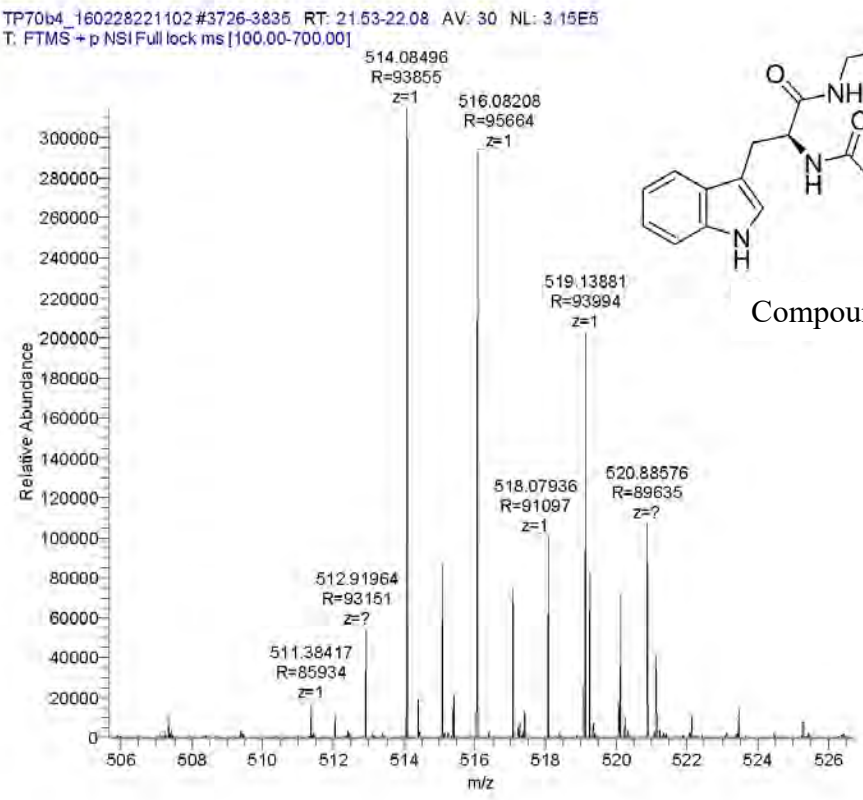

Compound **11**

COMPOUND 12

Compound Name: *N*-(4-Chloro-benzyl)-2-[2-(2,6-dichloro-phenyl)-acetylamino]-3-(1H-indol-3-yl)-propionamide

Obtained Weight & Yield: 80 mg, 40%

Appearance: White crystal

Solubility: EtOAc, Acetone, ACN

Melting Point: 265-256 ºC

TLC Conditions: EtOAc/Hexane (50/50)

IR Analysis: νmax/cm^{-1}

3410 (NH), 3292 (NH), 3252 (NH), 1641 (CON)

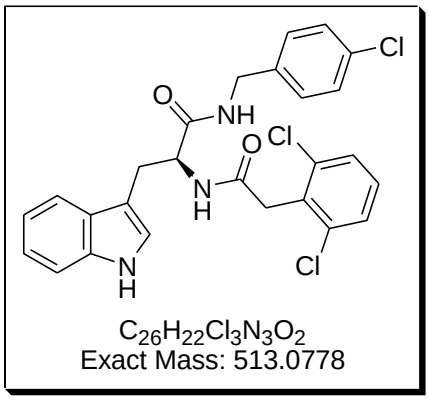

$C_{26}H_{22}Cl_3N_3O_2$
Exact Mass: 513.0778

^{1}H NMR Analysis:

^{1}H NMR (400 MHz, DMSO-d_6) δ 10.85 (s, 1H), 8.49 (t, J = 4.0 Hz, 1H), 8.40 (d, J = 8.2 Hz, 1H), 7.60 (d, J = 7.9 Hz, 1H), 7.41 (d, J = 7.9 Hz, 2H), 7.34 (d, J = 8.1 Hz, 1H), 7.28 (ddd, J = 8.6, 4.7, 2.5 Hz, 3H), 7.13 (d, J = 2.2 Hz, 1H), 7.11 – 7.03 (m, 3H), 7.00 – 6.94 (m, 1H), 4.60 (dd, J = 8.0 Hz, 1H), 4.24 (ddd, $J_{A'X'}$ = 8.0, $J_{B'X'}$ = 4.0, $J_{A'B'}$= 16 Hz, 2H), 3.84 (q, J = 16.3 Hz, 2H), 3.07 (ddd, J_{AX} = 6, J_{BX}= 8.0, J_{AB}= 12 Hz, 2H).

^{13}C NMR Analysis:

^{13}C NMR (101 MHz, DMSO-d_6) δ 171.9, 167.8, 138.7, 136.5, 136.0 (Cx2), 133.1, 131.6, 129.6, 129.2 (C x 2), 128.5 (C x 2), 128.5 (C x 2), 127.8, 124.1, 121.3, 118.9, 118.7, 111.7, 110.4, 54.3, 41.8, 37.9, 28.6.

HPLC:

RP-HPLC Alltima™ C18 5 µm 150 mm x4.6 mm, 10–100% B in 15 min, R_t = 6.54 min, 100%

Mass Spectral Analysis: LRMS (ESI+) m/z 513, 514 [M+H, ^{35}Cl]$^+$ 95%. HRMS (ES+) for $C_{26}H_{22}Cl_3N_3O_2$, calculated 514.0850, found 514.0850.

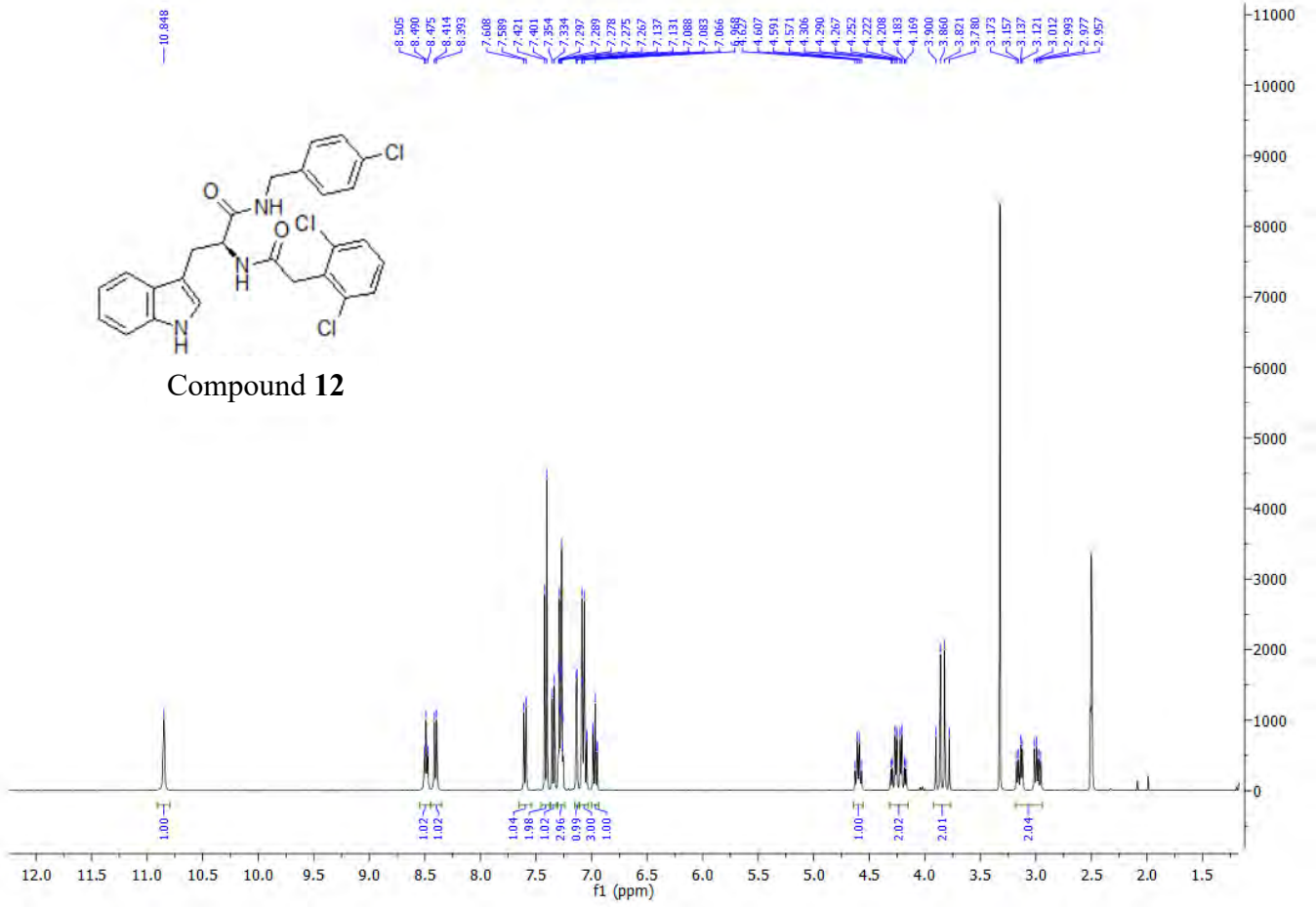
10.848
8.505
8.490
8.475
8.414
8.393
7.608
7.589
7.421
7.401
7.354
7.334
7.297
7.289
7.278
7.275
7.267
7.137
7.131
7.088
7.083
7.066
4.607
4.591
4.571
4.306
4.290
4.267
4.252
4.222
4.208
4.183
4.169
3.900
3.860
3.821
3.780
3.173
3.157
3.137
3.121
3.012
2.993
2.977
2.957
Cl
O
NH
O
Cl
N
H
N
H
Cl
1.00
1.02
1.02
1.04
1.98
1.02
2.96
0.99
3.00
1.00
1.00
2.02
2.01
2.04
f1 (ppm)

Compound **12**

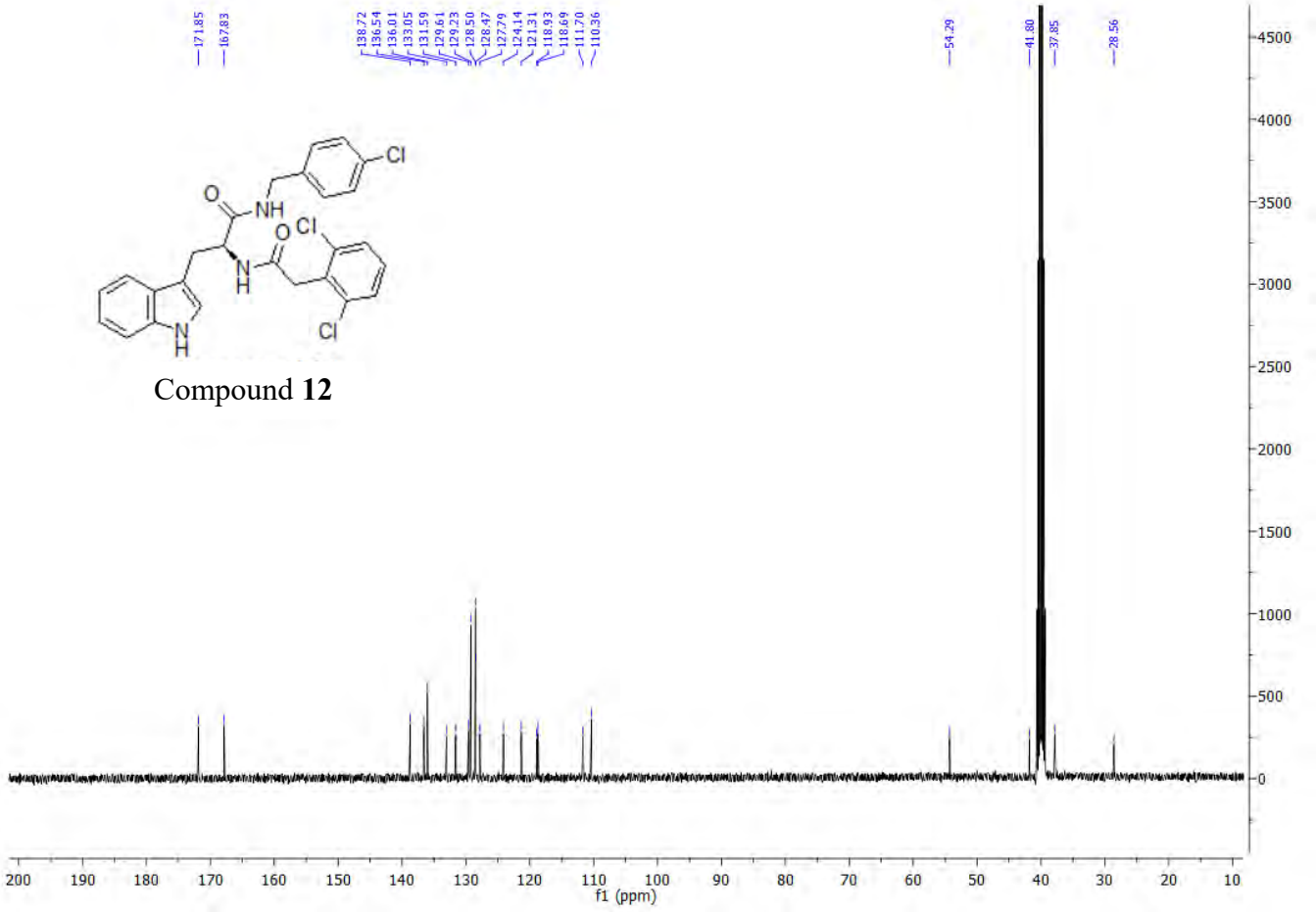
171.85
167.83
138.72
136.54
136.01
133.05
131.59
129.61
129.23
128.50
128.47
127.79
124.14
121.31
118.93
118.69
111.70
110.36
54.29
41.80
37.85
28.56
Cl
O
NH
O
Cl
N
H
N
H
Cl
4500
4000
3500
3000
2500
2000
1500
1000
500
0
200
190
180
170
160
150
140
130
120
110
100
90
80
70
60
50
40
30
20
10
f1 (ppm)

Compound **12**

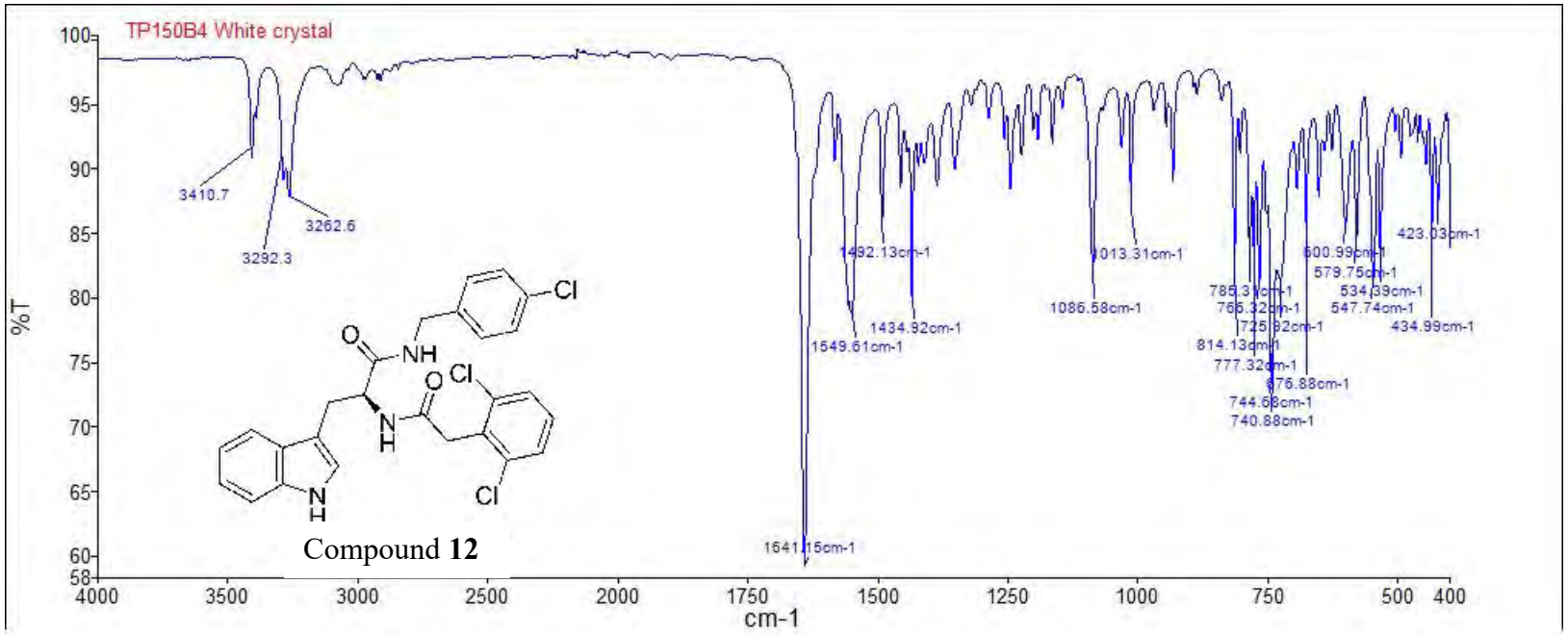
TP150B4 White crystal
%T
cm-1
3410.7
3292.3
3262.6
1641.15cm-1
1549.61cm-1
1492.13cm-1
1434.82cm-1
1086.58cm-1
1013.31cm-1
814.13cm-1
777.32cm-1
744.68cm-1
740.88cm-1
600.99cm-1
579.75cm-1
547.74cm-1
534.39cm-1
434.99cm-1
423.03cm-1
Cl
Cl
Cl
O
NH
O
N
H
N
H

Compound **12**

SHIMADZU LabSolutions **Analysis Report**

<Sample Information>

Sample Name	: TP150B4		
Sample ID	: TP150B4		
Data Filename	: TP150B4.lcd		
Method Filename	: 10-100 over 15 mins.lcm		
Batch Filename	: TRIEU Second Third Generation and New pro.lcb		
Vial #	: 1-1	Sample Type	: Unknown
Injection Volume	: 30 uL		
Date Acquired	: 5/09/2014 10:35:48 AM	Acquired by	: System Administrator
Date Processed	: 5/09/2014 11:05:49 AM	Processed by	: System Administrator

<Chromatogram>

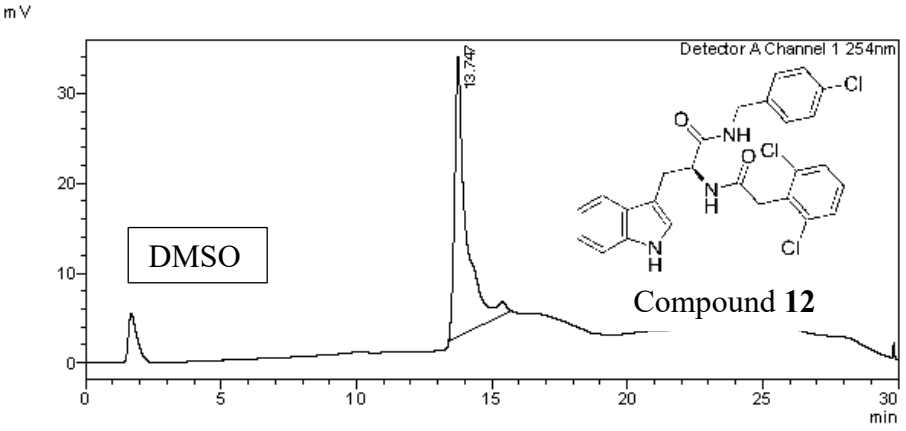

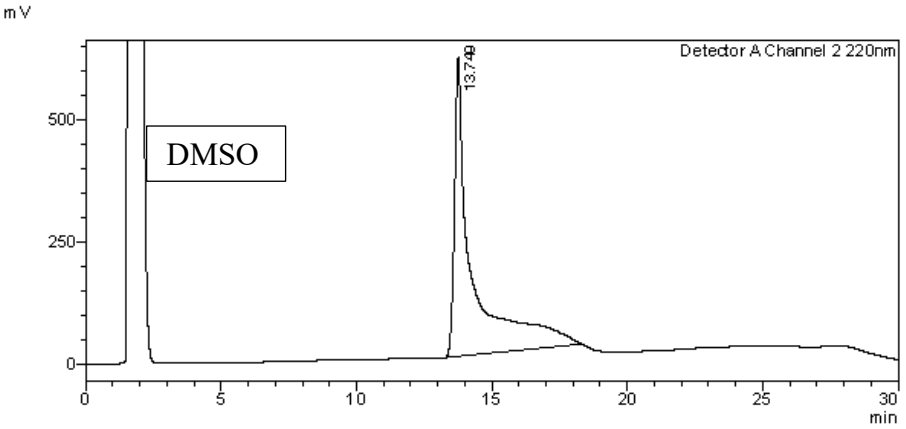

<Peak Table>

Detector A Channel 1 254nm

C:\LabSolutions\Data\Project1\TRIEU\TP150B4.lcd

Peak#	Ret. Time	Area	Height	Conc.	Unit	Mark	Name
1	13.747	938151	31154	100.000		M	
Total		938151	31154				

Detector A Channel 2 220nm

Peak#	Ret. Time	Area	Height	Conc.	Unit	Mark	Name
1	13.749	28196177	611041	100.000		M	
Total		28196177	611041				

==== Shimadzu LCMSsolution Data Report ====

<Chromatogram>

Sample Information

Acquired by	: Admin
Date Acquired	: 9/22/2015 1:10:30 PM
Sample Type	: Unknown
Level#	: 0
Sample Name	: TP150B4
Sample ID	:
ISTD Amount	: (Level1 Conc.)
Sample Amount	: 1
Dilution Factor	: 1
Tray#	: 1
Vial#	: 41
Injection Volume	: 5
Data File	: TP150B4.lcd
Method File	: FIA-ESI_Scan(+).lcm
Original Method	: C:\LabSolutions\Data\Kelly\FIA-ESI_Scan(+).lcm
Report Format	: DefaultLCMS.lcr
Tuning File	: C:\LabSolutions\Data\AutoTuning\Autotune_ESI_26AUG15.lct
Processed by	: Admin
Modified Date	: 9/22/2015 1:12:00 PM

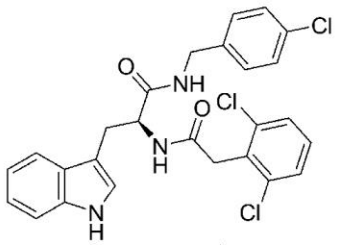

Compound **12**

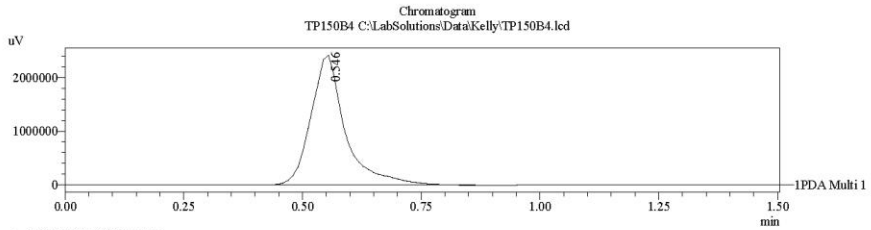

1 PDA Multi 1 / 254nm 4nm

<Spectrum>

Retention Time:1.020(Scan#:103)
Max Peak:428 Base Peak:156.85(385786)
Spectrum:Averaged 0.520-1.340(53-135)
Background:Averaged 0.020-0.497(3-51) Polarity:Pos Segment1 - Event1

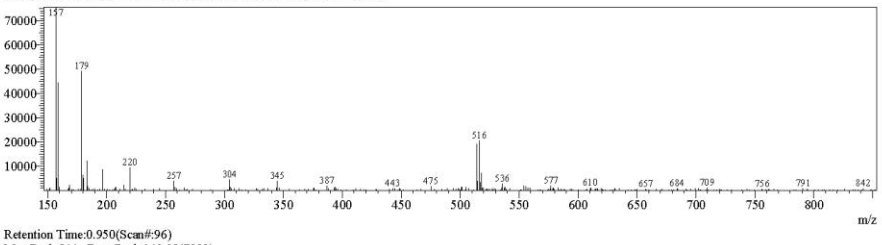

Retention Time:0.950(Scan#:96)
Max Peak:514 Base Peak:249.05(7999)
Spectrum:Averaged 0.530-1.350(54-136)
Background:Averaged 0.030-0.497(4-52) Polarity:Neg Segment1 - Event2

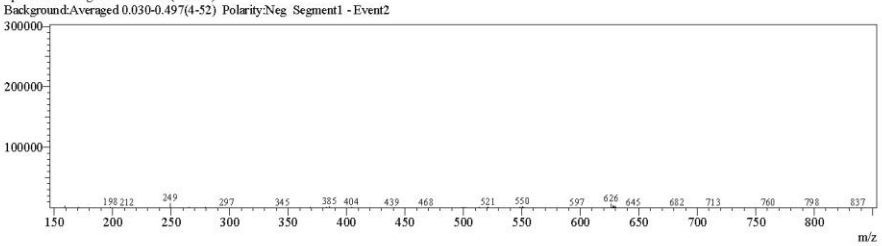

C:¥LabSolutions¥Data¥Kelly¥TP150B4.lcd

Compound	Chemical Formula	Predicted monoisotopic neutral MW	Predicted MH+	MH+ Measured	Main MS Ions	Main MS/MS Fragments
TP 150B4	$C_{26}H_{22}Cl_3N_3O_2$	513.0776	514.0850	514.08496	514.08496*	345.0559 159.0919 187.0869

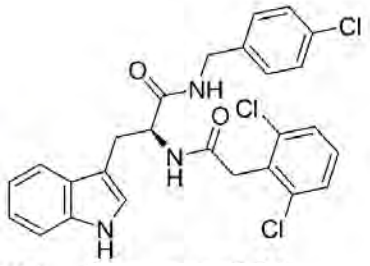

Compound **12**

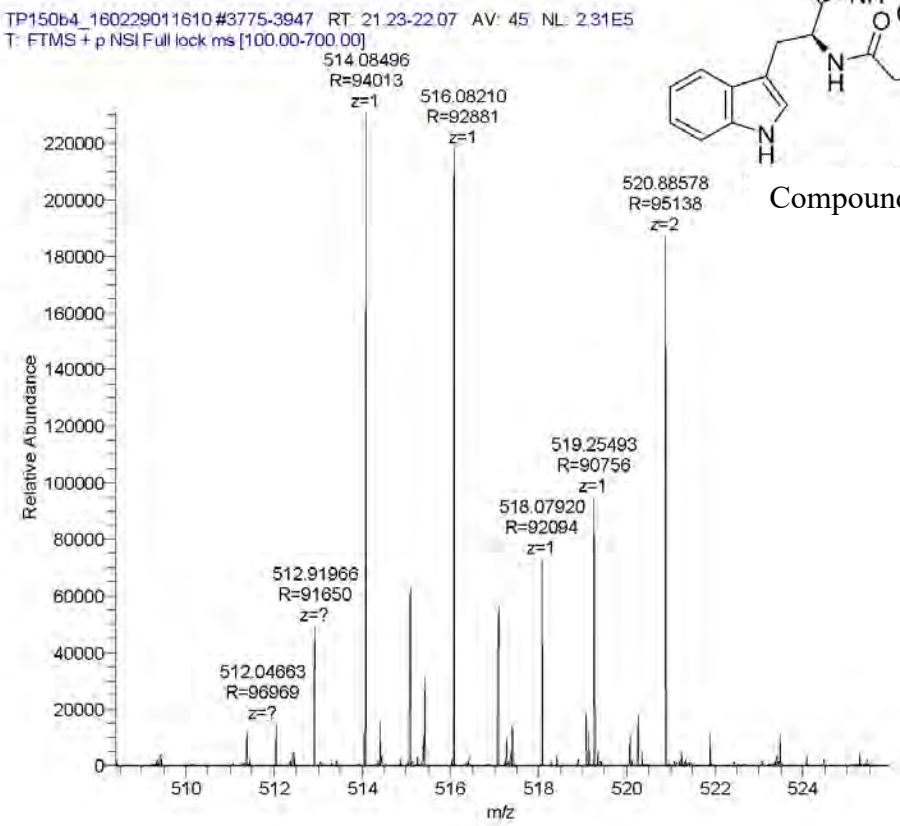

COMPOUND 13

Compound Name: *N*-(4-Chloro-benzyl)-2-[2-(4-chloro-phenyl)-acetylamino]-3-(1*H*-indol-3-yl)-propionamide

Obtained Weight & Yield: 60 mg, 32%

Appearance: White crystal

Solubility: EtOAc, Acetone, ACN

Melting Point: 205.2-206.3 ºC

TLC Conditions: EtOAc/Hexane (50/50)

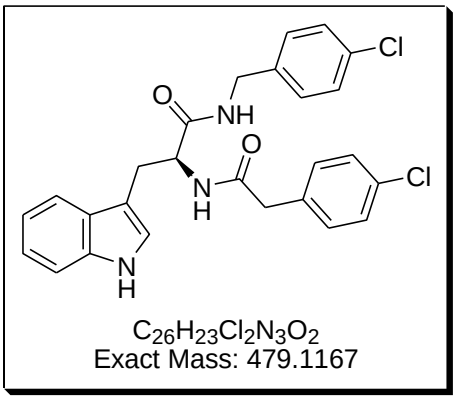

$C_{26}H_{23}Cl_2N_3O_2$
Exact Mass: 479.1167

IR Analysis: νmax/cm^{-1}

3410 (NH), 3292 (NH), 3061 (CH), 1635 (CON)

^{1}H NMR Analysis:

^{1}H NMR (400 MHz, DMSO-d_6) δ 10.84 (s, 1H), 8.55 (t, J = 6.0 Hz, 1H), 8.38 (d, J = 8.2 Hz, 1H), 7.60 (d, J = 7.9 Hz, 1H), 7.36 (d, J = 8.1 Hz, 1H), 7.32 – 7.21 (m, 4H), 7.16 – 7.01 (m, 6H), 7.01 – 6.90 (m, 1H), 4.59 (dd, J = 8 Hz, 1H), 4.23 (ddd, $J_{A'X'}$ = 8, $J_{B'X'}$ = 6.0, $J_{A'B'}$ = 16 Hz, 2H), 3.44 (dd, J = 19.8, 14.4 Hz, 2H), 3.05 (ddd, J_{AX} = 6, J_{BX} = 8, J_{AB} = 16 Hz, 2H).

^{13}C NMR Analysis:

^{13}C NMR (101 MHz, DMSO-d_6) δ 172.0, 170.0, 138.7, 136.6, 135.8, 131.6, 131.4, 131.3 (C x 2), 129.2 (C x 2), 128.5 (C x 2), 128.4 (C x 2), 127.7, 124.2, 121.4, 119.0, 118.7, 111.7, 110.4, 54.1, 41.8, 41.7, 28.5.

HPLC:

RP-HPLC Alltima™ C18 5 µm 150 mm x 4.6 mm, 10–100% B in 15 min, R_t = 13.69 min, 100%.

Mass Spectral Analysis: LRMS (ESI+) m/z 479, 480 $[M+H, {}^{35}Cl]^+$, 100%. HRMS (ES+) for $C_{26}H_{23}Cl_2N_3O_2$, calculated 480.1240, found 480.1240.

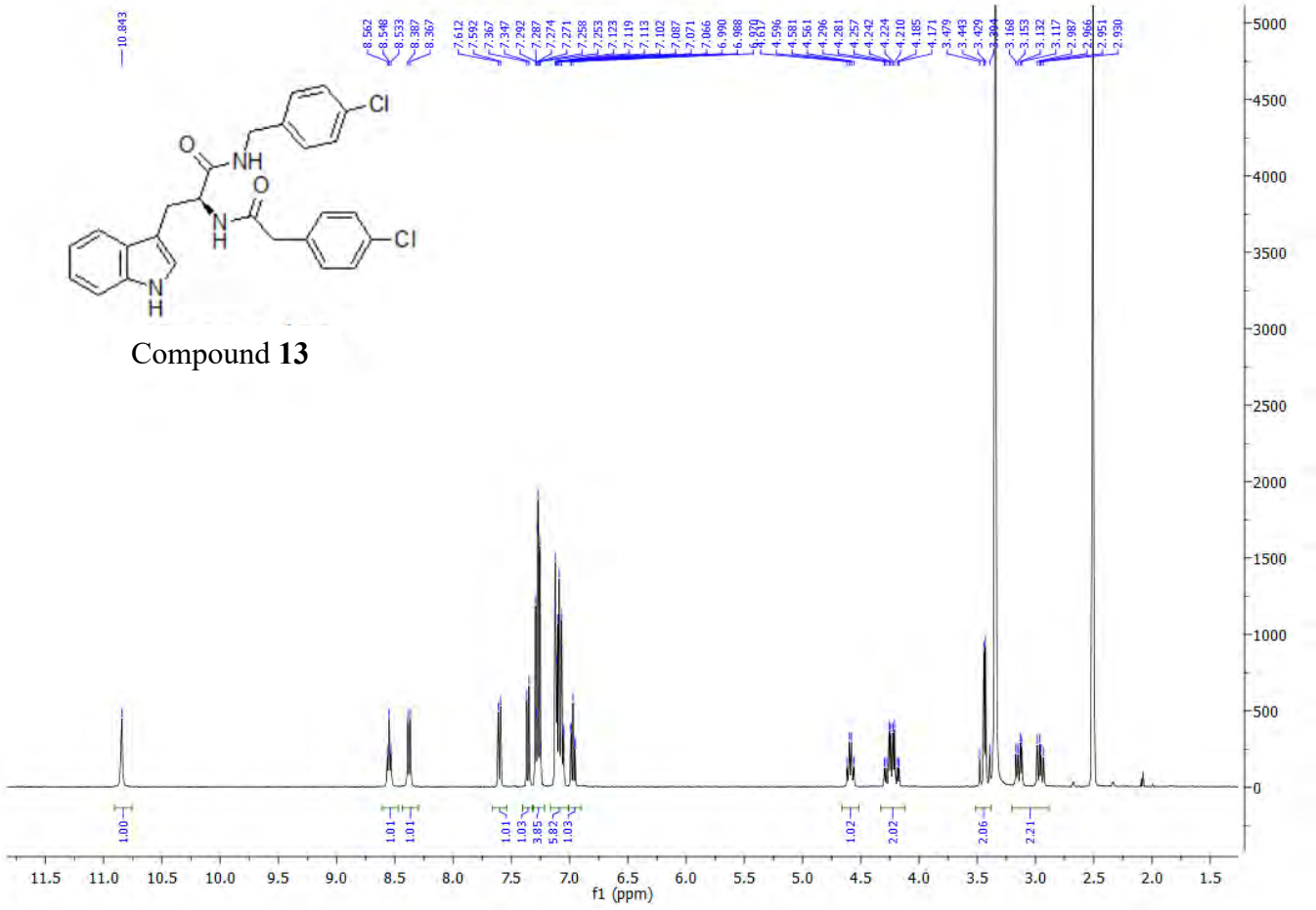

Compound **13**

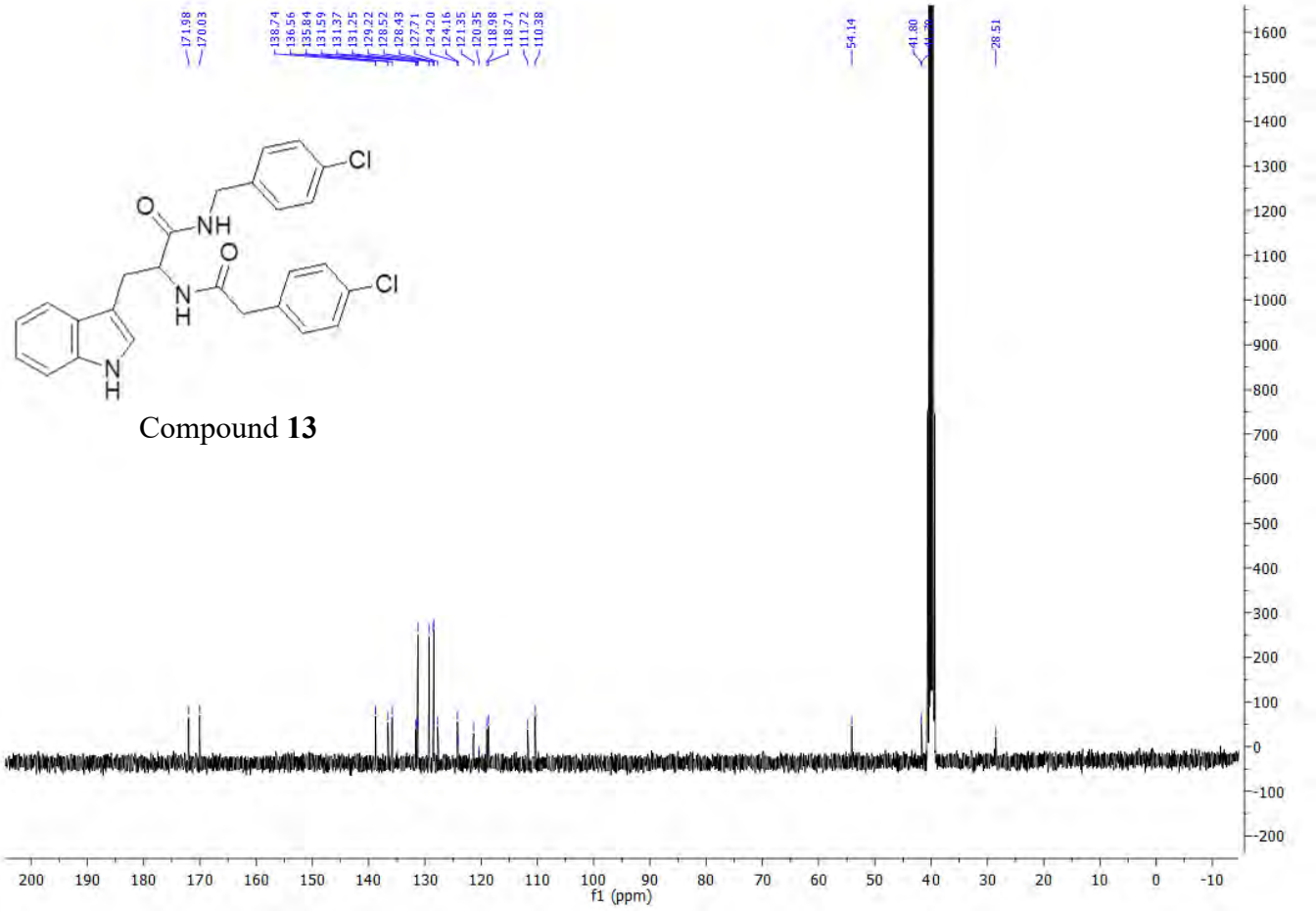
171.98
170.03
138.74
136.56
135.84
131.59
131.37
131.25
129.22
128.52
128.43
127.71
124.20
124.16
121.35
120.35
118.98
118.71
111.72
110.38
54.14
41.80
28.51
Cl
Cl
O
NH
O
N
H
N
H
f1 (ppm)

Compound **13**

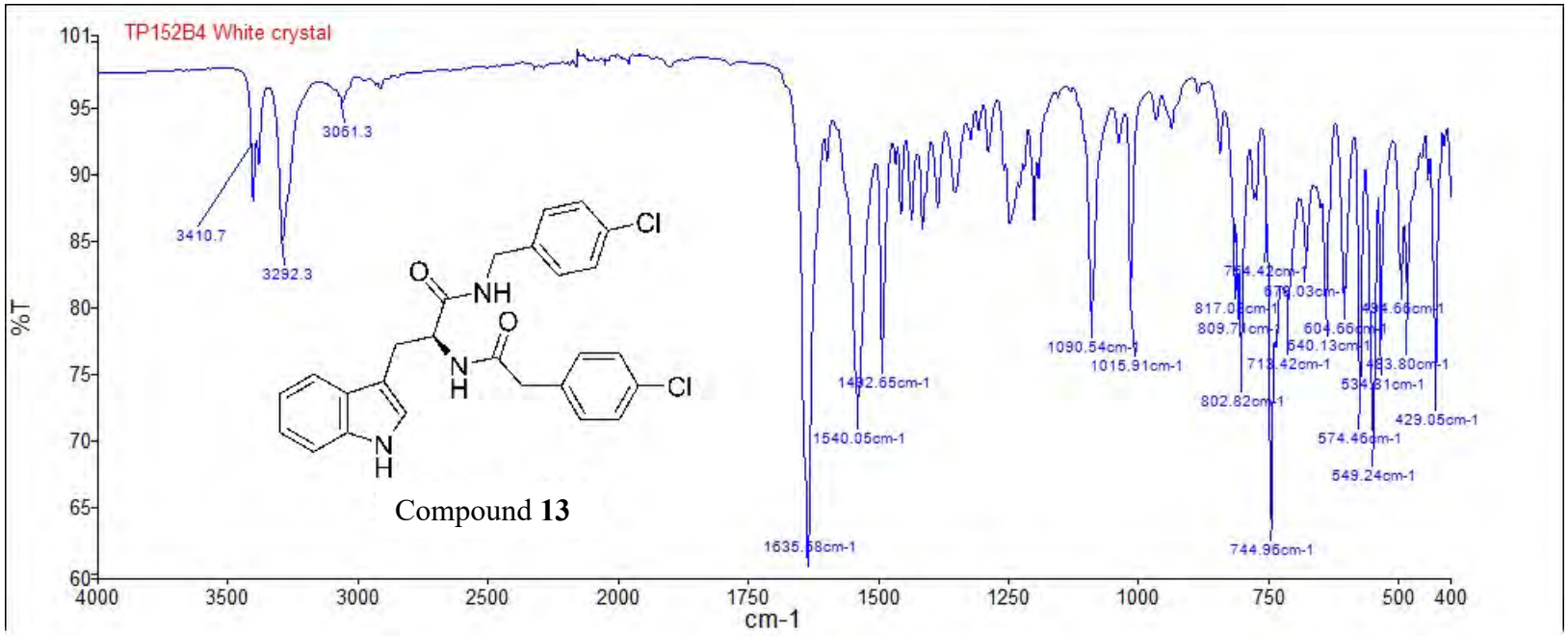
TP152B4 White crystal
%T
cm-1
3410.7
3292.3
3061.3
1635.68cm-1
1540.05cm-1
1492.65cm-1
1090.54cm-1
1015.91cm-1
802.82cm-1
744.96cm-1
574.46cm-1
549.24cm-1
429.05cm-1
Cl
Cl
NH
O
N
H
O
N
H

Compound **13**

SHIMADZU LabSolutions Analysis Report

<Sample Information>

Sample Name	: TP152B4		
Sample ID	: TP152B4		
Data Filename	: TP152B4.lcd		
Method Filename	: 10-100 over 15 mins.lcm		
Batch Filename	: TP174-176B3 10-100 over 15mins.lcb		
Vial #	: 1-11	Sample Type	: Unknown
Injection Volume	: 15 uL		
Date Acquired	: 6/08/2014 2:32:40 PM	Acquired by	: System Administrator
Date Processed	: 6/08/2014 3:02:42 PM	Processed by	: System Administrator

<Chromatogram>

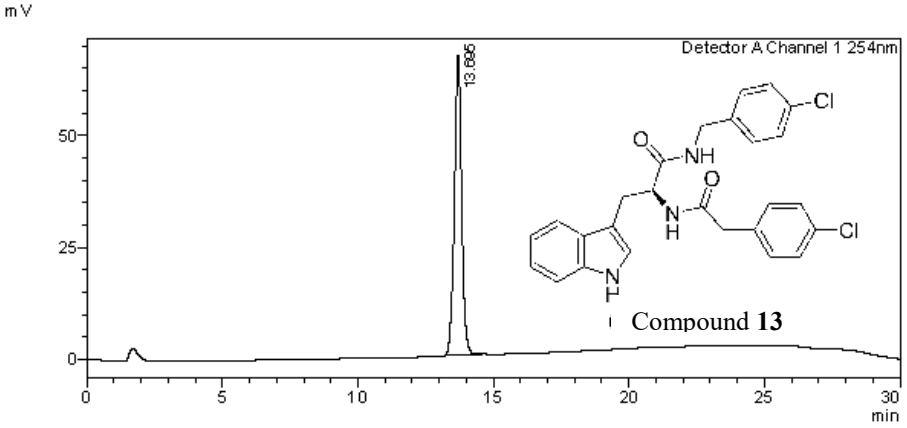

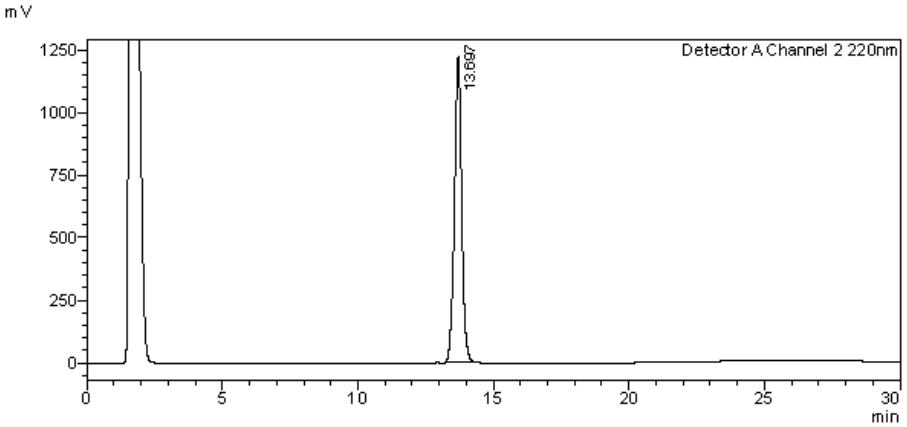

<Peak Table>

Detector A Channel 1 254nm

C:\LabSolutions\Data\Project1\TRIEU\TP152B4.lcd

Peak#	Ret. Time	Area	Height	Conc.	Unit	Mark	Name
1	13.695	1205928	66620	100.000		M	
Total		1205928	66620				

Detector A Channel 2 220nm

Peak#	Ret. Time	Area	Height	Conc.	Unit	Mark	Name
1	13.697	22112589	1216961	100.000		M	
Total		22112589	1216961				

==== Shimadzu LCMSsolution Data Report ====

<Chromatogram>

Sample Information

Acquired by	: Admin
Date Acquired	: 9/22/2015 1:15:26 PM
Sample Type	: Unknown
Level#	: 0
Sample Name	: TP152B4
Sample ID	:
ISTD Amount	: (Level1 Conc.)
Sample Amount	: 1
Dilution Factor	: 1
Tray#	: 1
Vial#	: 43
Injection Volume	: 5
Data File	: TP152B4.lcd
Method File	: FIA-ESI_Scan(+).lcm
Original Method	: C:\LabSolutions\Data\Kelly\FIA-ESI_Scan(+).lcm
Report Format	: DefaultLCMS.lcr
Tuning File	: C:\LabSolutions\Data\AutoTuning\Autotune_ESI_26AUG15.lct
Processed by	: Admin
Modified Date	: 9/22/2015 1:16:58 PM

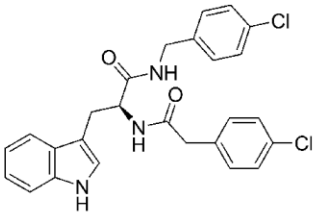

Compound **13**

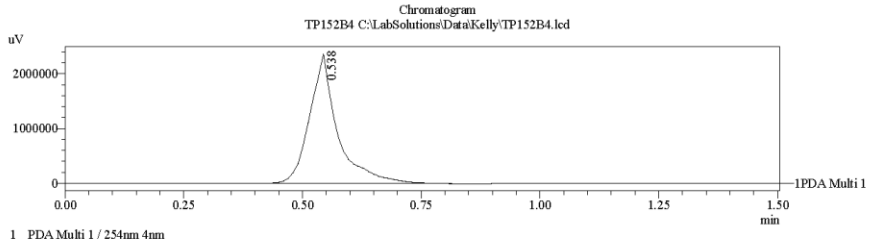

1 PDA Multi 1 / 254nm 4nm

<Spectrum>

Retention Time:1.020(Scan#:103)
Max Peak:459 Base Peak:480.10(20224)
Spectrum:Averaged 0.620-1.220(63-123)
Background:Averaged 0.060-0.514(7-53) Polarity:Pos Segment1 - Event1

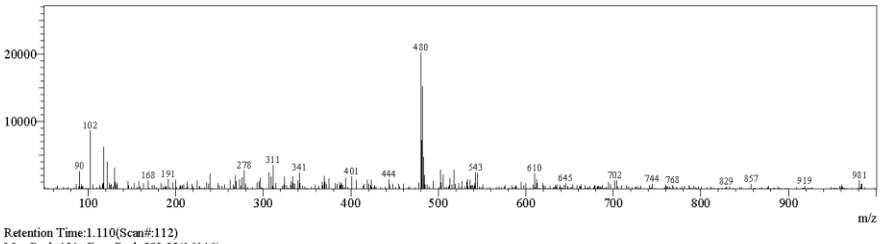

Retention Time:1.110(Scan#:112)
Max Peak:454 Base Peak:592.25(16146)
Spectrum:Averaged 0.630-1.230(64-124)
Background:Averaged 0.070-0.514(8-54) Polarity:Neg Segment1 - Event2

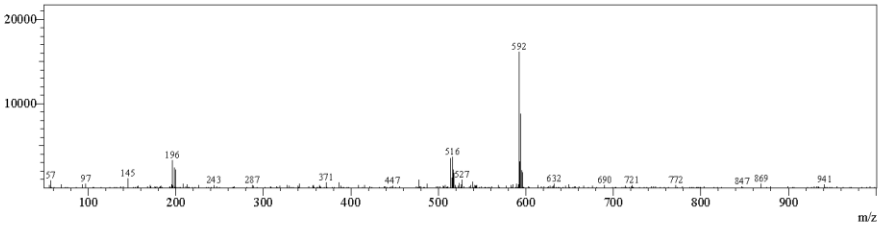

C:¥LabSolutions¥Data¥Kelly¥TP152B4.lcd

Compound	Chemical Formula	Predicted monoisotopic neutral MW	Predicted MH+	MH+ Measured	Main MS Ions	Main MS/MS Fragments
TP 152B4	$C_{26}H_{23}Cl_2N_3O_2$	479.1167	480.1240	480.12396	480.12396*	311.0950 159.0920 187.0870

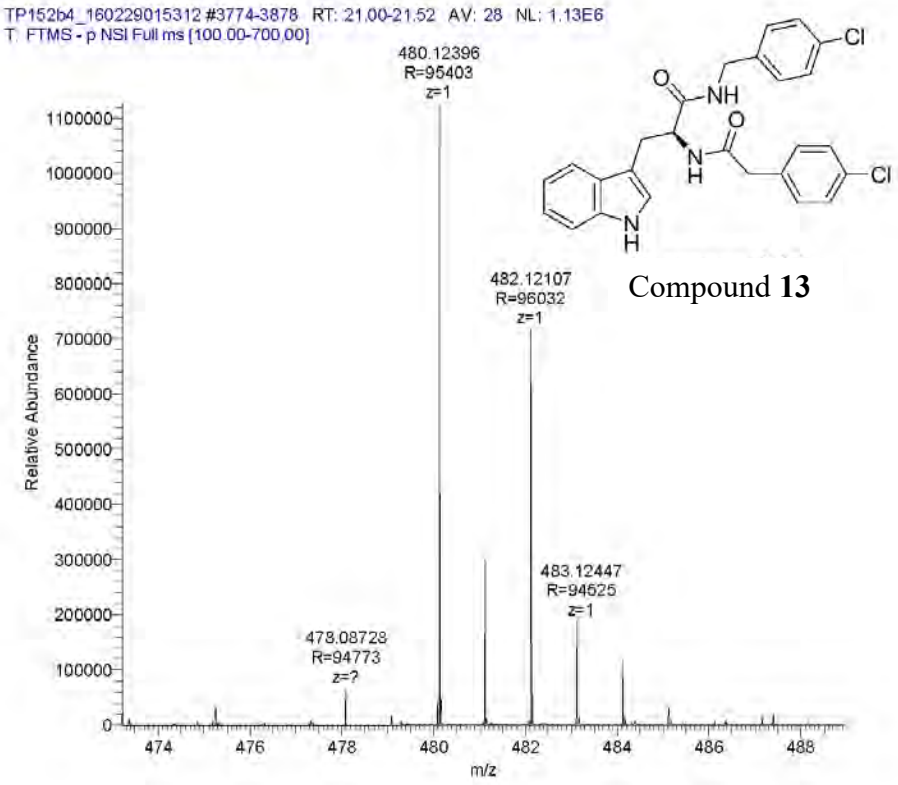

Compound **13**

COMPOUND 14

Compound Name: *1H*-Indole-2-carboxylic acid [1-(4-chloro-benzylcarbamoyl)-2-(*1H*-indol-3-yl)-ethyl]-amide (L-isomer)

Obtained Weight & Yield: 97 mg, 50%

Appearance: White powder

Solubility: Acetone, ACN

Melting Point: 229.5-230.7 ºC

TLC Conditions: EtOAc/Hexane (50/50)

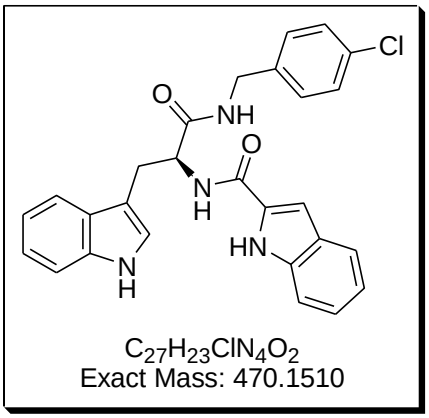

IR Analysis: νmax/cm^{-1}

3422 (NH), 3381 (NH), 3316 (NH), 1630 (CON)

^{1}H NMR Analysis:

^{1}H NMR (400 MHz, DMSO-*d*$_6$) δ (400 MHz, DMSO-*d*$_6$) δ 11.53 (s, 1H), 10.80 (s, 1H), 8.70 (t, *J* = 6.0 Hz, 1H), 8.57 (d, *J* = 8.1 Hz, 1H), 7.71 (d, *J* = 7.8 Hz, 1H), 7.62 (d, *J* = 8.0 Hz, 1H), 7.41 (d, *J* = 8.2 Hz, 1H), 7.33 (dd, *J* = 7.7, 5.5 Hz, 3H), 7.25 – 7.14 (m, 5H), 7.09 – 6.96 (m, 3H), 4.80 (dd, *J* = 9.2, 5.0 Hz, 1H), 4.31 (dd, $J_{A'X'}$ = $J_{B'X'}$ = 6.0, $J_{A'B'}$ = 16.0 Hz, 2H), 3.24 (ddd, J_{AX} = 5.0, J_{BX} = 9.6, J_{AB} = 14.4 Hz, 2H).

^{13}C NMR Analysis:

^{13}C NMR (101 MHz, DMSO-*d*$_6$) δ 172.3, 161.5, 138.9, 136.9, 136.5, 131.7, 129.3 (C x 2), 128.6 (C x 2), 127.7, 127.5, 124.3, 123.8, 122.0, 121.4, 120.2, 119.0, 118.7, 112.7, 111.8, 110.8, 103.8, 54.5, 41.9, 28.2.

HPLC:

RP-HPLC Alltima™ C18 5 µm 150 mm x 4.6 mm, 10–100% B in 15 min, R_t = 13.35 min, 100%.

Mass Spectral Analysis: LRMS (APCI+) m/z 470, 471 [M+H, ^{35}Cl]$^{+}$, 90%. HRMS (ES+) for $C_{27}H_{23}ClN_4O_2$ calculated 471.1582, found 471.1582.

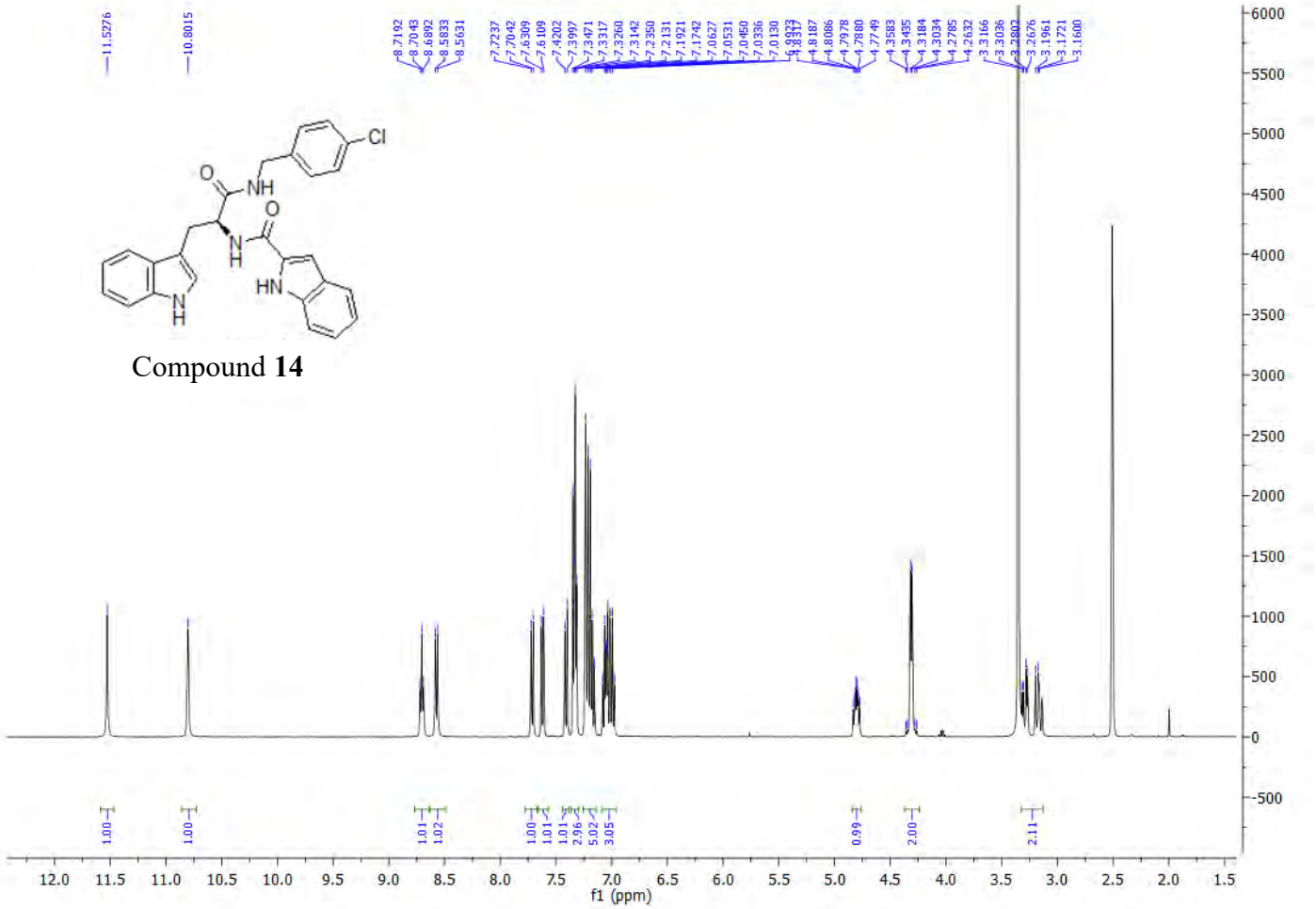
11.5276
10.8015
8.7192
8.7043
8.6892
8.5833
8.5631
7.7237
7.7042
7.6309
7.6109
7.4202
7.3997
7.3471
7.3317
7.3260
7.3142
7.2350
7.2131
7.1921
7.1742
7.0627
7.0531
7.0450
7.0336
7.0130
6.9923
4.8317
4.8187
4.8086
4.7978
4.7880
4.7749
4.3583
4.3435
4.3184
4.3034
4.2785
4.2632
3.3166
3.3036
3.2802
3.2676
3.1961
3.1721
3.1600
Cl
O
NH
N
H
O
HN
N
H
1.00
1.00
1.01
1.02
1.00
1.01
2.96
5.02
3.05
0.99
2.00
2.11
6000
5500
5000
4500
4000
3500
3000
2500
2000
1500
1000
500
0
-500
12.0
11.5
11.0
10.5
10.0
9.5
9.0
8.5
8.0
7.5
7.0
6.5
6.0
5.5
5.0
4.5
4.0
3.5
3.0
2.5
2.0
1.5
f1 (ppm)

Compound **14**

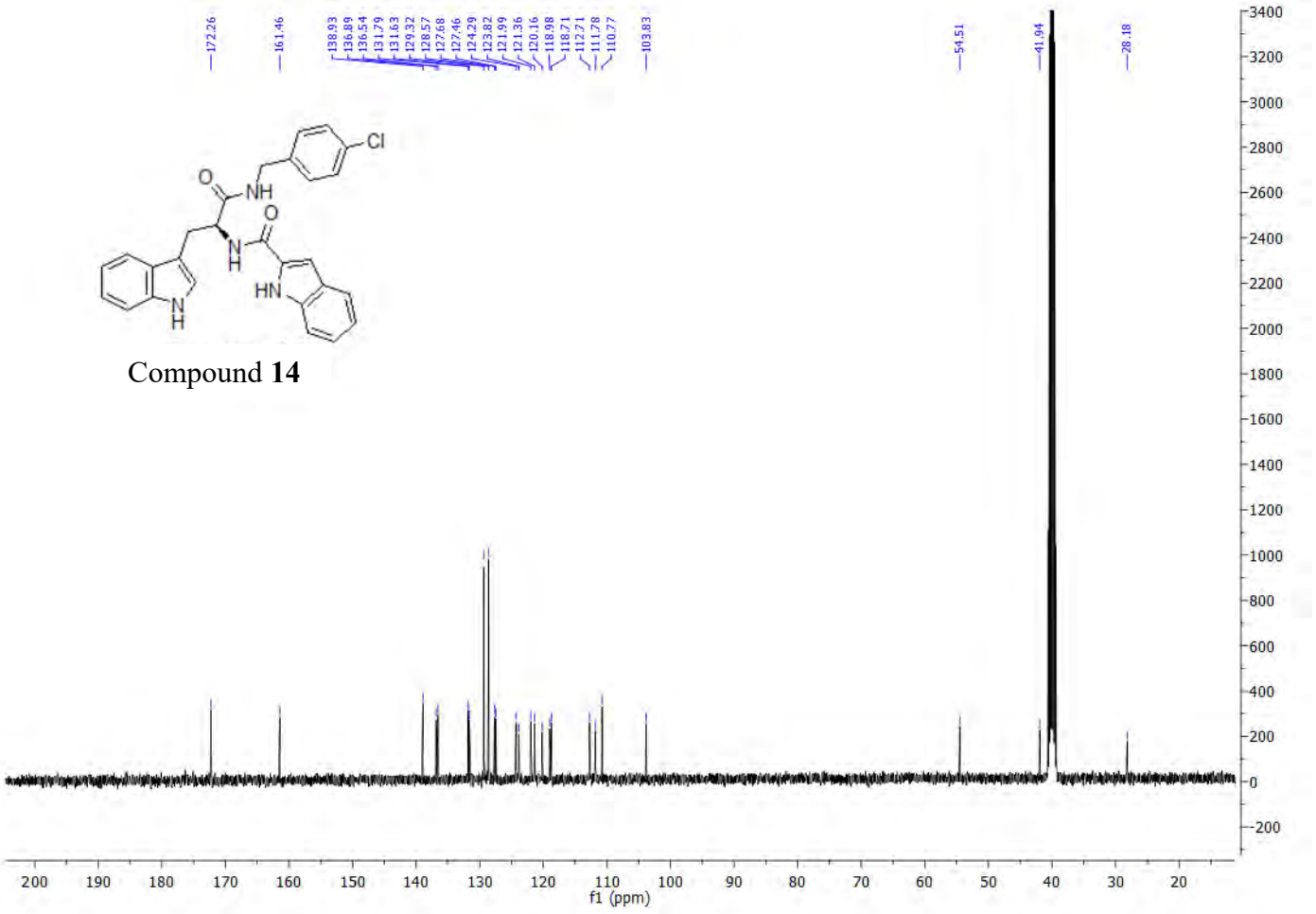
172.26
161.46
138.93
136.89
136.54
131.79
131.63
129.32
128.57
127.68
127.46
124.29
123.82
121.99
121.36
120.16
118.98
118.71
112.71
111.78
110.77
103.83
54.51
41.94
28.18
Cl
O
NH
O
N
H
HN
N
H
3400
3200
3000
2800
2600
2400
2200
2000
1800
1600
1400
1200
1000
800
600
400
200
0
-200
200
190
180
170
160
150
140
130
120
110
100
90
80
70
60
50
40
30
20
f1 (ppm)

Compound **14**

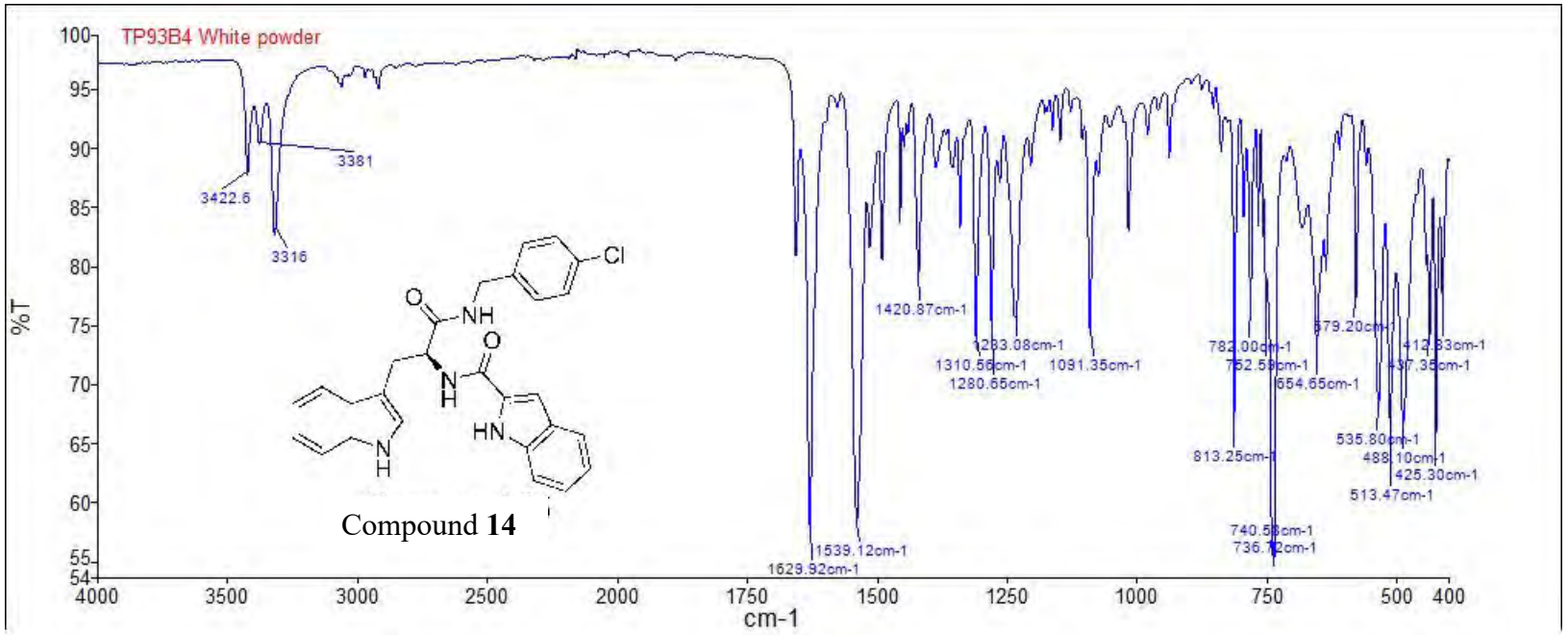
TP93B4 White powder
%T
cm-1
3422.6
3381
3316
1629.92cm-1
1539.12cm-1
1420.87cm-1
1310.56cm-1
1280.65cm-1
1091.35cm-1
813.25cm-1
740.58cm-1
736.72cm-1
654.65cm-1
535.80cm-1
513.47cm-1
425.30cm-1
Cl
NH
O
N
H
HN

Compound **14**

SHIMADZU LabSolutions Analysis Report

<Sample Information>

Sample Name	: TP93B4		
Sample ID	: TP93B4		
Data Filename	: TP93B4.lcd		
Method Filename	: 10-100 over 15 mins.lcm		
Batch Filename	: TRIEU Second Third Generation and New pro.lcb		
Vial #	: 1-5	Sample Type	: Unknown
Injection Volume	: 30 uL		
Date Acquired	: 5/09/2014 12:37:27 PM	Acquired by	: System Administrator
Date Processed	: 5/09/2014 1:07:28 PM	Processed by	: System Administrator

<Chromatogram>

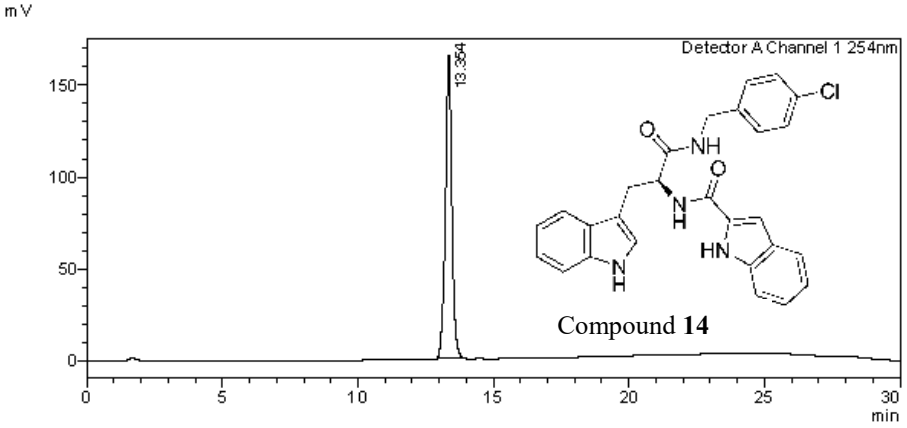

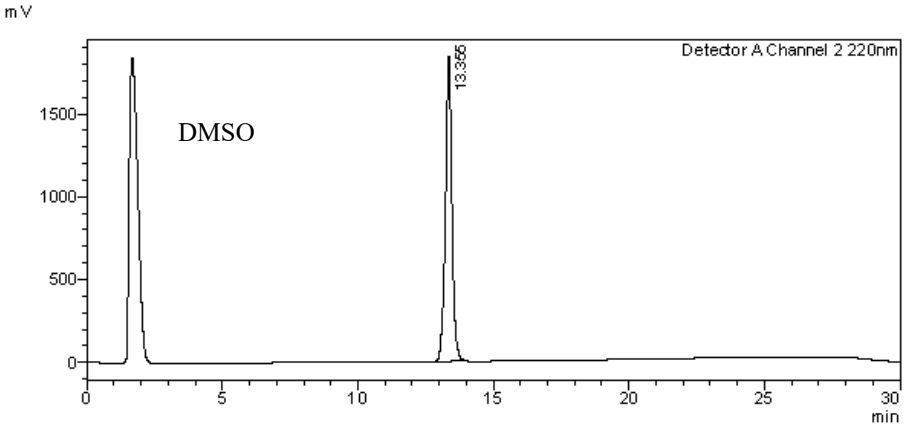

<Peak Table>

Detector A Channel 1 254nm

C:\LabSolutions\Data\Project1\TRIEU\TP93B4.lcd

Peak#	Ret. Time	Area	Height	Conc.	Unit	Mark	Name
1	13.354	2726844	164567	100.000		M	
Total		2726844	164567				

Detector A Channel 2 220nm

Peak#	Ret. Time	Area	Height	Conc.	Unit	Mark	Name
1	13.355	30658702	1835217	100.000		M	
Total		30658702	1835217				

==== Shimadzu LCMSsolution Data Report ====

<Chromatogram>

Sample Information

Acquired by	: Admin
Date Acquired	: 11/18/2014 2:11:44 PM
Sample Type	: Unknown
Level#	: 0
Sample Name	: tp93b4tp_APCI+
Sample ID	:
ISTD Amount	: (Level1 Conc.)
Sample Amount	: 1
Dilution Factor	: 1
Tray#	: 1
Vial#	: 5
Injection Volume	: 10
Data File	: tp93b4tp_APCI+.lcd
Method File	: FIA-APCI_scan(+).lcm
Original Method	: C:\LabSolutions\Data\Pete\FIA-APCI_scan(+).lcm
Report Format	: DefaultLCMS.lcr
Tuning File	: C:\LabSolutions\LCsolution\Log\Tuning\Autotune_030908.lct
Processed by	: Admin
Modified Date	: 11/18/2014 2:13:17 PM

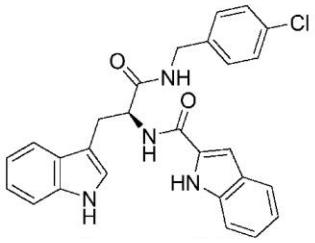

Compound **14**

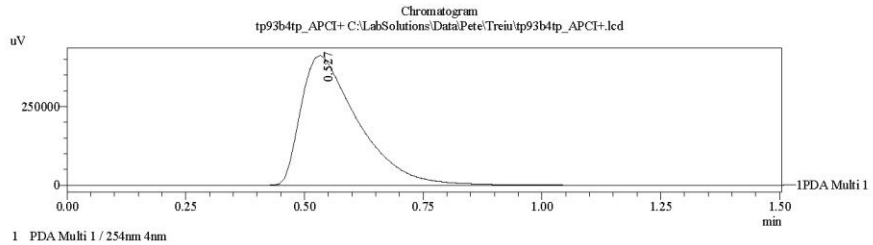

1 PDA Multi 1 / 254nm 4nm

<Spectrum>

Retention Time:0.600(Scan#:61)
Max Peak:591 Base Peak:168.80(427108)
Spectrum:Averaged 0.440-0.900(45-91)
Background:Averaged 0.060-0.354(7-37) Polarity:Pos Segment1 - Event1

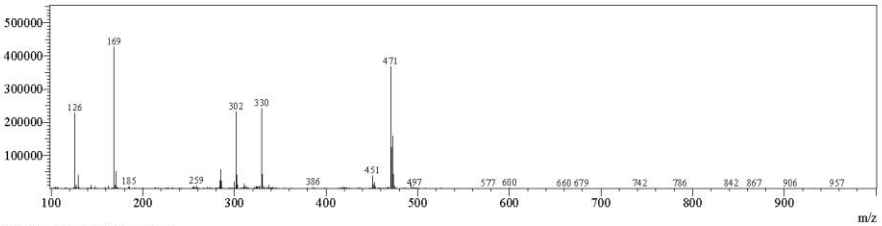

Retention Time:0.610(Scan#:62)
Max Peak:621 Base Peak:112.65(629426)
Spectrum:Averaged 0.450-0.910(46-92)
Background:Averaged 0.070-0.354(8-38) Polarity:Neg Segment1 - Event2

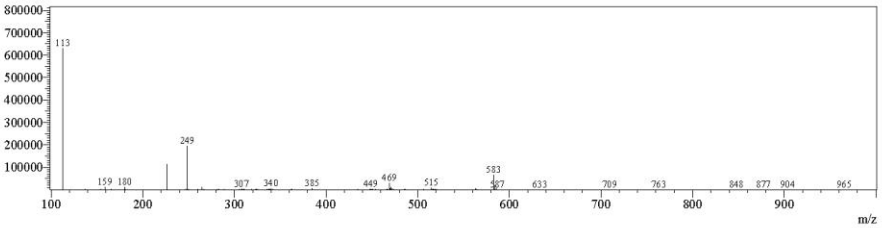

C:¥LabSolutions¥Data¥Pete¥Treiu¥tp93b4tp_APCI+.lcd

Compound	Chemical Formula	Predicted monoisotopic neutral MW	Predicted MH+	MH+ Measured	Main MS Ions	Main MS/MS Fragments
TP 93B4	$C_{27}H_{23}ClN_4O_2$	470.1510	471.15823	471.15821	471.15821*	n/a

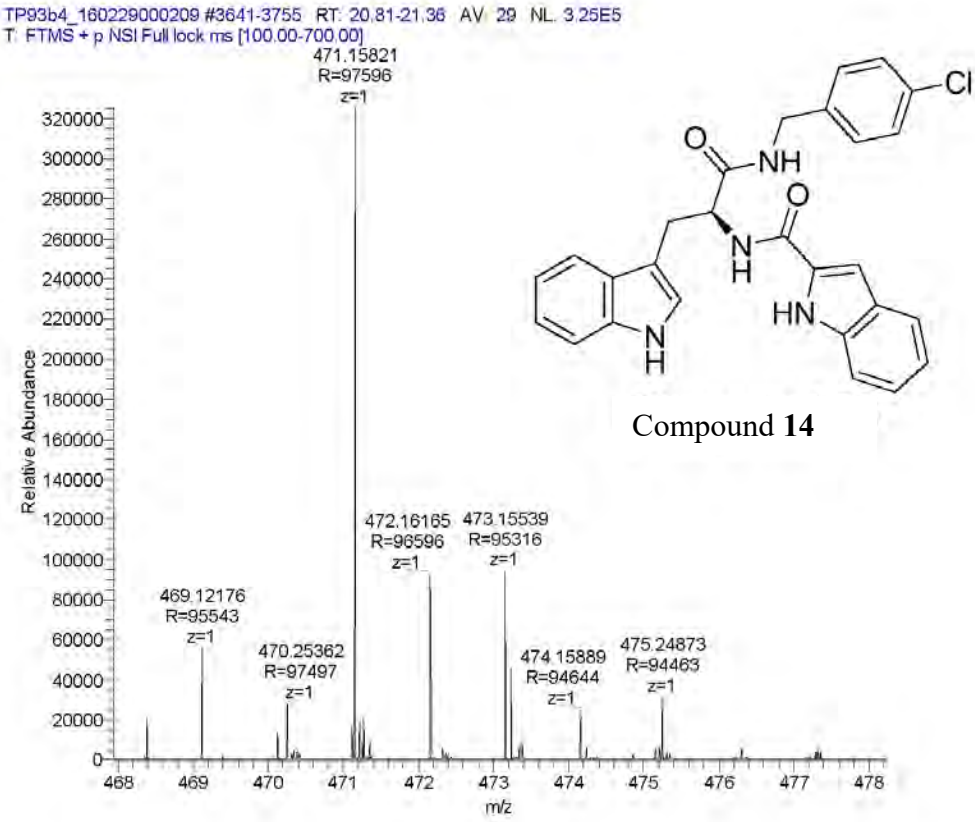

Compound **14**

COMPOUND 14a

Compound Name: *1H*-Indole-2-carboxylic acid [1-(4-chloro-benzylcarbamoyl)-2-(*1H*-indol-3-yl)-ethyl]-amide (D-isomer)

Obtained Weight & Yield: 156 mg, 48%

Appearance: Off-white powder

Solubility: EtOAc, Acetone, ACN

Melting Point: 227-227.5 ºC

TLC Conditions: EtOAc/Hexane (50/50)

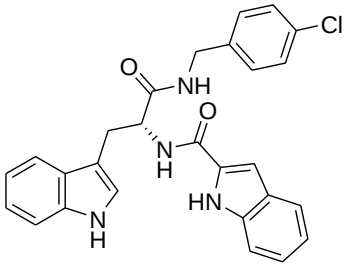

$C_{27}H_{23}ClN_4O_2$
Exact Mass: 470.1510
D-ISOMER

IR Analysis: νmax/cm^{-1}

3420 (NH), 3382 (NH), 3325 (NH), 1630 (CONH), 1656 (CON), 737 (CH-aromatics)

^{1}H NMR Analysis:

^{1}H (400 MHz, DMSO-d_6) δ 11.53 (s, 1H), 10.81 (d, J = 1.6 Hz, 1H), 8.71 (t, J = 6.0 Hz, 1H), 8.58 (d, J = 8.1 Hz, 1H), 7.72 (d, J = 7.8 Hz, 1H), 7.63 (d, J = 8.0 Hz, 1H), 7.45 – 7.39 (m, 1H), 7.37 – 7.30 (m, 3H), 7.26 – 7.14 (m, 5H), 7.11 – 6.95 (m, 3H), 4.82 (dd, J = 9.2, 5.2 Hz, 1H), 4.32 (dd, $J_{A'X'}$ =$J_{B'X'}$ = 6.0, $J_{A'B'}$= 16.0 Hz, 2H), 3.23 (ddd, J_{AX} = 5.2, J_{BX} = 9.6, J_{AB} = 14.4 Hz, 2H)..

^{13}C NMR Analysis:

^{13}C NMR (101 MHz, DMSO-d_6) δ 172.3, 161.5, 138.9, 136.9, 136.6, 131.8, 131.7, 129.3 (C x 2), 128.6 (C x 2), 127.7, 127.5, 124.3, 123.8, 122.0, 121.4, 120.2, 119.0, 118.7, 112.7, 111.8, 110.8, 103.9, 54.5, 42.0, 28.2.

HPLC:

RP-HPLC Alltima™ C18 5 µm 150 mm x 4.6 mm, 10–100% B in 15 min, R_t = 6.44 min, 100%.

Mass Spectral Analysis: LRMS (ESI+) m/z 470, 470 [M+H, ^{35}Cl]$^{+}$, 80%. HRMS (ES+) for $C_{27}H_{23}ClN_4O_2$ calculated 471.1582, found 471.1584.

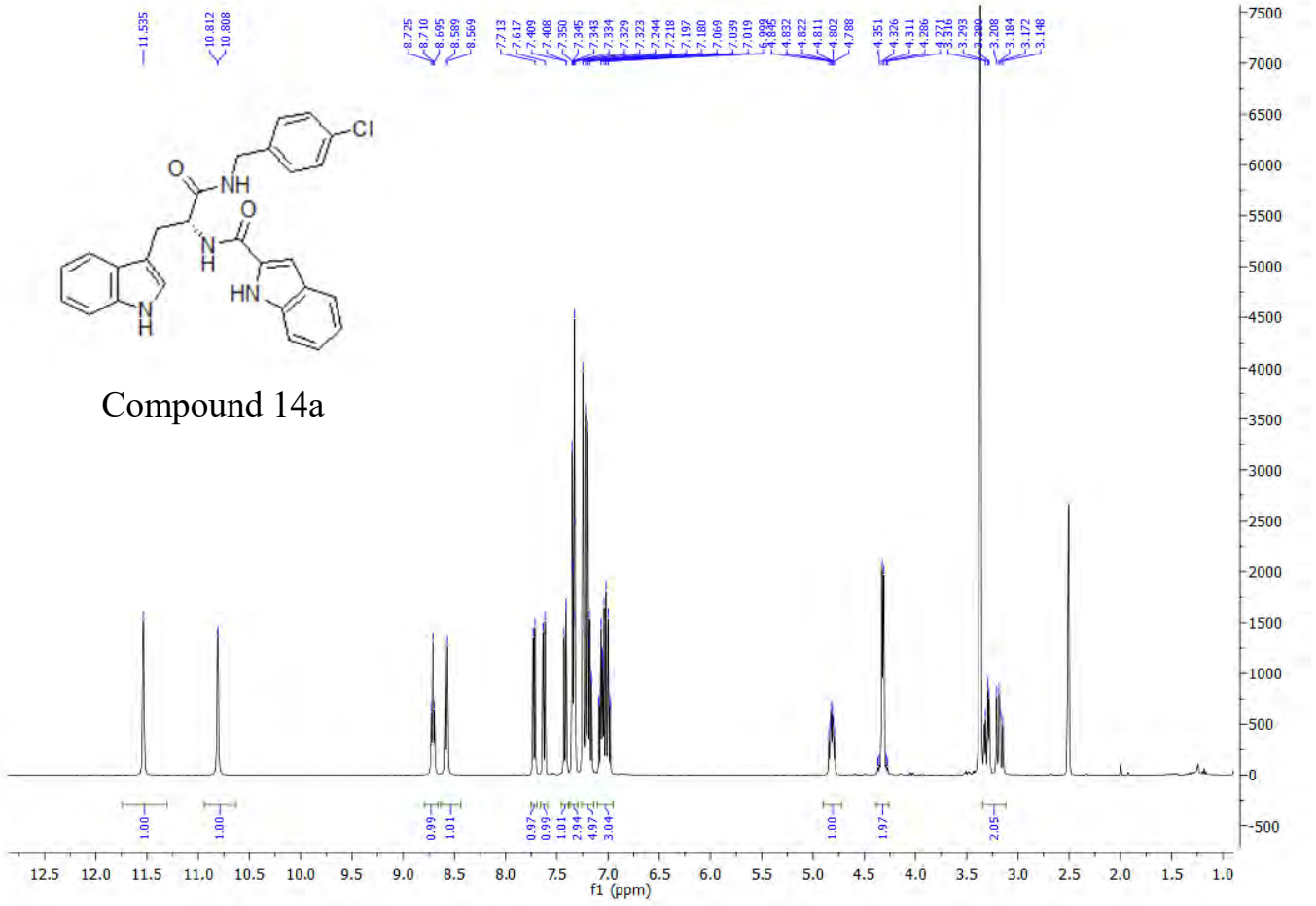

Compound 14a

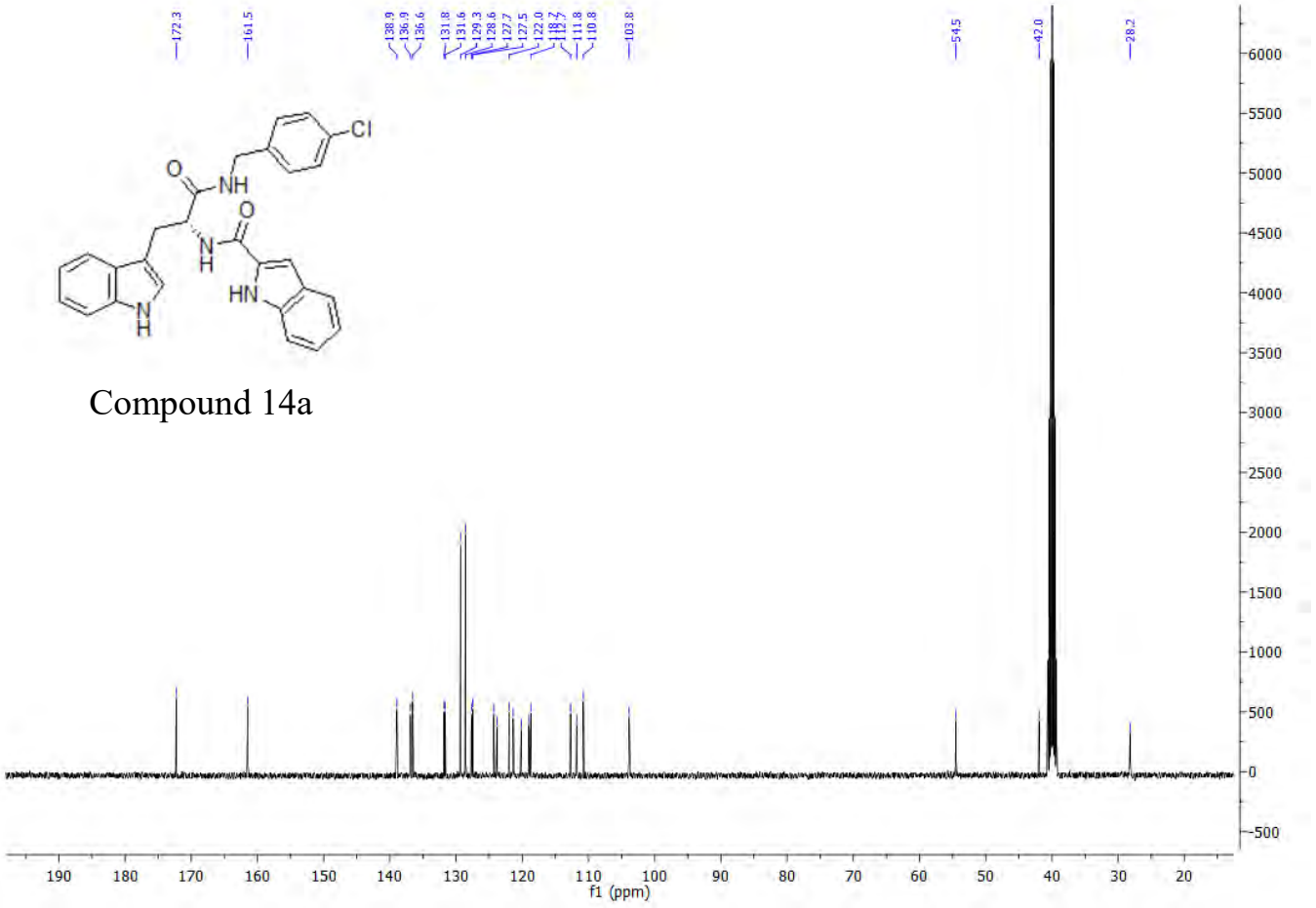

Compound 14a

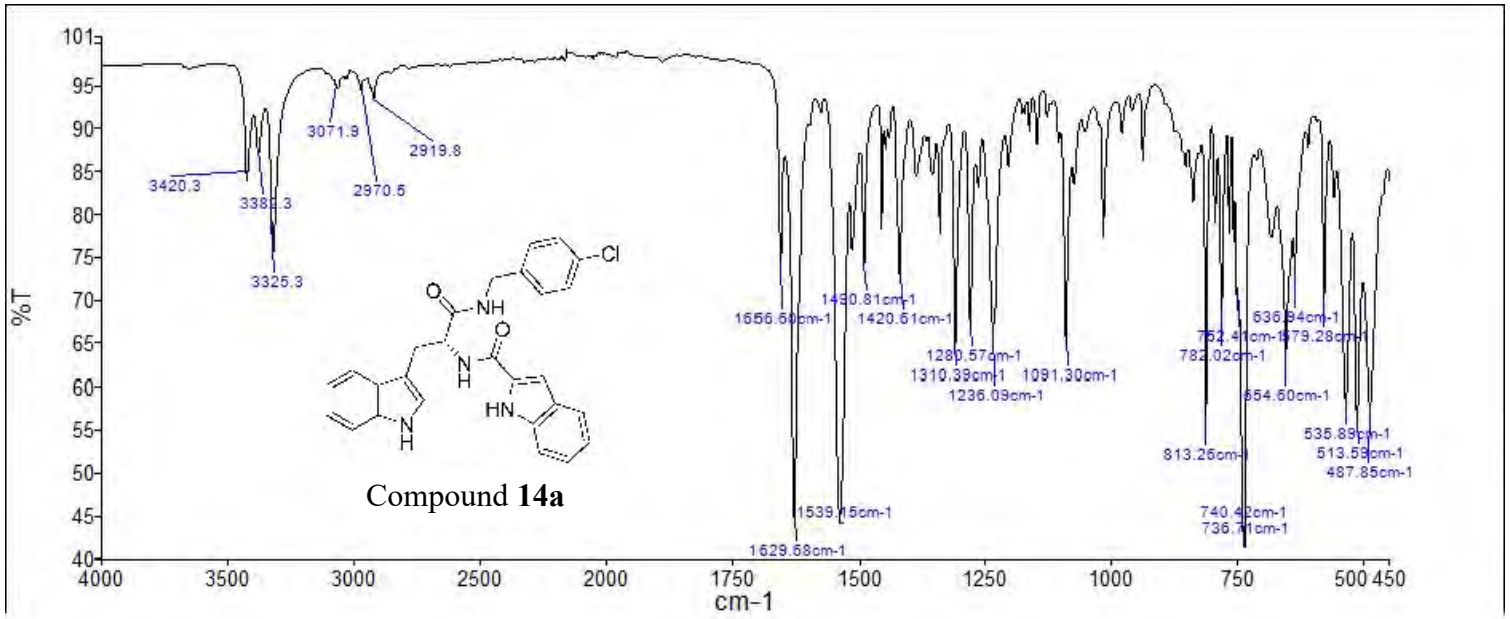

Compound **14a**

==== Shimadzu LCMSsolution Analysis Report ====

Acquired by	: Admin
Sample Name	: TP154B5 Diso
Sample ID	:
Vail #	: 55
Injection Volume	: 20 uL
Data File Name	: TP154B5 Diso.lcd
Method File Name	: Econosphere C18 EPS 5u lot 50195421 part 70070 150mm id 4.6mm.lcm
Batch File Name	: Second Isomers 10112015.lcb
Report File Name	: DefaultLCMS.lcr
Data Acquired	: 11/10/2015 11:30:26 AM
Data Processed	: 11/10/2015 11:58:21 AM

<Chromatogram>

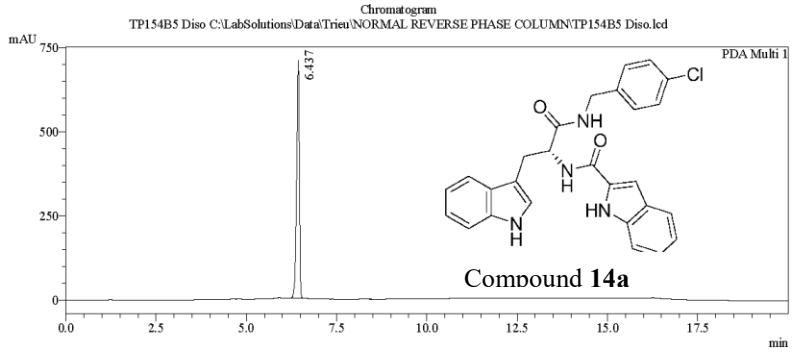

PeakTable

PDA Ch1 254nm 4nm

Peak#	Ret. Time	Area	Height	Area %	Height %
1	6.437	3727817	707496	100.000	100.000
Total		3727817	707496	100.000	100.000

PeakTable

PDA Ch2 220nm 4nm

Peak#	Ret. Time	Area	Height	Area %	Height %
1	6.448	27969882	3850186	100.000	100.000
Total		27969882	3850186	100.000	100.000

==== Shimadzu LCMSsolution Data Report ====

<Chromatogram>

Sample Information

Acquired by	: Admin
Date Acquired	: 7/31/2015 12:46:08 PM
Sample Type	: Unknown
Level#	: 0
Sample Name	: TP154B5 ESI POS
Sample ID	:
ISTD Amount	: (Level1 Conc.)
Sample Amount	: 1
Dilution Factor	: 1
Tray#	: 1
Vial#	: 56
Injection Volume	: 5
Data File	: TP154B5 ESI POS.lcd
Method File	: FIA-ESI_Scan(+).lcm
Original Method	: C:\LabSolutions\Data\Trieu\Mass spec files\FIA-ESI_Scan(+).lcm
Report Format	: DefaultLCMS.lcr
Tuning File	: C:\LabSolutions\LCsolution\Log\Tuning\Autotune_030908.lct
Processed by	: Admin
Modified Date	: 7/31/2015 12:47:41 PM

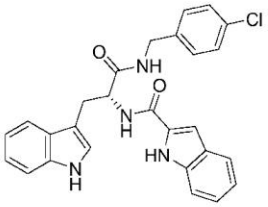

Compound **14a**

Chromatogram

TP154B5 ESI POS C:\LabSolutions\Data\Trieu\NORMAL REVERSE PHASE COLUMN\TP154B5 ESI POS.lcd

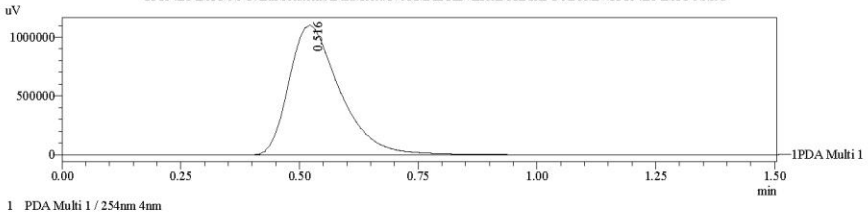

1 PDA Multi 1 / 254nm 4nm

<Spectrum>

Retention Time:0.820(Scan#:83)
Max Peak:394 Base Peak:82.65(36935)
Spectrum:Averaged 0.680-1.140(69-115)
Background:Averaged 0.080-0.448(9-45) Polarity:Pos Segment1 - Event1

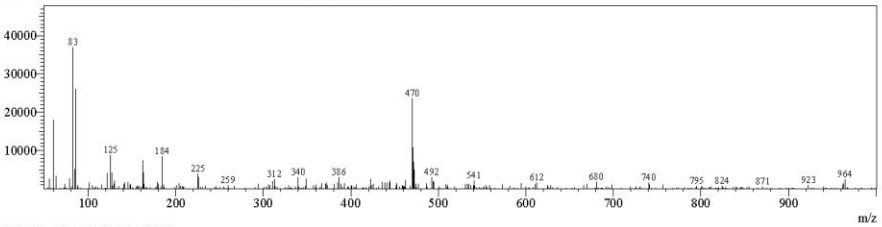

Retention Time:0.830(Scan#:84)
Max Peak:474 Base Peak:312.40(59823)
Spectrum:Averaged 0.690-1.150(70-116)
Background:Averaged 0.090-0.448(10-46) Polarity:Neg Segment1 - Event2

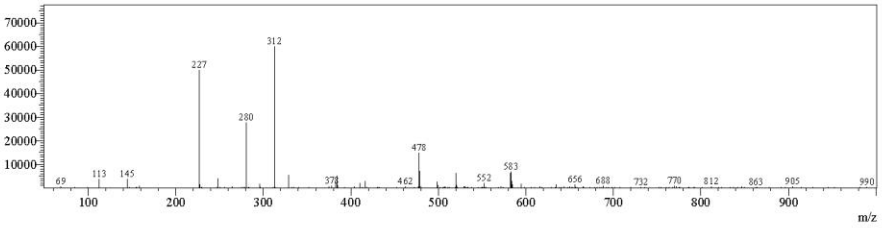

C:¥LabSolutions¥Data¥Trieu¥NORMAL REVERSE PHASE COLUMN¥TP154B5 ESI POS.lcd

Compound	Chemical Formula	Predicted monoisotopic neutral MW	Predicted MH+	MH+ Measured	Main MS Ions	Main MS/MS Fragments
TP154 B5	$C_{27}H_{23}ClN_4O_2$	470.15823	471.1510	471.15844	471.15844 302.12936 114.04477	302.1294 **285.1028** **144.0448**

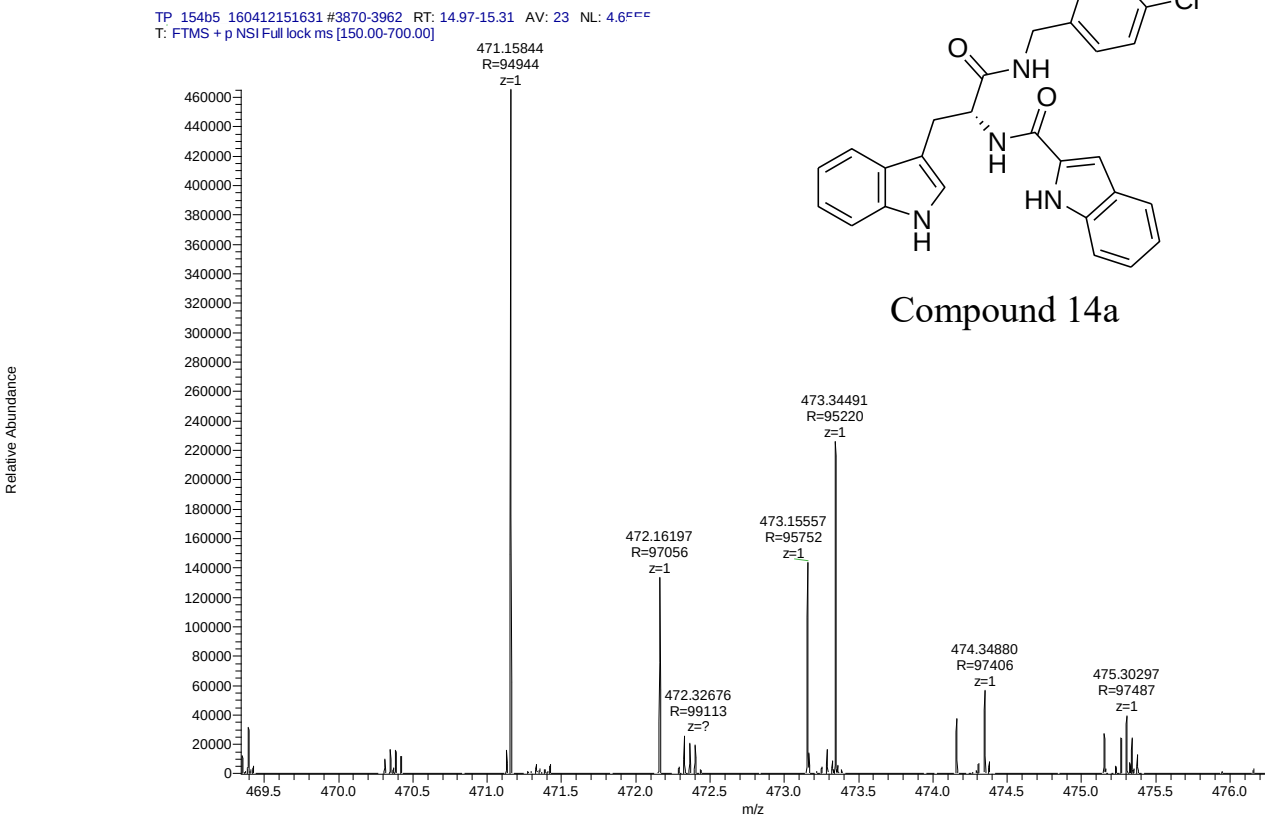

Compound 14a

COMPOUND 15

Compound Name: Naphthalene-1-carboxylic acid [1-(4-chloro-benzylcarbamoyl)-2-(*1H*-indol-3-yl)-ethyl]-amide

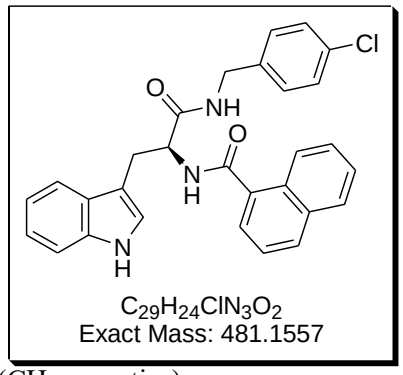

Obtained Weight & Yield: 57 mg, 41%

Appearance: Off-white powder

Solubility: EtOAc, Acetone, ACN

Melting Point: 165.7-166.5 ºC

TLC Conditions: EtOAc/Hexane (50/50)

IR Analysis: νmax/cm^{-1}

3398 (NH), 3268 (bp NH), 3049 (CH), 1627 (CON), 739 (CH-aromatics)

^{1}H NMR Analysis:

^{1}H NMR (400 MHz, DMSO-d_6) δ 10.89 (s, 1H), 8.73−8.67 (m, 2H) (overlapped two NH amides), 8.02 – 7.86 (m, 3H), 7.74 (d, J = 7.8 Hz, 1H), 7.57 – 7.47 (m, 3H), 7.47 – 7.32 (m, 4H), 7.27 (d, J = 8.5 Hz, 3H), 7.11 (dd, J = 11.1, 3.9 Hz, 1H), 7.02 (dd, J = 11.0, 3.9 Hz, 1H), 4.93 (ddd, J = 9.3, 5.2 Hz, 1H), 4.37 (ddd, $J_{A'X'}$ =$J_{B'X'}$ = 8.0, $J_{A'B'}$= 16.0 Hz, 2H), 3.23 (ddd, J_{AX} = 5.2, J_{BX}= 9.6, J_{AB} = 14.4 Hz, 2H).

^{13}C NMR Analysis:

^{13}C NMR (101 MHz, DMSO-d_6) δ 172.3, 169.0, 139.0, 136.7, 135.0, 133.5, 131.7, 130.2 (C x 2), 129.4 (C x 2), 128.6 (C x 3), 127.8, 126.9, 126.6, 126.0, 125.8, 125.3, 124.4, 121.4, 119.1, 118.7, 111.8, 110.7, 54.8, 42.0, 28.1.

HPLC:

RP-HPLC Alltima™ C18 5 µm 150 mm x 4.6 mm, 10–100% B in 15 min, R_t = 13.6 min, 99.1%

Mass Spectral Analysis: LRMS (APCI+) m/z 481, 482 $[M+H, {}^{35}Cl]^+$, 90%. HRMS (ES+) for $C_{29}H_{24}ClN_3O_2$, calculated 482.1630, found 482.1630.

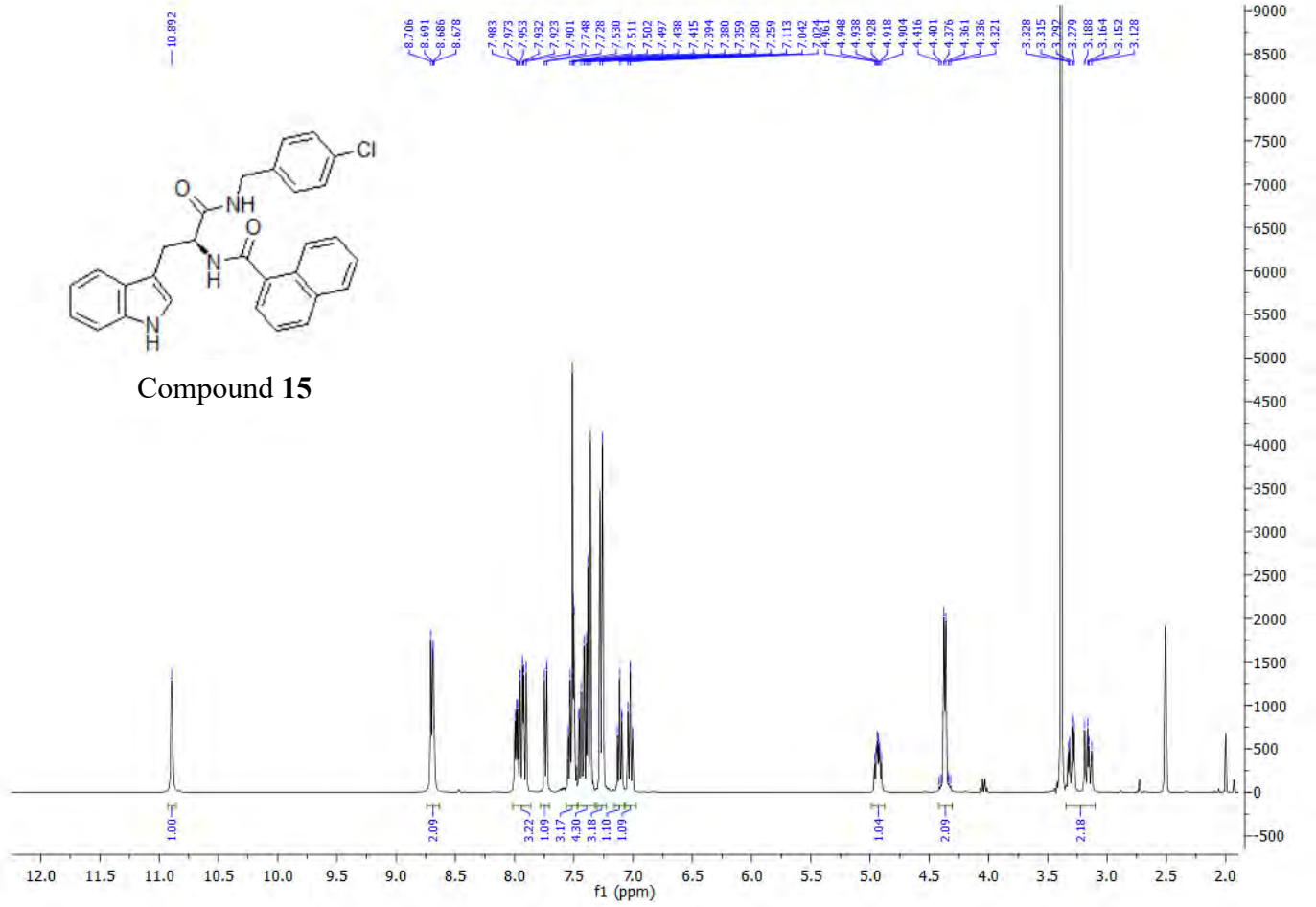

Compound **15**

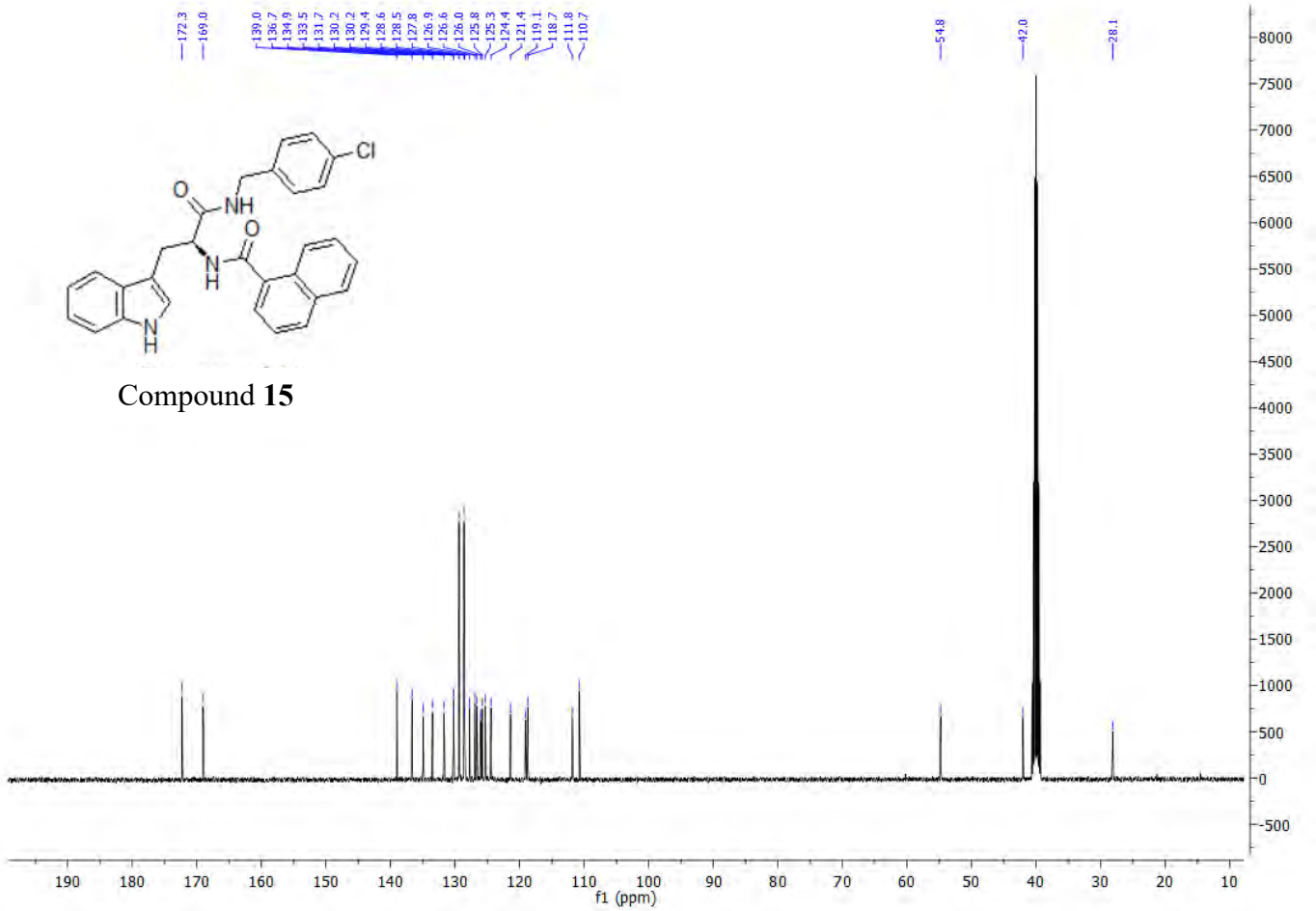
172.3
169.0
139.0
136.7
134.9
133.5
131.7
130.2
129.4
128.6
128.5
127.8
126.9
126.6
126.0
125.8
125.3
124.4
121.4
119.1
118.7
111.8
110.7
54.8
42.0
28.1
Cl
O
NH
O
N
H
N
H
8000
7500
7000
6500
6000
5500
5000
4500
4000
3500
3000
2500
2000
1500
1000
500
0
-500
190
180
170
160
150
140
130
120
110
100
90
80
70
60
50
40
30
20
10
f1 (ppm)

Compound **15**

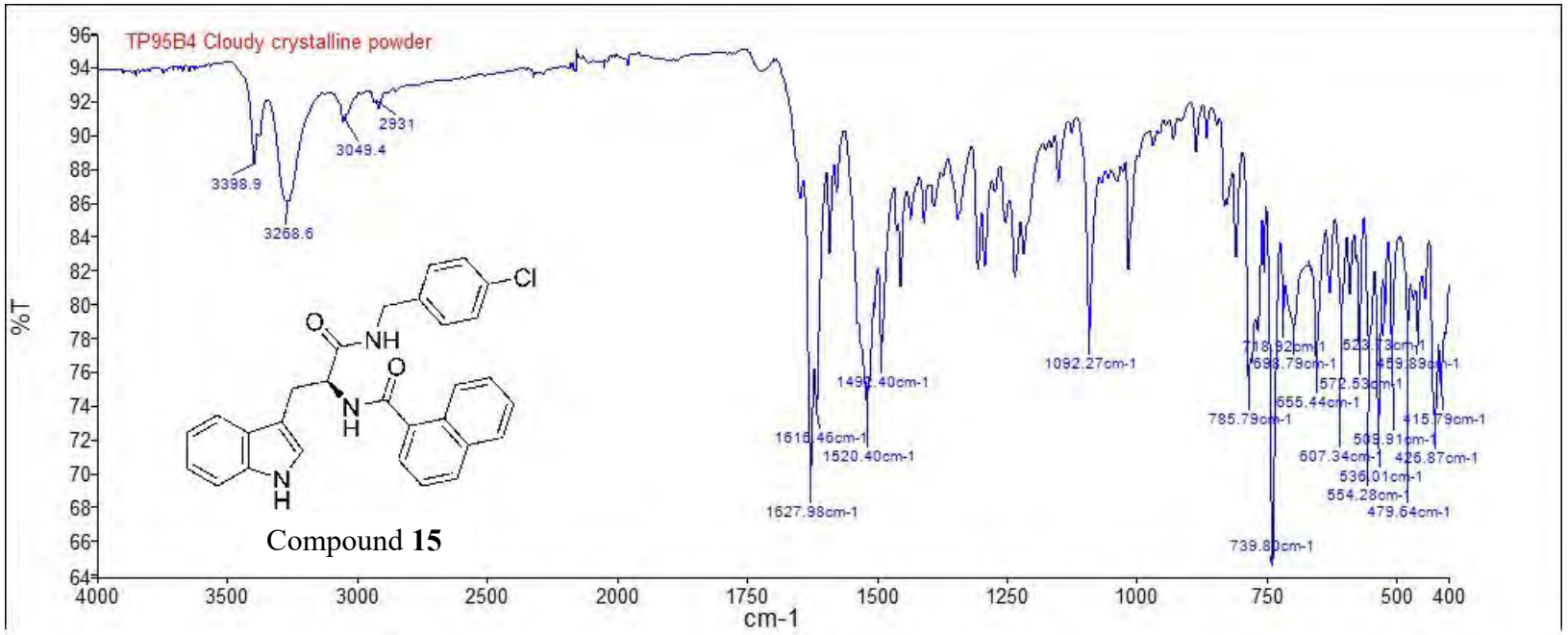
TP95B4 Cloudy crystalline powder
%T
cm-1
3398.9
3268.6
3049.4
2931
1627.98cm-1
1616.46cm-1
1520.40cm-1
1492.40cm-1
1092.27cm-1
739.80cm-1
785.79cm-1
655.44cm-1
607.34cm-1
554.28cm-1
536.01cm-1
509.91cm-1
479.64cm-1
426.87cm-1
415.79cm-1
572.53cm-1
Cl
NH
N
H
O
O
N
H

Compound **15**

SHIMADZU LabSolutions **Analysis Report**

<Sample Information>

Sample Name	: TP95B4		
Sample ID	: TP95B4		
Data Filename	: TP95B4.lcd		
Method Filename	: 10-100 over 15 mins.lcm		
Batch Filename	: TRIEU Second Third Generation and New pro.lcb		
Vial #	: 1-6	Sample Type	: Unknown
Injection Volume	: 30 uL		
Date Acquired	: 5/09/2014 1:07:52 PM	Acquired by	: System Administrator
Date Processed	: 5/09/2014 1:37:54 PM	Processed by	: System Administrator

<Chromatogram>

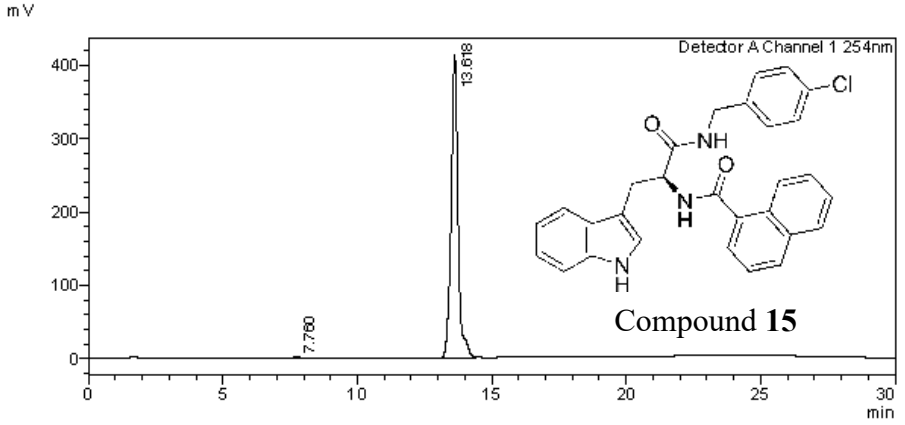

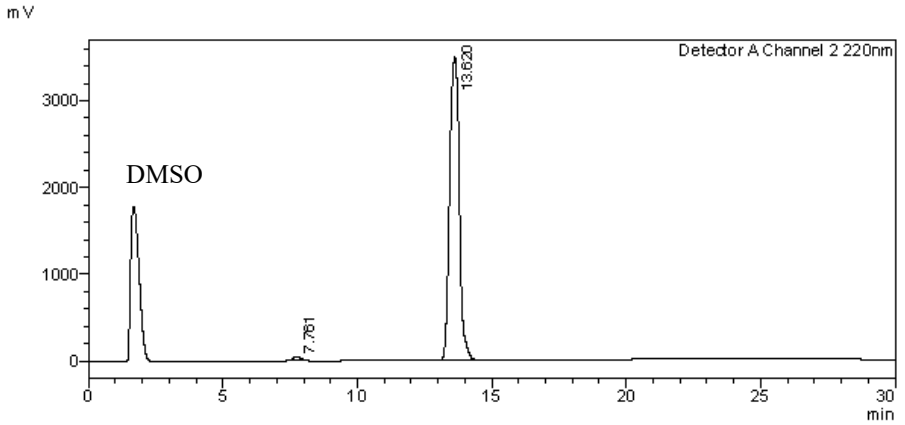

<Peak Table>

Detector A Channel 1 254nm

C:\LabSolutions\Data\Project1\TRIEU\TP95B4.lcd

Total		7234925	414636				

Detector A Channel 2 220nm

Peak#	Ret. Time	Area	Height	Conc.	Unit	Mark	Name
1	7.761	785103	41668	0.904		M	
2	13.620	86104280	3490680	99.096		M	
Total		86889383	3532349				

==== Shimadzu LCMSsolution Data Report ====

<Chromatogram>

Sample Information

Acquired by	: Admin
Date Acquired	: 11/18/2014 2:24:15 PM
Sample Type	: Unknown
Level#	: 0
Sample Name	: TP95B4_APCI+
Sample ID	:
ISTD Amount	: (Level1 Conc.)
Sample Amount	: 1
Dilution Factor	: 1
Tray#	: 1
Vial#	: 10
Injection Volume	: 10
Data File	: TP95B4_APCI+.lcd
Method File	: FIA-APCI_scan(+).lcm
Original Method	: C:\LabSolutions\Data\Pete\FIA-APCI_scan(+).lcm
Report Format	: DefaultLCMS.lcr
Tuning File	: C:\LabSolutions\LCsolution\Log\Tuning\Autotune_030908.lct
Processed by	: Admin
Modified Date	: 11/18/2014 2:25:47 PM

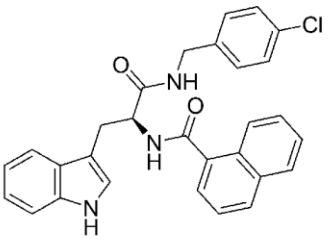

Compound **15**

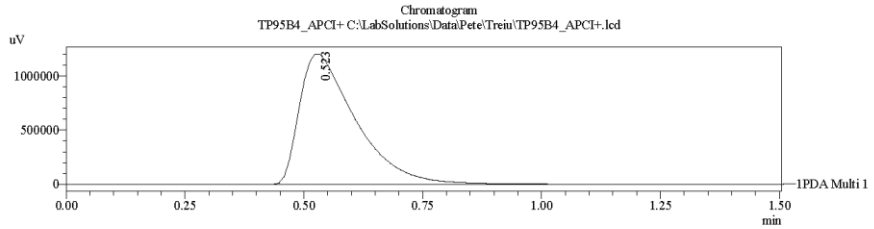

1 PDA Multi 1 / 254nm 4nm

<Spectrum>

Retention Time:0.580(Scan#:59)
Max Peak:652 Base Peak:340.90(659689)
Spectrum:Averaged 0.460-0.960(47-97)
Background:Averaged 0.040-0.347(5-35) Polarity:Pos Segment1 - Event1

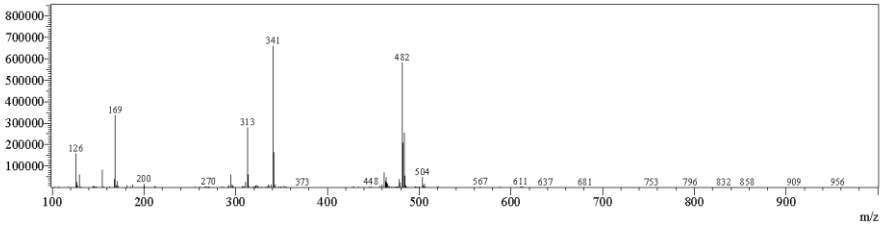

Retention Time:0.630(Scan#:64)
Max Peak:610 Base Peak:112.60(815311)
Spectrum:Averaged 0.470-0.970(48-98)
Background:Averaged 0.050-0.347(6-36) Polarity:Neg Segment1 - Event2

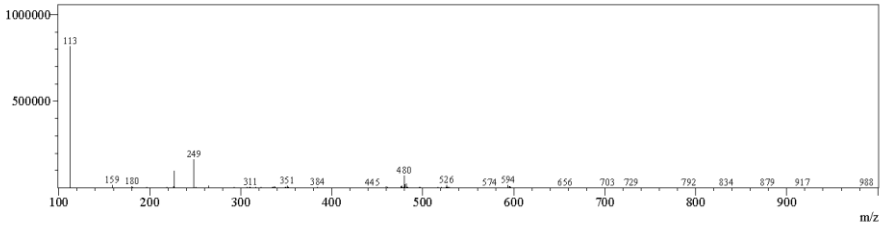

C:¥LabSolutions¥Data¥Pete¥Treiu¥TP95B4_APCI+.lcd

Compound	Chemical Formula	Predicted monoisotopic neutral MW	Predicted MH+	MH+ Measured	Main MS Ions	Main MS/MS Fragments
TP 95B4	$C_{29}H_{24}ClN_3O_2$	481.1557	482.1630	482.16300	482.16300*	313.1342 155.0495 130.0656

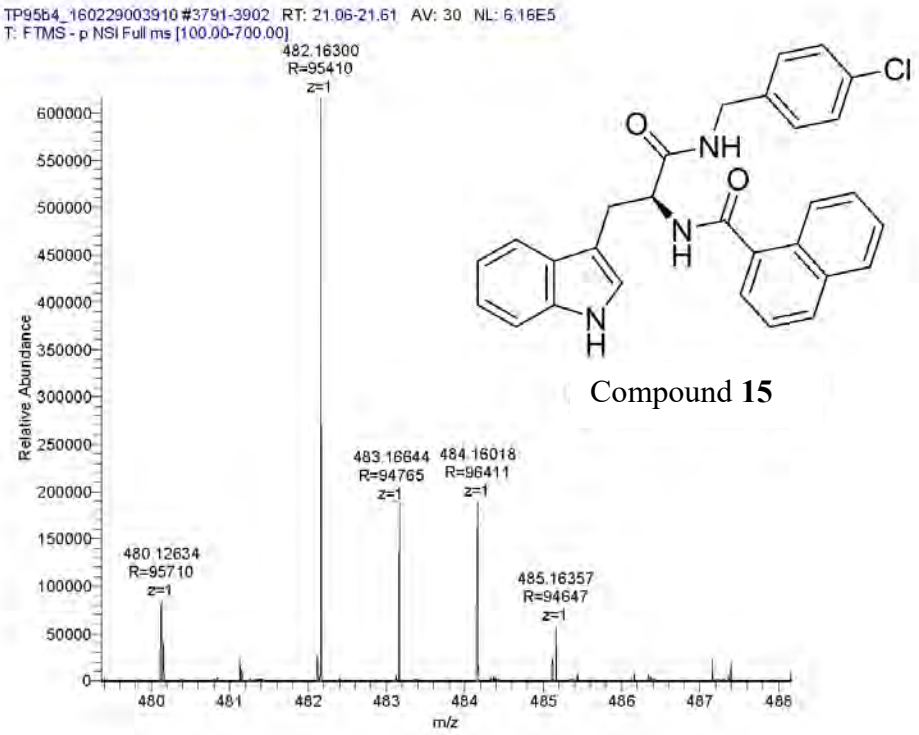

Compound **15**

COMPOUND 16

Compound Name: 4-Benzoyl-*N*-[1-(4-chloro-benzylcarbamoyl)-2-(*1H*-indol-3-yl)- ethyl]-benzamide

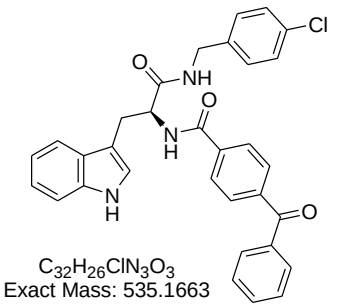

$C_{32}H_{26}ClN_3O_3$
Exact Mass: 535.1663

Obtained Weight & Yield: 120 mg, 45%

Appearance: White powder **Solubility:** EtOAc, Acetone, ACN **Melting Point:** 202 − 202.5 ºC

TLC Conditions: EtOAc/Hexane (50/50)

IR Analysis: νmax/cm^{-1}

3440 (NH), 3304 (NH), 1662 (CO), 1632 (CON), 743 (CH-aromatics)

^{1}H NMR Analysis:

^{1}H NMR (400 MHz, DMSO-d_6) δ 10.80 (s, 1H), 8.80 (d, J = 8.0 Hz, 1H), 8.68 (t, J = 5.9 Hz, 1H), 8.00 (d, J = 8.4 Hz, 2H), 7.81 – 7.66 (m, 6H), 7.58 (t, J = 7.6 Hz, 2H), 7.33 (dd, J = 8.2, 3.5 Hz, 3H), 7.21 (dd, J = 9.2, 5.3 Hz, 3H), 7.03 (dt, J = 30.0, 7.0 Hz, 2H), 4.81 (dd, J = 9.3, 5.2 Hz, 1H), 4.30 (ddd, $J_{A'X'}$ = 5.6, $J_{B'X'}$ = 4.4, $J_{A'B'}$ = 15.6 Hz, 2H), 3.25 (ddd, J_{AX} = 5.2, J_{BX} = 9.7, J_{AB} = 14.4 Hz, 2H).

^{13}C NMR Analysis:

^{13}C NMR (101 MHz, DMSO-d_6) δ 195.9, 172.1, 166.0, 139.7, 138.9, 137.8, 137.1, 136.6, 133.5, 131.7, 130.2 (C x 2), 129.8 (C x 2), 129.3 (C x 2), 129.1 (C x 2), 128.6 (C x 2), 128.2 (C x 2), 127.7, 124.2, 121.4, 119.0, 118.7, 111.8, 110.8, 55.0, 42.0, 28.0.

HPLC:

RP-HPLC Alltima™ C18 5 µm 150 mm x 4.6 mm, 10–100% B in 15 min, R_t = 14.1 min, 100%

Mass Spectral Analysis: LRMS (APCI+) m/z 535, 536 [M+H, ^{35}Cl]$^{+}$, 20%. HRMS (ES+), for $C_{32}H_{26}ClN_3O_3$, calculated 536.1735, found 536.1735.

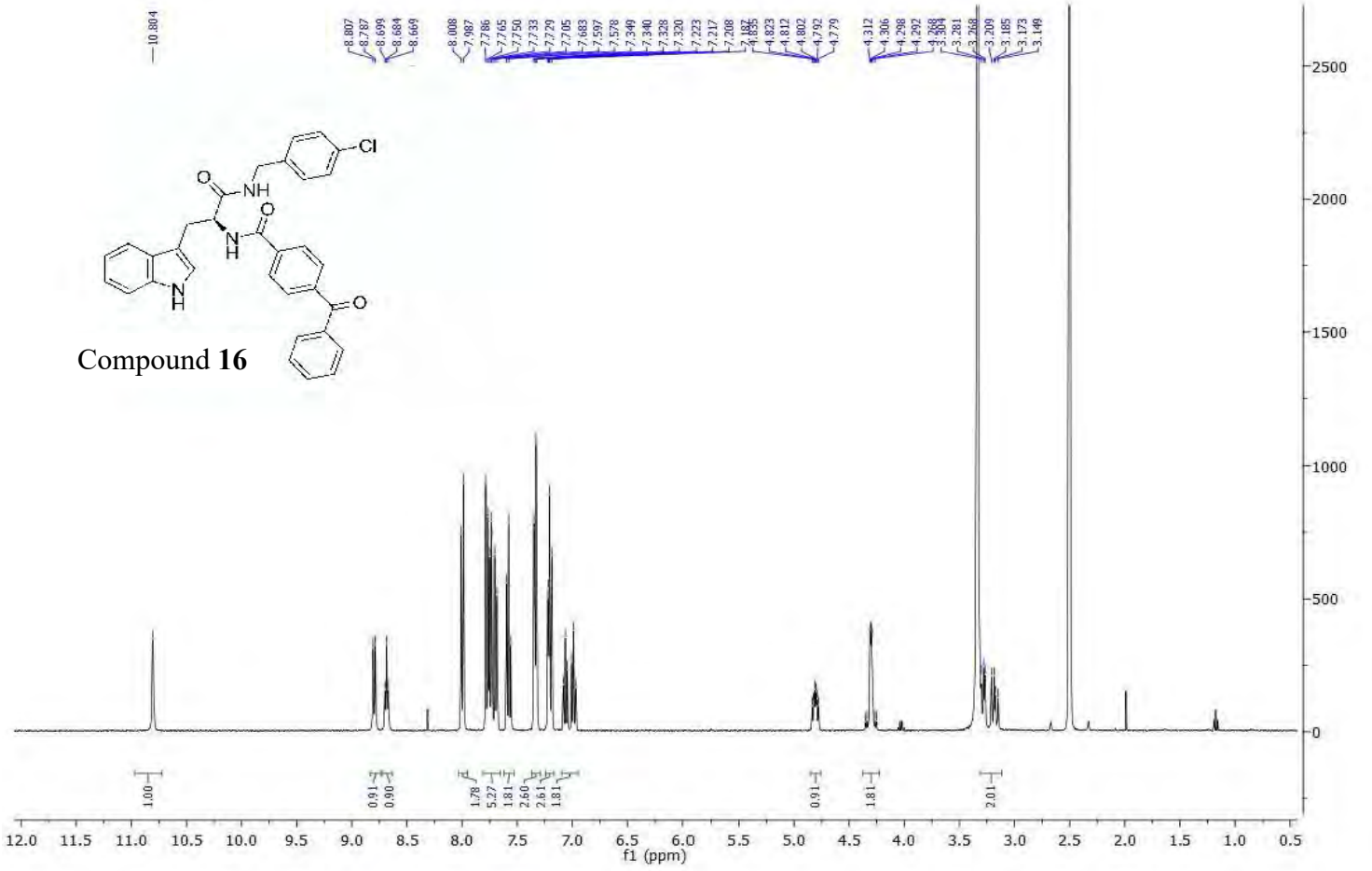
Cl
O
NH
O
N
H
N
H
O
O
10.804
8.807
8.787
8.699
8.684
8.669
8.008
7.987
7.786
7.765
7.750
7.733
7.729
7.705
7.683
7.597
7.578
7.349
7.340
7.328
7.320
7.223
7.217
7.208
4.823
4.812
4.802
4.792
4.779
4.312
4.306
4.298
4.292
3.281
3.268
3.209
3.185
3.173
3.149
2500
2000
1500
1000
500
0
1.00
0.91
0.90
1.78
5.27
1.81
2.60
2.61
1.81
0.91
1.81
2.01
12.0
11.5
11.0
10.5
10.0
9.5
9.0
8.5
8.0
7.5
7.0
6.5
6.0
5.5
5.0
4.5
4.0
3.5
3.0
2.5
2.0
1.5
1.0
0.5
f1 (ppm)

Compound **16**

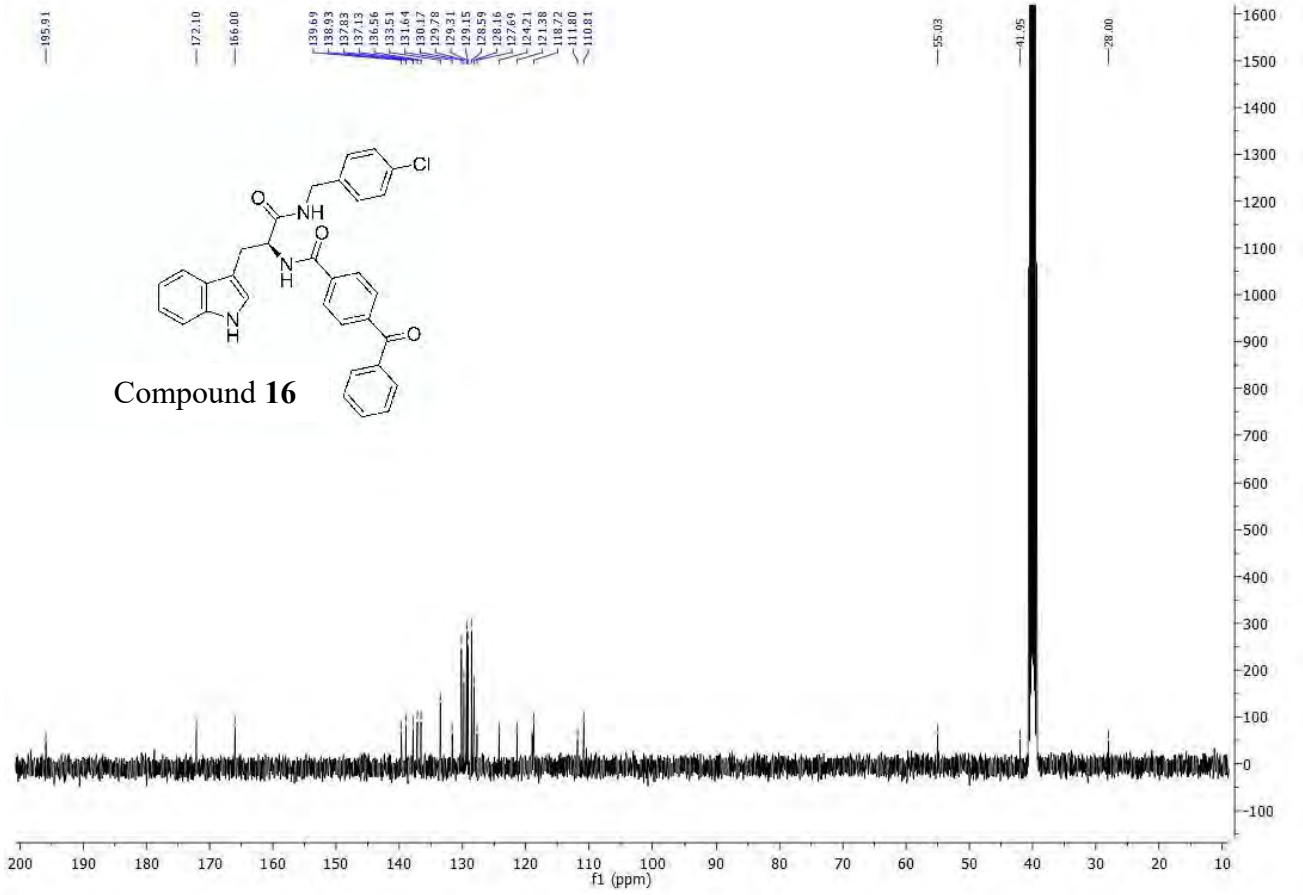
195.91
172.10
166.00
139.69
138.93
137.83
137.13
136.56
133.51
131.64
130.17
129.78
129.31
129.15
128.59
128.16
127.69
124.21
121.38
118.72
111.80
110.81
55.03
41.95
28.00
Cl
O
NH
O
N
H
N
H
O
f1 (ppm)

Compound **16**

SHIMADZU LabSolutions

Analysis Report

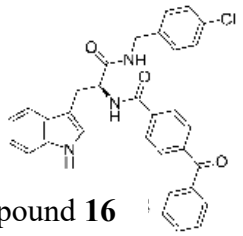

Compound **16**

<Sample Information>

Sample Name	: TP67B4		
Sample ID	: TP67B4		
Data Filename	: TP67B4.lcd		
Method Filename	: 10-100 over 15 mins.lcm		
Batch Filename	: TRIEU Second Third Generation and New pro.lcb		
Vial #	: 1-2	Sample Type	: Unknown
Injection Volume	: 30 uL		
Date Acquired	: 5/09/2014 11:06:13 AM	Acquired by	: System Administrator
Date Processed	: 5/09/2014 11:36:15 AM	Processed by	: System Administrator

<Chromatogram>

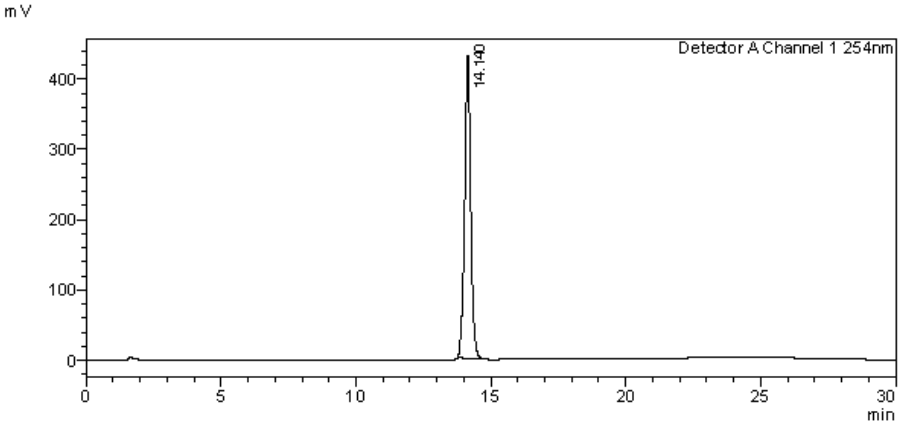

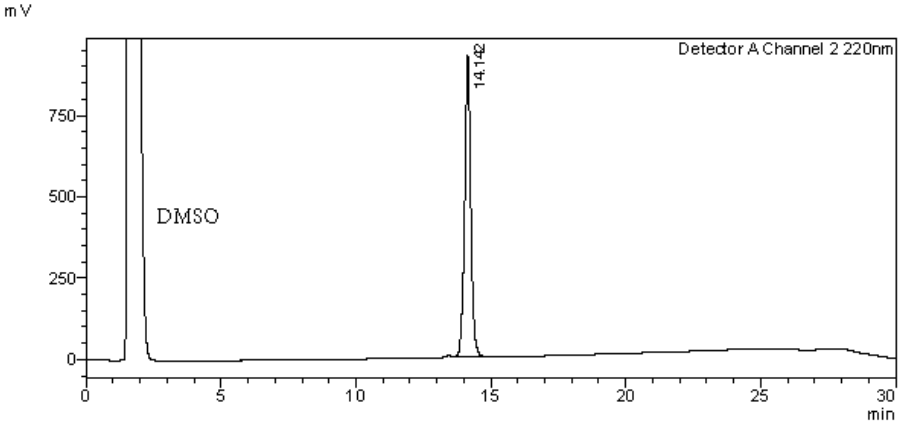

<Peak Table>

Detector A Channel 1 254nm

Peak#	Ret. Time	Area	Height	Conc.	Unit	Mark	Name
1	14.140	6746503	429754	100.000		M	
Total		6746503	429754				

Detector A Channel 2 220nm

Peak#	Ret. Time	Area	Height	Conc.	Unit	Mark	Name
1	14.142	14576069	923318	100.000		M	
Total		14576069	923318				

==== Shimadzu LCMSsolution Data Report ====

<Chromatogram>

Sample Information

Acquired by	: Admin
Date Acquired	: 11/18/2014 3:12:16 PM
Sample Type	: Unknown
Level#	: 0
Sample Name	: TP67B4_APCI-
Sample ID	:
ISTD Amount	: (Level1 Conc.)
Sample Amount	: 1
Dilution Factor	: 1
Tray#	: 1
Vial#	: 11
Injection Volume	: 10
Data File	: TP67B4_APCI-.lcd
Method File	: FIA-APCI_scan(-).lcm
Original Method	: C:\LabSolutions\Data\Pete\FIA-APCI_scan(-).lcm
Report Format	: DefaultLCMS.lcr
Tuning File	: C:\LabSolutions\LCsolution\Log\Tuning\Autotune_030908.lct
Processed by	: Admin
Modified Date	: 11/18/2014 3:13:47 PM

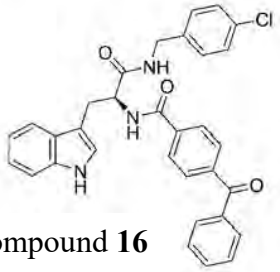

Compound **16**

Chromatogram
TP67B4_APCI- C:\LabSolutions\Data\Pete\Treiu\TP67B4_APCI-.lcd

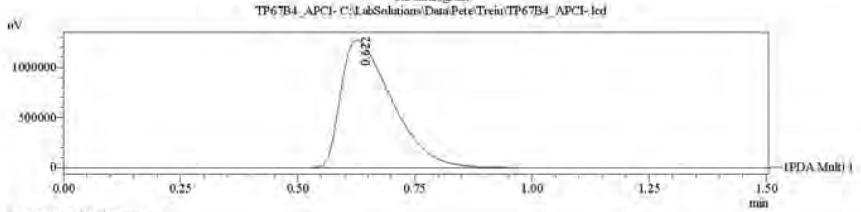

1 PDA Multi 1 / 254nm 4nm

<Spectrum>

Retention Time:0.760(Scan#:77)
Max Peak:599 Base Peak:156.70(619591)
Spectrum:Averaged 0.520-1.100(53-111)
Background:Averaged 0.080-0.460(9-47) Polarity:Pos Segment1 - Event1

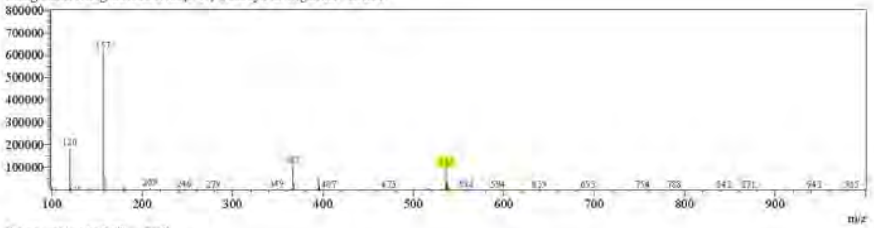

Retention Time:0.710(Scan#:72)
Max Peak:541 Base Peak:112.55(291891)
Spectrum:Averaged 0.530-1.110(54-112)
Background:Averaged 0.090-0.460(10-48) Polarity:Neg Segment1 - Event2

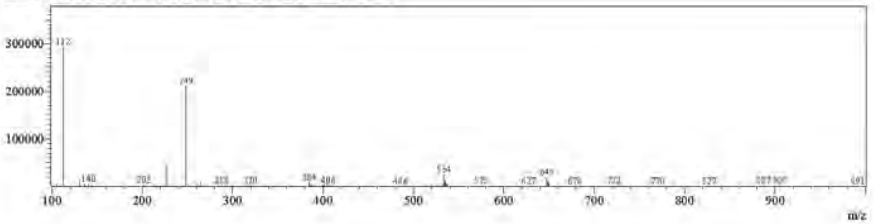

C:¥LabSolutions¥Data¥Pete¥Treiu¥TP67B4_APCI-.lcd

Compound	Chemical Formula	Predicted monoisotopic neutral MW	Predicted MH+	MH+ Measured	Main MS Ions	Main MS/MS Fragments
TP 67B4	$C_{32}H_{24}ClN_3O_3$	535.1663	536.1735	536.1735	536.17351*	367.1444 209.5099 130.0654

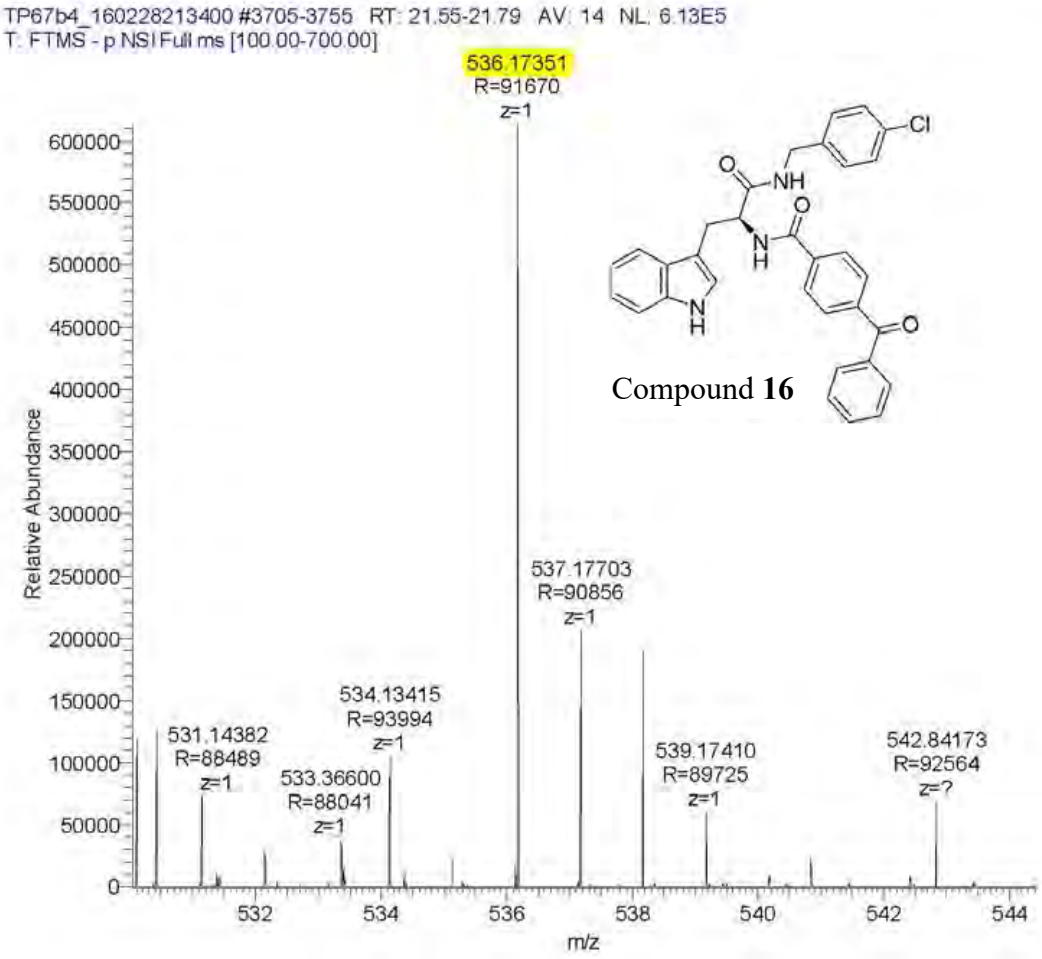

Compound **16**

COMPOUND 17

Compound Name: *N*-[1-(4-Chloro-benzylcarbamoyl)-2-(*1H*-indol-3-yl)-ethyl]-3,3,3-trifluoro-2-methoxy-2-phenyl-propionamide

Obtained Weight & Yield: 171 mg, 71%

Appearance: White powder

Solubility: DMSO

Melting Point: 171 − 172^{0}C

TLC Conditions: EtOAc/Hexane (50/50)

IR Analysis: νmax/cm^{-1}

3310 (bp,NH), 2925 (CH), 1657 (CON), 741 (CH-aromatics)

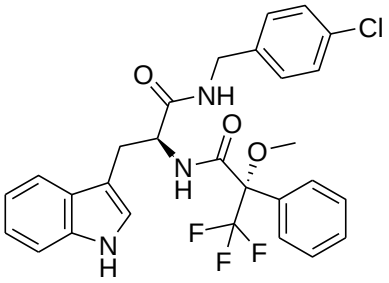

$C_{28}H_{25}ClF_3N_3O_3$
Mol. Wt.: 543.9646

^{1}H NMR Analysis:

^{1}H NMR (400 MHz, DMSO-d_6) δ 10.82 (s, 1H), 8.70 (t, J = 8.0 Hz, 1H), 8.17 (d, J = 8.5 Hz, 1H), 7.62 (d, J = 7.9 Hz, 1H), 7.43 – 7.32 (m, 4H), 7.30 – 7.18 (m, 4H), 7.13 – 7.01 (m, 3H), 7.01 – 6.90 (m, 2H), 4.81 (dd, J = 8.0, 4.0 Hz, 1H), 4.32 (ddd, $J_{A'X'}$ = 6.0, $J_{B'X'}$ = 8.0, $J_{A'B'}$ = 16.0 Hz, 2H), 3.27 (s, 3H), 3.15 (ddd, J_{AX} = 4, J_{BX} = 8, J_{AB} = 16.0 Hz, 2H).

^{13}C NMR Analysis:

^{13}C NMR (101 MHz, DMSO-d_6) δ 171.4, 165.6, 138.6, 136.6, 132.8, 131.8, 129.8, 129.4 (C x 4), 128.7 (C x 2), 128.6 (C x 4), 127.8, 124.4, 121.4, 119.0, 118.7, 111.7, 109.9, *84.4, 84.2, 83.9, 83.7*, 55.2, 53.8, 42.0, 28.1.

Note: CF_3 splitting are detected at 84.0 (q, J = 25.2 Hz) and presented in italic values

Mass Spectral Analysis: LRMS (APCI+) m/z 543, 544 [M+ H, ^{35}Cl]$^+$, 50%. HRMS (ES+) for $C_{28}H_{25}ClF_3N_3O_3$, calculated 543.1646, found 544.1611

HPLC:

RP-HPLC Alltima™ C18 5µm 150 mm x 4.6 mm, 10–100% B in 15 min, R_t = 14.5 min, 100%

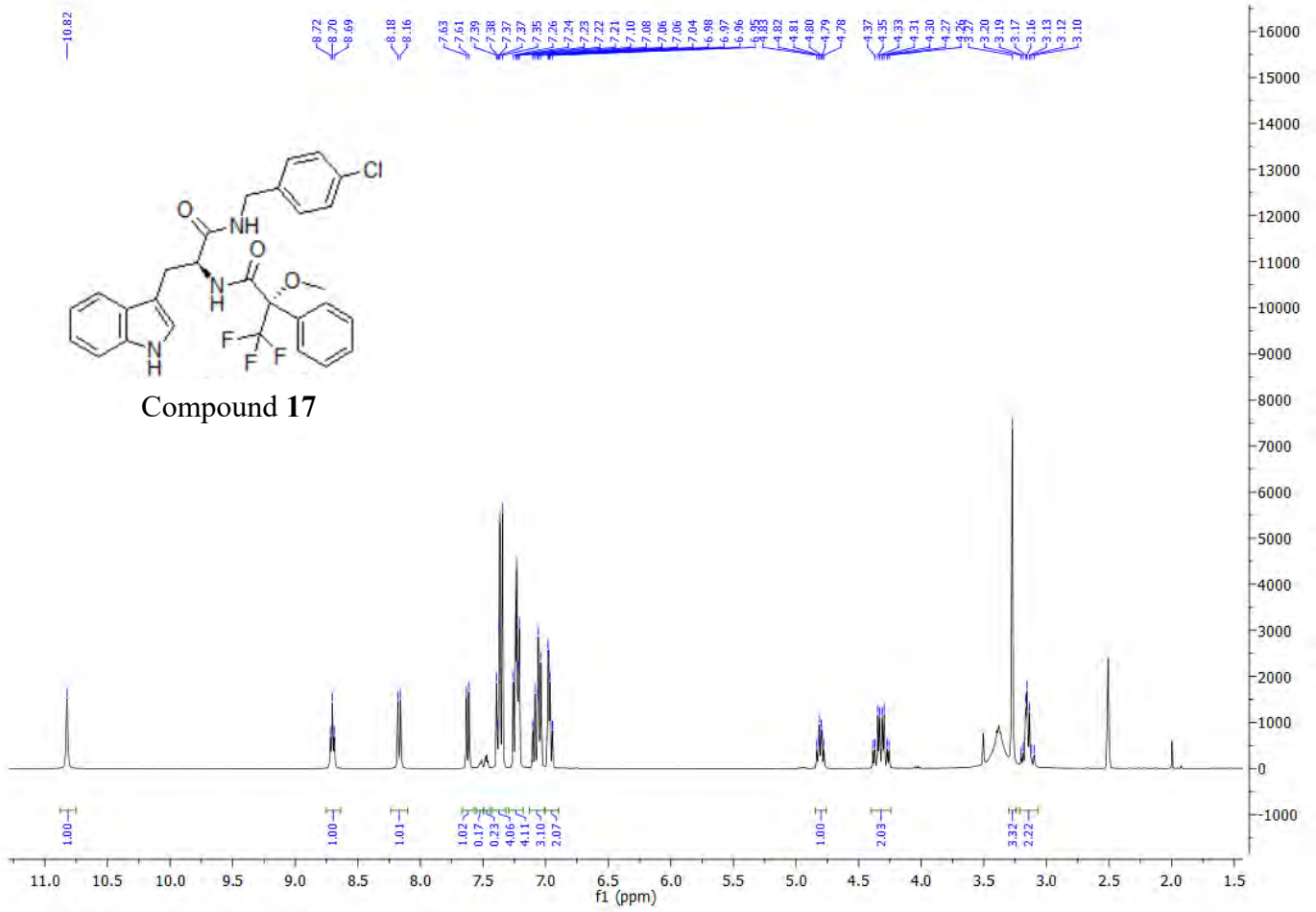

Compound **17**

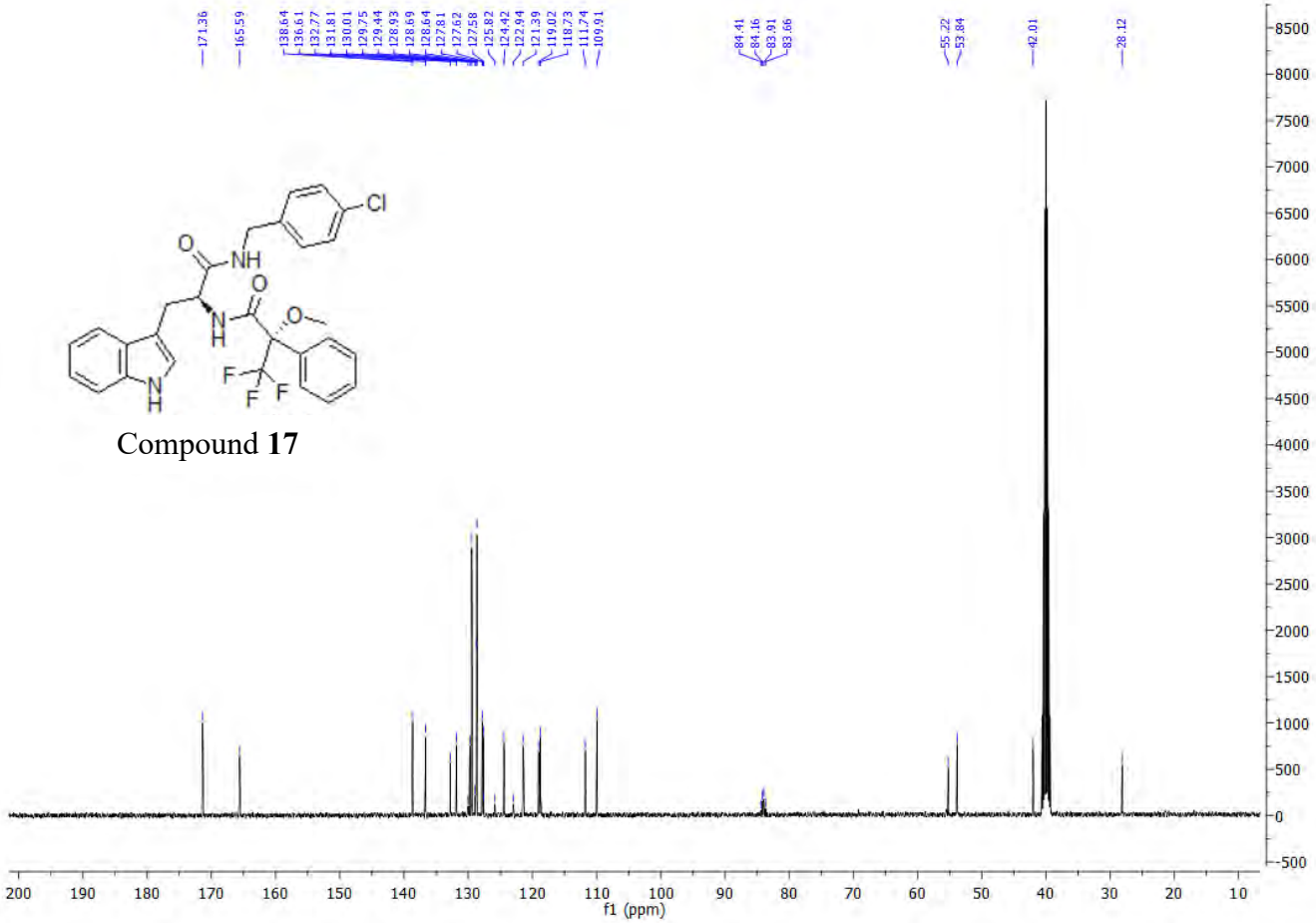
171.36
165.59
138.64
136.61
132.77
131.81
130.01
129.75
129.44
128.93
128.69
128.64
127.81
127.62
127.58
125.82
124.42
122.94
121.39
119.02
118.73
111.74
109.91
84.41
84.16
83.91
83.66
55.22
53.84
42.01
28.12
Cl
O
NH
O
N
H
O
F
F
F
N
H
8500
8000
7500
7000
6500
6000
5500
5000
4500
4000
3500
3000
2500
2000
1500
1000
500
0
-500
200
190
180
170
160
150
140
130
120
110
100
90
80
70
60
50
40
30
20
10
f1 (ppm)

Compound **17**

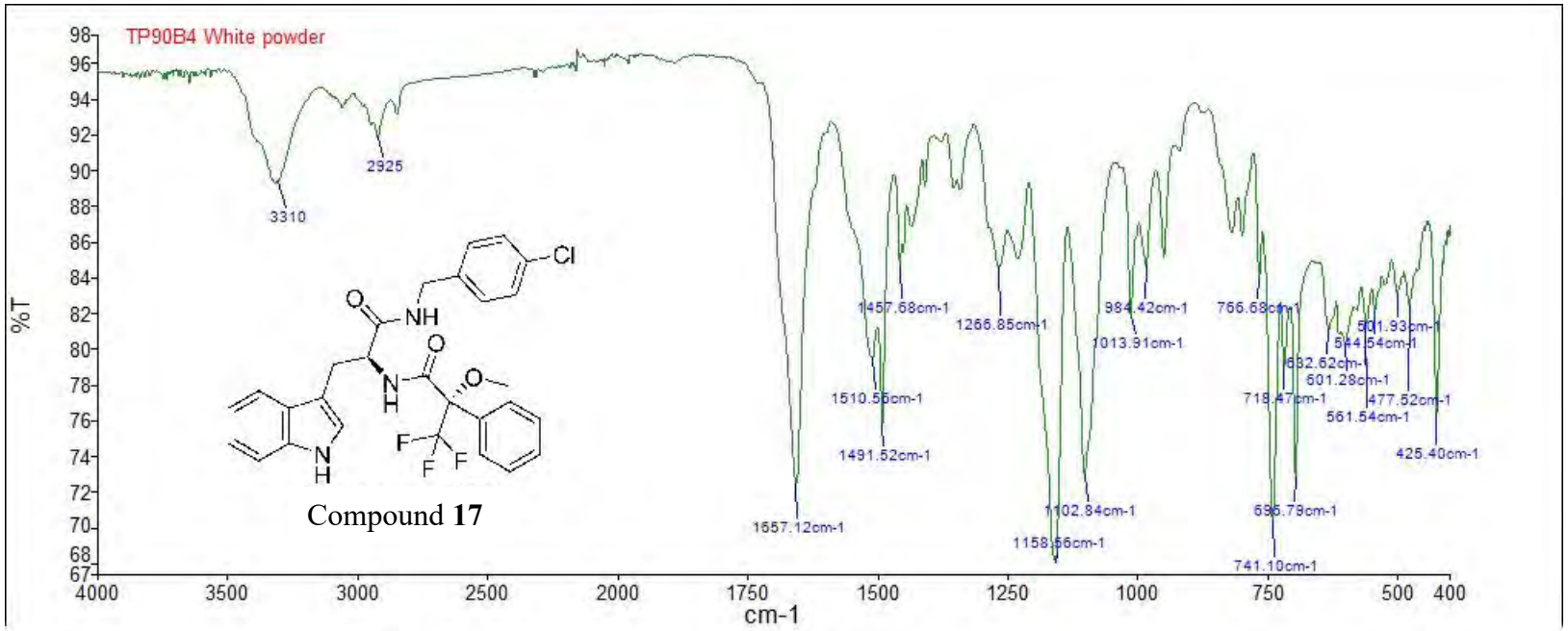
TP90B4 White powder
%T
cm-1
3310
2925
1657.12cm-1
1510.56cm-1
1491.52cm-1
1457.68cm-1
1266.85cm-1
1102.84cm-1
1158.56cm-1
1013.91cm-1
984.42cm-1
766.68cm-1
741.10cm-1
696.79cm-1
718.47cm-1
632.62cm-1
601.28cm-1
561.54cm-1
544.54cm-1
511.93cm-1
477.52cm-1
425.40cm-1
Cl
NH
O
N
H
F
F
F

Compound **17**

SHIMADZU LabSolutions Analysis Report

<Sample Information>

Sample Name	: TP90B4		
Sample ID	: TP90B4		
Data Filename	: TP90B4.lcd		
Method Filename	: 10-100 over 15 mins.lcm		
Batch Filename	: TRIEU Second Third Generation and New pro.lcb		
Vial #	: 1-4	Sample Type	: Unknown
Injection Volume	: 30 uL		
Date Acquired	: 5/09/2014 12:07:03 PM	Acquired by	: System Administrator
Date Processed	: 5/09/2014 12:37:04 PM	Processed by	: System Administrator

<Chromatogram>

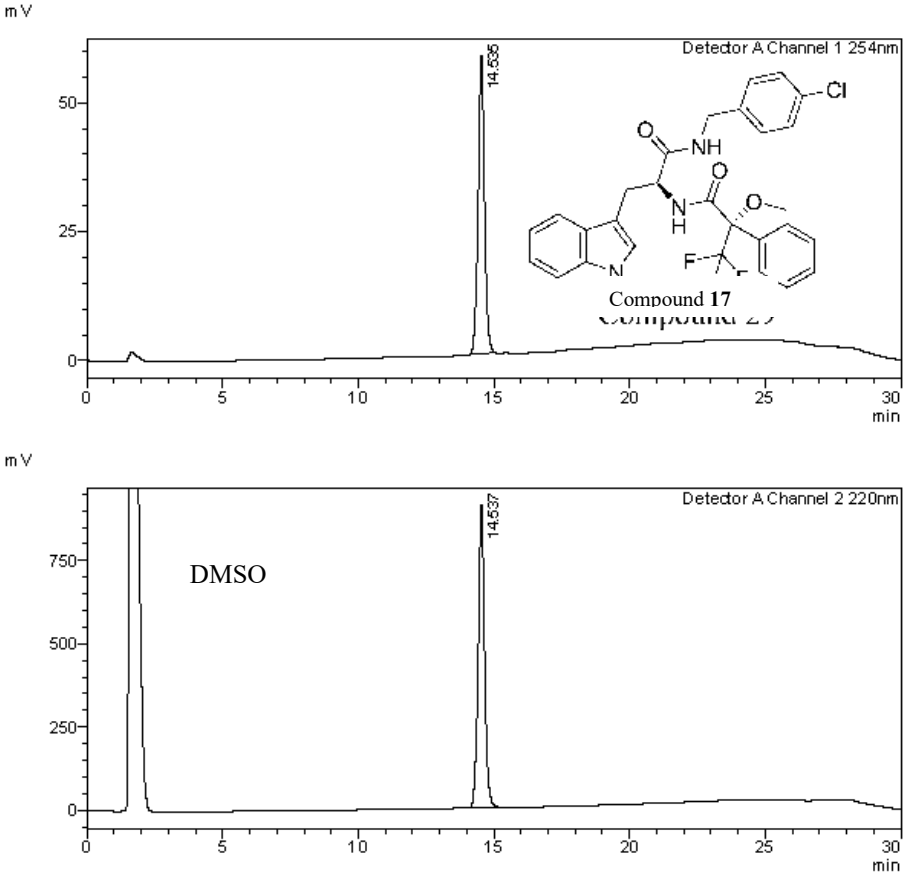

<Peak Table>

Detector A Channel 1 254nm

Peak#	Ret. Time	Area	Height	Conc.	Unit	Mark	Name
1	14.535	938906	57714	100.000		M	
Total		938906	57714				

Detector A Channel 2 220nm

Peak#	Ret. Time	Area	Height	Conc.	Unit	Mark	Name
1	14.537	14861604	906516	100.000		M	
Total		14861604	906516				

==== Shimadzu LCMSsolution Data Report ====

<Chromatogram>

Sample Information

Acquired by	: Admin
Date Acquired	: 11/18/2014 2:31:44 PM
Sample Type	: Unknown
Level#	: 0
Sample Name	: TP90B4_APCI+
Sample ID	:
ISTD Amount	: (Level1 Conc.)
Sample Amount	: 1
Dilution Factor	: 1
Tray#	: 1
Vial#	: 13
Injection Volume	: 10
Data File	: TP90B4_APCI+.lcd
Method File	: FIA-APCI_scan(+).lcm
Original Method	: C:\LabSolutions\Data\Pete\FIA-APCI_scan(+).lcm
Report Format	: DefaultLCMS.lcr
Tuning File	: C:\LabSolutions\LCsolution\Log\Tuning\Autotune_030908.lct
Processed by	: Admin
Modified Date	: 11/18/2014 2:33:17 PM

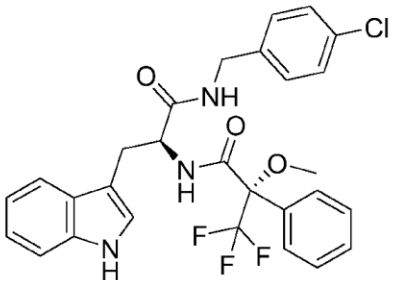

Compound **17**

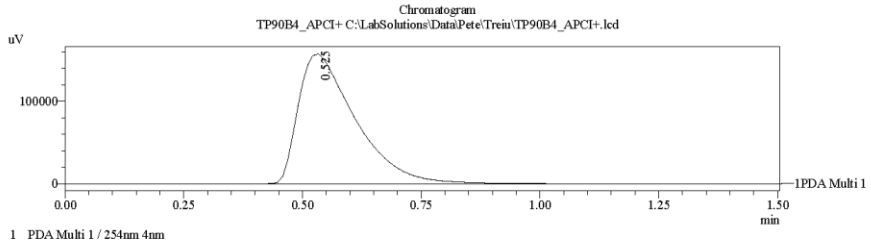

1 PDA Multi 1 / 254nm 4nm

<Spectrum>

Retention Time:0.580(Scan#:59)
Max Peak:582 Base Peak:168.80(561191)
Spectrum:Averaged 0.440-0.940(45-95)
Background:Averaged 0.060-0.345(7-35) Polarity:Pos Segment1 - Event1

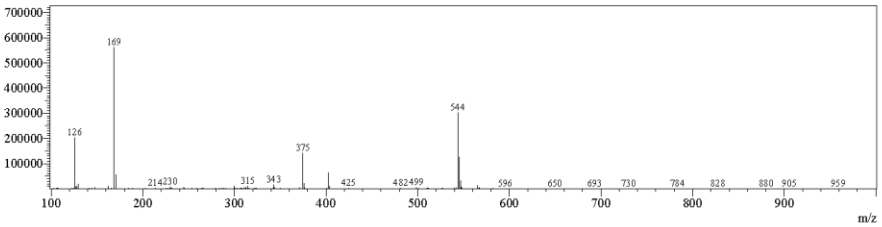

Retention Time:0.570(Scan#:58)
Max Peak:577 Base Peak:112.65(614763)
Spectrum:Averaged 0.450-0.950(46-96)
Background:Averaged 0.070-0.345(8-36) Polarity:Neg Segment1 - Event2

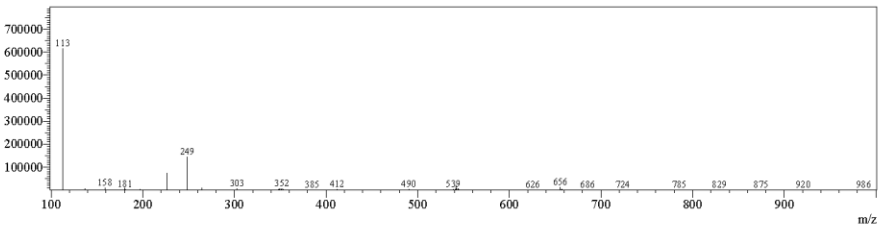

C:¥LabSolutions¥Data¥Pete¥Treiu¥TP90B4_APCI+.lcd

Compound	Chemical Formula	Predicted monoisotopic neutral MW	Predicted MH^+	MH^+ Measured	Main MS Ions	Main MS/MS Fragments
Compound **17**	$C_{28}H_{25}ClF_3N_3O_3$	543.1537	544.1609	544.1610	544.1610	375.1319

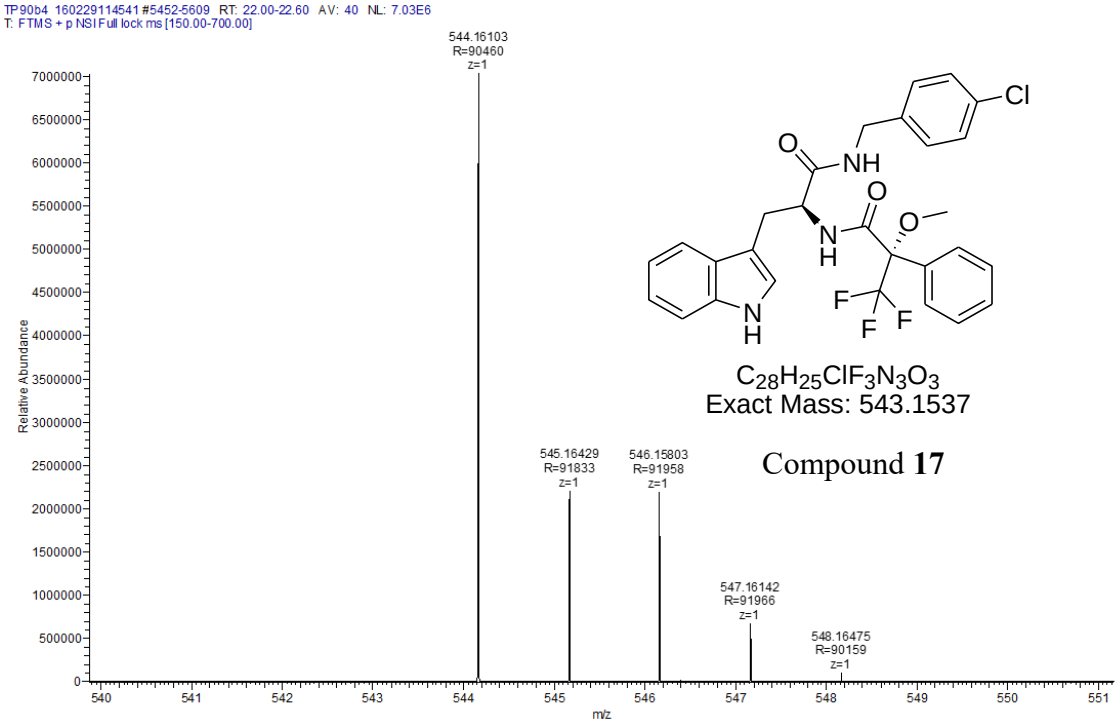

B. The benzo[1,3]dioxol-5-ylmethyl-[2-(*1H*-indol-3-yl)-ethyl]-amine analogues

COMPOUND 5

Compound Name: *N*-(1,3-benzodioxol-4-ylmethyl)-N-[2-(*1H*-indol-3-yl)ethyl]-napthalene-carboxamide

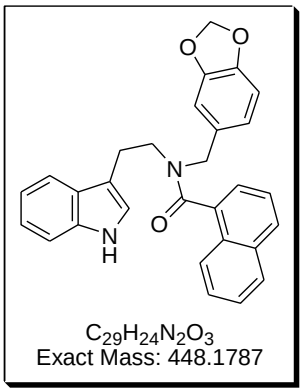

Obtained Weight & Yield: 110 mg, 67%

Appearance: White crystalline powder

Solubility: Acetone, DMSO

Melting Point: 199 − 200 ºC

TLC Conditions: EtOAc/Hexane (50/50)

IR Analysis: νmax/cm^{-1}

3215 (NH), 1608 (CON), 743 (CH- aromatics)

Proton and carbon spectra displays an atropisomeric property of compound **5, with the approximate ratio 1:0.66 calculated based on the proton benzodioxole C<u>H</u>2 peaks at 6.05 and 5.97 ppm, respectively.As the spectra is complex with both splitting and overlapping, the proton NMR is reported separately for splitting peaks where possible. In case of complex overlapping (aromatic region), the proton NMR is assigned as a whole. Carbon peaks are all included. This format will be applied to all atropisomeric mixtures.*

^{1}H NMR

^{1}H NMR (400 MHz, DMSO-d_6) δ 10.91 (s, 0.67H), 10.71 (s, 1H), 8.07 – 7.89 (m, 3.33H), 7.75 – 7.64 (m, 1H), 7.64 – 7.44 (m, 7H), 7.42 – 7.16 (m, 3.3H), 7.14 – 7.06 (m, 1.67H), 7.06 – 6.78 (m, 5.33H), 6.71 – 6.56 (m, 2.33H), 6.39 (d, *J* = 7.9 Hz, 1H), 6.05 (s, 2H), 5.97 (s, 1.33H), 5.01 – 4.70 (m, 2H), 4.26 −4.02 (m, 2H), 3.43 (d, *J* = 20.9 Hz, 0.67H), 3.26 – 2.98 (m, 3.33H), 2.91 −2.66 (m, 2H).

^{13}C NMR

^{13}C NMR (101 MHz, DMSO-d_6) δ 170.4, 170.0, 148.0, 148.0, 147.1, 147.0, 136.8, 136.4, 135.1, 135.0, 133.5 133.4, 132.3, 130.7, 129.5, 129.2, 129.0, 128.9, 128.9, 127.7, 127.5, 127.1, 126.9, 125.8, 125.0, 124.7, 124.1, 123.6, 123.3, 122.1, 121.5, 121.3, 121.1, 118.9, 118.8, 118.5, 118.0, 111.9, 111.8, 111.7, 110.7, 109.1, 108.8, 108.7, 108.1, 101.5, 51.8, 49.2, 47.1, 44.5, 24.9, 23.1.

RP-HPLC Alltima™ C18 5 μm 150 mm x 4.6 mm, 10–100% B in 15 min, R_t = 18.1 min, 100%.

LRMS (APCI +) m/z 448, 449 $[M+H]^+$, 100%. HRMS (ES+) for $C_{29}H_{24}N_2O_3$, calculated 449.1860, found 449.1859.

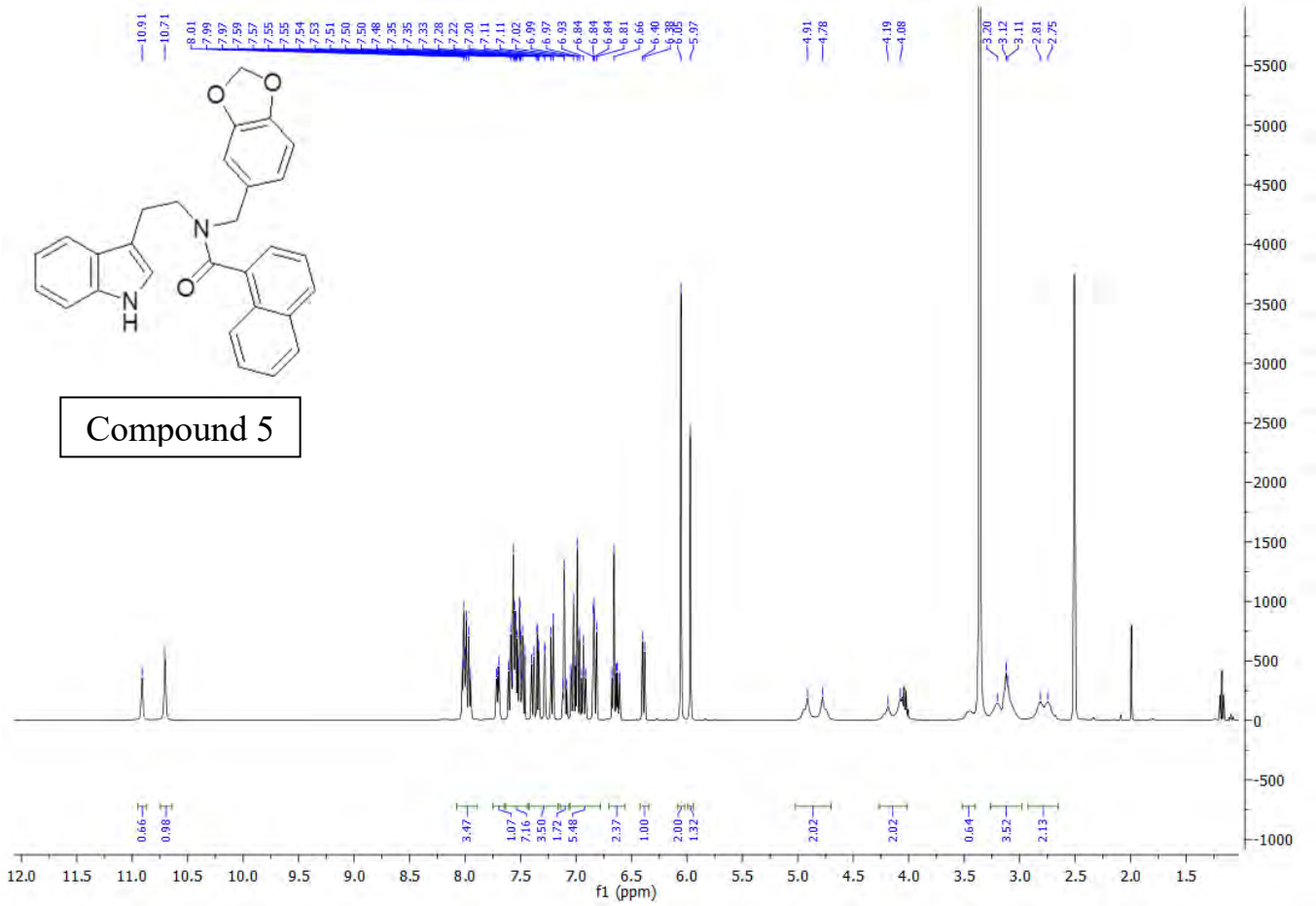
Compound 5
f1 (ppm)

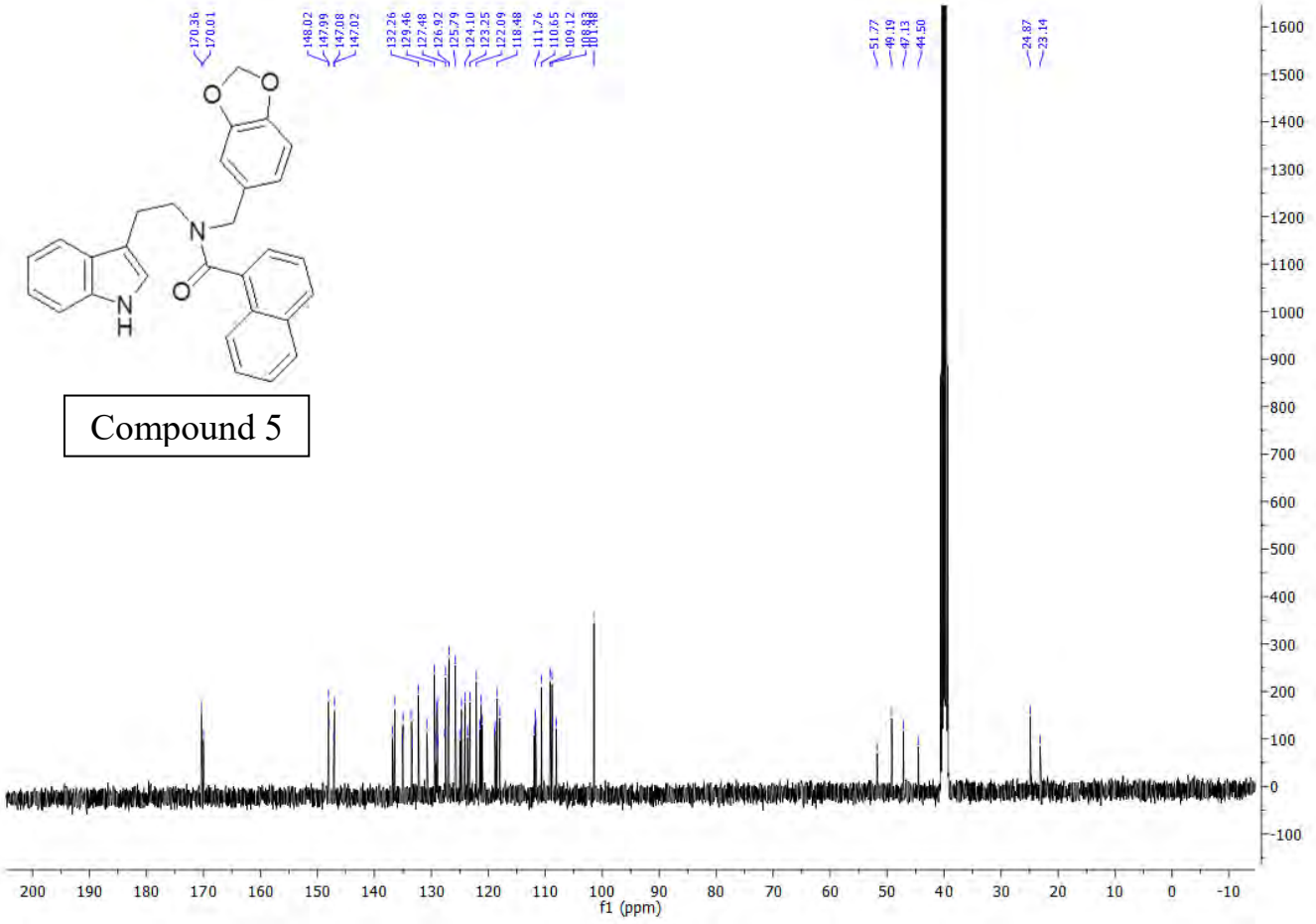
170.36
170.01
148.02
147.99
147.08
147.02
132.26
129.46
127.48
126.92
125.79
124.10
123.25
122.09
118.48
111.76
110.65
109.12
101.88
51.77
49.19
47.13
44.50
24.87
23.14
O
O
N
O
N
H
1600
1500
1400
1300
1200
1100
1000
900
800
700
600
500
400
300
200
100
0
-100
200 190 180 170 160 150 140 130 120 110 100 90 80 70 60 50 40 30 20 10 0 -10
f1 (ppm)

Compound 5

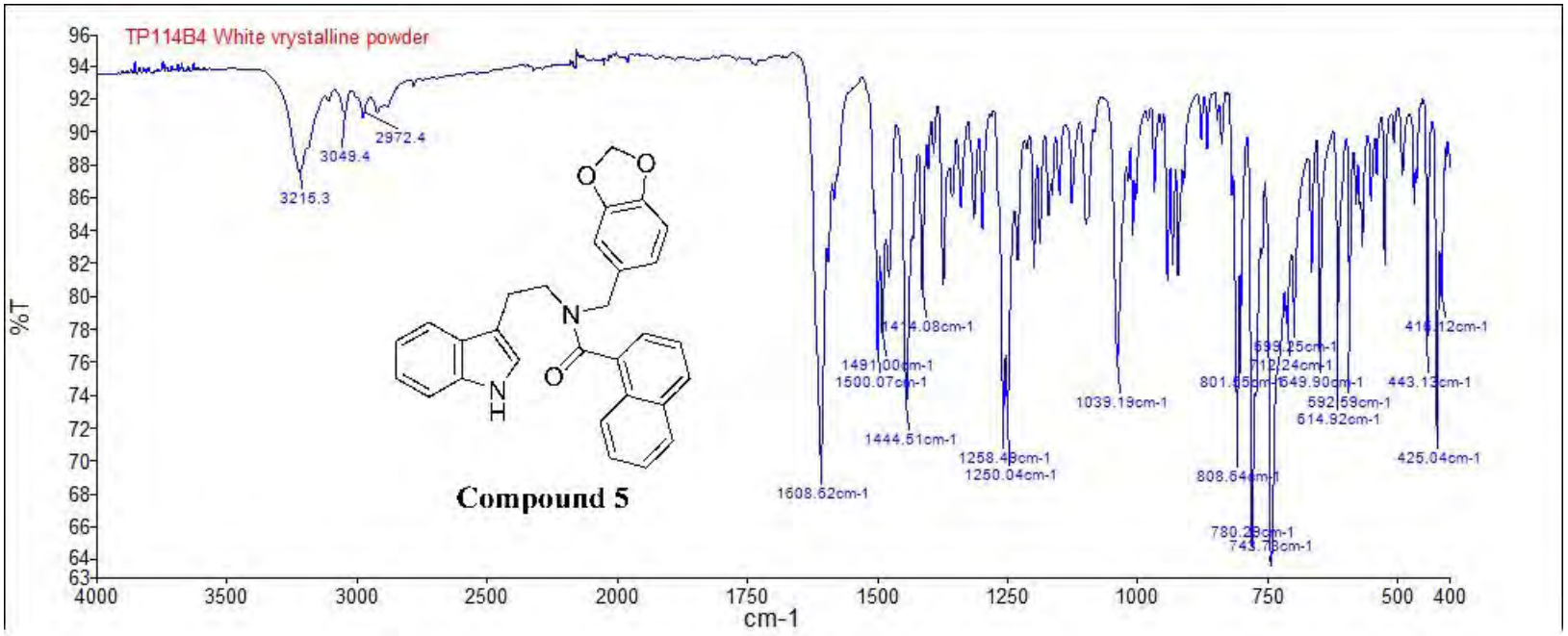
TP114B4 White vrystalline powder
%T
cm-1
3215.3
3049.4
2972.4
1608.62cm-1
1500.07cm-1
1491.00cm-1
1444.51cm-1
1258.43cm-1
1250.04cm-1
1039.19cm-1
808.64cm-1
780.23cm-1
743.78cm-1
714.24cm-1
649.90cm-1
592.59cm-1
514.92cm-1
443.13cm-1
425.04cm-1
Compound 5

SHIMADZU LabSolutions Analysis Report

<Sample Information>

Sample Name	: TP114B4 ISOMERS		
Sample ID	: TP114B4 ISOMERS		
Data Filename	: TP114B4 ISOMERS001.lcd		
Method Filename	: 30-100 over 15 mins.lcm		
Batch Filename	: TRIEU Third Generation.lcb		
Vial #	: 1-40	Sample Type	: Unknown
Injection Volume	: 10 uL		
Date Acquired	: 16/06/2014 1:51:51 PM	Acquired by	: System Administrator
Date Processed	: 6/10/2015 11:08:41 AM	Processed by	: System Administrator

<Chromatogram>

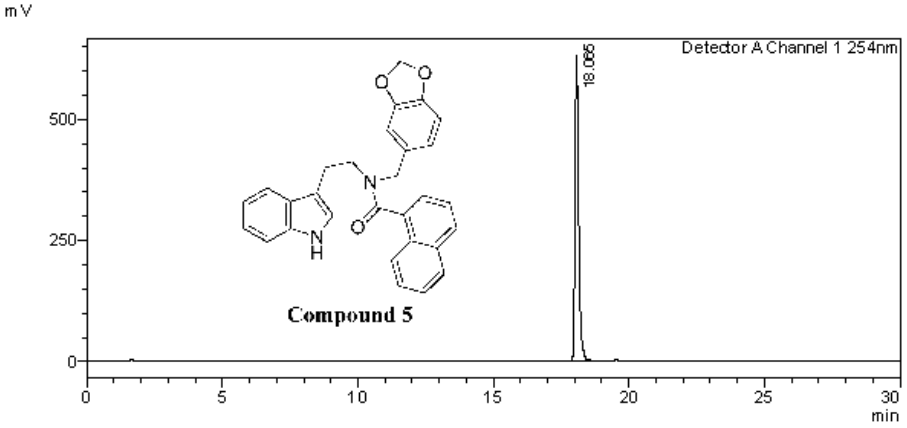

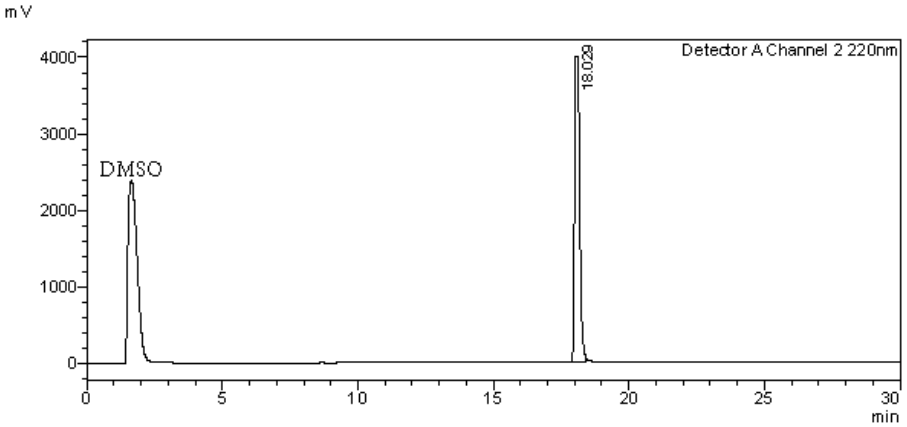

<Peak Table>

Detector A Channel 1 254nm

C:\LabSolutions\Data\Project1\Flash\TP114B4 ISOMERS001.lcd

Peak#	Ret. Time	Area	Height	Height%	Area%
1	18.065	5817007	629410	100.000	100.000
Total		5817007	629410	100.000	100.000

Detector A Channel 2 220nm

Peak#	Ret. Time	Area	Height	Height%	Area%
1	18.029	53101298	3982079	100.000	100.000
Total		53101298	3982079	100.000	100.000

==== Shimadzu LCMSsolution Data Report ====

<Chromatogram>

Sample Information

Acquired by	: Admin
Date Acquired	: 7/17/2014 11:19:39 AM
Sample Type	: Unknown
Level#	: 0
Sample Name	: TP114134_APCI(+)
Sample ID	:
ISTD Amount	: (Level1 Conc.)
Sample Amount	: 1
Dilution Factor	: 1
Tray#	: 1
Vial#	: 4
Injection Volume	: 10
Data File	: TP114134_APCI(+).lcd
Method File	: FIA-APCI_scan(+).lcm
Original Method	: C:\LabSolutions\Data\Pete\FIA-APCI_scan(+).lcm
Report Format	: DefaultLCMS.lcr
Tuning File	: C:\LabSolutions\LCsolution\Log\Tuning\Autotune_030908.lct
Processed by	: Admin
Modified Date	: 7/17/2014 11:21:10 AM

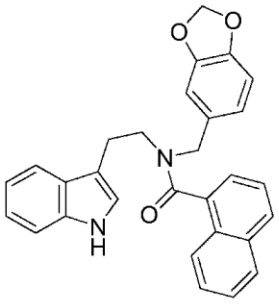

Compound 5

Chromatogram
TP114134_APCI(+) C:\LabSolutions\Data\Pete\Treiu\TP114134_APCI(+).lcd

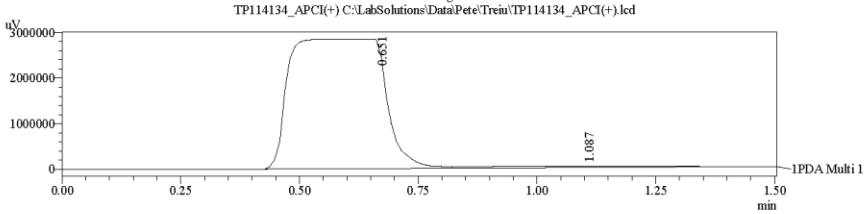

1 PDA Multi 1 / 254nm 4nm

<Spectrum>

Retention Time:0.660(Scan#:67)
Max Peak:579 Base Peak:448.60(432699)
Spectrum:Averaged 0.600-1.220(61-123)
Background:Averaged 0.080-0.420(9-43) Polarity:Pos Segment1 - Event1

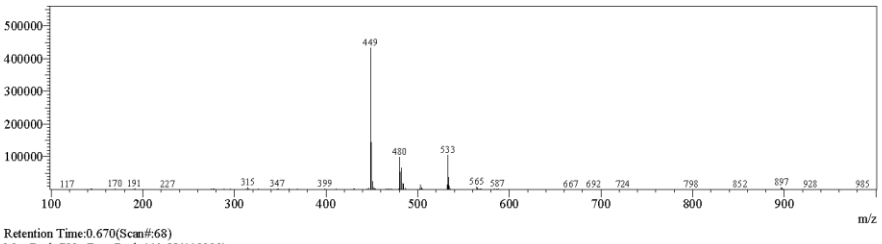

Retention Time:0.670(Scan#:68)
Max Peak:703 Base Peak:112.55(418908)
Spectrum:Averaged 0.610-1.230(62-124)
Background:Averaged 0.090-0.420(10-44) Polarity:Neg Segment1 - Event2

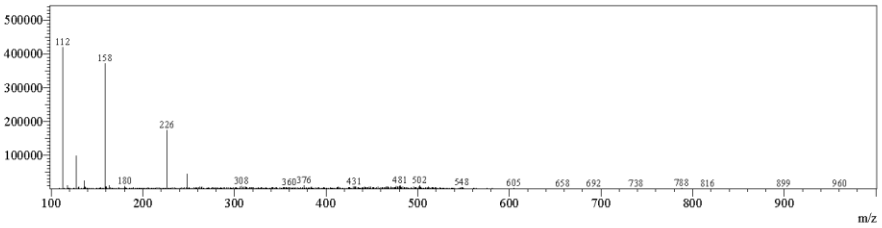

C:¥LabSolutions¥Data¥Pete¥Treiu¥TP114134_APCI(+).lcd

Compound	Chemical Formula	Predicted monoisotopic neutral MW	Predicted MH+	MH+ Measured	Main MS Ions	Main MS/MS Fragments
TP 114B4	$C_{29}H_{24}N_2O_3$	448.1787	449.1860	449.18588	449.1859	135.0444 155.0494 327.1496

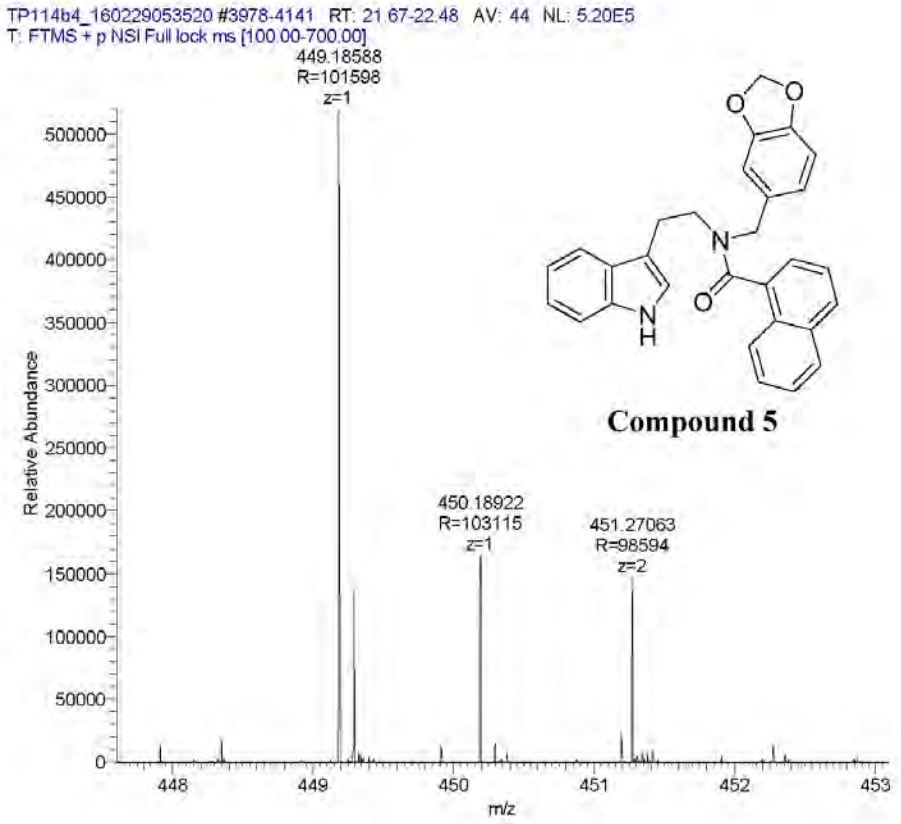

COMPOUND 20

Compound Name: *N*-(1,3-benzodioxol-4-ylmethyl)-N-[2-(*1H*-indol-3-yl)ethyl]-*1H*-indole-2-carboxamide

Obtained Weight & Yield: 140 mg, 67%

Appearance: White floppy precipitate

Solubility: Acetone, DMSO

Melting Point: 198-199 ºC

TLC Conditions: EtOAc/Hexane (50/50)

IR Analysis: νmax/cm^{-1}

3440 (NH), 3274 (NH), 1620 (CON)

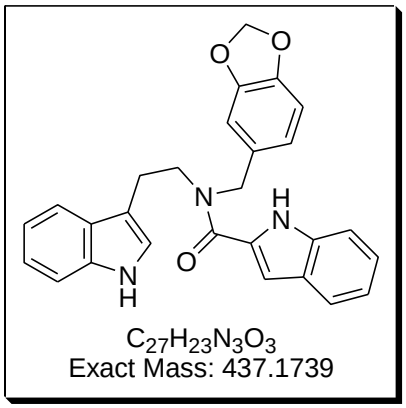

$C_{27}H_{23}N_3O_3$
Exact Mass: 437.1739

^{1}H NMR Analysis:

^{1}H NMR (400 MHz, DMSO-d_6) δ 11.72 (s, 1H), 10.86 (s, 1H), 7.72 – 7.29 (m, 4H), 7.20 (dd, J = 9.2, 4.8 Hz, 2H), 7.13 – 6.58 (m, 7H), 6.01 (s, 2H), 4.81 (bs, 2H), 3.76 (bs, 2H), 3.09 (s, 2H).

^{13}C NMR Analysis:

^{13}C NMR (101 MHz, DMSO-d_6) δ 163.7, 148.1, 147.0, 136.7, 136.4, 131.9, 130.5, 127.5, 123.8, 123.3, 121.9, 121.5, 120.2, 118.8, 118.7, 112.5, 111.9, 111.2, 108.8, 107.7, 103.7, 101.5, 52.4, 48.6, 47.7, 24.7, 23.3.

HPLC:

RP-HPLC Alltima™ C18 5 μm 150 mm x 4.6 mm, 10–100% B in 15 min, R_t = 14.7 min, 100%.

Mass Spectral Analysis: LRMS (APCI +) m/z 437, 438 $[M+H]^+$, 70%. HRMS (ES+) for $C_{27}H_{23}N_3O_3$, calculated 438.1812, found 439.1811.

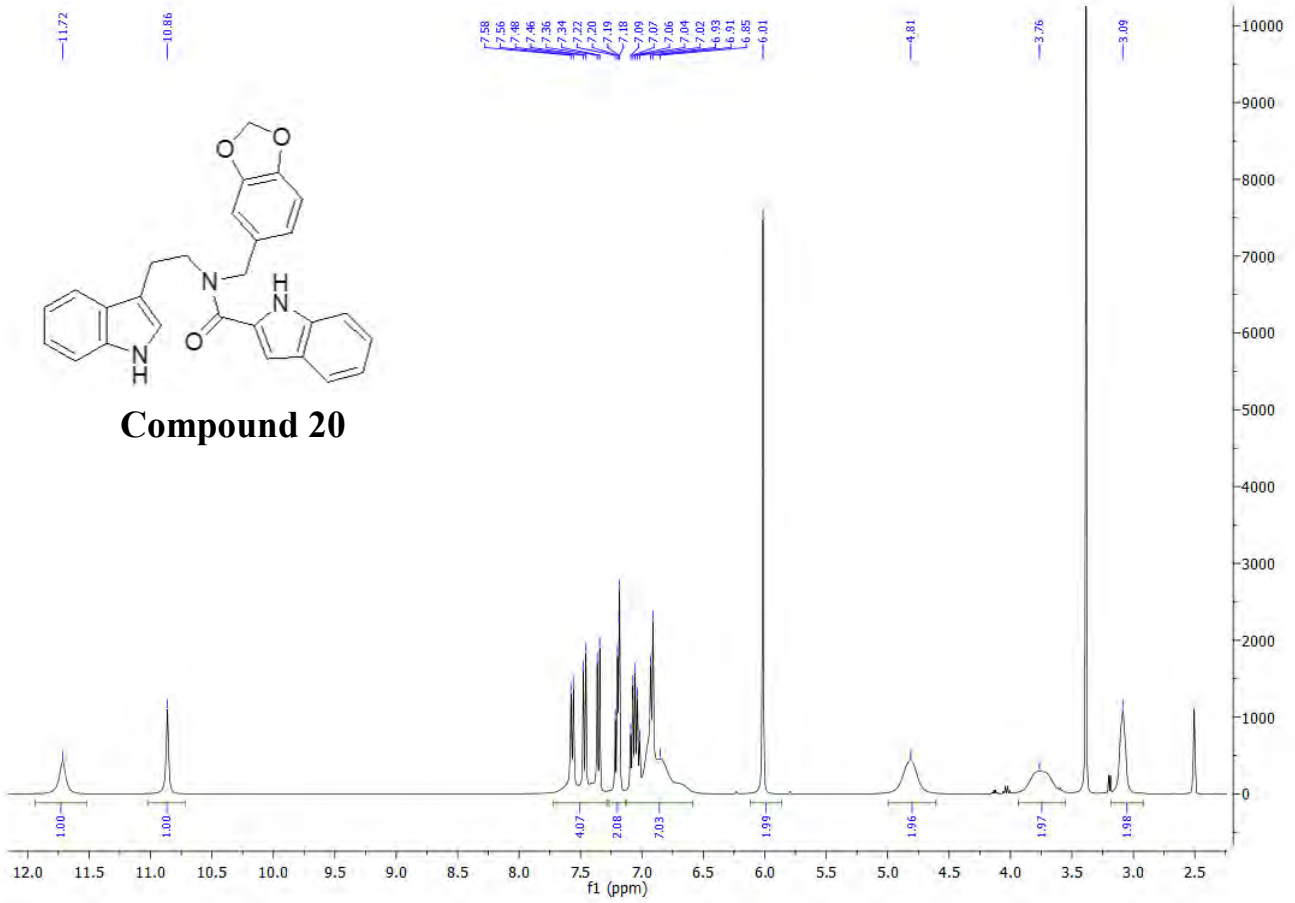
11.72
10.86
7.58
7.56
7.48
7.46
7.36
7.34
7.22
7.20
7.19
7.18
7.09
7.07
7.06
7.04
7.02
6.93
6.91
6.85
6.01
4.81
3.76
3.09
O
O
N
H
N
O
N
H
1.00
1.00
4.07
2.08
7.03
1.99
1.96
1.97
1.98
f1 (ppm)

Compound 20

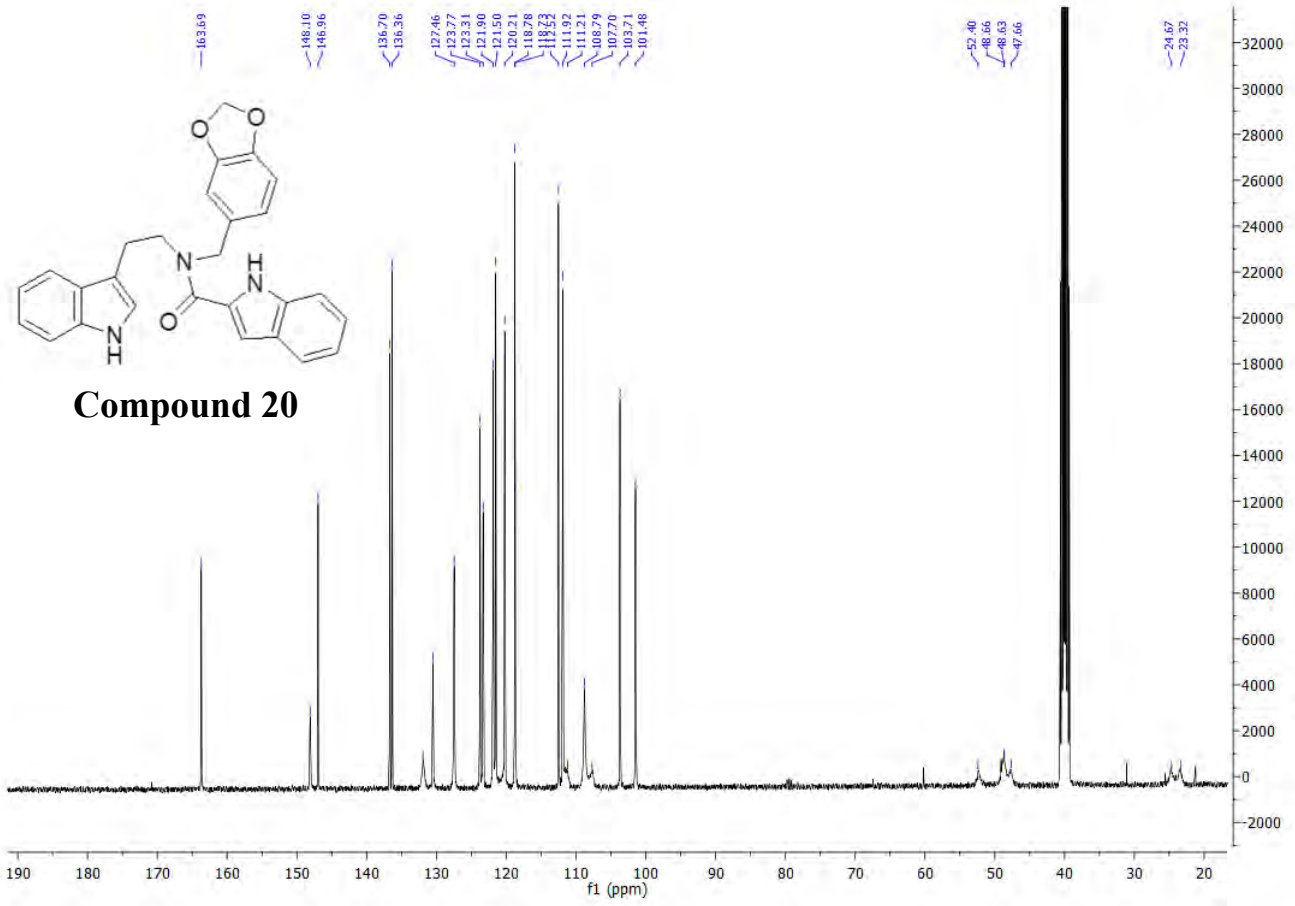
163.69
148.10
146.96
136.70
136.36
127.46
123.77
123.31
121.90
121.50
120.21
118.78
111.92
111.21
108.79
107.70
103.71
101.48
52.40
48.66
48.63
47.66
24.67
23.32
O
O
N
H
N
O
H
N
Compound 20
32000
30000
28000
26000
24000
22000
20000
18000
16000
14000
12000
10000
8000
6000
4000
2000
0
-2000
190
180
170
160
150
140
130
120
110
100
90
80
70
60
50
40
30
20
f1 (ppm)

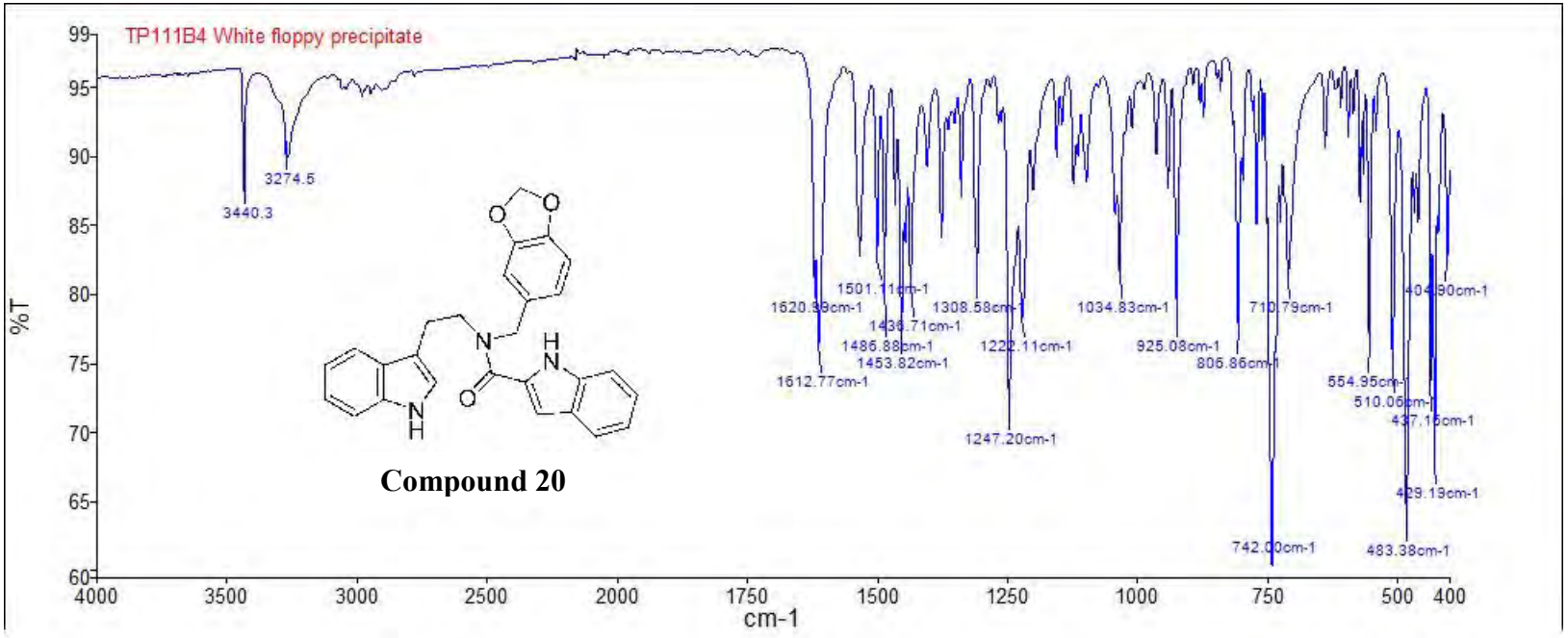
TP111B4 White floppy precipitate
%T
cm-1
3440.3
3274.5
1612.77cm-1
1620.99cm-1
1501.11cm-1
1486.88cm-1
1453.82cm-1
1436.71cm-1
1308.58cm-1
1247.20cm-1
1222.11cm-1
1034.83cm-1
925.08cm-1
805.86cm-1
710.79cm-1
742.00cm-1
554.95cm-1
510.06cm-1
483.38cm-1
429.19cm-1
437.15cm-1
404.90cm-1
O
O
N
H
N
O
H
N

Compound 20

SHIMADZU LabSolutions Analysis Report

<Sample Information>

Sample Name	: TP111B4		
Sample ID	: TP111B4		
Data Filename	: TP111B4.lcd		
Method Filename	: 10-100 over 15 mins.lcm		
Batch Filename	: TP174-176B3 10-100 over 15mins.lcb		
Vial #	: 1-9	Sample Type	: Unknown
Injection Volume	: 10 uL		
Date Acquired	: 6/08/2014 1:31:51 PM	Acquired by	: System Administrator
Date Processed	: 6/08/2014 2:01:53 PM	Processed by	: System Administrator

<Chromatogram>

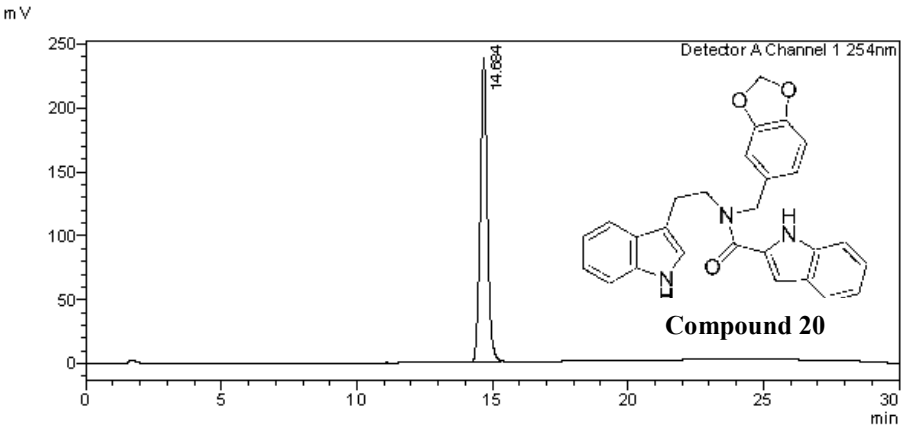

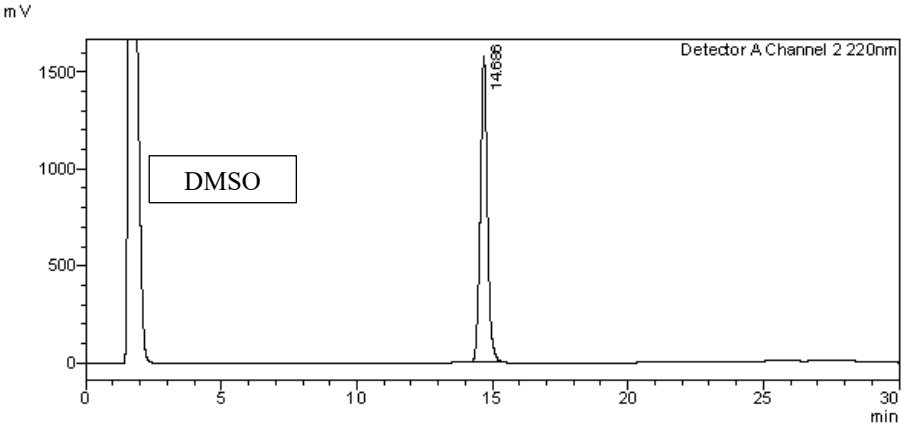

<Peak Table>

Detector A Channel 1 254nm

C:\LabSolutions\Data\Project1\TRIEU\TP111B4.lcd

Peak#	Ret. Time	Area	Height	Conc.	Unit	Mark	Name
1	14.684	4357192	237781	100.000		M	
Total		4357192	237781				

Detector A Channel 2 220nm

Peak#	Ret. Time	Area	Height	Conc.	Unit	Mark	Name
1	14.686	28741726	1575553	100.000		M	
Total		28741726	1575553				

Compound	Chemical Formula	Predicted monoisotopic neutral MW	Predicted MH+	MH+ Measured	Main MS Ions	Main MS/MS Fragments
TP 111B4	$C_{27}H_{23}N_3O_3$	437.1739	438.18122	438.18110	439.18110*	n/a

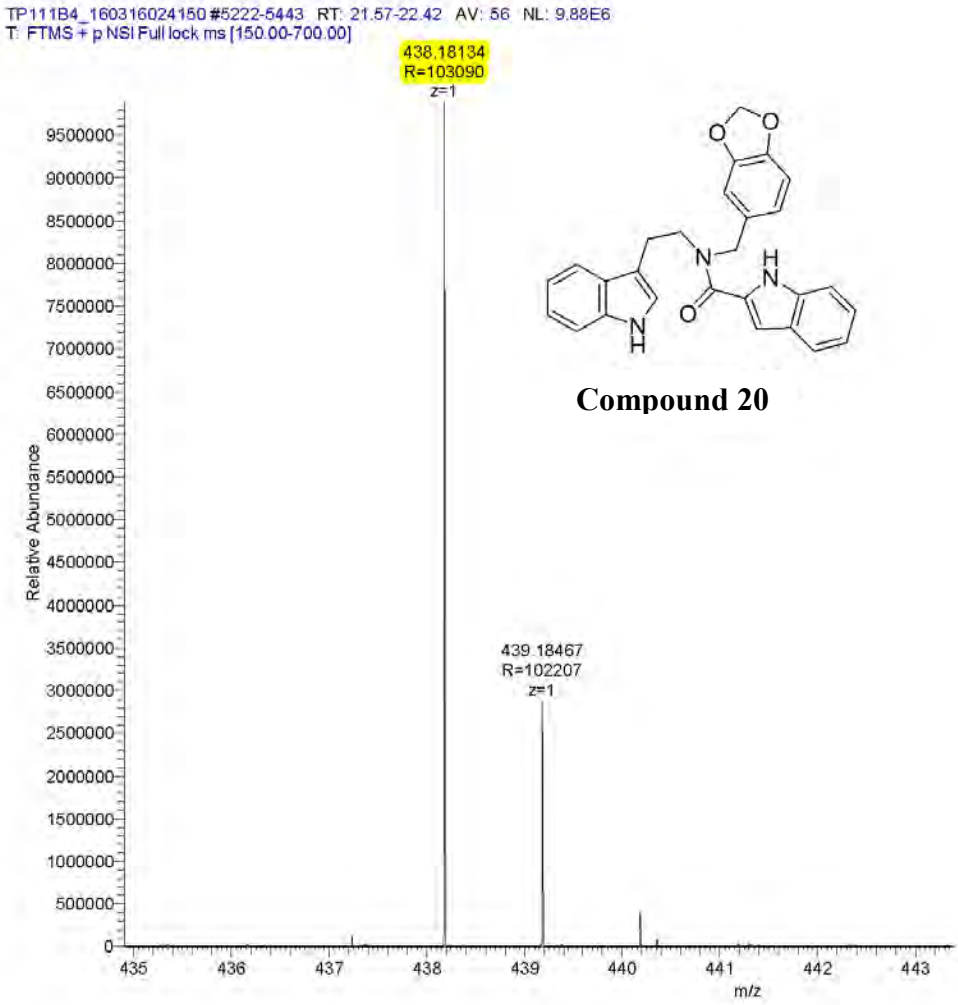

Compound 20

COMPOUND 21

Compound Name: Benzo[*b*]thiophene-2-carboxylic acid benzo[1,3]dioxol-5-ylmethyl-[2-(1*H*-indol-3-yl)-ethyl]-amide

Obtained Weight & Yield: 118 mg, 53%

Appearance: Milky powder/ off white precipitate

Solubility: DMSO

Melting Point: 166 − 167 ºC

TLC Conditions: EtOAc/Hexane (50/50)

IR Analysis: νmax/cm^{-1}

3331 (NH), 1627 (CON)

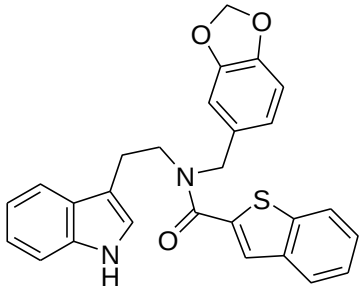

$C_{27}H_{22}N_2O_3S$
Exact Mass: 454.1351

^{1}H NMR Analysis:

^{1}H NMR (400 MHz, DMSO-d_6) δ 10.85 (s, 1H), 8.00 (d, J = 8.2 Hz, 1H), 7.81 (s, 1H), 7.70 – 6.64 (m, 11H), 6.02 (s, 2H), 4.73 (s, 2H), 3.65 (s, 2H), 3.12 – 2.91 (m, 2H)

^{13}C NMR Analysis:

^{13}C NMR (101 MHz, DMSO-d_6) δ 164.5, 148.1, 147.0, 139.7, 139.1, 137.7, 136.6, 131.5, 127.5, 126.32, 125.3 (Cx2), 125.2, 123.5, 122.9, 121.5 (Cx2), 118.7 (Cx2), 118.6, 111.9, 110.9, 108.8, 101.5, 49.6, 48.4, 24.7

HPLC:

RP-HPLC Alltima™ C18 5 µm 150 mm x 4.6 mm, 10–100% B in 15 min, R_t = 14.97 min, 100%.

Mass Spectral Analysis: LRMS (APCI +) m/z 454, 455 $[M+H]^+$, 100%. HRMS (ES+) for $C_{27}H_{22}N_2O_3S$, calculated 455.1424, found 455.1423.

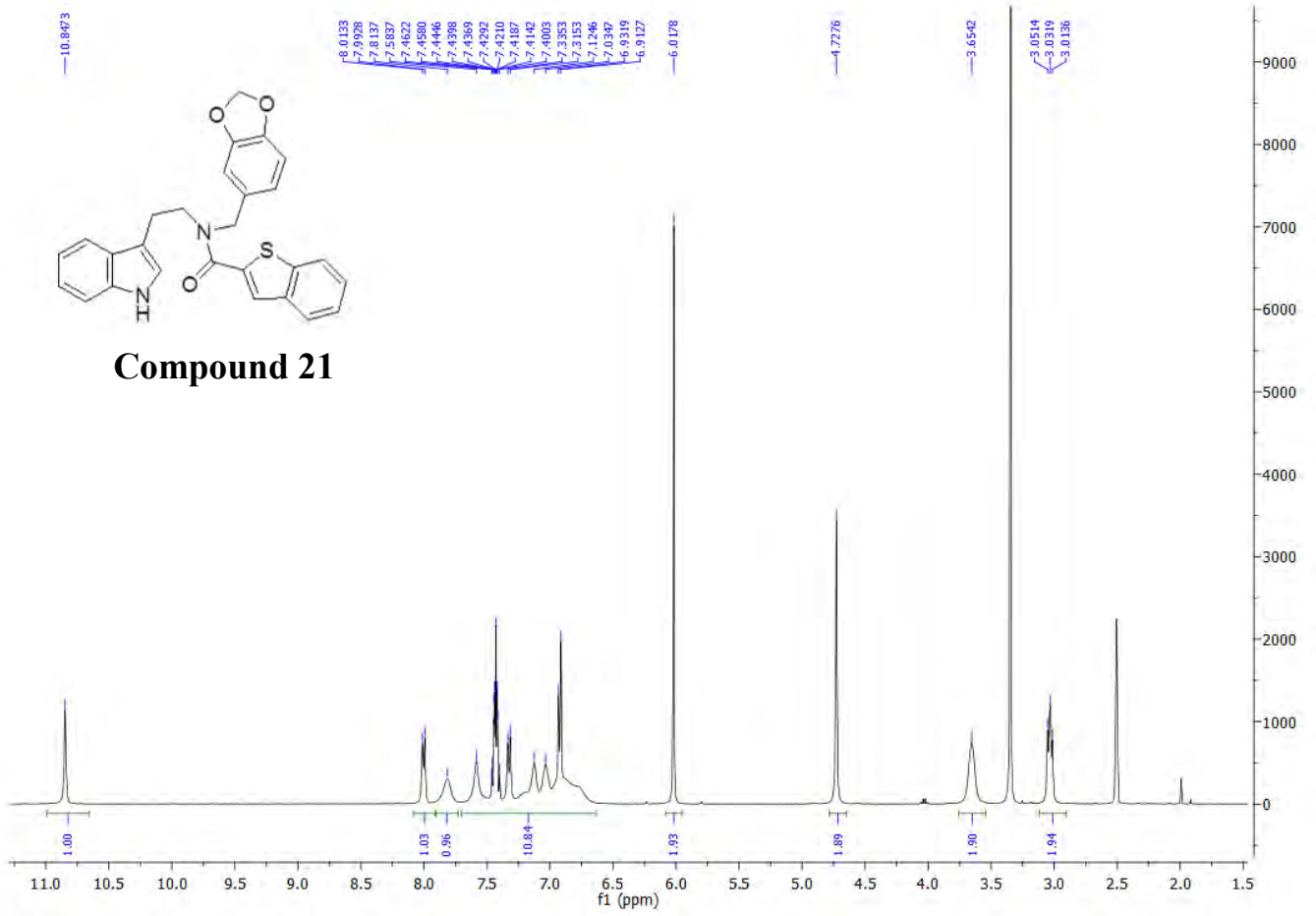
10.8473
8.0133
7.9928
7.8137
7.5837
7.4622
7.4580
7.4446
7.4398
7.4369
7.4292
7.4210
7.4187
7.4142
7.4003
7.3353
7.3153
7.1246
7.0347
6.9319
6.9127
6.0178
4.7276
3.6542
3.0514
3.0319
3.0136
O
O
N
S
O
N
H
9000
8000
7000
6000
5000
4000
3000
2000
1000
0
1.00
1.03
0.96
10.84
1.93
1.89
1.90
1.94
11.0
10.5
10.0
9.5
9.0
8.5
8.0
7.5
7.0
6.5
6.0
5.5
5.0
4.5
4.0
3.5
3.0
2.5
2.0
1.5
f1 (ppm)

Compound 21

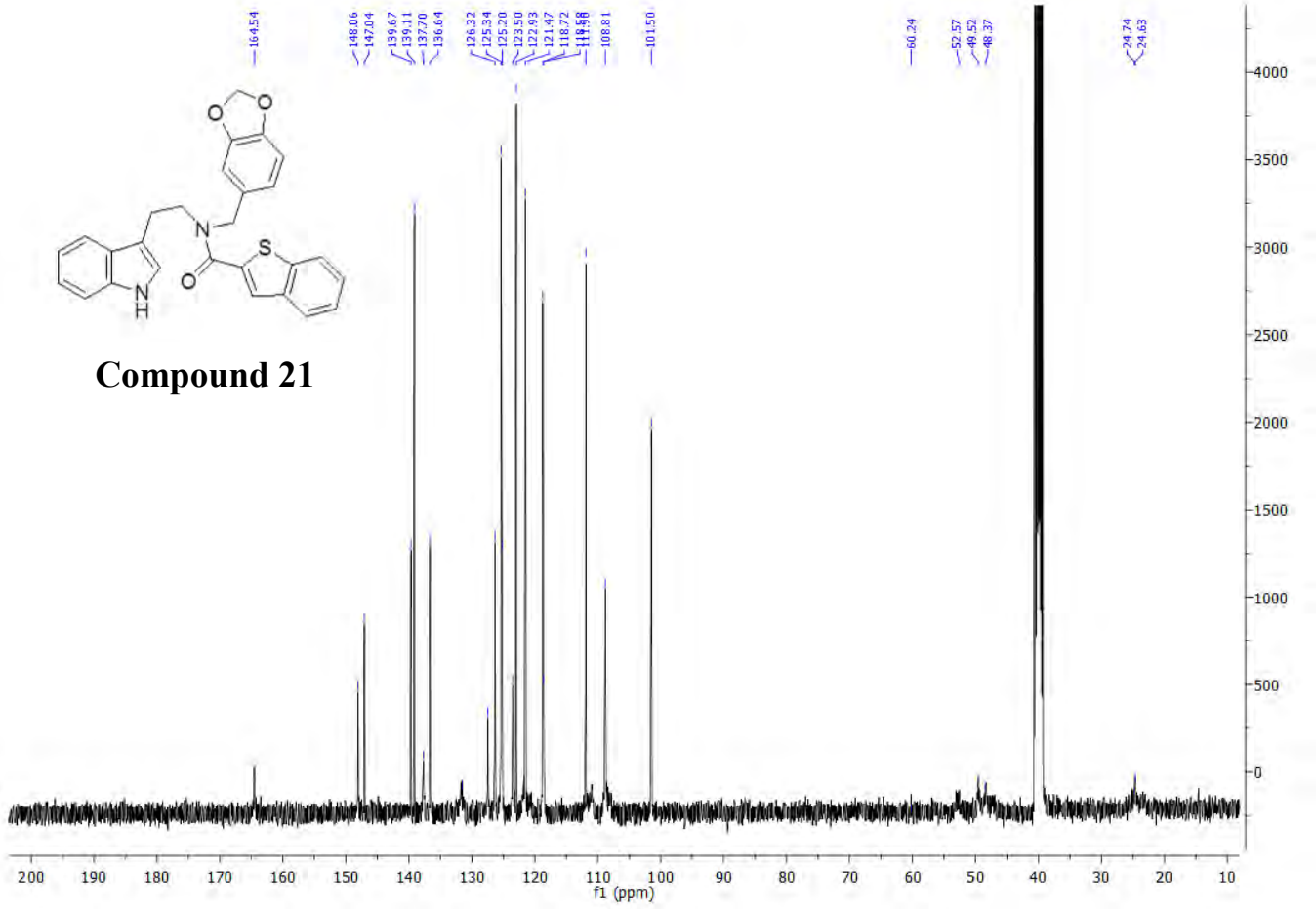
164.54
148.06
147.04
139.67
139.11
137.70
136.64
126.32
125.34
125.20
123.50
122.93
121.47
118.72
108.81
101.50
60.24
52.57
49.52
48.37
24.74
24.63
O
O
N
S
O
H
4000
3500
3000
2500
2000
1500
1000
500
0
200
190
180
170
160
150
140
130
120
110
100
90
80
70
60
50
40
30
20
10
f1 (ppm)

Compound 21

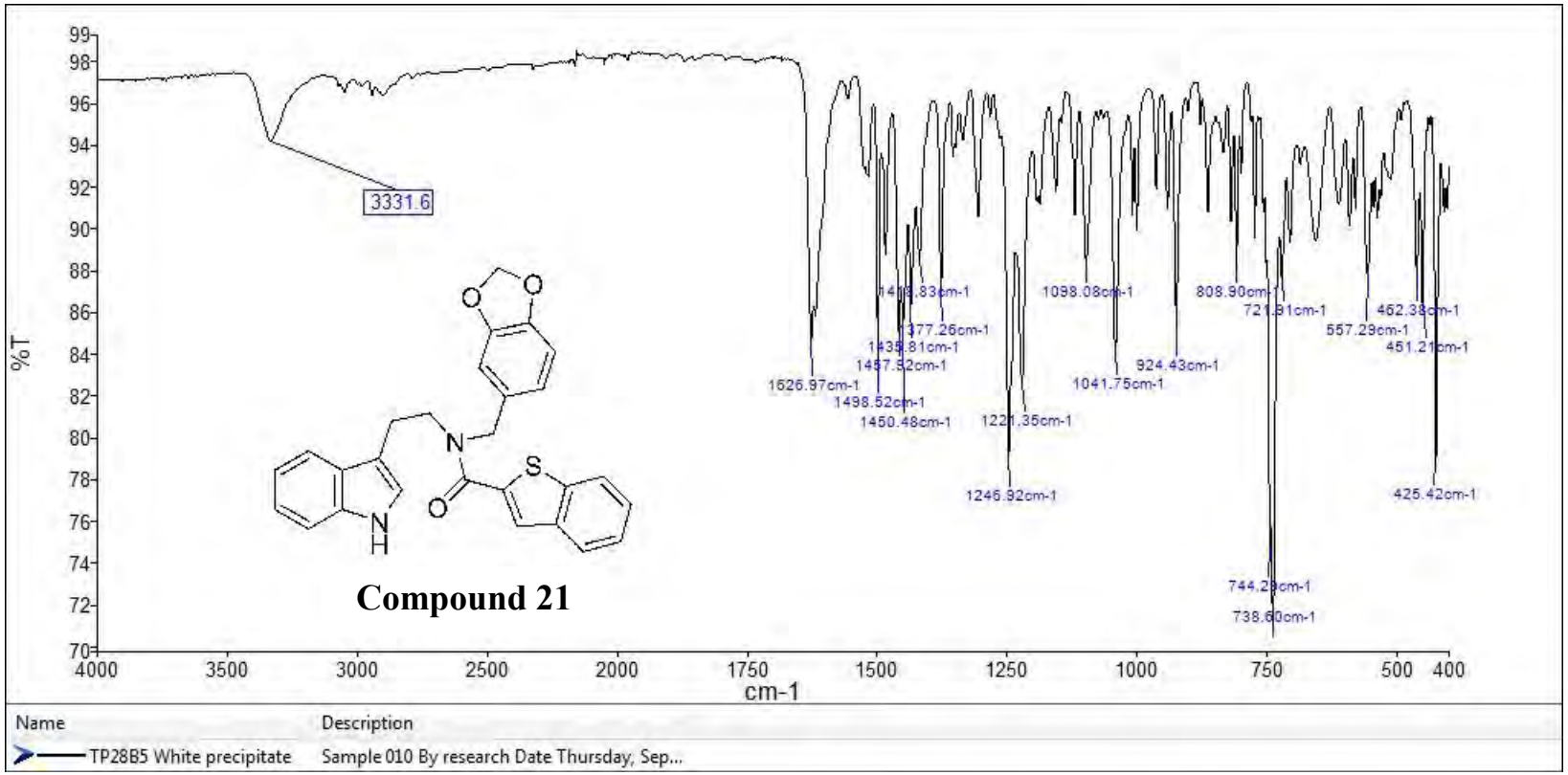
3331.6
1626.97cm-1
1498.52cm-1
1450.48cm-1
1435.81cm-1
1457.52cm-1
1377.26cm-1
1221.35cm-1
1246.92cm-1
1098.08cm-1
1041.75cm-1
924.43cm-1
808.90cm-1
721.91cm-1
744.23cm-1
738.60cm-1
557.29cm-1
462.38cm-1
451.21cm-1
425.42cm-1
%T
cm-1
Name
Description
TP28B5 White precipitate
Sample 010 By research Date Thursday, Sep...

Compound 21

SHIMADZU LabSolutions **Analysis Report**

<Sample Information>

Sample Name	: TP28B5		
Sample ID	: TP28B5		
Data Filename	: TP28B5.lcd		
Method Filename	: 10-100 over 15 mins.lcm		
Batch Filename	: TRIEU Second Third Generation and New pro.lcb		
Vial #	: 1-7	Sample Type	: Unknown
Injection Volume	: 30 uL		
Date Acquired	: 5/09/2014 1:38:17 PM	Acquired by	: System Administrator
Date Processed	: 5/09/2014 2:08:18 PM	Processed by	: System Administrator

<Chromatogram>

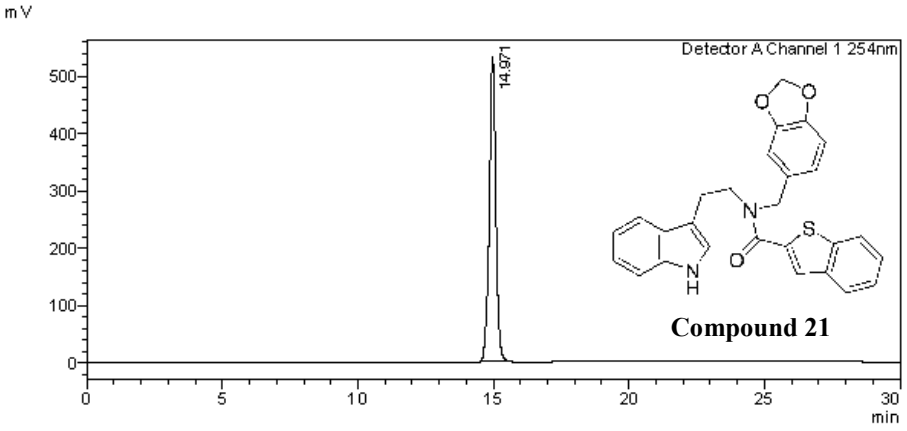

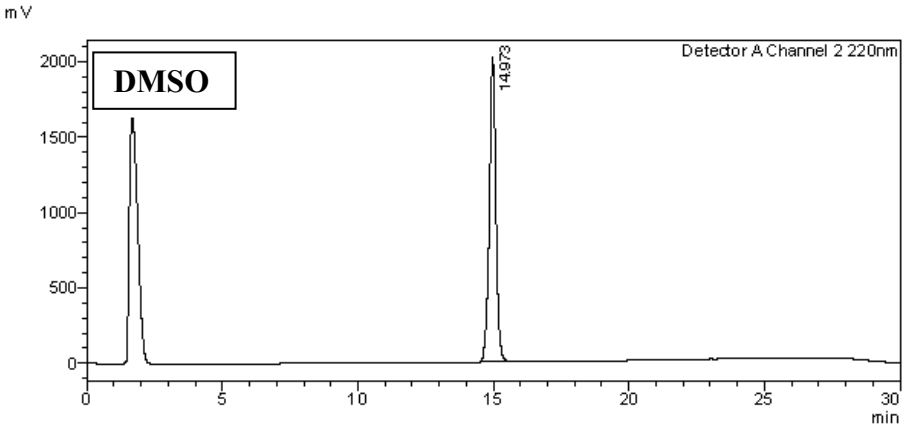

<Peak Table>

Detector A Channel 1 254nm

C:\LabSolutions\Data\Project1\TRIEU\TP28B5.lcd

Peak#	Ret. Time	Area	Height	Conc.	Unit	Mark	Name
1	14.971	8655283	530748	100.000		M	
Total		8655283	530748				

Detector A Channel 2 220nm

Peak#	Ret. Time	Area	Height	Conc.	Unit	Mark	Name
1	14.973	33111569	2016825	100.000		M	
Total		33111569	2016825				

==== Shimadzu LCMSsolution Data Report ====

<Chromatogram>

Sample Information

Acquired by	: Admin
Date Acquired	: 11/18/2014 2:09:14 PM
Sample Type	: Unknown
Level#	: 0
Sample Name	: TP28b5_APCI+
Sample ID	:
ISTD Amount	: (Level1 Conc.)
Sample Amount	: 1
Dilution Factor	: 1
Tray#	: 1
Vial#	: 4
Injection Volume	: 10
Data File	: TP28b5_APCI+.lcd
Method File	: FIA-APCI_scan(+).lcm
Original Method	: C:\LabSolutions\Data\Pete\FIA-APCI_scan(+).lcm
Report Format	: DefaultLCMS.lcr
Tuning File	: C:\LabSolutions\LCsolution\Log\Tuning\Autotune_030908.lct
Processed by	: Admin
Modified Date	: 11/18/2014 2:10:47 PM

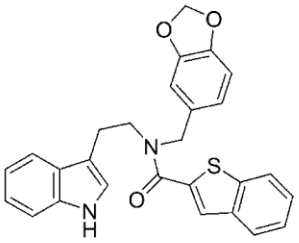

Compound 21

Chromatogram
TP28b5_APCI+ C:\LabSolutions\Data\Pete\Treiu\TP28b5_APCI+.lcd

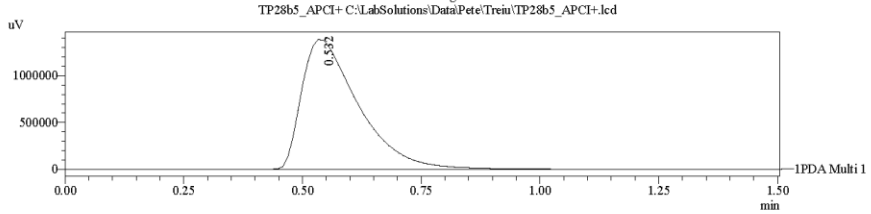

1 PDA Multi 1 / 254nm 4nm

<Spectrum>

Retention Time:0.580(Scan#:59)
Max Peak:584 Base Peak:454.70(1072828)
Spectrum:Averaged 0.460-0.980(47-99)
Background:Averaged 0.060-0.357(7-37) Polarity:Pos Segment1 - Event1

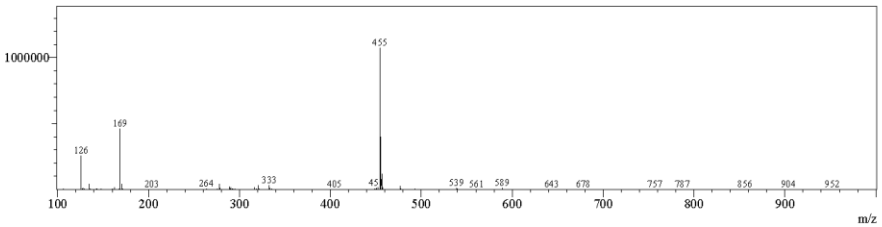

Retention Time:0.650(Scan#:66)
Max Peak:566 Base Peak:112.60(469733)
Spectrum:Averaged 0.470-0.990(48-100)
Background:Averaged 0.070-0.357(8-38) Polarity:Neg Segment1 - Event2

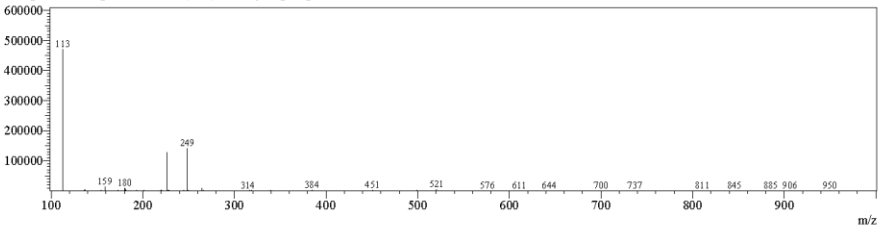

C:¥LabSolutions¥Data¥Pete¥Treiu¥TP28b5_APCI+.lcd

Compound	Chemical Formula	Predicted monoisotopic neutral MW	Predicted MH+	MH+ Measured	Main MS Ions	Main MS/MS Fragments
TP 2885	$C_{27}H_{22}N_2O_3S$	454.1351	455.14239	455.14231	455.14231*	n/a

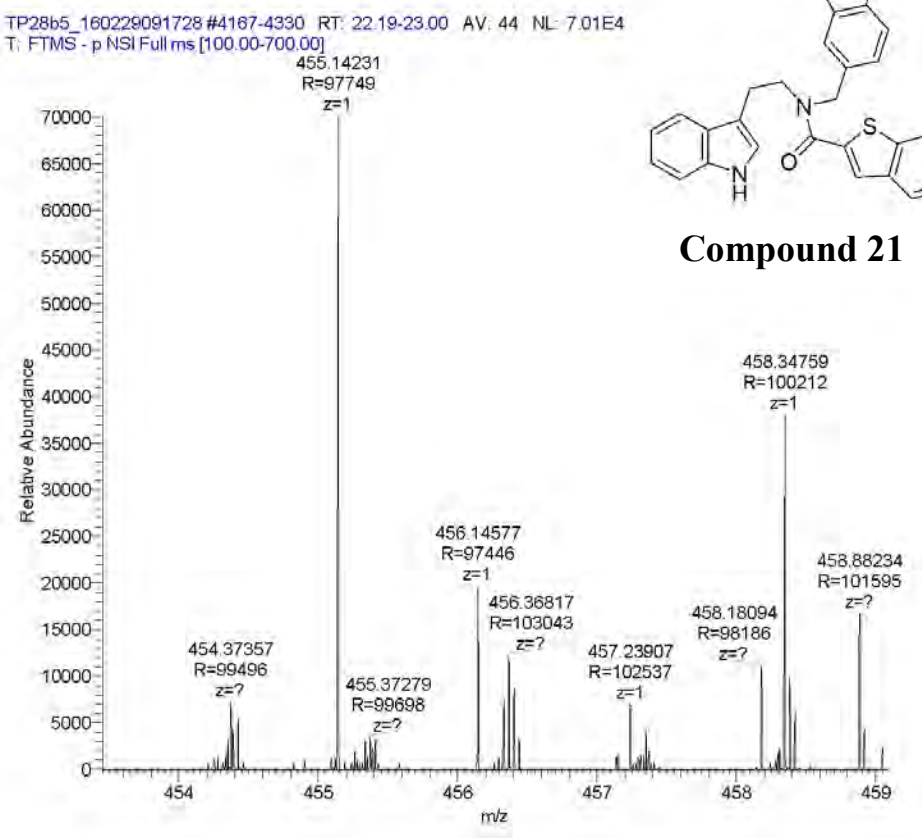

Compound 21

COMPOUND 22

Compound Name: Benzofuran-2-carboxylic acid benzo[1,3]dioxol-5-ylmethyl-[2-(*1H*-indol-3-yl)-ethyl]-amide

Obtained Weight & Yield: 156 mg, 63%

Appearance: Off white precipitate

Solubility: DMSO

Melting Point: 173 − 173.6 ºC

TLC Conditions: EtOAc/Hexane (50/50)

IR Analysis: νmax/cm^{-1}

3316 (NH), 1627 (CON), 737 (CH-aromatics)

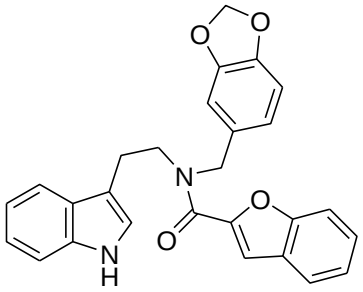

$C_{27}H_{22}N_2O_4$
Exact Mass: 438.1580

^{1}H NMR Analysis:

^{1}H NMR (400 MHz, DMSO-d_6) δ 10.83 (s, 1H), 7.72 (d, J = 5.8 Hz, 1H), 7.62 (d, J = 8.3 Hz, 1H), 7.58 – 7.26 (m, 5H), 7.19 – 6.71 (m, 6H), 6.01 (s, 2H), 4.72 (s, 2H), 3.91 −3.51 (m, 2H), 3.05 (s, 2H).

^{13}C NMR Analysis:

^{13}C NMR (101 MHz, DMSO-d_6) δ 154.4, 149.3, 148.0, 147.0, 136.7, 131.7, 129.0, 127.4, 127.2, 126.9, 124.1, 123.6, 122.9, 122.0, 121.4, 118.7, 118.5, 112.2, 111.9, 111.1, 109.0, 108.8, 101.5, 48.7, 48.8, 25.1.

HPLC:

RP-HPLC Alltima™ C18 5 μm 150 mm x 4.6 mm, 10–100% B in 15 min, R_t = 7.12 min, 100%.

Mass Spectral Analysis: LRMS **(**APCI+/-) m/z 438, 439 $[M+H]^+$, 100%. HRMS (ES+) for $C_{27}H_{22}N_2O_4$, calculated 439.1652, found 439.1652.

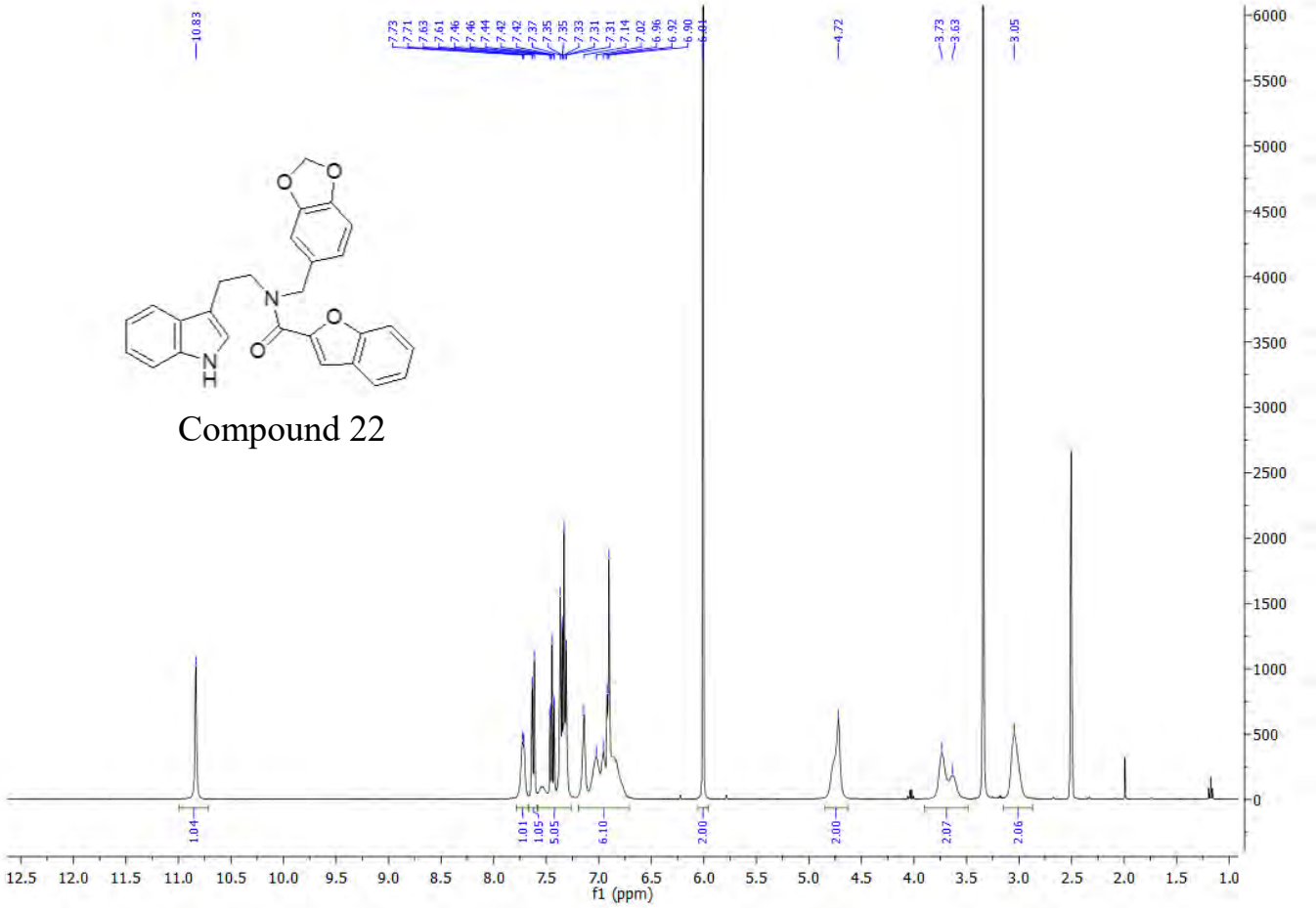
10.83
7.73
7.71
7.63
7.61
7.46
7.46
7.44
7.42
7.42
7.37
7.35
7.35
7.33
7.31
7.31
7.14
7.02
6.96
6.92
6.90
4.72
3.73
3.63
3.05
1.04
1.01
1.05
5.05
6.10
2.00
2.00
2.07
2.06
f1 (ppm)

Compound 22

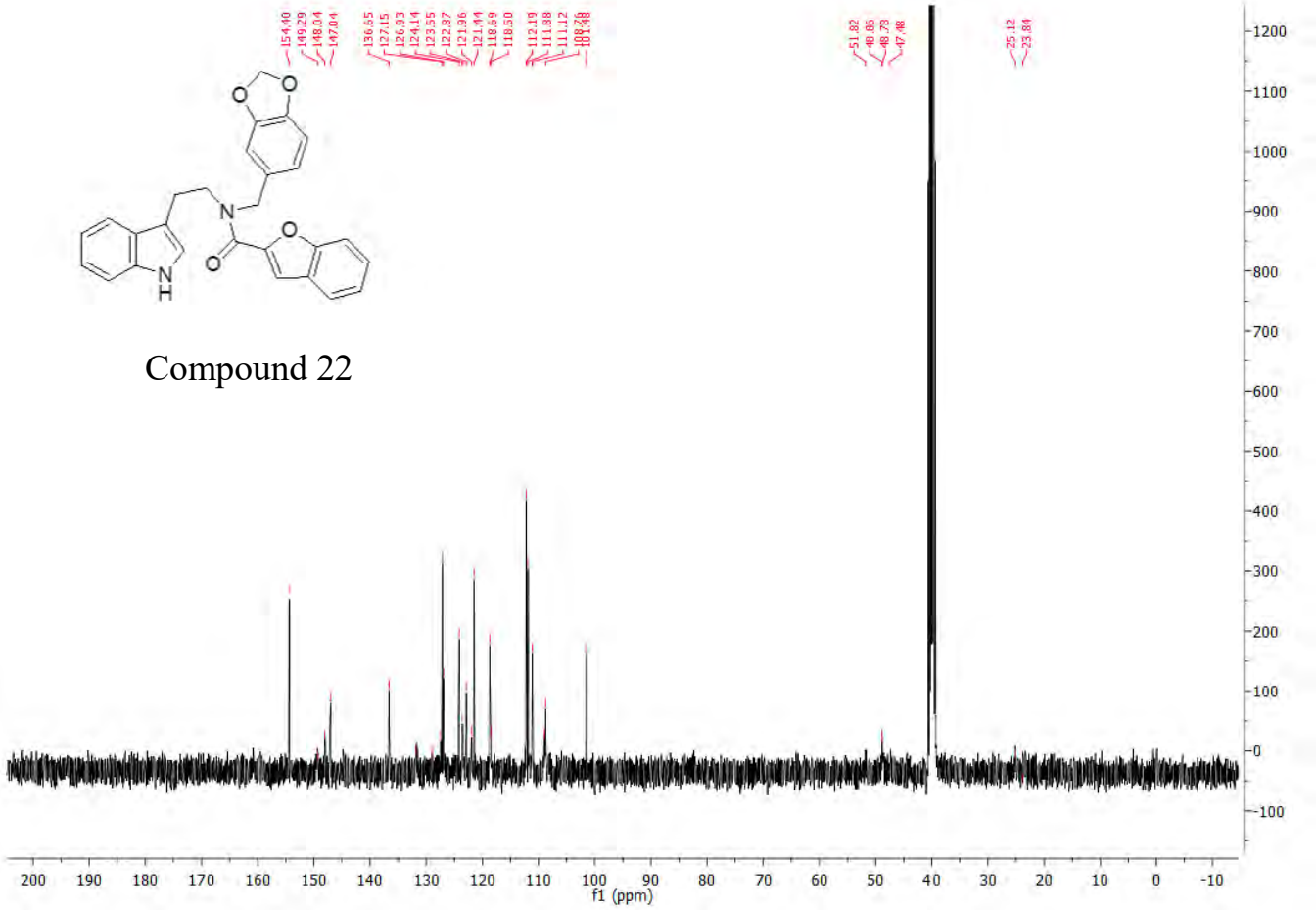
154.40
149.29
148.04
147.04
136.65
127.15
126.93
124.14
123.55
122.87
121.96
121.44
118.69
118.50
112.19
111.88
111.12
101.73
101.48
51.82
48.86
48.78
47.48
25.12
23.84
O
O
N
O
O
N
H
1200
1100
1000
900
800
700
600
500
400
300
200
100
0
-100
200
190
180
170
160
150
140
130
120
110
100
90
80
70
60
50
40
30
20
10
0
-10
f1 (ppm)

Compound 22

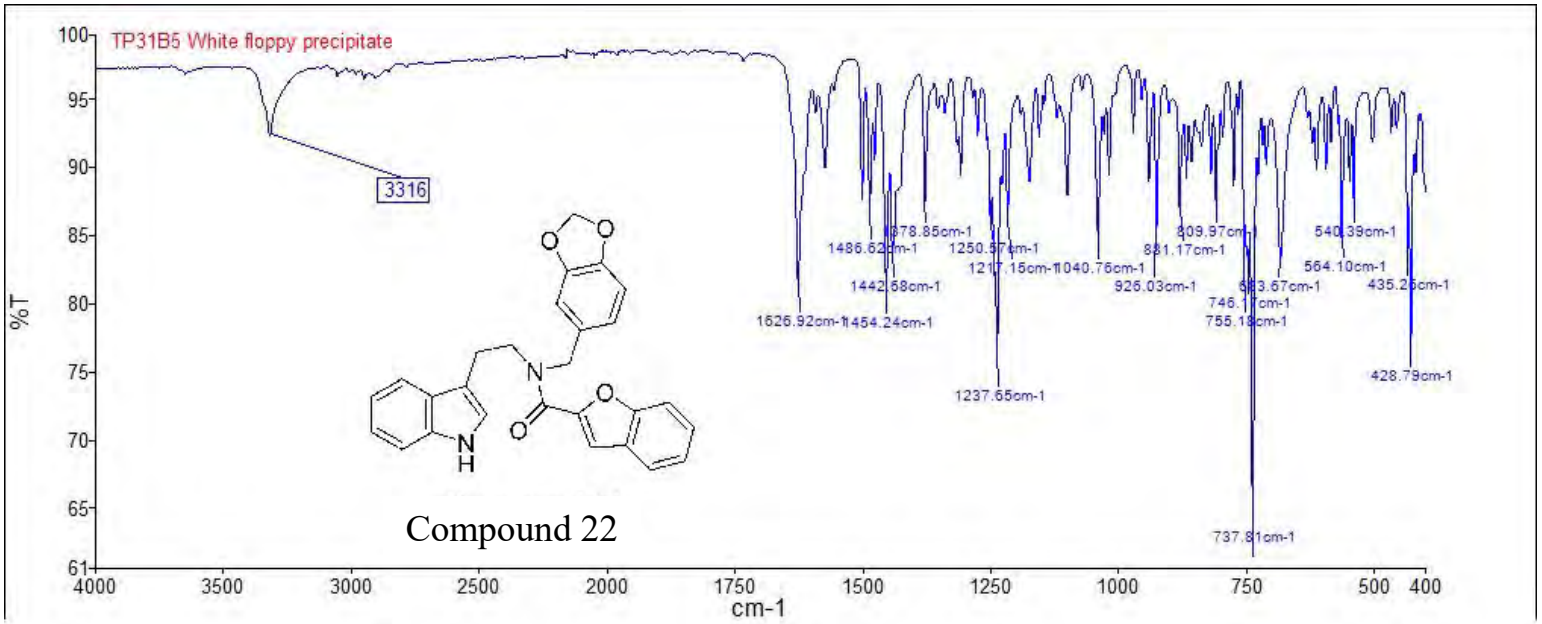
TP31B5 White floppy precipitate
%T
cm-1
3316
1626.92cm-1
1454.24cm-1
1442.68cm-1
1237.65cm-1
1040.76cm-1
926.03cm-1
737.81cm-1
428.79cm-1
564.10cm-1
540.39cm-1
435.26cm-1
Compound 22

==== Shimadzu LCMSsolution Analysis Report ====

Acquired by	: Admin
Sample Name	: TP31B5
Sample ID	:
Vail #	: 57
Injection Volume	: 20 uL
Data File Name	: TP31B5.lcd
Method File Name	: Econosphere C18 EPS 5u lot 50195421 part 70070 150mm id 4.6mm.lcm
Batch File Name	: Second and third 23092015.lcb
Report File Name	: DefaultLCMS.lcr
Data Acquired	: 9/23/2015 5:53:12 PM
Data Processed	: 9/25/2015 4:15:40 PM

<Chromatogram>

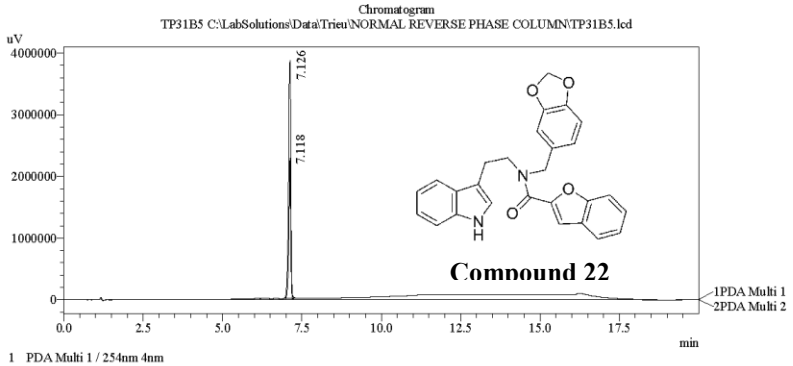

1 PDA Multi 1 / 254nm 4nm
2 PDA Multi 2 / 220nm 4nm

PeakTable

PDA Ch1 254nm 4nm

Peak#	Ret. Time	Area	Height	Area %	Height %
1	7.118	8897445	2284787	100.000	100.000
Total		8897445	2284787	100.000	100.000

PeakTable

PDA Ch2 220nm 4nm

Peak#	Ret. Time	Area	Height	Area %	Height %
1	7.126	19630044	3828232	100.000	100.000
Total		19630044	3828232	100.000	100.000

==== Shimadzu LCMSsolution Data Report ====

<Chromatogram>

Sample Information

Acquired by	: Admin
Date Acquired	: 11/12/2014 10:20:37 AM
Sample Type	: Unknown
Level#	: 0
Sample Name	: tp31b5_ APCI-
Sample ID	:
ISTD Amount	: (Level1 Conc.)
Sample Amount	: 1
Dilution Factor	: 1
Tray#	: 1
Vial#	: 2
Injection Volume	: 10
Data File	: tp31b5_ APCI-.lcd
Method File	: FIA-APCI_scan(-).lcm
Original Method	: C:\LabSolutions\Data\Kelly\FIA-APCI_scan(-).lcm
Report Format	: DefaultLCMS.lcr
Tuning File	: C:\LabSolutions\LCsolution\Log\Tuning\Autotune_030908.lct
Processed by	: Admin
Modified Date	: 11/12/2014 10:22:09 AM

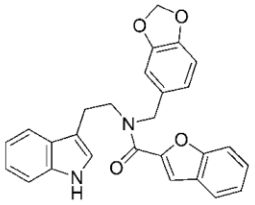

Compound 22

Chromatogram

tp31b5_ APCI- C:\LabSolutions\Data\Pete\Treiu\tp31b5_ APCI-.lcd

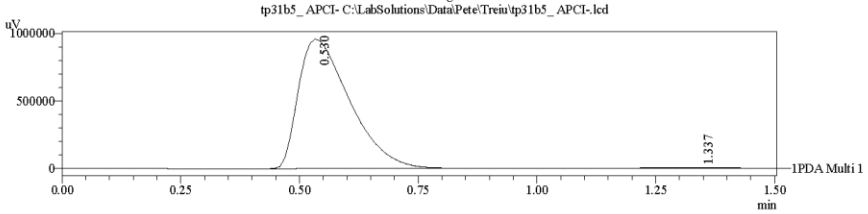

1 PDA Multi 1 / 254nm 4nm

<Spectrum>

Retention Time:0.600(Scan#:61)
Max Peak:593 Base Peak:438.95(1093426)
Spectrum:Averaged 0.480-0.900(49-91)
Background:Averaged 0.100-0.353(11-37) Polarity:Pos Segment1 - Event1

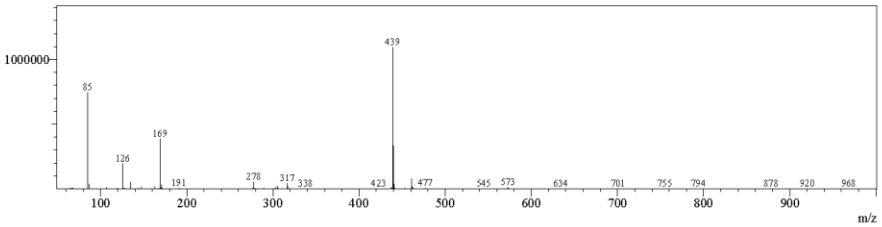

Retention Time:0.610(Scan#:62)
Max Peak:455 Base Peak:112.60(536544)
Spectrum:Averaged 0.490-0.910(50-92)
Background:Averaged 0.110-0.353(12-38) Polarity:Neg Segment1 - Event2

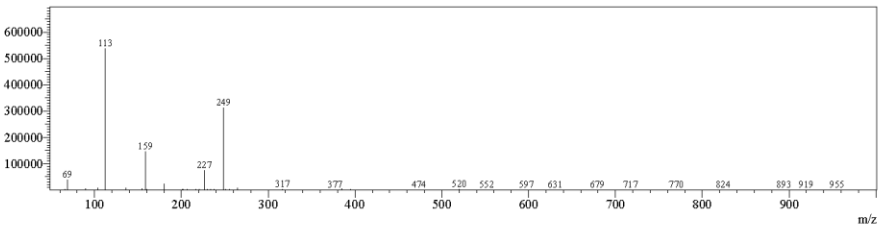

C:¥LabSolutions¥Data¥Pete¥Treiu¥tp31b5_ APCI-.lcd

Compound	Chemical Formula	Predicted monoisotopic neutral MW	Predicted MH+	MH+ Measured	Main MS Ions	Main MS/MS Fragments
TP 31B5	$C_{27}H_{22}N_2O_4$	438.1580	439.16523	439.16523	439.16523	n/a

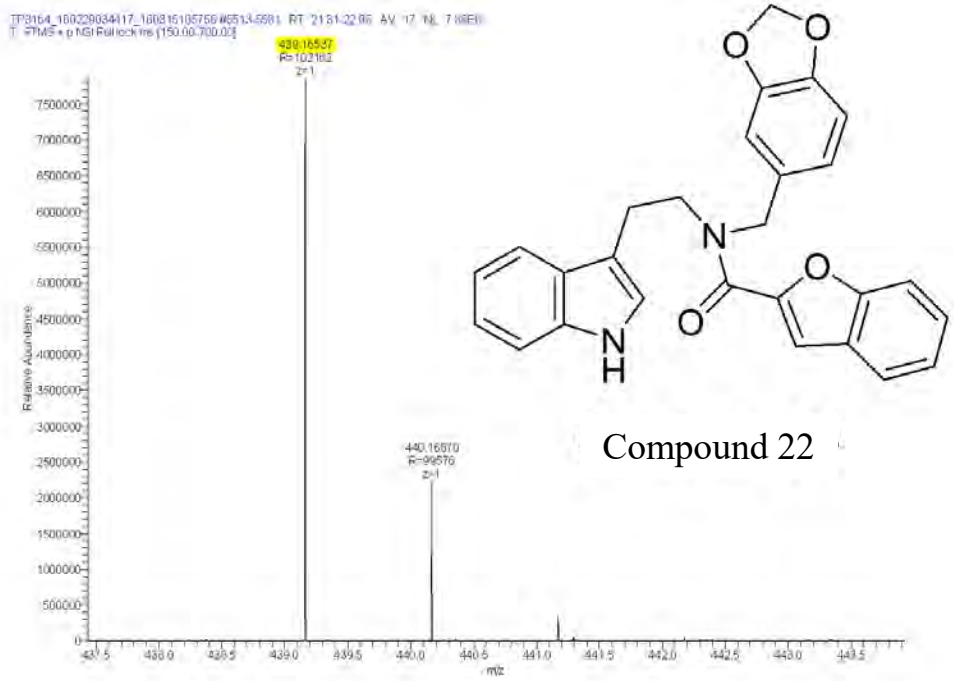

Compound 22

COMPOUND 23

Compound Name: *N*-Benzo[1,3]dioxol-5-ylmethyl-4-chloro-*N*-[2-(*1H*-indol-3-yl)-ethyl]-benzamide

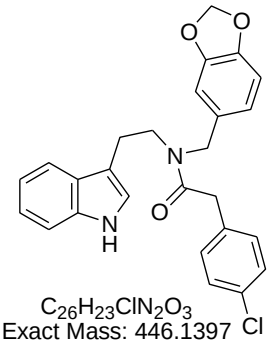

$C_{26}H_{23}ClN_2O_3$
Exact Mass: 446.1397

Obtained Weight & Yield: 90 mg, 58%

Appearance: White powder

Solubility: EtOAc, Acetone, ACN

Melting Point: 132-133 °C

TLC Conditions: EtOAc/Hexane (50/50)

IR Analysis: νmax/cm^{-1}

3203 (NH), 1626 (CON), 1500 (C=C aromatic), 1251 (C-N), 747 (C-H aromatic)

*This is a mixture of atropisomers of compound **35** with the ratio approximately 2.0 : 1.2 calculated on the CH_2 splitting peaks at 2.93 and 2.84 ppm of the proton NMR. The exact structure for each of the atropisomer remains to be confirmed. As the spectra is complex with both splitting and overlapping, the proton NMR is reported separately for splitting peaks where possible. In case of complex overlapping (aromatic region), the proton NMR is assigned as a whole.*

^{1}H NMR Analysis: Calculated separately for splitting peaks

1H NMR (400 MHz, DMSO-d_6) δ 10.89 (s, 2H), 10.79 (s, 1H), 7.50 (t, J = 6.8 Hz, 3H), 7.40-7.26 (m, 9H), 7.23 (d, J = 8.4 Hz, 2H), 7.15 (d, J = 1.9 Hz, 2H), 7.12-6.91 (m, 11H), 6.90-6.82 (m, 3H), 6.82 – 6.62 (m, 6H), 6.03-5.94 (m, 6H), 4.57-4.46 (m, 6H), 3.59 – 3.43 (m, 10H), 2.93 (t, J = 7.2 Hz, 4H), 2.89 – 2.78 (m, 2H).

^{13}C NMR Analysis: Calculated separately for splitting peaks

^{13}C NMR (101 MHz, DMSO-d_6) δ 170.1 and 170.0 (1C), 147.6 and 147.4 (1C), 146.5 and 146.3 (1C), 136.2 (1C), 135.1 and 135.0 (1C), 132.1, 131.3 and 131.2 (2C), 131.1 and 130.9 (1C), 128.1 and 127.9 (2C), 127.1 and 127.0 (1C), 123.4, 122.7, 121.2 and 121.1 (1C), 120.9 and 120.2 (1C), 118.5 and 118.3 (1C), 118.2 and 118.1 (1C), 111.5 and 111.4 (1C), 110.9, 108.3 and 108.1 (1C), 107.4, 101.0 and 100.9 (1C), 50.8 and 47.1 (1C), 47.5 and 46.4 (1C), 38.9 and 38.3(1C), 23.8 and 23.0 (1C).

HPLC: RP-HPLC Alltima™ C18 5 µm 150 mm x 4.6 mm, 10–100% B in 15 min, R_t = 14.76 min, 100%.

Mass Spectral Analysis (Low res): m/z APCI (+) 446, 447 $[M+H]^+$ 100%. HRMS (ES+) calculated for $C_{26}H_{23}ClN_2O_3$ 446.1397, found 447.1467.

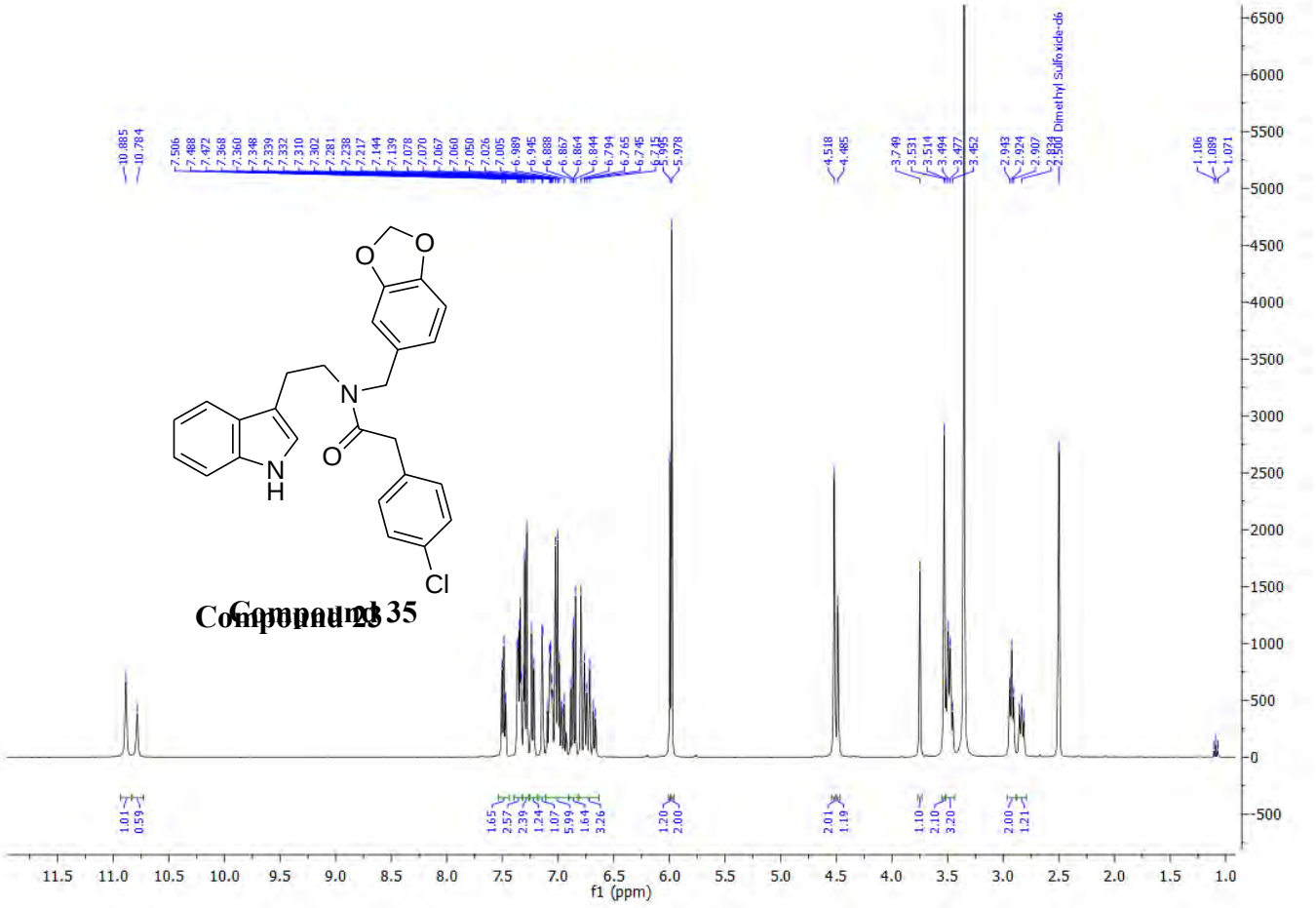
Compound 35
Dimethyl Sulfoxide-d6
f1 (ppm)

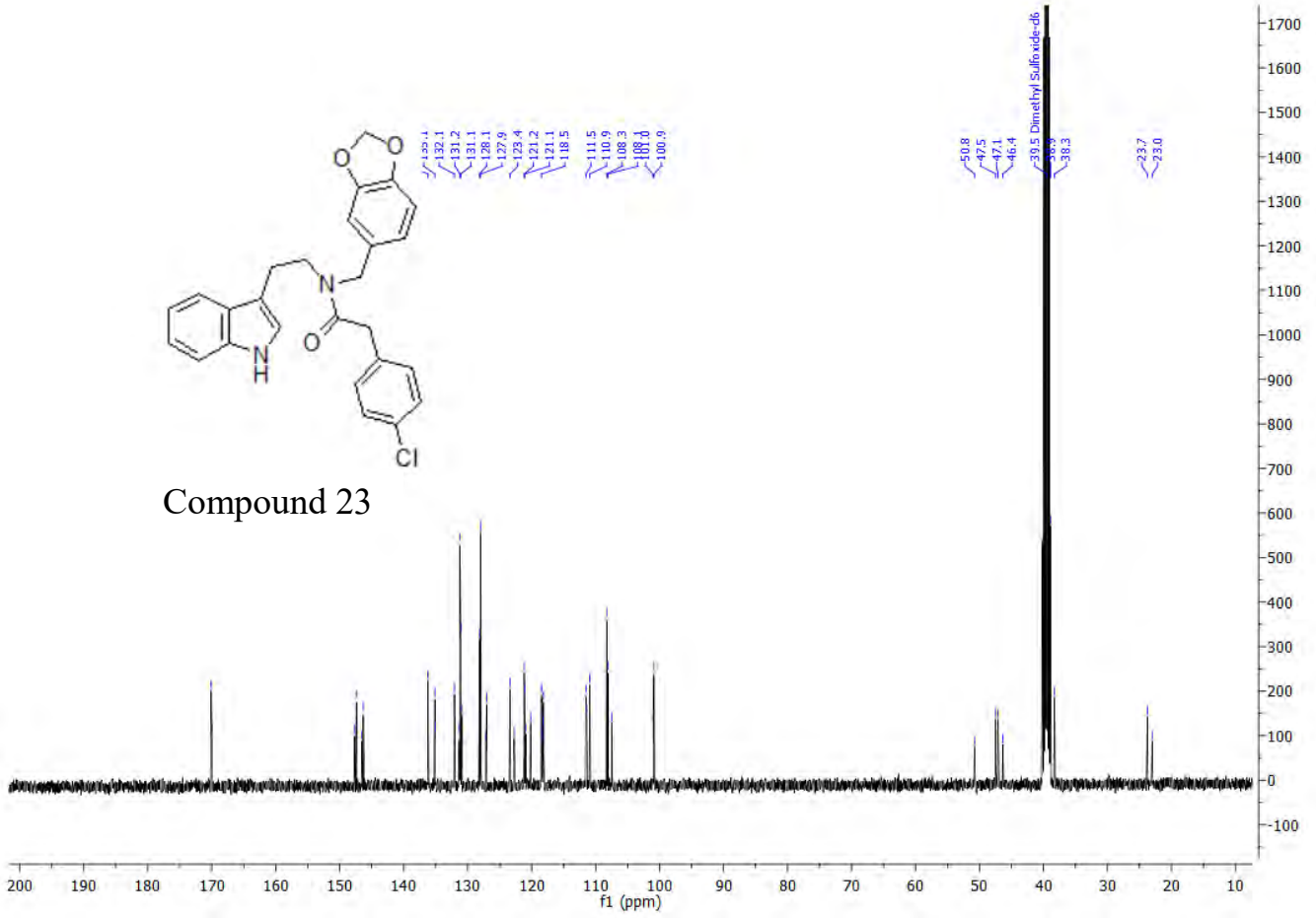
O
O
N
H
O
Cl
132.1
131.2
131.1
128.1
127.9
123.4
121.2
121.1
118.5
111.5
110.9
108.3
101.0
100.9
50.8
47.5
47.1
46.4
39.5 Dimethyl Sulfoxide-d6
38.9
38.3
23.7
23.0
1700
1600
1500
1400
1300
1200
1100
1000
900
800
700
600
500
400
300
200
100
0
-100
200
190
180
170
160
150
140
130
120
110
100
90
80
70
60
50
40
30
20
10
f1 (ppm)

Compound 23

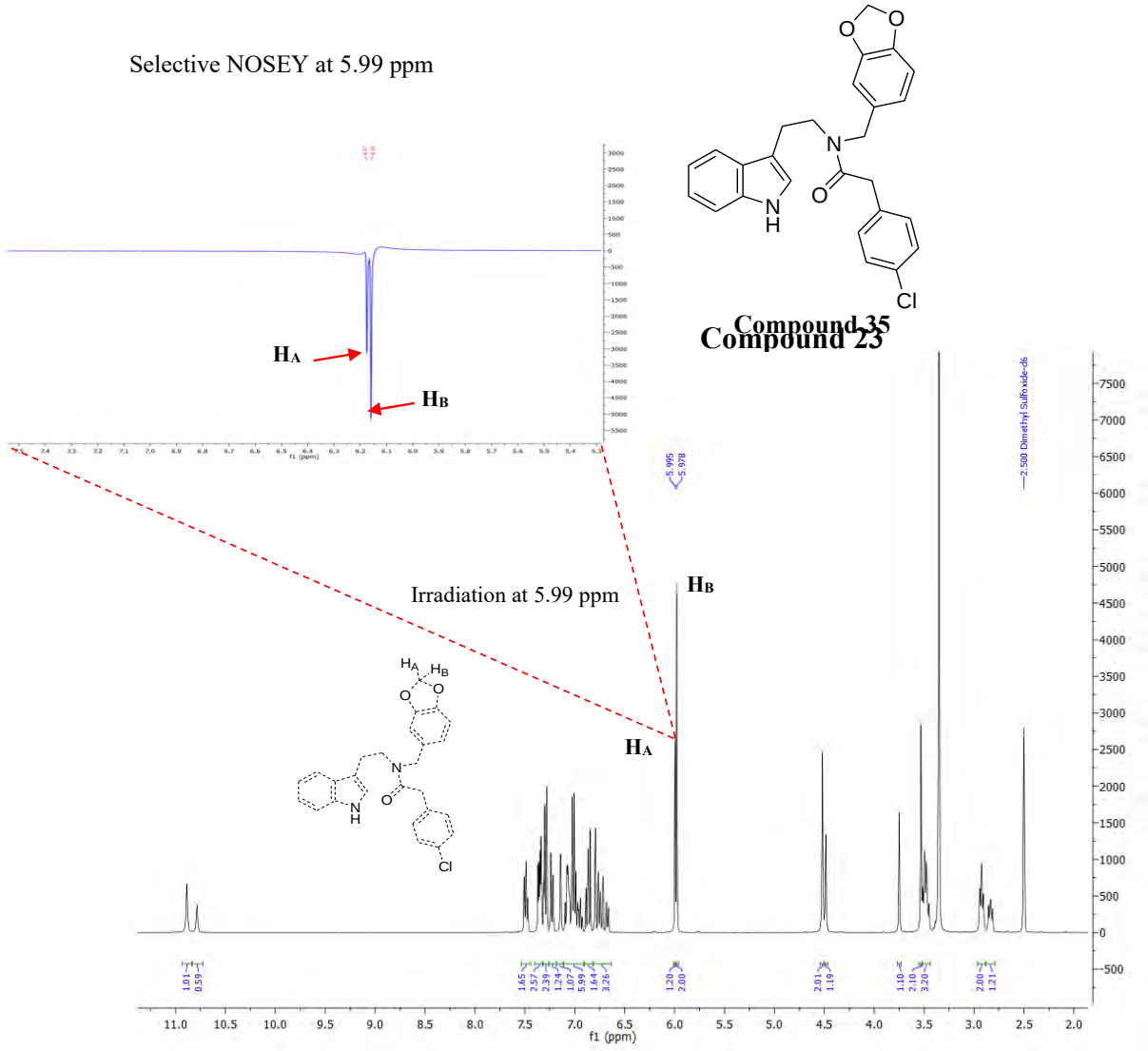
Selective NOSEY at 5.99 ppm
Compound 35
Compound 23
HA
HB
Irradiation at 5.99 ppm
HB
HA
f1 (ppm)

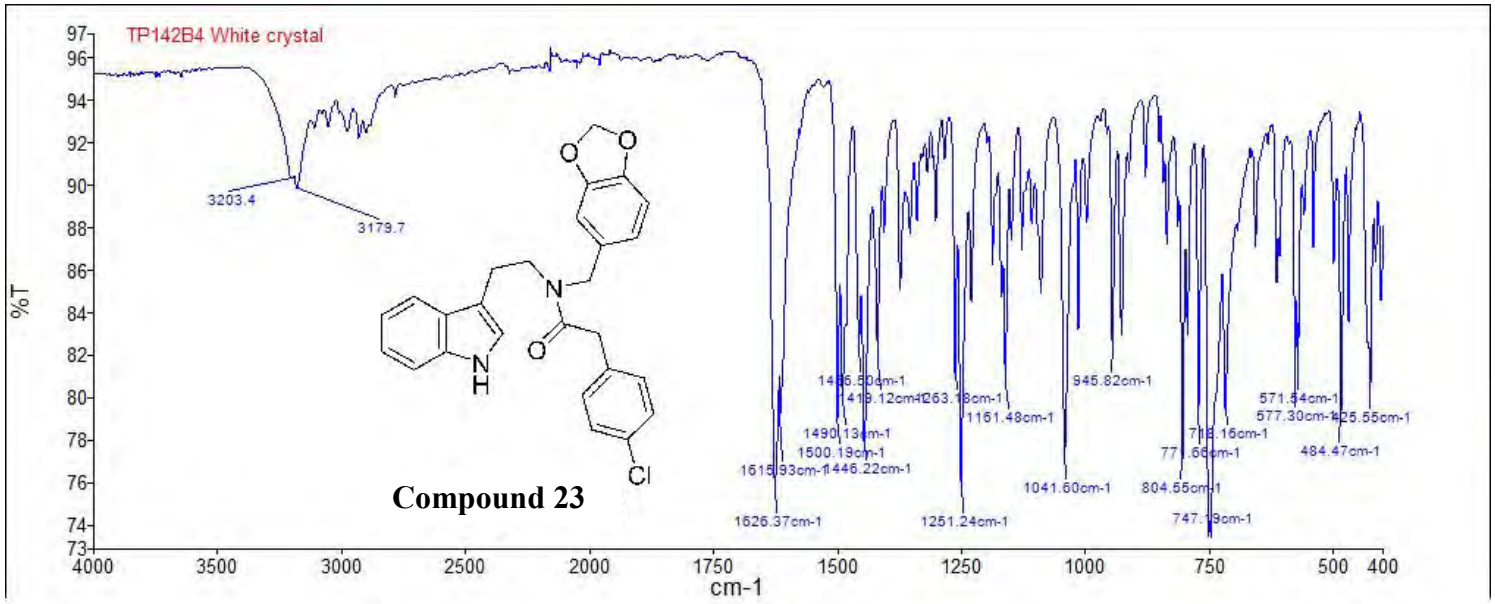
TP142B4 White crystal
%T
cm-1
3203.4
3179.7
1626.37cm-1
1615.93cm-1
1500.19cm-1
1490.13cm-1
1446.22cm-1
1419.12cm-1
1251.24cm-1
1041.60cm-1
945.82cm-1
804.55cm-1
747.19cm-1
484.47cm-1
O
O
N
H
O
Cl

Compound 23

SHIMADZU LabSolutions **Analysis Report**

<Sample Information>

Sample Name	: TP142B4		
Sample ID	: TP142B4		
Data Filename	: TP142B4.lcd		
Method Filename	: 10-100 over 15 mins.lcm		
Batch Filename	: TRIEU Second Third Generation and New pro.lcb		
Vial #	: 1-12	Sample Type	: Unknown
Injection Volume	: 30 uL		
Date Acquired	: 8/09/2014 12:07:19 PM	Acquired by	: System Administrator
Date Processed	: 8/09/2014 12:37:20 PM	Processed by	: System Administrator

<Chromatogram>

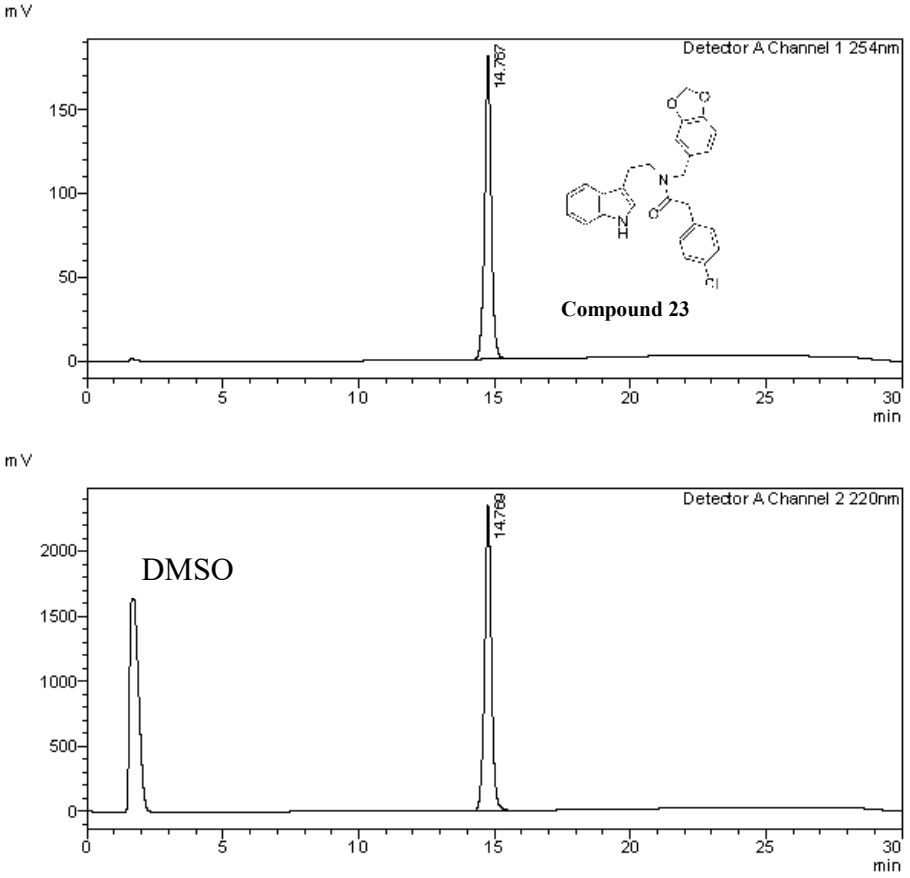

<Peak Table>

Detector A Channel 1 254nm

C:\LabSolutions\Data\Project1\TRIEU\TP142B4.lcd

Peak#	Ret. Time	Area	Height	Conc.	Unit	Mark	Name
1	14.767	3008239	180337	100.000		M	
Total		3008239	180337				

Detector A Channel 2 220nm

Peak#	Ret. Time	Area	Height	Conc.	Unit	Mark	Name
1	14.769	40285389	2338461	100.000		M	
Total		40285389	2338461				

==== Shimadzu LCMSsolution Data Report ====

<Chromatogram>

Sample Information

Acquired by	: Admin
Date Acquired	: 11/12/2014 10:03:07 AM
Sample Type	: Unknown
Level#	: 0
Sample Name	: tp142b4_APCI+
Sample ID	:
ISTD Amount	: (Level1 Conc.)
Sample Amount	: 1
Dilution Factor	: 1
Tray#	: 1
Vial#	: 5
Injection Volume	: 10
Data File	: tp142b4_APCI+.lcd
Method File	: FIA-APCI_scan(+).lcm
Original Method	: C:\LabSolutions\Data\Kelly\FIA-APCI_scan(+).lcm
Report Format	: DefaultLCMS.lcr
Tuning File	: C:\LabSolutions\LCsolution\Log\Tuning\Autotune_030908.lct
Processed by	: Admin
Modified Date	: 11/12/2014 10:04:39 AM

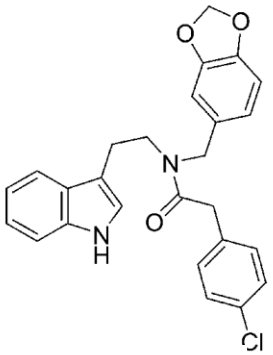

Compound 23

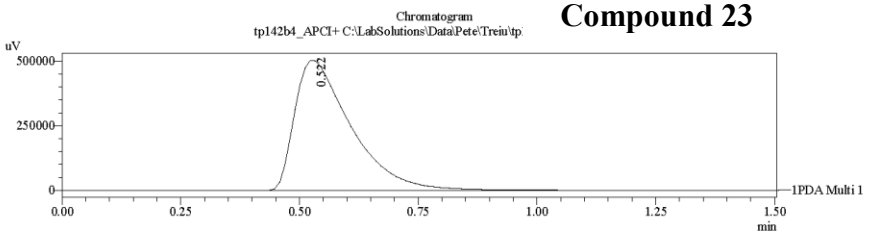

1 PDA Multi 1 / 254nm 4nm

<Spectrum>

Retention Time:0.640(Scan#:65)
Max Peak:638 Base Peak:446.70(863876)
Spectrum:Averaged 0.440-1.100(45-111)
Background:Averaged 0.040-0.403(5-41) Polarity:Pos Segment1 - Event1

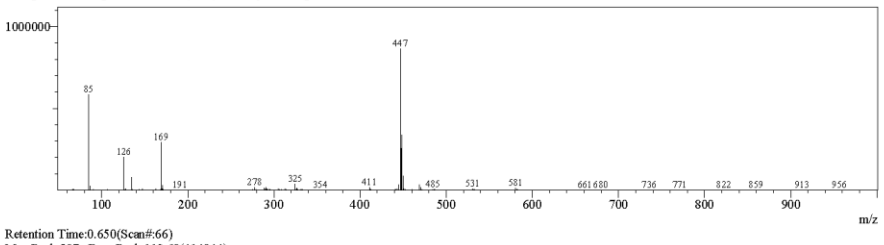

Retention Time:0.650(Scan#:66)
Max Peak:587 Base Peak:112.60(414044)
Spectrum:Averaged 0.450-1.110(46-112)
Background:Averaged 0.050-0.403(6-42) Polarity:Neg Segment1 - Event2

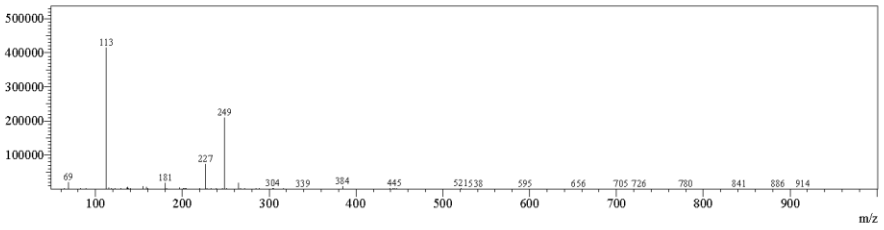

C:¥LabSolutions¥Data¥Pete¥Treiu¥tp142b4_APCI+.lcd

Compound	Chemical Formula	Predicted monoisotopic neutral MW	Predicted MH+	MH+ Measured	Main MS Ions	Main MS/MS Fragments
TP 142B4	$C_{26}H_{23}ClN_2O_3$	446.1397	447.14700	447.14688		
					447.14688*	Not triggered

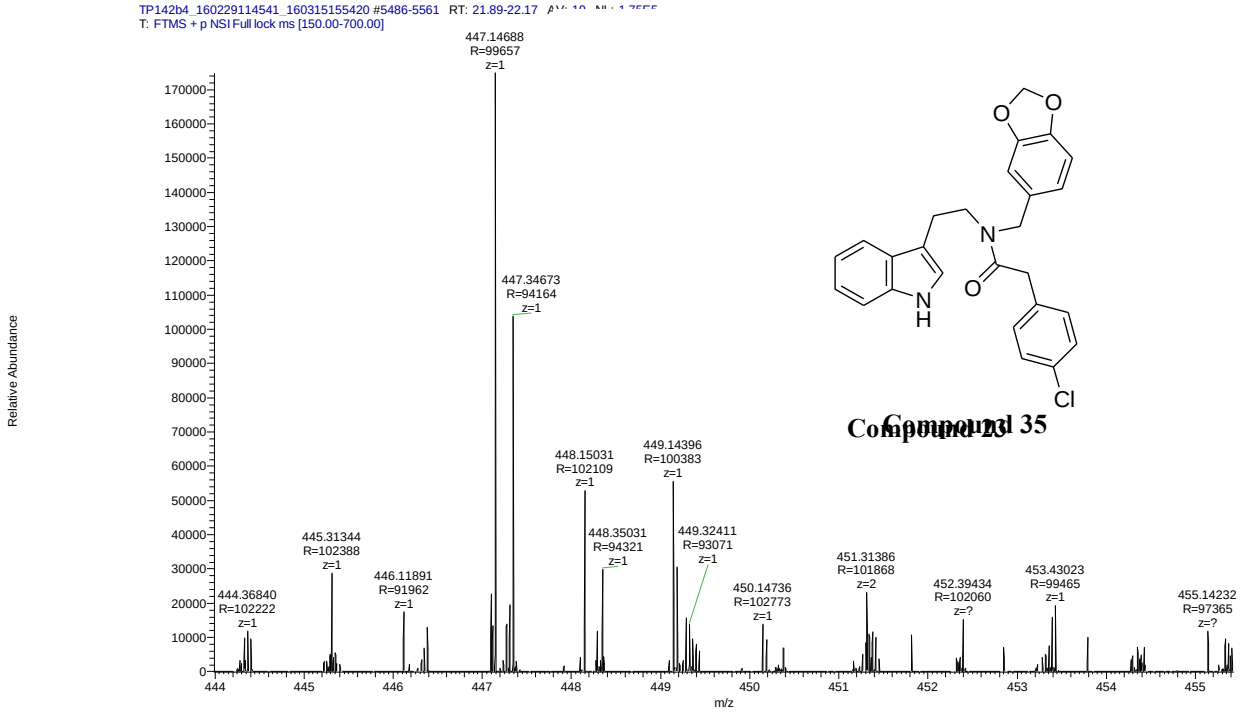

COMPOUND 24

Compound Name: *N*-Benzo[1,3]dioxol-5-ylmethyl-2,6-dichloro-*N*-[2-(*1H*-indol-3-yl)-ethyl]-benzamide

Obtained Weight & Yield: 100 mg, 65%

Appearance: White crystal

Solubility: EtOAc, Acetone, ACN

Melting Point: 157-158 ºC

TLC Conditions: EtOAc/Hexane (50/50)

IR Analysis: νmax/cm^{-1}

3280 (NH), 2937 (CH), 1626 (CON), 739 (CH- aromatics)

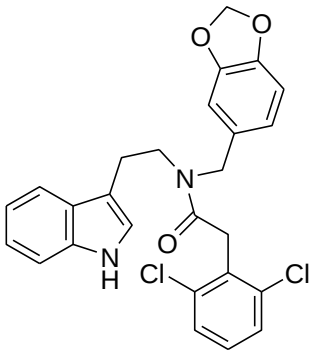

$C_{26}H_{22}Cl_2N_2O_3$
Exact Mass: 480.1007

*This is a mixture of atropisomers of compound **36** with the ratio approximately 2.0 : 1.3 calculated on the CH_2 splitting peaks at 5.99 and 6.02 ppm of the proton NMR.*

^{1}H NMR Analysis:

^{1}H NMR (400 MHz, DMSO-d_6) δ 10.90 (s, 1H), 10.80 (s, 0.7H), 7.59 – 7.25 (m, 8.3H), 7.21 (d, *J* = 2.2 Hz, 1H), 7.10 (s, 0.3H), 7.07 (dd, *J* = 15.0, 8.0 Hz, 2H), 7.03 – 6.91 (m, 2.3H), 6.88 (d, *J* = 7.7 Hz, 1.7H), 6.83 – 6.75 (m, 2.7H), 6.02 (s, 1.3H), 5.99 (s, 2H), 4.61 (s, 1.3H), 4.53 (s, 2H), 4.04 (s, 1.3H), 3.87 (s, 2H), 3.65 (t, *J* = 7.2 Hz, 2H), 3.58 – 3.44 (m, 1.3H), 3.04 (t, *J* = 7.1 Hz, 2H), 2.97 – 2.80 (m, 1.3H).

^{13}C NMR Analysis:

^{13}C NMR (101 MHz, DMSO-d_6) δ 168.2, 168.0, 148.1, 147.9, 147.0, 146.8, 136.8, 136.7, 135.9, 135.9, 133.7, 133.6, 132.5, 131.8, 129.6, 129.5, 128.5, 128.4, 127.6, 127.5, 124.0, 123.2, 121.5, 121.4, 120.5, 118.9, 118.7, 118.7, 118.5, 112.0, 111.8, 111.1, 108.9, 108.6, 107.8, 101.5, 101.4, 51.1, 47.9, 47.7, 47.5, 36.7, 35.9, 24.2, 23.6.

HPLC:

RP-HPLC Alltima™ C18 5 μm 150 mm x 4.6 mm, 10–100% B in 15 min, R_t = 18.81 min, 100%.

Mass Spectral Analysis: LRMS (ESI+) m/z 481, 481[M, ^{35}Cl]$^+$, 100%. HRMS (ES+) for $C_{26}H_{22}Cl_2N_2O_3$, calculated 480.1080, found 481.1079.

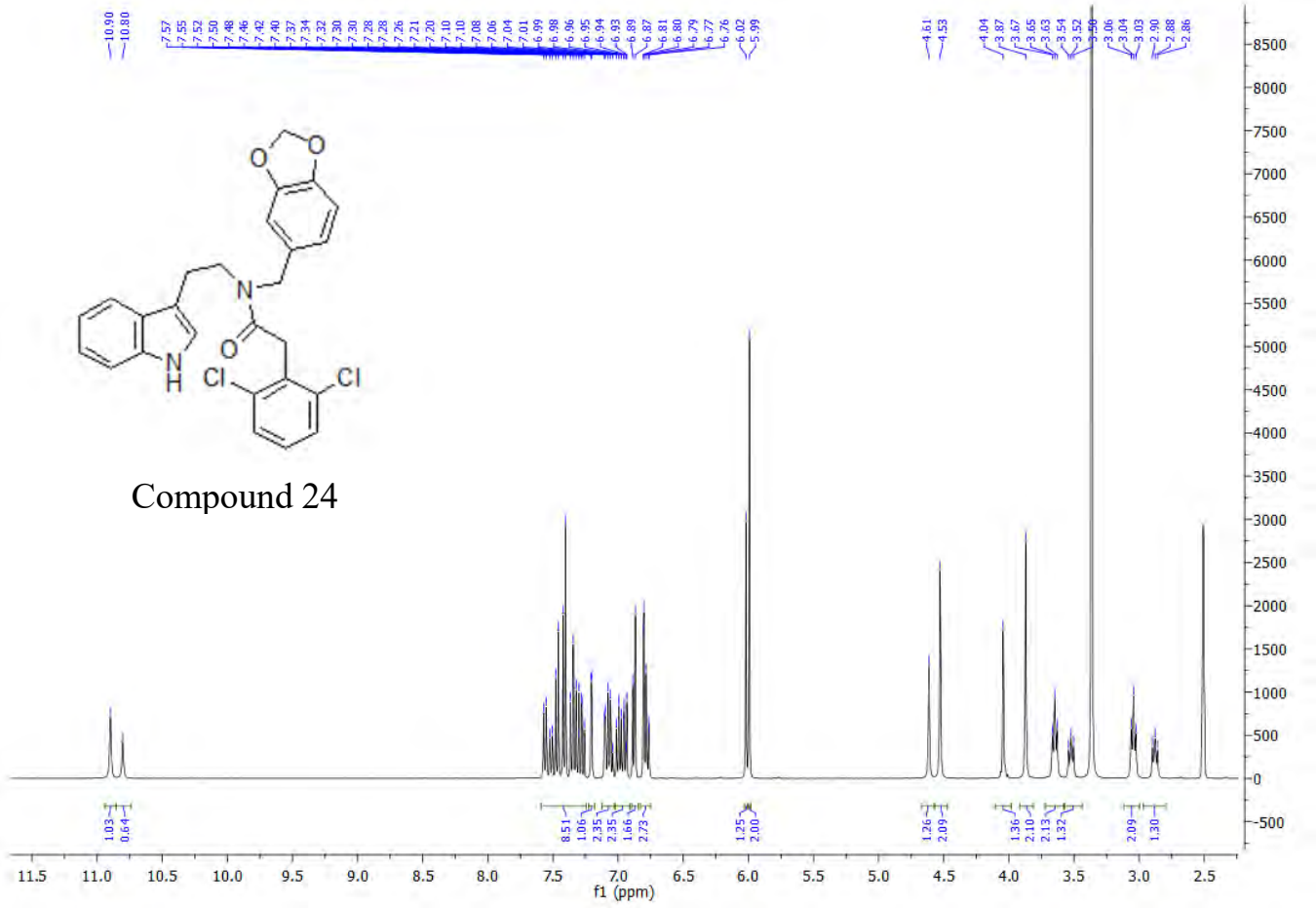
10.90
10.80
7.57
7.55
7.52
7.50
7.48
7.46
7.42
7.40
7.37
7.34
7.32
7.30
7.30
7.28
7.28
7.26
7.21
7.20
7.10
7.08
7.06
7.04
7.01
6.99
6.98
6.96
6.95
6.94
6.93
6.89
6.87
6.81
6.80
6.79
6.77
6.76
6.02
5.99
4.61
4.53
4.04
3.87
3.67
3.65
3.63
3.54
3.52
3.50
3.06
3.04
3.03
2.90
2.88
2.86
O
O
N
O
N
H
Cl
Cl
1.03
0.64
8.51
1.06
2.35
2.35
1.66
2.73
1.25
2.00
1.26
2.09
1.36
2.10
2.13
1.32
2.09
1.30
11.5
11.0
10.5
10.0
9.5
9.0
8.5
8.0
7.5
7.0
6.5
6.0
5.5
5.0
4.5
4.0
3.5
3.0
2.5
f1 (ppm)
8500
8000
7500
7000
6500
6000
5500
5000
4500
4000
3500
3000
2500
2000
1500
1000
500
0
-500

Compound 24

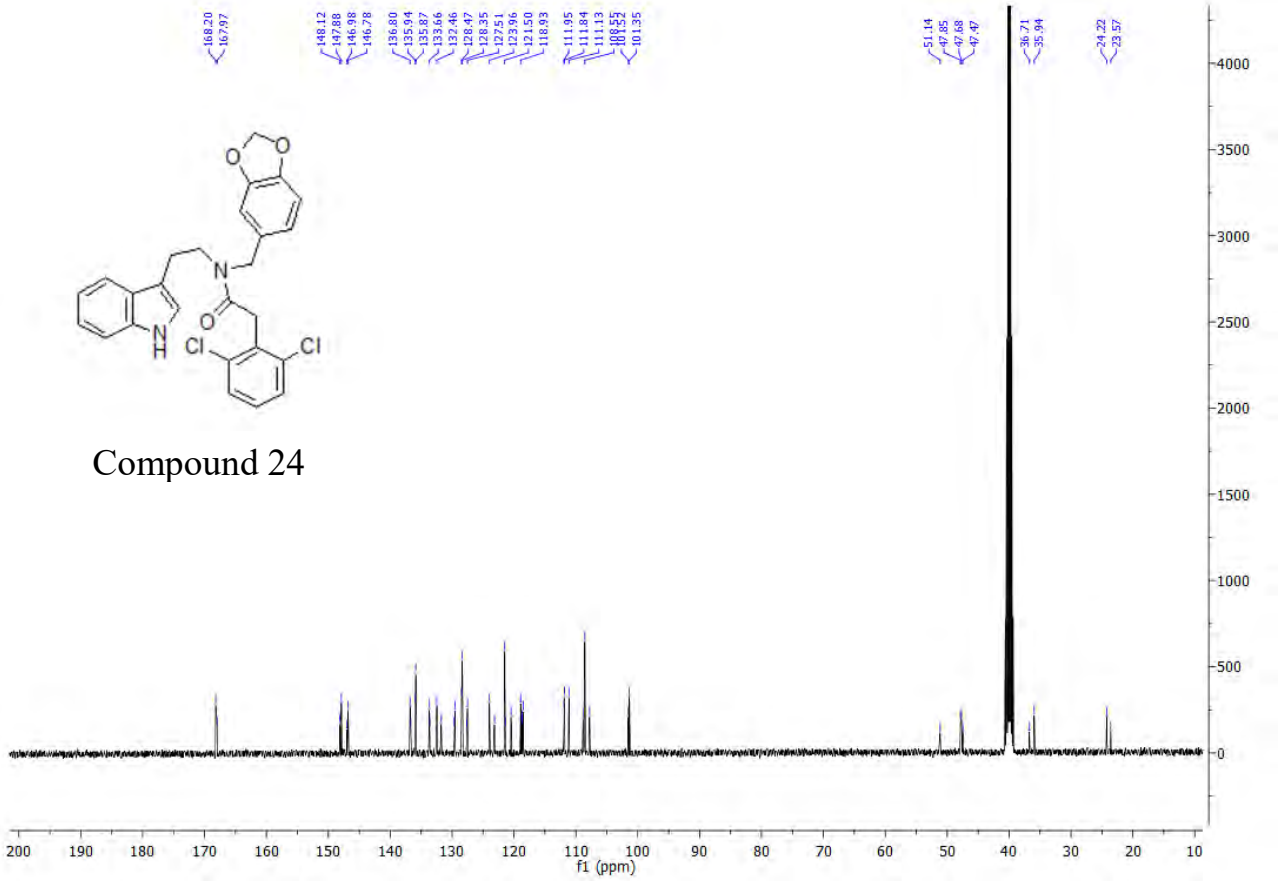
168.20
167.97
148.12
147.88
146.98
146.78
136.80
135.94
135.87
133.66
132.46
128.47
128.35
127.51
123.96
121.50
118.93
111.95
111.84
111.13
101.35
51.14
47.85
47.68
47.47
36.71
35.94
24.22
23.57
O
O
N
O
H
Cl
Cl
4000
3500
3000
2500
2000
1500
1000
500
0
200
190
180
170
160
150
140
130
120
110
100
90
80
70
60
50
40
30
20
10
f1 (ppm)

Compound 24

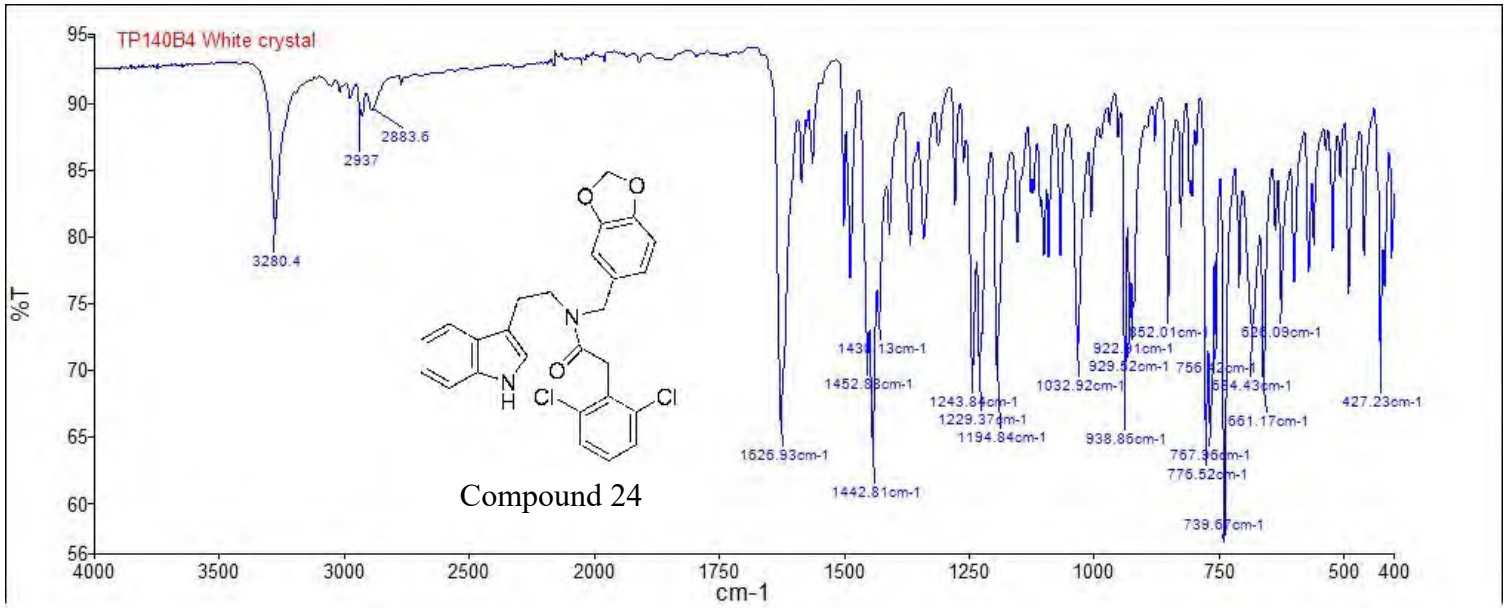
TP140B4 White crystal
%T
cm-1
3280.4
2937
2883.6
1626.93cm-1
1452.88cm-1
1442.81cm-1
1243.84cm-1
1229.37cm-1
1194.84cm-1
1032.92cm-1
938.86cm-1
776.52cm-1
661.17cm-1
427.23cm-1
Cl
Cl
O
O
N
H
O

Compound 24

SHIMADZU LabSolutions **Analysis Report**

<Sample Information>

Sample Name	: TP114B4 ISOMERS		
Sample ID	: TP114B4 ISOMERS		
Data Filename	: TP114B4 ISOMERS001.lcd		
Method Filename	: 30-100 over 15 mins.lcm		
Batch Filename	: TRIEU Third Generation.lcb		
Vial #	: 1-40	Sample Type	: Unknown
Injection Volume	: 10 uL		
Date Acquired	: 16/06/2014 1:51:51 PM	Acquired by	: System Administrator
Date Processed	: 24/06/2014 5:29:02 PM	Processed by	: System Administrator

<Chromatogram>

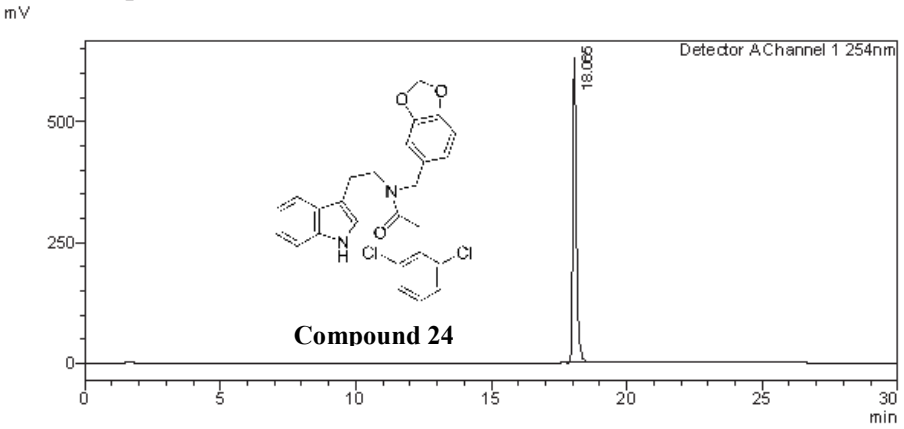

Detector A Channel 1 254nm

Peak#	Ret. Time	Area	Height	Conc.	Unit	Mark	Name
1	18.065	5792623	629051	100.000		M	
Total		5792623	629051				

C:\LabSolutions\Data\Project1\Flash\TP114B4 ISOMERS001.lcd

==== Shimadzu LCMSsolution Data Report ====

<Chromatogram>

Sample Information

Acquired by	: Admin
Date Acquired	: 10/6/2015 3:41:11 PM
Sample Type	: Unknown
Level#	: 0
Sample Name	: TP140B4_ESI+
Sample ID	:
ISTD Amount	: (Level1 Conc.)
Sample Amount	: 1
Dilution Factor	: 1
Tray#	: 1
Vial#	: 39
Injection Volume	: 10
Data File	: TP140B4_ESI+.lcd
Method File	: FIA-ESI_Scan(+).lcm
Original Method	: C:\LabSolutions\Data\Jen Baker\FIA-ESI_Scan(+).lcm
Report Format	: DefaultLCMS.lcr
Tuning File	: C:\LabSolutions\Data\AutoTuning\Autotune_ESI_26AUG15.lct
Processed by	: Admin
Modified Date	: 10/6/2015 3:42:42 PM

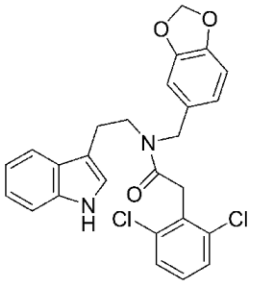

Compound 24

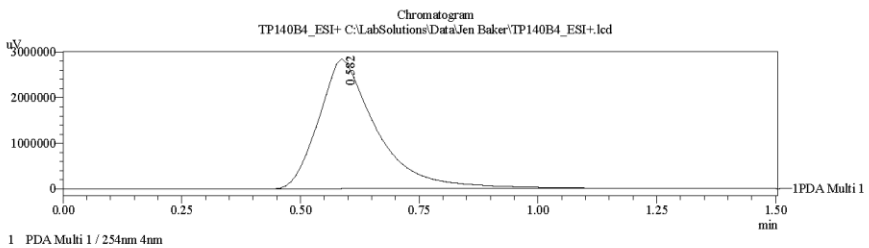

1 PDA Multi 1 / 254nm 4nm

<Spectrum>

Retention Time:1.040(Scan#:105)
Max Peak:477 Base Peak:82.95(126151)
Spectrum:Averaged 0.660-1.440(67-145)
Background:Averaged 0.000-0.686(1-69) Polarity:Pos Segment1 - Event1

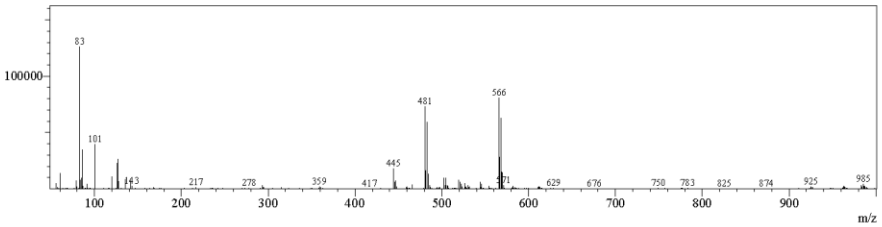

Retention Time:0.870(Scan#:88)
Max Peak:654 Base Peak:227.15(73987)
Spectrum:Averaged 0.670-1.450(68-146)
Background:Averaged 0.010-0.686(2-70) Polarity:Neg Segment1 - Event2

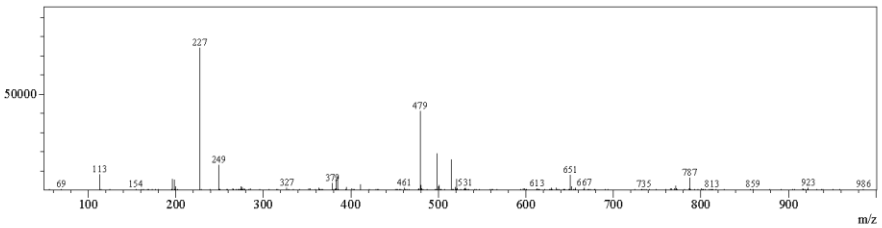

C:¥LabSolutions¥Data¥Jen Baker¥TP140B4_ESI+.lcd

Compound	Chemical Formula	Predicted monoisotopic neutral MW	Predicted MH+	MH+ Measured	Main MS Ions	Main MS/MS Fragments
TP 140B4	$C_{26}H_{22}Cl_2N_2O_3$	480.1007	481.1080	481.1079		135.0444
					481.1079	278.1180
						359.0720

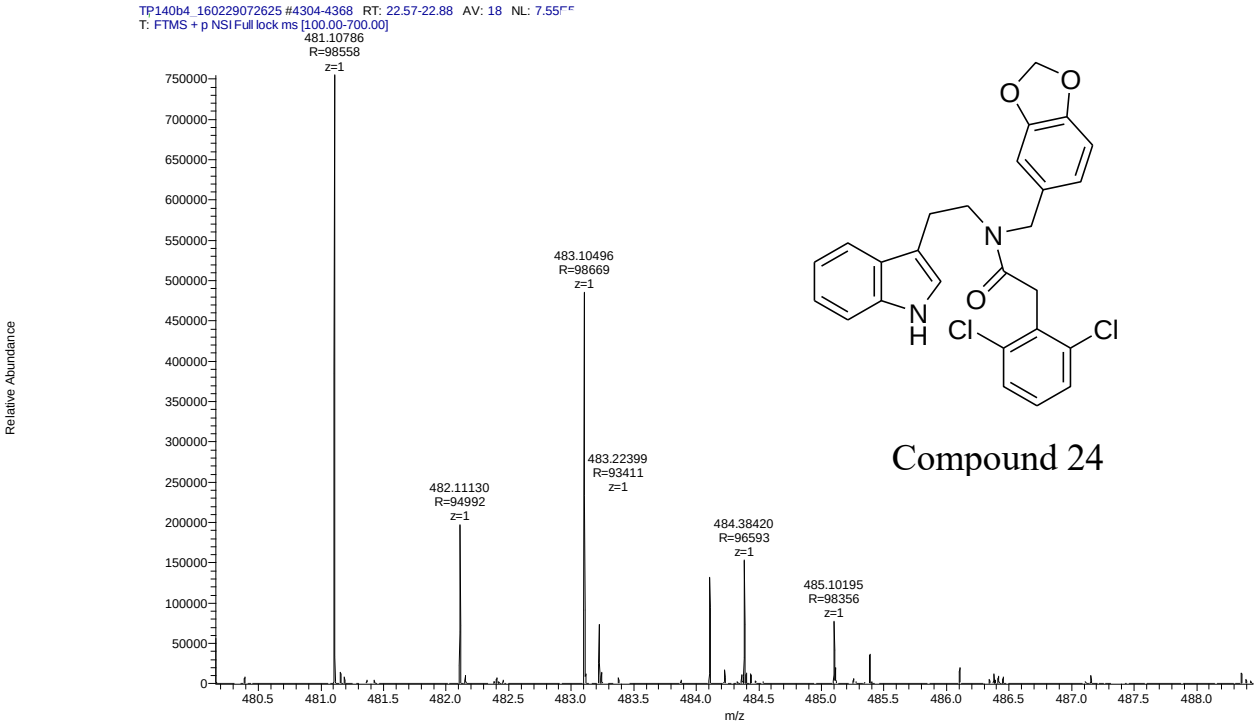

Compound 24

COMPOUND 25

Compound Name: *N*-Benzo[1,3]dioxol-5-ylmethyl-4-benzoyl-*N*-[2-(1*H*-indol-3-yl)-ethyl]-benzamide

Obtained Weight & Yield: 77 mg, 40%

Appearance: White sparkling crystalline powder

Solubility: EtOAc, Acetone, ACN

Melting Point: 181.2-181.7 ºC

TLC Conditions: EtOAc/Hexane (50/50)

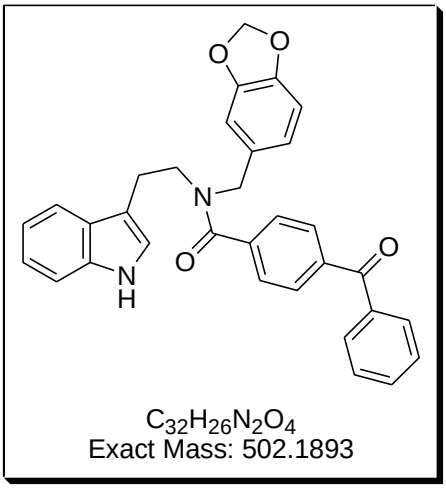

$C_{32}H_{26}N_2O_4$
Exact Mass: 502.1893

IR Analysis: νmax/cm^{-1}

3191 (NH), 2990 (CH), 1643 (CON), 742 (CH-aromatics)

^{1}H NMR Analysis:

*This is a mixture of atropisomers of compound **37** with the ratio approximately 2.0 : 0.9 calculated on the CH_2 splitting peaks at 4.75 and 6.02 ppm of the proton NMR.*

^{1}H NMR (400 MHz, DMSO-d_6) δ 10.83 (d, J = 10.1 Hz, 1.5H), 7.85 – 7.66 (m, 5.5H), 7.58 (dt, J = 18.2, 8.8 Hz, 6.5H), 7.41 – 7.17 (m, 4H), 7.11 – 6.85 (m, 7.5H), 6.84 – 6.56 (m, 2H), 6.01 (d, J = 13.2 Hz, 3H), 4.75 (s, 2H), 4.32 (s, 1H), 3.60 (d, J = 7.1 Hz, 1H), 3.36 – 3.30 (overlapped by water) (m, 2.5H), 3.03 (d, J = 7.1 Hz, 1H), 2.88 (t, J = 7.1 Hz, 2H).

^{13}C NMR Analysis:

^{13}C NMR (101 MHz, DMSO-d_6) δ 195.6, 170.6, 148.0, 146.9, 140.9, 137.4, 137.2, 136.6, 133.4, 132.0, 130.1, 130.0, 129.1, 127.4, 127.1, 126.8, 123.7, 121.8, 121.4, 118.7, 118.6, 118.1, 111.9, 110.8, 108.8, 108.7, 101.4, 52.4, 49.1, 46.9, 45.5, 24.2, 23.1.

HPLC:

RP-HPLC Alltima™ C18 5 μm 150 mm x 4.6 mm, 10–100% B in 15 min, R_t = 17.71 min, 100 %.

Mass Spectral Analysis: LRMS (APCI+/-) m/z 502, 503 $[M+H]^+$, 100%. HRMS (ES+) for $C_{32}H_{26}N_2O_4$, calculated 503.1965, found 503.1964.

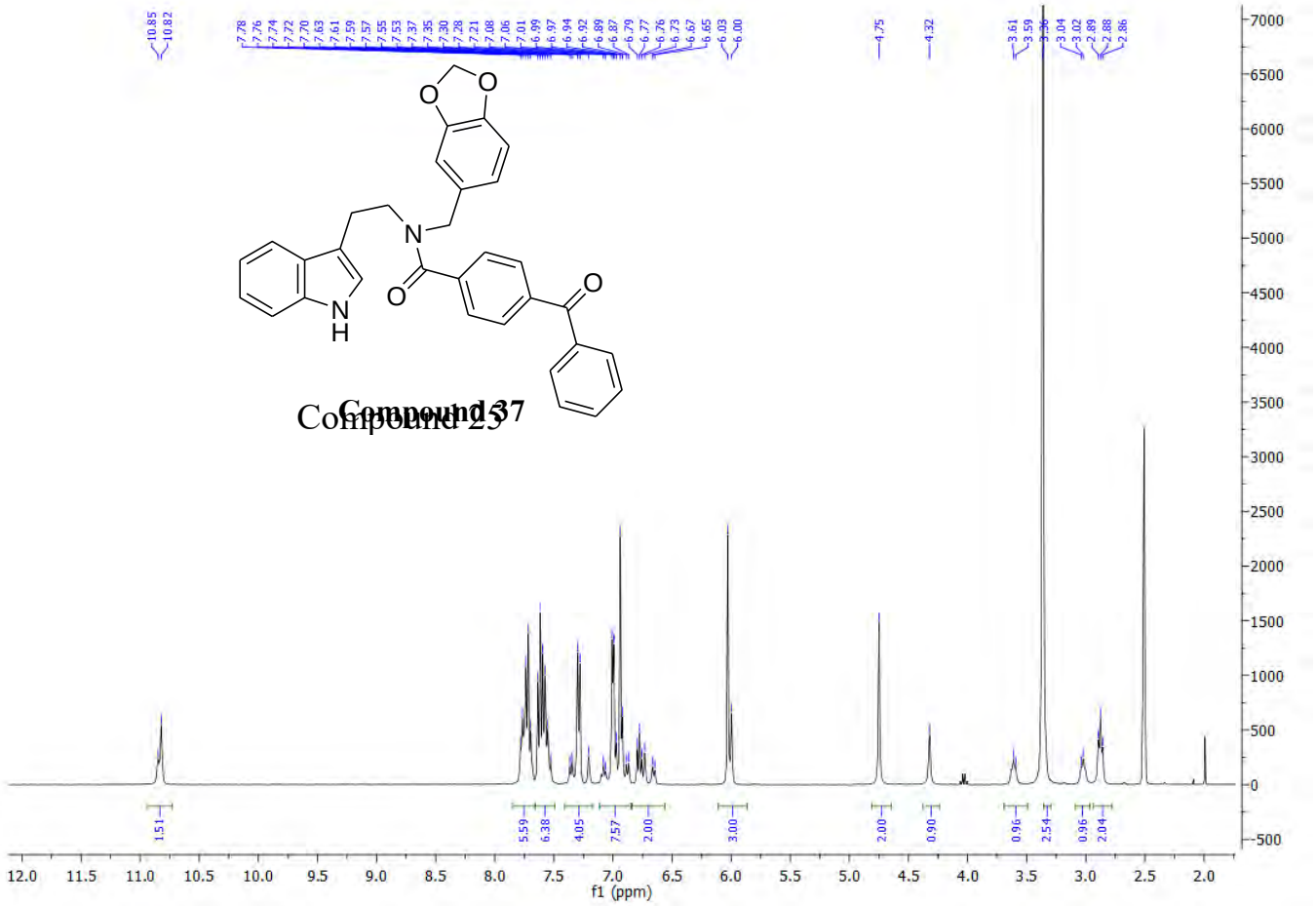
Compound 37
f1 (ppm)

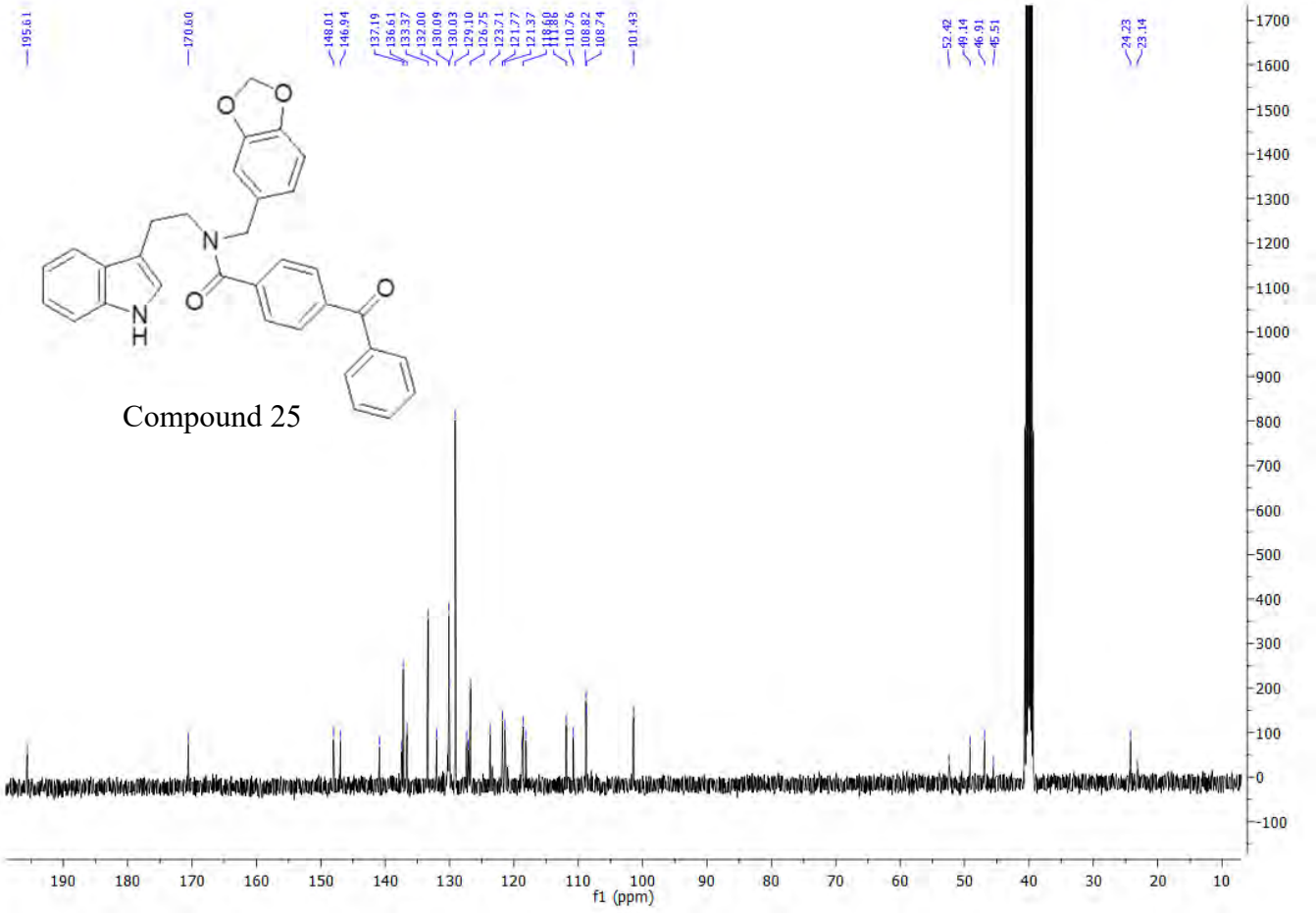
195.61
170.60
148.01
146.94
137.19
136.61
133.37
132.00
130.09
130.03
129.10
126.75
123.71
121.77
121.37
118.80
118.66
110.76
108.82
108.74
101.43
52.42
49.14
46.91
45.51
24.23
23.14
O
O
N
O
O
N
H
1700
1600
1500
1400
1300
1200
1100
1000
900
800
700
600
500
400
300
200
100
0
-100
190
180
170
160
150
140
130
120
110
100
90
80
70
60
50
40
30
20
10
f1 (ppm)

Compound 25

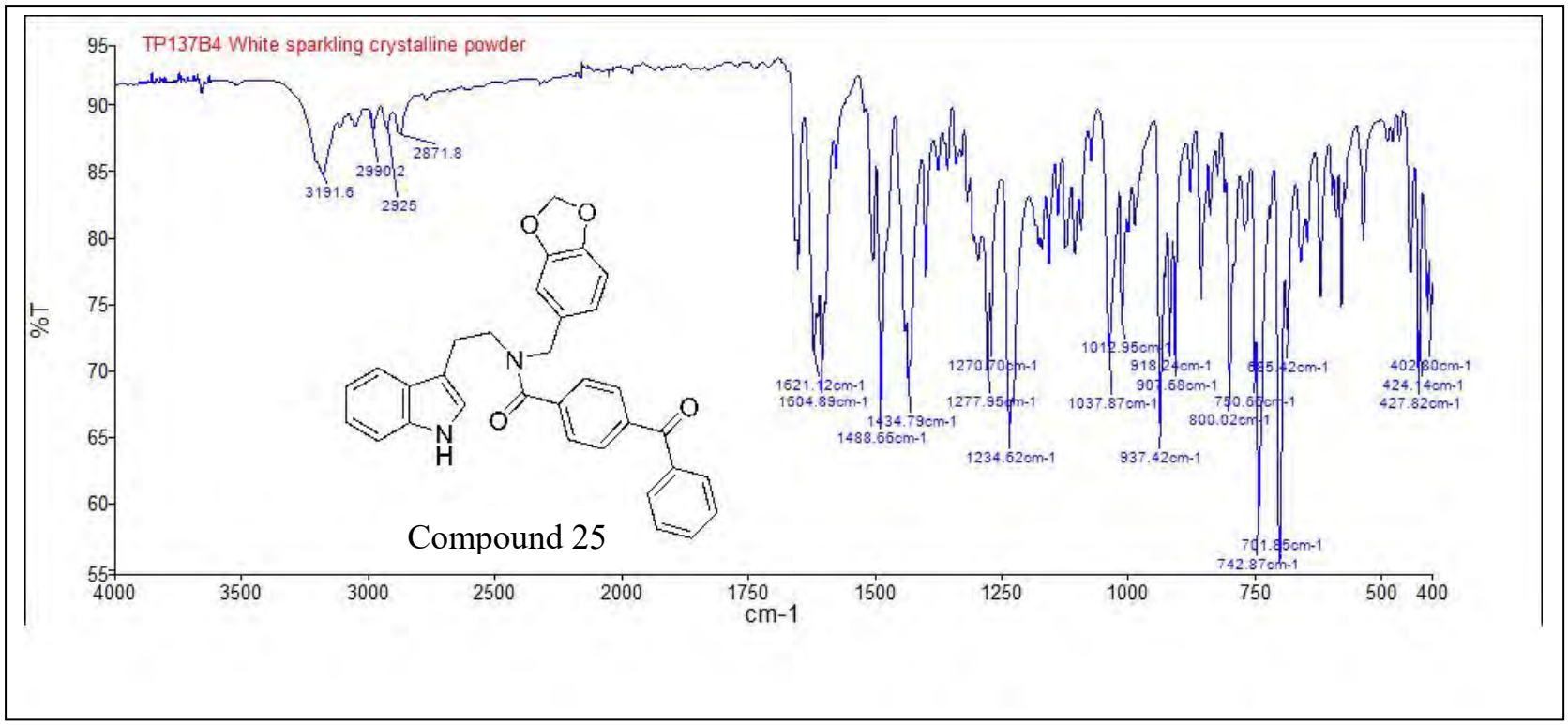
TP137B4 White sparkling crystalline powder
%T
cm-1
3191.6
2990.2
2925
2871.8
1621.12cm-1
1604.89cm-1
1488.66cm-1
1434.79cm-1
1277.95cm-1
1270.70cm-1
1234.62cm-1
1037.87cm-1
1012.95cm-1
937.42cm-1
907.68cm-1
800.02cm-1
742.87cm-1
701.85cm-1
427.82cm-1
424.14cm-1
Compound 25

SHIMADZU LabSolutions Analysis Report

<Sample Information>

Sample Name	: TP137B4 ISOMERS		
Sample ID	: TP137B4 ISOMERS		
Data Filename	: TP137B4 ISOMERS001.lcd		
Method Filename	: 30-100 over 15 mins.lcm		
Batch Filename	: TRIEU Third Generation.lcb		
Vial #	: 1-41	Sample Type	: Unknown
Injection Volume	: 10 uL		
Date Acquired	: 16/06/2014 2:22:15 PM	Acquired by	: System Administrator
Date Processed	: 16/06/2014 2:52:18 PM	Processed by	: System Administrator

<Chromatogram>

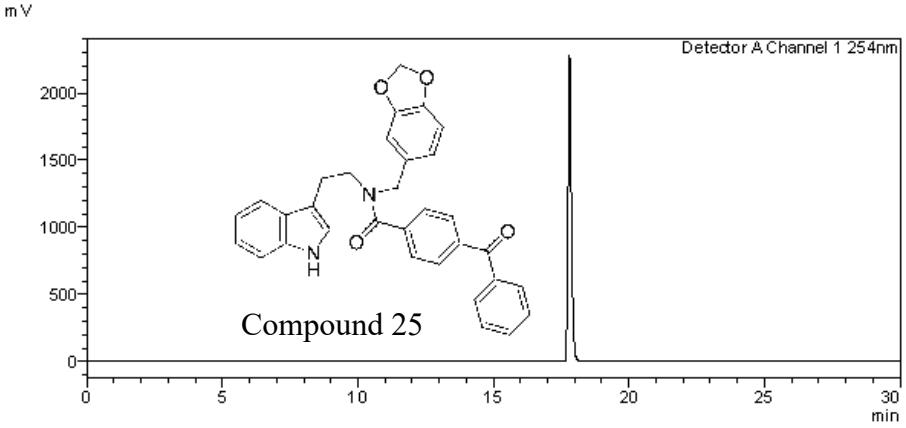

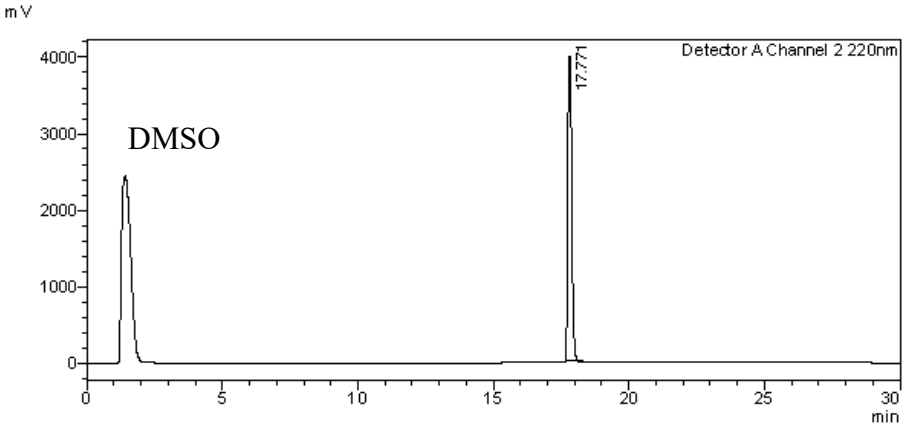

<Peak Table>

Detector A Channel 1 254nm

C:\LabSolutions\Data\Project1\Flash\TP137B4 ISOMERS001.lcd

Peak#	Ret. Time	Area	Height	Conc.	Unit	Mark	Name
Total							

Detector A Channel 2 220nm

Peak#	Ret. Time	Area	Height	Conc.	Unit	Mark	Name
1	17.771	39528115	3965481	100.000		M	
Total		39528115	3965481				

==== Shimadzu LCMSsolution Data Report ====

<Chromatogram>

Sample Information

Acquired by	: Admin
Date Acquired	: 7/17/2014 11:29:34 AM
Sample Type	: Unknown
Level#	: 0
Sample Name	: TP137134_APCI(-)
Sample ID	:
ISTD Amount	: (Level1 Conc.)
Sample Amount	: 1
Dilution Factor	: 1
Tray#	: 1
Vial#	: 3
Injection Volume	: 10
Data File	: TP137134_APCI(-).lcd
Method File	: FIA-APCI_scan(-).lcm
Original Method	: C:\LabSolutions\Data\Pete\FIA-APCI_scan(-).lcm
Report Format	: DefaultLCMS.lcr
Tuning File	: C:\LabSolutions\LCsolution\Log\Tuning\Autotune_030908.lct
Processed by	: Admin
Modified Date	: 7/17/2014 11:31:05 AM

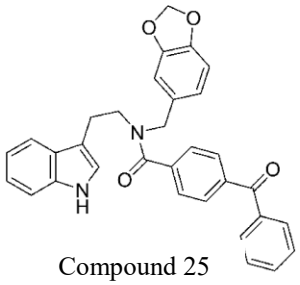

Compound 25

Chromatogram

TP137134_APCI(-) C:\LabSolutions\Data\Pete\Treiu\TP137134_APCI(-).lcd

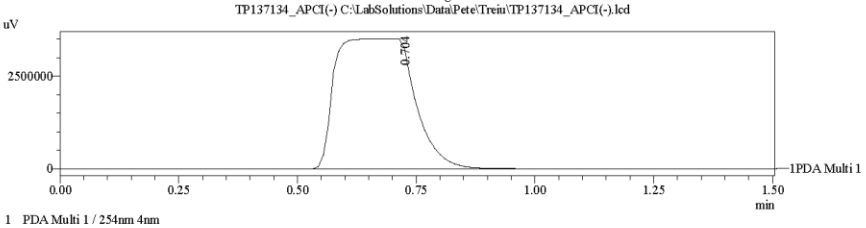

1 PDA Multi 1 / 254nm 4nm

<Spectrum>

Retention Time:0.640(Scan#:65)
Max Peak:570 Base Peak:502.90(638470)
Spectrum:Averaged 0.540-1.000(55-101)
Background:Averaged 0.080-0.316(9-33) Polarity:Pos Segment1 - Event1

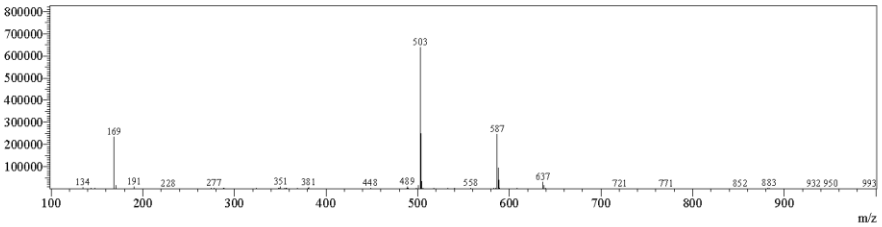

Retention Time:0.630(Scan#:64)
Max Peak:640 Base Peak:112.55(56468)
Spectrum:Averaged 0.550-1.010(56-102)
Background:Averaged 0.090-0.316(10-34) Polarity:Neg Segment1 - Event2

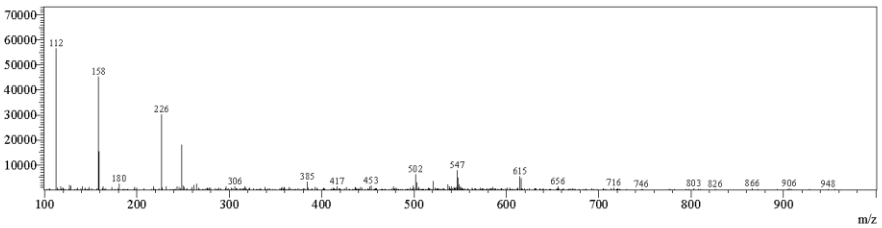

C:¥LabSolutions¥Data¥Pete¥Treiu¥TP137134_APCI(-).lcd

Compound	Chemical Formula	Predicted monoisotopic neutral MW	Predicted MH+	MH+ Measured	Main MS Ions	Main MS/MS Fragments
TP 137B4	$C_{32}H_{26}N_2O_4$	502.1893	503.19653	503.19636	503.19636[R]	135.0444 209.0602 381.1605

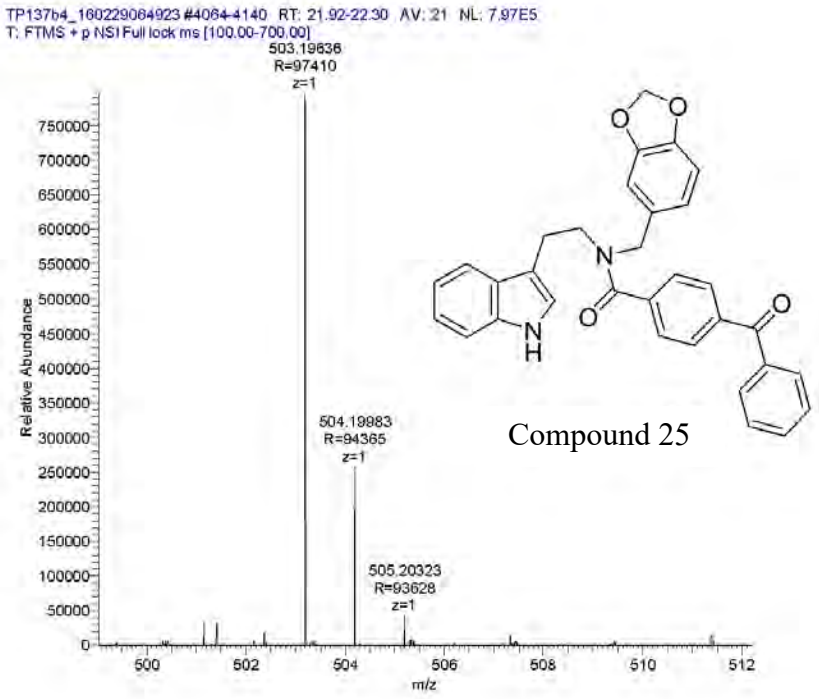

COMPOUND 26

Compound Name: 5-Methyl-pyrazine-2-carboxylic acid benzo[1,3]dioxol-5-ylmethyl-[2-(*1H*-indol-3-yl)-ethyl]-amide

Obtained Weight & Yield: 47 mg, 22%

Appearance: White floppy precipitate

Solubility: EtOAc, Acetone, ACN

Melting Point: 132 −133 ºC

TLC Conditions: EtOAc/Hexane (50/50)

IR Analysis: νmax/cm^{-1}

3316 (NH), 1632 (CON), 1632 (CON), 739 (CH-aromatic)

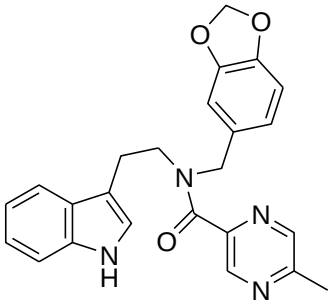

$C_{24}H_{22}N_4O_3$
Exact Mass: 414.1692

*This is a mixture of atropisomers of compound **38** with the ratio approximately 2 : 1 calculated on the CH_2 splitting peaks at 4.71 and 4.46 ppm of the proton NMR. ^{1}H NMR is reported as displayed on spectra. All peaks in ^{13}C NMR is reported*

^{1}H NMR Analysis:

^{1}H NMR (400 MHz, DMSO-d_6) δ 10.83 (s, 0.5H), 10.77 (s, 1H), 8.75 (d, *J* = 1.2 Hz, 0.5H), 8.56 (s, 0.5H), 8.34 (s, 1H), 8.19 (d, *J* = 1.3 Hz, 1H), 7.52 (d, *J* = 7.8 Hz, 0.5H), 7.34 (d, *J* = 8.1 Hz, 0.7H), 7.25 (d, *J* = 8.1 Hz, 1.2H), 7.16 (d, *J* = 2.0 Hz, 0.7H), 7.11 – 7.02 (m, 1.8H), 7.02 – 6.79 (m, 8H), 6.75 (d, *J* = 7.9 Hz, 0.5H), 6.01 (s, 2H), 5.99 (s, 0.8H), 4.71 (s, 2H), 4.46 (s, 1H), 3.60 (dt, *J* = 15.8, 7.5 Hz, 3.2H), 2.92 (dt, *J* = 13.8, 7.5 Hz, 3.2H), 2.54 (s, 1.8H), 2.41 (s, 3.2).

^{13}C NMR Analysis:

^{13}C NMR (101 MHz, DMSO-d_6) δ 167.2, 166.8, 155.0, 154.2, 147.9, 147.4, 147.1, 147.0, 146.9, 143.7, 143.2, 143.0, 142.0, 136.7, 136.6, 131.9, 131.3, 127.6, 127.1, 123.6, 123.3, 121.8, 121.6, 121.5, 121.3, 118.7, 118.5, 118.1, 111.9, 111.7, 110.9, 108.8, 108.7, 108.6, 108.5, 101.5, 101.4, 52.0, 48.6, 47.8, 46.192, 24.4, 23.1, 21.7, 21.5.

HPLC: RP-HPLC Alltima™ C18 5 μM 150 mm x 4.6 mm, 10–100% B in 15 min, R_t = 12.40 min, 100%.

Mass Spectral Analysis: LRMS (APCI +/-) m/z 414, 415 $[M+H]^+$, 100%. HRMS (ES+) for $C_{24}H_{22}N_4O_3$, calculated 415.1765, found 415.1761.

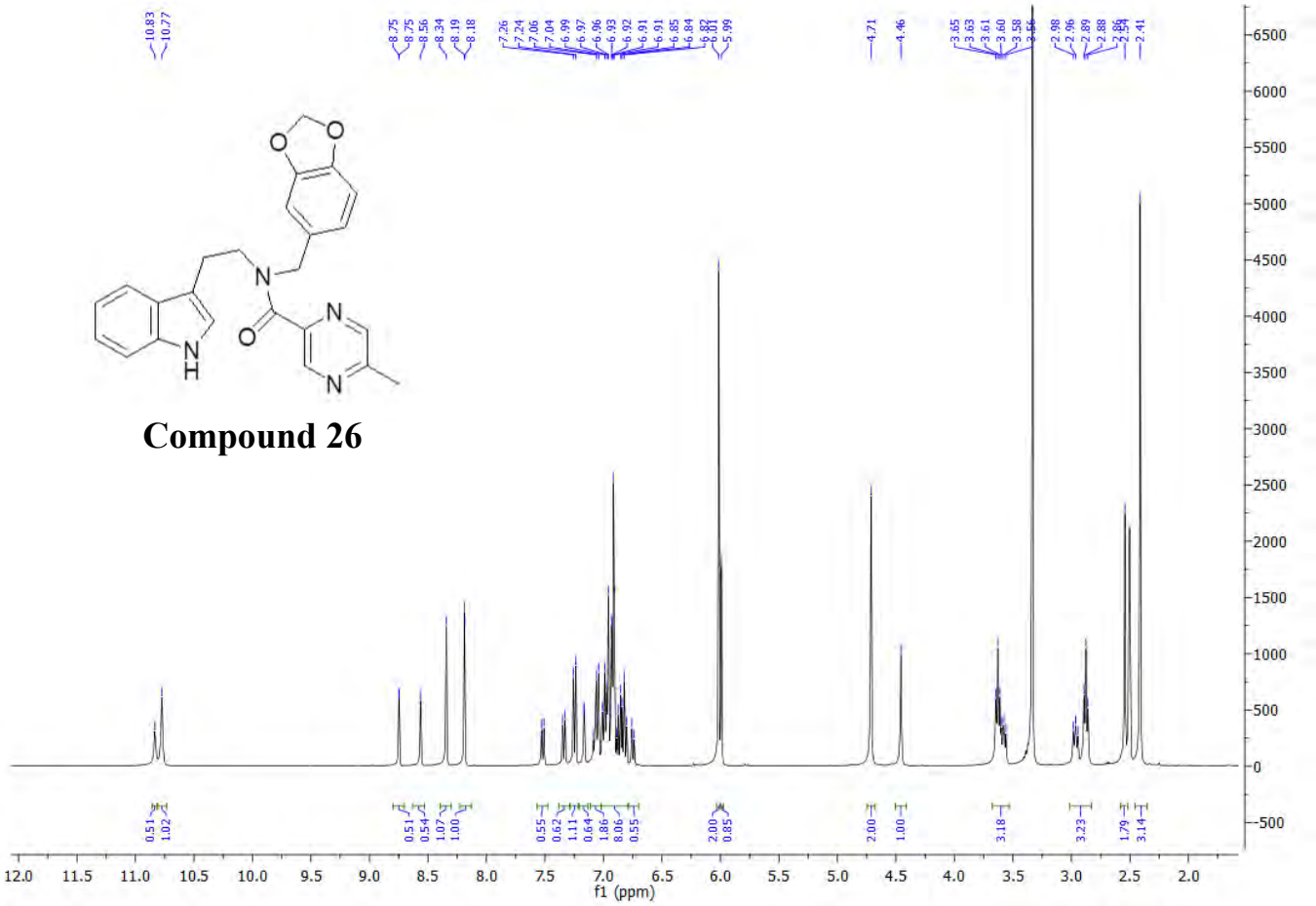
10.83
10.77
8.75
8.75
8.56
8.34
8.19
8.18
7.26
7.24
7.06
7.04
6.99
6.97
6.96
6.93
6.92
6.91
6.91
6.85
6.84
5.99
4.71
4.46
3.65
3.63
3.61
3.60
3.58
2.98
2.96
2.89
2.88
2.41
6500
6000
5500
5000
4500
4000
3500
3000
2500
2000
1500
1000
500
0
-500
0.51
1.02
0.51
0.54
1.07
1.00
0.55
0.62
1.11
0.64
1.86
8.06
0.55
2.00
0.85
2.00
1.00
3.18
3.23
1.79
3.14
12.0
11.5
11.0
10.5
10.0
9.5
9.0
8.5
8.0
7.5
7.0
6.5
6.0
5.5
5.0
4.5
4.0
3.5
3.0
2.5
2.0
f1 (ppm)

Compound 26

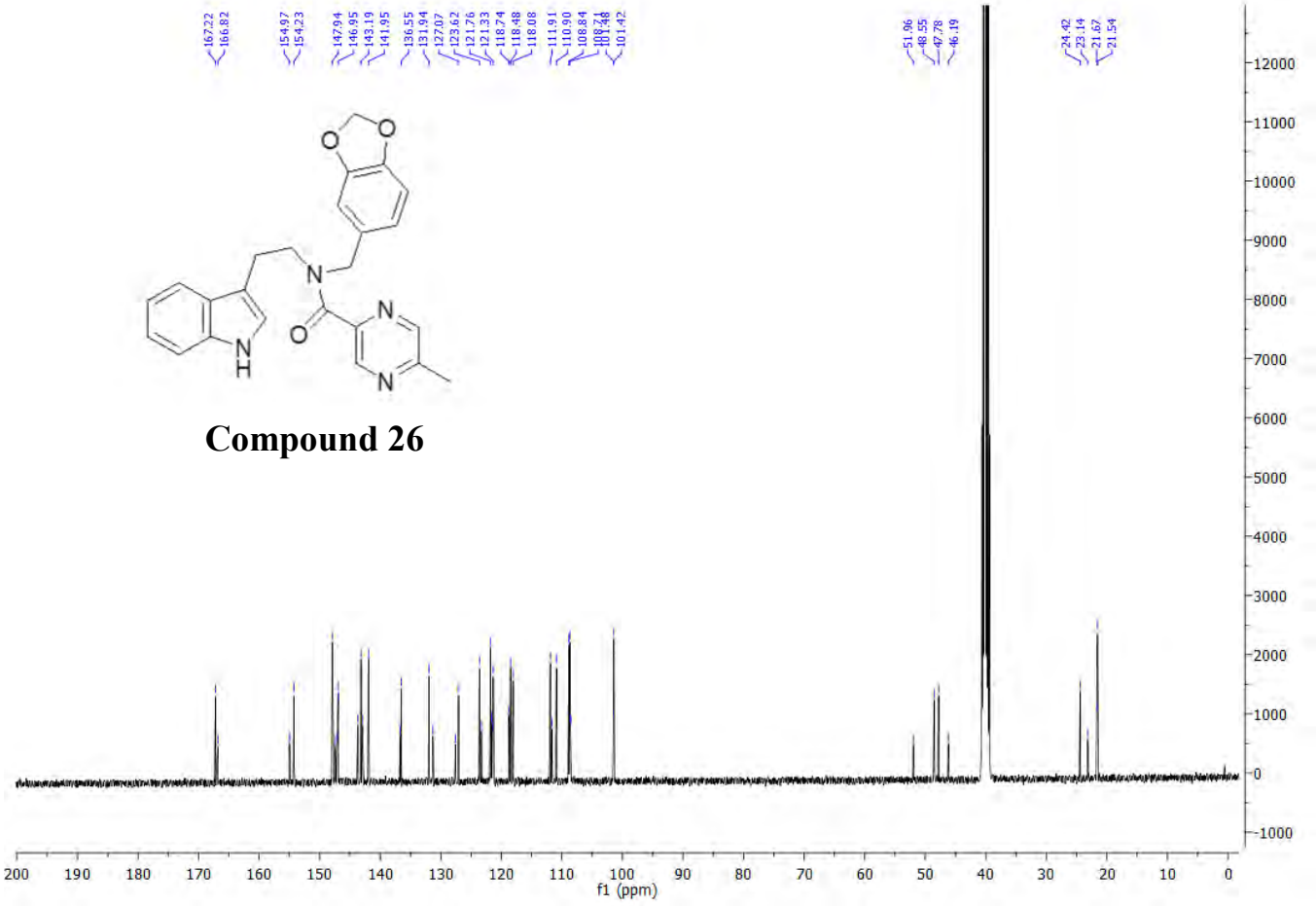
167.22
166.82
154.97
154.23
147.94
146.95
143.19
141.95
136.55
131.94
127.07
123.62
121.76
121.33
118.74
118.48
118.08
111.91
110.90
108.84
101.42
51.96
48.55
47.78
46.19
24.42
23.14
21.67
21.54
O
O
N
O
N
H
N
N
12000
11000
10000
9000
8000
7000
6000
5000
4000
3000
2000
1000
0
-1000
200
190
180
170
160
150
140
130
120
110
100
90
80
70
60
50
40
30
20
10
0
f1 (ppm)

Compound 26

1D Selective NOESY

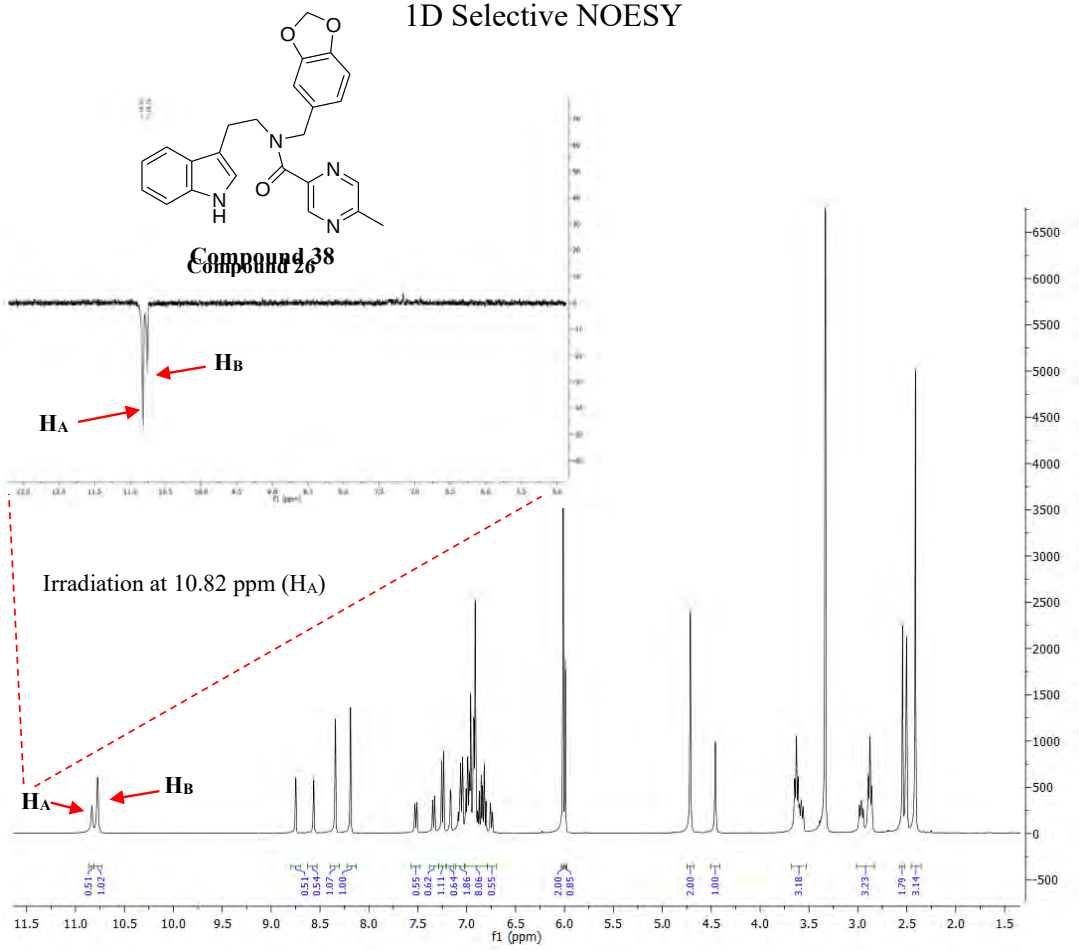

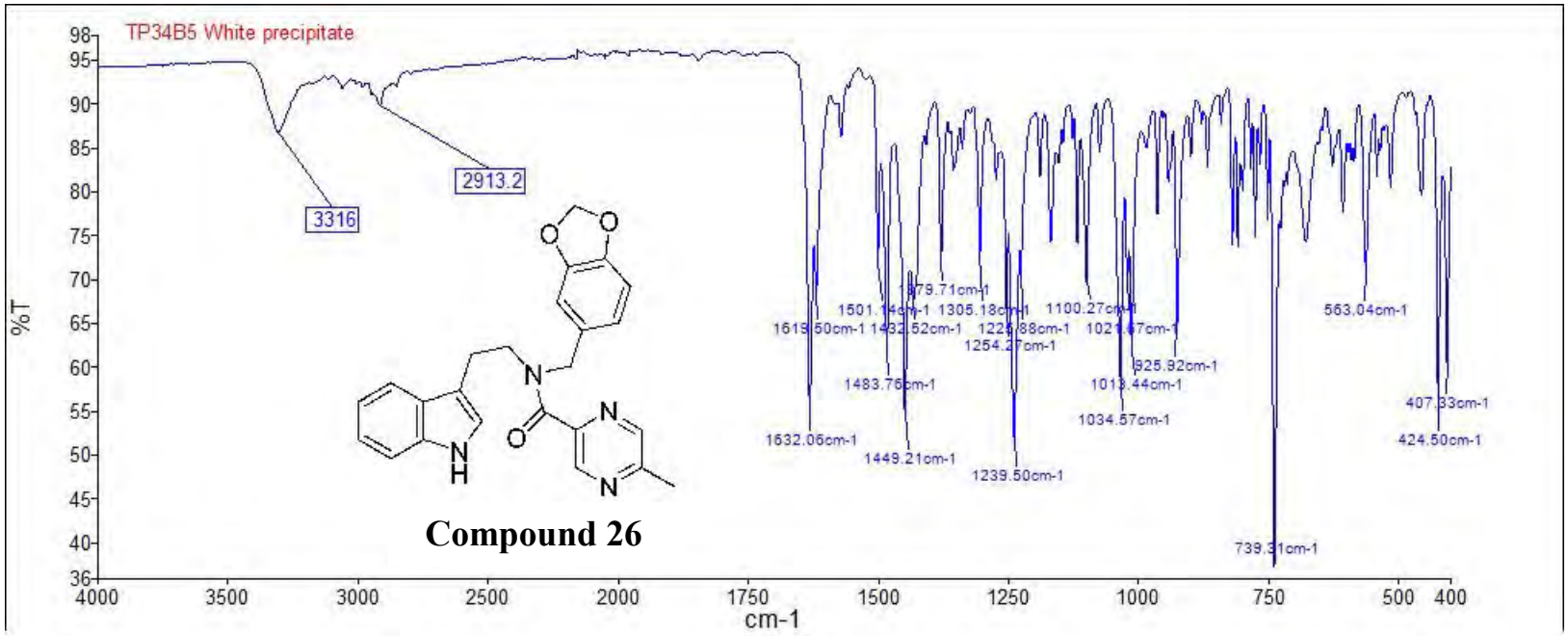
TP34B5 White precipitate
%T
cm-1
3316
2913.2
1632.06cm-1
1619.50cm-1
1501.14cm-1
1483.76cm-1
1449.21cm-1
1432.52cm-1
1379.71cm-1
1305.18cm-1
1254.27cm-1
1239.50cm-1
1225.88cm-1
1100.27cm-1
1034.57cm-1
1021.67cm-1
1013.44cm-1
925.92cm-1
739.31cm-1
563.04cm-1
424.50cm-1
407.33cm-1

Compound 26

SHIMADZU LabSolutions **Analysis Report**

<Sample Information>

Sample Name	: TP34B5		
Sample ID	: TP34B5		
Data Filename	: TP34B5.lcd		
Method Filename	: 10-100 over 15 mins.lcm		
Batch Filename	: TRIEU Second Third Generation and New pro.lcb		
Vial #	: 1-9	Sample Type	: Unknown
Injection Volume	: 30 uL		
Date Acquired	: 5/09/2014 2:39:07 PM	Acquired by	: System Administrator
Date Processed	: 5/09/2014 3:09:08 PM	Processed by	: System Administrator

<Chromatogram>

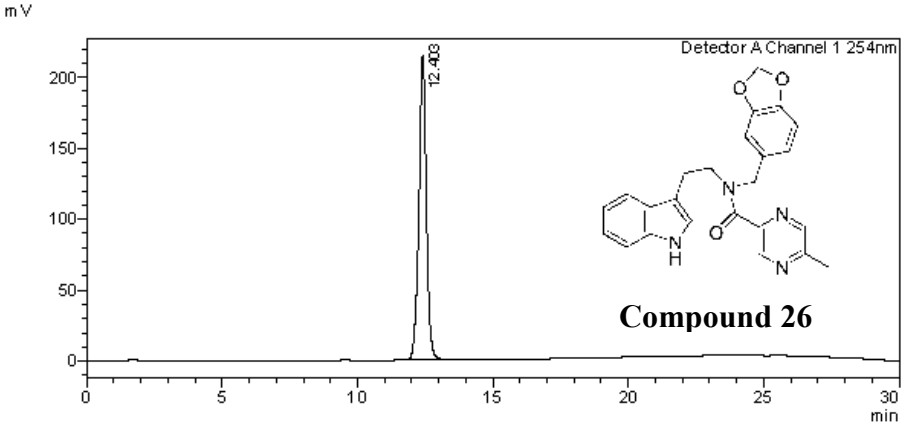

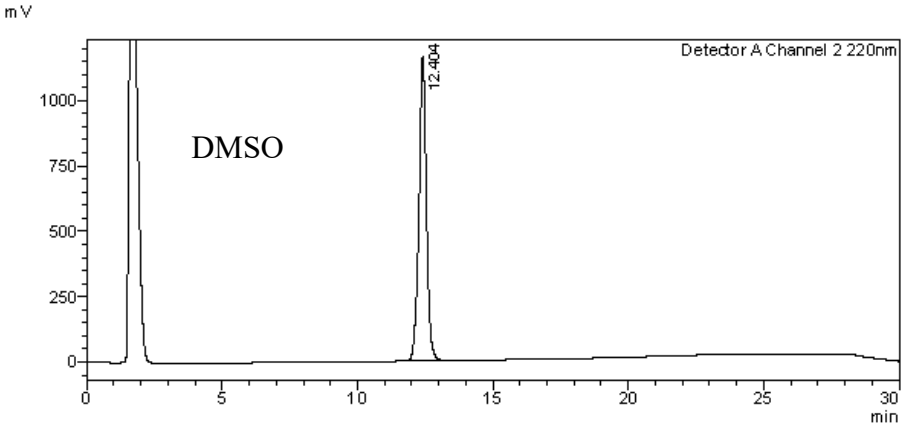

<Peak Table>

Detector A Channel 1 254nm

C:\LabSolutions\Data\Project1\TRIEU\TP34B5.lcd

Peak#	Ret. Time	Area	Height	Conc.	Unit	Mark	Name
1	12.403	4074948	214379	100.000		M	
Total		4074948	214379				

Detector A Channel 2 220nm

Peak#	Ret. Time	Area	Height	Conc.	Unit	Mark	Name
1	12.404	22146215	1160602	100.000		M	
Total		22146215	1160602				

==== Shimadzu LCMSsolution Data Report ====

<Chromatogram>

Sample Information

Acquired by	: Admin
Date Acquired	: 11/12/2014 9:58:08 AM
Sample Type	: Unknown
Level#	: 0
Sample Name	: tp34b5_APCI+
Sample ID	:
ISTD Amount	: (Level1 Conc.)
Sample Amount	: 1
Dilution Factor	: 1
Tray#	: 1
Vial#	: 3
Injection Volume	: 10
Data File	: tp34b5_APCI+.lcd
Method File	: FIA-APCI_scan(+).lcm
Original Method	: C:\LabSolutions\Data\Kelly\FIA-APCI_scan(+).lcm
Report Format	: DefaultLCMS.lcr
Tuning File	: C:\LabSolutions\LCsolution\Log\Tuning\Autotune_030908.lct
Processed by	: Admin
Modified Date	: 11/12/2014 9:59:39 AM

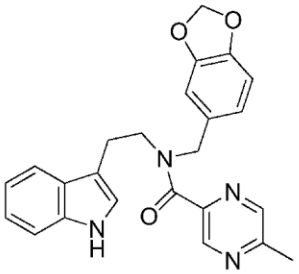

Compound 26

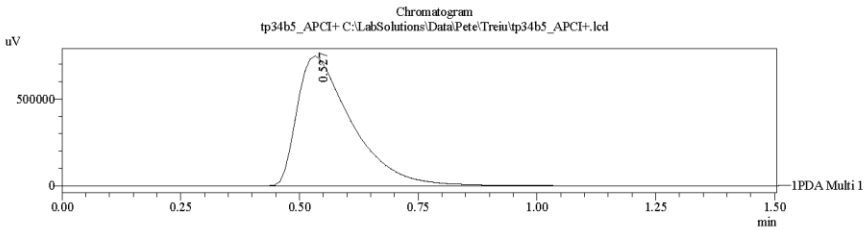

1 PDA Multi 1 / 254nm 4nm

<Spectrum>

Retention Time:0.600(Scan#:61)
Max Peak:595 Base Peak:414.75(969814)
Spectrum:Averaged 0.480-1.040(49-105)
Background:Averaged 0.060-0.384(7-39) Polarity:Pos Segment1 - Event1

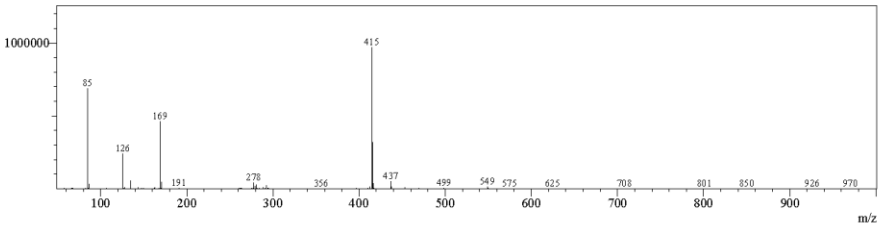

Retention Time:0.590(Scan#:60)
Max Peak:572 Base Peak:112.60(532108)
Spectrum:Averaged 0.490-1.050(50-106)
Background:Averaged 0.070-0.384(8-40) Polarity:Neg Segment1 - Event2

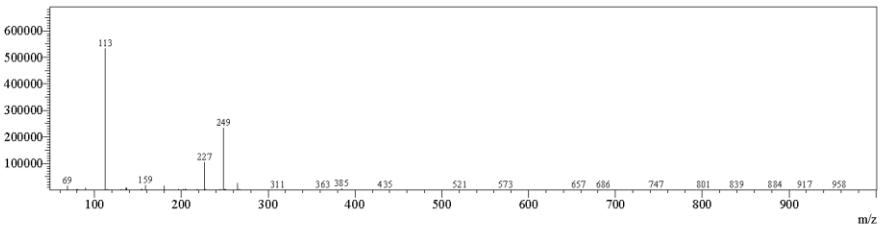

C:¥LabSolutions¥Data¥Pete¥Treiu¥tp34b5_APCI+.lcd

Compound	Chemical Formula	Predicted monoisotopic neutral MW	Predicted MH+	MH+ Measured	Main MS Ions	Main MS/MS Fragments
TP 28B5	$C_{27}H_{22}N_2O_3S$	454.1351	455.14239	455.14231	455.14231*	n/a

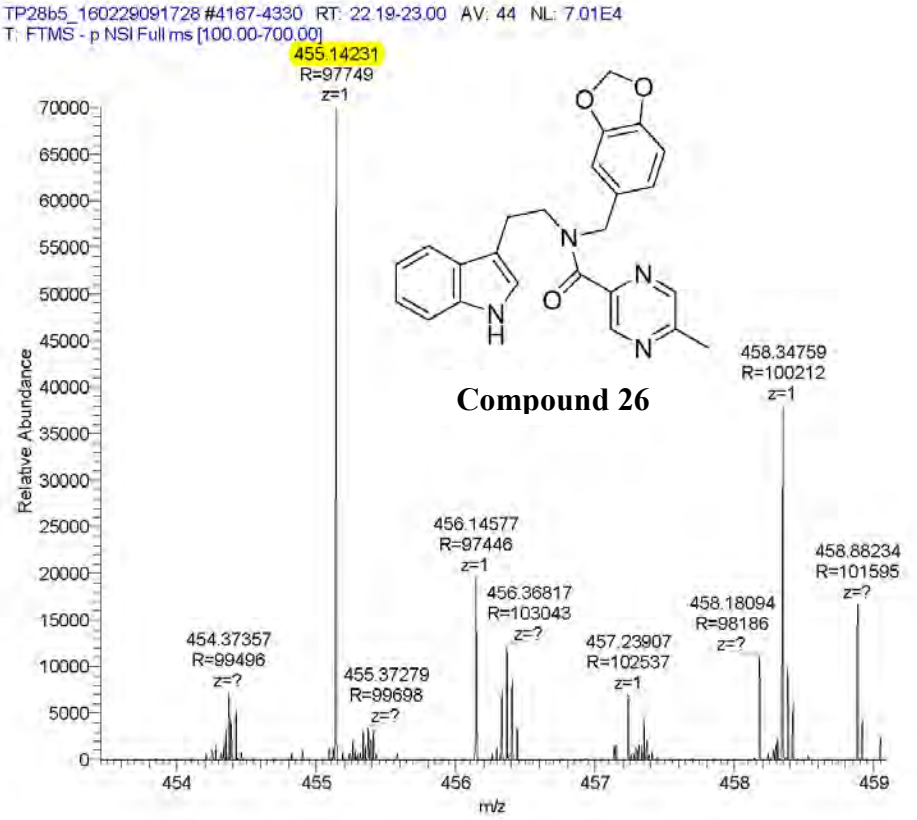

Compound 26

COMPOUND 27

Compound Name: 5-Methoxy-*1H*-indole-2-carboxylic acid benzo[1,3]dioxol-5-ylmethyl-[2-(*1H*-indol-3-yl)-ethyl]-amide

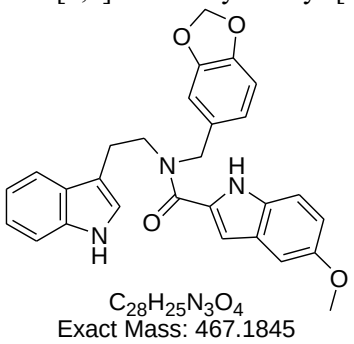

$C_{28}H_{25}N_3O_4$
Exact Mass: 467.1845

Obtained Weight & Yield: 149 mg, 62%

Appearance: Milky powder/ off white precipitate

Solubility: EtOAc, Acetone, ACN

Melting Point: 202-202.5 ºC

TLC Conditions: EtOAc/Hexane (50/50)

IR Analysis: νmax/cm^{-1}

3439 (NH), 3258 (NH), 1612 (CON), 1450 (C-C ring), 738 (C-H ring)

^{1}H NMR Analysis:

^{1}H NMR (400 MHz, DMSO-*d*$_6$) δ 11.57 (s, 1H), 10.86 (s, 1H), 7.68-7.26 (m, 3H), 7.19 (s, 1H), 7.13 – 6.48 (m, 8H), 6.01 (s, 2H), 4.81 (s, 2H), 3.73 (s, 5H), 3.08 (s, 2H).

^{13}C NMR Analysis:

^{13}C NMR (101 MHz, DMSO-*d*$_6$) δ 163.6, 154.2, 148.1, 146.9, 136.7, 132.0, 131.6, 130.8, 127.8, 127.6, 123.3, 121.5 (C x 2), 118.8 (C x 2), 115.0, 113.4, 111.9, 108.8, 103.5 (C x 2), 102.4, 101.5, 65.4, 55.7, 48.5, 48.1, 23.6.

HPLC:

RP-HPLC Alltima™ C18 5 μm 150 mm x 4.6 mm, 10–100% B in 15 min, R_t = 6.92 min, 100%.

Mass Spectral Analysis (Low res): LRMS (ESI+) m/z 467, 467 $[M]^+$, 100%. HRMS (ES+) for $C_{28}H_{25}N_3O_4$, calculated 468.1918, found 468.1919.

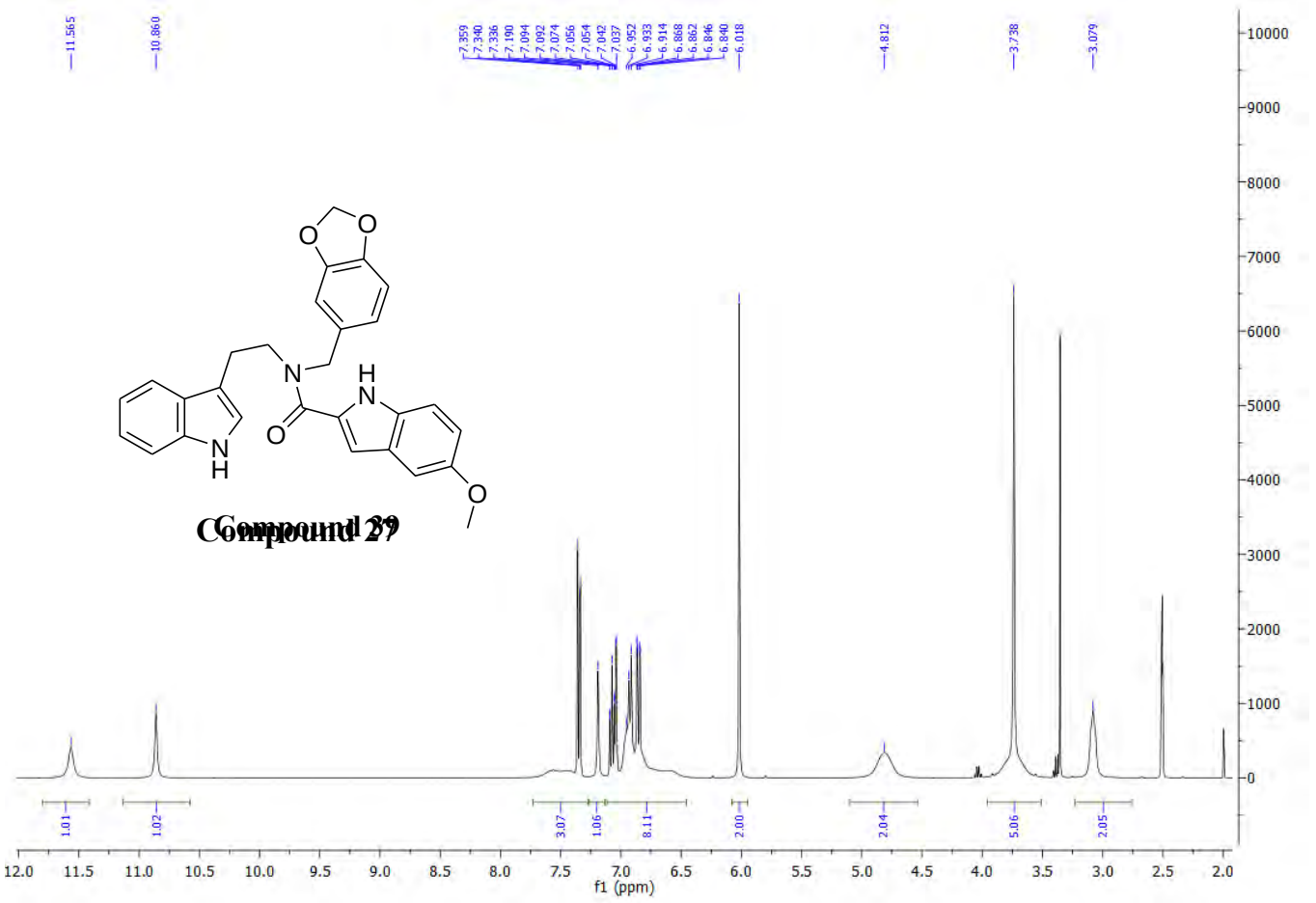
11.565
10.860
7.359
7.340
7.336
7.190
7.094
7.092
7.074
7.056
7.054
7.042
7.037
6.952
6.933
6.914
6.868
6.862
6.846
6.840
6.018
4.812
3.738
3.079
O
O
N
H
N
H
O
O
10000
9000
8000
7000
6000
5000
4000
3000
2000
1000
0
1.01
1.02
3.07
1.06
8.11
2.00
2.04
5.06
2.05
12.0
11.5
11.0
10.5
10.0
9.5
9.0
8.5
8.0
7.5
7.0
6.5
6.0
5.5
5.0
4.5
4.0
3.5
3.0
2.5
2.0
f1 (ppm)

Compound 29

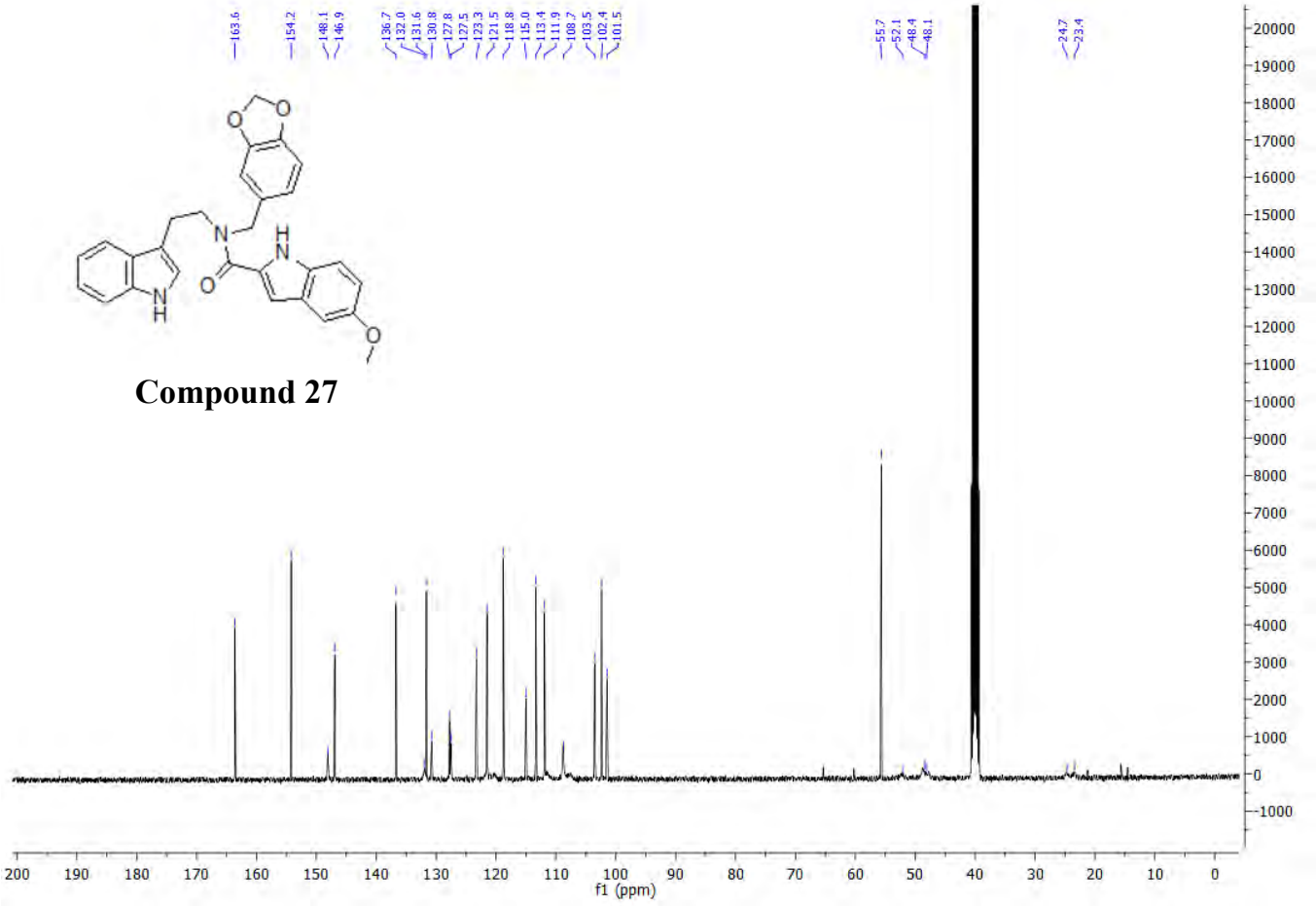
163.6
154.2
148.1
146.9
136.7
132.0
131.6
130.8
127.8
127.5
123.3
121.5
118.8
115.0
113.4
111.9
108.7
103.5
102.4
101.5
55.7
52.1
48.4
48.1
24.7
23.4
f1 (ppm)

Compound 27

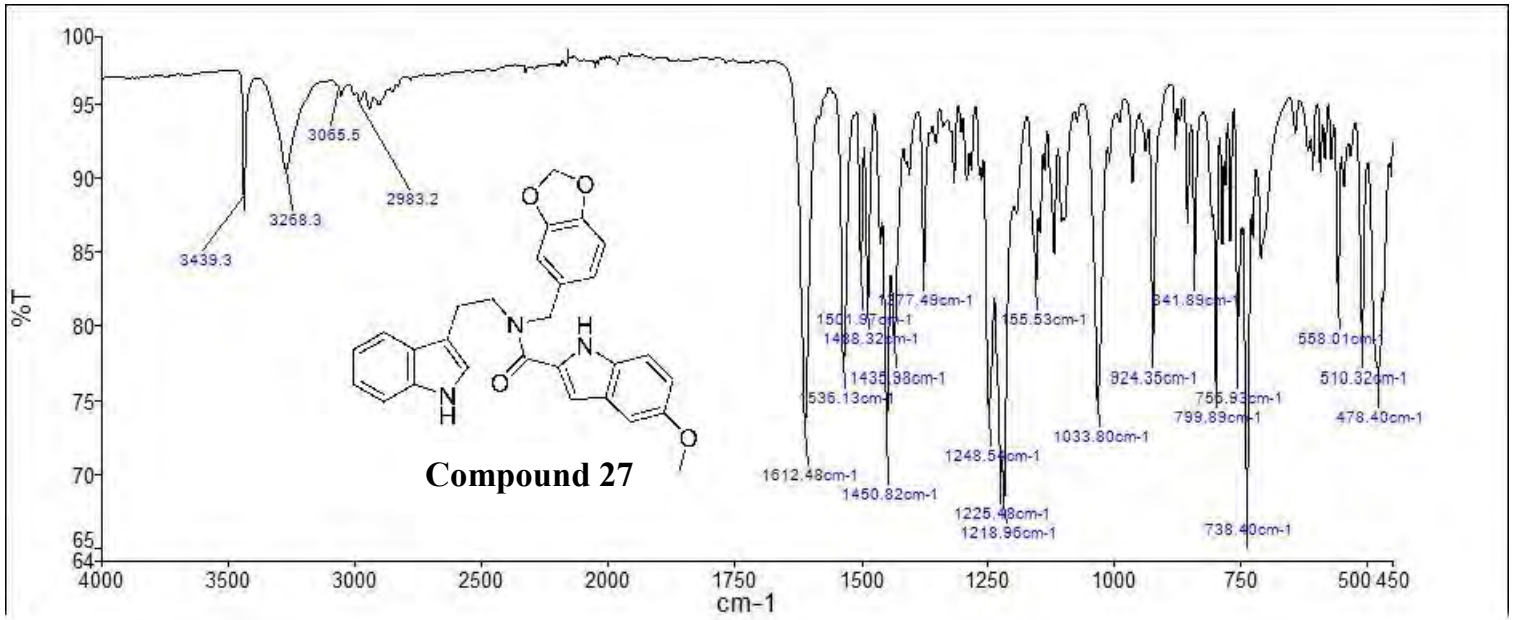
100
95
90
85
80
75
70
65
64
%T
4000
3500
3000
2500
2000
1750
1500
1250
1000
750
500 450
cm-1
3439.3
3268.3
3065.5
2983.2
1612.48cm-1
1450.82cm-1
1248.54cm-1
1225.48cm-1
1218.96cm-1
1033.80cm-1
924.35cm-1
738.40cm-1
558.01cm-1
510.32cm-1
478.40cm-1
Compound 27

==== Shimadzu LCMSsolution Data Report ====

<Chromatogram>

Sample Information

Acquired by	: Admin
Date Acquired	: 7/31/2015 12:36:14 PM
Sample Type	: Unknown
Level#	: 0
Sample Name	: TP140B5 ESI POS
Sample ID	:
ISTD Amount	: (Level1 Conc.)
Sample Amount	: 1
Dilution Factor	: 1
Tray#	: 1
Vial#	: 52
Injection Volume	: 5
Data File	: TP140B5 ESI POS.lcd
Method File	: FIA-ESI_Scan(+).lcm
Original Method	: C:\LabSolutions\Data\Trieu\Mass spec files\FIA-ESI_Scan(+).lcm
Report Format	: DefaultLCMS.lcr
Tuning File	: C:\LabSolutions\LCsolution\Log\Tuning\Autotune_030908.lct
Processed by	: Admin
Modified Date	: 7/31/2015 12:37:45 PM

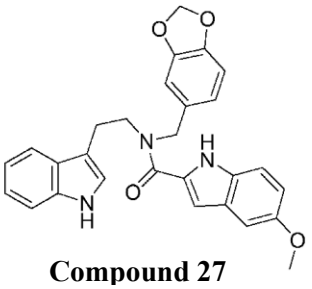

Compound 27

Chromatogram
TP140B5 ESI POS C:\LabSolutions\Data\Trieu\NORMAL REVERSE PHASE COLUMN\TP140B5 ESI POS.lcd

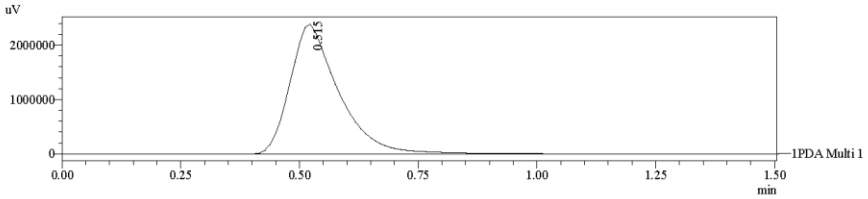

1 PDA Multi 1 / 254nm 4nm

<Spectrum>

Retention Time:0.640(Scan#:65)
Max Peak:369 Base Peak:82.60(38609)
Spectrum:Averaged 0.620-1.180(63-119)
Background:Averaged 0.120-0.506(13-51) Polarity:Pos Segment1 - Event1

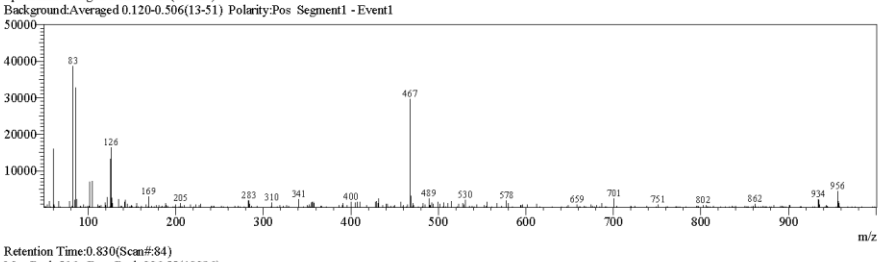

Retention Time:0.830(Scan#:84)
Max Peak:516 Base Peak:226.55(48236)
Spectrum:Averaged 0.630-1.190(64-120)
Background:Averaged 0.130-0.506(14-52) Polarity:Neg Segment1 - Event2

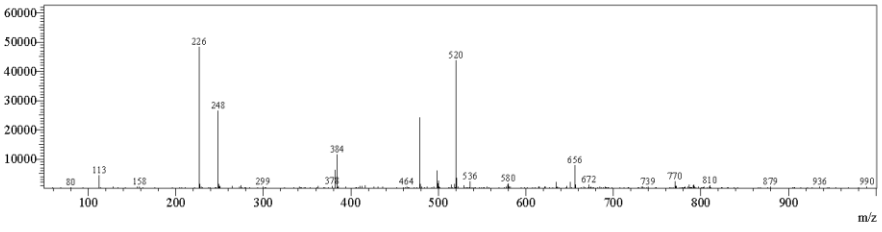

C:¥LabSolutions¥Data¥Trieu¥NORMAL REVERSE PHASE COLUMN¥TP140B5 ESI POS.lcd

==== Shimadzu LCMSsolution Analysis Report ====

Acquired by	: Admin
Sample Name	: TP140B5 Re
Sample ID	:
Vail #	: 56
Injection Volume	: 20 uL
Data File Name	: TP140B5 Re.lcd
Method File Name	: Econosphere C18 EPS 5u lot 50195421 part 70070 150mm id 4.6mm.lcm
Batch File Name	: Second and third 23092015.lcb
Report File Name	: DefaultLCMS.lcr
Data Acquired	: 9/23/2015 5:32:46 PM
Data Processed	: 9/25/2015 4:17:56 PM

<Chromatogram>

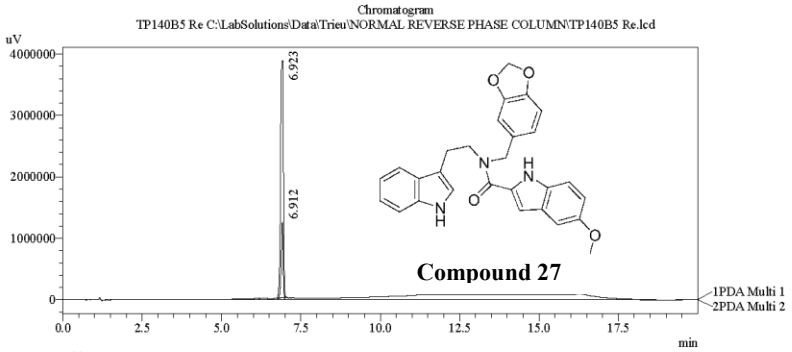

1 PDA Multi 1 / 254nm 4nm
2 PDA Multi 2 / 220nm 4nm

PeakTable

PDA Ch1 254nm 4nm

Peak#	Ret. Time	Area	Height	Area %	Height %
1	6.912	5407801	1253212	100.000	100.000
Total		5407801	1253212	100.000	100.000

PeakTable

PDA Ch2 220nm 4nm

Peak#	Ret. Time	Area	Height	Area %	Height %
1	6.923	23892199	3854292	100.000	100.000
Total		23892199	3854292	100.000	100.000

Compound	Chemical Formula	Predicted monoisotopic neutral MW	Predicted MH+	MH+ Measured	Main MS Ions	Main MS/MS Fragments
TP 140B5	$C_{28}H_{25}N_3O$	467.1845	468.19178	468.19186	468.19186*	n/a

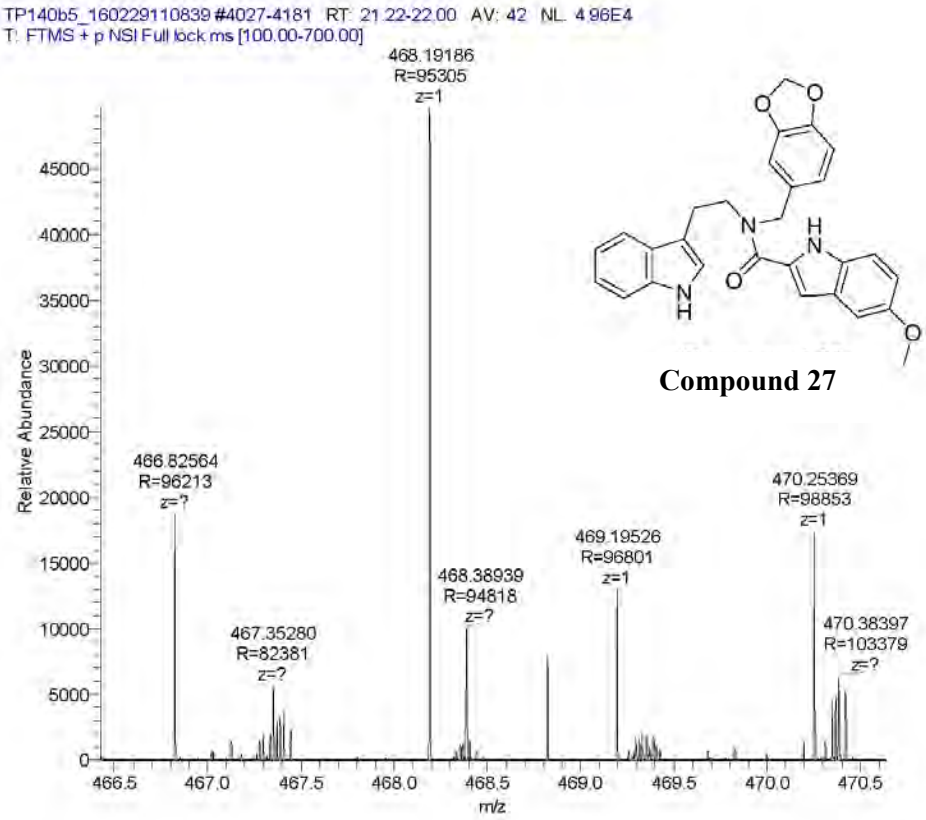

Compound 27

COMPOUND 28

Compound Name: 5-Chloro-1*H*-indole-2-carboxylic acid benzo[1,3]dioxol-5-ylmethyl-[2-(1*H*-indol-3-yl)-ethyl]-amide

Obtained Weight & Yield: 170 mg, 64%

Appearance: Off white precipitate

Solubility: EtOAc, Acetone, ACN

Melting Point: 194 −194.5 ºC

TLC Conditions: EtOAc/Hexane (50/50)

IR Analysis: νmax/cm^{-1}

3433 (NH), 3265 (NH), 1612 (CON), 739 (CH-aromatics)

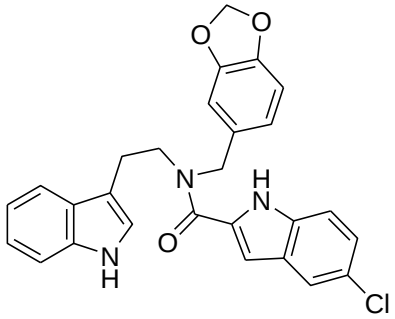

$C_{27}H_{22}ClN_3O_3$
Exact Mass: 471.1350

^{1}H NMR Analysis:

^{1}H NMR (400 MHz, DMSO-d_6) δ 11.93 (s, 1H), 10.87 (s, 1H), 7.73 – 7.26 (m, 4H), 7.25 – 7.13 (m, 2H), 7.08 (t, J = 7.5 Hz, 1H), 7.02 – 6.60 (m, 5H), 6.02 (s, 2H), 4.79 (br.s, 2H), 3.74 (br.s, 2H), 3.08 (s, 2H).

^{13}C NMR Analysis:

^{13}C NMR (101 MHz, DMSO-d_6) δ 163.4, 148.1, 147.0, 136.7, 134.8, 132.1, 128.5, 127.5, 124.7, 123.9 (Cx2), 123.4, 121.5, 121.4, 121.0, 118.8 (Cx2), 118.7, 114.1, 111.9, 108.8, 103.2 (Cx2), 101.5, 52.4, 48.9, 48.6, 47.6, 24.7, 23.4.

**Note: 52.38 and 48.59 are the splitting of 1 C (Ar-$\underline{C}H_2$-N-); 48.91 and 47.58 are the splitting of (CH_2-$\underline{C}H_2$-N-), and 24.68, 23.41 are the splitting of ($\underline{C}H_2$-CH_2-N-)*

UPLC:

Mobile phase A= 100% H_2O with 0.1% formic acid; Mobile phase B = 90% ACN : 10% H_2O and 0.1% formic acid

RP-HPLC Agilent Zorbax SB-C18 1.8 µm, 50 mm x 2.1 mm, isocratic 80% mobile phase B at 0.6 mL/min in 8 minutes, R_t = 5.05 min, 100%.

Mass Spectral Analysis: LRMS (ESI-) m/z 471, 470 [M-H, ^{35}Cl]$^{+}$, 100%; m/z 471, 472 [M+H, ^{35}Cl]$^{+}$, 100%. HRMS (ES+) for $C_{27}H_{22}ClN_3O_3$, calculated 472.1423, found 472.1422.

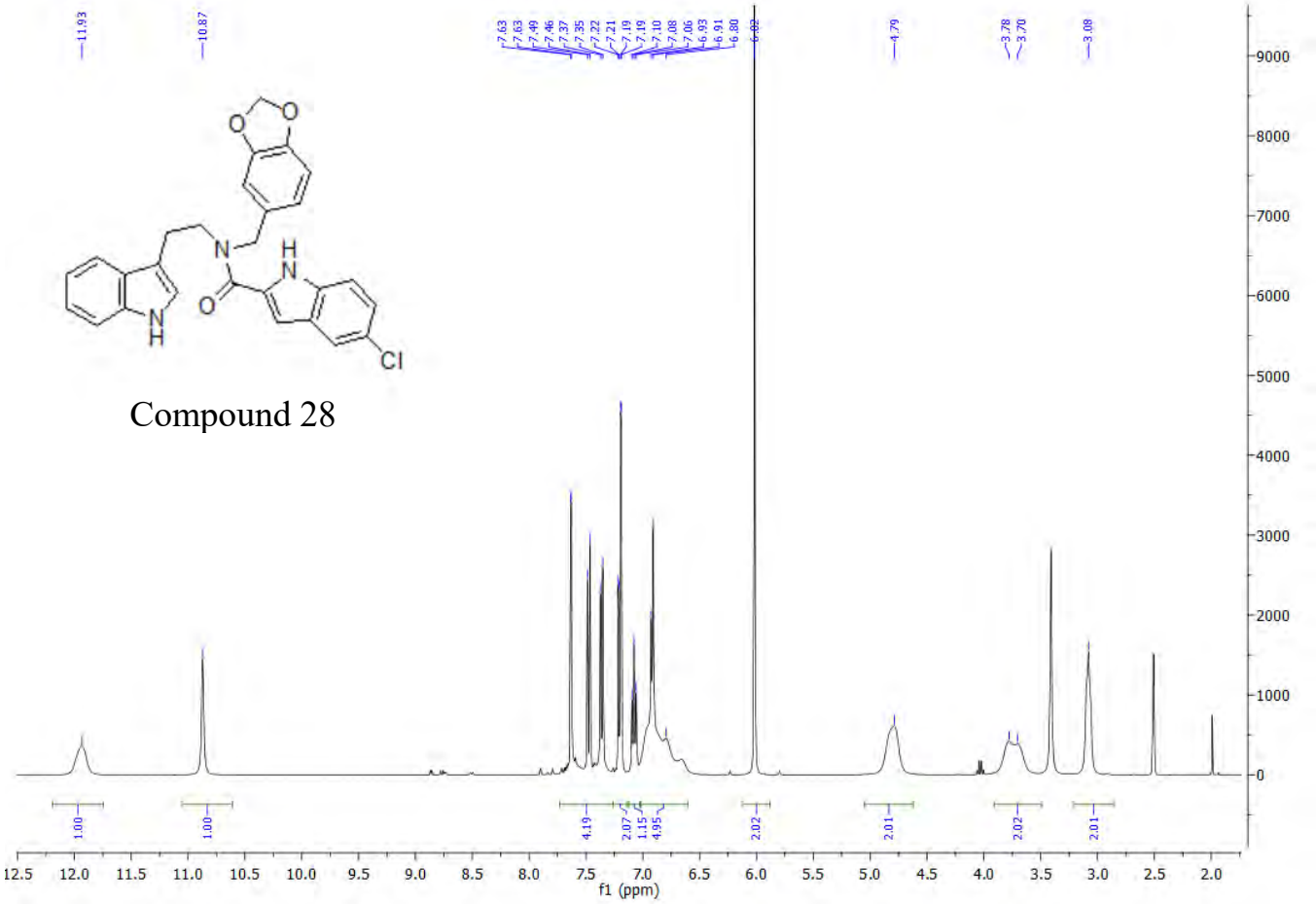
11.93
10.87
7.63
7.63
7.49
7.46
7.37
7.35
7.22
7.21
7.19
7.19
7.10
7.08
7.06
6.93
6.91
6.80
6.02
4.79
3.78
3.70
3.08
O
O
N
H
N
O
N
H
Cl
9000
8000
7000
6000
5000
4000
3000
2000
1000
0
1.00
1.00
4.19
2.07
1.15
4.95
2.02
2.01
2.02
2.01
12.5
12.0
11.5
11.0
10.5
10.0
9.5
9.0
8.5
8.0
7.5
7.0
6.5
6.0
5.5
5.0
4.5
4.0
3.5
3.0
2.5
2.0
f1 (ppm)

Compound 28

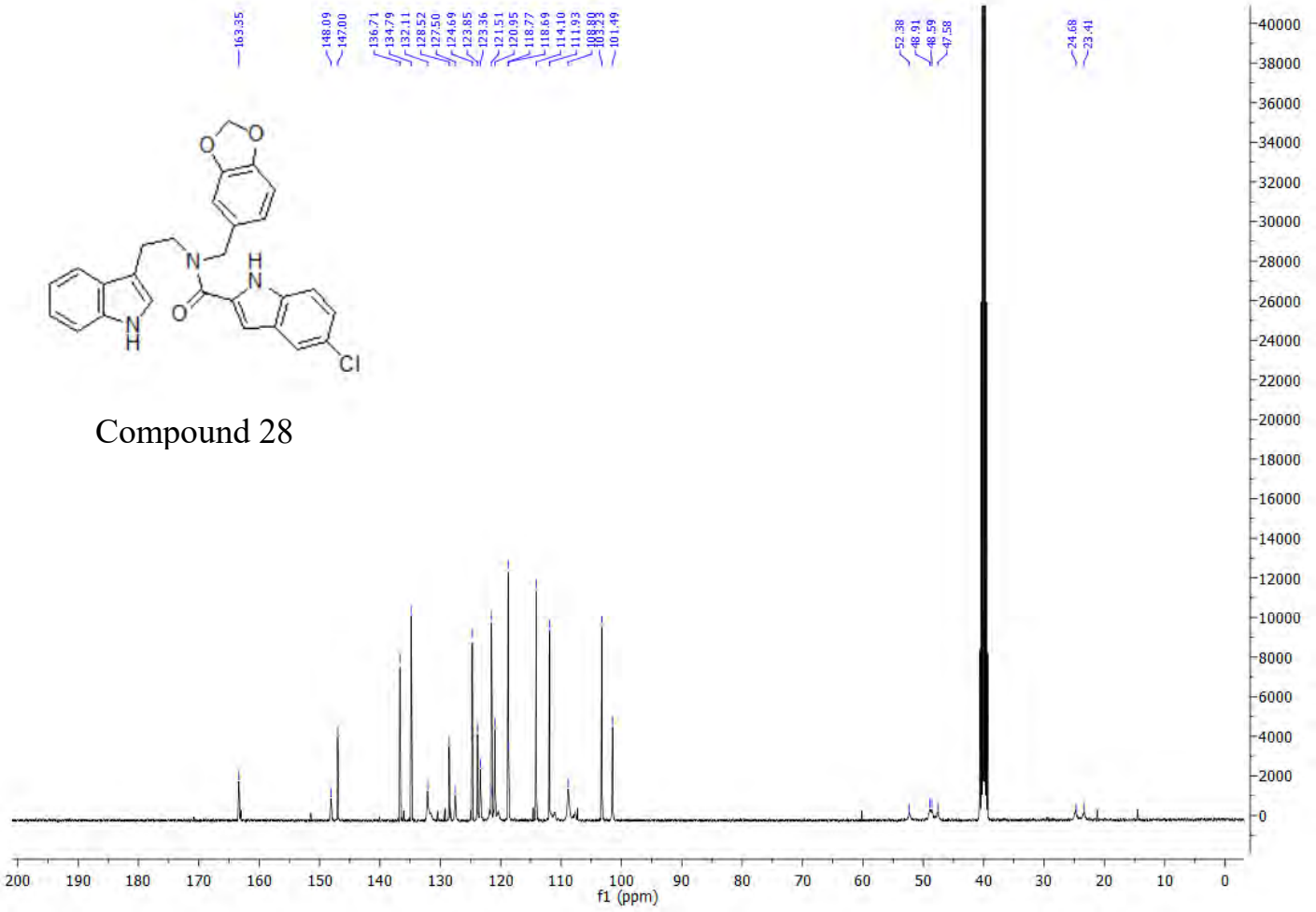
163.35
148.09
147.00
136.71
134.79
132.11
128.52
127.50
124.69
123.85
123.36
121.51
120.95
118.77
118.69
114.10
111.93
101.49
52.38
48.91
48.59
47.58
24.68
23.41
O
O
N
H
N
O
H
N
Cl
40000
38000
36000
34000
32000
30000
28000
26000
24000
22000
20000
18000
16000
14000
12000
10000
8000
6000
4000
2000
0
200
190
180
170
160
150
140
130
120
110
100
90
80
70
60
50
40
30
20
10
0
f1 (ppm)

Compound 28

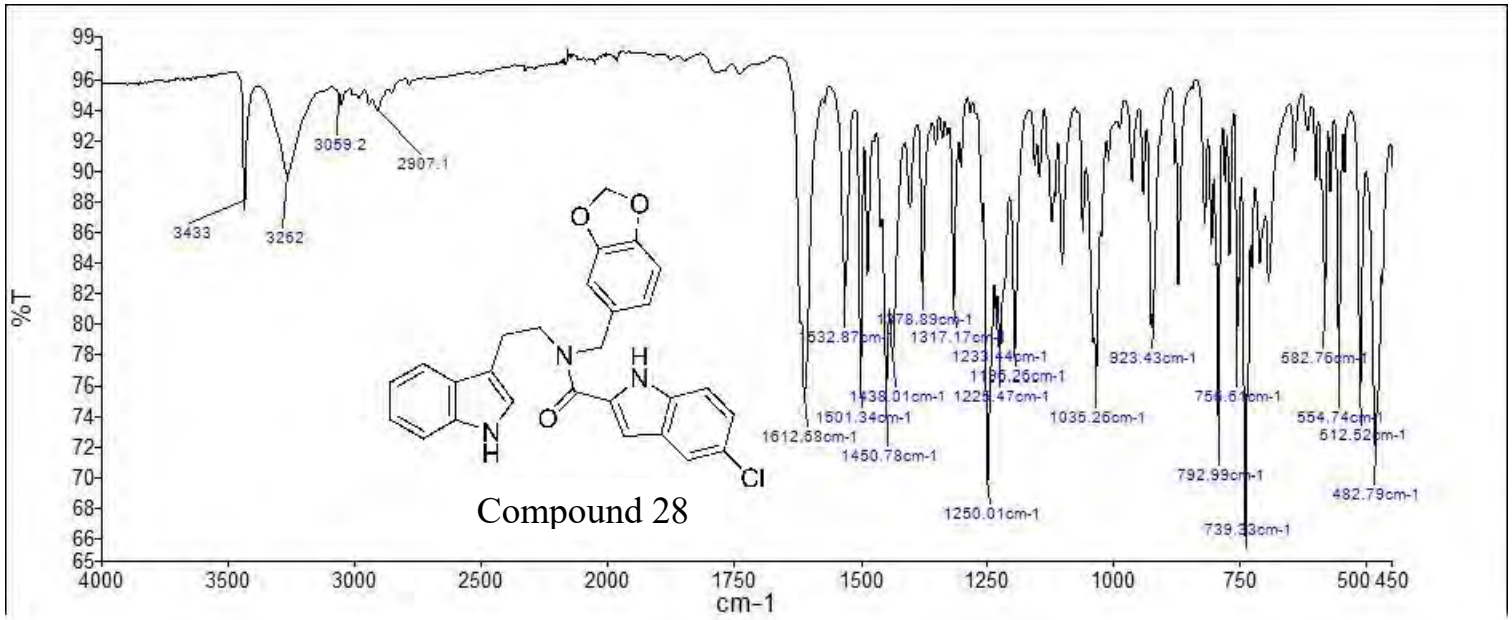
%T
cm-1
3433
3262
3059.2
2907.1
1612.68cm-1
1532.87cm-1
1501.34cm-1
1450.78cm-1
1438.01cm-1
1378.89cm-1
1317.17cm-1
1250.01cm-1
1233.44cm-1
1225.47cm-1
1035.26cm-1
923.43cm-1
792.99cm-1
739.33cm-1
582.76cm-1
554.74cm-1
512.52cm-1
482.79cm-1
Cl

Compound 28

LCMS Report

Agilent Technologies

Data file:	D:\Chem32\1\Data\Analyst\TP142B5 2016-01-18 12-05-58.D		
Sample name:	TP142B5		
Description:			
Sample amount:	5.000	Sample type:	Sample
Instrument:	LCMS	Location:	31
Injection date:	1/18/2016 12:07:31 PM	Injection:	1 of 1
Acq. method:	LCMS gradient initial.M	Injection volume:	10.000
Analysis method:	DEF_LC.M	Acq. operator:	SYSTEM
Last changed:	11/20/2006 9:14:44 PM		

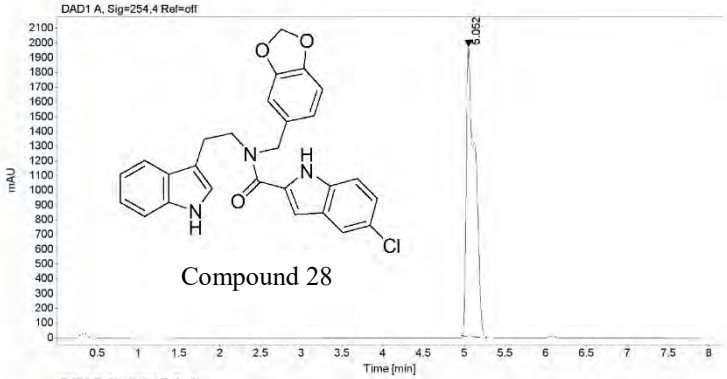

Compound 28

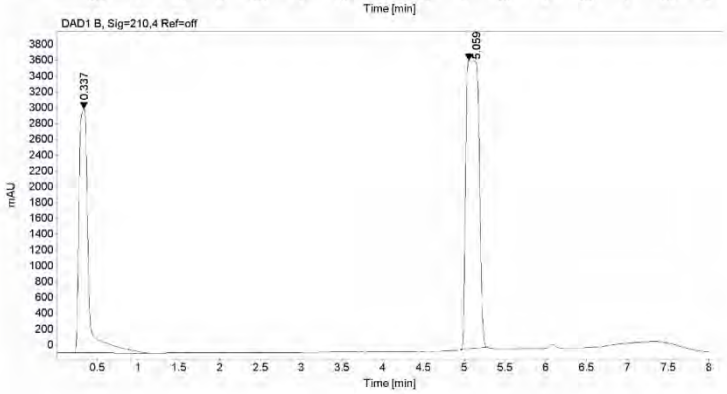

LCMS Report

Agilent Technologies

Signal: DAD1 A, Sig=254,4 Ref=off

RT [min]	Type	Width [min]	Area	Height	Area%	Name
5.052	MM	0.1210	14385.3301	1981.6835	100.0000	
	Sum		14385.3301			

Signal: DAD1 B, Sig=210,4 Ref=off

RT [min]	Type	Width [min]	Area	Height	Area%	Name
0.337	BB	0.1282	24911.3223	3084.0674	38.3123	
5.059	MM	0.1834	40110.4609	3645.2058	61.6877	
	Sum		65021.7832			

Signal: MSD1 TIC, MS File

RT [min]	Type	Width [min]	Area	Height	Area%	Name
0.369	BB	0.1810	7481543.0000	595334.3125	45.3819	
5.107	BB	0.1636	9004196.0000	734879.6875	54.6181	
	Sum		16485739.00			

Signal: MSD2 TIC, MS File

RT [min]	Type	Width [min]	Area	Height	Area%	Name
5.102	MM	0.1790	2261783.2500	210582.6719	100.0000	
	Sum		2261783.250			

Agilent Technologies

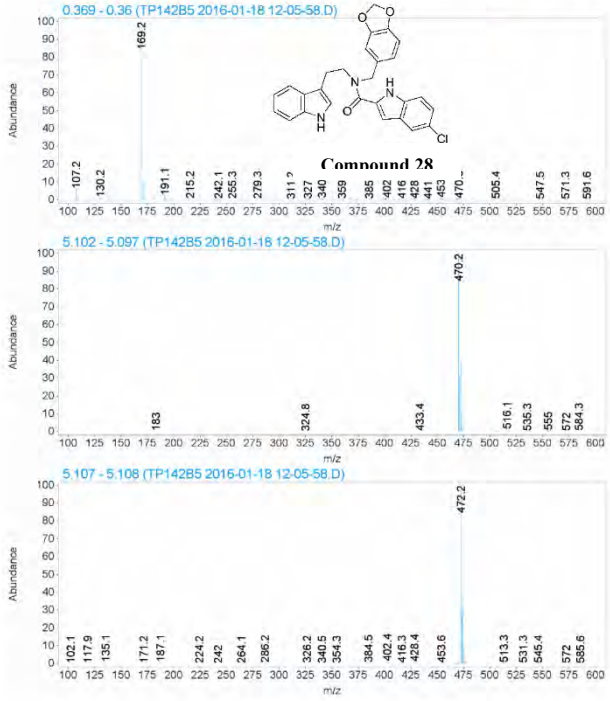

Compound 28

Compound	Chemical Formula	Predicted monoisotopic neutral MW	Predicted MH+	MH+ Measured	Main MS Ions	Main MS/MS Fragments
TP 142B5	$C_{27}H_{22}ClN_3O_3$	471.1350	472.14225	472.14215	472.1422	135.0444 187.0870 144.0810

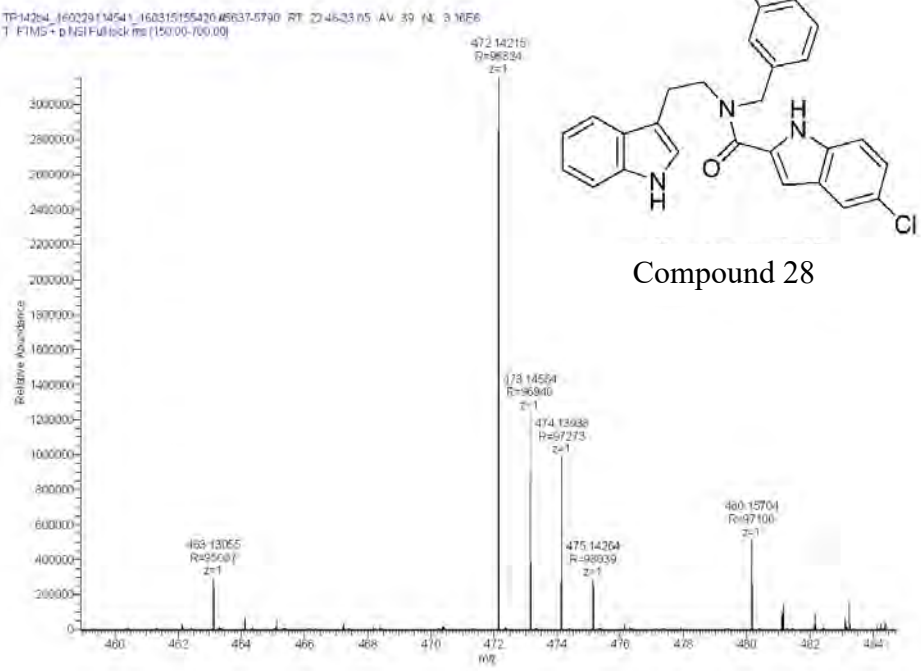

Compound 28

COMPOUND 29

Compound Name: *N-(*1,3-benzodioxol-4-ylmethyl)-*N*-[2-(*1H*-indol-3-yl)ethyl]-*1H*-indole-5-carboxamide

Obtained Weight & Yield: 158 mg, 67%

Appearance: White floppy precipitate

Solubility: DMSO

Melting Point: 162.5-163 ºC

TLC Conditions: EtOAc/Hexane (50/50)

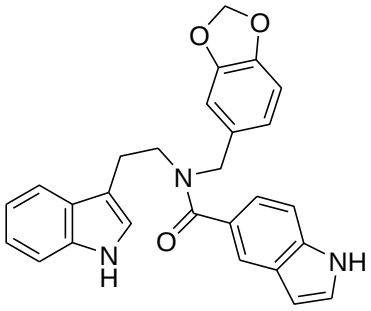

$C_{27}H_{23}N_3O_3$
Exact Mass: 437.1739

IR Analysis: νmax/cm^{-1}

3638 (NH), 3227 (NH), 1614 (CON), 740 (CH-aromatics)

^{1}H NMR Analysis:

^{1}H NMR (400 MHz, DMSO-*d*$_6$) δ 11.29 (s, 1H), 10.78 (s, 1H), 7.61 (s, 1H), 7.51 – 7.39 (m, 2H), 7.56 – 6.38 (m, 9H), 6.47 (s, 1H), 6.01 (s, 2H), 4.87 – 4.29 (m, 2H), 3.65 – 3.45 (m, 2H), 3.12 – 2.70 (m, 2H)

^{13}C NMR Analysis:

^{13}C NMR (101 MHz, DMSO-*d*$_6$) δ 186.0, 172.8, 148.0, 146.9, 136.6, 136.5, 127.8, 127.5, 127.0, 123.3, 121.4, 120.4, 119.1, 118.6, 111.8, 111.7, 108.7, 102.2, 101.4, 49.1, 47.3, 45.6, 24.6, 23.4.

**Note* : Signs of atropisomers for aliphatic CH_2, in which *47.3 is the splitting of 1 C (Ar-CH$_2$-N-); 49.1 and 45.6 are the splitting of (CH$_2$-CH$_2$-N-); 24.6 and 23.4 are the splitting of (CH$_2$-CH$_2$-N-).*

HPLC:

RP-HPLC Alltima™ C18 5 µm 150 mm x 4.6 mm, 10–100% B in 15 min, R_t = 6.48 min, 96%.

Mass Spectral Analysis: LRMS* (ESI+) m/z 437, 437 $[M]^+$, 70%. HRMS (ES+) for $C_{27}H_{23}N_3O_3$, calculated 438.1812, found 438.1812.

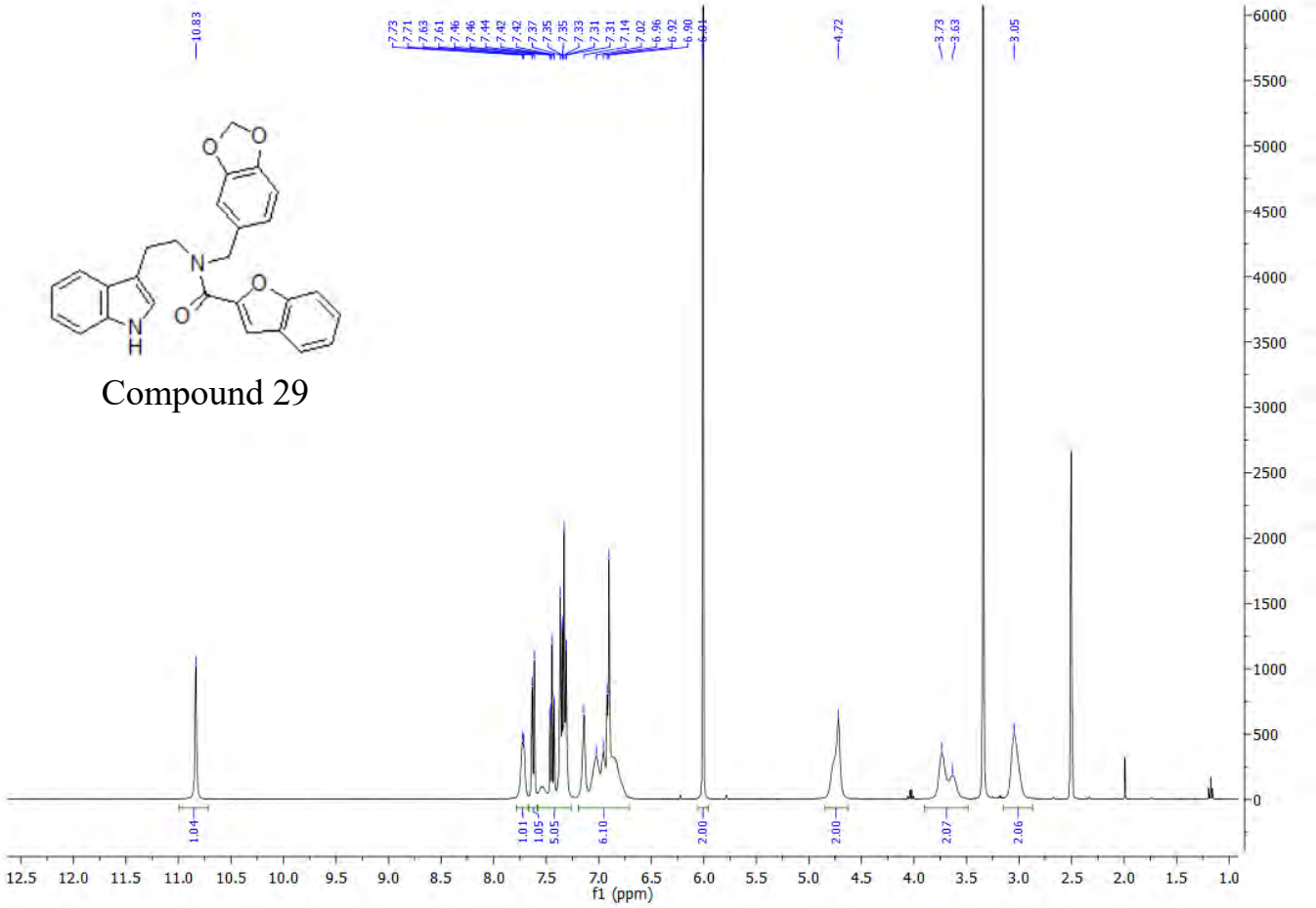
10.83
7.73
7.71
7.63
7.61
7.46
7.46
7.44
7.42
7.42
7.37
7.35
7.35
7.33
7.31
7.31
7.14
7.02
6.96
6.92
6.90
4.72
3.73
3.63
3.05
1.04
1.01
1.05
5.05
6.10
2.00
2.00
2.07
2.06
f1 (ppm)

Compound 29

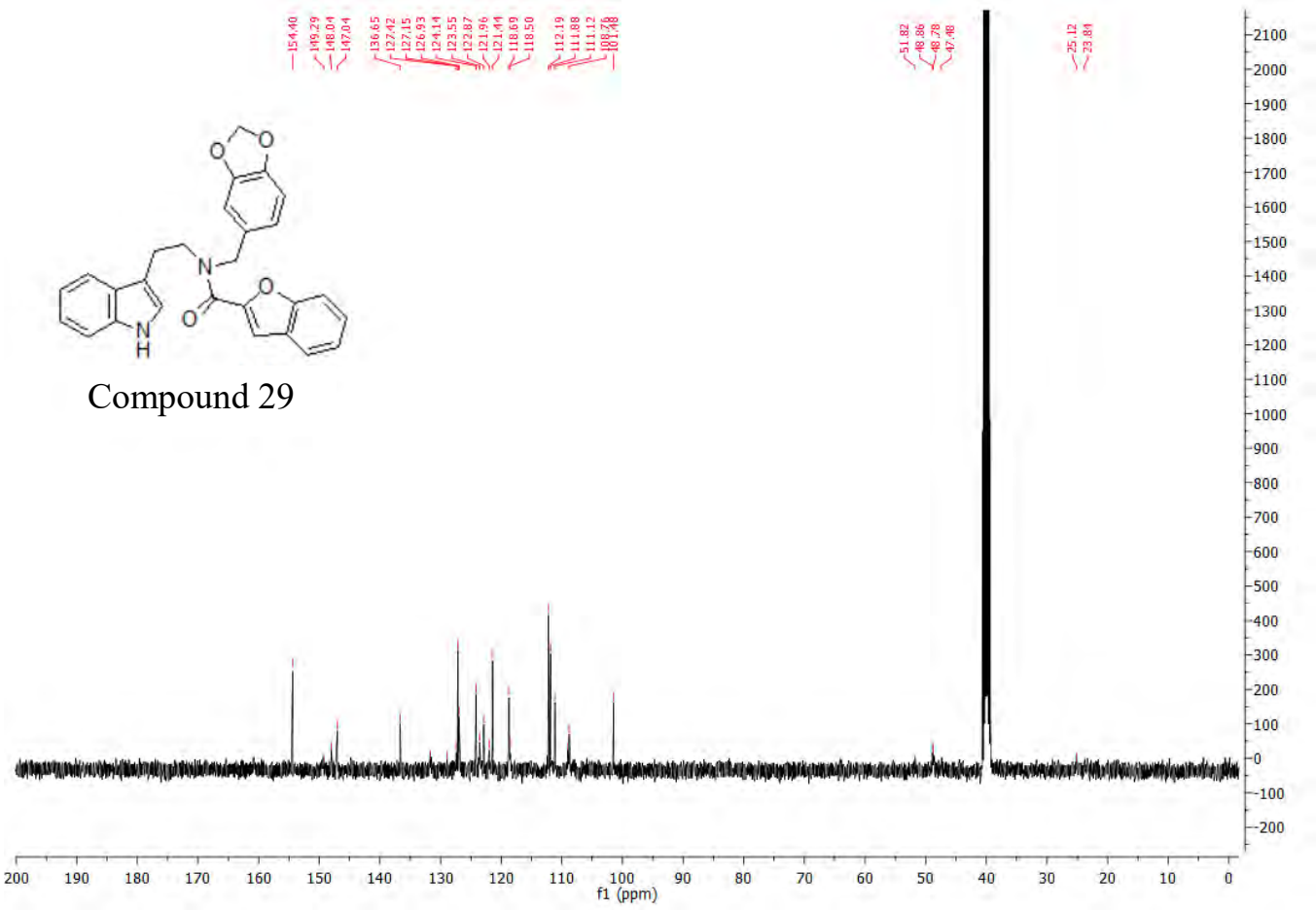
154.40
149.29
148.04
147.04
136.65
127.42
127.15
126.93
124.14
123.55
122.87
121.96
121.44
118.69
118.50
112.19
111.88
111.12
108.76
101.48
51.82
48.86
48.78
47.48
25.12
23.84
2100
2000
1900
1800
1700
1600
1500
1400
1300
1200
1100
1000
900
800
700
600
500
400
300
200
100
0
-100
-200
200 190 180 170 160 150 140 130 120 110 100 90 80 70 60 50 40 30 20 10 0
f1 (ppm)

Compound 29

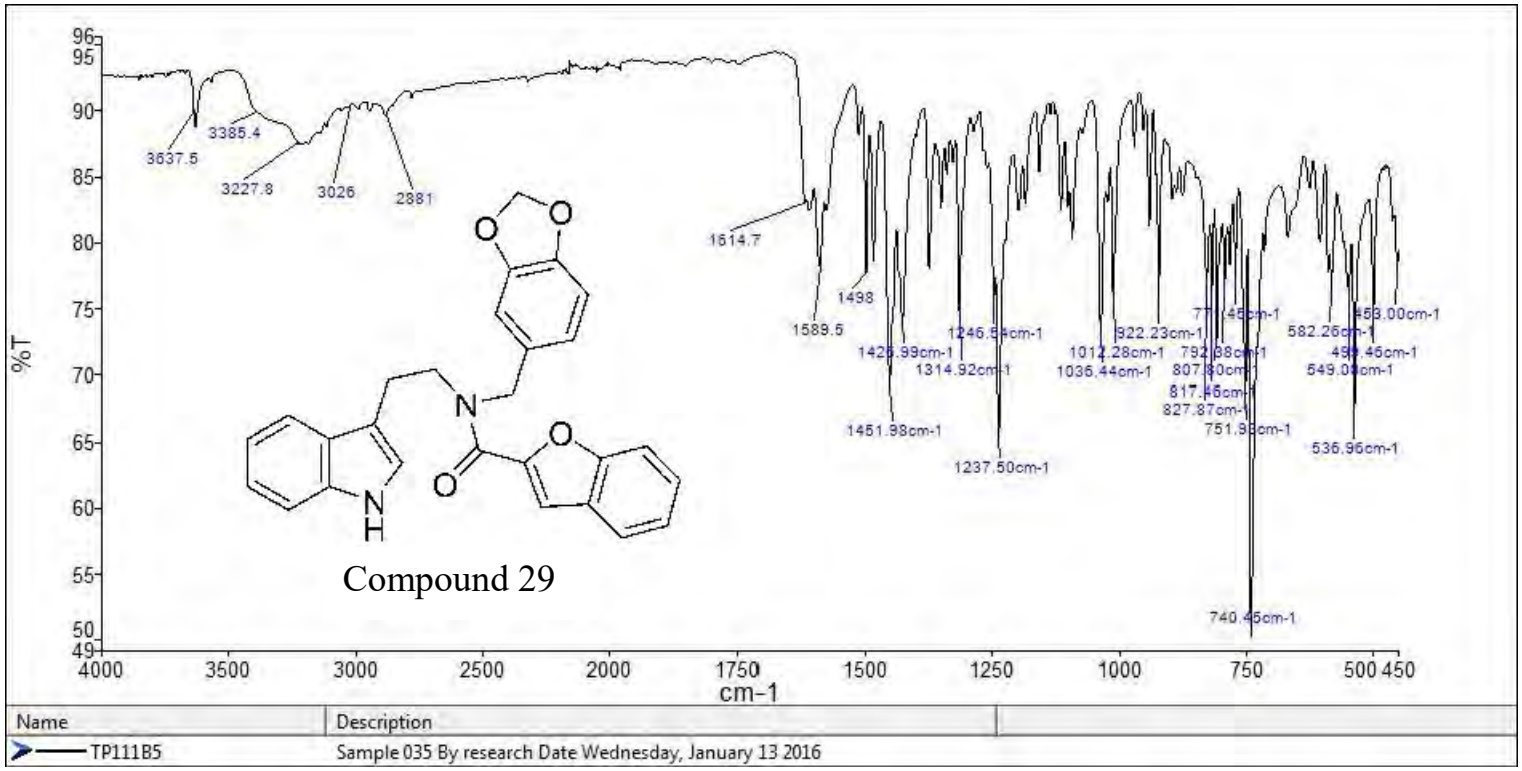
%T
cm-1
3637.5
3385.4
3227.8
3026
2881
1614.7
1589.5
1498
1451.98cm-1
1426.99cm-1
1314.92cm-1
1246.54cm-1
1237.50cm-1
1036.44cm-1
1012.28cm-1
922.23cm-1
827.87cm-1
807.30cm-1
751.98cm-1
740.45cm-1
582.26cm-1
549.01cm-1
536.96cm-1
Name
Description
TP111B5
Sample 035 By research Date Wednesday, January 13 2016

Compound 29

==== Shimadzu LCMSsolution Analysis Report ====

Acquired by	: Admin
Sample Name	: TP111B5 Re
Sample ID	:
Vail #	: 52
Injection Volume	: 20 uL
Data File Name	: TP111B5 Re.lcd
Method File Name	: Econosphere C18 EPS 5u lot 50195421 part 70070 150mm id 4.6mm.lcm
Batch File Name	: Second and third 23092015.lcb
Report File Name	: DefaultLCMS.lcr
Data Acquired	: 9/23/2015 4:10:56 PM
Data Processed	: 9/25/2015 4:24:03 PM

<Chromatogram>

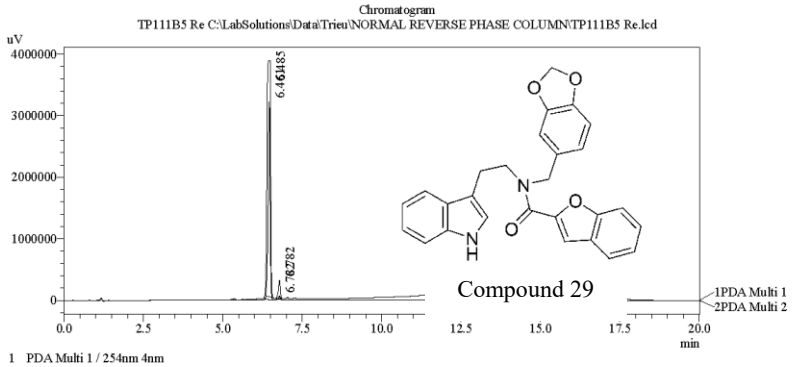

1 PDA Multi 1 / 254nm 4nm
2 PDA Multi 2 / 220nm 4nm

PeakTable

PDA Ch1 254nm 4nm

Peak#	Ret. Time	Area	Height	Area %	Height %
1	6.461	13516088	3212596	98.931	98.511
2	6.782	146024	48562	1.069	1.489
Total		13662112	3261158	100.000	100.000

PeakTable

PDA Ch2 220nm 4nm

Peak#	Ret. Time	Area	Height	Area %	Height %
1	6.485	29251714	3838659	95.911	92.725
2	6.782	1247061	301177	4.089	7.275
Total		30498775	4139836	100.000	100.000

==== Shimadzu LCMSsolution Data Report ====

<Chromatogram>

Sample Information

Acquired by	: Admin
Date Acquired	: 7/31/2015 12:41:11 PM
Sample Type	: Unknown
Level#	: 0
Sample Name	: TP111B5 ESI POS
Sample ID	:
ISTD Amount	: (Level1 Conc.)
Sample Amount	: 1
Dilution Factor	: 1
Tray#	: 1
Vial#	: 54
Injection Volume	: 5
Data File	: TP111B5 ESI POS.lcd
Method File	: FIA-ESI_Scan(+).lcm
Original Method	: C:\LabSolutions\Data\Trieu\Mass spec files\FIA-ESI_Scan(+).lcm
Report Format	: DefaultLCMS.lcr
Tuning File	: C:\LabSolutions\LCsolution\Log\Tuning\Autotune_030908.lct
Processed by	: Admin
Modified Date	: 7/31/2015 12:42:43 PM

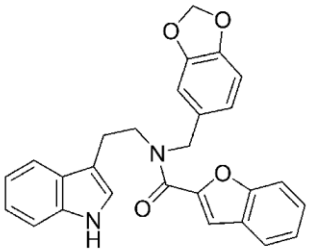

Compound 29

Chromatogram

TP111B5 ESI POS C:\LabSolutions\Data\Trieu\NORMAL REVERSE PHASE COLUMN\TP111B5 ESI POS.lcd

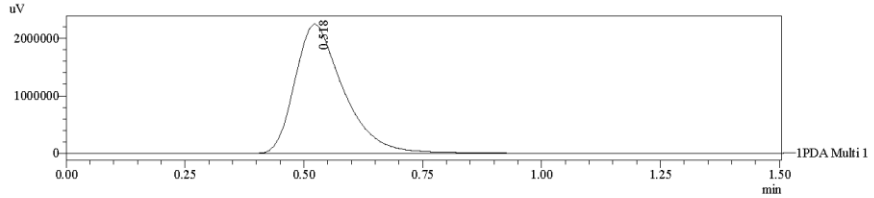

1 PDA Multi 1 / 254nm 4nm

<Spectrum>

Retention Time:0.800(Scan#:81)
Max Peak:353 Base Peak:437.45(54851)
Spectrum:Averaged 0.660-1.140(67-115)
Background:Averaged 0.160-0.487(17-49) Polarity:Pos Segment1 - Event1

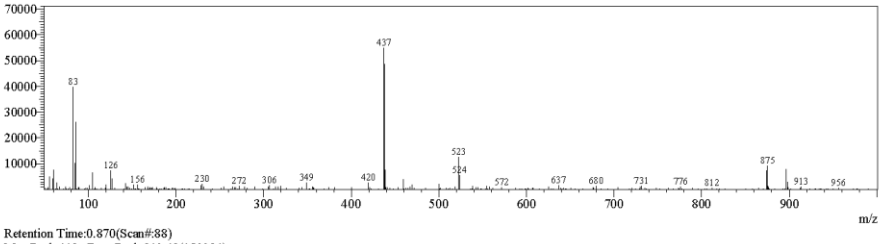

Retention Time:0.870(Scan#:88)
Max Peak:410 Base Peak:312.40(152234)
Spectrum:Averaged 0.670-1.150(68-116)
Background:Averaged 0.170-0.487(18-50) Polarity:Neg Segment1 - Event2

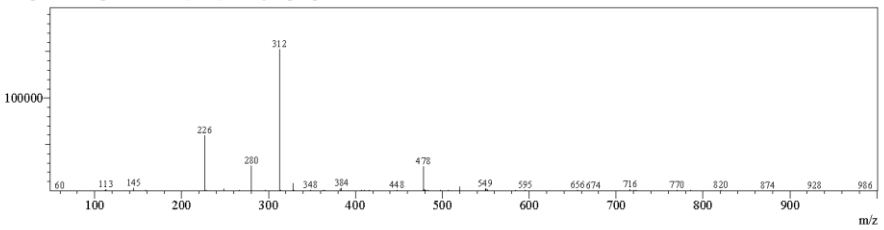

C:¥LabSolutions¥Data¥Trieu¥NORMAL REVERSE PHASE COLUMN¥TP111B5 ESI POS.lcd

Compound	Chemical Formula	Predicted monoisotopic neutral MW	Predicted MH+	MH+ Measured	Main MS Ions	Main MS/MS Fragments
TP 111B5	$C_{27}H_{23}N_3O_3$	437.1739	438.18122	438.18122	438.18122	135.0443 144.0446 278.1175

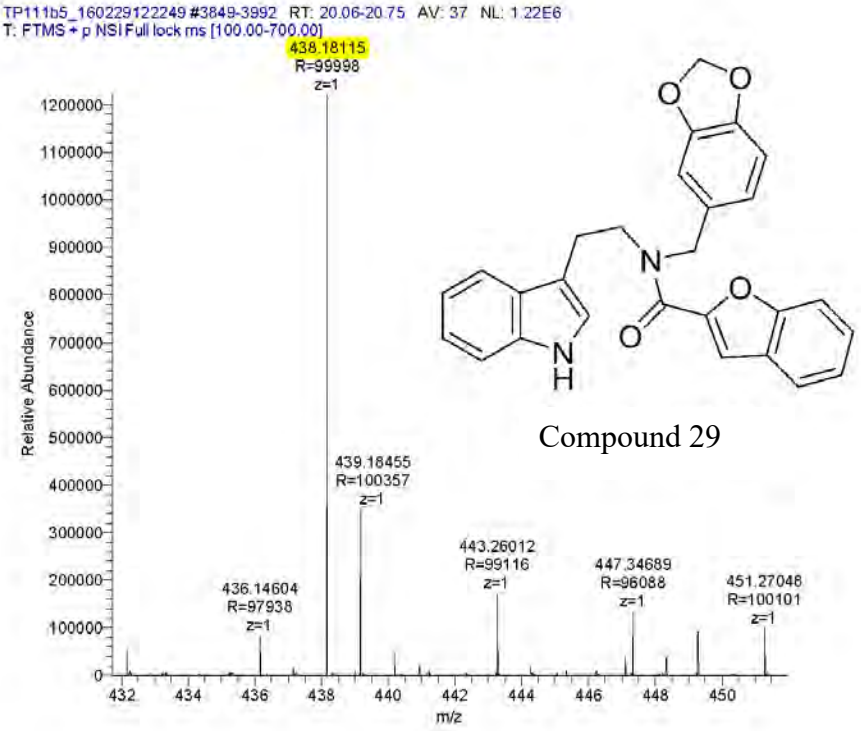

Compound 29

8.4. Appendix to Chapter 5

8.4.1. Compounds characterization

Compound **8a**

Compound Name: 2,4-Dimethyl-6-phenylimino-6*H*-[1,3]thiazine-5-carboxylic acid ethyl ester

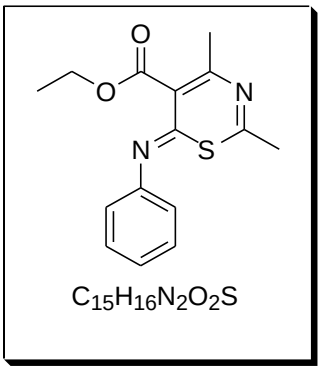

Obtained Weight & Yield: 200 mg, 65%

Appearance: Sparkling yellow precipitate

Solubility: MeOH, Acetone, ACN

Melting Point: 145.3- 146.5 °C

TLC Conditions: EtOAc/Hexane (50/50)

IR Analysis: vmax/cm^{-1} 2984 (CH), 1728 (COO), 1584, 1232 (CO)

^{1}H NMR Analysis:

^{1}H NMR (400 MHz, CDCl3) δ 7.65 – 7.43 (m, 3H), 7.25 – 7.09 (m, 2H), 4.42 (q, *J* = 7.1 Hz, 2H), 2.31 (s, 3H), 2.22 (s, 3H), 1.39 (t, *J* = 7.1 Hz, 3H).

^{13}C NMR Analysis:

^{13}C NMR (400 MHz, $CDCl_3$) δ 183.0, 166.1, 159.2, 153.9, 140.6, 132.3, 130.5 (Cx2), 129.7, 127.1 (Cx2), 62.0, 25.1, 21.9, 14.0.

HPLC:

RP-HPLC Alltima™ C18 5 µm 150 mm x 4.6 mm, 10-100% B in 15 min, R_t = 5.19 min, 100%.

Mass Spectral Analysis: LRMS (ESI+) m/z: 288, 288 $[M]^+$ 40%. HRMS (ES+) for $C_{15}H_{16}N_2O_2S$, calculated 289.1005, found 289.1004.

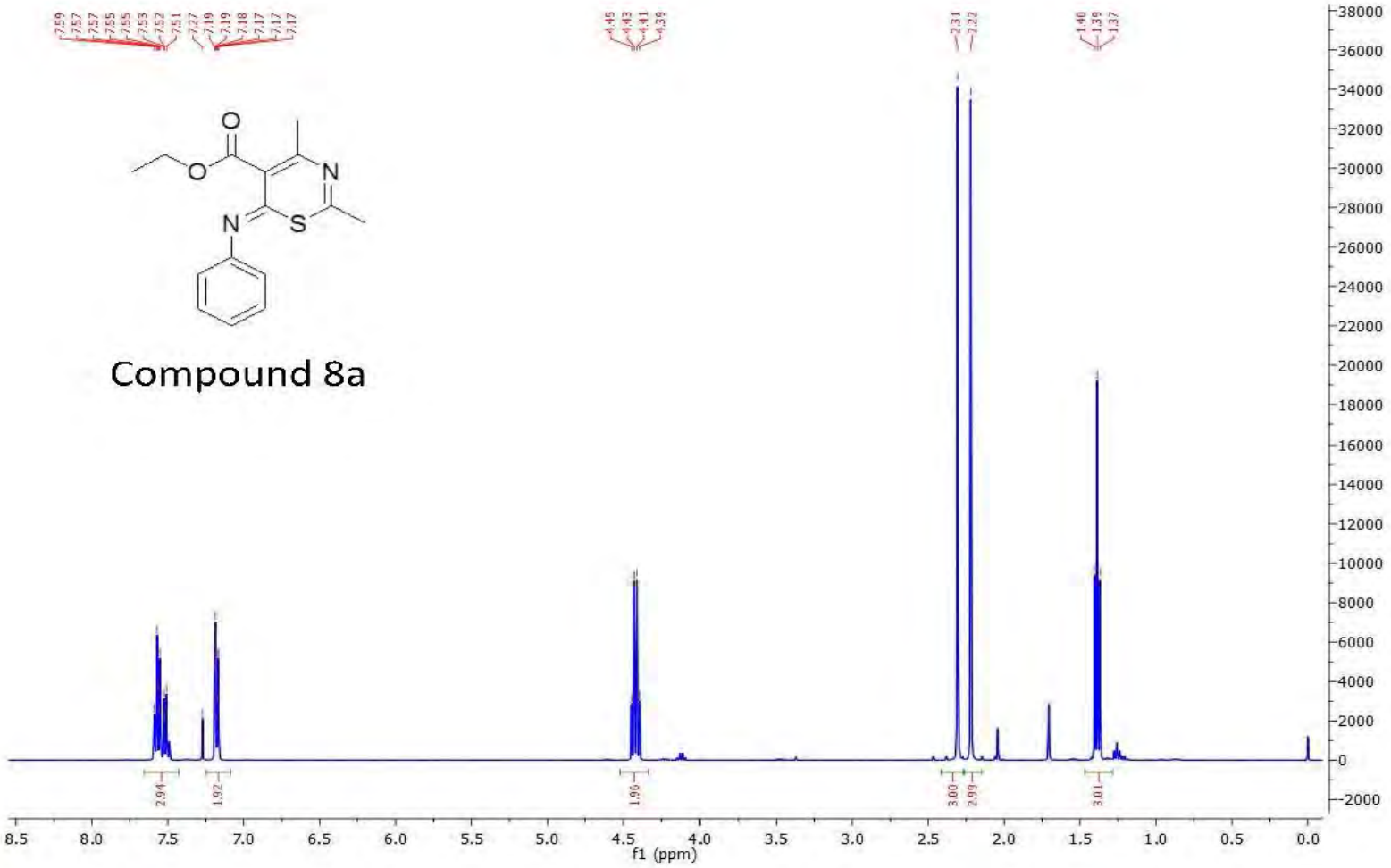
7.59
7.57
7.57
7.55
7.55
7.53
7.52
7.51
7.27
7.19
7.19
7.18
7.17
7.17
7.17
7.17
4.45
4.43
4.41
4.39
2.31
2.22
1.40
1.39
1.37
O
O
N
N
S
Compound 8a
38000
36000
34000
32000
30000
28000
26000
24000
22000
20000
18000
16000
14000
12000
10000
8000
6000
4000
2000
0
-2000
2.94
1.92
1.96
3.00
2.99
3.01
8.5
8.0
7.5
7.0
6.5
6.0
5.5
5.0
4.5
4.0
3.5
3.0
2.5
2.0
1.5
1.0
0.5
0.0
f1 (ppm)

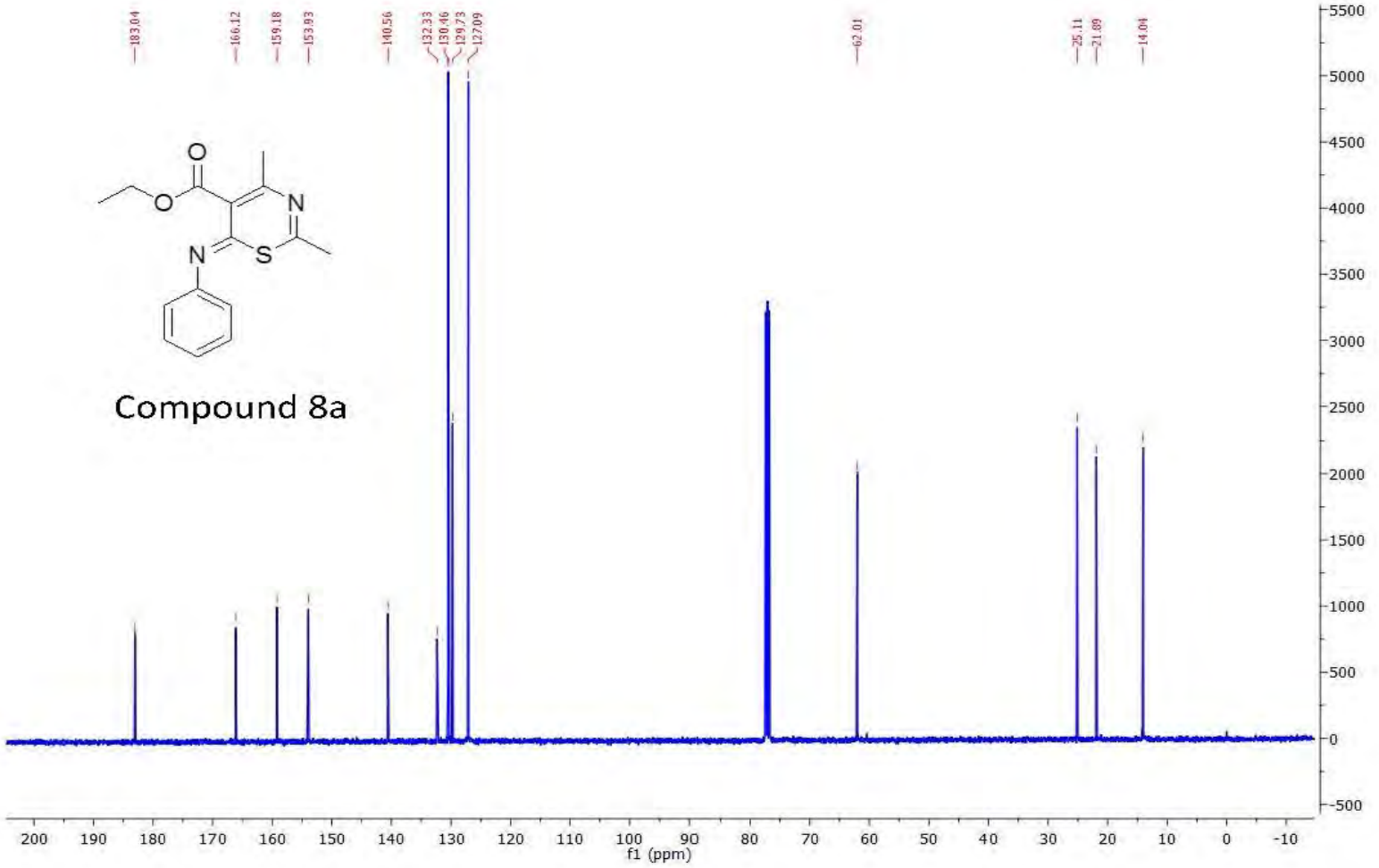
183.04
166.12
159.18
153.93
140.56
132.33
130.46
129.73
127.09
62.01
25.11
21.89
14.04
O
O
N
N
S
Compound 8a
5500
5000
4500
4000
3500
3000
2500
2000
1500
1000
500
0
-500
200 190 180 170 160 150 140 130 120 110 100 90 80 70 60 50 40 30 20 10 0 -10
f1 (ppm)

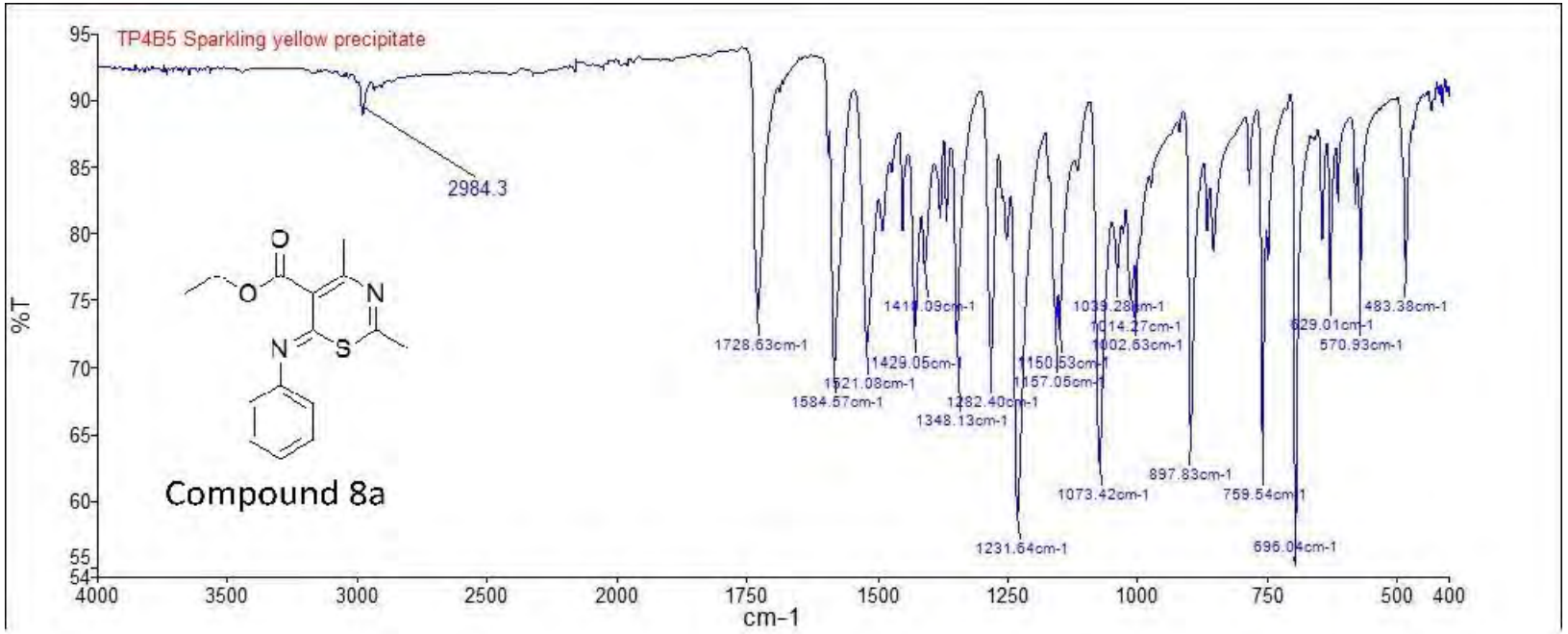
TP4B5 Sparkling yellow precipitate
2984.3
1728.63cm-1
1584.57cm-1
1521.08cm-1
1429.05cm-1
1348.13cm-1
1282.40cm-1
1231.64cm-1
1157.05cm-1
1150.53cm-1
1073.42cm-1
1039.28cm-1
1014.27cm-1
1002.63cm-1
897.83cm-1
759.54cm-1
696.04cm-1
629.01cm-1
570.93cm-1
483.38cm-1
Compound 8a
%T
cm-1

==== Shimadzu LCMSsolution Analysis Report ====

Acquired by	: Admin
Sample Name	: TP4B5Re
Sample ID	:
Vail #	: 51
Injection Volume	: 20 uL
Data File Name	: TP4B5Re.lcd
Method File Name	: Econosphere C18 EPS 5u lot 50195421 part 70070 150mm id 4.6mm.lcm
Batch File Name	: Indole deriv and third.lcb
Report File Name	: DefaultLCMS.lcr
Data Acquired	: 10/6/2015 12:58:28 PM
Data Processed	: 10/6/2015 1:21:28 PM

<Chromatogram>

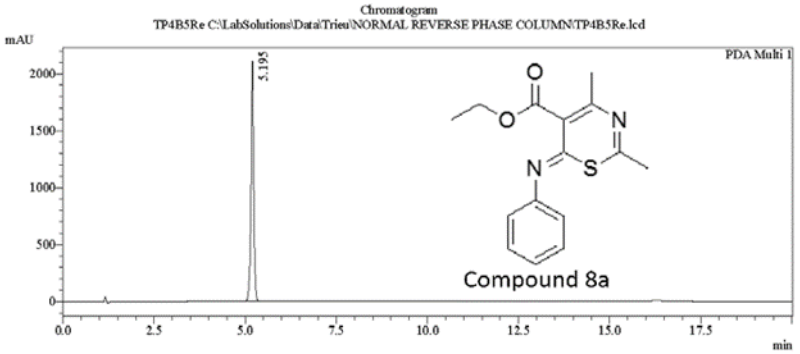

1 PDA Multi 1 / 254nm 4nm
2 PDA Multi 2 / 220nm 4nm

PeakTable

PDA Ch1 254nm 4nm

Peak#	Ret. Time	Area	Height	Area %	Height %
1	5.195	10583312	2107255	100.000	100.000
Total		10583312	2107255	100.000	100.000

PeakTable

PDA Ch2 220nm 4nm

Peak#	Ret. Time	Area	Height	Area %	Height %
1	5.227	30319270	3846336	100.000	100.000
Total		30319270	3846336	100.000	100.000

==== Shimadzu LCMSsolution Data Report ====

<Chromatogram>

Sample Information

Acquired by	: Admin
Date Acquired	: 8/11/2015 11:51:29 AM
Sample Type	: Unknown
Level#	: 0
Sample Name	: TP4B5
Sample ID	:
ISTD Amount	: (Level1 Conc.)
Sample Amount	: 1
Dilution Factor	: 1
Tray#	: 1
Vial#	: 6
Injection Volume	: 20
Data File	: TP4B5.lcd
Method File	: FIA-ESI_Scan(+).lcm
Original Method	: C:\LabSolutions\Data\Jen Baker\FIA-ESI_Scan(+).lcm
Report Format	: DefaultLCMS.lcr
Tuning File	: C:\LabSolutions\LCsolution\Log\Tuning\Autotune_030908.lct
Processed by	: Admin
Modified Date	: 8/11/2015 11:53:31 AM

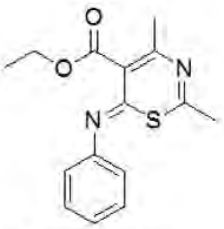

Compound 8a

Chromatogram
TP4B5 C:\LabSolutions\Data\Trieu\SECOND PROI\Mass\TP4B5.lcd

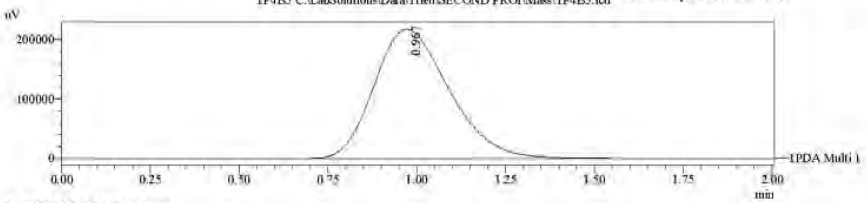

1 PDA Multi 1 / 254nm 4nm

<Spectrum>

Retention Time:1.320(Scan#:133)
Max Peak:351 Base Peak:156.50(701317)
Spectrum:Averaged 1.040-1.820(105-183)
Background:Averaged 0.180-0.741(19-75) Polarity:Pos Segment1 - Event1

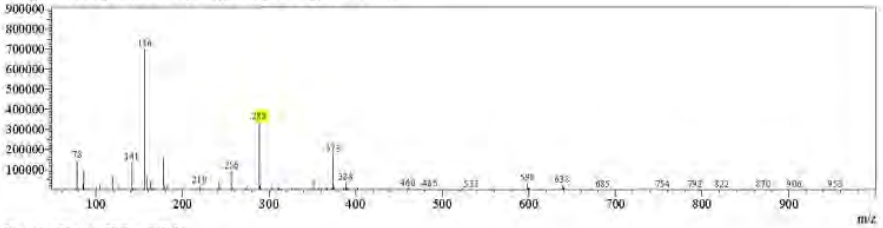

Retention Time:1.350(Scan#:136)
Max Peak:510 Base Peak:226.50(212889)
Spectrum:Averaged 1.050-1.830(106-184)
Background:Averaged 0.190-0.741(20-76) Polarity:Neg Segment1 - Event2

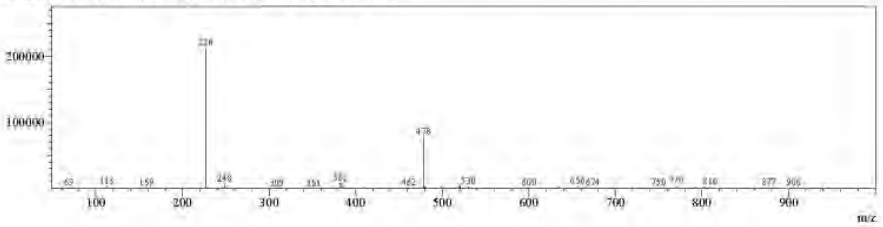

C:¥LabSolutions¥Data¥Trieu¥SECOND PROI¥Mass¥TP4B5.lcd

Compound	Chemical Formula	Predicted monoisotopic neutral MW	Predicted MH+	MH+ Measured	Main MS Ions	Main MS/MS Fragments
8a	$C_{15}H_{16}N_2O_2S$	288.0932	289.10053	289.10043		243.0591
					289.1004	261.0698
						172.0431

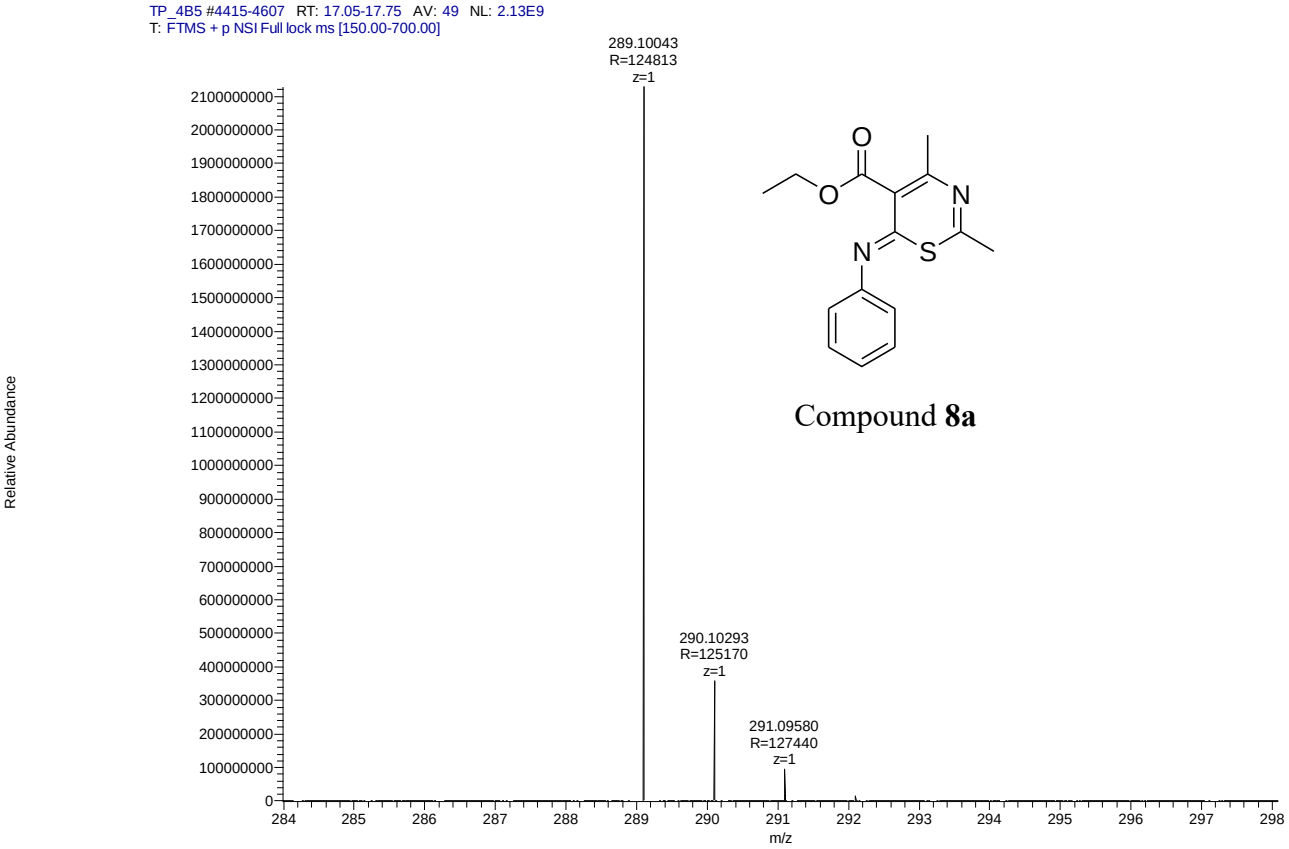

Compound **8a**

Compound 8b

Compound Name: 2,4-Dimethyl-6-p-tolylimino-6*H*-[1,3]thiazine-5-carboxylic acid ethyl ester

Obtained Weight & Yield: 100 mg, 18%

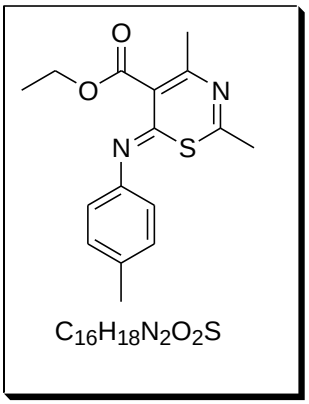

Appearance: Yellow precipitate

Solubility: MeOH, ACN, Acetone

Melting Point: 166.7-167.5 °C

TLC Conditions: EtOAc/n-Hexane (50/50)

IR Analysis: 2975 (CH), 1733 (COO), 1232 (CO)

^{1}H NMR Analysis:

^{1}H NMR (400 MHz, $CDCl_3$) δ 7.36 (d, *J* = 8.1 Hz, 2H), 7.05 (d, *J* = 8.3 Hz, 2H), 4.42 (q, *J* = 7.1 Hz, 2H), 2.43 (s, 3H), 2.30 (s, 3H), 2.22 (s, 3H), 1.39 (t, *J* = 7.1 Hz, 3H).

^{13}C NMR Analysis:

^{13}C NMR (101 MHz, $CDCl_3$) δ 183.11, 166.14, 159.45, 153.87, 139.87, 137.97, 132.27, 131.13 (Cx2), 126.69 (Cx2), 61.98, 25.11, 21.87, 21.37, 14.04.

HPLC RP-HPLC Alltima™ C18 5 µm 150 mm x 4.6 mm, 10–100% B in 15 min, R_t = 6.81 min, 100%.

Mass Spectral Analysis: LRMS (ESI+) m/z 302, 302 [M^+] (100%). HRMS (ES+) for $C_{16}H_{18}N_2O_2S$, calculated 303.1162, found 303.1160.

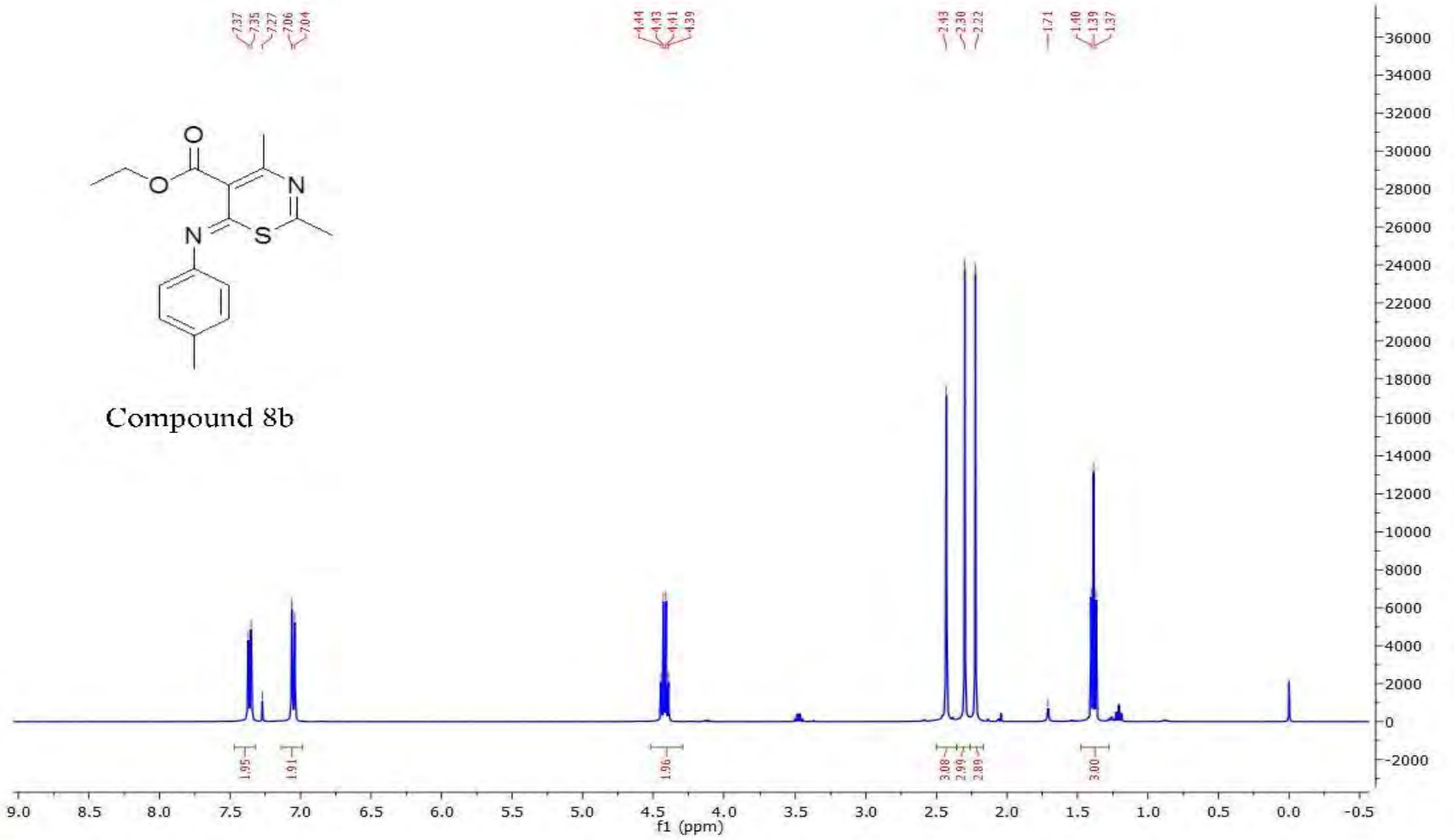
7.37
7.35
7.27
7.06
7.04
4.44
4.43
4.41
4.39
2.43
2.30
2.22
1.71
1.40
1.39
1.37
O
O
N
N
S
Compound 8b
1.95
1.91
1.96
3.08
2.99
2.89
3.00
f1 (ppm)

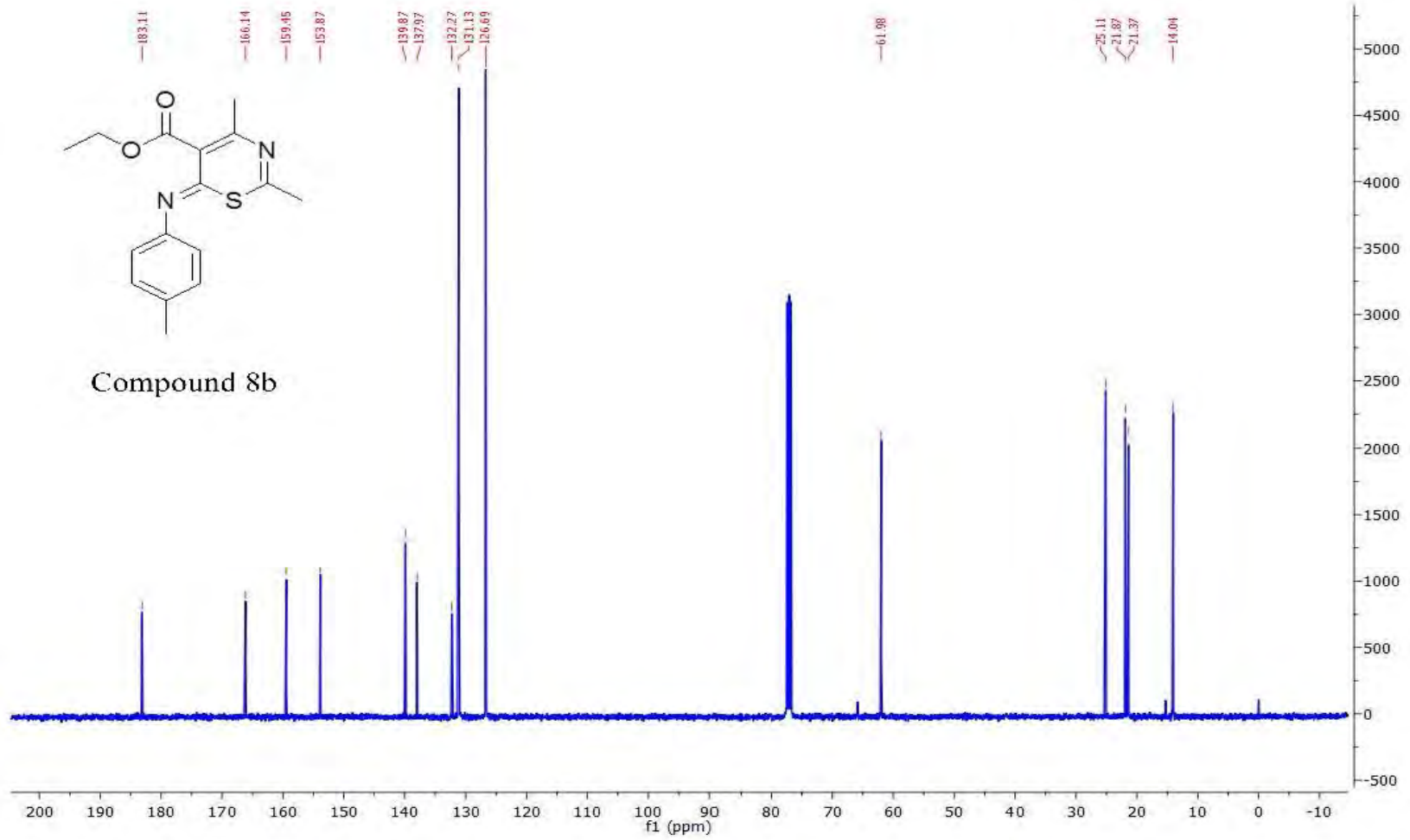
183.11
166.14
159.45
153.87
139.87
137.97
132.27
131.13
126.69
61.98
25.11
21.87
21.37
14.04
O
O
N
N
S
5000
4500
4000
3500
3000
2500
2000
1500
1000
500
0
-500
200
190
180
170
160
150
140
130
120
110
100
90
80
70
60
50
40
30
20
10
0
-10
f1 (ppm)

Compound 8b

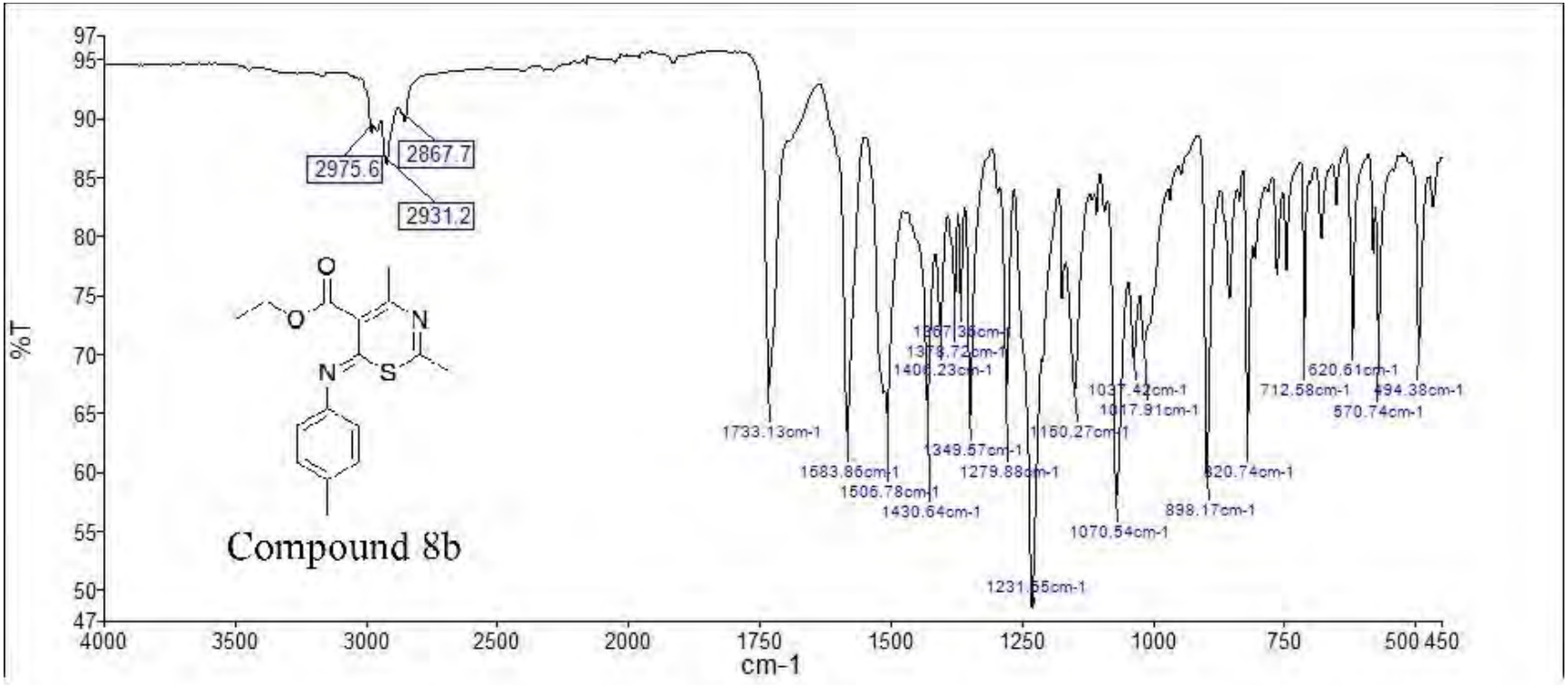
%T
cm-1
2975.6
2867.7
2931.2
1733.13cm-1
1683.86cm-1
1506.78cm-1
1430.64cm-1
1349.57cm-1
1279.88cm-1
1231.65cm-1
1160.27cm-1
1070.54cm-1
1037.42cm-1
1017.91cm-1
898.17cm-1
820.74cm-1
712.58cm-1
620.61cm-1
570.74cm-1
Compound 8b

==== Shimadzu LCMSsolution Analysis Report ====

Acquired by	: Admin
Sample Name	: TP102B5 Re
Sample ID	:
Vail #	: 58
Injection Volume	: 20 uL
Data File Name	: TP102B5 Re.lcd
Method File Name	: Platinum C18 EPS 3u lot 561094 part 50573 53mm id 7mm.lcm
Batch File Name	: Batch Second pro.lcb
Report File Name	: DefaultLCMS.lcr
Data Acquired	: 8/11/2015 7:33:18 PM
Data Processed	: 8/12/2015 1:29:14 PM

<Chromatogram>

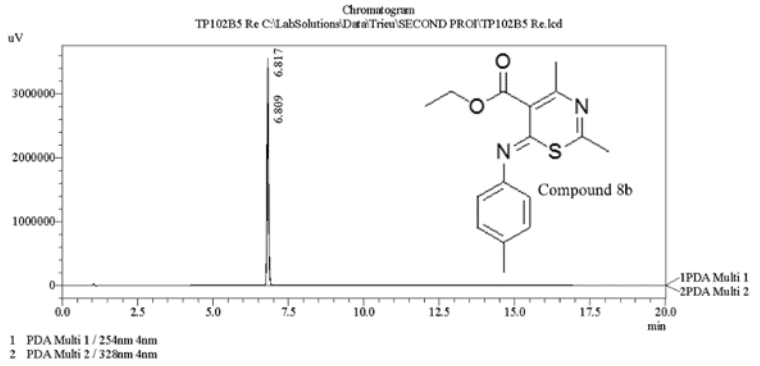

PeakTable

PDA Ch2 328nm 4nm

Peak#	Ret. Time	Area	Height	Area %	Height %
1	6.817	14829439	3561084	100.000	100.000
Total		14829439	3561084	100.000	100.000

PeakTable

PDA Ch1 254nm 4nm

Peak#	Ret. Time	Area	Height	Area %	Height %
1	6.809	8956246	2849511	100.000	100.000
Total		8956246	2849511	100.000	100.000

==== Shimadzu LCMSsolution Data Report ====

<Chromatogram>

Sample Information

Acquired by	: Admin
Date Acquired	: 8/12/2015 12:20:01 PM
Sample Type	: Unknown
Level#	: 0
Sample Name	: TP102B5 Re ESI +
Sample ID	:
ISTD Amount	: (Level1 Conc.)
Sample Amount	: 1
Dilution Factor	: 1
Tray#	: 1
Vial#	: 58
Injection Volume	: 3
Data File	: TP102B5 Re ESI +.lcd
Method File	: FIA-ESI_Scan(+).lcm
Original Method	: C:\LabSolutions\Data\Trieu\Mass spec files\FIA-ESI_Scan(+).lcm
Report Format	: Default.LCMS.lcr
Timing File	: C:\LabSolutions\LCsolution\Log\Timing\Autotune_030908.lcr
Processed by	: Admin
Modified Date	: 8/12/2015 12:22:05 PM

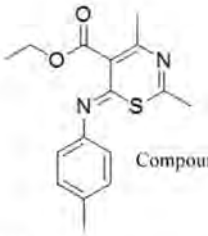

Compound 8b

Chromatogram

TP102B5 Re ESI + C:\LabSolutions\Data\Trieu\SECOND PROJ\Mass\TP102B5 Re ESI +.lcd

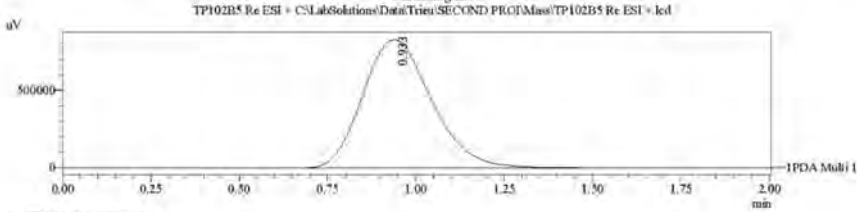

1 PDA Multi 1 / 254nm 4nm

<Spectrum>

Retention Time:1.240(Scan#:125)
Max Peak:342 Base Peak:302.55(1561248)
Spectrum:Averaged 0.980-1.740(99-175)
Background:Averaged 0.200-0.703(21-71) Polarity:Pos Segment1 - Event1

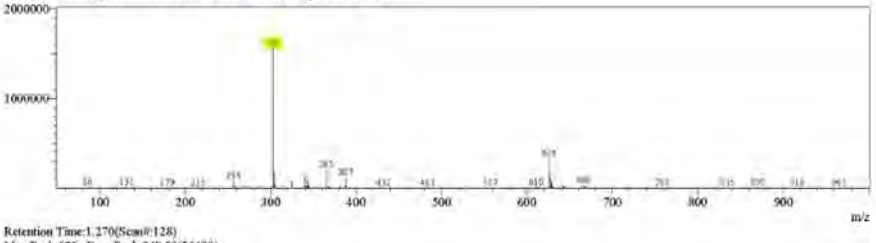

Retention Time:1.270(Scan#:128)
Max Peak:626 Base Peak:248.50(56430)
Spectrum:Averaged 0.990-1.750(100-176)
Background:Averaged 0.210-0.703(22-72) Polarity:Neg Segment1 - Event2

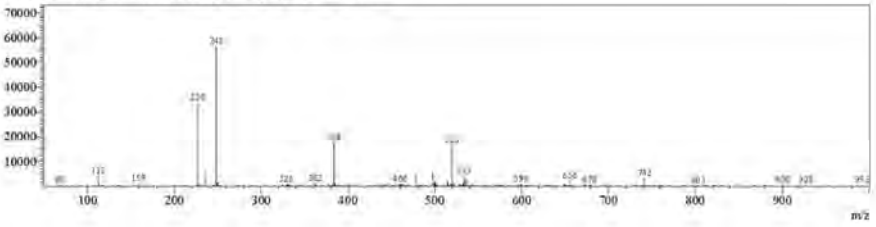

C:¥LabSolutions¥Data¥Trieu¥SECOND PROJ¥Mass¥TP102B5 Re ESI +.lcd

Compound	Chemical Formula	Predicted monoisotopic neutral MW	Predicted MH+	MH+ Measured	Main MS Ions	Main MS/MS Fragments
8b	$C_{16}H_{18}N_2O_2S$	302.1089	303.11618	303.11604		257.0747
					303.1160	275.0852
						172.0430

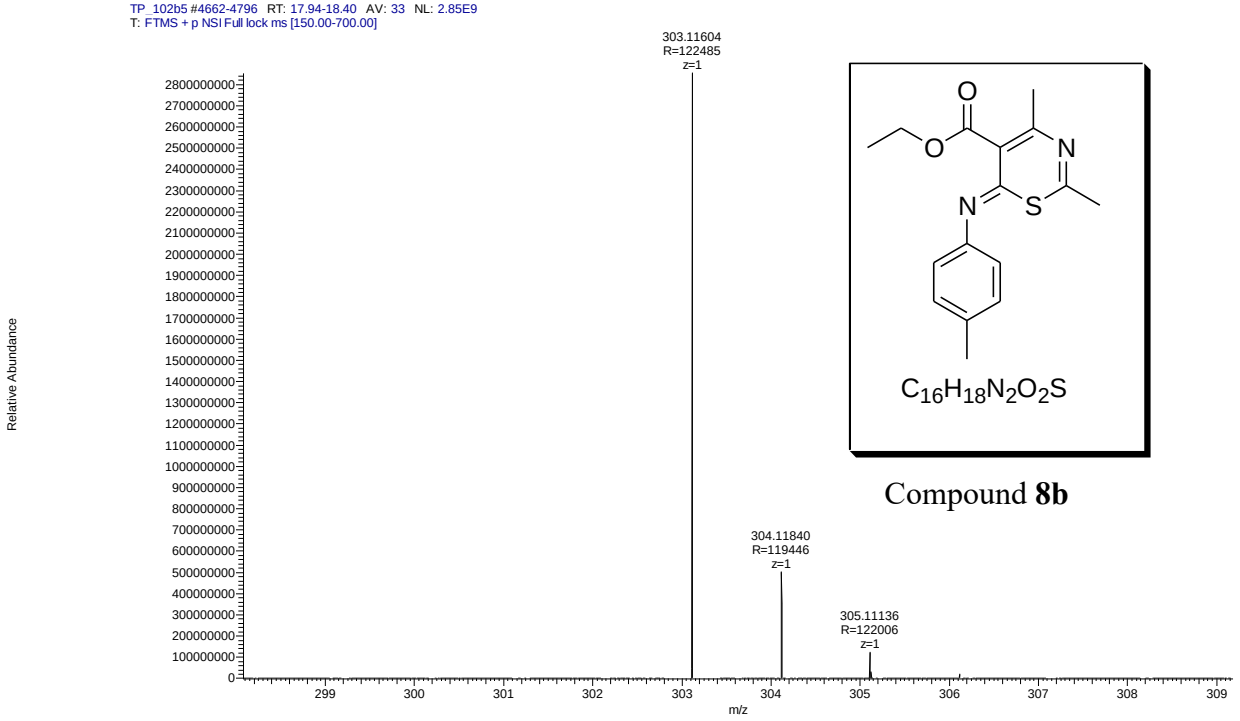

Compound 8c

Compound Name: 6-(4-Isopropyl-phenylimino)-2,4-dimethyl-6*H*-[1,3]thiazine-5-carboxylic acid ethyl ester

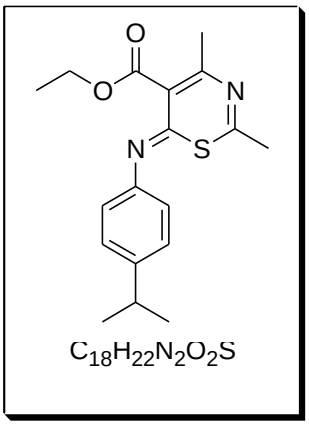

Obtained Weight & Yield: 392 mg, 50%

Appearance: Yellow precipitate

Solubility: MeOH, ACN, Acetone

Melting Point: 113.8-114.6 ºC

TLC Conditions: EtOAc/n-Hexane (50/50)

IR Analysis:

2989 (CH), 1727 (COO), 1233 (CO)

^{1}H NMR Analysis:
^{1}H NMR (400 MHz, $CDCl_3$) δ 7.40 (d, *J* = 8.3 Hz, 2H), 7.08 (d, *J* = 8.4 Hz, 2H), 4.40 (q, *J* = 7.1 Hz, 2H), 3.03-2.90 (m, 1H), 2.29 (s, 3H), 2.21 (s, 3H), 1.37 (t, *J* = 7.1 Hz, 3H), 1.29 (d, *J* = 6.9 Hz, 6H).

^{13}C NMR Analysis:
^{13}C NMR (101 MHz, $CDCl_3$) δ 183.0, 166.1, 159.5, 153.7, 150.3, 138.1, 132.2, 128.4 (C x 2), 126.7 (C x 2), 61.9, 33.8, 25.1, 23.8 (C x 2), 21.8, 14.0.

HPLC: RP-HPLC Alltima™ C18 5 µm 150 mm x 4.6 mm, 10-100% B in 15 min, R_t = 7.55 min, 94%.

Mass Spectral Analysis: LRMS (ESI+) m/z 330, 330 $[M]^+$ (100%). HRMS (ES+) for $C_{18}H_{22}N_2O_2S$, calculated 331.1475, found 331.1470.

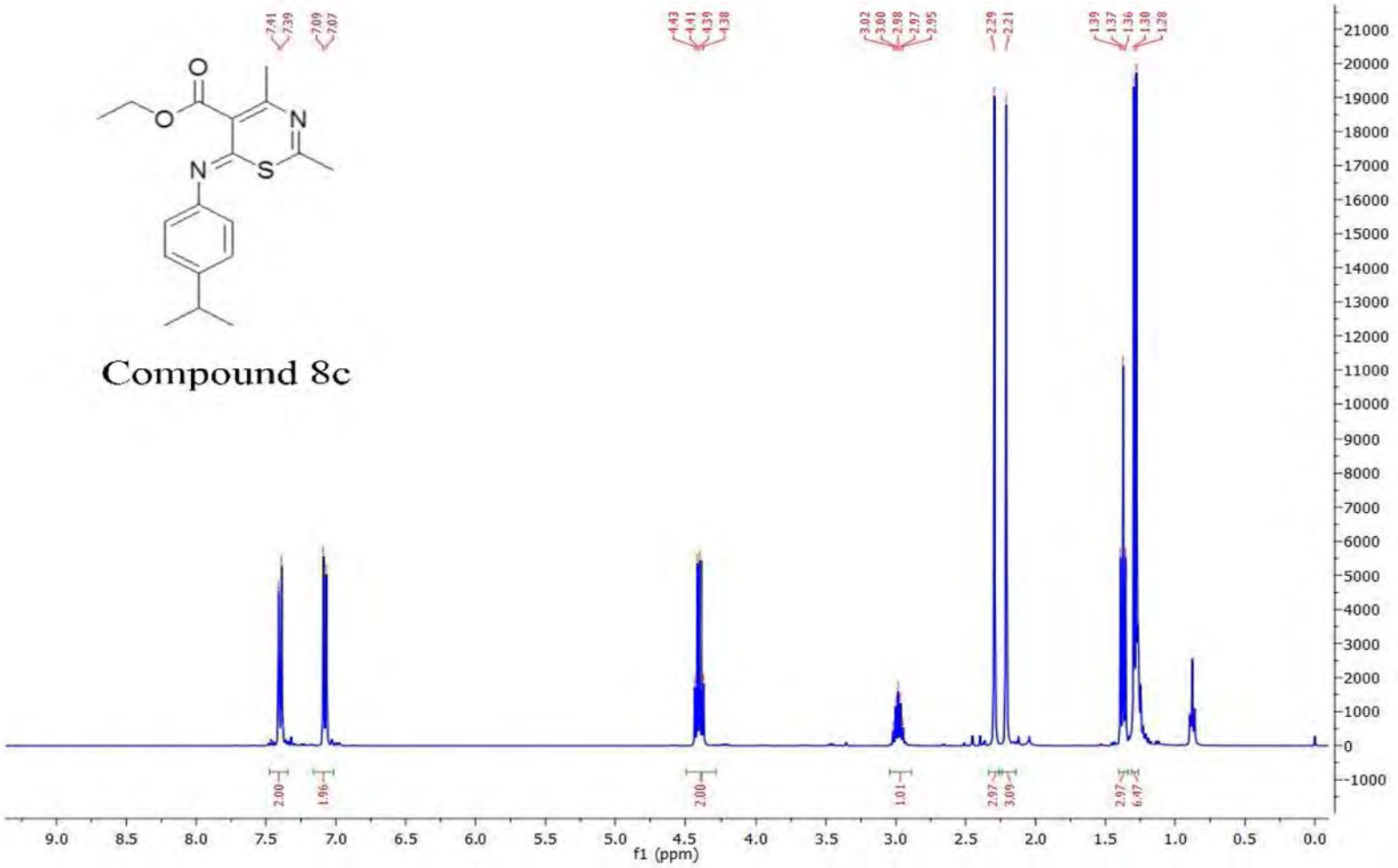
7.41
7.39
7.09
7.07
4.43
4.41
4.39
4.38
3.02
3.00
2.98
2.97
2.95
2.29
2.21
1.39
1.37
1.36
1.30
1.28
O
O
N
N
S
2.00
1.96
2.00
1.01
2.97
3.09
2.97
6.47
f1 (ppm)

Compound 8c

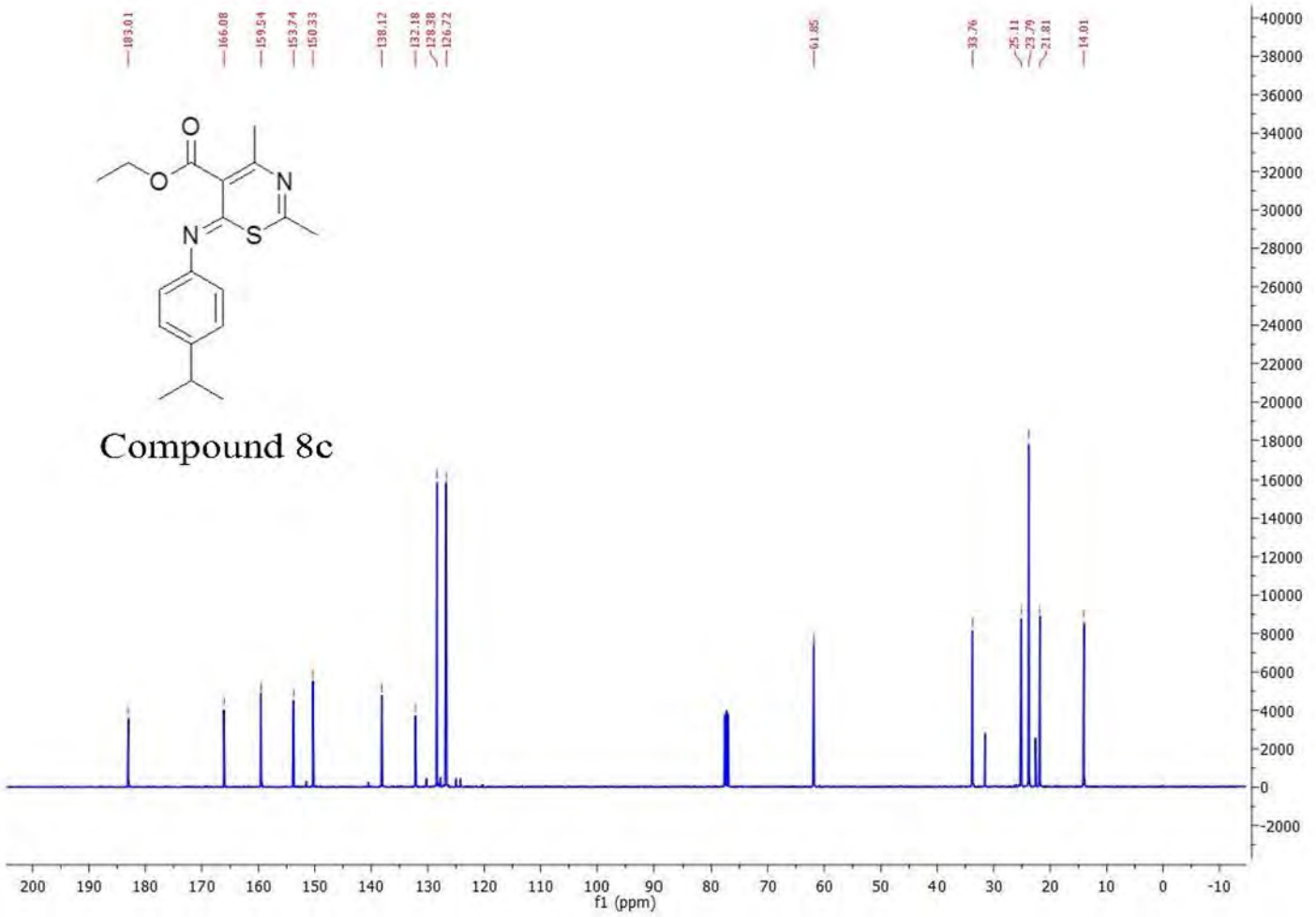
183.01
166.08
159.54
153.74
150.33
138.12
132.18
128.38
126.72
61.85
33.76
25.11
23.79
21.81
14.01
O
O
N
N
S
Compound 8c
f1 (ppm)

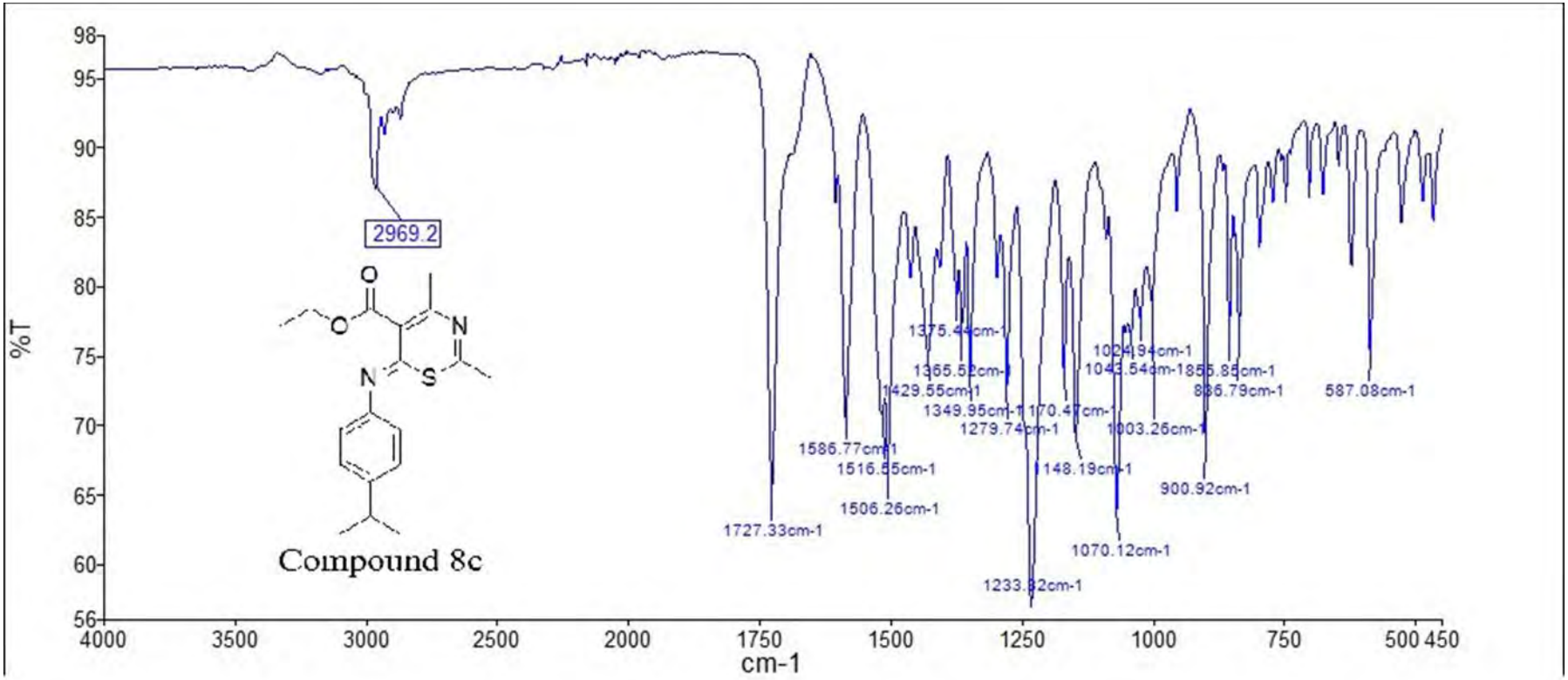
%T
cm-1
2969.2
1727.33cm-1
1586.77cm-1
1516.55cm-1
1506.26cm-1
1429.55cm-1
1375.44cm-1
1365.52cm-1
1349.95cm-1
1279.74cm-1
1233.32cm-1
1170.47cm-1
1148.19cm-1
1070.12cm-1
1043.54cm-1
1024.94cm-1
1003.26cm-1
900.92cm-1
886.79cm-1
855.85cm-1
587.08cm-1
Compound 8c

==== Shimadzu LCMSsolution Analysis Report ====

Acquired by	: Admin
Sample Name	: TP133B5 Re
Sample ID	:
Vail #	: 61
Injection Volume	: 20 uL
Data File Name	: TP133B5 Re.lcd
Method File Name	: Platinum C18 EPS 3u lot 561094 part 50573 53mm id 7mm.lcm
Batch File Name	: Batch Second pro.lcb
Report File Name	: DefaultLCMS.lcr
Data Acquired	: 8/11/2015 8:34:42 PM
Data Processed	: 8/12/2015 1:44:43 PM

<Chromatogram>

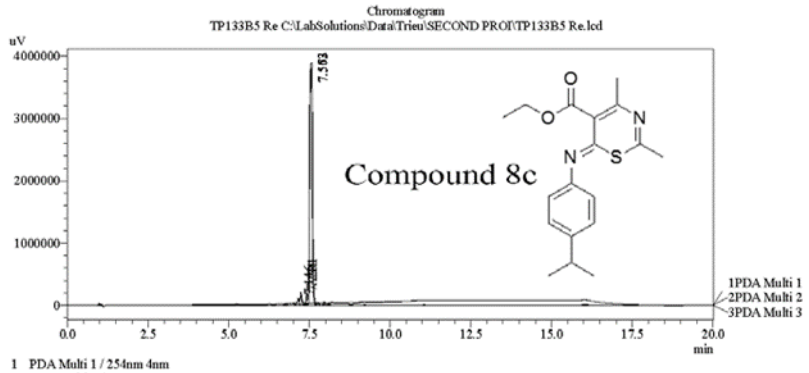

1 PDA Multi 1 / 254nm 4nm
2 PDA Multi 2 / 328nm 4nm
3 PDA Multi 3 / 220nm 4nm

PeakTable

PDA Ch1 254nm 4nm

Peak#	Ret. Time	Area	Height	Area %	Height %
1	7.146	443420	105687	2.204	2.597
2	7.231	600764	153863	2.987	3.781
3	7.552	19071287	3809833	94.809	93.622
Total		20115470	4069383	100.000	100.000

PeakTable

PDA Ch2 328nm 4nm

Peak#	Ret. Time	Area	Height	Area %	Height %
1	7.563	20011674	3591760	100.000	100.000
Total		20011674	3591760	100.000	100.000

PeakTable

PDA Ch3 220nm 4nm

Peak#	Ret. Time	Area	Height	Area %	Height %
1	7.231	1078094	182721	4.167	4.511
2	7.573	24793641	3867823	95.833	95.489
Total		25871735	4050544	100.000	100.000

==== Shimadzu LCMSsolution Data Report ====

<Chromatogram>

Sample Information

Acquired by	: Admin
Date Acquired	: 8/12/2015 12:28:58 PM
Sample Type	: Unknown
Level#	: 0
Sample Name	: TP133B5 Re ESI +
Sample ID	:
ISTD Amount	: (Level1 Conc.)
Sample Amount	: 1
Dilution Factor	: 1
Tray#	: 1
Vial#	: 61
Injection Volume	: 3
Data File	: TP133B5 Re ESI +.lcd
Method File	: FIA-ESI_Scan(+).lcm
Original Method	: C:\LabSolutions\Data\Trieu\Mass spec files\FIA-ESI_Scan(+).lcm
Report Format	: DefaultLCMS.lcr
Tuning File	: C:\LabSolutions\LCsolution\Log\Tuning\Autotune_030908.lct
Processed by	: Admin
Modified Date	: 8/12/2015 12:30:58 PM

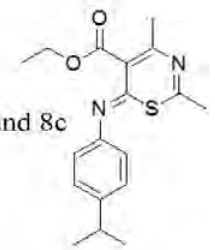

Compound 8c

Chromatogram

TP133B5 Re ESI + C:\LabSolutions\Data\Trieu\SECOND PROI\Mass\TP133B5 Re ESI +.lcd

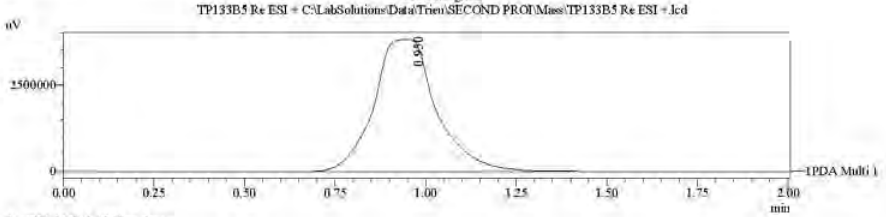

1 PDA Multi 1 / 254nm 4nm

<Spectrum>

Retention Time:1.260(Scan#:127)
Max Peak:420 Base Peak:330.40(1562688)
Spectrum:Averaged 0.940-1.760(95-177)
Background:Averaged 0.140-0.673(15-69) Polarity:Pos Segment1 - Event1

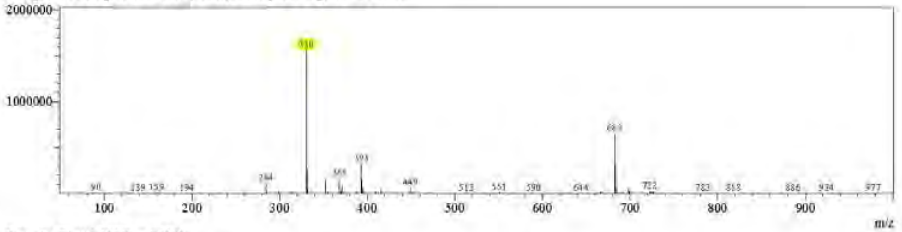

Retention Time:1.230(Scan#:124)
Max Peak:624 Base Peak:520.25(119015)
Spectrum:Averaged 0.950-1.770(96-178)
Background:Averaged 0.150-0.673(16-70) Polarity:Neg Segment1 - Event2

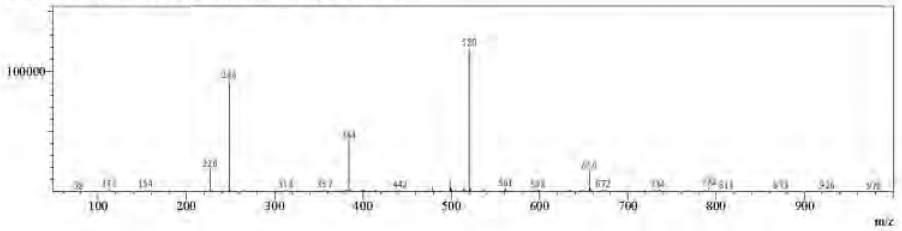

C:¥LabSolutions¥Data¥Trieu¥SECOND PROI¥Mass¥TP133B5 Re ESI +.lcd

Compound	Chemical Formula	Predicted monoisotopic neutral MW	Predicted MH+	MH+ Measured	Main MS Ions	Main MS/MS Fragments
8c	$C_{18}H_{22}N_2O_2S$	330.1402	331.14748	331.14700		285.1056
					331.1470	303.1163
						172.0428

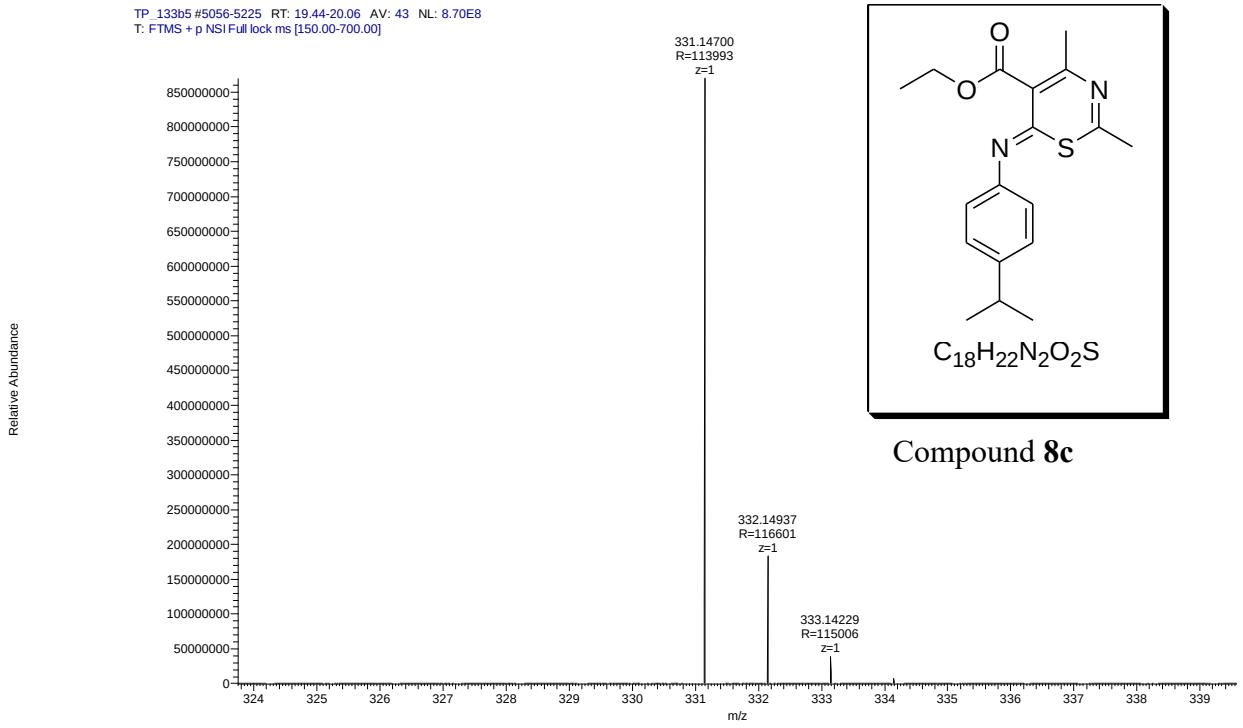

Compound **8c**

Compound 8d

Compound Name: 4-Methyl-2-phenyl-6-phenylimino-6*H*-[1,3]thiazine-5-carboxylic acid ethyl ester

Obtained Weight & Yield: 300 mg, 66%

Appearance: Yellow precipitate

Solubility: MeOH, ACN, Acetone

Melting Point: 178-179 °C

TLC Conditions: EtOAc/n-Hexane (50/50)

IR Analysis: 2994 (CH), 1729 (COO), 1239 (CO)

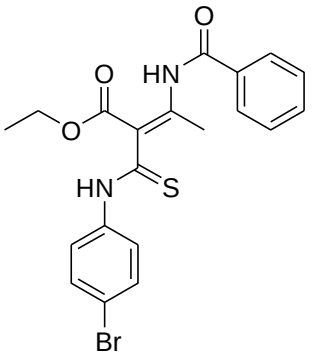

$C_{20}H_{19}BrN_2O_3S$
Exact Mass: 446.0300

^{1}H NMR Analysis:

^{1}H NMR (400 MHz, Acetone) δ 7.85 – 7.71 (m, 2H), 7.45 – 7.35 (m, 2H), 4.31 (q, *J* = 7.1 Hz, 2H), 2.26 (s, 3H), 2.21 (s, 3H), 1.32 (t, *J* = 7.1 Hz, 3H).

^{13}C NMR Analysis:

^{13}C NMR (400 MHz, Acetone) δ 182.7, 165.5, 159.5, 153.7, 140.4, 133.3(Cx2), 131.9, 129.9 (Cx2), 122.8, 61.2, 24.6, 21.1, 13.4.

HPLC RP-HPLC Alltima™ C18 5 μm 150 mm x 4.6 mm, 10–100% B in 15 min, R_t = 7.14 min, 100%.

Mass Spectral Analysis: LRMS (ESI+) m/z 366, 368 [M+ 2H; ^{79}Br, ^{81}Br]$^{+}$ (100%). HRMS (ES+) for $C_{15}H_{15}BrO_2S$ calculated 367.0110, found 367.0110 [M+ H; ^{79}Br, ^{81}Br]$^{+}$.

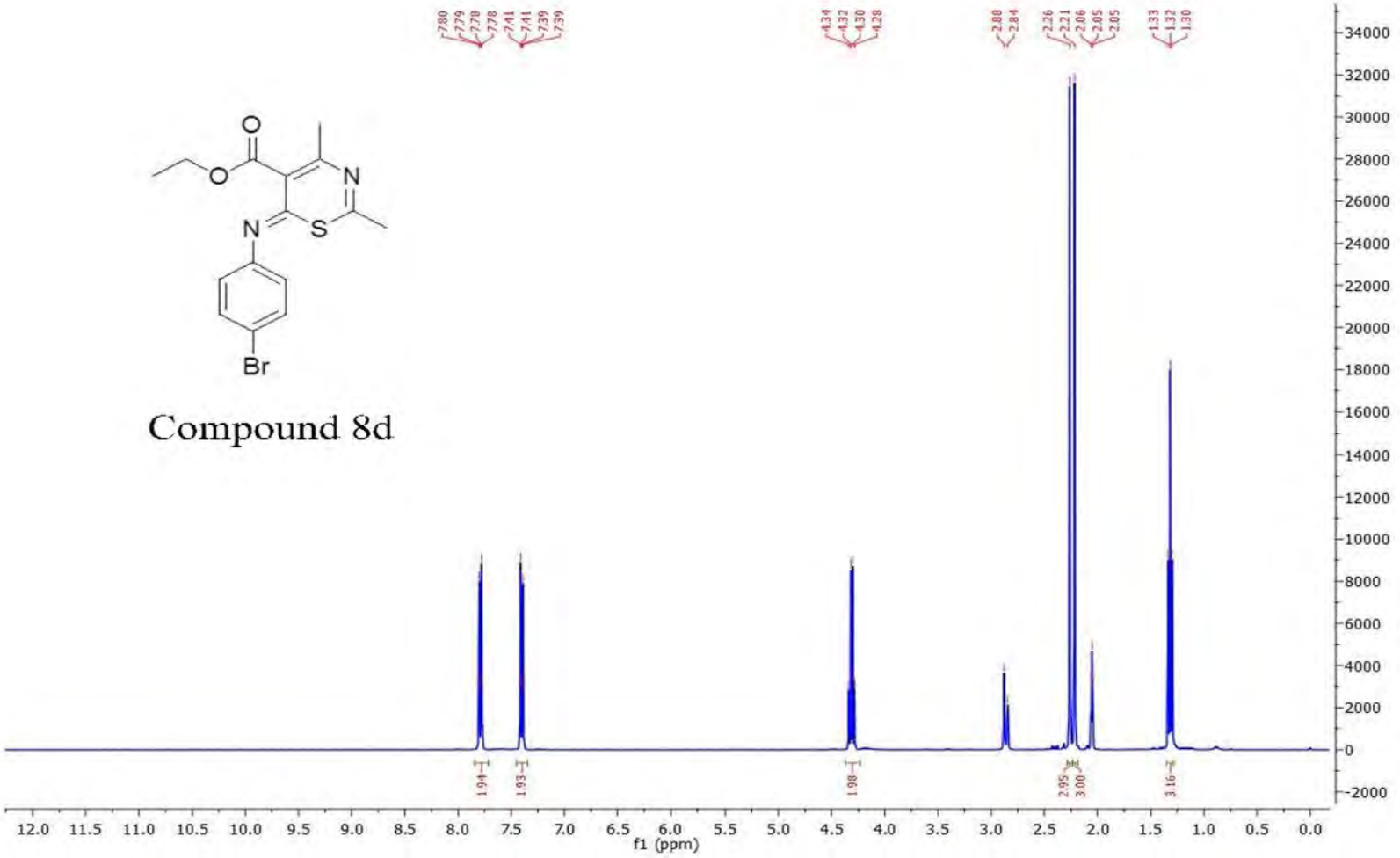
O
O
N
N
S
Br
7.80
7.79
7.78
7.78
7.41
7.41
7.39
7.39
4.34
4.32
4.30
4.28
2.88
2.84
2.26
2.21
2.06
2.05
2.05
1.33
1.32
1.30
1.94
1.93
1.98
2.95
3.00
3.16
f1 (ppm)

Compound 8d

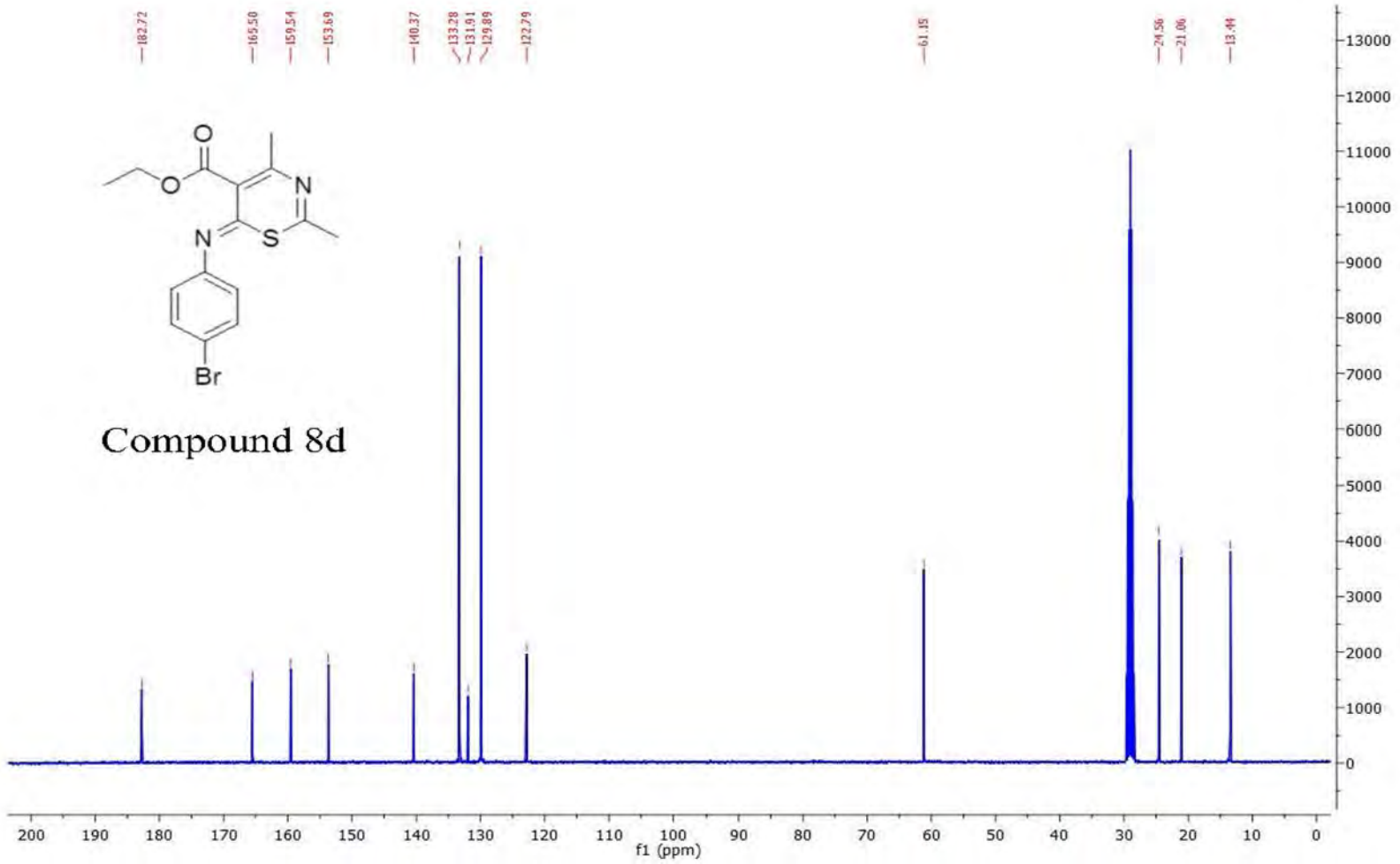
182.72
165.50
159.54
153.69
140.37
133.28
131.91
129.89
122.79
61.15
24.56
21.06
13.44
O
O
N
N
S
Br
Compound 8d
13000
12000
11000
10000
9000
8000
7000
6000
5000
4000
3000
2000
1000
0
200
190
180
170
160
150
140
130
120
110
100
90
80
70
60
50
40
30
20
10
0
f1 (ppm)

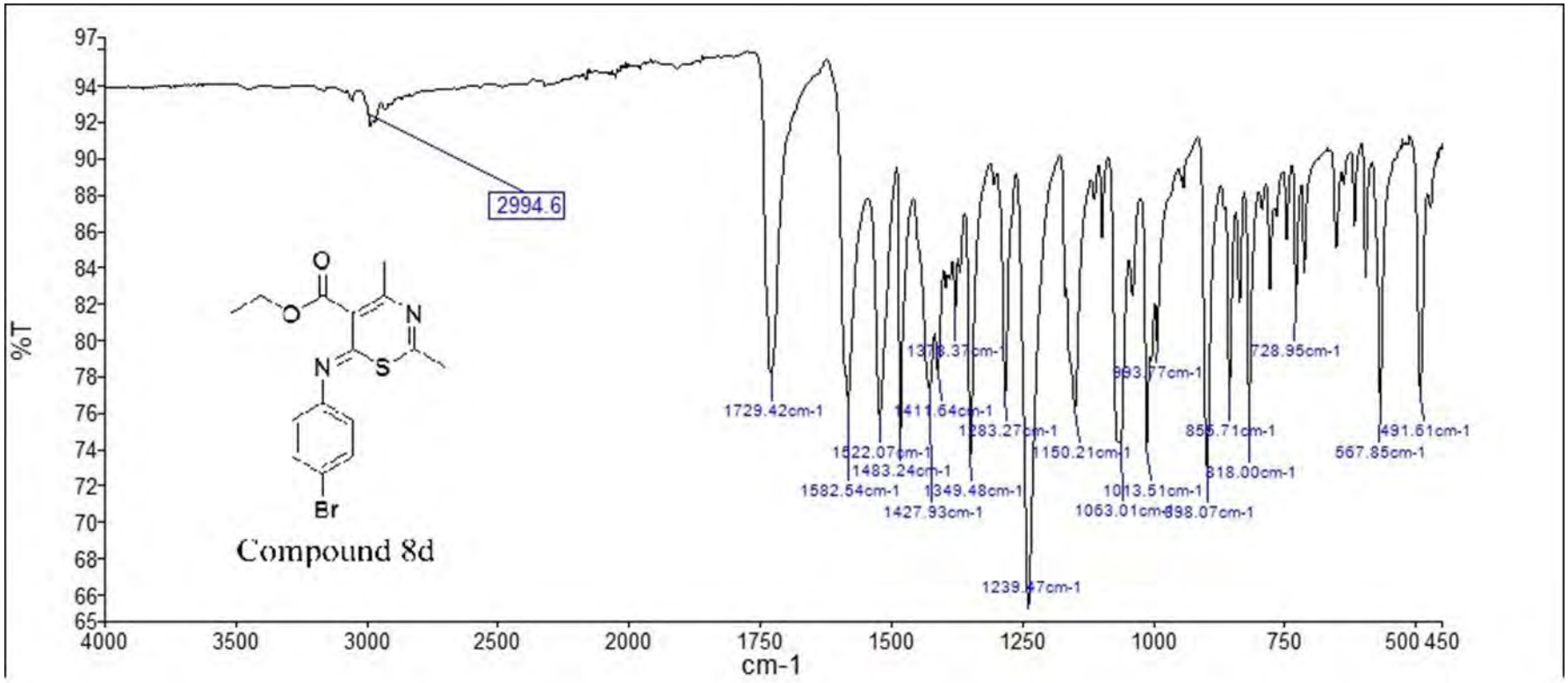
%T
cm-1
2994.6
1729.42cm-1
1582.54cm-1
1522.07cm-1
1483.24cm-1
1427.93cm-1
1411.64cm-1
1349.48cm-1
1283.27cm-1
1239.47cm-1
1150.21cm-1
1063.01cm-1
1013.51cm-1
993.77cm-1
898.07cm-1
855.71cm-1
818.00cm-1
728.95cm-1
567.85cm-1
491.61cm-1
Br
Compound 8d

==== Shimadzu LCMSsolution Analysis Report ====

Acquired by	: Admin
Sample Name	: TP54B5 Re
Sample ID	:
Vail #	: 60
Injection Volume	: 20 uL
Data File Name	: TP54B5 Re.lcd
Method File Name	: Platinum C18 EPS 3u lot 561094 part 50573 53mm id 7mm.lcm
Batch File Name	: Batch Second pro.lcb
Report File Name	: DefaultLCMS.lcr
Data Acquired	: 8/11/2015 8:14:14 PM
Data Processed	: 8/12/2015 1:49:21 PM

<Chromatogram>

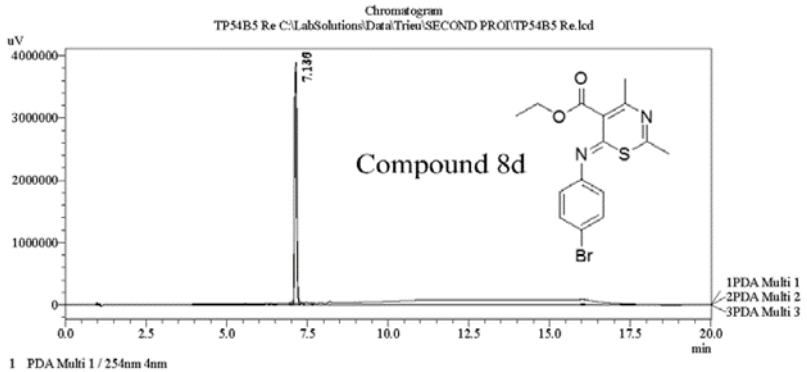

1 PDA Multi 1 / 254nm 4nm
2 PDA Multi 2 / 328nm 4nm
3 PDA Multi 3 / 220nm 4nm

PeakTable

PDA Ch1 254nm 4nm

Peak#	Ret. Time	Area	Height	Area %	Height %
1	7.130	14303819	3742268	100.000	100.000
Total		14303819	3742268	100.000	100.000

PeakTable

PDA Ch2 328nm 4nm

Peak#	Ret. Time	Area	Height	Area %	Height %
1	7.136	14473430	3568720	100.000	100.000
Total		14473430	3568720	100.000	100.000

PeakTable

PDA Ch3 220nm 4nm

Peak#	Ret. Time	Area	Height	Area %	Height %
1	7.147	21168731	3874538	100.000	100.000
Total		21168731	3874538	100.000	100.000

==== Shimadzu LCMSsolution Data Report ====

<Chromatogram>

Sample Information

Acquired by	: Admin
Date Acquired	: 8/12/2015 12:25:59 PM
Sample Type	: Unknown
Level#	: 0
Sample Name	: TP54B5 Re ESI +
Sample ID	:
ISTD Amount	: (Level1 Conc.)
Sample Amount	: 1
Dilution Factor	: 1
Tray#	: 1
Vial#	: 60
Injection Volume	: 3
Data File	: TP54B5 Re ESI +.lcd
Method File	: FIA-ESI_Scan(+).lcm
Original Method	: C:\LabSolutions\Data\Trieu\Mass spec files\FIA-ESI_Scan(+).lcm
Report Format	: DefaultLCMS.lcr
Tuning File	: C:\LabSolutions\LCsolution\Log\Tuning\Autotune_030908.lct
Processed by	: Admin
Modified Date	: 8/12/2015 12:28:03 PM

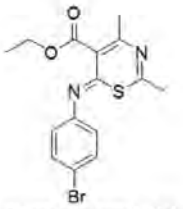

Compound 8d

Chromatogram

TP54B5 Re ESI + C:\LabSolutions\Data\Trieu\SECOND PROI\Mass\TP54B5 Re ESI +.lcd

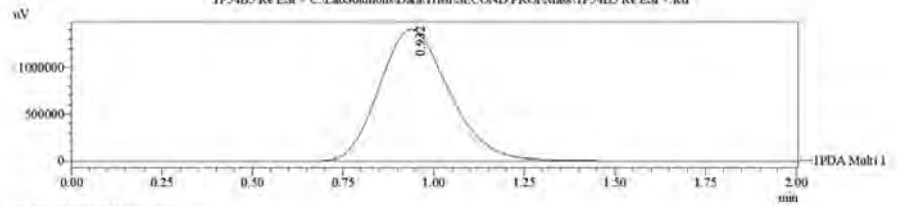

1 PDA Multi 1 / 254nm 4nm

<Spectrum>

Retention Time:1.280(Scan#:129)
Mnc Peak:599 Base Peak:368.35(1023640)
Spectrum:Averaged 1.000-1.640(101-165)
Background:Averaged 0.160-0.609(17-61) Polarity:Pos Segment1 - Event1

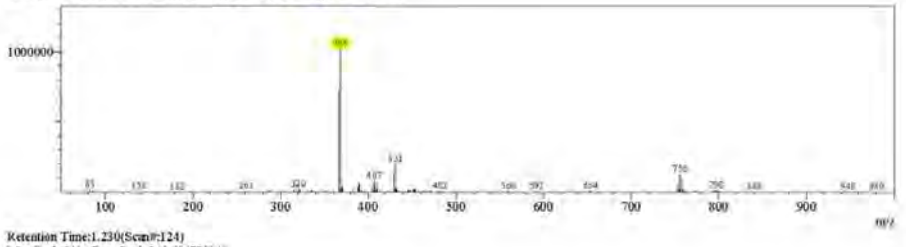

Retention Time:1.230(Scan#:124)
Mnc Peak:641 Base Peak:248.50(73834)
Spectrum:Averaged 1.010-1.650(102-166)
Background:Averaged 0.170-0.609(18-62) Polarity:Neg Segment1 - Event2

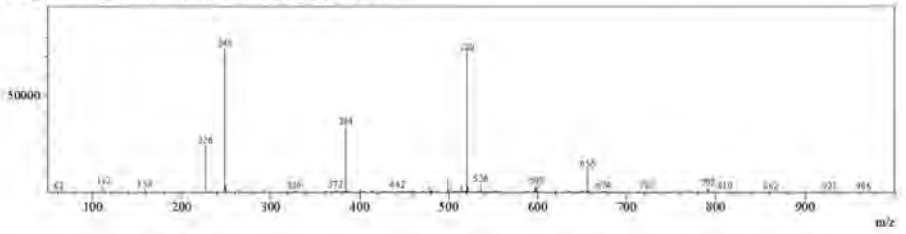

C:¥LabSolutions¥Data¥Trieu¥SECOND PROI¥Mass¥TP54B5 Re ESI +.lcd

Compound	Chemical Formula	Predicted monoisotopic neutral MW	Predicted MH+	MH+ Measured	Main MS Ions	Main MS/MS Fragments
8d	$C_{15}H_{15}BrN_2O_2S$	366.0038	367.0110	367.0110		320.9694
					367.0110	195.9759
						172.0429

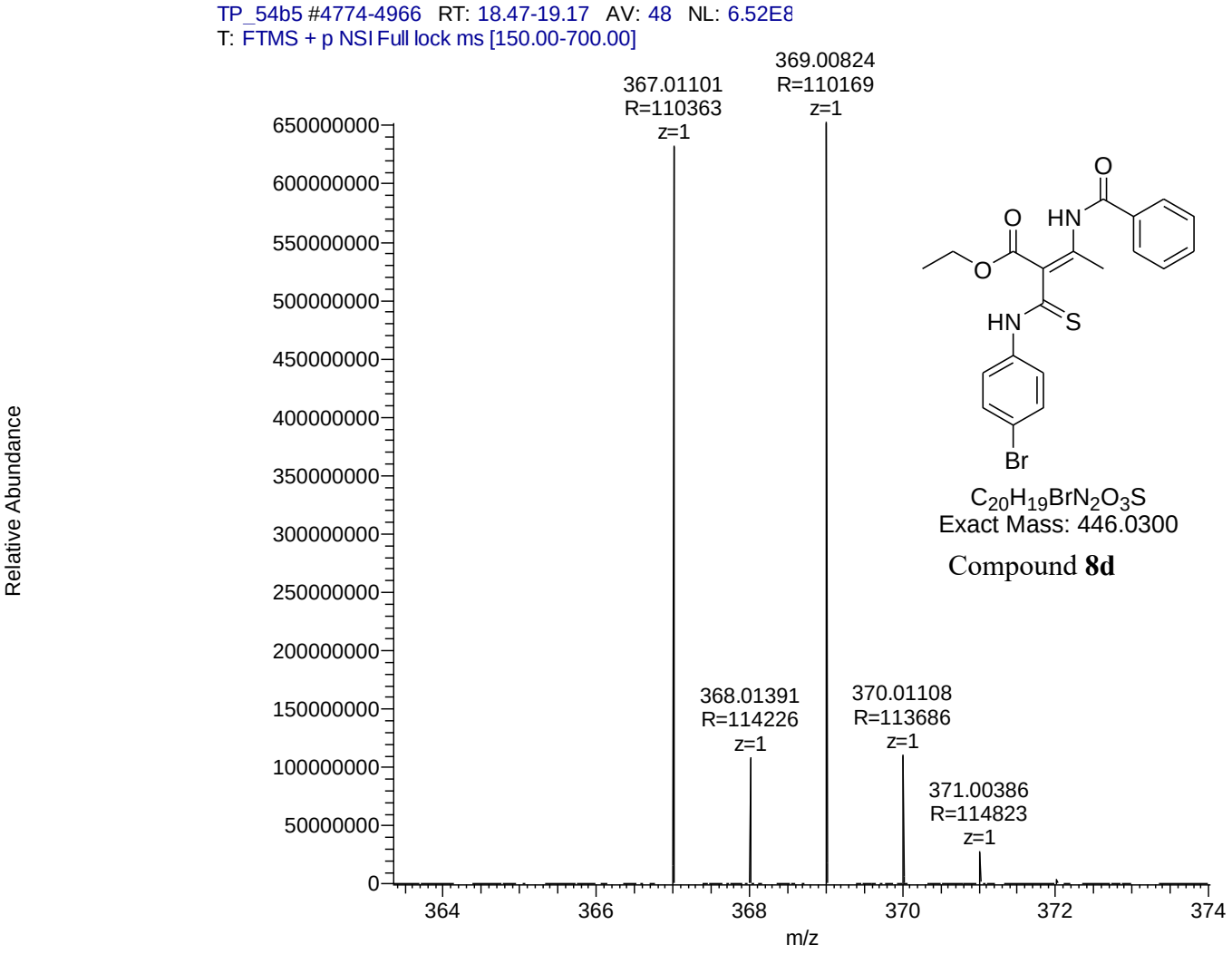

Compound **8e**

Compound Name: 2,4-Dimethyl-6-(4-trifluoromethyl-phenylimino)-6*H*-[1,3]thiazine-5-carboxylic acid ethyl ester

Obtained Weight & Yield: 300 mg, 35%

Appearance: Yellow precipitate

Solubility: MeOH, ACN, Acetone

Melting Point: 125.7-126.5

TLC Conditions: EtOAc/n-Hexane (50/50)

IR Analysis:
2982 (CH), 1728 (COO), 1235 (CO)

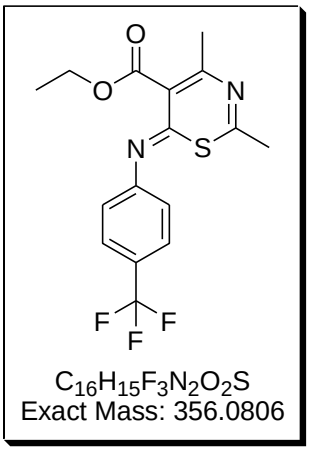

$C_{16}H_{15}F_3N_2O_2S$
Exact Mass: 356.0806

^{1}H NMR Analysis:
^{1}H NMR (400 MHz, CDCl3) δ 7.84 (d, *J* = 8.4 Hz, 2H), 7.35 (d, J = 8.3 Hz, 2H), 4.41 (q, *J* = 7.1 Hz, 2H), 2.32 (s, 3H), 2.21 (s, 3H), 1.38 (t, *J* = 7.1 Hz, 3H).

^{13}C NMR Analysis:
^{13}C NMR (101 MHz, $CDCl_3$) δ 182.8, 165.9, 158.5, 154.3, 143.5, 143.5, 132.3, 131.8 (q, *J* = 33.3Hz, 1H), 128.1 (C x 2), 127.7 (C x 2) (q, *J* = 4.1 Hz, 2H), 123.4 (q, *J* = 273 Hz, 1H), 62.1, 25.08, 21.9, 14.0.
* *CF3 splitting*

HPLC
RP-HPLC Alltima™ C18 5 µm 150 mm x4.6 mm, 10–100% B in 15 min, R_t = 7.22 min, 95%.

Mass Spectral Analysis: LRMS (ESI+) m/z : 356, 356 $[M+H]^+$ 100%. HRMS (ES+) for $C_{16}H_{15}F_3N_2O_2S$ calculated 357.0879, found 357.0886.

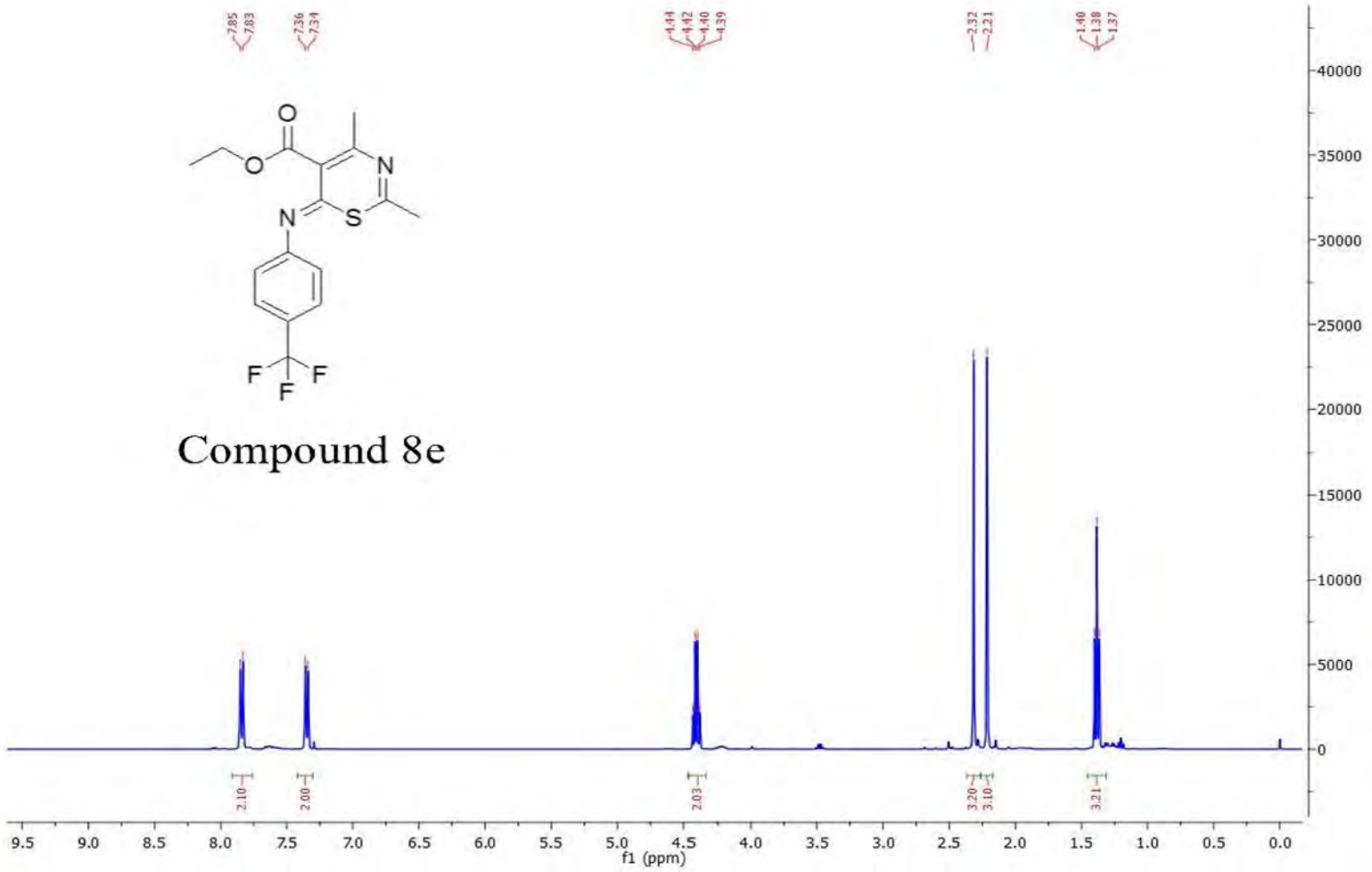
7.85
7.83
7.36
7.34
4.44
4.42
4.40
4.39
2.32
2.21
1.40
1.38
1.37
O
O
N
N
S
F
F
F
40000
35000
30000
25000
20000
15000
10000
5000
0
2.10
2.00
2.03
3.20
3.10
3.21
9.5
9.0
8.5
8.0
7.5
7.0
6.5
6.0
5.5
5.0
4.5
4.0
3.5
3.0
2.5
2.0
1.5
1.0
0.5
0.0
f1 (ppm)

Compound 8e

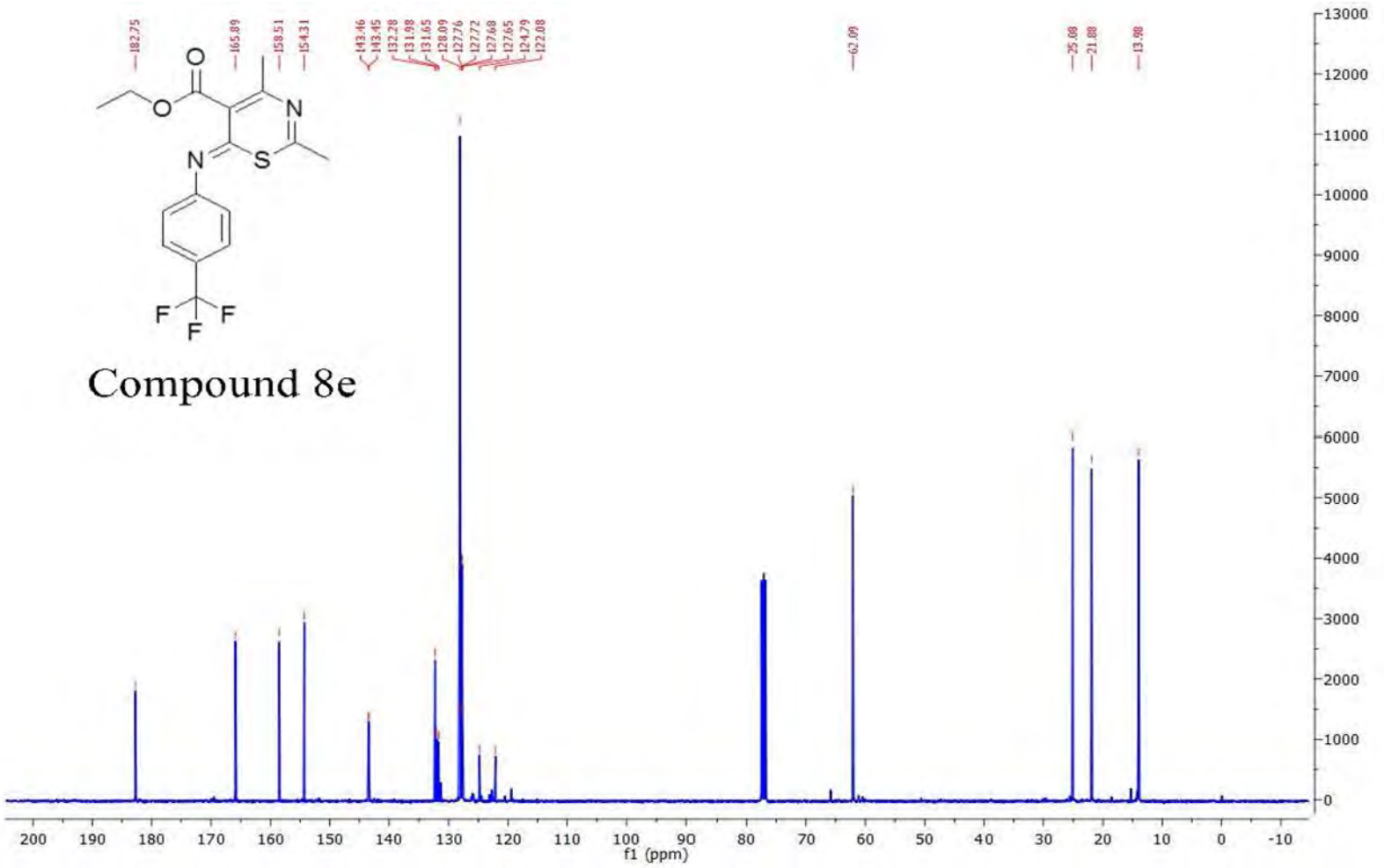
182.75
165.89
158.51
154.31
143.46
143.45
132.28
131.98
131.65
128.09
127.76
127.72
127.60
127.65
124.79
122.08
62.09
25.08
21.88
13.98
O
O
N
N
S
F
F
F
Compound 8e
13000
12000
11000
10000
9000
8000
7000
6000
5000
4000
3000
2000
1000
0
200
190
180
170
160
150
140
130
120
110
100
90
80
70
60
50
40
30
20
10
0
-10
f1 (ppm)

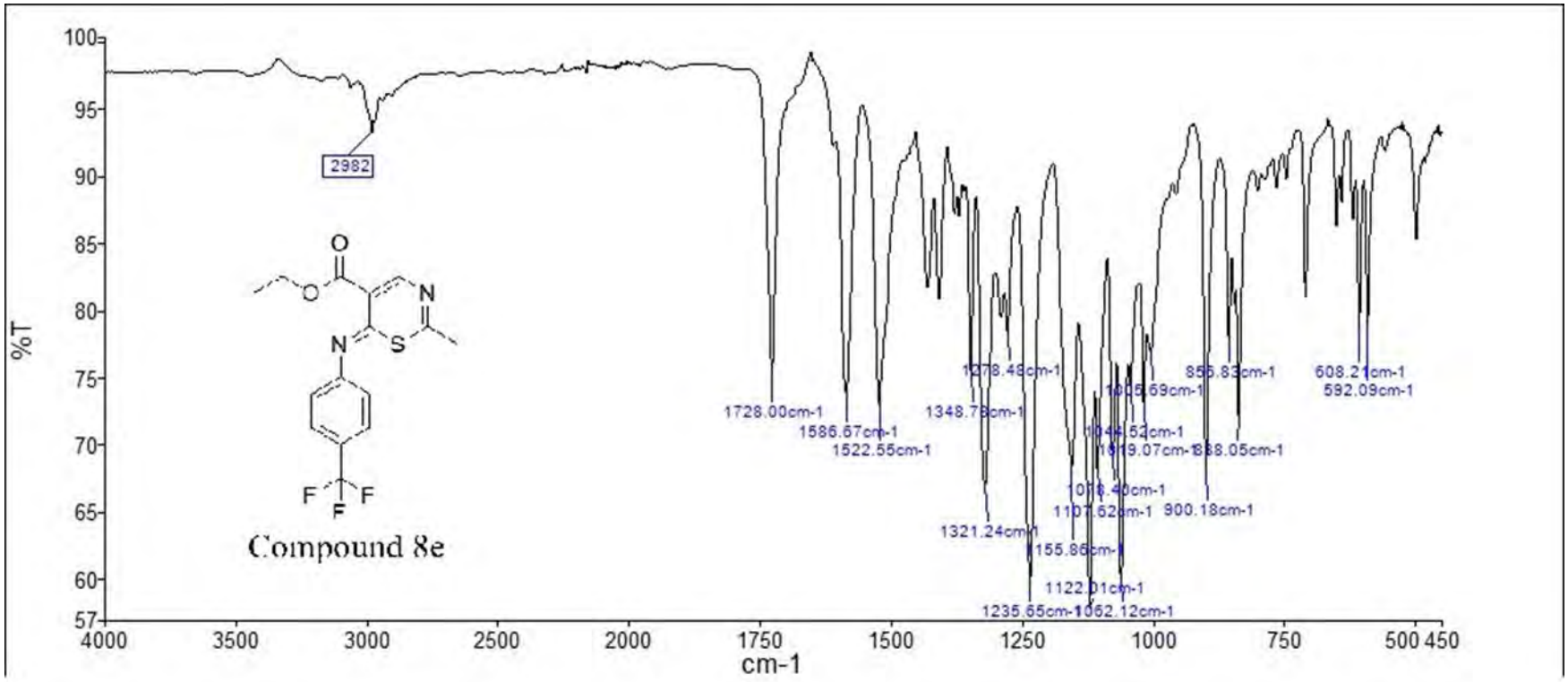
%T
cm-1
2982
1728.00cm-1
1586.67cm-1
1522.55cm-1
1348.78cm-1
1321.24cm-1
1235.65cm-1
1122.01cm-1
1062.12cm-1
900.18cm-1
856.83cm-1
608.21cm-1
592.09cm-1
Compound 8e

==== Shimadzu LCMSsolution Analysis Report ====

Acquired by	: Admin
Sample Name	: TP130B5 Re
Sample ID	:
Vail #	: 57
Injection Volume	: 20 uL
Data File Name	: TP130B5 Re.lcd
Method File Name	: Platinum C18 EPS 3u lot 561094 part 50573 53mm id 7mm.lcm
Batch File Name	: Batch Second pro.lcb
Report File Name	: DefaultLCMS.lcr
Data Acquired	: 8/11/2015 7:12:51 PM
Data Processed	: 8/12/2015 2:34:16 PM

<Chromatogram>

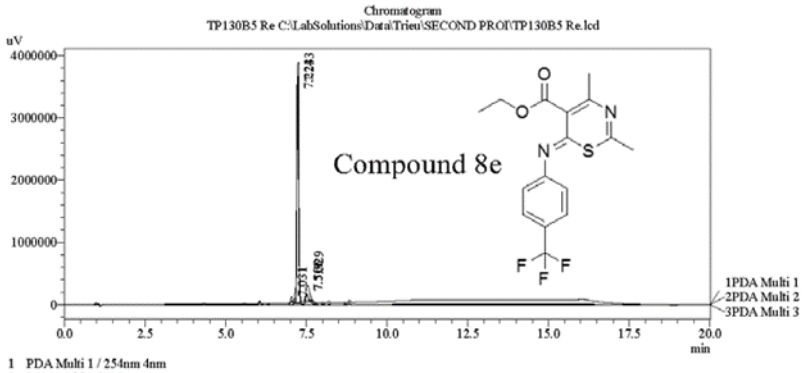

1 PDA Multi 1 / 254nm 4nm
2 PDA Multi 2 / 328nm 4nm
3 PDA Multi 3 / 220nm 4nm

PeakTable

PDA Ch1 254nm 4nm

Peak#	Ret. Time	Area	Height	Area %	Height %
1	7.224	11644696	3647701	97.155	96.855
2	7.511	340935	118433	2.845	3.145
Total		11985630	3766135	100.000	100.000

PeakTable

PDA Ch2 328nm 4nm

Peak#	Ret. Time	Area	Height	Area %	Height %
1	7.233	15463993	3575921	95.773	95.294
2	7.506	682536	176595	4.227	4.706
Total		17146529	3752515	100.000	100.000

PeakTable

PDA Ch3 220nm 4nm

Peak#	Ret. Time	Area	Height	Area %	Height %
1	7.031	64535	12877	0.318	0.310
2	7.243	19286914	3850569	95.034	95.757
3	7.529	943197	157754	4.648	3.923
Total		20294646	4131200	100.000	100.000

==== Shimadzu LCMSsolution Data Report ====

<Chromatogram>

Compound 8e

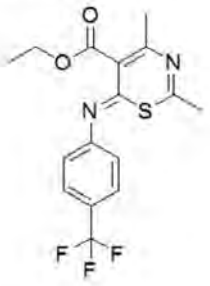

Sample Information

Acquired by	: Admin
Date Acquired	: 8/12/2015 12:17:02 PM
Sample Type	: Unknown
Level#	: 0
Sample Name	: TP130B5 Re ESI +
Sample ID	:
ISTD Amount	: (Level1 Conc.)
Sample Amount	: 1
Dilution Factor	: 1
Tray#	: 1
Vial#	: 57
Injection Volume	: 3
Data File	: TP130B5 Re ESI +.lcd
Method File	: FIA-ESI_Scan(+).lcm
Original Method	: C:\LabSolutions\Data\Trieu\Mass spec files\FIA-ESI_Scan(+).lcm
Report Format	: Default.LCMS.lcr
Tuning File	: C:\LabSolutions\LCsolution\Log\Tuning\Autotune_030908.lct
Processed by	: Admin
Modified Date	: 8/12/2015 12:19:03 PM

Chromatogram

TP130B5 Re ESI + C:\LabSolutions\Data\Trieu\SECOND PROJ\Mass\TP130B5 Re ESI +.lcd

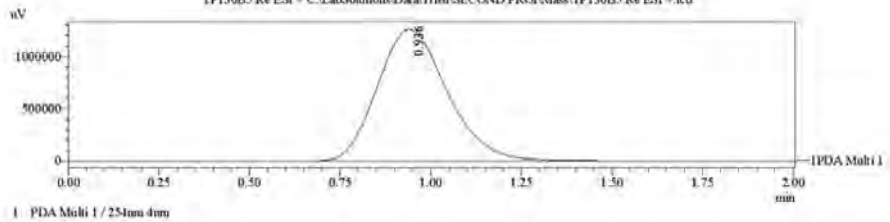

1 PDA Multi 1 / 254nm 4nm

<Spectrum>

Retention Time:1.220(Scan#:123)
Max Peak:573 Base Peak:356.50(1692999)
Spectrum:Averaged 1.000-1.780(101-179)
Background:Averaged 0.120-0.476(13-49) Polarity:Pos Segment1 - Event1

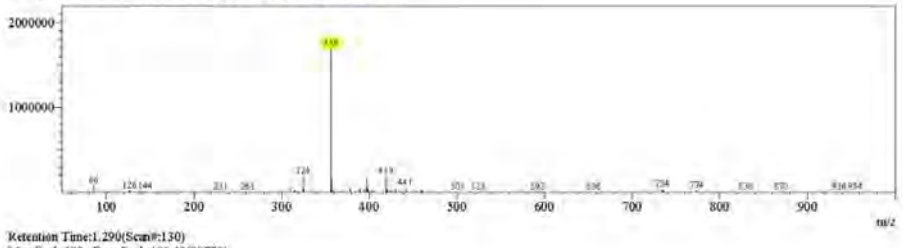

Retention Time:1.290(Scan#:130)
Max Peak:639 Base Peak:486.40(88770)
Spectrum:Averaged 1.010-1.790(102-180)
Background:Averaged 0.130-0.476(14-50) Polarity:Neg Segment1 - Event2

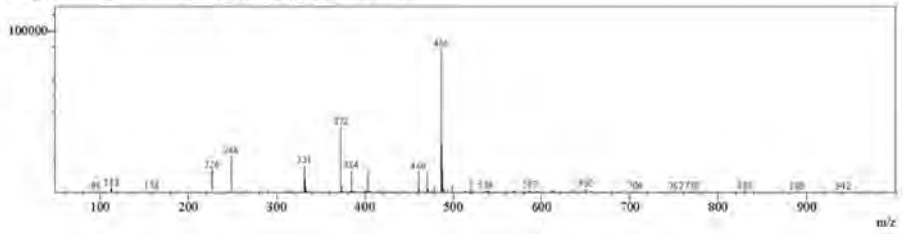

C:¥LabSolutions¥Data¥Trieu¥SECOND PROJ¥Mass¥TP130B5 Re ESI +.lcd

Compound	Chemical Formula	Predicted monoisotopic neutral MW	Predicted MH+	MH+ Measured	Main MS Ions	Main MS/MS Fragments
8e	$C_{16}H_{15}F_3N_2O_2S$	356.0806	357.08791	357.08857		311.0470
					357.0886	329.0576
						172.0433

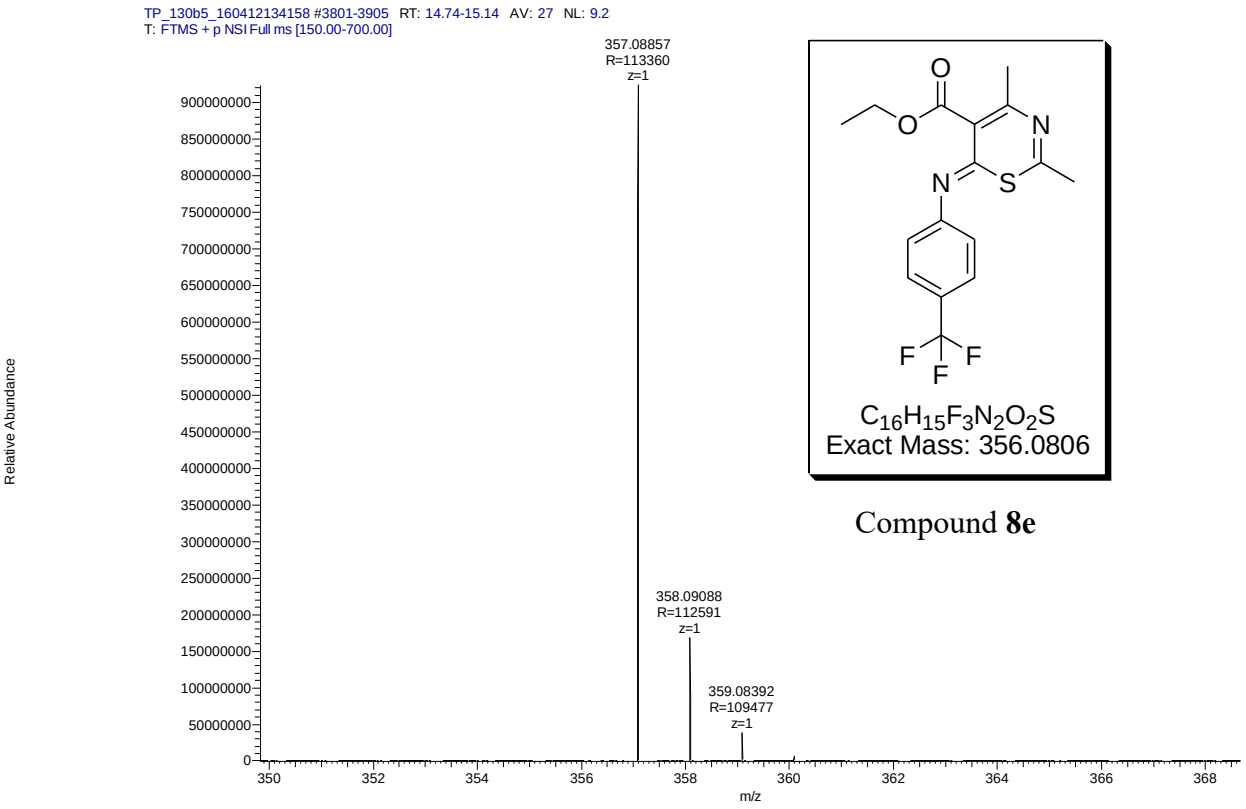

Compound **8e**

Compound 8f

Compound Name: 6-(3,5-Dichloro-phenylimino)-2,4-dimethyl-6*H*-[1,3]thiazine-5-carboxylic acid ethyl ester

Obtained Weight & Yield: 123 mg, 20%

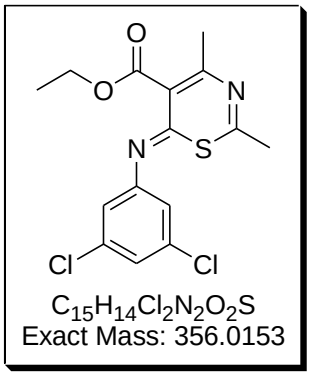

$C_{15}H_{14}Cl_2N_2O_2S$
Exact Mass: 356.0153

Appearance: Yellow precipitate

Solubility: MeOH, ACN, Acetone

Melting Point: 184.3-185.1 °C

TLC Conditions: EtOAc/n-Hexane (50/50)

IR Analysis:
3070 (CH), 2982 (CH), 1720 (COO), 1243 (CO)

^{1}H NMR Analysis:

^{1}H NMR (400 MHz, $CDCl_3$) δ 7.51 (t, *J* = 1.8 Hz, 1H), 7.14 (d, *J* = 1.8 Hz, 2H), 4.41 (q, *J* = 7.1 Hz, 2H), 2.29 (d, *J* = 7.4 Hz, 6H), 1.38 (t, *J* = 7.1 Hz, 3H).

13C NMR Analysis:

13C NMR (101 MHz, CDCl3) δ 182.7, 165.7, 158.3, 154.2, 141.9, 136.8 (Cx2), 132.3, 130.2, 126.3 (Cx2), 62.1, 25.1, 21.9, 14.0.

HPLC: RP-HPLC Alltima™ C18 5 μm 150 mm x 4.6 mm, 10–100% B in 15 min, R_t = 7.53 min, 96%.

Mass Spectral Analysis: LRMS (ESI+) m/z 356, 356 [M, $^{35}Cl]^+$ (100%). HRMS (ES+) for $C_{15}H_{14}Cl_2N_2O_2S$, calculated 357.0226, found 357.0226.

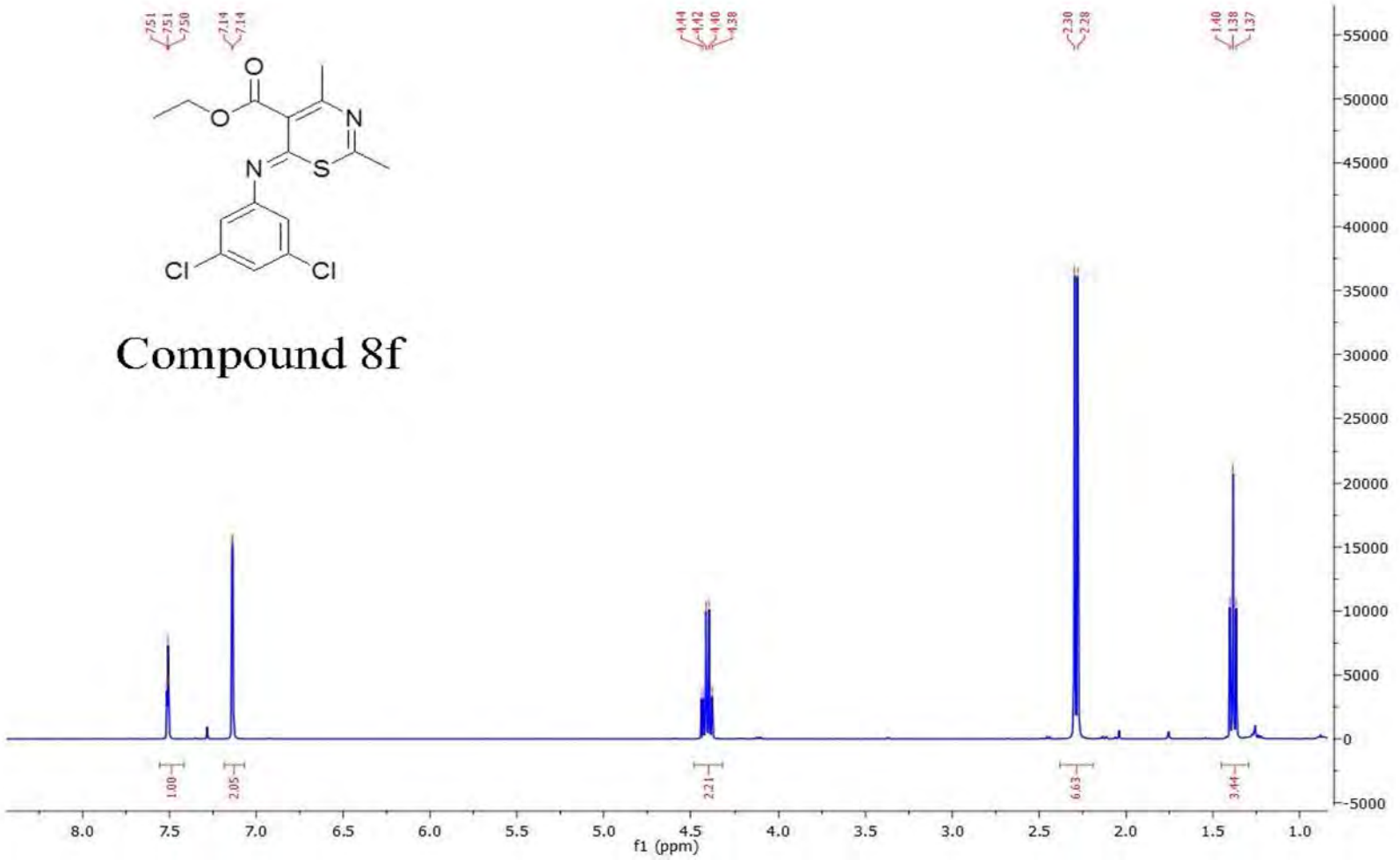
7.51
7.51
7.50
7.14
7.14
4.44
4.42
4.40
4.38
2.30
2.28
1.40
1.38
1.37
O
O
N
N
S
Cl
Cl
Compound 8f
55000
50000
45000
40000
35000
30000
25000
20000
15000
10000
5000
0
-5000
1.00
2.05
2.21
6.63
3.44
8.0
7.5
7.0
6.5
6.0
5.5
5.0
4.5
4.0
3.5
3.0
2.5
2.0
1.5
1.0
f1 (ppm)

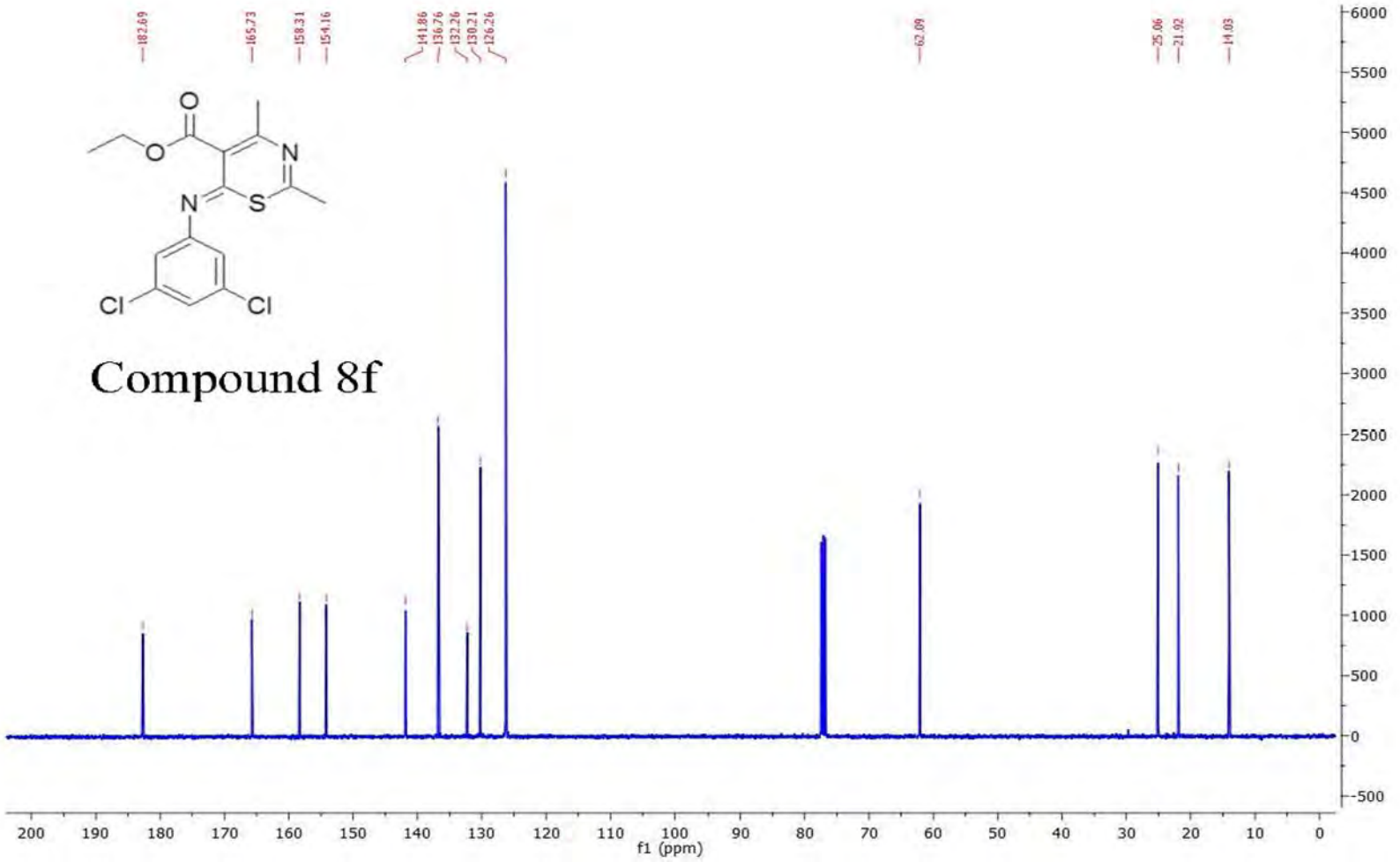
182.69
165.73
158.31
154.16
141.86
136.76
132.26
130.21
126.26
62.09
25.06
21.92
14.03
O
O
N
N
S
Cl
Cl
Compound 8f
6000
5500
5000
4500
4000
3500
3000
2500
2000
1500
1000
500
0
-500
200
190
180
170
160
150
140
130
120
110
100
90
80
70
60
50
40
30
20
10
0
f1 (ppm)

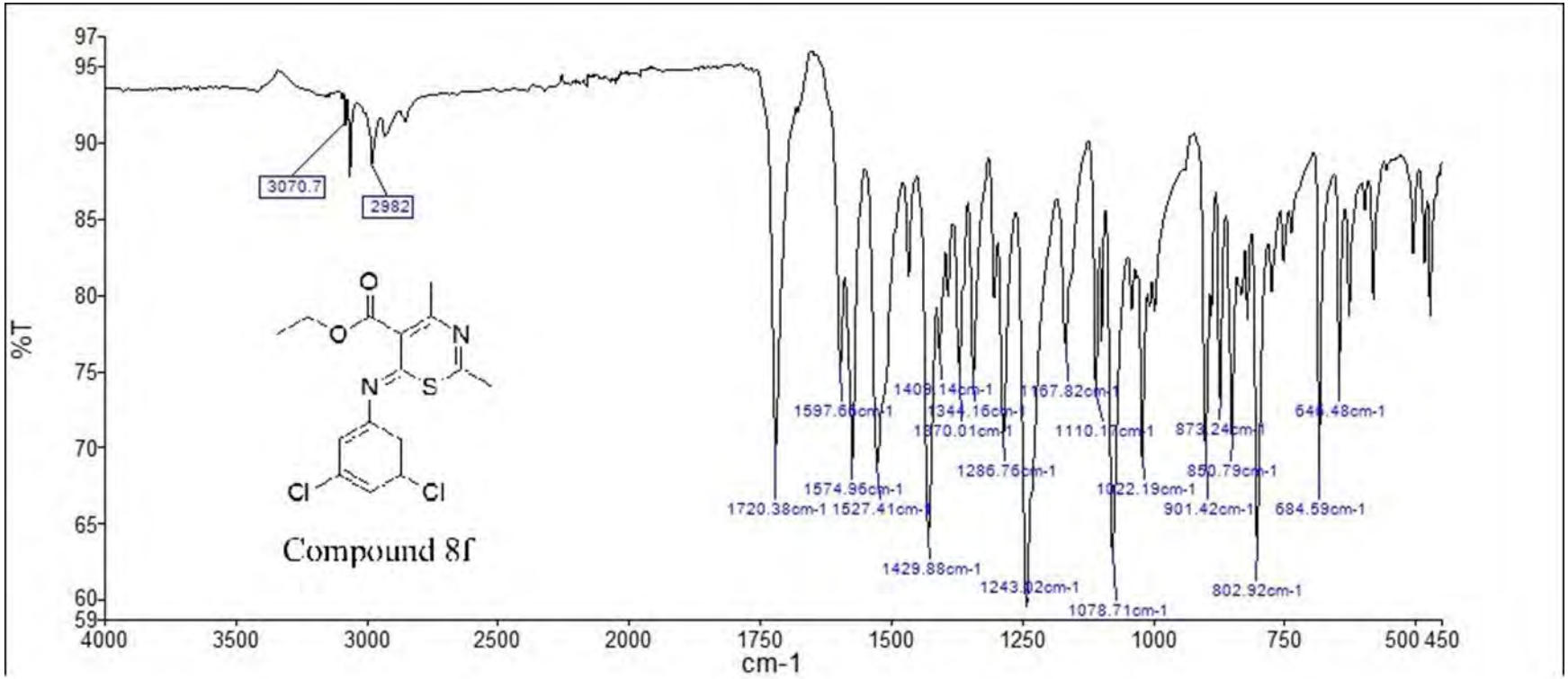
%T
cm-1
3070.7
2982
1720.38cm-1
1597.66cm-1
1574.96cm-1
1527.41cm-1
1429.88cm-1
1409.14cm-1
1370.01cm-1
1344.16cm-1
1286.76cm-1
1243.02cm-1
1167.82cm-1
1110.17cm-1
1078.71cm-1
1022.19cm-1
901.42cm-1
873.24cm-1
850.79cm-1
802.92cm-1
684.59cm-1
646.48cm-1
Cl
Cl
Compound 8f

==== Shimadzu LCMSsolution Analysis Report ====

Acquired by	: Admin
Sample Name	: TP123B5 Repeat
Sample ID	:
Vail #	: 65
Injection Volume	: 20 uL
Data File Name	: TP123B5 Repeat.lcd
Method File Name	: Platinum C18 EPS 3u lot 561094 part 50573 53mm id 7mm.lcm
Batch File Name	: Batch Second pro.lcb
Report File Name	: DefaultLCMS.lcr
Data Acquired	: 8/12/2015 2:09:20 PM
Data Processed	: 8/12/2015 2:42:54 PM

<Chromatogram>

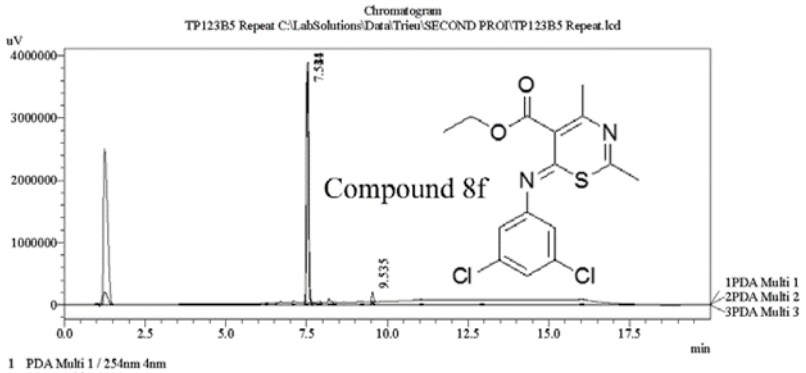

1 PDA Multi 1 / 254nm 4nm
2 PDA Multi 2 / 328nm 4nm
3 PDA Multi 3 / 220nm 4nm

PeakTable

PDA Ch1 254nm 4nm

Peak#	Ret. Time	Area	Height	Area %	Height %
1	7.524	14530588	3739370	100.000	100.000
Total		14530588	3739370	100.000	100.000

PeakTable

PDA Ch2 328nm 4nm

Peak#	Ret. Time	Area	Height	Area %	Height %
1	7.531	14957865	3573865	100.000	100.000
Total		14957865	3573865	100.000	100.000

PeakTable

PDA Ch3 220nm 4nm

Peak#	Ret. Time	Area	Height	Area %	Height %
1	7.541	21518553	3851394	97.183	96.063
2	9.535	623667	157842	2.817	3.937
Total		22142220	4009236	100.000	100.000

==== Shimadzu LCMSsolution Data Report ====

<Chromatogram>

Sample Information

Acquired by	: Admin
Date Acquired	: 8/12/2015 12:11:05 PM
Sample Type	: Unknown
Level#	: 0
Sample Name	: TP123B5 Re ESI +
Sample ID	:
ISTD Amount	: (Level1 Conc.)
Sample Amount	: 1
Dilution Factor	: 1
Tray#	: 1
Vial#	: 55
Injection Volume	: 3
Data File	: TP123B5 Re ESI +.lcd
Method File	: FIA-ESI_Scan(+).lcm
Original Method	: C:\LabSolutions\Data\Trieu\Mass spec files\FIA-ESI_Scan(+).lcm
Report Format	: Default.LCMS.lcr
Tuning File	: C:\LabSolutions\LCsolution\Log\Tuning\Autotune_030908.lct
Processed by	: Admin
Modified Date	: 8/12/2015 12:13:06 PM

Compound 8f

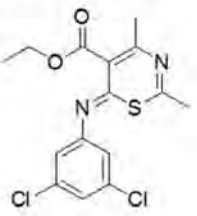

Chromatogram

TP123B5 Re ESI + C:\LabSolutions\Data\Trieu\SECOND PROI\Mass\TP123B5 Re ESI +.lcd

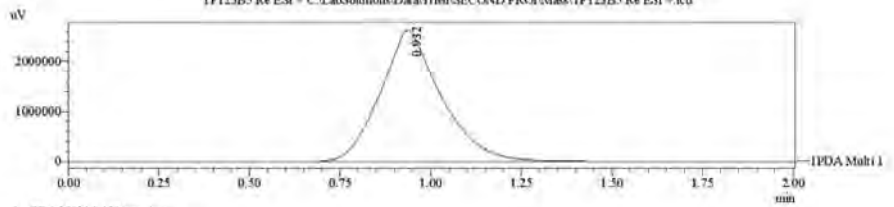

1 PDA Multi 1 / 254nm 4nm

<Spectrum>

Retention Time:1.280(Scan#:129)
Max Peak:680 Base Peak:356.25(878519)
Spectrum:Averaged 0.960-1.680(97-169)
Background:Averaged 0.120-0.539(13-55) Polarity:Pos Segment1 - Event1

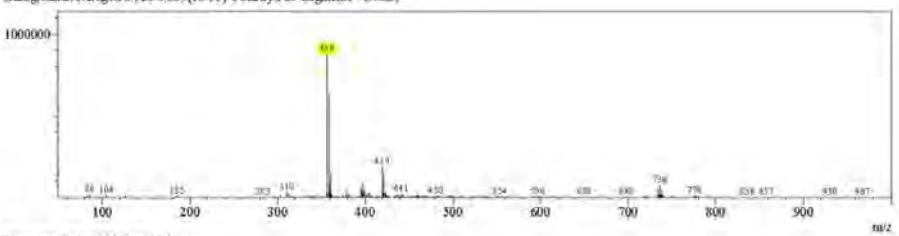

Retention Time:1.230(Scan#:124)
Max Peak:579 Base Peak:486.50(61784)
Spectrum:Averaged 0.970-1.690(98-170)
Background:Averaged 0.130-0.539(14-56) Polarity:Neg Segment1 - Event2

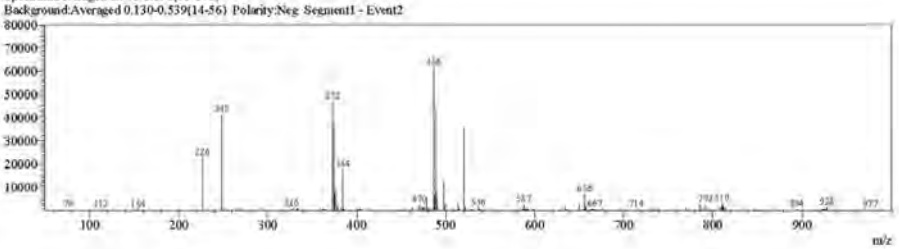

C:¥LabSolutions¥Data¥Trieu¥SECOND PROI¥Mass¥TP123B5 Re ESI +.lcd

Compound	Chemical Formula	Predicted monoisotopic neutral MW	Predicted MH+	MH+ Measured	Main MS Ions	Main MS/MS Fragments
8f	$C_{15}H_{14}Cl_2N_2O_2S$	356.0153	357.0226	357.0226		310.9810
					357.0226	328.9916
						172.0429

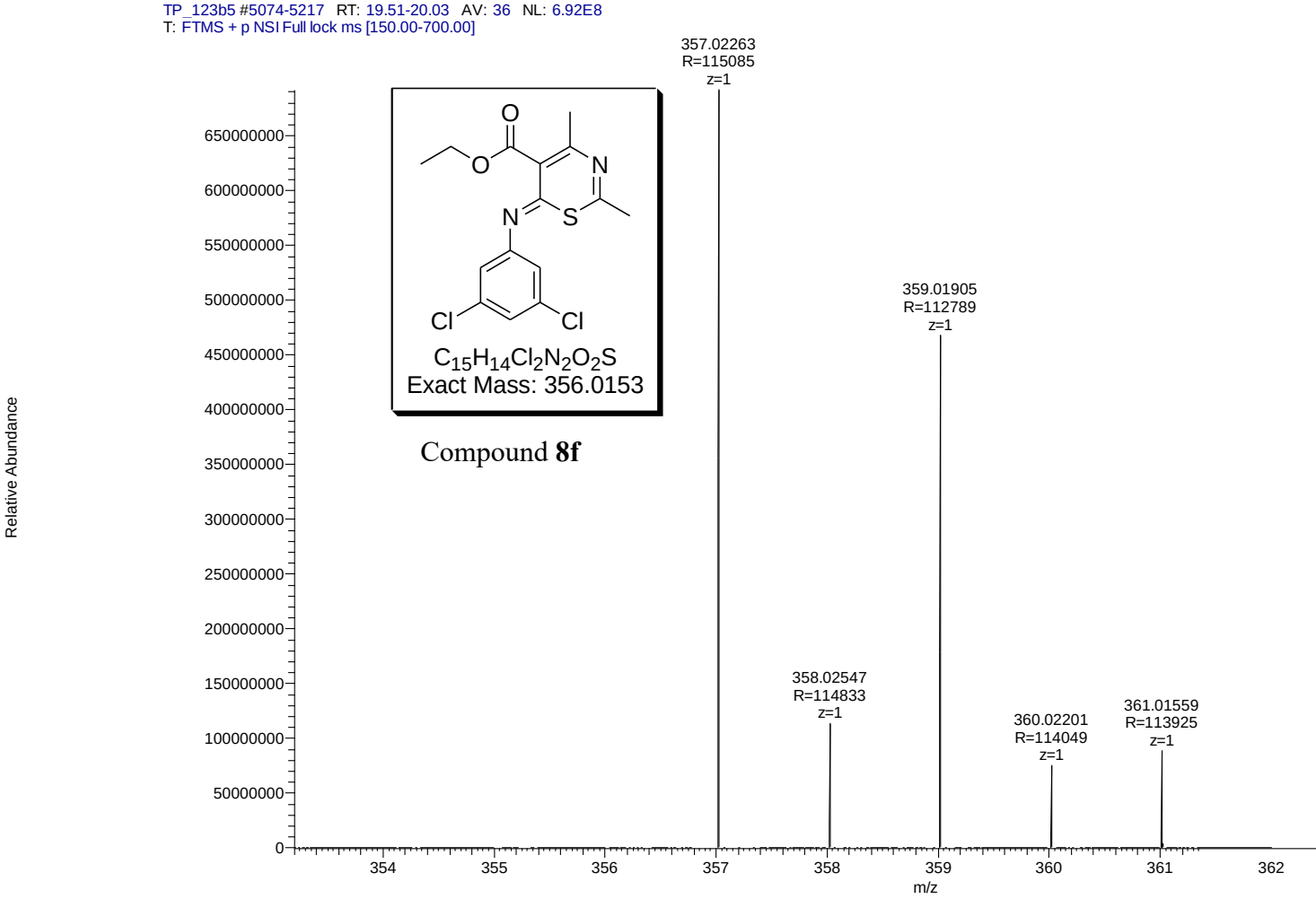

Compound **8g**

Compound Name: 6-(Benzo[1,3]dioxol-5-ylimino)-2,4-dimethyl-6*H*-[1,3]thiazine-5-carboxylic acid ethyl ester

Obtained Weight & Yield: 134 mg, 29%

Appearance: Yellow precipitate

Solubility: MeOH, ACN, Acetone

Melting Point: 146.5-147.3 °C

TLC Conditions: EtOAc/n-Hexane (50/50)

IR Analysis: 2982 (CH), 1733 (COO), 1250 (CO)

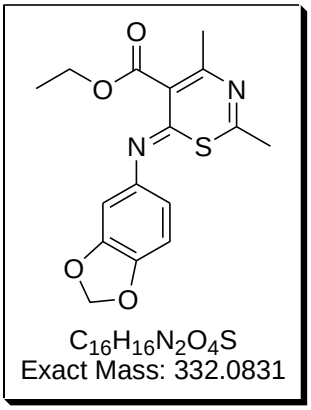

^{1}H NMR Analysis:
^{1}H NMR (400 MHz, $CDCl^3$) δ 6.94 (d, *J* = 7.9 Hz, 1H), 6.66 – 6.60 (m, 2H), 6.08 (d, *J* = 4.9 Hz, 2H), 4.42 (q, *J* = 7.1 Hz, 2H), 2.32-2.26 (m, 6H), 1.39 (t, *J* = 7.1 Hz, 3H).

^{13}C NMR Analysis:
^{13}C NMR (101 MHz, $CDCl_3$) δ 183.3, 166.1, 159.7, 153.8, 149.3, 148.6, 134.0, 132.2, 120.54, 109.4, 108.0, 102.3, 62.0, 25.0, 21.9, 14.0.

HPLC: RP-HPLC Alltima™ C18 5 µm 150 mm x 4.6 mm, 10-100% B in 15 min, R_t = 6.39 min, 100%.

Mass Spectral Analysis: LRMS (ESI+) m/z 332, 332 [M^+] (100%). HRMS (ES+) for $C_{16}H_{16}N_2O_4S$, calculated 333.0904, found 333.0902.

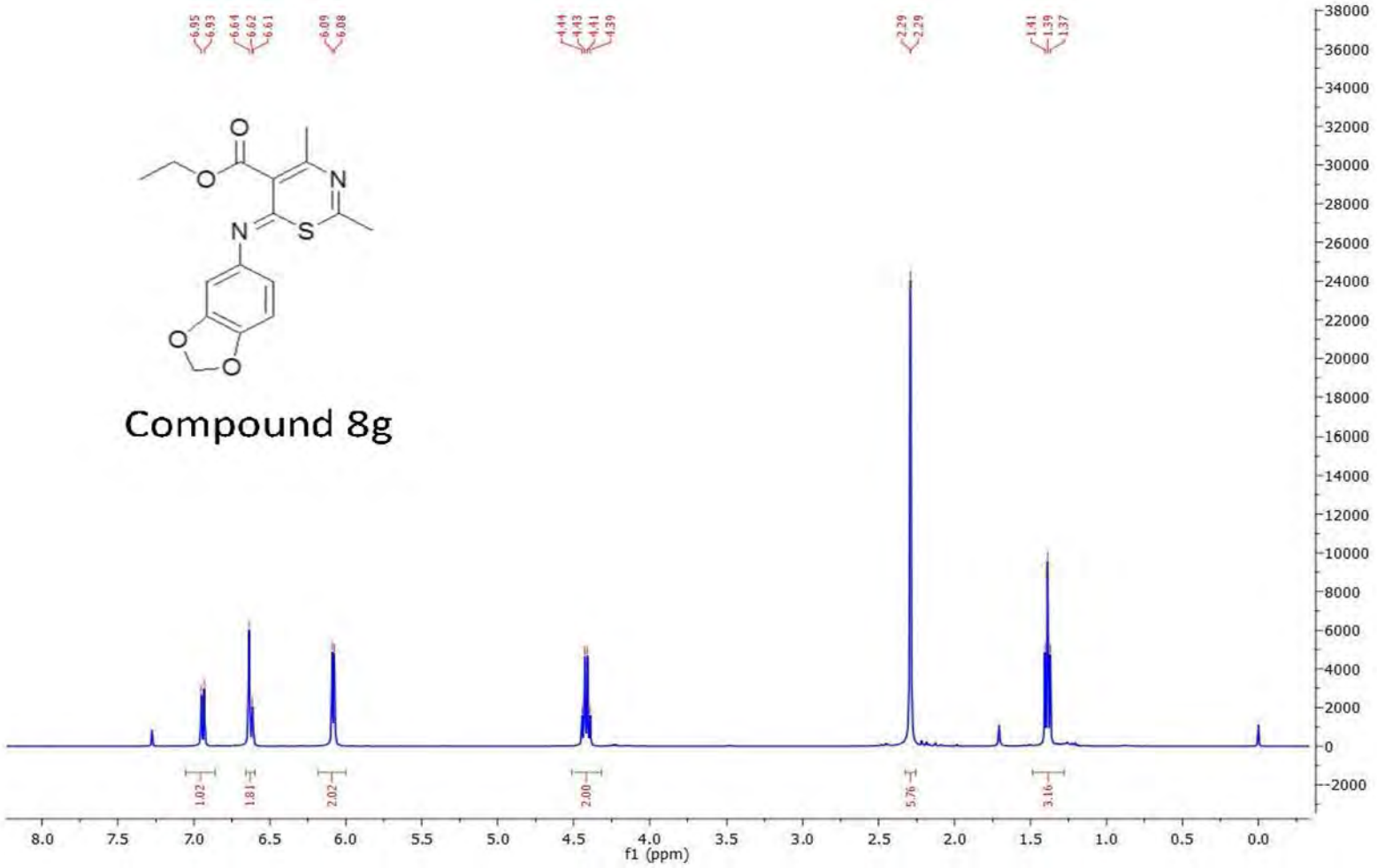
6.95
6.93
6.64
6.62
6.61
6.09
6.08
4.44
4.43
4.41
4.39
2.29
2.29
1.41
1.39
1.37
O
O
N
N
S
O
O
Compound 8g
38000
36000
34000
32000
30000
28000
26000
24000
22000
20000
18000
16000
14000
12000
10000
8000
6000
4000
2000
0
-2000
1.02
1.81
2.02
2.00
5.76
3.16
8.0
7.5
7.0
6.5
6.0
5.5
5.0
4.5
4.0
3.5
3.0
2.5
2.0
1.5
1.0
0.5
0.0
f1 (ppm)

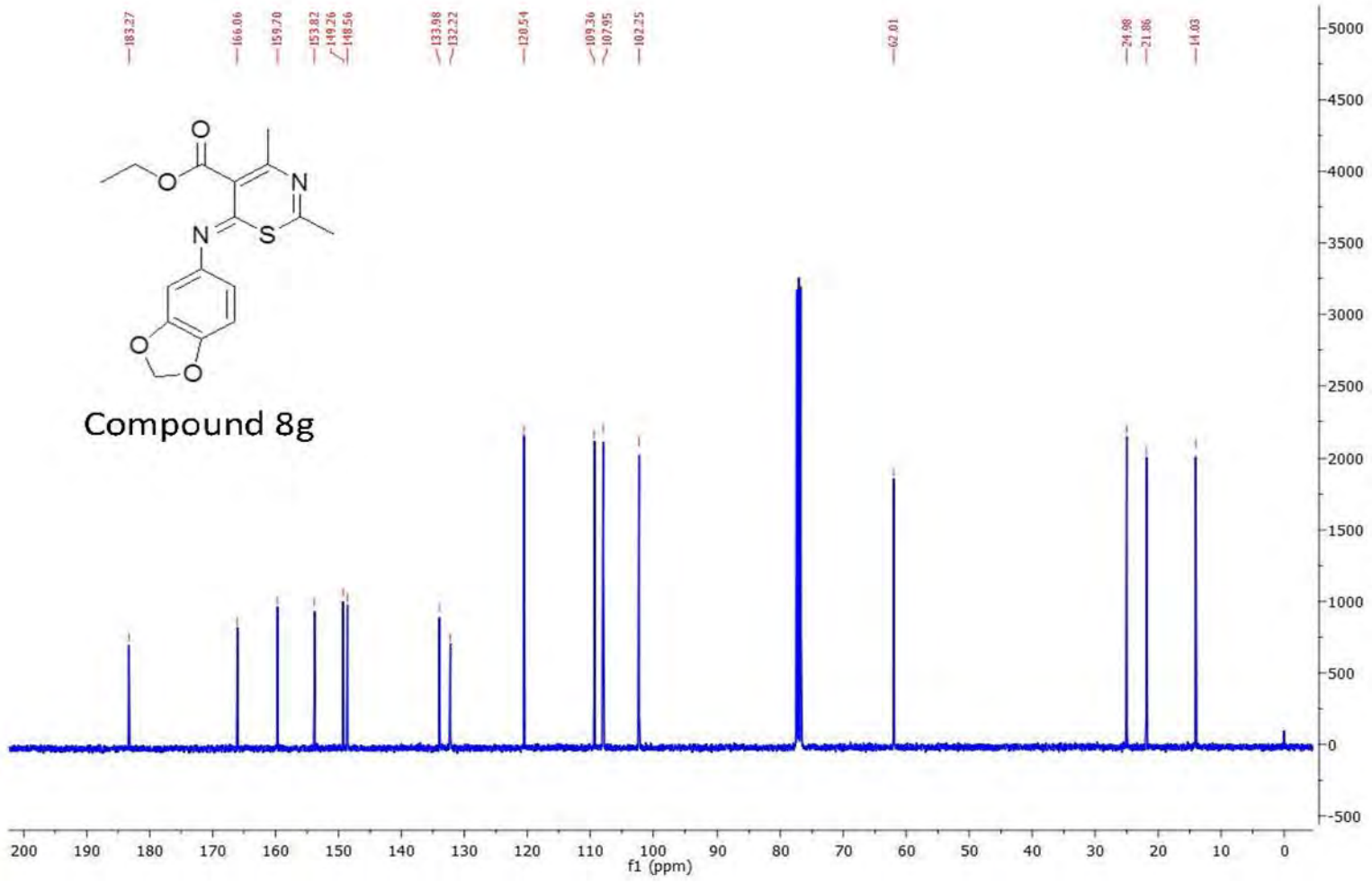
183.27
166.06
159.70
153.82
149.26
148.56
133.98
132.22
120.54
109.36
107.95
102.25
62.01
24.98
21.86
14.03
Compound 8g
f1 (ppm)

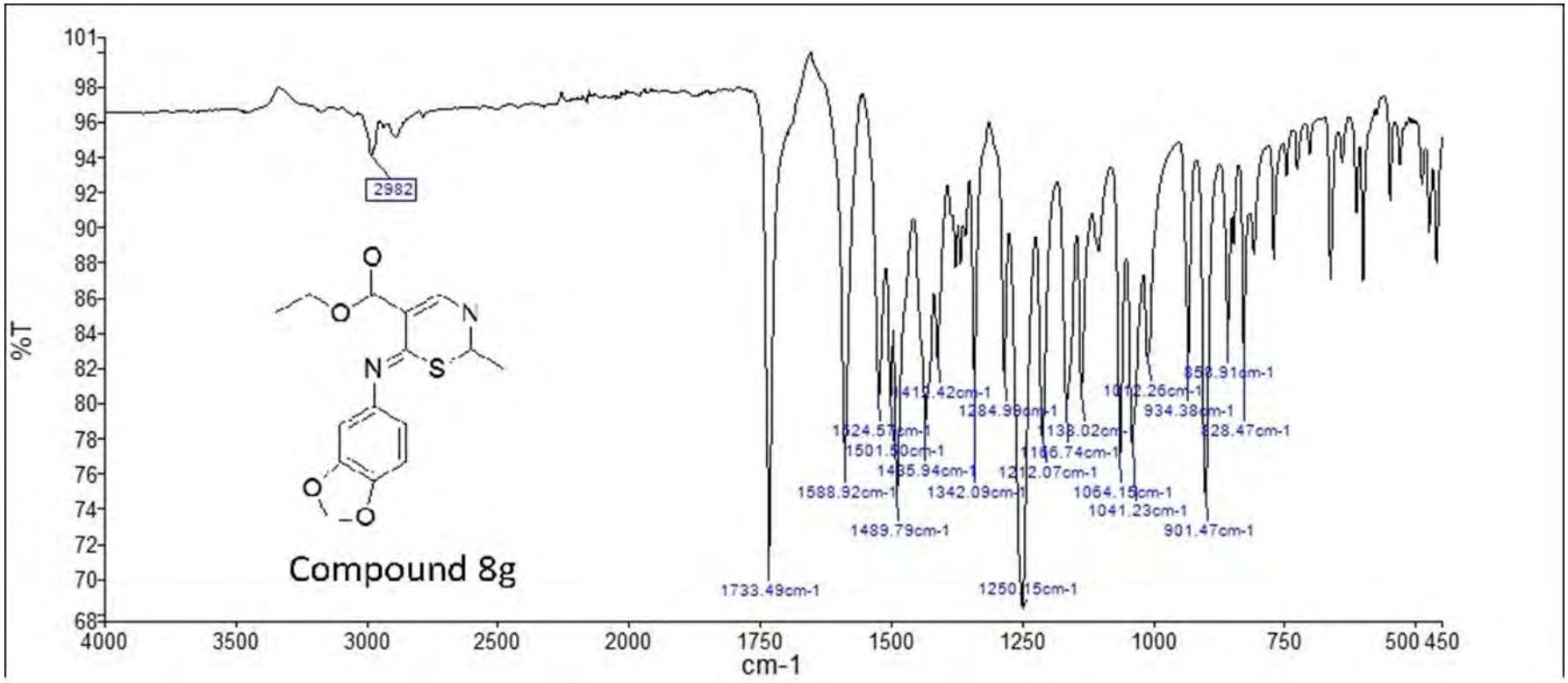
%T
cm-1
2982
1733.49cm-1
1588.92cm-1
1489.79cm-1
1342.09cm-1
1250.15cm-1
1212.07cm-1
1166.74cm-1
1064.15cm-1
1041.23cm-1
1012.26cm-1
934.38cm-1
901.47cm-1
828.47cm-1
Compound 8g

==== Shimadzu LCMSsolution Analysis Report ====

Acquired by	: Admin
Sample Name	: TP114B5 Re
Sample ID	:
Vail #	: 56
Injection Volume	: 20 uL
Data File Name	: TP114B5 Re.lcd
Method File Name	: Platinum C18 EPS 3u lot 561094 part 50573 53mm id 7mm.lcm
Batch File Name	: Batch Second pro.lcb
Report File Name	: DefaultLCMS.lcr
Data Acquired	: 8/11/2015 6:52:23 PM
Data Processed	: 8/12/2015 2:37:49 PM

<Chromatogram>

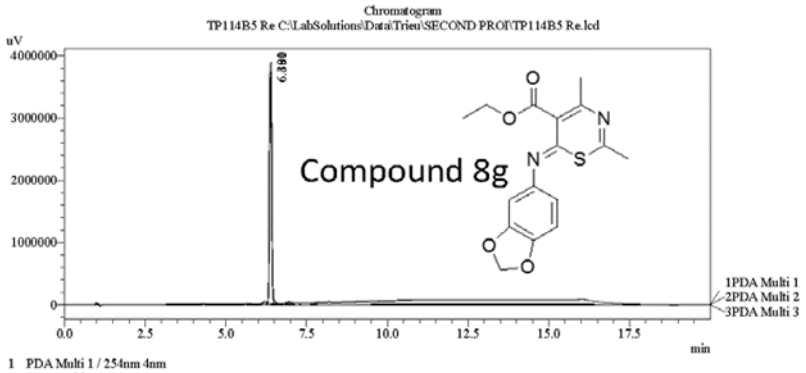

1 PDA Multi 1 / 254nm 4nm
2 PDA Multi 2 / 220nm 4nm
3 PDA Multi 3 / 328nm 4nm

PeakTable

PDA Ch1 254nm 4nm

Peak#	Ret. Time	Area	Height	Area %	Height %
1	6.381	14858626	3744314	100.000	100.000
Total		14858626	3744314	100.000	100.000

PeakTable

PDA Ch2 220nm 4nm

Peak#	Ret. Time	Area	Height	Area %	Height %
1	6.400	20911920	3878902	100.000	100.000
Total		20911920	3878902	100.000	100.000

PeakTable

PDA Ch3 328nm 4nm

Peak#	Ret. Time	Area	Height	Area %	Height %
1	6.390	17497253	3568074	100.000	100.000
Total		17497253	3568074	100.000	100.000

==== Shimadzu LCMSsolution Data Report ====

<Chromatogram>

Sample Information

Acquired by	: Admin
Date Acquired	: 8/12/2015 12:14:02 PM
Sample Type	: Unknown
Level#	: 0
Sample Name	: TP114B5 Re ESI +
Sample ID	:
ISTD Amount	: (Level1 Conc.)
Sample Amount	: 1
Dilution Factor	: 1
Tray#	: 1
Vial#	: 56
Injection Volume	: 3
Data File	: TP114B5 Re ESI +.lcd
Method File	: FIA-ESI_Scan(+).lcm
Original Method	: C:\LabSolutions\Data\Trieu\Mass spec files\FIA-ESI_Scan(+).lcm
Report Format	: Default\LCMS.lcr
Tuning File	: C:\LabSolutions\LCsolution\Log\Tuning\Autotune_030908.lct
Processed by	: Admin
Modified Date	: 8/12/2015 12:16:04 PM

Compound 8g

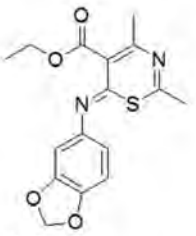

Chromatogram

TP114B5 Re ESI + C:\LabSolutions\Data\Trieu\SECOND PROJ\Mass\TP114B5 Re ESI +.lcd

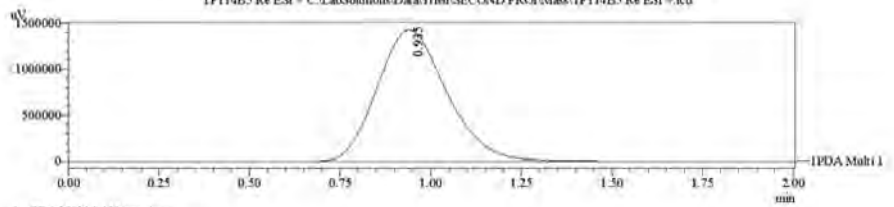

1 PDA Multi 1 / 254nm 4nm

<Spectrum>

Retention Time:1.280(Scan#:129)
Max Peak:526 Base Peak:332.50(1703194)
Spectrum:Averaged 0.960-1.720(97-173)
Background:Averaged 0.120-0.523(13-53) Polarity:Pos Segment1 - Event1

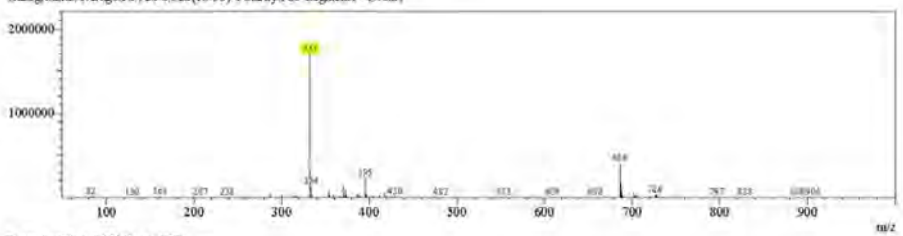

Retention Time:1.270(Scan#:128)
Max Peak:663 Base Peak:248.40(88794)
Spectrum:Averaged 0.970-1.730(98-174)
Background:Averaged 0.130-0.523(14-54) Polarity:Neg Segment1 - Event2

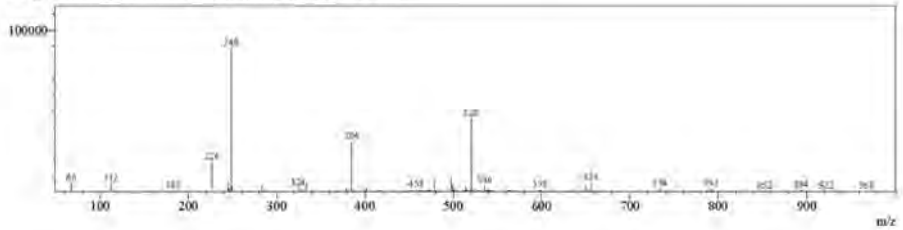

C:¥LabSolutions¥Data¥Trieu¥SECOND PROJ¥Mass¥TP114B5 Re ESI +.lcd

Compound	Chemical Formula	Predicted monoisotopic neutral MW	Predicted MH+	MH+ Measured	Main MS Ions	Main MS/MS Fragments
8g	$C_{16}H_{16}N_2O_4S$	332.0831	333.0904	339.0902		287.0484
					339.0902	333.0904
						305.0588

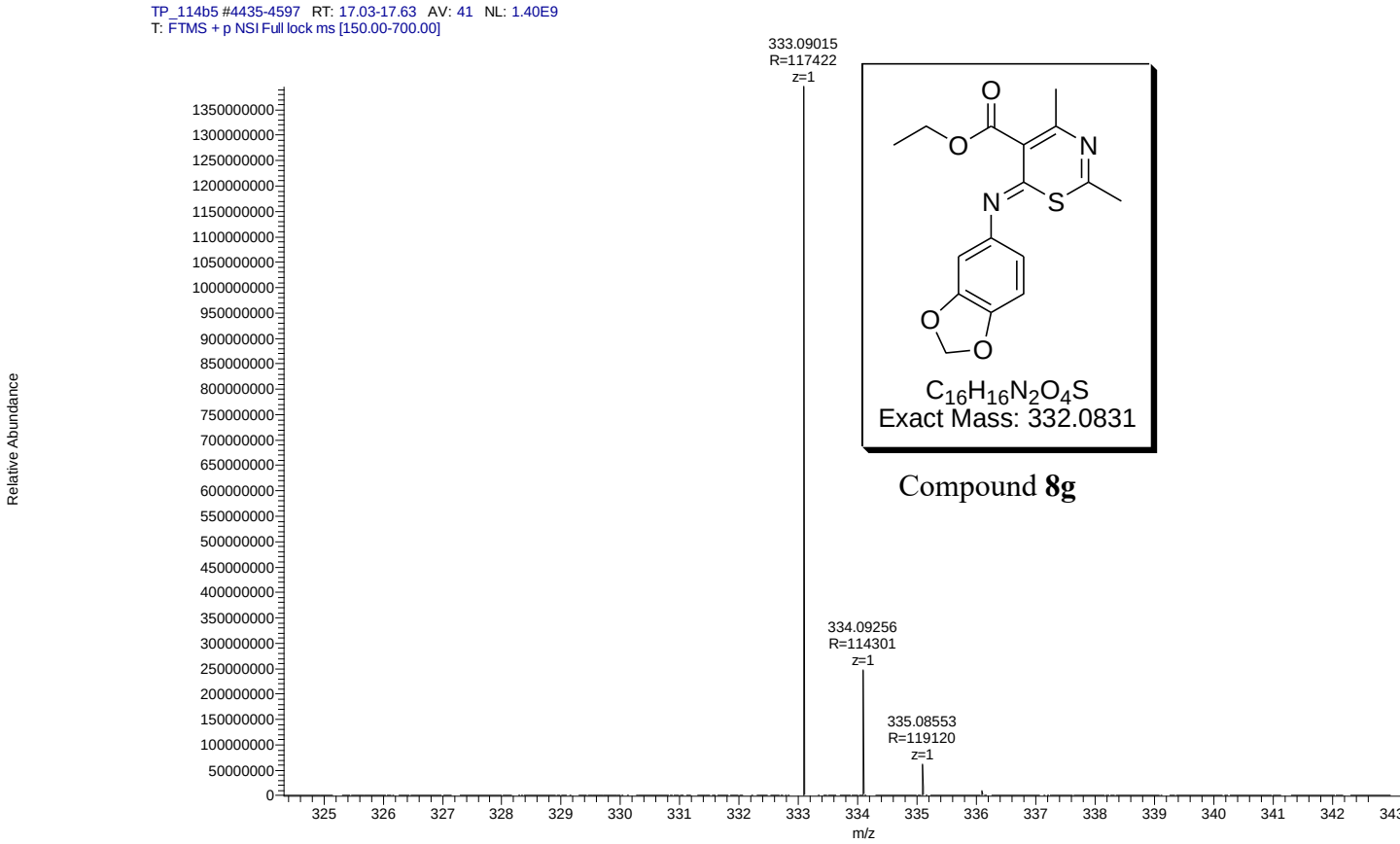

Compound **8g**

Compound **8h**

Compound Name: 2,4-Dimethyl-6-(naphthalen-1-ylimino)-6*H*-[1,3]thiazine-5-carboxylic acid ethyl ester

Obtained Weight & Yield: 96 mg, 20%

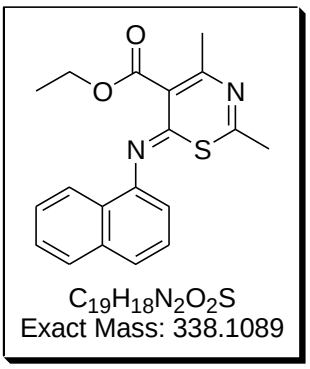

Appearance: Yellow precipitate

Solubility: MeOH, ACN, Acetone

Melting Point: 162.1-163 °C

TLC Conditions: EtOAc/n-Hexane (50/50)

IR Analysis:
2982 (CH), 1726 (COO), 1239 (CO)

^{1}H NMR Analysis:
^{1}H NMR (400 MHz, $CDCl_3$) δ 7.99 (d, *J* = 8.3 Hz, 1H), 7.95 (dd, *J* = 6.9, 2.2 Hz, 1H), 7.64 – 7.48 (m, 3H), 7.45 – 7.40 (m, 1H), 7.37 (dd, *J* = 7.3, 0.7 Hz, 1H), 4.51 – 4.32 (m, 2H), 2.37 (s, 3H), 2.13 (s, 3H), 1.39 (t, *J* = 7.1 Hz, 3H).

^{13}C NMR Analysis:
^{13}C NMR (400 MHz, CDCl3) δ 183.1, 166.2, 160.0, 154.0, 137.0, 134.6, 132.4, 130.2, 129.0, 128.2, 128.1, 127.1, 125.9, 125.5, 121.4, 62.0, 24.4, 22.0, 14.1

HPLC: RP-HPLC Alltima™ C18 5 µm 150 mm x 4.6 mm, 10-100% B in 15 min, R_t = 7.12 min, 100%.

Mass Spectral Analysis: LRMS (ESI+) m/z 338, 338 $[M]^+$ 100%. HRMS (ES+) for $C_{19}H_{18}N_2O_2S$, calculated 339.1162, found 339.1160.

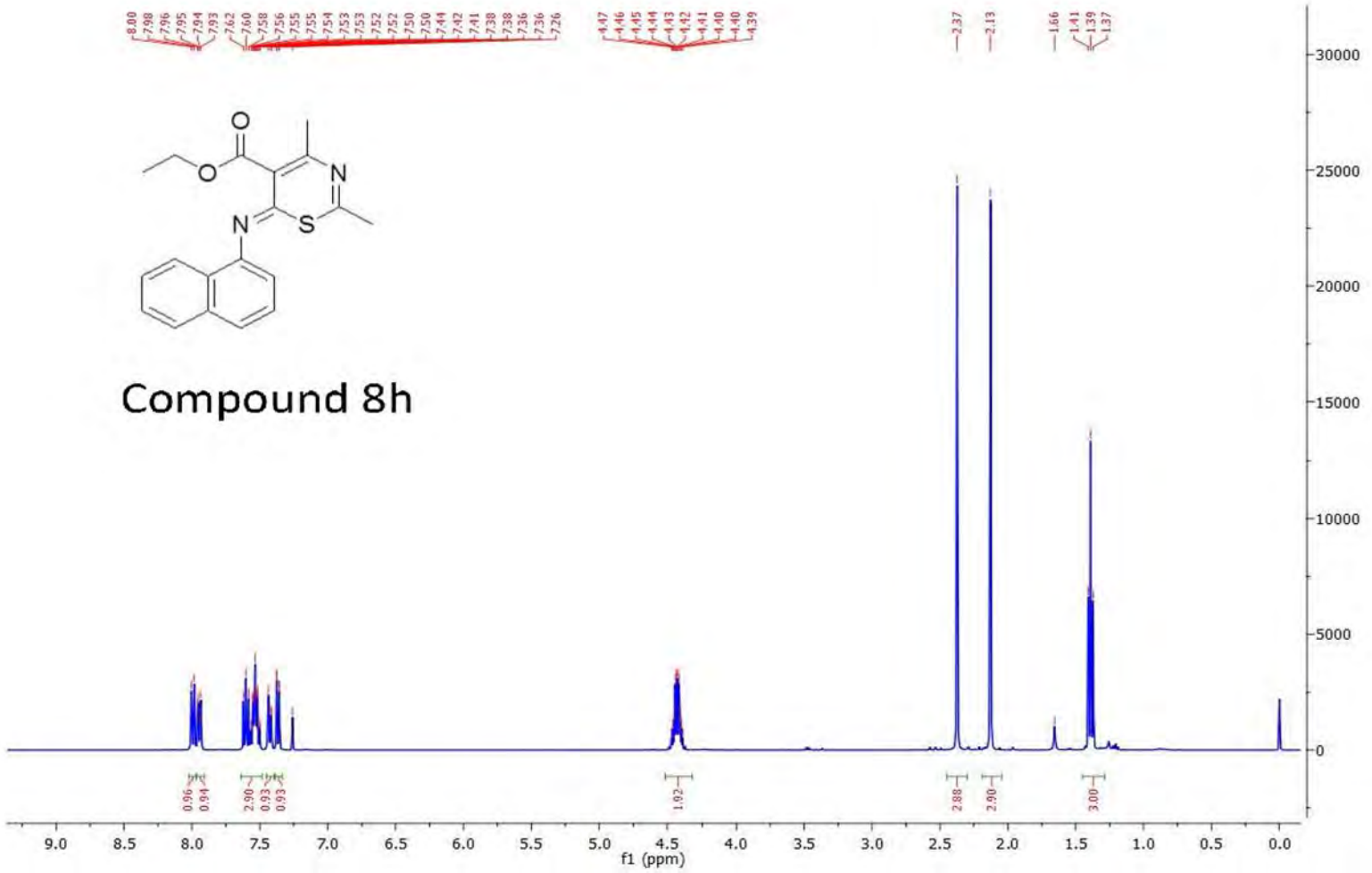
Compound 8h
f1 (ppm)

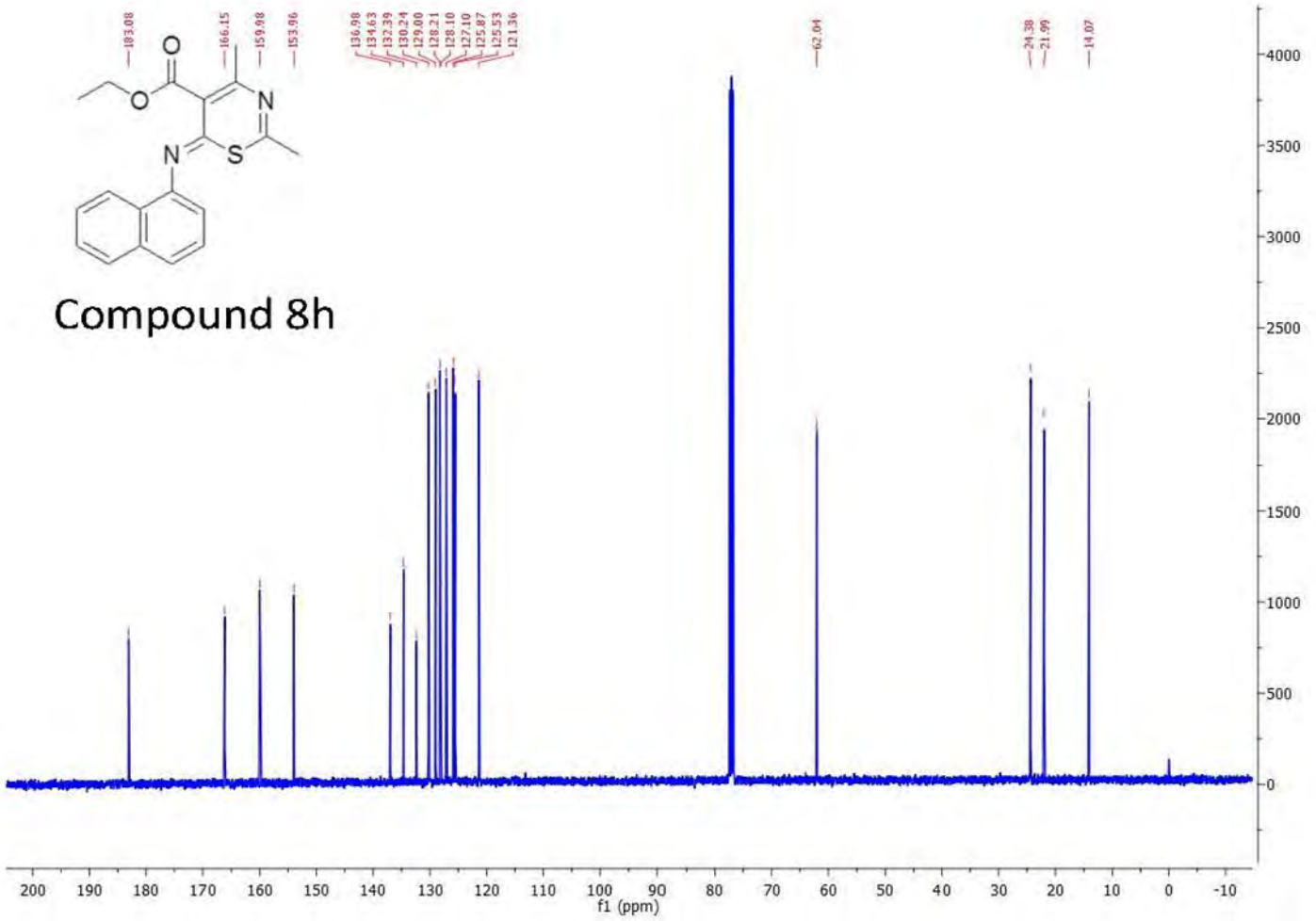
183.08
166.15
159.98
153.96
136.98
134.63
132.39
130.24
129.00
128.21
128.10
127.10
125.87
125.53
121.36
62.04
24.38
21.99
14.07
O
O
N
N
S
Compound 8h
4000
3500
3000
2500
2000
1500
1000
500
0
200 190 180 170 160 150 140 130 120 110 100 90 80 70 60 50 40 30 20 10 0 -10
f1 (ppm)

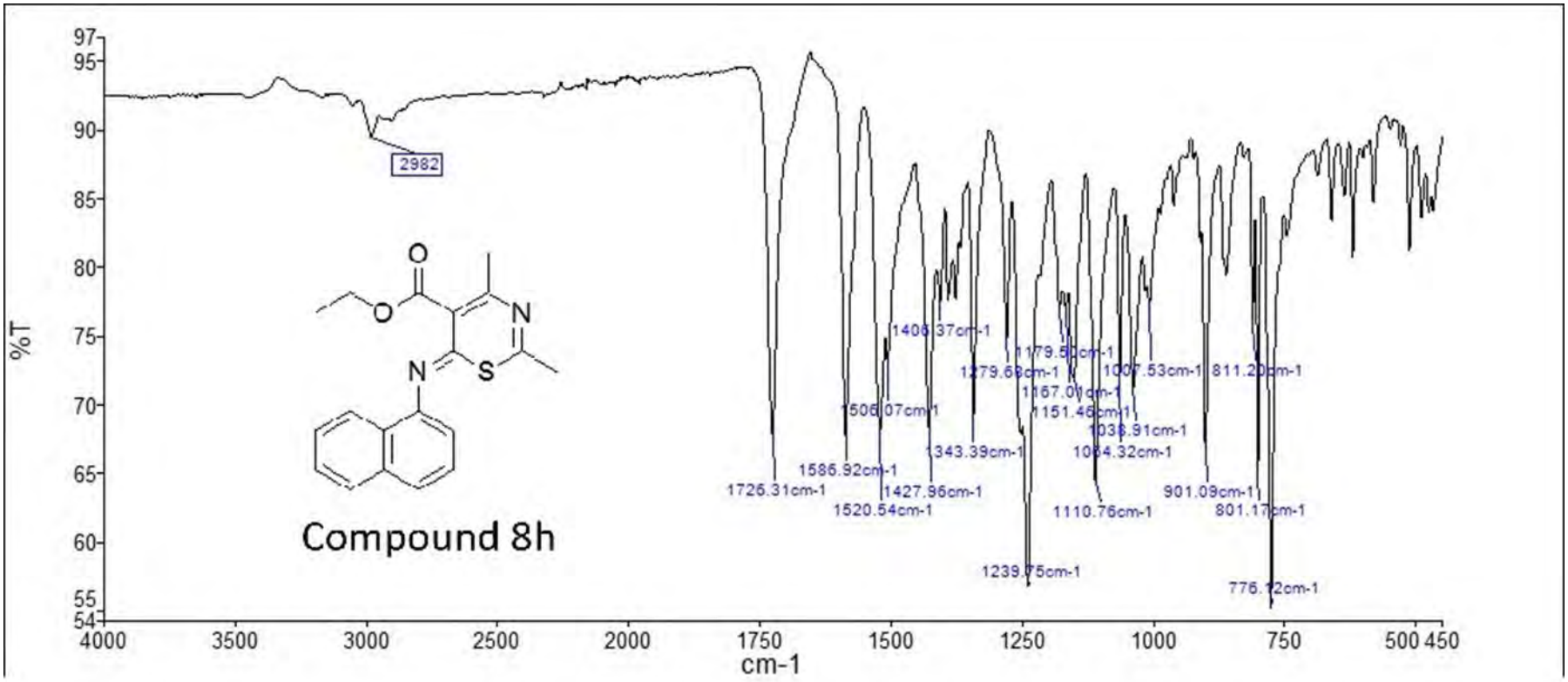
%T
cm-1
2982
1726.31cm-1
1586.92cm-1
1520.54cm-1
1506.07cm-1
1427.96cm-1
1343.39cm-1
1239.75cm-1
1110.76cm-1
1007.53cm-1
901.09cm-1
811.20cm-1
801.17cm-1
776.12cm-1
Compound 8h

==== Shimadzu LCMSsolution Analysis Report ====

Acquired by	: Admin
Sample Name	: TP65B5 Re
Sample ID	:
Vail #	: 53
Injection Volume	: 20 uL
Data File Name	: TP65B5 Re.lcd
Method File Name	: Platinum C18 EPS 3u lot 561094 part 50573 53mm id 7mm.lcm
Batch File Name	: Batch Second pro.lcb
Report File Name	: DefaultLCMS.lcr
Data Acquired	: 8/11/2015 5:51:02 PM
Data Processed	: 8/12/2015 2:52:17 PM

<Chromatogram>

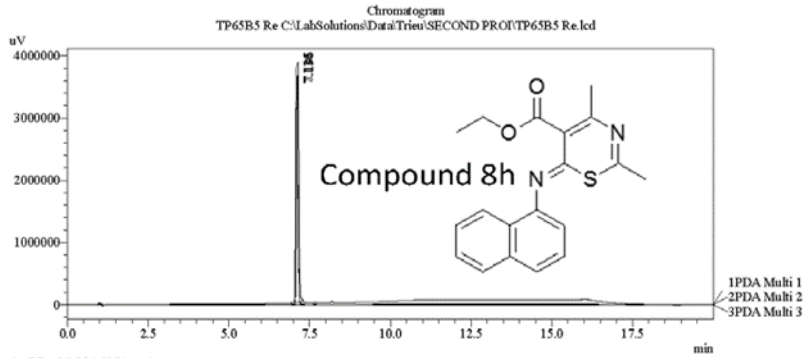

1 PDA Multi 1 / 254nm 4nm
2 PDA Multi 2 / 328nm 4nm
3 PDA Multi 3 / 220nm 4nm

PeakTable

PDA Ch1 254nm 4nm

Peak#	Ret. Time	Area	Height	Area %	Height %
1	7.115	13174604	3683077	100.000	100.000
Total		13174604	3683077	100.000	100.000

PeakTable

PDA Ch2 328nm 4nm

Peak#	Ret. Time	Area	Height	Area %	Height %
1	7.116	13671328	3553581	100.000	100.000
Total		13671328	3553581	100.000	100.000

PeakTable

PDA Ch3 220nm 4nm

Peak#	Ret. Time	Area	Height	Area %	Height %
1	7.136	24900670	3853095	100.000	100.000
Total		24900670	3853095	100.000	100.000

==== Shimadzu LCMSsolution Data Report ====

<Chromatogram>

Sample Information

Acquired by	: Admin
Date Acquired	: 8/12/2015 12:05:09 PM
Sample Type	: Unknown
Level#	: 0
Sample Name	: TP65B5 Re ESI +
Sample ID	:
ISTD Amount	: (Level1 Conc.)
Sample Amount	: 1
Dilution Factor	: 1
Tray#	: 1
Vial#	: 53
Injection Volume	: 5
Data File	: TP65B5 Re ESI +.lcd
Method File	: FIA-ESI_Scan(+).lcm
Original Method	: C:\LabSolutions\Data\Trieu\Mass spec files\FIA-ESI_Scan(+).lcm
Report Format	: DefaultLCMS.lcr
Tuning File	: C:\LabSolutions\LCsolution\Log\Tuning\Autotune_030908.lct
Processed by	: Admin
Modified Date	: 8/12/2015 12:07:10 PM

Compound 8h

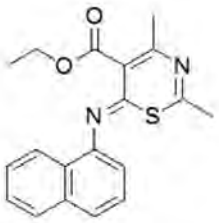

Chromatogram
TP65B5 Re ESI + C:\LabSolutions\Data\Trieu\SECOND PROI\Mass\TP65B5 Re ESI +.lcd

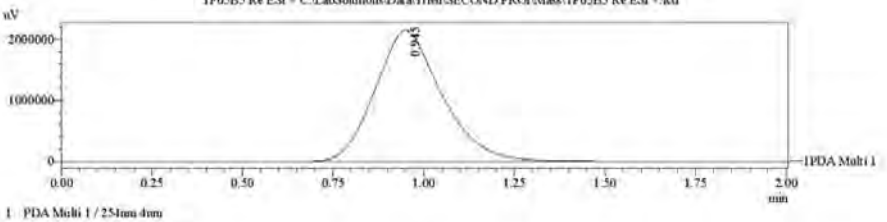

1 PDA Multi 1 / 254nm 4nm

<Spectrum>

Retention Time:1.280(Scan#:129)
Max Peak:522 Base Peak:338.55(1695807)
Spectrum:Averaged 0.980-1.740(99-175)
Background:Averaged 0.140-0.573(15-59) Polarity:Pos Segment1 - Event1

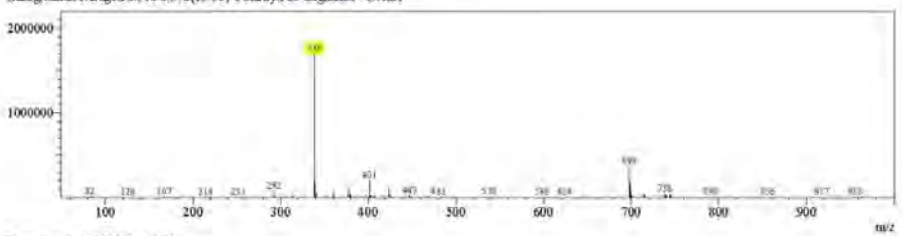

Retention Time:1.230(Scan#:124)
Max Peak:684 Base Peak:248.50(70740)
Spectrum:Averaged 0.990-1.750(100-176)
Background:Averaged 0.150-0.573(16-60) Polarity:Neg Segment1 - Event2

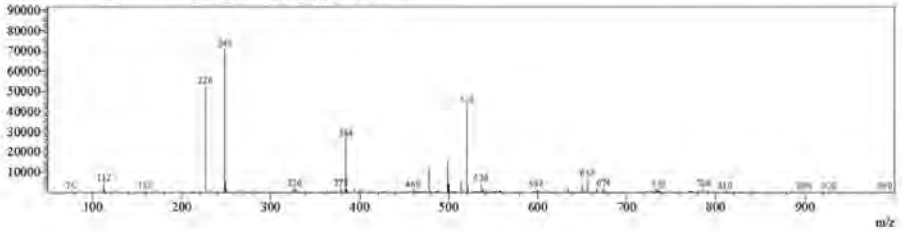

C:¥LabSolutions¥Data¥Trieu¥SECOND PROI¥Mass¥TP65B5 Re ESI +.lcd

Compound	Chemical Formula	Predicted monoisotopic neutral MW	Predicted MH+	MH+ Measured	Main MS Ions	Main MS/MS Fragments
8h	$C_{19}H_{18}N_2O_2S$	338.1089	339.1162	339.1160		293.0746
					339.1160	311.0853
						168.0810

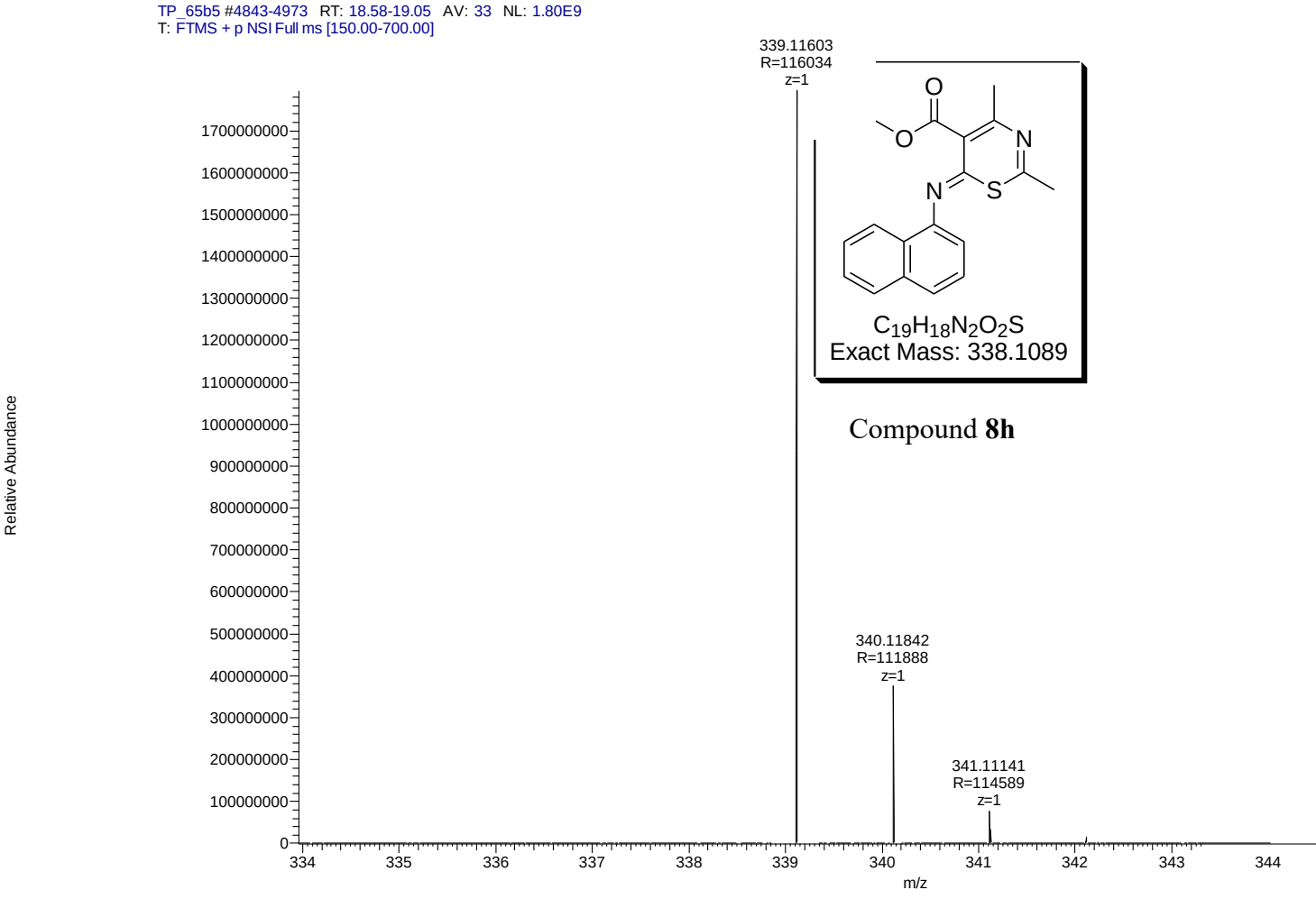

Compound **8i**

Compound Name: 6-Ethylimino-2,4-dimethyl-6H-[1,3]thiazine-5-carboxylic acid ethyl ester.

Obtained Weight & Yield: 30 mg, 14%

Appearance: Yellow precipitate

Solubility: MeOH, ACN, Acetone

Melting Point: 112.5-113.4 °C

TLC Conditions: EtOAc/n-Hexane (50/50)

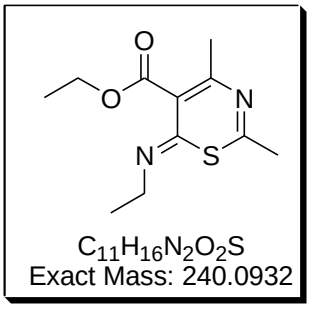

IR Analysis:

IR (cm^{-1}): 2969 (CH), 1732 (COO), 1267 (CO)

^{1}H NMR Analysis:

^{1}H NMR (400 MHz, $CDCl_3$) δ 4.72-4.61 (m, 2H), 4.53 – 4.33 (m, 2H), 2.69 (s, 3H), 2.22 (s, 3H), 1.48-1.37 (m, 6H).

^{13}C NMR Analysis:

^{13}C NMR (400 MHz, $CDCl_3$) δ 181.0, 166.3, 158.6, 153.4, 132.5, 61.9, 45.8, 23.8, 21.6, 14.0, 11.8.

HPLC: RP-HPLC Alltima™ C18 5 μm 150 mm x 4.6 mm, 10-100% B in 15 min, R_t = 5.83 min, 94%.

Mass Spectral Analysis: LRMS (ESI+) m/z: 240, 240 $[M]^+$ 100%. HRMS (ES+) for $C_{11}H_{16}N_2O_2S$, calculated 241.1005, found 241.1003.

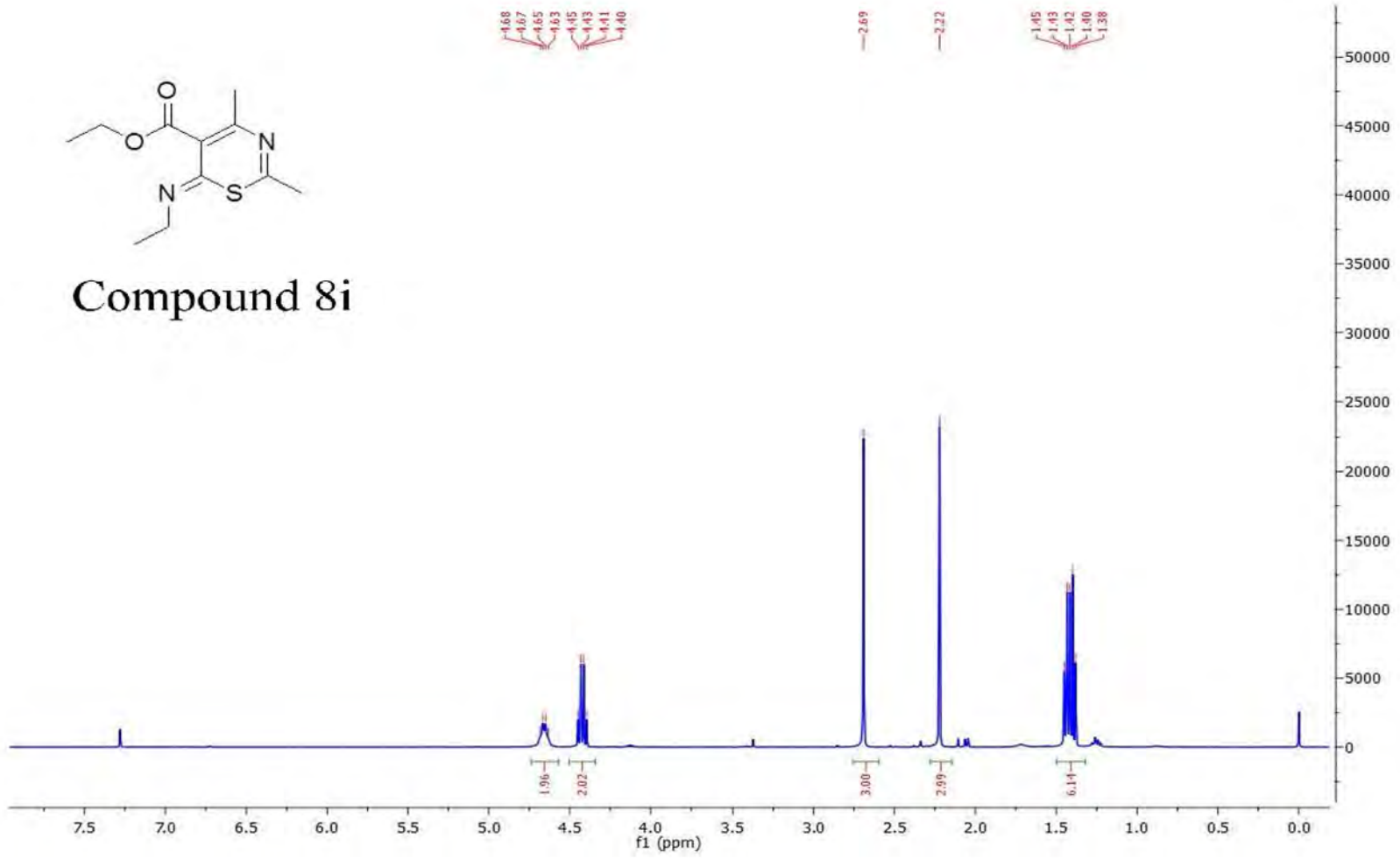
Compound 8i
4.68
4.67
4.65
4.63
4.45
4.43
4.41
4.40
2.69
2.22
1.45
1.43
1.42
1.40
1.38
1.96
2.02
3.00
2.99
6.14
f1 (ppm)

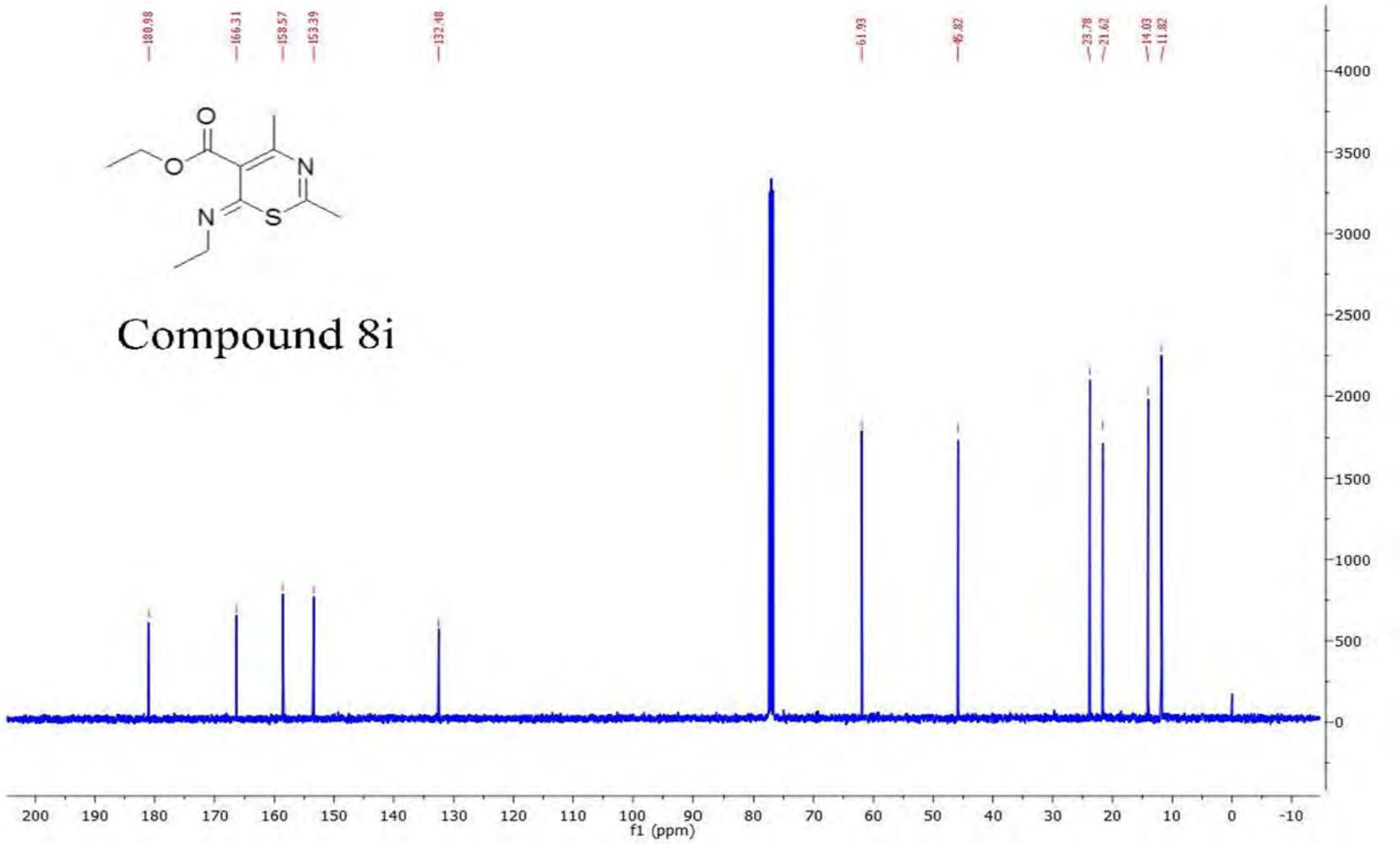
180.98
166.31
158.57
153.39
132.48
61.93
45.82
23.78
21.62
14.03
11.82
O
O
N
N
S
Compound 8i
4000
3500
3000
2500
2000
1500
1000
500
0
200 190 180 170 160 150 140 130 120 110 100 90 80 70 60 50 40 30 20 10 0 -10
f1 (ppm)

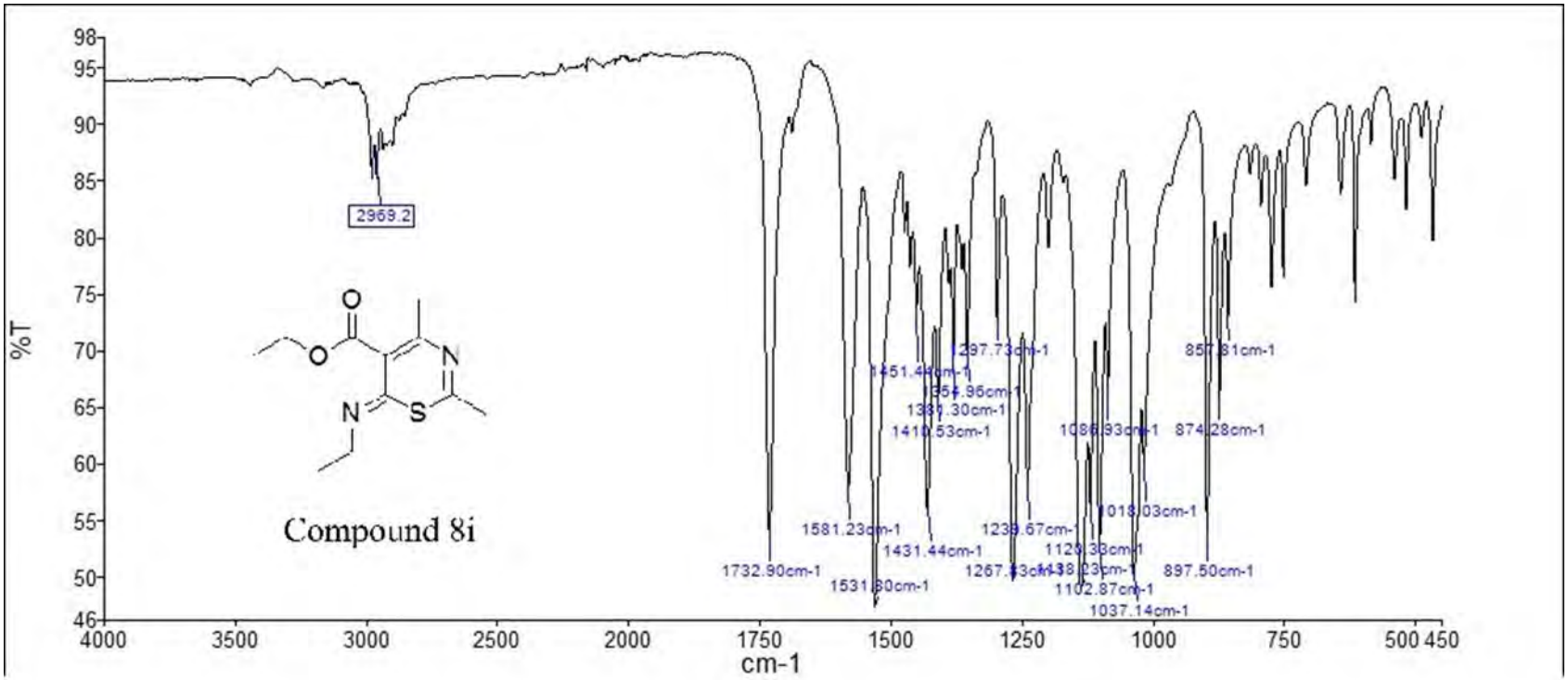
%T
cm-1
2969.2
Compound 8i
1732.90cm-1
1581.23cm-1
1531.80cm-1
1431.44cm-1
1410.53cm-1
1337.30cm-1
1297.73cm-1
1267.43cm-1
1238.67cm-1
1102.87cm-1
1037.14cm-1
897.50cm-1
874.28cm-1

==== Shimadzu LCMSsolution Analysis Report ====

Acquired by	: Admin
Sample Name	: TP56B5 Re
Sample ID	:
Vail #	: 59
Injection Volume	: 20 uL
Data File Name	: TP56B5 Re.lcd
Method File Name	: Platinum C18 EPS 3u lot 561094 part 50573 53mm id 7mm.lcm
Batch File Name	: Batch Second pro.lcb
Report File Name	: DefaultLCMS.lcr
Data Acquired	: 8/11/2015 7:53:46 PM
Data Processed	: 8/12/2015 2:10:58 PM

<Chromatogram>

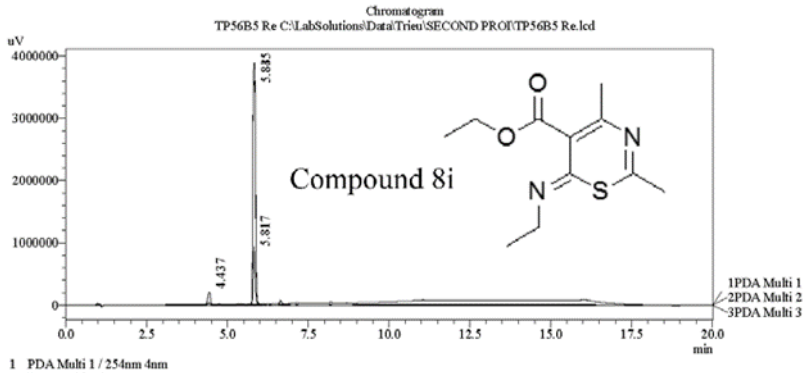

1 PDA Multi 1 / 254nm 4nm
2 PDA Multi 2 / 328nm 4nm
3 PDA Multi 3 / 220nm 4nm

PeakTable

PDA Ch1 254nm 4nm

Peak#	Ret. Time	Area	Height	Area %	Height %
1	4.437	77127	57334	1.704	5.711
2	5.817	4448442	946567	98.296	94.289
Total		4525569	1003901	100.000	100.000

PeakTable

PDA Ch2 328nm 4nm

Peak#	Ret. Time	Area	Height	Area %	Height %
1	5.845	21906920	3592877	100.000	100.000
Total		21906920	3592877	100.000	100.000

PeakTable

PDA Ch3 220nm 4nm

Peak#	Ret. Time	Area	Height	Area %	Height %
1	5.835	21079895	3880816	100.000	100.000
Total		21079895	3880816	100.000	100.000

==== Shimadzu LCMSsolution Data Report ====

<Chromatogram>

Sample Information

Acquired by	: Admin
Date Acquired	: 8/12/2015 12:23:00 PM
Sample Type	: Unknown
Level#	: 0
Sample Name	: TP56B5 Re ESI +
Sample ID	:
ISTD Amount	: (Level1 Conc.)
Sample Amount	: 1
Dilution Factor	: 1
Tray#	: 1
Vial#	: 59
Injection Volume	: 3
Data File	: TP56B5 Re ESI +.lcd
Method File	: FIA-ESI_Scan(+).lcm
Original Method	: C:\LabSolutions\Data\Trieu\Mass spec files\FIA-ESI_Scan(+).lcm
Report Format	: DefaultLCMS.lcr
Tuning File	: C:\LabSolutions\LCsolution\Log\Tuning\Autotune_030908.lct
Processed by	: Admin
Modified Date	: 8/12/2015 12:25:04 PM

Compound 8i

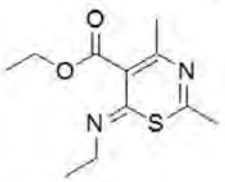

Chromatogram
TP56B5 Re ESI + C:\LabSolutions\Data\Trieu\SECOND PROJ\Mass\TP56B5 Re ESI +.lcd

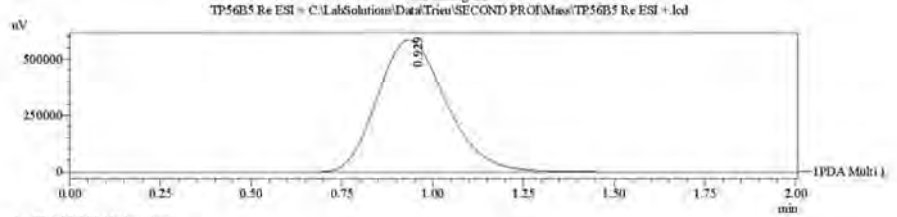

1 PDA Multi 1 / 254nm 4nm

<Spectrum>

Retention Time:1.240(Scan#:125)
Max Peak:951 Base Peak:240.55(1816794)
Spectrum:Averaged 0.960-1.610(97-165)
Background:None Polarity:Pos Segment1 - Event1

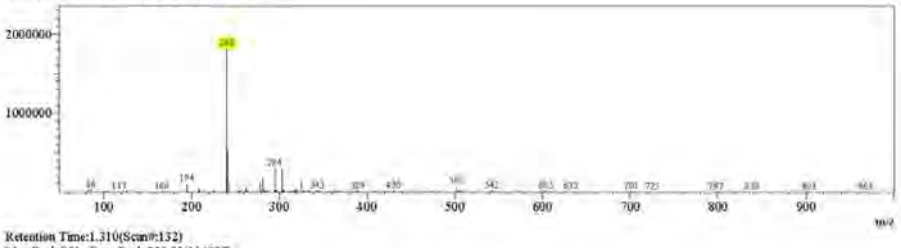

Retention Time:1.310(Scan#:132)
Max Peak:951 Base Peak:226.55(114327)
Spectrum:Averaged 0.970-1.650(98-166)
Background:None Polarity:Neg Segment1 - Event2

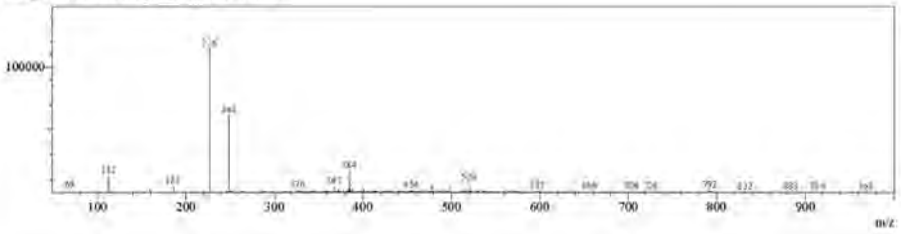

C:¥LabSolutions¥Data¥Trieu¥SECOND PROJ¥Mass¥TP56B5 Re ESI +.lcd

Compound	Chemical Formula	Predicted monoisotopic neutral MW	Predicted MH+	MH+ Measured	Main MS Ions	Main MS/MS Fragments
8i	$C_{11}H_{16}N_2O_2S$	240.0932	241.1005	241.1003		213.0694
					241.1003	195.0589
						167.0276

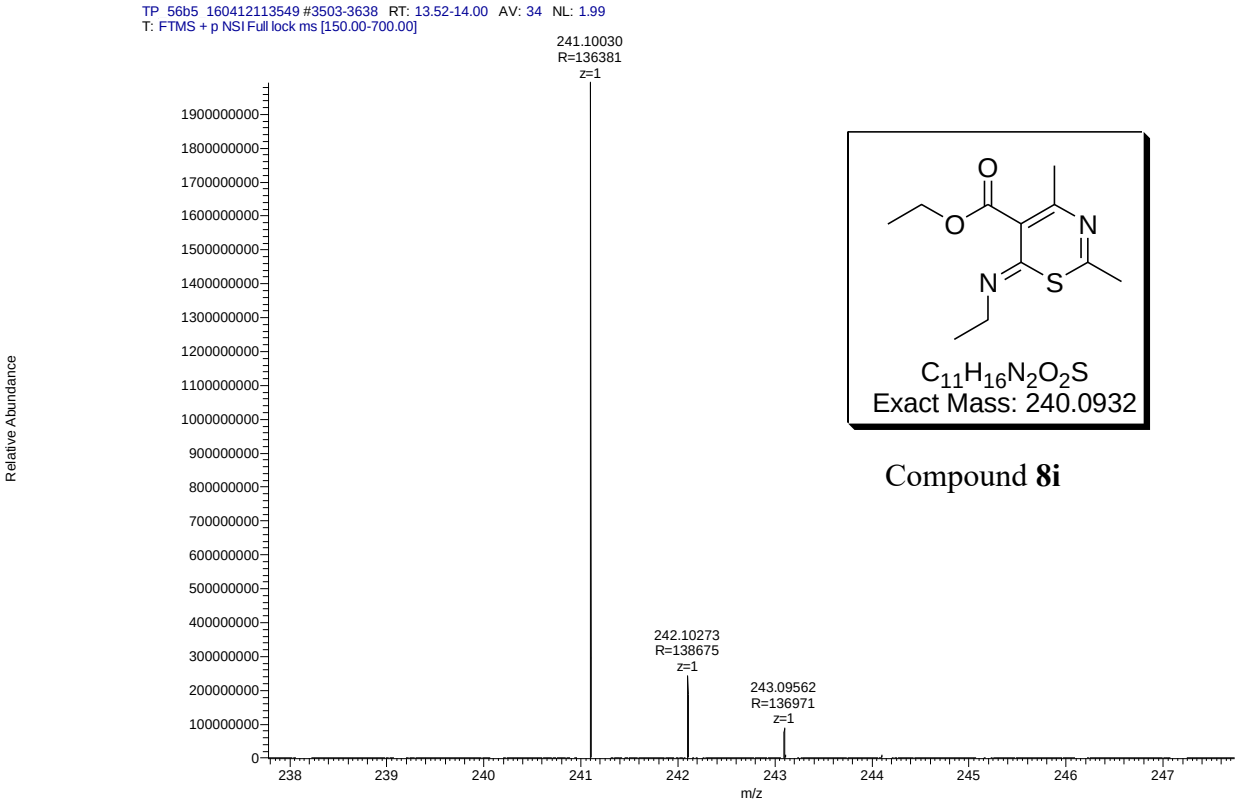

Compound **8i**

Compound **8k**

Compound Name: 2-Ethyl-4-methyl-6-phenylimino-6*H*-[1,3]thiazine-5-carboxylic acid ethyl ester

Obtained Weight & Yield: 41 mg, 17%

Appearance: Yellow precipitate

Solubility: MeOH, ACN, Acetone **Melting Point:** 87.5-88.3 °C

TLC Conditions: EtOAc/n-Hexane (50/50)
IR Analysis: 2988 (CH), 1728 (COO), 1237 (CO)

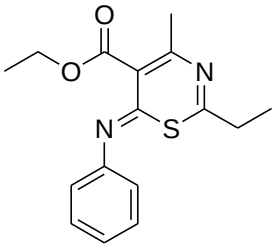

$C_{16}H_{18}N_2O_2S$
Exact Mass: 302.1089

^{1}H NMR Analysis:

^{1}H NMR (400 MHz, CDCl3) δ 7.59 – 7.47 (m, 3H), 7.20 – 7.13 (m, 2H), 4.42 (q, *J* = 7.1 Hz, 2H), 2.40 (d, *J* = 7.4 Hz, 2H), 2.33 (s, 3H), 1.39 (t, *J* = 7.1 Hz, 3H), 1.15 (t, *J* = 7.4 Hz, 3H).

^{13}C NMR Analysis:

^{13}C NMR (101 MHz, $CDCl_3$) δ 183.1, 166.3, 162.9, 154.1, 140.0, 132.1, 130.3 (Cx2), 129.7, 127.4 (Cx2), 62.0, 30.1, 22.0, 14.0, 11.4.

HPLC:

RP-HPLC Alltima™ C18 5 µm 150 mm x4.6 mm, 10-100% B in 15 min, R_t = 6.91 min, 100%.

Mass Spectral Analysis: LRMS **(ESI+)** m/z: 302, 302 $[M]^+$ 100%. HRMS (ES+) for $C_{16}H_{18}N_2O_2S$, calculated 303.1162, found 303.1157.

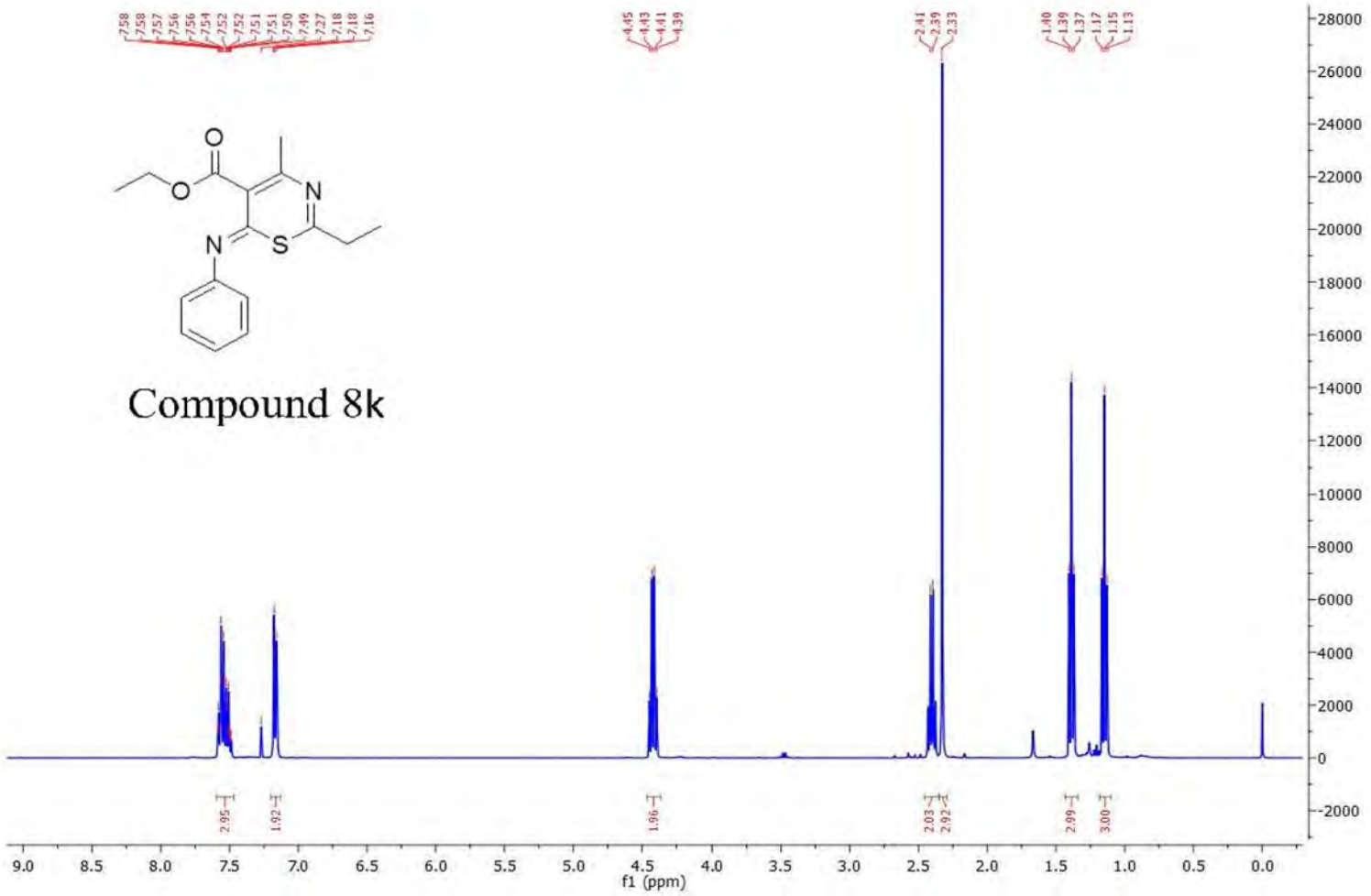
Compound 8k
f1 (ppm)

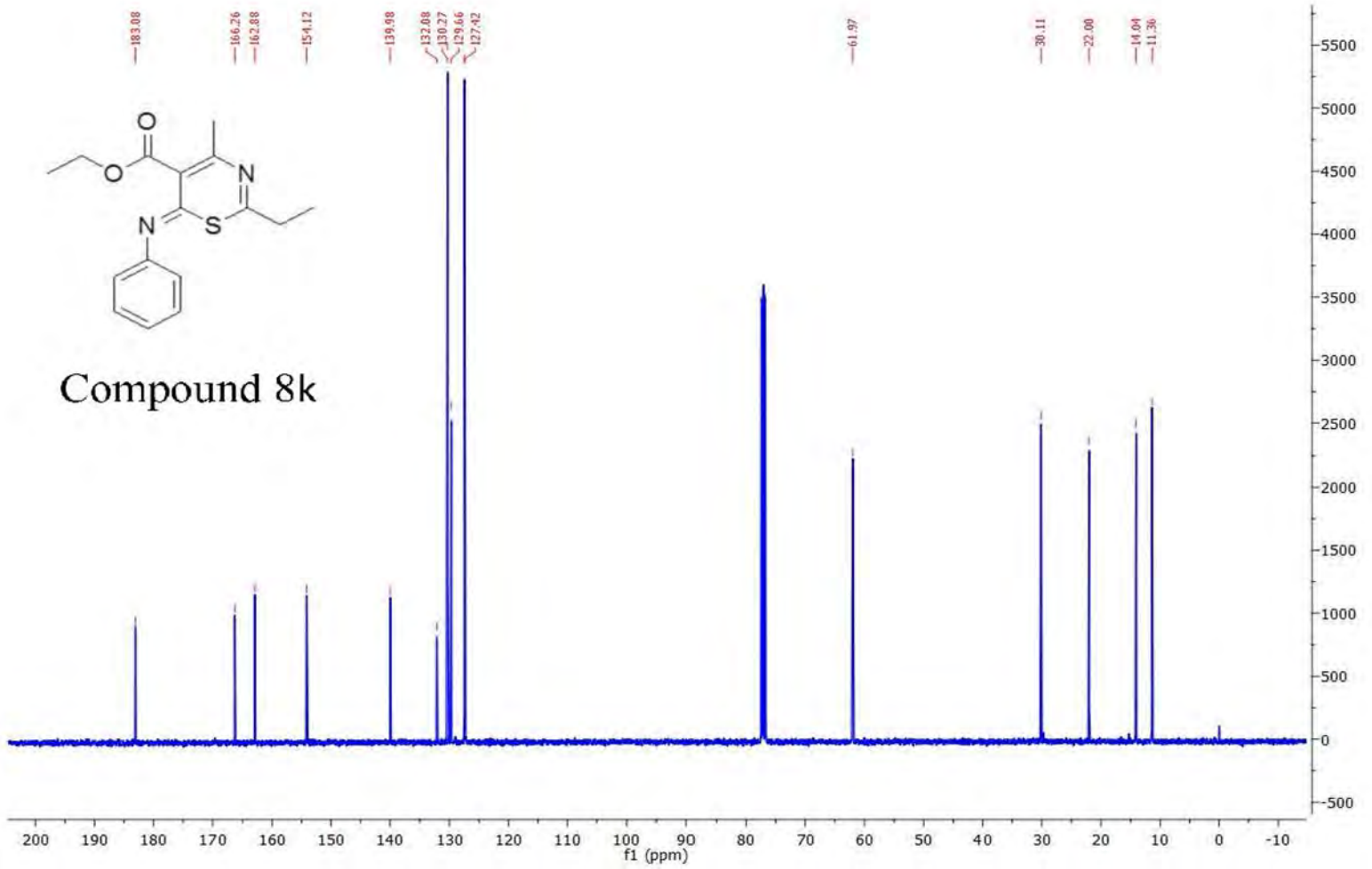
183.08
166.26
162.88
154.12
139.98
132.08
130.27
129.66
127.42
61.97
30.11
22.00
14.04
11.36
O
O
N
N
S
Compound 8k
5500
5000
4500
4000
3500
3000
2500
2000
1500
1000
500
0
-500
200 190 180 170 160 150 140 130 120 110 100 90 80 70 60 50 40 30 20 10 0 -10
f1 (ppm)

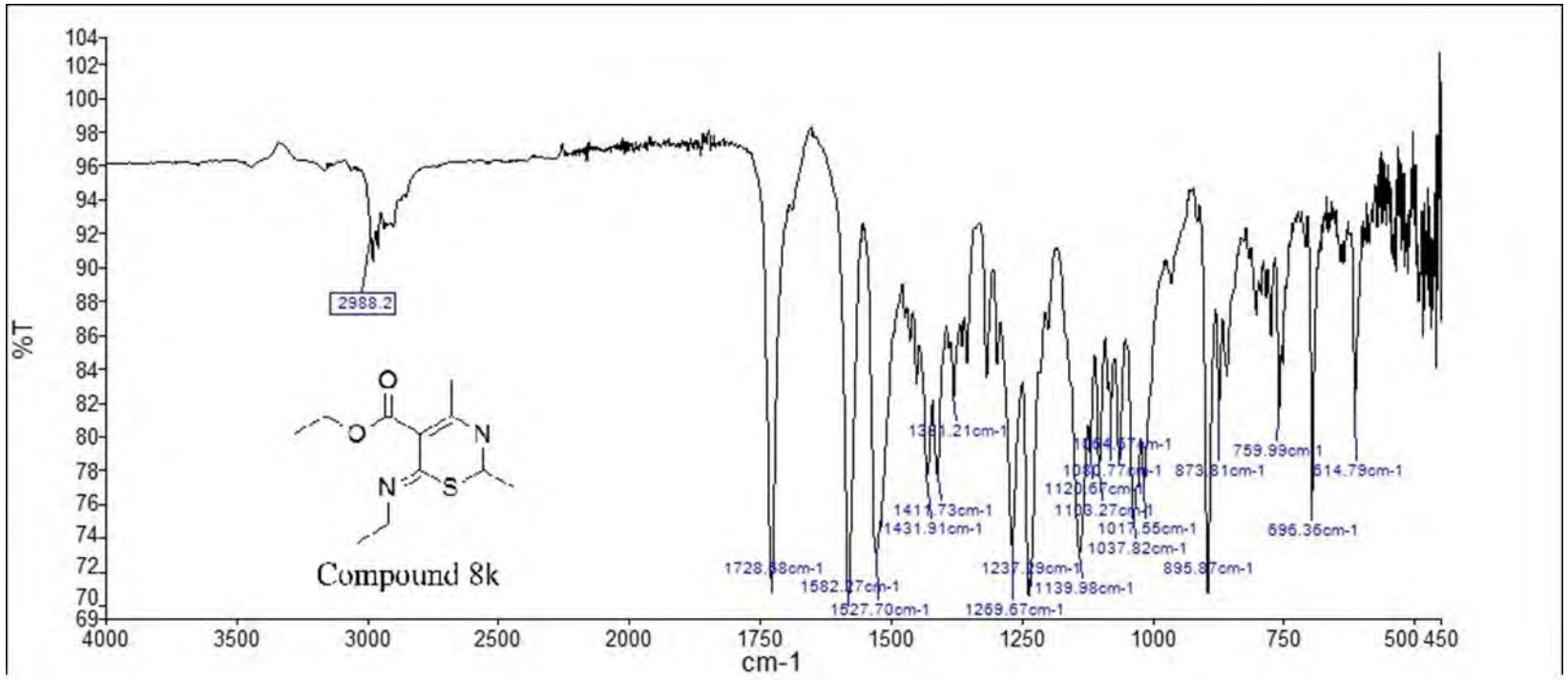
%T
cm-1
2988.2
1728.88cm-1
1582.07cm-1
1527.70cm-1
1431.91cm-1
1411.73cm-1
1269.67cm-1
1139.98cm-1
1037.82cm-1
1017.55cm-1
895.87cm-1
759.99cm-1
696.36cm-1
Compound 8k

==== Shimadzu LCMSsolution Analysis Report ====

Acquired by	: Admin
Sample Name	: TP96B5 Re
Sample ID	:
Vail #	: 54
Injection Volume	: 20 uL
Data File Name	: TP96B5 Re.lcd
Method File Name	: Platinum C18 EPS 3u lot 561094 part 50573 53mm id 7mm.lcm
Batch File Name	: Batch Second pro.lcb
Report File Name	: DefaultLCMS.lcr
Data Acquired	: 8/11/2015 6:11:28 PM
Data Processed	: 8/12/2015 2:49:25 PM

<Chromatogram>

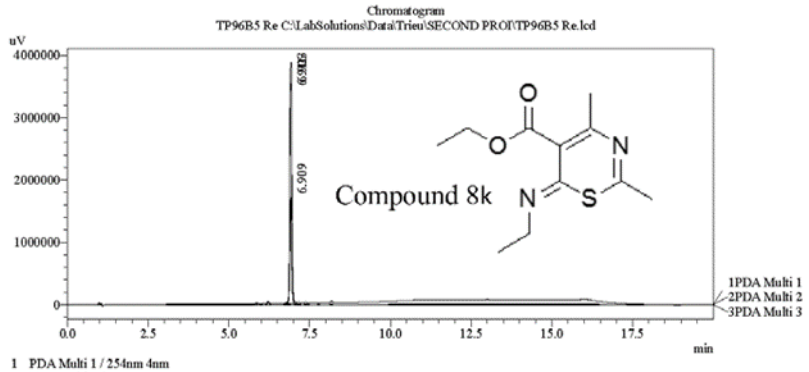

1 PDA Multi 1 / 254nm 4nm
2 PDA Multi 2 / 328nm 4nm
3 PDA Multi 3 / 220nm 4nm

PeakTable

PDA Ch1 254nm 4nm

Peak#	Ret. Time	Area	Height	Area %	Height %
1	6.909	6310514	1714955	100.000	100.000
Total		6310514	1714955	100.000	100.000

PeakTable

PDA Ch2 328nm 4nm

Peak#	Ret. Time	Area	Height	Area %	Height %
1	6.916	15430658	3548053	100.000	100.000
Total		15430658	3548053	100.000	100.000

PeakTable

PDA Ch3 220nm 4nm

Peak#	Ret. Time	Area	Height	Area %	Height %
1	6.923	18715655	3868330	100.000	100.000
Total		18715655	3868330	100.000	100.000

==== Shimadzu LCMSsolution Data Report ====

<Chromatogram>

Sample Information

Acquired by	: Admin
Date Acquired	: 8/12/2015 12:08:07 PM
Sample Type	: Unknown
Level#	: 0
Sample Name	: TP96B5 Re ESI +
Sample ID	:
ISTD Amount	: (Level1 Conc.)
Sample Amount	: 1
Dilution Factor	: 1
Tray#	: 1
Vial#	: 54
Injection Volume	: 5
Data File	: TP96B5 Re ESI +.lcd
Method File	: FIA-ESI_Scan(+).lcm
Original Method	: C:\LabSolutions\Data\Trieu\Mass spec files\FIA-ESI_Scan(+).lcm
Report Format	: DefaultLCMS.lcr
Tuning File	: C:\LabSolutions\LCsolution\Log\Tuning\Autotune_030908.lct
Processed by	: Admin
Modified Date	: 8/12/2015 12:10:08 PM

Compound 8k

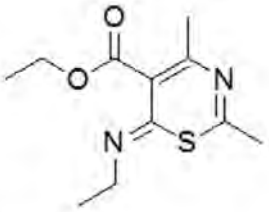

Chromatogram
TP96B5 Re ESI + C:\LabSolutions\Data\Trieu\SECOND PROI\Mass\TP96B5 Re ESI +.lcd

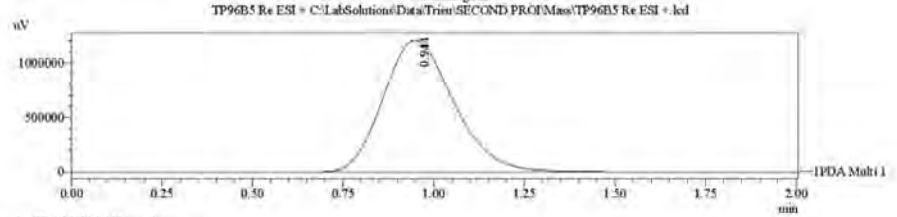

1 PDA Multi 1 / 254nm 4nm

<Spectrum>

Retention Time:1.300(Scan#:131)
Mnc Peak:483 Base Peak:302.55(1706321)
Spectrum:Averaged 0.980-1.700(99-171)
Background:Averaged 0.140-0.472(15-49) Polarity:Pos Segment1 - Event1

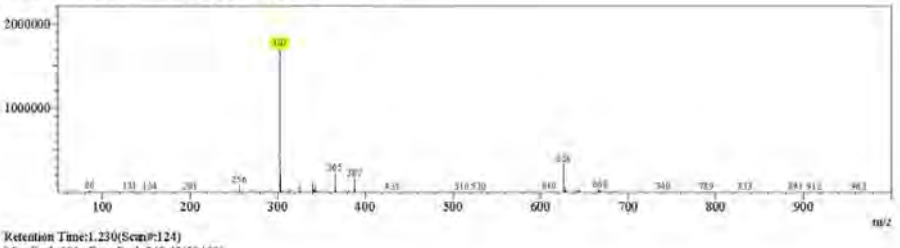

Retention Time:1.230(Scan#:124)
Mnc Peak:684 Base Peak:248.45(58460)
Spectrum:Averaged 0.990-1.710(100-172)
Background:Averaged 0.150-0.472(16-50) Polarity:Neg Segment1 - Event2

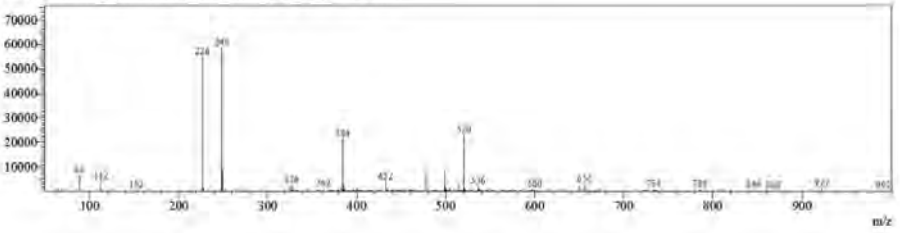

C:¥LabSolutions¥Data¥Trieu¥SECOND PROI¥Mass¥TP96B5 Re ESI +.lcd

Compound	Chemical Formula	Predicted monoisotopic neutral MW	Predicted MH+	MH+ Measured	Main MS Ions	Main MS/MS Fragments
8k	$C_{16}H_{18}N_2O_{2S}$	302.1089	303.1162	303.1157		257.0742
					303.1158	132.0809
						275.0849

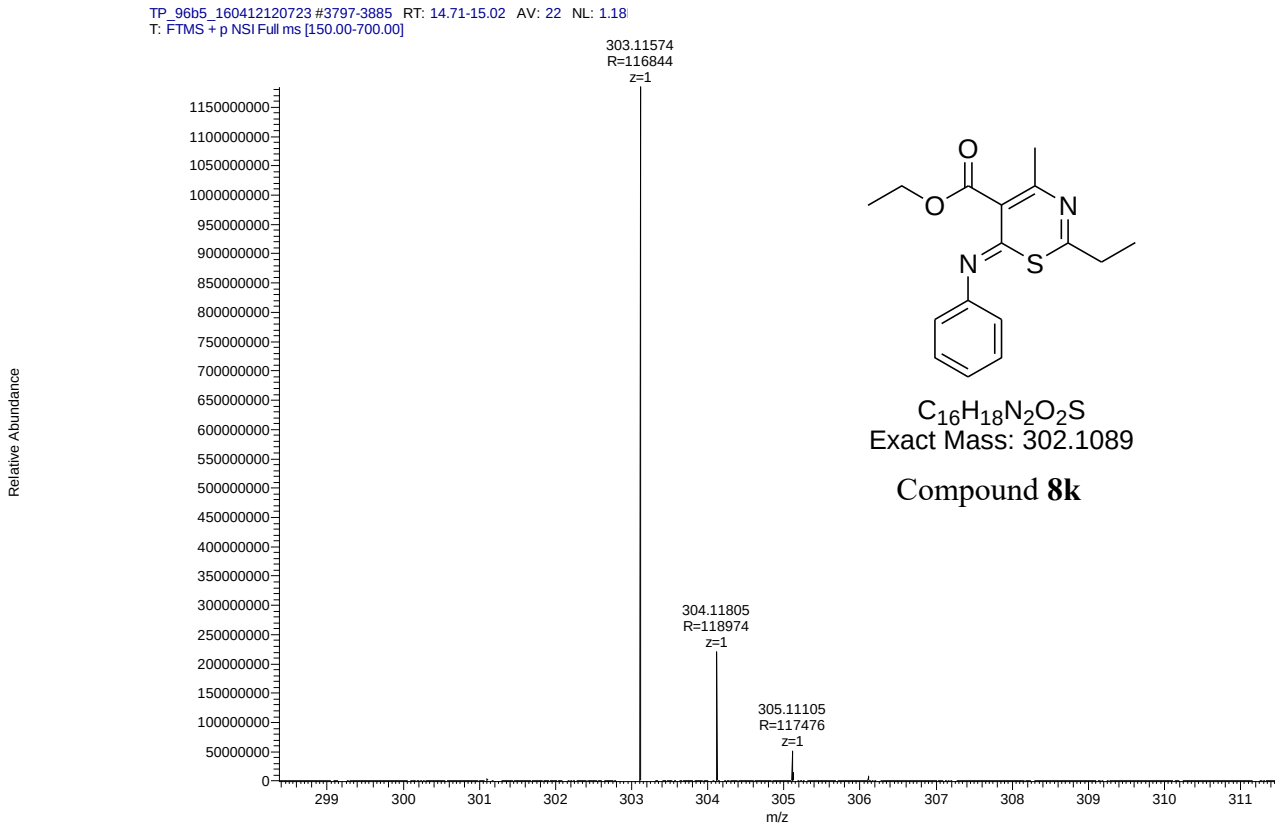

Compound **8l**

Compound Name: 4-Methyl-2-phenyl-6-phenylimino-6*H*-[1,3]thiazine-5-carboxylic acid ethyl ester

Obtained Weight & Yield: 30 mg, 21%

Appearance: Yellow precipitate

Solubility: MeOH, ACN, Acetone

Melting Point: 252-252.5 ºC

TLC Conditions: EtOAc/n-Hexane (50/50)

IR Analysis:

2982 (CH), 1725 (COO), 1231 (CO)

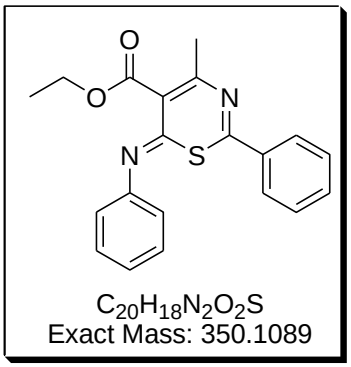

^{1}H NMR Analysis:

^{1}H NMR (400 MHz, $CDCl_3$) δ 7.35 – 7.17 (m, 8H), 7.15 – 7.03 (m, 2H), 4.47 (q, *J* = 7.1 Hz, 2H), 2.40 (s, 3H), 1.42 (t, *J* = 7.1 Hz, 3H).

^{13}C NMR Analysis:

^{13}C NMR (400 MHz, $CDCl_3$) δ 183.2, 166.1, 159.7, 153.8, 140.1, 134.5, 132.9, 129.9, 129.3 (Cx2), 129.2, 128.9 (Cx2), 128.7 (Cx2), 128.1 (Cx2), 62.2, 22.0, 14.1.

HPLC:

RP-HPLC Alltima™ C18 5 µm 150 mm x 4.6 mm, 10-100% B in 15 min, R_t = 7.26 min, 100%.

Mass Spectral Analysis: LRMS (ESI+) m/z: 350, 350 $[M]^+$ 100%. HRMS (ES+) for $C_{20}H_{18}N_2O_2S$ calculated 351.1162, found 351.1157.

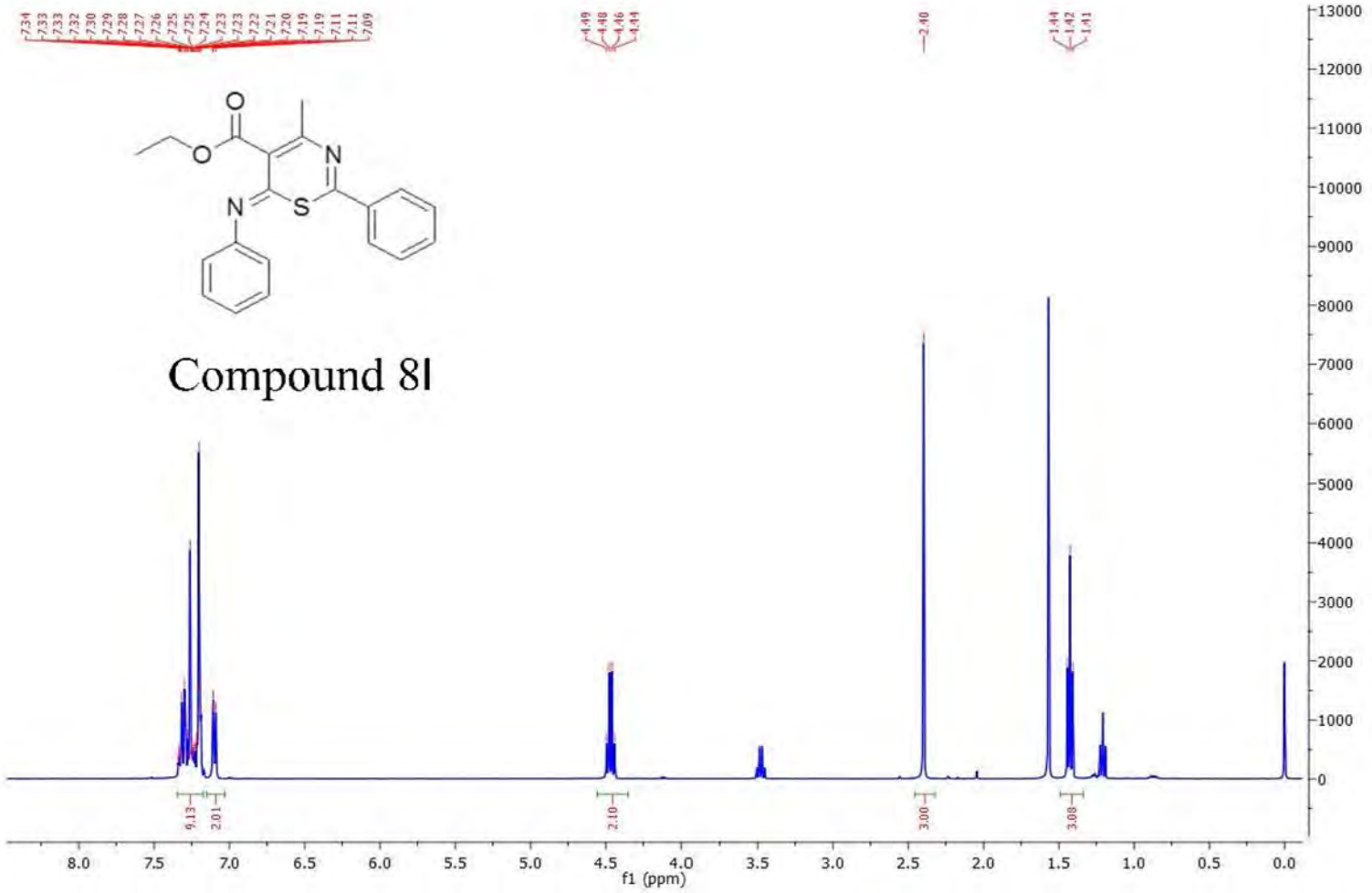
Compound 8l
f1 (ppm)

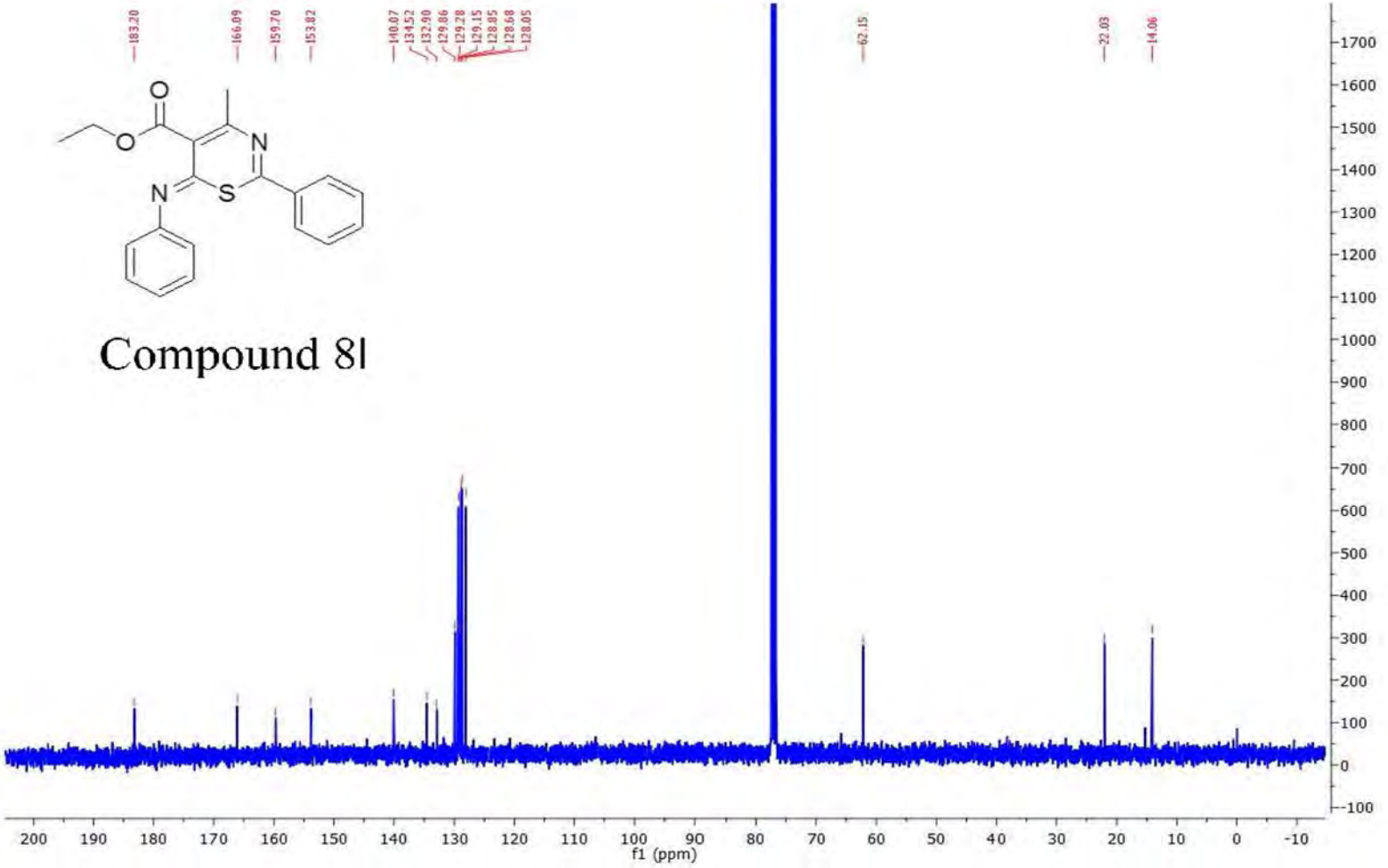
183.20
166.09
159.70
153.82
140.07
134.52
132.90
129.86
129.28
129.15
128.85
128.68
128.05
62.15
22.03
14.06
O
O
N
N
S
Compound 8l
f1 (ppm)

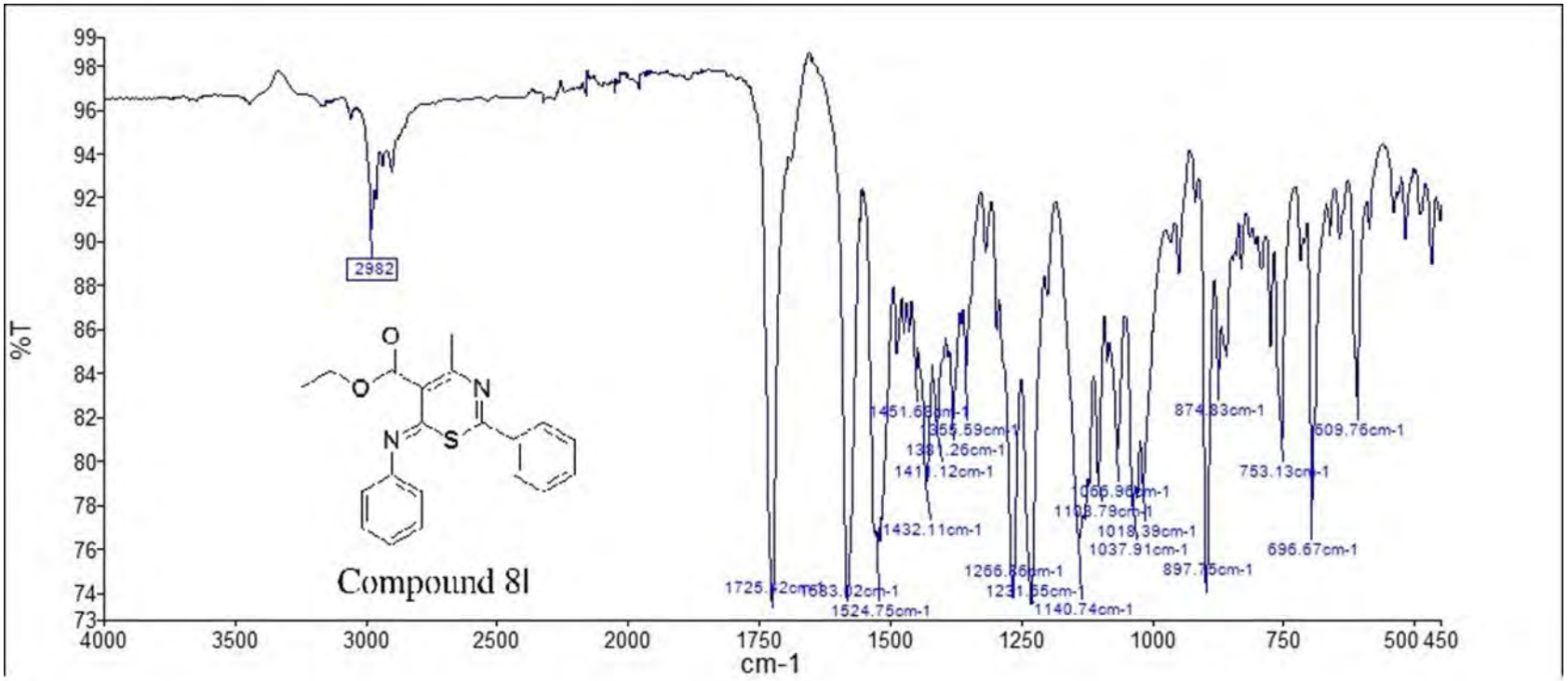
%T
cm-1
2982
1725.42cm-1
1683.02cm-1
1524.75cm-1
1451.68cm-1
1355.59cm-1
1381.26cm-1
1411.12cm-1
1432.11cm-1
1266.76cm-1
1231.55cm-1
1140.74cm-1
1103.79cm-1
1066.96cm-1
1018.39cm-1
1037.91cm-1
897.75cm-1
874.83cm-1
753.13cm-1
696.67cm-1
609.76cm-1
Compound 8l

==== Shimadzu LCMSsolution Analysis Report ====

Acquired by	: Admin
Sample Name	: TP21B5 Re
Sample ID	:
Vail #	: 51
Injection Volume	: 20 uL
Data File Name	: TP21B5 Re.lcd
Method File Name	: Platinum C18 EPS 3u lot 561094 part 50573 53mm id 7mm.lcm
Batch File Name	: Batch Second pro.lcb
Report File Name	: DefaultLCMS.lcr
Data Acquired	: 8/11/2015 5:10:06 PM
Data Processed	: 8/12/2015 1:39:29 PM

<Chromatogram>

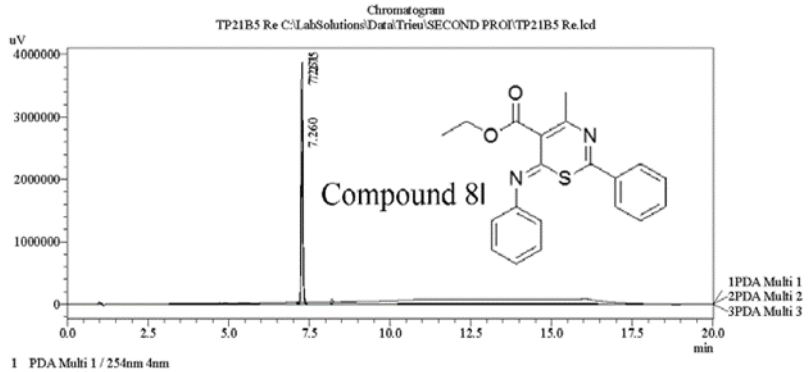

1 PDA Multi 1 / 254nm 4nm
2 PDA Multi 2 / 328nm 4nm
3 PDA Multi 3 / 220nm 4nm

PeakTable

PDA Ch1 254nm 4nm

Peak#	Ret. Time	Area	Height	Area %	Height %
1	7.261	10531364	3430838	100.000	100.000
Total		10531364	3430838	100.000	100.000

PeakTable

PDA Ch2 328nm 4nm

Peak#	Ret. Time	Area	Height	Area %	Height %
1	7.260	7278852	2441554	100.000	100.000
Total		7278852	2441554	100.000	100.000

PeakTable

PDA Ch3 220nm 4nm

Peak#	Ret. Time	Area	Height	Area %	Height %
1	7.275	17293760	3862225	100.000	100.000
Total		17293760	3862225	100.000	100.000

==== Shimadzu LCMSsolution Data Report ====

<Chromatogram>

Sample Information

Acquired by	: Admin
Date Acquired	: 8/12/2015 11:57:49 AM
Sample Type	: Unknown
Level#	: 0
Sample Name	: TP21B5 Re ESI +
Sample ID	:
ISTD Amount	: (Level1 Conc.)
Sample Amount	: 1
Dilution Factor	: 1
Tray#	: 1
Vial#	: 51
Injection Volume	: 5
Data File	: TP21B5 Re ESI +.lcd
Method File	: FIA-ESI_Scan(+).lcm
Original Method	: C:\LabSolutions\Data\Trieu\Mass spec files\FIA-ESI_Scan(+).lcm
Report Format	: DefaultLCMS.lcr
Tuning File	: C:\LabSolutions\LCsolution\Log\Tuning\Autotune_030908.lct
Processed by	: Admin
Modified Date	: 8/12/2015 11:59:20 AM

Compound 8l

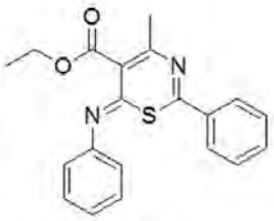

Chromatogram

TP21B5 Re ESI - C:\LabSolutions\Data\Trieu\SECOND PROJ\Mass\TP21B5 Re ESI +.lcd

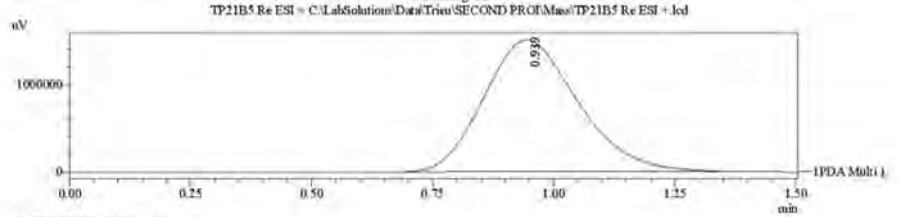

1 PDA Multi 1 / 254nm 4nm

<Spectrum>

Retention Time:1.220(Scan#:123)
Max Peak:455 Base Peak:350.40(1774195)
Spectrum:Averaged 0.960-1.440(97-145)
Background:Averaged 0.120-0.378(13-39) Polarity:Pos Segment1 - Event1

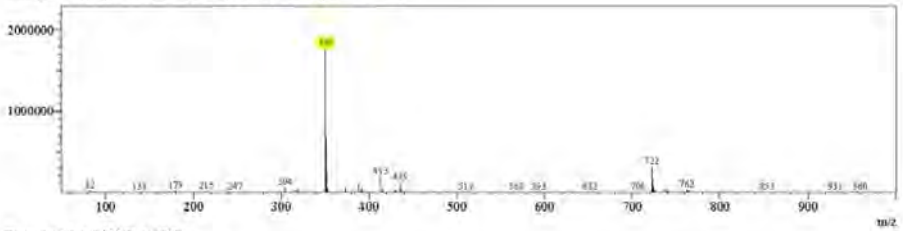

Retention Time:1.270(Scan#:128)
Max Peak:644 Base Peak:248.50(106203)
Spectrum:Averaged 0.970-1.450(98-146)
Background:Averaged 0.130-0.378(14-40) Polarity:Neg Segment1 - Event2

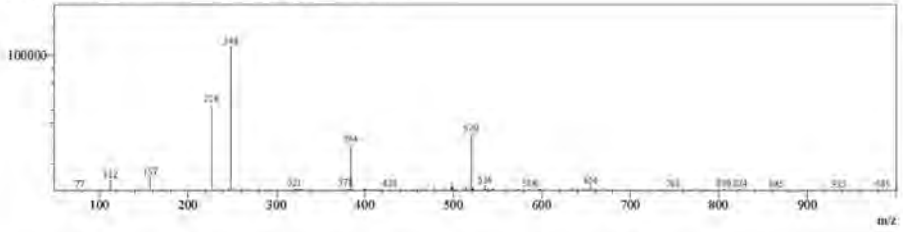

C:¥LabSolutions¥Data¥Trieu¥SECOND PROJ¥Mass¥TP21B5 Re ESI +.lcd

Compound	Chemical Formula	Predicted monoisotopic neutral MW	Predicted MH+	MH+ Measured	Main MS Ions	Main MS/MS Fragments
8l	$C_{20}H_{18}N_2O_2S$	350.1089	351.1162	351.1157		305.0740
					351.1157	323.0847
						180.0807

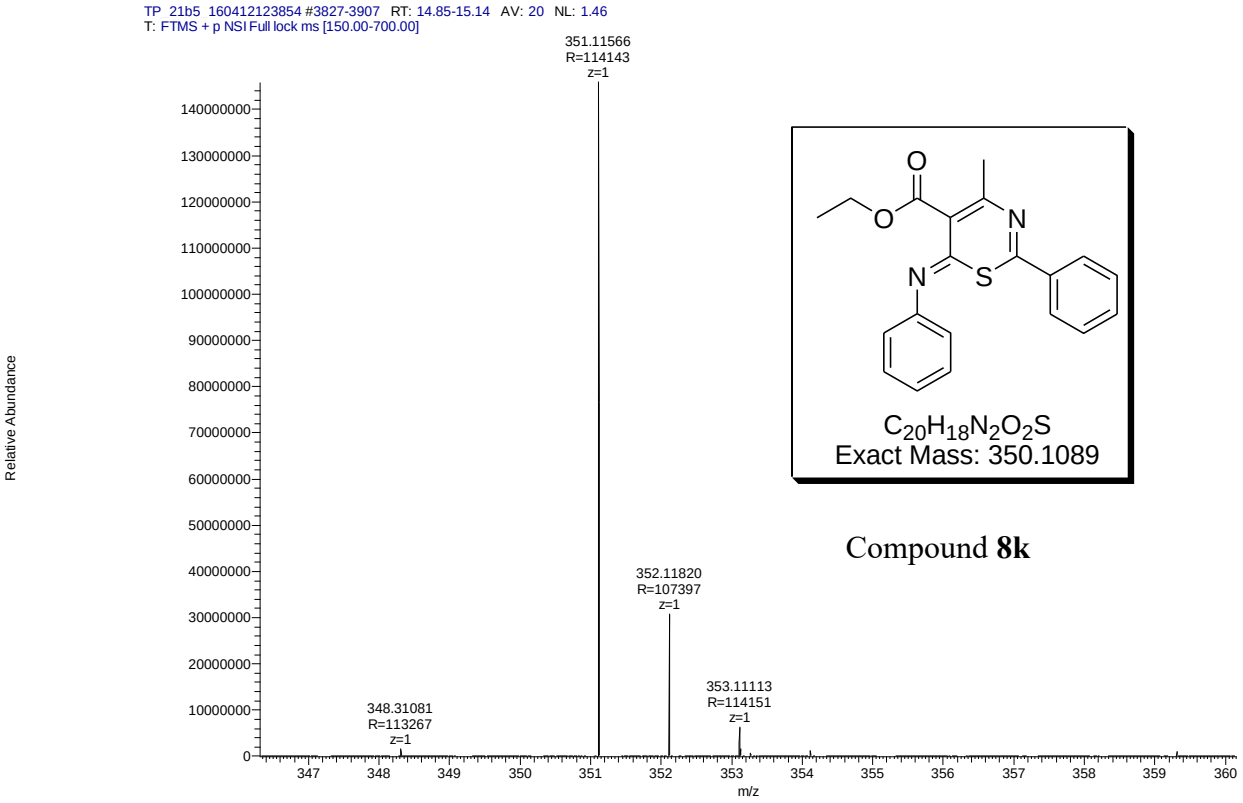

Compound **8k**

Compound **8m**

Compound Name: 4-Methyl-6-phenylimino-2-trifluoromethyl-6*H*-[1,3]thiazine-5-carboxylic acid ethyl ester

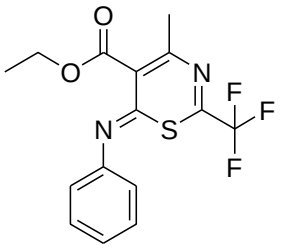

$C_{15}H_{13}F_3N_2O_2S$
Exact Mass: 342.0650

Obtained Weight & Yield: 60 mg, 12%

Appearance: Yellow precipitate

Solubility: MeOH, ACN, Acetone

Melting Point: 101.2-102.6 °C

TLC Conditions: EtOAc/n-Hexane (50/50)

IR Analysis: IR (cm-1): 2982 (CH), 1733 (COO), 1225 (CO)

^{1}H NMR Analysis:

^{1}H NMR (400 MHz, $CDCl_3$) δ 7.61 – 7.47 (m, 3H), 7.22-7.16 (m, 2H), 4.43 (q, *J* = 7.1 Hz, 2H), 2.38 (s, 3H), 1.39 (t, *J* = 7.1 Hz, 3H).

^{13}C NMR Analysis:

^{13}C NMR (101 MHz, CDCl3) δ 184.2, 164.9, 151.6, 146.4, 146.0, 137.0, 135.9, 130.5, 129.6, 129.0, 128.5, 128.5, 124.0, 121.5, 121.4, 121.1, 118.6, 115.9, 62.4, 21.6, 14.0.

HPLC: RP-HPLC Alltima™ C18 5 µm 150 mm x 4.6 mm, 10-100% B in 15 min, R_t = 7.48 min, 92%.

Mass Spectral Analysis: LRMS (ESI+) m/z: 342, 342 $[M]^+$ 100%. HRMS (ES+) for $C_{15}H_{13}F_3N_2O_2S$, calculated 343.0723, found 343.0721

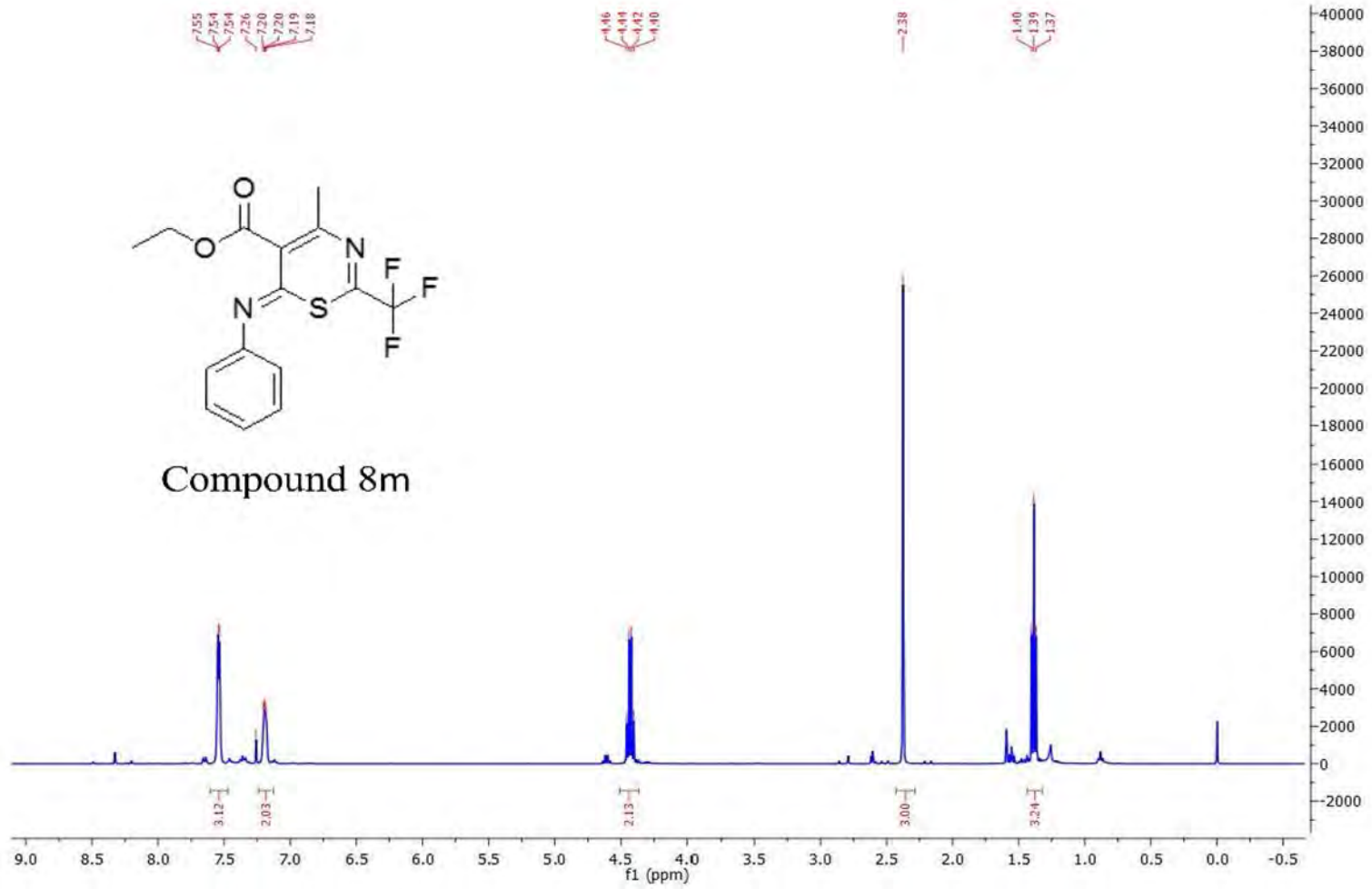
7.55
7.54
7.54
7.26
7.20
7.20
7.19
7.18
4.46
4.44
4.42
4.40
2.38
1.40
1.39
1.37
O
O
N
F
F
F
N
S
Compound 8m
3.12
2.03
2.13
3.00
3.24
f1 (ppm)

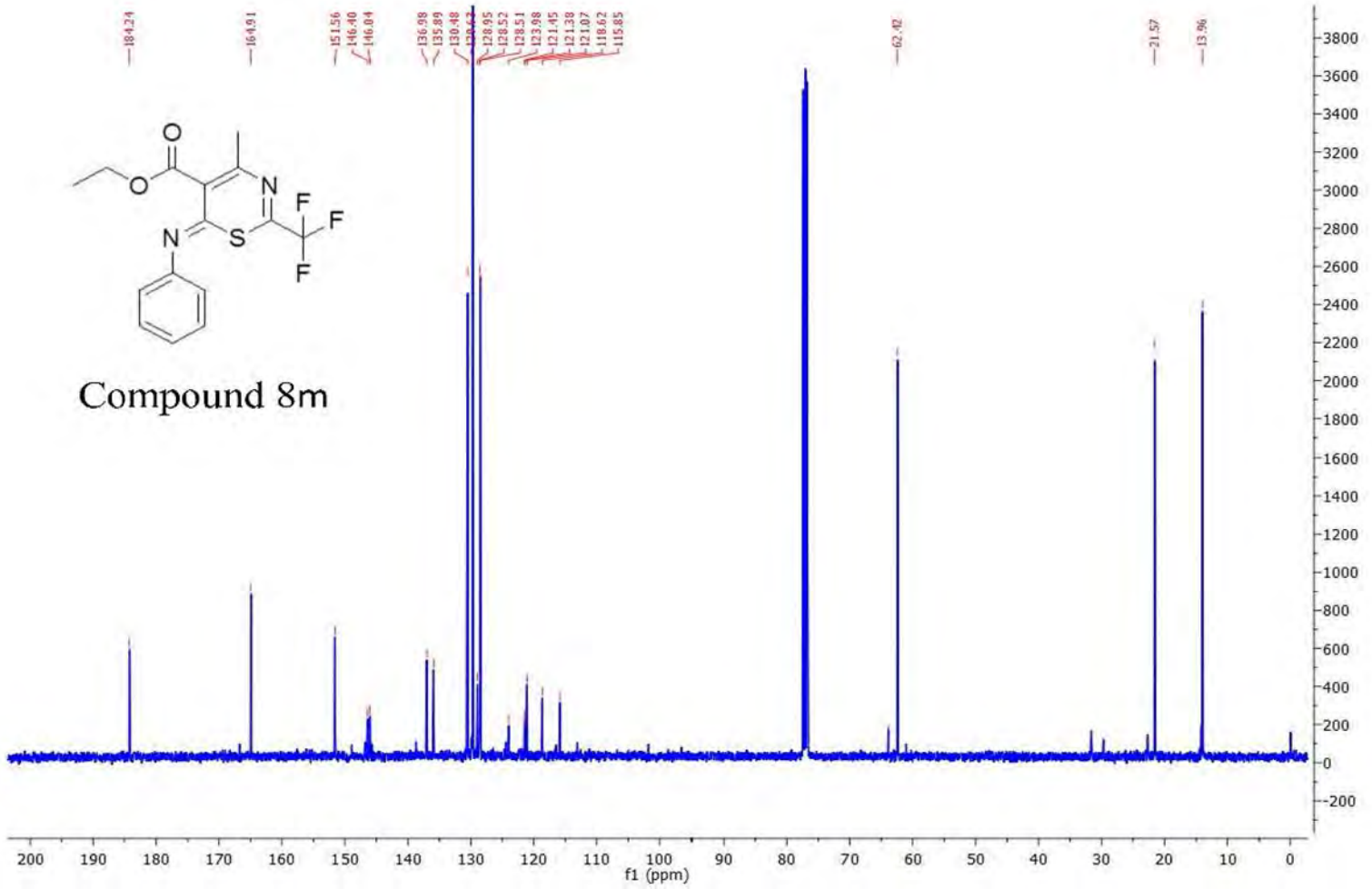
184.24
164.91
151.56
146.40
146.04
136.98
135.89
130.48
128.95
128.52
128.51
123.98
121.45
121.38
121.07
118.62
115.85
62.42
21.57
13.96
O
O
N
F
F
F
N
S
Compound 8m
f1 (ppm)

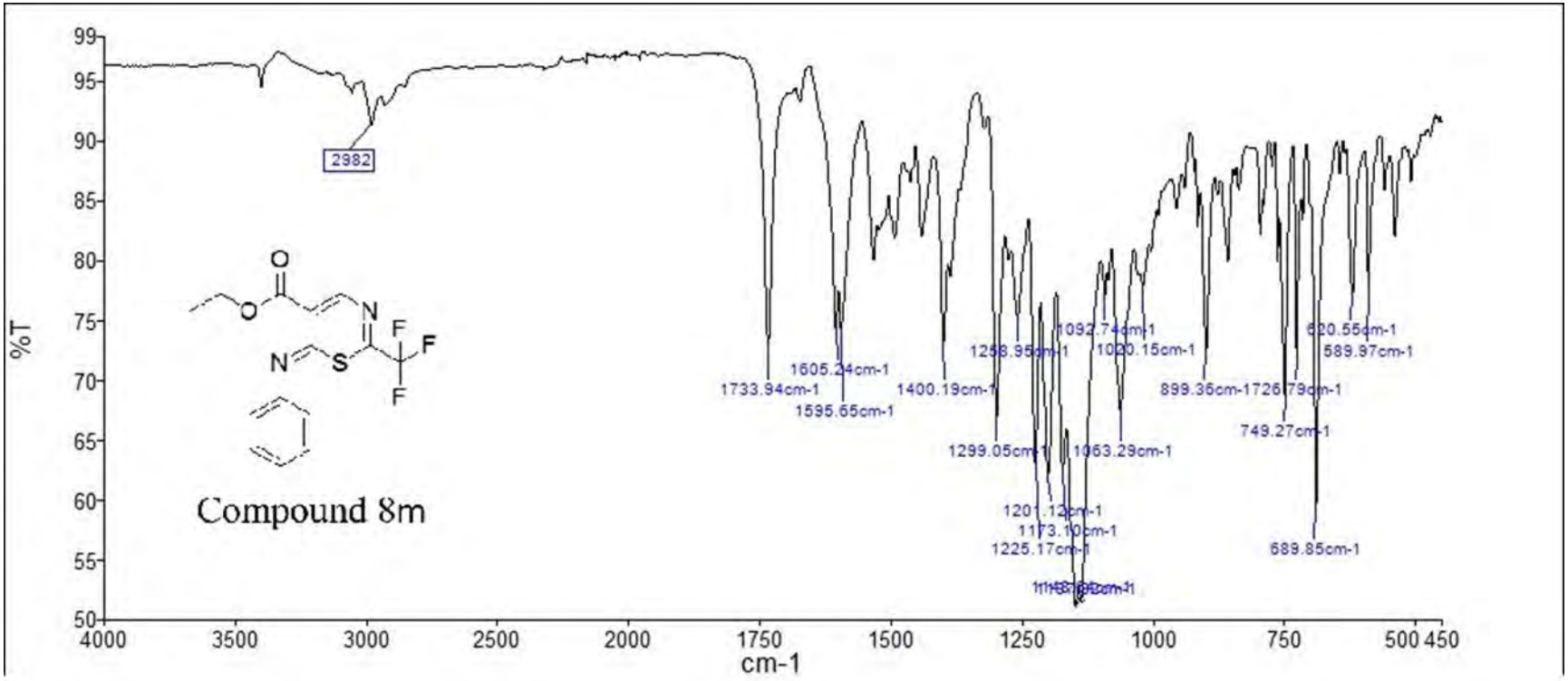
2982
1733.94cm-1
1605.24cm-1
1595.65cm-1
1400.19cm-1
1299.05cm-1
1092.74cm-1
1020.15cm-1
963.29cm-1
899.36cm-1
749.27cm-1
689.85cm-1
620.55cm-1
589.97cm-1
Compound 8m
%T
cm-1

==== Shimadzu LCMSsolution Analysis Report ====

Acquired by	: Admin
Sample Name	: TP92B5 product
Sample ID	:
Vail #	: 64
Injection Volume	: 50 uL
Data File Name	: TP92B5 product.lcd
Method File Name	: Platinum C18 EPS 3u lot 561094 part 50573 53mm id 7mm.lcm
Batch File Name	: Batch Second pro.lcb
Report File Name	: DefaultLCMS.lcr
Data Acquired	: 8/12/2015 1:36:54 PM
Data Processed	: 8/12/2015 2:26:01 PM

<Chromatogram>

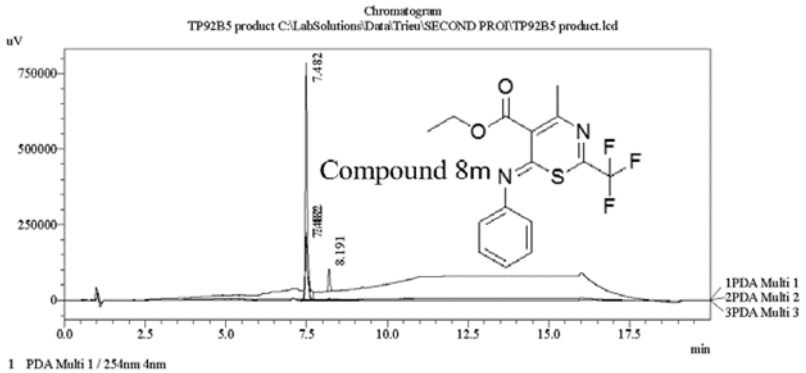

1 PDA Multi 1 / 254nm 4nm
2 PDA Multi 2 / 328nm 4nm
3 PDA Multi 3 / 220nm 4nm

PeakTable

PDA Ch1 254nm 4nm

Peak#	Ret. Time	Area	Height	Area %	Height %
1	7.482	1141897	212057	100.000	100.000
Total		1141897	212057	100.000	100.000

PeakTable

PDA Ch2 328nm 4nm

Peak#	Ret. Time	Area	Height	Area %	Height %
1	7.482	1053333	227658	100.000	100.000
Total		1053333	227658	100.000	100.000

PeakTable

PDA Ch3 220nm 4nm

Peak#	Ret. Time	Area	Height	Area %	Height %
1	7.482	3340928	784873	92.450	91.438
2	8.191	272841	73492	7.550	8.562
Total		3613770	858366	100.000	100.000

==== Shimadzu LCMSsolution Data Report ====

<Chromatogram>

Sample Information

Acquired by	: Admin
Date Acquired	: 8/12/2015 12:31:55 PM
Sample Type	: Unknown
Level#	: 0
Sample Name	: TP92B5 pro ESI +
Sample ID	:
ISTD Amount	: (Level1 Conc.)
Sample Amount	: 1
Dilution Factor	: 1
Tray#	: 1
Vial#	: 63
Injection Volume	: 3
Data File	: TP92B5 pro ESI +.lcd
Method File	: FIA-ESI_Scan(+).lcm
Original Method	: C:\LabSolutions\Data\Trieu\Mass spec files\FIA-ESI_Scan(+).lcm
Report Format	: DefaultLCMS.lcr
Tuning File	: C:\LabSolutions\LCsolution\Log\Tuning\Autotune_030908.lct
Processed by	: Admin
Modified Date	: 8/12/2015 12:33:56 PM

Compound 8m

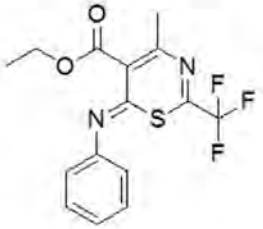

Chromatogram

TP92B5 pro ESI + C:\LabSolutions\Data\Trieu\SECOND PROJ\Mass\TP92B5 pro ESI +.lcd

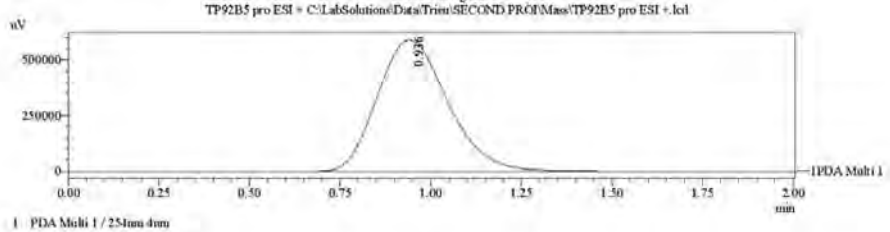

1 PDA Multi 1 / 254nm 4nm

<Spectrum>

Retention Time:1.280(Scan#:129)
Max Peak:565 Base Peak:342.45(439126)
Spectrum:Averaged 0.960-1.600(97-161)
Background:Averaged 0.080-0.555(9-57) Polarity:Pos Segment1 - Event1

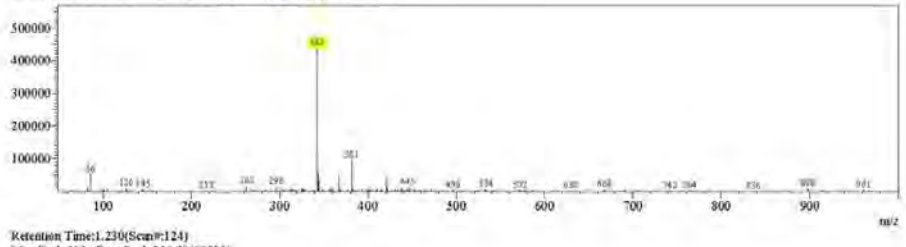

Retention Time:1.230(Scan#:124)
Max Peak:519 Base Peak:226.50(68528)
Spectrum:Averaged 0.970-1.610(98-162)
Background:Averaged 0.090-0.555(10-58) Polarity:Neg Segment1 - Event2

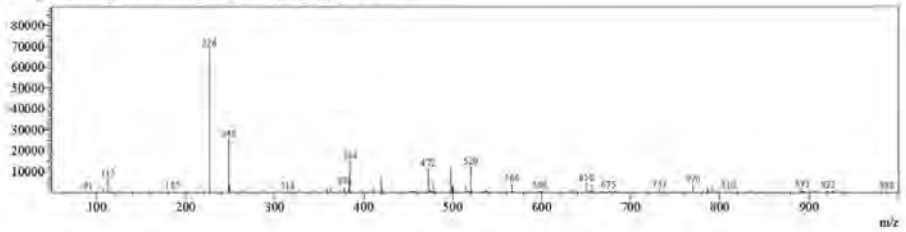

C:¥LabSolutions¥Data¥Trieu¥SECOND PROJ¥Mass¥TP92B5 pro ESI +.lcd

Compound	Chemical Formula	Predicted monoisotopic neutral MW	Predicted MH+	MH+ Measured	Main MS Ions	Main MS/MS Fragments
8m	$C_{15}H_{13}F_3N_2O_2S$	342.0650	343.0723	343.0721		315.0410
					224.0713	297.0304
						132.0446

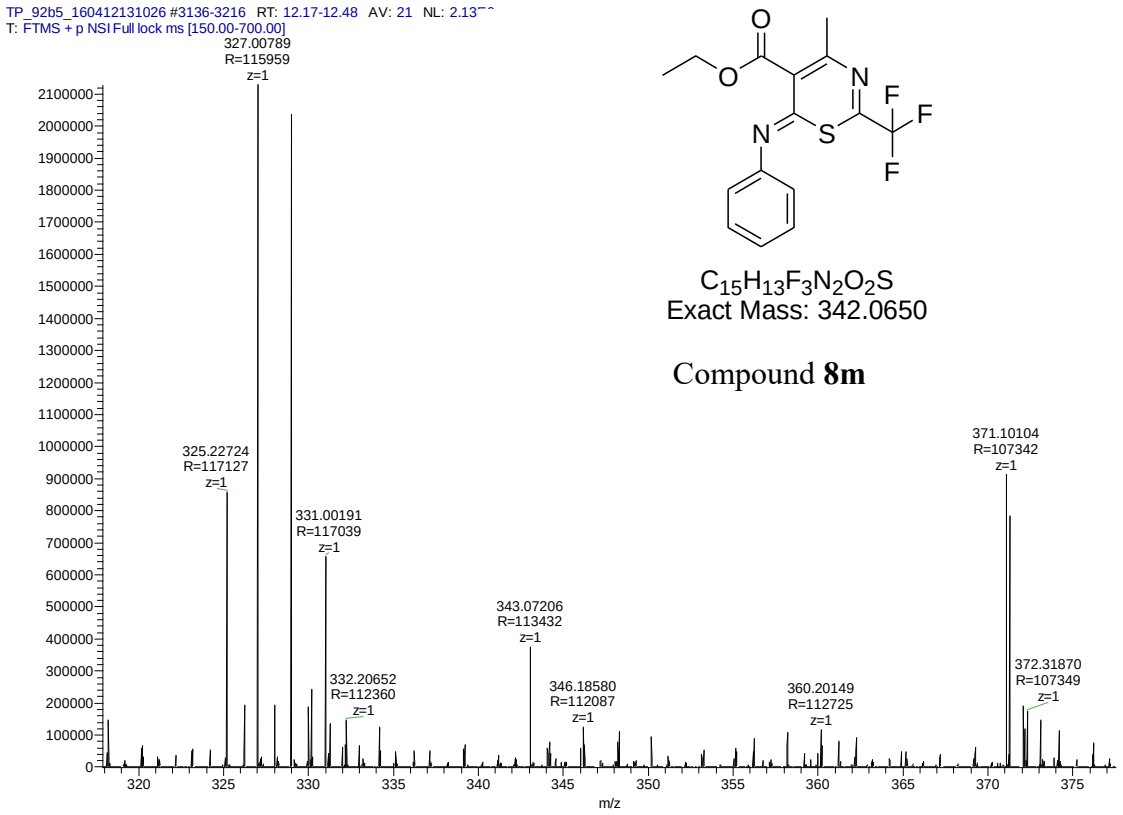

Compound **10a**

Compound Name: Ethyl (*E*)-3-benzamido-2-(phenylcarbamothioyl)but-2-enoate

Obtained Weight & Yield: 248 mg, 28%

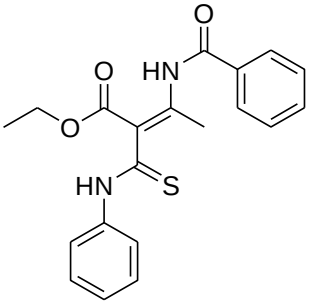

Appearance: Sparkling yellow precipitate

Solubility: MeOH, Acetone, ACN

TLC Conditions: EtOAc/Hexane (50/50)

IR Analysis: νmax/cm^{-1}
3185 (NH), 1697 (COO), 1665 (CON), 1234 (CO)

$C_{20}H_{20}N_2O_3S$
Exact Mass: 368.1195

The product is detected as a mixture of isomers, with the ration 2.3 : 1.0 calculated at 2.68 and 2.65 ppm, respectively. The 1H NMR is reported as a whole due to complex overlapping. All 13C NMR peaks are reported

^{1}H NMR Analysis:
^{1}H NMR (400 MHz, $CDCl_3$) δ 12.49 (d, J = 8.2 Hz, 1H), 10.03 (d, *J* = 46.0 Hz, 1H), 7.91 (dd, *J* = 10.6, 4.5 Hz, 3H), 7.61 – 7.04 (m, 7H), 4.19 – 3.90 (m, 2H), 2.66 (d, *J* = 11.6 Hz, 3H), 1.19 (dt, *J* = 14.5, 7.1 Hz, 3H).

^{13}C NMR Analysis:
^{13}C NMR (101 MHz, $CDCl_3$) δ 198.7, 194.3, 166.9, 166.6, 166.2, 165.8, 153.0, 151.4, 139.0, 138.4, 133.9, 133.6, 132.8, 132.6, 130.1, 129.5, 129.1 (C x 2), 129.0 (C x 2), 128.9, 128.8, 128.5, 127.7, 127.6 (C x 2), 127.3, 127.0, 123.0, 122.9 (C x 2), 116.3, 111.0, 61.3, 61.3, 19.4, 18.8, 14.1, 14.0.

RP-UPLC Agilent Zorbax SB™ C18 1.8 µm 50 mm x 2.1 mm, isocratic 50% B (9:1 ACN: Water) in 6 min, R_t = 4.1 min, 100% at 210, 254 and 320 nm.

Mass Spectral Analysis: LRMS (ESI+) m/z: 368, 369 [M+ H]+ 100%. HRMS (ES+) for $C_{20}H_{20}N_2O_3S$ calculated 369.1267, found 369.1270.

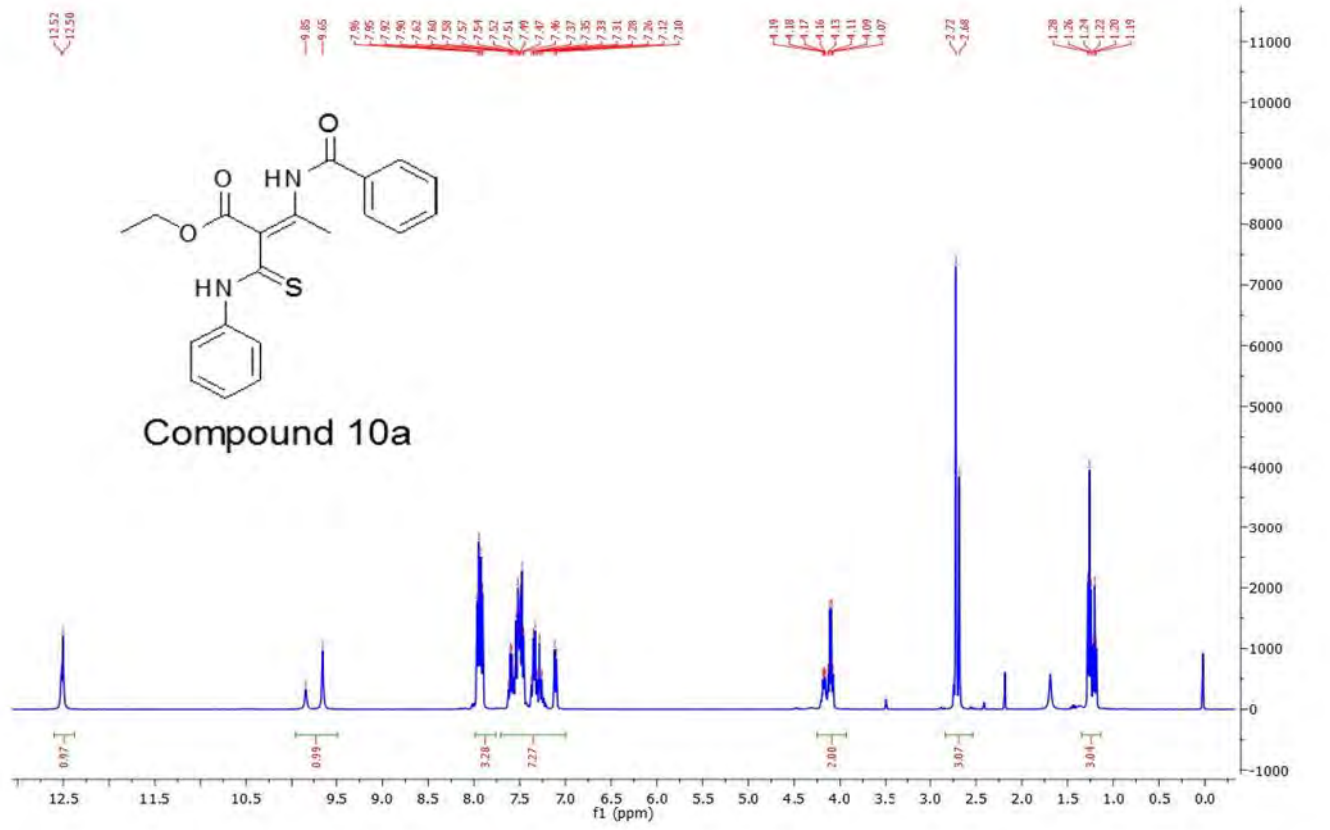
Compound 10a
f1 (ppm)

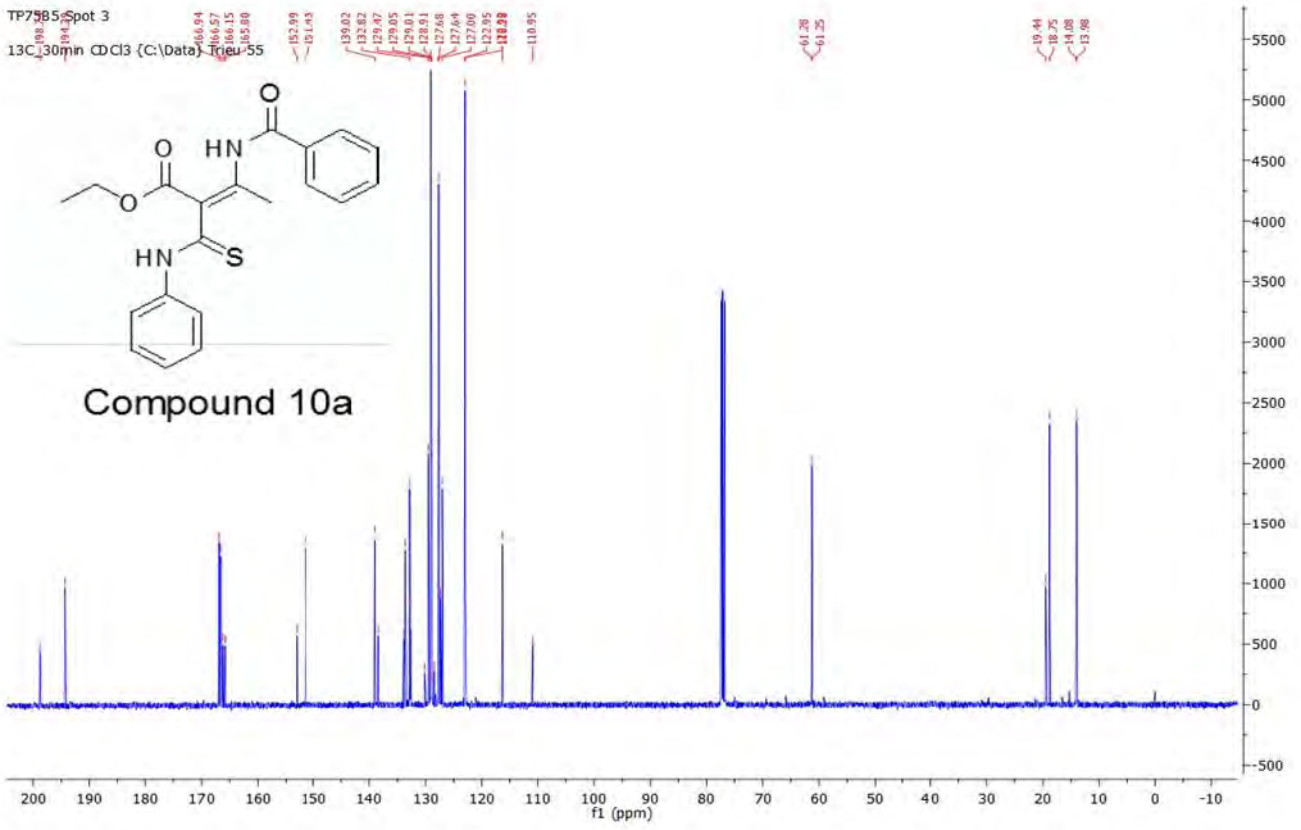
TP7585-Spot 3
13C_30min CDCl3 (C:\Data) Trieu-55
Compound 10a
f1 (ppm)

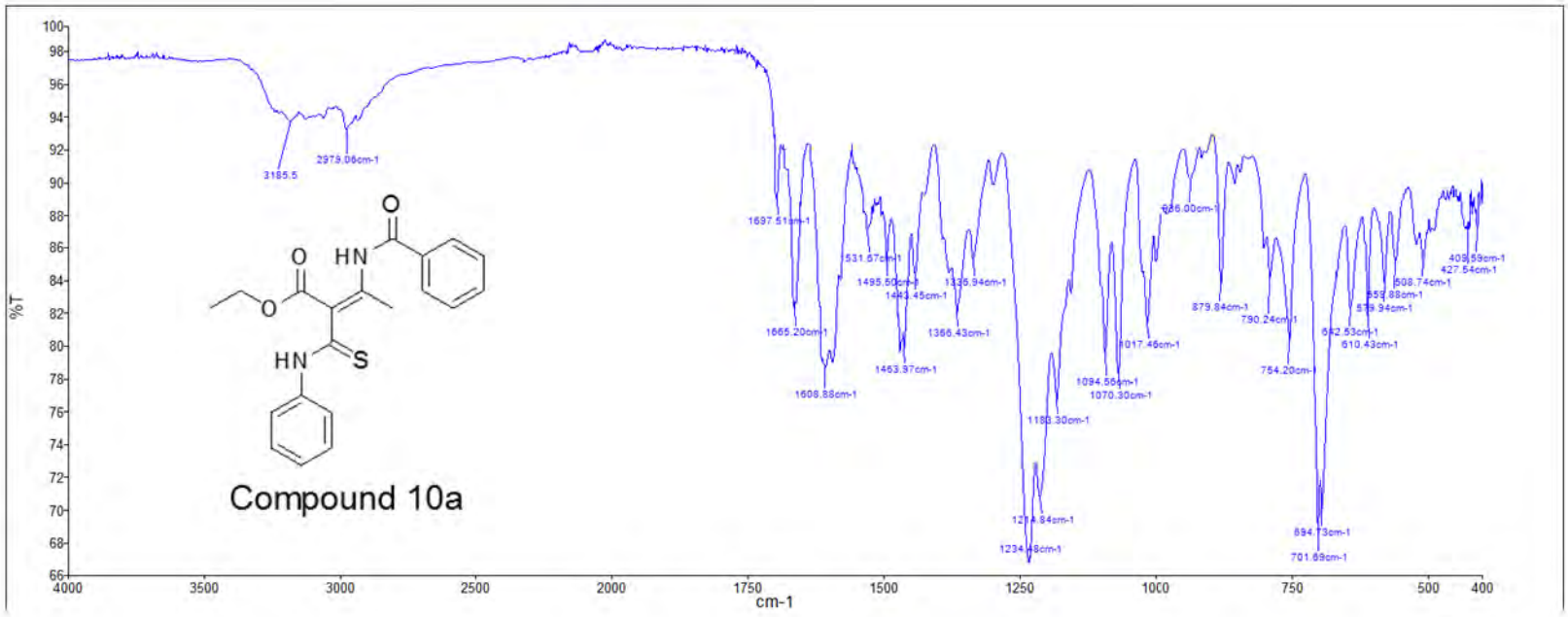
%T
cm-1
Compound 10a
3185.5
2979.06cm-1
1697.51cm-1
1665.20cm-1
1608.88cm-1
1531.67cm-1
1495.50cm-1
1463.97cm-1
1443.45cm-1
1366.43cm-1
1335.94cm-1
1180.30cm-1
1094.56cm-1
1070.30cm-1
1017.46cm-1
986.00cm-1
879.84cm-1
790.24cm-1
754.20cm-1
642.53cm-1
610.43cm-1
559.94cm-1
559.88cm-1
508.74cm-1
427.54cm-1
894.73cm-1
701.69cm-1

LCMS Report

Agilent Technologies

Data file:	D:\Chem32\1\Data\TP 2016-02-17 15-45-21\043-0101.D		
Sample name:	TP75B5		
Description:			
Sample amount:	0.000	Sample type:	Sample
Instrument:	LCMS	Location:	43
Injection date:	2/17/2016 3:47:04 PM	Injection:	1 of 1
Acq. method:	LCMS ISOCRATIC 50% B.M	Injection volume:	1.000
Analysis method:	LCMS ISOCRATIC 50%B.M	Acq. operator:	SYSTEM
Last changed:	2/17/2016 2:13:42 PM		

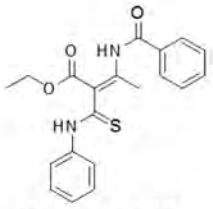

Compound 10a

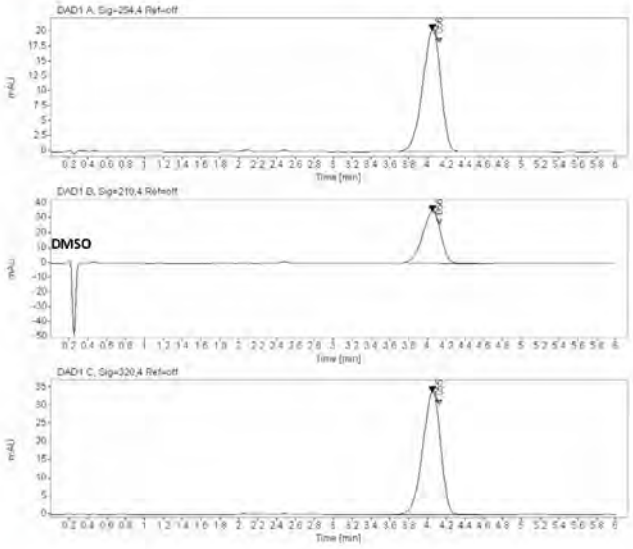

Signal: DAD1 A, Sig=254,4 Ref=off

RT [min]	Type	Width [min]	Area	Height	Area%	Name
4.056	BB	0.2114	275.4112	20.4119	100.0000	
		Sum	275.4112			

Signal: DAD1 B, Sig=210,4 Ref=off

RT [min]	Type	Width [min]	Area	Height	Area%	Name
4.056	BB	0.2114	471.9818	34.9771	100.0000	
		Sum	471.9818			

Signal: DAD1 C, Sig=320,4 Ref=off

RT [min]	Type	Width [min]	Area	Height	Area%	Name
4.055	BB	0.2103	453.7849	33.8671	100.0000	
		Sum	453.7849			

LCMS Report

Agilent Technologies

Data file:	D:\Chem32\1\Data\TP 2016-02-17 15-45-21\043-0101.D		
Sample name:	TP75B5		
Description:			
Sample amount:	0.000	Sample type:	Sample
Instrument:	LCMS	Location:	43
Injection date:	2/17/2016 3:47:04 PM	Injection:	1 of 1
Acq. method:	LCMS ISOCRATIC 50% B.M	Injection volume:	1.000
Analysis method:	LCMS ISOCRATIC 50%B.M	Acq. operator:	SYSTEM
Last changed:	2/17/2016 2:13:42 PM		

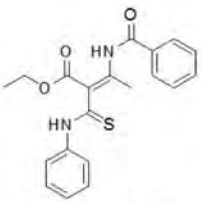

Compound 10a

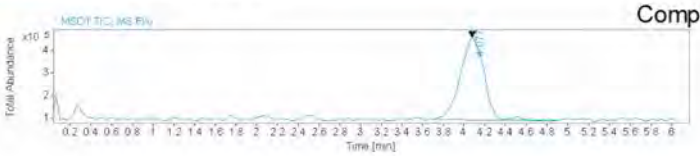

LCMS Report

Agilent Technologies

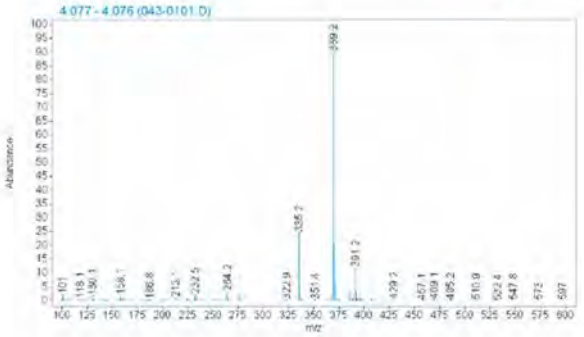

Compound	Chemical Formula	Predicted monoisotopic neutral MW	Predicted MH+	MH+ Measured	Main MS Ions	Main MS/MS Fragments
TP75 B5 **10a**	$C_{20}H_{20}N_2O_3S$	368.1195	369.1267	369.1270	369.1270	276.0696
					351.11595^	248.0747
						188.0712

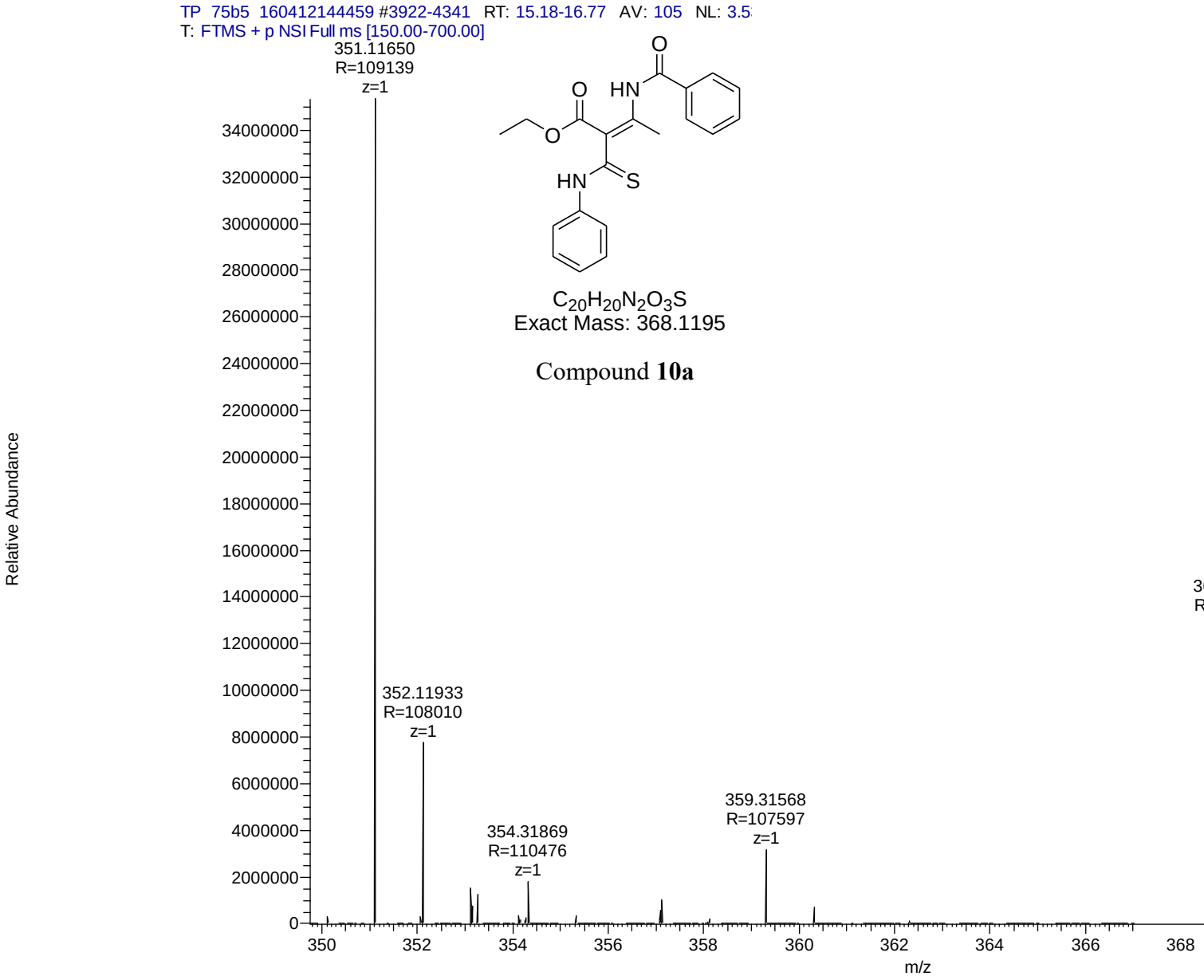

Compound **10b**

Compound Name: Ethyl-3-benzamido-2-((4-bromophenyl)carbamothioyl)but-2-enoate

Obtained Weight & Yield: 300 mg, 29%

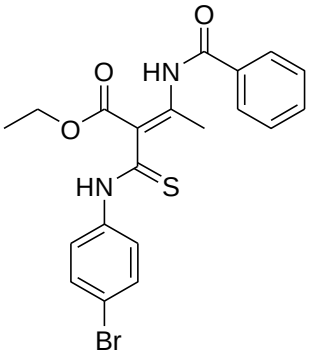

$C_{20}H_{19}BrN_2O_3S$
Exact Mass: 446.0300

Appearance: Sparkling yellow precipitate

Solubility: MeOH, Acetone, ACN

TLC Conditions: EtOAc/Hexane (50/50)

IR Analysis: νmax/cm^{-1}
3296 (NH), 1683 (COO), 1661 (CON), 1240 (CO)

The product is detected as a mixture of isomers, with the ration 12.8 : 1.0 calculated at 2.55 and 2.47 ppm, respectively. The 1H NMR is reported as a whole due to complex overlapping. All 13C NMR peaks are reported.

^{1}H NMR Analysis:
^{1}H NMR (400 MHz, DMSO-*d*$_6$) δ 12.31 (s, 1H), 12.11 (s, 1H), 8.01 – 7.83 (m, 4H), 7.74 – 7.06 (m, 5H), 4.28 – 4.06 (m, 2H), 2.55 (s, 2.7H), 2.47 (s, 0.2H), 1.25 – 1.05 (m, 3H).

^{13}C NMR Analysis:
^{13}C NMR (101 MHz, DMSO-*d*$_6$) δ 193.9, 167.3, 165.4, 150.7, 139.2, 134.1, 133.3, 132.1 (C x 2), 129.7 (C x 2), 127.7 (C x 2), 125.0 (C x 2), 118.8, 116.5, 61.4, 18.8, 14.5.

RP-UPLC Agilent Zorbax SB™ C18 1.8 µm 50 mm x 2.1 mm, isocratic 80% B (9:1 ACN: Water) in 6 min, R_t = 0.72 min, 100% at 210, 254 and 320 nm.

Mass Spectral Analysis: LRMS (ESI+) m/z: 446, 447 [M+ H; ^{79}Br, ^{81}Br]$^{+}$ 100%. HRMS (ES+) for $C_{20}H_{19}BrN_2O_3S$ calculated 447.0373, found 447.0370 [M+ H; ^{79}Br, ^{81}Br]$^{+}$.

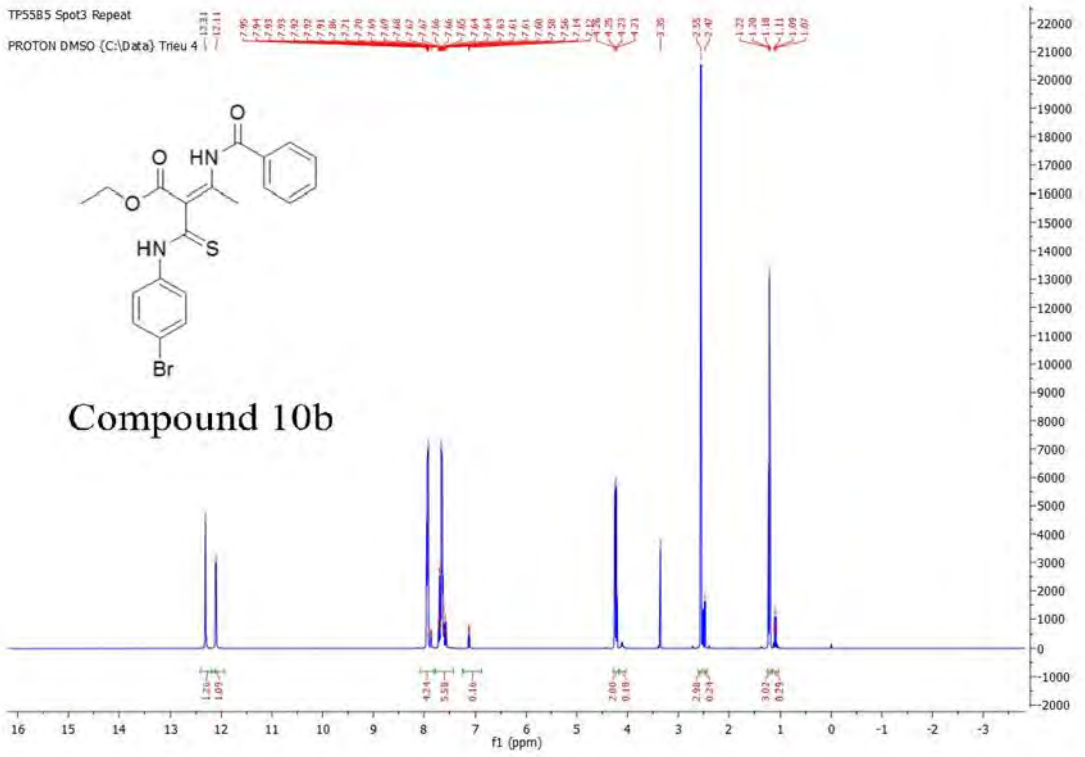
TP55B5 Spot3 Repeat
PROTON DMSO {C:\Data} Trieu 4
O
HN
O
O
HN
S
Br
Compound 10b
f1 (ppm)

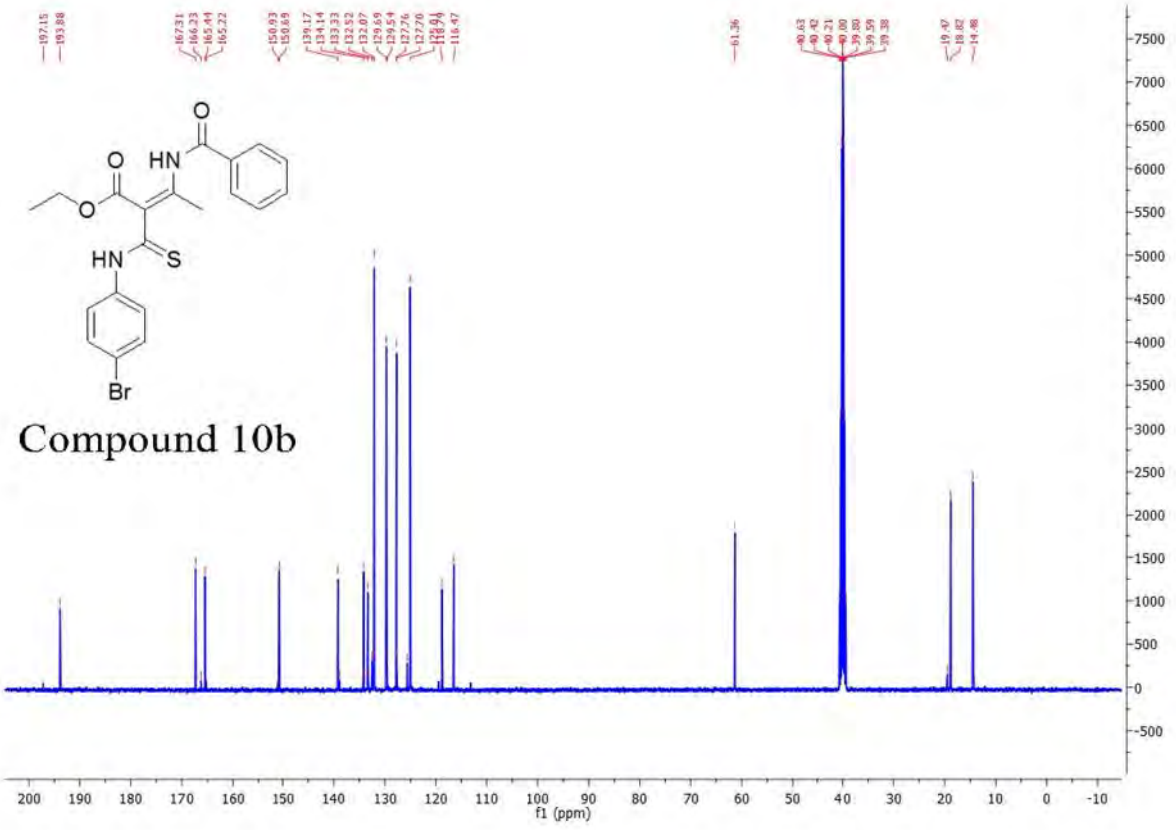
O
HN
O
O
HN
S
Br
Compound 10b
f1 (ppm)

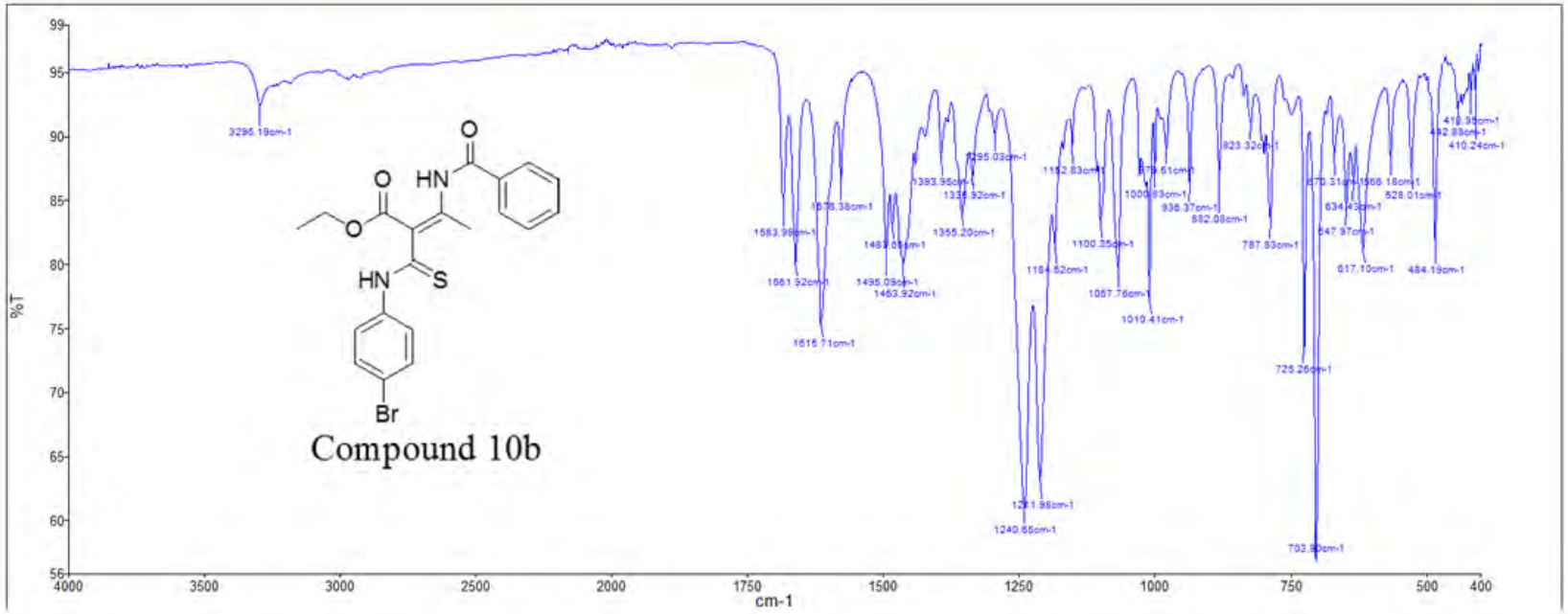
%T
cm-1
Compound 10b
Br

LCMS Report

Agilent Technologi

file:	D:\Chem32\1\Data\TP 2016-02-16 15-06-02\040-0201.D		
ple name:	TP55B5		
cription:			
ple amount:	0.000	Sample type:	Sample
rument:	LCMS	Location:	40
ction date:	2/16/2016 3:15:40 PM	Injection:	1 of 1
method:	LCMS ISOCRATIC 80% B.M	Injection volume:	10.000
lysis method:	LCMS ISOCRATIC 80%B.M	Acq. operator:	SYSTEM
changed:	1/28/2016 10:04:30 AM		

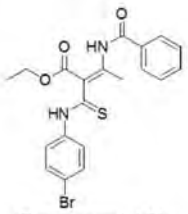

Compound 10b

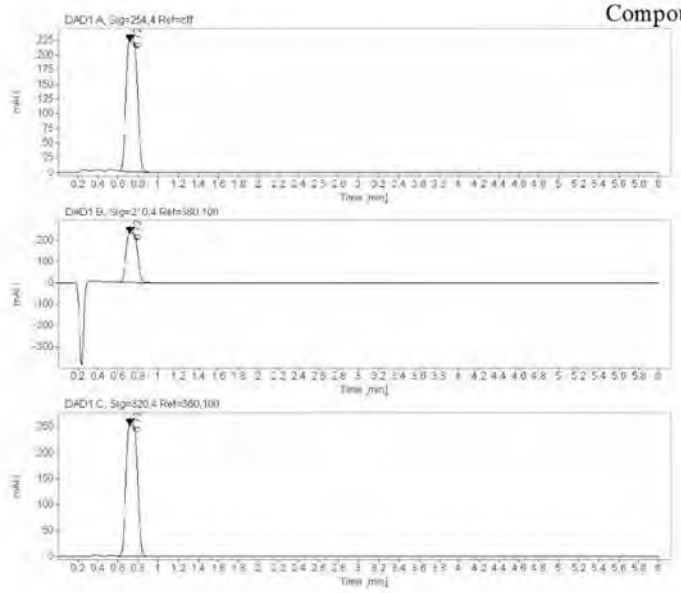

Signal: DAD1 A, Sig=254,4 Ref=off

RT [min]	Type	Width [min]	Area	Height	Area%	Name
0.720	BB	0.1049	1695.4336	222.4668	100.0000	
		Sum	1695.4336			

Signal: DAD1 B, Sig=210,4 Ref=360,100

RT [min]	Type	Width [min]	Area	Height	Area%	Name
0.720	BB	0.1050	1761.0068	230.8283	100.0000	
		Sum	1761.0068			

Signal: DAD1 C, Sig=320,4 Ref=360,100

RT [min]	Type	Width [min]	Area	Height	Area%	Name
0.720	BB	0.1047	1922.0504	252.9278	100.0000	
		Sum	1922.0504			

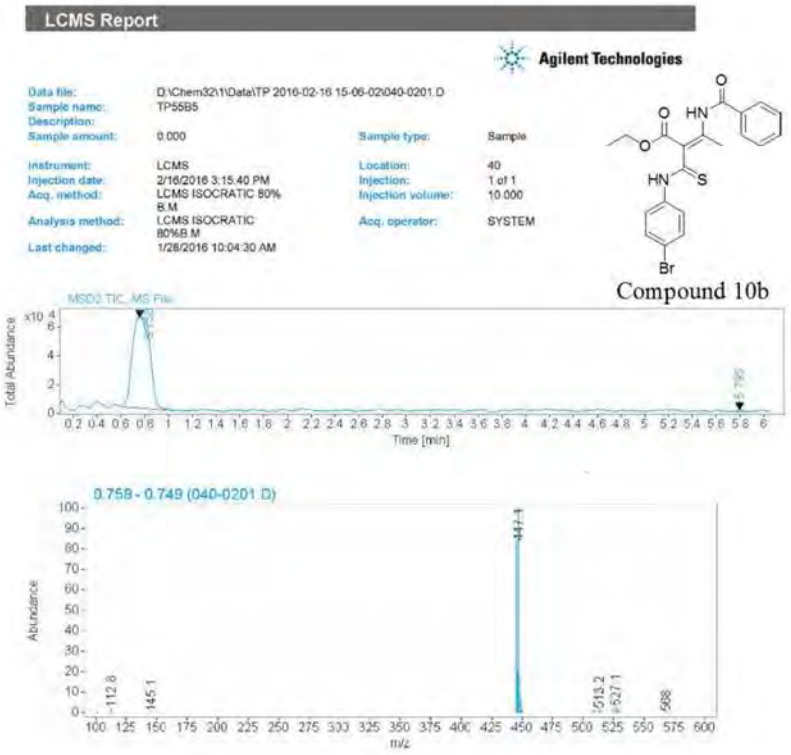
LCMS Report
Agilent Technologies
Data file: D:\Chem32\1\Data\TP 2016-02-16 15-06-02\040-0201.D
Sample name: TP55B5
Description:
Sample amount: 0.000
Sample type: Sample
Instrument: LCMS
Injection date: 2/16/2016 3:15:40 PM
Acq. method: LCMS ISOCRATIC 50% B.M
Analysis method: LCMS ISOCRATIC 80%B.M
Last changed: 1/28/2016 10:04:30 AM
Location: 40
Injection: 1 of 1
Injection volume: 10.000
Acq. operator: SYSTEM
Compound 10b
MSD2 TIC, MS File
Total Abundance
Time [min]
0.758 - 0.749 (040-0201.D)
Abundance
m/z

Compound	Chemical Formula	Predicted monoisotopic neutral MW	Predicted MH+	MH+ Measured	Main MS Ions	Main MS/MS Fragments
TP55 B5 **10b**	$C_{20}H_{19}BrN_2O_3S$	446.0300	447.0373	447.0370	447.0370	309.0234
					429.02646	276.0690
						105.0338